

U.S. ARMY Const. Eng. Res. Ctr. Shore Protect. Man.

1984



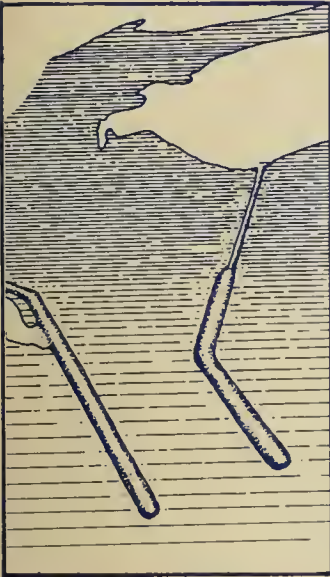
US Army Corps of Engineers

# SHORE PROTECTION MANUAL

## VOLUME I

Coastal Engineering Research Center

DEPARTMENT OF THE ARMY  
Waterways Experiment Station, Corps of Engineers  
PO Box 631  
Vicksburg, Mississippi 39180



1984

Approved For Public Release; Distribution Unlimited



Prepared for

DEPARTMENT OF THE ARMY  
US Army Corps of Engineers  
Washington, DC 20314

Reprint or republication of any of this material should give appropriate credit to the U.S. Army Engineer Waterways Experiment Station Coastal Engineering Research Center, P.O. Box 631, Vicksburg, Miss. 39180

This publication is intended as a guide for coastal engineering planning and design and is not intended to replace the judgement of a qualified design engineer on a particular project. The United States Government and the U.S. Army Corps of Engineers assume no liability for interpretations or implementations made by users of this publication.

The contents of this publication are not to be used for advertising, publication, or promotional purposes. Citation of trade names does not constitute an official endorsement or approval of the use of such commercial products.



edition

Vols. 1

ch Center 1984

RETURNED

NOV 27 1982

Top: Weir Jetty, Murrels Inlet, South Carolina

Bottom: Detached Breakwaters, Presque Isle, Pennsylvania



# SHORE PROTECTION MANUAL



## VOLUME I

(Chapters 1 Through 5)

DEPARTMENT OF THE ARMY  
Waterways Experiment Station, Corps of Engineers  
COASTAL ENGINEERING RESEARCH CENTER

1984

Fourth Edition

For sale by the Superintendent of Documents, U.S. Government Printing Office  
Washington, D.C. 20402 (2-part set; sold in sets only)

Original Printing ..... 1973  
Second Printing ..... 1974  
Second Edition ..... 1975  
Third Edition ..... 1977  
Fourth Edition ..... 1984

## PREFACE

The Coastal Engineering Research Center (CERC) of the U.S. Army Engineer Waterways Experiment Station (WES), and its predecessor, the Beach Erosion Board, has, since 1930, conducted studies on shore processes and methods of shore protection. CERC continues an extensive research and development program to improve both coastal engineering (including shore protection) and offshore engineering techniques. The scientific and engineering aspects of coastal processes and coastal and offshore structures are in the developmental stage, and the requirement for improved techniques for use in design and engineering of coastal structures is evident. This need was met in 1954, to the extent of available knowledge, by publication of "Shore Protection, Planning and Design," Technical Report Number 4 (TR 4); revised editions thereof appeared in 1957, 1961, and 1966.

This Shore Protection Manual (SPM), originally published in 1973, incorporated new material with appropriate information extracted from TR 4, and has expanded coverage within the coastal engineering field. Previous revised editions were published in 1975 and 1977. The present edition incorporates substantial revisions to all chapters of the SPM. This edition has been reduced from three volumes to two by moving Chapter 5 from Volume II to Volume I and including the appendices within Volume II.

This edition was prepared under the direction of Dr. Robert W. Whalin, Chief, CERC; Dr. Fred E. Camfield, Acting Chief, Engineering Development Division, and Chief, Coastal Design Branch; Mr. Neill E. Parker, former Chief, Engineering Development Division; Mr. Robert A. Jachowski, former Chief, Coastal Design Branch; and Dr. J. Richard Weggel, former Chief, Coastal Structures and Evaluation Branch. Chapter 1 was revised by Mr. James W. Eckert and Dr. Steven A. Hughes. Revisions to Chapter 2 were prepared by Dr. Fred E. Camfield and Mr. William N. Seelig. Chapter 3 was revised by Drs. Jon M. Hubertz, Edward F. Thompson, and C. Linwood Vincent, and Chapter 4 by Mr. William A. Birkemeier, Drs. Robert J. Hallemeier, Robert M. Sorensen, Edward F. Thompson, and Todd L. Walton, Jr., and Mr. Philip Vitale. Revisions to Chapter 5 were prepared by Mr. William Dally, Dr. Richard D. Hobson, Mr. Paul L. Knutsen, and Mr. Philip Vitale, and to Chapter 6 by Mr. James W. Eckert, Dr. Steven A. Hughes, and Mr. Paul L. Knutsen. Chapter 7 was revised by Dr. Fred E. Camfield, Mr. D. D. Davidson, Mr. James W. Eckert, Dr. Steven A. Hughes, Mr. Robert E. Ray, Ms. Debra L. Rouse, Mr. William N. Seelig, Mr. Orson P. Smith, and Dr. J. Richard Weggel. Chapter 8 was revised by Dr. J. Richard Weggel, Dr. Yen-hsi Chu, and Ms. Mary A. Cialone. The present index was prepared by Ms. Alfrieda S. Clark, Ms. Katherine M. Kennedy, and Mr. Paul A. Taccarino, Special Projects Branch, Technical Information Center. Editors for this edition were Ms. Betty Hall, Ms. Mozelle Jones, and Ms. Kathryn B. (Taffy) Stept. Editorial assistance was provided by Ms. Goldie Booth, Ms. Mary Pikul, and Ms. Josephine Head. Typing and composing were done by Ms. Peggy Johnson, Ms. Dorothy T. Lauria, and Ms. Mary L. Logan.

Commander and Director of WES during final preparation and publication of this edition was COL Tilford C. Creel, CE. Technical Director was Mr. F. R. Brown.

Comments or suggestions on material in this publication are invited.

This report is published under authority of Public Law 166, 79th Congress, approved July 31, 1945, as supplemented by Public Law 172, 88th Congress, approved November 7, 1963.

# TABLE OF CONTENTS

## VOLUME I

### CHAPTER 1. INTRODUCTION TO COASTAL ENGINEERING

I—Overview of Coastal Engineering and the SPM, page 1-1; II—The Coastal Area, page 1-2; III—The Beach and Nearshore System, page 1-4; IV—Dynamic Beach Response to the Sea, page 1-9; V—Causes of Shoreline Erosion, page 1-15; VI—Coastal Protection Methods and Navigation Works, page 1-17; VII—Conservation of Sand, page 1-25; Literature Cited, page 1-27

### CHAPTER 2. MECHANICS OF WAVE MOTION

I—Introduction, page 2-1; II—Wave Mechanics, page 2-1; III—Wave Refraction, page 2-60; IV—Wave Diffraction, page 2-75; V—Wave Reflection, page 2-109; VI—Breaking Waves, 2-129; Literature Cited, page 2-137; Bibliography, page 2-147

### CHAPTER 3. WAVE AND WATER LEVEL PREDICTIONS

I—Introduction, page 3-1; II—Characteristics of Ocean Waves, page 3-1; III—Wave Field, page 3-19; IV—Estimation of Surface Winds for Wave Prediction, page 3-27; V—Simplified Methods for Estimating Wave Conditions, page 3-39; VI—Wave Forecasting for Shallow Water, page 3-55; VII—Hurricane Waves, page 3-77; VIII—Water Level Fluctuations, page 3-88; Literature Cited, page 3-130; Bibliography, page 3-140

### CHAPTER 4. LITTORAL PROCESSES

I—Introduction, page 4-1; II—Littoral Materials, page 4-12; III—Littoral Wave Conditions, page 4-29; IV—Nearshore Currents, page 4-46; V—Littoral Transport, page 4-55; VI—Role of Foredunes in Shore Processes, page 4-108; VII—Sediment Budget, page 4-113; VIII—Engineering Study of Littoral Processes, page 4-133; IX—Tidal Inlets, page 4-148; Literature Cited, page 4-182; Bibliography, page 4-208

### CHAPTER 5. PLANNING ANALYSIS

I—General, page 5-1; II—Seawalls, Bulkheads, and Revetments, page 5-2; III—Protective Beaches, page 5-6; IV—Sand Dunes, page 5-24; V—Sand Bypassing, page 5-26; VI—Groins, page 5-35; VII—Jetties, page 5-56; VIII—Breakwaters, Shore-Connected, page 5-58; IX—Breakwaters, Offshore, page 5-61; X—Environmental Considerations, page 5-74; Literature Cited, page 5-75

## VOLUME II

### CHAPTER 6. STRUCTURAL FEATURES

I—Introduction, page 6-1; II—Seawalls, Bulkheads, and Revetments, page 6-1; III—Protective Beaches, page 6-14; IV—Sand Dunes, page 6-37; V—Sand Bypassing, page 6-53; VI—Groins, page 6-76; VII—Jetties, page 6-84; VIII—Breakwaters, Shore-Connected, page 6-88; IX—Breakwaters, Offshore, page 6-93; X—Construction Materials and Design Practices, page 6-95; Literature Cited, page 6-99

### CHAPTER 7. STRUCTURAL DESIGN: PHYSICAL FACTORS

I—Wave Characteristics, page 7-1; II—Wave Runup, Overtopping, and Transmission, page 7-16; III—Wave Forces, page 7-100; IV—Velocity Forces—Stability of Channel Revetments, page 7-249; V—Impact Forces, page 7-253; VI—Ice Forces, page 7-253; VII—Earth Forces, page 7-256; Literature Cited, page 7-261; Bibliography, page 7-277

### CHAPTER 8. ENGINEERING ANALYSIS: CASE STUDY

I—Introduction, page 8-1; II—Statement of Problem, page 8-1; III—Physical Environment, page 8-1; IV—Preliminary Design, page 8-46; V—Computation of Potential Longshore Transport, page 8-85; VI—Beachfill Requirements, page 8-90; Literature Cited, page 8-93

APPENDIX A. GLOSSARY, page A-1

APPENDIX B. LIST OF SYMBOLS, page B-1

APPENDIX C. MISCELLANEOUS TABLES AND PLATES, page C-1

APPENDIX D. INDEX, page D-1

# CHAPTER 1

## Introduction to Coastal Engineering



*Fort DeRussy, Oahu, Hawaii, 27 August 1970*



CONTENTS

CHAPTER 1

INTRODUCTION TO COASTAL ENGINEERING

	Page
I OVERVIEW OF COASTAL ENGINEERING AND THE SPM.....	1-1
II THE COASTAL AREA.....	1-2
III THE BEACH AND NEARSHORE SYSTEM.....	1-4
1. The Sea.....	1-4
2. The Beach and Nearshore Zone.....	1-7
IV DYNAMIC BEACH RESPONSE TO THE SEA.....	1-9
1. Normal Beach Response.....	1-9
2. Beach Response to Storms.....	1-10
3. Beach and Dune Recovery from Storm Attack.....	1-13
4. Littoral Transport.....	1-13
5. Effect of Inlets on Barrier Beaches.....	1-14
6. Beach Stability.....	1-15
V CAUSES OF SHORELINE EROSION.....	1-15
1. Natural Causes.....	1-15
2. Man-Induced Causes.....	1-16
VI COASTAL PROTECTION METHODS AND NAVIGATION WORKS.....	1-17
VII CONSERVATION OF SAND.....	1-25
LITERATURE CITED.....	1-27

TABLES

1-1 Causes of coastal erosion.....	1-16
------------------------------------	------

FIGURES

1-1 Visual definition of terms describing a typical beach profile.....	1-2
1-2 Large waves breaking over a breakwater.....	1-5
1-3 Wave characteristics.....	1-5
1-4 Undeveloped barrier island on the gulf coast of Alabama after Hurricane Frederic.....	1-8
1-5 Developed barrier island, Atlantic City, New Jersey.....	1-9
1-6 Sand dunes on Padre Island, Texas.....	1-11
1-7 Sand dunes at Nauset Spit, Cape Cod, Massachusetts.....	1-11
1-8 Schematic diagram of storm wave attack on beach and dune.....	1-12
1-9 Littoral barrier, Ocean City Inlet, Maryland.....	1-18
1-10 Damage after the 1962 storm, Rehoboth Beach, Delaware.....	1-20
1-11 Undermining of structures by storm waves, Potham Beach, Maine.....	1-21
1-12 Beach restoration, Dade County, Florida.....	1-22
1-13 Weir jetty at Murrells Inlet, South Carolina, 1981.....	1-25



## CHAPTER 1

### INTRODUCTION TO COASTAL ENGINEERING

#### I. OVERVIEW OF COASTAL ENGINEERING AND THE SPM

The Shore Protection Manual (SPM) assembles in a single source the current state-of-the-art of coastal engineering to provide appropriate guidance for application of techniques and methodology to the solution of coastal design problems. As the state-of-the-art advances, the manual is periodically revised. This is the fourth edition of the SPM and the seventh major revision of this material since its predecessor report "Shore Protection, Planning and Design" (TR-4) was originally published (U.S. Army, Corps of Engineers, 1954).

Coastal engineering, a specialized branch of the engineering profession, is a composite of the many physical science and engineering disciplines having application in the coastal area. Coastal engineering addresses both the natural and man-induced changes in the coastal zone, the structural and non-structural protection against these changes, and the desirable and adverse impacts of possible solutions to problem areas on the coast. Although the SPM focuses primarily on shore protection, i.e., coastal works designed to stabilize the shores against erosion due principally to water wave action, most of the material is also applicable to the design of harbor works and navigation channel improvements.

Because the nature and complexity of most coastal problems vary widely with location, the proper solution of any specific problem requires a systematic and thorough study. The first requisite for such a study is a clear definition of the problem, the causes, and the objectives to be met by the solution. Ordinarily, there will be more than one method of achieving the immediate objectives. Therefore, the immediate and long-term effects of each method should be studied, not only within the problem area but also in adjacent shore areas. All physical and environmental effects, advantageous and detrimental, should be considered in comparing the overall cost, including annual maintenance, and benefits to determine the justification of protection methods.

The SPM provides sufficient introductory material and engineering methodology to allow a person with an engineering background to obtain an understanding of coastal phenomena and to solve related engineering problems. The manual includes detailed summaries of applicable methods, techniques, and useful data pertinent to the solution of coastal engineering problems.

Chapter 1 presents a basic introduction to the subject. Chapter 2, "Mechanics of Wave Motion," reviews wave theories, wave refraction and diffraction, wave reflection, and breaking waves. Chapter 3, "Wave and Water Level Predictions," discusses wave forecasting and the water level fluctuations caused by tides, storm surges, and tsunamis. Chapter 4, "Littoral Processes," examines the characteristics and sources of littoral material, nearshore currents, littoral transport, and sand budget techniques. Chapter 5, "Planning Analyses," treats the functional planning of shore protection measures. Chapter 6, "Structural Features," illustrates the structural design

of various coastal or protective structures. Chapter 7, "Structural Design--Physical Factors," considers the effects of environmental forces on the design of protective works. Chapter 8, "Engineering Analysis--Case Study," presents a series of calculations for the preliminary design of a hypothetical structure. Each chapter includes a listing of bibliographic sources.

The SPM concludes with four supporting appendixes. Appendix A is a glossary of coastal engineering terms used. Appendix B lists and defines the symbols used. Appendix C is a collection of miscellaneous tables and plates that supplement the material in the chapters, and Appendix D is the subject index.

## II. THE COASTAL AREA

In any discussion on engineering, an agreement on the meaning of terms is necessary before effective communication can occur. Since the varied meanings of coastal engineering terms used over the years have complicated dialogue, the glossary in Appendix A has been assembled to establish a common vocabulary for the SPM. Figure 1-1 provides a visual definition of the terms discussed in this chapter.

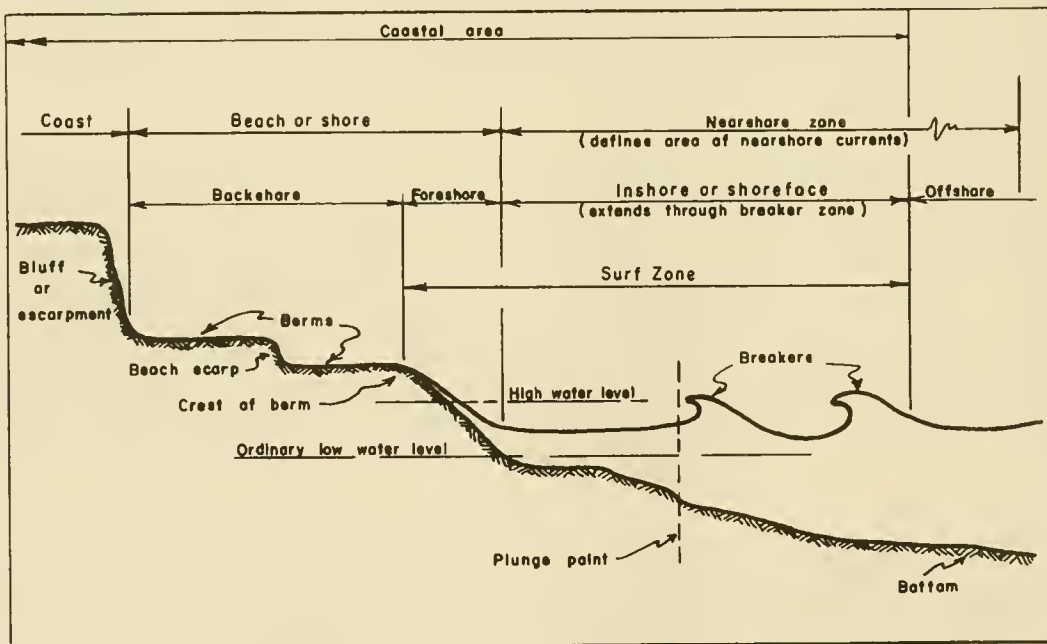


Figure 1-1. Visual definition of terms describing a typical beach profile.

Any overview of the coastal area quickly reveals a wide variability of coastal landforms. The "Report on the National Shoreline Study" (U.S. Army, Corps of Engineers, 1971) indicates that of the total 135,550 kilometers (84,240 miles) of U.S. shoreline, 55,550 kilometers (34,520 miles) (41 percent) is exposed shoreline and 80,000 kilometers (49,720 miles) (59 percent) is sheltered shoreline (i.e., in bays, estuaries, and lagoons). About 33,000 kilometers (20,500 miles) of the shoreline (or 24 percent of the total) is eroding. Of the total length of shoreline, exclusive of Alaska (59,450

kilometers or 36,940 miles), about 19,550 kilometers (12,150 miles) (33 percent) has beaches; the remaining 39,900 kilometers (24,790 miles) is rocky or otherwise lacks the typical beach characteristics described in Figure 1-1. Likewise the coast along shorelines varies. In New England, it is frequently rocky promontories while the south Atlantic and gulf coasts are generally low, dotted with backbays, wide estuaries, and marshes. Southern California with a history of a rising landmass has coastal cliffs of conglomerate material, some of which were at one time beaches. The coast of the north Pacific and Alaska is dominated by the basaltic deposits of postvolcanic activity, weathered by the action of water. Even on a more local scale, beaches and coasts can vary widely reflecting their differences in geologic history and recent wave and current action.

Where the land meets the ocean at a sandy beach, the shore has natural defenses against attack by waves, currents, and storms. The first of these defenses is the sloping nearshore bottom that causes waves to break offshore, dissipating their energy over the surf zone. The process of breaking often creates an offshore bar in front of the beach that helps to trip following waves. The broken waves re-form to break again, and may do this several times before finally rushing up the beach foreshore. At the top of wave uprush a ridge of sand is formed. Beyond this ridge, or crest of the berm, lies the flat beach berm that is reached only by higher storm waves.

During the early days of the United States, natural beach processes molded the shore as in ages past. As the country developed, shore activity was confined principally to harbor areas, and development along the shore progressed slowly as small, isolated fishing villages. As the national economy grew and transportation improved, more people began to use the beaches. Gradually, extensive housing and commercial, industrial, recreational, and resort developments replaced the fishing villages as the predominant coastal manmade features. Examples of this development are Atlantic City, Miami Beach, Honolulu, and Imperial Beach south of San Diego.

Numerous factors control the growth of development at beach areas, but undoubtedly the beach environment is the development's basic asset. The desire of visitors, residents, and industries to find accommodations as close to the ocean as possible has resulted in man's encroachment on the sea. In their eagerness to be as close as possible to the water, developers and property owners often forget that land in the coastal area comes and goes, and that land which nature provides at one time may later be reclaimed by the sea. Once the seaward limit of a development is established, this boundary between land and sea is perceived as fixed and must be held if large investments are to be preserved. Whether the problem is one of natural erosion processes working on the coastal land that threatens man's presence there, or erosion induced by man's encroachment on the sea, the results are similar. Erosion generally leads to either great monetary losses due to storm damage or even larger expenditures for shore protection to prevent the loss.

Another problem in the coastal area is the need for inland waterborne commerce on rivers and bays which must pass through the coastal area to reach deep water. Inlets which once migrated to suit the water and wave forces acting on them are now being pinned in place by jetties, creating accretion and erosion problems on their flanks.

Coastal engineering is the discipline which deals with these problems. To do this, the coastal engineer must not only design a solution but also have knowledge of the natural processes at work, the wind and water forces driving them, and the probable impact of the solution on the existing coastal system and environment. Coastal engineering is a very site-specific discipline, and solutions successful at one point may not work at another.

To achieve the objectives of coastal engineering, practitioners must utilize several disciplines. From field investigations and a knowledge of physics, they develop an understanding of the coastal processes at the project site. Then using models, both physical and numerical, they study the possible solutions and their impacts. However, no factor is more important for the engineer than past experience. Monitoring of constructed projects provides tremendous assistance towards planning the next.

The coastal engineer's work is divided into three phases: understanding the nearshore physical system and the shoreline's response to it; designing coastal works to meet project objectives within the bounds of acceptable coastal impact; and overseeing the construction of coastal works and monitoring their performance to ensure that projects function as planned.

### III. THE BEACH AND NEARSHORE SYSTEM

The beach and nearshore zone of a coast is the region where the forces of the sea react against the land. The physical system within this region is composed primarily of the motion of the sea, which supplies energy to the system, and the shore, which absorbs this energy. Because the shoreline is the intersection of the air, land, and water, the physical interactions which occur in this region are unique, very complex, and difficult to fully understand. As a consequence, a large part of the understanding of the beach and nearshore physical system is simply descriptive in nature.

#### 1. The Sea.

Water covers 71 percent of the Earth, and thus a large part of the Sun's radiant energy that is not reflected back into space is absorbed by the water of the oceans. This absorbed energy warms the water, which in turn warms the air above the oceans, and forms air currents caused by differences in air temperature. These air currents blow across the water, returning some energy to the water by generating *wind waves*. The waves then travel across the oceans until they reach land where their remaining energy is expended on the shore. The power in the waves as they arrive in the nearshore zone can vary from 1.39 megawatts per kilometer (3,000 horsepower per mile) of beach on a relatively calm day (0.6-meter or 2-foot waves) to 25 times this amount or more during a storm.

The motions of the sea which contribute to the beach and nearshore physical system include waves, tides, currents, storm surges, and tsunamis. Wind waves are by far the largest contribution of energy from the sea to the beach and nearshore physical system. As winds blow over the water, waves are generated in a variety of sizes from ripples to large ocean waves as high as 30 meters (100 feet) (see Fig. 1-2).



Figure 1-2. Large waves breaking over a breakwater.

Wind waves, which are also known as oscillatory waves, are usually defined by their height, length, and period (see Fig. 1-3). Wave height is the vertical distance from the top of the crest to the bottom of the trough. Wavelength is the horizontal distance between successive crests. Wave period is the time between successive crests passing a given point. As waves propagate in deep water, only the waveform and part of the energy move forward; the water particles move in a nearly circular path.

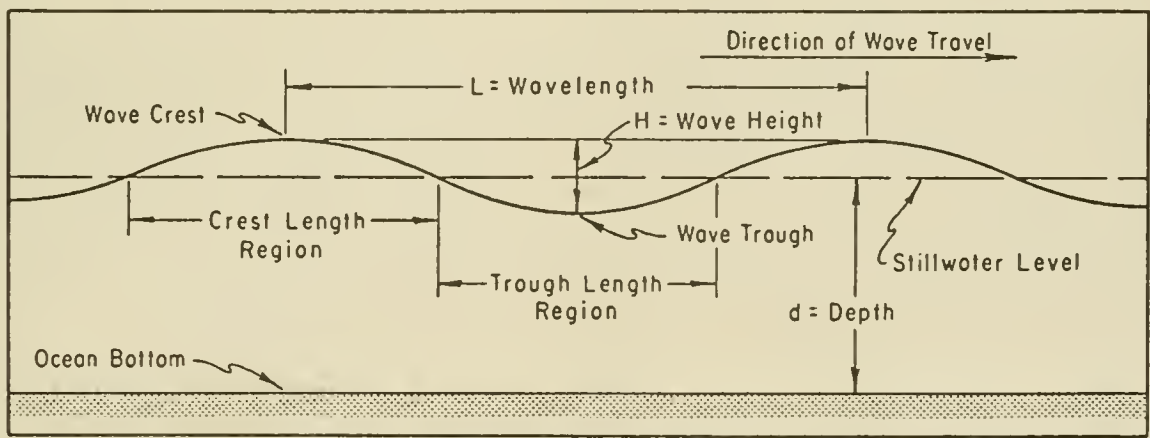


Figure 1-3. Wave characteristics.

The height, length, and period of wind waves at a site in the open ocean are determined by the *fetch* (the distance the wind blows over the sea in generating the waves), the windspeed, the duration (the length of time the wind blows), the *decay distance* (the distance the wave travels after leaving the generating area), and the water depth. Generally, increases in fetch, windspeed, or duration result in larger wind waves. The water depth, if shallow enough, will also affect the size of waves generated. The wind simultaneously generates waves of many heights, lengths, and periods as it blows over the sea.

If winds of a local storm blow toward the shore, the waves will reach the beach in nearly the same waveform in which they are generated. Under these conditions, the waves are steep; i.e., the wavelength is 10 to 20 times the wave height. Such waves are called *seas*. If waves are generated by a distant storm, they may travel through hundreds or even thousands of miles of calm wind areas before reaching the shore. Under these conditions, waves *decay*--short, steep waves are transformed into relatively long, low waves which reach the shore. Such waves, which have lengths from 30 to more than 500 times the wave height, are called *swell*.

*Tides* are created by the gravitational force of the Moon and, to a lesser extent, the Sun. These forces of attraction, and the fact that the Sun, Moon, and Earth are always in motion relative to each other, cause waters of ocean basins to be set in motion. These tidal motions of water masses are a form of very long period wave motion, resulting in a rise and fall of the water surface at a point. There are normally two tides per day, but some localities have only one per day. Tides constantly change the level at which waves attack the beach.

The range of tides varies tremendously with geographic location. Some areas, such as Eastport, Maine, experience an average tidal range of about 5.5 meters (18 feet) while other locations, such as Mobile, Alabama, experience variations of about 0.6 meter. Even more dramatic is the difference between mean tidal ranges at Anchorage (7.9 meters or 26 feet) and Kodiak Island (2.1 meters or 7 feet), Alaska. These sites are only 415 kilometers (224 nautical miles) apart.

*Currents* and *surges* sometimes play an important role in the nearshore physical system. When water in one area becomes higher than water in another area, water from the higher elevation flows toward the lower level, creating a current. Significant currents generated by tides occur at inlets to lagoons and bays or at entrances to harbors. Tidal currents in these constricted places flow in when the tide is rising (floodtide) and flow out as the tide falls (ebbtide). Exceptions can occur at times of high river discharge or strong winds. Currents can be caused by differences in water elevation due to (a) wind, (b) waves breaking on a beach, and (c) river discharge. The river discharge to the sea introduces currents into the nearshore zone.

Wind creates currents as it blows over the water surface, producing a stress on surface water particles and starting the movement of the particles in the direction in which the wind is blowing. Thus, a surface current is created. When the surface current reaches a barrier, such as the coast, water

tends to pile up against the land. Strong winds create *wind setup* or *storm surges* in this way. The height of storm surge depends on wind speed and direction, fetch, atmospheric pressure, offshore bathymetry, and nearshore slope. In violent storms, storm surge may raise the water level at the shore as much as 6 meters (20 feet). In the United States, larger surges occur on the gulf coast because of the shallower and broader shelf off that coast compared to the shelf off both the Atlantic and Pacific coasts. Storm surges may also be increased by a funneling effect in converging shorelines within estuaries.

When waves approach the beach at an angle, they create a current in shallow water parallel to the shore, known as the *longshore current*. This current, under certain conditions, may turn and flow seaward in what is known as a *rip current*.

*Tsunamis* are waves created by earthquakes or other tectonic disturbances on the ocean bottom. These long-period waves can travel across entire oceans at speeds exceeding 800 kilometers (500 miles) per hour. Tsunamis can cause extensive damage at times, but fortunately major tsunamis do not occur frequently.

## 2. The Beach and Nearshore Zone.

The shoreline, the intersection of the land and the sea, is where tides, winds, and waves attack the land; and it is where the land responds to this attack by a variety of "give and take" measures which effectively dissipate the sea's energy. The shores of the United States include practically all known landforms of many clastic materials from various stages of geologic evolution. The areas most directly affected by the forces of the sea are the *beach* and the *nearshore zone* regions that experience the full impact of the sea's energy. Hence, they are the most dynamic areas in the coastal zone.

*Beach sediments* on most beaches range from fine sands to cobbles. The size and character of sediments and the slope of the beach are related to the forces to which the beach is exposed and the type of material available on the coast. Much of the beach material originates many miles inland where weathering of the mountains produces small rock fragments that are supplied to the beach by streams and rivers. When these fragments reach the shore as sand, they are moved alongshore by waves and currents. This longshore transport is a constant process, and great volumes may be transported. Beach material is also derived from erosion of the coastal formations caused by waves and currents and, in some cases, by onshore movement of sediment from deeper water. In some regions, a sizable fraction of the beach material is composed of marine shell fragments, coral reef fragments, or volcanic materials. Clay and silt do not usually exist on ocean beaches because the waves create such turbulence in the water along the shore that these fine particles are kept in suspension. The particles settle and deposit on the bottom only after moving away from the beaches into the quieter water of lagoons and estuaries or the deeper water offshore.

*Beach characteristics* are usually described in terms of average size of the sand particles that make up the beach, range and distribution of sizes of the sand particles, sand composition, elevation and width of berm, slope or

steepness of the foreshore, the existence (or lack) of a bar, and the general slope of the inshore zone fronting the beach. Generally, the larger the sand particles the steeper the beach slope. Beaches with gently sloping foreshores and inshore zones usually have a preponderance of the finer sizes of sand. Daytona Beach, Florida, is a good example of a gently sloping beach composed of fine sand.

*Barrier islands* are an important part of the physical system in some areas (see Fig. 1-4). These are long narrow islands or spits lying parallel to the mainland. Most of the coast on the U.S. Atlantic south of Long Island and along the gulf is composed of barrier islands. During severe storms these barrier islands provide protection for the mainland by absorbing the brunt of the wave attack. However, many barrier islands are so highly developed that the protection of their beaches has become an important consideration (see Fig. 1-5).



Figure 1-4. Undeveloped barrier island on the gulf coast of Alabama after Hurricane Frederic.

*Lagoons* are shallow bodies of water separating the barrier beach from the mainland. They are usually connected to the sea by narrow channels through which tidal currents flow. Lagoons provide a habitat for a wide variety of wildlife, and many lagoons serve as safe harbors and navigable waterways.

An *inlet* is the narrow opening between the lagoon and the ocean. Inlets occur at fairly regular intervals along a barrier island chain, and they often, when improved, provide a navigation passage to the sea. When barrier beach dunes are breached by storm wave attack, the result may be the cutting of a new inlet. An inlet can permit beach material removed by storms to enter a lagoon and be deposited there. It may also allow some bottom material from a lagoon to be carried oceanward by tidal currents and then be transported along the shore by wave action. Over time, changing conditions may cause some inlets to close and new inlets to open.



Figure 1-5. Developed barrier island, Atlantic City, New Jersey.

#### IV. DYNAMIC BEACH RESPONSE TO THE SEA

The beach constantly adjusts its profile to provide the most efficient means of dissipating incoming wave energy. This adjustment is the beach's natural dynamic response to the sea. Although an equilibrium is sometimes reached between the beach and the sea, the "peace" is short-lived and the "battle" soon begins anew.

There are two general types of dynamic beach response to wave motion: response to normal conditions and response to storm conditions. Normal conditions prevail most of the time, and the wave energy is easily dissipated by the beach's natural defense mechanisms. However, when storm conditions generate waves containing increased amounts of energy, the coast must respond with extraordinary measures, such as sacrificing large sections of beach and dune. In time the beach may recover, but often not without a permanent loss.

##### 1. Normal Beach Response.

As a wave moves toward shore, it encounters the first beach defense in the form of the sloping nearshore bottom. When the wave reaches a water depth equal to about 1.3 times the wave height, the wave collapses or breaks. Thus a wave 0.9 meter (3 feet) high will break in a depth of about 1.2 meters (4 feet). Breakers are classified as four types--plunging, spilling, surging, or collapsing. The form of breakers is controlled by wave steepness and nearshore bottom slope. Breaking results in a dissipation of wave energy by the generation of turbulence in the water and by the transport of sediment lifted off the bottom and tossed around by the turbulent water. Broken waves often re-form to break again, losing additional energy. Finally, the water travels forward as a foaming, turbulent mass and expends most of its remaining energy in a rush up the beach slope. If there is an increase in the incoming

wave energy, the beach adjusts its profile to facilitate the dissipation of the additional energy. This is most frequently done by the seaward transport of beach material to an area where the bottom water velocities are sufficiently reduced to cause sediment deposition. Eventually enough material is deposited to form an offshore bar which causes the waves to break farther seaward, widening the surf zone over which the remaining energy must be dissipated. Tides compound the dynamic beach response by constantly changing the elevation at which the water intersects the shore and by providing tidal currents. Thus, the beach is always adjusting to changes in both wave energy and water level.

*Natural protective dunes* are formed by winds blowing onshore over the foreshore and berm, transporting sand landward from the beach (see Figs. 1-6 and 1-7). Grass and sometimes bushes and trees grow on the dunes, and the dunes become a natural levee against sea attack. Dunes provide a reservoir of beach sand which in turn provides the final natural protection line against wave attack.

## 2. Beach Response to Storms.

The subtle changes in the beach which occur during normal conditions are nearly imperceptible to the untrained observer, but the beach's defense mechanisms become obvious when storms attack. Storms do not occur often, but their effects are often devastating in terms of shoreline erosion.

During storms, strong winds generate high, steep waves. In addition, these winds often create a storm surge which raises the water level and exposes to wave attack higher parts of the beach not ordinarily vulnerable to waves. The storm surge allows the large waves to pass over the offshore bar formation without breaking. When the waves finally break, the remaining width of the surf zone is not sufficient to dissipate the increased energy contained in the storm waves. The remaining energy is spent in erosion of the beach, berm, and sometimes dunes which are now exposed to wave attack by virtue of the storm surge. The eroded material is carried offshore in large quantities where it is deposited on the nearshore bottom to form an offshore bar. This bar eventually grows large enough to break the incoming waves farther offshore, forcing the waves to spend their energy in the surf zone. This process is illustrated in Figure 1-8.

Beach berms are built naturally by waves to about the highest elevation reached by normal storm waves. When storm waves erode the berm and carry the sand offshore, the protective value of the berm is reduced and large waves can overtop the beach. The width of the berm at the time of a storm is thus an important factor in the amount of upland damage a storm can inflict.

In severe storms, such as hurricanes, the higher water levels resulting from storm surges allow waves to erode parts of a dune. It is not unusual for 18- to 30-meter-wide (60- to 100- foot) dunes to disappear in a few hours. Storm surges are especially damaging if they occur concurrently with high astronomical tides.



Figure 1-6. Sand dunes on Padre Island, Texas.

1976



Figure 1-7. Sand dunes at Nauset Spit, Cape Cod, Massachusetts.

1977

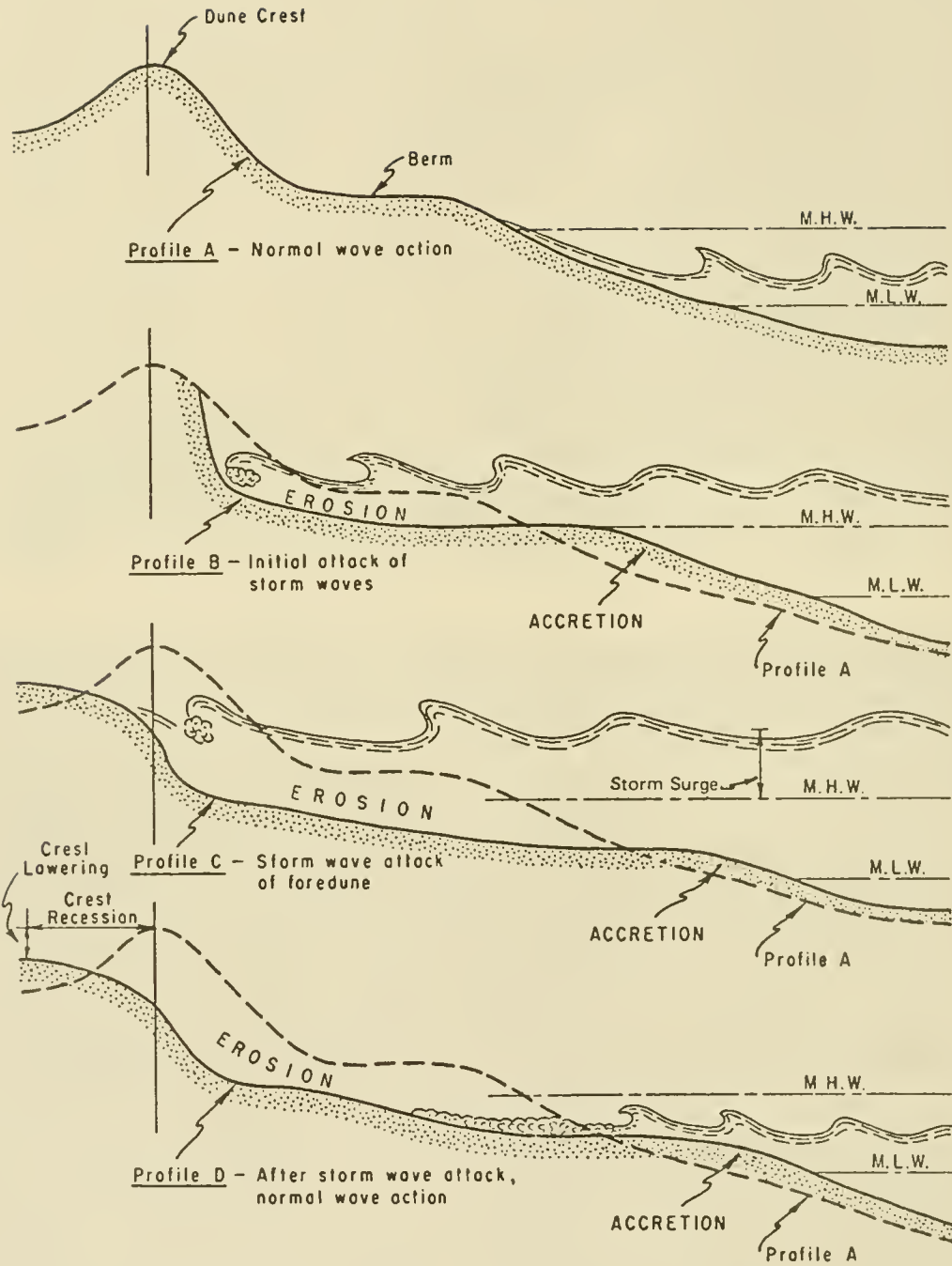


Figure 1-8. Schematic diagram of storm wave attack on beach and dune.

In essence, the dynamic response of a beach under storm attack is a sacrifice of some beach, and often dune, to provide material for an offshore bar. This bar protects the shoreline from further erosion. After a storm or storm season, natural defenses may again be re-formed by normal wave and wind action.

Besides causing erosion of the shoreline, storm surges can damage shore structures that are inadequately protected and located close to the water by either direct wave attack or undermining of the structure.

At locations where there is a low section of protective dunes, or when the storm conditions are particularly severe, the storm surge and wave action may succeed in completely overtopping the dunes causing extensive coastal flooding. When this occurs, beach and dune sediments are swept landward by the water, and in the case of barrier islands, are deposited as *overwash fans* on the backshore or in the lagoon. This process results in a loss of sand from the dynamic beach system. Often, storm overwash and storm flooding return flow will erode enough sand to cut a new tidal inlet through the barrier island. Depending on various factors, the new inlet may become a permanent feature of the coastline.

### 3. Beach and Dune Recovery from Storm Attack.

Following a storm there is a return to more normal conditions which are dominated by low, long swells. These waves transport sand from the offshore bar, built during the storm, and place the material on the beach. Winds then transport the sand onto the dunes where it is trapped by the vegetation. In this manner the beach begins to recover from the storm attack. The rebuilding process takes much longer than the short span of erosion which took place. Therefore, a series of violent local storms over a short period of time can result in severe erosion of the shore because the natural protection does not have time to rebuild between storms. Sometimes full recovery of the beach never occurs because sand is deposited too far offshore during the storm to be returned to the beach by the less steep, normal waves which move material shoreward. This is particularly true in the Great Lakes and in bays and estuaries where waves are fetch-limited and do not develop into long swell waves.

Alternate erosion and accretion may be seasonal on some beaches; the winter storm waves erode the beach, and the summer swell (waves) rebuilds it. Beaches also appear to follow long-term cyclic patterns, where they may erode for several years and then accrete for several years.

### 4. Littoral Transport.

Another dynamic feature of the beach and nearshore physical system is *littoral transport*, defined as the movement of sediments in the nearshore zone by waves and currents. Littoral transport is divided into two general classes: transport parallel to the shore (longshore transport) and transport perpendicular to the shore (onshore-offshore transport). The material that is transported is called *littoral drift*.

Onshore-offshore transport is determined primarily by wave steepness,

sediment size, and beach slope. In general, high steep waves move material offshore, and low waves of long period (low steepness waves) move material onshore. The onshore-offshore process associated with storm waves is illustrated in Figure 1-8.

Longshore transport results from the stirring up of sediment by the breaking wave and the movement of this sediment by both the component of the wave energy in an alongshore direction and the longshore current generated by the breaking wave. The direction of longshore transport is directly related to the direction of wave approach and the angle of the wave (crest) to the shore. Thus, due to the variability of wave approach, longshore transport direction can vary from season to season, day to day, or hour to hour. Reversals of transport direction are quite common for most U.S. coasts. Direction may vary at random, but in most areas the net effect is seasonal.

The rate of longshore transport is dependent on the angle of wave approach, duration, and wave energy. Thus, high storm waves will generally move more material per unit time than that moved by low waves. However, if low waves exist longer than high waves, the low waves may be more significant in moving sand than the high waves.

Because reversals in transport direction occur, and because different types of waves transport material at different rates, two components of the longshore transport rate become important. The first is the net rate, the net amount of material passing a particular point in the predominant direction during an average year. The second component is the gross rate, the total of all material moving past a given point in a year regardless of direction. Most shores consistently have a net annual longshore transport in one direction. Determining the direction and average net and gross annual amount of longshore transport is important in developing shore protection plans. In inland seas, such as the Great Lakes, a longshore transport rate in one direction can normally be expected to be no more than about 115,000 cubic meters (150,000 cubic yards) per year. For open ocean coasts, the net rate of transport may vary from 75,000 to more than 1.5 million cubic meters (100,000 to 2 million cubic yards) per year. The rate depends on the local shore conditions and shore alinement, as well as the energy and direction of wave approach.

##### 5. Effect of Inlets on Barrier Beaches.

Inlets may have significant effects on adjacent shores by interrupting the longshore transport and trapping onshore-offshore moving sand. During ebb-tide, sand transported to the inlet by waves is carried seaward a short distance and deposited on an outer bar. When this bar becomes large enough, the waves begin to break on it, moving the sand over the bar back toward the beach. During floodtide, when water flows through the inlet into the lagoon, sand in the inlet is carried a short distance into the lagoon and deposited. This process creates shoals in the landward end of the inlet known as *middle-ground shoals* or *inner bars*. Later, ebb flows may return some of the material in these shoals to the ocean, but some is always lost from the littoral system and thus from the downdrift beaches. In this way, tidal inlets store sand and reduce the supply of sand to adjacent shores. Estimates of the amount of material deposited in the middleground shoals range from 100,000 to 160,000 cubic meters (130,000 to 210,000 cubic yards) per year for inlets on the east

coast of Florida (Walton and Adams, 1976), but quantities elsewhere vary widely according to local conditions.

## 6. Beach Stability.

Although a beach may be temporarily eroded by storm waves and later partly or wholly restored by swells, and erosion and accretion patterns may occur seasonally, the long-range condition of the beach--whether eroding, stable, or accreting--depends on the rates of supply and loss of littoral material. The shore accretes or progrades when the rate of supply exceeds the rate of loss. The shore is considered stable (even though subject to storm and seasonal changes) when the long-term rates of supply and loss are equal. Thus, conservation of sand is an important aspect of shore protection.

## V. CAUSES OF SHORELINE EROSION

Before embarking upon any method of coastal protection, it is important to identify and understand both the short- and long-term causes of coastal erosion. Failure to do this may result in the design and placement of shore protection measures which actually accelerate the process that the protection measure was intended to alleviate. Although the most serious incidents of coastal erosion occur during storms, there are many other causes, both natural and man-induced, which need to be examined.

Natural causes of erosion are those which occur as a result of the response of the beach to the effects of nature. Man-induced erosion occurs when human endeavors impact on the natural system. Much of the man-induced erosion is caused by a lack of understanding and can be successfully alleviated by good coastal zone management. However, in some cases coastal erosion can be due to construction projects that are of economic importance to man. When the need for such projects is compelling, the coastal engineer must understand the effects that the work will have on the natural system and then strive to greatly reduce or eliminate these effects through designs which work in harmony with nature.

Natural and man-induced causes of erosion, as discussed below, are given in Table 1-1.

### 1. Natural Causes.

a. Sea Level Rise. A long-term rise in sea level relative to the land exists in many areas of the world. This rise results in a slow, long-term recession of the shoreline, partly due to direct flooding and partly as a result of profile adjustment to the higher water level.

b. Variability in Sediment Supply to the Littoral Zone. Changes in the world's weather pattern that cause droughts can result in a reduction in the occurrence of floods on rivers supplying sediment to the coastal zone.

c. Storm Waves. Steep waves from a coastal storm cause sand to be transported offshore with temporary storage in a bar or shoal. Later partial recovery of the beach may be made through natural transport of this material onshore by longer period, flatter waves. But, in most cases, some material is permanently lost into the greater offshore depths.

d. Wave and Surge Overwash. Overwash is a phenomenon which occurs during periods of storm surge and severe wave action. Waves and overflowing water erode the beach and transport and deposit this material shoreward of the beach, or as an overwash fan on the bay side of low-lying barrier islands.

e. Deflation. The removal of loose material from a beach by wind action can be a significant cause of erosion. In many parts of the world, major natural dune fields exist well behind the active beach zone. These dunes can represent a large volume of beach sediment.

f. Longshore Sediment Transport. Sand is transported alongshore by waves breaking at an angle to the shore. If the sediment carrying capacity of the longshore current generated by these waves exceeds the quantity of sediment naturally supplied to the beach, erosion of the beach results.

g. Sorting of Beach Sediment. Sorting of beach sediment by wave action results in the selective redistribution of sediment particles (sand, shell, and shingle) along a beach profile according to size or hydraulic properties. This mechanism is particularly important in designing beach nourishment projects because the selective loss of finer material to the offshore region and the retention of the coarse material in the surf zone require the placement of additional fill in order to balance this loss. Best results are usually achieved when the fill material is similar in grain-size distribution to the native beach material.

Table 1-1. Causes of coastal erosion.

Natural	Man-induced
a. Sea level rise	a. Land subsidence from removal of subsurface resources
b. Variability in sediment supply to the littoral zone	b. Interruption of material in transport
c. Storm waves	c. Reduction of sediment supply to the littoral zone
d. Wave and surge overwash	d. Concentration of wave energy on beaches
e. Deflation	e. Increase water level variation
f. Longshore sediment transport	f. Change natural coastal protection
g. Sorting of beach sediment	g. Removal of material from the beach

2. Man-Induced Causes.

a. Land Subsidence from Removal of Subsurface Resources. The removal of natural resources, such as gas, oil, coal, and groundwater underlying the coastal zone, may cause subsidence of the beach. This has the same effect as a sea level rise.

b. Interruption of Material in Transport. This factor is probably the most important cause of man-induced erosion. Improvement of inlets by both channel dredging and channel control and by harbor structures impounds littoral material (see Fig. 1-9). Often, the material is permanently lost from the downcoast beach regime either by the deposition of dredged material outside of the active littoral zone or the building of bars, shoals, and wider updrift beaches. This can be mitigated by sand-bypassing systems. Construction of protective works at the source of littoral material, such as an eroding cliff or bluff, can also result in disruption of supply. Realignment of the shoreline by the use of such structures as groins also interrupts the transport of littoral material. These structures may not only reduce the rate of a longshore transport but also may reduce littoral material reaching downcoast beaches by entrapment.

c. Reduction of Sediment Supply to the Littoral Zone. In some areas the transport of sediment to the coast by rivers form the major source of material to the littoral zone. Dams constructed on these rivers not only form sediment traps but also reduce peak floodflows, thereby reducing the sediment supply to the coast which results in coastal erosion.

d. Concentration of Wave Energy on Beaches. The building of coastal structures (such as a vertical wall) either in the active beach zone or on the backshore can increase the amount of wave energy being dissipated by the beach material fronting the structure, resulting in an increase in the rate of erosion.

e. Increase Water Level Variation. The deepening and widening of navigation inlets may adversely affect the tidal range within a harbor or bay, and may permit larger waves to enter the harbor area and adjacent beaches. An increase in tidal range will expose more of the harbor or bay beach face to the erosive effects of waves and cause a change in the beach profile.

f. Change Natural Coastal Protection. The dredging of nearshore bars and shoals can change the pattern of energy dissipation on a beach face. If the change increases the wave energy acting on a given section of beach, erosion will likely result at that section. Onshore, the leveling of dunes, destruction of beach vegetation, paving of large backshore areas, and construction of boat channels on the backside of a narrow barrier island can further increase the overwash erosion and island breaching potential.

g. Removal of Material from the Beach. Excavation of beach material is undertaken in many parts of the world. This material is sometimes mined for the minerals it contains; in other places it is used for construction purposes (landfills, construction aggregate). For whatever purpose, it is a direct loss of available supply of material for littoral transport.

## VI. COASTAL PROTECTION METHODS AND NAVIGATION WORKS

The sloping beach and beach berm are the outer line of defense in absorbing most wave energy; dunes are the last zone of defense in absorbing the energy of storm waves that overtop the berm. Although dunes erode during severe storms, they are often substantial enough to afford complete protection to the



circa 1974

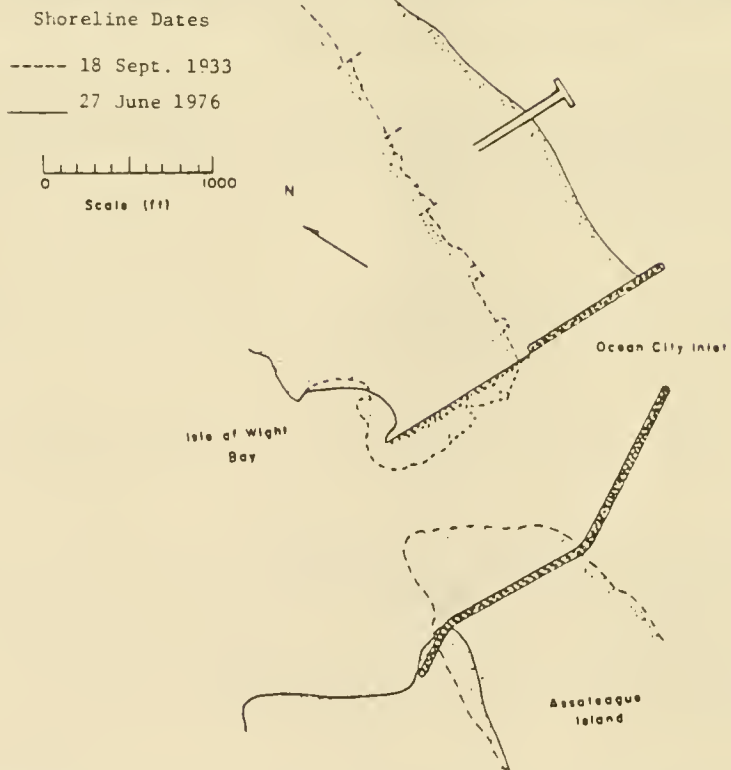


Figure 1-9. Littoral barrier, Ocean City Inlet, Maryland (after Dean and Perlin, 1977).

land behind them. Even when breached by severe storm waves, dunes may gradually rebuild naturally (over a period of several years) to provide protection during future storms.

Continuing encroachment on the sea with manmade development has often taken place without proper regard for the protection provided by dunes. Large dune areas have been leveled to make way for real estate developments, or have been lowered to permit easy access to and view of the beach area. Where there is inadequate dune or similar protection, storm waves may attack beach-front structures (see Fig. 1-10), and wave overwash may flood and damage backshore property. Even when coastal flooding does not occur, high storm surges and associated waves can undermine and damage structures placed too close to the beach (Fig. 1-11).

When the natural protection system fails during large storms, the first solutions frequently chosen are quasi-natural methods such as beach nourishment or artificial sand-dune building. Such solutions retain the beach as a very effective wave energy dissipater and the dune as a flexible last line of defense. However, even these methods provide only a temporary solution to chronic long-term erosion caused by the diminishing supply of sediment in the littoral system and by the slow sea level rise.

The method of placing beach fill to ensure sand supply at the required replenishment rate is important. Where stabilization of an eroding beach is the problem, suitable beach material may be stockpiled at the updrift sector of the problem area. The establishment and periodic replenishment of such a stockpile is termed artificial beach nourishment. To restore an eroded beach and stabilize it at the restored position, fill is placed directly along the eroded sector, and then the beach is artificially nourished by the stockpiling method.

When conditions are suitable for artificial nourishment, long reaches of shore may be protected by this method at a relatively low cost per linear meter of protected shore. An equally important advantage is that artificial nourishment directly remedies the basic cause of most erosion problems--a deficiency in natural sand supply--and benefits rather than damages the adjacent shore. An added consideration is that a widened beach has value as a recreation feature. One of the most recent beach restoration projects began in 1977 along 17 kilometers (10.5 miles) of beach in Dade County, Florida (including Miami Beach). This project is shown in Figure 1-12.

Where beaches and dunes protect shore developments, additional protective works may not be required. However, when natural forces do create erosion, storm waves may overtop the beach and damage backshore structures. Manmade structures must then be constructed to provide protection. In general, measures designed to stabilize the shore fall into two classes: (1) structures to prevent waves from reaching a harbor area (e.g., breakwaters, seawalls, bulkheads, revetments) and (2) manmade structures, such as groins and jetties, used to retard the longshore transport of littoral drift. These may be used in conjunction with seawalls or beach fills or both.

Separate protection for short reaches of eroding shores (e.g., individual shore-front lots) within a larger zone of eroding shore, is a difficult and

costly approach. Such protection often fails at flanks of these reaches as the adjacent unprotected shores continue to recede. Partial or inadequate protective measures may even accelerate erosion of adjacent shores. Coordinated action under a comprehensive plan that considers erosion processes over the full length of the regional shore compartment is much more effective and economical.

Onshore structures, termed *bulkheads*, *seawalls*, and *revetments*, provide protection, based on their use and design, for the upper beach which fronts backshore development or erodible bluffs. Shore-front owners have resorted to this shore armoring by wave-resistant walls of various types when justified by the economic or esthetic value of what is protected.



Figure 1-10. Damage after the 1962 storm, Rehoboth Beach, Delaware.

Bulkheads and seawalls are similar in design with slightly differing purposes. Bulkheads are primarily soil-retaining structures which are designed to also resist wave attack. Conversely, seawalls are principally structures designed to resist wave attack but also may retain some soil to assist in resisting wave forces. The land behind seawalls is usually a recent fill area. Bulkheads and seawalls may be built of many materials including steel, timber, or concrete piling, gabions, or rubble-mound structures.



Figure 1-11. Undermining of structures by storm waves, Potham Beach, Maine.

For ocean-exposed locations vertical bulkheads alone do not provide a long-term solution because of foreshore erosion and flanking. Unless combined with other types of protection, the bulkhead must be enlarged into a massive seawall capable of withstanding the direct onslaught of the waves. Seawalls may have vertical, curved, stepped, or sloping faces. Although seawalls protect the upland, they often create a local problem. Downward forces of water, produced by waves striking the wall, can rapidly remove sand from in front of the wall. A stone apron is often necessary to prevent excessive scouring and undermining.

A revetment armors the existing slope face of a dune or embankment. It is usually composed of one or more layers of quarystone or precast concrete armor units, with a filter layer overlaying a graded in situ soil slope. Revetments are of little benefit if placed at the toe of a marginally stable slope since they are usually only a protective armor and not a retaining structure. Because the sloping face of the quarystone revetment is a good energy dissipater, revetments have a less adverse effect on the beach in front of them than a smooth-faced vertical bulkhead.



Before



After

Figure 1-12. Beach Restoration, Dade County, Florida.

*Breakwaters* are wave energy barriers designed to protect any landform or water area behind them from the direct assault of waves. However, because of the higher cost of these offshore structures over onshore structures (e.g., seawalls), breakwaters have been mainly used for harbor protection and navigational purposes. In recent years shore-parallel, detached, segmented breakwaters have been used for shore protection structures.

Breakwaters have both beneficial and detrimental effects on the shore. All breakwaters reduce or eliminate wave action in their lee (shadow). However, whether they are offshore, detached, or shore-connected structures, the reduction or elimination of wave action also reduces the longshore transport in the shadow. For offshore breakwaters this leads to a sand accretion in the lee of the breakwater in the form of a sandbar (called a tombolo) which grows from the shore toward the structure, as well as the associated downdrift beach erosion.

Shore-connected breakwaters provide protection to harbors from wave action and have the advantage of a shore arm to facilitate construction and maintenance of the structure. In recent years, shore-parallel breakwaters built of short detached groupings have provided adequate large storm protection without adversely affecting the longshore transport.

At a harbor breakwater, the longshore movement of sand generally can be restored by pumping sand from the side where sand accumulates through a pipeline to the eroded downdrift side. This type of operation has been in use for many years at such places as Santa Barbara, California, and Channel Islands Harbor, California.

Offshore breakwaters have also been used in conjunction with navigation structures to control channel silting. If the offshore breakwater is placed immediately updrift from a navigation opening, the structure impounds sand in its lee, prevents it from entering the navigation channel, and affords shelter for a floating dredge plant to pump out the impounded material across the channel to the downdrift beach. This method has been successfully used at Channel Islands Harbor near Port Hueneme, California.

While breakwaters have been built of everything from sunken ships to large fabric bags filled with concrete, the primary material in the United States is a rubble-mound section with armor stone encasing underlayers and core material. Some European and Japanese breakwaters use a submerged mound foundation in deeper water topped with a concrete superstructure, thereby reducing the width and overall quantity of fill material necessary for harbor protection.

*Groins* are barrier-type structures that extend from the backshore into the littoral zone. Groins are generally constructed in series, referred to as a groin field or system, along the entire length of beach to be protected. The basic purposes of a groin are to modify the longshore movement of sand and to either accumulate sand on the shore or retard sand losses. Trapping of sand by a groin is done at the expense of the adjacent downdrift shore unless the groin or groin system is artificially filled with sand to its entrapment capacity from other sources. To reduce the potential for damage to property downdrift of a groin, some limitation must be imposed on the amount of sand permitted to be impounded on the updrift side. Since more and more shores are being protected, and less and less sand is available as natural supply, it is now desirable, and frequently necessary, to place sand artificially to fill the area between the groins, thereby ensuring an uninterrupted passage of the sand to the downdrift beaches.

Groins that have been constructed in various configurations using timber, steel, concrete, or quarrystone are classified as high or low, long or short,

permeable or impermeable, and fixed or adjustable, according to their design and construction. A high groin, extending through the surf zone for ordinary or moderate storm waves, initially entraps nearly all of the longshore moving sand within that intercepted area until the accumulated sand fills the entrapment area and the sand passes around the seaward end of the groin to the down-drift beach. Low groins (top profile no higher than that of desired beach dimensions or natural beach elevation) trap sand like high groins. However, some of the sand also passes over the top of the structure. Permeable groins permit some of the wave energy and movement of sand through the structure.

*Jetties* are structures used at inlets to stabilize the position of the navigation channel, to shield vessels from wave forces, and to control the movement of sand along the adjacent beaches so as to minimize the movement of sand into the channel. The sand transported into an inlet will interfere with navigation and will usually necessitate more frequent dredging to maintain the navigation depth. Because of the longshore transport reversals common at many sites, jetties are often required on both sides of the inlet to achieve complete channel protection. Jetties are built from a variety of materials, e.g., timber, steel, concrete, and quarrystone. Most of the larger structures are of rubble-mound construction with quarrystone armor and a core of less permeable material to prevent sand passing through. It is the impoundment of sand at the updrift jetty which creates the major impact. When fully developed, the fillet of impounded sand extends well updrift on the beach and outward toward the tip of the jetty.

Like the groin, the jetty's major adverse impact is the erosion of the downdrift beach. Before the installation of a jetty, nature supplies sand by intermittently transporting it across the inlet along the outer bar. The reduction or cessation of this sand transport due to the presence of a jetty leaves the downdrift beach with an inadequate natural supply of sand to replace that carried away by littoral currents.

To minimize the downdrift erosion, some projects provide for dredging the sand impounded by the updrift jetty and pumping it through a pipeline (bypassing the inlet) to the downdrift eroding beach. This provides for nourishment of the downdrift beach and may also reduce shoaling of the entrance channel. If the sand impounded at the updrift jetty extends to the head or seaward end of the jetty, it will move around the jetty and into the channel causing a navigation hazard. Therefore, the updrift impounded sand should be bypassed to the downcoast beach, not only to reduce downdrift erosion but also to help maintain a safe navigation channel.

A more recent development for sand bypassing provides a low section or weir in the updrift jetty over which sand moves into a sheltered predredged, deposition basin. By dredging the basin periodically, channel shoaling is reduced or eliminated. The dredged material is normally pumped across the navigation channel (inlet) to provide nourishment for the downdrift shore. A *weir jetty* of this type at Murrells Inlet, South Carolina, is shown in Figure 1-13.

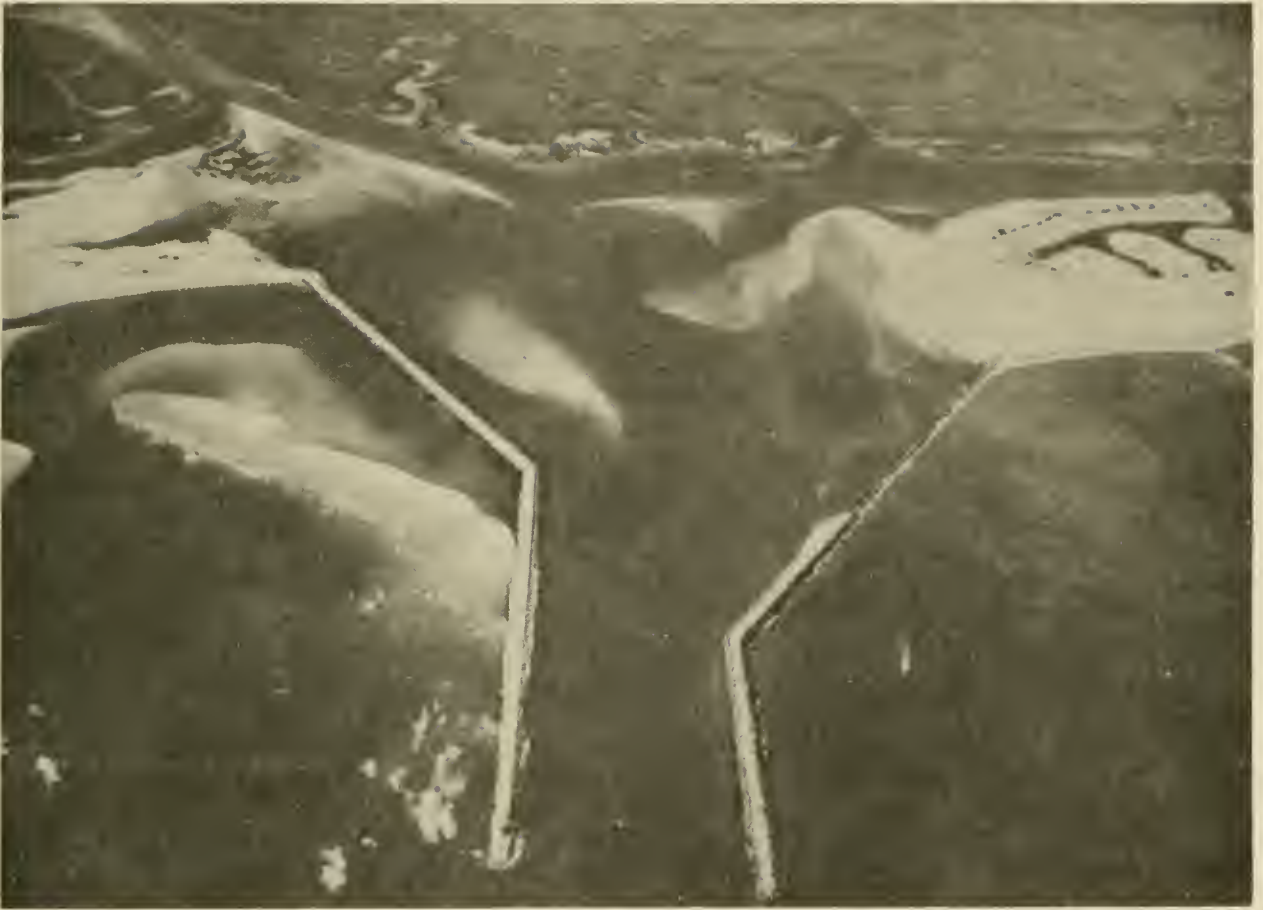


Figure 1-13. Weir jetty at Murrells Inlet, South Carolina, 1981.

## VII. CONSERVATION OF SAND

Throughout this chapter the primary importance of an adequate sand supply has been clearly shown. Where sand is available in abundant quantities, protective measures are generally not required or greatly simplified. When dunes and broad, gently sloping beaches can no longer be provided, it is necessary to resort to alternative structures, causing the recreational attraction of the seashore to be lost or greatly diminished. Because sand is a diminishing resource in many coastal areas, its conservation is an important factor in the preservation of our coastal areas and must be included in long-range planning.

Sand was once available to the shores in adequate supply from streams and rivers and by natural erosion of coastal formations. Now development in the watershed areas and along previously eroding shores has progressed to a stage where large areas of the coast now receive little or no sand through natural geologic processes. Continued land development along both inland rivers and coastal areas has been accompanied by erosion control methods which have

deprived the coastal areas of sediment formerly available through the natural erosion process. These methods reduce the amount of sand transported along the coast. It thus becomes apparent that sand must be conserved. This does not mean local hoarding of beach sand at the expense of adjoining areas, but rather the elimination of wasteful practices and the prevention of losses from the coastal zone whenever feasible.

Fortunately, nature provides extensive storage of beach sand in bays, lagoons, estuaries, and offshore areas that can be used as a source of beach and dune replenishment where the ecological balance will not be disrupted. Massive dune deposits are also available at some locations, though these must be used with caution to avoid exposing the area to flood hazard. The sources are not always located in the proper places for economic utilization nor are they considered permanent. When these sources are depleted, increasing costs must be faced for the preservation of the beaches. Offshore sand deposits will probably become the most important source in the future.

Mechanical bypassing of sand at structured coastal inlets is one means of conservation that will come into increasing practice. Mining of beach sand for commercial purposes, formerly a common procedure, is rapidly being reduced as coastal communities learn the need for regulating this practice. Modern hopper dredges equipped with a pump-out capability and split-hulled dredges are being used to facilitate nearshore discharge of sands from navigation channel maintenance dredging. On the California coast where large volumes of sand are lost into deep submarine canyons near the coast, facilities are being considered that will trap the sand before it reaches the submarine canyon and transport it mechanically to a point where it can resume advantageous long-shore transport. Dune planting with appropriate grasses and shrubs reduces landward windborne losses and aids in dune preservation.

The protection of coastal areas is not a simple problem; neither is it insurmountable. It is a task and a responsibility that has increased tremendously in importance in the past 50 years, and is destined to become a necessity in future years. While the cost will mount as time passes, it will be possible through careful planning, adequate management, and sound engineering to do the job of protecting coastal areas properly and economically.

#### LITERATURE CITED

- DEAN, R.G., and PERLIN, M., "Coastal Engineering Study of Ocean City Inlet, Maryland," *Coastal Sediments '77*, American Society of Civil Engineers, Nov. 1977, pp. 520-542.
- U.S. ARMY, CORPS OF ENGINEERS, "Shore Protection, Planning and Design," TR-4, Beach Erosion Board, Washington, D.C., 1954.
- U.S. ARMY, CORPS OF ENGINEERS, "Report on the National Shoreline Study," Washington, D.C., Aug. 1971.
- WALTON, T.L., and ADAMS, W.D., "Capacity of Inlet Outer Bars to Store Sand," *Proceedings of the 15th Conference on Coastal Engineering*, American Society of Civil Engineers, Ch. 112, 1976, pp. 1919-1937.



# CHAPTER 2

## Mechanics of Wave Motion



*Leo Carrillo State Beach, California, July 1968*



CONTENTS

CHAPTER 2

MECHANICS OF WAVE MOTION

	Page
I INTRODUCTION.....	2-1
II WAVE MECHANICS.....	2-1
1. General.....	2-1
2. Wave Fundamentals and Classification of Waves.....	2-3
3. Elementary Progressive Wave Theory (Small-Amplitude Wave Theory).....	2-6
4. Higher Order Wave Theories.....	2-31
5. Stokes' Progressive, Second-Order Wave Theory.....	2-34
6. Cnoidal Waves.....	2-44
7. Solitary Wave Theory.....	2-55
8. Stream-Function Wave Theory.....	2-59
III WAVE REFRACTION.....	2-60
1. Introduction.....	2-60
2. General--Refraction by Bathymetry.....	2-62
IV WAVE DIFFRACTION.....	2-75
1. Introduction.....	2-75
2. Diffraction Calculations.....	2-77
3. Refraction and Diffraction Combined.....	2-109
V WAVE REFLECTION.....	2-109
1. General.....	2-109
2. Reflection from Impermeable, Vertical Walls (Linear Theory)....	2-112
3. Reflections in an Enclosed Basin.....	2-113
4. Wave Reflection from Plane Slopes, Beaches, Revetments, and Breakwaters.....	2-116
5. Wave Reflection from Bathymetric Variation.....	2-122
6. Refraction of Reflected Waves.....	2-124
VI BREAKING WAVES.....	2-129
1. Deep Water.....	2-129
2. Shoaling Water.....	2-129
LITERATURE CITED.....	2-137
BIBLIOGRAPHY.....	2-147

TABLES

2-1 Distribution of wave heights in a short train of waves.....	2-30
2-2 Example computations of values of $C_1/C_2$ for refraction analysis.....	2-68
2-3 $\alpha_2$ correction factor for multiple layers of armor units.....	2-121

CONTENTS--Continued

FIGURES

	Page
2-1 Approximate distribution of ocean surface wave energy illustrating the classification of surface waves by wave band, primary disturbing force, and primary restoring force.....	2-5
2-2 Definition of terms--elementary, sinusoidal, progressive wave.....	2-8
2-3 Local fluid velocities and accelerations.....	2-14
2-4 Water particle displacements from mean position for shallow-water and deepwater waves.....	2-17
2-5 Formation of wave groups by the addition of two sinusoids having different periods.....	2-24
2-6 Summary of linear (Airy) wave theory--wave characteristics.....	2-32
2-7 Regions of validity for various wave theories.....	2-33
2-8 Comparison of second-order Stokes' profile with linear profile.....	2-40
2-9 Cnoidal wave surface profiles as a function of $k^2$ .....	2-47
2-10 Cnoidal wave surface profiles as a function of $k^2$ .....	2-48
2-11 Relationship between $k^2$ , $H/d$ , and $T\sqrt{g/d}$ .....	2-49
2-12 Relationships between $k^2$ and $L^2H/d^3$ .....	2-50
2-13 Relationships between $k^2$ and $L^2H/d^3$ and between $(y_c-d)/H$ , $(y_t-d)/H + 1$ and $L^2H/d^3$ .....	2-51
2-14 Relationship between $T\sqrt{g/d} y_t/d$ , $H/y_t$ , and $L^2H/d^3$ .....	2-52
2-15 Relationship between $C/\sqrt{gy_t}$ , $H/y_t$ , and $L^2H/d^3$ .....	2-53
2-16 Functions M and N in solitary wave theory.....	2-58
2-17 Wave refraction at Westhampton Beach, Long Island, New York.....	2-61
2-18 Refraction template.....	2-65
2-19 Changes in wave direction and height due to refraction on slopes, with straight, parallel depth contours.....	2-67
2-20 Use of the refraction template.....	2-69
2-21 Refraction of diagram using R/J method.....	2-70
2-22 Use of fan-type refraction diagram.....	2-72

CONTENTS

FIGURES--Continued

	Page
2-23 Refraction along a straight beach with parallel bottom contours.....	2-73
2-24 Refraction by a submarine ridge (a) and submarine canyon (b).....	2-73
2-25 Refraction along an irregular shoreline.....	2-73
2-26 Wave incident on a breakwater--(a) no diffraction and (b) diffraction effects.....	2-76
2-27 Wave diffraction at Channel Islands Harbor breakwater, California...	2-77
2-28 Wave diffraction diagram--15° wave angle.....	2-78
2-29 Wave diffraction diagram--30° wave angle.....	2-79
2-30 Wave diffraction diagram--45° wave angle.....	2-80
2-31 Wave diffraction diagram--60° wave angle.....	2-81
2-32 Wave diffraction diagram--75° wave angle.....	2-82
2-33 Wave diffraction diagram--90° wave angle.....	2-83
2-34 Wave diffraction diagram--105° wave angle.....	2-84
2-35 Wave diffraction diagram--120° wave angle.....	2-85
2-36 Wave diffraction diagram--135° wave angle.....	2-86
2-37 Wave diffraction diagram--150° wave angle.....	2-87
2-38 Wave diffraction diagram--165° wave angle.....	2-88
2-39 Wave diffraction diagram--180° wave angle.....	2-89
2-40 Diffraction for a single breakwater normal incidence.....	2-91
2-41 Schematic representation of wave diffraction overlay.....	2-92
2-42 Generalized diffraction diagram for a breakwater gap width of 2 wavelengths.....	2-93
2-43 Contours of equal diffraction coefficient gap width = 0.5 wavelength.....	2-94
2-44 Contours of equal diffraction coefficient gap width = 1 wavelength.....	2-94
2-45 Contours of equal diffraction coefficient gap width = 1.41 wavelengths.....	2-95

CONTENTS

FIGURES--Continued

	Page
2-46	Contours of equal diffraction coefficient gap width = 1.64 wave-lengths.....2-95
2-47	Contours of equal diffraction coefficient gap width = 1.78 wave-lengths.....2-96
2-48	Contours of equal diffraction coefficient gap width = 2 wave-lengths.....2-96
2-49	Contours of equal diffraction coefficient gap width = 2.50 wave-lengths.....2-97
2-50	Contours of equal diffraction coefficient gap width = 2.95 wave-lengths.....2-97
2-51	Contours of equal diffraction coefficient gap width = 3.82 wave-lengths.....2-98
2-52	Contours of equal diffraction coefficient gap width = 5 wave-lengths.....2-98
2-53	Diffraction for breakwater gap width $> 5L$ .....2-99
2-54	Wave incidence oblique to breakwater gap.....2-100
2-55	Diffraction for a breakwater gap of one wavelength width where $\phi = 0^\circ$ and $15^\circ$ .....2-101
2-56	Diffraction for a breakwater gap of one wavelength width where $\phi = 30^\circ$ and $45^\circ$ .....2-102
2-57	Diffraction for a breakwater gap of one wavelength width where $\phi = 60^\circ$ and $75^\circ$ .....2-103
2-58	Diffractions diagram for a gap of two wavelengths and a $45^\circ$ approach compared with that for a gap width $\sqrt{2}$ wavelengths with a $90^\circ$ approach.....2-104
2-59	Approximate method for computing wave diffraction around an offshore breakwater.....2-106
2-60	Wave diffraction pattern behind an offshore breakwater three wavelengths long for waves approaching at a $30^\circ$ angle.....2-108
2-61	Single breakwater, refraction-diffraction combined.....2-110
2-62	Wave reflection at Hamlin Beach, New York.....2-111
2-63	Standing wave (clapotis) system, perfect reflection from a vertical barrier, linear theory.....2-114

CONTENTS

FIGURES--Continued

	Page
2-64 Definition of wave reflection terms.....	2-117
2-65 Wave reflection coefficients for slopes, beaches, and rubble- mound breakwaters as a function of the surf similarity parameter $\xi$ .....	2-118
2-66 Correction factor $\alpha_1$ , due to slope roughness and the extent of wave breaking at the toe of a structure.....	2-120
2-67 Wave reflection coefficients for smooth steps, $\ell/(d_1 + d_2) \approx 6$ and $\ell/(d_1 + d_2) \approx 12$ .....	2-123
2-68 Wave reflection coefficients for sinusoidal underwater bars with $L/\ell = 2.0$ .....	2-125
2-69 Definition sketch of trapped wave rays.....	2-127
2-70 Solution of equations for trapped reflected waves with angle $\alpha$ shown in degrees.....	2-128
2-71 Wave of limiting steepness in deep water.....	2-129
2-72 Breaker height index versus deepwater wave steepness, $H_o/gT^2$ .....	2-131
2-73 Dimensionless depth at breaking versus breaker steepness.....	2-132
2-74 Spilling breaking wave.....	2-133
2-75 Plunging breaking wave.....	2-133
2-76 Surging breaking wave.....	2-134
2-77 Collapsing breaking wave.....	2-134



## CHAPTER 2

### MECHANICS OF WAVE MOTION

#### I. INTRODUCTION

The effects of water waves are of paramount importance in the field of coastal engineering. Waves are the major factor in determining the geometry and composition of beaches and significantly influence the planning and design of harbors, waterways, shore protection measures, coastal structures, and other coastal works. Surface waves generally derive their energy from the winds. A significant amount of this wave energy is finally dissipated in the nearshore region and on the beaches.

Waves provide an important energy source for forming beaches; sorting bottom sediments on the shoreface; transporting bottom materials onshore, offshore, and alongshore; and for causing many of the forces to which coastal structures are subjected. An adequate understanding of the fundamental physical processes in surface wave generation and propagation must precede any attempt to understand complex water motion in the nearshore areas of large bodies of water. Consequently, an understanding of the mechanics of wave motion is essential in the planning and design of coastal works.

This chapter presents an introduction to surface wave theories. Surface and water particle motion, wave energy, and theories used in describing wave transformation due to interaction with the bottom and with structures are described to provide an elementary physical and mathematical understanding of wave motion, and to indicate limitations of selected theories. A number of wave theories have been omitted. References are cited to provide information on theories not discussed and to supplement the theories presented.

The reader is cautioned that man's ability to describe wave phenomena is limited, especially when the region under consideration is the coastal zone. Thus, the results obtained from the wave theories presented should be carefully interpreted for application to the actual design of coastal structures or description of the coastal environment.

#### II. WAVE MECHANICS

##### 1. General.

Waves in the ocean often appear as a confused and constantly changing sea of crests and troughs on the water surface because of the irregularity of wave shape and the variability in the direction of propagation. This is particularly true while the waves are under the influence of the wind. The direction of wave propagation can be assessed as an average of the directions of individual waves. The sea surface is difficult to describe because of the interaction between individual waves. Faster waves overtake and pass through slower ones from various directions. Waves sometimes reinforce or cancel each other by this interaction, often collide with each other, and are transformed into turbulence and spray. When waves move out of the area where they are directly affected by the wind, they assume a more ordered state with the appearance of definite crests and troughs and with a more rhythmic rise and

fall. These waves may travel hundreds or thousands of kilometers after leaving the area in which they were generated. Wave energy is dissipated internally within the fluid, by interaction with the air above, by turbulence on breaking, and at the bottom in shallow depths.

Waves that reach coastal regions expend a large part of their energy in the nearshore region. As the wave nears the shore, the wave energy may be dissipated as heat through turbulent fluid motion induced by breaking and through bottom friction and percolation. While the heat is of little concern to the coastal engineer, breaking is important because it affects both beaches and manmade shore structures. Thus, shore protection measures and coastal structure designs are dependent on the ability to predict waveforms and fluid motion beneath waves, and on the reliability of such predictions. Prediction methods generally have been based on simple waves where elementary mathematical functions can be used to describe wave motion. For some situations, these simple formulas provide reliable predictions of wave conditions; however, for other situations the predictions may be unsatisfactory for engineering applications. Although many theoretical concepts have evolved in the past two centuries for describing complex sea waves, complete agreement between theory and observation is not always found.

In general, actual water-wave phenomena are complex and difficult to describe mathematically because of nonlinearities, three-dimensional characteristics, and apparent random behavior. However, there are two classical theories, one developed by Airy (1845) and the other by Stokes (1880), that describe simple waves. The Airy and Stokes theories generally predict wave behavior better where water depth relative to wavelength is not too small. For shallow water, a cnoidal wave theory often provides an acceptable approximation of simple waves. For very shallow water near the breaker zone, solitary wave theory satisfactorily predicts certain features of the wave behavior. These theories are described according to their fundamental characteristics, together with the mathematical equations that describe wave behavior. Many other wave theories have been presented in the literature which, for some specific situations, may predict wave behavior more satisfactorily than the theories presented here. These other theories are not included, since it is beyond the scope of this manual to cover all theories.

The most elementary wave theory, referred to as small-amplitude or linear wave theory, was developed by Airy (1845). This wave theory is of fundamental importance since it is not only easy to apply, but also reliable over a large segment of the whole wave regime. Mathematically, the Airy theory can be considered a first approximation of a complete theoretical description of wave behavior. A more complete theoretical description of waves may be obtained as the sum of an infinite number of successive approximations, where each additional term in the series is a correction to preceding terms. For some situations, waves are better described by these higher order theories, which are usually referred to as finite-amplitude theories. The first finite-amplitude theory, known as the trochoidal theory, was developed by Gerstner (1802). It is so called because the free-surface or wave profile is a trochoid. This theory is mentioned only because of its classical interest. It is not recommended for application, since the water particle motion predicted is not that observed in nature. The trochoidal theory does, however, predict wave profiles quite accurately. Stokes (1880) developed a finite-amplitude theory that is more satisfactory than the trochoidal theory. Only the second-order

Stokes' equations are presented, but the use of higher order approximations is sometimes justified for the solution of practical problems.

For shallow-water regions, cnoidal wave theory, originally developed by Korteweg and De Vries (1895), provides a rather reliable prediction of the waveform and associated motions for some conditions. However, cnoidal wave theory has received little attention with respect to the actual application in the solution of engineering problems. This may be due to the difficulties in making computations. Recently, the work involved in using cnoidal wave theory has been substantially reduced by the introduction of graphical and tabular forms of functions (Wiegel, 1960; Masch and Wiegel, 1961); however, application of the theory is still complex. At the limit of cnoidal wave theory, certain aspects of wave behavior may be described satisfactorily by the solitary wave theory. Unlike the cnoidal wave theory, the solitary wave theory is easy to use because it reduces to functions that may be evaluated without recourse to special tables.

The development of individual wave theories is omitted, and only the results are presented since the purpose is to present only that information that may be useful for the solution of practical engineering problems. Many publications are available, such as Wiegel (1964), Kinsman (1965), and Ippen (1966a), which cover in detail the development of some of the theories mentioned above, as well as others. The mathematics used here generally is restricted to elementary arithmetic and algebraic operations. Emphasis is placed on the selection of an appropriate theory in accordance with its application and limitations.

Numerous example problems are provided to illustrate the theory involved and to provide some practice in using the appropriate equations or graphical and tabular functions. Some of the sample computations give more significant digits than are warranted for practical applications. For instance, a wave height could be determined to be 3.048 meters for certain conditions purely based on theoretical considerations. This accuracy is unwarranted because of the uncertainty in the basic data used and the assumption that the theory is representative of real waves. A practical estimate of the wave height given above would be 3.0 meters. When calculating real waves, the final answer should be rounded off.

## 2. Wave Fundamentals and Classification of Waves.

Any adequate physical description of a water wave involves both its surface form and the fluid motion beneath the wave. A wave that can be described in simple mathematical terms is called a *simple wave*. Waves that are composed of several components and difficult to describe in form or motion are termed *complex waves*. *Sinusoidal* or *simple harmonic waves* are examples of *simple waves* since their surface profile can be described by a single sine or cosine function. A wave is *periodic* if its motion and surface profile recur in equal intervals of time. A waveform which moves relative to a fixed point is called a *progressive wave*; the direction in which it moves is termed the *direction of wave propagation*. If a waveform merely moves up and down at a fixed position, it is called a *complete standing wave* or a *clapotis*. A progressive wave is called a wave of *permanent form* if it is propagated without experiencing any changes in free-surface configuration.

Water waves are considered *oscillatory* or *nearly oscillatory* if the water particle motion is described by orbits that are closed or nearly closed for each wave period. The linear, or Airy, theory describes pure oscillatory waves. Most finite-amplitude wave theories describe nearly oscillatory waves since the fluid is moved a small amount in the direction of wave advance by each successive wave. This motion is termed *mass transport* of the waves. When water particles advance with the wave and do not return to their original position, the wave is called a *wave of translation*. A solitary wave is an example of a wave of translation.

It is important to distinguish between the various types of water waves that may be generated and propagated. One way to classify waves is by wave period  $T$  (the time for a wave to travel a distance of one wavelength), or by the reciprocal of  $T$ , the wave frequency  $f$ . Figure 2-1 is an illustration of classification by period or frequency given by Kinsman (1965). The figure shows the relative amount of energy contained in ocean waves having a particular frequency. Of primary concern are the waves referred to in Figure 2-1 as gravity waves, which have periods from 1 to 30 seconds. A narrower range of wave periods, from 5 to 15 seconds, is usually more important in coastal engineering problems. Waves in this range are referred to as *gravity waves* since gravity is the principal restoring force; i.e., the force due to gravity attempts to return the fluid to its equilibrium position. Figure 2-1 also shows that a large amount of the total wave energy is associated with waves classified as gravity waves; hence, gravity waves are extremely important in dealing with the design of coastal and offshore structures.

Gravity waves can be further separated into two states:

(a) Seas, when the waves are under the influence of wind in a generating area, and

(b) swell, when the waves move out of the generating area and are no longer subjected to significant wind action.

Seas are usually made up of steeper waves with shorter periods and lengths, and the surface appears much more disturbed than for swell. Swell behaves much like a free wave (i.e., free from the disturbing force that caused it), while seas consist to some extent of forced waves (i.e., waves on which the disturbing force is applied continuously).

Ocean waves are complex. Many aspects of the fluid mechanics necessary for a complete discussion have only a minor influence on solving most coastal engineering problems. Thus, a simplified theory that omits most of the complicating factors is useful. The assumptions made in developing the simple theory should be understood, because not all the assumptions are justified in all problems. When an assumption is not valid in a particular problem, a more complete theory should be employed.

The most restrictive of common assumptions is that waves are small perturbations on the surface of a fluid which is otherwise at rest. This leads to a wave theory that is variously called small-amplitude theory, linear theory, or Airy theory. The small-amplitude theory provides insight for all periodic wave behavior and a description of the periodic flow that is adequate for most practical problems. This theory cannot account for mass transport due to

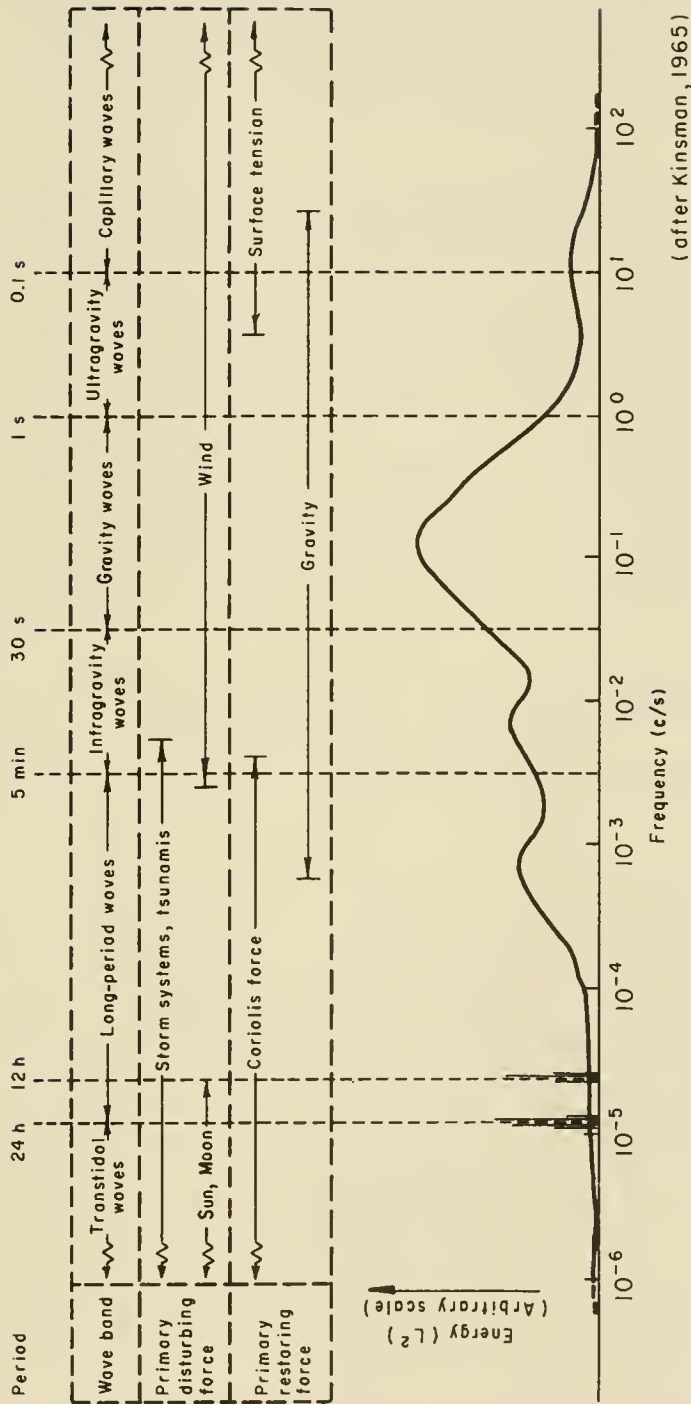


Figure 2-1. Approximate distribution of ocean surface wave energy illustrating the classification of surface waves by wave band, primary disturbing force, and primary restoring force.

waves (Sec. II,5,c), or the fact that wave crests depart farther from the mean water level (MWL) than do the troughs. More general theories such as *finite-amplitude*, or *nonlinear wave theories* are required to account for these phenomena as well as most interactions between waves and other flows. Non-linear wave theories also permit a more accurate evaluation of some wave properties than can be obtained with linear theory.

Several assumptions commonly made in developing a simple wave theory are listed below:

(a) The fluid is homogeneous and incompressible; therefore, the density  $\rho$  is a constant.

(b) Surface tension can be neglected.

(c) Coriolis effect can be neglected.

(d) Pressure at the free surface is uniform and constant.

(e) The fluid is ideal or inviscid (lacks viscosity).

(f) The particular wave being considered does not interact with any other water motions.

(g) The bed is a horizontal, fixed, impermeable boundary, which implies that the vertical velocity at the bed is zero.

(h) The wave amplitude is small and the waveform is invariant in time and space.

(i) Waves are plane or long crested (two dimensional).

The first three assumptions are acceptable for virtually all coastal engineering problems. It will be necessary to relax assumptions (d), (e), and (f) for some specialized problems not considered in this manual. Relaxing the three final assumptions is essential in many problems, and is considered later in this chapter.

In applying assumption (g) to waves in water of varying depth as is encountered when waves approach a beach, the local depth is usually used. This can be justified, but not without difficulty, for most practical cases in which the bottom slope is flatter than about 1 on 10. A progressive wave moving into shallow water will change its shape significantly. Effects due to viscosity and vertical velocity on a permeable bottom may be measurable in some situations, but these effects can be neglected in most engineering problems.

### 3. Elementary Progressive Wave Theory (Small-Amplitude Wave Theory).

The most fundamental description of a simple sinusoidal oscillatory wave is by its length  $L$  (the horizontal distance between corresponding points on two successive waves), height  $H$  (the vertical distance to its crest from the preceding trough), period  $T$  (the time for two successive crests to pass a

given point), and depth  $d$  (the distance from the bed to the stillwater level, SWL). (See App. B for a list of common symbols.)

Figure 2-2 shows a two-dimensional, simple progressive wave propagating in the positive  $x$ -direction, using the symbols presented above. The symbol  $\eta$  denotes the displacement of the water surface relative to the SWL and is a function of  $x$  and time  $t$ . At the wave crest,  $\eta$  is equal to the amplitude of the wave  $a$  or one-half of the wave height.

Small-amplitude wave theory and some finite-amplitude wave theories can be developed by the introduction of a velocity potential  $\phi(x, z, t)$ . Horizontal and vertical components of the water particle velocities are defined at a point  $(x, z)$  in the fluid as  $u = \partial\phi/\partial x$  and  $w = \partial\phi/\partial z$ . The velocity potential, Laplace's equation, and Bernoulli's dynamic equation together with the appropriate boundary conditions, provide the necessary information to derive the small-amplitude wave formulas. Such a development has been shown by Lamb (1932), Eagleson and Dean (1966, see Ippen, 1966b), and others.

a. Wave Celerity, Length, and Period. The speed at which a waveform propagates is termed the phase velocity or wave celerity  $C$ . Since the distance traveled by a wave during one wave period is equal to one wavelength, the wave celerity can be related to the wave period and length by

$$C = \frac{L}{T} \quad (2-1)$$

An expression relating the wave celerity to the wavelength and water depth is given by

$$C = \sqrt{\frac{gL}{2\pi} \tanh\left(\frac{2\pi d}{L}\right)} \quad (2-2)$$

From equation (2-1), it is seen that equation (2-2) can be written as

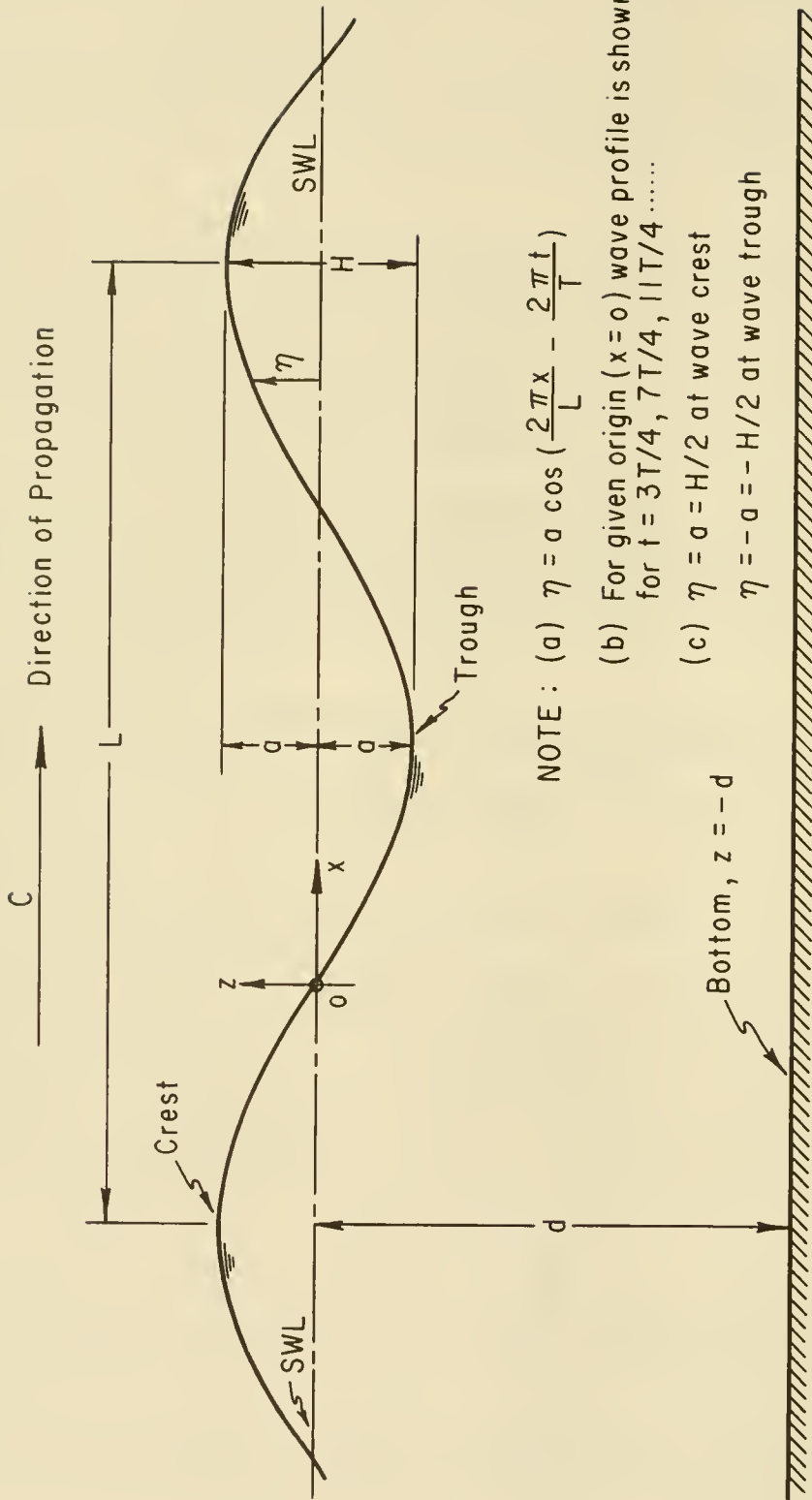
$$C = \frac{gT}{2\pi} \tanh\left(\frac{2\pi d}{L}\right) \quad (2-3)$$

The values  $2\pi/L$  and  $2\pi/T$  are called the wave number  $k$  and the wave angular frequency  $\omega$ , respectively. From equations (2-1) and (2-3) an expression for wavelength as a function of depth and wave period may be obtained.

$$L = \frac{gT^2}{2\pi} \tanh\left(\frac{2\pi d}{L}\right) \quad (2-4a)$$

Use of equation (2-4a) involves some difficulty since the unknown  $L$  appears on both sides of the equation. Tabulated values of  $d/L$  and  $d/L_0$  ( $d/L_0$  is the deepwater wavelength) in Tables C-1 and C-2 in Appendix C may be used to simplify the solution of equation (2-4a). Eckart (1952) gives an approximate expression for equation (2-4a), which is correct to within about 5 percent. This expression is given by

$$L \approx \frac{gT^2}{2\pi} \sqrt{\tanh\left(\frac{4\pi^2 d}{T^2 g}\right)} \quad (2-4b)$$



NOTE : (a)  $\eta = a \cos \left( \frac{2\pi x}{L} - \frac{2\pi t}{T} \right)$

(b) For given origin ( $x = 0$ ) wave profile is shown for  $t = 3T/4, 7T/4, 11T/4, \dots$

(c)  $\eta = a = H/2$  at wave crest  
 $\eta = -a = -H/2$  at wave trough

Figure 2-2. Definition of terms--elementary, sinusoidal, progressive wave.

Equation (2-4b) explicitly gives  $L$  in terms of wave period  $T$  and is sufficiently accurate for many engineering calculations. The maximum error of 5 percent occurs when  $2\pi d/L \approx 1$ .

Gravity waves may also be classified by the water depth in which they travel. The following classifications are made according to the magnitude of  $d/L$  and the resulting limiting values taken by the function  $\tanh(2\pi d/L)$ :

Classification	$d/L$	$2\pi d/L$	$\tanh(2\pi d/L)$
Deep water	$> 1/2$	$> \pi$	$\approx 1$
Transitional	$1/25$ to $1/2$	$1/4$ to $\pi$	$\tanh(2\pi d/L)$
Shallow water	$< 1/25$	$< 1/4$	$\approx 2\pi d/L$

In deep water,  $\tanh(2\pi d/L)$  approaches unity and equations (2-2) and (2-3) reduce to

$$C_o = \sqrt{\frac{gL_o}{2\pi}} = \frac{L_o}{T} \quad (2-5)$$

and

$$C_o = \frac{gT}{2\pi} \quad (2-6)$$

Although *deep water* actually occurs at an infinite depth,  $\tanh(2\pi d/L)$ , for most practical purposes, approaches unity at a much smaller  $d/L$ . For a relative depth of one-half (i.e., when the depth is one-half the wavelength),  $\tanh(2\pi d/L) = 0.9964$ .

Thus, when the relative depth  $d/L$  is greater than one-half, the wave characteristics are virtually independent of depth. Deepwater conditions are indicated by the subscript  $o$  as in  $L_o$  and  $C_o$ . The period  $T$  remains constant and independent of depth for oscillatory waves; hence, the subscript is omitted (Ippen, 1966b, pp. 21-24). If units of meters and seconds are specified, the constant  $g/2\pi$  is equal to 1.56 meters per second squared and

$$C_o = \frac{gT}{2\pi} = \frac{9.8}{2\pi} T = 1.56T \text{ m/s} \quad (2-7a)$$

and

$$L_o = \frac{gT^2}{2\pi} = \frac{9.8}{2\pi} T^2 = 1.56T^2 \text{ m} \quad (2-8a)$$

If units of feet and seconds are specified, the constant  $g/2\pi$  is equal to 5.12 feet per second squared and

$$C_o = \frac{gT}{2\pi} = 5.12T \text{ ft/s} \quad (2-7b)$$

and

$$L_o = \frac{gT^2}{2\pi} = 5.12T^2 \text{ ft} \quad (2-8b)$$

If equations (2-7a) and (2-7b) are used to compute wave celerity when the relative depth is  $d/L = 0.25$ , the resulting error will be about 9 percent. It is evident that a relative depth of 0.5 is a satisfactory boundary separating deepwater waves from waves in water of transitional depth. If a wave is traveling in *transitional* depths, equations (2-2) and (2-3) must be used without simplification. Care should be taken to use equations (2-2) and (2-3) when necessary; i.e., when the relative depth is between one-half and one-twenty-fifth.

When the relative water depth becomes shallow, i.e.,  $2\pi d/L < 1/4$  or  $d/L < 1/25$ , equation (2-2) can be simplified to

$$C = \sqrt{gd} \quad (2-9)$$

This relation, attributed to Lagrange, is of importance when dealing with long-period waves, often referred to as long waves. Thus, when a wave travels in shallow water, wave celerity depends only on water depth.

b. The Sinusoidal Wave Profile. The equation describing the free surface as a function of time  $t$  and horizontal distance  $x$  for a simple sinusoidal wave can be shown to be

$$\eta = a \cos \left( \frac{2\pi x}{L} - \frac{2\pi t}{T} \right) = \frac{H}{2} \cos \left( \frac{2\pi x}{L} - \frac{2\pi t}{T} \right) \quad (2-10)$$

where  $\eta$  is the elevation of the water surface relative to the SWL, and  $H/2$  is one-half the wave height equal to the wave amplitude  $a$ . This expression represents a periodic, sinusoidal, progressive wave traveling in the positive  $x$ -direction. For a wave moving in the negative  $x$ -direction, the minus sign before  $2\pi t/T$  is replaced with a plus sign. When  $(2\pi x/L - 2\pi t/T)$  equals 0,  $\pi/2$ ,  $\pi$ ,  $3\pi/2$ , the corresponding values of  $\eta$  are  $H/2$ , 0,  $-H/2$ , and 0, respectively.

c. Some Useful Functions. It can be shown by dividing equation (2-3) by equation (2-6), and equation (2-4) by equation (2-8) that

$$\frac{C}{C_o} = \frac{L}{L_o} = \tanh \left( \frac{2\pi d}{L} \right) \quad (2-11)$$

If both sides of equation (2-11) are multiplied by  $d/L$ , it becomes

$$\frac{d}{L_o} = \frac{d}{L} \tanh \left( \frac{2\pi d}{L} \right) \quad (2-12)$$

The term  $d/L_o$  has been tabulated by Wiegel (1954) as a function of  $d/L$  and is presented in Appendix C, Table C-1. Table C-2 includes  $d/L$  as a function

of  $d/L_0$ , in addition to other useful functions such as  $2\pi d/L$  and  $\tanh(2\pi d/L)$ . These functions simplify the solution of wave problems described by the linear theory.

An example problem illustrating the use of linear wave theory and the tables in Appendix C follows.

\*\*\*\*\* EXAMPLE PROBLEM 1 \*\*\*\*\*

GIVEN: A wave with a period  $T = 10$  seconds is propagated shoreward over a uniformly sloping shelf from a depth  $d = 200$  meters (656 feet) to a depth  $d = 3$  meters (9.8 feet).

FIND: The wave celerities  $C$  and lengths  $L$  corresponding to depths  $d = 200$  meters (656 feet) and  $d = 3$  meters (9.8 feet).

SOLUTION:

Using equation (2-8a),

$$L_0 = \frac{gT^2}{2\pi} = \frac{9.8}{2\pi} T^2 = 1.56T^2 \text{ m (5.12T}^2 \text{ ft)}$$

$$L_0 = 1.56T^2 = 1.56(10)^2 = 156 \text{ m (512 ft)}$$

For  $d = 200$  meters

$$\frac{d}{L_0} = \frac{200}{156} = 1.2821$$

From Table C-1 it is seen that for values of

$$\frac{d}{L_0} > 1.0$$

$$\frac{d}{L_0} = \frac{d}{L}$$

therefore,

$$L = L_0 = 156 \text{ m (512 ft)} \left( \text{deepwater wave, since } \frac{d}{L} > \frac{1}{2} \right)$$

By equation (2-1)

$$C = \frac{L}{T} = \frac{156}{T}$$

$$C = \frac{156}{10} = 15.6 \text{ m/s (51.2 ft/s)}$$

For  $d = 3$  meters

$$\frac{d}{L_0} = \frac{3}{156} = 0.0192$$

Entering Table C-1 with  $d/L_0$  it is found that,

$$\frac{d}{L} = 0.05641$$

hence,

$$L = \frac{3}{0.05641} = 53.2 \text{ m (174 ft)} \left( \text{transitional depth, since } \frac{1}{25} < \frac{d}{L} < \frac{1}{2} \right)$$

$$C = \frac{L}{T} = \frac{53.2}{10} = 5.32 \text{ m/s (17.4 ft/s)}$$

An approximate value of  $L$  can also be found by using equation (2-4b)

$$L \approx \frac{gT^2}{2\pi} \sqrt{\tanh\left(\frac{4\pi^2 d}{T^2 g}\right)}$$

which can be written in terms of  $L_0$  as

$$L \approx L_0 \sqrt{\tanh\left(\frac{2\pi d}{L_0}\right)}$$

therefore,

$$L \approx 156 \sqrt{\tanh\frac{2\pi(3)}{156}}$$

$$L \approx 156 \sqrt{\tanh(0.1208)}$$

$$L \approx 156 \sqrt{0.1202} = 54.1 \text{ m (177.5 ft)}$$

which compares with  $L = 53.3$  meters obtained using Table C-1. The error in this case is 1.5 percent. Note that Plate C-1 could also have been used to determine  $d/L$ .

\*\*\*\*\*

d. Local Fluid Velocities and Accelerations. In wave force studies, it is often desirable to know the local fluid velocities and accelerations for various values of  $z$  and  $t$  during the passage of a wave. The horizontal component  $u$  and the vertical component  $w$  of the local fluid velocity are given by the following equations (with  $X$  and  $t$  as defined in Figure 2-2):

$$u = \frac{H}{2} \frac{gT}{L} \frac{\cosh[2\pi(z+d)/L]}{\cosh(2\pi d/L)} \cos\left(\frac{2\pi x}{L} - \frac{2\pi t}{T}\right) \quad (2-13)$$

$$w = \frac{H}{2} \frac{gT}{L} \frac{\sinh[2\pi(z+d)/L]}{\cosh(2\pi d/L)} \sin\left(\frac{2\pi x}{L} - \frac{2\pi t}{T}\right) \quad (2-14)$$

These equations express the local fluid velocity components any distance ( $z + d$ ) above the bottom. The velocities are harmonic in both  $x$  and  $t$ . For a given value of the phase angle  $\theta = (2\pi x/L - 2\pi t/T)$ , the hyperbolic functions  $\cosh$  and  $\sinh$ , as functions of  $z$  result in an approximate exponential decay of the magnitude of velocity components with increasing distance below the free surface. The maximum positive horizontal velocity occurs when  $\theta = 0, 2\pi, \text{etc.}$ , while the maximum horizontal velocity in the negative direction occurs when  $\theta = \pi, 3\pi, \text{etc.}$  On the other hand, the maximum positive vertical velocity occurs when  $\theta = \pi/2, 5\pi/2, \text{etc.}$ , and the maximum vertical velocity in the negative direction occurs when  $\theta = 3\pi/2, 7\pi/2, \text{etc.}$  (see Fig. 2-3).

The local fluid particle accelerations are obtained from equations (2-13) and (2-14) by differentiating each equation with respect to  $t$ . Thus,

$$\alpha_x = + \frac{g\pi H}{L} \frac{\cosh[2\pi(z + d)/L]}{\cosh(2\pi d/L)} \sin \left( \frac{2\pi x}{L} - \frac{2\pi t}{T} \right) \quad (2-15)$$

$$\alpha_z = - \frac{g\pi H}{L} \frac{\sinh[2\pi(z + d)/L]}{\cosh(2\pi d/L)} \cos \left( \frac{2\pi x}{L} - \frac{2\pi t}{T} \right) \quad (2-16)$$

Positive and negative values of the horizontal and vertical fluid accelerations for various values of  $\theta = 2\pi x/L - 2\pi t/T$  are shown in Figure 2-3.

The following problem illustrates the computations required to determine local fluid velocities and accelerations resulting from wave motions.

\* \* \* \* \* EXAMPLE PROBLEM 2 \* \* \* \* \*

GIVEN: A wave with a period  $T = 8$  seconds, in a water depth  $d = 15$  meters (49 feet), and a height  $H = 5.5$  meters (18.0 feet).

FIND: The local horizontal and vertical velocities  $u$  and  $w$ , and accelerations  $\alpha_x$  and  $\alpha_z$  at an elevation  $z = -5$  meters (-16.4 feet) below the SWL when  $\theta = 2\pi x/L - 2\pi t/T = \pi/3$  ( $60^\circ$ ).

SOLUTION: Calculate

$$L_o = 1.56T^2 = 1.56(8)^2 = 99.8 \text{ m (327 ft)}$$

$$\frac{d}{L_o} = \frac{15}{99.8} = 0.1503$$

From Table C-1 in Appendix C for a value of

$$\frac{d}{L_o} = 0.1503$$

$$\frac{d}{L} \approx 0.1835; \cosh \frac{2\pi d}{L} = 1.742$$

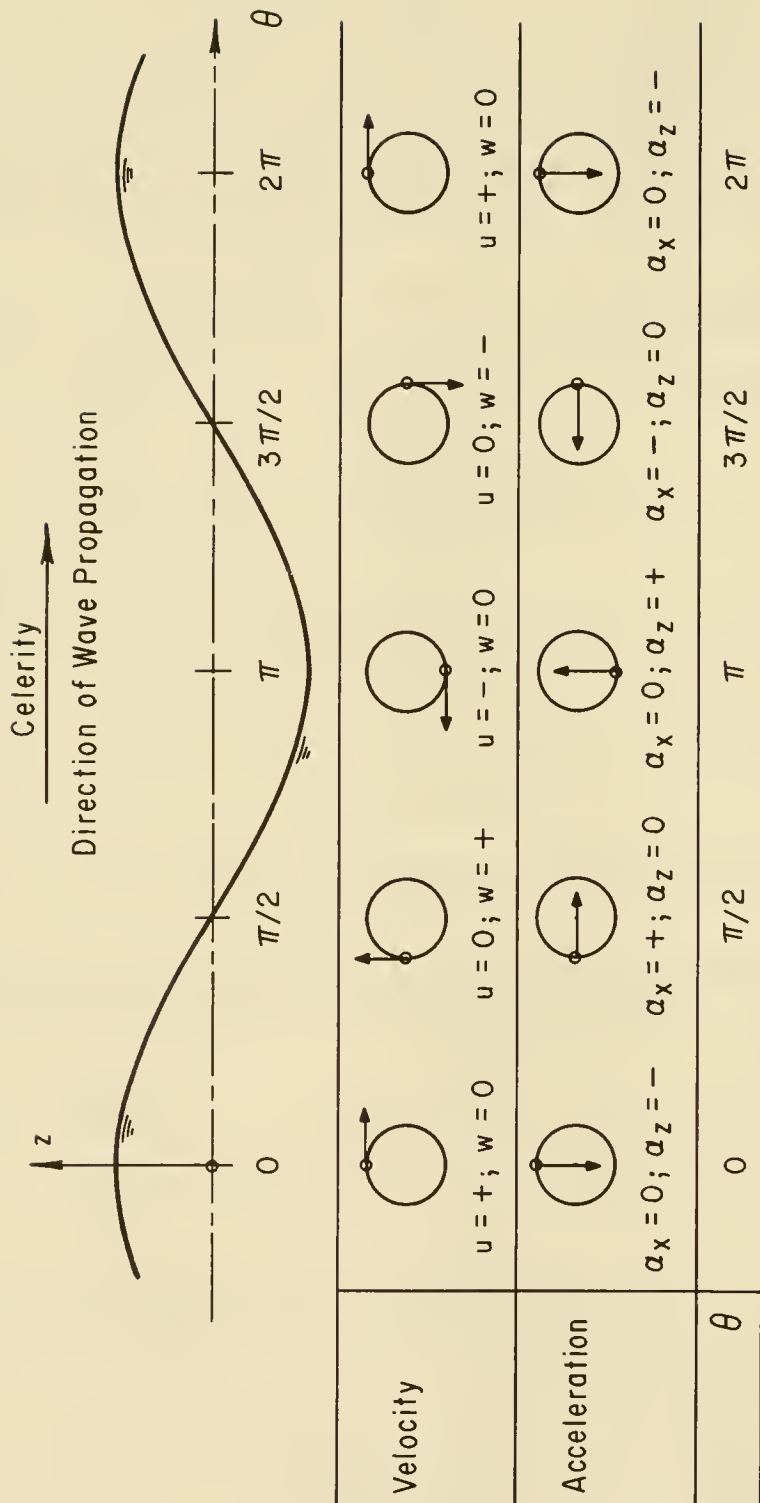


Figure 2-3. Local fluid velocities and accelerations.

hence,

$$L = \frac{15}{0.1835} = 81.7 \text{ m (268 ft)}$$

Evaluation of the constant terms in equations (2-13) to (2-16) gives

$$\frac{HgT}{2L} \frac{1}{\cosh(2\pi d/L)} = \frac{5.5 (9.8)(8)}{2 (81.7)} \frac{1}{1.742} = 1.515$$

$$\frac{Hg\pi}{L} \frac{1}{\cosh(2\pi d/L)} = \frac{5.5 (9.8)(3.1416)}{81.7} \frac{1}{1.742} = 1.190$$

Substitution into equation (2-13) gives

$$u = 1.515 \cosh \left[ \frac{2\pi(15 - 5)}{81.7} \right] [\cos 60^\circ] = 1.515 [\cosh(0.7691)] (0.500)$$

From Table C-1 find

$$\frac{2\pi d}{L} = 0.7691$$

and by interpolation

$$\cosh(0.7691) = 1.3106$$

and

$$\sinh(0.7691) = 0.8472$$

Therefore,

$$u = 1.515 (1.3106) (0.500) = 0.99 \text{ m/s (3.26 ft/s)}$$

$$w = 1.515 (0.8472) (0.866) = 1.11 \text{ m/s (3.65 ft/s)}$$

$$\alpha_x = 1.190 (1.3106) (0.866) = 1.35 \text{ m/s}^2 (4.43 \text{ ft/s}^2)$$

$$\alpha_z = -1.190 (0.8472) (0.500) = -0.50 \text{ m/s}^2 (1.65 \text{ ft/s}^2)$$

Figure 2-3, a sketch of the local fluid motion, indicates that the fluid under the crest moves in the direction of wave propagation and returns during passage of the trough. Linear theory does not predict any mass transport; hence, the sketch shows only an oscillatory fluid motion.

\*\*\*\*\*

e. Water Particle Displacements. Another important aspect of linear wave mechanics deals with the displacement of individual water particles within the wave. Water particles generally move in elliptical paths in shallow or transitional water and in circular paths in deep water. If the mean particle position is considered to be at the center of the ellipse or circle, then vertical particle displacement with respect to the mean position cannot exceed one-half the wave height. Thus, since the wave height is assumed to be small, the displacement of any fluid particle from its mean position is small.

Integration of equations (2-13) and (2-14) gives the horizontal and vertical particle displacement from the mean position, respectively (see Fig. 2-4).

Thus,

$$\xi = -\frac{HgT^2}{4\pi L} \frac{\cosh[2\pi(z+d)/L]}{\cosh(2\pi d/L)} \sin\left(\frac{2\pi x}{L} - \frac{2\pi t}{T}\right) \quad (2-17)$$

$$\zeta = +\frac{HgT^2}{4\pi L} \frac{\sinh[2\pi(z+d)/L]}{\cosh(2\pi d/L)} \cos\left(\frac{2\pi x}{L} - \frac{2\pi t}{T}\right) \quad (2-18)$$

The above equations can be simplified by using the relationship

$$\left(\frac{2\pi}{T}\right)^2 = \frac{2\pi g}{L} \tanh \frac{2\pi d}{L}$$

Thus,

$$\xi = -\frac{H}{2} \frac{\cosh[2\pi(z+d)/L]}{\sinh(2\pi d/L)} \sin\left(\frac{2\pi x}{L} - \frac{2\pi t}{T}\right) \quad (2-19)$$

$$\zeta = +\frac{H}{2} \frac{\sinh[2\pi(z+d)/L]}{\sinh(2\pi d/L)} \cos\left(\frac{2\pi x}{L} - \frac{2\pi t}{T}\right) \quad (2-20)$$

Writing equations (2-19) and (2-20) in the forms,

$$\sin^2\left(\frac{2\pi x}{L} - \frac{2\pi t}{T}\right) = \left[\frac{\xi}{a} \frac{\sinh(2\pi d/L)}{\cosh[2\pi(z+d)/L]}\right]^2$$

$$\cos^2\left(\frac{2\pi x}{L} - \frac{2\pi t}{T}\right) = \left[\frac{\zeta}{a} \frac{\sinh(2\pi d/L)}{\sinh[2\pi(z+d)/L]}\right]^2$$

and adding give

$$\frac{\xi^2}{A^2} + \frac{\zeta^2}{B^2} = 1 \quad (2-21)$$

in which

$$A = \frac{H}{2} \frac{\cosh[2\pi(z+d)/L]}{\sinh(2\pi d/L)} \quad (2-22)$$

$$B = \frac{H}{2} \frac{\sinh[2\pi(z+d)/L]}{\sinh(2\pi d/L)} \quad (2-23)$$

Equation (2-21) is the equation of an ellipse with a major (horizontal) semi-axis equal to A and a minor (vertical) semi-axis equal to B. The lengths of A and B are measures of the horizontal and vertical displacements of the water particles. Thus, the water particles are predicted to move in

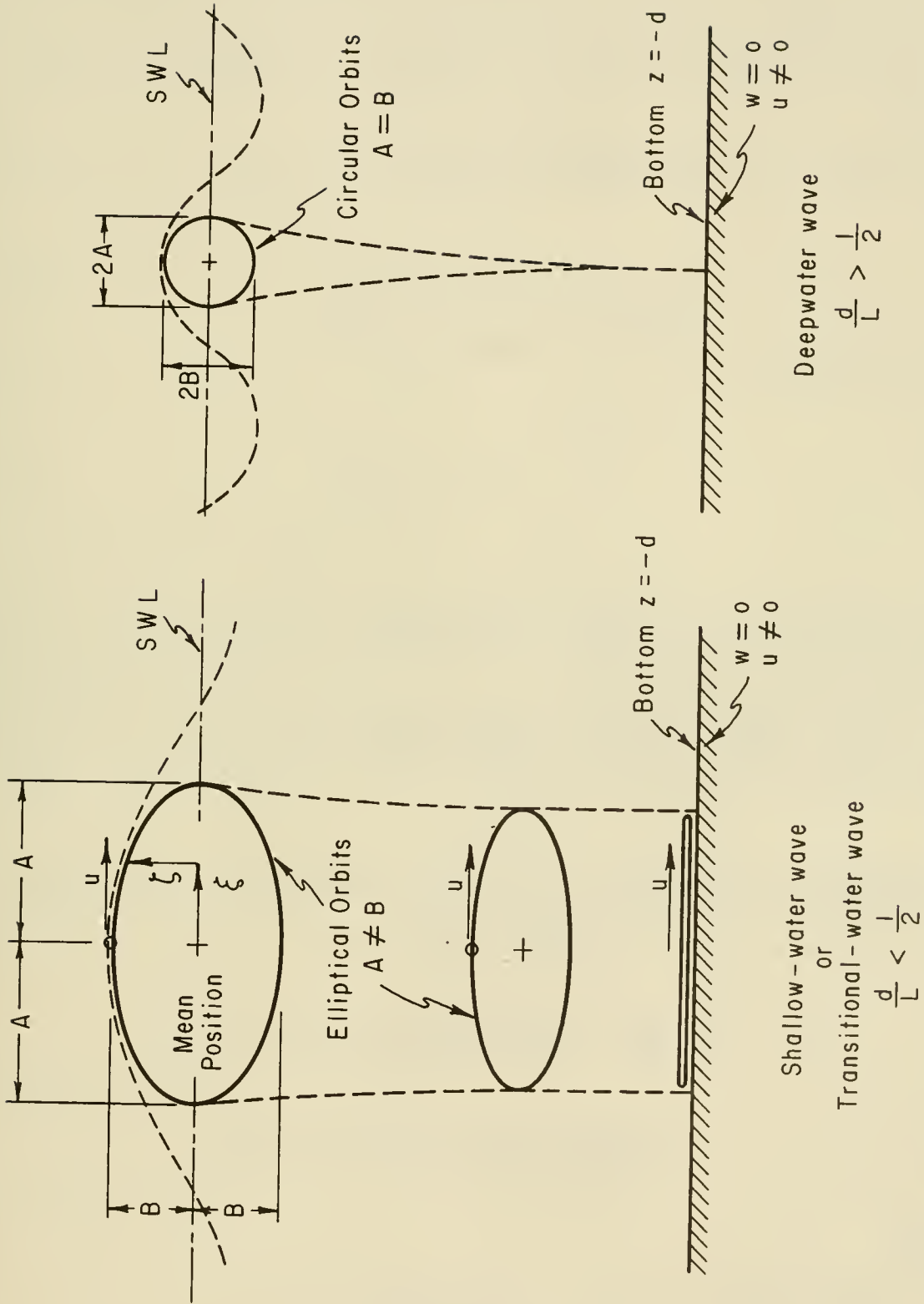


Figure 2-4. Water particle displacements from mean position for shallow-water and deepwater waves.

closed orbits by linear wave theory; i.e., each particle returns to its initial position after each wave cycle. Morison and Crooke (1953) compared laboratory measurements of particle orbits with wave theory and found, as had others, that particle orbits were not completely closed. This difference between linear theory and observations is due to the mass transport phenomenon, which is discussed in a subsequent section.

Examination of equations (2-22) and (2-23) shows that for deepwater conditions, A and B are equal and particle paths are circular. The equations become

$$A = B = \frac{H}{2} e^{2\pi z/L} \quad \text{for } \frac{d}{L} > \frac{1}{2} \quad (2-24)$$

For shallow-water conditions, the equations become

$$A = \frac{H}{2} \frac{L}{2\pi d}$$

$$B = \frac{H}{2} \frac{z + d}{d}$$

for  $\frac{d}{L} < \frac{1}{25}$  (2-25)

Thus, in deep water, the water particle orbits are circular. The more shallow the water, the flatter the ellipse. The amplitude of the water particle displacement decreases exponentially with depth and in deepwater regions becomes small relative to the wave height at a depth equal to one-half the wavelength below the free surface; i.e., when  $z = L_0/2$ . This is illustrated in Figure 2-4. For shallow regions, horizontal particle displacement near the bottom can be large. In fact, this is apparent in offshore regions seaward of the breaker zone where wave action and turbulence lift bottom sediments into suspension.

The vertical displacement of water particles varies from a minimum of zero at the bottom to a maximum equal to one-half the wave height at the surface.

\*\*\*\*\* EXAMPLE PROBLEM 3 \*\*\*\*\*

PROVE:

(a) 
$$\left(\frac{2\pi}{T}\right)^2 = \frac{2\pi g}{L} \tanh\left(\frac{2\pi d}{L}\right)$$

(b) 
$$u = \frac{\pi H}{T} \frac{\cosh[2\pi(z + d)/L]}{\sinh(2\pi d/L)} \cos\left(\frac{2\pi x}{L} - \frac{2\pi t}{T}\right)$$

SOLUTION:

(a) Equation (2-3),

$$C = \frac{gT}{2\pi} \tanh\left(\frac{2\pi d}{L}\right)$$

Equation (2-1),

$$C = \frac{L}{T}$$

Therefore, equating (2-1) and (2-3),

$$\frac{L}{T} = \frac{gT}{2\pi} \tanh\left(\frac{2\pi d}{L}\right)$$

and multiplying both sides by  $(2\pi)^2/LT$

$$\frac{(2\pi)^2}{LT} \frac{L}{T} = \frac{(2\pi)^2}{LT} \frac{gT}{2\pi} \tanh\left(\frac{2\pi d}{L}\right)$$

Hence,

$$\left(\frac{2\pi}{T}\right)^2 = \frac{2\pi g}{L} \tanh\left(\frac{2\pi d}{L}\right)$$

(b) Equation (2-13) may be written

$$u = \frac{gTH}{2L} \frac{\cosh[2\pi(z+d)/L]}{\cosh(2\pi d/L)} \cos\left(\frac{2\pi x}{L} - \frac{2\pi t}{T}\right)$$

$$u = \frac{1}{C} \frac{gH}{2} \frac{\cosh[2\pi(z+d)/L]}{\cosh(2\pi d/L)} \cos\left(\frac{2\pi x}{L} - \frac{2\pi t}{T}\right)$$

since

$$\frac{T}{L} = \frac{1}{C}$$

Since

$$C = \frac{gT}{2\pi} \tanh\left(\frac{2\pi d}{L}\right)$$

$$u = \frac{\pi H}{T} \frac{1}{\tanh(2\pi d/L)} \frac{\cosh[2\pi(z+d)/L]}{\cosh(2\pi d/L)} \cos\left(\frac{2\pi x}{L} - \frac{2\pi t}{T}\right)$$

and since

$$\tanh\left(\frac{2\pi d}{L}\right) = \frac{\sinh(2\pi d/L)}{\cosh(2\pi d/L)}$$

therefore,

$$u = \frac{\pi H}{T} \frac{\cosh[2\pi(z+d)/L]}{\sinh(2\pi d/L)} \cos\left(\frac{2\pi x}{L} - \frac{2\pi t}{T}\right)$$

\*\*\*\*\*

GIVEN: A wave in a depth  $d = 12$  meters (39.4 feet), height  $H = 3$  meters (9.8 feet), and a period  $T = 10$  seconds. The corresponding deepwater wave height is  $H_0 = 3.13$  meters (10.27 feet).

FIND:

- (a) The horizontal and vertical displacement of a water particle from its mean position when  $z = 0$ , and when  $z = -d$ .
- (b) The maximum water particle displacement at an elevation  $z = 7.5$  meters (-24.6 feet) when the wave is in infinitely deep water.
- (c) For the deepwater conditions of (b) above, show that the particle displacements are small relative to the wave height when  $z = -L_0/2$ .

SOLUTION:

(a)  $L_0 = 1.56T^2 = 1.56(10)^2 = 156 \text{ m (512 ft)}$

$$\frac{d}{L_0} = \frac{12}{156} = 0.0769$$

From Appendix C, Table C-1

$$\sinh\left(\frac{2\pi d}{L}\right) = 0.8306$$

$$\tanh\left(\frac{2\pi d}{L}\right) = 0.6389$$

When  $z = 0$ , equation (2-22) reduces to

$$A = \frac{H}{2} \frac{1}{\tanh(2\pi d/L)}$$

and equation (2-23) reduces to

$$B = \frac{H}{2}$$

Thus,

$$A = \frac{3}{2} \frac{1}{(0.6389)} = 2.35 \text{ m (7.70 ft)}$$

$$B = \frac{H}{2} = \frac{3}{2} = 1.5 \text{ m (4.92 ft)}$$

When  $z = -d$ ,

$$A = \frac{H}{2 \sinh(2\pi d/L)} = \frac{3}{2(0.8306)} = 1.81 \text{ m (5.92 ft)}$$

and,  $B = 0$ .

(b) With  $H_0 = 3.13$  meters and  $z = -7.5$  meters (-24.6 feet), evaluate the exponent of  $e$  for use in equation (2-24), noting that  $L = L_0$ ,

$$\frac{2\pi z}{L} = \frac{2\pi(-7.5)}{156} = -0.302$$

thus,

$$e^{-0.302} = 0.739$$

Therefore,

$$A = B = \frac{H_0}{2} e^{2\pi z/L} = \frac{3.13}{2} (0.739) = 1.16 \text{ m (3.79 ft)}$$

The maximum displacement or diameter of the orbit circle would be  $2(1.16) = 2.32$  meters (7.61 feet).

(c) 
$$z = -\frac{L_0}{2} = \frac{-156}{2} = -78.0 \text{ m (255.9 ft)}$$

$$\frac{2\pi z}{L} = \frac{2\pi(-78)}{156} = -3.142$$

Therefore,

$$e^{-3.142} = 0.043$$

and,

$$A = B = \frac{H_0}{2} e^{2\pi z/L} = \frac{3.13}{2} (0.043) = 0.067 \text{ m (0.221 ft)}$$

Thus, the maximum displacement of the particle is 0.067 meters which is small when compared with the deepwater height,  $H_0 = 3.13$  meters (10.45 feet).

\*\*\*\*\*

f. Subsurface Pressure. Subsurface pressure under a wave is the summation of two contributing components, dynamic and static pressures, and is given by

$$p' = \rho g \frac{\cosh[2\pi(z+d)/L]}{\cosh(2\pi d/L)} \frac{H}{2} \cos\left(\frac{2\pi x}{L} - \frac{2\pi t}{T}\right) - \rho g z + p_a \quad (2-26)$$

where  $p'$  is the total or absolute pressure,  $p_a$  the atmospheric pressure and  $\rho = w/g$  the mass density of water (for salt water,  $\rho = 1025$  kilograms per cubic meter (2.0 slugs per cubic foot); for fresh water,  $\rho = 1000$  kilograms per cubic meter (1.94 slugs per cubic foot)). The first term of equation (2-26) represents a dynamic component due to acceleration, while the second term is the static component of pressure. For convenience, the pressure is usually taken as the gage pressure defined as

$$p = p' - p_a = \rho g \frac{\cosh [2\pi(z+d)/L]}{\cosh (2\pi d/L)} \frac{H}{2} \cos \left( \frac{2\pi x}{L} - \frac{2\pi t}{T} \right) - \rho g z \quad (2-27)$$

Equation (2-27) can be written as

$$p = \rho g \eta \frac{\cosh[2\pi(z + d)/L]}{\cosh(2\pi d/L)} - \rho g z \quad (2-28)$$

since

$$\eta = \frac{H}{2} \cos \left( \frac{2\pi x}{L} - \frac{2\pi t}{T} \right)$$

The ratio

$$K_z = \frac{\cosh[2\pi(z + d)/L]}{\cosh(2\pi d/L)} \quad (2-29)$$

is termed the pressure response factor. Hence, equation (2-28) can be written as

$$p = \rho g (\eta K_z - z) \quad (2-30)$$

The pressure response factor  $K$  for the pressure at the bottom when  $z = -d$ ,

$$K_z = K = \frac{1}{\cosh(2\pi d/L)} \quad (2-31)$$

is tabulated as a function of  $d/L_0$  and  $d/L$  in Tables C-1 and C-2 of Appendix C.

It is often necessary to determine the height of surface waves based on subsurface measurements of pressure. For this purpose, it is convenient to rewrite equation (2-30) as

$$\eta = \frac{N(p + \rho g z)}{\rho g K_z} \quad (2-32)$$

where  $z$  is the depth below the SWL of the pressure gage, and  $N$  a correction factor equal to unity if the linear theory applies. Several empirical studies have found  $N$  to be a function of period, depth, wave amplitude, and other factors. In general,  $N$  decreases with decreasing period, being greater than 1.0 for long-period waves and less than 1.0 for short-period waves.

A complete discussion of the interpretation of pressure gage wave records is beyond the scope of this manual. For a more detailed discussion of the variation of  $N$  with wave parameters, the reader is referred to Draper (1957), Grace (1970), and Esteva and Harris (1971).

\*\*\*\*\* EXAMPLE PROBLEM 5 \*\*\*\*\*

GIVEN: An average maximum pressure  $p = 124$  kilonewtons per square meter is measured by a subsurface pressure gage located in salt water 0.6 meter (1.97 feet) above the bed in water depth  $d = 12$  meters (39 feet). The average frequency  $f = 0.0666$  cycles per second (hertz).

FIND: The height of the wave H assuming that linear theory applies and the average frequency corresponds to the average wave amplitude.

SOLUTION:

$$T = \frac{1}{f} = \frac{1}{(0.0666)} \approx 15 \text{ s}$$

$$L_o = 1.56T^2 = 1.56(15)^2 = 351 \text{ m (1152 ft)}$$

$$\frac{d}{L_o} = \frac{12}{351} \approx 0.0342$$

From Table C-1 of Appendix C, entering with  $d/L_o$ ,

$$\frac{d}{L} = 0.07651$$

hence,

$$L = \frac{12}{(0.07651)} = 156.8 \text{ m (515 ft)}$$

and

$$\cosh\left(\frac{2\pi d}{L}\right) = 1.1178$$

Therefore, from equation (2-29)

$$K_z = \frac{\cosh[2\pi(z + d)/L]}{\cosh(2\pi d/L)} = \frac{\cosh[2\pi[-11.4 + 12]/156.8]}{1.1178} = \frac{1.0003}{1.1178} = 0.8949$$

Since  $\eta = a = H/2$  when the pressure is maximum (under the wave crest), and  $N = 1.0$  since linear theory is assumed valid,

$$\frac{H}{2} = \frac{N(p + \rho g z)}{\rho g K_z} = \frac{1.0 [124 + (10.06)(-11.4)]}{(10.06)(0.8949)} = 1.04 \text{ m (3.44 ft)}$$

Therefore,

$$H = 2(1.04) = 2.08 \text{ m (6.3 ft)}$$

Note that the tabulated value of K in Appendix C, Table C-1, could not be used since the pressure was not measured at the bottom.

\*\*\*\*\*

g. Velocity of a Wave Group. The speed with which a group of waves or a wave train travels is generally not identical to the speed with which individual waves within the group travel. The group speed is termed the group velocity  $C_g$ ; the individual wave speed is the phase velocity or wave celerity

given by equation (2-2) or (2-3). For waves propagating in deep or transitional water with gravity as the primary restoring force, the group velocity will be less than the phase velocity. (For those waves propagated primarily under the influence of surface tension, i.e. capillary waves, the group velocity may exceed the velocity of an individual wave.)

The concept of group velocity can be described by considering the interaction of two sinusoidal wave trains moving in the same direction with slightly different wavelengths and periods. The equation of the water surface is given by

$$\eta = \eta_1 + \eta_2 = \frac{H}{2} \cos \left( \frac{2\pi x}{L_1} - \frac{2\pi t}{T_1} \right) + \frac{H}{2} \cos \left( \frac{2\pi x}{L_2} - \frac{2\pi t}{T_2} \right) \quad (2-33)$$

where  $\eta_1$  and  $\eta_2$  are the contributions of each of the two components. They may be summed since superposition of solutions is permissible when the linear wave theory is used. For simplicity, the heights of both wave components have been assumed equal. Since the wavelengths of the two component waves,  $L_1$  and  $L_2$ , have been assumed slightly different for some values of  $x$  at a given time, the two components will be in phase and the wave height observed will be  $2H$ ; for some other values of  $x$ , the two waves will be completely out of phase and the resultant wave height will be zero. The surface profile made up of the sum of the two sinusoidal waves is given by equation (2-33) and is shown in Figure 2-5. The waves shown in Figure 2-5 appear to be traveling in groups described by the equation of the envelope curves

$$\eta_{envelope} = \pm H \cos \left[ \pi \left( \frac{L_2 - L_1}{L_1 L_2} \right) x - \pi \left( \frac{T_2 - T_1}{T_1 T_2} \right) t \right] \quad (2-34)$$

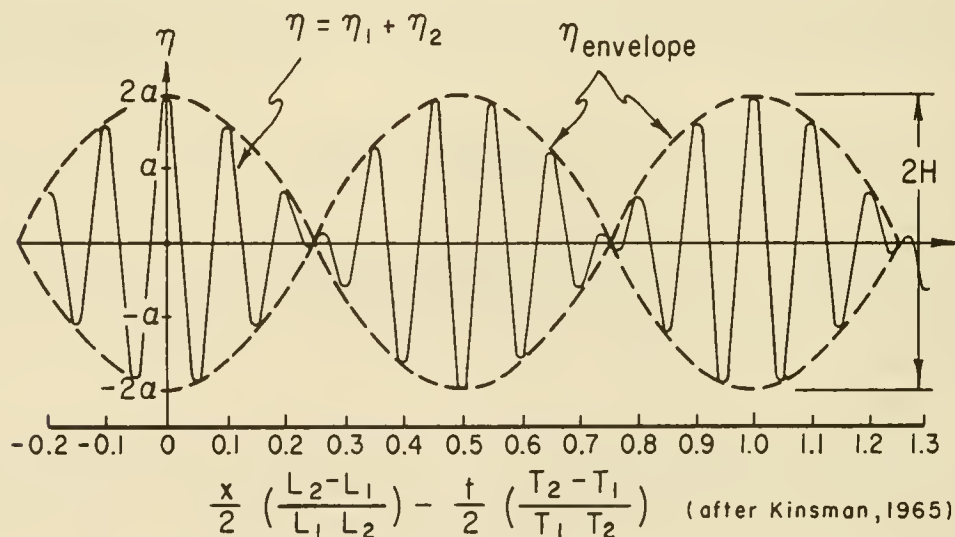


Figure 2-5. Formation of wave groups by the addition of two sinusoids having different periods.

It is the speed of these groups (i.e., the velocity of propagation of the envelope curves) that represents the group velocity. The limiting speed of the wave groups as they become large (i.e., as the wavelength  $L_1$  approaches

$L_2$  and consequently the wave period  $T_1$  approaches  $T_2$ ) is the group velocity and can be shown to be equal to

$$C_g = \frac{1}{2} \frac{L}{T} \left[ 1 + \frac{4\pi d/L}{\sinh(4\pi d/L)} \right] = nC \quad (2-35)$$

where

$$n = \frac{1}{2} \left[ 1 + \frac{4\pi d/L}{\sinh(4\pi d/L)} \right]$$

In deep waters, the term  $(4\pi d/L)/\sinh(4\pi d/L)$  is approximately zero and

$$C_g = \frac{1}{2} \frac{L_o}{T} = \frac{1}{2} C_o \quad (\text{deep water}) \quad (2-36)$$

or the group velocity is one-half the phase velocity. In shallow water,  $\sinh(4\pi d/L) \approx 4\pi d/L$  and

$$C_g = \frac{L}{T} = C \approx \sqrt{gd} \quad (\text{shallow water}) \quad (2-37)$$

hence, the group and phase velocities are equal. Thus, in shallow water, because wave celerity is fully determined by the depth, all component waves in a wave train will travel at the same speed precluding the alternate reinforcing and canceling of components. In deep and transitional water, wave celerity depends on the wavelength; hence, slightly longer waves travel slightly faster and produce the small phase differences resulting in wave groups. These waves are said to be *dispersive* or propagating in a *dispersive medium*; i.e., in a medium where their celerity is dependent on wavelength.

Outside of shallow water, the phase velocity of gravity waves is greater than the group velocity; an observer that follows a group of waves at group velocity will see waves that originate at the rear of the group move forward through the group traveling at the phase velocity and disappear at the front of the wave group.

Group velocity is important because it is with this velocity that wave energy is propagated. Although mathematically the group velocity can be shown rigorously from the interference of two or more waves (Lamb, 1932), the physical significance is not as obvious as it is in the method based on the consideration of wave energy. Therefore an additional explanation of group velocity is provided on wave energy and energy transmission.

h. Wave Energy and Power. The total energy of a wave system is the sum of its kinetic energy and its potential energy. The kinetic energy is that part of the total energy due to water particle velocities associated with wave motion. Potential energy is that part of the energy resulting from part of the fluid mass being above the trough: the wave crest. According to the Airy theory, if the potential energy is determined relative to SWL, and all waves are propagated in the same direction, potential and kinetic energy components are equal, and the total wave energy in one wavelength per unit crest width is given by

$$E = E_k + E_p = \frac{\rho g H^2 L}{16} + \frac{\rho g H^2 L}{16} = \frac{\rho g H^2 L}{8} \quad (2-38)$$

Subscripts k and p refer to kinetic and potential energies. Total average wave energy per unit surface area, termed the *specific energy* or *energy density*, is given by

$$\bar{E} = \frac{E}{L} = \frac{\rho g H^2}{8} \quad (2-39)$$

Wave energy flux is the rate at which energy is transmitted in the direction of wave propagation across a vertical plane perpendicular to the direction of wave advance and extending down the entire depth. The average energy flux per unit wave crest width transmitted across a vertical plane perpendicular to the direction of wave advance is

$$\bar{P} = \bar{E} n C = \bar{E} C_g \quad (2-40)$$

Energy flux  $\bar{P}$  is frequently called *wave power* and

$$n = \frac{1}{2} \left[ 1 + \frac{4\pi d/L}{\sinh(4\pi d/L)} \right]$$

If a vertical plane is taken other than perpendicular to the direction of wave advance,  $P = E C_g \sin \phi$ , where  $\phi$  is the angle between the plane across which the energy is being transmitted and the direction of wave advance.

For deep and shallow water, equation (2-40) becomes

$$\bar{P}_o = \frac{1}{2} \bar{E}_o C_o \quad (\text{deep water}) \quad (2-41)$$

$$\bar{P} = \bar{E} C_g = \bar{E} C \quad (\text{shallow water}) \quad (2-42)$$

An energy balance for a region through which waves are passing will reveal that, for steady state, the amount of energy entering the region will equal amount leaving the region provided no energy is added or removed from the system. Therefore, when the waves are moving so that their crests are parallel to the bottom contours,

$$\bar{E}_o n_o C_o = \bar{E} n C$$

or since

$$n_o = \frac{1}{2}$$

$$\frac{1}{2} \bar{E}_o C_o = \bar{E} n C \quad (2-43)$$

When the wave crests are not parallel to the bottom contours, some parts of the wave will be traveling at different speeds and the wave will be refracted; equation (2-43) does not apply (see Sec. III).

The following problem illustrates some basic principles of wave energy and energy flux:

\*\*\*\*\* EXAMPLE PROBLEM 6 \*\*\*\*\*

GIVEN: A deepwater oscillatory wave with a wavelength  $L_o = 156$  meters (512 feet), a height  $H_o = 2$  meters (6.56 feet), and a celerity  $C_o = 15.6$  meters per second, moving shoreward with its crest parallel to the depth contours. Any effects due to reflection from the beach are negligible.

FIND:

- (a) Derive a relationship between the wave height in any depth of water and the wave height in deep water, assuming that wave energy flux per unit crest width is conserved as a wave moves from deep water into shoaling water.
- (b) Calculate the wave height for the given wave when the depth is 3 meters (9.84 feet).
- (c) Determine the rate at which energy per unit crest width is transported toward the shoreline and the total energy per unit width delivered to the shore in 1 hour by the given waves.

SOLUTION:

- (a) Since the wave crests are parallel to the bottom contours, refraction does not occur, therefore  $H_o = H'_o$  (see Sec. III).

From equation (2-43),

$$\frac{1}{2} \bar{E}_o C_o = n \bar{E} C$$

The expressions for  $\bar{E}_o$  and  $\bar{E}$  are

$$\bar{E}_o = \frac{\rho g H_o'^2}{8}$$

and

$$\bar{E} = \frac{\rho g H^2}{8}$$

where  $H'_o$  represents the wave height in deep water if the wave is not refracted.

Substituting into the above equation gives

$$\frac{1}{2} C_o \frac{\rho g H_o'^2}{8} = n C \frac{\rho g H^2}{8}$$

Therefore,

$$\left(\frac{H}{H'_0}\right)^2 = \frac{1}{2} \frac{1}{n} \frac{C_0}{C}$$

and since from equations (2-3) and (2-6)

$$\frac{C}{C_0} = \tanh\left(\frac{2\pi d}{L}\right)$$

and from equation (2-35) where

$$n = \frac{1}{2} \left[ 1 + \frac{4\pi d/L}{\sinh(4\pi d/L)} \right]$$

$$\frac{H}{H'_0} = \sqrt{\frac{1}{\tanh(2\pi d/L)} \frac{1}{\left[ 1 + \frac{(4\pi d/L)}{\sinh(4\pi d/L)} \right]}} = K_s \quad (2-44)$$

where  $K_s$  or  $H/H'_0$  is termed the *shoaling coefficient*. Values of  $H/H'_0$  as a function of  $d/L_0$  and  $d/L$  have been tabulated in Tables C-1 and C-2 of Appendix C.

(b) For the given wave,  $d/L_0 = 3/156 = 0.01923$ . From Table C-1 or from an evaluation of equation (2-44) above,

$$\frac{H}{H'_0} = 1.237$$

Therefore,

$$H = 1.237(2) = 2.474 \text{ m (8.117 ft)}$$

(c) The rate at which energy is being transported toward shore is the wave energy flux.

$$\bar{P} = \frac{1}{2} \bar{E}_0 C_0 = n \bar{E} C$$

Since it is easier to evaluate the energy flux in deep water, the left side of the above equation will be used.

$$\bar{P} = \frac{1}{2} \bar{E}_0 C_0 = \frac{1}{2} \frac{\rho g (H'_0)^2}{8} 15.6 = \frac{1}{2} \frac{10,050(2)^2}{8} 15.6$$

$$\bar{P} = 39,195 \text{ N}\cdot\text{m/s per m of wave crest}$$

$$\bar{P} = \frac{8811}{550} = 16.02 \text{ hp/ft of wave crest}$$

This represents an expenditure of

$$39,195 \frac{\text{N}\cdot\text{m}}{\text{s}} \times 3600 \frac{\text{s}}{\text{h}} = 14.11 \times 10^7 \text{ J}$$

of energy each hour on each meter of beach ( $31.72 \times 10^6$  foot-pounds each hour on each foot of beach).

\* \* \* \* \*

The mean rate of energy transmission associated with waves propagating into an area of calm water provides a better physical description of the concept of group velocity. Sverdrup and Munk (1947) provide an excellent discussion of this subject. Quoting from Technical Report No. 2, by the Beach Erosion Board (U.S. Army, Corps of Engineers, 1942):

"As the first wave in the group advances one wave length, its form induces corresponding velocities in the previously undisturbed water and the kinetic energy corresponding to those velocities must be drawn from the energy flowing ahead with the form. If there is equipartition of energy in the wave, half of the potential energy which advanced with the wave must be given over to the kinetic form and the wave loses height. Advancing another wave length another half of the potential energy is used to supply kinetic energy to the undisturbed liquid. The process continues until the first wave is too small to identify. The second, third, and subsequent waves move into water already disturbed and the rate at which they lose height is less than for the first wave. At the rear of the group, the potential energy might be imagined as moving ahead, leaving a flat surface and half of the total energy behind as kinetic energy. But the velocity pattern is such that flow converges toward one section thus developing a crest and diverges from another section forming a trough. Thus the kinetic energy is converted into potential and a wave develops in the rear of the group.

"This concept can be interpreted in a quantitative manner, by taking the following example from R. Gatewood (Gaillard 1904, p. 50). Suppose that in a very long trough containing water originally at rest, a plunger at one end is suddenly set into harmonic motion and starts generating waves by periodically imparting an energy  $E/2$  to the water. After a time interval of  $n$  periods there are  $n$  waves present. Let  $m$  be the position of a particular wave in this group such that  $m=1$  refers to the wave which has just been generated by the plunger,  $m=(n+1)/2$  to the center wave, and  $m=n$  to the wave furthest advanced. Let the waves travel with constant velocity  $C$ , and neglect friction.

"After the first complete stroke one wave will be present and its energy is  $E/2$ . One period later this wave has advanced one wave length but has left one-half of its energy or  $E/4$

behind. It now occupies a previously undisturbed area to which it has brought energy  $E/4$ . In the meantime, a second wave has been generated, occupying the position next to the plunger where  $E/4$  was left behind by the first wave. The energy of this second wave equals  $E/4 + E/2 = 3E/4$ . Repeated applications of this reasoning lead to the results shown in Table 2-1.

Table 2-1. Distribution of wave heights in a short train of waves.

Series number, n	Wave number, m							Total energy of group
	1	2	3	4	5	6	7	
1	$1/2E$	---	---	---	---	---	---	$1/2E$
2	$3/4$	$1/4E$	---	---	---	---	---	$2/2$
3	$7/8$	$4/8$	$1/8E$	---	---	---	---	$3/2$
4	$15/16$	$11/16$	$5/16$	$1/16E$	---	---	---	$4/2$
5	$31/32$	$26/32$	$16/32$	$6/32$	$1/32E$	---	---	$5/2$
6	$63/64$	$57/64$	$42/64$	$22/64$	$7/64$	$1/64E$	---	$6/2$

"The series number  $n$  gives the total number of waves present and equals the time in periods since the first wave entered the area of calm; the wave number  $m$  gives the position of the wave measured from the plunger and equals the distance from the plunger expressed in wave lengths. In any series,  $n$ , the deviation of the energy from the value  $E/2$  is symmetrical about the center wave. Relative to the center wave all waves nearer the plunger show an excess of energy and all waves beyond the center wave show a deficit. For any two waves at equal distances from the center wave the excess equals the deficiency. In every series,  $n$ , the energy first decreases slowly with increasing distance from the plunger, but in the vicinity of the center wave it decreases rapidly. Thus, there develops an "energy front" which advances with the speed of the central part of the wave system, that is, with half the wave velocity.

"According to the last line in Table 2-1 a definite pattern develops after a few strokes: the wave closest to the plunger has an energy  $E(2^n-1)/2^n$  which approaches the full amount  $E$ , the center wave has an energy  $E/2$ , and the wave which has traveled the greatest distance has very little energy ( $E/2^n$ )."

With a large number of waves (a large  $n$ ), energy decreases with increasing  $m$ , and the leading wave eventually loses its identity. At the group center, energy increases and decreases rapidly--to nearly maximum and to nearly zero. Consequently, an energy front is located at the center wave group for deep-water conditions. If waves had been examined for shallow rather than deep water, the energy front would have been found at the leading edge of the

group. For any depth, the ratio of group to phase velocity ( $C_g/C$ ) generally defines the energy front. Also, wave energy is transported in the direction of phase propagation, but moves with the group velocity rather than phase velocity.

1. Summary of Linear Wave Theory. Equations describing water surface profile particle velocities, particle accelerations, and particle displacements for linear (Airy) theory are summarized in Figure 2-6.

#### 4. Higher Order Wave Theories.

The solution of the hydrodynamic equations for gravity wave phenomena can be improved. Each extension of the theories usually produces better agreement between theoretical and observed wave behavior. The extended theories can explain phenomena such as mass transport that cannot be explained by the linear theory. If the precise measurements for amplitude and period are known, the extended theories will provide estimates of such derived quantities as the velocity and pressure fields due to waves that are more accurate than that provided by linear theory. In shallow water, the maximum possible wave height is determined by the depth and can be estimated without wave records.

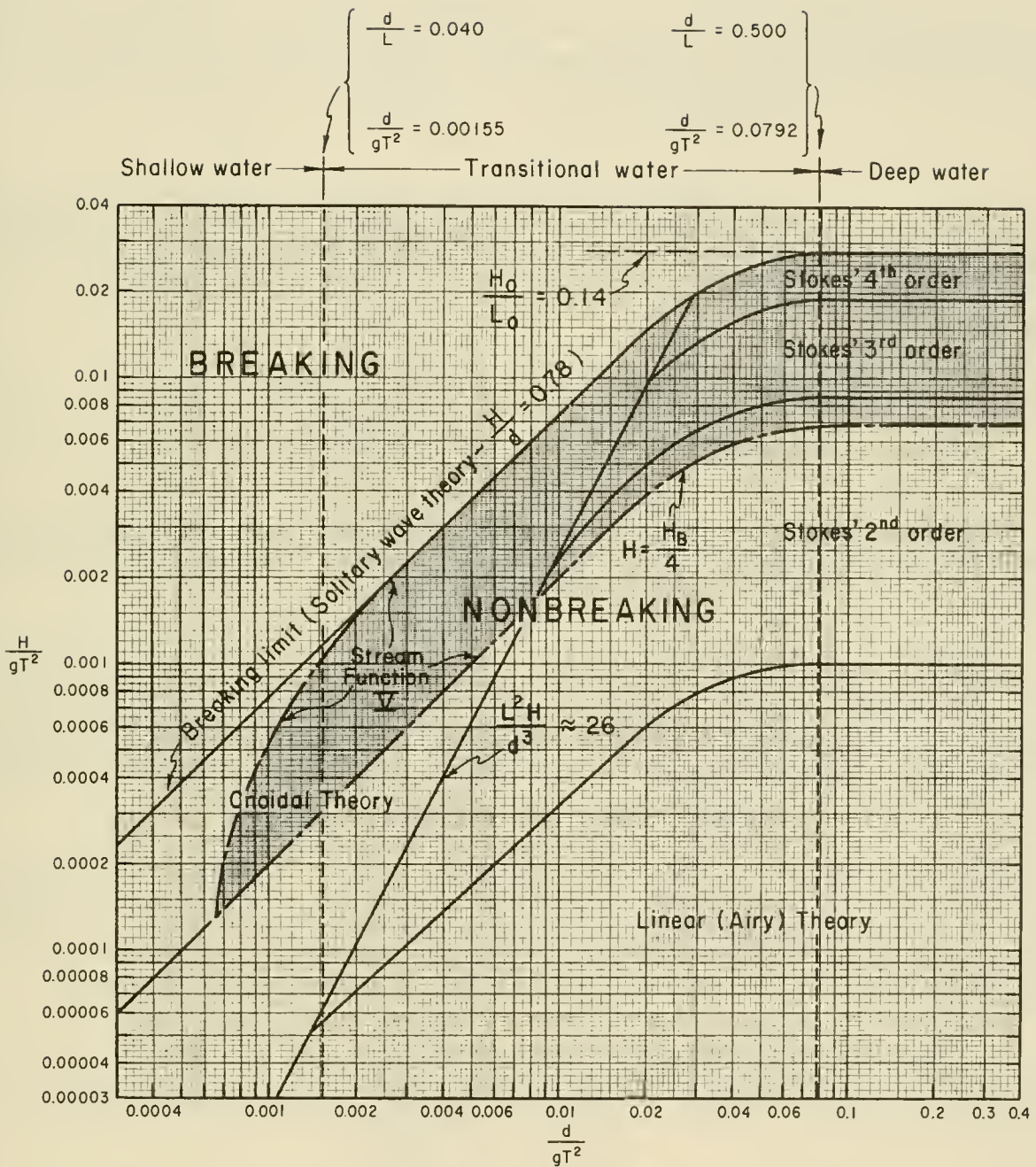
When concern is primarily with the oscillating character of waves, estimates of amplitude and period must be determined from empirical data. In such problems, the uncertainty of the accurate wave height and period leads to a greater uncertainty of the ultimate answer than does neglecting the effect of nonlinear processes. Therefore, it is unlikely that the extra work involved in using nonlinear theories is justified.

The engineer must define regions where various wave theories are valid. Since investigators differ on the limiting conditions for the several theories, some overlap must be permitted in defining the regions. Le Mehaute (1969) presented Figure 2-7 to illustrate the approximate limits of validity for several wave theories. Theories discussed here are indicated as the Stokes third- and fourth-order theories. Dean (1974), after considering three analytic theories, presents a slightly different analysis. Dean (1974) and Le Mehaute (1969) agree in recommending cnoidal theory for shallow-water waves of low steepness, and Stokes' higher order theories for steep waves in deep water, but differ in regions assigned to Airy theory. Dean indicates that tabulated stream-function theory is most internally consistent over most of the domain considered. For the limit of low steepness waves in transitional and deep water, the difference between stream-function theory and Airy theory is small. Other wave theories may also be useful in studying wave phenomena. For given values of  $H$ ,  $d$ , and  $T$ , Figure 2-7 may be used as a guide in selecting an appropriate theory. The magnitude of the Ursell or Stokes parameter  $U_R$  shown in the figure may be used to establish the boundaries of regions where a particular wave theory should be used. The parameter was first noted by Stokes (1847) when he stated that the parameter must be small if his equations were to remain valid for long waves. The parameter is defined by

$$U_R = \frac{L^2 H}{d^3} \quad (2-45)$$

RELATIVE DEPTH	SHALLOW WATER $\frac{d}{L} < \frac{1}{25}$	TRANSITIONAL WATER $\frac{1}{25} < \frac{d}{L} < \frac{1}{2}$	DEEP WATER $\frac{d}{L} > \frac{1}{2}$
1. Wave profile	Same As $\rightarrow$	$\eta = \frac{H}{2} \cos \left[ \frac{2\pi x}{L} - \frac{2\pi t}{T} \right] = \frac{H}{2} \cos \theta$	Same As $\leftarrow$
2. Wave celerity	$C = \frac{L}{T} = \sqrt{gd}$	$C = \frac{L}{T} = \frac{gT}{2\pi} \tanh \left( \frac{2\pi d}{L} \right)$	$C = C_0 = \frac{L}{T} = \frac{gT}{2\pi}$
3. Wavelength	$L = T \sqrt{gd} = CT$	$L = \frac{gT^2}{2\pi} \tanh \left( \frac{2\pi d}{L} \right)$	$L = L_0 = \frac{gT^2}{2\pi} = C_0 T$
4. Group velocity	$C_g = C = \sqrt{gd}$	$C_g = nC = \frac{1}{2} \left[ 1 + \frac{4\pi d/L}{\sinh(4\pi d/L)} \right] \cdot C$	$C_g = \frac{1}{2} C = \frac{gT}{4\pi}$
5. Water Particle Velocity (a) Horizontal (b) Vertical	$u = \frac{H}{2} \sqrt{\frac{g}{d}} \cos \theta$ $w = \frac{HT}{T} \left( 1 + \frac{z}{d} \right) \sin \theta$	$u = \frac{HT}{2} \frac{\cosh \left[ \frac{2\pi(z+d)/L}{\cosh(2\pi d/L)} \right]}{\cosh(2\pi d/L)} \cos \theta$ $w = \frac{HT}{2} \frac{\sinh \left[ \frac{2\pi(z+d)/L}{\cosh(2\pi d/L)} \right]}{\cosh(2\pi d/L)} \sin \theta$	$u = \frac{\pi H}{T} e^{\frac{2\pi z}{L}} \cos \theta$ $w = \frac{\pi H}{T} e^{\frac{2\pi z}{L}} \sin \theta$
6. Water Particle Accelerations (a) Horizontal (b) Vertical	$a_x = \frac{H\pi}{T} \sqrt{\frac{g}{d}} \sin \theta$ $a_z = -2H \left( \frac{\pi}{T} \right)^2 \left( 1 + \frac{z}{d} \right) \cos \theta$	$a_x = \frac{g\pi H}{L} \frac{\cosh \left[ \frac{2\pi(z+d)/L}{\cosh(2\pi d/L)} \right]}{\cosh(2\pi d/L)} \sin \theta$ $a_z = -\frac{g\pi H}{L} \frac{\sinh \left[ \frac{2\pi(z+d)/L}{\cosh(2\pi d/L)} \right]}{\cosh(2\pi d/L)} \cos \theta$	$a_x = 2H \left( \frac{\pi}{T} \right)^2 e^{\frac{2\pi z}{L}} \sin \theta$ $a_z = -2H \left( \frac{\pi}{T} \right)^2 e^{\frac{2\pi z}{L}} \cos \theta$
7. Water Particle Displacements (a) Horizontal (b) Vertical	$\xi = -\frac{HT}{4\pi} \sqrt{\frac{g}{d}} \sin \theta$ $\zeta = \frac{H}{2} \left( 1 + \frac{z}{d} \right) \cos \theta$	$\xi = -\frac{H}{2} \frac{\cosh \left[ \frac{2\pi(z+d)/L}{\sinh(2\pi d/L)} \right]}{\sinh(2\pi d/L)} \sin \theta$ $\zeta = \frac{H}{2} \frac{\sinh \left[ \frac{2\pi(z+d)/L}{\sinh(2\pi d/L)} \right]}{\sinh(2\pi d/L)} \cos \theta$	$\xi = -\frac{H}{2} e^{\frac{2\pi z}{L}} \sin \theta$ $\zeta = \frac{H}{2} e^{\frac{2\pi z}{L}} \cos \theta$
8. Subsurface Pressure	$p = \rho g (\gamma - z)$	$p = \rho g \gamma \frac{\cosh \left[ \frac{2\pi(z+d)/L}{\cosh(2\pi d/L)} \right]}{\cosh(2\pi d/L)} - \rho g z$	$p = \rho g \eta e^{\frac{2\pi z}{L}} - \rho g z$

Figure 2-6. Summary of linear (Airy) wave theory---wave characteristics.



(after Le Mehaute, 1969)

Figure 2-7. Regions of validity for various wave theories.

For linear theory to predict accurately the wave characteristics, both the wave steepness  $H/gT^2$  and the Ursell parameter must be small, as shown in Figure 2-7.

### 5. Stokes' Progressive, Second-Order Wave Theory.

Wave formulas presented in the preceding sections on linear wave theory are based on the assumption that the motions are so small that the free surface can be described to the first order of approximation by equation (2-10):

$$\eta = \frac{H}{2} \cos \left( \frac{2\pi x}{L} - \frac{2\pi t}{T} \right) = \frac{H}{2} \cos \theta \quad \text{or} \quad a \cos \theta$$

More specifically, it is assumed that wave amplitude is small, and the contribution made to the solution by higher order terms is negligible. A more general expression would be

$$\begin{aligned} \eta = & a \cos(\theta) + a^2 B_2(L,d) \cos(2\theta) \\ & + a^3 B_3(L,d) \cos(3\theta) + \dots a^n B_n(L,d) \cos(n\theta) \end{aligned} \quad (2-46)$$

where  $a = H/2$ , for first and second orders, but  $a < H/2$  for orders higher than the second, and  $B^2$ ,  $B^3$ , etc. are specified functions of the wavelength  $L$  and depth  $d$ .

Linear theory considers only the first term on the right side of equation (2-46). To consider additional terms represents a higher order of approximation of the free-surface profile. The order of the approximation is determined by the highest order term of the series considered. Thus, the ordinate of the free surface to the third order is defined by the first three terms in equation (2-46).

When the use of a higher order theory is warranted, wave tables, such as those prepared by Skjelbreia (1959) and Skjelbreia and Hendrickson (1962), should be used to reduce the possibility of numerical errors made in using the equations. Although Stokes (1847, 1880) first developed equations for finite-amplitude waves, the equations presented here are those of Miche (1944).

a. Wave Celerity, Length, and Surface Profile. It can be shown that, for second-order theories, expressions for wave celerity (eq. 2-3) and wavelength (eq. 2-4) are identical to those obtained by linear theory. Therefore,

$$C = \frac{gT}{2\pi} \tanh \left( \frac{2\pi d}{L} \right)$$

and

$$L = \frac{gT^2}{2\pi} \tanh \left( \frac{2\pi d}{L} \right)$$

The above equations, corrected to the third order, are given by:

$$C = \frac{gT}{2\pi} \tanh\left(\frac{2\pi d}{L}\right) \left\{ 1 + \left(\frac{\pi H}{L}\right)^2 \left[ \frac{5 + 2 \cosh(4\pi d/L) + 2 \cosh^2(4\pi d/L)}{8 \sinh^4(2\pi d/L)} \right] \right\} \quad (2-47)$$

and

$$L = \frac{gT^2}{2\pi} \tanh\left(\frac{2\pi d}{L}\right) \left\{ 1 + \left(\frac{\pi H}{L}\right)^2 \left[ \frac{5 + 2 \cosh(4\pi d/L) + 2 \cosh^2(4\pi d/L)}{8 \sinh^4(2\pi d/L)} \right] \right\} \quad (2-48)$$

The equation of the free surface for second-order theory is

$$\begin{aligned} \eta = & \frac{H}{2} \cos\left(\frac{2\pi x}{L} - \frac{2\pi t}{T}\right) \\ & + \left(\frac{\pi H^2}{8L}\right) \frac{\cosh(2\pi d/L)}{\sinh^3(2\pi d/L)} \left[ 2 + \cosh(4\pi d/L) \right] \cos\left(\frac{4\pi x}{L} - \frac{4\pi t}{T}\right) \end{aligned} \quad (2-49)$$

For deep water, ( $d/L > 1/2$ ) equation (2-49) becomes,

$$\eta = \frac{H_0}{2} \cos\left(\frac{2\pi x}{L_0} - \frac{2\pi t}{T}\right) + \frac{\pi H_0^2}{4L_0} \cos\left(\frac{4\pi x}{L_0} - \frac{4\pi t}{T}\right) \quad (2-50)$$

**b. Water Particle Velocities and Displacements.** The periodic  $x$  and  $z$  components of the water particle velocities to the second order are given by

$$\begin{aligned} u = & \frac{HgT}{2L} \frac{\cosh[2\pi(z+d)/L]}{\cosh(2\pi d/L)} \cos\left(\frac{2\pi x}{L} - \frac{2\pi t}{T}\right) \\ & + \frac{3}{4} \left(\frac{\pi H}{L}\right)^2 C \frac{\cosh[4\pi(z+d)/L]}{\sinh^4(2\pi d/L)} \cos\left(\frac{4\pi x}{L} - \frac{4\pi t}{T}\right) \end{aligned} \quad (2-51)$$

$$\begin{aligned} w = & \frac{\pi H}{L} C \frac{\sinh[2\pi(z+d)/L]}{\sinh(2\pi d/L)} \sin\left(\frac{2\pi x}{L} - \frac{2\pi t}{T}\right) \\ & + \frac{3}{4} \left(\frac{\pi H}{L}\right)^2 C \frac{\sinh[4\pi(z+d)/L]}{\sinh^4(2\pi d/L)} \sin\left(\frac{4\pi x}{L} - \frac{4\pi t}{T}\right) \end{aligned} \quad (2-52)$$

Second-order equations for water particle displacements from their mean position for a finite-amplitude wave are

$$\xi = -\frac{HgT^2}{4\pi L} \frac{\cosh[2\pi(z+d)/L]}{\cosh(2\pi d/L)} \sin\left(\frac{2\pi x}{L} - \frac{2\pi t}{T}\right) + \frac{\pi H^2}{8L} \frac{1}{\sinh^2(2\pi d/L)} \quad (2-53)$$

$$\left\{1 - \frac{3}{2} \frac{\cosh[4\pi(z+d)/L]}{\sinh^2(2\pi d/L)}\right\} \sin\left(\frac{4\pi x}{L} - \frac{4\pi t}{T}\right) + \left(\frac{\pi H}{L}\right)^2 \frac{Ct}{2} \frac{\cosh[4\pi(z+d)/L]}{\sinh^2(2\pi d/L)}$$

and

$$\zeta = \frac{HgT^2}{4\pi L} \frac{\sinh[2\pi(z+d)/L]}{\cosh(2\pi d/L)} \cos\left(\frac{2\pi x}{L} - \frac{2\pi t}{T}\right) + \frac{3}{16} \frac{\pi H^2}{L} \frac{\sinh[4\pi(z+d)/L]}{\sinh^4(2\pi d/L)} \cos\left(\frac{4\pi x}{L} - \frac{4\pi t}{T}\right) \quad (2-54)$$

c. Mass Transport Velocity. The last term in equation (2-53) is of particular interest; it is not periodic, but is the product of time and a constant depending on the given wave period and depth. The term predicts a continuously increasing net particle displacement in the direction of wave propagation. The distance a particle is displaced during one wave period when divided by the wave period gives a mean drift velocity,  $\bar{U}(z)$ , called the mass transport velocity. Thus,

$$\bar{U}(z) = \left(\frac{\pi H}{L}\right)^2 \frac{C}{2} \frac{\cosh[4\pi(z+d)/L]}{\sinh^2(2\pi d/L)} \quad (2-55)$$

Equation (2-53) indicates that there is a net transport of fluid by waves in the direction of wave propagation. If the mass transport, indicated by equation (2-55) leads to an accumulation of mass in any region, the free surface must rise, thus generating a pressure gradient. A current, formed in response to this pressure gradient, will reestablish the distribution of mass. Theoretical and experimental studies of mass transport have been conducted by Mitchim (1940), Miche (1944), Ursell (1953), Longuet-Higgins (1953, 1960), and Russell and Osorio (1958). Their findings indicate that the vertical distribution of the mass transport velocity is modified so that the net transport of water across a vertical plane is zero.

d. Subsurface Pressure. The pressure at any distance below the fluid surface is given by

$$p = \rho g \frac{H}{2} \frac{\cosh[2\pi(z+d)/L]}{\cosh(2\pi d/L)} \cos\left(\frac{2\pi x}{L} - \frac{2\pi t}{T}\right) - \rho g z + \frac{3}{8} \rho g \frac{\pi H^2}{L} \frac{\tanh(2\pi d/L)}{\sinh^2(2\pi d/L)} \left\{ \frac{\cosh[4\pi(z+d)/L]}{\sinh^2(2\pi d/L)} - \frac{1}{3} \right\} \cos\left(\frac{4\pi x}{L} - \frac{4\pi t}{T}\right) - \frac{1}{8} \rho g \frac{\pi H^2}{L} \frac{\tanh(2\pi d/L)}{\sinh^2(2\pi d/L)} \left\{ \cosh \frac{4\pi(z+d)}{L} - 1 \right\} \quad (2-56)$$

e. Maximum Steepness of Progressive Waves. A progressive gravity wave is physically limited in height by depth and wavelength. The upper limit or breaking wave height in deep water is a function of the wavelength and, in shallow and transitional water, is a function of both depth and wavelength.

Stokes (1880) predicted theoretically that a wave would remain stable only if the water particle velocity at the crest was less than the wave celerity or phase velocity. If the wave height were to become so large that the water particle velocity at the crest exceeded the wave celerity, the wave would become unstable and break. Stokes found that a wave having a crest angle less than  $120^\circ$  would break (angle between two lines tangent to the surface profile at the wave crest). The possibility of the existence of a wave having a crest angle equal to  $120^\circ$  was shown by Wilton (1914). Michell (1893) found that in deep water the theoretical limit for wave steepness was

$$\left(\frac{H_o}{L_o}\right)_{max} = 0.142 \approx \frac{1}{7} \quad (2-57)$$

Havelock (1918) confirmed Michell's findings.

Miche (1944) gives the limiting steepness for waves traveling in depths less than  $L_o/2$  without a change in form as

$$\left(\frac{H}{L}\right)_{max} = \left(\frac{H_o}{L_o}\right)_{max} \tanh\left(\frac{2\pi d}{L}\right) = 0.142 \tanh\left(\frac{2\pi d}{L}\right) \quad (2-58)$$

Laboratory measurements by Danel (1952) indicate that the above equation is in close agreement with an envelope curve to laboratory observations. Additional discussion of breaking waves in deep and shoaling water is presented in Section VI.

f. Comparison of the First- and Second-Order Theories. A comparison of first- and second-order theories is useful to obtain insight about the choice of a theory for a particular problem. It should be kept in mind that linear (or first-order) theory applies to a wave that is symmetrical about the SWL and has water particles that move in closed orbits. On the other hand, Stokes' second-order theory predicts a waveform that is unsymmetrical about the SWL but still symmetrical about a vertical line through the crest and has water particle orbits that are open.

\* \* \* \* \* EXAMPLE PROBLEM 7 \* \* \* \* \*

GIVEN: A wave traveling in water depth  $d = 6$  meters (19.7 feet), with a wavelength  $L = 60$  meters (196.9 feet) and a height  $H = 1$  meter (3.28 feet).

FIND:

- (a) Compare the wave profiles given by the first- and second-order theories.
- (b) What is the difference between the first- and second-order horizontal velocities at the surface under both the crest and trough?

- (c) How far in the direction of wave propagation will a water particle move from its initial position during one wave period when  $z = 0$ ?
- (d) What is the pressure at the bottom under the wave crest as predicted by both the first- and second-order theories?
- (e) What is the wave energy per unit width of crest predicted by the first-order theory?

SOLUTION:

(a) The first-order profile equation (2-10) is

$$\eta = \frac{H}{2} \cos \theta$$

where

$$\theta = \left( \frac{2\pi x}{L} - \frac{2\pi t}{T} \right)$$

and the second-order profile equation (2-49) is

$$\eta = \frac{H}{2} \cos \theta + \frac{\pi H^2}{8L} \frac{\cosh(2\pi d/L)}{\sinh^3(2\pi d/L)} \left[ 2 + \cosh \left( \frac{4\pi d}{L} \right) \right] \cos 2\theta$$

for

$$\frac{d}{L} = \frac{6}{60} = 0.1$$

and from Table C-2

$$\cosh \left( \frac{2\pi d}{L} \right) = 1.2040$$

$$\sinh \left( \frac{2\pi d}{L} \right) = 0.6705$$

$$\cosh \left( \frac{4\pi d}{L} \right) = 1.8991$$

$$\frac{\pi H^2}{8L} \frac{\cosh(2\pi d/L)}{\sinh^3(2\pi d/L)} \left[ 2 + \cosh \left( \frac{4\pi d}{L} \right) \right] = 0.102 \text{ m (0.334 ft)}$$

Therefore,

$$\eta = 0.5 \cos \theta + 0.102 \cos 2\theta$$

$$\eta_{c,2} = 0.602 \text{ m (1.975 ft)}$$

$$\eta_{t,2} = -0.398 \text{ m (1.306 ft)}$$

where  $\eta_{c,2}$  and  $\eta_{t,2}$  are the values of  $\eta$  at the crest (i.e.,  $\cos \theta = 1$ ,  $\cos 2\theta = 1$ ) and trough (i.e.,  $\cos \theta = -1$ ,  $\cos 2\theta = 1$ ) according to second-order theory.

Figure 2-8 shows the surface profile  $\eta$  as a function of  $\theta$ . The second-order profile is more peaked at the crest and flatter at the trough than the first-order profile. The height of the crest above SWL is greater than one-half the wave height; consequently the distance below the SWL of the trough is less than one-half the height. Moreover, for linear theory, the elevation of the water surface above the SWL is equal to the elevation below the SWL; however, for second-order theory there is more height above SWL than below.

(b) For convenience, let

$u_{c,1}$  = value of  $u$  at crest according to first-order theory,

$u_{t,1}$  = value of  $u$  at trough according to first-order theory,

$u_{c,2}$  = value of  $u$  at a crest according to second-order theory,

$u_{t,2}$  = value of  $u$  at a trough according to second-order theory.

According to first-order theory, a crest occurs at  $z = H/2$ ,  $\cos \theta = 1$  and a trough at  $z = -H/2$ ,  $\cos \theta = -1$ . Equation (2-13) therefore implies

$$u_{c,1} = \frac{Hg}{2L} \frac{T \cosh[2\pi(z+d)/L]}{\cosh(2\pi d/L)}$$

with

$$z = \frac{H}{2}$$

and

$$u_{t,1} = -\frac{HgT}{2L} \frac{\cosh[2\pi(z+d)/L]}{\cosh(2\pi d/L)}$$

with

$$z = -\frac{H}{2}$$

According to second-order theory, a crest occurs at  $z = \eta_{c,2} = 0.602$  meter (2.48 feet),  $\cos \theta = \cos 2\theta = 1$  and a trough at  $z = \eta_{t,2} = -0.398$  meter (1.52 feet),  $\cos \theta = -1$ ,  $\cos 2\theta = 1$ . Equation (2-51) therefore implies

$$u_{c,2} = \frac{HgT}{2L} \frac{\cosh[2\pi(z+d)/L]}{\cosh(2\pi d/L)} + \frac{3}{4} \left( \frac{\pi H}{L} \right)^2 C \frac{\cosh[4\pi(z+d)/L]}{\sinh^4(2\pi d/L)}$$

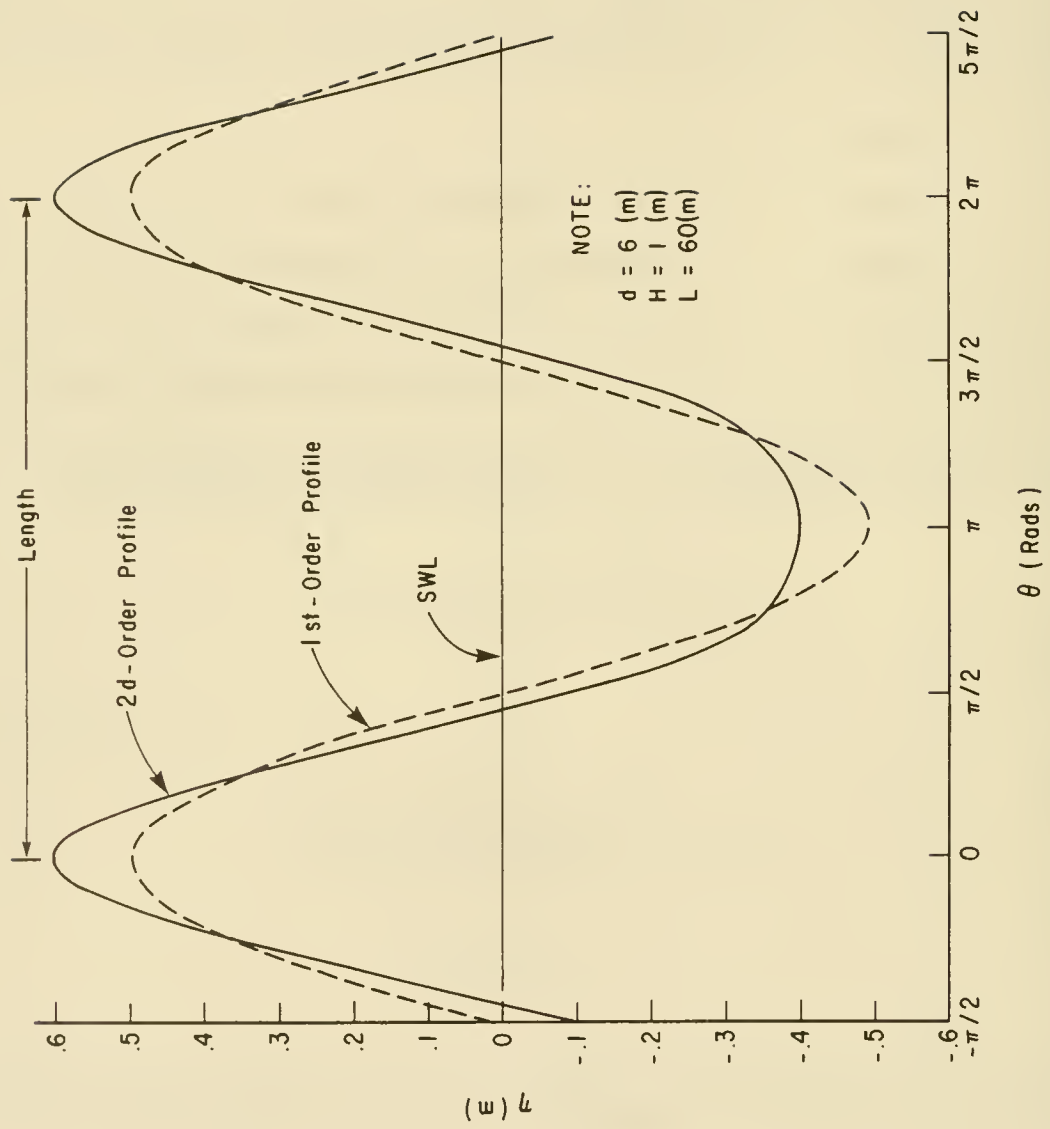


Figure 2-8. Comparison of second-order Stokes' profile with linear profile.

with

$$z = \eta_{c,2} = + 0.602 \text{ m (2.48 ft)}$$

and

$$u_{t,2} = - \frac{HgT}{2L} \frac{\cosh[2\pi(z+d)/L]}{\cosh(2\pi d/L)} \\ + \frac{3}{4} \left( \frac{\pi H}{L} \right)^2 C \frac{\cosh[4\pi(z+d)/L]}{\sinh^4(2\pi d/L)}$$

with

$$z = \eta_{t,2} = - 0.398 \text{ m (1.52 ft)}$$

Entering Table C-2 with  $d/L = 0.10$ , find  $\tanh(2\pi d/L) = 0.5569$ .

From equation (2-3) which is true for both first- and second-order theories,

$$C^2 = \frac{gL}{2\pi} \tanh\left(\frac{2\pi d}{L}\right) = \frac{(9.8)(60)(0.5569)}{2\pi} = 52.12 \text{ m/s}^2 \text{ (571 ft/s}^2\text{)}$$

or

$$C = 7.22 \text{ m/s (23.68 ft/s)}$$

As a consequence,

$$\frac{T}{L} = \frac{1}{C} = 0.1385 \text{ s/m (0.0422 s/ft)}$$

Referring again to Table C-2, it is found that when

$$z = \frac{H}{2}$$

$$\cosh\left[\frac{2\pi(z+d)}{L}\right] = \cosh[2\pi(0.108)] = 1.241$$

and when

$$z = -\frac{H}{2}$$

$$\cosh\left[\frac{2\pi(z+d)}{L}\right] = \cosh[2\pi(0.092)] = 1.171$$

Thus, the value of  $u$  at a crest and trough, respectively, according to first-order theory is

$$u_{c,1} = \frac{1}{2} (9.8)(0.1385) \frac{1.241}{1.2040} = 0.700 \text{ m/s (2.29 ft/s)}$$

$$u_{t,1} = -\frac{1}{2} (9.8)(0.1385) \frac{1.171}{1.2040} = -0.660 \text{ m/s (2.17 ft/s)}$$

Entering Table C-2 again, it is found that when

$$z = \eta_{c,2} = 0.602 \text{ m (2.48 ft)}$$

$$\cosh \left[ \frac{2\pi(z+d)}{L} \right] = \cosh[2\pi(0.1100)] = 1.249$$

$$\cosh \left[ \frac{4\pi(z+d)}{L} \right] = \cosh[4\pi(0.1100)] = 2.118$$

When

$$z = \eta_{t,2} = -0.398 \text{ m (1.52 ft)}$$

$$\cosh \left[ \frac{2\pi(z+d)}{L} \right] = \cosh[2\pi(0.0934)] = 1.177$$

$$\cosh \left[ \frac{4\pi(z+d)}{L} \right] = \cosh[4\pi(0.0934)] = 1.772$$

Thus, the value of  $u$  at a crest and trough according to second-order theory is

$$\begin{aligned} u_{c,2} &= \frac{1}{2} (9.8)(0.1385) \frac{1.249}{1.2040} + \frac{3}{4} \left( \frac{1\pi}{60} \right)^2 (7.22) \frac{2.118}{0.202} \\ &= 0.718 \text{ m/s (2.36 ft/s)} \end{aligned}$$

$$\begin{aligned} u_{t,2} &= -\frac{1}{2} (9.8)(0.1385) \frac{1.177}{1.2040} + \frac{3}{4} \left( \frac{1\pi}{60} \right)^2 (7.22) \frac{1.772}{0.202} \\ &= -0.553 \text{ m/s (1.75 ft/s)} \end{aligned}$$

(c) To find the horizontal distance that a particle moves during one wave period at  $z = 0$ , equation (2-55) can be written as

$$\bar{U}(z) = \frac{\Delta X(z)}{T} = \left( \frac{\pi H}{L} \right)^2 \frac{C}{2} \frac{\cosh[4\pi(z+d)/L]}{\sinh^2(2\pi d/L)}$$

where  $\Delta X(z)$  is the net horizontal distance traveled by a water particle,  $z$  feet below the surface, during one wave period.

For the example problem when

$$z = 0$$

$$\begin{aligned} \Delta X(0) &= T \left( \frac{\pi H}{L} \right)^2 \frac{\cosh(4\pi d/L)}{\sinh^2(2\pi d/L)} \frac{C}{2} \\ &= \frac{(\pi H)^2}{2L} \frac{\cosh(4\pi d/L)}{\sinh^2(2\pi d/L)} = \frac{(\pi 1)^2 (1.899)}{2(60)(0.6705)^2} = 0.347 \text{ m (1.14 ft)} \end{aligned}$$

(d) The first-order approximation for pressure under a wave is

$$p = \frac{\rho g H}{2} \frac{\cosh[2\pi(z+d)/L]}{\cosh(2\pi d/L)} \cos \theta - \rho g z$$

when

$$\theta = 0 \text{ (i.e., the wave crest), } \cos \theta = 1$$

and when

$$z = -d, \cosh \left[ \frac{2\pi(z+d)}{L} \right] = \cosh(0) = 1.0$$

Therefore,

$$\begin{aligned} p &= \frac{(1025)(9.8)(1)}{2} \frac{1}{1.204} - (1025) 9.8(-6) \\ &= 4171 + 60,270 = 64,441 \text{ N/m}^2 \text{ (1,345 lbs/ft}^2\text{)} \end{aligned}$$

at a depth of 6 meters (20 feet) below the SWL. The second-order terms according to equation (2-56) are

$$\begin{aligned} &\frac{3}{8} \rho g \frac{\pi H^2}{L} \frac{\tanh(2\pi d/L)}{\sinh^2(2\pi d/L)} \left\{ \frac{\cosh[4\pi(z+d)/L]}{\sinh^2(2\pi d/L)} - \frac{1}{3} \right\} \cos 2\theta \\ &- \frac{1}{8} \rho g \frac{\pi H^2}{L} \frac{\tanh(2\pi d/L)}{\sinh^2(2\pi d/L)} \left\{ \cosh \frac{4\pi(z+d)}{L} - 1 \right\} \end{aligned}$$

Substituting in the equation:

$$\begin{aligned} &\frac{3}{8} (1025)(9.8) \frac{\pi(1)^2}{60} \frac{(0.5569)}{(0.6705)^2} \left[ \frac{1}{(0.6705)^2} - \frac{1}{3} \right] (1) \\ &- \frac{1}{8} (1025)(9.8) \frac{\pi(1)^2}{60} \frac{(0.5569)}{(0.6705)^2} (0) = 462 \text{ N/m}^2 \text{ (10 lbs/ft}^2\text{)} \end{aligned}$$

Thus, second-order theory predicts a pressure,

$$p = 64,441 + 462 = 64,903 \text{ N/m}^2 \text{ (1,356 lbs/ft}^2\text{)}$$

(e) Evaluation of the hydrostatic pressure component (60,270 newtons per square meter) (1,288 pounds per square foot) indicates that Airy theory gives a dynamic component of 4171 newtons per square meter (107 pounds per square foot) while Stokes theory gives 4633 newtons per square meter (121 pounds per square foot). Stokes theory shows a dynamic pressure component about 11 percent greater than Airy theory. Using equation (2-38), the energy in one wavelength per unit width of crest given by the first-order theory is

$$E = \frac{\rho g H^2 L}{8} = \frac{(1025)(9.8)(1)^2(60)}{8} = 75,338 \text{ N/m (16,940 ft-lbs/ft)}$$

\*\*\*\*\*

### 6. Cnoidal Waves.

Long, finite-amplitude waves of permanent form propagating in shallow water are frequently best described by *cnoidal* wave theory. The existence in shallow water of such long waves of permanent form may have first been recognized by Boussinesq (1877). However, the theory was originally developed by Korteweg and DeVries (1895). The term *cnoidal* is used since the wave profile is given by the Jacobian elliptical cosine function usually designated *cn*.

In recent years, cnoidal waves have been studied by many investigators. Wiegel (1960) summarized much of the existing work on cnoidal waves and presented the principal results of Korteweg and DeVries (1895) and Keulegan and Patterson (1940) in a more usable form. Masch and Wiegel (1961) presented such wave characteristics as length, celerity and period in tabular and graphical form to facilitate application of cnoidal theory.

The approximate range of validity for the cnoidal wave theory as determined by Laitone (1963) and others is  $d/L < 1/8$ ; and the Ursell or Stokes parameter, is  $L^2 H/d^3 > 26$  (see Fig. 2-7). As wavelength becomes long and approaches infinity, cnoidal wave theory reduces to the solitary wave theory which is described in the next section. Also, as the ratio of wave height to water depth becomes small (infinitesimal wave height), the wave profile approaches the sinusoidal profile predicted by the linear theory.

Description of local particle velocities, local particle accelerations, wave energy, and wave power for cnoidal waves is difficult; hence their description is not included here, but can be obtained in graphical form from Wiegel (1960, 1964) and Masch (1964).

Wave characteristics are described in parametric form in terms of the modulus *k* of the elliptic integrals. While *k* itself has no physical significance, it is used to express the relationships between the various wave

parameters. Tabular presentations of the elliptic integrals and other important functions can be obtained from the above references. The ordinate of the water surface  $y_s$  measured above the bottom is given by

$$y_s = y_t + H \operatorname{cn}^2 \left[ 2K(k) \left( \frac{x}{L} - \frac{t}{T} \right), k \right] \quad (2-59a)$$

where

$y_t$  = distance from the bottom to the wave trough

$\operatorname{cn}$  = elliptic cosine function

$K(k)$  = complete elliptic integral of the first kind

$k$  = modulus of the elliptic integrals

The argument of  $\operatorname{cn}^2$  is frequently denoted simply by  $( )$ ; thus, equation (2-59a) above can be written as

$$y_s = y_t + H \operatorname{cn}^2 ( ) \quad (2-59b)$$

The elliptic cosine is a periodic function where  $\operatorname{cn}^2 [2K(k) ((x/L) - (t/T))]$  has a maximum amplitude equal to unity. The modulus  $k$  is defined over the range between 0 and 1. When  $k = 0$ , the wave profile becomes a sinusoid, as in the linear theory; when  $k = 1$ , the wave profile becomes that of a solitary wave.

The distance from the bottom to the wave trough  $y_t$ , as used in equations (2-59a) and (2-59b), is given by

$$\frac{y_t}{d} = \frac{y_c}{d} - \frac{H}{d} = \frac{16d^2}{3L^2} K(k) [K(k) - E(k)] + 1 - \frac{H}{d} \quad (2-60)$$

where  $y_c$  is the distance from the bottom to the crest, and  $E(k)$  the complete elliptic integral of the second kind. Wavelength is given by

$$L = \sqrt{\frac{16d^3}{3H}} kK(k) \quad (2-61)$$

and wave period by

$$T \sqrt{\frac{g}{d}} = \sqrt{\frac{16y_t}{3H} \frac{d}{y_t} \left[ \frac{kK(k)}{1 + \frac{H}{y_t} k^2 \left( \frac{1}{2} - \frac{E(k)}{K(k)} \right)} \right]} \quad (2-62)$$

Cnoidal waves are periodic and of permanent form; thus  $L = CT$ .

Pressure under a cnoidal wave at any elevation  $y$  above the bottom depends on the local fluid velocity, and is therefore complex. However, it may be approximated in a hydrostatic form as

$$p = \rho g(y_s - y) \quad (2-63)$$

i.e., the pressure distribution may be assumed to vary linearly from  $\rho g y_s$  at the bed to zero at the surface.

Figures 2-9 and 2-10 show the dimensionless cnoidal wave surface profiles for various values of the square of the modulus of the elliptic integrals  $k^2$ , while Figures 2-11 to 2-15 present dimensionless plots of the parameters which characterize cnoidal waves. The ordinates of Figures 2-11 and 2-12 should be read with care, since values of  $k^2$  are extremely close to 1.0 ( $k^2 = 1 - 10^{-1} = 1 - 0.1 = 0.90$ ). It is the exponent  $\alpha$  of  $k^2 = 1 - 10^{-\alpha}$  that varies along the vertical axis of Figures 2-11 and 2-12.

Ideally, shoaling computations might best be performed using cnoidal wave theory since this theory best describes wave motion in relatively shallow (or shoaling) water. Simple, completely satisfactory procedures for applying cnoidal wave theory are not available. Although linear wave theory is often used, cnoidal theory may be applied by using figures such as 2-9 to 2-15.

The following problem illustrates the use of these figures.

\* \* \* \* \* EXAMPLE PROBLEM 8 \* \* \* \* \*

GIVEN: A wave traveling in water depth  $d = 3$  meters (9.84 ft), with a period  $T = 15$  seconds, and a height  $H = 1.0$  meter (3.3 ft).

FIND:

- (a) Using cnoidal wave theory, find the wavelength  $L$  and compare this length with the length determined using Airy theory.
- (b) Determine the celerity  $C$ . Compare this celerity with the celerity determined using Airy theory.
- (c) Determine the distance above the bottom of the wave crest  $y_c$  and wave trough  $y_t$ .
- (d) Determine the wave profile.

SOLUTION:

- (a) Calculate

$$\frac{H}{d} = \frac{1}{3} = 0.33$$

and

$$T \sqrt{\frac{g}{d}} = 15 \sqrt{\frac{9.8}{3}} = 27.11$$

From Figure 2-11, entering  $H/d$  and  $T \sqrt{g/d}$ , determine the square of the modulus of the complete elliptical integrals  $k^2$ .

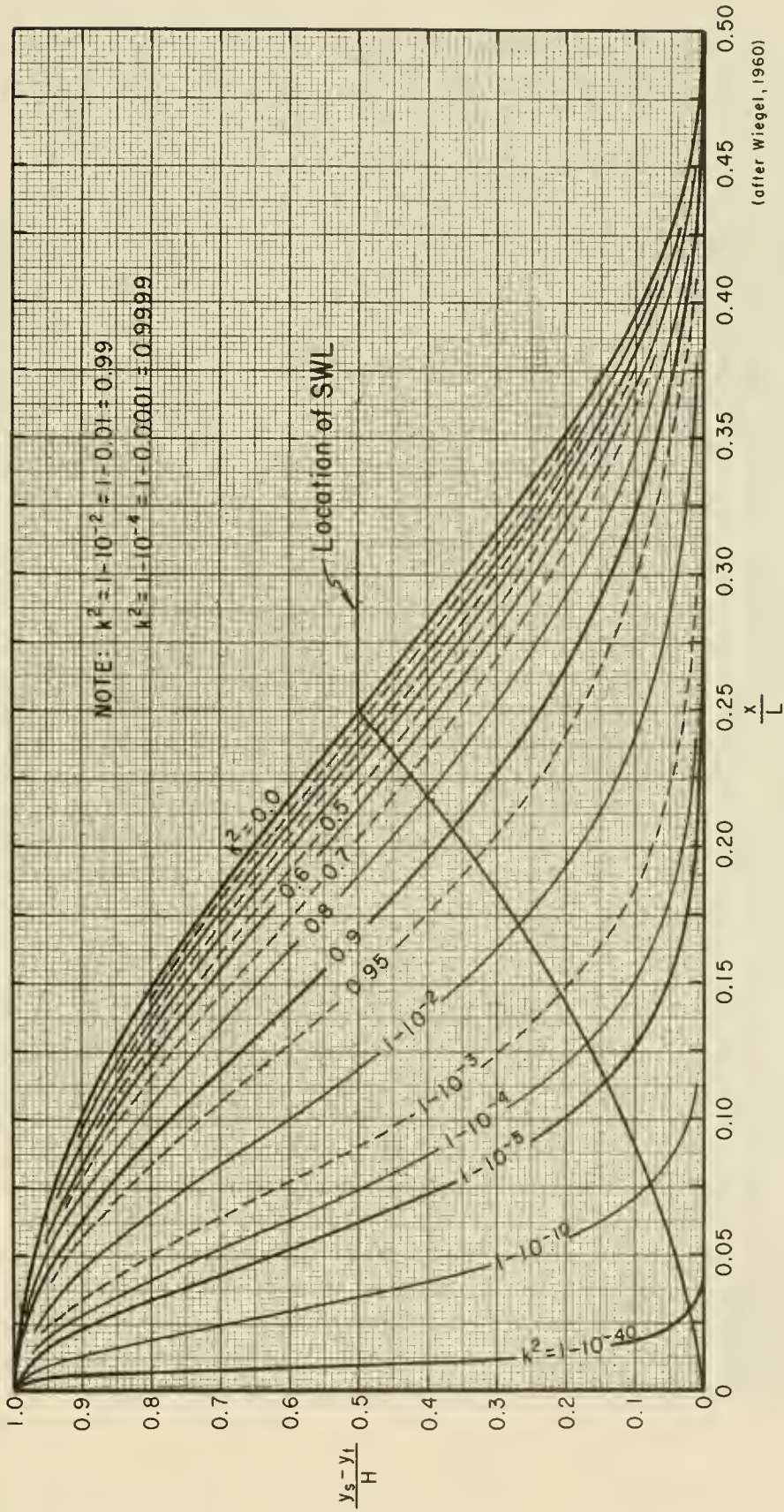


Figure 2-9. Cnoidal wave surface profiles as a function of  $k^2$ .

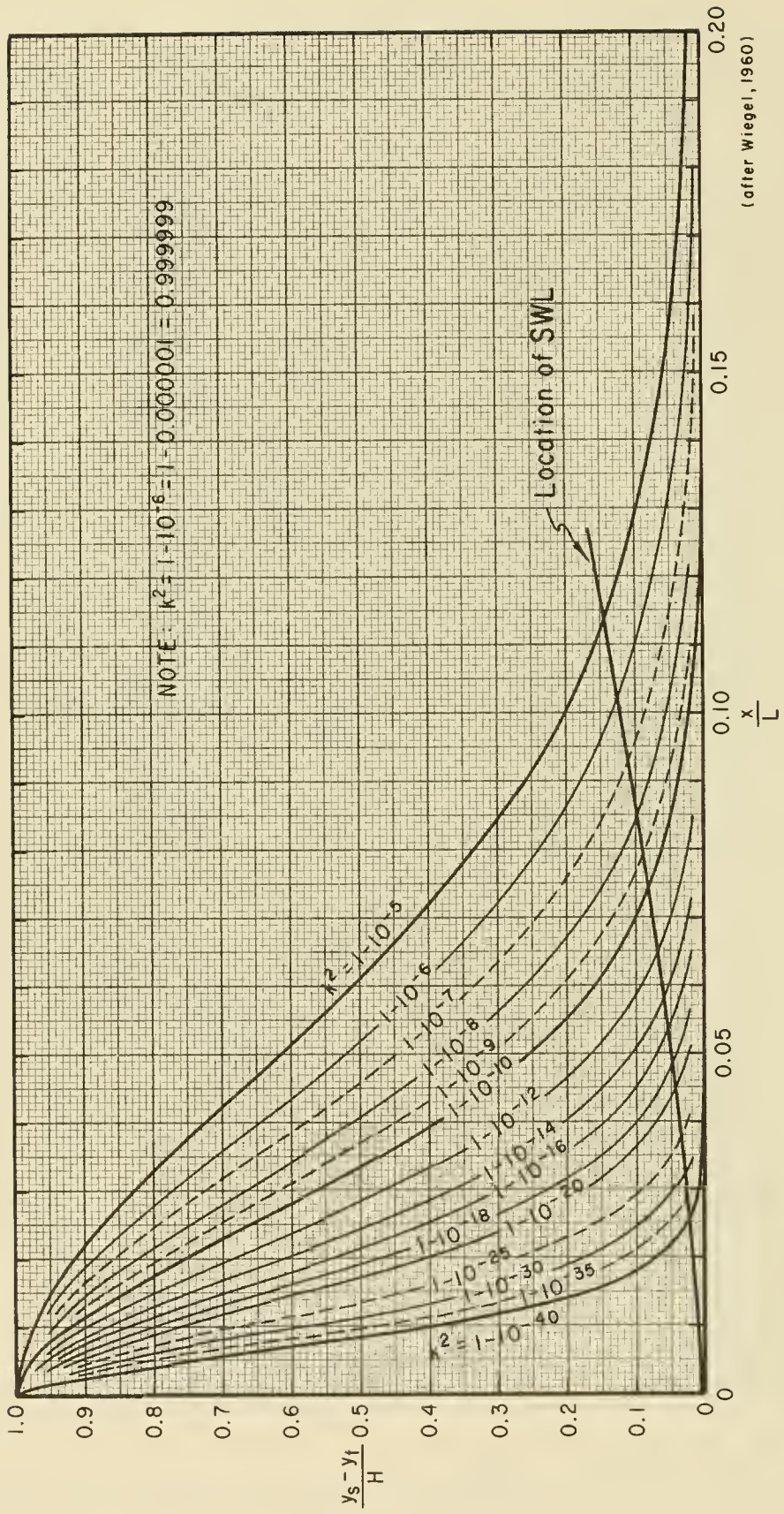


Figure 2-10. Cnoidal wave surface profiles as a function of  $k^2$ .

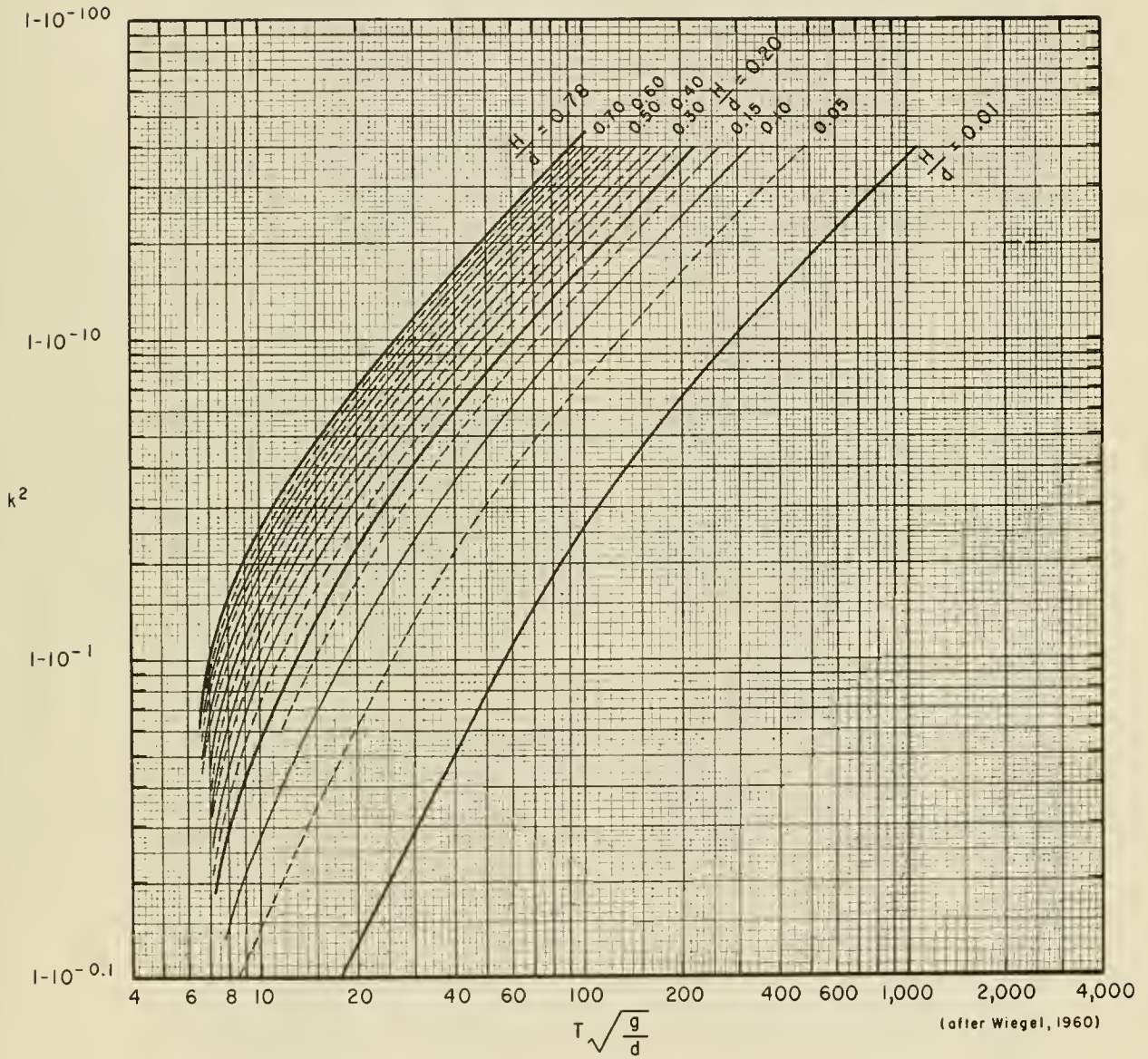
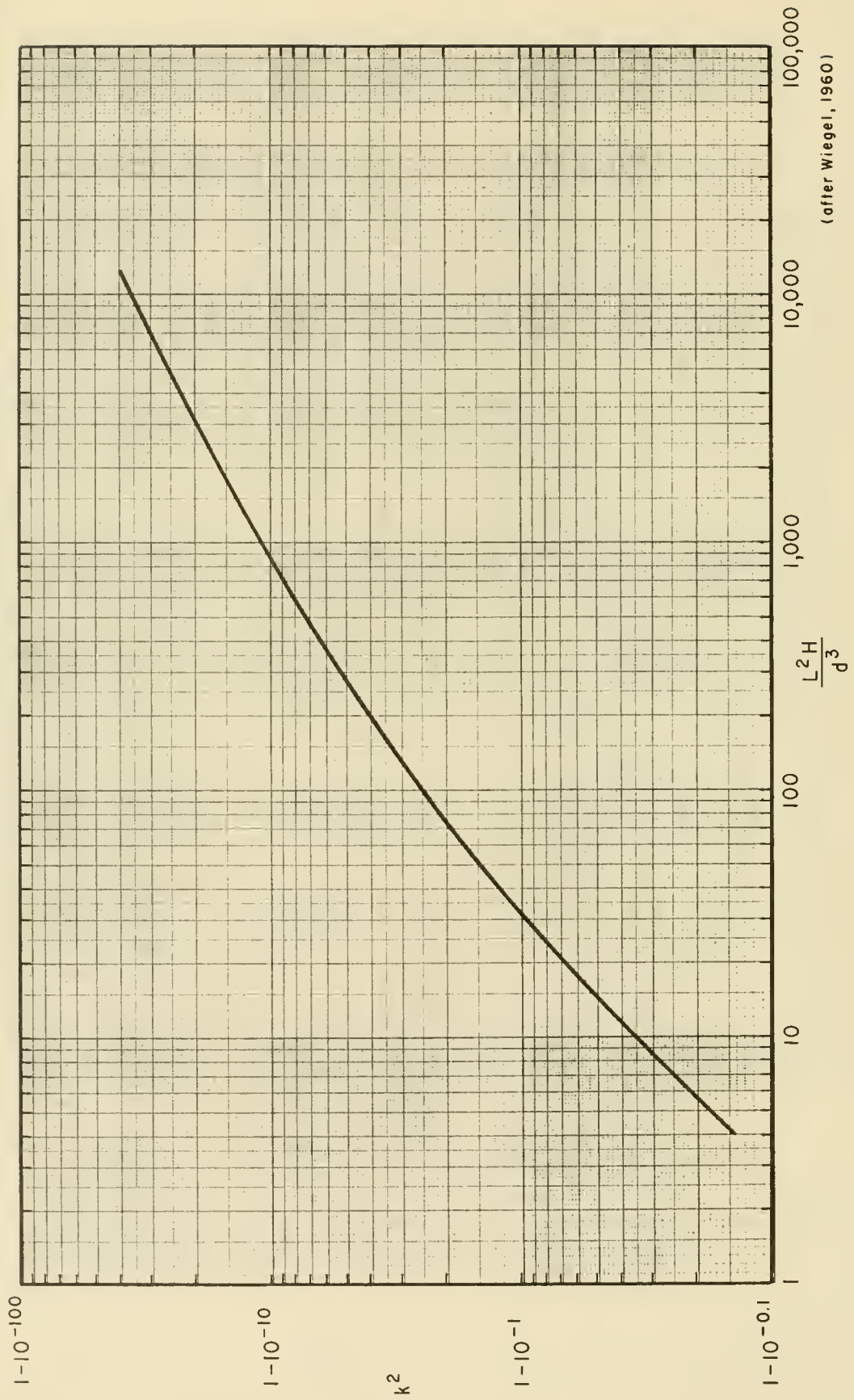


Figure 2-11. Relationship between  $k^2$ ,  $H/d$ , and  $T\sqrt{g/d}$ .



(after Wiegel, 1960)

Figure 2-12. Relationships between  $k^2$  and  $L^2H/d^3$ .

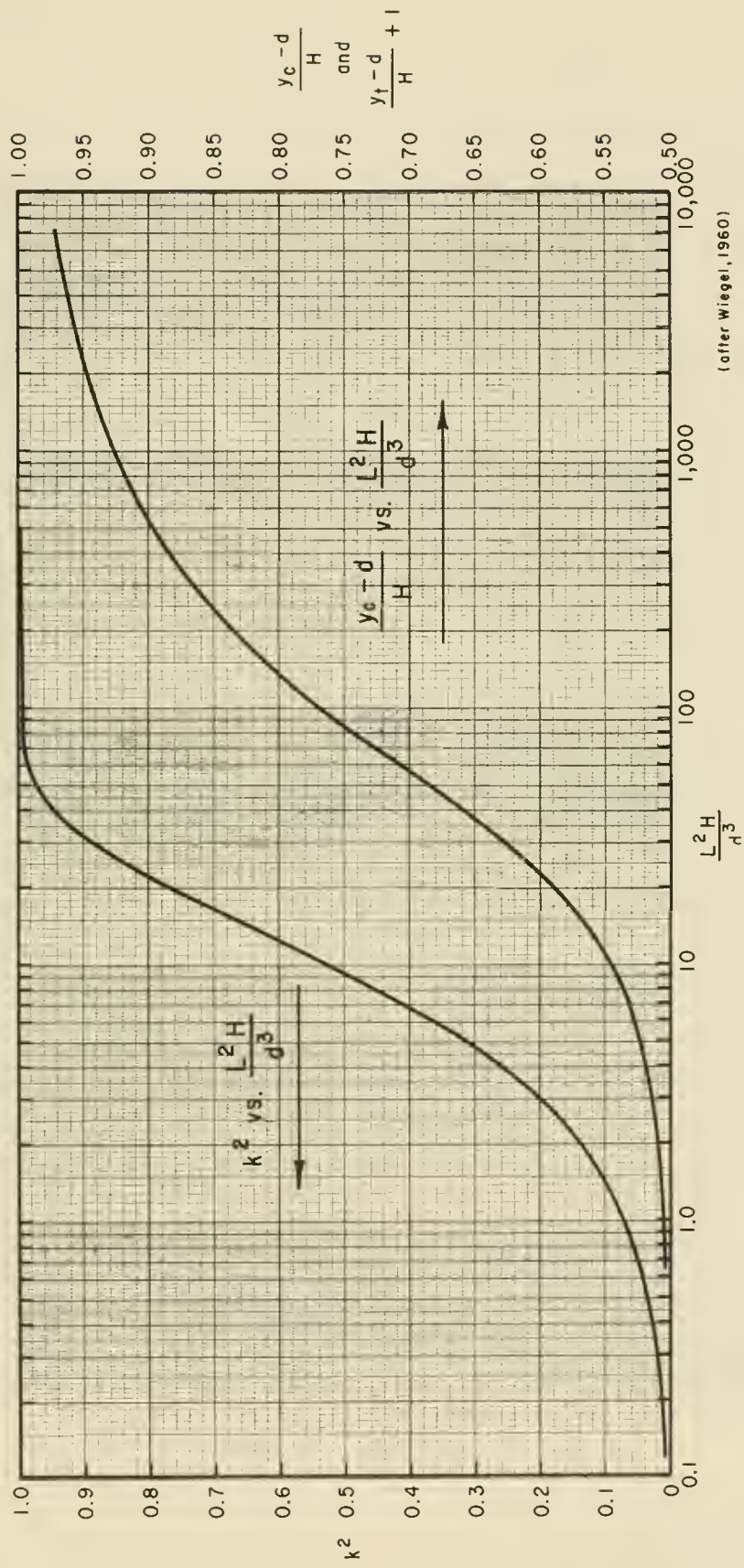


Figure 2-13. Relationships between  $k^2$  and  $L^2H/d^3$  and between  $(y_c-d)/H$ ,  $(y_t-d)/H + 1$  and  $L^2H/d^3$ .

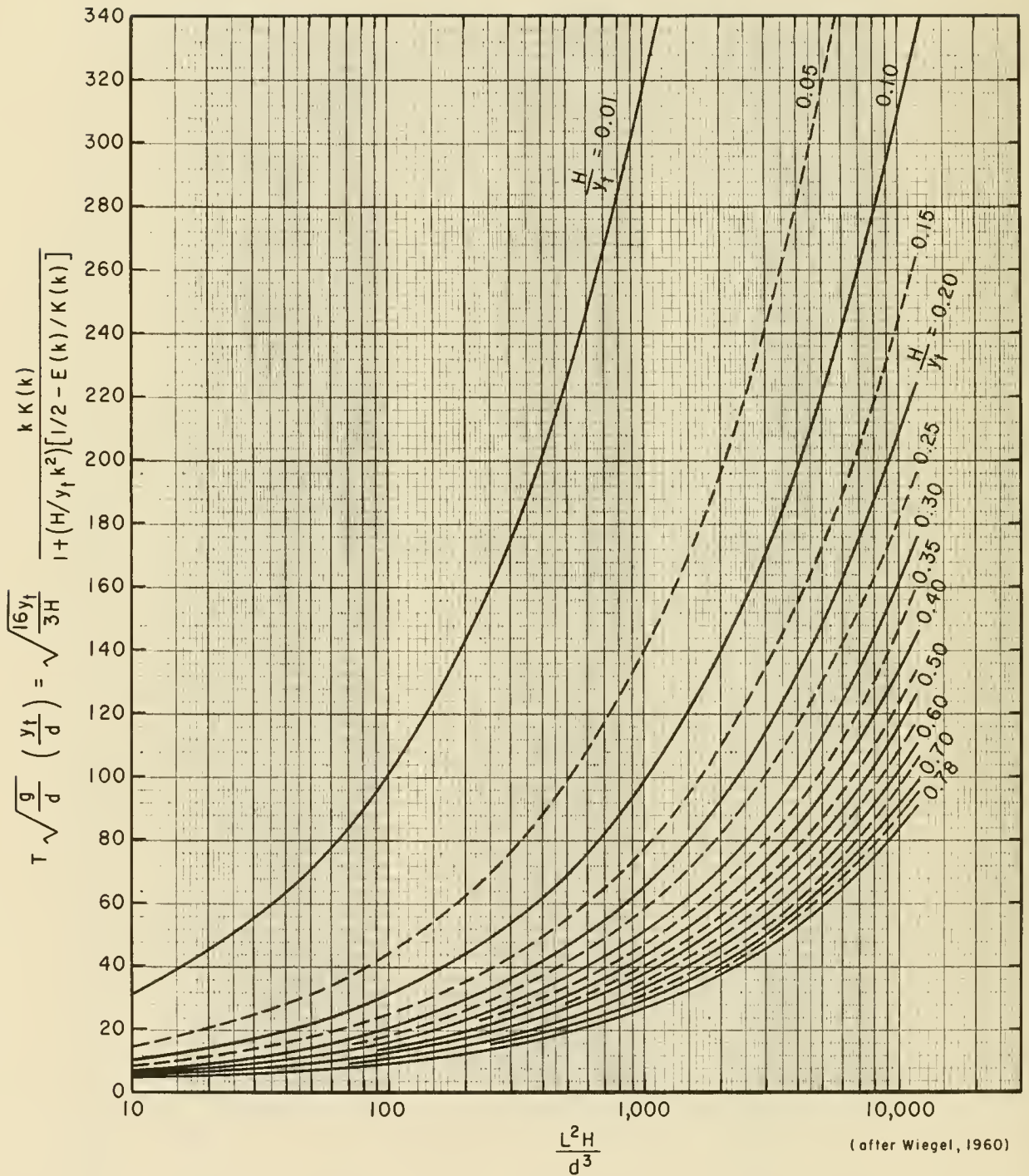


Figure 2-14. Relationship between  $T \sqrt{g/d} y_t/d$ ,  $H/y_t$ , and  $L^2H/d^3$ .

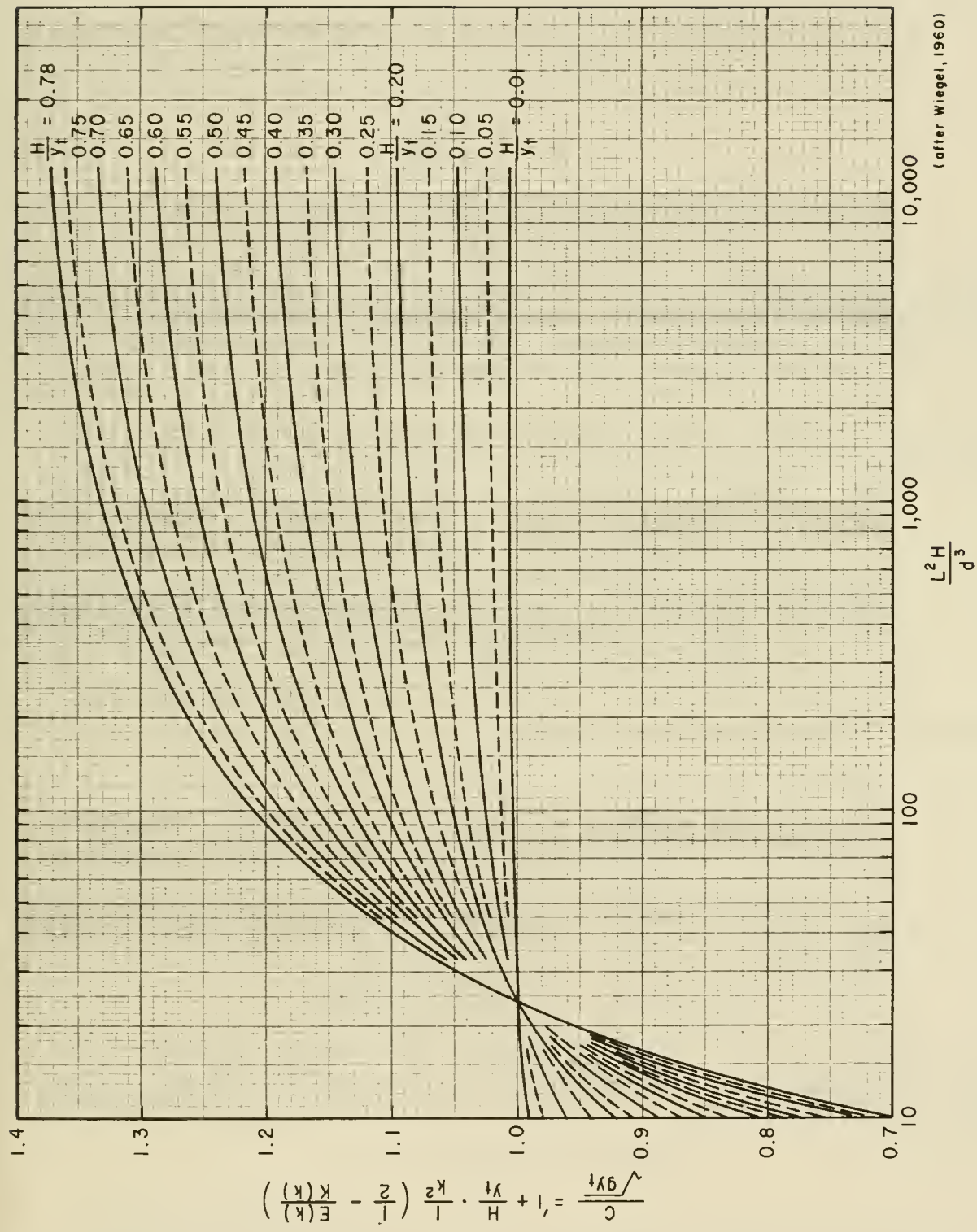


Figure 2-15. Relationship between  $C/\sqrt{gy_t}$ ,  $H/y_t$ , and  $L^2H/d^3$ .

$$k^2 = 1 - 10^{-5.10}$$

Entering Figure 2-12 with the value of  $k^2$  gives

$$\frac{L^2 H}{d^3} = 290$$

or

$$L = \sqrt{\frac{290 d^3}{H}} = \sqrt{\frac{290(3)^3}{1}}$$

$$L = 88.5 \text{ m (290.3 ft)}$$

From Airy theory,

$$L = \frac{gT^2}{2\pi} \tanh\left(\frac{2\pi d}{L}\right) = 80.6 \text{ m (264.5 ft)}$$

To check whether the wave conditions are in the range for which cnoidal wave theory is valid, calculate  $d/L$  and the Ursell or Stokes parameter  $L^2 H/d^3$ .

$$\frac{d}{L} = \frac{3}{88.5} = 0.0339 < \frac{1}{8} \text{ O.K.}$$

$$\frac{L^2 H}{d^3} = \frac{1}{(d/L)^2} \left(\frac{H}{d}\right) = 290 > 26 \text{ O.K.}$$

Therefore, cnoidal theory is applicable.

(b) Wave celerity is given by

$$C = \frac{L}{T} = \frac{88.5}{15} = 5.90 \text{ m/s (19.36 ft/s)}$$

while the Airy theory predicts

$$C = \frac{L}{T} = \frac{80.6}{15} = 5.37 \text{ m/s (17.63 ft/s)}$$

Thus if it is assumed that the wave period is the same for cnoidal and Airy theories then

$$\frac{C_{\text{cnoidal}}}{C_{\text{Airy}}} = \frac{L_{\text{cnoidal}}}{L_{\text{Airy}}} \approx 1$$

(c) The percentage of the wave height above the SWL may be determined from Figure 2-13. Entering the figure with  $L^2 H/d^3 = 290$ , the value of  $(y_c - d)/H$  is found to be 0.865 or 86.5 percent. Therefore,

$$y_c = 0.865 H + d$$

$$y_c = 0.865(1) + 3 = 0.865 + 3 = 3.865 \text{ m (12.68 ft)}$$

Also from Figure 2-13,

$$\frac{(y_t - d)}{H} + 1 = 0.865$$

thus,

$$y_t = (0.865 - 1)(1) + 3 = 2.865 \text{ m (9.40 ft)}$$

- (d) The dimensionless wave profile is given in Figure 2-9 and is approximately the one drawn for  $k^2 = 1 - 10^{-5}$ . The results obtained in (c) above can also be checked by using Figure 2-9. For the wave profile obtained with  $k^2 = 1 - 10^{-5}$ , it is seen that the SWL is approximately  $0.14 H$  above the wave trough or  $0.86 H$  below the wave crest.

The results for the wave celerity determined under (b) above can now be checked with the aid of Figure 2-15. Calculate

$$\frac{H}{y_t} = \frac{(1)}{2.865} = 0.349$$

Entering Figure 2-15 with

$$\frac{L^2 H}{d^3} = 290$$

and

$$\frac{H}{y_t} = 0.349$$

it is found that

$$\frac{C}{\sqrt{g y_t}} = 1.126$$

Therefore,

$$C = 1.126 \sqrt{(9.8)(2.865)} = 5.97 \text{ m/s (19.57 ft/s)}$$

The difference between this number and the 5.90 meters per second (18.38 ft/s) calculated under (b) above is the result of small errors in reading the curves.

\*\*\*\*\*

## 7. Solitary Wave Theory.

Waves considered in the previous sections were oscillatory or nearly oscillatory waves. The water particles move backward and forward with the

passage of each wave, and a distinct wave crest and wave trough are evident. A solitary wave is neither oscillatory nor does it exhibit a trough. In the pure sense, the solitary waveform lies entirely above the stillwater level. The solitary wave is a wave of translation relative to the water mass.

The first systematic observations and experiments on waves can probably be attributed to Russell (1838, 1844). Russell first recognized the existence of a solitary wave, and the report (Russell, 1844) of his first observation is worth noting.

"I believe I shall best introduce this phenomenon by describing the circumstances of my own first acquaintance with it. I was observing the motion of a boat which was rapidly drawn along a narrow channel by a pair of horses, when the boat suddenly stopped--not so the mass of water in the channel which it had put in motion; it accumulated round the prow of the vessel in a state of violent agitation, then suddenly leaving it behind, rolled forward with great velocity, assuming the form of a large solitary elevation, a rounded, smooth and well-defined heap of water, which continued its course along the channel apparently without change of form or diminution of speed. I followed it on horseback, and overtook it still rolling on at a rate of some eight or nine miles an hour, preserving its original figure some thirty feet long and a foot to a foot and a half in height. Its height gradually diminished, and after a chase of one or two miles I lost it in the windings of the channel. Such, in the month of August 1834, was my first chance interview with that singular and beautiful phenomenon which I have called the Wave of Translation, a name which it now very generally bears; which I have since found to be an important element in almost every case of fluid resistance, and ascertained to be the type of that great moving elevation of the sea, which, with the regularity of a planet, ascends our rivers and rolls along our shores.

"To study minutely this phenomenon with a view to determine accurately its nature and laws, I have adopted other more convenient modes of producing it than that which I have just described, and have employed various methods of observation. A description of these will probably assist me in conveying just conceptions of the nature of this wave."

The study of waves developed from this chance observation in 1834. While Russell's studies were empirical in nature, his results agree well with later theoretical results. The original theoretical developments were made by Boussinesq (1872) Rayleigh (1876), and McCowan (1891), and more recently by Keulegan and Patterson (1940), Keulegan (1948), and Iwasa (1955).

In nature it is difficult to form a truly solitary wave, because at the trailing edge of the wave there are usually small dispersive waves. However, long waves such as tsunamis and waves resulting from large displacements of water caused by such phenomena as landslides and earthquakes sometimes behave approximately like solitary waves. When an oscillatory wave moves into

shallow water, it may often be approximated by a solitary wave (Munk, 1949). As an oscillatory wave moves into shoaling water, the wave amplitude becomes progressively higher, the crests become shorter and more pointed, and the trough becomes longer and flatter.

The solitary wave is a limiting case of the cnoidal wave. When  $k^2 = 1$ ,  $K(k) = K(1) = \infty$ , and the elliptic cosine reduces to the hyperbolic secant function,  $y_t = d$ , and equation (2-59) reduces to

$$y_s = d + H \operatorname{sech}^2 \left[ \sqrt{\frac{3}{4} \frac{H}{d^3}} (x - Ct) \right]$$

or

$$\eta = H \operatorname{sech}^2 \left[ \sqrt{\frac{3}{4} \frac{H}{d^3}} (x - Ct) \right] \quad (2-64)$$

where the origin of  $x$  is at the wave crest. The volume of water within the wave above the stillwater level per unit crest width is

$$V = \left[ \frac{16}{3} d^3 H \right]^{1/2} \quad (2-65)$$

An equal amount of water per unit crest length is transported forward past a vertical plane that is perpendicular to the direction of wave advance. Several relations have been presented to determine the celerity of a solitary wave; these equations differ depending on the degree of approximation. Laboratory measurements by Daily and Stephan (1953) indicate that the simple expression

$$C = \sqrt{g(H + d)} \quad (2-66)$$

gives a reasonably accurate approximation to the celerity.

The water particle velocities for a solitary wave, as found by McCowan (1891) and given by Munk (1949), are

$$u = CN \frac{1 + \cos(My/d) \cosh(Mx/d)}{[\cos(My/d) + \cosh(Mx/d)]^2} \quad (2-67)$$

$$w = CN \frac{\sin(My/d) \sinh(Mx/d)}{[\cos(My/d) + \cosh(Mx/d)]^2} \quad (2-68)$$

where  $M$  and  $N$  are the functions of  $H/d$  shown in Figure 2-16, and  $y$  is measured from the bottom. The expression for horizontal velocity  $u$  is often used to predict wave forces on marine structures sited in shallow water. The maximum velocity  $u_{max}$  occurs when  $x$  and  $t$  are both equal to zero; hence,

$$u_{max} = \frac{CN}{1 + \cos(My/d)} \quad (2-69)$$

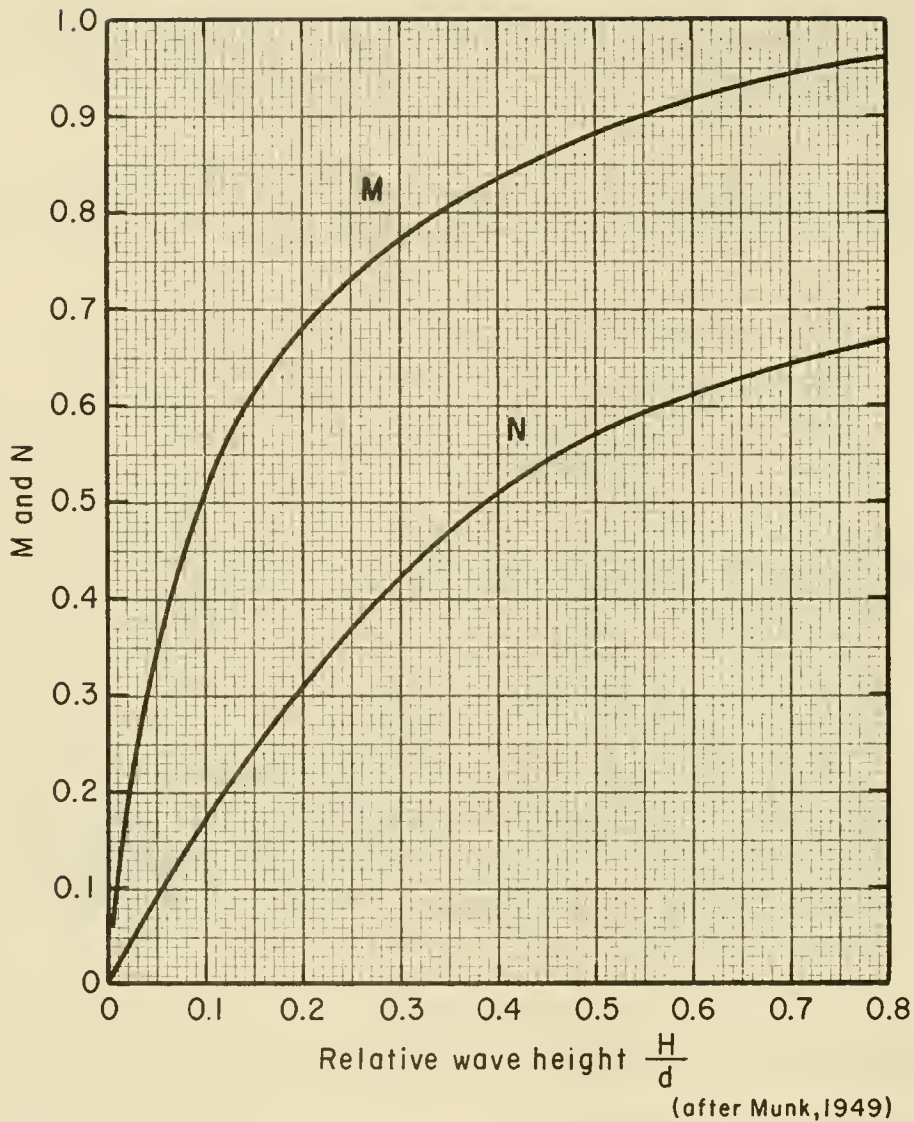


Figure 2-16. Functions M and N in solitary wave theory.

Total energy in a solitary wave is about evenly divided between kinetic and potential energy. Total wave energy per unit crest width is

$$E = \frac{8}{3\sqrt{3}} \rho g H^{3/2} d^{3/2} \quad (2-70)$$

and the pressure beneath a solitary wave depends on the local fluid velocity, as does the pressure under a cnoidal wave; however, it may be approximated by

$$p = \rho g (y_s - y) \quad (2-71)$$

Equation (2-71) is identical to that used to approximate the pressure beneath a cnoidal wave.

As a solitary wave moves into shoaling water it eventually becomes unstable and breaks. McCowan (1891) assumed that a solitary wave breaks when the

water particle velocity at the wave crest becomes equal to the wave celerity. This occurs when

$$\left(\frac{H}{d}\right)_{\max} = 0.78 \quad (2-72a)$$

Laboratory investigations have shown that the value of  $(H/d)_{\max} = 0.78$  agrees better with observations for oscillatory waves than for solitary waves. Ippen and Kulin (1954), Galvin (1969), and Camfield and Street (1969) have shown that the nearshore slope has a substantial effect on this ratio. Other factors such as bottom roughness may also be involved. Galvin tested periodic waves with periods from 1 to 6 seconds on slopes of  $m = 0.0, 0.05, 0.10,$  and  $0.20,$  and found that  $H_b/d_b$  ratios were approximately equal to 0.83, 1.05, 1.19, and 1.32, respectively. Camfield and Street tested single solitary waves on slopes from  $m = 0.01$  to  $m = 0.20$  and found an empirical relationship between the slope and the breaker height-to-water depth ratio given by

$$\frac{H_b}{d_b} = 0.75 + 25m - 112m^2 + 3870m^3 \quad (2-72b)$$

It was found that waves did not break when the slope  $m$  was greater than about 0.18. It was also noted that as the slope increased the breaking position moved closer to the shoreline. This accounts for the large values of  $H_b/d_b$  for large slopes; i.e., as  $d_b \rightarrow 0$ . In general, it must be concluded that for some conditions, equation (2-72) is unsatisfactory for predicting breaking depth. Further discussion of the breaking of waves with experimental results is in Section VI.

## 8. Stream-Function Wave Theory.

In recent years, numerical approximations to solutions of hydrodynamic equations describing wave motion have been proposed and developed by Dean (1965a, 1965b, 1967) and Monkmeyer (1970). The approach by Dean, termed a symmetric, stream-function theory, is a nonlinear wave theory that is similar to higher order Stokes' theories. Both are constructed of sums of sine or cosine functions that satisfy the original differential equation (Laplace equation). The theory, however, determines the coefficient of each higher order term so that a best fit, in the least squares sense, is obtained to the theoretically posed, dynamic, free-surface boundary condition. Assumptions made in the theory are identical to those made in the development of the higher order Stokes' solutions. Consequently, some of the same limitations are inherent in the stream-function theory; however, it represents a better solution to the equations used to approximate the wave phenomena. It is more important that the stream-function representation appears to more accurately predict the wave phenomena observed in laboratory wave studies (Dean and Le Mehaute, 1970), and may possibly describe naturally occurring wave phenomena better than other theories.

The long, tedious computations involved in evaluating the terms of the series expansions that make up the higher order stream-function solutions make it desirable to use tabular or graphical presentations of the solutions. These tables, their use, and their range of validity have been developed by Dean (1974).

### III. WAVE REFRACTION

#### 1. Introduction.

Equation (2-2) shows that wave celerity depends on the water depth in which the wave propagates. If the wave celerity decreases with depth, wavelength must also decrease proportionally. Variation in wave velocity occurs along the crest of a wave moving at an angle to underwater contours because the part of the wave in deeper water is moving faster than the part in shallower water. This variation causes the wave crest to bend toward alignment with the contours (see Fig. 2-17). This bending effect, called refraction, depends on the relation of water depth to wavelength. It is analogous to refraction for other types of waves; i.e., light and sound.

In practice, refraction is important for several reasons:

(1) Refraction, coupled with shoaling, determines the wave height in any particular water depth for a given set of incident deepwater wave conditions; i.e., wave height, period, and direction of propagation in deep water. Refraction therefore has significant influence on the wave height and distribution of wave energy along a coast.

(2) The change in wave direction of different parts of the wave results in convergence or divergence of wave energy and materially affects the forces exerted by waves on structures.

(3) Refraction contributes to the alteration of bottom topography by its effect on the erosion and deposition of beach sediments. Munk and Traylor (1947) confirmed earlier work indicating the possible interrelationships between refraction, wave energy distribution along a shore, and the erosion and deposition of beach materials.

(4) A general description of the nearshore bathymetry of an area can sometimes be obtained by analyzing aerial photography of wave refraction patterns. While the techniques for performing such analyses are not well developed, an experienced observer can obtain a general picture of simple bottom topography.

In addition to refraction caused by variations in bathymetry, waves may be refracted by currents or any other phenomenon that causes one part of a wave to travel slower or faster than another part. At a coastal inlet, refraction may be caused by a gradient in the current. Refraction by a current occurs when waves intersect the current at an angle. The extent to which the current will refract incident waves depends on the initial angle between the wave crests and the direction of current flow, the characteristics of the incident waves, and the strength of the current. In at least two situations, wave refraction by currents may be of practical importance. At tidal entrances, ebb currents run counter to incident waves and consequently increase wave height and steepness. Also, major ocean currents such as the Gulf Stream may have some effect on the height, length, and direction of the approach of waves reaching the coasts. A quantitative evaluation of the effects of refraction by currents is difficult. Additional research is needed in this area. No detailed discussion of this problem is presented here, but an introduction is presented by Johnson (1947).

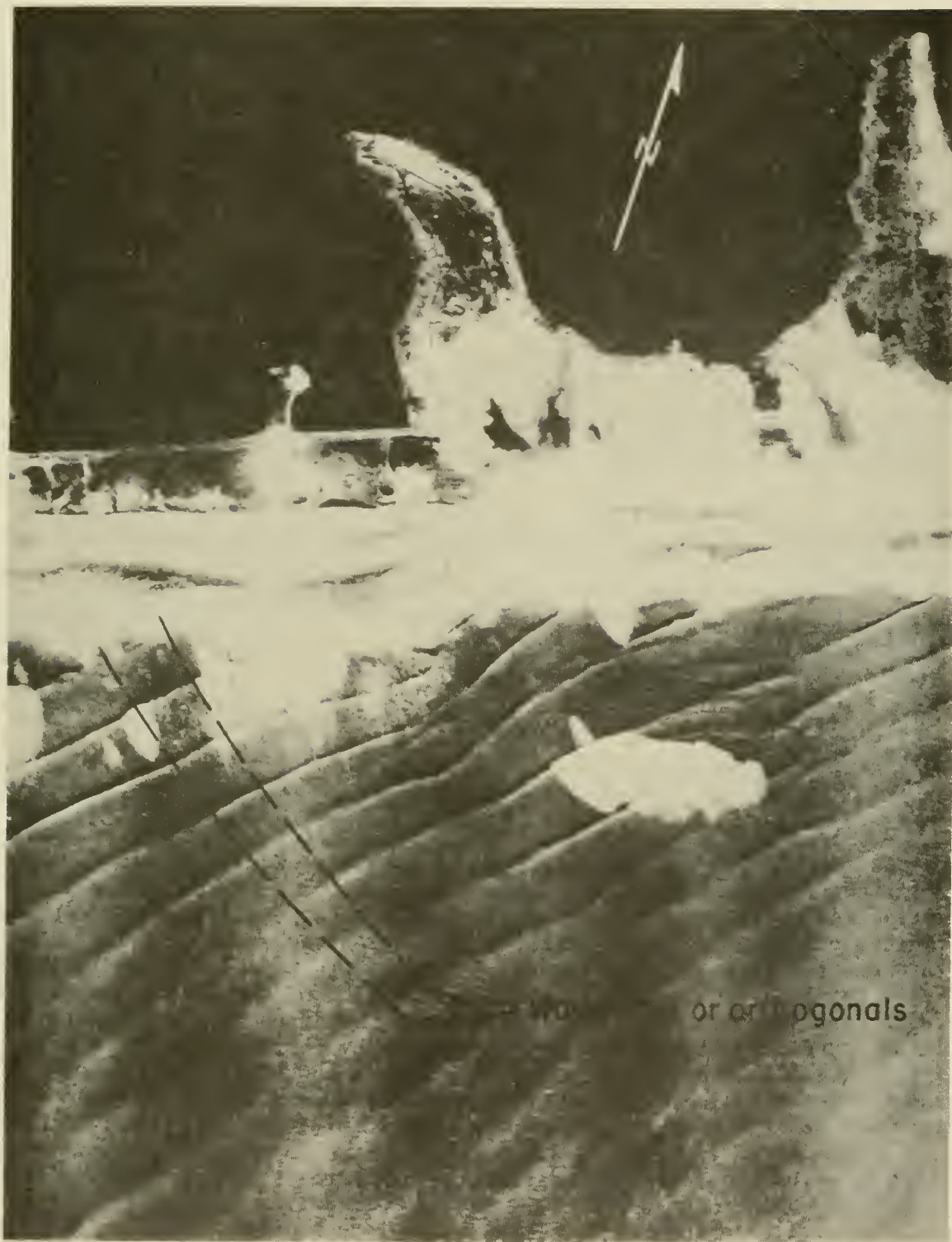


Figure 2-17. Wave refraction at Westhampton Beach, Long Island, New York.

The decrease in wave celerity with decreasing water depth can be considered similar to the decrease in the speed of light with an increase in the refractive index of the transmitting medium. Using this analogy, O'Brien (1942) suggested the use of Snell's law of geometrical optics for solving the problem of water-wave refraction by changes in depth. The validity of this approach has been verified experimentally by Chien (1954), Ralls (1956), and Wiegel and Arnold (1957). Chao (1970) showed analytically that Fermat's principle and hence Snell's law followed from the governing hydrodynamic equations, and was a valid approximation when applied to the refraction problem. Generally, two basic techniques of refraction analysis are available--graphical and numerical. Several graphical procedures are available, but fundamentally all methods of refraction analyses are based on Snell's law.

The assumptions usually made are

(1) Wave energy between wave rays or orthogonals remains constant. (Orthogonals are lines drawn perpendicular to the wave crests, and extend in the direction of wave advance.) (See Fig. 2-17.)

(2) Direction of wave advance is perpendicular to the wave crest; i.e., in the direction of the orthogonals.

(3) Speed of a wave with a given period at a particular location depends only on the depth at that location.

(4) Changes in bottom topography are gradual.

(5) Waves are long-crested, constant period, small-amplitude, and monochromatic.

(6) Effects of currents, winds, and reflections from beaches, and underwater topographic variations are considered negligible.

## 2. General--Refraction by Bathymetry.

In water deeper than one-half the wavelength, the hyperbolic tangent function in the formula

$$C^2 = \frac{gL}{2\pi} \tanh \left( \frac{2\pi d}{L} \right)$$

is nearly equal to unity, and equation (2-2) reduces to

$$C_o^2 = \frac{gL}{2\pi}$$

In this equation, the velocity  $C_o$  does not depend on depth; therefore, in those regions deeper than one-half the wavelength (deep water), refraction by bathymetry will not be significant. Where the water depth is between one-half and one-twenty-fifth the wavelength (transitional water), and in the region where the water depth is less than one-twenty-fifth, the wavelength (shallow water), refraction effects may be significant. In transitional water, wave

velocity must be computed from equation (2-2); in shallow water,  $\tanh(2\pi d/L)$  becomes nearly equal to  $2\pi d/L$  and equation (2-2) reduces to equation (2-9).

$$C^2 = gd \quad \text{or} \quad C = (gd)^{1/2}$$

Both equations (2-2) and (2-9) show the dependence of wave velocity on depth. To a first approximation, the total energy in a wave per unit crest width may be written as

$$E = \frac{\rho g H^2 L}{8}$$

It has been noted that not all the wave energy  $E$  is transmitted forward with the wave; only one-half is transmitted forward in deep water. The amount of energy transmitted forward for a given wave remains nearly constant as the wave moves from deep water to the breaker line if energy dissipation due to bottom friction ( $K_f = 1.0$ ), percolation, and reflected wave energy is negligible.

In refraction analyses, it is assumed that for a wave advancing toward shore, no energy flows laterally along a wave crest; i.e., the transmitted energy remains constant between orthogonals. In deep water the wave energy transmitted forward across a plane between two adjacent orthogonals (the average energy flux) is

$$\bar{P}_o = \frac{1}{2} b_o \bar{E}_o C_o \quad (2-73)$$

where  $b_o$  is the distance between the selected orthogonals in deep water. The subscript  $o$  always refers to deepwater conditions. This power may be equated to the energy transmitted forward between the same two orthogonals in shallow water

$$\bar{P} = nb \bar{E}C \quad (2-74)$$

where  $b$  is the spacing between the orthogonals in the shallower water. Therefore,  $(1/2) b_o \bar{E}_o C_o = nb \bar{E}C$ , or

$$\frac{\bar{E}}{\bar{E}_o} = \frac{1}{2} \left( \frac{1}{n} \right) \left( \frac{b_o}{b} \right) \left( \frac{C_o}{C} \right) \quad (2-75)$$

From equation (2-39),

$$\frac{H}{H_o} = \sqrt{\frac{\bar{E}}{\bar{E}_o}} \quad (2-76)$$

and combining equations (2-75) and (2-76),

$$\frac{H}{H_o} = \sqrt{\left( \frac{1}{2} \right) \left( \frac{1}{n} \right) \left( \frac{C_o}{C} \right)} \sqrt{\left( \frac{b_o}{b} \right)} \quad (2-77)$$

The term  $\sqrt{(1/2) (1/n) (C_0/C)}$  is known as the *shoaling coefficient*  $K_S$  or  $H/H_0$ . This shoaling coefficient is a function of wavelength and water depth.  $K_S$  and various other functions of  $d/L$ , such as  $2\pi d/L$ ,  $4\pi d/L$ ,  $\tanh(2\pi d/L)$ , and  $\sinh(4\pi d/L)$  are tabulated in Appendix C (Table C-1 for even increments of  $d/L_0$  and Table C-2 for even increments of  $d/L$ ).

Equation (2-77) enables determination of wave heights in transitional or shallow water, knowing the deepwater wave height when the relative spacing between orthogonals can be determined. The square root of this relative spacing,  $\sqrt{b_0/b}$ , is the *refraction coefficient*  $K_R$ .

Various methods may be used for constructing refraction diagrams. The earliest approaches required the drawing of successive wave crests. Later approaches permitted the immediate construction of orthogonals, and also permitted moving from the shore to deep water (Johnson, O'Brien, and Isaacs, 1948; Arthur, Munk, and Isaacs, 1952; Kaplan, 1952; and Saville and Kaplan, 1952).

The change of direction of an orthogonal as it passes over relatively simple hydrography may be approximated by

$$\sin \alpha_2 = \left( \frac{C_2}{C_1} \right) \sin \alpha_1 \quad (\text{Snell's law}) \quad (2-78a)$$

where

$\alpha_1$  = the angle a wave crest (perpendicular to an orthogonal) makes with the bottom contour over which the wave is passing

$\alpha_2$  = a similar angle measured as the wave crest (or orthogonal) passes over the next bottom contour

$C_1$  = the wave velocity (eq. 2-2) at the depth of the first contour

$C_2$  = the wave velocity at the depth of the second contour

From this equation, a template may be constructed which will show the angular change in  $\alpha$  that occurs as an orthogonal passes over a particular contour interval to construct the changed-direction orthogonal. Such a template is shown in Figure 2-18. In application to wave refraction problems, it is simplest to construct this template on a transparent material.

Refraction may be treated analytically at a straight shoreline with parallel offshore contours, by using Snell's law directly:

$$\sin \alpha = \left( \frac{C}{C_0} \right) \sin \alpha_0 \quad (2-78b)$$

where  $\alpha$  is the angle between the wave crest and the shoreline, and  $\alpha_0$  is the angle between the deepwater wave crest and the shoreline.

For example, if  $\alpha_0 = 30^\circ$  and the period and depth of the wave are such that  $C/C_0 = 0.5$ , then

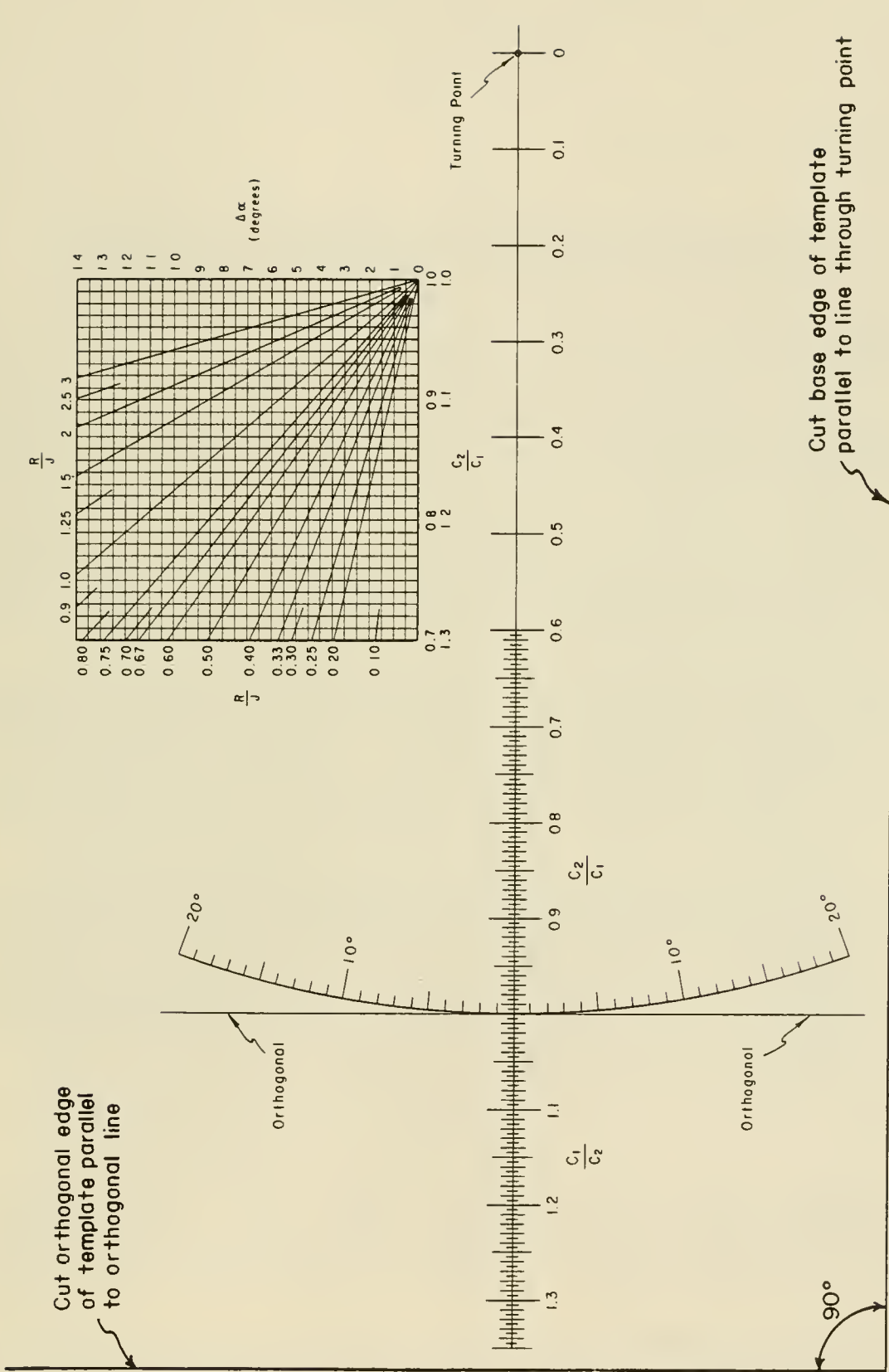


Figure 2-18. Refraction template.

$$\alpha = \sin^{-1} [0.5(0.5)] = 14.5^\circ$$

$$\cos \alpha = 0.968$$

and

$$\cos \alpha_o = 0.866$$

From the geometry of the wave rays,

$$K_R = \left( \frac{b_o}{b} \right)^{1/2} = \left( \frac{\cos \alpha_o}{\cos \alpha} \right)^{1/2} = \left( \frac{0.866}{0.968} \right)^{1/2} = 0.945$$

Figure 2-19 shows the relationships between  $\alpha$ ,  $\alpha_o$ , period, depth, and  $K_R$  in graphical form.

a. Procedures in Refraction Diagram Construction--Orthogonal Method. Charts showing the bottom topography of the study area are obtained. Two or more charts of differing scales may be required, but the procedures are identical for charts of any scale. Underwater contours are drawn on the chart, or on a tracing paper overlay, for various depth intervals. The depth intervals chosen depend on the degree of accuracy desired. If overlays are used, the shoreline should be traced for reference. In tracing contours, small irregularities must be *smoothed out*, since bottom features that are comparatively small with respect to the wavelength do not affect the wave appreciably.

The range of wave periods and directions to be investigated is determined by a hindcasting study of historical weather charts or from other historical records relating to wave period and direction. For each wave period and direction selected, a separate diagram must be prepared.  $C_1/C_2$  values for each contour interval may then be marked between contours. The method of computing  $C_1/C_2$  is shown by Table 2-2; a tabulation of  $C_1/C_2$  for various contour intervals and wave periods is given in Table C-4 of Appendix C.

To construct orthogonals from deep to shallow water, the deepwater direction of wave approach is first determined. A deepwater wave front (crest) is drawn as a straight line perpendicular to this wave direction, and suitably spaced orthogonals are drawn perpendicular to this wave front and parallel to the chosen direction of wave approach. Closely spaced orthogonals give more detailed results than widely spaced orthogonals. These lines are extended to the first depth contour shallower than  $L_o/2$  where

$$L_o = \frac{9.8}{2\pi} T^2$$

b. Procedure When  $\alpha$  Is Less Than  $80^\circ$ . Recall that  $\alpha$  is the angle a wave crest makes with the bottom contour. Starting with any one orthogonal and using the refraction template in Figure 2-18, the following steps are performed in extending the orthogonal to shore:

- (1) Sketch a contour midway between the first two contours to be crossed, extend the orthogonal to the midcontour, and construct a tangent to the midcontour at this point.

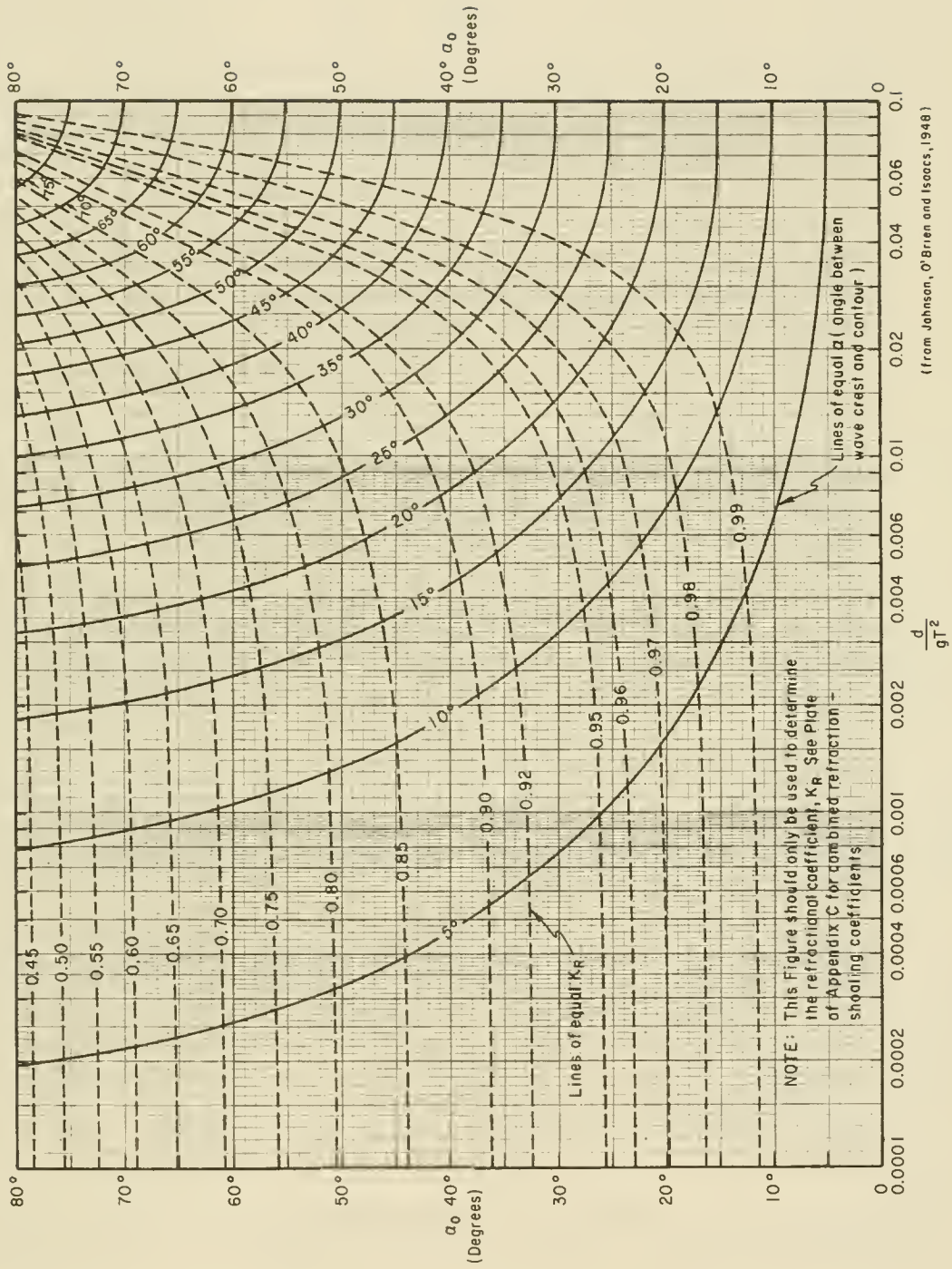


Figure 2-19. Changes in wave direction and height due to refraction on slopes with straight, parallel depth contours.

Table 2-2. Example computations of values of  $C_1/C_2$  for refraction analysis.<sup>1</sup>

T = 10 s				
1	2	3	4	5
d (m)	$\frac{d}{L_0}$	$\tanh \frac{2\pi d}{L}$	$\frac{C_1}{C_2}$	$\frac{C_2}{C_1}$
2	0.0128	0.280	1.40	0.72
4	0.0256	0.391	1.21	0.83
6	0.0384	0.472	1.14	0.88
8	0.0513	0.537		

<sup>1</sup>Column 1 gives depths corresponding to chart contours. These would extend from 2 meters to a depth equal to  $L_0/2$ . Column 2 is column 1 divided by  $L_0$  corresponding to the given period. Column 3 is the value of  $\tanh 2\pi d/L$  found in Table C-1 of Appendix C, corresponding to the value of  $d/L_0$  in column 2. This term is also  $C/C_0$ . Column 4 is the quotient of successive terms in column 3. Column 5 is the reciprocal of column 4.

(2) Lay the line on the template labeled *orthogonal* along the incoming orthogonal with the point marked 1.0 at the intersection of the orthogonal and midcontour (Fig. 2-20, top). This establishes the turning point.

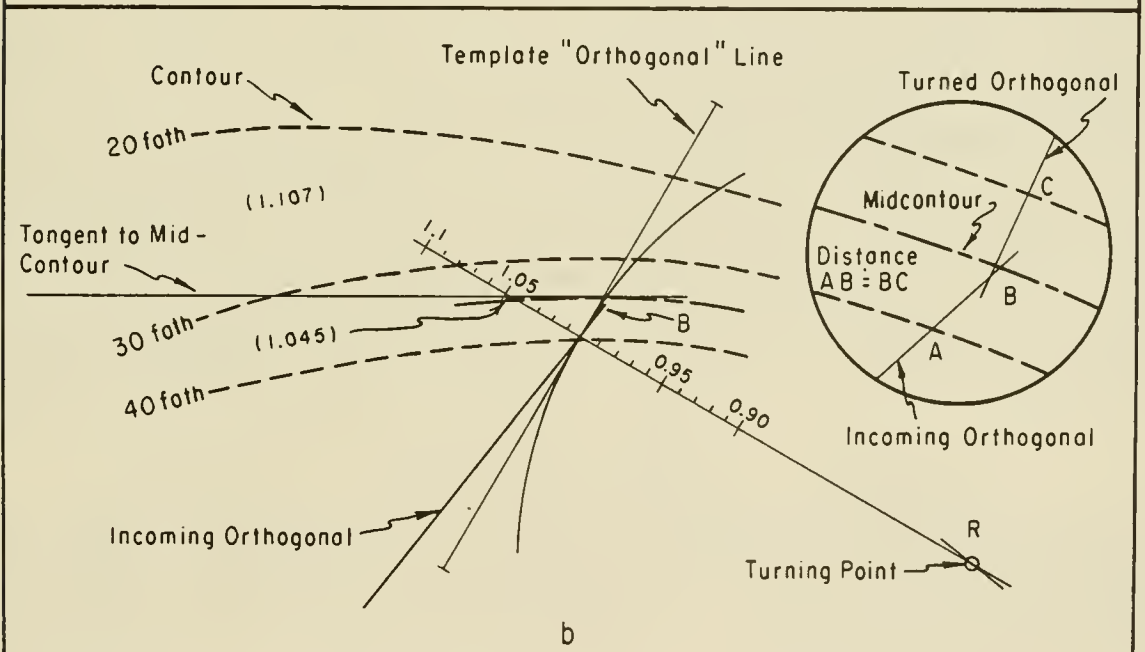
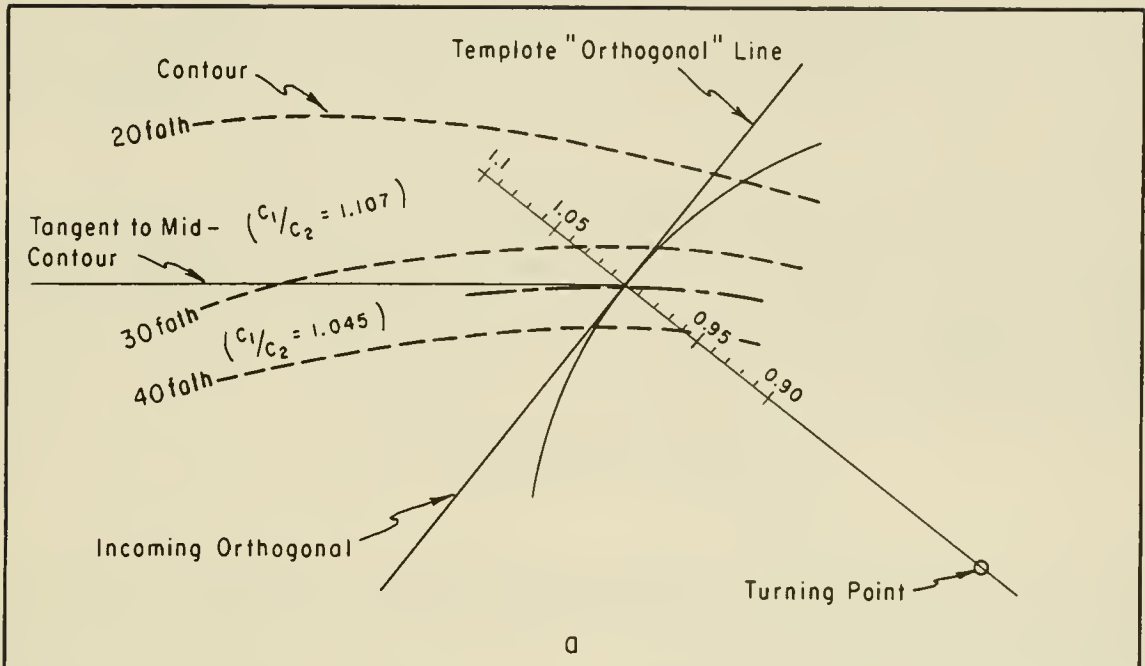
(3) Rotate the template about the *turning point* until the  $C_1/C_2$  value corresponding to the contour interval being crossed intersects the tangent to the midcontour. The orthogonal line on the chart now lies in the direction of the turned orthogonal on the template (Fig. 2-20, bottom).

(4) Place a triangle along the base of the template (this edge should be parallel to the line through the turning point), and construct a line parallel to the template orthogonal line so that it intersects the incoming orthogonal at point B. This intersection point is to be equidistant along the incoming and turned orthogonal lines (see insert to Fig. 2-20,b where  $AB = BC$ ). This intersection point is not necessarily on the midcontour line.

(5) Repeat the above steps for successive contour intervals.

If the orthogonal is being constructed from shallow to deep water, the same procedure may be used, except that  $C_2/C_1$  values are used instead of  $C_1/C_2$ .

A template suitable for attachment to a drafting machine can be made, (Palmer, 1957) and may make the procedure simpler if many diagrams are to be used.



NOTE: The template has been turned about R until the value  $c_1/c_2 = 1.045$  intersects the tangent to the midcontour. The template "orthogonal" line lies in the direction of the turned orthogonal. This direction is to be laid off at some point "B" on the incoming orthogonal, which is equidistant from the two contours along the incoming and outgoing orthogonals.

Figure 2-20. Use of the refraction template.

c. Procedure When  $\alpha$  Is Greater Than  $80^\circ$ --The R/J Method. In any depth, when  $\alpha$  becomes greater than  $80^\circ$ , the above procedure cannot be used. The orthogonal no longer appears to cross the contours, but tends to run almost parallel to them. In this case, the contour interval must be crossed in a series of steps. The entire interval is divided into a series of smaller intervals. At the midpoint of the individual subintervals, orthogonal angle turnings are made.

As can be seen in Figure 2-21, the interval to be crossed is divided into segments or boxes by transverse lines. The spacing R of transverse lines is arbitrarily set as a ratio of the distance J, between the contours. For the complete interval to be crossed,  $C_2/C_1$  is computed or found from Table C-4 of Appendix C ( $C_2/C_1$ , not  $C_1/C_2$ ).

- J = Distance between contours at turning points, ●
- R = Distance along orthogonal
- T = 12 s
- $L_0 = 737$  ft
- For contour interval from 40 fath to 30 fath  $C_1/C_2 = 1.045$ ,  $C_2/C_1 = 0.957$

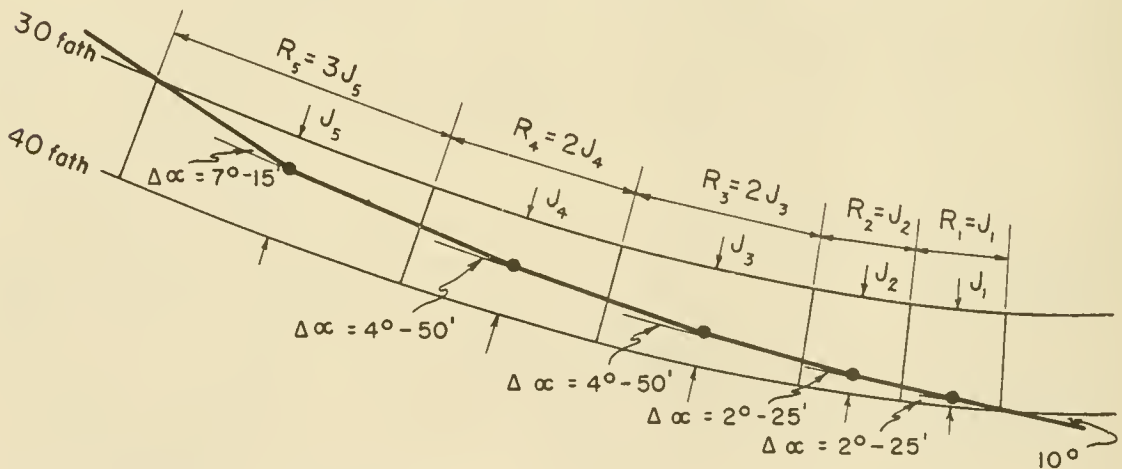


Figure 2-21. Refraction diagram using R/J method.

On the template (Fig. 2-18), a graph showing orthogonal angle turnings  $\Delta\alpha$  is plotted as a function of the  $C_2/C_1$  value for various values of the ratio R/J. The  $\Delta\alpha$  value is the angle turned by the incoming orthogonal in the center of the subinterval.

The orthogonal is extended to the middle of the box,  $\Delta\alpha$  is read from the graph, and the orthogonal turned by that angle. The procedure is repeated for each box in sequence, until  $\alpha$  at a plotted or interpolated contour becomes smaller than  $80^\circ$ . At this point, this method of orthogonal construction must be stopped, and the preceding technique for  $\alpha$  smaller than  $80^\circ$  used; otherwise, errors will result.

d. Refraction Fan Diagrams. It is often convenient, especially where sheltering landforms shield a stretch of shore from waves approaching in certain directions, to construct refraction diagrams from shallow water toward deep water. In these cases, a sheaf or fan of orthogonals may be projected

seaward in directions some 5° or 10° apart (see Fig. 2-22,a). With the deep-water directions thus determined by the individual orthogonals, companion orthogonals may be projected shoreward on either side of the seaward projected ones to determine the refraction coefficient for the various directions of wave approach (see Fig. 2-22,b).

e. Other Graphical Methods of Refraction Analysis. Another graphical method for the construction of refraction diagrams is the wave front method (Johnson, O'Brien, and Isaacs, 1948). This method applies particularly to very long waves where the crest alignment is also desired. The method is not explained here where many diagrams are required because it would be over-balanced by the advantages of the orthogonal method. The orthogonal method permits the direct construction of orthogonals and determination of the refraction coefficient, without the intermediate step of first constructing successive wave crests. Thus, when the wave crests are not required, significant time is saved by using the orthogonal method.

f. Computer Methods for Refraction Analysis. Harrison and Wilson (1964) developed a method for the numerical calculation of wave refraction by use of an electronic computer. Wilson (1966) extended the method so that, in addition to the numerical calculation, the actual plotting of refraction diagrams is accomplished automatically by use of a computer. Numerical methods are a practical means of developing wave refraction diagrams when an extensive refraction study of an area is required, and when they can be relied upon to give accurate results. However, the interpretation of computer output requires care, and the limitations of the particular scheme used should be considered in the evaluation of the results. For a discussion of some of these limitations, see Coudert and Raichlen (1970). For additional references, the reader is referred to the works of Keller (1958), Mehr (1962), Griswold (1963), Wilson (1966), Lewis, Bleistein, and Ludwig, (1967), Dobson (1967), Hardy (1968), Chao (1970), and Keulegan and Harrison (1970), in which a number of available computer programs for calculation of refraction diagrams are presented. Most of these programs are based on an algorithm derived by Munk and Arthur (1951) and, as such, are fundamentally based on the geometrical optics approximation (Fermat's principle).

g. Interpretation of Results and Diagram Limitations. Some general observations of refraction phenomena are in Figures 2-23, 2-24, and 2-25. These figures show the effects of several common bottom features on passing waves. Figure 2-23 shows the effect of a straight beach with parallel, evenly spaced bottom contours on waves approaching from an angle. Wave crests turn toward alignment with the bottom contours as the waves approach shore. The refraction effects on waves normally incident on a beach fronted by a submarine ridge or submarine depression are illustrated in Figure 2-24 (a and b). The ridge tends to focus wave action toward the section of beach where the ridge line meets the shoreline. The orthogonals in this region are more closely spaced; hence  $\sqrt{b_0/b}$  is greater than 1.0 and the waves are higher than they would be if no refraction occurred. Conversely, a submarine depression will cause orthogonals to diverge, resulting in low heights at the shore ( $b_0/b$  less than 1.0). Similarly, heights will be greater at a headland than in a bay. Since the wave energy contained between two orthogonals is constant, a larger part of the total energy expended at the shore is focused on projections from the shoreline; consequently, refraction straightens an

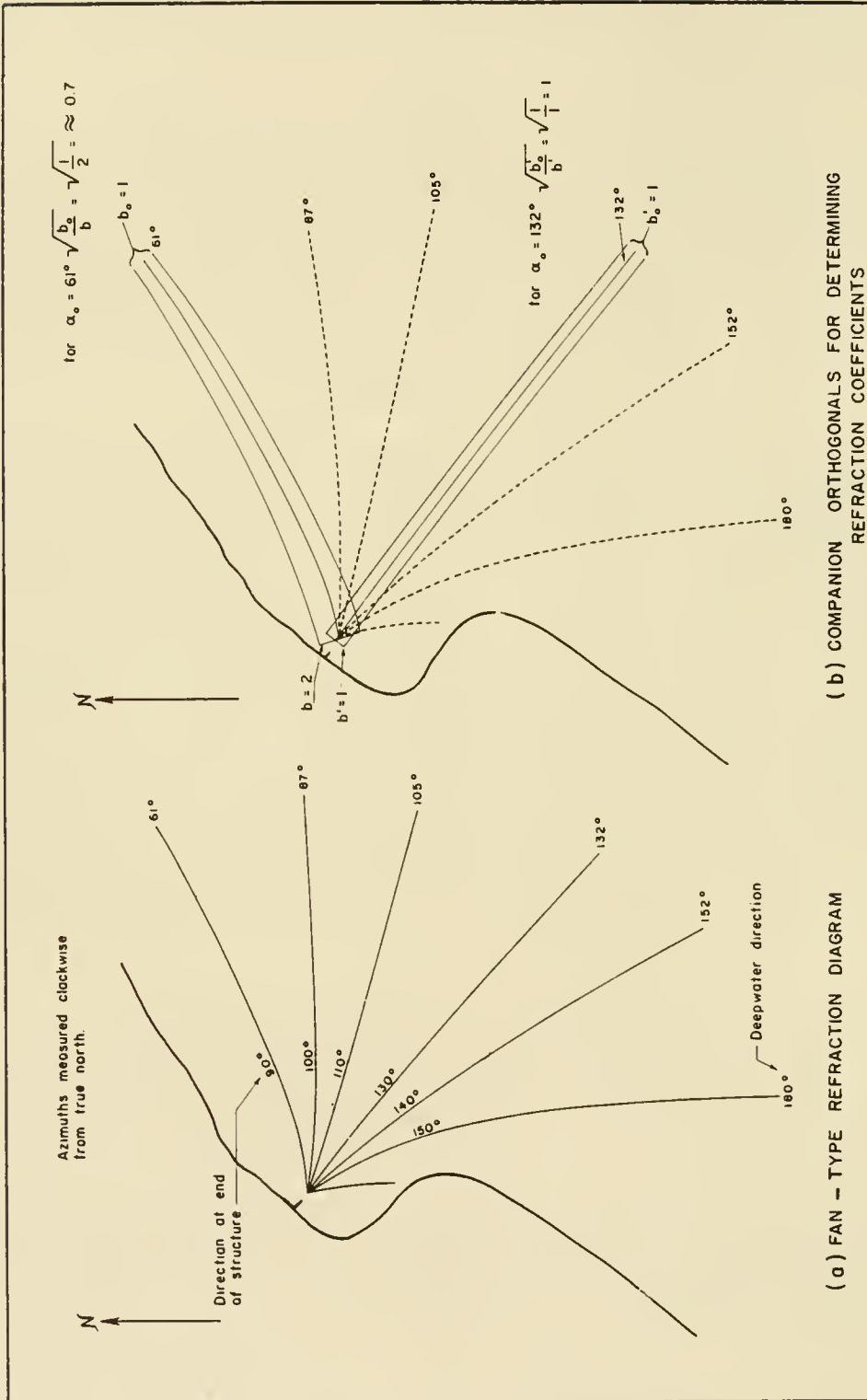


Figure 2-22. Use of fan-type refraction diagram.

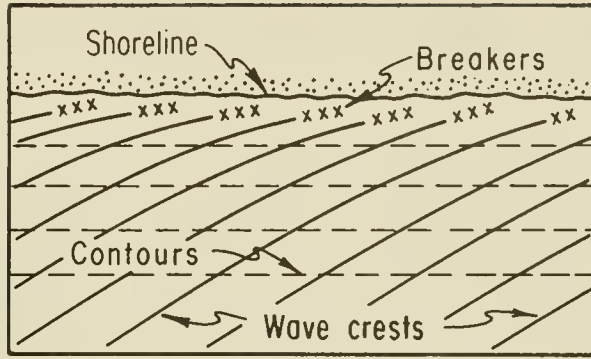


Figure 2-23. Refraction along a straight beach with parallel bottom contours.

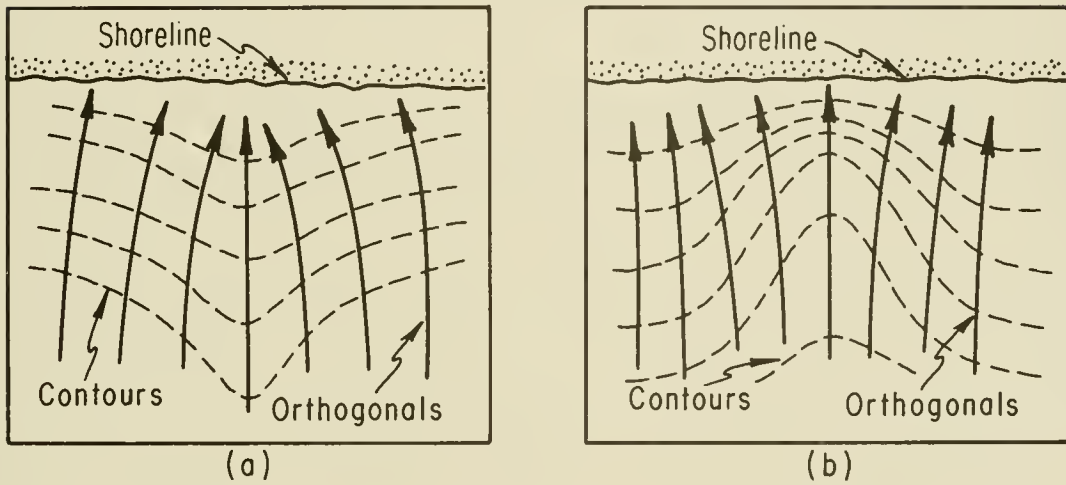


Figure 2-24. Refraction by a submarine ridge (a) and submarine canyon (b).

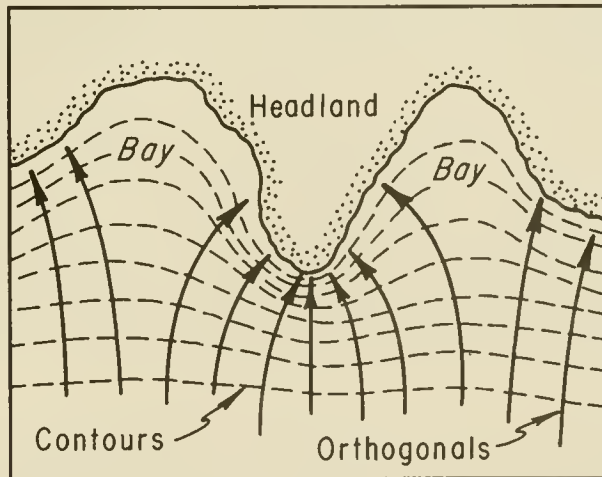


Figure 2-25. Refraction along an irregular shoreline.

irregular coast. Bottom topography can be inferred from refraction patterns in aerial photography. The pattern in Figure 2-17 indicates the presence of a submarine ridge.

Refraction diagrams can provide a measure of changes in waves approaching a shore. However, the accuracy of refraction diagrams is limited by the validity of the theory of construction and the accuracy of depth data. The orthogonal direction change (eq. 2-78a) is derived for straight parallel contours. It is difficult to carry an orthogonal accurately into shore over complex bottom features (Munk and Arthur, 1951). Moreover, the equation is derived for small waves moving over mild slopes.

Dean (1974) considered the combined effects of refraction and shoaling, including nonlinearities applied to a slope with depth contours parallel to the beach but not necessarily of constant slope. He found that nonlinear effects can significantly increase (in comparison with linear theory) both amplification and angular turning of waves of low steepness in deep water.

Strict accuracy for height changes cannot be expected for slopes steeper than 1:10, although model tests have shown that direction changes nearly as predicted even over a vertical discontinuity (Wiegel and Arnold, 1957). Accuracy where orthogonals bend sharply or exhibit extreme divergence or convergence is questionable. This phenomenon has been studied by Beitinjani and Brater (1965), Battjes (1968), and Whalin (1971). Where two orthogonals meet, a caustic develops. A caustic is an envelope of orthogonal crossings caused by convergence of wave energy at the caustic point. An analysis of wave behavior near a caustic is not available; however, qualitative analytical results show that wave amplitude decays exponentially away from a caustic in the shadow zone, and that there is a phase shift of  $\pi/2$  across the caustic (Whalin 1971). Wave behavior near a caustic has also been studied by Pierson (1950), Chao (1970), and others. Little quantitative information is available for the area beyond a caustic.

h. Refraction of Ocean Waves. Unlike monochromatic waves, actual ocean waves are complicated. Their crest lengths are short; their form does not remain permanent; and their speed, period, and direction of propagation vary from wave to wave.

Pierson (1951), Longuet-Higgins (1957), and Kinsman (1965) have suggested a solution to the ocean-wave refraction problem. The sea-surface waves in deep water become a number of component monochromatic waves, each with a distinct frequency and direction of propagation. The energy or height of each component in the spectrum may then be found and conventional refraction analysis techniques applied. Near the shore, the wave energy propagated in a particular direction is approximated as the linear sum of the wave components of all frequencies refracted in the given direction from all the deepwater directional components.

The work required from this analysis, even for a small number of individual components, is laborious and time consuming. Research by Borgman (1969) and Fan and Borgman (1970) has used the idea of directional spectra which may provide a technique for rapidly solving complex refraction problems.

## IV. WAVE DIFFRACTION

### 1. Introduction.

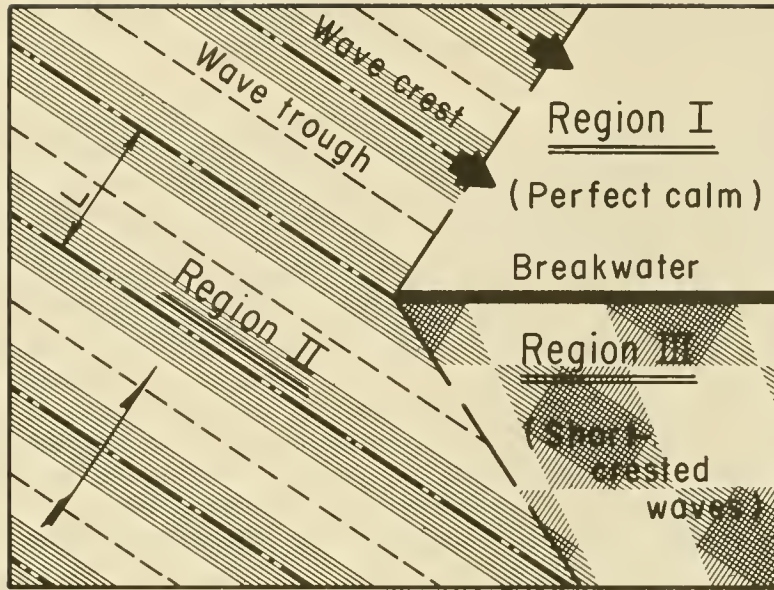
Diffraction of water waves is a phenomenon in which energy is transferred laterally along a wave crest. It is most noticeable where an otherwise regular train of waves is interrupted by a barrier such as a breakwater or small island. If the lateral transfer of wave energy along a wave crest and across orthogonals did not occur, straight, long-crested waves passing the tip of a structure would leave a region of perfect calm in the lee of the barrier, while beyond the edge of the structure the waves would pass unchanged in form and height. The line separating two regions would be a discontinuity. A part of the area in front of the barrier would, however, be disturbed by both the incident waves and by those waves reflected by the barrier. The three regions are shown in Figure 2-26(a) for the hypothetical case if diffraction did not occur, and in Figure 2-26(b) for the actual phenomenon as observed. The direction of the lateral energy transfer is also shown in Figure 2-26(a). Energy flow across the discontinuity is from Region II into Region I. In Region III, the superposition of incident and reflected waves results in the appearance of short-crested waves if the incident waves approach the breakwater obliquely. A partial standing wave will occur in Region III if the waves approach perpendicular to the breakwater. This process is also similar to that for other types of waves, such as light or sound waves.

Calculation of diffraction effects is important for several reasons. Wave height distribution in a harbor or sheltered bay is determined to some degree by the diffraction characteristics of both the natural and manmade structures affording protection from incident waves. Therefore, a knowledge of the diffraction process is essential in planning such facilities. The proper design and location of harbor entrances to reduce such problems as silting and harbor resonance also require a knowledge of the effects of wave diffraction. The prediction of wave heights near the shore is affected by diffraction caused by naturally occurring changes in hydrography. An aerial photograph illustrating the diffraction of waves by a breakwater is shown in Figure 2-27.

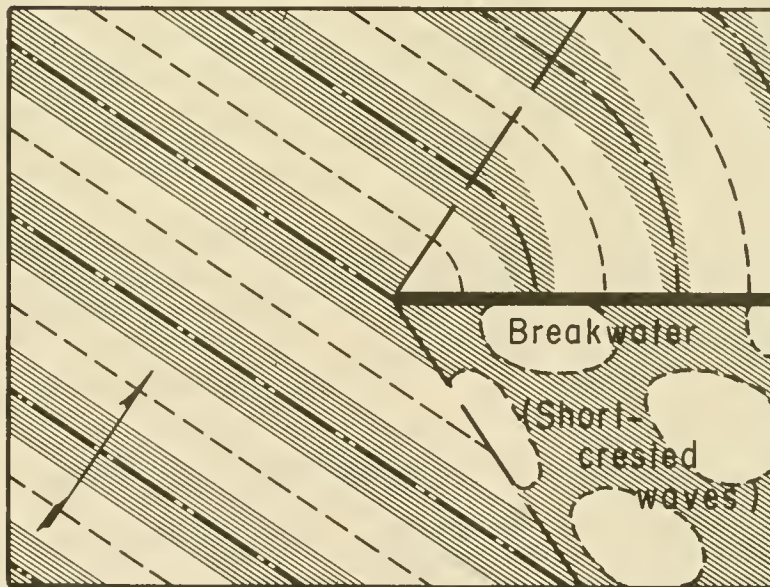
Putnam and Arthur (1948) presented experimental data verifying a method of solution proposed by Penny and Price (1944) for wave behavior after passing a single breakwater. Wiegel (1962) used a theoretical approach to study wave diffraction around a single breakwater. Blue and Johnson (1949) dealt with the problem of wave behavior after passing through a gap, as between two breakwater arms.

The assumptions usually made in the development of diffraction theories are

- (1) Water is an ideal fluid; i.e., inviscid and incompressible.
- (2) Waves are of small amplitude and can be described by linear wave theory.
- (3) Flow is irrotational and conforms to a potential function, which satisfies the Laplace equation.
- (4) Depth shoreward of the breakwater is constant.



a. No diffraction.



b. Diffraction effects.

Figure 2-26. Wave incident on a breakwater--(a) no diffraction and (b) diffraction effects.



Figure 2-27. Wave diffraction at Channel Islands Harbor breakwater, California.

If this last assumption is not valid then the processes of both refraction and diffraction come into play.

## 2. Diffraction Calculations.

a. Waves Passing a Single Breakwater. From a presentation by Wiegel (1962), diffraction diagrams have been prepared which, for a uniform depth adjacent to an impervious structure, show lines of equal wave height reduction. These diagrams are shown in Figures 2-28 to 2-39; the graph coordinates are in units of wavelength. Wave height reduction is given in terms of a diffraction coefficient  $K'$  which is defined as the ratio of a wave height  $H$

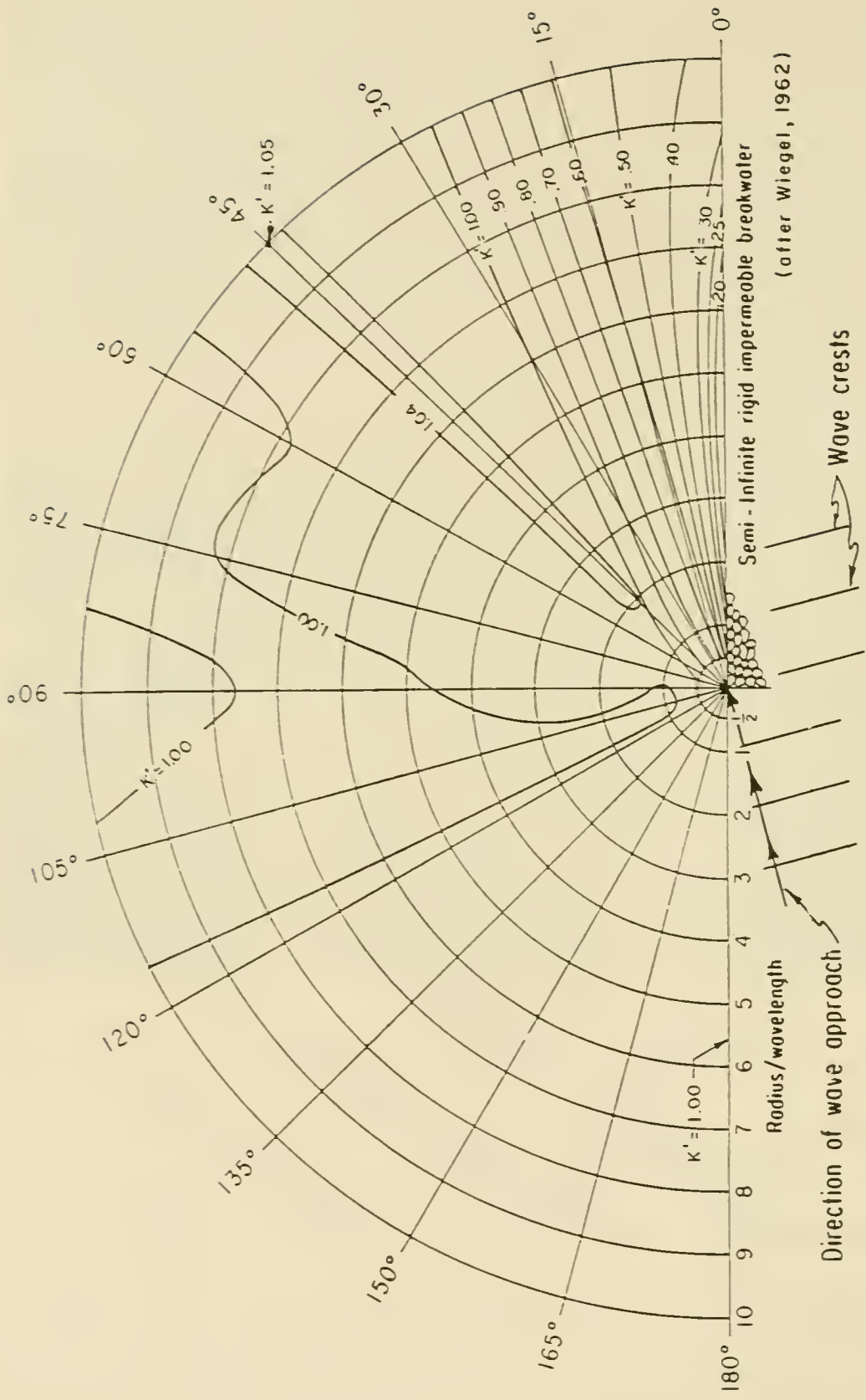


Figure 2-28. Wave diffraction diagram--15° wave angle.

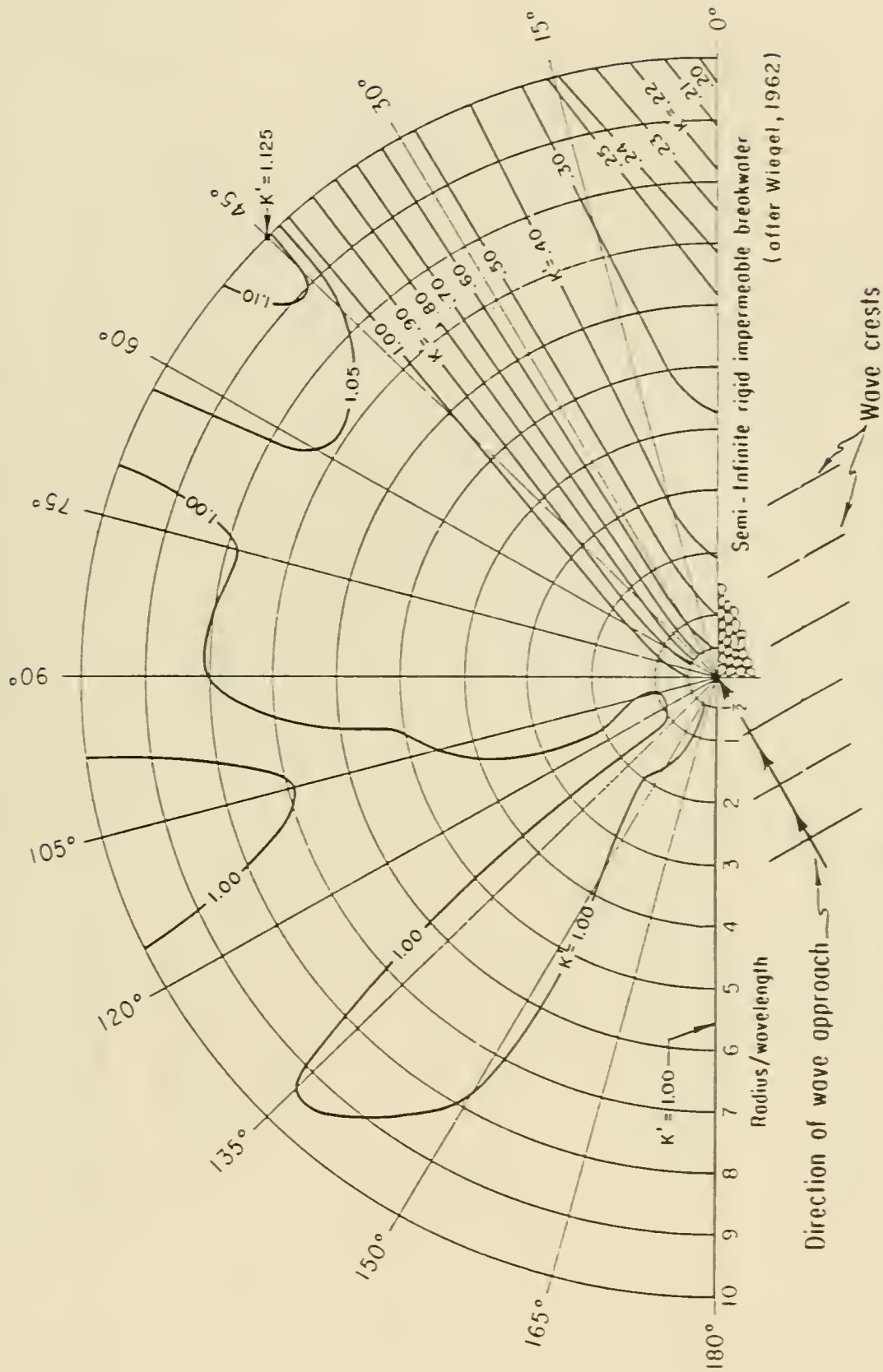


Figure 2-29. Wave diffraction diagram--30° wave angle.

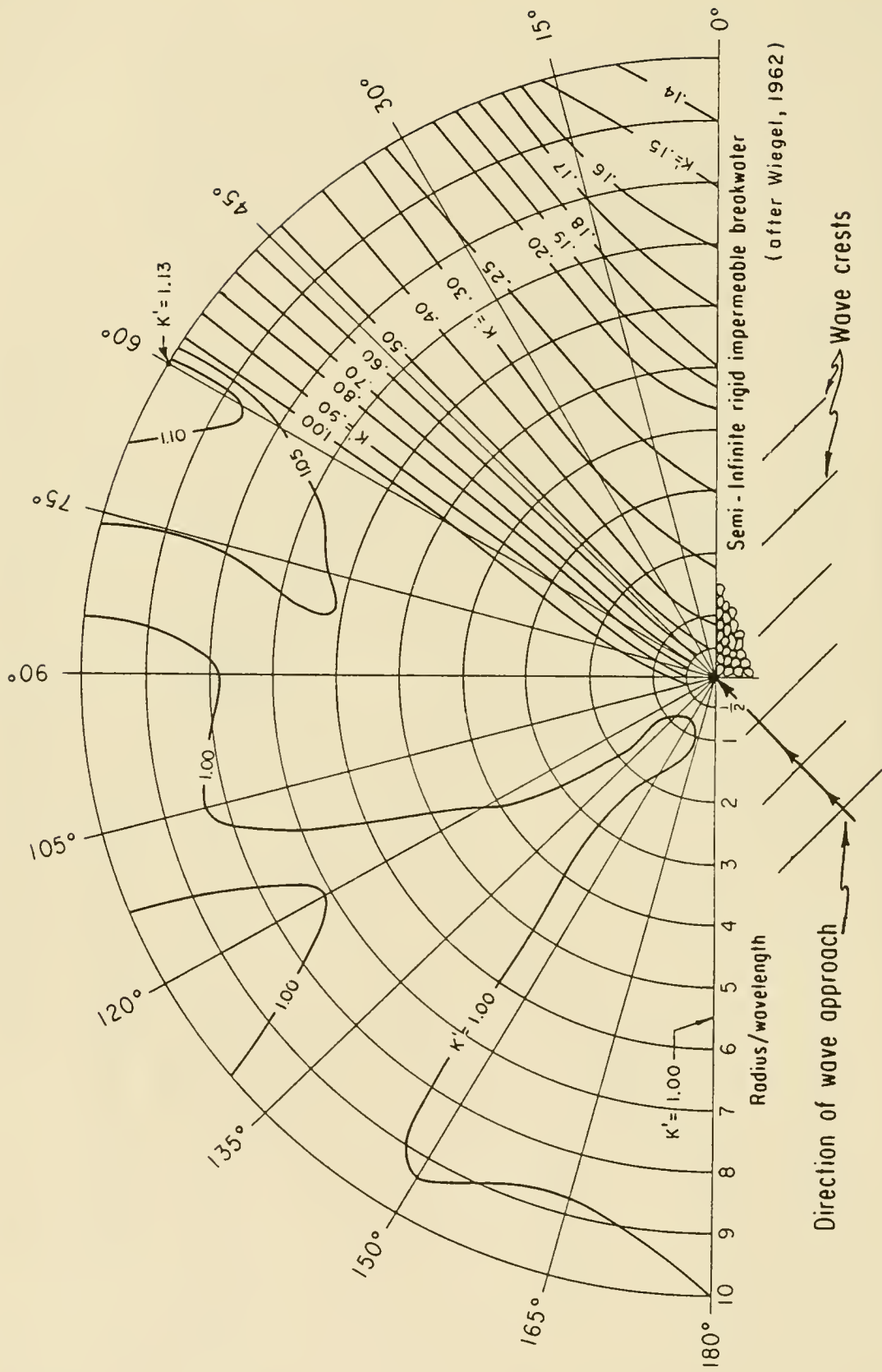


Figure 2-30. Wave diffraction diagram-- $45^\circ$  wave angle.

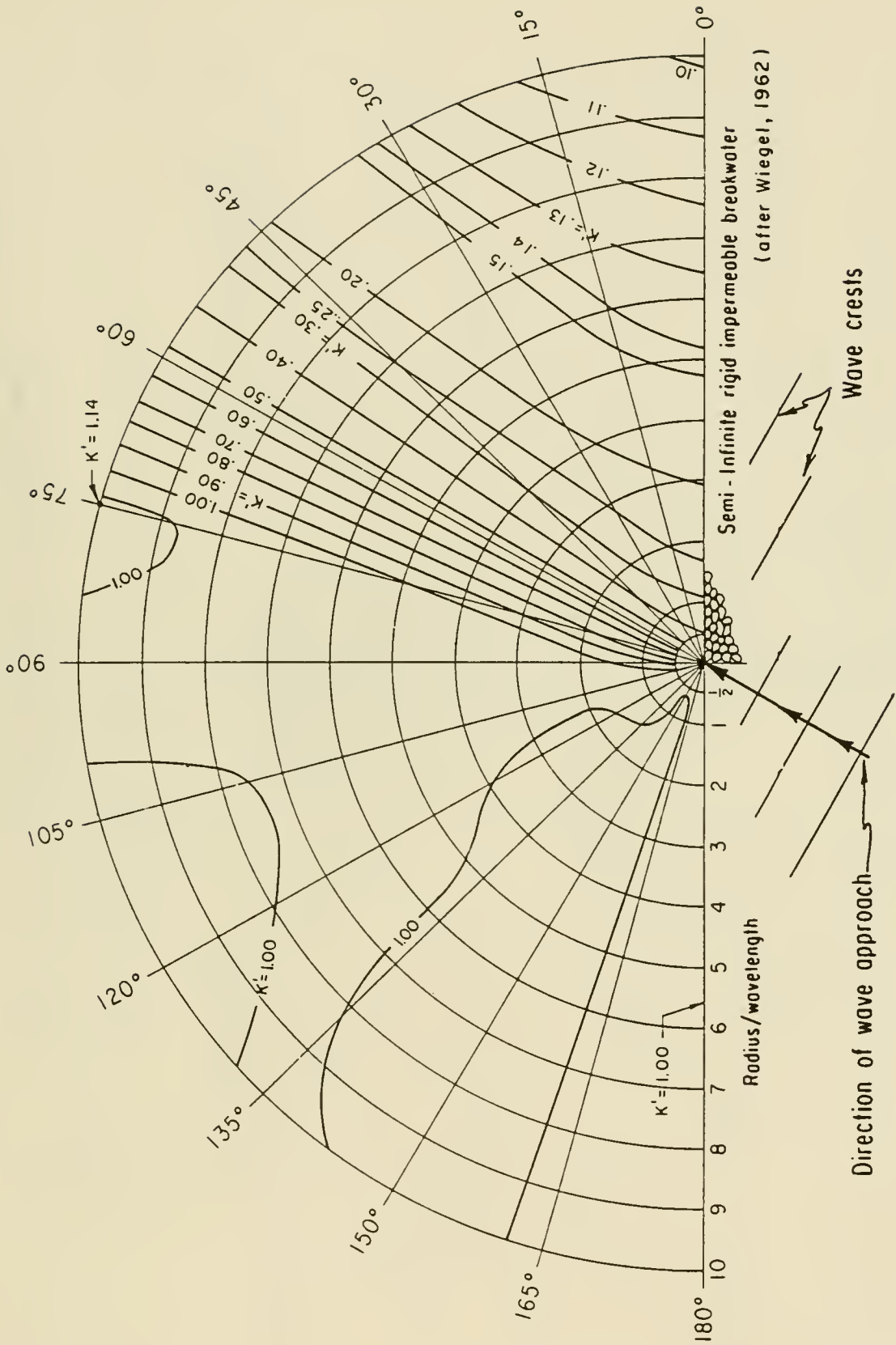


Figure 2-31. Wave diffraction diagram--60° wave angle.

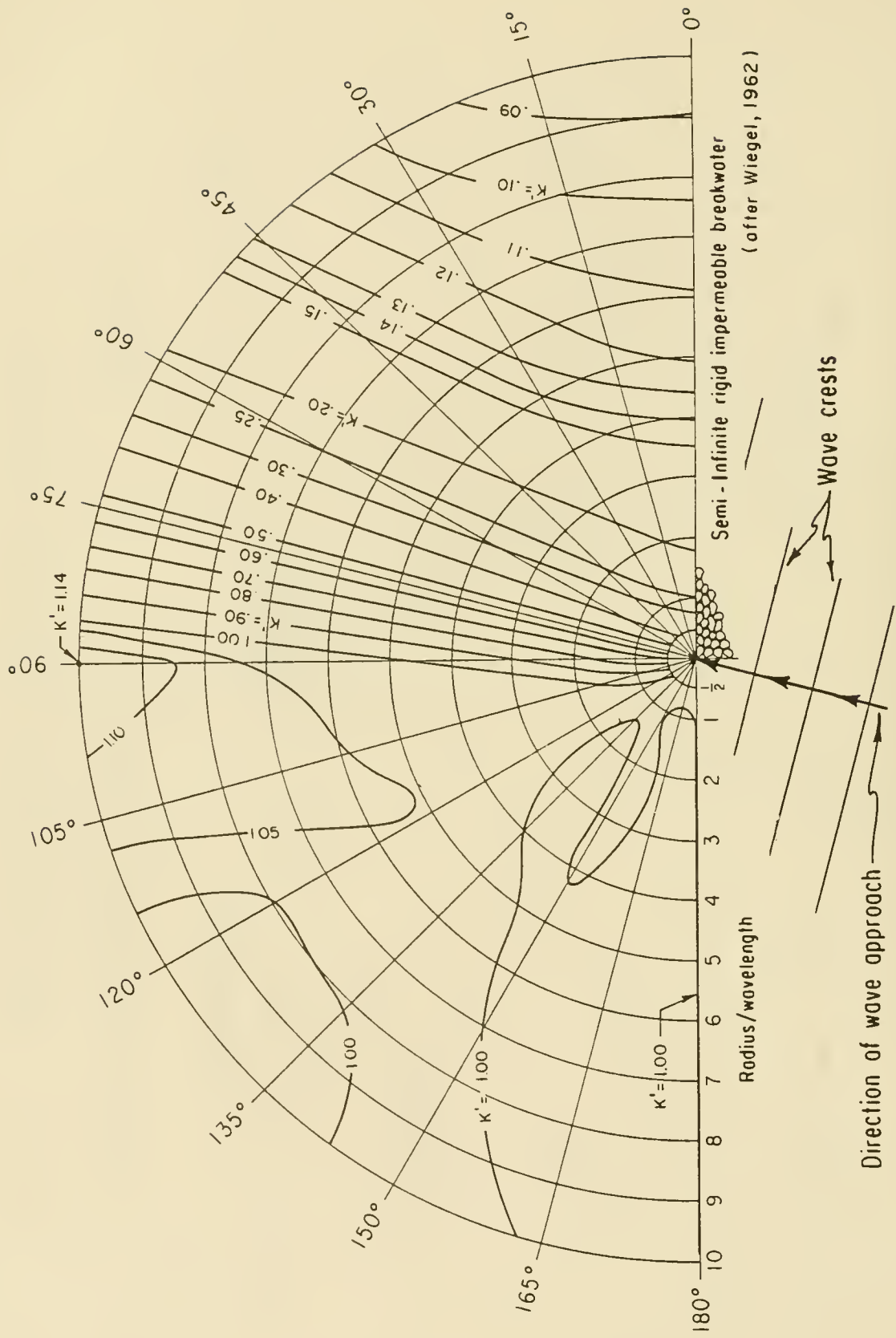


Figure 2-32. Wave diffraction diagram--75° wave angle.

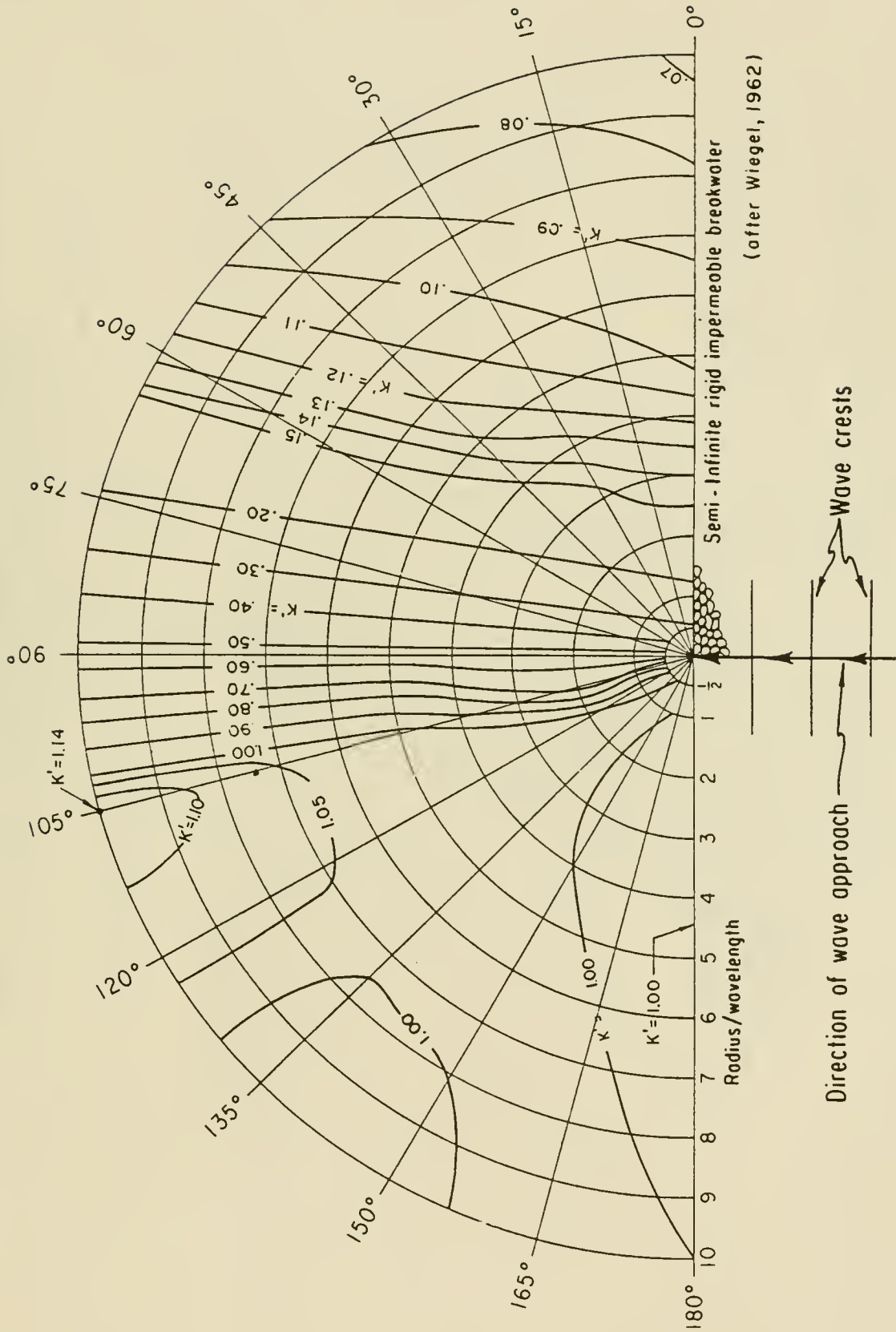


Figure 2-33. Wave diffraction diagram--90° wave angle.

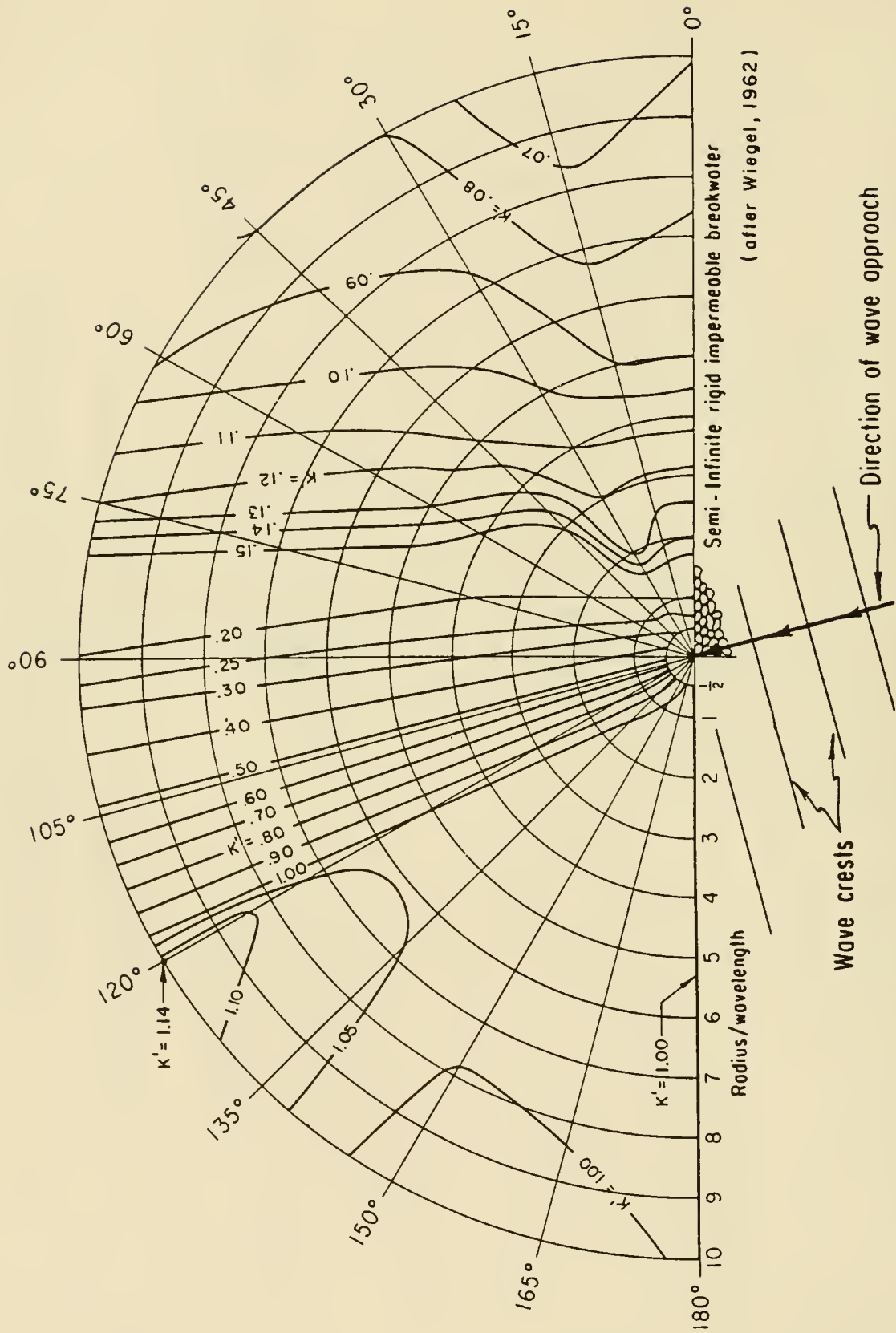


Figure 2-34. Wave diffraction diagram--105° wave angle.

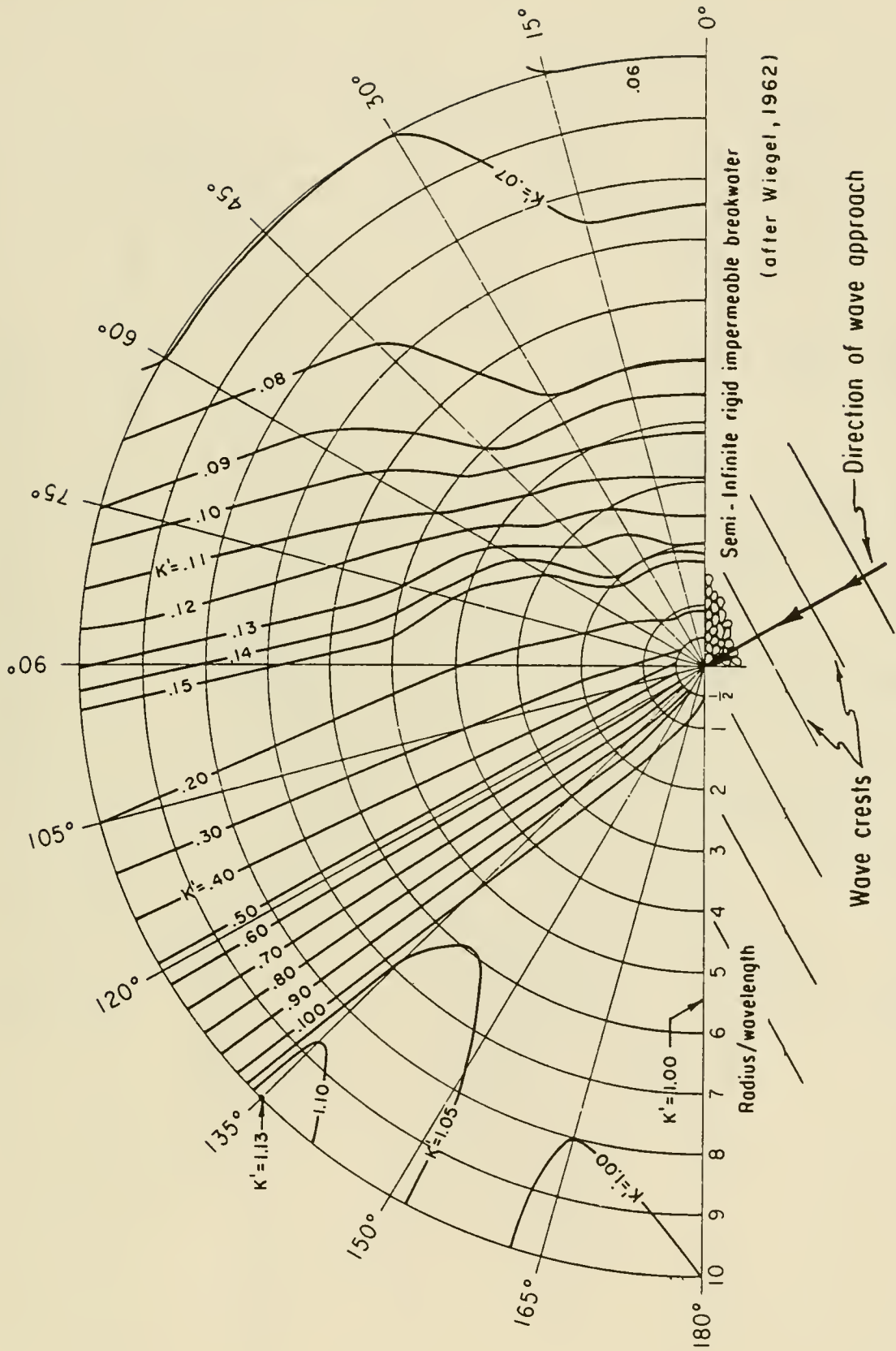


Figure 2-35. Wave diffraction diagram--120° wave angle.

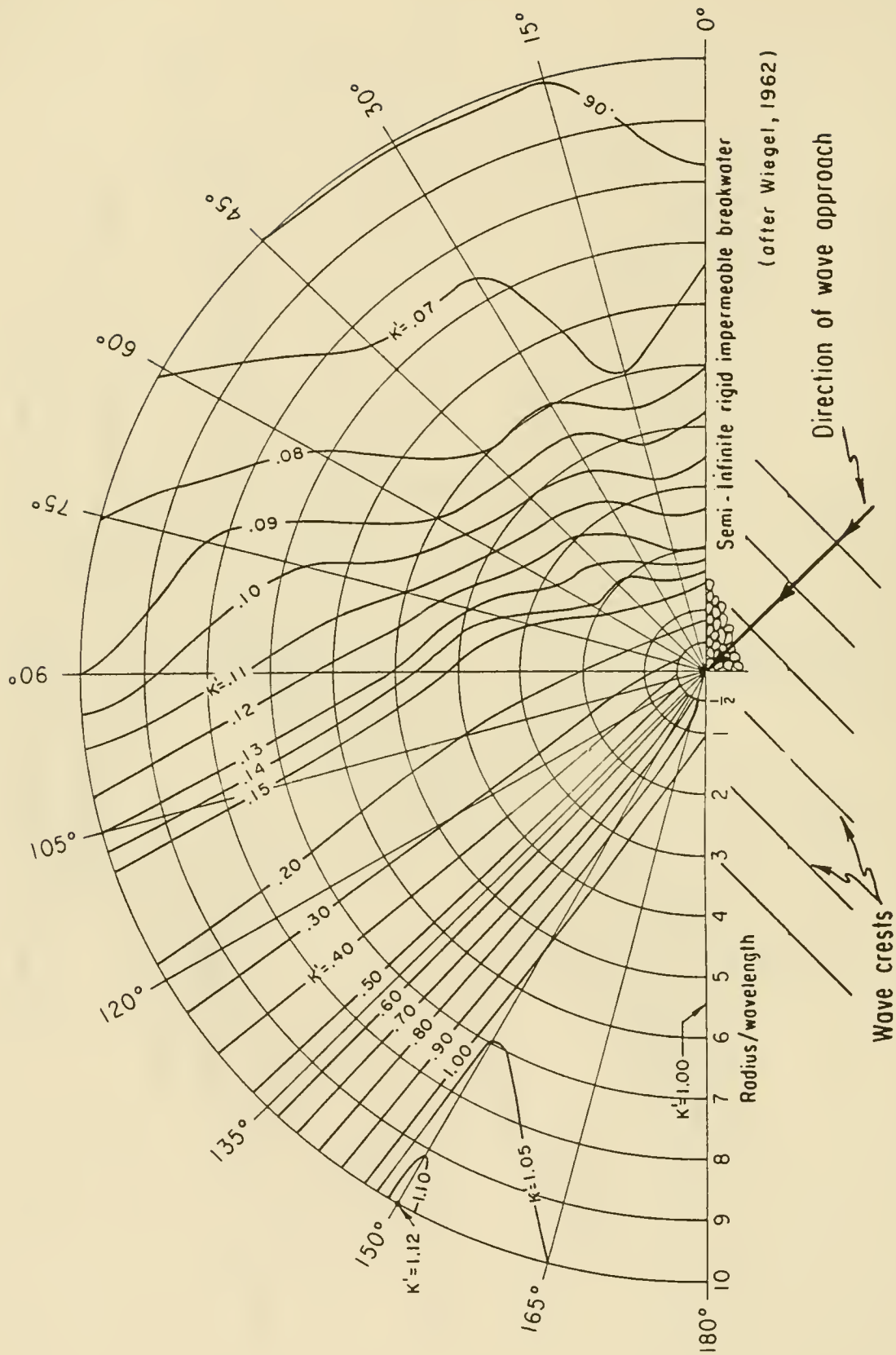


Figure 2-36. Wave diffraction diagram--135° wave angle.

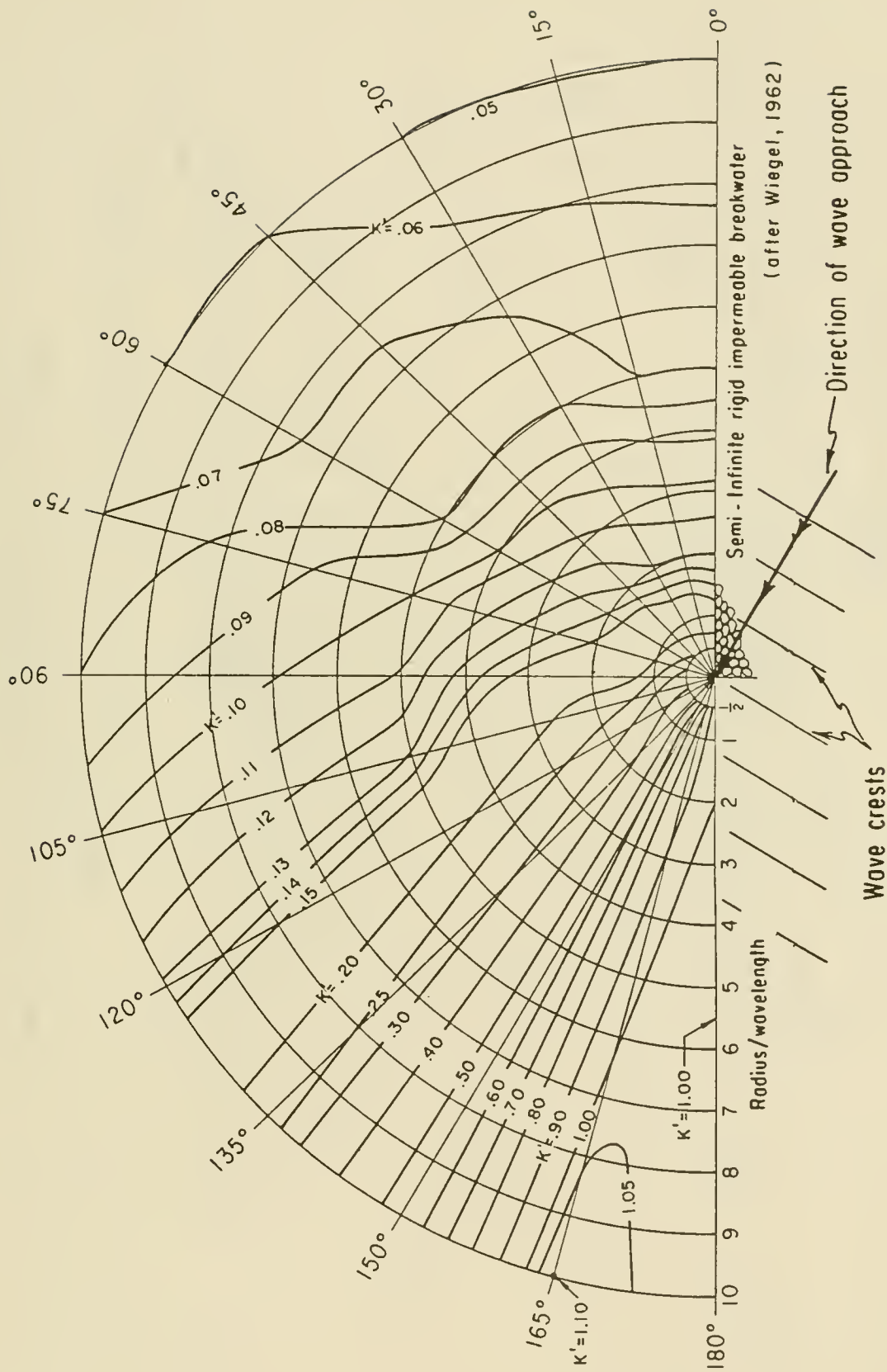


Figure 2-37. Wave diffraction diagram--150° wave angle.

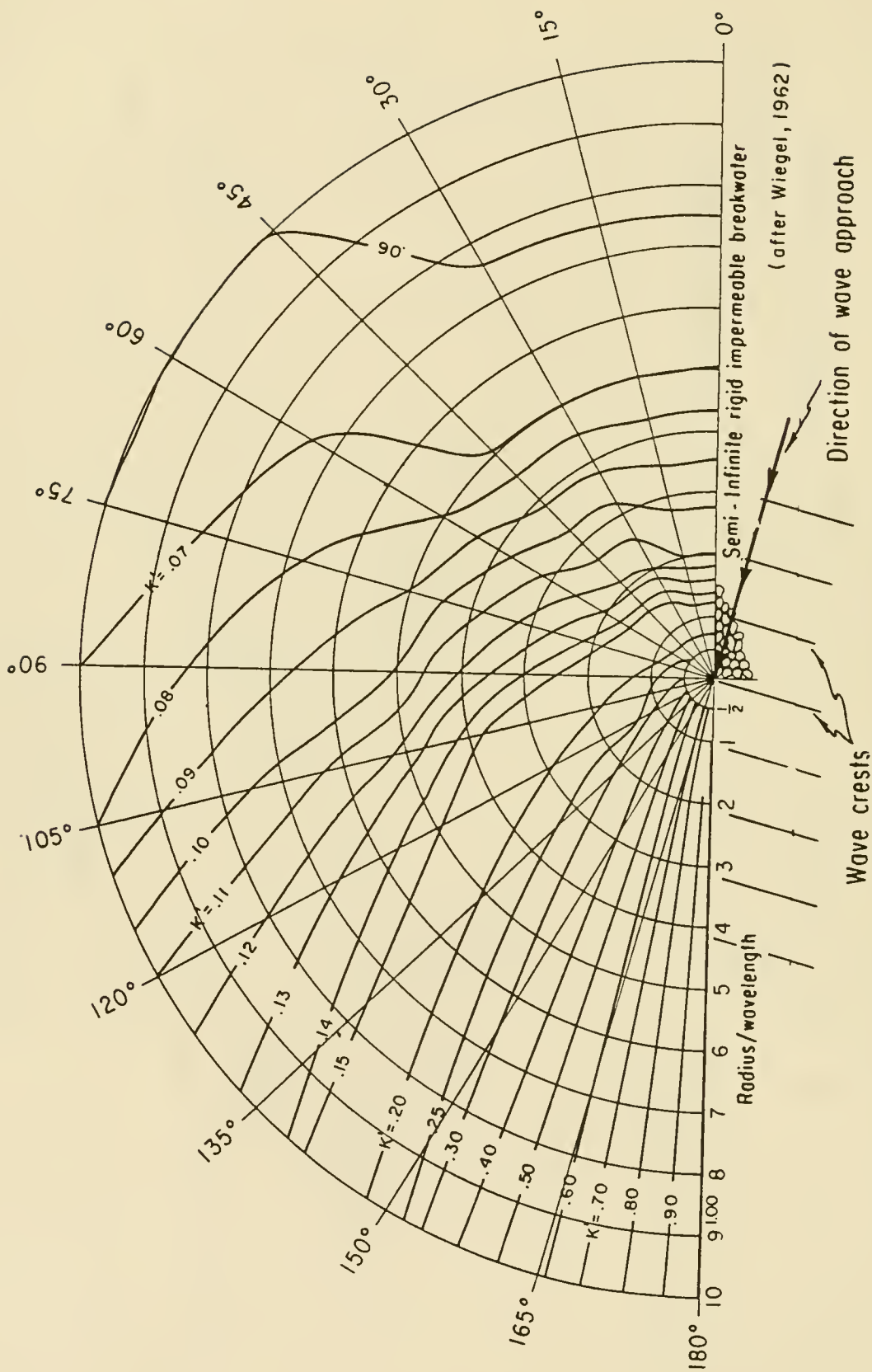


Figure 2-38. Wave diffraction diagram--165° wave angle.

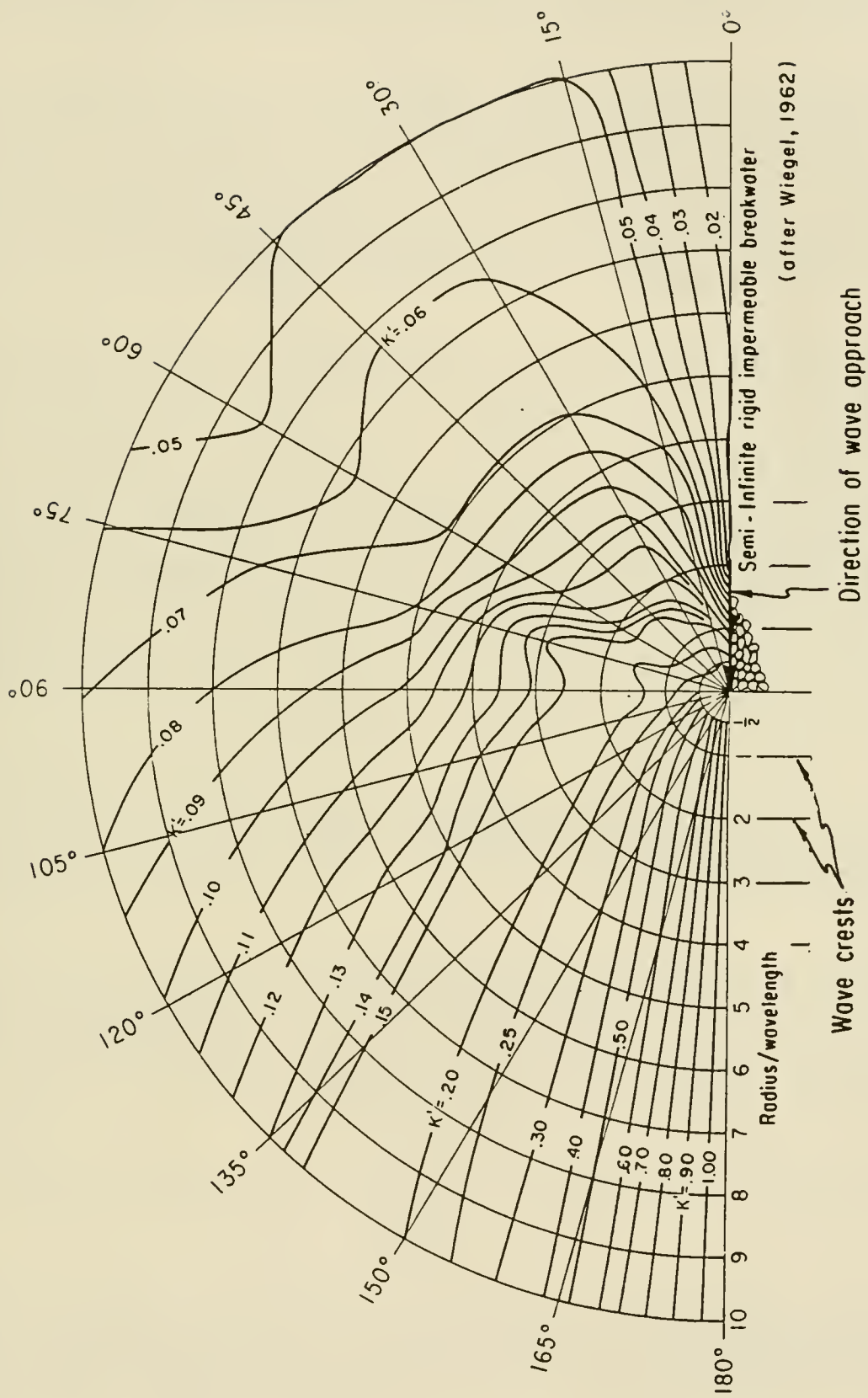


Figure 2-39. Wave diffraction diagram--180° wave angle.

in the area affected by diffraction to the incident wave height  $H_1$  in the area unaffected by diffraction. Thus,  $H$  and  $H_1$  are determined by  $H = K'H_1$ .

The diffraction diagrams shown in Figures 2-28 to 2-39 are constructed in polar coordinate form with arcs and rays centered at the structure's tip. The arcs are spaced one *radius-wavelength* unit apart and rays  $15^\circ$  apart. In application, a given diagram must be scaled up or down so that the particular wavelength corresponds to the scale of the hydrographic chart being used. Rays and arcs on the diffraction diagrams provide a coordinate system that makes it relatively easy to transfer lines of constant  $K'$  on the scaled diagrams.

When applying the diffraction diagrams to actual problems, the wavelength must first be determined based on the water depth at the toe of the structure. The wavelength  $L$  in water depth  $d_s$ , may be found by computing  $d_s/L_0 = d_s/5.12T^2$  and using Appendix C, Table C-1, to find the corresponding value of  $d_s/L$ . Dividing  $d_s$  by  $d_s/L$  will give the shallow-water wavelength  $L$ . It is then useful to construct a scaled diffraction diagram overlay template to correspond to the hydrographic chart being used. In constructing this overlay, first determine how long each of its radius-wavelength units must be. As noted previously, one radius-wavelength unit on the overlay must be identical to one wavelength on the hydrographic chart. The next step is to sketch all overlay rays and arcs on clear plastic or translucent paper. This allows the scaled lines of equal  $K'$  to be penciled in for each angle of wave approach that may be considered pertinent to the problem. After studying the wave field for one angle of wave approach,  $K'$  lines may be erased for a subsequent analysis of a different angle of wave approach.

The diffraction diagrams in Figures 2-28 to 2-39 show the breakwater extending to the right as seen looking toward the area of wave diffraction; however, for some problems the structure may extend to the left. All diffraction diagrams presented may be reversed by simply turning the transparency over to the opposite side.

Figure 2-40 illustrates the use of a template overlay and also indicates the angle of wave approach which is measured counterclockwise from the breakwater. This angle would be measured clockwise from the breakwater if the diagram were turned over. The figure also shows a rectangular coordinate system with distance expressed in units of wavelength. Positive  $x$  direction is measured from the structure's tip along the breakwater, and positive  $y$  direction is measured into the diffracted area.

The following problem illustrates determination of a single wave height in the diffraction area.

\*\*\*\*\* EXAMPLE PROBLEM 9 \*\*\*\*\*

GIVEN: Waves with a period  $T = 8$  seconds and height  $H = 3$  meters (9.84 feet) impinge upon a breakwater at an angle of  $135^\circ$ . The water depth at the tip of the breakwater toe is  $d_s = 5$  meters (16.40 feet). Assume that the hydrographic chart being used has a scale of 1:1600 (1 centimeter = 16 meters).

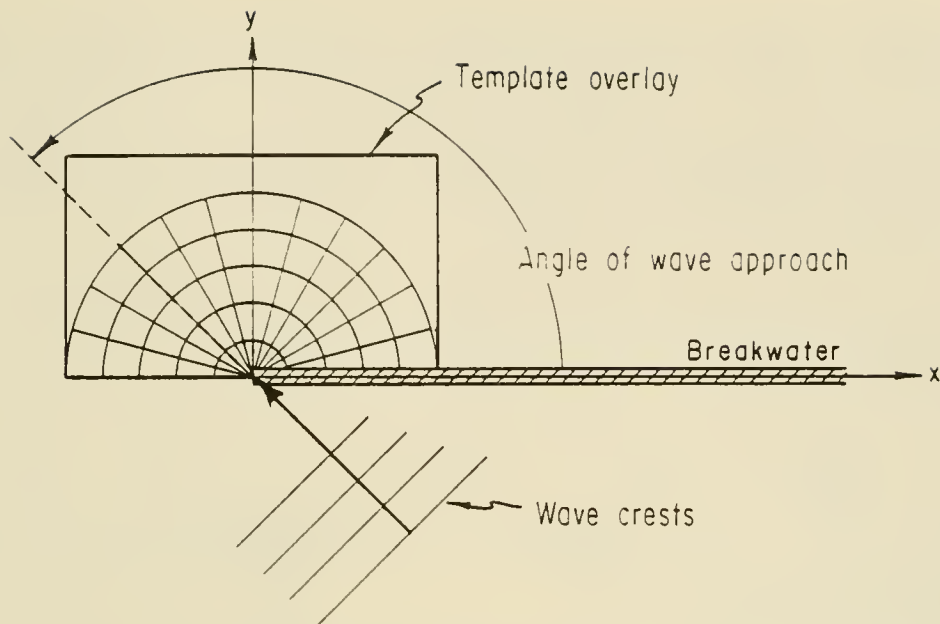


Figure 2-40. Diffraction for a single breakwater normal incidence.

FIND: The wave height at a point P having coordinates in units of wavelength  $x = 3$  and  $y = 4$ . (Polar coordinates of  $x$  and  $y$  are  $r = 5$  at  $53^\circ$ .)

SOLUTION:

Since  $d_s = 5$  meters,  $T = 8$  seconds,

$$\frac{d_s}{L_o} = \frac{d_s}{1.56T^2} = \frac{5}{(1.56)(64)} = 0.0501$$

Using Table C-1 with

$$\frac{d}{L_o} = \frac{d_s}{L_o} = 0.0501$$

the corresponding value of

$$\frac{d}{L} \text{ or } \frac{d_s}{L} = 0.0942$$

therefore,

$$L = \frac{d_s}{\left(\frac{d_s}{L}\right)} = \frac{5}{0.0942} = 53.06 \text{ m (174 ft)}$$

Because 1 centimeter represents 16 meters on the hydrographic chart and  $L = 53.06$  meters, the wavelength is 0.0332 meter or 3.32 centimeters (1.31 inches) on the chart. This provides the necessary information for scaling Figure 2-36 to the hydrographic chart being used. Thus 3.32 centimeters represents a radius-wavelength unit.

For this example point P and those lines of equal  $K'$  situated nearest P are shown on a schematic overlay (Fig. 2-41). This overlay is based on Figure 2-36 since the angle of wave approach is  $135^\circ$ . It should be noted that Figure 2-41, being a schematic rather than a true representation of the overlay, is not drawn to the hydrographic chart scale calculated in the problem. From the figure it is seen that  $K'$  at point P is approximately 0.086. Thus the diffracted wave height at this point is

$$H = K'H_i = (0.086)(3) = 0.258 \text{ m, say } 0.26 \text{ m (0.853 ft)}$$

The above calculation indicates that a wave undergoes a substantial height reduction in the area considered.

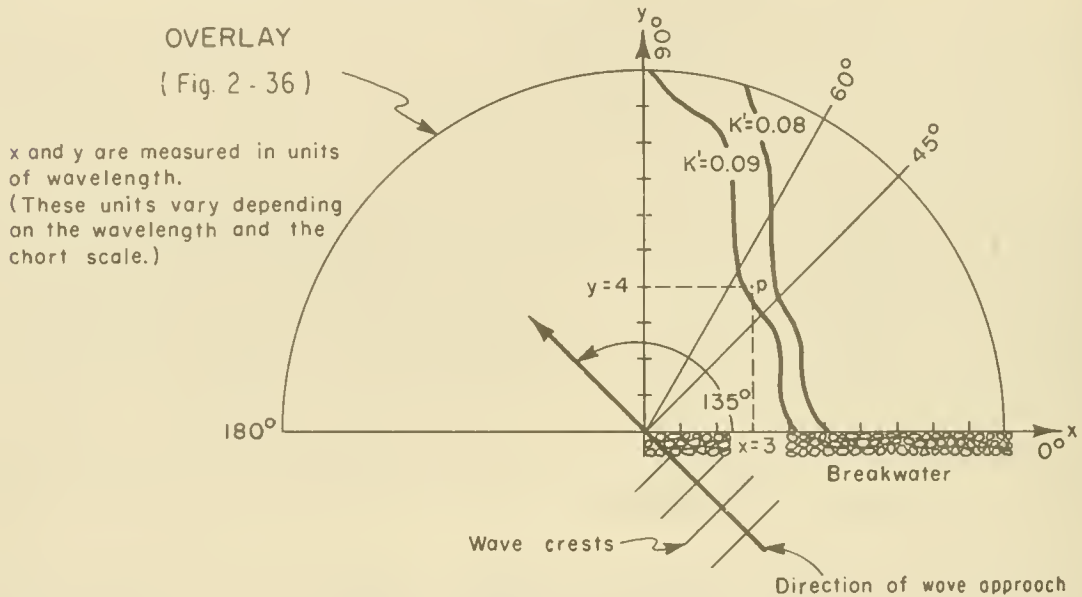


Figure 2-41. Schematic representation of wave diffraction overlay.

\*\*\*\*\*

b. Waves Passing a Gap of Width Less Than Five Wavelengths at Normal Incidence. The solution of this problem is more complex than that for a single breakwater, and it is not possible to construct a single diagram for all conditions. A separate diagram must be drawn for each ratio of gap width to wavelength  $B/L$ . The diagram for a  $B/L$  ratio of 2 is shown in Figure 2-42 which also illustrates its use. Figures 2-43 to 2-52 (Johnson, 1952) show lines of equal diffraction coefficient for  $B/L$  ratios of 0.50, 1.00, 1.41, 1.64, 1.78, 2.00, 2.50, 2.95, 3.82, and 5.00. A sufficient number of diagrams have been included to represent most gap widths encountered in practice. In all but Figure 2-48 ( $B/L = 2.00$ ), the wave crest lines have been omitted. Wave crest lines are usually of use only for illustrative purposes. They are, however, required for an accurate estimate of the combined effects of refraction and diffraction. In such cases, wave crests may be approximated with sufficient accuracy by circular arcs. For a single breakwater, the arcs will be centered on the breakwater toe. That part of the wave crest extending into unprotected water beyond the  $K' = 0.5$  line may be approximated by a straight line. For a breakwater gap, crests that are more than eight wavelengths

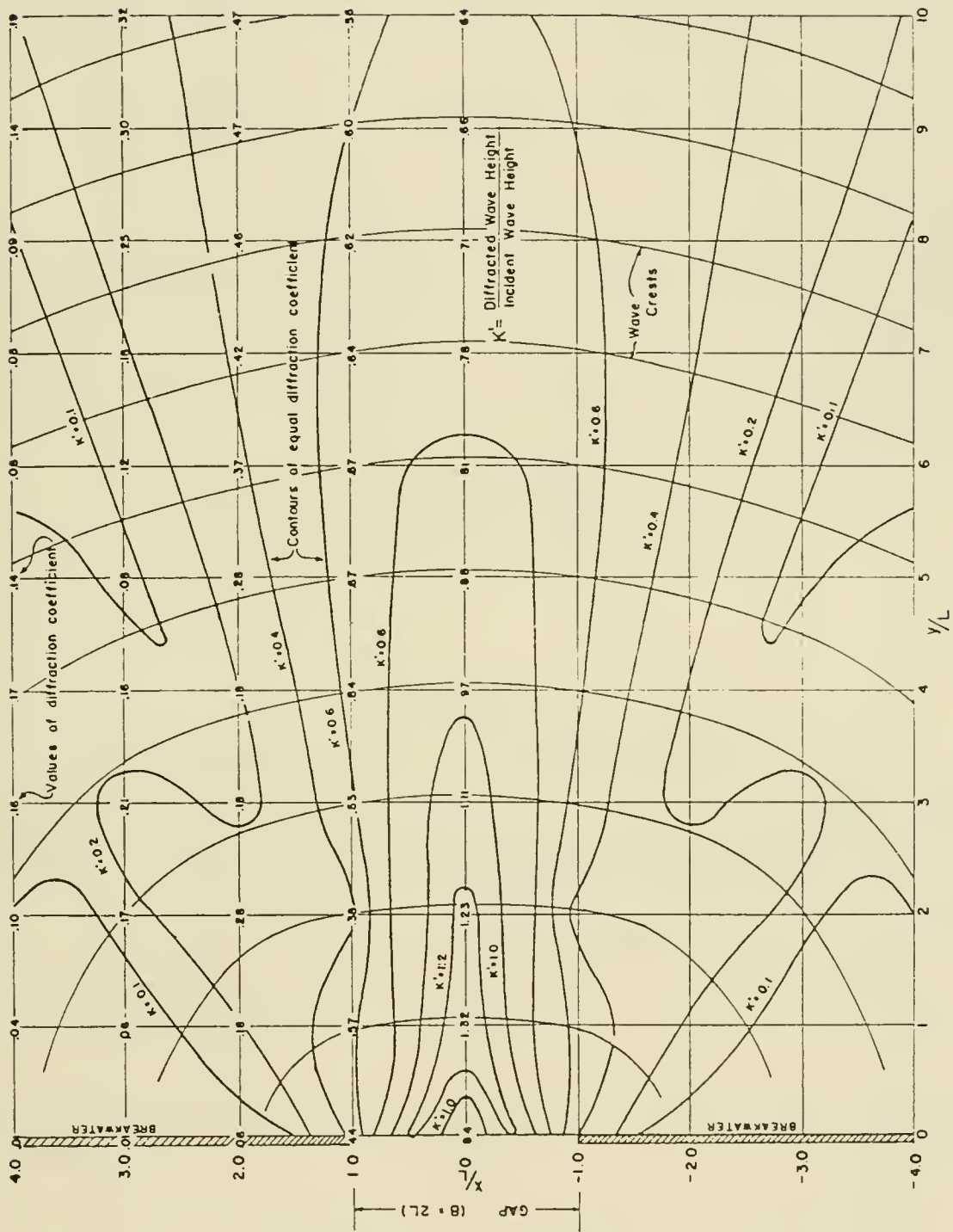


Figure 2-42. Generalized diffraction diagram for a breakwater gap width of two wavelengths ( $B/L = 2$ ).

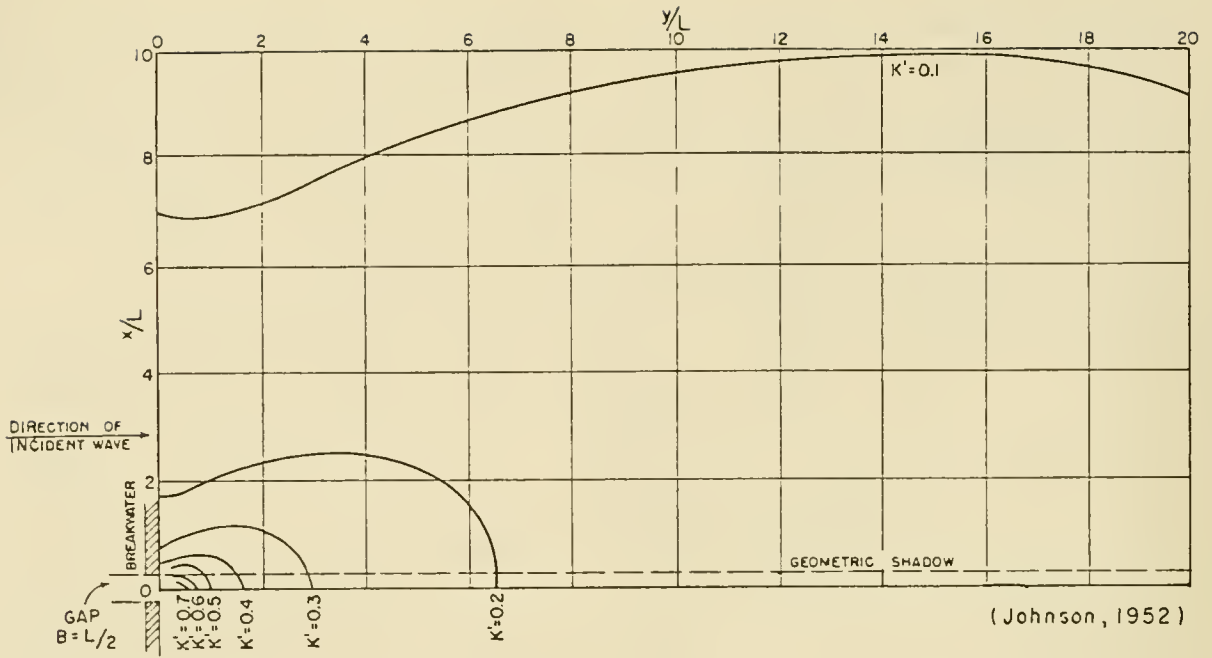


Figure 2-43. Contours of equal diffraction coefficient gap width = 0.5 wavelength ( $B/L = 0.5$ ).

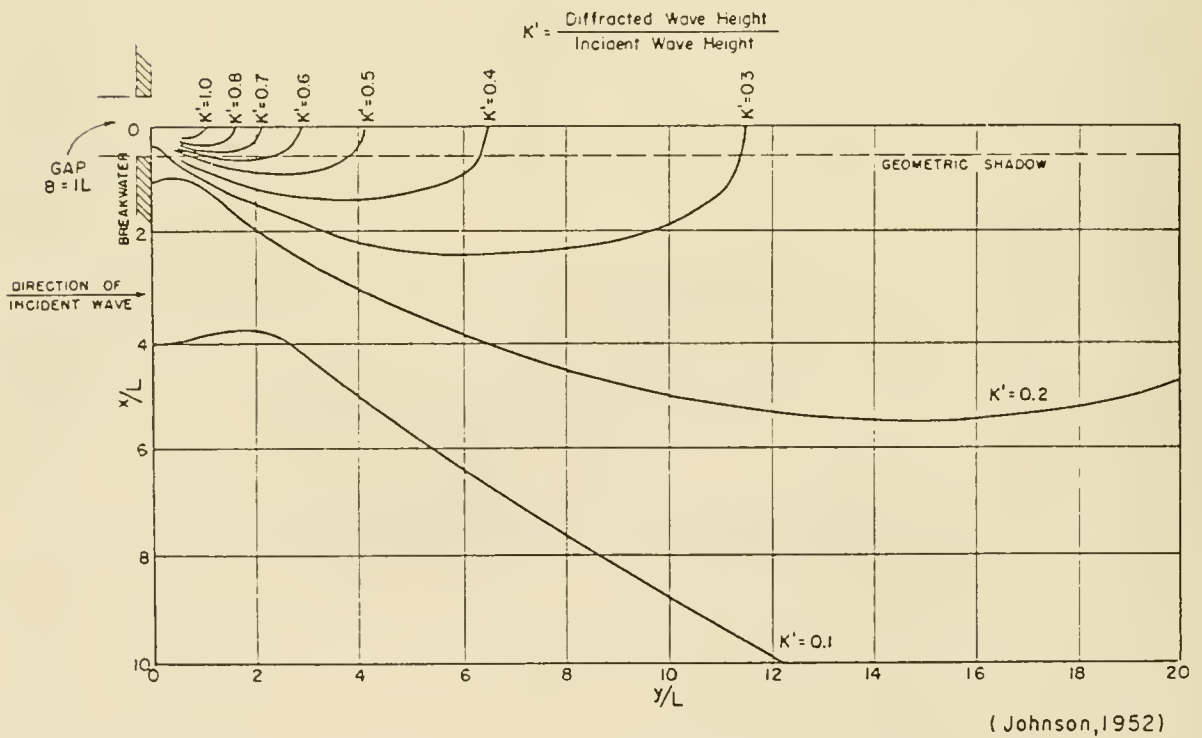


Figure 2-44. Contours of equal diffraction coefficient gap width = 1 wavelength ( $B/L = 1$ ).

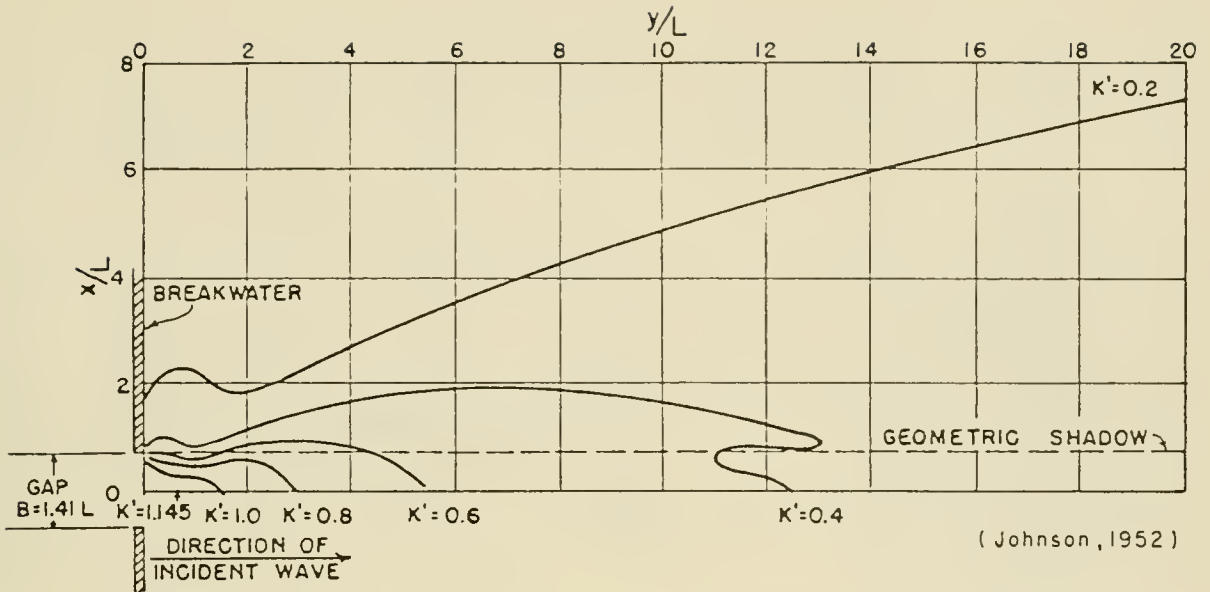


Figure 2-45. Contours of equal diffraction coefficient gap width = 1.41 wavelengths ( $B/L = 1.41$ ).

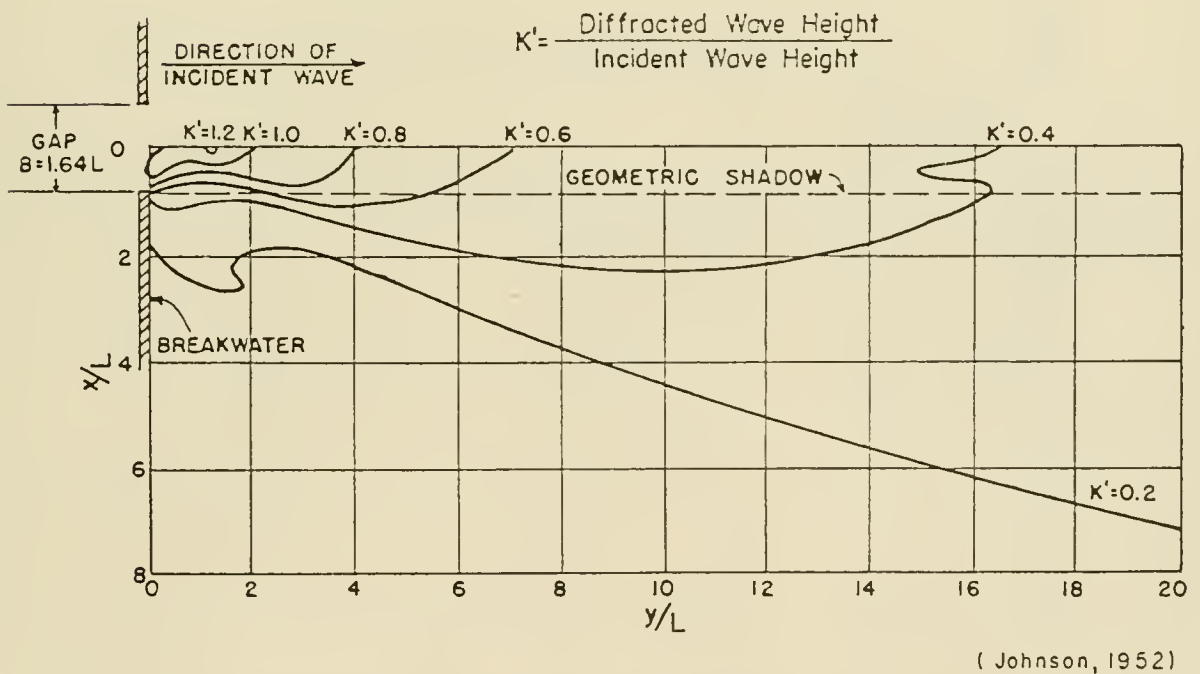


Figure 2-46. Contours of equal diffraction coefficient gap width = 1.64 wavelengths ( $B/L = 1.64$ ).

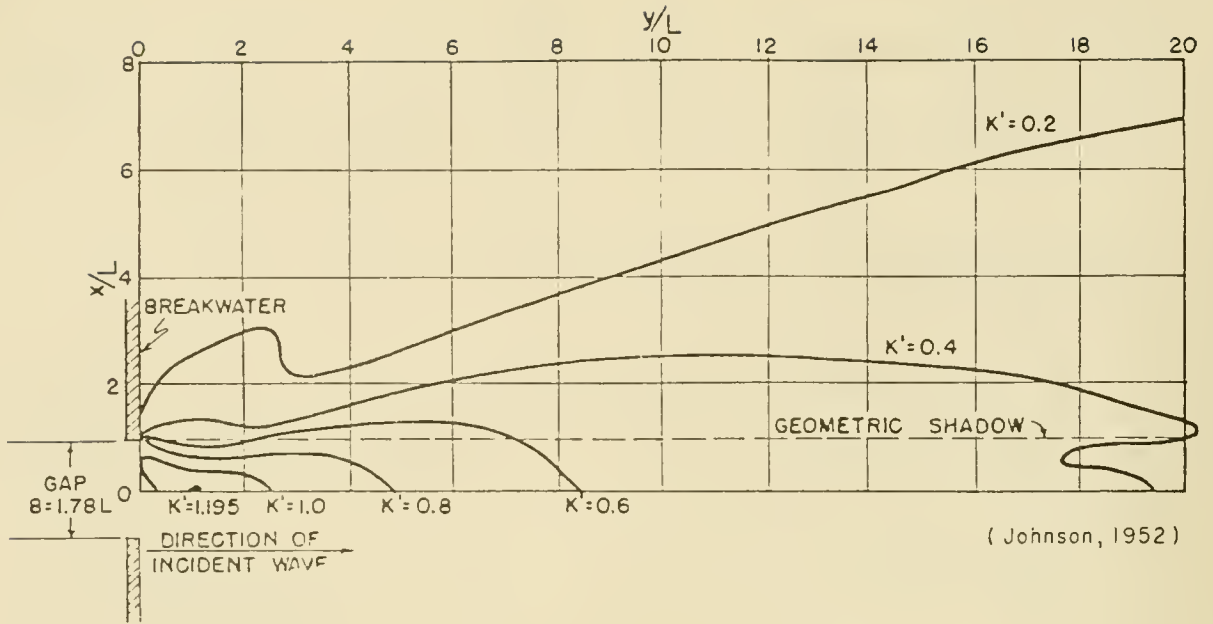


Figure 2-47. Contours of equal diffraction coefficient gap width = 1.78 wavelengths ( $B/L = 1.78$ ).

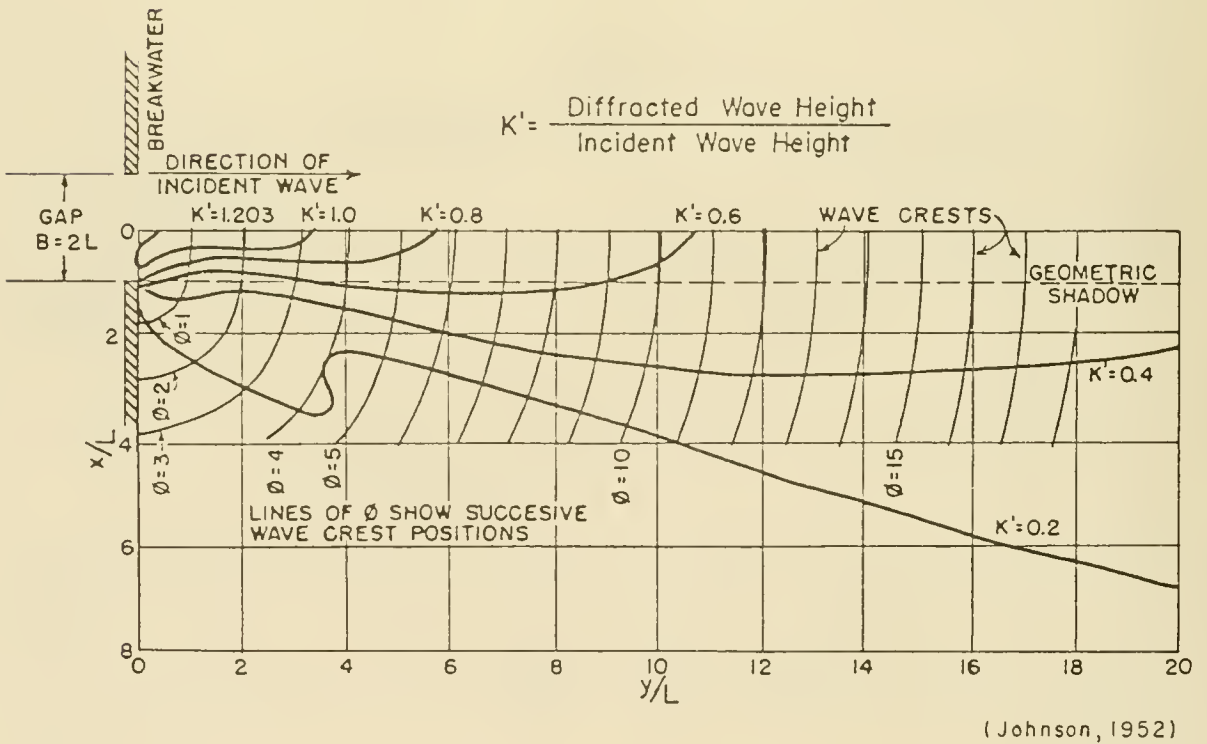


Figure 2-48. Contours of equal diffraction coefficient gap width = 2 wavelengths ( $B/L = 2$ ).

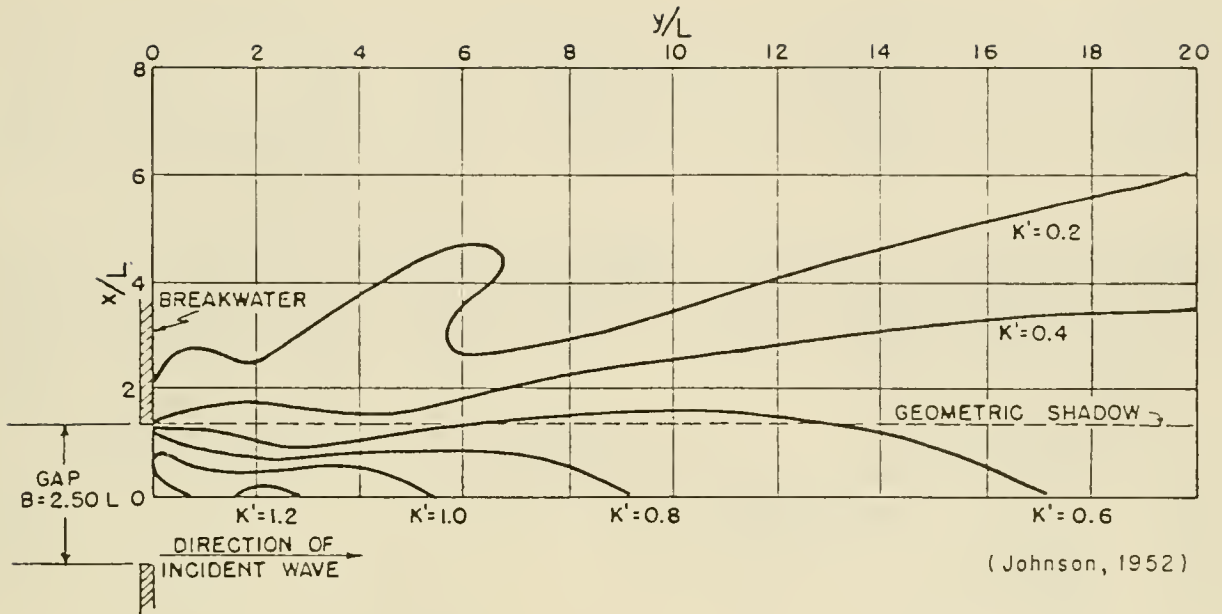


Figure 2-49. Contours of equal diffraction coefficient gap width = 2.50 wavelengths ( $B/L = 2.50$ ).

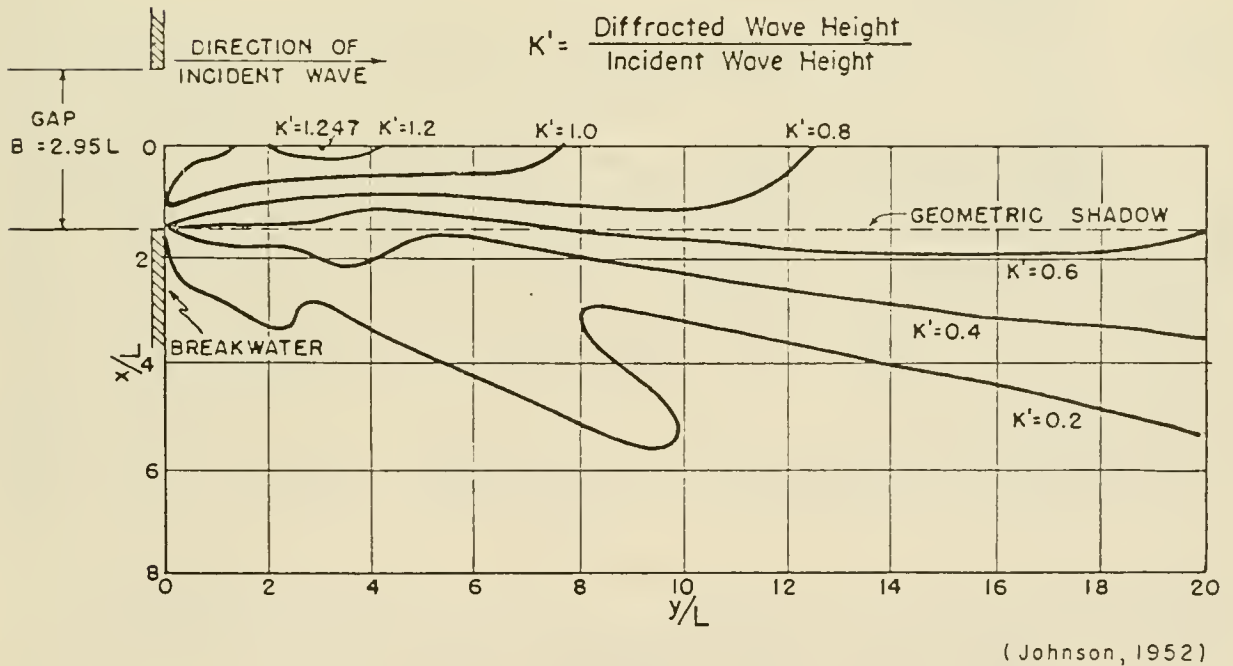


Figure 2-50. Contours of equal diffraction coefficient gap width = 2.95 wavelengths ( $B/L = 2.95$ ).

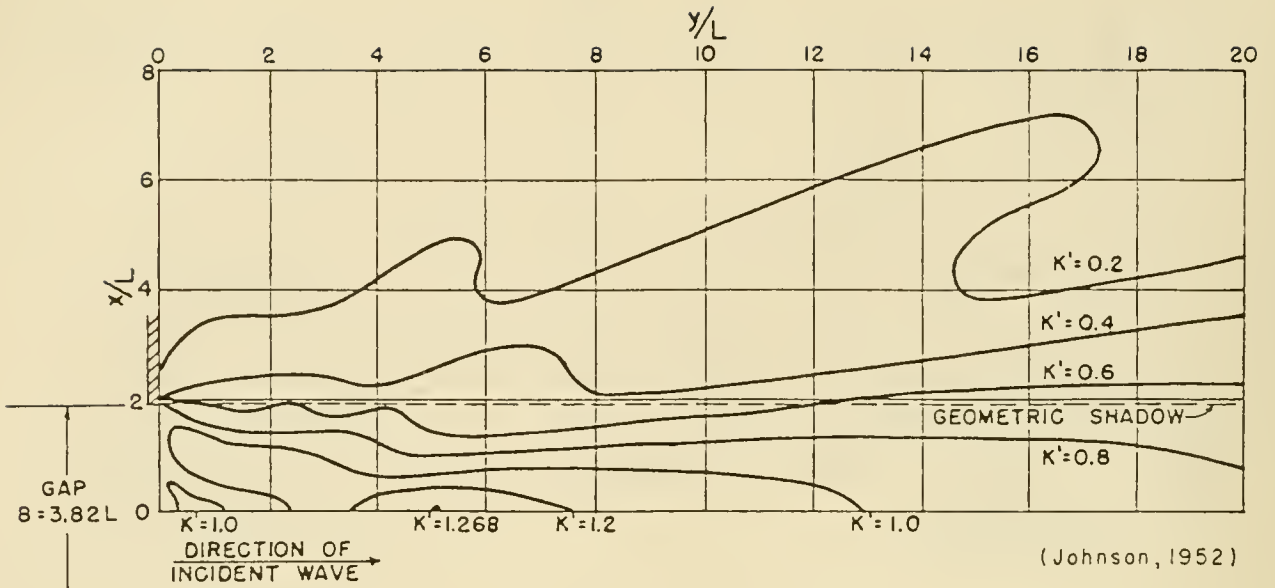


Figure 2-51. Contours of equal diffraction coefficient gap width = 3.82 wavelengths ( $B/L = 3.82$ ).

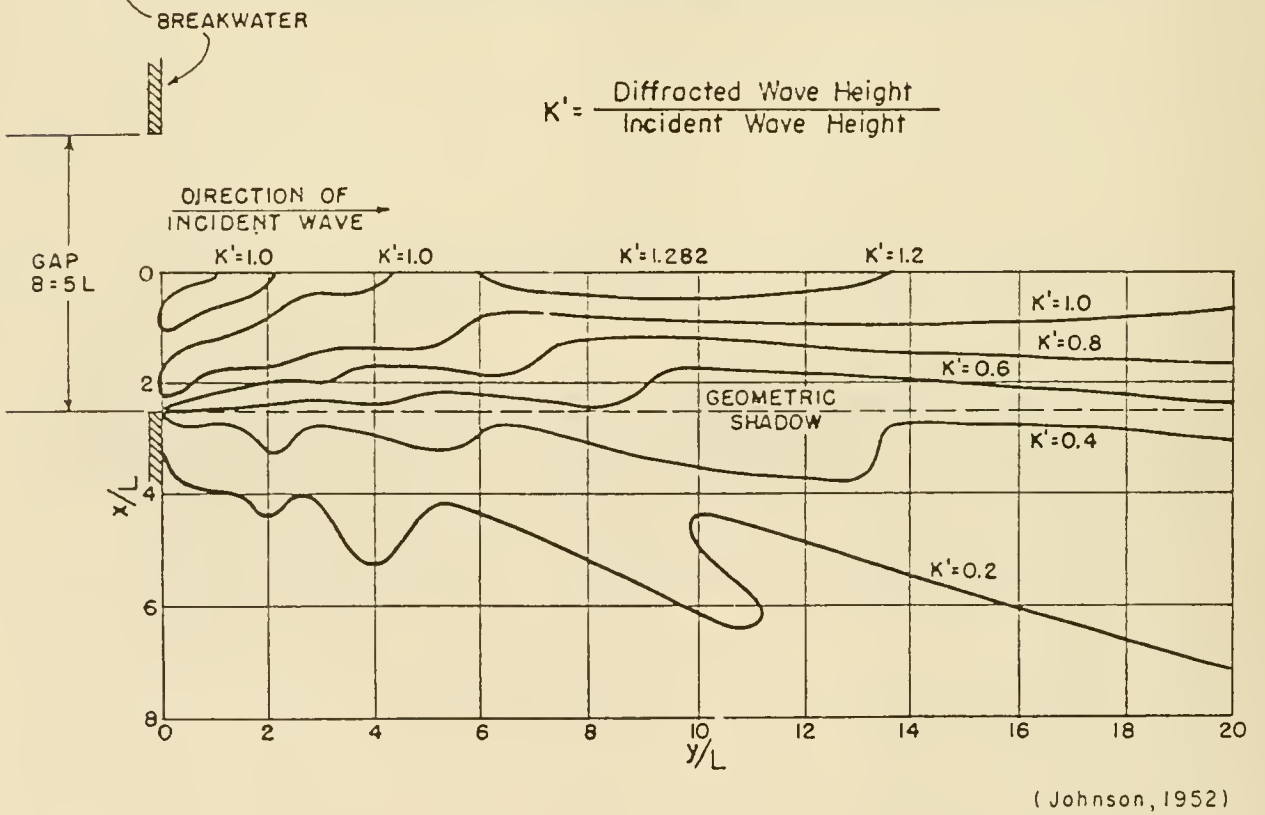


Figure 2-52. Contours of equal diffraction coefficient gap width = 5 wavelengths ( $B/L = 5$ ).

behind the breakwater may be approximated by an arc centered at the middle of the gap; crests to about six wavelengths may be approximated by two arcs, centered on the two ends of the breakwater and connected by a smooth curve (approximated by a circular arc centered at the middle of the gap). Only one-half of the diffraction diagram is presented on the figures since the diagrams are symmetrical about the line  $x/L = 0$ .

c. Waves Passing a Gap of Width Greater Than Five Wavelengths at Normal Incidence. Where the breakwater gap width is greater than five wavelengths, the diffraction effects of each wing are nearly independent, and the diagram (Fig. 2-33) for a single breakwater with a  $90^\circ$  wave approach angle may be used to define the diffraction characteristic in the lee of both wings (see Fig. 2-53).

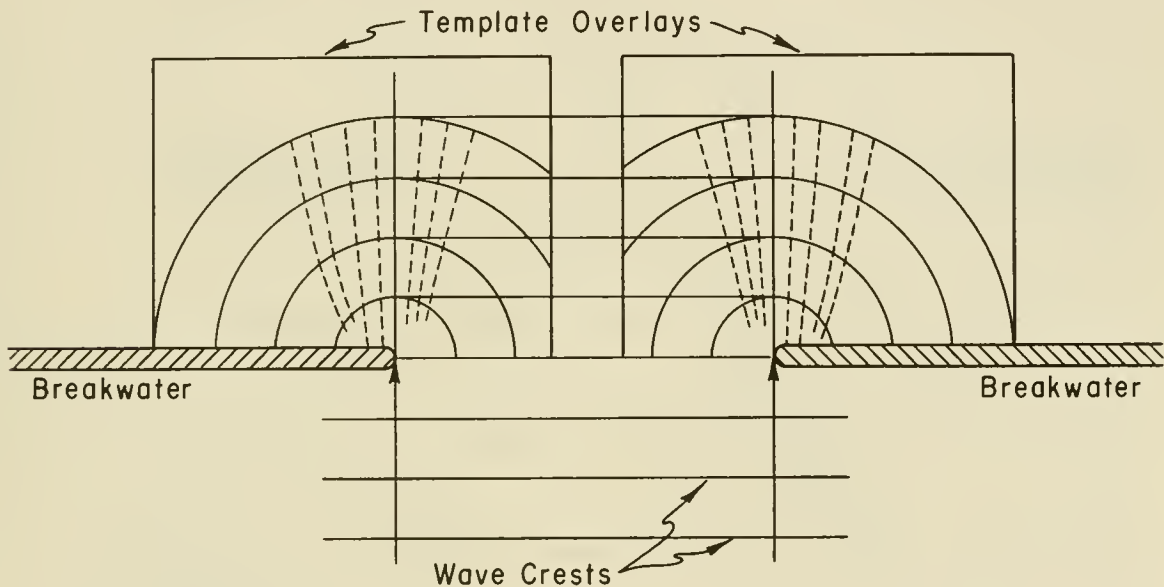
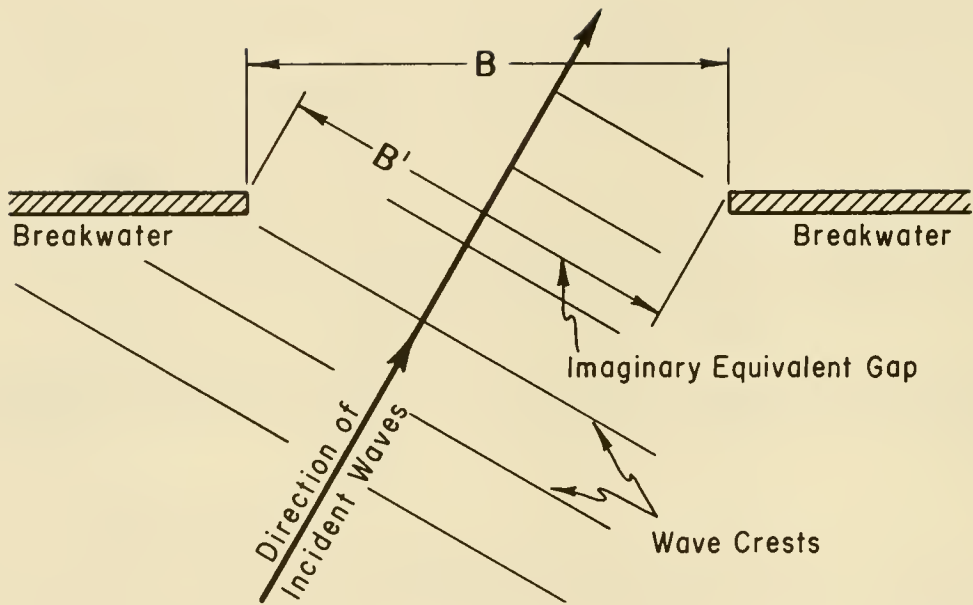


Figure 2-53. Diffraction for breakwater gap of width  $> 5L$  ( $B/L > 5$ ).

d. Diffraction at a Gap-Oblique Incidence. When waves approach at an angle to the axis of a breakwater, the diffracted wave characteristics differ from those resulting when waves approach normal to the axis. An approximate determination of diffracted wave characteristics may be obtained by considering the gap to be as wide as its projection in the direction of incident wave travel as shown in Figure 2-54. Calculated diffraction diagrams for wave approach angles of  $0^\circ$ ,  $15^\circ$ ,  $30^\circ$ ,  $45^\circ$ ,  $60^\circ$  and  $75^\circ$  are shown in Figures 2-55, 2-56, and 2-57. Use of these diagrams will give more accurate results than the approximate method. A comparison of a  $45^\circ$  incident wave using the approximate method and the more exact diagram method is shown in Figure 2-58.

e. Other Gap Geometries. Memos (1976, 1980a, 1980b, and 1980c) developed an approximate analytical solution for diffraction through a gap formed at the intersection of two breakwater legs with axes that are not collinear but intersect at an angle. The point of intersection of the breakwater axes coincides with the tip of one of the breakwaters. His solution can be developed for various angles of wave approach. Memos (1976) presented diffraction patterns for selected angles of approach.



(Johnson, 1952)

Figure 2-54. Wave incidence oblique to breakwater gap.

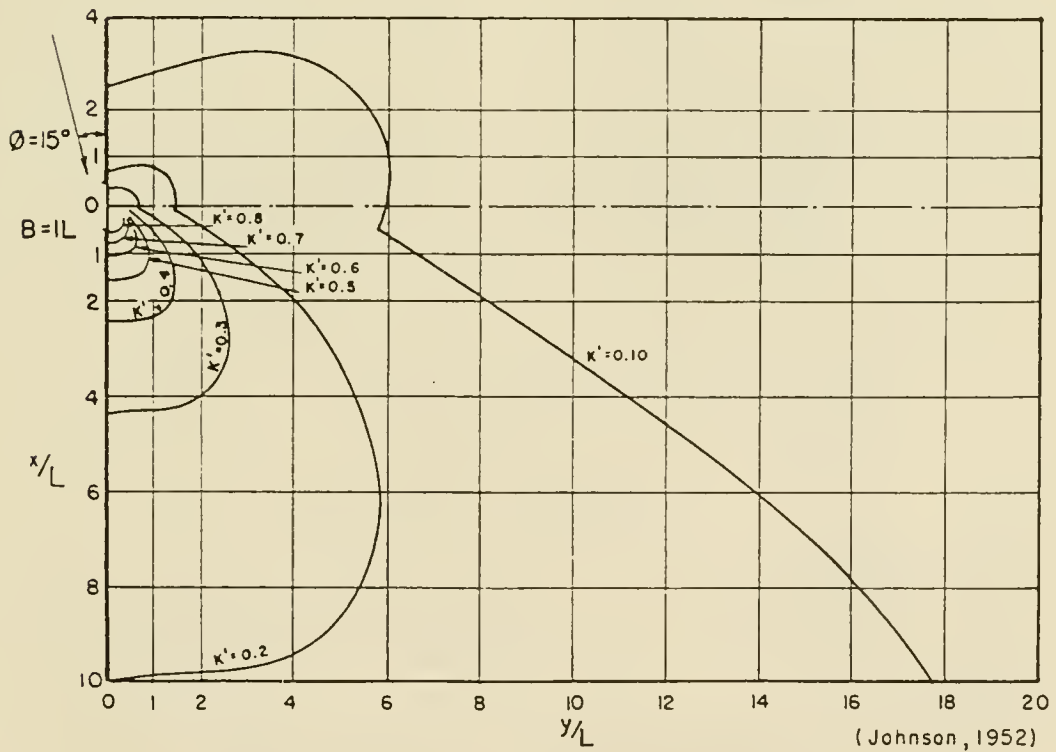
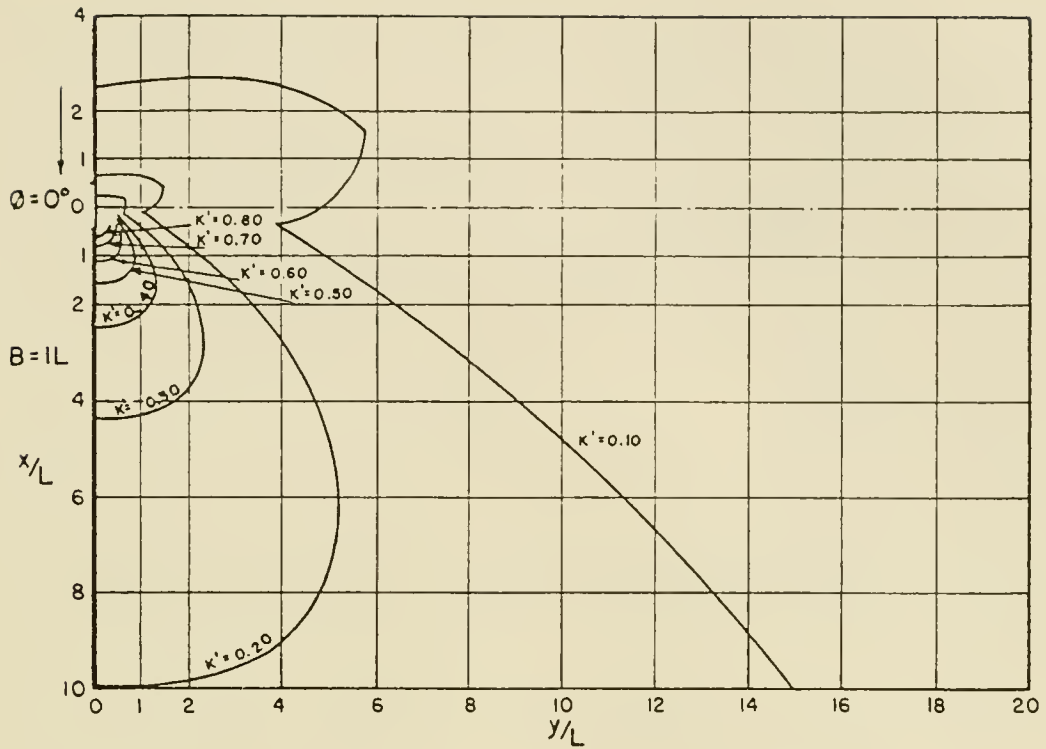


Figure 2-55. Diffraction for a breakwater gap of one wavelength width where  $\phi = 0^\circ$  and  $15^\circ$ .

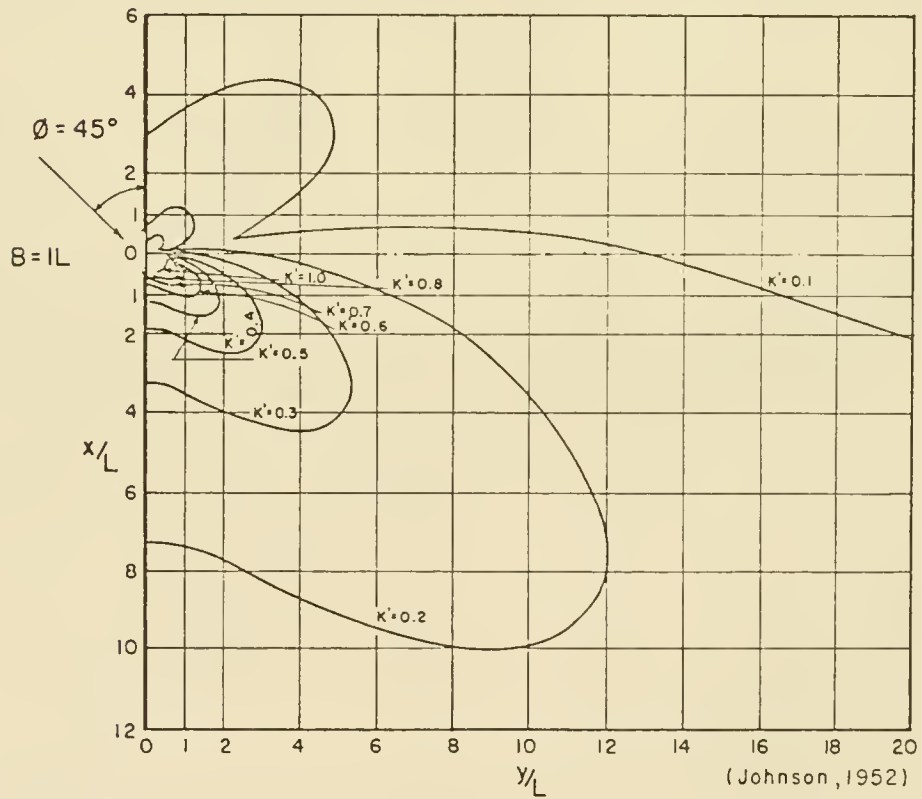
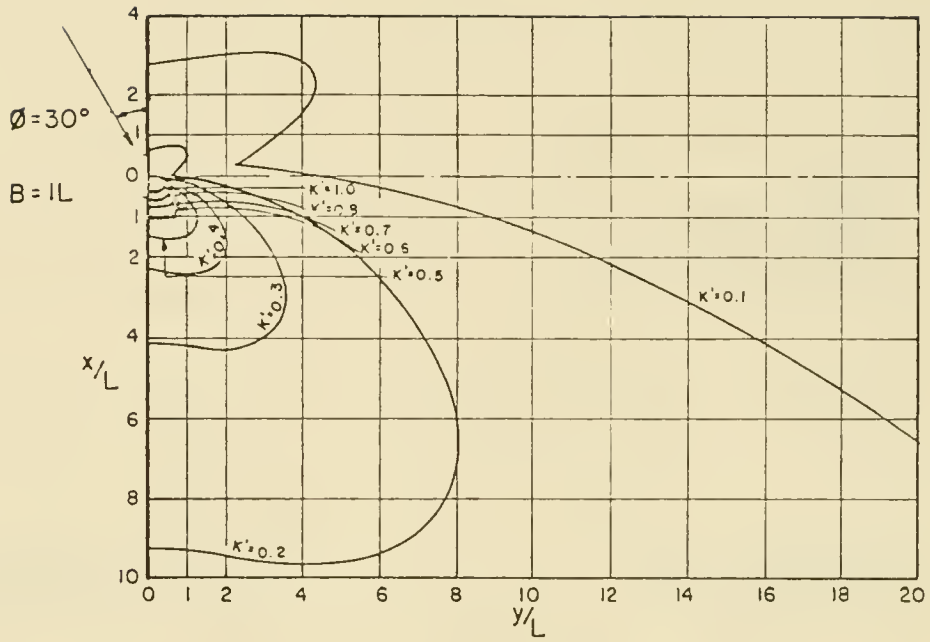


Figure 2-56. Diffraction for a breakwater gap of one wavelength width where  $\phi = 30^\circ$  and  $45^\circ$ .

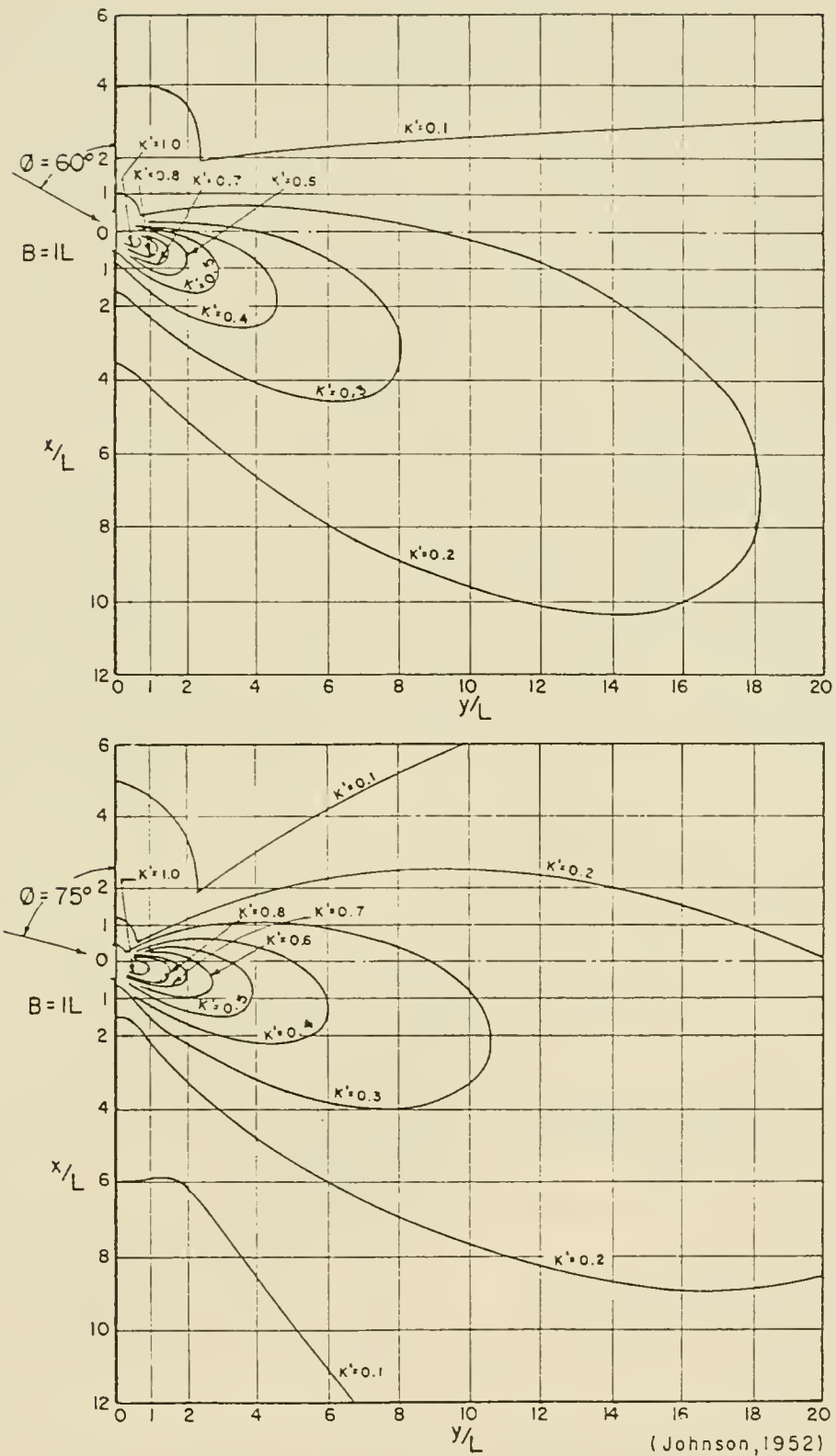
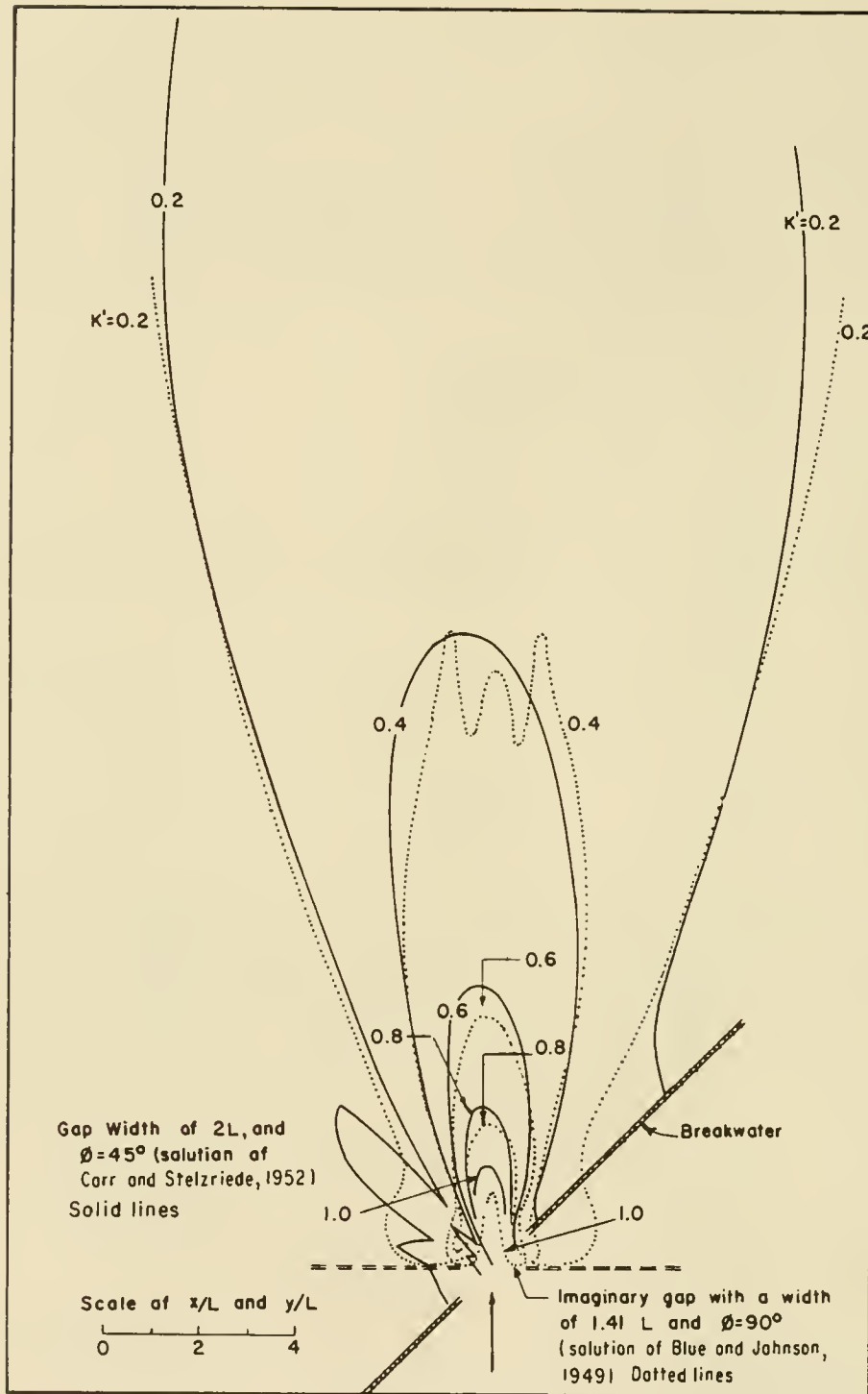


Figure 2-57. Diffraction for a breakwater gap of one wavelength width where  $\phi = 60^\circ$  and  $75^\circ$ .



(Johnson, 1952)

Figure 2-58. Diffraction diagram for a gap of two wavelengths and a  $45^\circ$  approach compared with that for a gap width  $\sqrt{2}$  wavelengths with a  $90^\circ$  approach.

f. Diffraction Around an Offshore Breakwater. In recent years there has been increased interest in using offshore breakwaters as shoreline stabilization structures. Reorientation of the shoreline in response to the waves diffracted around the breakwater tips is of interest. The diffraction pattern in the lee of a single breakwater can be approximated by superimposing two semi-infinite breakwater diffraction patterns. One diffraction diagram is centered at each end of the breakwater and a combined diffraction coefficient determined (Harms, 1979; Harms, et al., 1979). The approximate superposition solution is valid about two wavelengths behind the breakwater and beyond. Close to the breakwater and in front of it the solution is not valid. For waves approaching perpendicular to the breakwater, the diffraction pattern for one end is the mirror image of the pattern for the other end. For nonperpendicular wave approach, the diffraction pattern for one end is the mirror image for the supplementary angle of the diffraction pattern for the other end, as shown on Figure 2-59. If the incident waves are long crested and monochromatic, the wave propagating around each breakwater tip will either reinforce or cancel each other depending on their relative phase. To calculate the relative phase angle of the two wave components, crest patterns must be constructed. Behind the breakwater in the shadow zone the crests can be approximated by circular arcs centered at each breakwater tip. On the wave crest diagram where two crests or two troughs intersect, the two wave components will be in phase; where a wave crest crosses a wave trough, the waves will be 180° out of phase (see Fig. 2-59). Lines of constant phase difference could be constructed. These would be lines radiating outward from the breakwater as shown in Figure 2-59. The diffraction coefficient for the composite wave field can be calculated from the diffraction coefficients of the waves coming around each breakwater tip by

$$K'^2 = K'_L{}^2 + K'_R{}^2 + 2K'_L K'_R \cos \theta$$

where

$K'$  = combined diffraction coefficient

$K'_L$  = diffraction coefficient for the waves coming around the left tip of the breakwater

$K'_R$  = diffraction coefficient for the waves coming around the right tip of the breakwater

$\theta$  = phase difference between the two component waves at the point of interest

Application of the approximate method is illustrated here by an example problem.

\*\*\*\*\* EXAMPLE PROBLEM 10 \*\*\*\*\*

GIVEN: A breakwater 200 meters (656 feet) long is built in water 5 meters (16.4 feet) deep. Waves with a period  $T = 10$  seconds and a height  $H = 3$  meters (9.8 feet) approach at such an angle that the incoming wave crests make a 30° angle with the breakwater's axis.

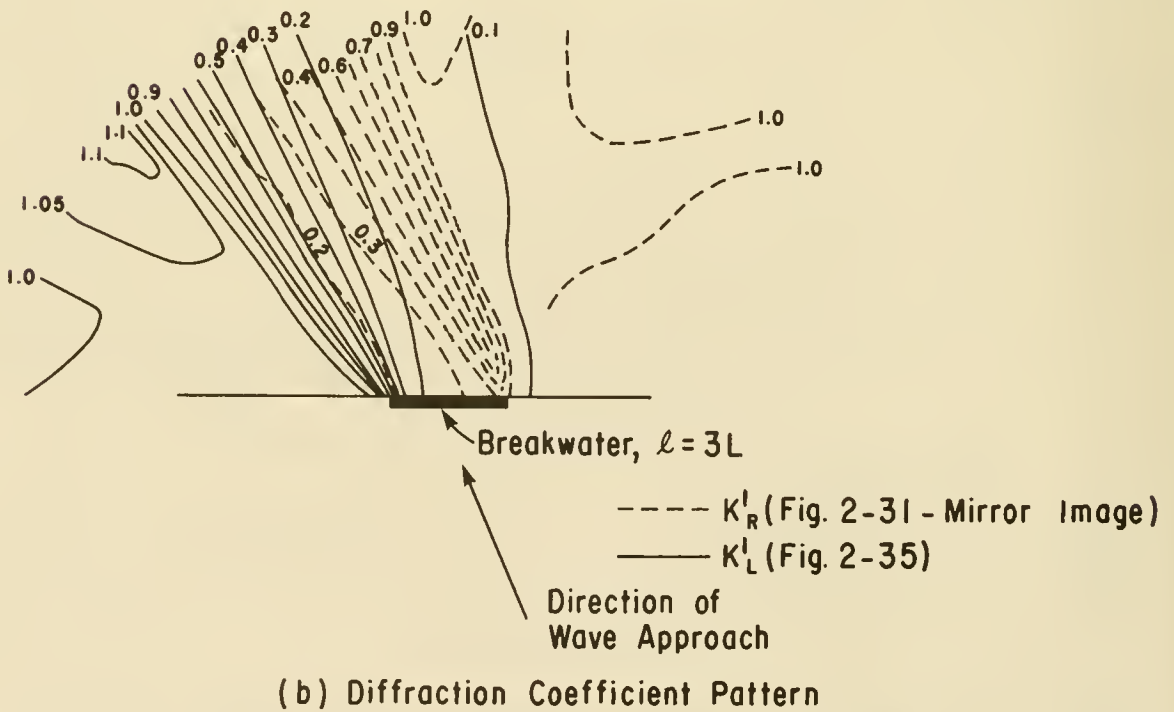
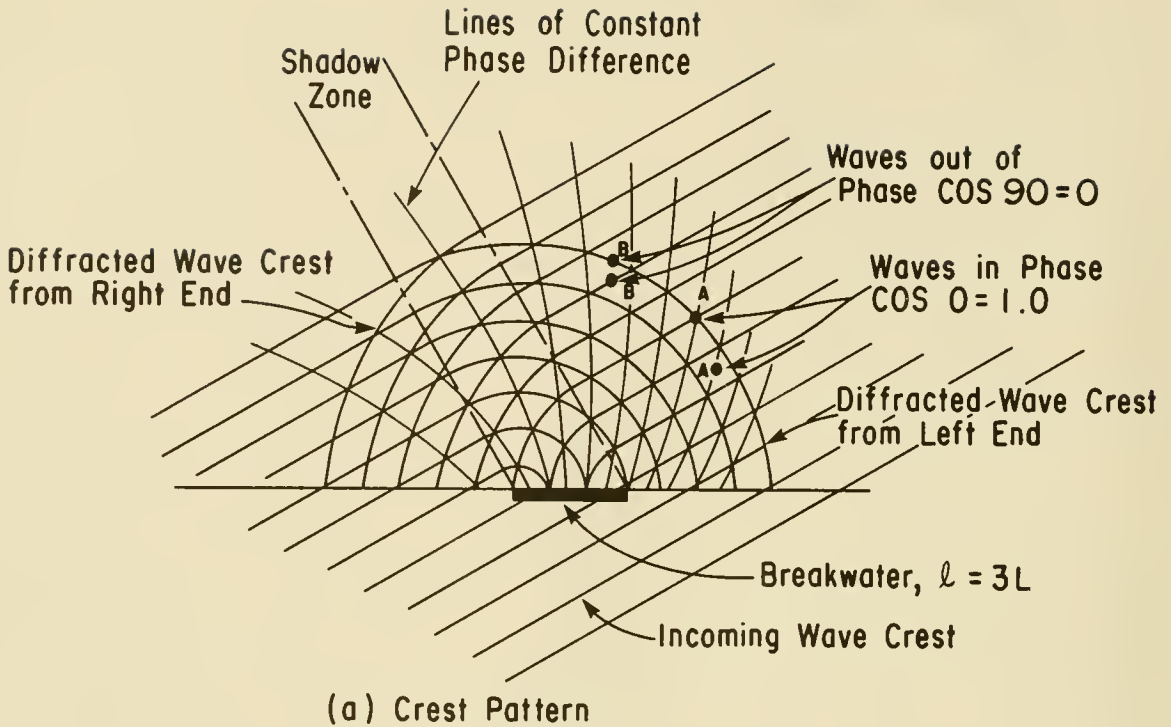


Figure 2-59. Approximate method for computing wave diffraction around an offshore breakwater.

FIND: The approximate diffraction pattern in the lee of the breakwater and the wave height three wavelengths behind the center of the breakwater.

SOLUTION: Determine the wavelength in the water depth  $d = 5$  meters.

$$L_o = \frac{gT^2}{2\pi} = 1.56(10)^2 = 156 \text{ m (512 ft)}$$

$$\frac{d}{L_o} = \frac{5}{156} = 0.0321$$

Enter Table C-1, Appendix C, with the calculated value of  $d/L_o$  and find

$$\frac{d}{L} = 0.0739$$

Therefore,  $L = 5/0.0739 = 67.7$  meters (222 ft). The breakwater is therefore  $200/67.7 = 2.95$  wavelengths long (say, three wavelengths). The appropriate semi-infinite breakwater diffraction patterns are given in Figure 2-35 and in the mirror image of Figure 2-31. The diffraction patterns are scaled in accordance with the calculated wavelength.

\* \* \* \* \*

From the mirror image of Figure 2-31, the diffraction coefficient three wavelengths behind the center of the breakwater gives  $K_R = 0.6$ . From Figure 2-35,  $K_L$  equals 0.15 for the same point. The relative phase angle between the two waves coming around the two ends is  $\theta \cong 182^\circ$  and the combined diffraction coefficient

$$K' = \sqrt{K_R'^2 + K_L'^2 + 2K_L' K_R' \cos \theta}$$

$$K' = \sqrt{(0.6)^2 + (0.15)^2 + 2(0.6)(0.15) \cos 182^\circ}$$

(2-79)

$$K' = \sqrt{0.36 + 0.0225 + (0.18)(-0.999)}$$

$$K' = \sqrt{0.2026} = 0.450$$

Therefore,  $H = 0.450 (3) = 1.35$  meters (4.44 feet). The approximate diffraction pattern can be constructed by determining the diffraction coefficients at various locations behind the breakwater and drawing contour lines of equal diffraction coefficient. The pattern for the example problem is shown in Figure 2-60. The same procedure of superimposing diffraction diagrams could be used for a series of offshore breakwaters using diffraction patterns for wave propagation through a breakwater gap. Equation 2-79 applies to this situation as well. The results of the preceding analysis is approximate. Montefusco (1968) and Goda, Yoshimura, and Ito (1971) have worked out analytical solutions, and others (e.g., Harms, 1979; Harms, et al., 1979) have developed

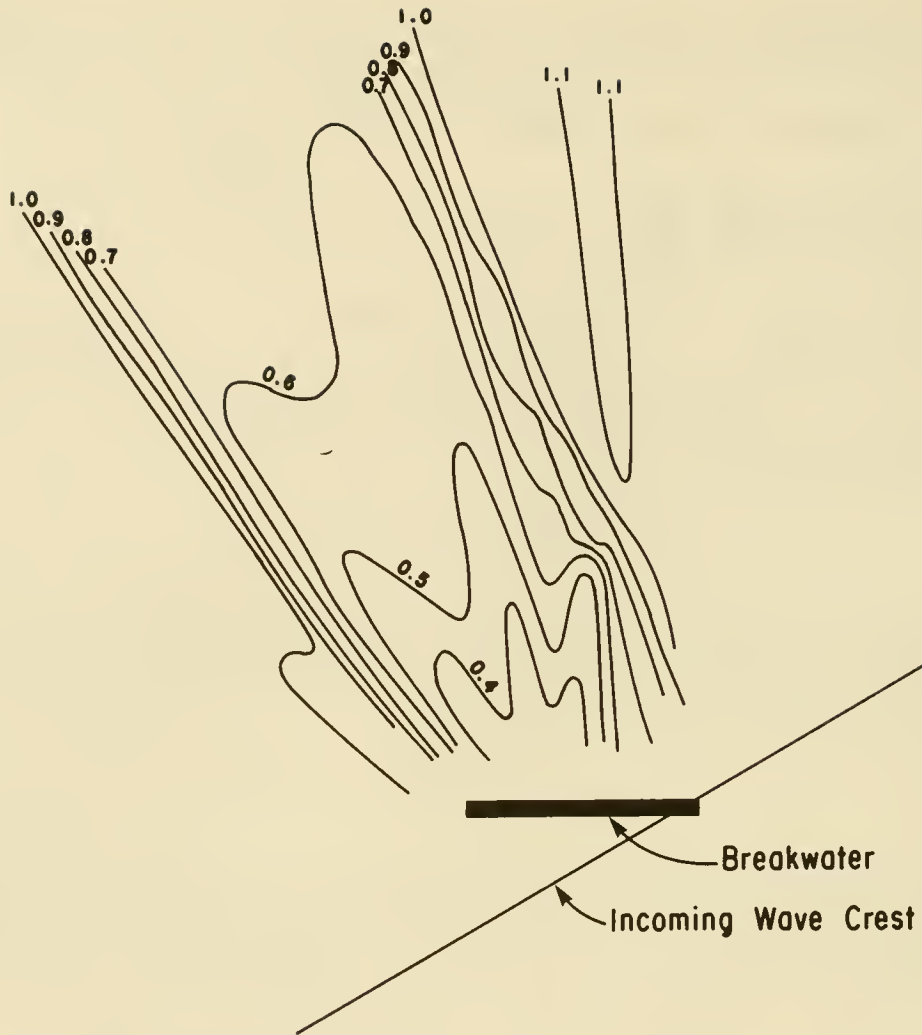


Figure 2-60. Wave diffraction pattern behind an offshore breakwater three wavelengths long for waves approaching at a  $30^\circ$  angle.

numerical computer solutions to the offshore structure diffraction problem for structures of arbitrary planform. Better accuracy in proximity to the structure and definition of the reflected wave field in front of the structure are given by these solutions.

g. Diffraction of Irregular Waves. The preceding discussions of diffraction phenomena deal only with monochromatic waves. Waves in the real world are usually made up of many components having different periods or frequencies (see Ch. 3). The combination of wave heights and frequencies present in the sea forms what is termed a wave spectrum. For a wave spectrum, each wave frequency is diffracted in accordance with its local wavelength. For diffraction around offshore breakwaters, the handlike pattern of Figure 2-59 will not be well defined because of the range of phase differences among the many wave components propagating around each breakwater tip. Diffraction of irregular waves by a breakwater gap has been studied by Wiegel, Al-Kazily, and Raissi (1971), Raissi and Wiegel (1978), and Goda, Takayama, and Suzuki (1978). The study by Goda, Takayama, and Suzuki takes into account an initial spreading of

the incident wave direction and presents diffraction diagrams for various gap widths. This work and the resulting diffraction diagrams are presented in Chapter 7.

### 3. Refraction and Diffraction Combined.

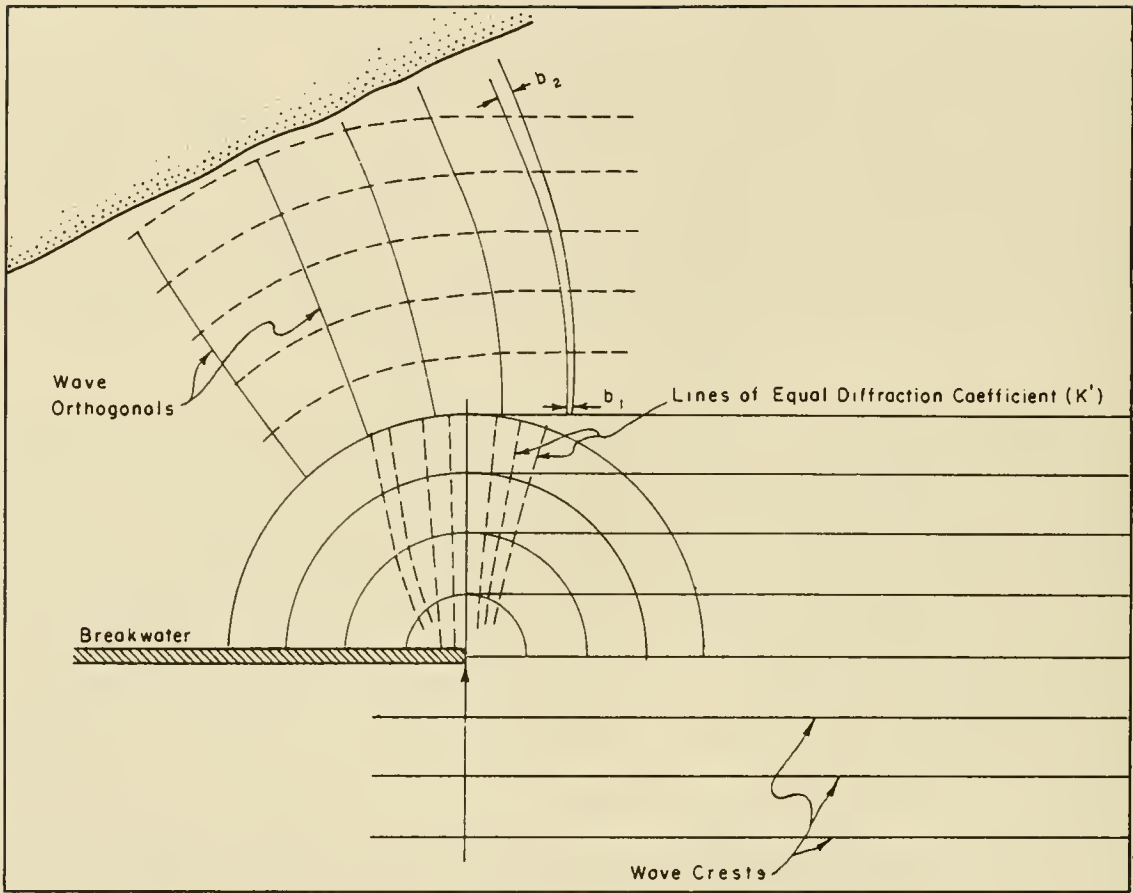
Usually the bottom seaward and shoreward of a breakwater is not flat; therefore, refraction occurs in addition to diffraction. Although a general unified theory of the two has only been developed for a few special cases, some insight into the problem is presented by Battjes (1968), and Berkoff (1972). Battjes (1968) shows that contrary to what numerous investigators have stated, there is no lateral transfer of energy along a wave crest but that all energy flux is along an orthogonal. Berkoff (1972) develops the equations that govern the combined refraction-diffraction phenomenon and uses finite-element models to numerically calculate the propagation of long waves around an island and over a parabolic shoal. He also investigated the response of a rectangular harbor with constant bottom slope to incident shore waves.

More recently, Liu and Lozano (1979), Lozano (1980), and Liu (1982) studied analytically the behavior of waves in the vicinity of a thin groin extending seaward from a sloping beach. Liu (1982) compared their analytical results with the experimental data obtained by Hales (1980) of combined refraction-diffraction around a jetty on a sloping beach with good agreement. Lozano and Liu (1980) compared the analytical solution with experimental data obtained by Whalin (1972) for wave propagation over a semicircular shoal, again with good agreement in the shadow region of the structure. An approximate picture of wave changes may be obtained by (a) constructing a refraction diagram shoreward to the breakwater; (b) at this point, constructing a diffraction diagram carrying successive crests three or four wavelengths shoreward, if possible; and (c) with the wave crest and wave direction indicated by the last shoreward wave crest determined from the diffraction diagram, constructing a new refraction diagram to the breaker line. The work of Mobarek (1962) on the effect of bottom slope on wave diffraction indicates that the method presented here is suitable for medium-period waves. For long-period waves the effect of shoaling (Sec. III,2) should be considered. For the condition when the bottom contours are parallel to the wave crests, the sloping bottom probably has little effect on diffraction. A typical refraction-diffraction diagram and the method for determining combined refraction-diffraction coefficients are shown in Figure 2-61.

## V. WAVE REFLECTION

### 1. General.

Water waves may be either partially or totally reflected from both natural and manmade barriers (see Fig. 2-62). Wave reflection may often be as important a consideration as refraction and diffraction in the design of coastal structures, particularly for structures associated with harbor development. Reflection of waves implies a reflection of wave energy as opposed to energy dissipation. Consequently, multiple reflections and absence of sufficient energy dissipation within a harbor complex can result in a buildup of energy which appears as wave agitation and surging in the harbor. These surface fluctuations may cause excessive motion of moored ships and other floating



Overall refraction-diffraction coefficient is given  
 by  $(K_R)(K^1)\sqrt{b_1/b_2}$   
 Where  $K_R$  = Refraction coefficient to breakwater  
 $K^1$  = Diffraction coefficient at point on  
 diffracted wave crest from which  
 orthogonal is drawn.  
 $b_1$  = Orthogonal spacing at diffracted wave  
 crest.  
 $b_2$  = Orthogonal spacing nearer shore.

Figure 2-61. Single breakwater, refraction-diffraction combined.



Figure 2-62. Wave reflection at Hamlin Beach, New York.

facilities, and result in the development of great strains on mooring lines. Therefore seawalls, bulkheads, and revetments inside of harbors should dissipate rather than reflect incident wave energy whenever possible. Natural beaches in a harbor are excellent wave energy dissipaters, and proposed harbor modifications which would decrease beach areas should be carefully evaluated prior to construction. Hydraulic model studies are often necessary to evaluate such proposed changes. The importance of wave reflection and its effect on harbor development are discussed by Bretschneider (1966), Lee (1964), and LeMehaute (1965); harbor resonance is discussed by Raichlen (1966).

A measure of how much a barrier reflects waves is given by the ratio of the reflected wave height  $H_r$  to the incident wave height  $H_i$  which is termed the reflection coefficient  $\chi$ ; hence  $\chi = H_r/H_i$ . The magnitude of  $\chi$  varies from 1.0 for total reflection to 0 for no reflection; however, a small value of  $\chi$  does not necessarily imply that wave energy is dissipated by a structure since energy may be transmitted through some structures such as permeable, rubble-mound breakwaters. A transmission coefficient may be defined as the ratio of transmitted wave height  $H_t$  to incident wave height  $H_i$ . In general, both the reflection coefficient and the transmission coefficient will depend on the geometry and composition of a structure and the incident wave characteristics such as wave steepness and relative depth  $d/L$  at the structure site.

## 2. Reflection from Impermeable, Vertical Walls (Linear Theory).

Impermeable vertical walls will reflect most incident wave energy unless they are fronted by rubble toe protection or are extremely rough. The reflection coefficient  $\chi$  is therefore equal to approximately 1.0, and the height of a reflected wave will be equal to the height of the incident wave. Although some experiments with smooth, vertical, impermeable walls appear to show a significant decrease of  $\chi$  with increasing wave steepness, Domzig (1955) and Goda and Abe (1968) have shown that this paradox probably results from the experimental technique, based on linear wave theory, used to determine  $\chi$ . The use of a higher order theory to describe the water motion in front of the wall gives a reflection coefficient of 1.0 and satisfies the conservation of energy principle.

Wave motion in front of a perfectly reflecting vertical wall subjected to monochromatic waves moving in a direction perpendicular to the barrier can be determined by superposing two waves with identical wave numbers, periods and amplitudes but traveling in opposite directions. The water surface of the incident wave is given to a first-order (linear) approximation by equation (2-10)

$$\eta_i = \frac{H_i}{2} \cos \left( \frac{2\pi x}{L} - \frac{2\pi t}{T} \right)$$

and the reflected wave by

$$\eta_r = \frac{H_r}{2} \cos \left( \frac{2\pi x}{L} + \frac{2\pi t}{T} \right)$$

Consequently, the water surface is given by the sum of  $\eta_i$  and  $\eta_r$ , or, since  $H_i = H_r$ ,

$$\eta = \eta_i + \eta_r = \frac{H_i}{2} \left[ \cos \left( \frac{2\pi x}{L} - \frac{2\pi t}{T} \right) + \cos \left( \frac{2\pi x}{L} + \frac{2\pi t}{T} \right) \right]$$

which reduces to

$$\eta = H_i \cos \frac{2\pi x}{L} \cos \frac{2\pi t}{T} \quad (2-80)$$

Equation 2-80 represents the water surface for a standing wave or *clapotis* which is periodic in time and in  $x$  having a maximum height of  $2H_i$  when both  $\cos(2\pi x/L)$  and  $\cos(2\pi t/T)$  equal 1. The water surface profile as a function of  $2\pi x/L$  for several values of  $2\pi t/T$  is shown in Figure 2-63. There are some points (nodes) on the profile where the water surface remains at the SWL for all values of  $t$  and other points (antinodes) where the water particle excursion at the surface is  $2H_i$  or twice the incident wave height. The equations describing the water particle motion show that the velocity is always horizontal under the nodes and always vertical under the antinodes. At intermediate points, the water particles move along diagonal lines as shown in Figure 2-63. Since water motion at the antinodes is purely vertical, the presence of a vertical wall at any antinode will not change the flow pattern described since there is no flow across the vertical barrier and equivalently, there is no flow across a vertical line passing through an antinode. (For the linear theory discussion here, the water contained between any two antinodes will remain between those two antinodes.) Consequently, the flow described here is valid for a barrier at  $2\pi x/L = 0$  ( $x = 0$ ) since there is an antinode at that location.

### 3. Reflections in an Enclosed Basin.

Some insight can be obtained about the phenomenon of the resonant behavior of harbors and other enclosed bodies of water by examining the standing wave system previously described. The possible resonant oscillations between two vertical walls can be described by locating the two barriers so that they are both at antinodes; e.g., barriers at  $x = 0$  and  $\pi$  or  $x = 0$  and  $2\pi$ , etc., represent possible modes of oscillation. If the barriers are taken at  $x = 0$  and  $x = \pi$ , there is one-half of a wave in the basin, or if  $l_B$  is the basin length,  $l_B = L/2$ . Since the wavelength is given by equation (2-4)

$$L = \frac{gT^2}{2\pi} \tanh \left( \frac{2\pi d}{L} \right)$$

the period of this fundamental mode of oscillation is

$$T = \left[ \frac{4\pi l_B}{g \tanh(\pi d/l_B)} \right]^{1/2} \quad (2-81)$$

The next possible resonant mode occurs when there is one complete wave in the basin (barriers at  $x = 0$  and  $x = 2\pi$ ) and the next mode when there are 3/2 waves in the basin (barriers at  $x = 0$  and  $x = 3\pi/2$ , etc.). In general,  $l_B = jL/2$ , where  $j = 1, 2, \dots$ . In reality, the length of a natural or manmade basin  $l_B$  is fixed and the wavelength of the resonant wave contained in the basin will be the variable; hence,

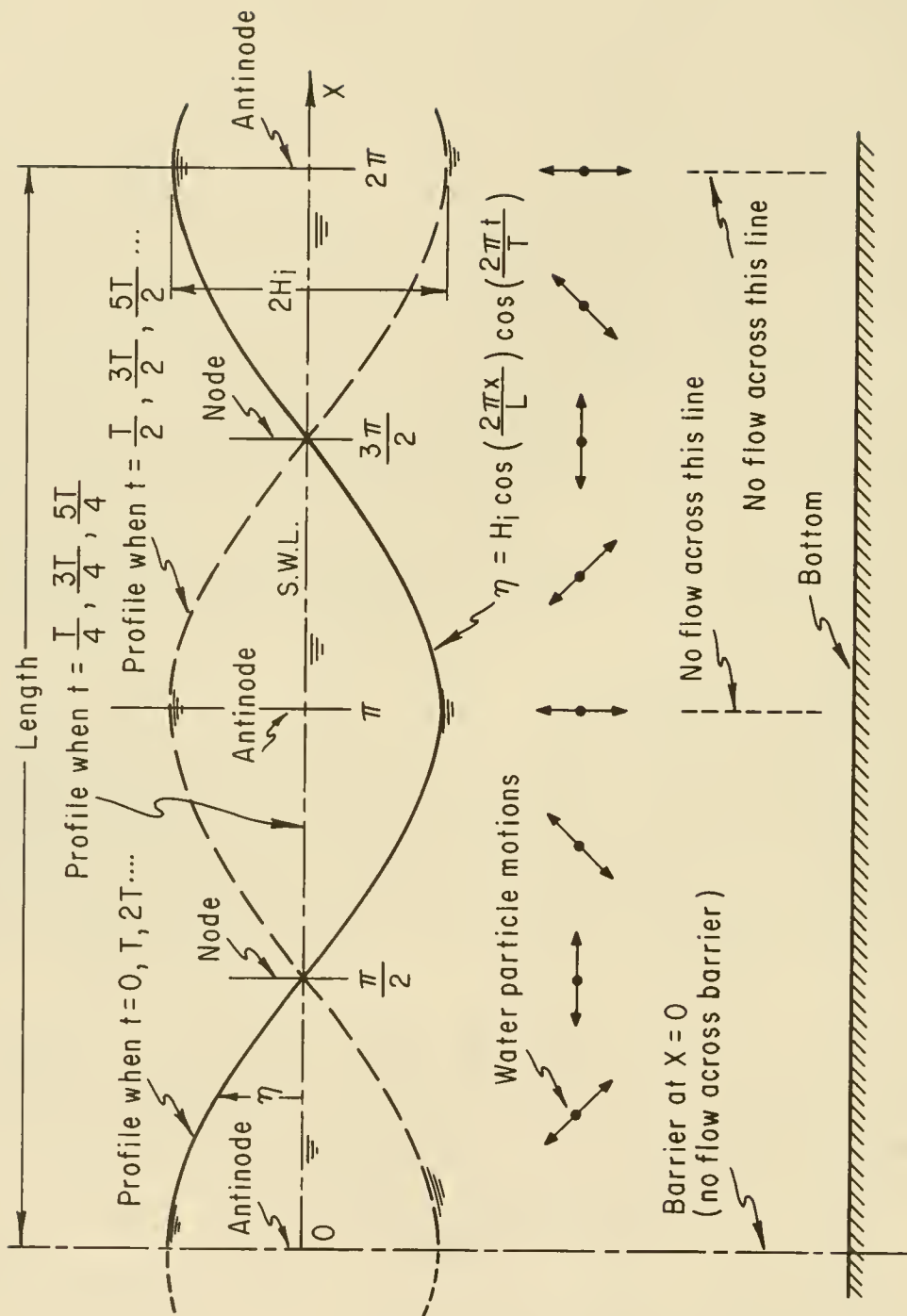


Figure 2-63. Standing wave (clapotis) system, perfect reflection from a vertical barrier, linear theory.

$$L = \frac{2\ell_B}{j} \quad j = 1, 2, \dots \quad (2-82)$$

may be thought of as defining the wavelengths capable of causing resonance in a basin of length  $\ell_B$ . The general form of equation (2-81) is found by substituting equation (2-82) into the expression for the wavelength; therefore,

$$T_j = \left[ \frac{4\pi\ell_B}{jg \tanh(\pi jd/\ell_B)} \right]^{1/2}, \quad j = 1, 2, \dots \quad (2-83)$$

For an enclosed harbor, of approximately rectangular planform with length  $\ell_B$ , waves entering through a breakwater gap having a predominant period close to one of those given by equation (2-83) for small values of  $j$  may cause significant agitation unless some effective energy dissipation mechanism is present. The addition of energy to the basin at the resonant (or excitation) frequency ( $f_j = 1/T_j$ ) is said to *excite* the basin.

Equation (2-83) was developed by assuming the end boundaries to be vertical; however, it is still approximately valid so long as the end boundaries remain highly reflective to wave motion. Sloping boundaries, such as beaches, while usually effective energy dissipaters, may be significantly reflective if the incident waves are extremely long. The effect of sloping boundaries and their reflectivity to waves of differing characteristics is given in Section V,4.

Long-period resonant oscillations in large lakes and other large enclosed bodies of water are termed *seiches*. The periods of seiches may range from a few minutes up to several hours, depending on the geometry of the particular basin. In general, these basins are shallow with respect to their length; hence,  $\tanh(\pi jd/\ell_B)$  in equation (2-83) becomes approximately equal to  $\pi jd/\ell_B$  and

$$T_j = \frac{2\ell_B}{j} \frac{1}{(gd)^{1/2}} \quad j = 1, 2, \dots \text{ (small values)} \quad (2-84)$$

Equation (2-84) is termed Merian's equation. In natural basins, complex geometry and variable depth will make the direct application of equation (2-84) difficult; however, it may serve as a useful first approximation for enclosed basins. For basins open at one end, different modes of oscillation exist since resonance will occur when a node is at the open end of the basin and the fundamental oscillation occurs when there is one-quarter of a wave in the basin; hence,  $\ell_B' = L/4$  for the fundamental mode and  $T = 4\ell_B'/\sqrt{gd}$ . In general  $\ell_B' = (2j - 1)L/4$ , and

$$T_j = \frac{4\ell_B'}{(2j - 1)} \frac{1}{(gd)^{1/2}} \quad j = 1, 2, \dots \text{ (small values)} \quad (2-85)$$

Note that higher modes occur when there are 3, 5, ...,  $2j - 1$ , etc., quarters of a wave within the basin.

GIVEN: Lake Erie has a mean depth  $d = 18.6$  meters (61 feet) and its length  $l_B$  is 354 kilometers (220 miles)

FIND: The fundamental period of oscillation  $T_j$ , if  $j = 1$ .

SOLUTION: From equation (2-84) for an enclosed basin,

$$T_1 = \frac{2l_B}{j} \frac{1}{(gd)^{1/2}}$$

$$T_1 = \frac{2(354,000)}{1} \frac{1}{[9.8(18.6)]^{1/2}}$$

$$T_1 = 52\,440 \text{ s or } 14.57 \text{ h}$$

Considering the variability of the actual lake cross section, this result is surprisingly close to the actual observed period of 14.38 hours (Platzman and Rao, 1963). Such close agreement may not always result.

\*\*\*\*\*

Note: Additional discussion of seiching is presented in Chapter 3, Section VIII, 4.

4. Wave Reflection from Plane Slopes, Beaches, Revetments, and Breakwaters.

The amount of wave energy reflected from a beach or a manmade structure depends on the slope, roughness, and permeability of the beach or structure, and also on the wave steepness and angle of wave approach. Battjes (1974) found that the surf similarity parameter given by

$$\xi = \frac{1.0}{\cot\theta \sqrt{H_1/L_0}} \tag{2-86}$$

is an important parameter for determining the amount of reflection of waves approaching a beach or structure at a right angle. In equation (2-86),  $\theta$  is the angle the beach or structure slope makes with a horizontal,  $H_1$  the incident wave height, and  $L_0$  the deepwater wavelength (see Fig. 2-64). The amount of reflection is given by the reflection coefficient

$$X = \frac{H_r}{H_1} \tag{2-87}$$

in which  $H_r$  is the height of the reflected wave, and  $H_1$  the height of the incident wave.

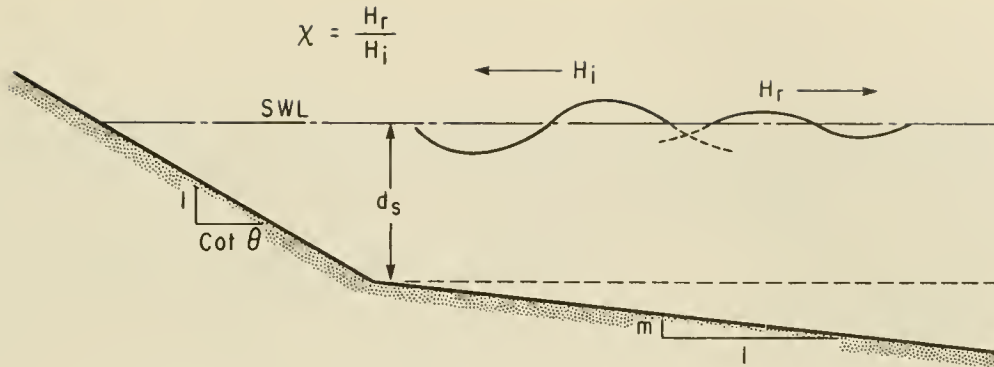


Figure 2-64. Definition of wave reflection terms.

Based on a compilation of measurements from several sources, Seelig and Ahrens (1981) developed the curves in Figure 2-65. These curves can be used to obtain a high estimate of the reflection coefficient for smooth slopes, sand beaches, and rubble-mound breakwaters (curves A, B, and C, respectively). The curves show that the wave reflection coefficient decreases as either the wave steepness increases or as the slope angle  $\theta$  decreases.

\*\*\*\*\* EXAMPLE PROBLEM 12 \*\*\*\*\*

**GIVEN:** An incident wave with period  $T = 10$  seconds and a wave height  $H_i = 2$  meters (6.56 feet) impinges on a slope.

**FIND:**

- (a) The height of the wave reflected from an impermeable slope with  $\cot\theta = 5.0$ .
- (b) Compare the reflection coefficient obtained in (a) above with that obtained for a beach with  $\cot\theta = 50$ .

**SOLUTION:** Calculate

(a) 
$$L_o = \frac{gT^2}{2\pi} = \frac{9.8(100)}{2\pi} = 156 \text{ m (512 ft)}$$

and from equation (2-86)

$$\xi = \frac{1.0}{5.0 \sqrt{2/156}} = 1.77$$

The reflection coefficient from curve A for plane slopes in Figure 2-65 is  $\chi = 0.29$ ; therefore, the reflected wave height is  $H_r = 0.29(2) = 0.58$  meter (1.90 feet).

(b) For a 1 on 50 sloped beach,

$$\xi = \frac{1.0}{50.0 \sqrt{2/156}} = 0.18$$

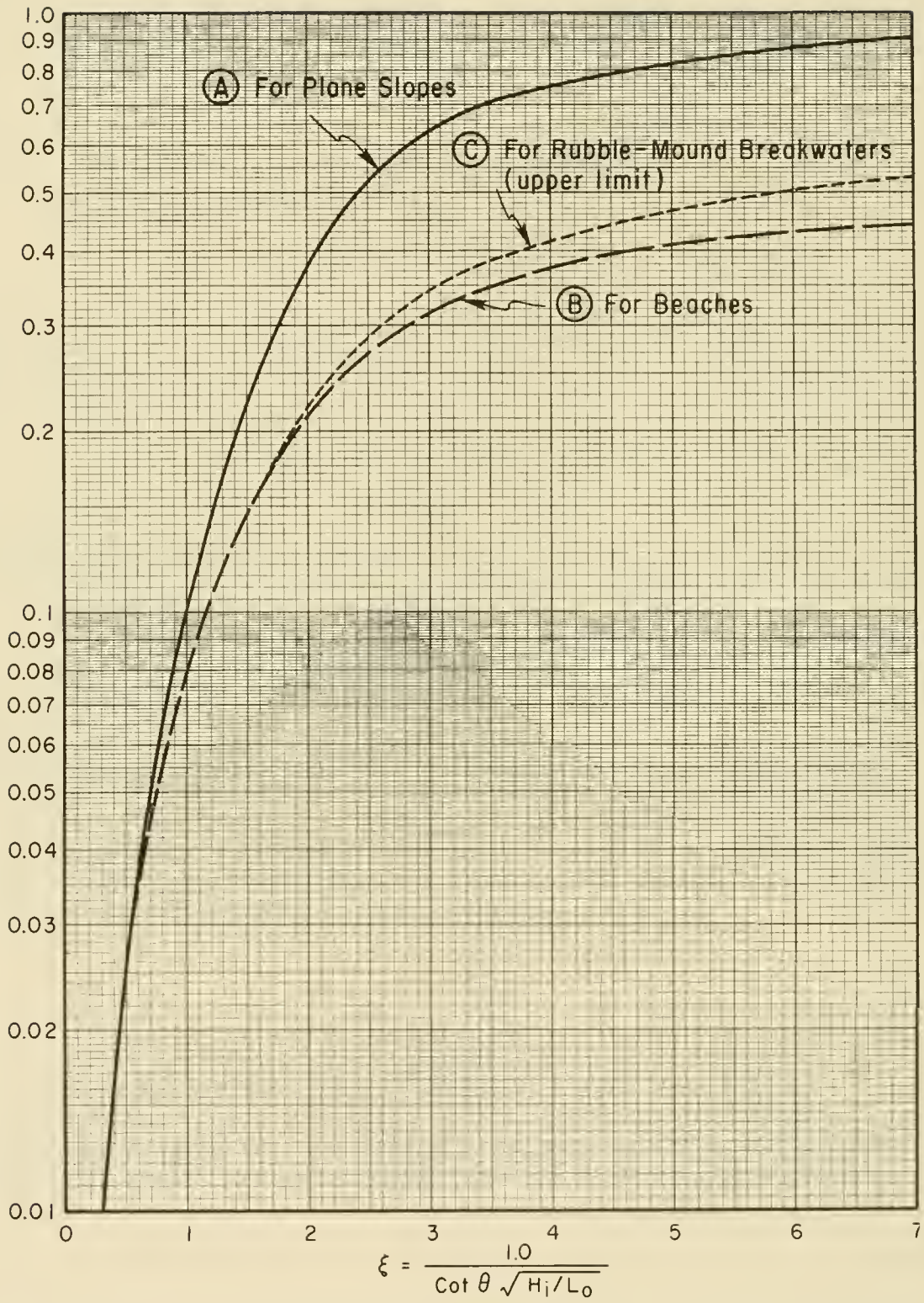


Figure 2-65. Wave reflection coefficients for slopes, beaches, and rubble-mound breakwaters as a function of the surf similarity parameter  $\xi$ .

From curve B in Figure 2-65,  $\chi < 0.01$  for the beach. The 1 on 50 beach slope reflects less wave energy and is a better wave energy dissipater than the 1 on 5 structure slope.

\*\*\*\*\*

The preceding example problem and Figure 2-65 indicate that the reflection coefficient depends on incident wave steepness. A beach or structure will selectively dissipate wave energy, dissipating the energy of relatively steep waves while reflecting the energy of longer, flatter waves.

\*\*\*\*\* EXAMPLE PROBLEM 13 \*\*\*\*\*

GIVEN: Waves with a height  $H_1 = 3.0$  meters (9.84 feet) and a period  $T = 7$  seconds are normally incident to a rubble-mound breakwater with a slope of 1 on 2 ( $\cot\theta = 2.0$ ).

FIND: A high estimate (upper bound) of the reflection coefficient.

SOLUTION: Calculate

$$L_o = \frac{gT^2}{2\pi} = \frac{9.8(7.0)^2}{2\pi} = 76.4 \text{ m (251 ft)}$$

and from equation (2-86)

$$\xi = \frac{1.0}{2.0 \sqrt{3.0/76.4}} = 2.52$$

From curve C in Figure 2-64,  $\chi = 0.29$  which is the desired upper bound on  $\chi$ . The actual reflection coefficient depends on wave transmission, internal dissipation, overtopping, and many other factors. Techniques described in Seelig and Ahrens (1981) and laboratory tests by Seelig (1980) should be used to obtain better wave reflection coefficient estimates for breakwaters.

\*\*\*\*\*

Revetments faced with armor stone dissipate more wave energy and allow less reflection than smooth slopes; therefore, reflection coefficient values from curve A in Figure 2-65 should be multiplied by two reduction factors,  $\alpha_1$  and  $\alpha_2$ . The reduction factor  $\alpha_1$ , given in Figure 2-66, accounts for reduction due to relative armor size and wave breaking at the structure toe. In Figure 2-66,  $d_g$  is the armor diameter,  $L$  the wavelength at the toe of the structure, and  $H_b$  the maximum possible breaker height at the structure toe (see Ch. 7 for estimating  $H_b$ ). The factor  $\alpha_2$  depends on the number of armor layers  $n$  and the ratio of armor unit diameter  $d_g$  to the incident wave height  $H_1$ . Table 2-3 gives an estimate of  $\alpha_2$  based on laboratory tests.

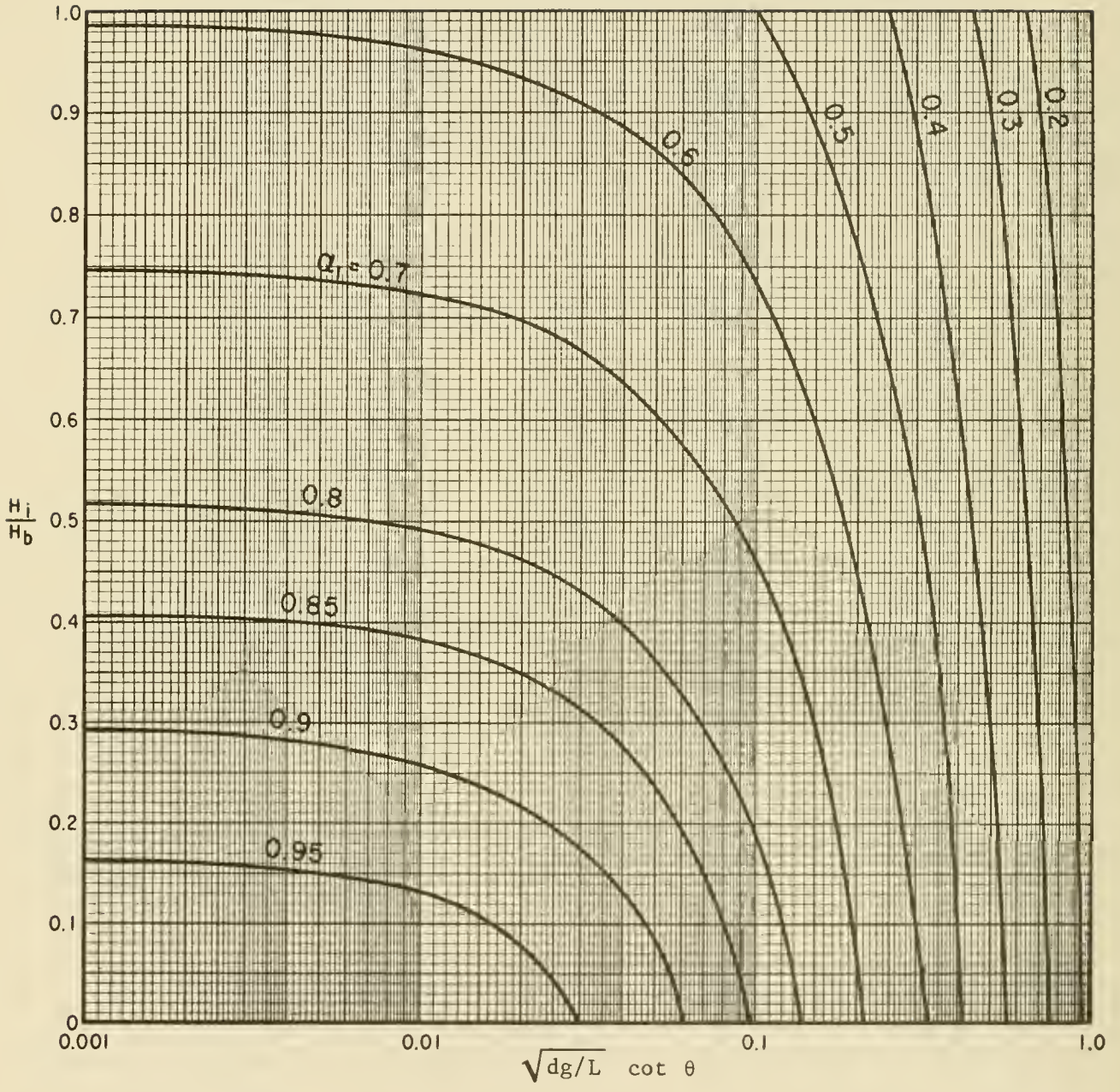


Figure 2-66. Correction factor  $\alpha_1$ , due to slope roughness and the extent of wave breaking at the toe of a structure.

Table 2-3.  $\alpha_2$  correction factor for multiple layers of armor units.<sup>1</sup>

$\frac{d_g}{H_i}$	n			
	1	2	3	4
<0.75	1.00	0.93	0.88	0.78
0.75 to 2.0	1.00	0.71	0.70	0.69
>2.0	1.00	0.58	0.52	0.49

<sup>1</sup>Derived from data with  $\cot\theta = 2.5$ ,  $d_g/d_s = 0.15$ ,  $0.004 < d_s/gT^2 < 0.03$ .

\*\*\*\*\* EXAMPLE PROBLEM 14 \*\*\*\*\*

GIVEN: A wave with a period  $T = 10$  seconds and a height  $H_1 = 2$  meters (6.56 feet) impinges on a revetment having two layers of armor units with diameter  $d_g = 1$  meter (3.28 feet). The structure slope is  $\cot\theta = 5$ ; the breaker height is  $H_b = 3.60$  meters (11.8 feet); the wavelength at breaking is  $L_b = 65.2$  meters (214 feet).

FIND: Determine the reflection coefficient.

SOLUTION: Calculate the dimensionless parameters

$$\sqrt{d_g/L} \cot\theta - \sqrt{1/65.2(5)} = 0.62$$

$$\frac{H_1}{H_b} = \frac{2.0}{3.60} = 0.56$$

and

$$\frac{d_g}{H_i} = \frac{1.0}{2.0} = 0.5$$

From Figure 2-66 with  $\sqrt{d_g/L} \cot\theta = 0.62$  and  $H_1/H_b = 0.56$ , read  $\alpha_1 = 0.29$ . From Table 2-3 with  $d_g/H_i < 0.75$  and  $n = 2$ , read  $\alpha_2 = 0.93$ . The reflection coefficient  $\chi = 0.29$  from the earlier example for a smooth slope is multiplied by  $\alpha_1$  and  $\alpha_2$  so that

$$\chi = \alpha_1 \alpha_2 (0.29) = (0.29)(0.93)(0.29) = 0.08$$

The two layers of armor units reduce the reflection coefficient to less than 30 percent of the smooth slope reflection coefficient.

\*\*\*\*\*

### 5. Wave Reflection from Bathymetric Variation.

Any change in bathymetry such as a shoal or offshore bar results in some reflection of an incident wave. Reflection from complex bathymetric changes can be determined mathematically (Long, 1973) or by physical models (Whalin, 1972). Estimates of wave reflection from simple bathymetric changes can be calculated using linear wave theory. Two examples for normally incident waves are presented here. The first example is for a smooth step and the second for a series of sinusoidal offshore bars. Nonlinear effects and wave energy dissipation are neglected so reflection coefficient estimates will be high.

Wave reflection coefficients for smooth sloped steps have been determined by Rosseau (1952; also see Webb, 1965) for several shapes. Linear wave theory was used. The water depth decreases from  $d_1$  to  $d_2$  over a length  $\ell$ . Reflection coefficients for the cases of  $\ell/(d_1 + d_2) = 6$  and 12 are given as a function of  $d_1/d_2$  for various values of  $d_1/(gT^2)$  in Figure 2-67 (a and b). These graphs indicate that for a given  $\ell/(d_1 + d_2)$ , wave reflection increases as the step size  $d_1/d_2$  increases and as the wave period increases. Maximum reflection occurs as  $T$  approaches infinity independent of  $\ell$ , as the upper curves in Figure 2-67 (a and b) show. Wave reflection decreases for a given wave condition and step size as  $\ell/(d_1 + d_2)$  becomes larger; i.e., a flatter step.

\*\*\*\*\* EXAMPLE PROBLEM 15 \*\*\*\*\*

GIVEN: A wave with a period  $T = 10$  seconds and a height  $H = 1$  meter in a water depth  $d_1 = 6$  meters (19.7 feet) travels over a smooth step in the hydrography into a reduced depth  $d_2 = 2$  meters (6.56 feet). The step is 50 meters (164 feet) long.

FIND: The height of the reflected wave.

SOLUTION: Calculate

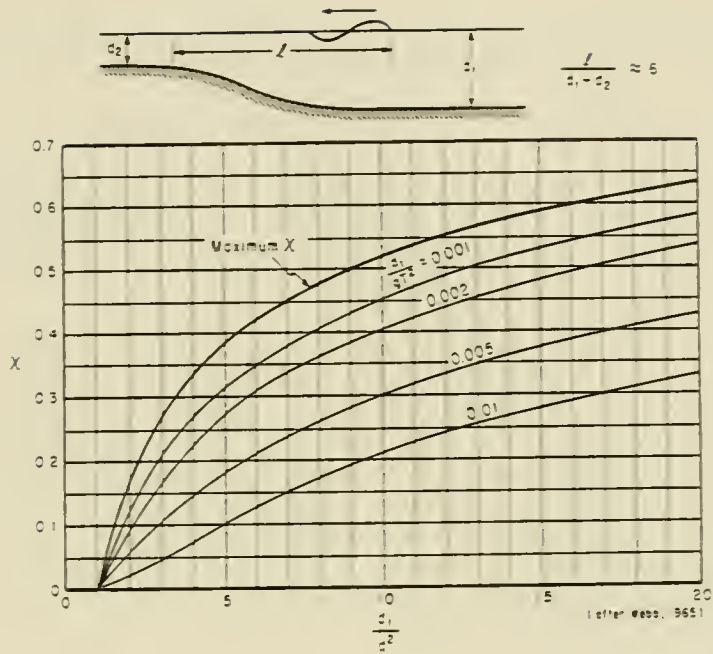
$$\frac{\ell}{d_1 + d_2} = \frac{50}{6 + 2} = 6.25$$

Therefore, Figure 2-67,a, is used. Enter the figure with

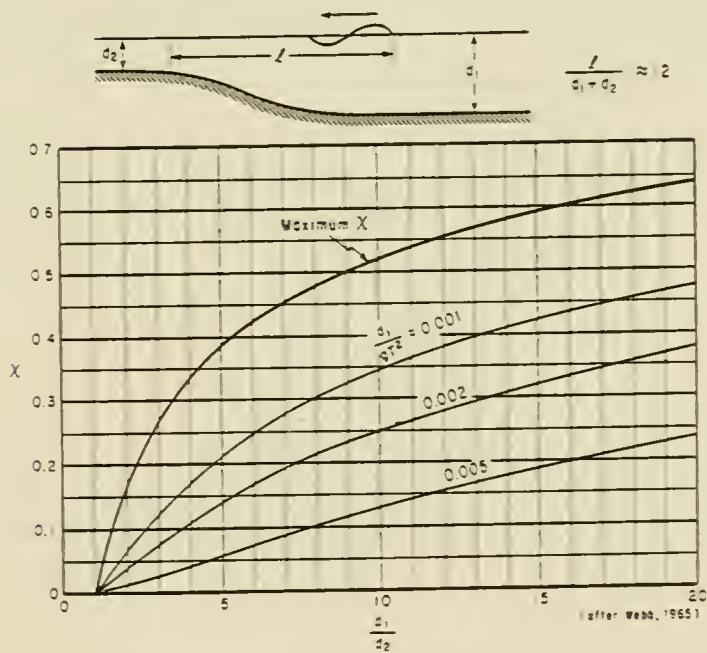
$$\frac{d_1}{d_2} = \frac{6}{2} = 3.0$$

and

$$\frac{d_1}{gT^2} = \frac{6}{9.8(10^2)} = 0.0061$$



a.  $l/(d_1 + d_2) \approx 6$



b.  $l/(d_1 + d_2) \approx 12$

Figure 2-67. Wave reflection coefficients for smooth steps,  $l/(d_1 + d_2) \approx 6$  and  $l/(d_1 + d_2) \approx 12$ .

to estimate a reflection coefficient,  $\chi = 0.095$ . The reflected wave height is, therefore,  $H_r = 0.095(1) = 0.095$  meter (0.3 foot).

\*\*\*\*\*

Wave reflection from sinusoidal-shaped bed forms on a flat bottom was analyzed by Davies (1980) using linear wave theory. His analysis shows that the wave reflection coefficient is periodic in the ratio of wavelength  $L$  to bed form length  $\ell$ , and that it is maximum when  $L = 2\ell$ .

Figure 2-68 gives the reflection coefficient for the case of  $L = 2\ell$  for bedform steepnesses,  $b/\ell = 1/20$  and  $b/\ell = 1/40$ , where  $b$  is the amplitude of the bars. Reflection coefficients are given for various numbers of bars as a function of the ratio of the bar amplitude to water depth. These figures show that for  $L/\ell = 2$  the reflection coefficient increases as the number of bars increases, as the ratio of bar amplitude to water depth increases, and as bar steepness decreases. Wave reflection coefficients will be smaller than those given in Figure 2-68 if  $L/\ell$  is not equal to 2, if the wave is nonlinear, if wave energy dissipation is significant, or if the bars are not sinusoidal in shape.

\*\*\*\*\* EXAMPLE PROBLEM 16 \*\*\*\*\*

GIVEN: Two sinusoidal bars are located in a water depth  $d = 3$  meters (9.8 feet) with an amplitude  $b = 1$  meter (3.28 feet) and a length  $\ell = 20$  meters (65 feet). A normally incident wave with a period  $T = 8$  seconds has a length  $L = 50$  meters (164 feet) and height of 1 meter (3.28 feet).

FIND: The height of the reflected wave.

SOLUTION: Calculate

$$\frac{b}{\ell} = \frac{1.0}{20.0} = \frac{1}{20}$$

and

$$\frac{b}{d} = \frac{1.0}{3} = 0.33$$

Enter the upper part of Figure 2-68 with  $b/d = 0.33$  and read  $\chi = 0.50$ . This is an upper bound on the reflection coefficient. The actual reflection coefficient may be smaller due to nonlinear wave effects, energy dissipation, or if the ratio  $L/\ell$  is not equal to 2. The maximum reflected wave height is, therefore,  $H_r = 0.50(1) = 0.50$  meter (1.64 feet).

\*\*\*\*\*

## 6. Refraction of Reflected Waves.

A substantial increase in reflected wave energy may result where structures are built along a section of coastline with no beach fronting the structure. In cases where the structure is nearly parallel with the bottom contours, and the wave direction and offshore bathymetry near the end of the structure result in wave reflection at a large angle, the structure may

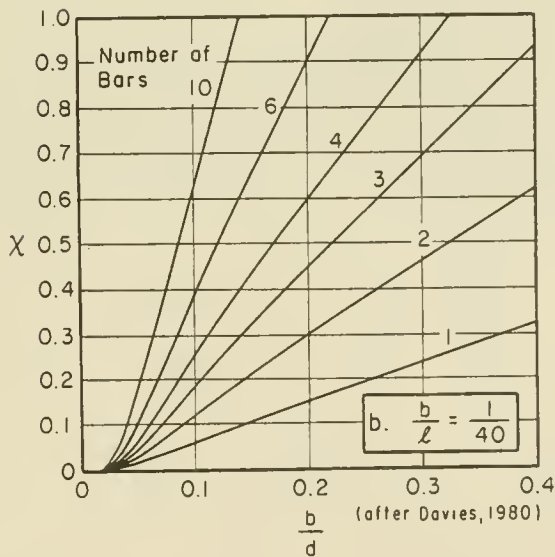
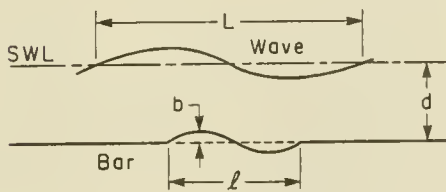
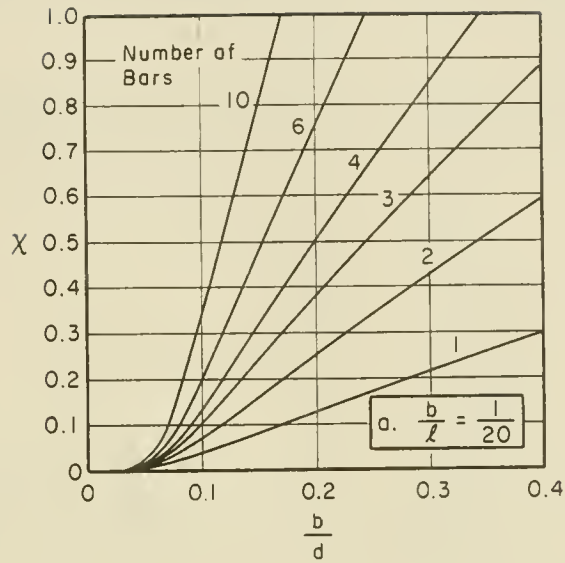


Figure 2-68. Wave reflection coefficients for sinusoidal underwater bars with  $L/l = 2.0$ .

combine with a steep bottom slope  $m$  to form a waveguide which traps wave energy along the shoreline. This trapped energy may increase wave heights and therefore increase erosion along an adjacent section of shoreline. Trapped wave rays are illustrated in Figure 2-69.

The seaward distance  $X$  that the slope must extend to trap waves, and the distance  $Y$  that a reflected wave ray will travel before returning to the shoreline are given by Camfield (1982) in dimensionless form as

$$\frac{X_m}{d_s} = \frac{1}{\sin^2 \alpha} - 1 \quad (2-88a)$$

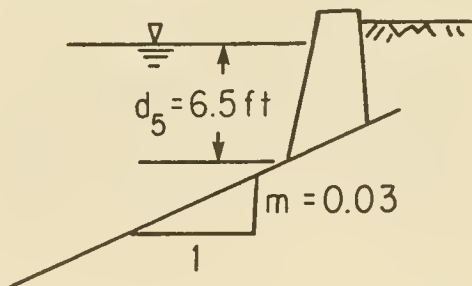
$$\frac{Y_m}{d_s} = \frac{1}{\sin^2 \alpha} [\pi - 2\alpha + \sin(2\alpha)] \quad (2-88b)$$

where  $d_s$  is the water depth at the toe of the structure, and  $\alpha$  is the reflected wave angle in radians (see Fig. 2-69). The bottom slope  $m$  is assumed to be uniform, and the waves are assumed to be shallow-water waves (i.e., the wavelength is assumed to exceed 2.0 times the water depth). For convenience, equations (2-88a) and (2-88b) are solved graphically in Figure 2-70 with  $\alpha$  given in degrees.

The values of  $d_s$  and  $m$  are known for a particular structure or proposed structure under investigation. The value of  $\alpha$  can be determined from existing wave refraction methods for incident waves as discussed in Section III. Where solutions of equations (2-88a) and (2-88b) show that wave energy will be trapped, a more extensive investigation should be undertaken to determine the effects along the shoreline.

\*\*\*\*\* EXAMPLE PROBLEM 17 \*\*\*\*\*

GIVEN: A vertical bulkhead is located along a shoreline in a 2.0-meter (6.5 foot) water depth as shown. The bottom slope  $m$  is 0.03 and is uniform to a depth of 20 meters (66 feet). Refraction studies show that waves will have an angle of incidence at the wall of  $25^\circ$  (0.436 radian); i.e., they will be reflected at that angle.



FIND: Determine if waves may be trapped along the shoreline.

SOLUTION: For the given reflection angle  $\alpha = 25^\circ$ , Figure 2-70 gives

$$\frac{X_m}{d_s} = 4.6$$

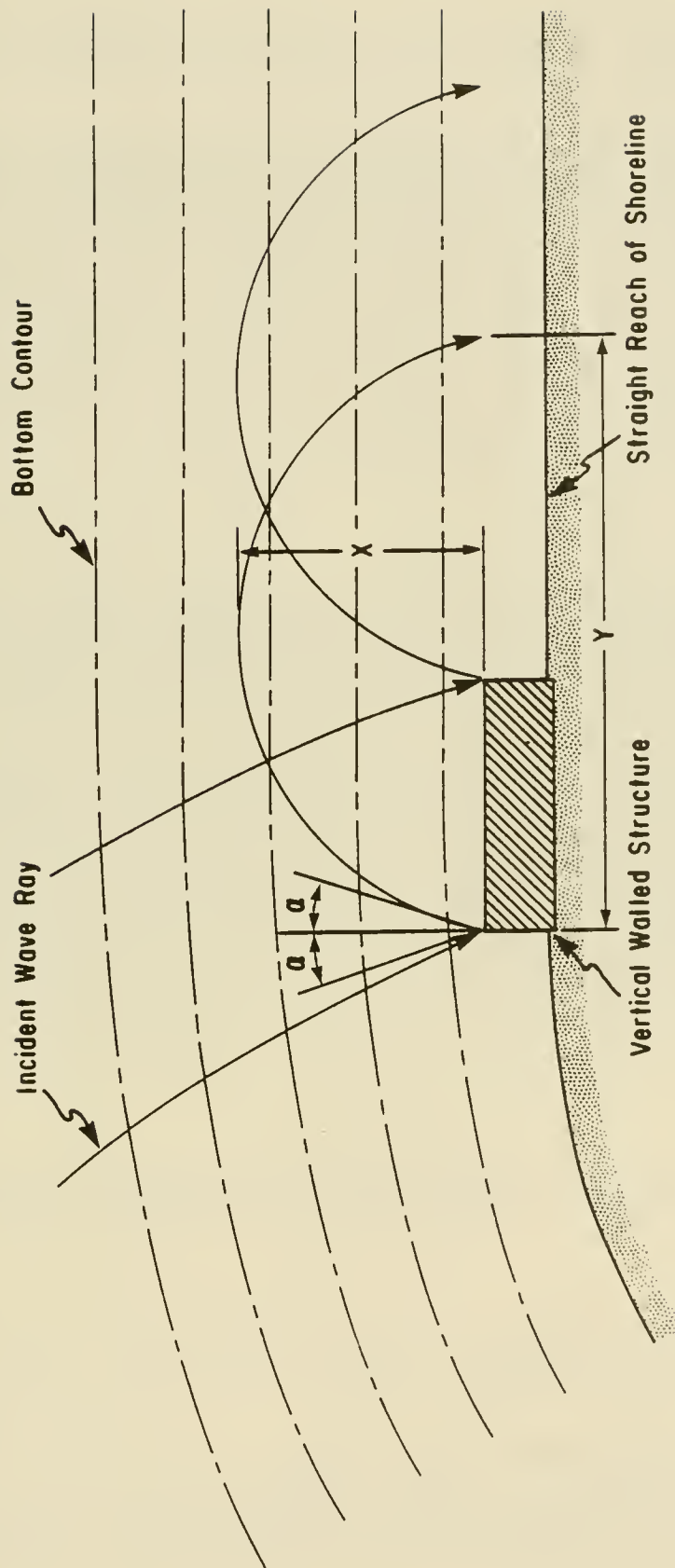


Figure 2-69. Definition sketch of trapped wave rays.

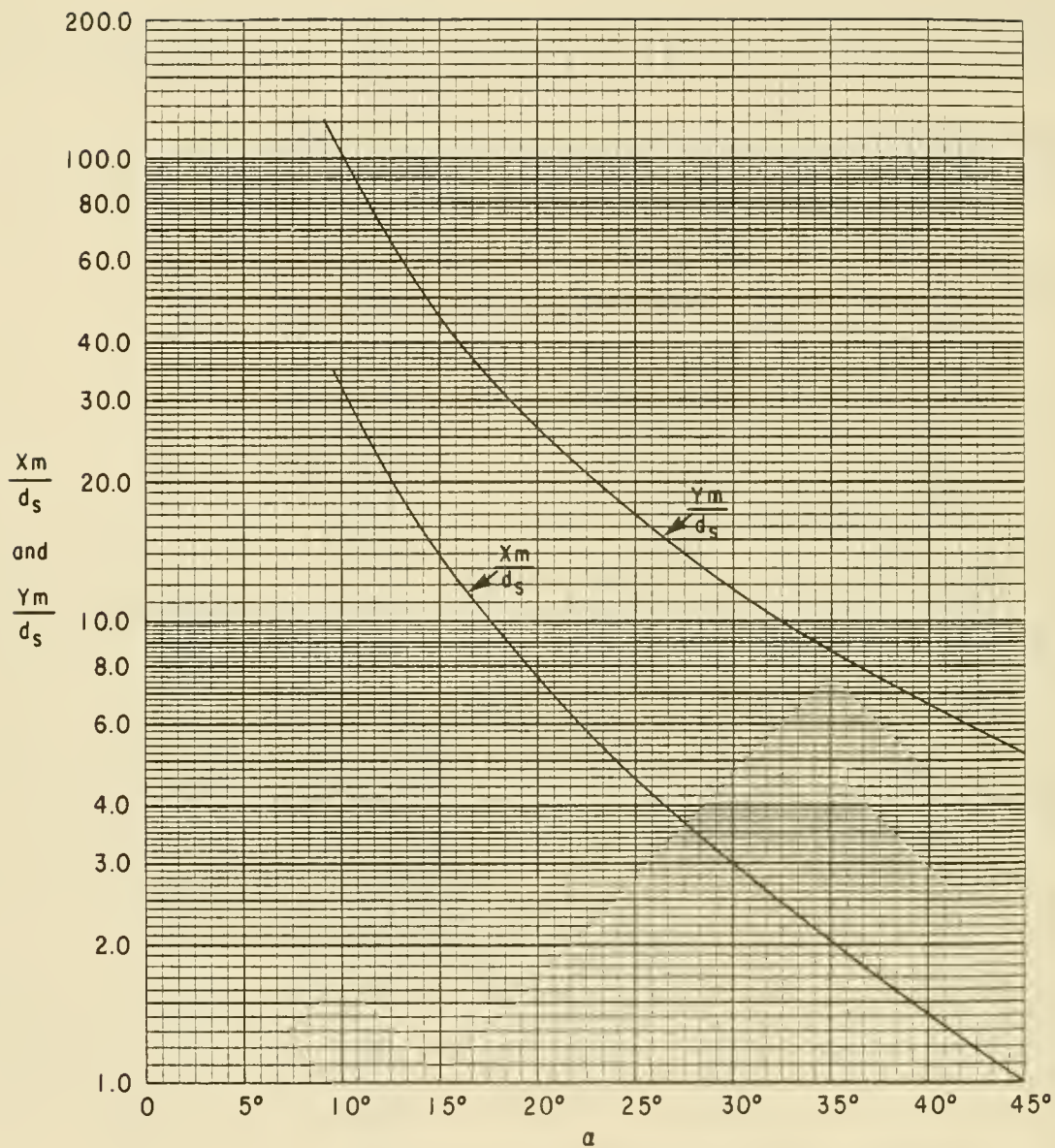


Figure 2-70. Solution of equations for trapped reflected waves with angle  $\alpha$  shown in degrees (from Camfield, 1982).

For

$$m = 0.03 \text{ and } d_s = 2.0 \text{ meters (6.5 ft)}$$

$$X = 4.5(2.0)/0.03 = 307 \text{ meters (997 ft)}$$

The water depth at that distance from shore is

$$d = d_s + mX = 2.0 + 0.03(307)$$

$$d = 11.2 \text{ m (36.8 ft)}$$

$d < 20$  meters (66 feet), so the slope extends a sufficient distance offshore to trap waves. From Figure 2-70

$$\frac{Y_m}{d_s} = 17$$

$$Y = 17(2.0)/0.03 = 1133 \text{ m (3,718 ft)}$$

For a long, relatively straight reach of coastline (greater than 1133 meters long in this example), further investigation is needed to determine the effects of trapped wave energy.

\*\*\*\*\*

## VI. BREAKING WAVES

### 1. Deep Water.

The maximum height of a wave traveling in deep water is limited by a maximum wave steepness for which the waveform can remain stable. Waves reaching the limiting steepness will begin to break and in so doing will dissipate a part of their energy. Based on theoretical considerations, Michell (1893) found the limiting steepness to be given by

$$\frac{H_o}{L_o} = 0.142 \approx \frac{1}{7} \tag{2-89}$$

which occurs when the crest angle as shown in Figure 2-71 is  $120^\circ$ . This limiting steepness occurs when the water particle velocity at the wave crest just equals the wave celerity; a further increase in steepness would result in particle velocities at the wave crest greater than the wave celerity and, consequently, instability.

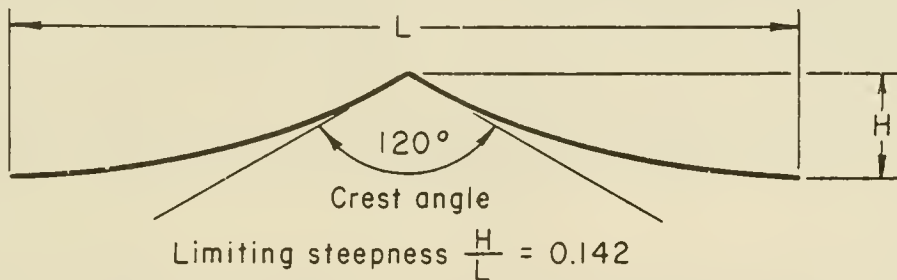


Figure 2-71. Wave of limiting steepness in deep water.

### 2. Shoaling Water.

When a wave moves into shoaling water, the *limiting steepness* which it can attain decreases, being a function of both the relative depth  $d/L$  and the beach slope  $m$ , perpendicular to the direction of wave advance. A wave of given deepwater characteristics will move toward a shore until the water

becomes shallow enough to initiate breaking; this depth is usually denoted as  $d_b$  and termed the breaking depth. Munk (1949) derived several relationships from a modified solitary wave theory relating the breaker height  $H_b$ , the breaking depth  $d_b$ , the unrefracted deepwater wave height  $H'_0$ , and the deepwater wavelength  $L_0$ . His expressions are given by

$$\frac{H_b}{H'_0} = \frac{1}{3.3(H'_0/L_0)^{1/3}} \quad (2-90)$$

and

$$\frac{d_b}{H_b} = 1.28 \quad (2-91)$$

The ratio  $H_b/H'_0$  is frequently termed the breaker height index. Subsequent observations and investigations by Iversen (1952, 1953) Galvin (1969), and Goda (1970) among others, have established that  $H_b/H'_0$  and  $d_b/H_b$  depend on beach slope and on incident wave steepness. Figure 2-72 shows Goda's empirically derived relationships between  $H_b/H'_0$  and  $H'_0/L_0$  for several beach slopes. Curves shown on the figure are fitted to widely scattered data; however they illustrate a dependence of  $H_b/H'_0$  on the beach slope. Empirical relationships derived by Weggel (1972) between  $d_b/H_b$  and  $H_b/gT^2$  for various beach slopes are presented in Figure 2-73. It is recommended that Figures 2-72 and 2-73 be used, rather than equations (2-90) and (2-91), for making estimates of the depth at breaking or the maximum breaker height in a given depth since the figures take into consideration the observed dependence of  $d_b/H_b$  and  $H_b/H'_0$  on beach slope. The curves in Figure 2-73 are given by

$$\frac{d_b}{H_b} = \frac{1}{b - (aH_b/gT^2)} \quad (2-92)$$

where  $a$  and  $b$  are functions of the beach slope  $m$ , and may be approximated by

$$a = 43.75(1 - e^{-19m}) \quad (2-93)$$

$$b = \frac{1.56}{(1 + e^{-19.5m})} \quad (2-94)$$

Breaking waves have been classified as spilling, plunging, or surging depending on the way in which they break (Patrick and Wiegel, 1955), and (Wiegel, 1964). Spilling breakers break gradually and are characterized by *white water* at the crest (see Fig. 2-74). Plunging breakers curl over at the crest with a plunging forward of the mass of water at the crest (see Fig. 2-75). Surging breakers build up as if to form a plunging breaker but the base of the wave surges up the beach before the crest can plunge forward (see Fig. 2-76). Further subdivision of breaker types has also been proposed. The term collapsing breaker is sometimes used (Galvin, 1968) to describe breakers in the transition from plunging to surging (see Fig. 2-77). In actuality, the

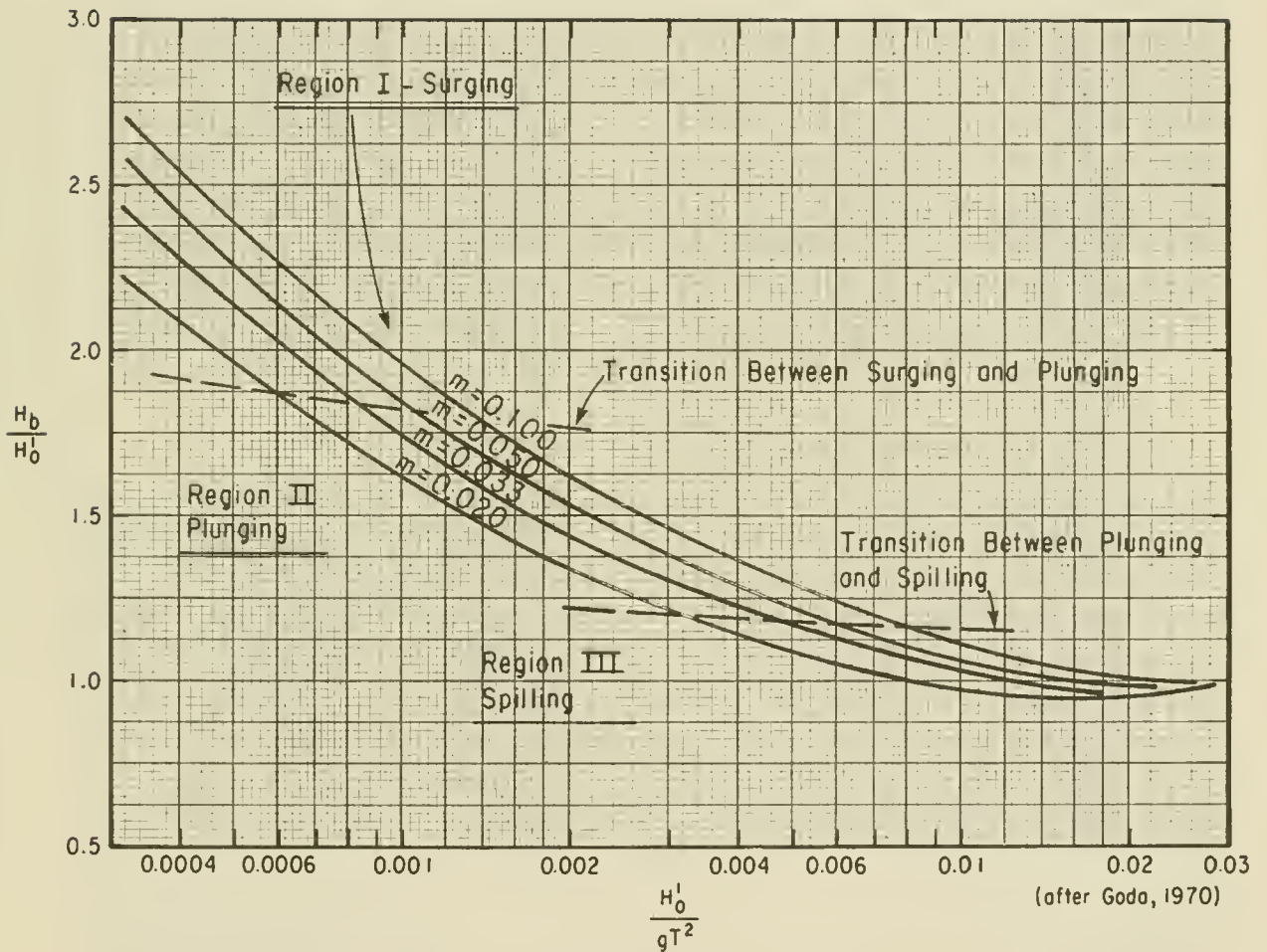


Figure 2-72. Breaker height index versus deepwater wave steepness,  $H_0'/gT^2$ .

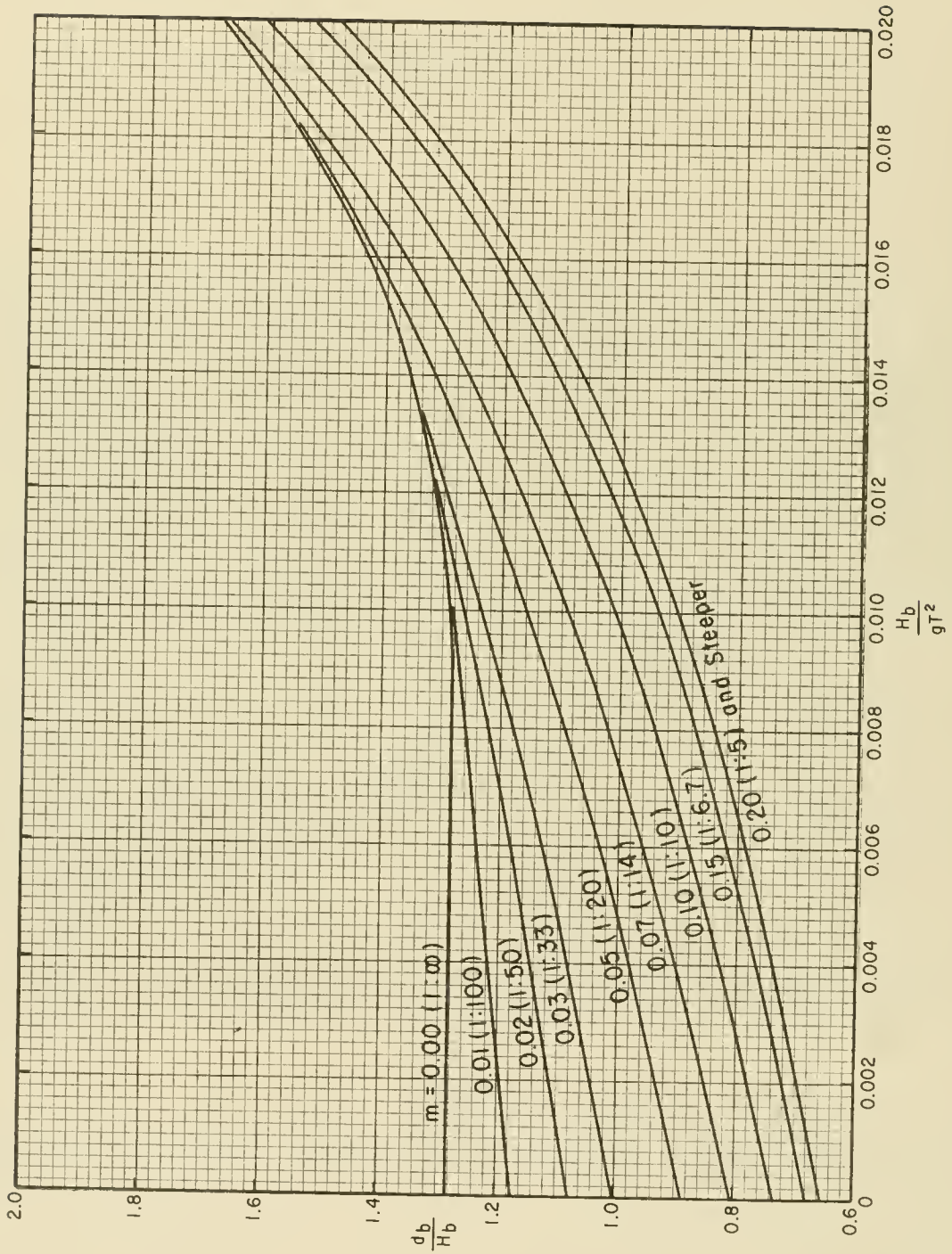


Figure 2-73. Dimensionless depth at breaking versus breaker steepness.



Figure 2-74. Spilling breaking wave.



Figure 2-75. Plunging breaking wave.



Figure 2-76. Surging breaking wave.

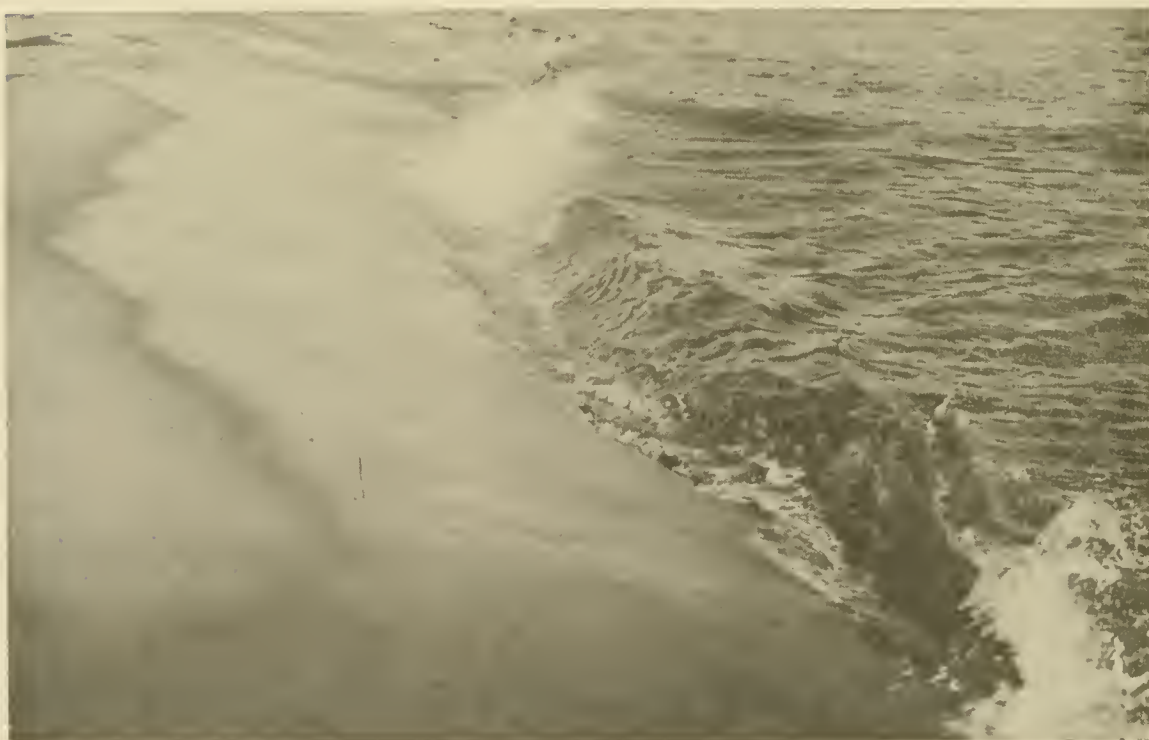


Figure 2-77. Collapsing breaking wave.

transition from one breaker type to another is gradual without distinct dividing lines; however, Patrick and Wiegel (1955) presented ranges of  $H'_0/L_0$  for several beach slopes for which each type of breaker can be expected to occur. This information is also presented in Figure 2-72 in the form of three regions on the  $H_b/H'_0$  vs  $H'_0/L_0$  plane. An example illustrating the estimation of breaker parameters follows.

\*\*\*\*\* EXAMPLE PROBLEM 18 \*\*\*\*\*

GIVEN: A beach having a 1 on 20 slope; a wave with deepwater height  $H_0 = 2$  meters (6.56 ft) and a period  $T = 10$  seconds. Assume that a refraction analysis gives a refraction coefficient  $K_R = (b_0/b)^{1/2} = 1.05$  at the point where breaking is expected to occur.

FIND: The breaker height  $H_b$  and the depth  $d_b$  at which breaking occurs.

SOLUTION: The unrefracted deepwater height  $H'_0$  can be found from

$$\frac{H'_0}{H_0} = K_R = \left(\frac{b_0}{b}\right)^{1/2} \quad (\text{see Sec. III,2})$$

hence,

$$H'_0 = 1.05(2) = 2.10 \text{ m (6.89 ft)}$$

and,

$$\frac{H'_0}{gT^2} = \frac{2.10}{9.8(10)^2} = 0.00214$$

From Figure 2-72 entering with  $H'_0/gT^2 = 0.00214$  and intersecting the curve for a slope of 1:20 ( $m = 0.05$ ) result in  $H_b/H'_0 = 1.50$ . Therefore,

$$H_b = \left(\frac{H_b}{H'_0}\right) H'_0$$

$$H_b = 1.50(2.10) = 3.15 \text{ m (10.33 ft)}$$

To determine the depth at breaking, calculate

$$\frac{H_b}{gT^2} = \frac{3.15}{9.8(10)^2} = 0.00321$$

and enter Figure 2-73 for  $m = 0.050$ .

$$\frac{d_b}{H_b} = 0.96$$

Thus  $d_b = 0.96(3.15) = 3.02$  meters (9.92 feet), and therefore the wave will break when it is approximately  $3.02/(0.05) = 60.4$  meters (198 feet) from the shoreline, assuming a constant nearshore slope. The initial value selected for the refraction coefficient should now be checked to determine if it is correct for the actual breaker location as found in the solution. If necessary, a corrected value for the refraction coefficient should be used and the breaker height recomputed. The example wave will result in a plunging breaker (see Fig. 2-72).

\* \* \* \* \*

## LITERATURE CITED

- AIRY, G.B., "On Tides and Waves," *Encyclopaedia Metropolitana*, 1845.
- ARTHUR, R.S., MUNK, W.H., and ISAACS, J.D., "The Direct Construction of Wave Rays," *Transactions of the American Geophysical Union*, Vol. 33, No. 6, 1952, pp. 855-865.
- BATTJES, J.A., "Refraction of Water Waves," *Journal of the Waterways and Harbors Division*, American Society of Civil Engineers, Vol. 94, WW4, No. 6206, Nov. 1968.
- BATTJES, J.A., "A Computation of Set-Up, Longshore Currents, Run-Up and Overtopping Due to Wind-Generated Waves," Ph.D. Dissertation, Delft University of Technology, The Netherlands, July 1974.
- BEITINJANI, K.I., and BRATER, E.F., "Study on Refraction of Waves in Prismatic Channels," *Journal of the Waterways and Harbors Division*, Vol. 91, WW3, No. 4434, 1965, pp. 37-64.
- BERKOFF, J.C.W., "Computation of Combined Refraction-Diffraction," *Proceedings of the 13th International Conference on Coastal Engineering*, American Society of Civil Engineers, Ch. 24, July 1972, pp. 471-490.
- BLUE, F.L., Jr., and JOHNSON, J.W., "Diffraction of Water Waves Passing Through a Breakwater Gap," *Transactions of the American Geophysical Union*, Vol. 30, No. 5, Oct. 1949, pp. 705-718.
- BORGMAN, L.E., "Directional Spectra Models for Design Use," HEL-1-12, University of California, Berkeley, Calif., 1969.
- BOUSSINESQ, J., "Theory of Waves and Swells Propagated in a Long Horizontal Rectangular Canal, and Imparting to the Liquid Contained in this Canal Approximately Equal Velocities from the Surface to the Bottom," *Journal de Mathematiques Pures et Appliquees*, Vol. 17, Series 2, 1872.
- BOUSSINESQ, J., "Essai sur la Theorie des Eaux Courantes," *Mem. divers Savants a L'Academie des Science*, No. 32, 1877, p. 56.
- BRETSCHNEIDER, C.L., "Wave Refraction, Diffraction and Reflection," *Estuary and Coastline Hydrodynamics*, A.T. Ippen, ed., McGraw-Hill, Inc., N.Y., 1966, pp. 257-280.
- CAMFIELD, F.E., "Calculation of Trapped Reflected Waves," *Journal of the Waterways, Port, Coastal and Ocean Division*, American Society of Civil Engineers, Vol. 108, No. WW1, Feb. 1982.
- CAMFIELD, F.E., and STREET, R.L., "Shoaling of Solitary Waves on Small Slopes," *Journal of the Waterways and Harbors Division*, Vol. 95, No. WW1, Feb. 1969.
- CARR, J.H., and STELZRIEDE, M.E., "Diffraction of Water Waves by Breakwaters," *Gravity Waves*, Circular No. 521, National Bureau of Standards, Washington, D.C., Nov. 1952, pp. 109-125.

- CHAO, Y.Y., "The Theory of Wave Refraction in Shoaling Water," TR-70-7, Department of Meteorology and Oceanography, New York University, N.Y., 1970.
- CHIEN, N., "Ripple Tank Studies of Wave Refraction," *Transactions of the American Geophysical Union*, Vol. 35, No. 6, 1954, pp. 897-904.
- COUDERT, J.F., and RAICHLEN, F., "Wave Refraction Near San Pedro Bay, California," *Journal of the Waterways, Harbors and Coastal Engineering Division*, WW3, 1970, pp. 737-747.
- DAILY, J.W., and STEPHAN, S.C., Jr., "Characteristics of a Solitary Wave," *Transactions of the American Society of Civil Engineers*, Vol. 118, 1953, pp. 575-587.
- DANEL, P., "On the Limiting Clapotis," *Gravity Waves*, Circular No. 521, National Bureau of Standards, Washington D.C., 1952, pp. 35-38.
- DAVIES, A.G., "Some Interactions Between Surface Water Waves and Ripples and Dunes on the Seabed," Report No. 108, Institute of Oceanographic Sciences, Taunton, England, unpublished, 1980.
- DEAN, R.G., "Stream Function Representation of Nonlinear Ocean Waves," *Journal of the Geophysical Research*, Vol. 70, No. 18, Sept. 1965a.
- DEAN, R.G., "Stream Function Wave Theory; Validity and Application," *Proceedings of the Santa Barbara Specialty Conference*, Ch. 12, Oct. 1965b.
- DEAN, R.G., "Relative Validities of Water Wave Theories," *Proceedings of the Conference on Civil Engineering in the Oceans I*, Sept. 1967.
- DEAN, R.G., "Evaluation and Development of Water Wave Theories for Engineering Application," SR-1, Vol. II, Coastal Engineering Research Center, U. S. Army Engineer Waterways Experiment Station, Vicksburg, Miss., Nov. 1974.
- DEAN, R.G., and LE MEHAUTE, B., "Experimental Validity of Water Wave Theories," *Proceedings of the Meeting on National Structural Engineering*, American Society of Civil Engineers, 1970.
- DOBSON, R.S., "Some Applications of Digital Computers to Hydraulic Engineering Problems," TR-80, Ch. 2, Department of Civil Engineering, Stanford University, Palo Alto, Calif., June 1967.
- DOMZIG, H., "Wellendruck und druckerzeugender Seegang," *Mitteilungen der Hannoverschen Versuchsanstalt für Grundbau und Wasserbau*, Hannover, Germany, 1955.
- DRAPER, L., "Attenuation of Sea Waves with Depth," *La Houille Blanche*, Vol. 12, No. 6, 1957, pp. 926-931.
- EAGLESON, P.S., and DEAN, R.G., "Small Amplitude Wave Theory," *Estuary and Coastline Hydrodynamics*, A.T. Ippen, ed., McGraw-Hill, Inc., N.Y., 1966, pp. 1-92.

- ECKART, C., "The Propagation of Gravity Waves from Deep to Shallow Water," *Gravity Waves*, Circular No. 521, National Bureau of Standards, Washington, D.C., 1952.
- ESTEVA, D., and HARRIS, D.L., "Comparison of Pressure and Staff Wave Gage Records," *Proceedings of the 12th Conference on Coastal Engineering*, American Society of Civil Engineers, 1971 (also Reprint 2-71, Coastal Engineering Research Center, U. S. Army Engineer Waterways Experiment Station, Vicksburg, Miss., NTIS 732 637).
- FAN, S.S., and BORGMAN, L.E., "Computer Modeling of Diffraction of Wind Waves," *Proceedings of the 12th Conference on Coastal Engineering*, American Society of Civil Engineers, Sept. 1970.
- GAILLARD, D.D., "Wave Action in Relation to Engineering Structures," Professional Paper No. 31, U.S. Army, Corps of Engineers, Washington, D.C., 1904.
- GALVIN, C.J., Jr., "Breaker Type Classification on Three Laboratory Beaches," *Journal of Geophysical Research*, Vol. 73, No. 12, 1968 (also Reprint 3-68, Coastal Engineering Research Center, U. S. Army Engineer Waterways Experiment Station, Vicksburg, Miss., NTIS 673 621).
- GALVIN, C.J., Jr., "Breaker Travel and Choice of Design Wave Height," *Journal of the Waterways and Harbors Division*, WW2, No. 6569, 1969, pp. 175-200 (also Reprint 4-70, Coastal Engineering Research Center, U. S. Army Engineer Waterways Experiment Station, Vicksburg, Miss., NTIS 712 652).
- GERSTNER, F., "Theorie die Wellen," *Abhandlungen der Koniglichen Bohmischen Gesellschaft der Wissenschaften*, Prague, Czechoslovakia, 1802.
- GODA, Y., "A Synthesis of Breaker Indices," *Transactions of the Japanese Society of Civil Engineers*, Vol. 2, Pt. 2, 1970.
- GODA, Y., and ABE, Y., "Apparent Coefficient of Partial Reflection of Finite Amplitude Waves," Report No. 3, Vol. 7, Port and Harbor Research Institute, Nagase, Yokosuka, Japan, Sept. 1968.
- GODA, Y., TAKAYAMA, T., and SUZUKI, Y., "Diffraction Diagrams for Directional Random Waves," Ch. 35, *Proceedings of the 16th International Conference on Coastal Engineering*, American Society of Civil Engineers, 1978, pp. 628-650.
- GODA, Y., YOSHIMURA, J., and ITO, M., "Reflection and Diffraction of Water Waves by an Insular Breakwater," *Report of the Port and Harbor Research Institute* (in Japanese), Vol. 10, No. 2, June 1971, pp. 4-51.
- GRACE, R.A., "How to Measure Waves," *Ocean Industry*, Vol. 5, No. 2, 1970, pp. 65-69.
- GRISWOLD, G.M., "Numerical Calculation of Wave Refraction," *Journal of Geophysical Research*, Vol. 68, No. 6, 1963.
- HALES, L.Z., "Erosion Control of Scour During Construction, Report 3, Experimental Measurements of Refraction, Diffraction and Current Patterns Near Jetties," Report No. HL 80-3, U.S. Army Engineer Waterways Experiment Station, Vicksburg, Miss., 1980.

- HARDY, J.R., "Some Grid and Projection Problems in the Numerical Calculation of Wave Refraction," *Journal of Geophysical Research*, Vol. 73, No. 22, Nov. 1968.
- HARMS, N.W., "Diffraction of Water Waves by Isolated Structures," *Journal of the Waterway, Port, Coastal and Ocean Division*, No. WW2, May 1979.
- HARMS, N.W., et al., "Computer Manual for Calculation Wave-Height Distributions about Offshore Structures," Water Resources and Environmental Engineering Research Report No. 79-4, State University of New York at Buffalo, Buffalo, N.Y., Sept. 1979.
- HARRISON, W., and WILSON, W.S., "Development of a Method for Numerical Calculation of Wave Refraction," TM-6, Coastal Engineering Research Center, U. S. Army Engineer Waterways Experiment Station, Vicksburg, Miss., Oct. 1964.
- HAVELOCK T.H., "Periodic Irrotational Waves of Finite Height," *Proceedings of the Royal Society of London*, Vol. 95, Series A, No. A665, 1918, pp. 37-51.
- IPPEN A., and KULIN G., "The Shoaling and Breaking of the Solitary Wave," *Proceedings of the Fifth Conference on Coastal Engineering*, American Society of Civil Engineers, 1954, pp. 27-49.
- IPPEN, A.T., "Waves and Tides in Coastal Processes," *Journal of the Boston Society of Civil Engineers*, Vol. 53, No. 2, 1966a., pp. 158-181.
- IPPEN, A.T., ed., *Estuary and Coastline Hydrodynamics*, McGraw-Hill, Inc., N.Y., 1966b.
- IVERSEN, H.W., "Laboratory Study of Breakers," *Gravity Waves*, Circular No. 521, National Bureau of Standards, Washington, D.C., 1952.
- IVERSEN, H.W., "Waves and Breakers in Shoaling Water," *Proceedings of the Third Conference on Coastal Engineering*, American Society of Civil Engineers, 1953.
- IWASA, Y., "Analytical Consideration on Cnoidal and Solitary Waves," *Memoirs of the Faculty of Engineering*, Reprint, Kyoto University, Japan, 1955.
- JOHNSON, J.W., "The Refraction of Surface Waves by Currents," *Transactions of the American Geophysical Union*, Vol. 28, No. 6, 1947, pp. 867-874.
- JOHNSON, J.W., "Generalized Wave Diffraction Diagrams," *Proceedings of the Second Conference on Coastal Engineering*, American Society of Civil Engineers, 1952.
- JOHNSON, J.W., O'BRIEN, M.P., and ISAACS, J.D., "Graphical Construction of Wave Refraction Diagrams," HO No. 605, TR-2, U.S. Naval Oceanographic Office, Washington, D.C., Jan. 1948.
- KAPLAN, K., "Effective Height of Seawalls," Vol. 6, Bulletin No. 2, U.S. Army, Corps of Engineers, Beach Erosion Board, Washington, D.C., 1952.

- KELLER, J.B., "Surface Waves on Water of Non-uniform Depth," *Journal of Fluid Mechanics*, Vol. 4, 1958, pp. 607-614.
- KEULEGAN, G.H., "Gradual Damping of Solitary Waves," *Journal of Research of the National Bureau of Standards*, Reprint, Vol. 40, 1948, pp. 487-498.
- KEULEGAN, G.H., and HARRISON, J., "Tsunami Refraction Diagrams by Digital Computer," *Journal of the Waterways, Harbors and Coastal Engineering Division*, American Society of Civil Engineers, Vol. 96, WW2, No. 7261, May 1970, pp. 219-233.
- KEULEGAN, G.H., and PATTERSON, G.W., "Mathematical Theory of Irrotational Translation Waves," RP No. 1272, National Bureau of Standards, Washington, D.C., 1940, pp. 47-101.
- KINSMAN, B., *Wind Waves, Their Generation and Propagation on the Ocean Surface*, Prentice Hall, Inc., Englewood Cliffs, N.J., 1965.
- KORTEWEG, D.J., and DE VRIES, G., "On the Change of Form of Long Waves Advancing in a Rectangular Canal, and on a New Type of Long Stationary Waves," *Philosophical Magazine*, 5th Series, 1895, pp. 422-443.
- LAITONE, E.V., "Higher Approximation to Non-linear Water Waves and the Limiting Heights of Cnoidal, Solitary and Stokes Waves," TM-133, U.S. Army, Corps of Engineers, Beach Erosion Board, Washington, D.C., 1963.
- LAMB, H., *Hydrodynamics*, 6th ed., Cambridge University Press, London, England, 1932.
- LEE, C., "On the Design of Small Craft Harbors," *Proceedings of the Ninth Conference on Coastal Engineering*, American Society of Civil Engineers, June 1964.
- LE MEHAUTE, B., "Wave Absorbers in Harbors," Contract Report No. 2-122, U.S. Army Engineer Waterways Experiment Station, Vicksburg, Miss., June 1965.
- LE MEHAUTE, B., "An Introduction to Hydrodynamics and Water Waves," *Water Wave Theories*, Vol. II, TR ERL 118-POL-3-2, U.S. Department of Commerce, ESSA, Washington, D.C., 1969.
- LEWIS, R.M., BLEISTEIN, N., and LUDWIG, D., "Uniform Asymptotic Theory of Creeping Waves," *Communications on Pure and Applied Mathematics*, Vol. 20, No. 2, 1967.
- LIU, P.L-F., "Combined Refraction and Diffraction: Comparison Between Theory and Experiments," *Journal of Geophysical Research*, Vol. 87, No. C8, July 1982, pp. 5723-5730.
- LIU, P.L-F., and LOZANO, C., "Combined Wave Refraction and Diffraction," *Proceedings of the Coastal Structures '79 Conference*, 1979.
- LONG, R.B., "Scattering of Surface Waves by an Irregular Bottom," *Journal of Geophysical Research*, Vol. 78, No. 33, Nov. 1973, pp. 7861-7870.

- LONGUET-HIGGINS, M.S., "Mass Transport in Water Waves," *Philosophical Transactions of the Royal Society of London*, Series A, Vol. 245, No. 903, 1953.
- LONGUET-HIGGINS, M.S., "On the Transformation of a Continuous Spectrum by Refraction," *Proceedings of the Cambridge Philosophical Society*, Vol. 53, Part I, 1957, pp. 226-229.
- LONGUET-HIGGINS, M.S., "Mass Transport in the Boundary Layer at a Free Oscillating Surface," Vol. 8, National Institute of Oceanography, Wormley, Surrey, England, 1960.
- LOZANO, C., "Uniform Approximation to Surface Gravity Waves Around a Breakwater on Waters of Variable Depth," Technical Report 37, Applied Mathematics Institute, University of Delaware, Newark, Del., 1980.
- LOZANO, C., and LIU, P.L-F., "Refraction-Diffraction Model for Linear Surface Water Waves," *Journal of Fluid Mechanics*, Vol. 101, Pt. 4, Dec. 1980.
- McCOWAN, J., "On the Solitary Wave," *Philosophical Magazine*, 5th Series, Vol. 32, No. 194, 1891, pp. 45-58.
- MASCH, F.D., "Cnoidal Waves in Shallow Water," *Proceedings of the Ninth Conference of Coastal Engineering*, American Society of Civil Engineers, Ch. 1, 1964.
- MASCH, F.D., and WIEGEL, R.L., "Cnoidal Waves. Tables of Functions," Council on Wave Research, The Engineering Foundation, Richmond, Calif., 1961.
- MEHR, E., "Surf Refraction--Computer Refraction Program," Statistical Laboratory, New York University, N.Y., Sept. 1962.
- MEMOS, C.D., "Diffraction of Waves Through a Gap Between Two Inclined Breakwaters," Ph.D. Thesis, University of London, London, England, 1976.
- MEMOS, C.D., "An Extended Approach to Wave Scattering Through a Harbor Entrance," *Bulletin of the Permanent International Association of Navigation Congresses*, Vol. I, No. 35, 1980a, pp. 20-26.
- MEMOS, C.D., "Energy Transmission by Surface Waves Through an Opening," *Journal of Fluid Mechanics*, Vol. 97, Pt. 3, 1980b, pp. 557-568.
- MEMOS, C.D., "Water Waves Diffracted by Two Breakwaters," *Journal of Hydraulic Research*, Vol. 18, No. 4, 1980c, pp. 343-357.
- MICHE, M., "Mouvements Ondulatoires de la Mer en Profondeur Constante ou Decroissante," *Annales des Ponts et Chaussees*, 1944, pp. 25-78, 131-164, 270-292, and 369-406.
- MICHELL, J.H., "On the Highest Waves in Water," *Philosophical Magazine*, 5th Series, Vol. 36, 1893, pp. 430-437.
- MITCHIM, C.F., "Oscillatory Waves in Deep Water," *The Military Engineer*, Mar. 1940, pp. 107-109.

- MOBAREK, I., "Effect of Bottom Slope on Wave Diffraction," HEL-1-1, University of California, Berkeley, Calif., Nov. 1962.
- MONKMEYER, P.L., "Higher Order Theory for Symmetrical Gravity Waves," Ch. 33, *Proceedings of the 12th Conference on Coastal Engineering*, American Society of Civil Engineers, 1970.
- MONTEFUSCO, L., "The Diffraction of a Plane Wave by an Isolated Breakwater," *Meccanica*, Vol. 3, 1968, pp. 156-166.
- MORISON, J.R., and CROOKE, R.C., "The Mechanics of Deep Water, Shallow Water, and Breaking Waves," TM-40, U.S. Army, Corps of Engineers, Beach Erosion Board, Washington, D.C., Mar. 1953.
- MUNK, W.H., "The Solitary Wave Theory and Its Application to Surf Problems," *Annals of the New York Academy of Sciences*, Vol. 51, 1949, pp. 376-462.
- MUNK, W.H., and ARTHUR, R.S., "Wave Intensity Along a Refracted Ray," *Symposium on Gravity Waves*, Circular No. 521, National Bureau of Standards, Washington, D.C., 1951.
- MUNK, W.H., and TRAYLOR, M.A., "Refraction of Ocean Waves," *Journal of Geology*, Vol. LV, No. 1, 1947.
- O'BRIEN, M.P., "A Summary of the Theory of Oscillatory Waves," TR 2, U.S. Army, Corps of Engineers, Beach Erosion Board, Washington, D.C., 1942.
- PALMER, R.Q., "Wave Refraction Plotter," Vol. 11, Bulletin No. 1, U.S. Army, Corps of Engineers, Beach Erosion Board, Washington, D.C., 1957.
- PATRICK, D.A., and WIEGEL, R.L., "Amphibian Tractors in the Surf," *Proceedings of the First Conference on Ships and Waves*, Council on Wave Research and Society of Naval Architects and Marine Engineers, 1955.
- PENNEY, W.G., and PRICE, A.T., "Diffraction of Sea Waves by a Breakwater," *Artificial Harbors*, Technical History No. 26, Sec. 3-D, Directorate of Miscellaneous Weapons Development, 1944.
- PIERSON, W.J., Jr., "The Interpretation of Crossed Orthogonals in Wave Refraction Phenomena," TM-21, U.S. Army, Corps of Engineers, Beach Erosion Board, Washington, D.C., Nov. 1950.
- PIERSON, W.J., Jr., "The Accuracy of Present Wave Forecasting Methods with Reference to Problems in Beach Erosion on the New Jersey and Long Island Coasts," TM-24, U.S. Army, Corps of Engineers, Beach Erosion Board, Washington, D.C., Apr. 1951.
- PLATZMAN, G.W., and RAO, D.B., "The Free Oscillations of Lake Erie," TR-8, U.S. Weather Bureau, Washington, D.C., Sept. 1963.
- PUTNAM, J.A., and ARTHUR, R.S., "Diffraction of Water Waves by Breakwaters," *Transactions of the American Geophysical Union*, Vol. 29, No. 4, 1948, pp. 317-374.

- RAICHLIN, F., "Long Period Oscillations in Basins of Arbitrary Shapes," Ch. 7, *Proceedings of the Santa Barbara Specialty Conference on Coastal Engineering*, American Society of Civil Engineers, 1966, pp. 115-148.
- RAISSI, H., and WIEGEL, R.L., "Wind Generated Wave Diffraction by Breakwater Gap," *Proceedings of the 16th International Conference on Coastal Engineering*, American Society of Civil Engineers, Ch. 34, Aug. 1978, pp. 609-627.
- RALLS, G.C., "A Ripple Tank Study of Wave Refraction," *Journal of the Waterways and Harbors Division*, Vol. 82, WW1, No. 911, Mar. 1956.
- RAYLEIGH, L., "On Waves," *Philosophical Magazine and Journal of Science*, Vol. 1, No. 4, 1876, pp. 257-279.
- ROSSEAU, M., "Contribution a la theorie des ondes liquides de gravite en profondeur variable, Publ. Sci, et Tech. du Ministere de l'Air, No. 275, 1952.
- RUSSELL, J.S., "Report of the Committee on Waves," *Seventh Meeting of the British Association for the Advancement of Science*, 1838, p. 417.
- RUSSELL, J.S., "Report on Waves," *Proceedings of the 14th Meeting of the British Association for the Advancement of Science*, 1844, p. 311.
- RUSSELL, R.C.H., and OSORIO, J.D.C., "An Experimental Investigation of Drift Profiles in a Closed Channel," *Proceedings of the Sixth Conference on Coastal Engineering*, American Society of Civil Engineers, 1958, pp. 171-183.
- SAVILLE, T., Jr., and KAPLAN, K., "A New Method for the Graphical Construction of Wave Refraction Diagrams," Vol. 6, Bulletin No. 3, U.S. Army, Corps of Engineers, Beach Erosion Board, Washington, D.C., 1952, pp. 23-24.
- SEELIG, W.N., "Two-Dimensional Tests of Wave Transmission and Reflection Characteristics of Laboratory Breakwaters," TR 80-1, Coastal Engineering Research Center, U. S. Army Engineer Waterways Experiment Station, Vicksburg, Miss., June 1980.
- SEELIG, W.N., and AHRENS, J.P., "Estimation of Wave Reflection and Energy Dissipation Coefficients for Beaches, Revetments, and Breakwaters," TP 81-1, Coastal Engineering Research Center, U. S. Army Engineer Waterways Experiment Station, Vicksburg, Miss., Feb. 1981.
- SKJELBREIA, L., "Gravity Waves. Stokes' Third Order Approximation. Tables of Functions," University of California, Council on Wave Research, The Engineering Foundation, Berkeley, Calif., 1959.
- SKJELBREIA, L., and HENDRICKSON, J.A., *Fifth Order Gravity Wave Theory and Tables of Functions*, National Engineering Science Co., Pasadena, Calif., 1962.
- SOMMERFELD, A., "Mathematische Theorie der Diffraction," *Mathematische Annals*, Vol. 47, 1896, pp. 317-374.

- STOKES, G.G., "On the Theory of Oscillatory Waves," *Transactions of the Cambridge Philosophical Society*, Vol. 8, 1847, pp. 441-455.
- STOKES, G.C., "On the Theory of Oscillatory Waves," *Mathematical and Physical Papers*, Vol. 1, Cambridge University Press, London, England, 1880.
- SVERDRUP, H.U., and MUNK, W.H., "Wind, Sea, and Swell: Theory of Relations for Forecasting," TR-1, H.O. No. 601, U.S. Naval Hydrographic Office, Washington, D.C., 1947, p. 7.
- U.S. ARMY, CORPS OF ENGINEERS, "A Summary of the Theory of Oscillatory Waves," TR-2, Beach Erosion Board, Washington, D.C., 1942.
- URSELL, F., "Mass Transport in Gravity Waves," *Proceedings of the Cambridge Philosophical Society*, Vol. 49, Pt. 1, 1953, pp. 145-150.
- WEBB, L.M., "Contributions to the Mono Lake Experiments, Linear Theory of the Propagation of Periodic Waves Over a Continental Slope," Report No. S256-2, National Engineering Science Co., Pasadena, Calif., Oct. 1965.
- WEGGEL, J.R., "Maximum Breaker Height," *Journal of the Waterways, Harbors and Coastal Engineering Division*, Vol. 98, WW4, Nov. 1972.
- WHALIN, R.W., "The Limit of Applicability of Linear Wave Refraction Theory in a Convergence Zone," Report No. H-71-3, U.S. Army Engineer Waterways Experiment Station, Vicksburg, Miss., 1971, p. 156.
- WHALIN, R.W., "Wave Refraction Theory in a Convergence Zone," *Proceedings of the 13th Conference on Coastal Engineering*, American Society of Civil Engineers, Ch. 23, July 1972, pp. 451-470.
- WIEGEL, R.L., *Oceanographical Engineering*, Fluid Mechanics Series, Prentice Hall, Inc. Englewood Cliffs, N.J., 1904.
- WIEGEL, R.L., *Gravity Waves. Tables of Functions*, University of California, Council on Wave Research, The Engineering Foundation, Berkeley, Calif., 1954.
- WIEGEL, R.L., "A Presentation of Cnoidal Wave Theory for Practical Application," *Journal of Fluid Mechanics*, Vol. 7, Pt. 2, 1960, pp. 273-286.
- WIEGEL, R.L., "Diffraction of Waves by a Semi-infinite Breakwater," *Journal of the Hydraulics Division*, Vol. 88, No. HY1, Jan. 1962, pp. 27-44.
- WIEGEL, R.L., AL-KAZILY, M.F., and RAISSI, H., "Wind Generated Wave Diffraction by a Breakwater," Technical Report HEL 1-19, Hydraulic Engineering Laboratory, University of California, Berkeley, Calif., 1971.
- WIEGEL, R.L., and ARNOLD, A.L., "Model Study of Wave Refraction," TM-103, U.S. Army, Corps of Engineers, Beach Erosion Board, Washington, D.C., Dec. 1957.
- WILLIAMS, L.C., "CERC Wave Gages," TM-30, Coastal Engineering Research Center, U. S. Army Engineer Waterways Experiment Station, Vicksburg, Miss., Dec. 1969.

WILSON, W.S., "A Method for Calculating and Plotting Surface Wave Rays," TM-17, Coastal Engineering Research Center, U. S. Army Engineer Waterways Experiment Station, Vicksburg, Miss., Feb. 1966.

WILTON, J.R., "On Deep Water Waves," *Philosophical Magazine*, 6th Series, 1914, pp. 385-394.

## BIBLIOGRAPHY

- CALDWELL, J.M., "Reflection of Solitary Waves," TM-11, U.S. Army, Corps of Engineers, Beach Erosion Board, Washington, D.C., Nov. 1949.
- DEAN, R.G., "Reprints on Stream Function Wave Theory and Application to Wave Force Calculations," Engineering and Industrial Experiment Station, College of Engineering, University of Florida, Gainesville, Fla., 1970.
- FAN, S.S., "Diffraction of Wind Waves," HEL-1-10, Hydraulics Laboratory, University of California, Berkeley, Calif., Aug. 1968.
- GRESLAU, L., and MAHE Y., "Study of the Reflection Coefficient of a Wave on an Inclined Plane," *Proceedings of the Fifth Conference on Coastal Engineering*, American Society of Civil Engineers, 1954.
- HEALY, J.J., "Wave Damping Effect of Beaches," *Proceedings of the Conference on International Hydraulics*, American Society of Civil Engineers, 1953.
- HOM-MA, M., HORIKAWA, K., and KOMORI, S., "Response Characteristics of Underwater Wave Gauge," *Proceedings of the 10th Conference on Coastal Engineering*, American Society of Civil Engineers, Vol. 1, 1966, pp. 99-114.
- HUNT, I.A., "Winds, Wind Setup and Seiches on Lake Erie," Lake Survey, U.S. Army, Corps of Engineers, Detroit, Mich., 1959.
- JOHNSON, J.W., "Engineering Aspects of Diffraction and Refraction," *Transactions of the American Society of Civil Engineers*, Vol. 118, No. 2556, 1953, pp. 617-652.
- LACOMB H., "The Diffraction of a Swell--A Practical Approximate Solution and Its Justification," *Gravity Waves*, Circular No. 521, National Bureau of Standards, Washington, D.C., 1952, pp. 129-140.
- LIU, P.L-F., "Scattering of Water Waves by a Pair of Semi-Infinite Barriers," *Journal of Applied Mechanics*, Vol. 42, 1975, pp. 777-779.
- LOWELL, S.C., "The Propagation of Waves in Shallow Water," *Communications on Pure and Applied Mathematics*, Vol. 12, Nos. 2 and 3, 1949.
- MATTSSON, A., "Reflection of Gravity Waves," *Congress on the International Association of Hydraulic Research*, London, England, 1963.
- MORSE, P.M., and RUBINSTEIN, P.J., "The Diffraction of Waves by Ribbons and Slits," *Physical Reviews*, Vol. 54, Dec. 1938, pp. 895-898.
- NIELSEN, A.H., "Diffraction of Periodic Waves Along a Vertical Breakwater of Small Angles of Incidence," HEL-1-2, Institute of Engineering Research, University of California, Berkeley, Calif., Dec. 1962.

- ORR, T.E., and HERBICH, J.B., "Numerical Calculation of Wave Refraction by Digital Computer," COE Report No. 114, Sea Grant Publication No. 209, Department of Coastal and Ocean Engineering, Texas A&M University, College Station, Tex., Dec. 1969.
- PENNEY, W.G., and PRICE, A.T., "The Diffraction Theory of Sea Waves by Breakwater and the Shelter Afforded by Breakwater," *Philosophical Transactions of the Royal Society (London)*, Series A, Vol. 244, Mar. 1952, pp. 253-263.
- PIERSON, W.J., Jr., "Observing and Forecasting Ocean Waves," H.O. No. 603, U.S. Naval Oceanographic Office, Washington, D.C., 1965.
- POCINKI, L.S., "The Application of Conformal Transformations to Ocean Wave Refraction Problems," Department of Meteorology and Oceanography, New York University, N.Y., 1950.
- SILVESTER, R., "Design Wave for Littoral Drift Model," *Journal of the Waterways and Harbors Division*, Vol. 89, WW3, No. 360, Aug. 1963.
- WORTHINGTON, H.W., and HERBICH, J.B., "A Computer Program to Estimate the Combined Effects of Refraction and Diffraction of Water Waves," Sea Grant Publication, No. 219, Texas A&M University, College Station, Tex., Aug. 1970.

# CHAPTER 3

## Wave and Water Level Predictions



*Ocean City, New Jersey, 9 March 1962*



# CONTENTS

## CHAPTER 3

### WAVE AND WATER LEVEL PREDICTIONS

	Page
I INTRODUCTION.....	3-1
II CHARACTERISTICS OF OCEAN WAVES.....	3-1
1. Significant Wave Height and Period.....	3-2
2. Wave Height Variability.....	3-2
3. Energy Spectra of Waves.....	3-11
4. Directional Spectra of Waves.....	3-14
5. Comparability of Wave Height Parameters.....	3-14
III WAVE FIELD.....	3-19
1. Development of a Wave Field.....	3-19
2. Verification of Wave Hindcasting.....	3-21
3. Decay of a Wave Field.....	3-21
IV ESTIMATION OF SURFACE WINDS FOR WAVE PREDICTION.....	3-24
1. Winds Over Water.....	3-24
2. Procedure for Adjusting Winds Observed Over Water.....	3-32
3. Procedure for Estimating Overwater Winds from Nearby Land Winds.....	3-32
4. Wind Information from Surface Pressure.....	3-33
V SIMPLIFIED METHODS FOR ESTIMATING WAVE CONDITIONS.....	3-39
1. Delineating a Fetch.....	3-39
2. Simplified Wave-Prediction Models.....	3-42
3. Formulas for Predicting Waves in Deep Water.....	3-44
4. Narrow Fetch Conditions.....	3-51
5. Effects of Moving Storms and a Variable Wind Speed and Direction.....	3-53
VI WAVE FORECASTING FOR SHALLOW WATER.....	3-55
1. Forecasting Curves.....	3-55
2. Propagation Over Flooded, Vegetated Land.....	3-66
VII HURRICANE WAVES.....	3-77
1. Description of Hurricane Waves.....	3-77
2. Model Wind and Pressure Fields for Hurricanes.....	3-81
3. Prediction Technique.....	3-83
VIII WATER LEVEL FLUCTUATIONS.....	3-88
1. Astronomical Tides.....	3-89
2. Tsunamis.....	3-92
3. Lake Levels.....	3-93
4. Seiches.....	3-96
5. Wave Setup.....	3-99
6. Storm Surge and Wind Setup.....	3-107
LITERATURE CITED.....	3-130
BIBLIOGRAPHY.....	3-140

CONTENTS--Continued

TABLES

	Page
3-1	Classes of commonly used wave height parameters.....3-15
3-2	Deepwater wave forecasting equation.....3-48
3-3	Tidal ranges.....3-92
3-4	Fluctuations in water levels, Great Lakes System (1900 through 1977).....3-96
3-5	Maximum deviations from mean lake levels.....3-97
3-6	Highest and lowest water levels.....3-116

FIGURES

3-1	Sample wave records--(a) Chesapeake Bay Bridge Tunnel, Portal Island, significant height 1.7 meters, period 4 seconds; (b) Huntington Beach, California, significant height 1.7 meters, period 8 seconds.....3-3
3-2	Waves in a coastal region.....3-4
3-3	Theoretical and observed wave height distributions.....3-7
3-4	Theoretical and observed wave height distributions.....3-8
3-5	Theoretical wave height distributions.....3-9
3-6	Typical wave spectra from the Atlantic coast.....3-13
3-7	Dimensionless wave profiles for the 40 cases.....3-16
3-8	Theoretical and observed relationship between height and standard deviation of sea-surface elevations as a function of relative water depth.....3-17
3-9	Observed and hindcasted significant wave heights versus time, December 1959, at and near the weather station J in the north Atlantic.....3-22
3-10	Corps of Engineers numerical wave model results.....3-23
3-11	Atmospheric boundary layer over waves.....3-25
3-12	Duration of the fastest mile windspeed as a function of windspeed.....3-28
3-13	Ratio of windspeed of any duration, $U_A$ , to the 1-hour windspeed, $U_{3600}$ .....3-29
3-14	Amplification ratio, $R_T$ , accounting for effects of air-sea temperature difference.....3-31
3-15	Ratio, $R_L$ , of windspeed over water, $U_W$ , to windspeed over land, $U_L$ , as a function of windspeed over land, $U_L$ .....3-31
3-16	Surface synoptic chart for 0030Z, 27 October 1950.....3-36
3-17	Sample plotted report.....3-37

## CONTENTS

### FIGURES--Continued

	Page
3-18 Geostrophic wind scale.....	3-38
3-19 Ratio $R_g$ of windspeed $U$ at 10-meter elevation to geostrophic windspeed $U_g$ .....	3-40
3-20 Possible fetch limitations.....	3-41
3-21 Forecasting curves for wave height. Constant water depth.....	3-45
3-22 Forecasting curves for wave period. Constant water depth.....	3-46
3-23 Nomograms of deepwater significant wave prediction curves as functions of windspeed, fetch length, and wind duration (metric units).....	3-49
3-24 Nomograms of deepwater significant wave prediction curves as functions of windspeed, fetch length, and wind duration (English units).....	3-50
3-25 Narrow fetch data from reservoirs.....	3-54
3-26 Narrow fetch data.....	3-54
3-27 Forecasting curves for shallow-water waves; constant depths = 5 feet and 1.5 meters.....	3-56
3-28 Forecasting curves for shallow-water waves; constant depths = 10 feet and 3.0 meters.....	3-57
3-29 Forecasting curves for shallow-water waves; constant depths = 15 feet and 4.5 meters.....	3-58
3-30 Forecasting curves for shallow-water waves; constant depths = 20 feet and 6.0 meters.....	3-59
3-31 Forecasting curves for shallow-water waves; constant depths = 25 feet and 7.5 meters.....	3-60
3-32 Forecasting curves for shallow-water waves; constant depths = 30 feet and 9.0 meters.....	3-61
3-33 Forecasting curves for shallow-water waves; constant depths = 35 feet and 10.5 meters.....	3-62
3-34 Forecasting curves for shallow-water waves; constant depths = 40 feet and 12.0 meters.....	3-63
3-35 Forecasting curves for shallow-water waves; constant depths = 45 feet and 13.5 meters.....	3-64
3-36 Forecasting curves for shallow-water waves; constant depths = 50 feet and 15 meters.....	3-65
3-37 Bottom friction factors.....	3-68
3-38 Relationship for friction loss over a bottom of constant depth....	3-69
3-39 Typical hurricane wave spectra from the Atlantic coast of the United States.....	3-78

CONTENTS

FIGURES--Continued

	Page
3-40 Single-peaked spectrum near the center of Hurricane David, West Palm Beach, Florida.....	3-79
3-41 Compositive wave charts.....	3-80
3-42 Pressure and wind distribution in model hurricane.....	3-82
3-43 Isolines of relative significant wave height for slow-moving hurricane.....	3-85
3-44 Typical tide curves along Atlantic and gulf coasts.....	3-90
3-45 Typical tide curves along Pacific coasts of the United States.....	3-91
3-46 Sample tsunami records from tide gages.....	3-94
3-47 Typical water level variations in Great Lakes.....	3-95
3-48 Long wave surface profiles.....	3-97
3-49 Definition sketch of wave setup.....	3-100
3-50 $S_w/H_b$ versus $H_b/gT^2$ .....	3-103
3-51 Definition sketch.....	3-105
3-52 Measured random wave setup on a 1-on-30 flat slope.....	3-108
3-53 Predicted random wave setup on plane slopes for $\frac{d}{H_o} = 0.5$ .....	3-109
3-54 Storm surge and observed tide chart, Hurricane Carla, 7-12 September 1961.....	3-112
3-55 High water mark chart for Texas, Hurricane Carla, 7-12 September 1961.....	3-114
3-56 Notation and reference frame.....	3-120
3-57 Storm surge chart, Hurricane Carol, 30 and 31 August 1954.....	3-124
3-58 Lake surface contours on Lake Okeechobee, Florida, Hurricane on 26 and 27 August 1949.....	3-128

## CHAPTER 3

### WAVE AND WATER LEVEL PREDICTIONS

#### I. INTRODUCTION

Chapter 2 treated phenomena associated with surface waves as though each phenomenon could be considered separately without regard to other phenomena. Surface waves were discussed from the standpoint of motions and transformations without regard to wave generation. Furthermore, the water level, *stillwater level (SWL)*, on which the waves propagated was assumed known.

In this chapter, wave observations are presented to show characteristics of surface waves in nature. The characteristics of real waves are much less regular than those implied by theory. Also presented are procedures for representing the complexity of the real sea by a small number of parameters. Deviations between the actual waves and the parameter values are discussed.

Theory for wave generation is reviewed to show progress in explaining and predicting the actual complexity of the sea. Wave prediction is called *hindcasting* when based on past meteorological conditions and *forecasting* when based on predicted conditions. The same procedures are used for hindcasting and forecasting; the only difference is the source of meteorological data. The most advanced prediction techniques currently available can be used only in a few laboratories because of the need for computers, the sophistication of the models, and the need for correct weather data. However, simplified wave prediction techniques, suitable for use by field offices, are presented. While simplified prediction systems will not solve all problems, they can be used to indicate probable wave conditions for some design studies.

Prediction theories are reviewed to give the reader more perspective for the simplified prediction methods provided. This will justify confidence in some applications of the simplified procedures, will aid in recognizing unexpected difficulties when they occur, and will indicate some conditions in which they are not adequate. The problem of obtaining wind information for wave hindcasting is discussed, and specific instructions for estimating wind parameters are given.

Many factors govern water levels at a shore during a storm. Other than the tide, the principal factor is the effect of wind blowing over water. Some of the largest increases in water level are due to severe storms, such as hurricanes, which can cause storm surges higher than 7.0 meters (22 feet) at some locations on the open coast and even higher water levels in bays and estuaries. Estimating water levels caused by meteorological conditions is complex, even for the simplest cases; the best approaches available for predicting these water levels are elaborate numerical models which require use of a computer.

#### II. CHARACTERISTICS OF OCEAN WAVES

The earlier discussion of waves was concerned with idealized, monochromatic waves. The pattern of waves on any body of water exposed to winds

generally contains waves of many periods. Typical records from a recording gage during periods of steep waves (Fig. 3-1) indicate that heights and periods of real waves are not constant as is assumed in theory. Wavelengths and directions of propagation are also variable (see Fig. 3-2). Further, the surface profile for waves near breaking in shallow water or for very steep waves in any water depth is distorted, with high narrow crests and broad flat troughs (see Ch. 2, II, 5 and 6 and higher waves in Fig. 3-1,a). Real ocean waves are so complex that some idealization is required.

## 1. Significant Wave Height and Period.

An early idealized description of ocean waves postulated a *significant height* and *significant period* that would represent the characteristics of the real sea in the form of monochromatic waves. The representation of a wave field by significant height and period has the advantage of retaining much of the insight gained from theoretical studies. Its value has been demonstrated in the solution of many engineering problems. For some problems this representation appears adequate; for others it is useful, but not entirely satisfactory.

To apply the significant wave concept it is necessary to define the height and period parameters from wave observations. Munk (1944) defined *significant wave height*, as the *average height of the one-third highest waves*, and stated that it was about equal to the average height of the waves as estimated by an experienced observer. This definition, while useful, has some drawbacks in wave record analysis. It is not always clear which irregularities in the wave record should be counted to determine the total number of waves on which to compute the average height of the one-third highest. The significant wave height is written as  $H_{1/3}$  or simply  $H_s$ .

The significant wave period obtained by visual observations of waves is likely to be the average period of 10 to 15 successive prominent waves. When determined from gage records, the significant period is apt to be the average period of all waves whose troughs are below and whose crests are above the mean water level (zero up-crossing method). Most modern gage record analyses provide a wave period corresponding to the highest peak of the spectrum (see Ch. 3, II, 3, Energy Spectra of Waves), which has greater dynamic importance than significant period, although the two parameters are generally comparable.

## 2. Wave Height Variability.

When the heights of individual waves on a deepwater wave record are ranked from the highest to lowest, the frequency of occurrence of waves above any given value is given to a close approximation by the cumulative form of the Rayleigh distribution. This fact can be used to estimate the average height of the one-third highest waves from measurements of a few of the highest waves, or to estimate the height of a wave of any arbitrary frequency from a knowledge of the significant wave height. According to the Rayleigh distribution function, the probability that the wave height  $H$  is more than some arbitrary value of  $H$  referred to as  $\hat{H}$  is given by

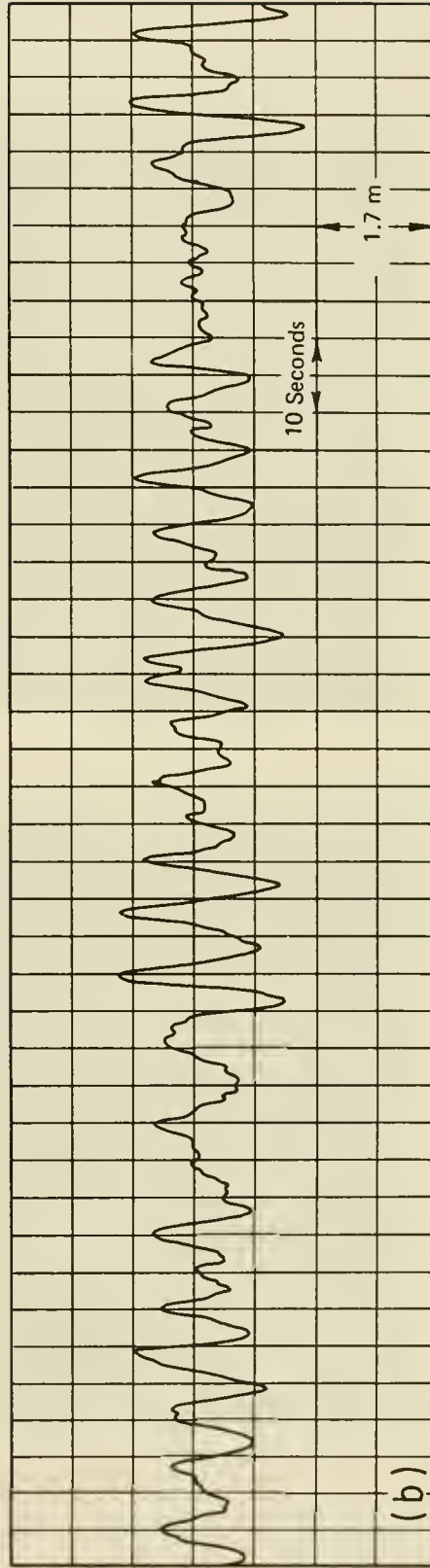
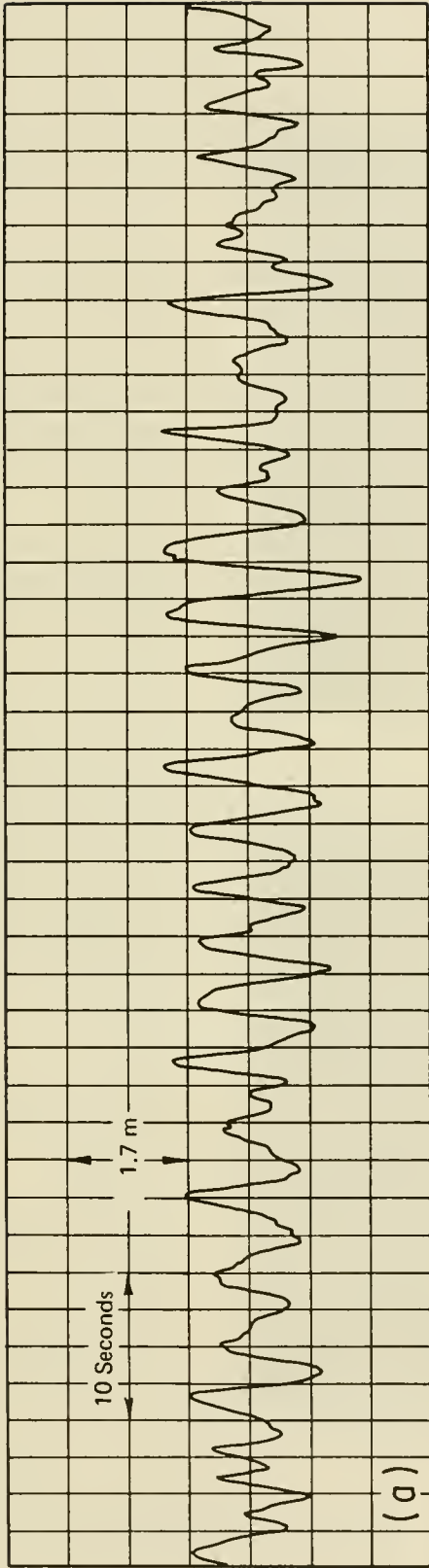


Figure 3-1. Sample wave records--(a) Chesapeake Bay Bridge Tunnel, Portal Island, significant height 1.7 meters (5.5 feet), period 4 seconds; (b) Huntington Beach, California, significant height 1.7 meters, period 8 seconds.

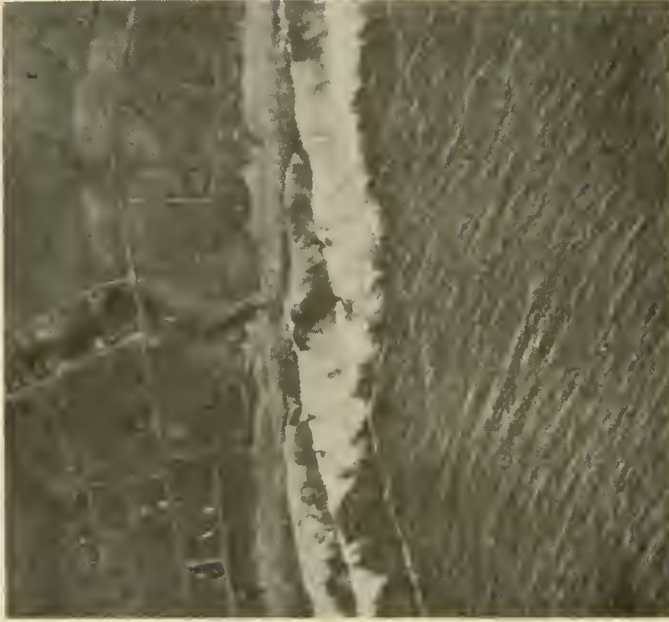
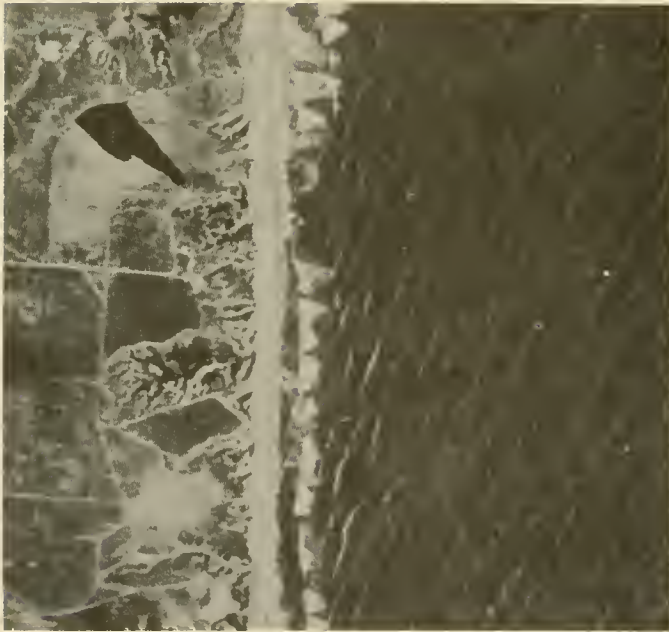


Figure 3-2. Waves in a coastal region. (The left photo shows two wave trains approaching the shore simultaneously forming an irregular pattern of short-crested waves. The right photo shows long swell obscured by local wind waves until almost the breaking point.)

$$P(H > \hat{H}) = e^{-\left(\frac{\hat{H}}{H_{rms}}\right)^2} \quad (3-1)$$

where  $H_{rms}$  is a parameter of the distribution, and  $P(H > \hat{H})$  is the number  $n$  of waves larger than  $\hat{H}$  divided by the total number  $N$  of waves in the record. Thus  $P$  has the form  $n/N$ . The value  $H_{rms}$  is called the *root-mean-square height* and is defined by

$$H_{rms} = \sqrt{\frac{1}{N} \sum_{j=1}^N H_j^2} \quad (3-2)$$

It was shown in Chapter 2, Section II,3,h (Wave Energy and Power) that the total energy per unit surface area for a train of sinusoidal waves of height  $H$  is given by

$$\bar{E} = \frac{\rho g H^2}{8}$$

The average energy per unit surface area for a number of sinusoidal waves of variable height is given by

$$(\bar{E})_A = \frac{\rho g}{8} \frac{1}{N} \sum_{j=1}^N H_j^2 \quad (3-3)$$

where  $H_j$  is the height of successive individual waves and  $(\bar{E})_A$  the average energy per unit surface area of all waves considered. Thus  $H_{rms}$  is a measure of average wave energy. Calculation of  $H_{rms}$  by equation (3-2) is somewhat more subjective than direct evaluation of the  $H_g$  in which more emphasis is placed on the larger, better defined waves. The calculation of  $H_{rms}$  can be made more objective by substituting  $n/N$  for  $P(H > \hat{H})$  in equation (3-1) and taking natural logarithms of both sides to obtain

$$\ln(n) = \ln(N) - (H_{rms}^{-2}) \hat{H}^2 \quad (3-4)$$

By making the substitutions

$$y(n) = \ln(n), \quad a = \ln(N), \quad b = -H_{rms}^{-2}, \quad x(n) = \hat{H}^2(n)$$

Equation (3-4) may be written as

$$y(n) = a + bx(n) \quad (3-5)$$

The constants  $a$  and  $b$  can be found graphically or by fitting a least squares regression line to the observations. The parameters  $N$  and  $H_{rms}$  may be computed from  $a$  and  $b$ . The value of  $N$  found in this way is the value that provides the best fit between the observed distribution of identified waves and the Rayleigh distribution function. It is generally a little larger than the number of waves actually identified in the record. This seems reasonable because some very small waves are generally neglected in interpreting the record. When the observed wave heights are scaled by  $H_{rms}$ ;

i.e., made dimensionless by dividing each observed height by  $H_{rms}$ ; data from all observations may be combined into a single plot. Points from scaled 15-minute samples are superimposed on Figure 3-3 to show the scatter to be expected from analyzing individual observations in this manner.

Data from 72 scaled 15-minute samples representing 11,678 observed waves have been combined in this manner to produce Figure 3-4. The theoretical height appears to be about 5 percent greater than the observed height for a probability of 0.01 and 15 percent greater at a probability of 0.0001. It is possible that the difference between the actual and the theoretical heights of highest waves is due to breaking of the highest waves before they reach the coastal wave gages. Hence the Rayleigh distribution may be taken as an approximate distribution in shallow water, but is probably conservative.

Equation (3-1) can be established rigorously for restrictive conditions and empirically for a much wider range of conditions. If equation (3-1) is used, the probability density function can be obtained in the form

$$f[(\hat{H} - \Delta H) \leq H \leq (\hat{H} + \Delta H)] = \left(\frac{2}{H_{rms}^2}\right) H e^{-\left(\frac{\hat{H}}{H_{rms}}\right)^2} \quad (3-6)$$

The height of the wave with any given probability  $n/N$  of being exceeded may be determined approximately from curve a in Figure 3-5 or from the equation

$$\frac{\hat{H}}{H_{rms}} = \left[-\text{Ln}\left(\frac{n}{N}\right)\right]^{1/2} \quad (3-7)$$

The average height of all waves with heights greater than  $\hat{H}$ , denoted  $\bar{H}(\hat{H})$ , can be obtained from the equation

$$\bar{H}(\hat{H}) = \frac{\int_{\hat{H}}^{\infty} H^2 e^{-\left(\frac{H}{H_{rms}}\right)^2} dH}{\int_{\hat{H}}^{\infty} H e^{-\left(\frac{H}{H_{rms}}\right)^2} dH} \quad (3-8)$$

Alternatively, the ratio  $\bar{H}(\hat{H})/H_{rms}$  can be estimated from curve b in Figure 3-5, where  $P$  is the probability of  $\hat{H}$  being exceeded. By setting  $\hat{H} = 0$ , all waves are considered and it is found that the average wave height is given by

$$\bar{H} = 0.886 H_{rms} \quad (3-9)$$

and the significant wave height is given by

$$H_s = 1.416 H_{rms} \approx \sqrt{2} H_{rms} \quad (3-10)$$

In the analysis system used by CERC from 1960 to 1970, and whenever digital recordings cannot be used, the average period of a few of the best formed waves is selected as the significant wave period. An estimated number of

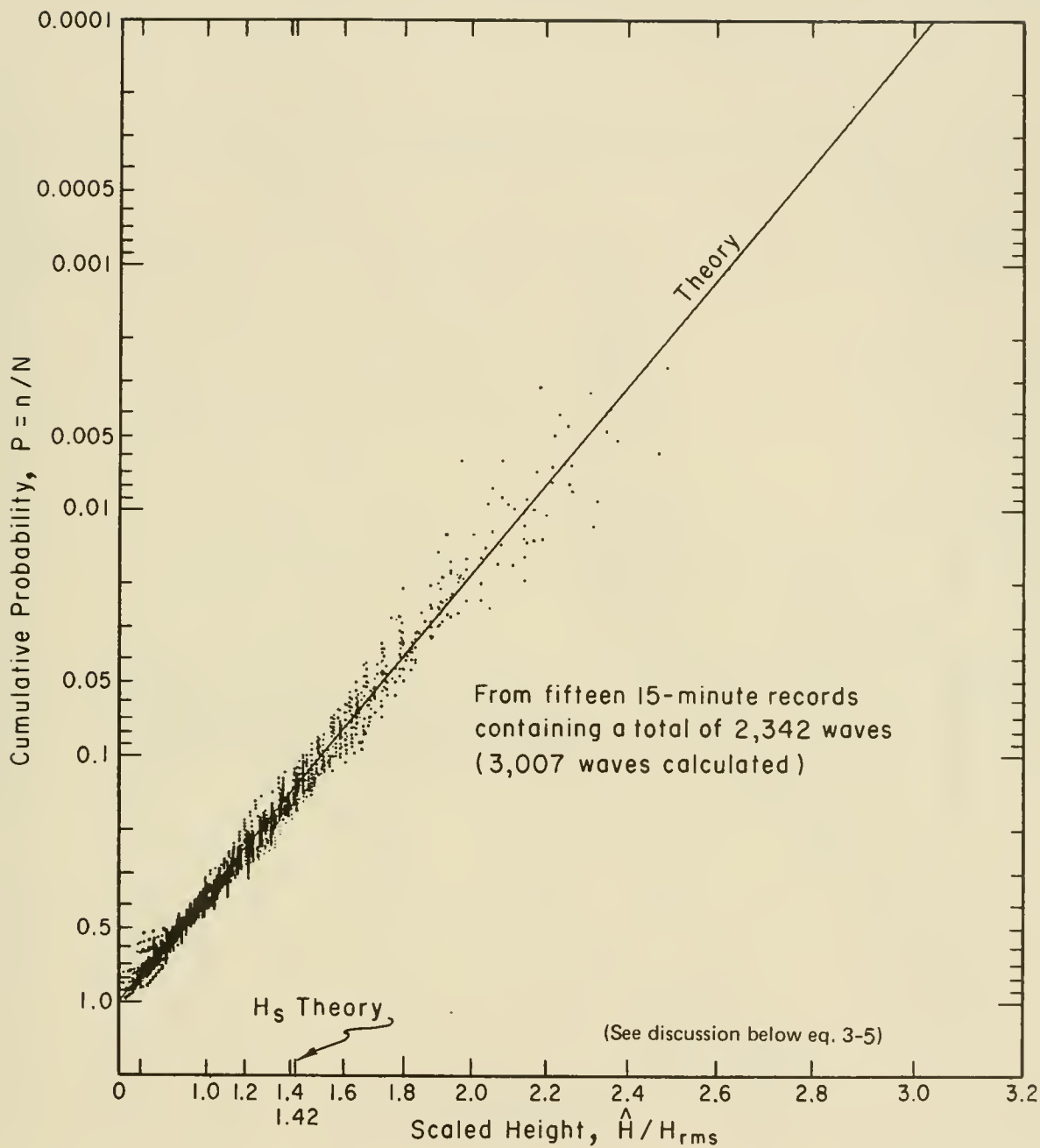


Figure 3-3. Theoretical and observed wave height distributions. (Observed distributions for 15 individual 15-minute observations from several Atlantic coast wave gages are superimposed on the Rayleigh distribution curve.)

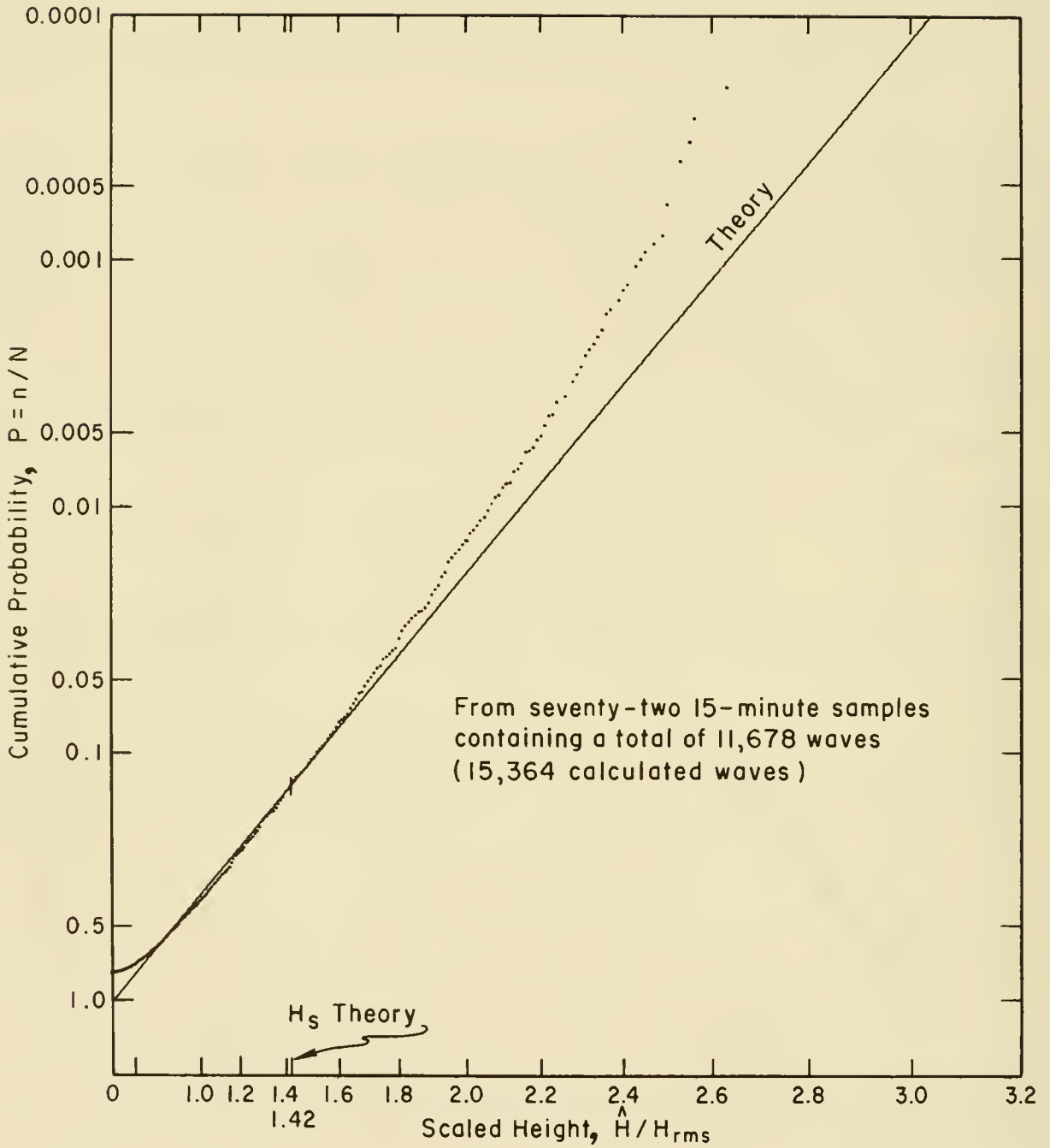


Figure 3-4. Theoretical and observed wave height distributions. (Observed waves from 72 individual 15-minute observations from several Atlantic coast wave gages are superimposed on the Rayleigh distribution curve.)

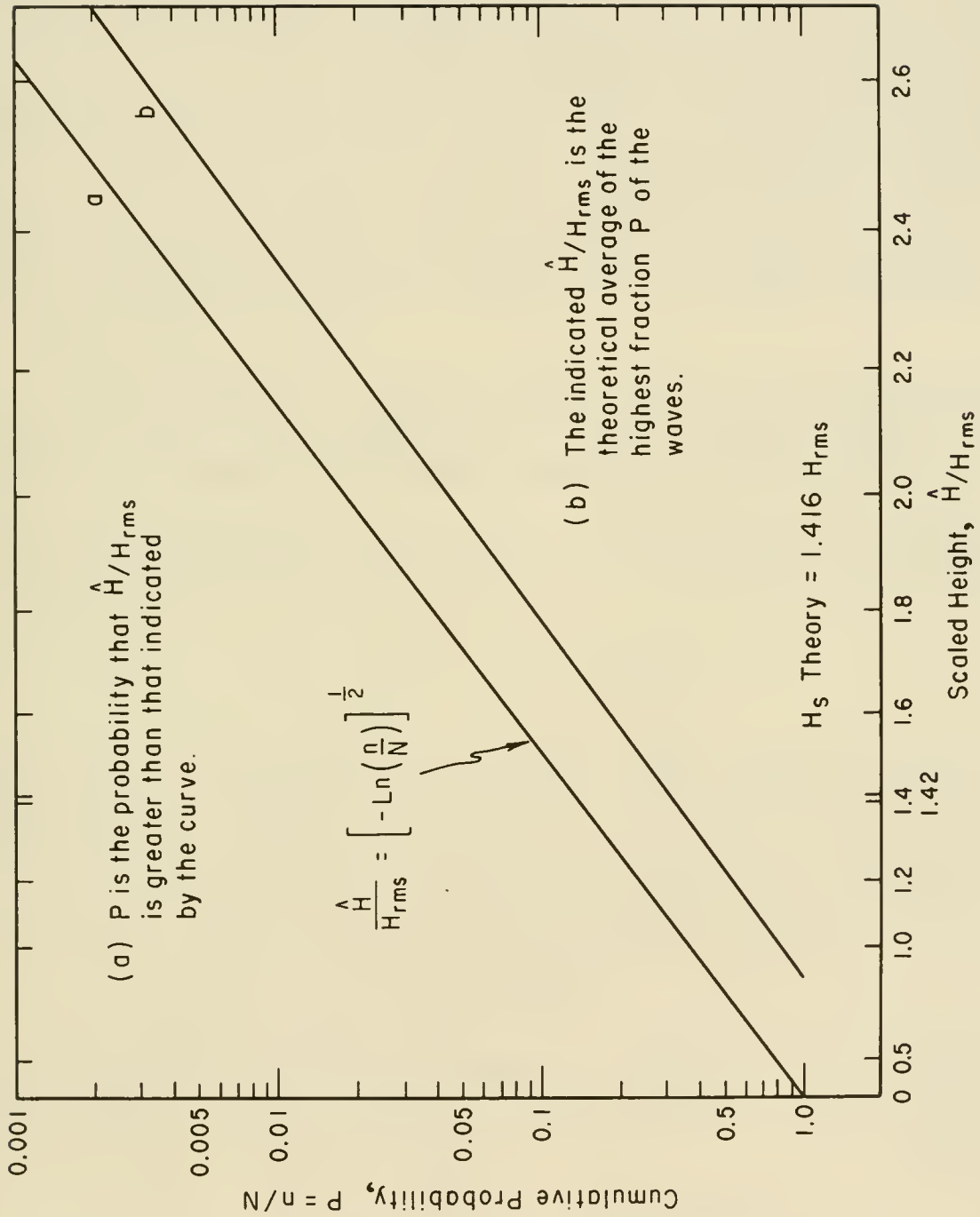


Figure 3-5. Theoretical wave height distributions.

equivalent waves in the record is obtained by dividing the duration of the record by this significant period. The highest waves are then ranked in order, with the highest wave ranked 1. The height of the wave ranked 0.135 times the total number of waves is taken as the significant wave height. The derivation of this technique is based on the assumption that the Rayleigh distribution law is exact. Harris (1970) and Thompson (1977) showed that this procedure agrees closely with values obtained by more rigorous procedures which require the use of a computer. These procedures are described in Chapter 3, Section II,3 (Energy Spectra of Waves).

The following problem illustrates the use of the theoretical wave height distribution curves given in Figure 3-5.

\*\*\*\*\* EXAMPLE PROBLEM 1 \*\*\*\*\*

GIVEN: Based on an analysis of wave records at a coastal location, the significant wave height  $H_g$  was estimated to be 3 meters (9.84 feet).

FIND:

- (a)  $H_{10}$  (average of the highest 10 percent of all waves).
- (b)  $H_1$  (average of the highest 1 percent of all waves).

SOLUTION:  $\hat{H} = H_g = 3$  meters

Using equation (3-10)

$$H_g = 1.416 H_{rms}$$

or

$$H_{rms} = \frac{H_g}{1.416} = \frac{3}{1.416} = 2.12 \text{ m (6.95 ft)}$$

(a) From Figure 3-5, curve b, it is seen that for  $P = 0.1$  (10 percent)

$$\frac{H_{10}}{H_{rms}} \approx 1.80; H_{10} = 1.80 H_{rms} = 1.80 (2.12) = 3.82 \text{ m (12.53 ft)}$$

(b) Similarly, for  $P = 0.01$  (1 percent)

$$\frac{H_1}{H_{rms}} \approx 2.36; H_1 = 2.36 H_{rms} = 2.36 (2.12) = 5.0 \text{ m (16.41 ft)}$$

Note that

$$\frac{H_{10}}{H_g} = \frac{3.82}{3} \text{ or } H_{10} = 1.27 H_g$$

and

$$\frac{H_1}{H_s} = \frac{5.0}{3} \text{ or } H_1 = 1.67 H_s$$

\*\*\*\*\*

Goodknight and Russell (1963) analyzed wave gage observations taken on an oil platform in the Gulf of Mexico during four hurricanes. They found agreement adequate for engineering application between such important parameters as  $H_s$ ,  $H_{10}$ ,  $H_{max}$ ,  $H_{rms}$ , and  $\bar{H}$ , although they did not find consistently good agreement between measured wave height distributions and the entire Rayleigh distribution. Borgman (1972) and Earle (1975) substantiate this conclusion using wave observations from other hurricanes. These findings are consistent with Figures 3-3 and 3-4, based on wave records obtained by CERC from shore-based gages. The CERC data include waves from both extra-tropical storms and hurricanes.

### 3. Energy Spectra of Waves.

The significant wave analysis, although simple in concept, is difficult to do objectively and does not provide all the information needed in engineering design. Also, it can be misleading in terms of available wave energy when applied in very shallow water where wave shapes are not sinusoidal.

Figure 3-1 indicates that the wave field might be better described by a sum of sinusoidal terms. That is, the curves in Figure 3-1 might be better represented by expressions of the type

$$n(t) = \sum_{j=1}^N a_j \cos(\omega_j t - \phi_j) \tag{3-11}$$

where  $n(t)$  is the departure of the water surface from its average position as a function of time,  $a_j$  the amplitude,  $\omega_j$  the frequency, and  $\phi_j$  the phase of the  $j^{th}$  wave at the time  $t = 0$ . The values of  $\omega$  are arbitrary, and  $\omega$  may be assigned any value within suitable limits. In analyzing records, however, it is convenient to set  $\omega_j = 2\pi j/D$ , where  $j$  is an integer and  $D$  the duration of the observation. The  $a_j$  will be large only for those  $\omega_j$  that are prominent in the record. When analyzed in this manner, the significant period may be defined as  $D/j$ , where  $j$  is the value of  $j$  corresponding to the largest  $a_j$ .

It was shown by Kinsman (1965) that the average energy of the wave train is proportional to the average value of  $[n(t)]^2$ . This is identical to  $\sigma^2$ , where  $\sigma$  is the standard deviation of the wave record. It can also be shown that

$$\sigma^2 = \frac{1}{2} \sum_{j=1}^N a_j^2 \tag{3-12}$$

In deep water, a useful estimate of significant height that is fundamentally related to wave energy is defined as

$$H_{m_0} = 4\sigma \quad (3-13)$$

Experimental results and calculations based on the Rayleigh distribution function show that when wave shapes are not severely deformed by shallow-water depth or high wave steepness, the following approximation can be used

$$H_{m_0} \approx H_s \quad (3-14)$$

Recalling that (eq. 3-10)

$$H_s \approx \sqrt{2} H_{rms}$$

then

$$\sigma \approx 0.25 \sqrt{2} H_{rms} \quad (3-15)$$

or

$$H_{rms} \approx 2 \sqrt{2} \sigma \quad (3-16)$$

These approximations may be poor when waves are breaking or near breaking (see Chapter 3, Section II,5, Comparability of Wave Height Parameters).

The variation of  $a_j^2$  with frequency can be used to estimate the distribution of wave energy as a function of frequency. This distribution is called the energy spectrum, often expressed as

$$E(\omega_j) (\Delta\omega)_j = \frac{a_j^2}{2} \quad (3-17)$$

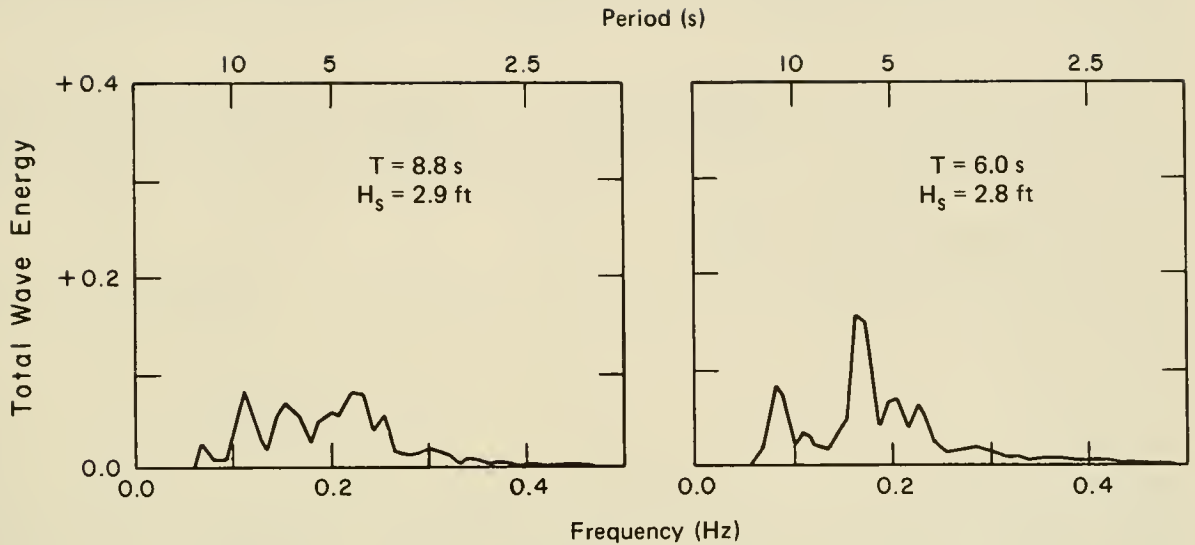
where  $E(\omega_j)$  is the energy density in the  $j^{th}$  component of the energy spectrum and  $(\Delta\omega)_j$  is the frequency bandwidth (difference between successive  $\omega_j$ ).

Equation (3-17) can be combined with equation (3-12) and  $N$  made to approach infinity to give

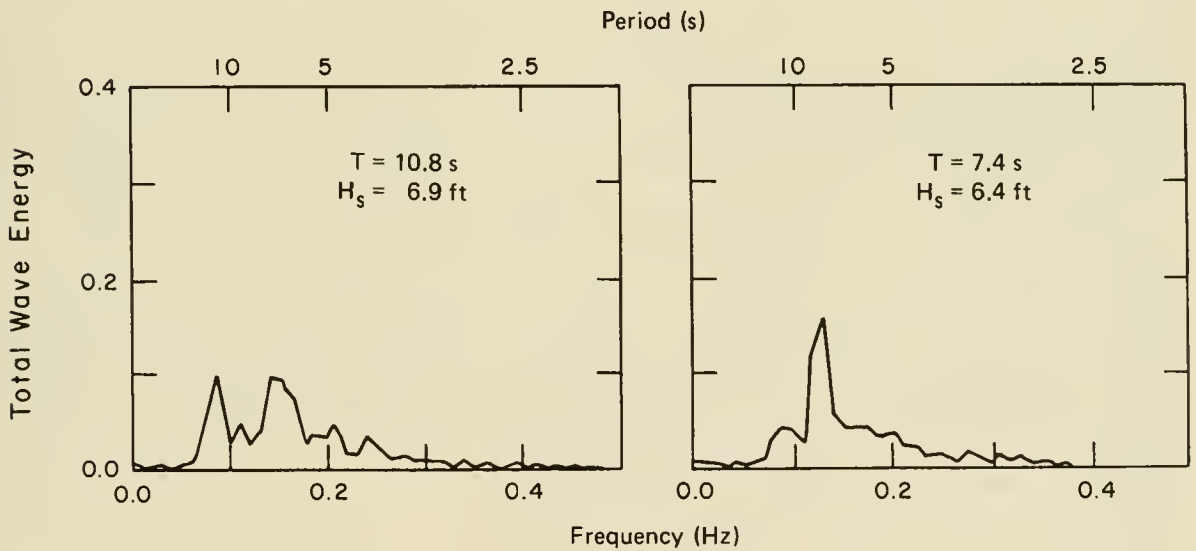
$$\sigma^2 = \int_0^{\infty} E(\omega) d\omega \quad (3-18)$$

where  $E(\omega)$  is the continuous energy spectrum.

The spectrum  $E(\omega)$  or  $E(\omega_j)$  permits specific parts of the total wave energy to be assigned to specific frequency intervals. Frequencies associated with large values of  $E(\omega)$  are dominant frequencies (periodicities) in a wave field. Frequencies associated with small values of  $E(\omega)$  are usually unimportant. It is common for ocean wave spectra to show two or more dominant frequencies, indicating the presence of two or more wave trains (see Figure 3-6). The spectrum allows easy identification of all prominent frequencies present and an assessment of their relative importance. Thus it also permits a first approximation in the calculation of velocities and accelerations from



Savannah Coast Guard Light Tower



Nags Head, N.C.

Figure 3-6. Typical wave spectra from the Atlantic coast. (The ordinate scale is the fraction of total wave energy in each frequency band of 0.011 hertz (1 hertz is 1 cycle per second). A linear frequency scale is shown at the bottom of each graph and a nonlinear period scale at the top of each graph).

a wave height record for a complex wave field. Since wave period is proportional to the reciprocal of frequency, important wave periods are also identified. Thompson (1980) provides further interpretations of coastal wave spectra.

The international standard unit for frequency measure is the *hertz*, defined as one cycle per second. The unit *radians per second* is also widely used. One hertz is equivalent to  $2\pi$  radians per second.

#### 4. Directional Spectra of Waves.

A more complete description of the wave field must recognize that not all waves are traveling in the same direction. This may be written as

$$\eta(x,y,t) = \sum a_j \cos \left[ \omega_j t - \phi_j - k_j (x \cos \theta_j + y \sin \theta_j) \right] \quad (3-19)$$

where  $k_j = 2\pi/L_j$ ,  $\phi_j$  is the angle between the  $x$  axis and the direction of wave propagation, and  $\theta_j$  is the phase of the  $j^{\text{th}}$  wave at  $t = 0$ . The energy density  $E(\theta, \omega)$  represents the concentration of energy at a particular wave direction  $\theta$  and frequency  $\omega$ ; therefore, the total energy is obtained by integrating  $E(\theta, \omega)$  over all directions and frequencies. Thus

$$E = \int_0^{2\pi} \int_0^{\infty} E(\theta, \omega) d\omega d\theta \quad (3-20)$$

The directional spectrum  $E(\theta, \omega)$  can be used to identify prominent frequencies and propagation directions; when these represent individual wave trains, they provide important information for many coastal engineering applications.

The concept of directional wave spectra is essential for advanced wave prediction models. Such models estimate wave growth, decay, and propagation under varying wind conditions in terms of directional spectra. Directional spectra are becoming increasingly available from gage measurements through the use of multiple, closely spaced pressure or staff gages; a pressure gage in combination with velocity measurements in the horizontal plane; or measurements of pitch and roll in a floating buoy. Remote sensing techniques for estimating directional spectra from imagery obtained by satellite are also a promising source of directional spectra.

#### 5. Comparability of Wave Height Parameters.

The wave height parameters discussed in Chapter 3, Sections II,1 and 2 based on statistics of the heights of individual waves in a record, may be referred to as "statistical-based" parameters. Wave height parameters introduced in Chapter 3, Section II, 3 are defined in terms of the standard deviation of sea-surface *elevations* as represented by all data values in the wave record. These parameters represent a fundamentally different class called "energy-based" parameters.

A third class of wave height parameters is defined in terms of idealized waves of uniform height and period. These "monochromatic-based" parameters

are sometimes encountered in laboratory and theoretical work. Commonly used wave height parameters in each of the three classes are listed in Table 3-1.

TABLE 3-1. Classes of commonly used wave height parameters.

Base	Parameter
Statistical	$H_{\max}$ , $H_1$ , $H_{1/3}$ , $H_s$ , $\bar{H}$ , $H_{rms}$
Energy	$H_{m_0}$ , $\sigma$
Monochromatic	$H_b$ , $H$

Wave height parameters within each class are clearly and easily inter-related. However, confusion can arise when parameters from different classes must be related. The primary source of confusion is the fundamental differences in the definition bases. Efforts to specify the relationship between parameters in different classes are further complicated by a dependence on water depth and wave characteristics such as steepness. For example, the relationship between the height of a wave and the potential energy contained in the deformed water surface changes as the wave profile changes shape in shallow water. Wave profiles computed by the stream-function theory (Chapter 2, Section II,h; Dean, 1974) for 40 cases clearly illustrate the dramatic differences induced by high wave steepness and shallow water (Fig. 3-7). These differences should be recognized by coastal engineers dealing with breaking or near-breaking wave conditions.

Dean's (1974) computations provide an approximate means of relating statistical-based with energy-based wave parameters. Although Dean's computations represent uniform waves propagating over a flat bottom, they can be expected to provide useful insight on how the ratio of wave height to the standard deviation of the wave profile can vary with water depth and wave steepness (Fig. 3-8).  $H_b$  is a combined depth-limited and steepness-limited breaking wave height that can be estimated as a function of  $H/gT^2$  and  $d/gT^2$  by the breaking limit curve in Figure 2-7 in Chapter 2. To aid in estimating a realistic practical limit on the ratio  $H_s/H_{m_0}$  for real ocean waves, the upper envelope of estimates from two comprehensive field experiments in which wave measurements were collected along a shore-perpendicular line of gages extending through and beyond the surf zone is also shown. The figure indicates that  $H_s$  is approximately equal to  $H_{m_0}$  in deep water, but can be at least 30 percent greater in shallow water for breaking waves. Thus, it is important to distinguish between  $H_s$  and  $H_{m_0}$  for depth-limited breaking waves.

Since monochromatic waves are actually a different phenomenon than irregular waves with the most satisfactory way to relate monochromatic-based

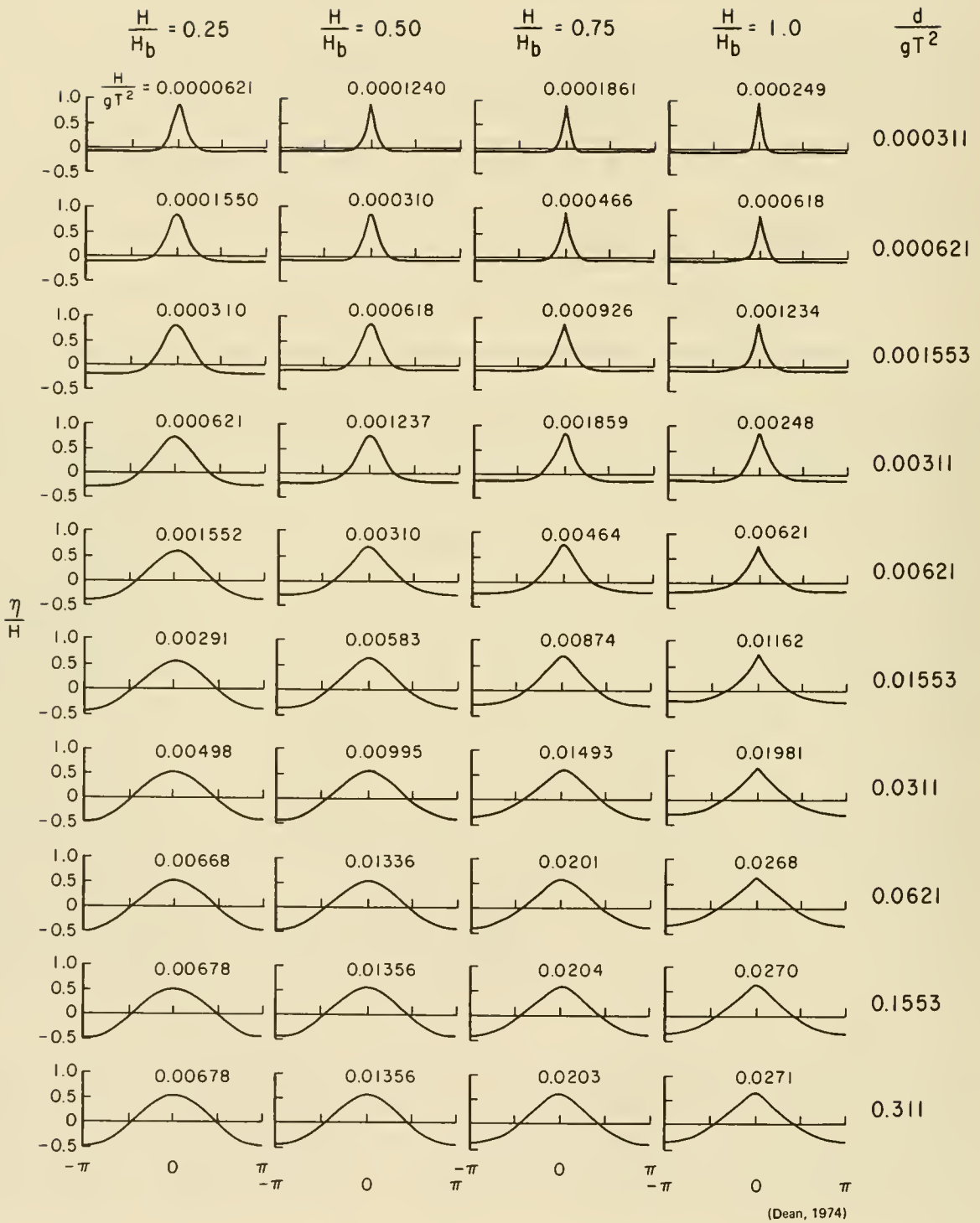


Figure 3-7. Dimensionless wave profiles for the 40 cases (Dean, 1974). (Numbers on each plot represent the value of  $H/gT^2$  for each case.)

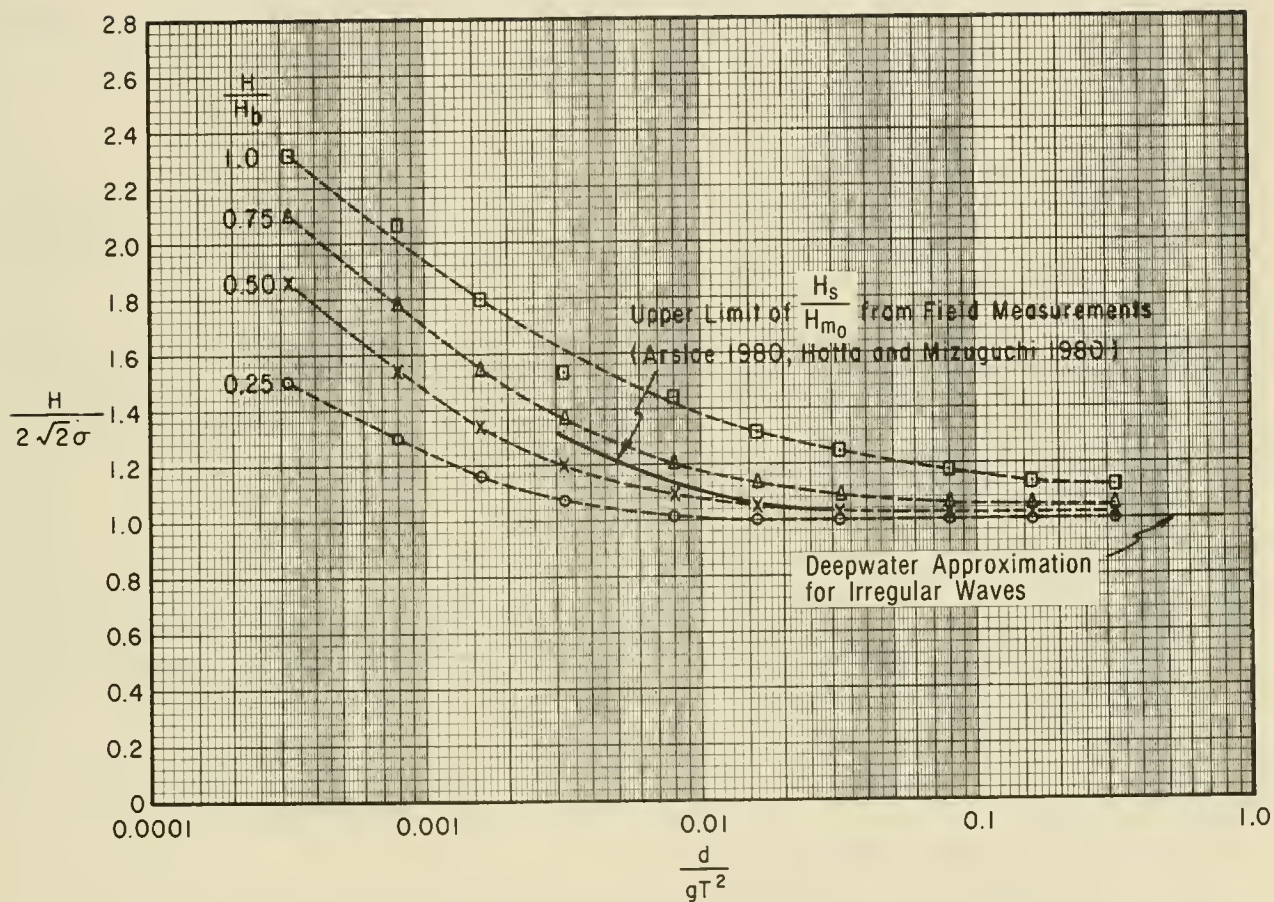


Figure 3-8. Theoretical and observed relationship between height and standard deviation of sea-surface elevations as a function of relative water depth. (Dashed curves represent the stream-function wave theory (Dean, 1974). The solid curve represents the upper limit of short-term measurements from two field experiments (Thompson and Seelig, 1984; Hotta and Mizuguchi, 1980).)

height parameters with parameters from the other two classes depends on the particular application. A rational approach for some applications is to equate the average total wave energy in both monochromatic and irregular wave trains. Thus, for sinusoidal, nonbreaking waves using relationships from Chapter 3, Sections II,2 and II,3

$$\frac{\rho g H^2}{8} = \rho g \sigma^2 \quad (3-21)$$

$$\frac{\rho g H^2}{8} = \rho g \frac{H_{m0}^2}{16} \quad (3-22)$$

$$H^2 = \frac{H_{m0}^2}{2} \quad (3-23)$$

or

$$H \approx H_{m0} / \sqrt{2} \quad (3-24)$$

Thus the height  $H$ , representing a monochromatic wave train with the same energy as an irregular wave train with significant height  $H_{m0}$ , is equal to  $0.71 H_{m0}$  for deep water. A precise computation of the relationship in shallow water is much more difficult. Equation (3-24) is expected to be a reasonable approximation for shallow water.

\*\*\*\*\* EXAMPLE PROBLEM 2 \*\*\*\*\*

GIVEN: Based on wave hindcasts from a spectral model, the energy-based wave height parameter  $H_{m0}$  and the peak spectral period  $T_p$  were estimated to be 3.0 meters (10 feet) and 9 seconds in a water depth of 6 meters (19.7 feet).

FIND:

- (a) An approximate value of  $H_s$ .
- (b) An approximate value of  $H_1$ .

SOLUTION:

$$(a) \quad \frac{d}{gT_p^2} = \frac{6.0}{9.81(9)^2} = 0.00755$$

It is evident from Figure 2-7 in Chapter 2 that the relative depth  $d/gT_p^2$  is sufficiently small that breaking is depth-limited. Thus

$$\frac{H_b}{d} = 0.78$$

$$H_b = 0.78 (6.0) = 4.7 \text{ m (15.4 ft)}$$

$$\frac{H_{m0}}{H_b} = \frac{3.0}{4.7} = 0.64$$

Enter Figure 3-8 with known values of  $d/gT_p^2$  and  $H_{m0}/H_b$ .

Note that  $H/H_b$  in Figure 3-8 is a ratio of wave heights which may be approximately estimated as  $H_s/H_b$  for irregular waves; however, only the energy-based parameter  $H_{m0}$  is known in this example. If the computed value of  $H_s$  differs greatly from  $H_{m0}$ , it may be necessary to return to

Figure 3-8 with a revised ratio  $\frac{H_s}{H_{m0}}$ . Using the vertical axis of Figure 3-8, estimate

$$\frac{H_s}{H_{m0}} = 1.16$$

This answer seems reasonable in light of the envelope of the field data shown in Figure 3-8. It does not seem necessary to repeat the analysis with a revised ratio  $H_s/H_b$ . Thus

$$H_s = 1.16(3.0) = 3.5 \text{ m (11.5 ft)}$$

(b)  $H_1 = 1.67 H_s$  from example in Chapter 3, Section II,2

$$H_1 = 1.67(3.5) = 5.8 \text{ m (19.0 ft)}$$

Note that this value is greater than  $H_b$ . Since  $H_b$  is the maximum allowable individual wave height, the computed value for  $H_1$  is too high in this example. Use instead  $H_1 = H_b = 4.7 \text{ m (} H_1 = H_b = 15.4 \text{ ft)}$ .

\*\*\*\*\*

### III. WAVE FIELD

#### 1. Development of a Wave Field.

Descriptions of the mechanism of wave generation by wind have been given, and significant progress in explaining the mechanism was reported by Miles (1957), Phillips (1957), and Hasselmann et al. (1973).

The Miles-Phillips-Hasselmann theory, as extended and corrected by experimental data, permits the formulation of a differential equation governing the growth of wave energy. This equation can be written in a variety of ways (Inoue, 1966, 1967; Barnett, 1968; Hasselmann, et al., 1976). Numerical models have been developed that solve these equations for oceanic and Great Lakes conditions (Inoue, 1967; Barnett, 1968; Hasselmann, et al., 1976; Resio and Vincent, 1977a; Resio, 1981). This approach will not be discussed in detail because the applications of such models require specialized expertise. A brief discussion of the physical concepts employed in the computer wave forecast, however, is presented to show the shortcomings and merits of simpler procedures that can be used in wave forecasting.

Growth and dissipation of wave energy are very sensitive to wave frequency and wave direction relative to the wind direction. Thus it is desirable to

consider each narrow band of directions and frequencies separately. A change in wave energy depends on the advection of energy into and out of a region; transformation of the wind's kinetic energy into the energy of water waves; dissipation of wave energy into turbulence by friction, viscosity, and breaking; and transformation of wave energy at one frequency into wave energy at other frequencies.

Phillips (1957) showed that the turbulence associated with the flow of wind near the water would create traveling pressure pulses. These pulses generate waves traveling at a speed appropriate to the dimensions of the pressure pulse. Wave growth by this process is most rapid when the waves are short and when their speed is identical with the component of the wind velocity in the direction of wave travel. The empirical data analyzed by Inoue (1966, 1967) indicates that the effect of turbulent pressure pulses is real, but it is only about one-twentieth as large as the original theory indicated.

Miles (1957) showed that the waves on the sea surface must be matched by waves on the bottom surface of the atmosphere. The speed of air and water must be equal at the water surface. Under most meteorological conditions, the airspeed increases from near 0 to 60-90 percent of the free air value within 20 meters (66 feet) of the water surface. Within a shear zone of this type, energy is extracted from the mean flow of the wind and transferred to the waves. The magnitude of this transfer at any frequency is proportional to the wave energy already present at that frequency. Growth is normally most rapid at high frequencies. The energy transfer is also a complex function of the wind profile, the turbulence of the airstream, and the vector difference between wind and wave velocities.

The theories of Miles and Phillips predict that waves grow most rapidly when the component of the windspeed in the direction of wave propagation is equal to the speed of wave propagation.

The wave generation process discussed by Phillips is very sensitive to the structure of the turbulence. This is affected significantly by any existing waves and the temperature gradient in the air near the water surface. The turbulence structure in an offshore wind is also affected by land surface roughness near the shore.

The wave generation process discussed by Miles is very sensitive to the vertical profile of the wind. This is determined largely by turbulence in the windstream, the temperature profile in the air, and by the roughness of the sea surface.

Measurements of the rate of wave growth due to Miles' mechanism indicated that only about 20 percent of the growth could be accounted for by direct wind input to waves. Hasselmann (1962) suggested a mechanism by which the wave field could shift energy within itself. He proposed that resonant interactions among waves of different frequencies and directions could lead to an energy transfer from the region of the spectrum just above the peak frequency to both lower and higher frequencies. The wave energy transferred to low frequencies is seen as wave growth, and the energy input is generally larger than the energy contributed to those frequencies directly by the wind. Measurements of the wave-wave interactions are in reasonable agreement with theoretical values (Hasselmann et al., 1973).

The current picture of wave-field development is complex. Energy from the wind is transferred to intermediate and short waves in the spectrum. The energy in these waves serves as a pool from which the wave-wave interactions draw energy, resulting in the growth of the longer waves in the spectrum. The dominant wave energy in a growing sea is seen to shift to lower frequencies.

Often the sea is made up of a number of different wave trains. If there is any significant wind, a wind sea will develop. It is initially composed of short waves, but with time the wind sea waves become longer and eventually may be the same length as the preexisting wave trains. If the wind is at an angle different from the direction of propagation of the existing wave trains, the sea surface can appear quite irregular. If the difference between wind direction and the direction of propagation of the preexisting waves is small, then wind seas can override the existing waves which then disappear. Often the wind field is not uniform. If the wind field is curved, then the sea surface can be a mixture of waves from different directions due to the same wind field. Storm systems may move faster than the surface wave energy generated by the storm; as a result, wave energy can be left behind by one part of the storm while local generation is occurring again. Consequently, wave prediction in larger waterbodies is best accomplished using numerical prediction schemes. Simplified wave prediction formulas should be used only in cases where the presence of energy from other wave trains can be neglected.

## 2. Verification of Wave Hindcasting.

Inoue (1967) prepared hindcasts for weather station J (located near 53° N., 18° W.), for the period 15 to 28 December 1959, using a differential equation embodying the Miles-Phillips-Hasselmann theory to predict wave growth. A comparison of significant wave heights from shipboard observations and by hindcasting at two separate locations near the weather ships is shown in Figure 3-9. The calculations required meteorological data from 519 grid points over the Atlantic Ocean. The agreement between observed and computed values seems to justify confidence in the basic prediction model. Observed meteorological data were interpolated in time and space to provide the required data, thus these predictions were hindcasts. Bunting and Moskowitz (1970) and Bunting (1970) have compared forecast wave heights with observations using the same model with comparable results.

Wave hindcasts were developed by the U.S. Army Engineer Waterways Experiment Station using models developed by Resio and Vincent (1977) and Resio (1981). These models were based on the Miles-Hasselmann mechanisms and demonstrate skill in both Great Lakes and oceanic conditions (Fig. 3-10). The results of these models and the results from similarly formulated models (Hasselmann et al., 1976) suggest that deepwater waves can be estimated reasonably well if adequate meteorological data are available.

## 3. Decay of a Wave Field.

Wind energy can be transferred directly to the waves only when the component of the surface wind in the direction of wave travel exceeds the speed of wave propagation. Winds may decrease in intensity or change in direction to such an extent that wave generation ceases, or the waves may

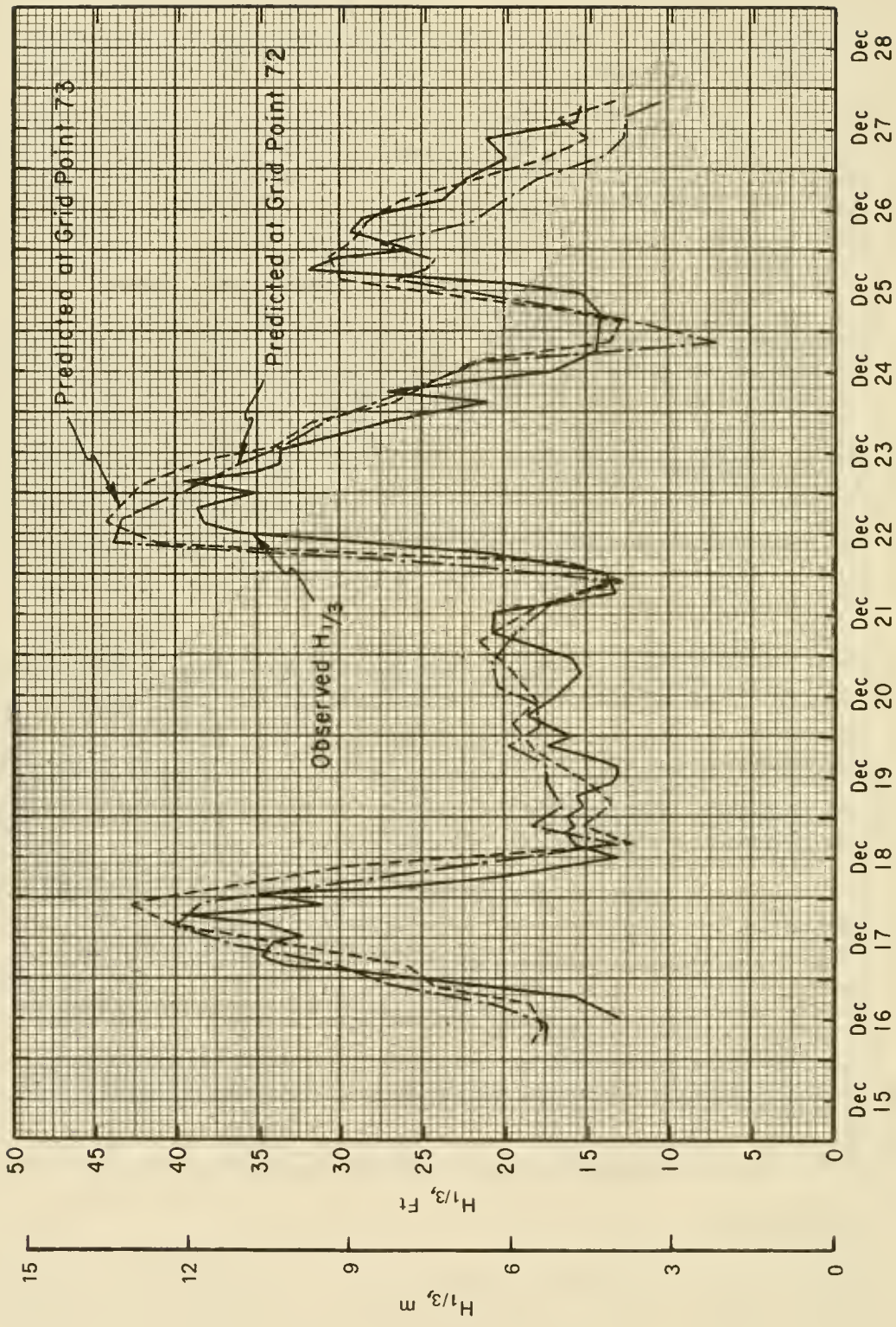
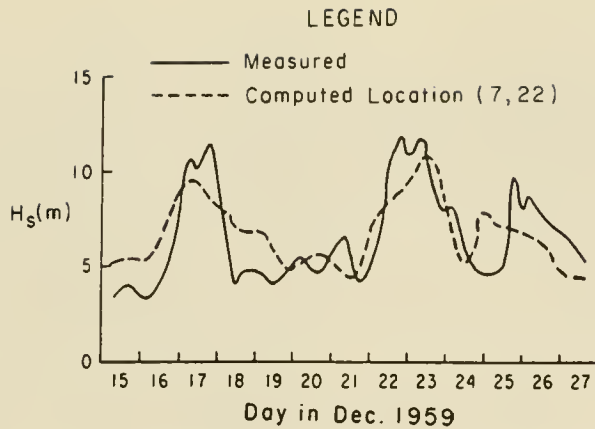
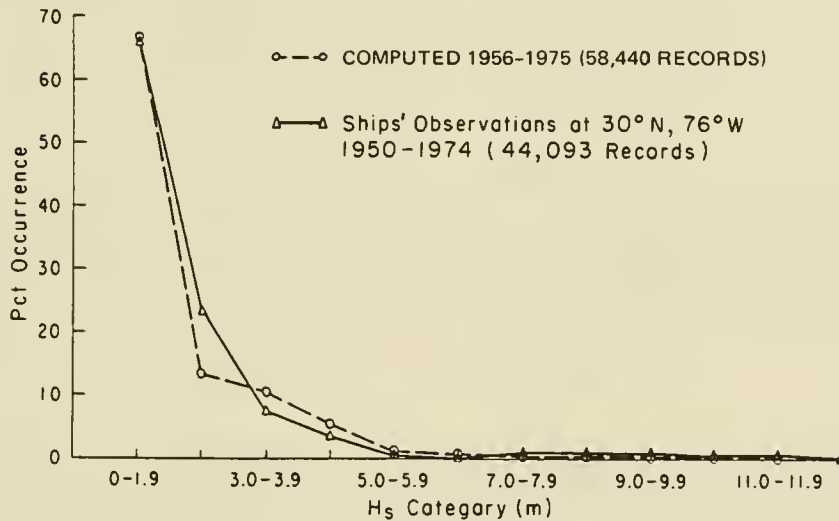


Figure 3-9. Observed and hindcasted significant wave heights versus time (GMT), December 1959, at and near the weather station J in the north Atlantic.



- a. Comparison plot of  $H_s$  versus time for a period in December 1959. Locations of measured and predicted values separated by about 140 km.



- b. Plot of percent occurrence versus  $H_s$  for ships' records and computed data.



- c. Great Lakes hindcast comparisons.

Figure 3-10. Corps of Engineers numerical wave model results.

propagate out of the generation area. When any of these events occurs, the wave field begins to decay. Wave energy travels at a speed which increases with the wave period, thus the energy packet leaving the generating area spreads out over a larger area with increasing time. The apparent period at the energy front increases and the wave height decreases. If the winds subside before the sea is fully arisen, the longer waves may begin to decay while the shorter waves are still growing. This possibility is recognized in advanced wave prediction techniques. The hindcast spectra, computed by the Inoue (1967) model and published by Guthrie (1971), show many examples of this for low swell, as do the aerial photographs and spectra given by Harris (1971). This swell is frequently overlooked in visual observations and even in the subjective analysis of pen-and-ink records from coastal wave gages.

Most coastal areas of the United States are situated so that most of the waves reaching them are generated in water too deep for depth to affect wave generation. In many of these areas, wave characteristics may be determined by first analyzing meteorological data to find deepwater conditions. Then by analyzing refraction (Chapter 2, Section II,2, Refraction by Bathymetry), the changes in wave characteristics as the wave moves through shallow water to the shore may be estimated. In other areas, in particular along the North Atlantic coast, where bathymetry is complex, refraction procedure results are frequently difficult to interpret, and the conversion of deepwater wave data to shallow-water and near-shore data becomes laborious and sometimes inaccurate.

Along the gulf coast and in many inland lakes, generation of waves by wind is appreciably affected by water depth. In addition, the nature and extent of transitional and shallow-water regions complicate ordinary refraction analysis by introducing a bottom friction factor and associated wave energy dissipation.

#### IV. ESTIMATION OF SURFACE WINDS FOR WAVE PREDICTION

Wind waves grow as a result of a flux of momentum and energy from the air above the waves into the wave field. Most theories of wave growth consider that this input of energy and momentum depends on the surface stress, which is highly dependent upon windspeed and other factors that describe the atmospheric boundary layer above the waves. Winds for wave prediction are normally obtained either from direct observations over the fetch, by projection of values over the fetch from observations over land, or by estimates based on weather maps. Methods for estimating the windspeeds needed in Chapter 3, Section V, to hindcast waves from these basic data types will be provided in Chapter 3, Sections 2, 3, and 4. Prior to that, the following brief discussion of the wind field above waves will be provided as background.

##### 1. Winds Over Water.

For discussion purposes, the wind will be considered to be driven by large-scale pressure gradients in the atmosphere that have been in a near-steady state. The winds above the wave field, then, can be considered as a profile (Fig. 3-11). Some 1000 meters or so above the surface, the winds are driven mainly by geostrophic balance between Coriolis and local pressure gradient forces. Below this level, the frictional effects due to the presence

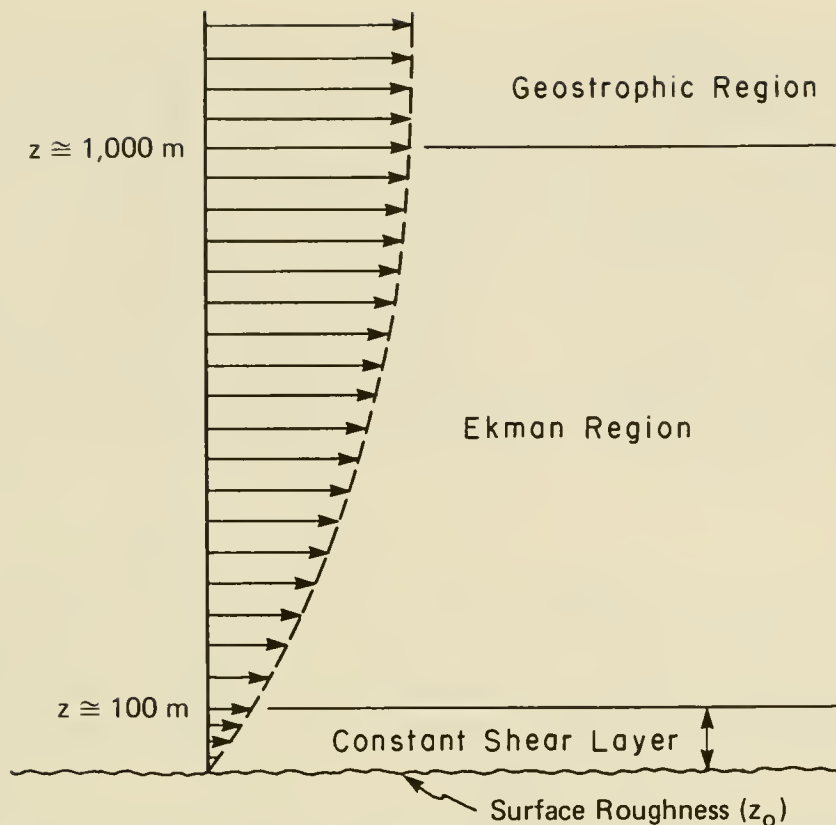


Figure 3-11. Atmospheric boundary layer over waves.

of the ocean distort the wind field; thus, wind speed and direction become dependent upon elevation above the mean surface, roughness of the surface, air-sea temperature differences, and horizontal temperature gradients. To simplify the discussion, temperature gradients in the horizontal plane will be ignored because their effect can rarely be taken into account in a simplified prediction scheme.

Below the geostrophic region, the boundary layer may be divided into two sections, a constant stress layer 10 to 100 meters in height and above that an Ekman layer. Emphasis is placed on the constant stress layer. A detailed description of the boundary layer mechanics is given in Resio and Vincent (1977b).

In the constant stress layer, it is possible to write an equation for the vertical variation in windspeed

$$U(z) = \frac{U_*}{0.4} \left[ \ln \left( \frac{z}{z_0} \right) - \Psi \left( \frac{z}{L} \right) \right] \quad (3-25)$$

where

$U_*$  = the friction velocity (the shear stress is given by  $\rho U_*^2$ )

$z_0$  = the surface roughness

$\Psi$  represents the effects of stability of the air column on the wind velocity

$L$  = a length scale associated with the mixing process and is dependent upon air-sea temperature difference.

As seen in this simple case, the velocity at an elevation  $z$  is dependent upon the shear stress through  $U_*$ , the surface roughness, and the air-sea temperature difference. To complicate matters, the surface roughness is directly related to the friction velocity. Since the shear stress is most directly related to wave growth, the relationship between observed windspeed and shear stress must, at a minimum, be dependent upon local windspeed and air-sea temperature difference,  $\Delta T_{as}$ .

To more accurately estimate the effect a particular windspeed will have on wave generation,  $\Delta T_{as}$ ,  $U_*$ , and  $z_0$  must be known. The wave growth curves in Chapter 3, Section VI are given in terms of an equivalent windspeed observed at  $z = 10$  meters for neutral stability so that the values are commensurate with units of measurement in normal use. Thus, observed windspeeds must be increased or decreased to account for the effect of the other factors.

In Chapter 3, Section IV, 2 to 6, specific instructions for estimating winds for use in the wave growth curves and formulas of Chapter 3, Section V will be given for the major wind observation conditions with which the engineer must normally deal. In addition, a procedure for estimating surface winds from pressure charts will be given. To make the wind transformations required in Section IV, 2 to 6, combinations of five adjustment factors will be used. These adjustment factors are discussed below.

a. Elevation. If the winds are not measured at the 10 meter elevation, the windspeed must be adjusted accordingly. It is possible, but normally not feasible, to solve equation (3-25) for  $U_*$  at the observed elevation  $z$  and then estimate  $U$  at 10 meters. The simple approximation

$$U(10) = U(z) \left(\frac{10}{z}\right)^{1/7} \quad (3-26)$$

can be used if  $z$  is less than 20 meters.

b. Duration-Averaged Windspeed. Windspeeds are frequently observed and reported as the fastest mile or extreme velocity (considered synonymous). (Daily fastest mile windspeed equals fastest speed (in miles per hour) at which wind travels 1 mile measured during a 24-hour period.)

Studies have indicated that the fastest mile windspeed values are obtained from a short time period generally less than 2 minutes in duration (U.S. Army Engineer Division, Missouri River, 1959). It is most probable that on a national basis many of the fastest mile windspeeds have resulted from short duration storms such as those associated with squall lines or thunderstorms. Therefore, *the fastest mile measurement, because of its short duration, should not be used alone to determine the windspeed for wave generation.* On the other hand, lacking other wind data, the measurement can be modified to a time-dependent average windspeed using the procedure discussed below.

To use the procedures for adjusting the windspeed discussed later, which are ultimately used in the wave forecasting models, the fastest mile windspeed must be converted to a time-dependent average windspeed, such as the 10-, 25-, 50-minute average windspeed.

Figures 3-12 and 3-13 allow conversion of the fastest mile to the average windspeed. The procedures for using these figures are illustrated by an example problem.

\*\*\*\*\* EXAMPLE PROBLEM 3 \*\*\*\*\*

GIVEN: Fastest mile windspeed,  $U_f = 29 \text{ m/s}$  (65 mph).

FIND: Twenty-five-minute average windspeed,  $U_{t=25 \text{ min}}$ .

SOLUTION:

$$t = \frac{3600}{U_f(\text{mph})} = \frac{3600}{65} = 55.4 \text{ s (time to travel 1 mile)}$$

or

$$t = \frac{1609}{U_f(\text{m/s})} = \frac{1609}{29} = 55.4 \text{ s,}$$

and

$$U_f = U_{t=55.4 \text{ s}} = 29 \text{ m/s (65 mph)}$$

From Figure 3-13 for  $t = 55$  seconds,  $\frac{U_{t=55}}{U_{3600}} = 1.25$ , and the 1-hour average windspeed is

$$U_{t=3600 \text{ s}} = \left( \frac{U_{t=55}}{U_{3600}} \right) = \frac{29}{1.25} = 23.2 \text{ m/s or } \frac{65}{1.25} = 52.0 \text{ mph}$$

Using Figure 3-13 again, find  $\frac{U_{t=25 \text{ min}}}{U_{3600}}$  for  $t = 25$  minutes or 1500 seconds

$$\frac{U_{t=25 \text{ min}}}{U_{3600}} = 1.015$$

Solving for  $U_{t=25 \text{ min}}$

$$U_{t=25 \text{ min}} = \left( \frac{U_{t=25 \text{ min}}}{U_{3600}} \right) U_{3600} = 1.015 (23.2) = 23.5 \text{ m/s (52.8 mph)}$$

\*\*\*\*\*

If the fastest mile windspeed observations (or any duration windspeed observations that can be converted by the procedure just outlined) are available at 1-hour increments, the procedure may be used to compute hourly average winds or some fraction thereof. If a duration of more than 1 hour is needed, the hourly average values may then be averaged to achieve the desired duration. If the hourly averages vary considerably (say more than 3 to 5 meters per second), then the assumption of constant wind made in the use of wave growth formulas is not valid and the accuracy of the wave predictions is questionable. If wind observations are available on a 3-hour basis, the same

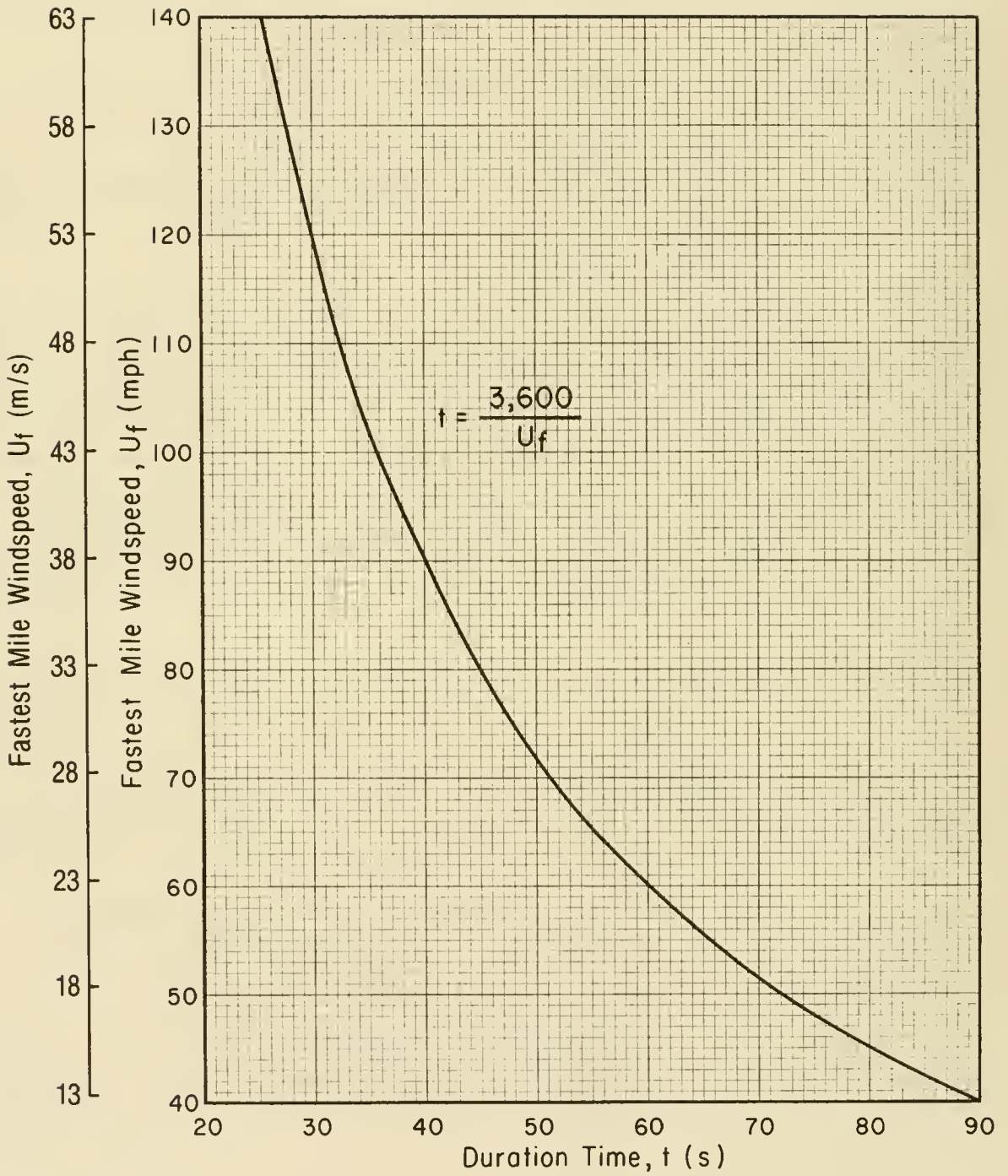
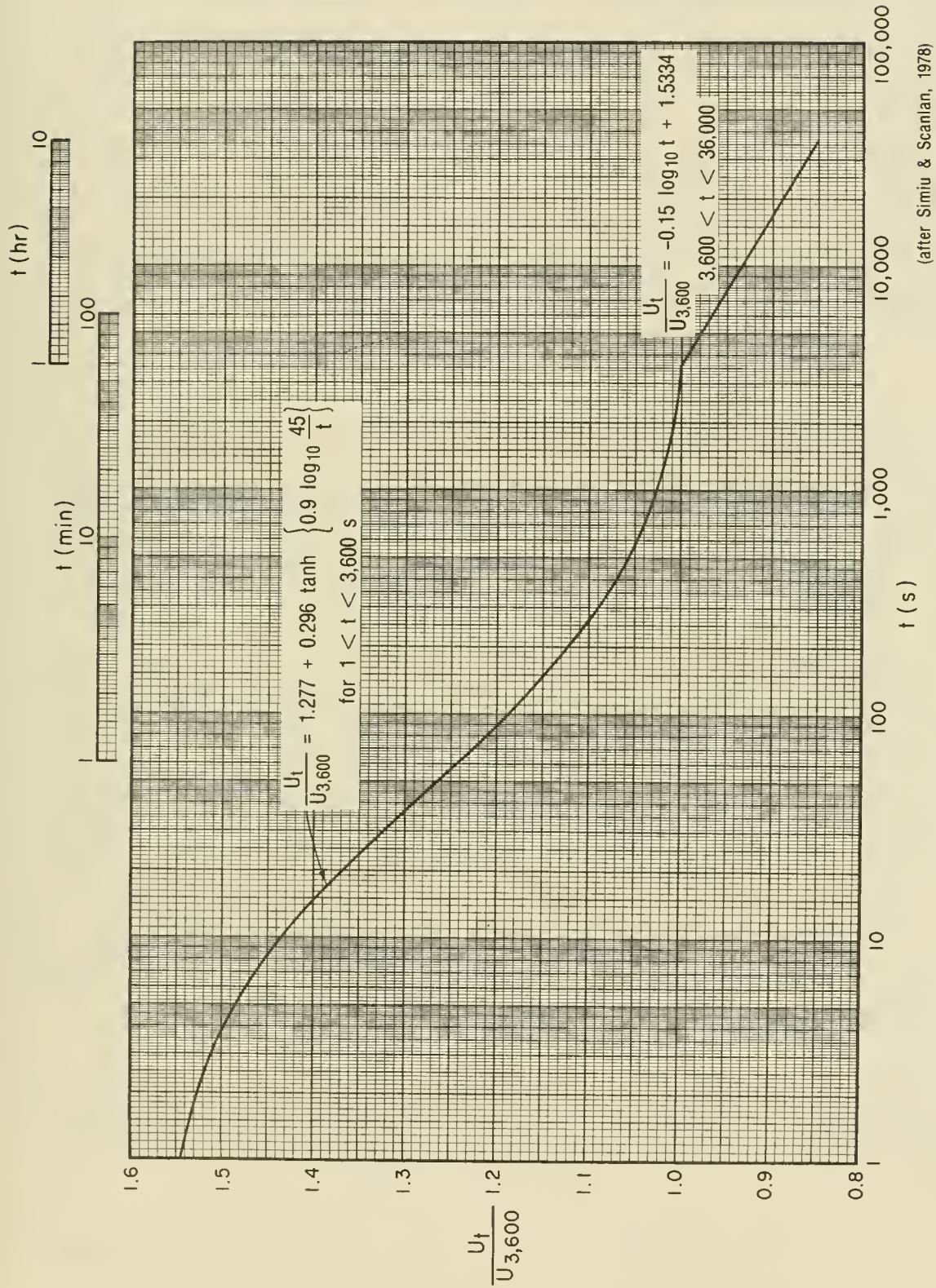


Figure 3-12. Duration of the fastest mile windspeed as a function of windspeed.



(after Simiu & Scanlan, 1978)

Figure 3-13. Ratio of windspeed of any duration,  $U_t$ , to the 1-hour windspeed,  $U_{3600}$ .

method may be applied to obtain a 3-hour average; however, the assumption of constant wind again may not be valid.

If thunderstorms or other brief, severe winds are included in the data, the method may overestimate results; but often there are no other data available.

c. Stability Correction. If the air-sea temperature difference  $\Delta T_{as} = T_a - T_s$  is zero, the boundary layer has neutral stability and no windspeed correction is necessary. If  $\Delta T_{as}$  is negative, the boundary layer is unstable and the windspeed is more effective in causing wave growth. If  $\Delta T_{as}$  is positive, the boundary layer is stable and the windspeed is less effective. The correction factor,  $R_T$ , is a function of  $\Delta T_{as}$  and was defined by Resio and Vincent (1977b) to account for this effect. An effective windspeed is obtained by

$$U = R_T U(10) \quad (3-27)$$

where  $R_T$  is read from Figure 3-14. This correction can be substantial. For example, if the winds are estimated for a  $\Delta T_{as}$  of  $+10^\circ\text{C}$  and  $\Delta T_{as}$  is actually  $-10^\circ\text{C}$ , the error in  $U_*$  is 50 percent.  $\Delta T_{as}$  may vary seasonally. In the fall a lake's water may still be warm, but cold winds may blow across it; in the spring, the reverse may be true. Investigation of the values of  $T_{as}$  is usually warranted, and the a priori assumption of a neutrally stable boundary layer should be questioned. In the absence of temperature information,  $R_T = 1.1$  should be assumed.

d. Location Effects. Often overwater wind data are not available, but data from nearby land sites are. It is possible to translate overland winds to overwater winds if they are the result of the same pressure gradient and the only major difference is the surface roughness (Resio and Vincent, 1977b). For first-order airport weather stations around the Great Lakes, the relationship between overwater winds to nearby overland winds is given for neutral stability by  $R_L$  in Figure 3-15; this can be used as an approximation for other areas unless the landscape roughness characteristics are markedly different. The land anemometer site should be close enough to the body of water so that the winds are caused by the same atmospheric pressure gradient. Thunderstorms and squall lines are small-scale phenomena and violate the assumption that overland winds and overwater winds are from the same pressure gradient. If the anemometer site is adjacent to shore, winds blowing off the water require no adjustment for location effects; i.e.,  $R_L = 1$ . A stability adjustment  $R_T$  should be used, however.

e. Coefficient of Drag. The wave growth formulas and nomograms are expressed in terms of wind-stress factor  $U_A$  (adjusted windspeed). After the appropriate windspeed conversions are made, the windspeed is converted to a wind-stress factor by either of the following formulas:

$$U_A = 0.71 U^{1.23} \quad (U \text{ in m/s}) \quad (3-28a)$$

$$U_A = 0.589 U^{1.23} \quad (U \text{ in mph}) \quad (3-28b)$$

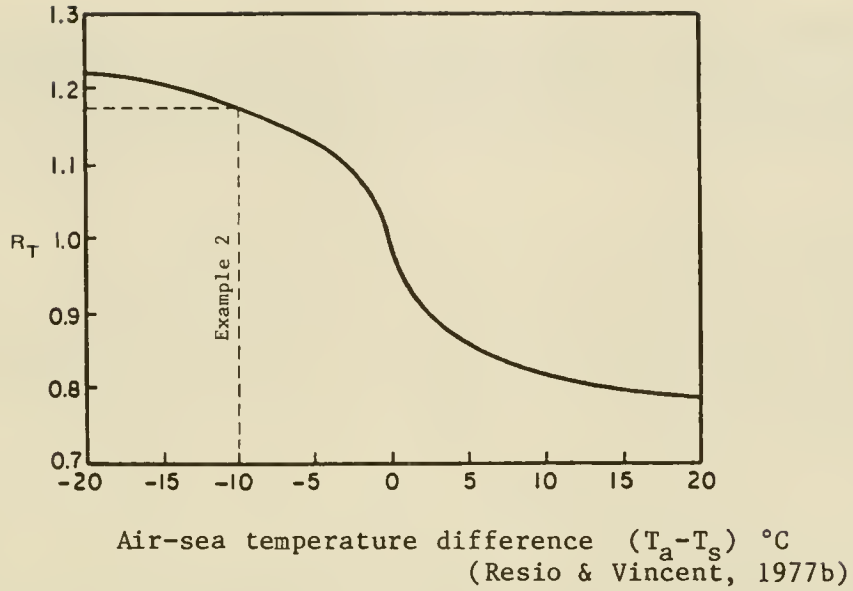


Figure 3-14. Amplification ratio,  $R_T$ , accounting for effects of air-sea temperature difference.

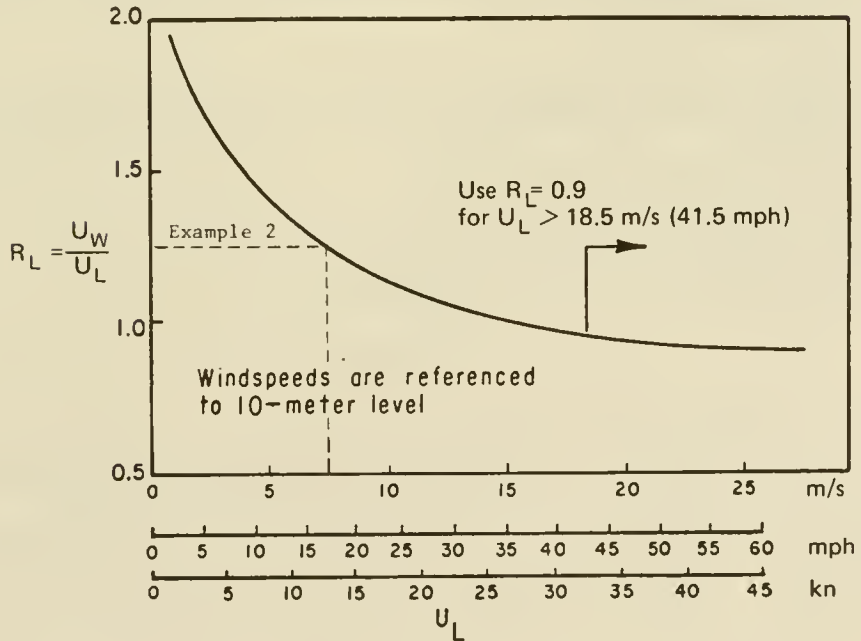


Figure 3-15. Ratio,  $R_L$ , of windspeed over water,  $U_W$ , to windspeed over land,  $U_L$ , as a function of windspeed over land,  $U_L$ .

The wind-stress factor accounts for the nonlinear relationship between wind stress and windspeed.

The approximations and adjustments used are made to reduce biases in wind data and to provide a reasonable means of providing information where adequate measurements are not available. The collection of overwater wind data at a site is preferable. Even if data can only be collected for a short period, say 1 year, it may be of value in relating overland wind data to overwater values.

## 2. Procedure for Adjusting Winds Observed Over Water.

Wind data gathered over the water are normally the most desirable for wave prediction. Most overwater wind data are gathered by observers on ships as visual observations of unknown quality. Cardone et al. (1969) reviewed bias in ship-observed windspeeds and suggested that a correction of

$$W = 2.16 \left( \frac{7}{9} \right) W_s \quad (3-29)$$

where  $W_s$  is the ship-reported windspeed in knots and  $W$  is the corrected windspeed in knots. In most cases, the elevation above the water surface where ship windspeeds are measured is variable and unknown. Other wind measurements may be taken on lightships or with automatic buoys. The following procedures should be used in correcting winds observed over water for use in the wave prediction formulas:

(a) If the winds are from ships, they should be corrected for bias by equation (3-29).

(b) If the winds are measured at an elevation other than 10 meters, equation (3-26) should be used to correct the windspeed.

(c) The windspeed should be adjusted for the stability effect from Figure 3-14.

(d) The duration-averaged windspeed is estimated by Chapter 3, Section IV,1,b.

(e) The windspeed is converted to the wind stress factor (Chapter 3, Section IV,1,e).

## 3. Procedure for Estimating Overwater Winds from Nearby Land Winds.

The following procedure should be used to obtain the overwater windspeeds from observations nearby on land. In the Great Lakes this procedure was successfully used to obtain estimates up to 113 kilometers (70 miles) away from wind stations normally within 16 kilometers (10 miles) of the lake; this was possible because of the size of the lakes and storm systems and the flatness of the topography. Also, multiple stations were used to obtain some spatial variability.

(a) The location of nearby anemometer sites should be checked to see if they are sheltered by major topographic features. The method should not be used for thunderstorms or any other condition that violates the assumption that the winds over the water are driven by the same pressure gradient at the land. The overland anemometer should be located at a large clearing, such as at an airport.

(b) The windspeeds should be adjusted for different observation elevations with equation (3-26). Note that the elevation of wind instruments at a site may have been changed sometime during the period of record. This possibility must be checked carefully and the wind data adjusted accordingly.

(c) If the anemometer is located immediately adjacent to the water-body, then onshore winds do not require adjustment for  $R_L$ . For sites some distance from the water or for winds blowing offshore at a site adjacent to the water, the windspeeds should be adjusted by  $R_L$  from Figure 3-15. If the fetch is less than 16 kilometers, then  $R_L$  can be set to 1.2, with the assumption that the boundary layer is not in full adjustment to the water surface.

(d) The adjustment for stability  $R_T$  from Figure 3-14 should be applied.

(e) The duration adjustment in Chapter 3, Section IV,1,b should be made.

(f) The windspeed should be converted to the wind stress factor by Chapter 3, Section IV,1,e.

This method is an approximation that can vary as the landscape characteristics change. It is highly desirable to obtain local wind data to calibrate the method for specific sites. Topographic funneling effects should not be present, or the wind data must be adjusted to account for the funneling.

#### 4. Wind Information from Surface Pressure.

Direct observations of wind may not always be available. It is possible to estimate windspeeds by analysis of pressure charts. The free air windspeed is first estimated from sea level pressure charts. Corrections to the free air wind are then made. Estimation from pressure charts can be subject to considerable error and should be used only for large areas over which pressure gradients can be smoothed. This method is not recommended for areas of high topographic relief; estimated values should be compared with other observations to confirm their validity.

a. Free Air Wind. Surface wind-field estimates that are fairly accurate can often be determined from analysis of the isobaric patterns of synoptic weather charts.

Horizontal pressure gradients arise in the atmosphere primarily because of density differences, which in turn are generated primarily by temperature

differences. Wind results from nature's efforts to eliminate the pressure gradients, but is modified by many other factors.

The pressure gradient is nearly always in approximate equilibrium with the acceleration produced by the rotation of the earth. The *geostrophic wind* is defined by assuming that exact equilibrium exists, and it is given by

$$U_g = \frac{1}{\rho_a f} \frac{dp}{dn} \quad (3-30)$$

where

$U_g$  = windspeed

$\rho_a$  = air density

$f$  = coriolis parameter =  $2\omega \sin \phi$

$\omega$  =  $7.292 \times 10^{-5}$  rad/s

$\phi$  = latitude

$\frac{dp}{dn}$  = horizontal gradient of atmospheric pressure

The geostrophic wind blows parallel to the isobars with low pressure to the left, when looking in the direction toward which the wind is blowing, in the Northern Hemisphere and low pressure to the right in the Southern Hemisphere. Geostrophic wind is usually the best simple estimate of the true wind in the free atmosphere.

When the trajectories of air particles are curved, equilibrium windspeed is called *gradient wind*. In the Northern Hemisphere, gradient wind is stronger than geostrophic wind for flow around a high-pressure area and weaker than geostrophic wind for flow around low pressure. The magnitude of the difference between geostrophic and gradient winds is determined by the curvature of the trajectories. If the pressure pattern does not change with time and friction is neglected, trajectories are parallel with the isobars. The isobar curvature can be measured from a single weather map, but at least two maps must be used to estimate trajectory curvature. There is a tendency by some analysts to equate the isobars and trajectories at all times and to compute the gradient wind correction from the isobar curvature. When the curvature is small and the pressure is changing, this tendency may lead to incorrect adjustments. Corrections to the geostrophic wind that cannot be determined from a single weather map are usually neglected, even though they may be more important than the isobaric curvature effect.

When forecasting for oceans or other large bodies of water, the most common form of meteorological data used is the synoptic surface weather chart. (*Synoptic* means that the charts are drawn by analysis of many individual items of meteorological data obtained simultaneously over a wide area.) These charts depict lines of equal atmospheric pressure, called isobars. Wind estimates at sea based on an analysis of the sea level atmospheric pressure are generally more reliable than wind observations because pressure, unlike wind, can be measured accurately on a moving ship. Pressures are recorded in millibars, 1,000 dynes per square centimeter; 1,000

millibars (a bar) equals 750 mm (29.53 inches) of mercury and is 98.7 percent of normal atmospheric pressure.

A simplified surface chart for the Pacific Ocean drawn for 27 October 1950 at 0030Z (0030 Greenwich mean time) is shown in Figure 3-16. Note the area labeled L in the right center of the chart and the area labeled H in the lower left corner of the chart. These are low- and high-pressure areas; the pressures increase moving outward from L (isobars 972, 975, etc.) and decrease moving outward from H (isobars 1026, 1023, etc.)

Scattered about the chart are small arrow shafts with a varying number of feathers or barbs. The direction of a shaft shows the direction of the wind; each one-half feather represents a unit of 5 knots (2.5 meters per second) in windspeed. Thus, in Figure 3-16 near the point 35°N. latitude, 135°W. longitude, there are three such arrows, two with 3-1/2 feathers which indicate a wind force of 31 to 35 knots (15 to 17.5 meters per second) and one with 3 feathers indicating a force of 26 to 30 knots (13 to 15 meters per second).

On an actual chart, much more meteorological data than wind speed and direction are shown for each station. This is accomplished by using coded symbols, letters, and numbers placed at definite points in relation to the station dot. A sample plotted report, showing the amount of information possible to report on a chart, is shown in Figure 3-17. Not all of the data shown on this plot are included in each report, and not all of the data in the report are plotted on each map.

Figure 3-18 may be used to facilitate computation of the geostrophic windspeed. The figure is a graphic solution of equation (3-30). A measure of the average pressure gradient over the area is required. Most synoptic charts are drawn with either a 3- or 4-millibar spacing. Sometimes when isobars are crowded, intermediate isobars are omitted. Either of these standard spacings is adequate as a measure of the geographical distance between isobars. Using Figure 3-18, the distance between isobars on a chart is measured in degrees of latitude (an average spacing over a fetch is ordinarily used), and the latitude position of the fetch is determined. Using the spacing as ordinate and location as abscissa, the plotted or interpolated slant line at the intersection of these two values gives the geostrophic windspeed. For example, in Figure 3-16, a chart with 3-millibar isobar spacing, the average isobar spacing (measured normal to the isobars) over  $F_2$ , located at 37°N. latitude, is 0.70° of latitude. Using the scales on the bottom and left side of Figure 3-18, a geostrophic wind of 345 meters per second (67 knots) is found.

b. Procedure for Estimating Surface Wind from Free Air Wind. After the free air wind has been estimated by the method above, the windspeed at the surface (10-meter level) must be estimated. First the geostrophic windspeed is converted to the 10-meter level velocity by multiplying by  $R_g$  as given in Figure 3-19;  $R_g$  is a function of the geostrophic windspeed (free air windspeed)  $U_g$ . The resulting velocity is then adjusted for stability effects by the factor  $R_T$  given in Figure 3-14 and discussed in Chapter 3, Section IV, 2. The duration-averaged windspeed is estimated in Chapter 3, Section IV,1,b. The wind stress factor is computed from the windspeed in Chapter 3, Section IV,1,e.

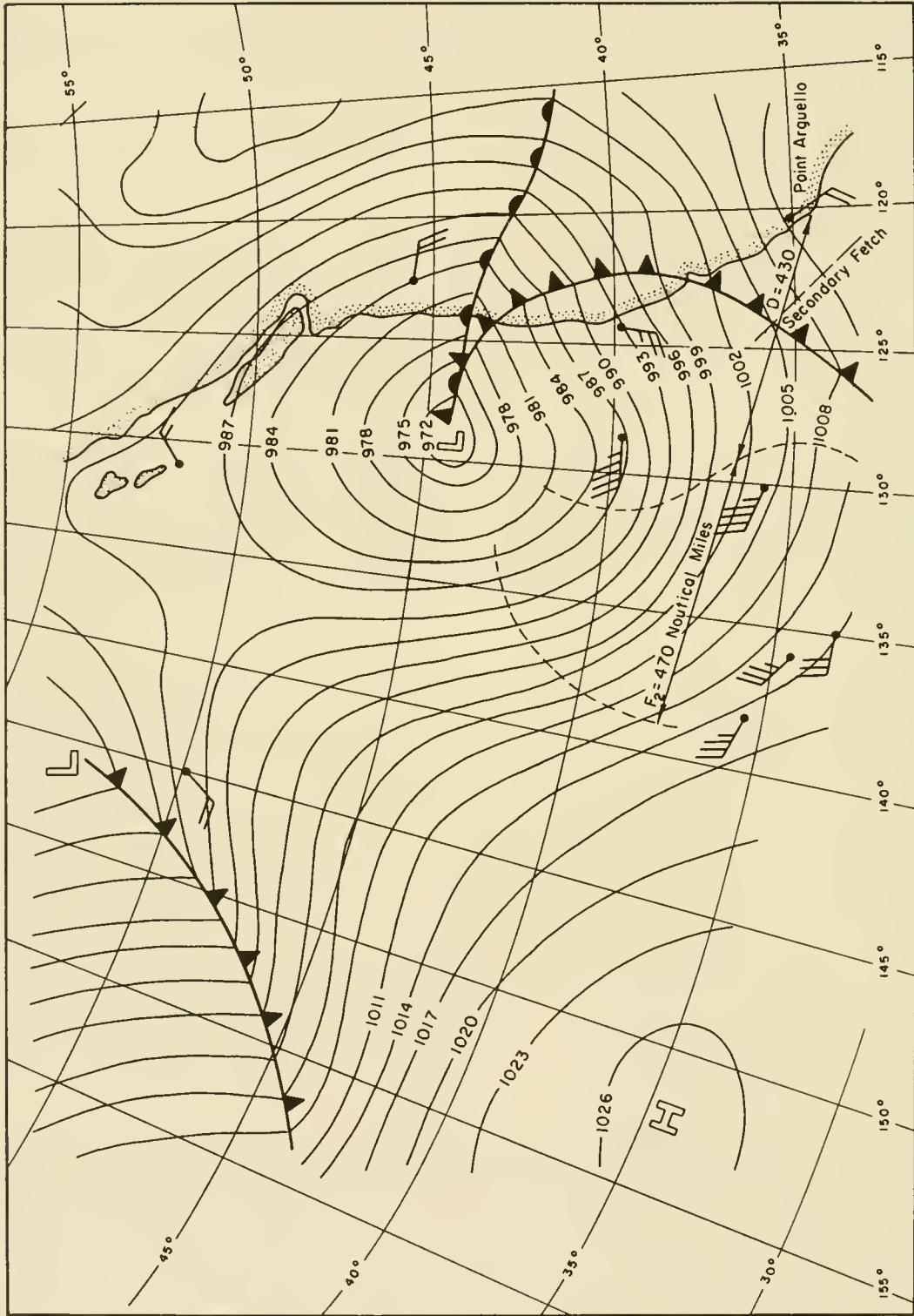
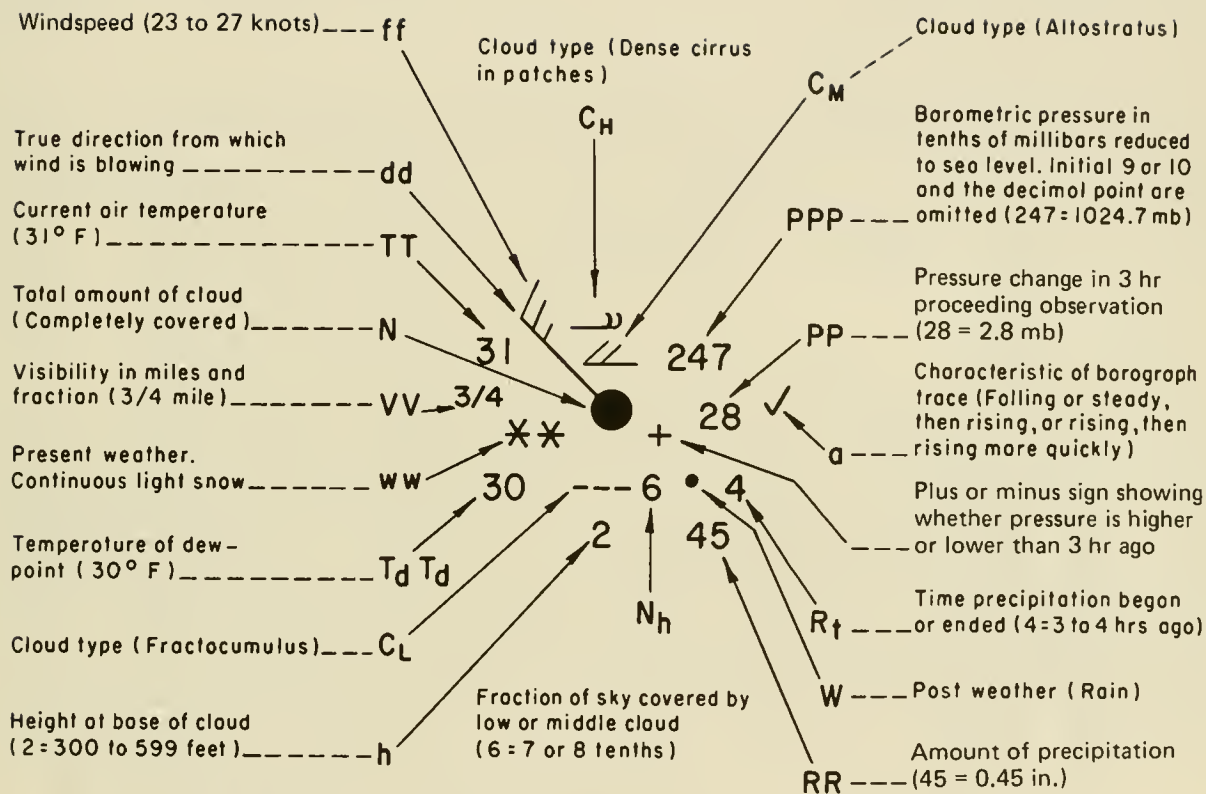


Figure 3-16. Surface synoptic chart for 0030Z, 27 October 1950.



NOTE: The letter symbols for each weather element are shown above.

Courtesy U.S. Weather Bureau  
abridged from W.M.O. Code

Figure 3-17. Sample plotted report.

$$U_g = \frac{1}{\rho_0 f} \frac{\Delta p}{\Delta n}$$

For  $T = 10^\circ \text{C}$

$\Delta p = 3 \text{ mb and } 4 \text{ mb}$

$\Delta n = \text{isobar spacing measured in degrees latitude}$

$\rho = 1013.3 \text{ mb}$

$\rho_0 = 1.247 \times 10^{-3} \text{ gm/cm}^3$

$f = \text{Coriolis parameter} = 2 \omega \sin \phi$

where

$\omega = \text{angular velocity of earth, } 0.2625 \text{ rad/hr}$

$\phi = \text{latitude in degrees}$

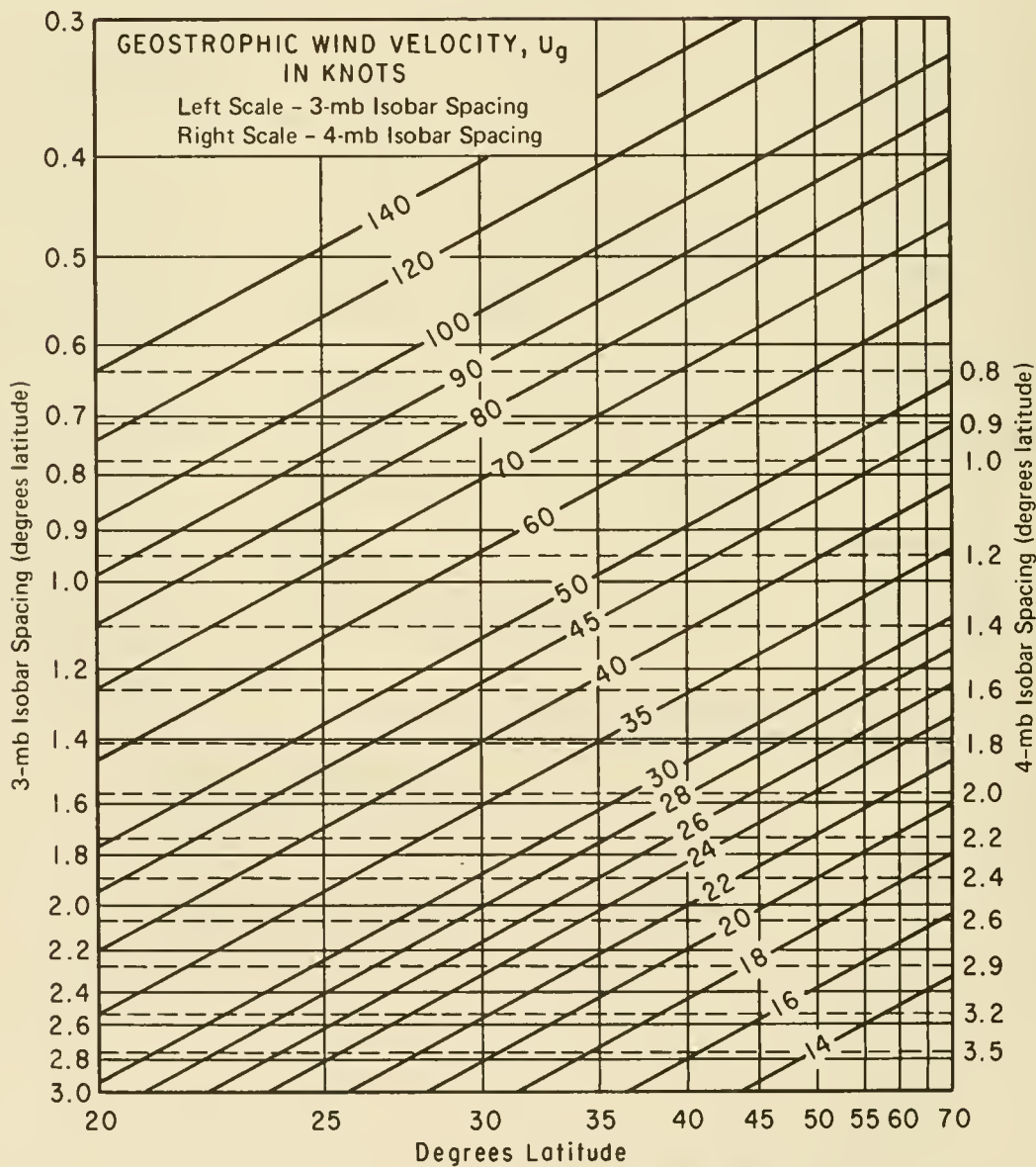


Figure 3-18. Geostrophic wind scale.

## V. SIMPLIFIED METHODS FOR ESTIMATING WAVE CONDITIONS

When estimates of wave heights, periods, and directions are needed, the most accurate procedures are the numerical methods discussed in Chapter 3, Section III. However, there are often cases where neither the time available nor the cost justifies using complex numerical methods. In these cases, a simplified method may be justified. Chapter 3, Section V,3 presents a series of equations and nomograms that give significant wave height by  $H_{m0}$  and period of the spectral peak,  $T_m$  for a given windspeed and fetch or duration. Estimating surface winds is treated in Chapter 3, Section IV. Estimating fetch length is treated in Chapter 3, Section V,1.

The spectrally based significant wave height  $H_{m0}$  is four times the square root of the variance of the sea surface elevation. In deep water  $H_{m0}$  is approximately equal to the significant wave height  $H_s$ , which is based on counting and measuring individual waves (see Chapter 3, Section II,5). In shallow water,  $H_{m0}$  becomes less than  $H_s$ . In both deep and shallow water,  $H_{m0}$  is based on the wave energy; this is not true for  $H_s$ .

The following assumptions pertain to these methods. The methods will be used for cases where fetches are short (80 to 120 kilometers (50 to 75 miles) or less) and the wind can be assumed uniform and constant over the fetch. Cases where the wind field varies rapidly in time or with distance over the fetch or where swell from distant sources propagates into the area are best treated numerically. Since these conditions are rarely met and wind fields are not usually estimated accurately, do not assume the results are more accurate than warranted by the accuracy of the input or the simplicity of the method. Good, unbiased estimates of all parameters for input to the wave equations should be sought and the results interpreted conservatively. Individual input parameters should not each be estimated conservatively, since to do so may bias the results.

### 1. Delineating a Fetch.

A fetch has been defined subjectively as a region in which the windspeed and direction are reasonably constant. Confidence in the computed results begins to deteriorate when wind direction variations exceed  $15^\circ$ ; confidence deteriorates significantly when direction deviations exceed  $45^\circ$ . The computed results are sensitive to changes in windspeed as small as 1 knot (0.5 meter per second), but it is not possible to estimate the windspeed over any sizable region with this precision. For practical wave predictions it is usually satisfactory to regard the windspeed as reasonably constant if variations do not exceed 5 knots (2.5 meters per second) from the mean. A coastline upwind from the point of interest always limits a fetch. An upwind limit to the fetch may also be provided by curvature or spreading of the isobars as indicated in Figure 3-20 (Shields and Burdwell, 1970) or by a definite shift in wind direction. Frequently the discontinuity at a weather front will limit a fetch, although this is not always so.

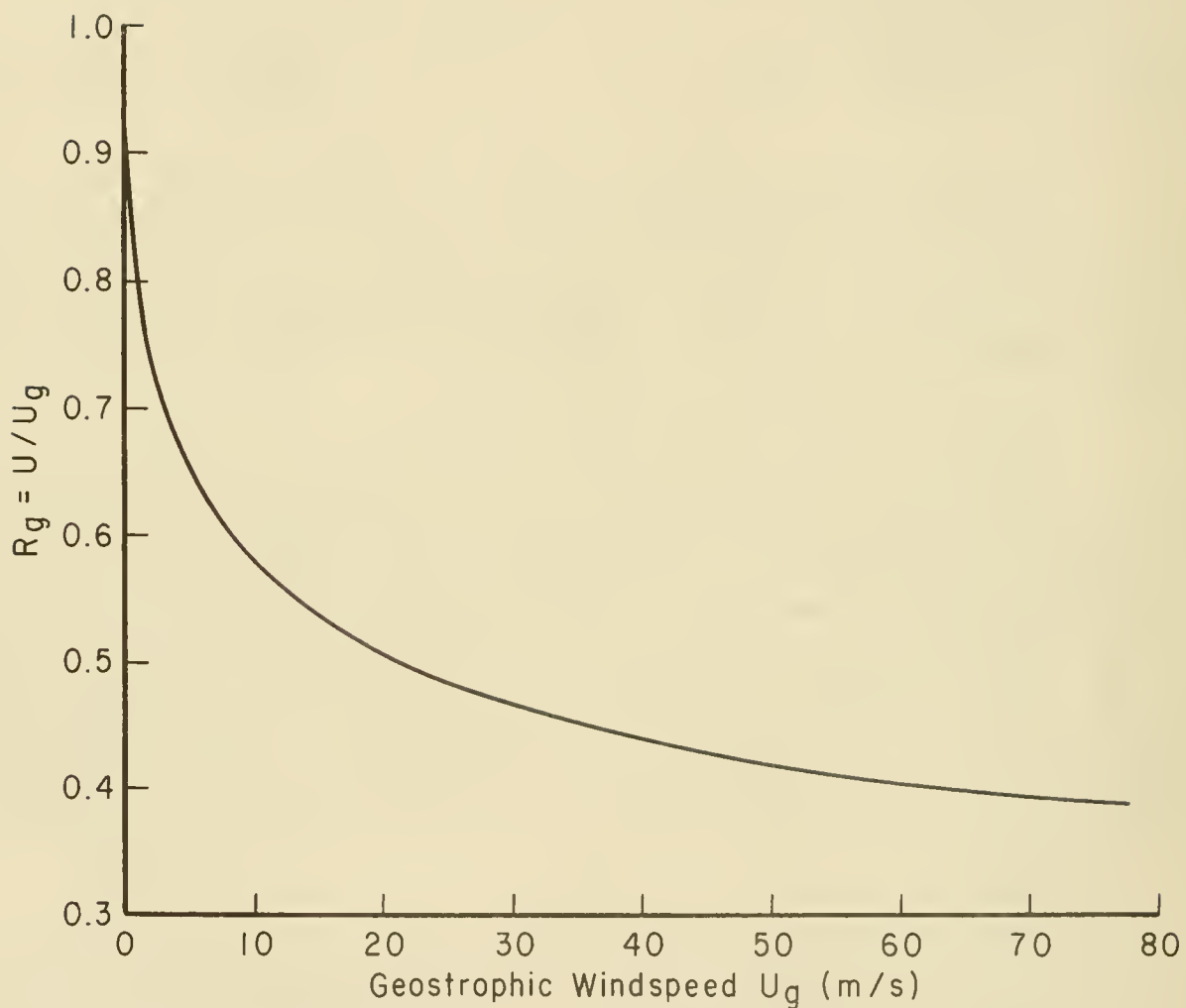


Figure 3-19. Ratio  $R_g$  of windspeed  $U$  at 10-meter elevation to geostrophic windspeed  $U_g$  (modified from Resio and Vincent, 1977b).

Estimates of the duration of the wind are also needed for wave prediction. Computer results, especially for short durations and high windspeeds may be sensitive to differences of only a few minutes in the duration. Complete synoptic weather charts are prepared only at 6-hour intervals. Thus interpolation to determine the duration may be necessary. Linear interpolation is adequate for most uses, and, when not obviously incorrect, is usually the best procedure. Care should be taken not to interpolate if short-duration phenomena, such as frontal passage or thunderstorms, are present.

The effect of fetch width on limiting ocean wave growth in a generating area may usually be neglected since nearly all ocean fetches have widths about as large as their lengths. In inland waters (bays, rivers, lakes, and reservoirs), fetches are limited by landforms surrounding the body of water. Fetches that are long in comparison to width are frequently found. It is not clear what measure of width is important in limiting the growth of waves.

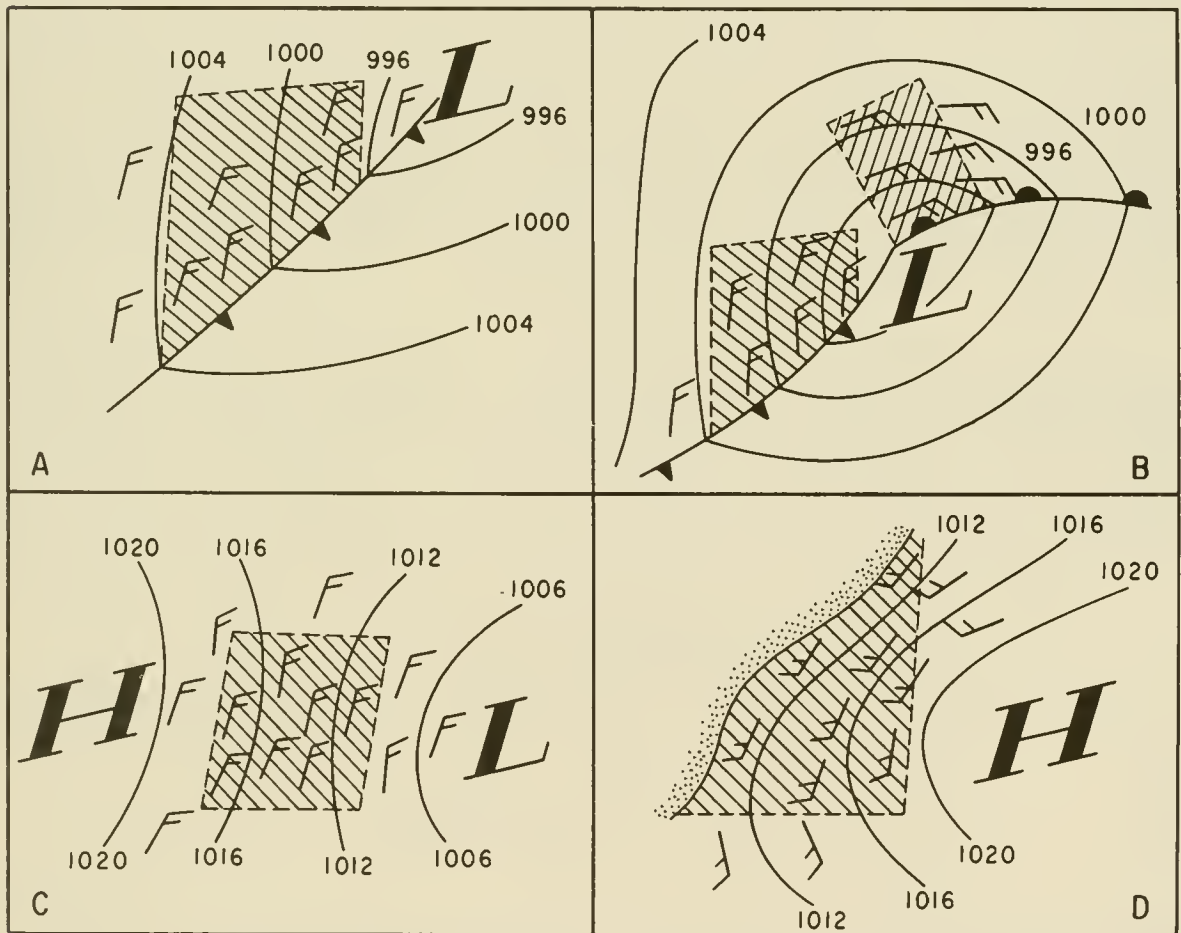


Figure 3-20. Possible fetch limitations.

Shorelines are usually irregular, and a more general method for estimating fetch must be applied. A recommended procedure for determining the fetch length consists of constructing nine radials from the point of interest at 3-degree intervals and extending these radials until they first intersect the shoreline. The length of each radial is measured and arithmetically averaged. While 3-degree spacing of the radials is used in this example, any other small angular spacing could be used.

## 2. Simplified Wave-Prediction Models.

Use of the wave prediction models discussed in Chapter 3, Section III (Wave Field) requires an enormous computational effort and more meteorological data than is likely to be found outside of a major forecasting center or laboratory.

The U.S. Navy operates an oceanic forecast facility at Monterey, California, and the Corps of Engineers is developing a wave climate for U.S. coastal areas using a sophisticated numerical model. The results of the latter study are being published as a series of climatological reports by the U.S. Army Engineer Waterways Experiment Station.

Computational effort required for the model discussed in Chapter 3, Section III,1 (Development of a Wave Field) can be greatly reduced by the use of simplified assumptions, with only a slight loss in accuracy for wave height calculations, but sometimes with significant loss of detail on the distribution of wave energy with frequency. One commonly used approach is to assume that both duration and fetch are large enough to permit an equilibrium state between the mean wind, turbulence, and waves. If this condition exists, all other variables are determined by the windspeed.

Pierson and Moskowitz (1964) consider three analytic expressions which satisfy all the theoretical constraints for an equilibrium spectrum. Empirical data described by Moskowitz (1964) were used to show that the most satisfactory of these is

$$E(\omega) d\omega = (\alpha g^2 / \omega^5) e^{-\beta(\omega_0^4 / \omega^4)} d\omega \quad (3-31)$$

where

$$\alpha = 8.1 \times 10^{-3} \quad (\text{dimensionless constant})$$

$$\beta = 0.74 \quad (\text{dimensionless constant})$$

$$\omega_0 = g/U$$

g = acceleration of gravity

U = windspeed reported by weather ships

$\omega$  = wave frequency considered

Equation (3-31) may be expressed in many other forms. Bretschneider (1959, 1963) gave an equivalent form, but with different values for  $\alpha$  and  $\beta$ . A similar expression was also given by Roll and Fischer (1956). The condition in which waves are in equilibrium with the wind is called a *fully arisen sea*. The assumption of a universal form for the fully arisen sea permits the

computation of other wave characteristics such as total wave energy, significant wave height, and period of maximum energy. The equilibrium state between wind and waves rarely occurs in the ocean and may never occur for higher windspeeds.

A more general model may be constructed by assuming that the sea is calm when the wind begins to blow. Integration of the equations governing wave growth then permits the consideration of changes in the shape of the spectrum with increasing fetch and duration. If enough wave and wind records are available, empirical data may be analyzed to provide similar information. Pierson, Neumann, and James (1955) introduced this type of wave prediction scheme based almost entirely on empirical data. Inoue (1966, 1967) repeated this exercise in a manner more consistent with the Miles-Phillips theory, using a differential equation for wave growth. Inoue was a member of Pierson's group when this work was carried out, and his prediction scheme may be regarded as a replacement for the earlier Pierson-Neuman-James (PNJ) wave prediction model. The topic has been extended by Silvester and Vongvisessomjai (1971) and others.

These simplified wave prediction schemes are based on the implicit assumption that the waves being considered are due entirely to a wind blowing at a constant speed and direction and for a given duration.

In principle it would be possible to consider some effects of variable wind velocity by tracing each wave train. Once waves leave a generating area and become swell, the wave energy is then propagated according to the group velocity. The total energy at a point and the square of the significant wave height could be obtained by adding contributions from individual wave trains. Without a computer, this procedure is too laborious and theoretically inaccurate.

A more practical procedure is to relax the restrictions implied by derivation of these schemes. Thus wind direction may be considered constant if it varies from the mean by less than some finite value, say 30°. Windspeed may be considered constant if it varies from the mean by less than ± 5 knots (± 2.5 meters per second) or 1/2 barb on the weather map. (The uncertainty inherent in this assumption is not much greater than the uncertainty inherent in wind reports from ships.) In this procedure, average values are used and are assumed constant over the fetch area and for a particular duration.

Hasselmann et al. (1973) have demonstrated that the spectrum of an actively growing wind sea can be reasonably well represented by one family of spectral shapes. The shape of the wind sea spectrum is given by

$$E(f) = \frac{\alpha g^2}{(2\pi)^4 f^5} e^a \gamma^b \quad (3-32)$$

where

$$a = - \left[ \frac{5}{4} \left( \frac{f_m}{f} \right)^4 \right]$$

$$b = \exp - \left[ \frac{(f - f_m)^2}{2 \sigma^2 f_m^2} \right]$$

$f_m$  is the frequency of the spectral peak, and  $\alpha$ ,  $\sigma$ , and  $\gamma$  are coefficients either fit to an observed spectrum or calculated as functions of dimensionless fetch (Hasselmann et al., (1973, 1976). This formula is called the Joint North Sea Wave Project (JONSWAP) spectral shape after the field experiment on which it is based. Frequently, a single peaked spectrum is fitted to this form if parametric analytic spectra are required for mathematical analysis.

Similar formulas can also be developed empirically from wind and wave observations. A combined empirical-analytical procedure was used by Sverdrup and Munk (1947) in the first widely used wave prediction system. The Sverdrup-Munk prediction curves were revised by Bretschneider (1952, 1958) using empirical data. This prediction system is therefore often called the Sverdrup-Munk-Bretschneider (SMB) method.

More recent field data (Mitsuyasu, 1968; Hasselman et al., 1973) have resulted in some revisions to this method. The resulting curves are given in the next section. This wave prediction system is convenient when limited data and time are available.

### 3. Formulas for Predicting Waves in Deep Water.

It is desirable to have a simple method for making wave estimates. This is possible only if the geometry of the waterbody is relatively simple and if the wave conditions are either fetch-limited or duration-limited. Under fetch-limited conditions, winds have blown constantly long enough for wave heights at the end of the fetch to reach equilibrium. Under duration-limited conditions, the wave heights are limited by the length of time the wind has blown. These two conditions represent asymptotic approximations to the general problem of wave growth. In most cases the wave growth pattern at a site is a combination of the two cases. Equations (3-33) to (3-38) (Table 3-2) were obtained by simplifying the equation used to develop the parametric model (Hasselmann et al., 1976). Two dimensionless plots for wave growth are given in Figures 3-21 and 3-22, which also include adjustments for shallow water discussed in Chapter 3, Section IV.

In the fetch-limited case, the parameters required are the fetch,  $F$  and the wind-stress factor  $U_A$  (adjusted windspeed), where  $U_A$  has been adjusted as described in Chapter 3, Section IV, and represents a relatively constant average value over the fetch. The spectral wave height  $H_{m_0}$  and peak spectral period  $T_m$  are the parameters predicted.

$$\frac{gH_{m_0}}{U_A^2} = 1.6 \times 10^{-3} \left( \frac{gF}{U_A^2} \right)^{1/2} \quad (3-33)$$

$$\frac{gT_m}{U_A} = 2.857 \times 10^{-1} \left( \frac{gF}{U_A^2} \right)^{1/3} \quad (3-34)$$



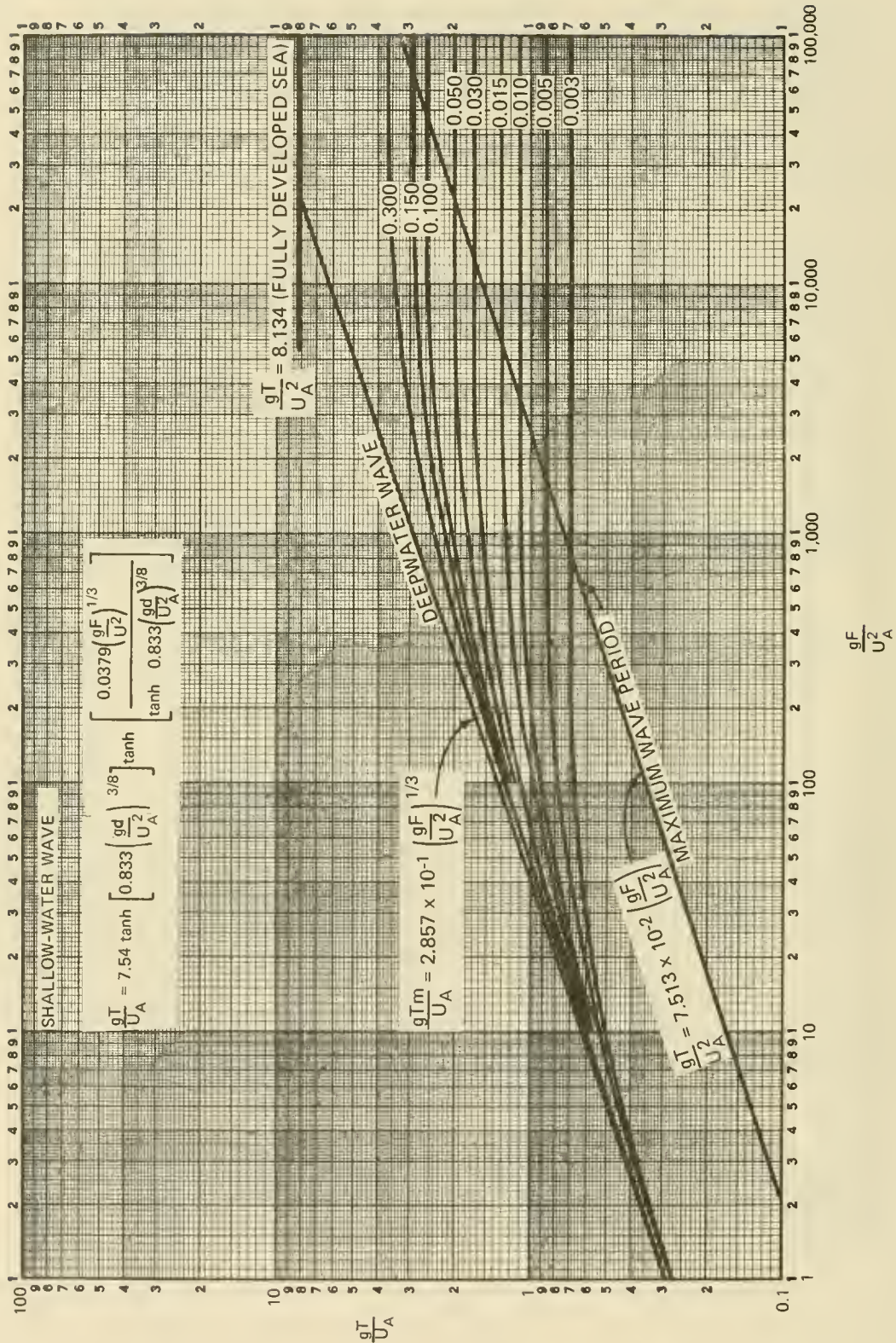


Figure 3-22. Forecasting curves for wave period. Constant water depth.

and

$$\frac{gt}{U_A} = 6.88 \times 10^1 \left( \frac{gF}{U_A^2} \right)^{2/3} \quad (3-35)$$

Note that  $T_{1/3}$  is given as  $0.95 T_m$ . The preceding equations are valid up to the fully developed wave conditions given by

$$\frac{gH_{m0}}{U_A^2} = 2.433 \times 10^{-1} \quad (3-36)$$

$$\frac{gT_m}{U_A} = 8.134 \quad (3-37)$$

$$\frac{gt}{U_A} = 7.15 \times 10^4 \quad (3-38)$$

where

$H_{m0}$  = the spectrally based significant wave height

$T_m$  = the period of the peak of the wave spectrum

F = the fetch

t = the duration

$U_A$  = the wind-stress factor

Often in applying the wave growth formulas, the engineer must determine if the design situation is fetch limited or duration limited. In these cases estimates of a one half- to 5-, etc. hour windspeeds with some return period (often 25 or 50 years) may be available. The objective is to find the largest wave height that occurs under these conditions. For example, a given return period, the 30-minute windspeed, will be higher than the 1- to 3-, etc. hour windspeeds, but because of its short duration it may produce a smaller wave height than the 1-hour windspeed.

A given calculation for a duration should be checked to ensure that it has not exceeded the maximum wave height or period possible for the given wind-stress factor and fetch. The nomograms in Figures 3-23 and 3-24 show wave prediction curves of empirical values which can be used to check the reasonableness of the mathematical solutions. For example, for  $U_A = 20$  meters per second a duration of 5 hours yields a height of 2.5 meters. However, if the fetch were only 30 kilometers long, the maximum wave height can only be 1.75 meters for a wind-stress factor of 20 meters per second. If the wind-stress factor is 20 meters per second and its duration is only 3 hours, the fetch-limited wave height of 2.5 meters for a fetch of 30 kilometers would not be reached; therefore, the wave height is duration limited. It is essential that fetch-limited wave calculations be checked to see if they are duration limited; likewise, duration-limited cases should be

Table 3-2. Deepwater wave forecasting equation.

Dimensionless	Metric Units	
	H(m), T(s), U <sub>A</sub> (m/s), F(m), t(a)	H(m), T(s), U <sub>A</sub> (m/s), F(km), t(hr)
<u>FETCH LIMITED (F, U)</u>		
$\frac{8H_{m_0}}{U_A^2} = 1.6 \times 10^{-3} \left( \frac{gF}{U_A^2} \right)^{1/2}$ (3-33)	$H_{m_0} = 5.112 \times 10^{-4} U_A F^{1/2}$ (3-33a)	$H_{m_0} = 1.616 \times 10^{-2} U_A F^{1/2}$ (3-33b)
$\frac{8T_m}{U_A} = 2.857 \times 10^{-1} \left( \frac{gF}{U_A^2} \right)^{1/3}$ (3-34)	$T_m = 6.238 \times 10^{-2} (U_A F)^{1/3}$ (3-34a)	$T_m = 6.238 \times 10^{-1} (U_A F)^{1/3}$ (3-34b)
$\frac{gt}{U_A} = 6.88 \times 10^1 \left( \frac{gF}{U_A^2} \right)^{2/3}$ (3-35)	$t = 3.215 \times 10^1 \left( \frac{F^2}{U_A} \right)^{1/3}$ (3-35a)	$t = 8.93 \times 10^{-1} \left( \frac{F^2}{U_A} \right)^{1/3}$ (3-35b)
<u>FULLY DEVELOPED</u>		
$\frac{8H_{m_0}}{U_A^2} = 2.433 \times 10^{-1}$ (3-36)	$H_{m_0} = 2.482 \times 10^{-2} U_A^2$ (3-36a)	$H_{m_0} = 2.4821 \times 10^{-2} U_A^2$ (3-36b)
$\frac{8T_m}{U_A} = 8.134$ (3-37)	$T_m = 8.30 \times 10^{-1} U_A$ (3-37a)	$T_m = 8.30 \times 10^{-1} U_A$ (3-37b)
$\frac{gt}{U_A} = 7.15 \times 10^4$ (3-38)	$t = 7.296 \times 10^3 U_A$ (3-38a)	$t = 2.027 U_A$ (3-38b)
<u>NOTATIONS</u>	$g = 9.8 \text{ m/s}^2$	$g = 9.8 \text{ m/s}^2$ 1 kilometer = 1000 m 1 hour = 3600 a

	English Units	
	H(ft), T(a), U <sub>A</sub> (ft/s), F(ft), t(a)	H(ft), T(s), U <sub>A</sub> (mi/hr), F(mi), t(hr)
<u>FETCH LIMITED (F, U)</u>		
$H_{m_0} = 2.82 \times 10^{-4} U_A F^{1/2}$ (3-33c)	$H_{m_0} = 3.01 \times 10^{-2} U_A F^{1/2}$ (3-33d)	$H_{m_0} = 3.714 \times 10^{-2} U_A F^{1/2}$ (3-33e)
$T_m = 2.825 \times 10^{-2} (U_A F)^{1/3}$ (3-34c)	$T_m = 5.59 \times 10^{-1} (U_A F)^{1/3}$ (3-34d)	$T_m = 6.14 \times 10^{-1} (U_A F)^{1/3}$ (3-34e)
$t = 2.16 \times 10^1 \left( \frac{F^2}{U_A} \right)^{1/3}$ (3-35c)	$t = 1.603 \left( \frac{F^2}{U_A} \right)^{1/3}$ (3-35d)	$t = 1.680 \left( \frac{F^2}{U_A} \right)^{1/3}$ (3-35e)
<u>FULLY DEVELOPED</u>		
$H_{m_0} = 7.553 \times 10^{-3} U_A^2$ (3-36c)	$H_{m_0} = 1.625 \times 10^{-2} U_A^2$ (3-36d)	$H_{m_0} = 2.154 \times 10^{-2} U_A^2$ (3-36e)
$T_m = 2.53 \times 10^{-1} U_A$ (3-37c)	$T_m = 3.706 \times 10^{-1} U_A$ (3-37d)	$T_m = 4.244 \times 10^{-1} U_A$ (3-37e)
$t = 2.220 \times 10^3 U_A$ (3-38c)	$t = 9.045 \times 10^{-1} U_A$ (3-38d)	$t = 1.04 U_A$ (3-38e)
<u>NOTATIONS</u>	$g = 32.2 \text{ ft/s}^2$	$g = 32.2 \text{ ft/s}^2$ 1 nautical mile = 6080 ft 1 knot = 1.689 ft/s 1 hour = 3600 a

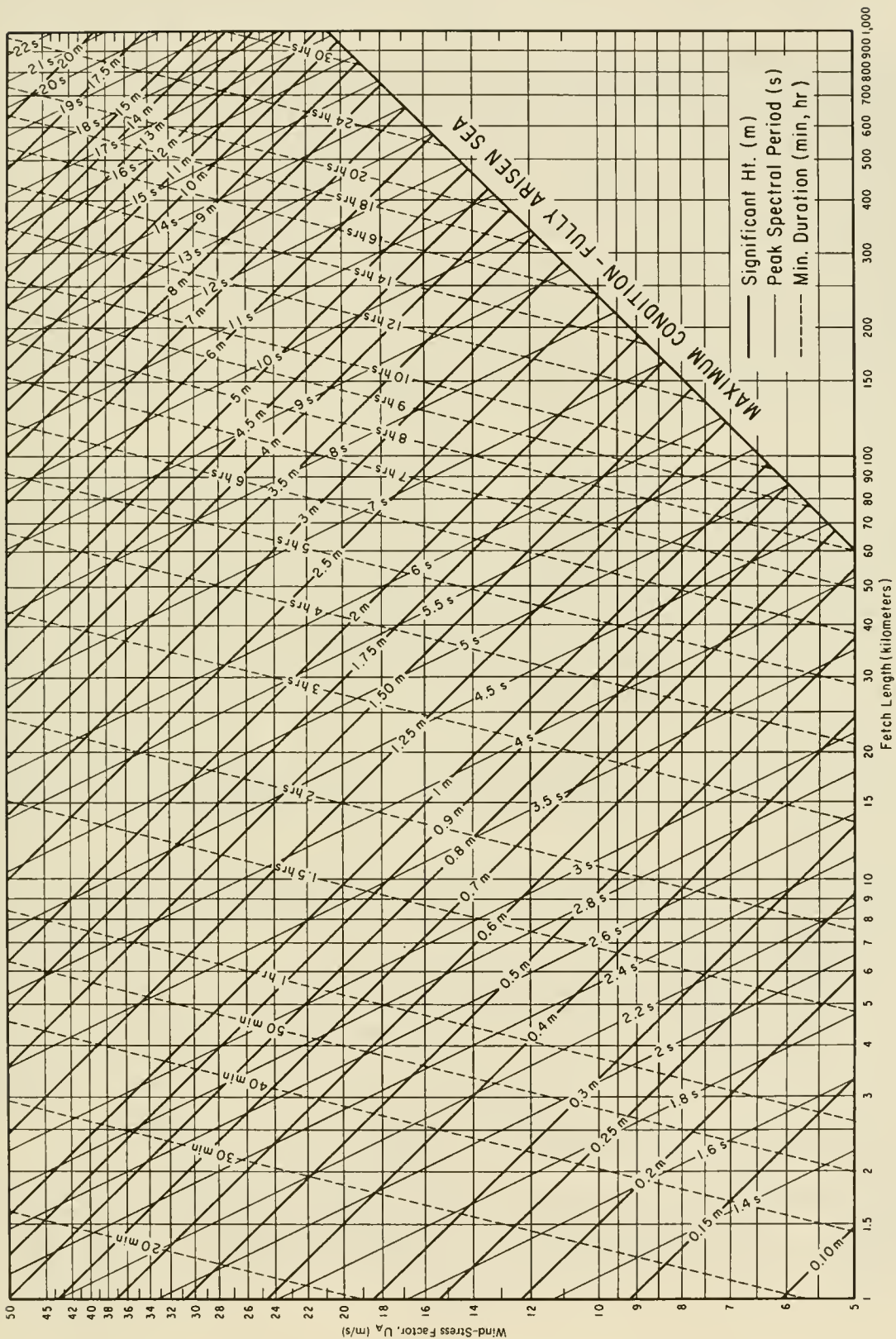
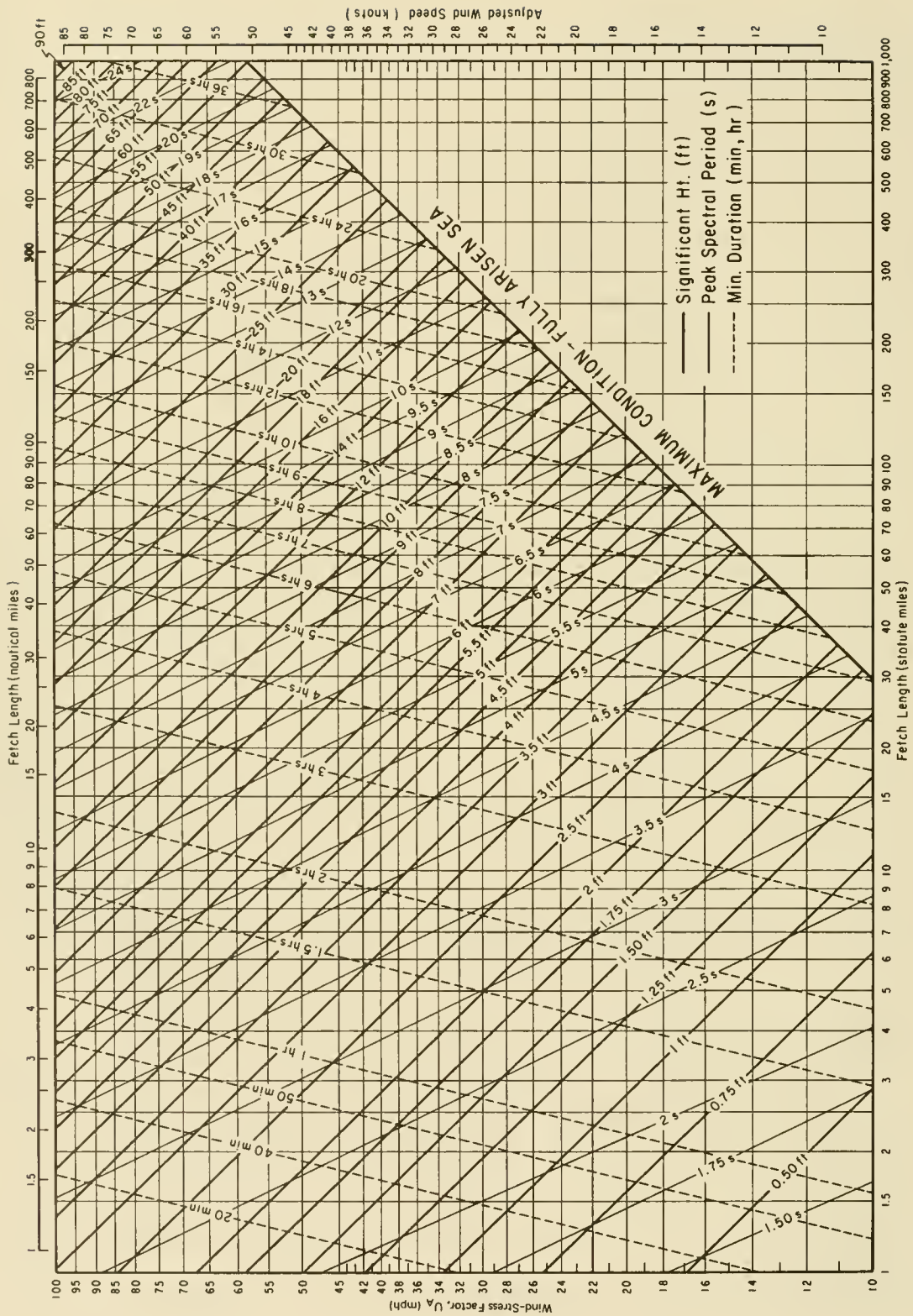


Figure 3-23. Nomograms of deepwater significant wave prediction curves as functions of windspeed, fetch length, and wind duration (metric units).



checked to see if they are really fetch limited. If the formulas are used rather than the nomograms, wave conditions should also be checked to see if they exceed the fully developed condition.

Wave growth with duration is not as well understood as wave growth with fetch length. Equation (3-36) ensures that the growth of  $H_m$  and  $T_m$  with time reaches the fetch-limited value at about the same duration specified by equation (3-39). The approximation works well except for long dimensionless fetches (relatively long-fetch, low-wind-speed cases).

Inevitably, estimating wave height and period requires that checks be made between fetch, duration, and fully developed limitations. Many design situations require iteration between these approaches and the appropriate averaged durations. The wave growth formulas must use the wind-stress factor and not windspeed. The proper averaging times for the winds (as related to the duration and fetch) must be used. This approach is approximate, and the number of iterations and adjustments used should reflect this limited accuracy.

#### 4. Narrow Fetch Conditions.

When early users of the SMB curves applied them to reservoirs and small lakes, calculated wave heights were much larger than observed wave heights. It was thus assumed that the narrowness of the fetch was affecting wave growth. The concept of an effective fetch was introduced which reduced fetch length to account for the narrowness of the fetch. The adjustment provided improved wave estimates. When the growth curves presented here were applied to similar situations (Resio and Vincent, 1979) the effective fetch calculation resulted in wave heights that were too low, while a straight-line fetch provided wave heights closer to observed values (Fig. 3-25). Data from inland reservoirs were checked by computing  $H_s$  based on an effective fetch and on straight-line fetch (Fig. 3-26). The straight-line fetch shows reasonable agreement with the growth curves.

The reason an effective fetch adjustment is required for the SMB curves is that these curves overpredict wave heights for small values of  $F$  more than do recent data. The effective fetch method implicitly assumes a cosine directional spread for wind input to the sea. More recent data suggest that a cosine to the 10th power describes the directional distribution near the peak frequency of the spectrum. This is a much narrower spread. *Effective fetch should not be used with the growth curves presented herein.* There may be a critical fetch width where width becomes important, but this is not known at this time.

\* \* \* \* \* EXAMPLE PROBLEM 4 \* \* \* \* \*

GIVEN: Eight consecutive hourly observations of fastest mile windspeed  $U_0 = 20$  meters per second are observed at an elevation of  $Z_L = 6$  meters, approximately 5 kilometers inland from shore. The observation site is at an airport weather station. The air-sea temperature difference was estimated to be  $-6^\circ\text{C}$ .

FIND: The spectral significant wave height  $H_{m_0}$ , the period of the spectral peak  $T_m$ , and the significant period  $T_s$  for

- (a) Fetch = 10 kilometers.
- (b) Fetch = 100 kilometers.
- (c) Duration = 3 hours for each of the above fetches.

SOLUTION: The winds are observed over land, so the procedure of Chapter 3, Section IV,3 will be followed.

(a) Assume that there are no topographic convergences and that the winds are from a large-scale pressure system.

(b) The winds must be converted to a 10-meter level (Ch. 3, Sec. IV,a):

$$U_{10} = U_o (10/Z)^{1/7} = (20) \left(\frac{10}{6}\right)^{0.142} = 21.5 \text{ m/s (48.1 mi/hr)}$$

(c) Since the anemometer is located 5 kilometers inland, the location factor adjustment may be needed (Ch. 3, Sec. IV,1,d). For the 10-kilometer fetch Chapter 3, Section IV,3,c indicates  $R_L = 1.2$ . For the 100-kilometer fetch, Figure 3-15 is used to obtain  $R_L = 1.2$  also. So in both cases the windspeed is increased by 20 percent to 26 meters per second.

(d) The stability factor (Fig. 3-14) is 1.14 for an air-sea temperature difference of  $-6^\circ\text{C}$ . Thus the windspeed is further increased by 14 percent to 30 meters per second. (If the temperature difference had been  $+6^\circ$ , the windspeed would have been reduced to 84 percent of its value or 22 meters per second.)

(e) Since the fastest mile windspeed is given, the duration-averaged windspeed must be estimated. From Chapter 3, Section IV,1,b find  $U_{t=60 \text{ min}}$ .

$$t = \frac{1609}{29.4} = 54.7 \text{ seconds, say } 55$$

and

$$U_t/U_{3600} = 1.25$$

The 1-hour windspeed is

$$U_{3600} = \frac{U_{55}}{U_{55}/U_{3600}} = \frac{29.4}{1.25} = 23.5 \text{ m/s (52.6 mi/hr)}$$

Since the observations indicate that the wind was constant over the 8 hours, the 8-hour average windspeed can be assumed to be 23.5 meters per second. (If the windspeed were variable, an iteration on the duration-averaged winds would have to be made. For example, a 23.5-meter-per-second windspeed will give a wind-stress factor of 34.5 (see below). Entering Figure 3-23 with a fetch of 10 kilometers and a wind-stress factor of 34.5, the duration to reach the fetch-limited case is about 1 hour and 20 minutes, so the wind duration that should be considered is 1 hour and 20 minutes.

(f) The wind-stress factor is computed by equation (3-28a),

$$U_A = 0.71 (U)^{1.23} = 0.71 (23.5)^{1.23} = 34.5 \text{ m/s (77.2 mi/hr)}$$

for both the 100-kilometer and 10-kilometer fetches and 3-hour duration.

(g) For  $F = 10$  kilometers and  $U_A = 34.5$  meters per second, Fig. 3-23 gives  $H_m = 1.75$  meters and  $T_m = 4.4$  seconds, ( $T_{1/3} = 0.95 T_m$  and  $T_m = 4.2$  seconds).

(h) For  $F = 100$  kilometers and  $U_A = 34.5$  meters per second,

$$H_{m_0} = 5.5 \text{ m, } T_m = 9.4 \text{ s and } T_{1/3} = 8.9 \text{ s}$$

(i) For  $t = 3$  hours and  $U_A = 34.5$  meters per second,

$$H_{m_0} = 3.3 \text{ m, } T_m = 6.7 \text{ s, and } T_{1/3} = 6.4 \text{ s}$$

However, if the fetch was only 10 kilometers, the wave growth would become fetch limited after about 1 hour and 25 minutes and the wave height would be limited to the values obtained in (g) above. If the fetch is 100 kilometers and the wind duration is 3 hours, then the values in (h) above will not be reached because the duration is too short. Therefore, it is essential to check that what is expected to be a fetch-limited case is not duration limited.

If for a given wind-stress factor and fetch or duration the point of intersection on Figure 3-23 or 3-24 lies in the maximum condition fully arisen sea area, the maximum wave height for that wind-stress factor is the wave height.

\*\*\*\*\*

## 5. Effects of Moving Storms and a Variable Wind Speed and Direction.

The case of a variable windfield in space and time over a waterbody of irregular geometry is complex and must be treated using advanced numerical wave prediction models such as those of Resio (1981) and Hasselmann et al. (1976).

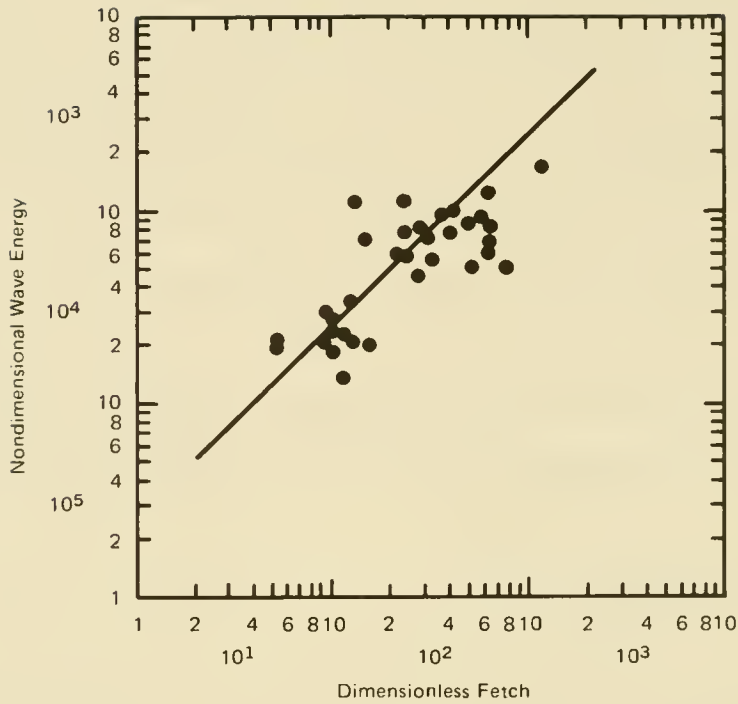


Figure 3-25. Narrow fetch data from reservoirs. (The fetch data are scaled by straight line fetch.)

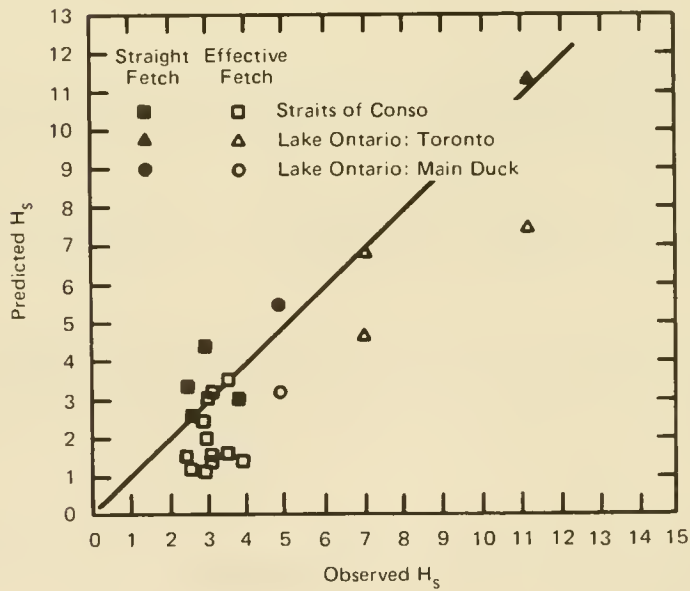


Figure 3-26. Narrow fetch data (Resio and Vincent, 1979). (Predictions are made with both an effective and a straight-line fetch, using the method given here.)

## VI. WAVE FORECASTING FOR SHALLOW WATER

### 1. Forecasting Curves.

Water depth affects wave generation. For a given set of wind and fetch conditions, wave heights will be smaller and wave periods shorter if generation takes place in transitional or shallow water rather than in deep water. Several forecasting approaches have been made, including the method given by Bretschneider as modified using the results of Ijima and Tang (1966). Bretschneider and Reid (1953) consider bottom friction and percolation in the permeable sea bottom.

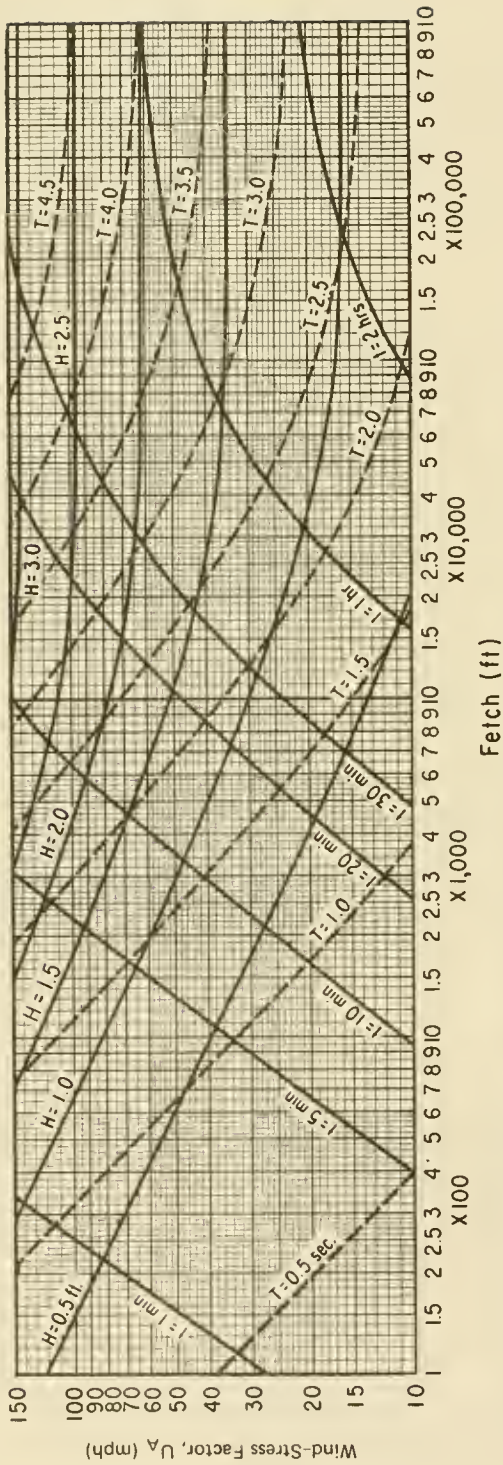
There is no single theoretical development for determining the actual growth of waves generated by winds blowing over relatively shallow water. The method presented here is based on successive approximations in which wave energy is added due to wind stress and subtracted due to bottom friction and percolation. This method uses deepwater forecasting relationships (Chapter 3, Section V) to determine the energy added due to wind stress. Wave energy lost due to bottom friction and percolation is determined from the relationships developed by Bretschneider and Reid (1953). Resultant wave heights and periods are obtained by combining the above relationships by numerical methods. The basic assumptions applicable to development of deepwater wave generation relationships as well as development of relationships for bottom friction loss (Putnam and Johnson, 1949) and percolation loss (Putnam, 1949) apply. The duration should be considered approximate.

These shallow-water forecasting curves (Fig. 3-27 through 3-36) represent an interim method for wave forecasting in shallow water. Modifications to the shallow-water forecasting equations were made to provide a transition between the revised deepwater forecasting equations and the shallow-water forecasting model. Research is underway that may revise the shallow-water forecasting model. Until the results of this new research are available, the curves should be used. The curves are plotted from the following equations:

$$\frac{gH}{U_A^2} = 0.283 \tanh \left[ 0.530 \left( \frac{gd}{U_A^2} \right)^{3/4} \right] \tanh \left\{ \frac{0.00565 \left( \frac{gF}{U_A^2} \right)^{1/2}}{\tanh \left[ 0.530 \left( \frac{gd}{U_A^2} \right)^{3/4} \right]} \right\} \quad (3-39)$$

$$\frac{gT}{U_A} = 7.54 \tanh \left[ 0.833 \left( \frac{gd}{U_A^2} \right)^{3/8} \right] \tanh \left\{ \frac{0.0379 \left( \frac{gF}{U_A^2} \right)^{1/3}}{\tanh \left[ 0.833 \left( \frac{gd}{U_A^2} \right)^{3/8} \right]} \right\} \quad (3-40)$$

Note: Waves in a water depth of 5 feet with wave periods less than 1.4 secs. are considered to be deepwater waves, i.e.,  $d/L^2 > 2.56$ .



Note: Waves in a water depth of 1.5 meters with wave periods less than 1.4 seconds are considered to be deepwater waves, i.e.,  $d/L^2 > 0.78$ .

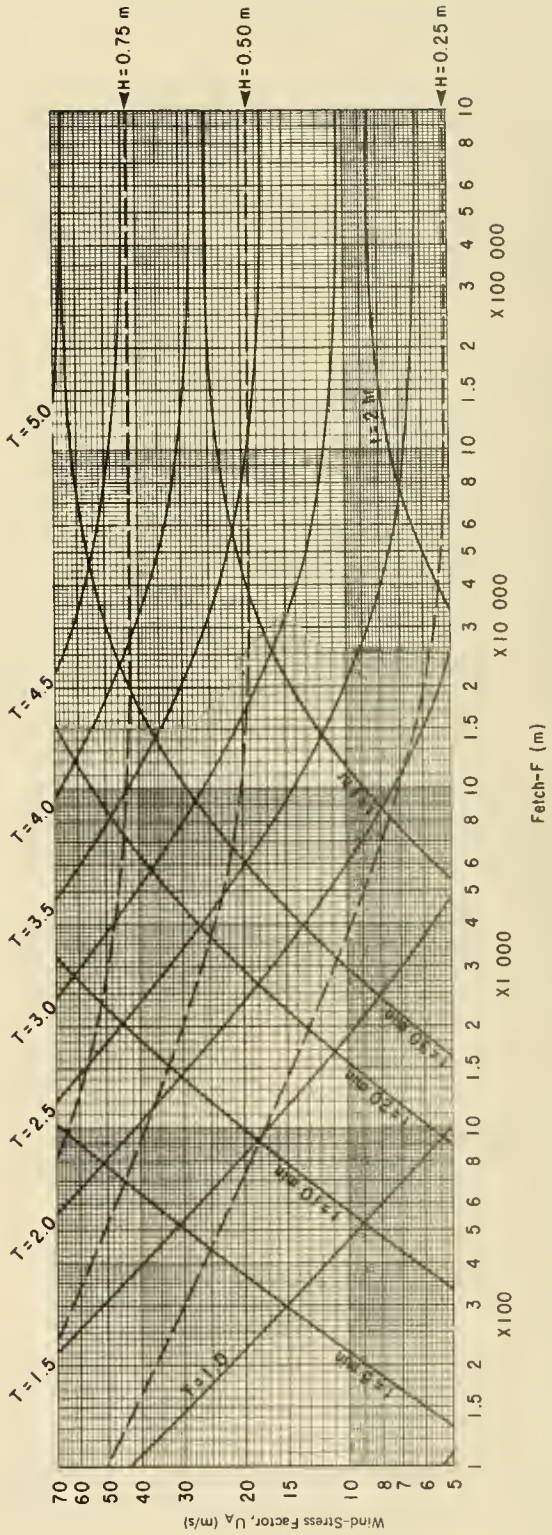
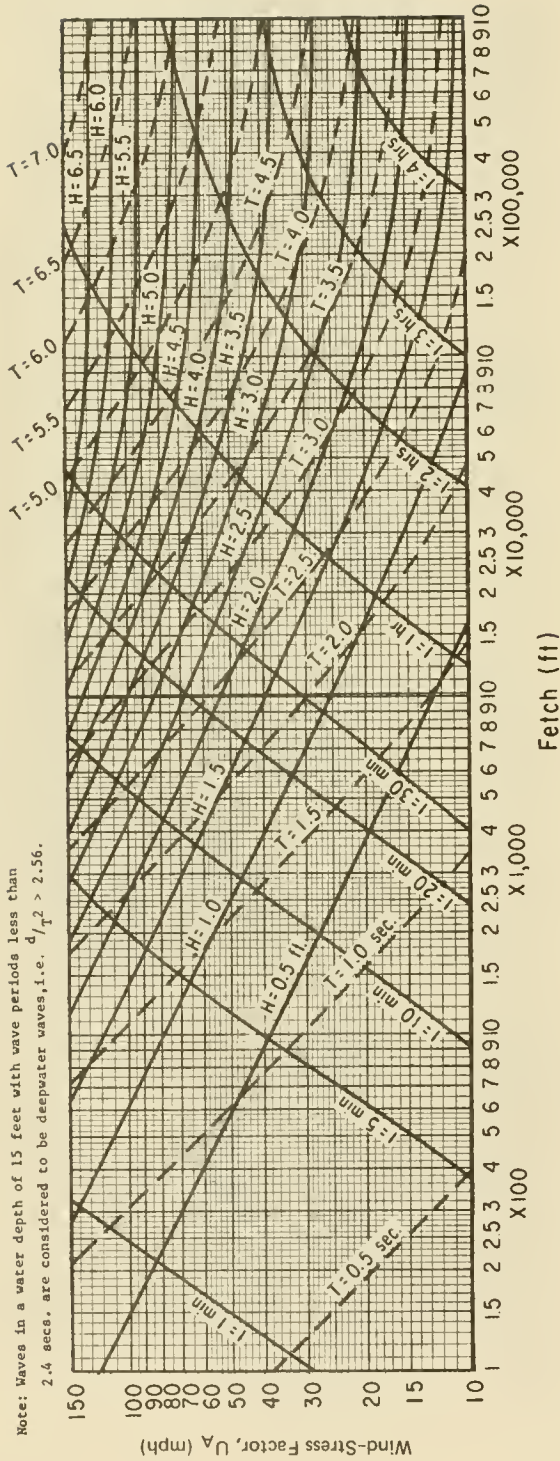


Figure 3-27. Forecasting curves for shallow-water waves; constant depths = 5 feet (upper graph) and 1.5 meters (lower graph).





Note: Waves in a water depth of 4.5 meters with wave periods less than 2.4 seconds are considered to be deepwater waves, i.e.,  $d/L_T > 0.78$ .

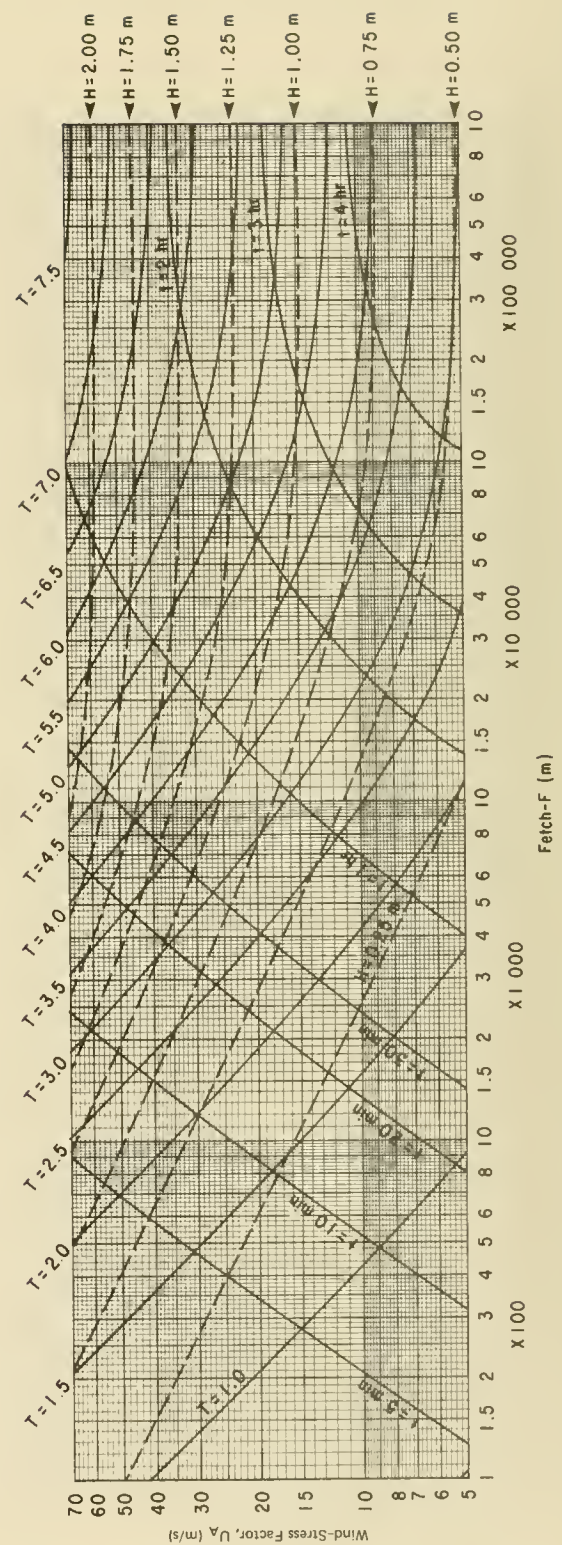
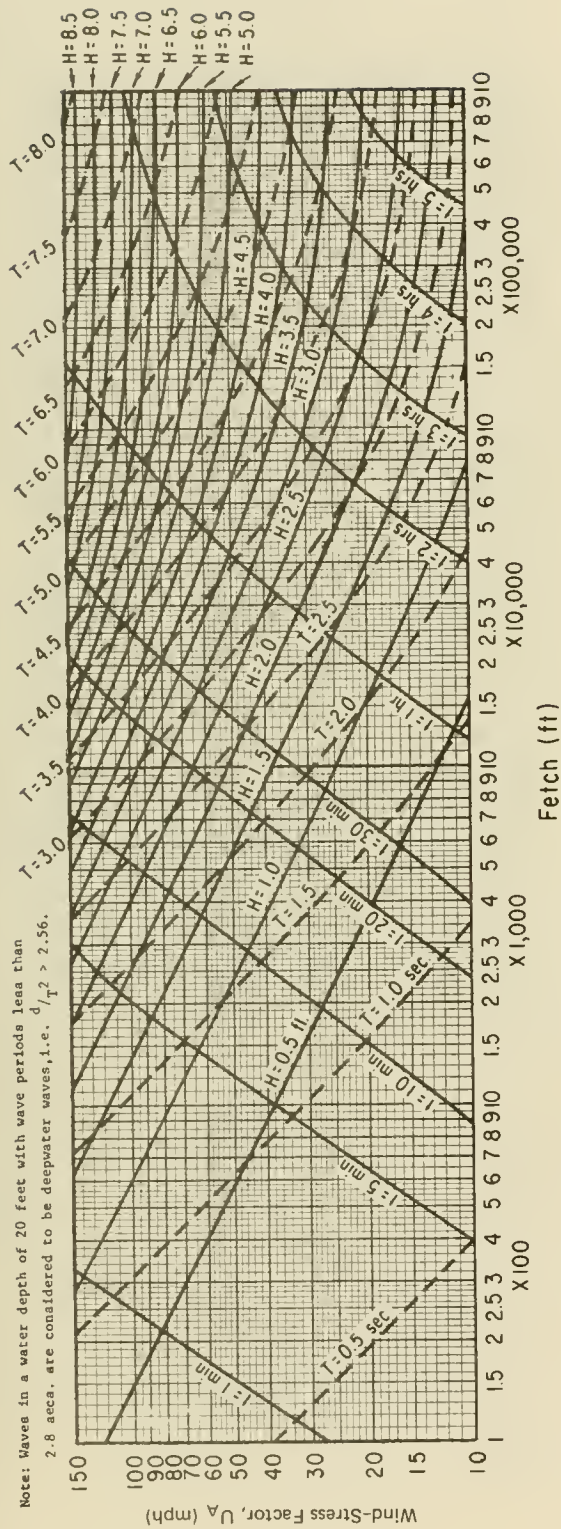


Figure 3-29. Forecasting curves for shallow-water waves; constant depths = 15 feet (upper graph) and 4.5 meters (lower graph).



Note: Waves in a water depth of 6.0 meters with wave periods less than 2.8 seconds are considered to be deepwater waves, i.e.,  $d/L^2 > 0.78$ .

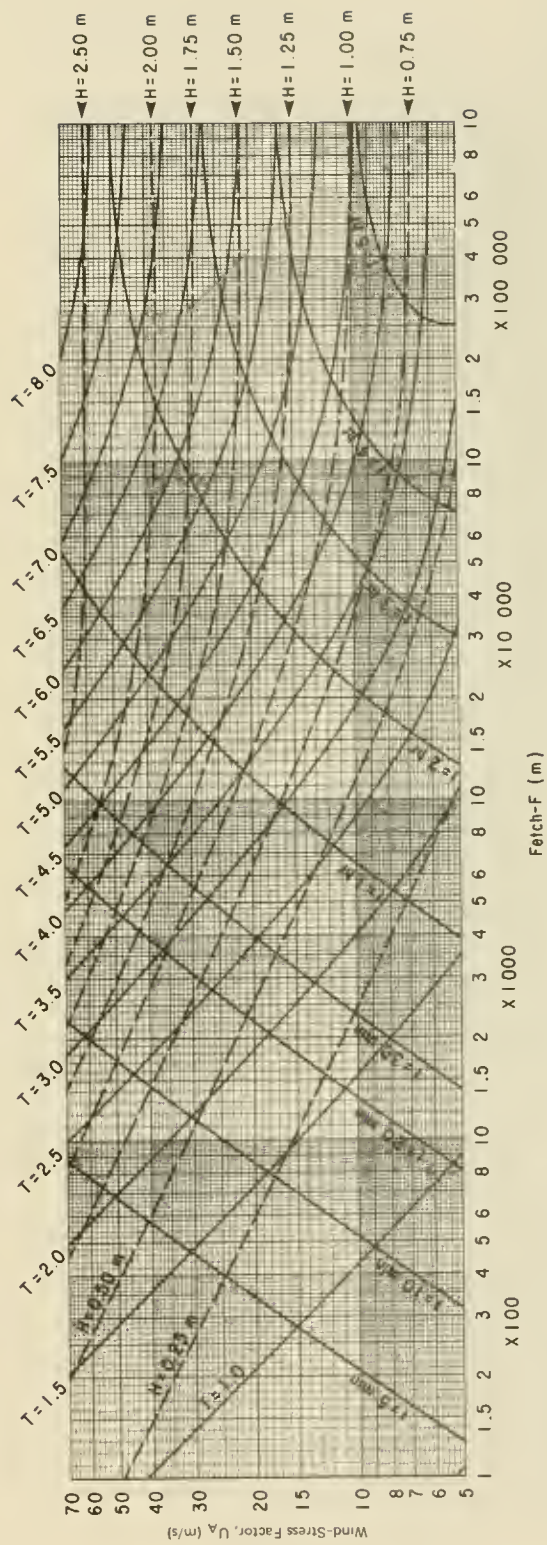
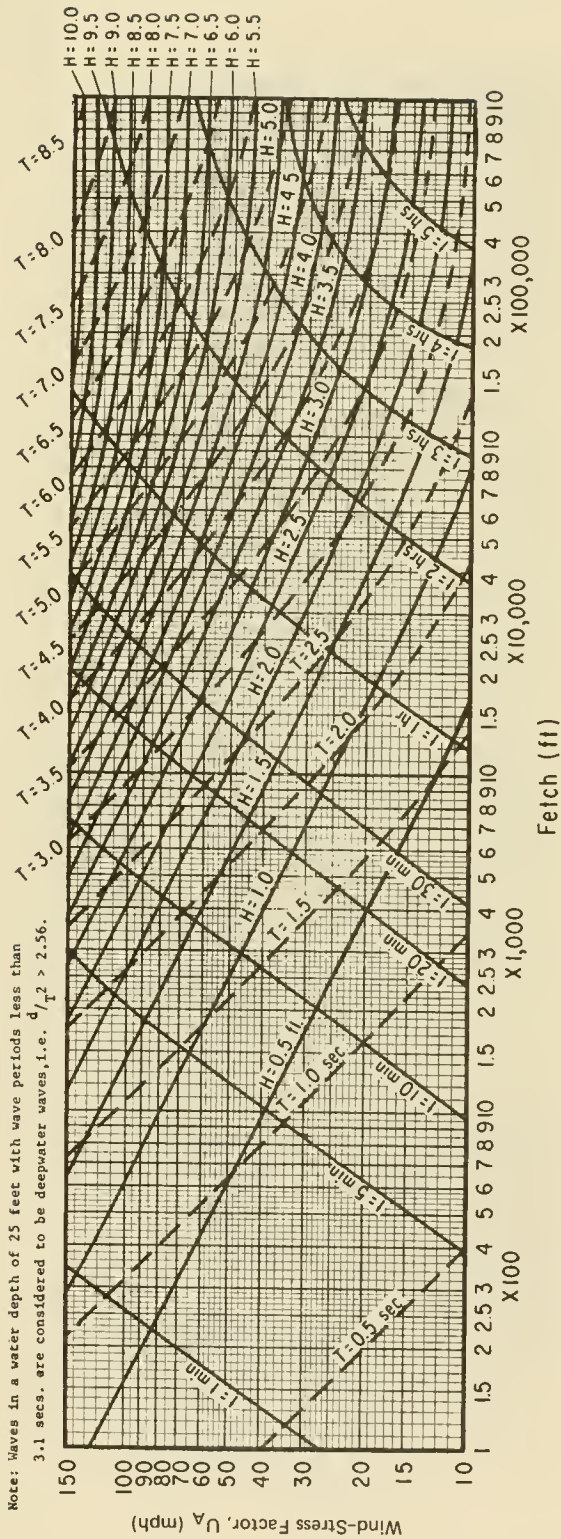


Figure 3-30. Forecasting curves for shallow-water waves; constant depths = 20 feet (upper graph) and 6.0 meters (lower graph).



Note: Waves in a water depth of 7.5 meters with wave periods less than 3.1 seconds are considered to be deepwater waves, i.e.,  $d/T^2 > 0.76$ .

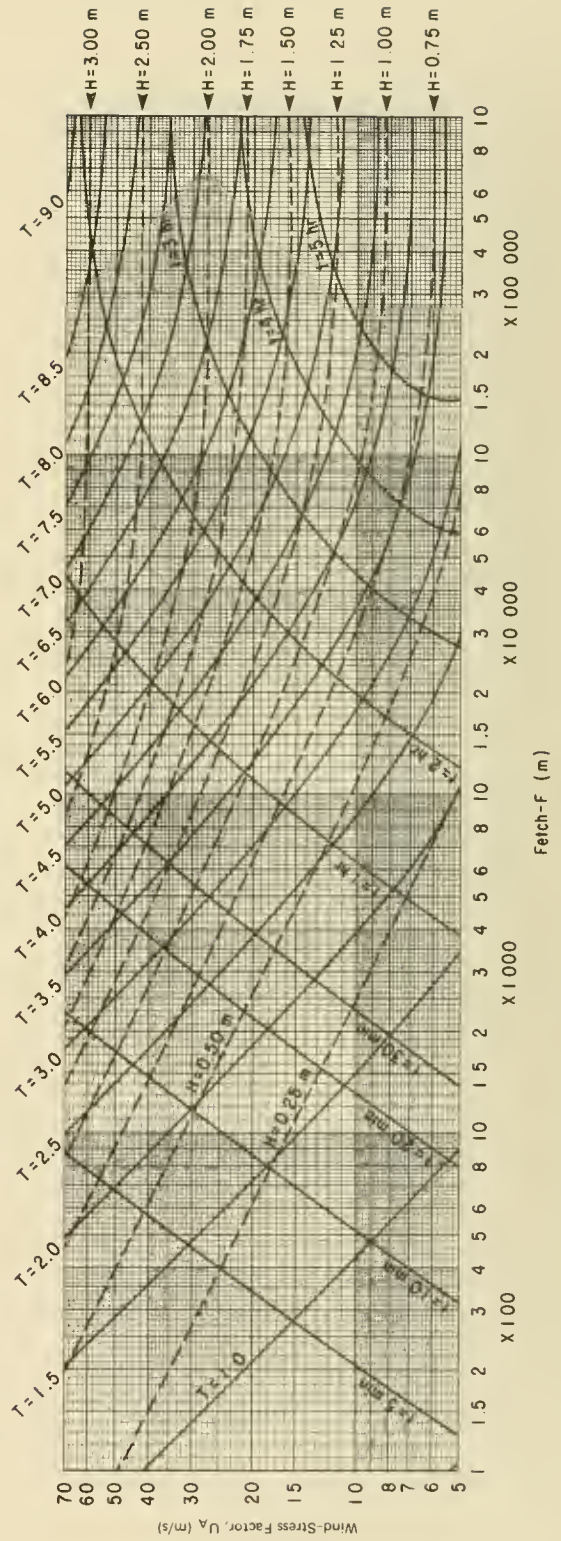
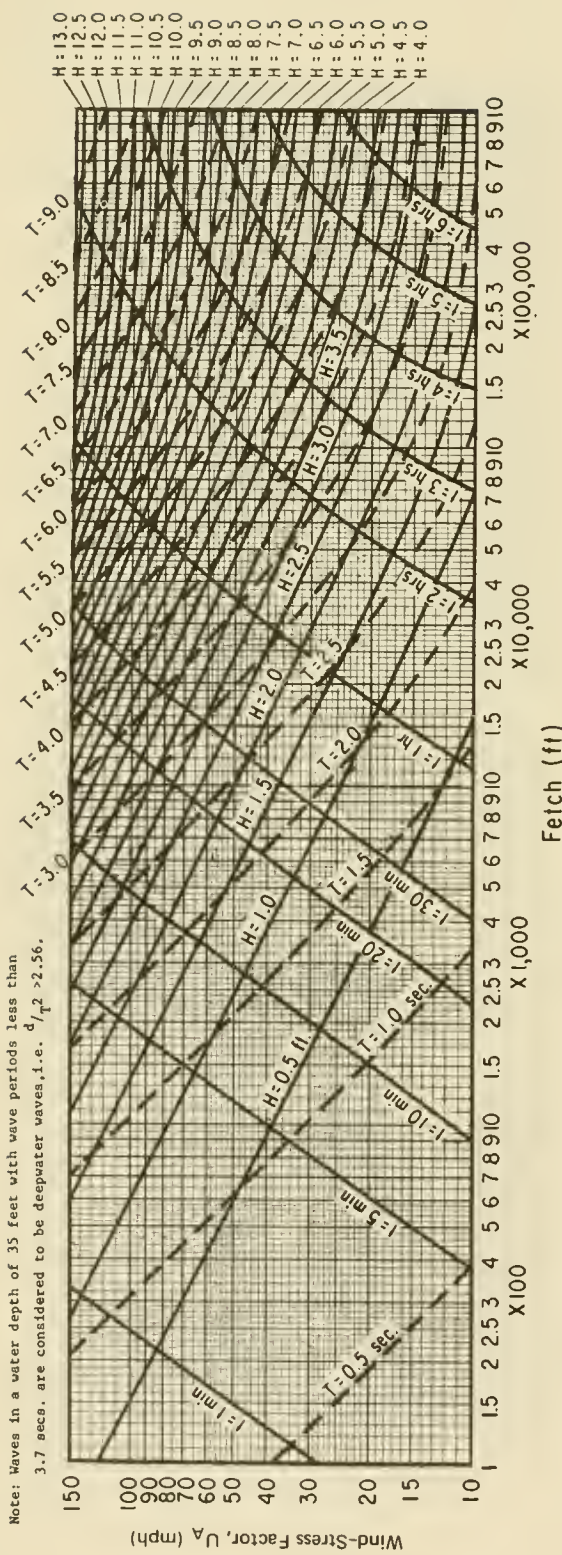


Figure 3-31. Forecasting curves for shallow-water waves; constant depths = 25 feet (upper graph) and 7.5 meters (lower graph).





Note: Waves in a water depth of 10.5 meters with wave periods less than 3.7 seconds are considered to be deepwater waves, i.e.,  $d/L_T > 0.78$ .

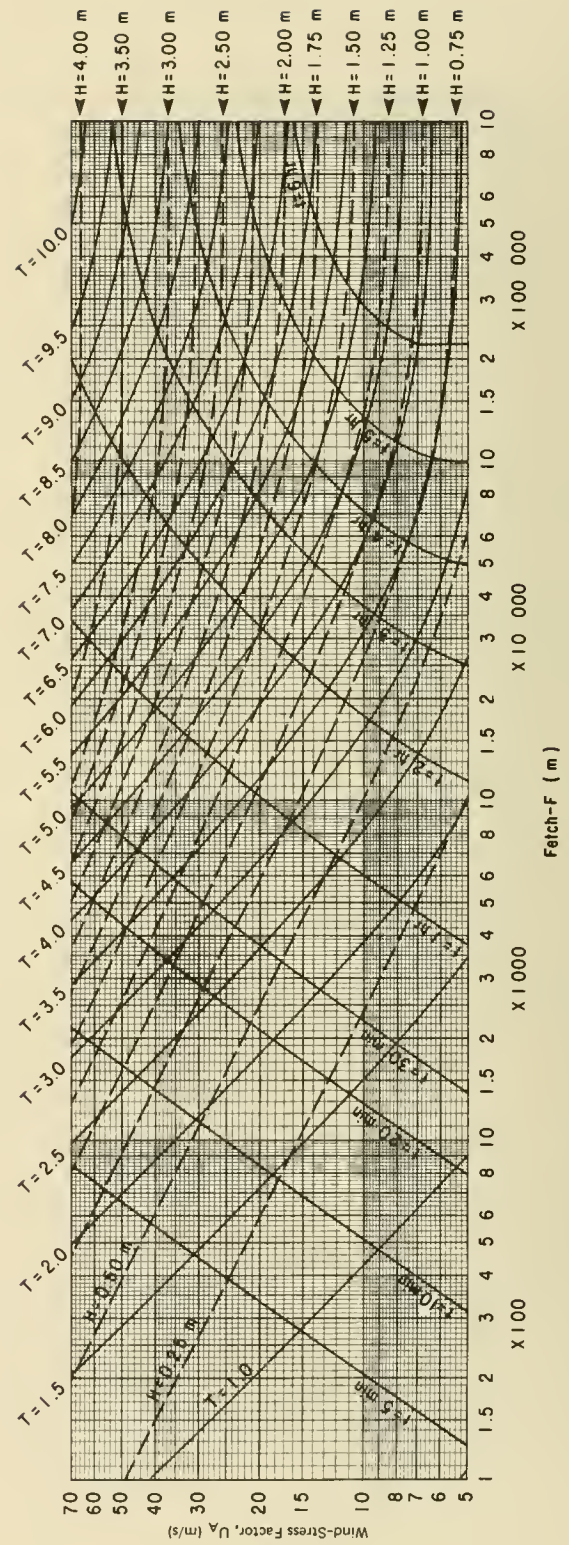
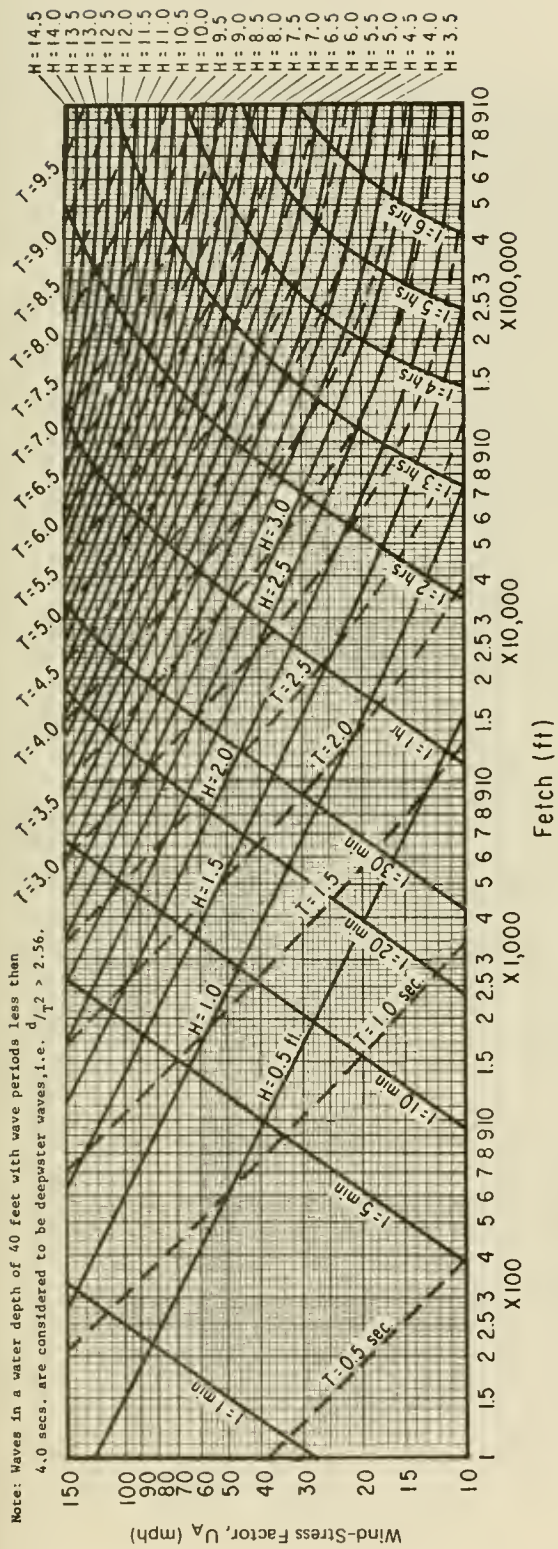


Figure 3-33. Forecasting curves for shallow-water waves; constant depths = 35 feet (upper graph) and 10.5 meters (lower graph).



Note: Waves in a water depth of 12.0 meters with wave periods less than 3.9 seconds are considered to be deepwater waves, i.e.,  $d/T^2 > 0.78$ .

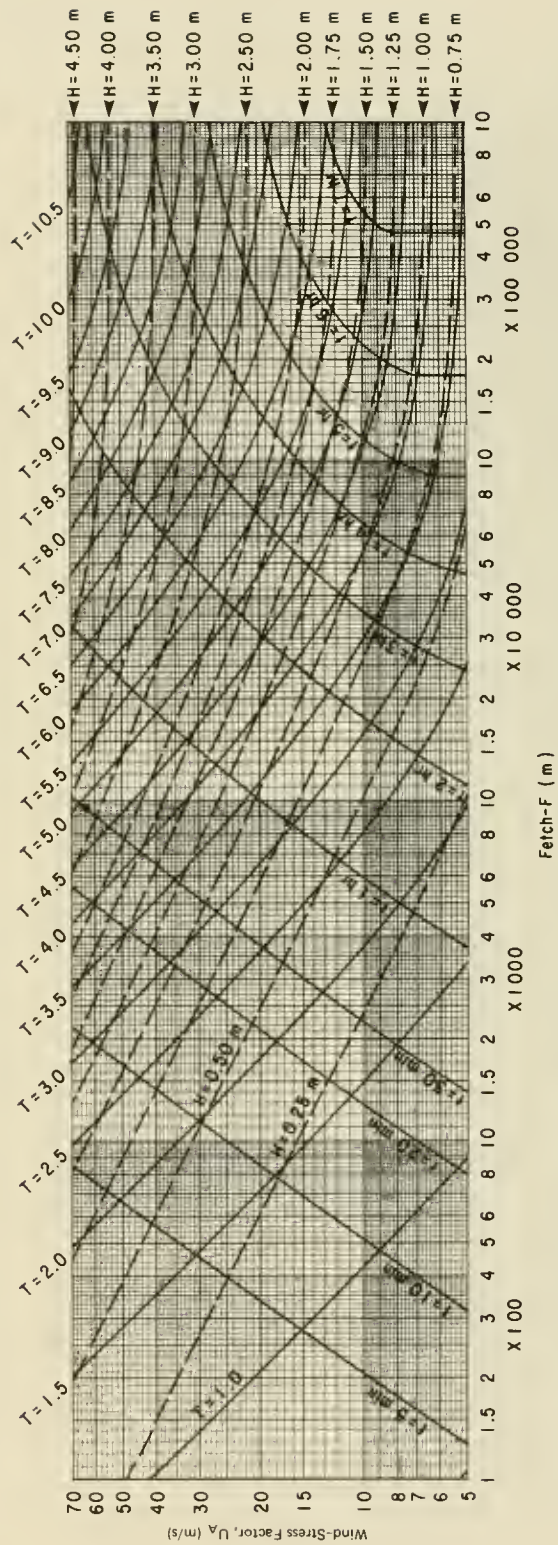
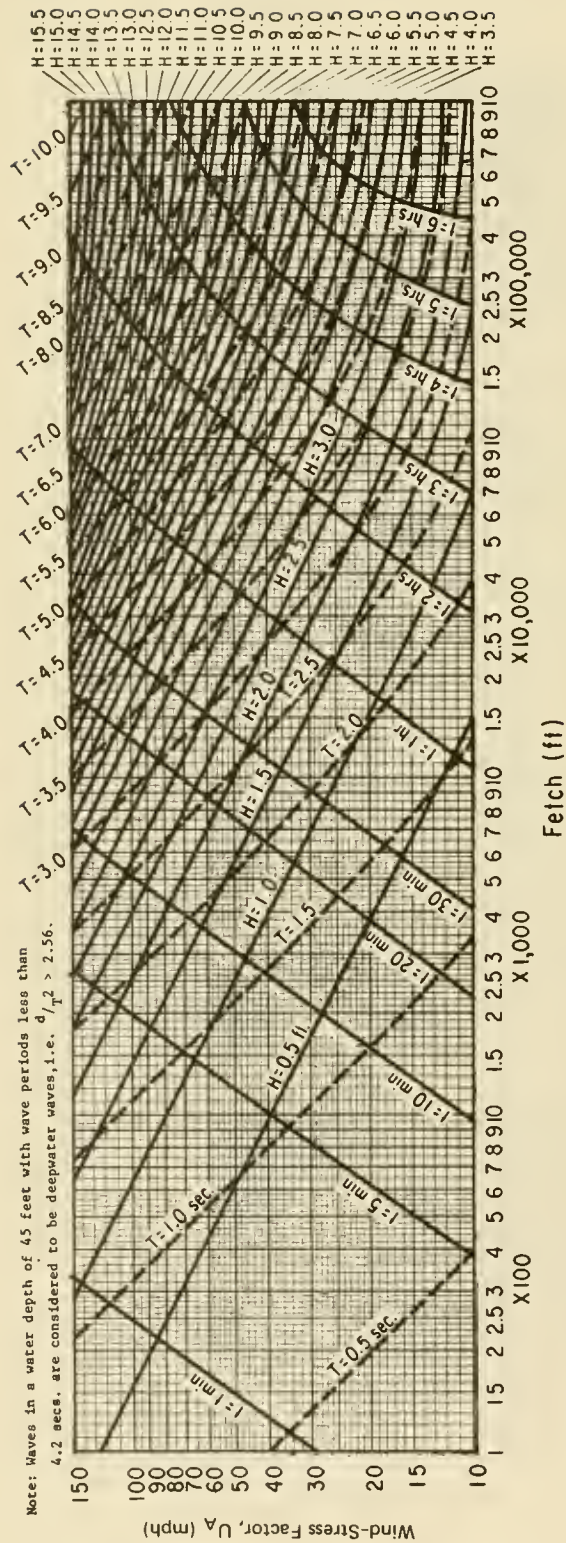


Figure 3-34. Forecasting curves for shallow-water waves; constant depths = 40 feet (upper graph) and 12.0 meters (lower graph).



Note: Waves in a water depth of 13.5 meters with wave periods less than 4.2 seconds are considered to be deepwater waves, i.e.,  $d/L^2 > 0.78$ .

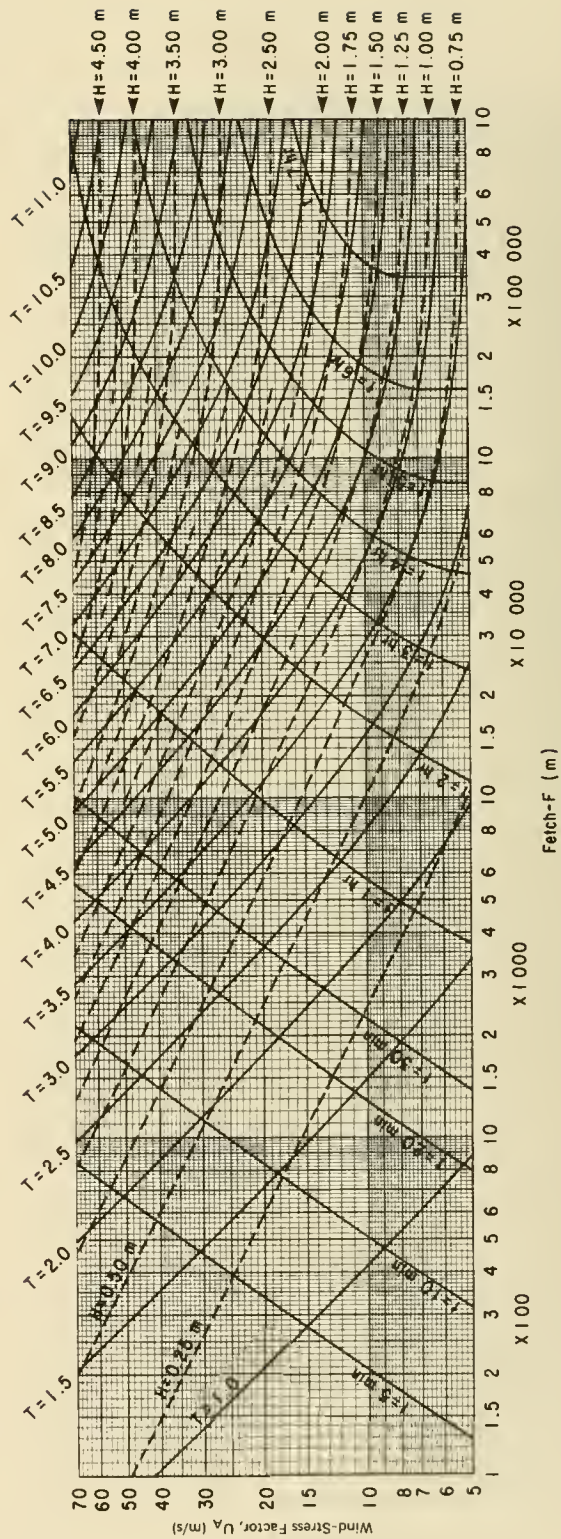
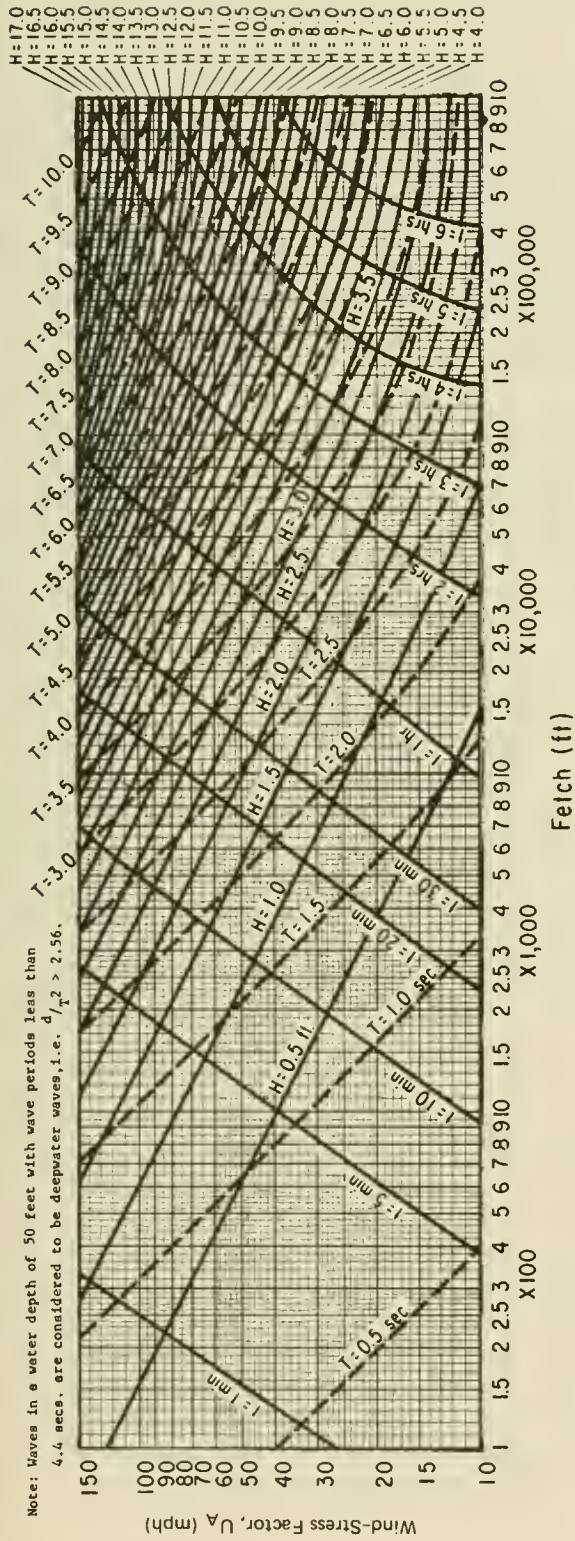


Figure 3-35. Forecasting curves for shallow-water waves; constant depths = 45 feet (upper graph) and 13.5 meters (lower graph).



Note: Waves in a water depth of 15.0 meters with wave periods less than 4.4 seconds are considered to be deepwater waves, i.e.,  $d/L^2 > 0.78$ .

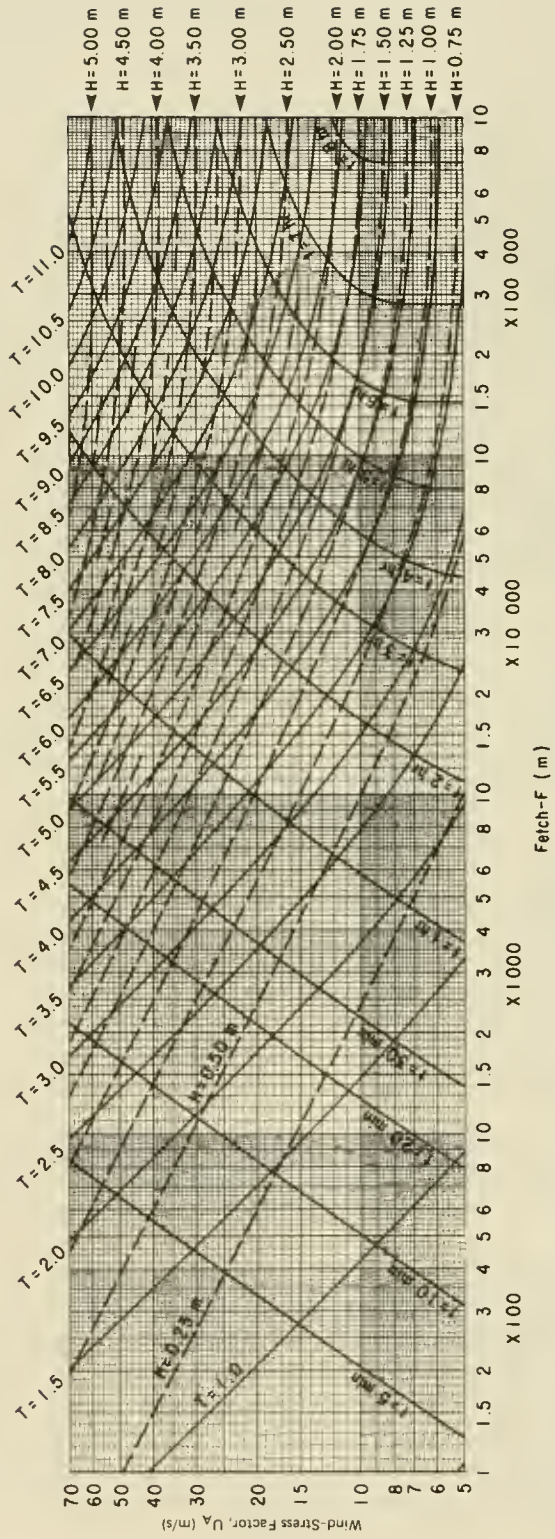


Figure 3-36. Forecasting curves for shallow-water waves; constant depths = 50 feet (upper graph) and 15.0 meters (lower graph).

and

$$\frac{gt}{U_A} = 5.37 \times 10^2 \left( \frac{gT}{U_A} \right)^{7/3} \quad (3-41)$$

The wind-stress factor  $U_A$  (adjusted windspeed) is obtained by estimating the surface wind  $U_s$  in meters per second via Chapter 3, Section IV and then setting  $U_A = 0.71 U_s^{1.23}$ . Each figure is plotted for a constant water depth  $d$ . Linear interpolation between figures is sufficiently accurate for determining intermediate wave heights and periods. For water depths greater than 15 meters (50 feet) and less than 90 meters (300 feet), use equations (3-39) to (3-41). For depths greater than 90 meters (300 feet), the revised deepwater forecasting equations should be used.

The minimum duration  $t$  has been added to the shallow-water forecasting curves to simplify determining the wind-stress factor  $U_A$ . Waves with periods less than a specified value are noted as deepwater waves on each figure. The duration equation used, therefore, is a transposed, simplified approximation of the deepwater duration equation.

\*\*\*\*\* EXAMPLE PROBLEM 5 \*\*\*\*\*

GIVEN: Fetch length  $F = 24.4 \text{ km}$  (80,000 ft)  
 Wind-stress factor  $U_A = 22 \text{ m/s}$  (50 mi/hr)  
 Constant depth  $d = 11 \text{ m}$  (35 ft)

FIND: Wave height  $H_s$   
 Wave period  $T$

SOLUTION:

From Figure 3-33a or equation (3-39) and (3-40)

$$H_s = 1.5 \text{ m} \quad (4.9 \text{ ft})$$

and

$$T = 4.4 \text{ s}$$

\*\*\*\*\*

2. Propagation Over Flooded, Vegetated Land.

When waves travel across a shallow flooded area, the initial heights and periods of the waves may increase; i.e., when the wind stress exceeds the frictional stress of the ground and vegetation underlying the shallow water. The initial wave heights may decay at other times when the frictional stress exceeds the wind stress.

Camfield (1977) presents an *approximate method* for estimating the growth or decay of wind waves passing over areas with high values of bottom friction. It is assumed that the high friction values can be accounted for by

adjusting the fetch length. Wave prediction curves for waves passing through shallow water with bottom friction  $f_f = 0.01$  are shown in Figures 3-21 and 3-22. For any given adjusted windspeed factor  $U_A$  and water depth  $d$  there is a maximum (depth-limited) significant wave height  $H_{sm}$  which is generated (long dashline in Fig. 3-21).

When the initial wave height  $H_i$  at the seaward or beginning edge of the fetch is less than  $H_{sm}$ , the wave increases in height. Where the bottom friction,  $f_f$  is greater than 0.01, the wave will not become as high as a wave traveling over a bottom where  $f_f = 0.01$ , if the segment of fetch distance  $\Delta x$  is the same in both cases. Therefore an adjusted fetch  $F_\alpha < \Delta x$  is used to describe the wave, using Figures 3-21 and 3-22 which were developed for the case of  $f_f = 0.01$ . For specific water depths, Figures 3-27 to 3-36 show the same results as Figures 3-21 and 3-22.

Where  $H_i > H_{sm}$ , the wave will decay. As a value of  $f_f > 0.01$  will cause a wave to decay a greater amount than if it were traveling over a bottom where  $f_f = 0.01$ , an adjusted fetch  $F_\alpha > \Delta x$  should be used in this case.

a. Fetch Adjustment. The fetch should be divided into segments to meet three conditions. First,

$$\Delta d < 0.25 d_i \quad (3-42)$$

where  $\Delta d$  is the change in depth over the distance across the segment in the direction of wave motion and  $d_i$  is the depth at the seaward or beginning edge of the segment; second

$$\Delta f_f < 0.25 f_{fi} \quad (3-43)$$

where  $\Delta f_f$  is the change in the bottom friction factor over the segment distance, and  $f_{fi}$  the bottom friction factor at the beginning edge of the segment; and third, after computation of the wave height at the end of the fetch,

$$\Delta H < 0.5 H_i \quad (3-44)$$

where  $\Delta H$  is the change in the wave height over the segment distance and  $H_i$  the wave height at the beginning edge of the segment. Each segment of the fetch can then be considered separately using the method indicated.

The bottom friction  $f_f$  can be obtained from Figure 3-37 for a known type of vegetation. The decay factor  $K_f$  may be obtained from Figure 3-38. Where  $H_i < H_{sm}$ , the wave will increase in height, and the adjusted fetch distance  $F_\alpha$  for a segment distance  $\Delta x$  is then determined using an adjustment factor  $\alpha$  which is defined as

$$\alpha = \frac{1 - K_{f.01}}{1 - K_{f\alpha}} \quad (3-45)$$

where  $K_{f.01}$  is the decay factor for a bottom friction factor  $f_f = 0.01$

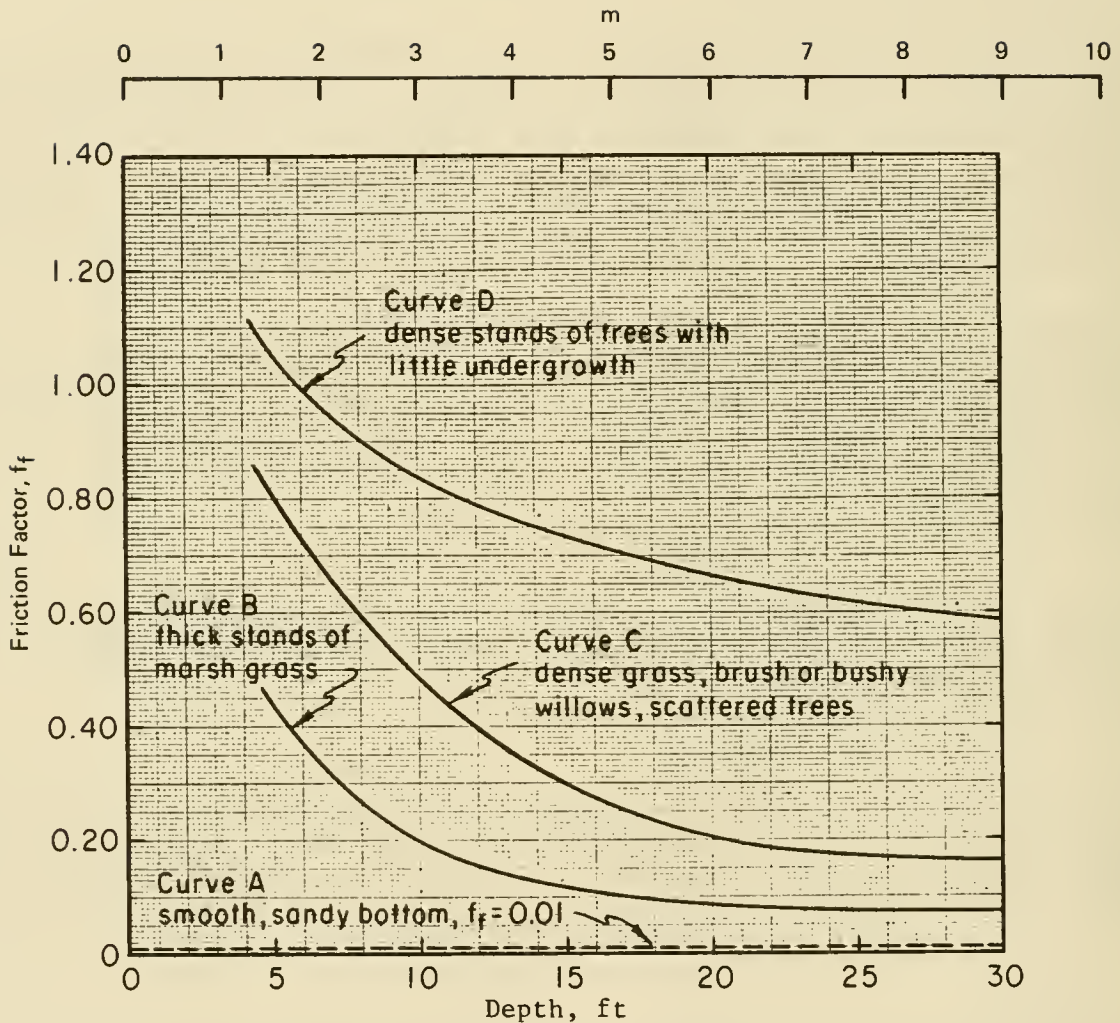


Figure 3-37. Bottom friction factors.

and  $K_{fa}$  is the decay factor for the actual bottom friction factor. The adjusted fetch length  $F_a$  is then given as

$$F_a = \alpha \Delta x \quad (3-46)$$

Where  $H_t > H_{sm}$ , the wave will decay and an adjustment factor  $\alpha_r$  is defined as

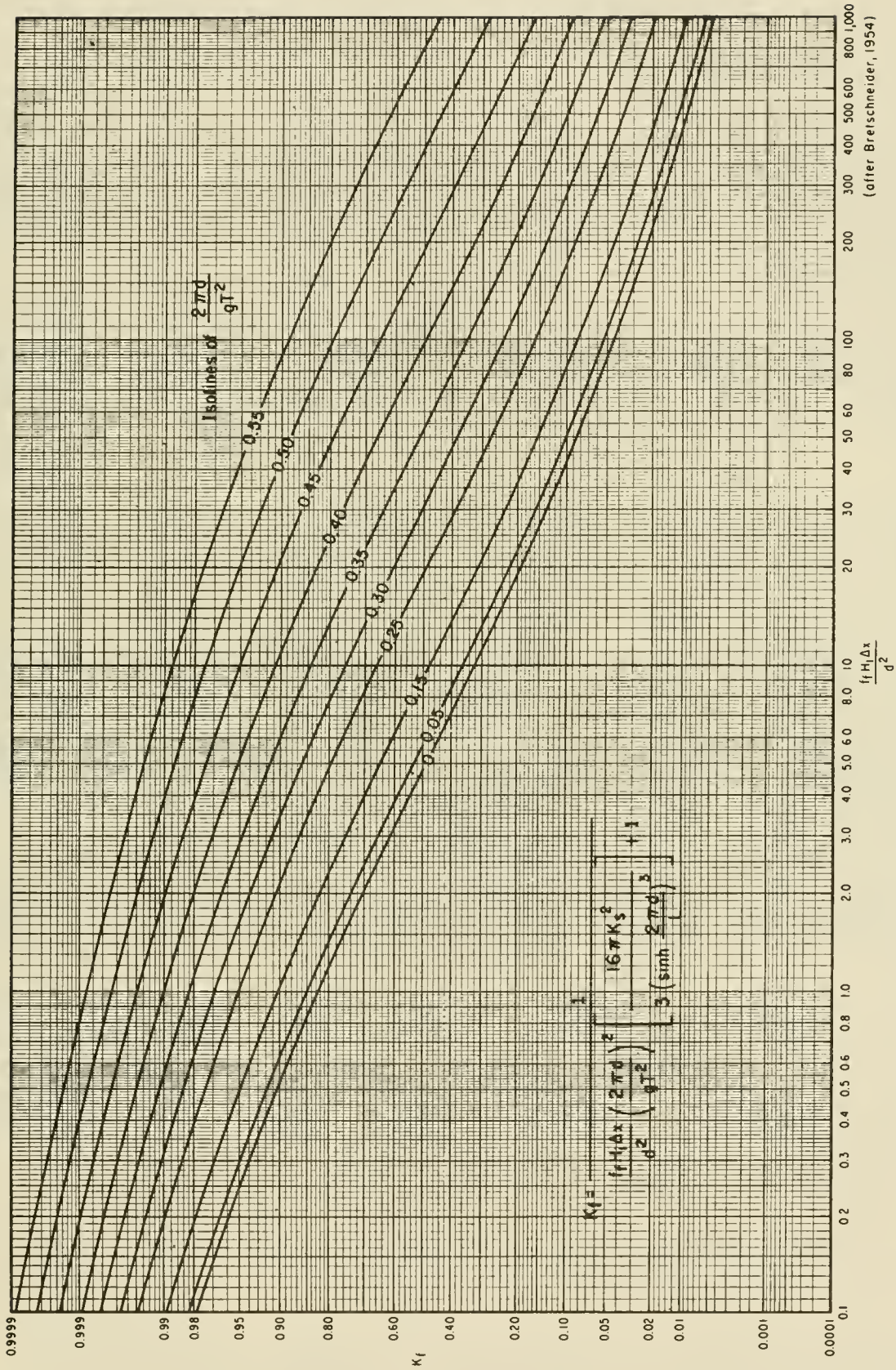


Figure 3-38. Relationship for friction loss over a bottom of constant depth.

$$\alpha_r = \frac{1 - K_f a}{1 - K_f .01} \quad (3-47)$$

and, for a decaying wave,

$$F_a = \alpha_r \Delta x \quad (3-48)$$

b. Wave Growth. For any given water depth, windspeed, and fetch length, a maximum significant wave height  $H_{sm}$  which is generated can be defined from Figure 3-21. If the initial wave height  $H_i$  at the seaward or beginning edge of the fetch segment is less than  $H_{sm}$ , it is assumed that the wave will increase in height.

To find the wave growth, first determine an equivalent fetch length  $F_e$  for the initial wave (obtained directly from Figure 3-21 using the given wave height, windspeed, and water depth). Secondly, the adjusted fetch  $F_a$  as discussed in Chapter 3, Section IV,2,a is determined using equations (3-45) and (3-46) and Figure 3-38. The total fetch is then given as

$$F = F_e + F_a \quad (3-49)$$

Reentering Figures 3-21 and 3-22 with the fetch length  $F$  and the adjusted windspeed factor  $U_A$  and water depth  $d$  the wave height and period at the end of the fetch segment,  $H_f$  and  $T$ , are determined.

c. Wave Decay. If the initial significant wave height  $H_i$  at the seaward or beginning edge of a segment of fetch exceeds the maximum significant wave height  $H_{sm}$  for the given water depth of the segment of fetch and the given windspeed, it may be assumed that the effects of the bottom friction will exceed the effects of the wind stress. Therefore, the wave will decay, will lose height, and over a long distance will approach a wave height equal to the maximum significant wave height.

The following steps are used to predict the decay of a wave:

(a) At the seaward end of fetch segment determine the maximum significant wave height  $H_{sm}$  that would be generated for a given windspeed and water depth, assuming an unlimited fetch and using Figure 3-21.

(b) Determine the maximum stable wave height  $H_m$  at the seaward edge of the fetch segment, where

$$H_m = 0.78 d \quad (3-50)$$

(c) Determine the fractional reduction  $R_i$  at the seaward edge of the segment of fetch under consideration. This is given by

$$R_i = \frac{H_m - H_i}{H_m - H_{sm}} \quad (3-51)$$

(d) Determine an equivalent initial wave height  $H_{ie}$ , assuming that fractional wave growth is proportional to fractional wave decay, by

$$H_{ie} = R_i H_{sm} \quad (3-52)$$

(e) Determine the equivalent fetch length  $F_e$  for the wave height  $H_{ie}$ .

(f) Determine an adjusted fetch length  $F_a$  for the segment length,  $\Delta x$  as discussed in Chapter 3, Section VI,2,a using equations (3-47) and (3-48).

(g) Determine the total fetch  $F$  from equation (3-49).

(h) Determine an equivalent wave height  $H_e$  for the total fetch and the given windspeed and water depth.

(i) Calculate the fractional growth by

$$G_i = \frac{H_e}{H_{sm}} \quad (3-53)$$

(j) Calculate the decayed wave height at the end of the fetch by

$$H_D = H_m - G_i (H_m - H_{sm}) \quad (3-54)$$

As a conservative estimate, it is assumed that the wave period remains constant as the wave decays.

\*\*\*\*\* EXAMPLE PROBLEM 6 \*\*\*\*\*

GIVEN: A flooded coastal area is covered with thick stands of tall grass.

The water depth  $d_i$  at the seaward edge of the area is 7 meters (23 feet), and at the landward edge of the area the depth is 4 meters (13 feet). The distance across the area in the direction of wave travel is 3050 meters (10,000 feet). The wave height  $H_i$  at the seaward edge of the area is limited to 0.9 meters (3 feet) by the flooded beach dune system seaward of the area being considered, and the wave period is 2.6 seconds. The adjusted windspeed factor is 31.3 meters per second (70 miles per hour or 103 feet per second).

FIND: The height and period of the significant wave at the landward edge of the area.

SOLUTION: From the long dashline in Figure 3-21, for an adjusted windspeed factor of 31.3 meters per second and a water depth of 7 meters,

$$\frac{gd}{U_A^2} = \frac{9.8 \times 7}{(31.3)^2} = 0.0700$$

giving (at the intersection of the above line with the long dashline)

$$\frac{gH}{U_A^2} = 0.02$$

so that the maximum significant wave height is

$$H_{sm} = \frac{0.02 U^2}{g} = \frac{0.02 (31.3)^2}{9.8} = 2.0 \text{ m (6.56 ft)}$$

Therefore, the initial wave will increase in height; the first step is to adjust the fetch (segment) for conformance with equations (3-42), (3-43), and (3-44).

$$0.25 d_i = 0.25 (7) = 1.75 \text{ m (5.74 ft)}$$

$$\Delta d = 7 - 4 = 3 \text{ m (9.84 ft)}$$

$$(\Delta d > 0.25 d_i)$$

Since this does not meet the condition of equation (3-42), the area should be divided into fetch segments. Assuming a uniform variation in depth, take the first segment as a distance  $\Delta x = 1525$  meters with a depth variation from 7 to 5.5 meters. Then

$$\Delta d = 7 - 5.5 = 1.5 \text{ m (4.92 ft)}$$

Thus,

$$\Delta d < 0.25 d_i \quad (3-42)$$

From Figure 3-37, curve B

$$f_f = 0.080 \text{ (depth = 7 meters)}$$

and

$$f_f = 0.095 \text{ (depth = 5.5 meters)}$$

therefore,

$$\Delta f_f = 0.095 - 0.080 = 0.015$$

$$0.25 f_{fi} = 0.25 (0.080) = 0.020$$

and

$$\Delta f_f < 0.25 f_{fi} \quad (3-43)$$

Equations (3-42) and (3-43) are satisfied, so the 1525-meter fetch segment is used. For a uniformly varying depth, the average depth can be taken as the average of the depths at the beginning and the end of the segment:

$$d = \frac{7 + 5.5}{2} = 6.25 \text{ m (20.5 ft)}$$

For a uniform type of vegetation, the friction factor will vary as a function of water depth as shown in Figure 3-37. As an approximation, the average friction factor can be taken as the average of the friction factors at the beginning and the end of the segment;

$$f_f = \frac{0.080 + 0.095}{2} = 0.088$$

Using Figure 3-21 for  $d = 6.25$  meters,  $H = 0.9$  meter, and  $U_A = 31.3$  meters per second with

$$\frac{gd}{U_A^2} = \frac{9.8 \times 6.25}{(31.3)^2} = 0.0626$$

$$\frac{gH_i}{U_A^2} = \frac{9.8 \times 0.9}{(31.3)^2} = 0.0090$$

it is found that

$$\frac{gF_e}{U_A^2} = 38$$

and

$$F_e = 38 \frac{U_A^2}{g} = 38 \frac{(31.3)^2}{9.8} = 3800 \text{ m}$$

For  $f_f = 0.01$ ,

$$\frac{f_f H_i \Delta x}{d^2} = \frac{0.01 \times 0.9 \times 1525}{(6.25)^2} = 0.351$$

and for  $f_f = 0.088$ ,

$$\frac{f_f H_i \Delta x}{d^2} = \frac{0.088 \times 0.9 \times 1525}{(6.25)^2} = 3.09$$

For the period  $T = 2.6$  seconds and  $d = 6.25$  meters

$$\frac{2\pi d}{gT^2} = \frac{2\pi (6.25)}{9.8 (2.6)^2} = 0.593$$

Using Figure 3-38, for  $2\pi d/(gT^2) = 0.593$

$$K_{f.01} = 0.9998 \text{ for } f_f = 0.01 \text{ and } \frac{f_f H_i \Delta x}{d^2} = 0.351$$

$$K_{f\alpha} = 0.998 \text{ for } f_f = 0.088 \text{ and } \frac{f_f H_i \Delta x}{d^2} = 3.09$$

From equation (3-45)

$$\alpha = \frac{1 - K_{f.10}}{1 - K_{f\alpha}} = \frac{1 - 0.9998}{1 - 0.998} = \frac{0.0002}{0.002} = 0.10$$

From equation (3-46)

$$F_\alpha = \alpha \Delta x = 0.10 (1525) = 152.5 \text{ m (500 ft)}$$

From equation (3-49)

$$F = F_e + F_a = 3800 + 153 = 3953 \text{ m (13,000 ft)}$$

For  $d = 6.25$  meters,  $U_A = 31.31$  meters per second, and  $F = 3953$  meters (from Figs. 3-21 and 3-22)

$$H_f = 0.92 \text{ m and } T = 2.84 \text{ sec}$$

$$\Delta H = 0.92 - 0.9 = 0.02 \text{ meter (0.7 ft)}$$

thus

$$\Delta H < 0.5 H_i \tag{3-44}$$

This satisfies the third basic requirement (eq. 3-44), and the solution may proceed to the next segment which is the remaining 1525 meters of the area, with the water depth varying from 5.5 to 4 meters.

$$0.25 d_i = 0.25 (5.5) = 1.38 \text{ m}$$

Since  $\Delta d = 5.5 - 4 = 1.5$  meters  $> 0.25 d_i$ , which does not satisfy equation (3-42) a shorter segment is required. For a 1000-meter segment, assuming a uniform depth variation, the depth will vary from 5.5 to 4.5 meters. This satisfies equation (3-42), and the solution can then proceed as above for a 1000-meter segment and then for a 525-meter segment.

\*\*\*\*\*  
\*\*\*\*\* EXAMPLE PROBLEM 7 \*\*\*\*\*

GIVEN: A coastal area is flooded by a storm surge so that the water depth over the area is 3 meters. The actual distance across the area in the direction of wave travel is 1000 meters. The area is covered with thick stands of tall grass and a small to moderate amount of brush or low, bushy trees in an even distribution. The windstress factor is 40 meters per second, and the initial wave height at the seaward edge of the area is 2 meters; the wave period is 4.7 seconds.

FIND: The wave height and period at the landward end of the area.

SOLUTION: Because of the constant depth and uniform friction effects, the first two fetch segment conditions are met. The third condition is tested after the wave height is determined. From the long dashline in Figure 3-21, for the windspeed of 40 meters per second and the water depth of 3 meters

$$\frac{gd}{U_A^2} = \frac{9.8 \times 3}{(40)^2} = 0.0184$$

giving (at the intersection of the above line with the long dashline)

$$\frac{gH}{U_A^2} = 0.0075$$

so that the maximum significant wave height is

$$H_{sm} = \frac{0.0075 U_A^2}{g} = \frac{0.0075 (40)^2}{9.8} = 1.22 \text{ m (4.02 ft)}$$

Since  $H_i$  is greater than  $H_{sm}$  (2 meters > 1.22 meters) then wave decay will occur. Therefore, the fractional reduction  $R_i$  must be determined using equation (3-51).

From equation (3-50),

$$H_m = 0.78d = 0.78 (3) = 2.34 \text{ m (7.68 ft)}$$

$$R_i = \frac{H_m - H_i}{H_m - H_{sm}} = \frac{2.34 - 2}{2.34 - 1.22} = 0.304$$

From equation (3-52), the equivalent initial wave height

$$H_{ie} = R_i H_{sm} = 0.304 \times 1.22 = 0.371 \text{ m (1.22 ft)}$$

from Figure 3-21, for

$$\frac{gH}{U_A^2} = \frac{9.8 (0.371)}{(40)^2} = 0.00227$$

and

$$\frac{gd}{U^2} = 0.0184$$

it is found that

$$\frac{gF_e}{U_A^2} = 2.25$$

from which  $F_e$  is found to be

$$F_e = 367 \text{ m (1205 ft)}$$

Since the vegetation does not match any of the curves in Figure 3-37, it is assumed that a moderate amount of brush will give a friction effect about halfway between curves B and C. From curve B, for  $d = 3$  meters,  $f_f$  is 0.20 and from curve C, for  $d = 3$  meters,  $f_f$  is 0.485. The bottom friction is then taken, in this case, as the average of the two values

$$f_f = \frac{0.20 + 0.485}{2} = 0.343$$

For  $f_f = 0.01$ ,

$$\frac{f_f H_i \Delta x}{d^2} = \frac{0.01 \times 2 \times 1000}{(3)^2} = 2.22$$

and for  $f_f = 0.343$ ,

$$\frac{f_f H_i \Delta x}{d^2} = \frac{0.343 \times 2 \times 1000}{(3)^2} = 76.22$$

For  $T = 4.7$  seconds and  $d = 3$  meters ,

$$\frac{2\pi d}{gT^2} = \frac{2\pi (3)}{9.8 (4.7)^2} = 0.087$$

Using Figure 3-38, for  $2\pi d/(gT^2) = 0.087$  ,

$$K_{f.01} = 0.76 \text{ for } f_f = 0.01 \text{ and } f_f H_i \Delta x/d^2 = 2.22$$

$$K_{fa} = 0.08 \text{ for } f_f = 0.343 \text{ and } f_f H_i \Delta x/d^2 = 76.22$$

From equation (3-47),

$$\alpha_r = \frac{1 - K_{fa}}{1 - K_{f.01}} = \frac{1 - 0.08}{1 - 0.76} = \frac{0.92}{0.24} = 3.83$$

From equation (3-48)

$$F_a = \alpha_r \Delta x = 3.83 (1000) = 3,830 \text{ m (12,566 ft)}$$

(i.e., the wave decay over 1000 meters of tall grass with some brush is equal to the wave decay over 3,830 meters of a sand bottom for indicated water depth and windspeed).

The total fetch, using equation (3-49) is

$$F = F_e + F_a = 367 + 3,830 = 4,197 \text{ m (13,770 ft)}$$

Using Figure 3-21 for a windspeed of 40 meters per second and a fetch of 2907 meters

$$\frac{gd}{U_A^2} = 0.0184 \text{ (as previously determined)}$$

$$\frac{gF}{U_A^2} = \frac{9.8 \times 4,197}{(40)^2} = 25.71$$

it is found that

$$\frac{gH}{U_A^2} = 0.0059$$

Solving for the equivalent wave height,

$$H_e = \frac{0.0059 U_A^2}{g} = \frac{0.0059 (40)^2}{9.8} = 0.963 \text{ m (3.16 ft)}$$

From equation (3-53), the fractional growth is

$$G_i = \frac{H_e}{H_{sm}} = \frac{0.963}{1.22} = 0.789$$

The decayed wave height is then given by equation (3-54) as

$$H_D = H_m - G_i (H_m - H_{sm}) = 2.34 - 0.789 (2.34 - 1.22) = 1.46 \text{ m (4.78 ft)}$$

The third condition for fetch segment is satisfactory, and

$$\Delta H < 0.5 H_z = 2 - 1.46 < 0.5 \quad (2)$$

Thus, at the end of the fetch segment, the wave height and period are approximated by

$$H_D = 1.46 \text{ meters (4.78 ft)}$$

$$T = 4.7 \text{ seconds}$$

\*\*\*\*\*

## VII. HURRICANE WAVES

When predicting wave generation by hurricanes, the determination of fetch and duration from a wind field is more difficult than it is for more normal weather conditions discussed earlier. The large changes in wind speed and direction with both location and time cause the difficulty. Estimation of the free air wind field must be approached through mathematical models because of the scarcity of observations in severe storms. However, the vertical temperature profile and atmospheric turbulence characteristics associated with hurricanes differ less from one storm to another than for other types of storms; thus the relation between the free air winds and the surface winds is less variable for hurricanes than for other storms.

### 1. Description Of Hurricane Waves.

In hurricanes, fetch areas in which wind speed and direction remain reasonably constant are always small; a fully arisen sea state never develops. In the high wind zones of a storm, however, long-period waves which can outrun the storm may be developed within fetches of 15 to 30 kilometers (10 to 20 miles) and over durations of a few hours. The wave field in front, or to either side, of the storm center will consist of a locally generated sea and a swell from other regions of the storm. Samples of wave spectra, obtained during Hurricane Agnes (1972) are shown in Figure 3-39. Most of the spectra display evidence of two or three distinct wave trains; thus, the physical interpretation of a *significant wave period* is not clear.

Other hurricane wave spectra computed with an analog spectrum analyzer from wave records obtained during Hurricane Donna (1959) have been published by Bretschneider (1963). Most of these spectra also contained two distinct peaks. However, near the center of a hurricane, very large single-peak spectra can occur as well (Fig. 40). Significant wave heights may exceed 15 meters (50 feet) in deep water, as in Hurricane Camille.

An indication of the distribution of waves throughout a hurricane can be obtained by plotting composite charts of shipboard wave observations. The position of a report is determined by its distance from the storm center and its direction from the storm track. Changes in storm intensity and shape are often small enough to permit all observations obtained during a period of 24 to 36 hours to be plotted on a single chart. Several plots of this type from Pore (1957) are given in Figure 3-41. Additional data of the same type have been presented by Arakawa and Suda (1953), Pore (1957), and Harris (1962).

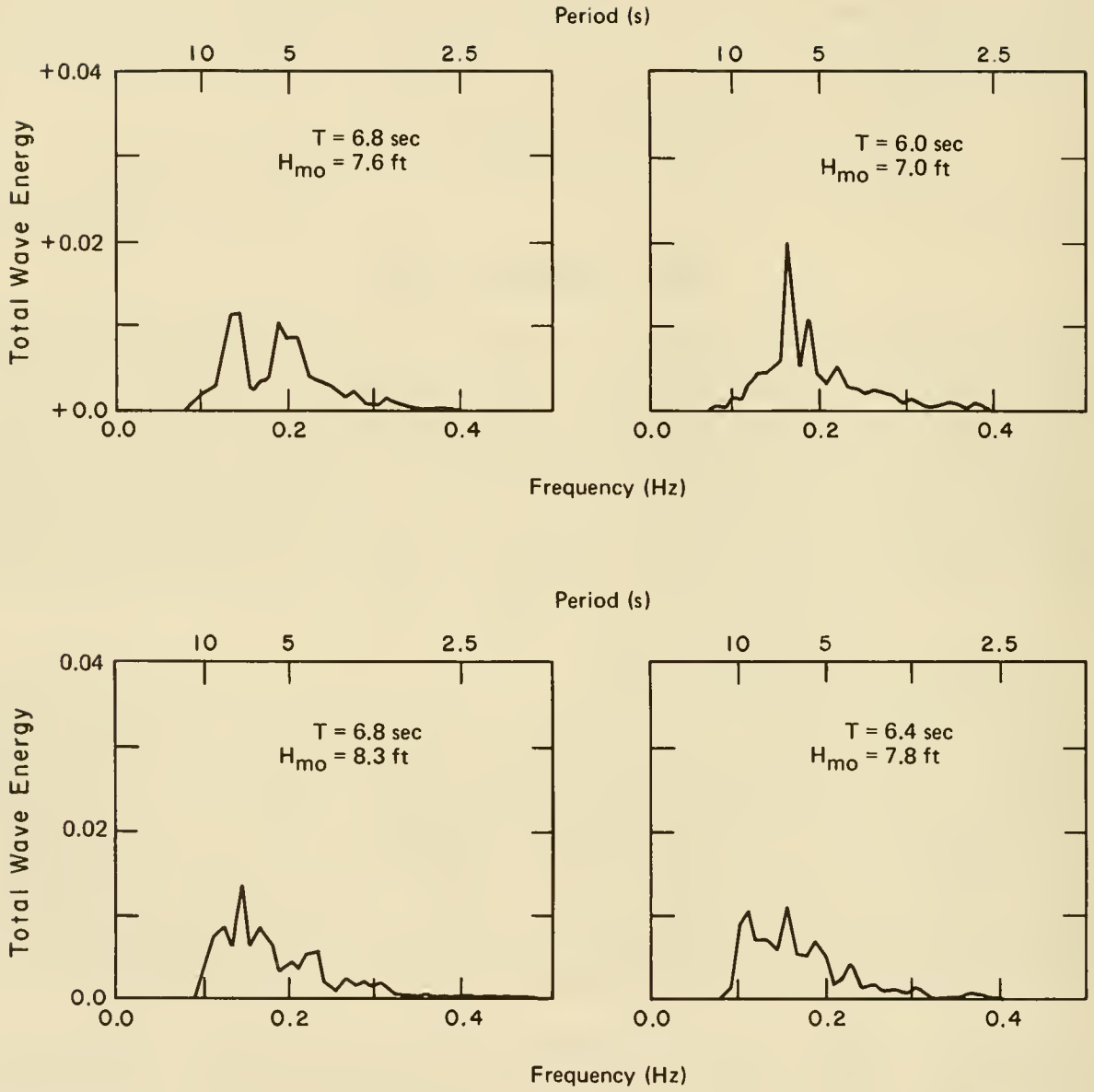


Figure 3-39. Typical hurricane wave spectra from the Atlantic coast of the United States. (The ordinate scale is the fraction of total wave energy in each frequency band of 0.0011 hertz (one hertz is 1 cycle per second.) A linear frequency scale is shown at bottom of each graph and a nonlinear period scale at top of each graph.)

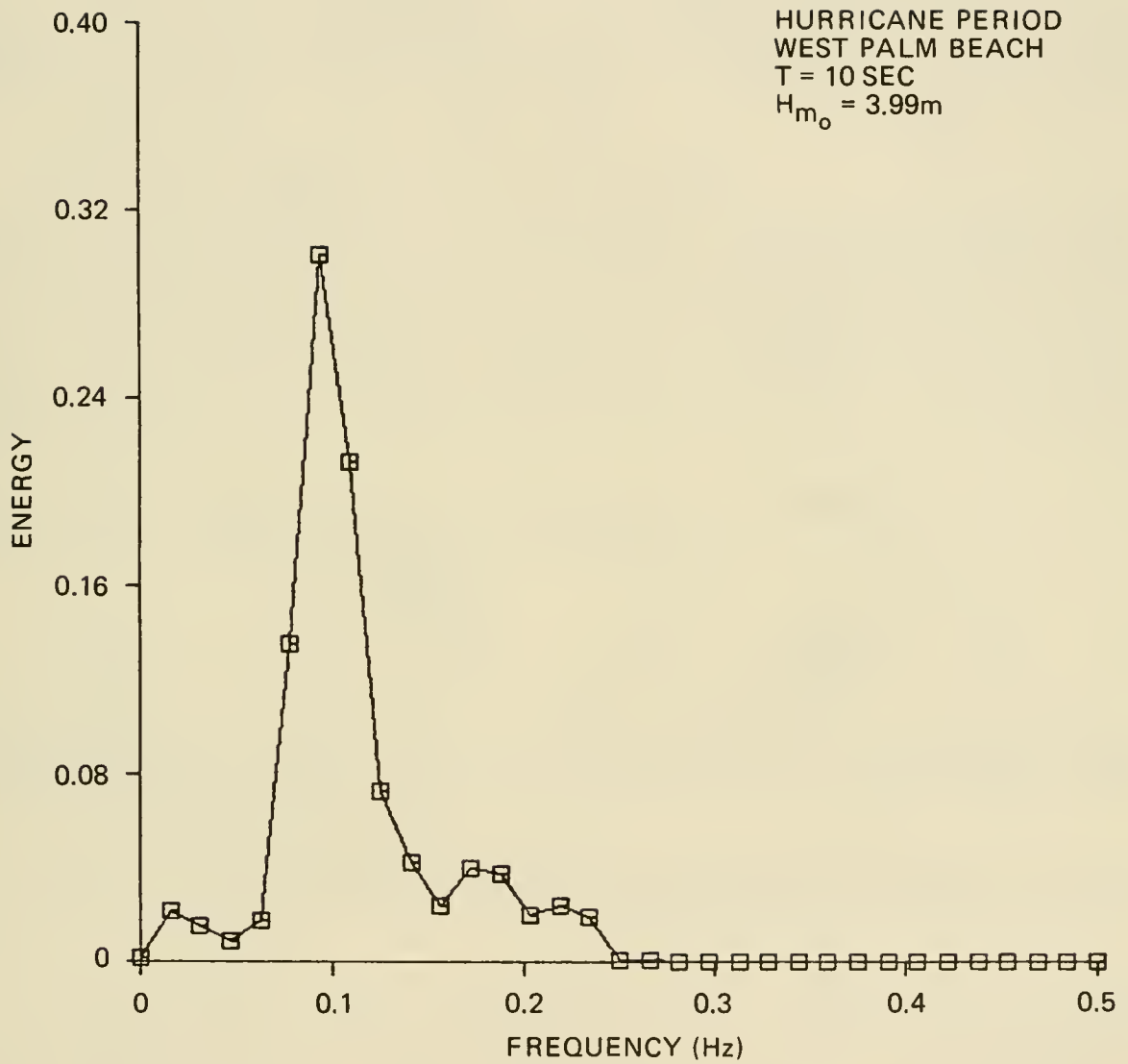
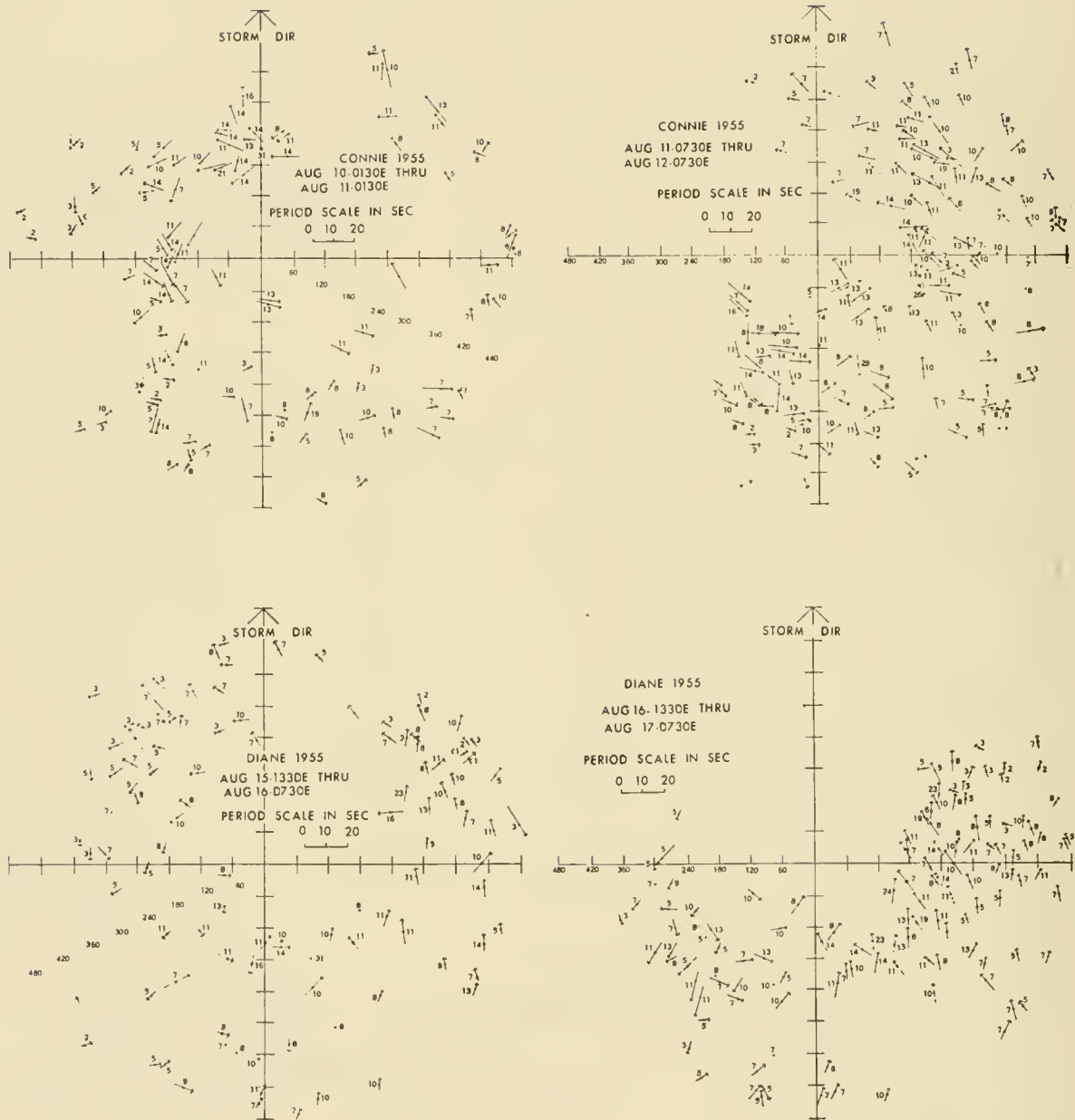


Figure 3-40. Single-peaked spectrum near the center of Hurricane David, West Palm Beach, Florida.



(after Pore, 1957)

Figure 3-41. Composite wave charts. (The wave height in feet is plotted beside the arrow indicating direction from which the waves came. The length of the arrow is proportional to the wave period. Dashed arrow indicates unknown period. Distances are marked along the radii at intervals of 60 nautical miles.)

Goodknight and Russell (1963) give a tabulation of the significant height and period for waves recorded on an oil drilling platform in approximately 10 meters (33 feet) of water, 2.5 kilometers (1.5 miles) from shore near Burrwood, Louisiana during Hurricanes Audrey (1957) and Ella (1950) and Tropical Storms Bertha (1957) and Esther (1957). These wave records were used to evaluate the applicability of the Rayleigh distribution function (Chapter 3, Section II,2 Wave Height Variability) to hurricane statistics for wave heights and periods. They concluded that the Rayleigh distribution function is adequate for deriving the ratios between  $H_s$ ,  $H_{10}$ ,  $H$ , etc., with sufficient accuracy for engineering design, but that its acceptance as a basic law for wave height distributions is questionable.

## 2. Model Wind and Pressure Fields for Hurricanes.

Many mathematical models have been proposed for use in studying hurricanes. Each is designed to simulate some aspect of the storm as accurately as possible without making excessively large errors in describing other aspects of the storm. Each model leads to a slightly different specification of the surface wind field. Available wind data are sufficient to show that some models duplicate certain aspects of the wind field better than certain other models; but there are not enough data for a determination of a *best model* for all purposes.

One of the simplest and earliest models for the hurricane wind field is the Rankin vortex. For this model, it is assumed that

$$\begin{aligned}
 U &= Kr \quad \text{for } r \leq R \\
 U &= \frac{KR^2}{r} \quad \text{for } r \geq R
 \end{aligned}
 \tag{3-55}$$

where  $K$  is a constant,  $R$  the radial distance from the storm center to the region of maximum windspeed, and  $r$  the radial distance from the storm center to any specified point in the storm system.

This model can be improved by adding a translational component to account for storm movement and a term producing cross-isobar flow toward the storm center.

Extensions of this model are still being used in some engineering studies (Collins and Viehman, 1971). This model gives an artificial discontinuity in the horizontal gradient of the windspeed at the radius of maximum winds and does not reproduce the well-known area of calm winds near the storm center.

A more widely used model was given by Myers (1954). A concise mathematical description of this model is given by Harris (1958) as follows:

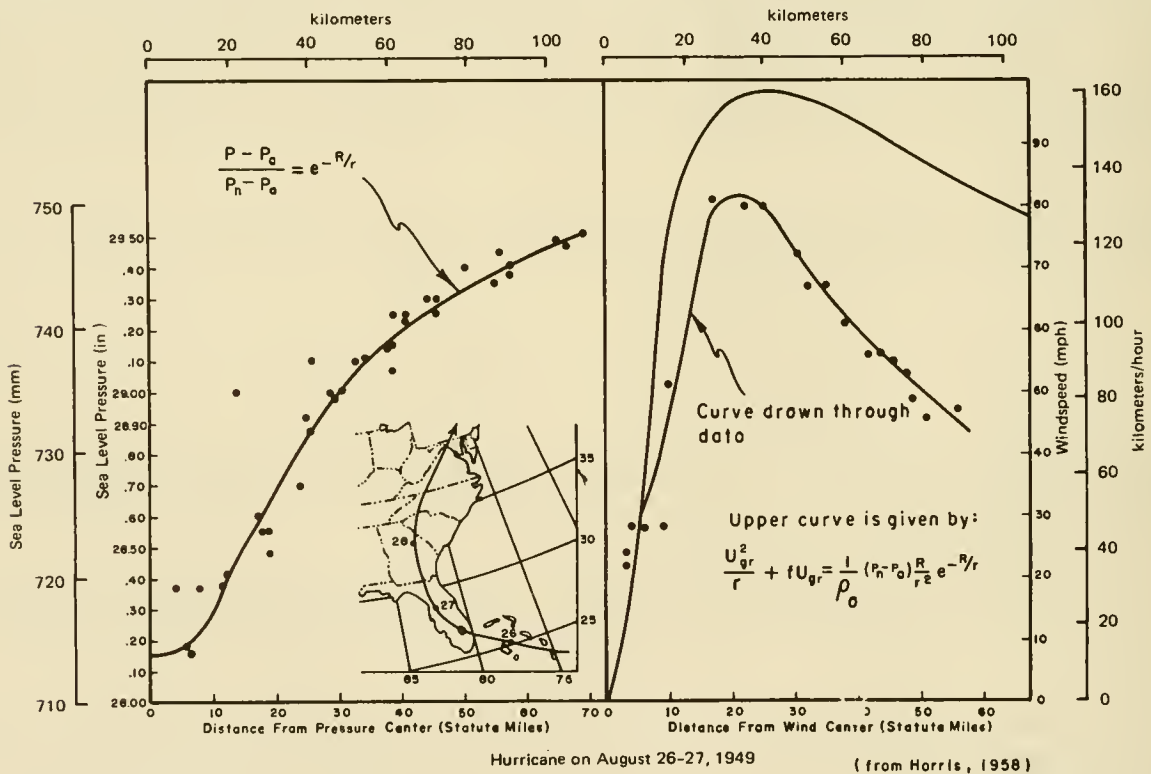
$$\frac{P - P_0}{P_n - P_0} = e^{-\frac{R}{r}}
 \tag{3-56}$$

$$\frac{U^2}{r} + fU = \frac{1}{\rho_a} (p_n - p_o) \frac{R}{2r} e^{-\frac{R}{r}} \quad (3-57)$$

where

- $p$  = the pressure at a point located at a distance  $r$  from the storm center
- $p_o$  = the central pressure
- $p_n$  = the pressure at the outskirts of the storm
- $\rho_a$  = the density of air
- $U_{gr}$  = the gradient windspeed
- $f$  = the Coriolis parameter

Agreement between this model and the characteristics of a well-observed hurricane is shown in Figure 3-42. The insert map gives the storm track; dots



a. Pressure profile.

b. Wind Profile.

Figure 3-42. Pressure and wind distribution in model hurricane. (Plotted dots represent observations.)

indicate the observed pressure at several stations in the vicinity of Lake Okeechobee, Florida; the solid line (Fig. 3-42a) gives the theoretical pressure profile fitted to three points within 80 kilometers (50 miles) of the storm center. The corresponding theoretical wind profile is given by the upper curve of Figure 3-42b. Observed winds at one station are indicated by dots below this curve. A solid line has been drawn through these dots by eye

to obtain a smooth profile. The observed windspeed varies in a systematic way from about 65 percent of the computed windspeed at the outer edge to almost 90 percent of the predicted value near the zone of maximum windspeed. Reasonably good agreement between the theoretical and observed windspeeds has been obtained in only a few storms. This lack of agreement between the theoretical and observed winds is due in part to the elementary nature of the model, but perhaps equally to the lack of accurate wind records near the center of hurricanes.

Parameters obtained from fitting this model to a large number of storms were given by Myers (1954). Parameters for these other storms (and for additional storms) are given by Harris (1958). Equation (3-57) will require some form of correction for a moving storm.

This model is purely empirical, but it has been used extensively and provides reasonable agreement with observations in many storms. Other equally valid models could be derived; however, alternative models should not be adopted without extensive testing.

In the northern hemisphere, windspeeds to the right of the storm track are always higher than those on the left, and a correction is needed when any stationary storm model is being used for a moving storm. The effect of storm motion on the wind field decreases with distance from the zone of highest windspeeds. Thus the vectorial addition of storm motion to the wind field of the stationary storm is not satisfactory. Jelesnianski (1966) suggests the following simple form for this correction,

$$U_{SM}(r) = \frac{Rr}{R^2 + r^2} V_F \quad (3-58)$$

where  $V_F$  is the velocity of the storm center and  $U_{SM}(r)$  is the convective term which is to be added vectorially to the wind velocity at each value of  $r$ . Wilson (1955, 1961) and Bretschneider (1959, 1972) have suggested other correction terms.

### 3. Prediction Technique.

The best method for calculating wave conditions in a hurricane is to use a numerical model such as discussed in Chapter 3, Section VIII,6; however, for a slowly moving hurricane, the following formulas can be used to obtain an estimate of the deepwater significant wave height and period at the point of maximum wind:

$$H_o = 5.03 e^{\frac{R\Delta p}{4700}} \left[ 1 + \frac{0.29 \alpha V_F}{\sqrt{U_R}} \right] \text{ Metric units} \quad (3-59a)$$

$$H_o = 16.5 e^{\frac{R\Delta p}{100}} \left[ 1 + \frac{0.208 \alpha V_F}{\sqrt{U_R}} \right] \text{ English units} \quad (3-59b)$$

and

$$T_s = 8.6 e^{\frac{R\Delta p}{9400}} \left[ 1 + \frac{0.145 \alpha V_F}{\sqrt{U_R}} \right] \text{ metric units} \quad (3-60a)$$

$$T_s = 8.6 e^{\frac{R\Delta p}{200}} \left[ 1 + \frac{0.104 \alpha V_F}{\sqrt{U_R}} \right] \text{ English units} \quad (3-60b)$$

where

$H_O$  = deepwater significant wave height in meters (feet)

$T_s$  = the corresponding significant wave period in seconds

$R$  = radius of maximum wind in kilometers (nautical miles)

$\Delta p$  =  $p_n - p_o$ , where  $p_n$  is the normal pressure of 760 millimeters (29.92 inches) of mercury, and  $p_o$  is the central pressure of the hurricane

$V_F$  = The forward speed of the hurricane in meters per second (knots)

$U_R$  = The maximum sustained windspeed in meters per second (knots), calculated for 10 meters (33 feet) above the mean sea surface at radius  $R$  where

$$U_R = 0.865 U_{max} \text{ (for stationary hurricane)} \quad (3-61)$$

$$U_R = 0.865 U_{max} + 0.5 V_F \text{ (for moving hurricane)} \quad (3-62)$$

$U_{max}$  = Maximum gradient windspeed 10 meters (33 feet) above the water surface; i.e.,

$$U_{max} = 0.447 [14.5 (p_n - p_o)^{1/2} - R(0.31f)] \quad \text{metric units} \quad (3-63a)$$

$$U_{max} = 0.868 [73 (p_n - p_o)^{1/2} - R(0.575f)] \quad \text{English units} \quad (3-63b)$$

$f$  = Coriolis parameter =  $2\omega \sin\phi$ , where  $\omega$  = angular velocity of Earth =  $2\pi/24$  radians per hour

Latitude ( $\phi$ )	25°	30°	35°	40°
$f$ (rad/hr)	0.221	0.262	0.300	0.337

$\alpha$  = a coefficient depending on the forward speed of the hurricane and the increase in effective fetch length because the hurricane is moving. It is suggested that for a slowly moving hurricane  $\alpha = 1.0$ .

Once  $H_0$  is determined for the point of maximum wind from equation (3-59) it is possible to obtain the approximate deepwater significant wave height  $H_0$  for other areas of the hurricane by use of Figure 3-43.

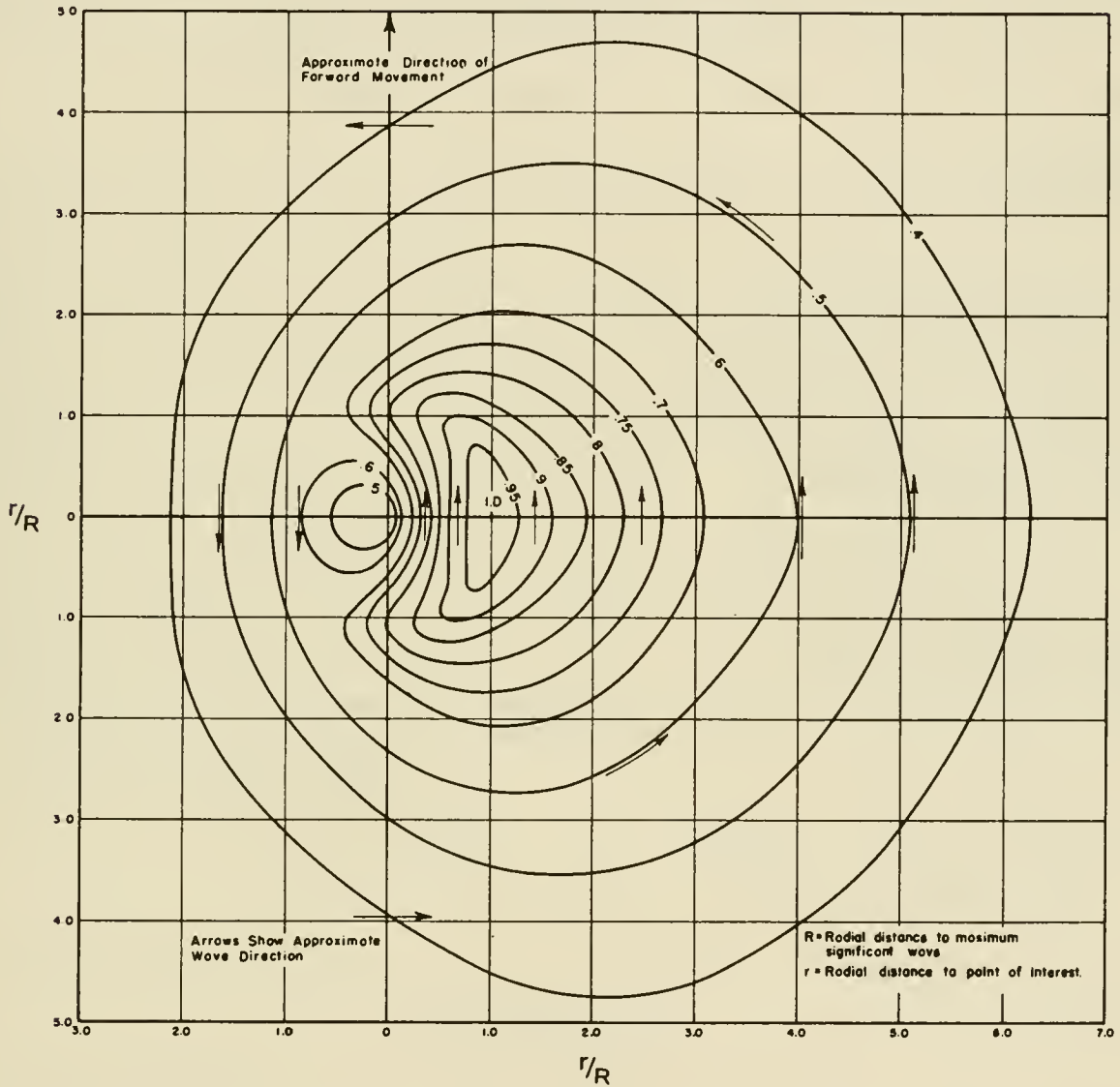


Figure 3-43. Isolines of relative significant wave height for slow-moving hurricane.

The corresponding approximate wave period may be obtained from

$$T = 12.1 \sqrt{\frac{H_0}{g}} \quad (3-64)$$

where  $H_o$  is the deepwater significant wave height in meters or feet (derived from empirical data showing that the wave steepness  $H/gT^2$  will be about 0.0068).

\*\*\*\*\* EXAMPLE PROBLEM 8 \*\*\*\*\*

GIVEN: A hurricane at latitude  $35^\circ$  N. with  $R = 67$  kilometers,  $\Delta p = 760 - 701 = 59$  millimeters of mercury, and forward speed  $V_F = 14$  meters per second. Assume for simplicity that  $\alpha = 1.0$ .

FIND: The deepwater significant wave height and period.

SOLUTION:

Using equation (3-63)

$$U_{max} = 0.447 [14.5 (p_n - p_o)^{1/2} - R (0.31f)]$$

$$U_{max} = 0.447 [14.5 (59)^{1/2} - 67 (0.31 \times 0.300)]$$

$$U_{max} = 0.447 (111.38 - 6.23) = 47.0 \text{ m/s}$$

Using equation (3-62)

$$U_R = 0.865 U_{max} + 0.5 V_F$$

$$U_R = 0.865 (47.0) + 0.5 (14) = 47.66 \text{ m/s}$$

Using equation (3-59a)

$$H_o = 5.03 e^{\frac{R\Delta p}{4700}} \left[ 1 + \frac{0.29 \alpha V_F}{\sqrt{U_R}} \right]$$

where the exponent is given by

$$\frac{R\Delta p}{4700} = \frac{67(59)}{4700} = 0.841$$

then

$$H_o = 5.03 (e^{0.841}) \left[ 1 + \frac{0.29 \times 1 \times 14}{\sqrt{47.66}} \right]$$

$$H_o = 5.03 (2.32) (1.588) = 18.5 \text{ m}$$

Using equation (3-60a)

$$T_s = 8.6 e^{\frac{R\Delta p}{9400}} \left[ 1 + \frac{0.145 \alpha V_F}{\sqrt{U_R}} \right]$$

where the exponent is given by

$$\frac{R\Delta p}{9400} = \frac{67(59)}{9400} = 0.421$$

$$T_s = 8.6 e^{0.421} \left[ 1 + \frac{0.145 \times 1 \times 14}{\sqrt{47.66}} \right]$$

$$T_s = 8.6(1.52) (1.294) = 16.9 \text{ s}$$

Alternately, by equation (3-64) it is seen that

$$T_s = 12.1 \sqrt{\frac{18.5}{9.81}} = 16.6 \text{ s}$$

Computing the values of wave height and period to three significant figures is not intended to imply the degree of accuracy of the method; it is done to reduce the computational error.

Referring to Figure 3-43,  $H_0 = 18.5$  meters corresponds to the relative significant wave height of 1.0 at  $r/R = 1.0$ , the point of maximum winds located, for this example 67 kilometers (36 nautical miles) to the right of the hurricane center. At that point the wave period  $T$  is about 16 seconds. At  $r/R = 1.0$  to the left of the hurricane center, from Figure 3-43 the ratio of relative significant height is about 0.62, when  $H_0 = 0.62 (18.5) = 11.5$  meters. This wave is moving in a direction opposite to that of the 18.5-meter wave. The significant wave period for the 11.5-meter wave is  $T_s = 12.1 \sqrt{11.5/9.81} = 13.1$  seconds, say 13 seconds.

The most probable maximum wave is assumed to depend on the number of waves considered applicable to the significant wave  $H_0 = 18.5$  meters. This number  $N$  depends on the length of the section of the hurricane for which near steady state exists and the forward speed of the hurricane. It has been found that maximum wave conditions occur over a distance equal to the radius of maximum wind. The time it takes the radius of maximum wind to pass a particular point is

$$t = \frac{R}{V_F} = \frac{67000 \text{ m}}{14 \text{ m/s}} = 4780 \text{ s} = 1.33 \text{ h} \quad (3-65)$$

the number of waves will be

$$N = \frac{t}{T_s} = \frac{4780}{16.6} \approx 288 \quad (3-66)$$

The most probable maximum waves can be obtained by using

$$H_n = 0.707 H_0 \sqrt{\log_e \frac{N}{n}} \quad (3-67)$$

For this example, the most probable maximum wave is obtained by setting  $n = 1$  and using equation (3-67)

$$H_1 = 0.707 (18.5) \sqrt{\log_e \frac{288}{1}} = 31.1 \text{ m}, \text{ say } 31 \text{ m}$$

Assuming that the 31-meter wave occurred, then the most probable second highest wave is obtained by setting  $n = 2$ , the third from  $n = 3$ , etc., thusly:

$$H_2 = 0.707 (18.5) \sqrt{\log_e \frac{288}{2}} = 29.2 \text{ m , say } 29 \text{ m}$$

$$H_3 = 0.707 (18.5) \sqrt{\log_e \frac{288}{3}} = 27.9 \text{ m , say } 28 \text{ m}$$

\* \* \* \* \*

### VIII. WATER LEVEL FLUCTUATIONS

The focus now changes from wave prediction to water level fluctuations in oceans and other bodies of water which have periods substantially longer than those associated with surface waves. Several known physical processes combine to cause these longer term variations of the water level.

The expression *water level* is used to indicate the mean elevation of the water when averaged over a period of time long enough (about 1 minute) to eliminate high-frequency oscillations caused by surface gravity waves. In the discussion of gravity waves the water level was also referred to as the *still-water level* (SWL) to indicate the elevation of the water if no gravity waves were present. In the field, water levels are determined by measuring water surface elevations in a stilling well. Inflow and outflow of the well is restricted so that the rapid responses produced by gravity waves are filtered out, thus reflecting only the mean water elevation. Measurements without a stilling well can be made and the results numerically filtered to obtain the stillwater level.

Water level fluctuations classified by the characteristics and types of motion which take place are identified as:

- (a) Astronomical tides
- (b) Tsunamis
- (c) Seiches
- (d) Wave setup
- (e) Storm surges
- (f) Climatological variations
- (g) Secular variations

The first five fluctuation categories have periods that range from a few minutes to a few days; the last two have periods that range from semiannual to many years long. Although important in long-term changes in water elevations, climatological and secular variations are not discussed here.

Forces caused by the gravitational attraction between the Moon, the Sun, and the rotating Earth result in periodic level changes in large bodies of water. The vertical rise and fall resulting from these forces is called the *tide* or *astronomical tide*; the horizontal movements of water are called *tidal currents*. The responses of water level changes to the tidal forces are modified in coastal regions because of variations in depths and lateral boundaries; tides vary substantially from place to place. Astronomical tide-generating forces are well understood and can be predicted many years in advance. The response to these forces can be determined from an analysis of tide gage records. Tide predictions are routinely made for many locations for which analyzed tide observations are available. In the United States, tide predictions are made by the National Ocean Service (NOS), National Oceanic and Atmospheric Administration (NOAA).

*Tsunamis* are long-period waves generated by several mechanisms: submarine earthquakes, submarine landslides, and underwater volcanos. These waves may travel distances of more than 8000 kilometers (5000 miles) across an ocean, with speeds at times exceeding 800 kilometers per hour (500 miles per hour). In open oceans, the heights of these waves are generally unknown but small; heights in coastal regions have been greater than 30 meters (100 feet).

*Seiches* are long-period standing waves that continue after the forces that start them have ceased to act. They occur commonly in enclosed or partially enclosed basins.

*Wave setup* is defined as the superelevation of the water surface due to the onshore mass transport of the water by wave action alone. Isolated observations have shown that wave setup does occur in the surf zone.

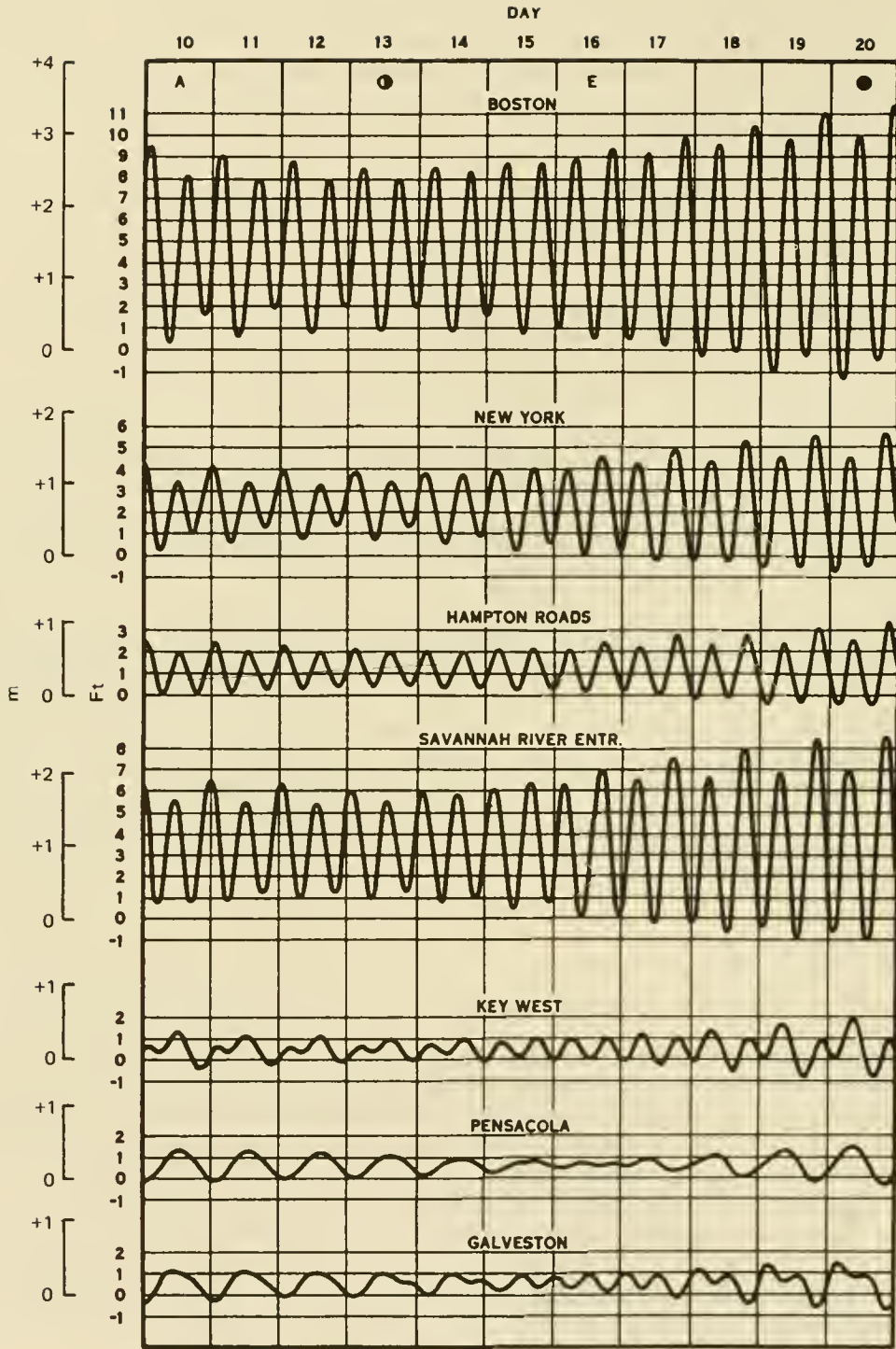
*Storm surges* are caused by moving atmospheric pressure jumps and by the wind stress accompanying moving storm systems. Storm systems are significant because of their frequency and potential for causing abnormal water levels at coastlines. In many coastal regions, maximum storm surges are produced by severe tropical cyclones called hurricanes (see Chapter 3, Section VII, for description and prediction of hurricane waves).

Prediction of water level changes is complex because many types of water level fluctuations can occur simultaneously. It is not unusual for surface wave setup, high astronomical tides, and storm surges to occur coincidentally at the shore on the open coast. It is difficult to determine how much rise can be attributed to each of these causes. Although astronomical tides can be predicted rather well where levels have been recorded for a year or more, there are many locations where this information is not available. Furthermore, the interactions between tides and storm surge in shallow water is not well defined.

#### 1. Astronomical Tides.

Tide is a periodic rising and falling of sea level caused by the gravitational attraction of the Moon, Sun, and other astronomical bodies acting on the rotating Earth. Tides follow the Moon more closely than they do the Sun. There are usually two high and two low waters in a tidal or lunar day. As the lunar day is about 50 minutes longer than the solar day, tides occur about 50 minutes later each day. Typical tide curves for various locations along the Atlantic, gulf, and Pacific coasts of the United States are shown in Figures 3-44 and 3-45. Along the Atlantic coast, the two tides each day are of nearly the same height. On the gulf coast, the tides are low but in some instances have a pronounced diurnal inequality. Pacific coast tides compare in height with those on the Atlantic coast but in most cases have a decided diurnal inequality (see App. A, Fig. A-10).

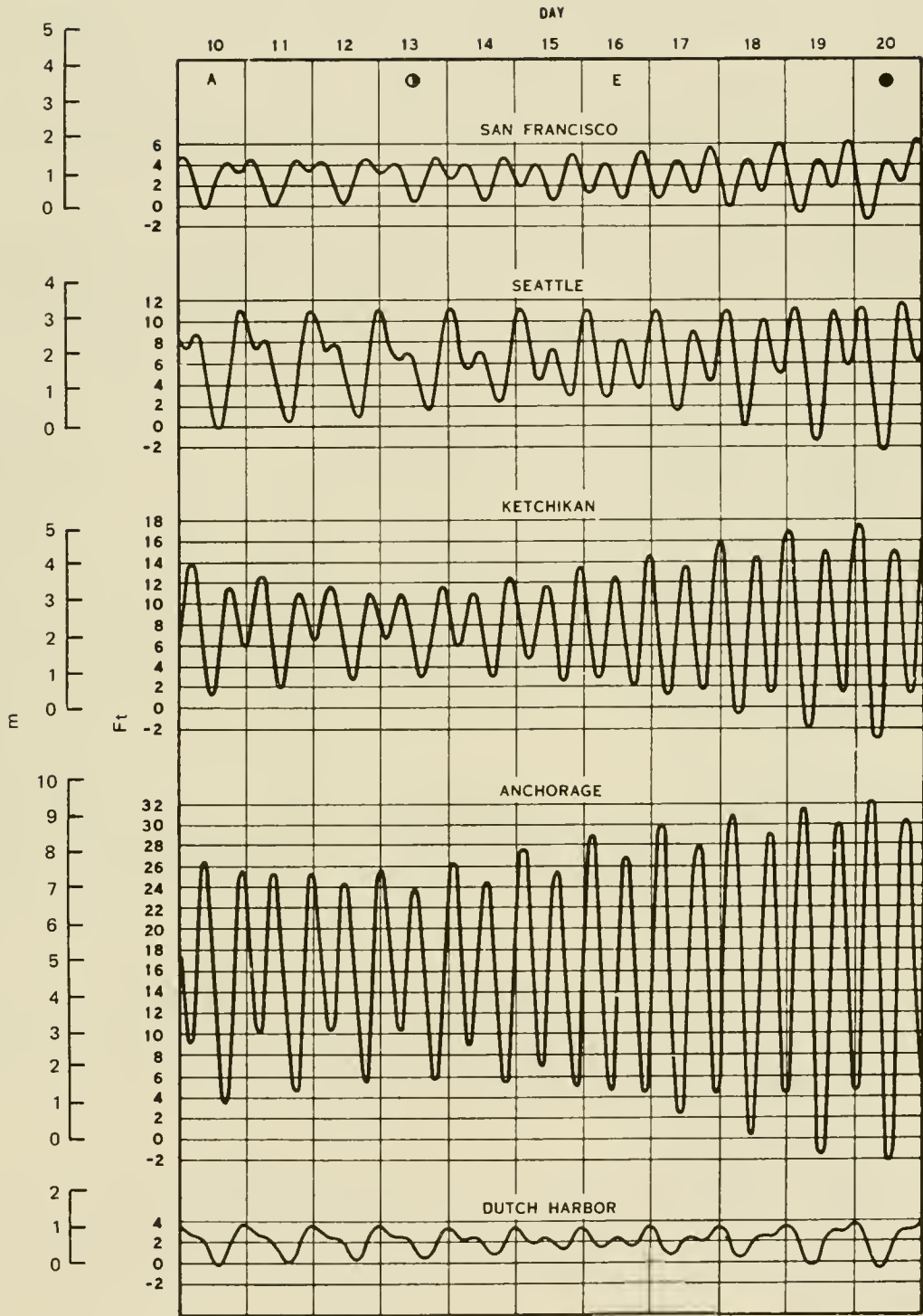
The dynamic theory of tides was formulated by Laplace (1775), and special solutions have been obtained by Doodson and Warburg (1941), among others. The use of simplified theories for the analysis and prediction of tides has been described by Schureman (1941), Defant (1961), and Ippen (1966). The computer program for tide prediction currently being used for official tide prediction in the United States is described by Pore and Cummings (1967).



Lunar data: max. S. declination, 9th; apogee, 10th; last quarter, 13th; on equator, 16th; new moon, 20th; perigee, 22d; max. N. declination, 23d.

(from National Ocean Survey, NOAA, Tide Tables)

Figure 3-44. Typical tide curves along Atlantic and gulf coasts.



Lunar data: max. S. declination, 9th, apogee, 10th, last quarter, 13th; on equator, 16th, new moon, 20th; perigee, 22d, max. N declination, 23d.

( from National Ocean Survey, NOAA, Tide Tables )

Figure 3-45. Typical tide curves along Pacific coasts of the United States.

Data concerning tidal ranges along the seacoasts of the United States are given to the nearest tenth of a meter or foot in Table 3-3. Spring ranges are shown for areas having approximately equal daily tides; diurnal ranges are shown for areas having either a diurnal tide or a pronounced diurnal inequality. Detailed data concerning tidal ranges are published annually in Tide Tables, U.S. Department of Commerce, National Ocean Service. Prediction, datum planes, and statistics of tidal data are discussed in Harris (1981).

Table 3-3. Tidal ranges.

Station	Approximate Ranges, meters (feet)		
	Mean	Diurnal	Spring
<b>Atlantic Coast</b>			
Calais, Maine	6.1 (20)		7.0 (23)
W. Quoddy Head, Maine	4.9 (16)		5.5 (18)
Englishman Bay, Maine	3.7 (12)		4.3 (14)
Belfast, Maine	3.0 (10)		3.4 (11)
Provincetown, Mass.	2.7 (9)		3.4 (11)
Chatham, Mass.	2.1 (7)		2.4 (8)
Cuttyhunk, Mass.	0.9 (3)		1.2 (4)
Saybrook, Conn.	1.2 (4)		1.2 (4)
Montauk Point, N.Y.	0.6 (2)		0.6 (2)
Sandy Hook, N.J.	1.5 (5)		1.8 (6)
Cape May, N.J.	1.2 (4)		1.5 (5)
Cape Henry, Va.	0.9 (3)		0.9 (3)
Charleston, S.C.	1.5 (5)		1.8 (6)
Savannah, Ga.	2.1 (7)		2.4 (8)
Mayport, Fla.	1.5 (5)		1.5 (5)
<b>Gulf Coast</b>			
Key West, Fla.	0.3 (1)		0.6 (2)
Apalachicola, Fla.		0.3 (1)	
Atchafalaya Bay, La.	0.3 (1)	0.6 (2)	
Port Isabel, Tex.	0.3 (1)	0.3 (1)	
<b>Pacific Coast</b>			
Point Loma, Calif.	1.2 (4)	1.5 (5)	
Cape Mendocino, Calif.	1.2 (4)	1.8 (6)	
Siuslaw River, Ore.	1.5 (5)	2.1 (7)	
Columbia River, Wash.	1.8 (6)	2.4 (8)	
Port Townsend, Wash.	2.1 (7)	3.0 (10)	
Puget Sound, Wash.	3.4 (11)	4.6 (15)	

## 2. Tsunamis.

Long-period gravity waves generated by such disturbances as earthquakes, landslides, volcano eruptions, and explosions near the sea surface are called tsunamis. The Japanese word *tsunamis* has been adopted to replace the expression *tidal wave* to avoid confusion with the astronomical tides.

Most tsunamis are caused by earthquakes that extend at least partly under the sea, although not all submarine earthquakes produce tsunamis. Severe tsunamis are rare events.

Tsunamis may be compared to the wave generated by dropping a rock in a pond. Waves (ripples) move outward from the source region in every direction. In general, the tsunami wave amplitudes decrease but the number of individual waves increases with distance from the source region. Tsunami waves may be reflected, refracted, or diffracted by islands, sea mounts, submarine ridges, or shores. The longest waves travel across the deepest part of the sea as shallow-water waves and can obtain speeds of several hundred kilometers per hour. The traveltime required for the first tsunami disturbance to arrive at any location can be determined within a few percent of the actual traveltime by the use of suitable tsunami traveltime charts.

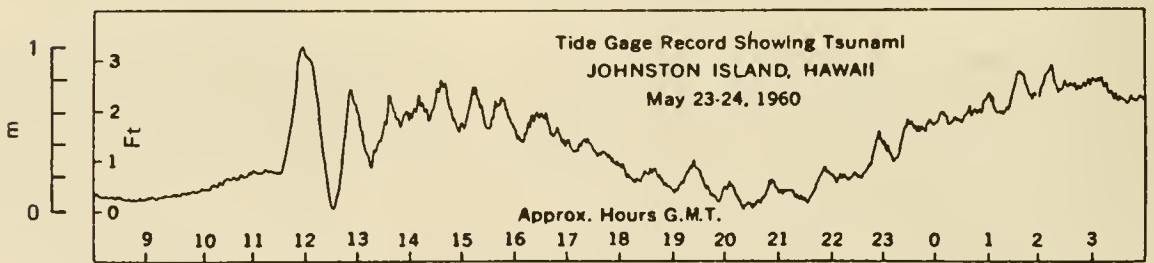
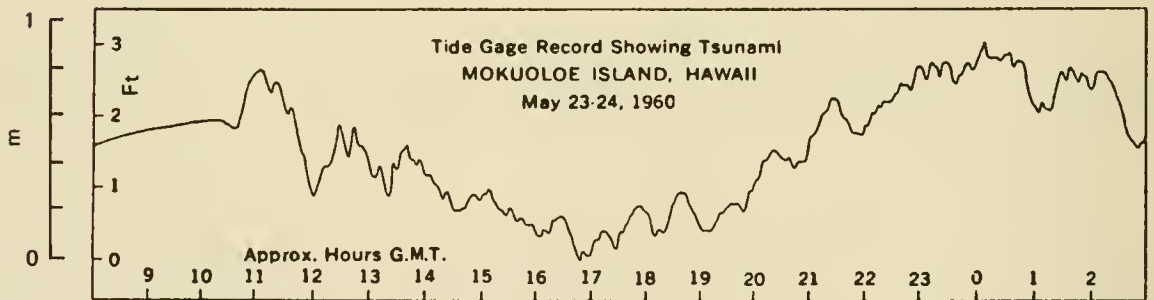
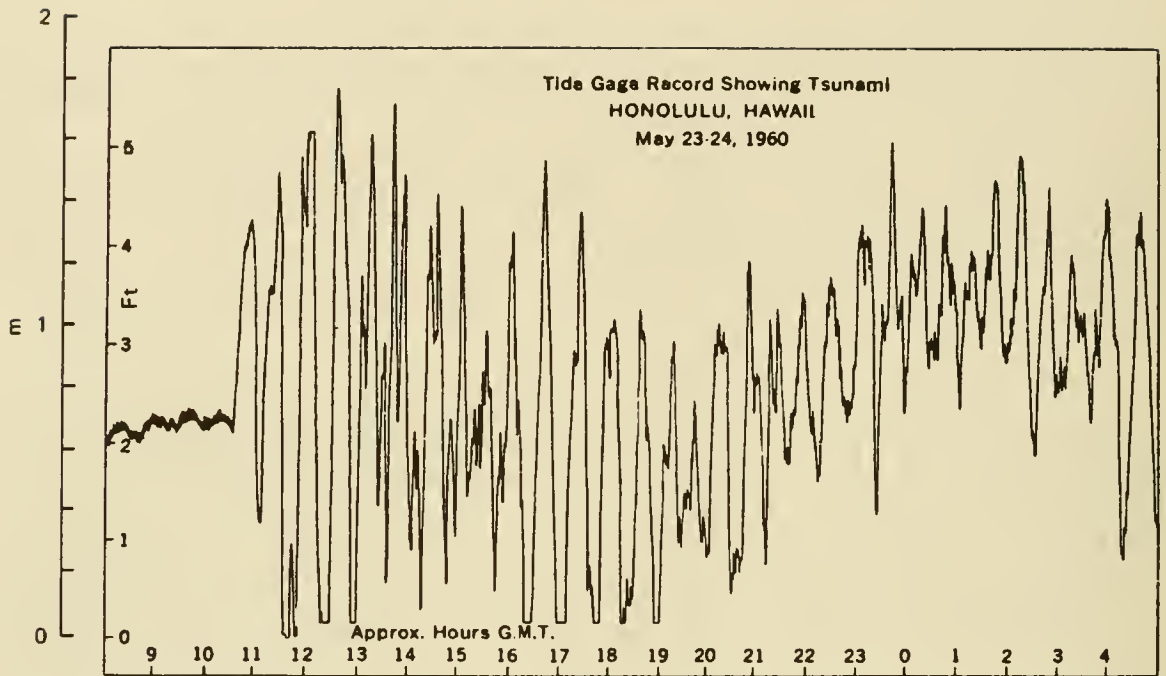
Tsunamis cross the sea as very long waves of low amplitude. A wavelength of 200 kilometers (124 miles) and an amplitude of 1 meter (3 feet) is not unreasonable. The wave may be greatly amplified by shoaling, diffraction, convergence, and resonance when it reaches land. Seawater has been carried higher than 11 meters (36 feet) above sea level in Hilo, Hawaii, by tsunamis. Tide gage records of the tsunami of 23-26 May 1960 at these locations are shown in Figure 3-46. The tsunami appears as a quasi-periodic oscillation, superimposed on the normal tide. The characteristic period of the disturbance, as well as the amplitude, is different at each of the three locations. It is generally assumed that the recorded disturbance results from forced oscillations of hydraulic basin systems and that the periods of greatest response are determined by basin geometry.

Theoretical and applied research dealing with tsunami problems has been greatly intensified since 1960. Preisendorfer (1971) lists more than 60 significant theoretical papers published since 1960. Recent research on tsunamis is discussed by Camfield (1980) and Murty (1977).

### 3. Lake Levels.

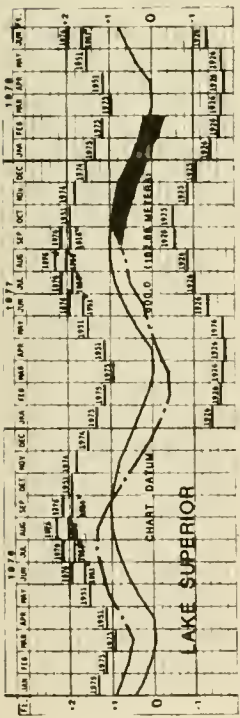
Lakes have insignificant tidal variations, but are subject to seasonal and annual hydrologic changes in water level and to water level changes caused by wind setup, barometric pressure variations, and seiches. Additionally, some lakes are subject to occasional water level changes by regulatory control works.

Water surface elevations of the Great Lakes vary irregularly from year to year. During each year, the water surfaces consistently fall to their lowest stages during the winter and rise to their highest stages during the summer. Nearly all precipitation in the watershed areas during the winter is snow or rainfall transformed to ice. When the temperature begins to rise there is substantial runoff--thus the higher stages in the summer. Typical seasonal and yearly changes in water levels for the Great Lakes are shown in Figure 3-47. The maximum and minimum monthly mean stages for the lakes are summarized in Table 3-4.

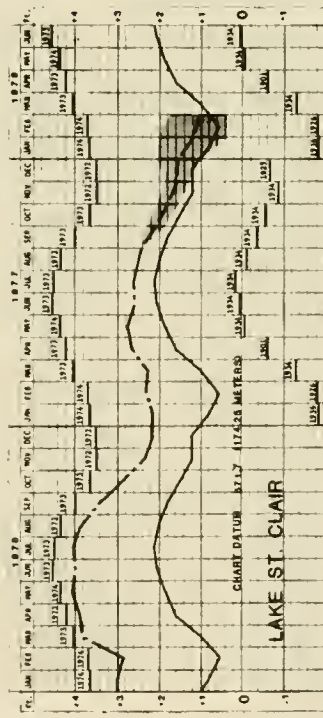
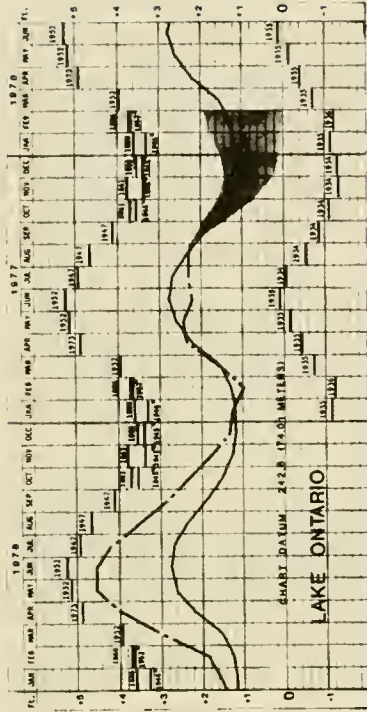
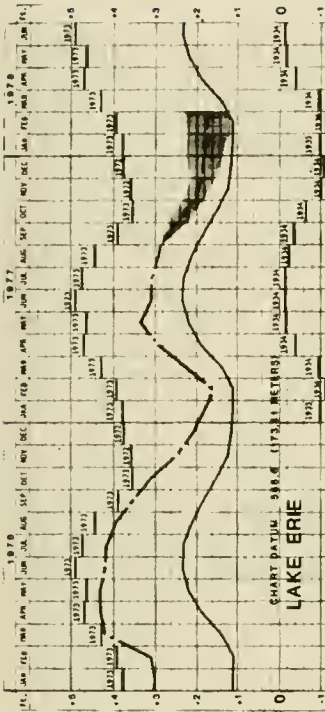
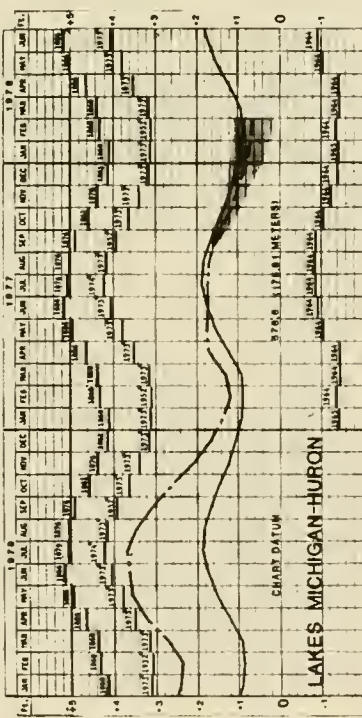


(from Symons and Zelter, 1960)

Figure 3-46. Sample tsunami records from tide gages.



ELEVATION IN FEET REFERRED TO CHART DATUM



**LEGEND**

RECORDED	LAKE LEVELS
PROBABLE	
1900-1976 AVERAGE	
MAXIMUM (1860 - 1976)	1865 1864 1864
MAXIMUM (1900 - 1976)	1974-1974-1973-1972
	MINIMUM 1936 1934 1926 1934

Hydrographs are in feet above(+) or below(-) Chart Datum, the plane on each lake to which navigation chart depths and Federal navigation improvement depths are referred. Chart Datum and all other elevations are in feet above mean water level at Father Point, Quebec (International Great Lakes Datum 1966).

Figure 3-47. Typical water level variations in Great Lakes.

Table 3-4. Fluctuations in water levels, Great Lakes System (1900 through 1977)<sup>1</sup>.

Lake	Datum <sup>2</sup> Factor	Low <sup>3</sup> Water Chart Datum	Alltime Monthly Means					
			Mean Surface Elevation	High, m (ft)	Date	Low, m (ft)	Date	Difference, m (ft)
Superior	0.52 (1.71)	182.9 (600.0)	183.0 (600.58)	183.5 (602.02)	8/1950	182.3 (598.23)	4/1926	1.1 (3.79)
Michigan-Huron	0.53 (1.74)	175.8 (576.8)	176.2 (578.23)	177.1 (581.04)	7/1974	175.4 (575.35)	3/1964	1.73 (5.69)
St. Clair <sup>1</sup>	0.55 (1.82)	174.2 (571.7)	174.7 (573.25)	175.6 (576.23)	6/1973	173.7 (569.86)	1/1936	3.67 (6.37)
Erie	0.59 (1.94)	173.3 (568.6)	173.8 (570.38)	174.8 (573.51)	6/1973	173.0 (567.49)	2/1936	1.83 (6.02)
Ontario	0.37 (1.23)	74.0 (242.8)	74.6 (244.70)	75.6 (248.06)	6/1952	76.6 (241.45)	11/1934	2.0 (6.61)

<sup>1</sup> Elevations are in meters (feet) above mean water level at Father Point, Quebec. International Great Lakes Datum (IGLD) (1955).

<sup>2</sup> To convert to 1935 Datum, add datum factor to IGLD (NOS 1935 = IGLD + datum factor).

<sup>3</sup> Low water datum is the zero plane on NOS Charts to which charts are referred. Thus the zero, (low water) datum on a NOS Lake Superior chart is 182 meters (600 feet) above mean water level at Father Point, Quebec.

In addition to seasonal and annual fluctuations, the Great Lakes are subject to occasional seiches of irregular amount and duration. These sometimes result from a resonant coupling which arises when the propagation speed of an atmospheric disturbance is nearly equal to the speed of free waves on a lake (Ewing, Press, and Donn, 1954; Harris, 1957; Platzman, 1958, 1965). The lakes are also affected by wind stresses which raise the water level at one end and lower it at the other. These mechanisms may produce changes in water elevation ranging from a few centimeters to more than 2 meters. Lake Erie, shallowest of the Great Lakes, is subject to greater wind-induced surface fluctuations, i.e. wind setup, than any other Lake. Wind setup is discussed in Chapter 3, Section VIII,6 (Storm Surge and Wind Setup).

In general, the maximum amount of these irregular changes in lake level must be determined for each location under consideration. Table 3-5 shows short-period observed maximum and minimum water level elevations at selected gage sites. More detailed data on seasonal lake levels and wind setup may be obtained for specific locations from the National Ocean Service, National Oceanic and Atmospheric Administration.

#### 4. Seiches.

Seiches are standing waves (Fig. 3-48) of relatively long periods that occur in lakes, canals, and bays and along open seacoasts. Lake seiches are usually the result of a sudden change, or a series of intermittent-periodic changes, in atmospheric pressure or wind velocity. Standing waves in canals can be initiated by suddenly adding or subtracting large quantities of water. Seiches in bays can be generated by local changes in atmospheric pressure and wind and by oscillations transmitted through the mouth of the bay from the open sea. Open-sea seiches can be caused by changes in atmospheric pressure and wind or by tsunamis. Standing waves of large amplitude are likely to be generated if the causative force which sets the water basin in

Table 3-5. Maximum deviations from mean lake levels <sup>1</sup>.

Location and Gage Location	Period of Gage Record	Maximum Recorded	
		Rise, m (ft)	Fall, m (ft)
Superior at Marquette	1903-1981	1.07 (3.5)	0.94 (3.1)
Michigan at Calumet Harbor (Chicago)	1903-1981	1.34 (4.4)	1.49 (4.9)
Huron at Harbor Beach	1902-1981	1.16 (3.8)	1.25 (4.1)
Erie at Buffalo	1900-1981	2.68 (8.8)	1.89 (6.2)
Erie at Toledo	1941-1981	1.92 (6.3)	2.71 (8.9)
Ontario at Oswego	1900-1981	1.31 (4.3)	1.16 (3.8)

<sup>1</sup>Deviations refer to differences between the mean surface elevation shown in Table 3-4 and the extreme instantaneous readings.

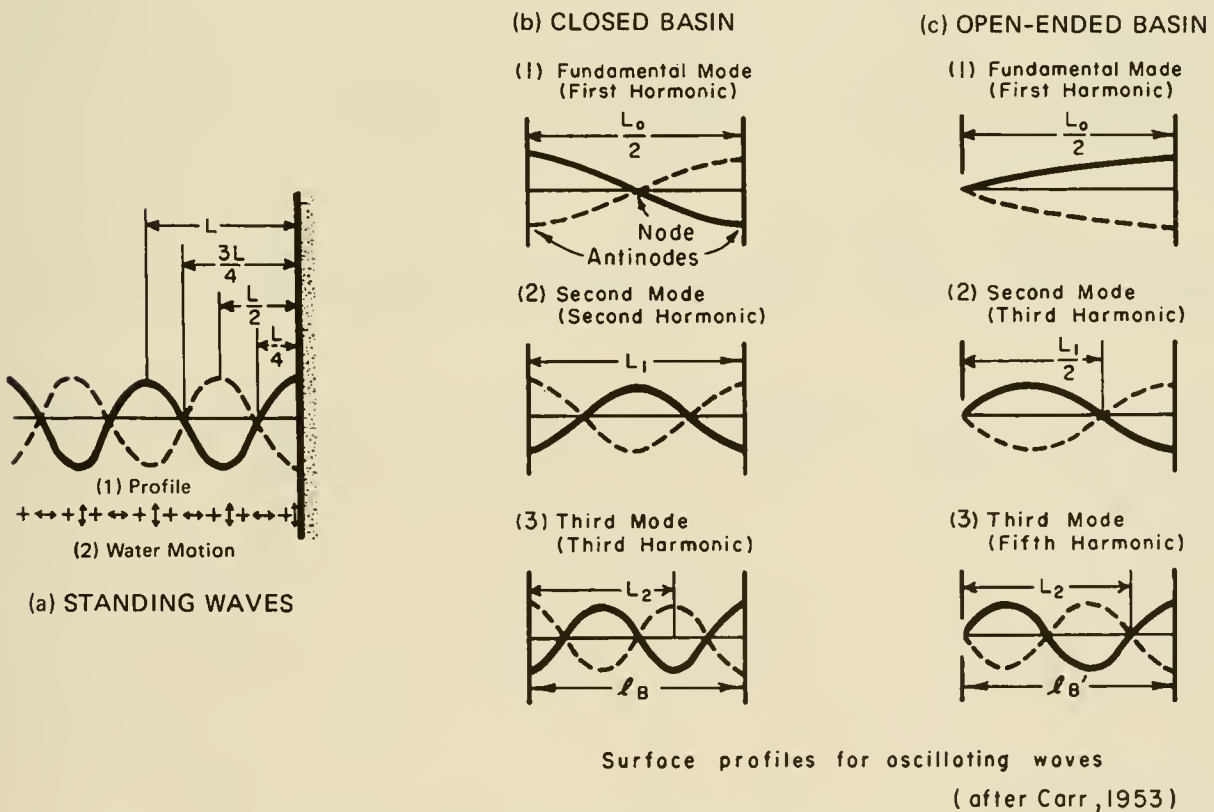


Figure 3-48. Long wave surface profiles.

motion is periodic in character, especially if the period of this force is the same as, or is in resonance with, the natural or free oscillating period of the basin (see Ch. 2, Sec. V, Wave Reflection).

Free oscillations have periods that are dependent upon the horizontal and vertical dimensions of the basin, the number of nodes of the standing wave (i.e., lines where deviation of the free surface from its undisturbed value is zero), and friction. The period of a true forced wave oscillation is the same as the period of the causative force. Forced oscillations, however, are usually generated by intermittent external forces, and the period of the oscillation is determined partly by the period of the external force and partly by the dimensions of the water basin and the mode of oscillation. Oscillations of this type have been called forced seiches (Chrystal, 1905) to distinguish them from free seiches in which the oscillations are free.

For the simplest form of a standing one-dimensional wave in a closed rectangular basin with vertical sides and uniform depth (Fig. 3-48b), wave antinodes (i.e., lines where deviation of the free surface from its undisturbed value is a relative maximum or minimum) are situated at the ends (longitudinal seiche) or sides (transverse seiche). The number of nodes and antinodes in a basin depends on which mode or modes of oscillation are present. If  $n$  = number of nodes along a given basin axis,  $d$  = basin depth, and  $\ell_B$  = basin length along that axis, then  $T_n$  the natural free oscillating period is given by

$$T_n = \frac{2\ell_B}{n\sqrt{gd}} \quad (3-70)$$

The fundamental and maximum period ( $T_n$  for  $n = 1$ ) becomes

$$T_1 = \frac{2\ell_B}{\sqrt{gd}} \quad (3-71)$$

Equation 3-69 is called Merian's formula (Sverdrup, Johnson, and Fleming, 1942).

In an open rectangular basin of length  $\ell_{B'}$  and constant depth  $d$ , the simplest form of a one-dimensional, nonresonant, standing longitudinal wave is one with a node at the opening, antinode at the opposite end, and  $n'$  nodes in between. (see Fig. 3-48c). The free oscillation period  $T'_{n'}$  in this case is

$$T'_{n'} = \frac{4\ell_{B'}}{(1 + 2n')\sqrt{gd}} \quad (3-72)$$

For the fundamental mode ( $n' = 0$ ),  $T'_{n'}$  becomes

$$T'_0 = \frac{4\ell_{B'}}{\sqrt{gd}} \quad (3-73)$$

The basin's total length is occupied by one-fourth of a wavelength.

This simplified theory must be modified for most actual basins, because of the variation in width and depth along the basin axes.

Defant (1961) outlines a method to determine the possible periods for one-dimensional free oscillations in long narrow lakes of variable width and depth. Defant's method is useful in engineering work because it permits computation of periods of oscillation, relative magnitudes of the vertical displacements along chosen axes, and the positions of nodal and antinodal lines. This method, applicable only to free oscillations, can be used to determine the modes of oscillation of multinodal and uninodal seiches. The theory for a particular forced oscillation was also derived by Defant and is discussed by Sverdrup, Johnson, and Fleming (1942). Hunt (1959) discusses some complexities involved in the hydraulic problems of Lake Erie and offers an interim solution to the problem of vertical displacement of water at the eastern end of the lake. More recently, work has been done by Platzman and Rao (1963), Simpson and Anderson (1964), Mortimer (1965), and Chen and Mei (1974). Rockwell (1966) computed the first five modes of oscillation for each of the Great Lakes by a procedure based on the work of Platzman and Rao (1965). Platzman (1972) has developed a method for evaluating natural periods for basins of general two-dimensional configuration.

## 5. Wave Setup.

Field observations indicate that part of the variation in mean nearshore water level is a function of the incoming wave field. However, these observations are insufficient to provide quantitative trends (Savage, 1957; Fairchild, 1958; Dorrestein, 1962; Galvin and Eagleson, 1965). A laboratory study by Saville (1961) indicated that for waves breaking on a slope there is a decrease in the mean water level relative to the stillwater level just prior to breaking, with a maximum depression or set-down at about the breaking point. This study also indicated that what is called wave setup occurs: from the breaking point the mean water surface slopes upward to the point of intersection with the shore. *Wave setup is defined as that superelevation of the mean water level caused by wave action alone.* This phenomenon is related to a conversion of kinetic energy of wave motion to a quasi-steady potential energy.

Two conditions that could produce wave setup should be examined. The simplest case is illustrated in Figure 3-49a in which the dashline represents the normal stillwater level; i.e., the water level that would exist if no wave action were present. The solid line represents the mean water level when wave shoaling and breaking occur. Also shown is a series of waves at an instant in time, illustrating the actual wave breaking and the resultant runup. As the waves approach the shore, the mean water level decreases to the minimum point  $d_b$  where the waves break. The difference in elevation between the mean water level and the normal stillwater level at this point is called the wave setdown,  $S_b$ . Beyond this point  $d_b$ , the mean water level rises until it intersects the shoreline. The total rise  $\Delta S$  between these points is the wave setup between the breaking zone and the shore. The net wave setup  $S_w$  is the difference between  $\Delta S$  and  $S_b$  and is the rise in the water surface at the shore above the normal stillwater level. In this case, the wave runup  $R$  is equal to the greatest height above normal stillwater level which is reached by the uprush of the waves breaking on the shore. For this type of problem the runup  $R$  includes the setup component and a separate computation

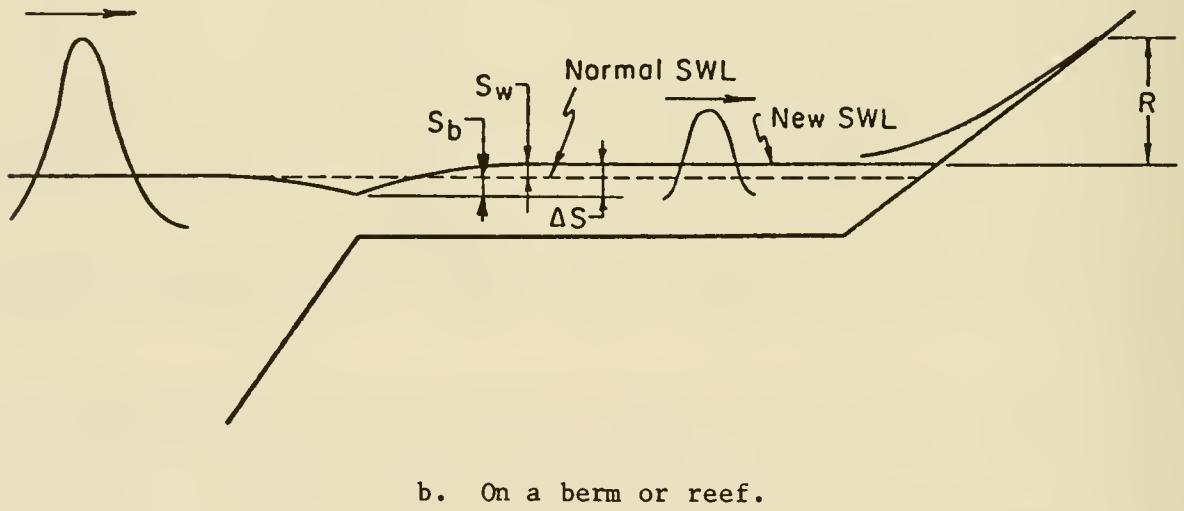
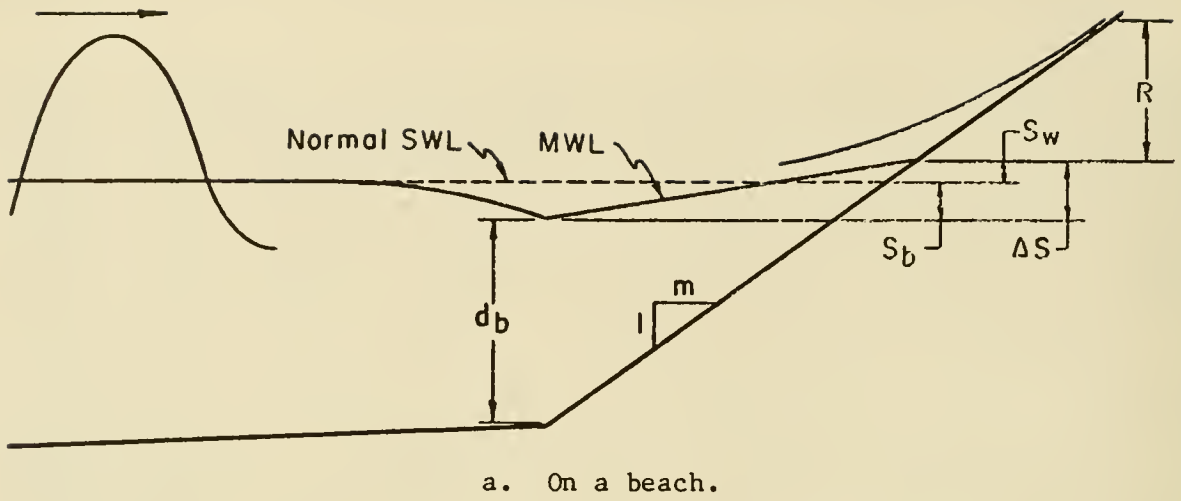


Figure 3-49. Definition sketch of wave setup.

for  $S_w$  is not needed. The reason for this is that laboratory measurements of wave runup are taken in reference to the stillwater level and already include the wave setup component.

Figure 3-49b illustrates a more complex situation involving wave setup. Here we have a beach fronted by a wide shelf. At some distance offshore the shelf abruptly drops off into the deep water. As waves approach the beach, the larger waves in the spectrum begin to break at the seaward edge of the shelf and a setup is produced. The increase in water level produced by this setup allows waves larger than would exist if based on the normal stillwater level to travel shoreward until they break on the beach. Calculations of wave runup on the beach would include the additional wave setup effects from the breaking of these smaller waves.

a. Wave Setup Due to Monochromatic Waves. Theoretical studies of wave setup have been made by Dorrestein (1962), Fortak (1962), Longuet-Higgins and Stewart (1960, 1962, 1963, 1964), Bowen, Inman, and Simmons (1968), Hwang and Divoky (1970), James (1974), and Goda (1975). Theoretical developments can account for many of the principal processes, but contain factors that are often difficult to specify in practical problems.

The computation of wave setup can be an important part of a thorough design effort requiring water level estimation. For major engineering structures such as nuclear powerplants it is quite important to consider all possible causes of water level rise. Wave runup computations alone will usually be sufficient, but in cases similar to that shown in Figure 3-49b, where large waves break offshore, an increase in the stillwater level on the berm or reef should be considered in determining the limit of wave runup.

In studies of coastal flooding by hurricanes, the effects of wave setup should be considered in the water level estimate. The procedure presented can be used to compute the wave setup for the cases shown in Figure 3-49.

R.O. Reid (Texas A & M University personal communication, 1972) has suggested the following approach for estimating the wave setup at shore, using the Longuet-Higgins and Stewart (1963) theory for the setdown at the breaking zone and solitary wave theory. The theory for setdown at the breaking zone indicates that

$$S_b = - \frac{g^{1/2} H'_0{}^2 T}{64 \pi d_b^{3/2}} \quad (3-74)$$

where

- $S_b$  = the setdown at the breaking zone
- $T$  = the wave period
- $H'_0$  = equivalent unrefracted deepwater significant wave height
- $d_b$  = the depth of water at the breaker point
- $g$  = the acceleration of gravity

The laboratory data of Saville (1961) give somewhat larger values than those obtained by use of equation (3-72). The net wave setup at the shore is

$$S_w = \Delta S - S_b \quad (3-75)$$

Equations (2-92), (2-93), and (2-94) define  $d_b$  in terms of the breaker height  $H_b$ , period  $T$ , and beach slope  $m$ .

$$d_b = \frac{H_b}{b - \left( a \frac{H_b}{gT^2} \right)}$$

where  $a$  and  $b$  are (approximately)

$$a = 43.75 \left( 1 - e^{-19m} \right)$$

$$b = \frac{1.56}{\left( 1 + e^{-19.5m} \right)}$$

Longuet-Higgins and Stewart (1963) have shown from an analysis of Saville's data (1961) that

$$\Delta S = 0.15 d_b \text{ (approximately)} \quad (3-76)$$

Combining equations (2-92), (2-93), and (2-94) with equations (3-72), (3-73), and (3-74) gives

$$S_w = 0.15 d_b - \frac{g^{1/2} \left( H'_0 \right)^2 T}{64 \pi d_b^{3/2}} \quad (3-77)$$

where

$$d_b = \frac{H_b}{\frac{1.56}{1 + e^{-19.5m}} - \frac{43.75 \left( 1 - e^{-19m} \right) H_b}{gT^2}} \quad (3-78)$$

Figure 3-50 is a plot of equation (3-75) in terms of  $S_w/H_b$  versus  $H_b/gT^2$  for slopes of  $m = 0.02, 0.033, 0.05,$  and  $0.10$  and is limited to values of  $0.0006 < H_b/gT^2 < 0.027$ .

Wave setup is a phenomenon involving the action of a train of many waves over a sufficient period of time to establish an equilibrium water level condition. The exact amount of time for equilibrium to be established is unknown, but a duration of 1 hour is considered an appropriate minimum value. The very high waves in the spectrum are too infrequent to make a significant contribution in establishing wave setup. For this reason, the significant wave height  $H_s$  represents the condition most suitable for design purposes.

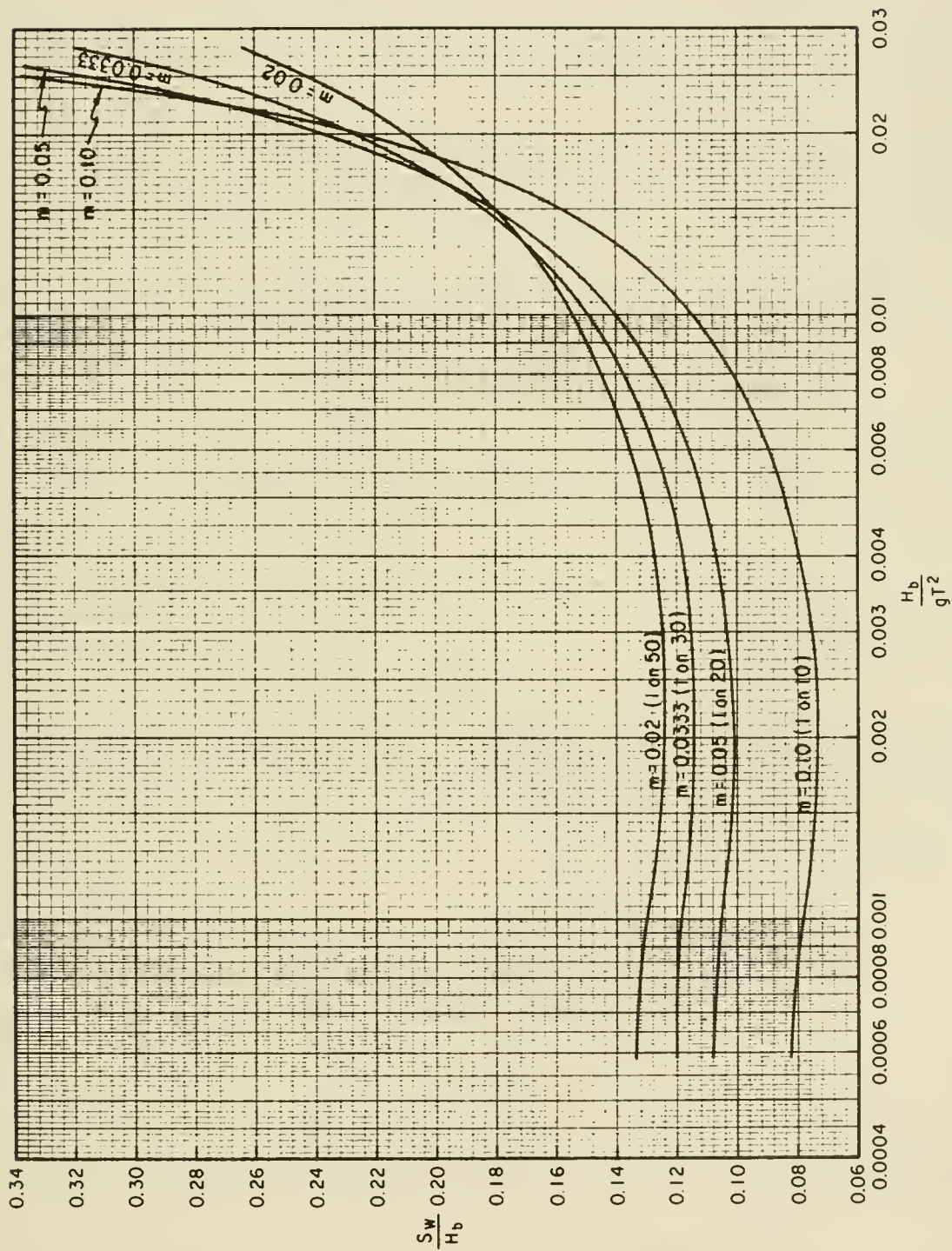


Figure 3-50.  $S_w/H_b$  versus  $H_b/gT^2$ .

The designer is cautioned, however, not to confuse the wave setup with wave runup. If an estimate of the highest elevation reached by wave runup on the shore is desired, the runup produced by a larger design wave can be estimated after considering the water level produced by wave setup (using  $H_{m0}$ ) and other effects (astronomical tide, wind setup, etc.). The selection of a design wave for runup considerations is left to the designer, based on the requirements of the project.

The wave setup estimates using the methods described in this section are based on the assumption that the waves approach normal to the coast. A wave that approaches the coast at an angle has components normal and parallel to the coast. The normal component produces wave setup; the parallel component produces a longshore current. It is reasonable to assume that the setup is a function of the cosine of the angle between the wave crest at breaking and the shore. Reducing the estimated wave setup in this manner is left to the judgment of the designer.

\*\*\*\*\* EXAMPLE PROBLEM 9 \*\*\*\*\*

GIVEN: A wave gage is located in 7 meters of water at mean low water. An analysis of the gage record for a period during a storm yields a significant wave height  $H_m = 6$  meters and period  $T_s = 12$  seconds.

Assume the direction of wave approach is normal to the coast which has straight and parallel depth contours (i.e., refraction coefficient = 1.0).

FIND: The maximum water level at the beach for which runup calculations can be made considering an initial stillwater level at mean low water.

SOLUTION: From the given conditions (shown in Figure 3-51) it is clear that the significant wave will break offshore of the shelf and induce a setup. First, define the unrefracted deepwater wave height  $H'_0$  and the breaker height  $H_b$ . From Table C-1, Appendix C,

$$\frac{d}{L_0} = \frac{7}{1.56 (12)^2} = 0.0311$$

$$\frac{H}{H'_0} = 1.118$$

and

$$H'_0 = 5.37 \text{ m}$$

From Figure 7-3 where  $m = 0.05$  and  $H'_0/gT^2 = 0.00380$

$$\frac{H_b}{H'_0} = 1.31$$

which gives

$$H_b = 7.03 \text{ meters}$$

From Figure 3-50, where  $H_b = 7.03$  ,  $H_b/gT^2 = 0.004976$  and  $m = 0.05$

$$\frac{S_w}{H_b} = 0.111$$

or

$$S_w = 0.78 \text{ m}$$

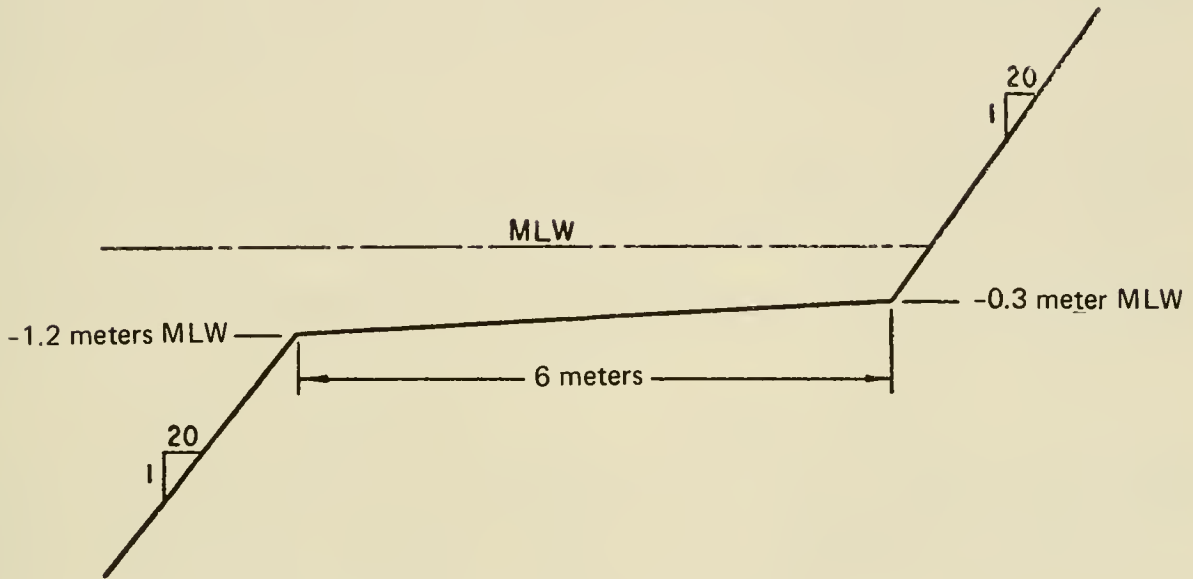


Figure 3-51. Definition sketch

Therefore, the new water level at the beach will be 0.78 meter at mean low water, which will result in a depth of 1.08 meters (3.6 feet) at the toe of the beach slope. The computation of the maximum runup height on the beach would involve the determination of the maximum breaking wave and run up for a range of wave periods. The highest runup elevation computed would be used for design purposes.

\*\*\*\*\*

\*\*\*\*\* EXAMPLE PROBLEM 10\*\*\*\*\*

GIVEN: A mathematical model simulation indicates that a particular section of coastline will experience a storm surge of +4.6 meters for a particular hurricane. The backshore area is protected by a continuous line of sand dunes whose lowest elevation is at about +6.1 meters. The estimated deepwater significant wave height and period are  $H_o = 9$  meters and  $T_s = 12$  seconds . The beach slope is a constant  $m = 0.05$

FIND: Whether continuous flooding of the backshore can be expected when wave setup is considered.

SOLUTION: First, assume that  $H_o = H'_o$  in this case. Then  $H_b$  can be found from Figure 7-3. With

$$\frac{H'_o}{gT^2} = 0.00637$$

and

$$m = 0.05$$

gives

$$\frac{H_b}{H'_o} = 1.15$$

or

$$H_b = 10.35 \text{ m}$$

From Figure 3-50, with  $H_b = 10.35$  meters

$$\frac{H_b}{gT^2} = 0.007327$$

and

$$m = 0.05$$

gives

$$\frac{S_w}{H_b} = 0.123$$

or

$$S_w = 1.27 \text{ m}$$

Therefore, the mean water level will be at elevation +5.87 meters which is 0.23 meter below the top of dunes. Extensive flooding should be expected as wave runup will overtop the dune crest, thus eroding it to a lower elevation and allowing continuous overflow.

\* \* \* \* \*

b. Wave Setup Due to Random Waves. Random wave setup produced by local storm waves (sea) may be somewhat different from the mean water level produced by monochromatic waves (swell) discussed in Chapter 3, Section VIII,5. Under sea conditions, groups of large waves may pump significant quantities of water toward the shoreline to cause setup, but some of this water can flow seaward during the relatively calm intervals between wave groups.

Let  $S$  be the mean water level position above the stillwater level ( $S$  is

negative for setdown) occurring at a point for random wave conditions. Figure 3-52 shows sample values of setup for a plane 1-on-30 laboratory slope. Setup occurs where the water depth-to-deepwater wave height ratio  $d/H'_0$  ranges from 0.9 to 1.1 where  $H'_0$  is the deepwater significant wave height, measured as  $H_{m0}$ . The amount of setup landward of this point increases as deepwater wave steepness decreases for a given value of deepwater wave height (Fig. 3-52). The increasing setup with decreasing steepness occurs in part because lower steepness waves are associated with decreased wave energy dissipation due to breaking; therefore, more wave energy is available to be converted into potential energy associated with wave setup. Note that at the initial stillwater level intercept ( $d = 0$ ) the setup is estimated to be on the order of twice the value at  $d/H'_0 = 0.5$ .

Setup observed on a 1-on-30 laboratory slope was used to calibrate a numerical procedure, and resulting predicted values of random (sea) wave setup are illustrated in Figure 3-53 for  $d/H'_0 = 0.5$ . Note that beach slope is predicted to have a small influence on setup for random (sea) wave conditions.

A simplified numerical procedure for predicting wave setup on a plane beach has been developed by Goda (1975).

## 6. Storm Surge and Wind Setup.

a. General. Reliable estimates of water level changes under storm conditions are essential for the planning and design of coastal engineering works. Determination of design water elevations during storms is a complex problem involving interaction between wind and water, differences in atmospheric pressure, and effects caused by other mechanisms unrelated to the storm. Winds are responsible for the largest changes in water level when considering only the storm surge generating processes. A wind blowing over a body of water exerts a horizontal force on the water surface and induces a surface current in the general direction of the wind. The force of wind on the water is partly due to inequalities of air pressures on the windward side of gravity waves and partly due to shearing stresses at the water surface. Horizontal currents induced by the wind are impeded in shallow water areas, thus causing the water level to rise downwind while at the windward side the water level falls. The term *storm surge* is used to indicate departure from normal water level due to the action of storms. The term *wind setup* is often used to indicate rises in lakes, reservoirs, and smaller bodies of water. A fall of water level below the normal level at the upwind side of a basin is generally referred to as *setdown*.

Severe storms may produce surges in excess of 8 meters (26 feet) on the open coast and even higher in bays and estuaries. Generally, setups in lakes and reservoirs are smaller, and setdown in these enclosed basins is about equivalent to the setup. Setdown in open oceans is insignificant because the volume of water required to produce the setup along the shallow regions of the coast is small compared to the volume of water in the ocean. However, setdown may be appreciable when a storm traverses a relatively narrow landmass such as southern Florida and moves offshore. High offshore winds in this case can cause the water level to drop as much as 1 meter or more.

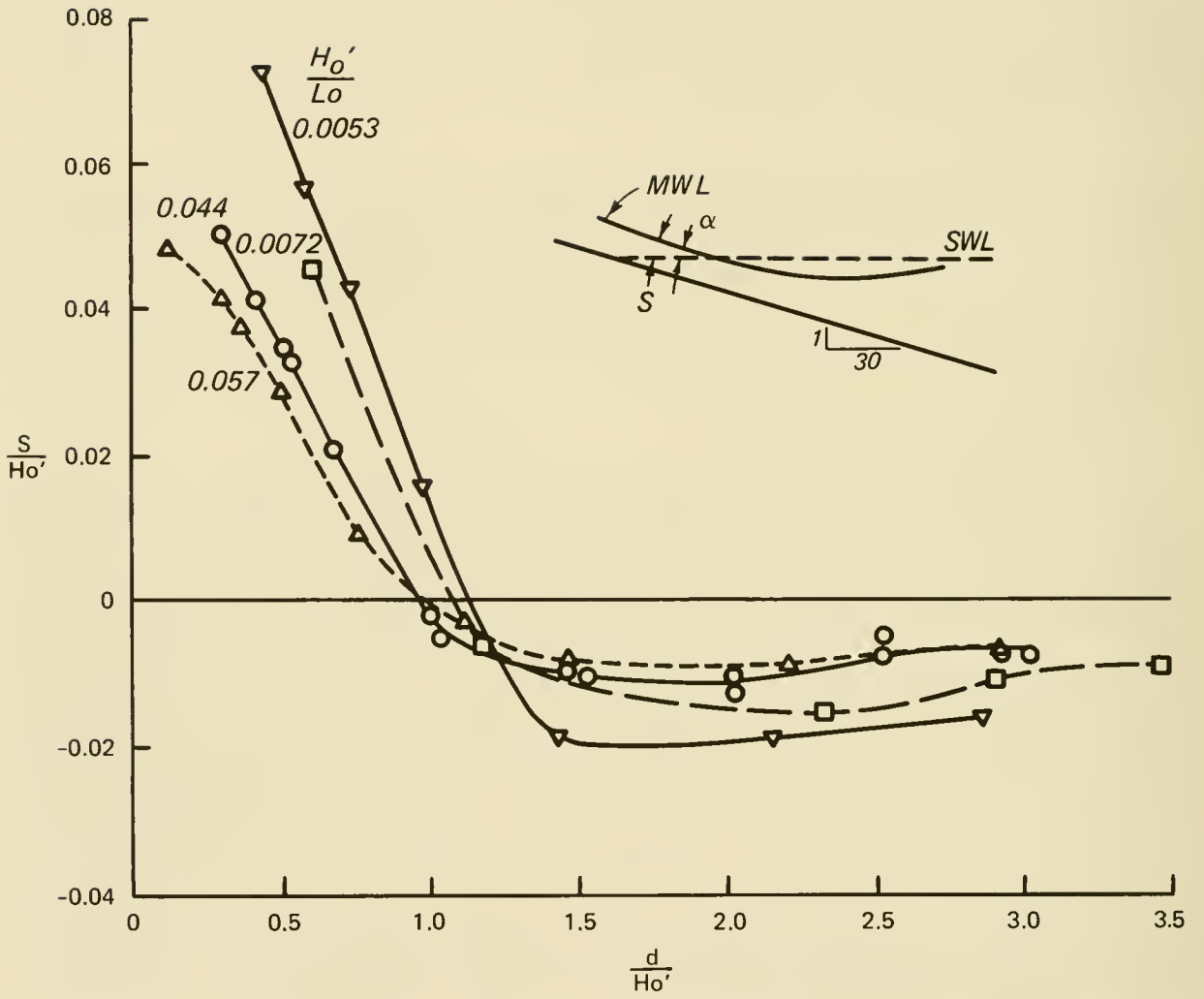


Figure 3-52. Measured random wave (sea) setup on a 1-on-30 flat slope.

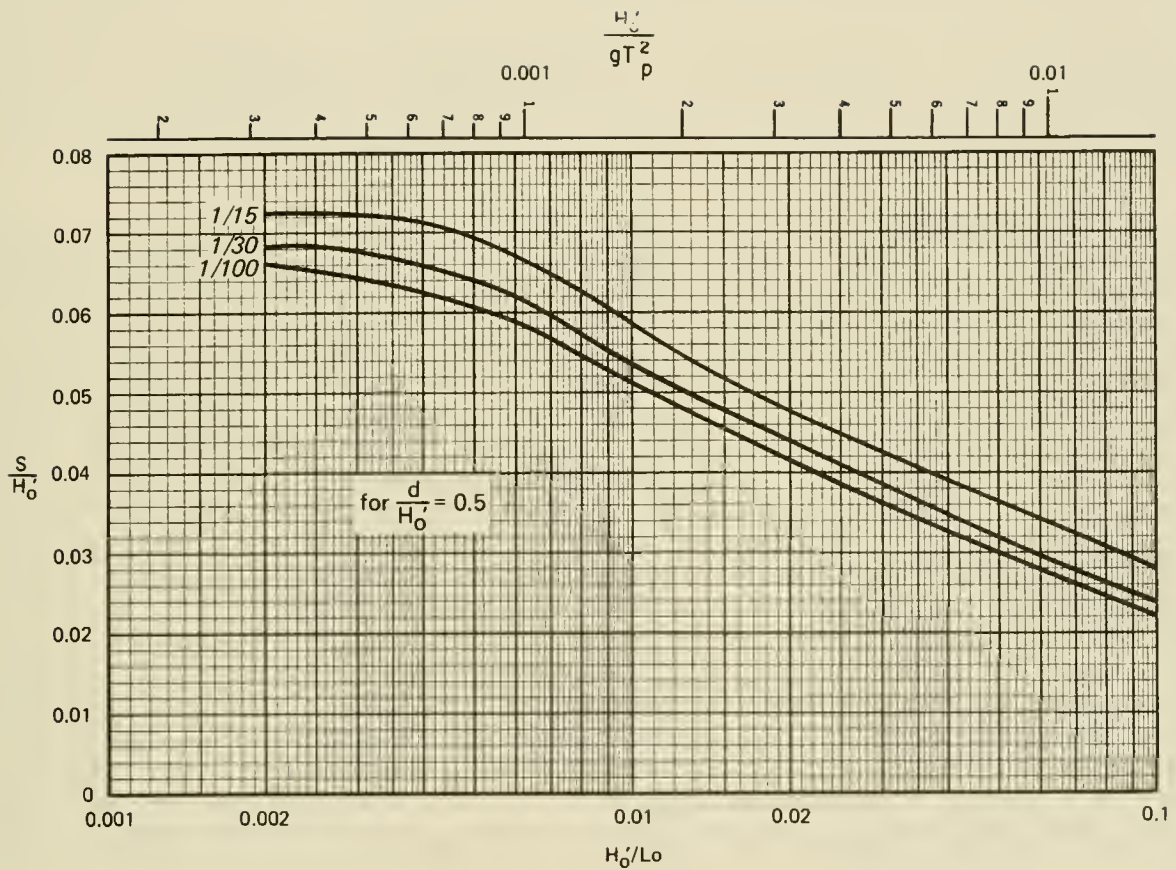


Figure 3-53. Predicted random wave (sea) setup on plane slopes for  $\frac{d}{H_0} = 0.5$ .

Setdown in semienclosed basins (bays and estuaries) also may be substantial, but the fall in water level is influenced by the coupling to the sea. Setdown produces some detrimental effects, such as making water-pumping facilities inoperable due to exposure of the intake, increasing the pumping heads of such facilities, and causing navigational hazards because of decreased depths.

However, rises in water level (setup rather than setdown) are of most concern. Abnormal rises in water level in nearshore regions will not only flood low-lying terrain, but provide a base on which high waves can attack the upper part of a beach and penetrate farther inland. Flooding of this type combined with the action of surface waves can cause severe damage to low-lying land and backshore improvements.

Wind-induced surge, accompanied by wave action, accounts for most of the damage to coastal engineering works and beach areas. Displacement of stone

armor units of jetties, groins, and breakwaters; scouring around structures; accretion and erosion of beach materials; cutting of new inlets through barrier beaches; and shoaling of navigational channels can often be attributed to storm surge and surface waves. Moreover, surge can increase hazards to navigation, impede vessel traffic, and hamper harbor operations. A knowledge of the increase and decrease in water levels that can be expected during the life of a coastal structure or project is necessary to design structures that will remain functional.

b. Storms. A storm is an atmospheric disturbance characterized by high winds which may or may not be accompanied by precipitation. Two distinctions are made in classifying storms: a storm originating in the tropics is called a *tropical storm*; a storm resulting from a cold or warm front is called an *extratropical storm*. Both these storms can produce abnormal rises in water level in shallow water near the edge of water bodies. The highest water levels produced along the entire gulf coast and from Cape Cod to the south tip of Florida on the east coast generally result from tropical storms. High water levels are rarely caused by tropical storms on the lower coast of California. Extreme water levels in some enclosed bodies, such as Lake Okeechobee, Florida, can also be caused by a tropical storm. Highest water levels at other coastal locations and most enclosed bodies of water result from extratropical storms.

A severe tropical storm is called a *hurricane* when the maximum sustained windspeeds reach 120 kilometers per hour (75 miles per hour or 65 knots). Hurricane winds may reach sustained speeds of more than 240 kilometers per hour (150 miles per hour or 130 knots). Hurricane season lasts from about June to November. Hurricanes, unlike less severe tropical storms, generally are well organized and have a circular wind pattern with winds revolving around a center or *eye* (not necessarily the geometric center). The eye is an area of low atmospheric pressure and light winds. Atmospheric pressure and windspeed increase rapidly with distance outward from the eye to a zone of maximum windspeed which may be anywhere from 7 to 110 kilometers (4 to 70 statute miles) from the center. From the zone of maximum wind to the periphery of the hurricane, the pressure continues to increase; however, the windspeed decreases. The atmospheric pressure within the eye is the best single index for estimating the surge potential of a hurricane. This pressure is referred to as the *central pressure index* (CPI). Generally for hurricanes of fixed size, the lower the CPI, the higher the windspeeds. Hurricanes may also be characterized by other important elements, such as the radius of maximum winds  $R$  which is an index of the size of the storm, and the speed of forward motion of the storm system  $V_F$ . A discussion of the formation, development, and general characteristics of hurricanes is given by Dunn and Miller (1964), Millar (1967), McBride (1981), and Ho et al. (1975).

Extratropical storms that occur along the northern part of the east coast of the United States accompanied by strong winds blowing from the northeast quadrant are called *northeasters*. Nearly all destructive northeasters have occurred in the period from November to April. A typical northeaster consists of a single center of low pressure about which the winds revolve, but wind patterns are less symmetrical than those associated with hurricanes.

c. Factors of Storm Surge Generation. The extent to which water levels will depart from normal during a storm depends on several factors. The factors are related to the

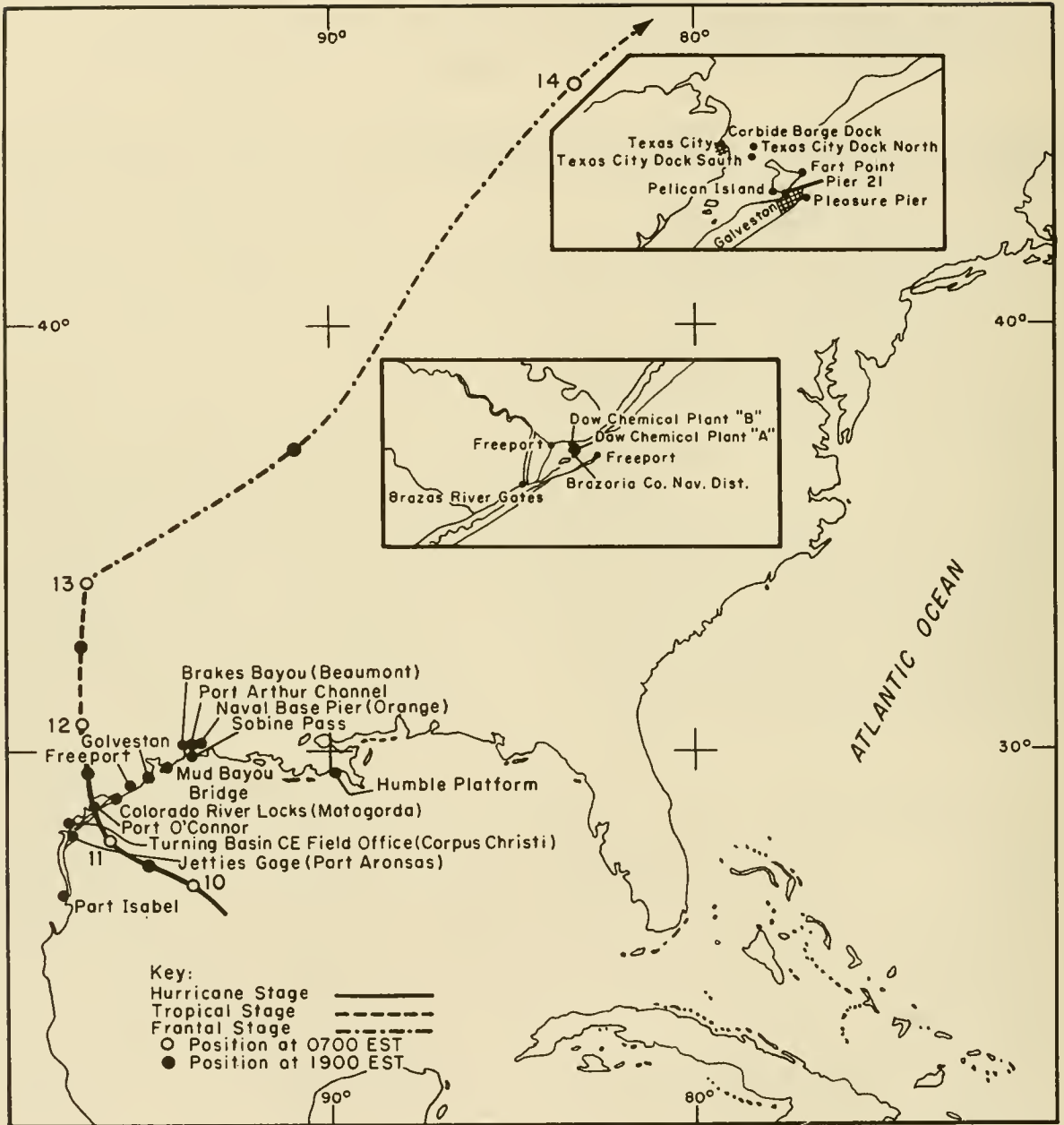
- (a) Characteristics and behavior of the storm
- (b) Hydrography of the basin
- (c) Initial state of the system
- (d) Other effects that can be considered external to the system

Several distinct factors that may be responsible for changing water levels during the passage of a storm may be identified as

- (a) Astronomical tides
- (b) Direct winds
- (c) Atmospheric pressure differences
- (d) Earth's rotation
- (e) Rainfall
- (f) Surface waves and associated wave setup
- (g) Storm motion effects

The elevation of setup or setdown in a basin depends on storm intensity, path or track, overwater duration, atmospheric pressure variation, speed of translation, storm size, and associated rainfall. Basin characteristics that influence water level changes are basin size and shape and bottom configuration and roughness. The size of the storm relative to the size of the basin is also important. The magnitude of storm surges is shown in Figures 3-54 and 3-55. Figure 3-54 shows the difference between observed water levels and predicted astronomical tide levels during Hurricane Carla (1961) at several Texas and Louisiana coastal tide stations. Figure 3-55 shows high water marks obtained from a storm survey made after Hurricane Carla. Harris (1963) gives similar data from other hurricanes.

d. Initial Water Level. Water surfaces on the open coast or in enclosed or semienclosed basins are not always at their normal level prior to the arrival of a storm. This departure of the water surface from its normal position in the absence of astronomical tides, referred to as an *initial water level*, is a contributing factor to the water level reached during the passage of a storm system. This level may be 0.6 meter (2 feet) above normal for some locations along the U.S. gulf coast. Some writers refer to this difference in water level as a *forerunner* in advance of the storm due to initial circulation and water transport by waves, particularly when the water level is above normal. Harris (1963), on the other hand, indicates that this general rise may be due to short-period anomalies in the mean sea level not related to hurricanes. Whatever the cause, the initial water level should be considered when evaluating the components of open-coast storm surge. The existence of an initial water level preceding the approach of Hurricane Carla is shown in Figure 3-54 and in a study of the synoptic weather charts for this storm (Harris, 1963). At 0700 hours (eastern standard time), 9 September 1961, the winds at Galveston, Texas, were about 16 kilometers per hour (10 miles per hour) but the open coast tide station (Pleasure Pier) shows the difference between the observed water level and astronomical tide to be above 0.6 meter (2 feet).



(from Harris, 1963)

Figure 3-54. Storm surge and observed tide chart, Hurricane Carla, 7-12 September 1961. (Insert maps are for Freeport and Galveston, Texas, areas.) (Continued.)

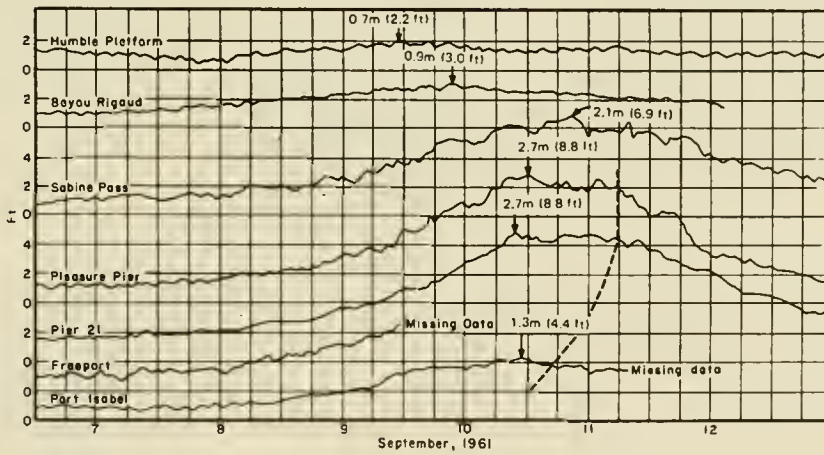
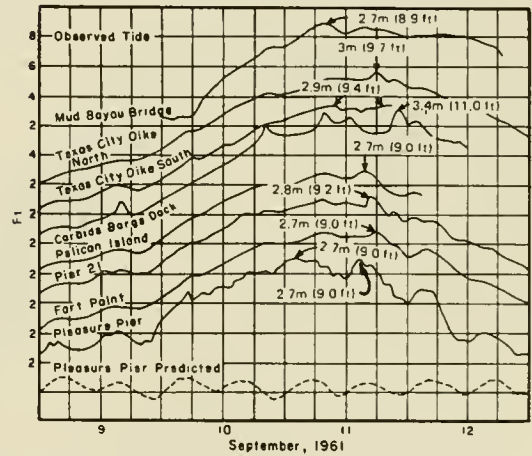
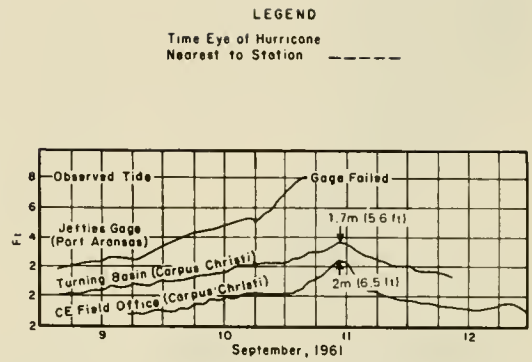
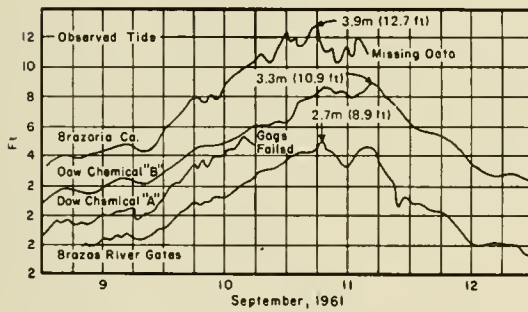
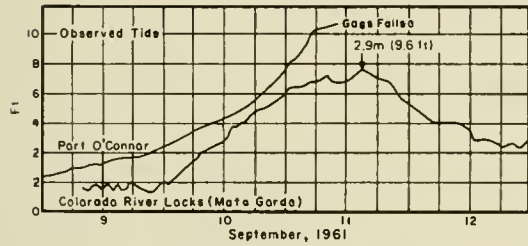
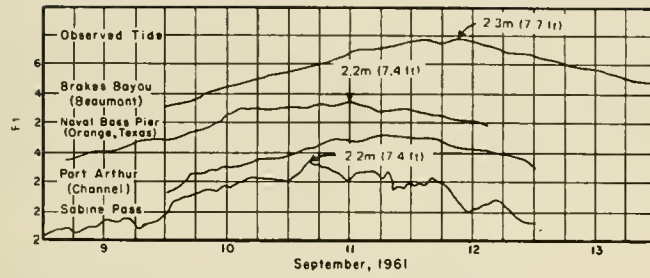
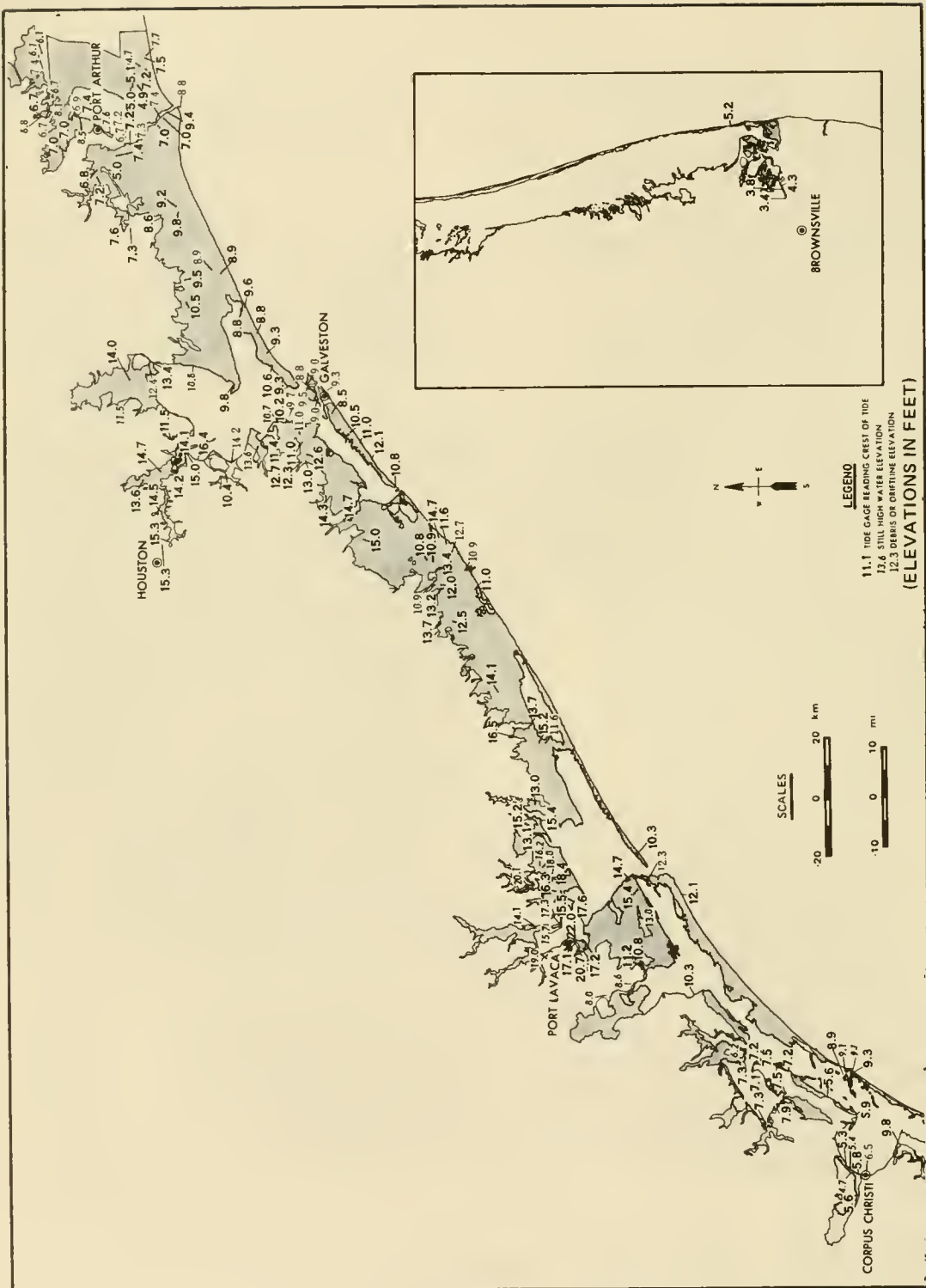


Figure 3-54. Concluded.



(from Harris, 1963)

Figure 3-55. High water mark chart for Texas, Hurricane Carla, 7-12 September 1961.  
 (Shaded area indicates the extent of flooding.)

Rises of this nature on the open coast can also affect levels in bays and estuaries.

There are other causes for departures of the water levels from normal in semienclosed and enclosed basins, such as the effects of evaporation and rainfall. Generally, rainfall plays a more dominant, role since these basins are affected by direct rainfall and can be greatly affected by rainfall runoff from rivers. The initial rise caused by rainfall is due to rains preceding the storm; rains during the passage of a storm have a time-dependent effect on the change in water level.

e. Storm Surge Prediction. The design of coastal engineering works is usually based on a life expectancy for the project and on the degree of protection the project is expected to provide. This design requires that the *design storm* have a specified frequency of occurrence for the particular area. An estimate of the frequency of occurrence of a particular storm surge is required. One method of making this estimate is to use frequency curves developed from statistical analyses of historical water level data. Table 3-6, based on National Ocean Service tide gage records, indicates observed extreme storm surge water levels including wave setup. The water levels are those actually recorded at the various tide stations and do not necessarily reflect the extreme water levels that may have occurred near the gages. Values in this table may differ from gage station values because of corrections for seasonal and secular anomalies. The frequency of occurrence for the highest and lowest water levels may be estimated by noting the length of time over which observations were made. The average yearly highest water level is an average of the highest water level from each year during the period of observation. Extreme water levels are rarely recorded by water level gages, partly because the gages tend to become inoperative with extremely high waves and partly because the peak storm surge often occurs between tide gage stations. Poststorm surveys showed water levels, the result of Hurricane Camille in August 1969, in excess of 6 meters (20 feet) MSL over many miles of the open gulf coast, with a peak value of 7.3 meters (24 feet) MSL near Pass Christian, Mississippi. High water levels in excess of 3.7 meters (12 feet) MSL on the open coast and 6 meters (20 feet) within bays were recorded along the Texas coast as the result of Hurricane Carla (September, 1961). Water levels above 4 meters (13 feet) MSL were recorded in the Florida Keys during Hurricane Donna (1960).

Accumulation of data over many years in some areas, such as regions near the North Sea, has led to relatively accurate empirical techniques of storm surge prediction for some locations. However, these empirical methods are not applicable to other locations. In general, not enough storm surge observations are available in the United States to make accurate predictions of storm surge. Therefore, it has been general practice to use hypothetical design storms and to estimate the storm-induced surge by physical or mathematical models. Mathematical models are usually used for predicting storm surge, since it is difficult to represent some of the storm surge generating processes (such as the direct wind effects and Coriolis effects) in physical laboratory models.

Table 3-6. Highest and lowest water levels.

Location	Observation Period	Mean Range meters (feet)	Highest Water Levels Above Mean High Water meters (feet)			Lowest Water Levels Below Low Water meters (feet)		
			Average Yearly Highest	Extreme High	Date of Record	Average Yearly Lowest	Extreme Low	Date of Record
ATLANTIC COAST Eastport, Maine	1930-69	5.54 (18.2)	1.19 (3.9)	1.49 (4.9)	21 Dec 68	1.19 (3.9)	1.34 (4.4)	7 Jan 43 23 May 59 30 Dec 63
Portland, Maine	1912-69	2.74 (9.0)	0.85 (2.8)	1.22 (4.0)	30 Nov 44 20 Nov 45	0.85 (2.8)	1.13 (3.7)	30 Nov 55
Bar Harbor, Maine	1947-70	32.0 (10.5)	0.94 (3.1)	1.31 (4.3)	29 Dec 59	0.85 (2.8)	1.10 (3.6)	30 Dec 53
Portsmouth, N.H.	1927-70	2.47 (8.1)	0.85 (2.8)	1.13 (3.7)	30 Nov 44 29 Dec 59	0.82 (2.7)	1.04 (3.4)	30 Nov 55
Boston, Mass.	1922-70	2.90 (9.5)	0.91 (3.0)	1.34 (4.4)	29 Dec 59	0.94 (3.1)	1.16 (3.8)	25 Jan 28 24 Mar 40
Woods Hole, Mass.	1933-70	0.55 (1.8)	0.88 (2.9)	2.80 (9.2)	21 Sept 38	0.61 (2.0)	0.82 (2.7)	8 Jan 68
Providence, R.I.	1938-47 1957-70	1.40 (4.6)	1.13 (3.7)	3.99 (13.1)	21 Sept 38	0.76 (2.5)	1.04 (3.4)	5 Jan 59
Newport, R.I.	1931-70	1.07 (3.5)	0.82 (2.7)	3.05 (10.0)	21 Sept 38	0.64 (2.1)	0.88 (2.9)	25 Jan 36
New London, Conn.	1938-70	0.79 (2.6)	0.98 (3.2)	2.47 (8.1)	21 Sept 38	0.70 (2.3)	1.04 (3.4)	11 Dec 43
Willets Point, N.Y.	1932-70	2.16 (7.1)	1.16 (3.8)	2.93 (9.6)	21 Sept 38	0.98 (3.2)	1.25 (4.1)	24 Mar 40
Battery, N.Y.	1920-70	1.37 (4.5)	0.88 (2.9)	1.74 (5.7)	12 Sept 60	0.91 (3.0)	1.22 (4.0)	8 Mar 32 5 Jan 59
Montauk, N.Y.	1948-70	0.64 (2.1)	0.98 (3.2)	2.01 (6.6)	31 Aug 54	0.58 (1.9)	0.79 (2.6)	8 Feb 51
Sandy Hook, N.J.	1933-70	1.40 (4.6)	0.94 (3.1)	1.74 (5.7)	12 Sept 60	0.88 (2.9)	1.25 (4.1)	31 Dec 62
Atlantic City, N.J.	1912-20 1923-70	1.25 (4.1)	0.85 (2.8)	1.58 (5.2)	14 Sept 44	0.52 (2.7)	1.13 (3.7)	8 Mar 32
Philadelphia, Pa.	1900-20 1922-70	1.80 (5.9)	0.67 (2.2)	1.43 (4.7)	25 Nov 50	0.94 (3.1)	2.04 (6.7)	31 Dec 62
Lewes, Del. Breakwater Harbor	1936-70	1.25 (4.1)	0.91 (3.0)	1.65 (5.4)	6 Mar 62	0.76 (2.5)	0.91 (3.0)	28 Mar 55
Baltimore, Md.	1902-70	0.33 (1.1)	0.70 (2.3)	2.04 (6.7)	23 Aug 33	1.04 (3.4)	1.52 (5.0)	24 Jan 08
Annapolis, Md.	1929-70	0.27 (0.9)	0.67 (2.2)	1.65 (5.4)	23 Aug 33	0.85 (2.8)	1.16 (3.8)	31 Dec 62
Solomons Island, Md.	1938-70	0.36 (1.2)	0.61 (2.0)	1.04 (3.4)	13 Aug 55	0.64 (2.1)	1.04 (3.4)	31 Dec 62
Washington, D.C.	1931-70	0.88 (2.9)	0.85 (2.8)	2.56 (8.4)	17 Oct 42	0.88 (2.9)	1.19 (3.9)	31 Dec 62
Portsmouth, Va.	1935-70	0.85 (2.8)	0.91 (3.0)	1.74 (5.7)	18 Sept 36	0.61 (2.0)	0.73 (2.4)	25 Jan 36 4 Dec 42 8 Feb 59

(Continued)

Table 3-6. Highest and lowest water levels (continued).

Location	Observation Period	Mean Range meters (feet)	Highest Water Levels Above Mean High Water meters (feet)			Lowest Water Levels Below Low Water meters (feet)		
			Average Yearly Highest	Extreme High	Date of Record	Average Yearly Lowest	Extreme Low	Date of Record
ATLANTIC COAST Norfolk, Va. Sewells Point	1928-70	0.76 (2.5)	0.85 (2.8)	1.83 (6.0)	23 Aug 33	0.64 (2.1)	0.91 (3.0)	23 Jan 28 26 Jan 28
Morehead City, N.C.	1953-57	0.85 (2.8)	--	1.28 (4.2)	15 Oct 54 19 Sept 55	--	0.52 (1.7)	11 Dec 54
Wilmington, N.C.	1935-70	1.10 (3.6)	0.52 (1.7)	1.31 (4.3)	15 Oct 54	0.43	0.61 (1.4)	3 Feb 40 (2.0)
Southport, N.C.	1933-53	1.25 (4.1)	0.73 (2.4)	1.04 (3.4)	2 Nov 47	0.37 (1.2)	0.58 (1.9)	28 Jan 34
Charleston, S.C.	1922-70	1.58 (5.2)	0.67 (2.2)	1.58 (5.2)	11 Aug 40	0.73 (2.4)	1.10 (3.6)	30 Nov 63
Fort Pulaski, Ga.	1936-70	2.10 (6.9)	0.76 (2.5)	1.28 (4.2)	15 Oct 47	0.88 (2.9)	1.34 (4.4)	20 Mar 36
Fernandina, Fla.	1897-1924 1939-1970	1.83 (6.0)	0.76 (2.5)	2.35 (7.7)	2 Oct 1898	0.76 (2.5)	1.19 (3.9)	24 Jan 1940
Mayport, Fla.	1928-70	1.37 (4.5)	0.58 (1.9)	0.91 (3.0)	9 Sept 64	0.61 (2.0)	0.98 (3.2)	24 Jan 40
Miami Beach, Fla.	1931-51 1955-70	0.76 (2.5)	0.49 (1.6)	1.19 (3.9)	8 Sept 65	3.96 (1.3)	0.49 (1.6)	24 Mar 36
GULF COAST Key West, Fla.	1926-70	0.39 (1.3)	0.40 (1.3)	0.76 (2.5)	8 Sept 65	0.37 (1.2)	0.49 (1.6)	19 Feb 28
St. Petersburg, Fla.	1947-70	0.70 <sup>1</sup> (2.3)	0.49 (1.6)	0.91 (3.0)	5 Sept 50	0.52 (1.7)	0.64 (2.1)	3 Jan 58
Cedar Key, Fla.	1914-25 1939-70	0.79 (2.6)	0.67 (2.2)	0.98 (3.2)	15 Feb 53 11 Sept 64	0.85 (2.8)	1.07 (3.5)	27 Aug 49 21 Oct 52 4 Feb 63
Pensacola, Fla.	1923-70	0.40 <sup>1</sup> (1.3)	0.49 (1.6)	2.32 (7.6)	20 Sept 26	0.43 (1.4)	0.67 (2.2)	6 Jan 24
Grand Isle, La. Humble Platform	1949-70	0.43 <sup>1</sup> (1.4)	0.46 (1.5)	0.67 (2.2)	25 Sept 53 22 Sept 56	0.43 (1.4)	0.52 (1.7)	22 Nov 49 3 Feb 51
Bayou Rigaud	1947-70	0.30 <sup>1</sup> (1.0)	0.60 (1.9)	1.19 (3.9)	24 Sept 56	0.33 (1.1)	0.46 (1.5)	3 Feb 51 13 Jan 64
Eugene Island, La.	1939-70	0.60 <sup>1</sup> (1.9)	0.76 (2.5)	1.83 (6.0)	27 Jun 57	0.49 (1.6)	0.73 (2.4)	25 Jan 40
Galveston, Tex.	1908-70	0.43 <sup>1</sup> (1.4)	0.67 (2.2)	3.08 (10.1)	16 and 17 Aug 15	0.79 (2.6)	1.62 (5.3)	11 Jan 08
Port Isabel, Tex.	1944-70	0.40 <sup>1</sup> (1.3)	0.46 (1.5)	1.16 (3.8)	11 Sept 61	0.43 (1.4)	0.52 (1.7)	31 Dec 56 7 Jan 62

(Continued)

<sup>1</sup>Diurnal Range.

Table 3-6. Highest and lowest water levels (concluded).

Location	Observation Period	Mean Range meters (feet)	Highest Water Levels Above Mean High Water meters (feet)			Lowest Water Levels Below Low Water meters (feet)		
			Average Yearly Highest	Extreme High	Date of Record	Average Yearly Lowest	Extreme Low	Date of Record
PACIFIC COAST <sup>2</sup> San Diego, Calif.	1906-70	1.73 (5.7)	0.55 (1.8)	0.79 (2.6)	20 Dec 68 29 Dec 59	0.61 (2.0)	0.85 (2.8)	17 Dec 33 17 Dec 37
La Jolla, Calif.	1925-53 1956-70	1.58 (5.2)	0.55 (1.8)	0.73 (2.4)	20 Dec 68	0.58 (1.9)	0.79 (2.6)	17 Dec 33
Los Angeles, Calif.	1924-70	1.65 (5.4)	0.55 (1.8)	0.70 (2.3)	19 and 20 Dec 68	0.55 (1.8)	0.79 (2.6)	26 Dec 32 17 Dec 33
Santa Monica, Calif.	1933-70	1.65 (5.4)	0.55 (1.8)	0.64 (2.1)	27 Dec 36 17 and 18 Jul 51	0.55 (1.8)	0.82 (2.7)	17 Dec 33
San Francisco, Calif.	1898-1970	1.73 (5.7)	0.46 (1.5)	0.70 (2.3)	24 Dec 40 19 Jan 69 9 Jan 70	0.64 (2.1)	0.82 (2.7)	26 Dec 32 17 Dec 33
Crescent City, Calif.	1933-46 1950-70	2.10 (6.9)	0.73 (2.4)	0.94 (3.1)	4 Feb 58	0.73 (2.4)	0.88 (2.9)	22 May 55
Astoria, Oreg.	1925-70	2.53 (8.3)	0.79 (2.6)	1.16 (3.8)	17 Dec 33	0.58 (1.9)	0.85 (2.8)	16 Jan 30
Neah Bay, Wash.	1935-70	2.50 (8.2)	0.88 (2.9)	1.25 (4.1)	30 Nov 51	0.94 (3.1)	1.16 (3.8)	29 Nov 36
Seattle, Wash.	1899-1970	3.44 (11.3)	0.67 (2.2)	1.01 (3.3)	6 Feb 04 5 Dec 67	1.19 (3.9)	1.43 (4.7)	4 Jan 16 20 Jun 51
Friday Harbor, Wash.	1934-70	2.35 (7.7)	0.70 (2.3)	0.98 (3.2)	30 Dec 52	0.98 (3.2)	1.22 (4.0)	7 Jan 47
Ketchikan, Alaska	1919-70	4.66 (15.3)	1.34 (4.4)	1.80 (5.9)	2 Dec 67	1.37 (4.5)	1.58 (5.2)	8 Dec 19 16 Jan 57 30 Dec 59
Juneau, Alaska	1936-41 1944-70	5.00 (16.4)	1.52 (5.0)	1.92 (6.3)	2 Nov 48	1.37 (4.5)	1.73 (5.7)	16 Jan 57
Skagway, Alaska	1945-62	5.09 (16.7)	1.49 (4.9)	2.04 (6.7)	22 Oct 45	1.52 (5.0)	1.83 (6.0)	16 Jan 57
Sitka, Alaska	1938-70	3.02 (9.9)	1.04 (3.4)	1.43 (4.7)	2 Nov 48	0.98 (3.2)	1.16 (3.8)	19 Jun 51 16 Jan 57
Yakutat, Alaska	1940-70	3.08 (10.1)	1.13 (3.7)	1.46 (4.8)	2 Nov 48	0.94 (3.1)	1.19 (3.9)	29 Dec 51 16 Jan 57
Seward, Alaska	1925-38	3.23 (10.6)	1.04 (3.4)	1.25 (4.1)	13 Oct 27	1.07 (3.5)	1.28 (4.2)	14 Jan 30
Kodiak Island, Alaska Womens Bay	1949-63	2.68 (8.8)	0.85 (2.8)	1.13 (3.7)	21 Nov 49	0.88 (2.9)	1.10 (3.6)	15 and 16 Jan 57
Unalaska Island, Alaska Dutch Harbor	1934-39 1946-70	1.13 (3.7)	0.61 (2.0)	0.88 (2.9)	14 and 15 Jan 38	0.61 (2.0)	0.82 (2.7)	13 Nov 50
Adak Island, Alaska Sweeper Cove	1943-70	1.13 (3.7) <sup>1</sup>	0.55 (1.8)	0.82 (2.7)	28 Dec 66	0.70 (2.3)	1.01 (3.3)	11 Nov 50
Attu Island, Alaska Massacre Bay	1943-69	1.01 (3.3)	0.49 (1.6)	0.73 (2.4)	6 Jan 66	0.52 (1.7)	0.73 (2.4)	12 and 13 Nov 50

<sup>2</sup> Tsunami levels not included.

(1) Hydrodynamic Equations. Equations that describe the storm surge generation processes are the continuity equation expressing conservation of mass and the equations of motion expressing Newton's second law. The derivations are not presented here; references are cited below. The equations of motion and continuity given here represent a simplification of the more complete equations. A more simplified form is obtained by vertically integrating all governing equations and then expressing everything in terms of either the mean horizontal current velocity or volume transport. Vertically integrated equations are generally preferred in storm surge calculations since interest is centered in the free-surface motion and mean horizontal flow. Integration of the equations for the storm surge problem are given by Haurwitz (1951), Welander (1961), Fortak (1962), Platzman (1963), Reid (1964), and Harris (1967).

The equations given here are obtained by assuming

- (a) Vertical accelerations are negligible
- (b) Curvature of the earth and effects of surface waves can be ignored
- (c) The fluid is inviscid
- (d) The bottom is fixed and impermeable

The notation and the coordinate scheme employed are shown schematically in Figure 3-56.  $D$  is the total water depth at time  $t$ , and is given by  $D = d + S$ , where  $d$  is the undisturbed water depth and  $S$  the height of the free surface above or below the undisturbed depth resulting from the surge. The Cartesian coordinate axes,  $x$  and  $y$ , are in the horizontal plane at the undisturbed water level, and the  $z$  axis is directed positively upward. The  $x$  axis is taken normal to the shoreline (positive in the shoreward direction), and the  $y$  axis is taken alongshore (positive to the left when facing the shoreline from the sea);  $\theta$  is the angle of wind measured counterclockwise from the  $x$  axis;  $W$  is windspeed.

The differential equations appropriate for tropical or extratropical storm surge problems on the open coast and in enclosed and semienclosed basins are as follows:

$$\frac{\partial U}{\partial t} + \underbrace{\frac{\partial M_{xx}}{\partial x} + \frac{\partial M_{xy}}{\partial y}}_{\text{Advection of Momentum}} = \underbrace{fV}_{\text{Coriolis}} - \underbrace{gD \frac{\partial S}{\partial x}}_{\text{Surface Slope}} + \underbrace{gD \frac{\partial \xi}{\partial x}}_{\text{Inverse Barometer}} + \underbrace{gD \frac{\partial \zeta}{\partial x}}_{\text{Astro. Tide Potential}} + \underbrace{\frac{\tau_{sx}}{\rho}}_{\text{Wind Stress}} - \underbrace{\frac{\tau_{bx}}{\rho}}_{\text{Bottom Stress}} + \underbrace{W_x P}_{\text{Rainfall Rate}} \quad (3-77)$$

$$\frac{\partial V}{\partial t} + \frac{\partial M_{yy}}{\partial y} + \frac{\partial M_{xy}}{\partial x} = -fU - gD \frac{\partial S}{\partial y} + gD \frac{\partial \xi}{\partial y} + gD \frac{\partial \zeta}{\partial y} + \frac{\tau_{sy}}{\rho} - \frac{\tau_{by}}{\rho} + W_y P \quad (3-78)$$

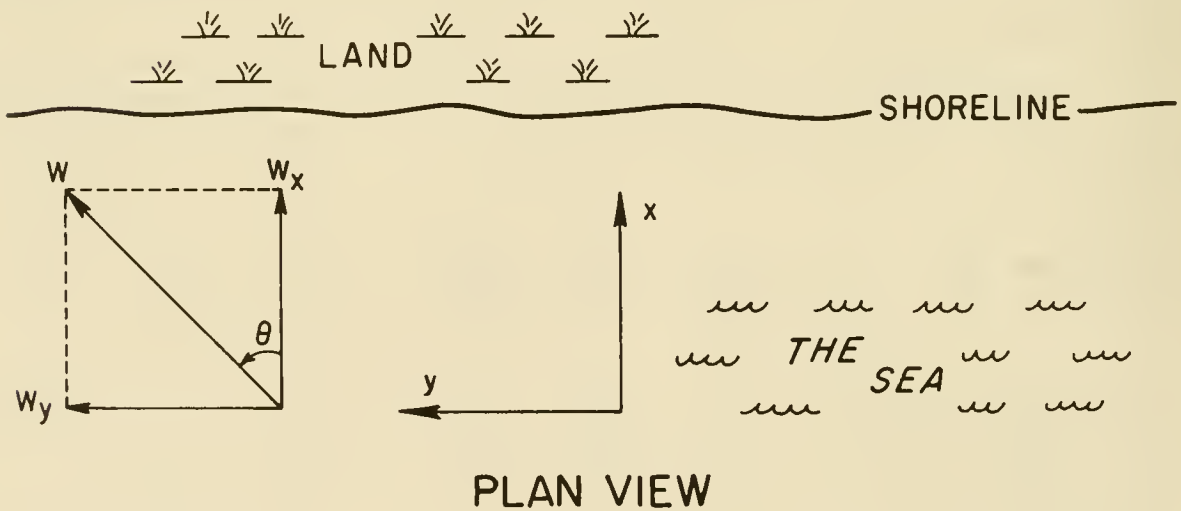
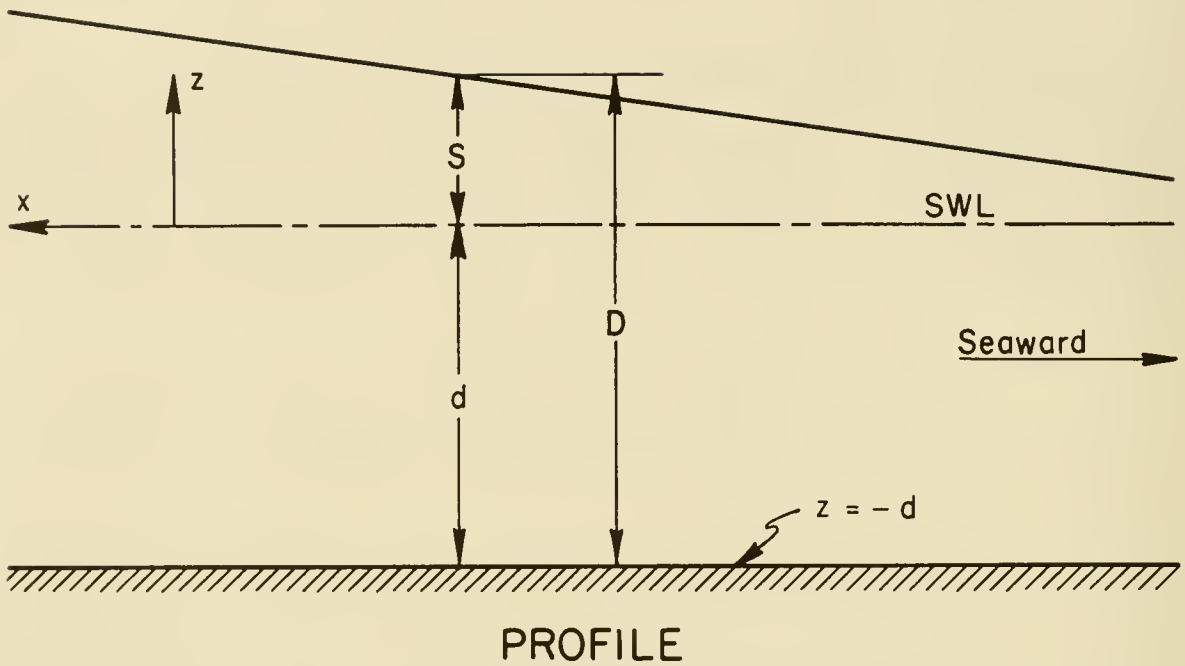


Figure 3-56. Notation and reference frame.

$$\frac{\partial S}{\partial t} + \frac{\partial U}{\partial x} + \frac{\partial V}{\partial y} = P \quad (3-79)$$

where

$$M_{xx} = \int_{-d}^S u^2 dz; \quad M_{yy} = \int_{-d}^S v^2 dz; \quad M_{xy} = \int_{-d}^S uv dz$$

$$U = \int_{-d}^S u dz; \quad V = \int_{-d}^S v dz$$

The symbols are defined as

$U, V$  =  $x$  and  $y$  components, respectively, of the volume transport per unit width

$t$  = time

$M_{xx}, M_{yy}, M_{xy}$  = momentum transport quantities

$f = 2\omega \sin \phi$  = Coriolis parameter

$\omega$  = angular velocity of earth ( $7.29 \times 10^{-5}$  radians per second)

$\phi$  = geographical latitude

$g$  = gravitational acceleration

$\xi$  = atmospheric pressure deficit in head of water

$\zeta$  = astronomical tide potential in head of water

$\tau_{sx}, \tau_{sy}$  =  $x$  and  $y$  components of surface wind stress

$\tau_{bx}, \tau_{by}$  =  $x$  and  $y$  components of bottom stress

$\rho$  = mass density of water

$W_x, W_y$  =  $x$  and  $y$  components of windspeed

$u, v$  =  $x$  and  $y$  components, respectively, of current velocity

$P$  = precipitation rate (depth/time)

Equations (3-77) and (3-78) are approximate expressions for the equations of motion, and equation (3-79) is the continuity relation for a fluid of constant density. These basic equations provide, for all practical purposes, a complete description of the water motions associated with nearly horizontal flows such as the storm surge problem. Since these equations satisfactorily describe the phenomenon involved, a nearly exact solution can be obtained only by using these relations in complete form.

It is possible to obtain useful approximations by ignoring some terms in

the basic equations when they are either equivalent to zero or are negligible, but accurate solutions can be achieved only by retaining the full two-dimensional characteristics of the surge problem. Various simplifications (discussed later) can be made by ignoring some of the physical processes. These simplifications may provide a satisfactory estimate, but it must always be considered as only an approximation.

In the past, simplified methods were used extensively to evaluate storm surge because it was necessary to make all computations manually. Manual solutions of the complete basic equations in two dimensions were prohibitively expensive because of the enormous computational effort. With high-speed computers it is possible to resolve the basic hydrodynamic relations efficiently and economically. As a result of computers, several workers have recently developed useful mathematical models for computing storm surge. These models have substantially improved accuracy and provide a means for evaluating the surge in the two horizontal dimensions. These more accurate methods are not covered here, but they are highly recommended for resolving storm surge problems where more exactness is warranted by the size or importance of the problem. A brief description of these methods and references to them follows.

Solutions to the basic equations given can be obtained by the techniques of numerical integration. The differential equations are approximated by finite differences resulting in a set of equations referred to as the numerical analogs. The finite-difference analogs, together with known input data and properly specified boundary conditions, allow evaluation at discrete points in space of both the fields of transport and water level elevations. Because the equations involve a transient problem, steps in time are necessary; the time interval required for these steps is restricted to a value between a few seconds and a few minutes, depending on the resolution desired and the maximum total water depth. Thus, solutions are obtained by a repetitive process where transport values and water level elevations are evaluated at all prescribed spatial positions for each time level throughout the temporal range.

These techniques have been applied to the study of long wave propagation in various waterbodies by numerous investigators. Some investigations of this type are listed below. Mungall and Matthews (1970) developed a variable boundary, numerical tidal model for a fiord inlet. The problem of surge on the open coast has been treated by Miyazaki (1963), Leendertse (1967), and Jelesnianski (1966, 1967, 1970, 1972, 1974, and 1976). Platzman (1958) developed a model for computing the surge on Lake Michigan resulting from a moving pressure front, and also developed a dynamical wind tide model for Lake Erie (Platzman, 1963). Reid and Bodine (1968) developed a numerical model for computing surges in a bay system, taking into account flooding of adjacent low-lying terrain and overtopping of low barrier islands.

Subsequently, Reid et al. (1977) added embedded channels to the model to simulate rivers and channels in a bay area. An alternative approach to resolving small-scale features such as channels and barriers is provided by the numerical model of Butler (1978a, 1978b, 1978c, 1979).

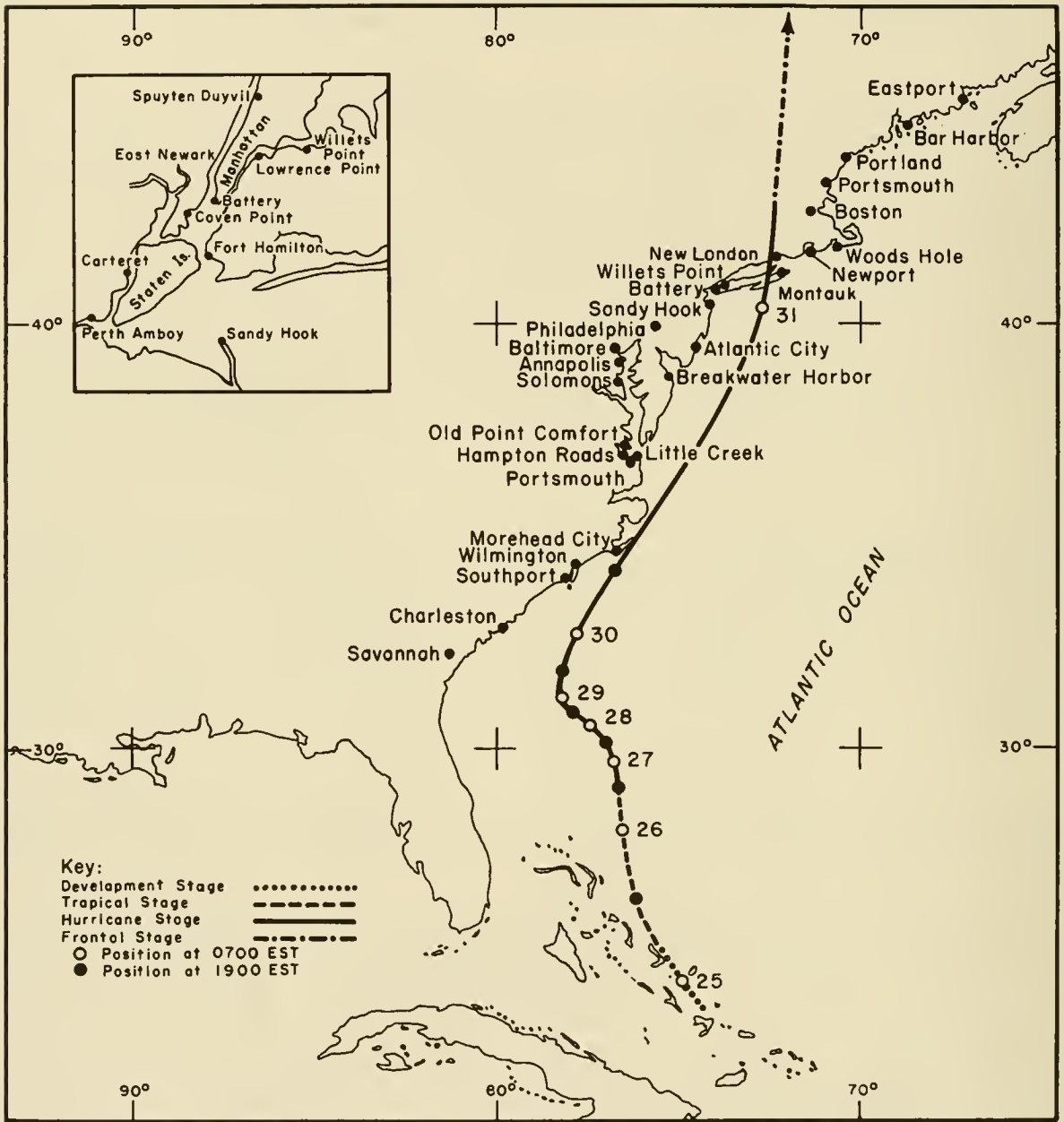
(2) Storm Surge on the Open Coast. Ocean basins are large and deep beyond the shallow waters of the Continental Shelf. The expanse of ocean

basins permits large tropical or extratropical storms to be situated entirely over water areas allowing tremendous energy to be transferred from the atmosphere to the water. Wind-induced surface currents, when moving from the deep ocean to the coast, are impeded by the shoaling bottom; this impediment causes an increase in water level over the Continental Shelf.

Onshore winds cause the water level to begin to rise at the edge of the Continental Shelf. The amount of rise increases shoreward to a maximum level at the shoreline. Storm surge at the shoreline can occur over long distances along the coast. The breadth and width of the surge will depend on the storm's size, intensity, track, and speed of forward motion, as well as the shape of the coastline and the offshore bathymetry. The highest water level, neglecting the contribution of astronomical tide, reached at a location along the coast during the passage of a storm is called the *maximum surge* for that location; the highest maximum surge is called the *peak surge*. Maximum water levels along a coast do not necessarily occur at the same time. The time of the maximum surge at one location may differ by several hours from the maximum surge at another location. The variations of maximum surge values and their times for many locations along the east coast during Hurricane Carol (1954) are shown in Figure 3-57. This hurricane moved a long distance along the coast before making landfall and altered the water levels along the entire east coast. The location of the peak surge relative to the location of the landfall where the eye crosses the shoreline depends on the seabed bathymetry, windfield, configuration of the coastline, and the path the storm takes over the shelf. For hurricanes moving more or less perpendicular to a coast with relatively straight bottom contours, the peak surge will occur close to the point where the region of maximum winds intersects the shoreline, approximately at a distance  $R$  to the right of the storm center. Peak surge is generally used by coastal engineers to establish design water levels at a site.

Attempts to evaluate theoretically storm surge on the open coast and in bays and estuaries require verification. The surge is verified by comparing the theoretical system response and computed water levels with those observed during an actual storm. The comparison is not always simple, because of the lack of field data. Most water level data obtained from past hurricanes were taken from high water marks in low-lying areas some distance inland from the open coast. The few water level recording stations along the open coast are too widely separated for satisfactory verification. Estimates of the water level on the open coast from levels observed at inland locations are unreliable, since corrective adjustments must be made to the data, and the transformation is difficult. An evaluation of certain storm surge models and examples of comparisons between model results and observations are provided by the Committee on Tidal Hydraulics (1980).

Systematic acquisition of hurricane data by a number of organizations and individuals began during the first quarter of this century. Harris (1963) presented water level data and synoptic weather charts for 28 hurricanes occurring from 1926 to 1961. Such data are useful for verifying surge prediction techniques.



(from Harris, 1963)

Figure 3-57. Storm surge chart, Hurricane Carol, 30 and 31 August 1954. (Insert map is for New York Harbor.) (Continued.)

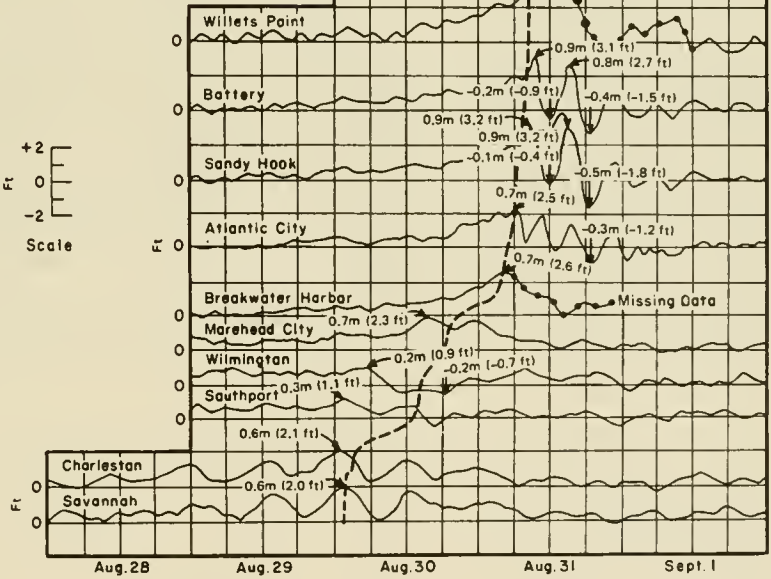
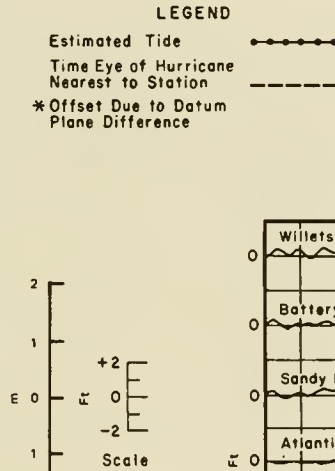
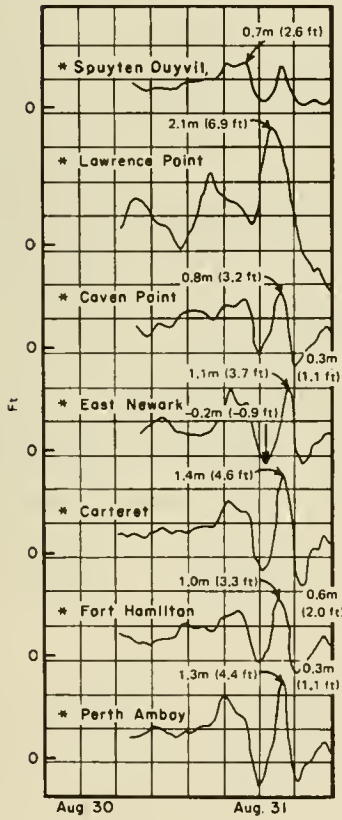
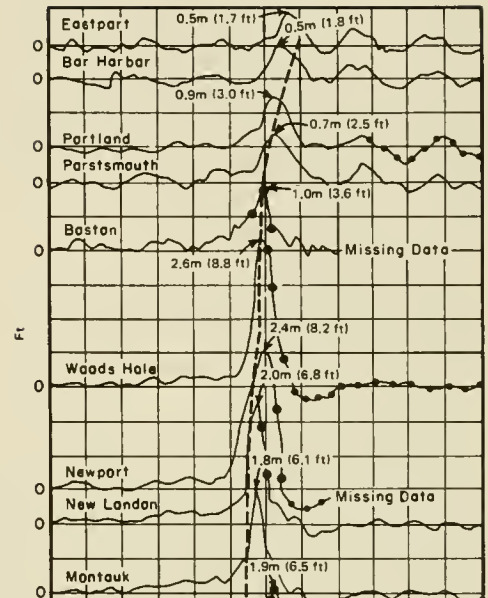
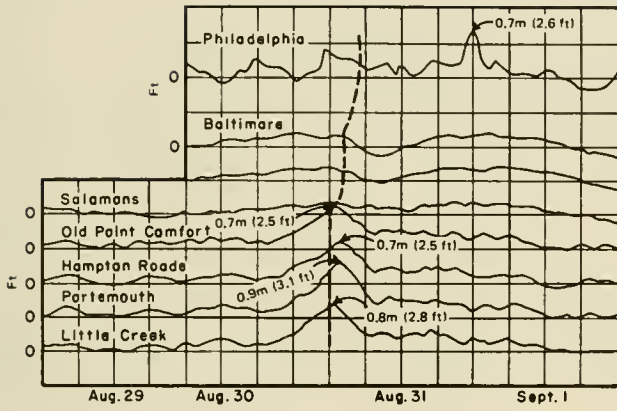


Figure 3-57. (Concluded).

Because of the limited availability of observed hurricane surge data for the open coast, design analysis for coastal structures is not always based on observed water levels. Consequently a statistical approach has evolved that takes into account the expected probability of the occurrence of a hurricane with a specific CPI at any particular coastal location. Statistical evaluations of hurricane parameters, based on detailed analysis of many hurricanes, have been compiled for coastal zones along the Atlantic and gulf coasts of the United States. The parameters evaluated were the radius of maximum wind  $R$ ; the minimum central pressure of the hurricanes  $p_o$ ; the forward speed of the hurricane  $V_F$  while approaching or crossing the coast; and the maximum sustained windspeed  $W$  at 10 meters (33 feet) above the mean water level.

Based on this analysis, the U.S. Weather Bureau (now the National Weather Service) and U.S. Army Corps of Engineers jointly established specific storm characteristics for use in the design of coastal structures. Because the parameters characterizing these storms are specified from statistical considerations and not from observations, the storms are termed *hypothetical hurricanes or hypohurricanes*. The parameters for such storms are assumed constant during the entire surge generation period. Examples of such hypothetical storms are the *Standard Project Hurricane* (SPH) and the *Probable Maximum Hurricane* (PMH) (National Weather Service, 1979). The mathematical model used for predicting the wind and pressure fields in the SPH is discussed in Chapter 3, Section VII,2 (Model Wind and Pressure Fields for Hurricanes). The SPH is defined as a "hypohurricane that is intended to represent the most severe combination of hurricane parameters that is reasonably characteristic of a region excluding extremely rare combinations." Most coastal structures built by the Corps of Engineers that are designed to withstand or protect against hurricanes are based on design water level associated with the SPH.

The construction of nuclear-powered electric generating stations in the coastal zone made necessary the definition of an extreme hurricane, the PMH. The PMH has been adopted for design purposes by the Nuclear Regulatory Commission to ensure public safety and the safety of nuclear-powered facilities. The PMH is defined as "hypothetical hurricane having that combination of characteristics which will make the most severe storm that is reasonably possible in the region involved if the hurricane should approach the point under study along a critical path and at an optimum rate of movement."

(3) Predicting Surge for Storms Other Than Hurricanes. Although the basic equations for water motion in response to atmospheric stresses are equally valid for nonhurricane tropical and extratropical storms, the structure of these storms is not nearly so simple as for hurricanes. Because the storms display much greater variability in structure, it is difficult to derive a standard wind field. Moreover, no system of storm parameters has been developed for these storms, such as has been done for hurricanes using such parameters as radius to maximum winds, forward motion of the storm center, and central pressure.

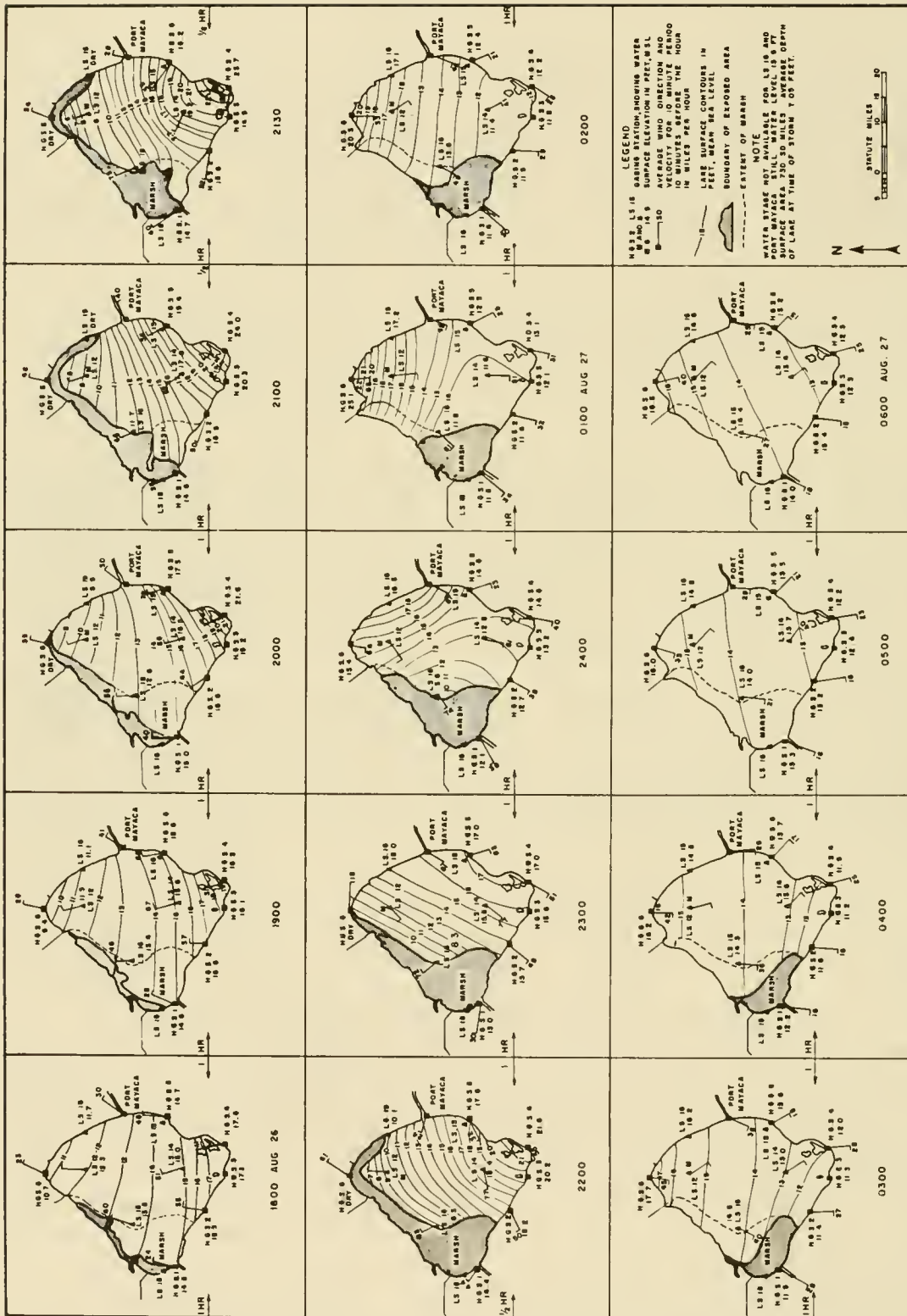
Criteria, however, have been established for a *Standard Project Northeaster* for the New England coast, north of Cape Cod (Peterson and Goodyear 1964). Specific standard project storms other than those for hurricanes are not presently available for other coastal locations. Estimates of design storm wind fields can be made by meteorologists working with climatological weather

maps and statistical wind records on land, assuming that the winds blow toward shore for a significant duration over a long, straight-line fetch. Once the wind field is determined, storm surge may be estimated by using a storm surge model.

(4) Storm Surge in Enclosed Basins. An example of an inclined water surface caused by wind shear stresses over an enclosed body of water occurred during passage of the hurricane of 26-27 August 1949 over the northern part of Lake Okeechobee, Florida. After the lake level was inclined by the wind, the wind direction shifted 180° within 3 hours, resulting in a turning of the height contours of the lake surface. However, the turning of the contours lagged behind the wind so that for a time the wind blew parallel to the water contours instead of perpendicular to them. Contour lines of the lake surface from 1800 hours on 26 August to 0600 hours on 27 August 1949 are shown in Figure 3-58. The map contours for 2300 hours on 26 August show the wind blowing parallel to the highest contours at two locations (Haurwitz, 1951; Saville, 1952; Sibul, 1955; Tickner, 1957; U.S. Army Engineer District, Jacksonville, 1955).

Recorded examples of wind setup on the Great Lakes are available from the U.S. Lake Survey, National Ocean Service, and NOAA. These observations have been used for the development of theoretical methods for forecasting water levels during approaching storms and for the planning and design of engineering works. As a result of the need to predict unusually high stages on the Great Lakes, numerous theoretical investigations have been made of setup for that area (Harris, 1953; Harris and Angelo, 1962; Platzman and Rao, 1963; Jelesnianski, 1958; Irish and Platzman 1962; Platzman, 1958, 1963, 1967).

Selection of hurricane parameters and the methods used for developing overwater windspeeds and directions for various coastal zones of the United States are discussed in detail by the National Weather Service (1979). The basic design storm data should be carefully determined, since errors may significantly affect the final results.



(U.S. Army of E, 1955)

Figure 3-58. Lake surface contours on Lake Okeechobee, Florida, Hurricane on 26 and 27 August 1949.

## LITERATURE CITED

- ARAKAWA, H., and SUDA, K., "Analysis of Winds, Wind Waves, and Swell Over the Sea to the East of Japan During the Typhoon of September 26, 1935," *Monthly Weather Review*, Vol. 81, No. 2, pp. 31-37, Feb. 1953.
- BARNETT, T.P., "On the Generation, Dissipation, and Prediction of Ocean Wind Waves," *Journal of Geophysical Research*, Vol. 73, No. 2, pp. 531-534, 1968.
- BELLAIRE, F.R., "The Modification of Warm Air Moving Over Cold Water," *Proceedings, Eighth Conference on Great Lakes Research*, 1965.
- BORGMAN, L.E., "The Extremal Rayleigh Distribution: A Simple Approximation for Maximum Ocean Wave Probabilities in a Hurricane with Varying Intensity," Stat. Lab Report No. 2004, University of Wyoming, Laramie, Wyo., Jan. 1972.
- BOWEN, A.J., INMAN, D.L., and SIMMONS, V.P., "Wave 'Setdown' and Set-up," *Journal of Geophysical Research*, Vol. 73, No. 8, 1968.
- BRETSCHNEIDER, C.L., "Revised Wave Forecasting Relationships," *Proceedings of the Second Conference on Coastal Engineering*, ASCE, Council on Wave Research, 1952.
- BRETSCHNEIDER, C.L., "Modification of Wave Height Due to Bottom Friction, Percolation, and Refraction," TM-45, U.S. Army Corps of Engineers, Beach Erosion Board, Washington, D.C., Oct. 1954.
- BRETSCHNEIDER, C.L., "Revisions in Wave Forecasting; Deep and Shallow Water," *Proceedings of the Sixth Conference on Coastal Engineering*, ASCE, Council on Wave Research, 1958.
- BRETSCHNEIDER, C.L., "Wave Variability and Wave Spectra for Wind-Generated Gravity Waves," TM-118, U.S. Army Corps of Engineers, Beach Erosion Board, Washington, D.C., Aug. 1959.
- BRETSCHNEIDER, C.L., "A One Dimensional Gravity Wave Spectrum," *Ocean Wave Spectra*, Prentice-Hall, New York, 1963.
- BRETSCHNEIDER, C.L., "A Non-Dimensional Stationary Hurricane Wave Model," *Offshore Technology Conference*, Preprint No. OTC 1517, Houston, Tex., May, 1972.
- BRETSCHNEIDER, C.L., and REID, R.O., "Change in Wave Height Due to Bottom Friction, Percolation and Refraction," *34th Annual Meeting of American Geophysical Union*, 1953.
- BUTLER, H. L., "Numerical Simulation of Tidal Hydrodynamics, Great Egg Harbor and Corson Inlets, New Jersey," Technical Report H-78-11, U.S. Army Engineer Waterways Experiment Station, Vicksburg, Miss., 1978a.
- BUTLER, H. L., "Coastal Flood Simulation in Stretched Coordinates," *Proceedings of the Sixteenth Coastal Engineering Conference*, ASCE, Vol. 1, p. 1030, 1978b.

- BUTLER, H. L., "Numerical Simulation of the Coos Bay-South Slough Complex," Technical Report H-78-22, U.S. Army Engineer Waterways Experiment Station, Vicksburg, Miss., 1978c.
- BUTLER, H. L., "Evolution of a Numerical Model for Simulating Long-Period Wave Behavior in Ocean-Estuarine Systems," in *Estuarine and Wetland Processes, with Emphasis on Modeling*, P. Hamilton and K. B. MacDonald, eds., *Proceedings, Symposium on Estuarine and Wetland Processes and Water Quality Modeling*, New Orleans, La., p. 147, 1979.
- BUNTING, D.C., "Evaluating Forecasts of Ocean-Wave Spectra," *Journal of Geophysical Research*, Vol. 75, No. 21, pp. 4131-4143, 1970.
- BUNTING, D.C., and MOSKOWITZ, L.I., "An Evaluation of a Computerized Numerical Wave Prediction Model for the North Atlantic Ocean," Technical Report No. TR 209, U.S. Naval Oceanographic Office, Washington, D.C., 1970.
- CAMFIELD, F.E., "Wind-Wave Propagation Over Flooded, Vegetated Land," Technical Paper No. 77-12, Coastal Engineering Research Center, U.S. Army Engineer Waterways Experiment Station, Vicksburg, Miss., 1977.
- CAMFIELD, F. E., "Tsunami Engineering," Special Report No. 6, Coastal Engineering Research Center, U.S. Army Engineer Waterways Experiment Station, Vicksburg, Miss., 1980.
- CARDONE, V. J., "Specification of Wind Distribution in the Marine Boundary Layer for Wave Forecasting," Technical Report No. 69-1, Geophysical Sciences Laboratory, New York University, N.Y., 1969.
- CARDONE, V. J., et al., "A Unified Program for the Specification of Hurricane Boundary Layer Winds Over Surfaces of Specified Roughness," U.S. Army Engineer Waterways Experiment Station, Vicksburg, Miss., 1969.
- CHEN, H. S., and MEI, C. C., "Oscillations and Wave Forces in an Offshore Harbor (Applications of the Hybrid Finite Element Method to Wave-Wave Scattering)," Report No. 190, MIT, Cambridge, Mass., 1974.
- CHRISTAL, G., "On the Hydrodynamical Theory of Seiches, with a Bibliographical Sketch," *Transactions of the Royal Society of Edinburgh*, Robert Grant and Son, London, Vol. XLI, Part 3, No. 25, 1905.
- COLLINS, J.I., and VIEHMAN, M.J., "A Simplified Empirical Model for Hurricane Wind Fields," *Offshore Technology Conference*, Vol. 1, Preprints, Houston, Tex., Apr. 1971.
- COMMITTEE ON TIDAL HYDRAULICS, "Evaluation of Numerical Storm Surge Models," Technical Bulletin No. 21, Office, Chief of Engineers, U.S. Army, Washington, D.C., 1980.
- DEAN, R. G., "Evaluation and Development of Water Wave Theories for Engineering Application", Special Report No. 1, Coastal Engineering Research Center, U.S. Army Engineer Waterways Experiment Station, Vicksburg, Miss., 1973.

- DEFANT, A., *Physical Oceanography*, Vol. 2, Pergamon Press, New York, 598 pp., 1961.
- DOODSON, A.T., and WARBURG, H.D., *Admiralty Manual of Tides*, Her Majesty's Stationery Office, London, 270 pp., 1941.
- DORRESTEIN, R., "Wave Setup on a Beach," *Proceedings, Second Technical Conference on Hurricanes*, National Hurricane Research Report No. 50, pp. 230-241, 1962.
- DUNN, G.E., and MILLER, B.I., *Atlantic Hurricanes*, Rev. ed., Louisiana State University Press, New Orleans, 1964.
- EARLE, M. D., "Extreme Wave Conditions During Hurricane Camille", *Journal of Geophysical Research*, Vol. 80, No. 3, 1975.
- EWING, J. A., "The Generation and Propagation of Sea Waves," *Dynamic Waves in Civil Engineering*, Wiley, New York, pp. 43-56, 1971.
- EWING, M., PRESS, F., and DONN, W.L., "An Explanation of the Lake Michigan Wave of 26 June 1954," *Science*, Vol. 120, pp. 684-686, 1954.
- FAIRCHILD, J.C., "Model Study of Wave Setup Induced by Hurricane Waves at Narragansett Pier, Rhode Island," *The Bulletin of the Beach Erosion Board*, Vol. 12, pp. 9-20, July 1958.
- FEUILLET, J., and SABATON, M., "Stability of Rubble Mound Breakwater," *Proceedings of the 17th Conference on Coastal Engineering*, Sydney, Australia, 1980.
- FORTAK, H., "Concerning the General Vertically Averaged Hydrodynamic Equations with Respect to Basic Storm Surge Equations," National Hurricane Research Project, Report No. 51, U.S. Weather Bureau, Washington, D.C., 1962.
- GALVIN, C.J., JR., and EAGLESON, P.S., "Experimental Study of Longshore Currents on a Plane Beach," TM-10, Coastal Engineering Research Center, U.S. Army Engineer Waterways Experiment Station, Vicksburg, Miss., Jan. 1965.
- GODA, Y., "Irregular Wave Deformation in the Surf Zone," *Coastal Engineering in Japan*, Vol. 18, pp. 13-26, 1975.
- GOODKNIGHT, R.C., and RUSSELL, T.L., "Investigation of the Statistics of Wave Heights," *Journal of the Waterways and Harbors Division*, ASCE, Vol. 89, No. WW2, Proc. Paper 3524, pp. 29-54, May 1963.
- GROSSKOPF, W.G., and VINCENT, C.L., "Energy Losses of Waves in Shallow Water", CETA-82-2, Coastal Engineering Research Center, U.S. Army Engineer Waterways Experiment Station, Vicksburg, Miss., 1982.
- GUTHRIE, R.C., "A Study of Ocean Wave Spectra for Relation to Ships Bending Stresses," Informal Report No. IR 71-12, U.S. Naval Oceanographic Office, Washington, D.C., 1971.

- HARRIS, D.L., "Wind Tide and Seiches in the Great Lakes," *Proceedings of the Fourth Conference on Coastal Engineering*, ASCE, pp. 25-51, 1953.
- HARRIS, D.L., "The Effect of a Moving Pressure Disturbance on the Water Level in a Lake," *Meteorological Monographs*, Vol. 2, No. 10, "Interaction of Sea Atmosphere: a Group of Contributions," pp. 46-57, 1957.
- HARRIS, D.L., "Meteorological Aspects of Storm Surge Generation," *Journal of the Hydraulics Division*, ASCE, No. HY7, Paper 1859, 25 pp, 1958.
- HARRIS, D.L., "Wave Patterns in Tropical Cyclones," *Mariners Weather Log*, Vol. 6, No. 5, pp. 156-160, Sept. 1962.
- HARRIS, D.L., "Characteristics of the Hurricane Storm Surge," Technical Paper No. 48, U.S. Dept. of Commerce, Washington, D.C., 1963.
- HARRIS, D.L., "A Critical Survey of the Storm Surge Protection Problem," *The 11th Symposium of Tsunami and Storm Surges*, pp. 47-65, 1967.
- HARRIS, D.L., "The Analysis of Wave Records," *Proceedings of the 12th Coastal Engineering Conference*, ASCE, Washington, D.C., 1970.
- HARRIS, D.L., "Characteristics of Wave Records in the Coastal Zone," Unpublished Manuscript, Coastal Engineering Research Center, U.S. Army Engineer Waterways Experiment Station, Vicksburg, Miss., 1971.
- HARRIS, D.L., "Tides and Tidal Datums in the United States," Special Report SR-7, Coastal Engineering Research Center, U.S. Army Engineer Waterways Experiment Station, Vicksburg, Miss. 1981.
- HARRIS, D.L., and ANGELO, A.T., "A Regression Model for the Prediction of Storm Surges on Lake Erie," *Proceedings, Fifth Conference on Great Lakes Research*, Toronto, 1962.
- HASSELMANN, K., "On the Nonlinear Energy Transfer in a Gravity-Wave Spectrum--General Theory," *Journal of Fluid Mechanics*, Vol. 12, Part 1, pp. 481-500, 1962.
- HASSELMANN, K., BARNETT, T. P., BONWS, E., CARLSON, H., CARTWRIGHT, D.C., ENKE, K., EWING, J., GIENAPP, H., HASSELMANN, D.E., KRUSEMAN, P., MEERBURG, A., MULLER, P., OLBERS, D. J., RICHTER, K., SELL, W., and WALDEN, H., "Measurements of Wind-Wave Growth and Swell Decay During the Joint North Sea Wave Project (JONSWAP), Deutsches Hydrographisches Institut, Hamburg, 95 pp., 1973.
- HASSELMANN, K., ROSS, D. B., MULLER, P., and SELL, W., "A Parametric Wave Prediction Model," *Journal of Physical Oceanography*, Vol. 6, pp. 200-228, 1976.
- HAURWITZ, B., "The Slope of Lake Surfaces under Variable Wind Stresses," TM-25, U.S. Army Corps of Engineers, Beach Erosion Board, Washington, D.C., Nov. 1951.

- HO, F. P., SCHWERDT, R. W., and GOODYEAR, H. V., "Some Climatological Characteristics of Hurricanes and Tropical Storms, Gulf and East Coasts of the United States, NOAA Technical Report NWS 15, 1975.
- HOTTA, S., and MIZUGUCHI, M., "A Field Study of Waves in the Surf Zone", *Coastal Engineering in Japan*, Vol. 23, 1980.
- HUNT, I.A., "Design of Seawalls and Breakwaters," *Proceedings, American Society of Civil Engineers*, ASCE, Waterways and Harbors Division, Vol. 85, No. WW3, Sept. 1959.
- HWANG, L., and DIVOKY, D., "Breaking Wave Setup and Decay on Gentle Slopes," *Proceedings of the 12th Coastal Engineering Conference*, ASCE, Vol. 1, 1970.
- IJIMA, T., and TANG, F.L.W., "Numerical Calculation of Wind Waves in Shallow Water," *Proceedings of 10th Conference on Coastal Engineering*, ASCE, Tokyo, Vol. 2, pp. 38-45, 1962.
- INOUE, T., "On the Growth of the Spectrum of a Wind Generated Sea According to a Modified Miles-Phillips Mechanism," Geophysical Sciences Laboratory Report No. TR-66-6, Department of Meteorology and Oceanography, New York University, N.Y., 1966.
- INOUE, T., "On the Growth of the Spectrum of a Wind Generated Sea According to a Modified Miles-Phillips Mechanism and its Application to Wave Forecasting," Geophysical Sciences Laboratory Report No. TR-67-5, Department of Meteorology and Oceanography, New York University, N.Y., 1967.
- IPPEN, A.T., "Estuary and Coastline Hydrodynamics," *Engineering Societies Monographs*, McGraw-Hill, New York, 1966.
- IRISH, S.M., and PLATZMAN, G.W., "An Investigation of the Meteorological Conditions Associated with Extreme Wind Tides on Lake Erie," *Monthly Weather Review*, Vol. 90, pp. 39-47, 1962.
- JAMES, I.D., "Non-Linear Waves in the Nearshore Region: Shoaling and Setup," *Estuarine and Coastal Marine Science*, Vol. 2, pp. 207-234, 1974.
- JELESNIANSKI, C.P., "The July 6, 1954, Water Wave on Lake Michigan Generated by a Pressure Jump Passage," Unpublished Master of Science Thesis, 1958.
- JELESNIANSKI, C.P., "Numerical Computations of Storm Surges Without Bottom Stress," *Monthly Weather Review*, Vol. 94, No. 6, pp. 379-394, 1966.
- JELESNIANSKI, C.P., "Numerical Computations of Storm Surges with Bottom Stress," *Monthly Weather Review*, Vol. 95, No. 11, pp. 740-756, 1967.
- JELESNIANSKI, C.P., "Bottom Stress Time-History in Linearized Equations of Motion of Storm Surges," *Monthly Weather Review*, Vol. 98, No. 6, pp. 462-478, 1970.

- JELESNIANSKI, C.P., "SPLASH (Special Program to List Amplitudes of Surges from Hurricanes); Part II: General Track and Variant Storm Conditions," NOAA Technical Memorandum NWS TDL-52, National Weather Service, Silver Spring, Md., 1972.
- JELESNIANSKI, C.P., "A Sheared Coordinate System for Storm Surge Equations of Motions with a Mildly Curved Coast," NOAA Technical Memorandum NWS TDL-61, National Weather Service, Silver Spring, Md., 1976.
- KINSMAN, B., *Wind Waves*, Prentice-Hall, Englewood Cliffs, N.J., 1965.
- LAPLACE, P.S., "Recherches sur plusieurs points du systeme du monde," *Memoirs, Academy of Royal Sciences*, Vol. 88, pp. 75-185, 1775.
- LEENDERTSE, J.J., "Aspects of a Computational Model for Long-Period Water Wave Propagation," Memorandum RM-5294-PR, prepared for U.S. Air Force, Project Rand, 1967.
- LONGUET-HIGGINS, M.S., and STEWART, R.W., "Changes in the Form of Short-Gravity Waves on Long Waves and Tidal Currents," *Journal of Fluid Mechanics*, Vol. 8, No. 565, 1960.
- LONGUET-HIGGINS, M.S., and STEWART, R.W., "Radiation Stress and Mass Transport in Gravity Waves, with Application to Surf Beat," *Journal of Fluid Mechanics*, Vol. 13, pp. 481-504, 1962.
- LONGUET-HIGGINS, M.S., and STEWART, R.W., "A Note on Wave Setup," *Journal of Marine Research*, Vol. 21(1), pp. 4-10, 1963.
- LONGUET-HIGGINS, M.S., and STEWART, R.W., "Radiation Stress in Water Waves; A Physical Discussion with Application," *Deep-Sea Research*, Vol. 11, pp. 529-562, 1964.
- McBRIDE, John L., *Journal of Atmospheric Sciences*, Parts I, II, III, Vol. 38, No. 6., pp. 1117-1166, June 1981.
- MILES, J.W., "On the Generation of Surface Waves by Shear Flows," *Journal of Fluid Mechanics*, Vol. 3, pp. 185-204, 1957.
- MILLAR, Banner I., "Characteristics of Hurricanes", *Science Magazine*, Sept. 22, 1967.
- MITSUYASU, H., "On the Growth of the Spectrum of Wind-Generated Waves (I)," Reports of the Research Institute of Applied Mechanics, Kyushu University, Fukuoka, Japan, Vol. 16, No. 55, pp. 459-482., 1968.
- MIYAZAKI, M., "A Numerical Computation of the Storm Surge of Hurricane Carla 1961 in the Gulf of Mexico," Technical Report No. 10, Department of Geophysical Sciences, University of Chicago, Chicago, Ill., 1963.
- MORTIMER, C.H., "Spectra of Long Surface Waves and Tides in Lake Michigan and at Green Bay, Wisconsin," *Proceedings, Eighth Conference on Great Lakes Research*, 1965.

- MUNGALL, J.C.H., and MATTHEWS, J.B., "A Variable-Boundary Numerical Tidal Model," Report No. R70-4, Office of Naval Research, Arlington, Va., 1970.
- MUNK, W.H., "Proposed Uniform Procedure for Observing Waves and Interpreting Instrument Records," Wave Project, Scripps Institute of Oceanography, LaJolla, Calif., 1944.
- MURTY, T. S., "Seismic Sea Waves--Tsunamis," Bulletin 198, Department of Fisheries and the Environment, Fisheries and Marine Service, Ottawa, Canada, 1977.
- MYERS, V.A., "Characteristics of United States Hurricanes Pertinent to Levee Design for Lake Okeechobee, Florida," Hydrometeorological Report No. 32, U.S. Weather Bureau, Washington, D.C., 1954.
- NATIONAL WEATHER SERVICE, "Meteorological Criteria for Standard Project Hurricane and Probable Maximum Hurricane Windfields, Gulf and East Coasts of the United States," NOAA Technical Report NWS 23, 1979.
- PETERSON, K.R., and GOODYEAR, H.V., "Criteria for a Standard Project Northeaster for New England North of Cape Cod," National Hurricane Research Project, Report No. 68, National Weather Service, Washington, D.C., 1964.
- PHILLIPS, O.M., "On the Generation of Waves by Turbulent Wind," *Journal of Fluid Mechanics*, Vol. 2, pp. 417-445, 1957.
- PIERSON, W.J., JR., and MOSKOWITZ, L., "A Proposed Spectral Form for Fully Developed Wind Seas Based on the Similarity Theory of S.A. Kitaigorodskii," *Journal of Geophysical Research*, Vol. 69, No. 24, pp. 5181-5190, 1964.
- PIERSON, W.J., JR., NEUMANN, G., and JAMES, R.W., "Practical Methods for Observing and Forecasting Ocean Waves by Means of Wave Spectra and Statistics," Publication No. 603, U.S. Navy Hydrographic Office, Washington, D.C., 1955.
- PLATZMAN, G.W., "A Numerical Computation of the Surge of 26 June 1954 on Lake Michigan," *Geophysics*, Vol. 6, 1958.
- PLATZMAN, G.W., "The Dynamic Prediction of Wind Tides on Lake Erie," *Meteorological Monographs*, Vol. 4, No. 26, 44 pp., 1963.
- PLATZMAN, G.W., "The Prediction of Surges in the Southern Basin of Lake Michigan," Part I, "The Dynamical Basis for Prediction," *Monthly Weather Review*, Vol. 93, pp. 275-281, 1965.
- PLATZMAN, G.W., "A Procedure for Operational Prediction of Wind Setup on Lake Erie," Technical Report to Environmental Science Services Administration, National Weather Service, 1967.
- PLATZMAN, G.W., "Two-Dimensional Free Oscillations in National Basins," *Journal of Physical Oceanography*, Vol. 2, pp. 117-138, 1972.
- PLATZMAN, G.W., and RAO, D.B., "Spectra of Lake Erie Water Levels," *Journal of Geophysical Research*, Vol. 69, pp. 2525-2535, Oct. 1963.

- PLATZMAN, G.W., and RAO, D.B., "The Free Oscillations of Lake Erie," *Studies on Oceanography*, University of Washington Press, Seattle, Wash., pp. 359-382, 1965.
- PORE, N.A., "Ocean Surface Waves Produced by Some Recent Hurricanes," *Monthly Weather Review*, Vol. 85, No. 12, pp. 385-392, Dec. 1957.
- PORE, N.A., and CUMMINGS, R.A., "A Fortran Program for the Calculation of Hourly Values of Astronomical Tide and Time and Height of High and Low Water," Technical Memorandum WBTM TDL-6, U.S. Department of Commerce, Environmental Science Services Administration, Washington, D.C., 1967.
- PREISENDORFER, R. W., "Recent Tsunami Theory", NOAA-JTRE-60, HIG-71-15, Hawaii Institute of Geophysics, University of Hawaii, Honolulu, 1971.
- PUTNAM, J.A., "Loss of Wave Energy Due to Percolation in a Permeable Sea Bottom," *Transactions of the American Geophysical Union*, Vol. 30, No. 3, pp. 349-357, 1949.
- PUTNAM, J.A., and JOHNSON, J.W., "The Dissipation of Wave Energy by Bottom Friction," *Transactions of the American Geophysical Union*, Vol. 30, No. 1, pp. 67-74, 1949.
- REID, R.O., "Short Course on Storm Surge," Summer Lectures, Texas A&M University, College Station, Tex., 1964.
- REID, R.O., and BODINE, B.R., "Numerical Model for Storm Surges, Galveston Bay," *Journal of the Waterways and Harbors Division*, ASCE, Vol. 94, No. WW1, Proc. Paper 5805, pp. 33-57, 1968.
- REID, R. O., VASTANO, A. C., and REID, T. J., "Development of Surge II Program with Application to the Sabine-Calcasieu Area for Hurricane Carla and Design Hurricanes," Technical Paper 77-13, Coastal Engineering Research Center, U. S. Army Engineer Waterways Experiment Station, Vicksburg, Miss., 1977.
- RESIO, D. T., "The Estimation of Wind Wave Generation in a Discrete Model," *Journal of Physical Oceanography*, Vol. 11, pp. 510-525, 1981.
- RESIO, D. T., and VINCENT, C. L., "Estimation of Winds Over the Great Lakes," MP H-76-12, U.S. Army Engineer Waterways Experiment Station, Vicksburg, Miss., 1976.
- RESIO, D. T., and VINCENT, C. L., "A Numerical Hindcast Model for Wave Spectra on Water Bodies with Irregular Shoreline Geometry; Report 1: Test of Non-dimensional Growth Rates," Miscellaneous Paper H-77-9, U.S. Army Engineer Waterways Experiment Station, Vicksburg, Miss., 1977a.
- RESIO, D. T., and VINCENT, C. L., "Estimation of Winds Over the Great Lakes," *Journal of the Waterway, Port, Coastal and Ocean Division, Proceedings of the American Society of Civil Engineers*, Vol. 103, No. WW2, p. 265, 1977b.
- RESIO, D. T., and VINCENT, C. L., "A Comparison of Various Numerical Wave Prediction Techniques," *Proceedings of the 11th Annual Ocean Technology Conference*, Houston, Tex., p. 2471, 1979.

- ROCKWELL, D.C., "Theoretical Free Oscillations of the Great Lakes," *Proceedings, Ninth Conference on Great Lakes Research*, pp. 352-368, 1966.
- ROLL, H.U., and FISHER, F., "Eine Kritische Bemerkung zum Neumann-Spektrum des Seeganges," *Deut. Hydrograph. Z.*, Vol. 9, No. 9, 1956.
- SAVAGE, R.P., "Model Tests of Wave Runup for the Hurricane Protection Project," *The Bulletin of the Beach Erosion Board*, Vol. 11, pp. 1-12, July 1957.
- SAVILLE, T., JR., "Wind Setup and Waves in Shallow Water," TM-27, U.S. Army Corps of Engineers, Beach Erosion Board, Washington, D.C., June 1952.
- SAVILLE, T., JR., "Experimental Determination of Wave Setup," *Proceedings, Second Technical Conference on Hurricanes*, National Hurricane Research Project, Report No. 50, pp. 242-252. 1961.
- SCHUREMAN, P., "Manual of Harmonic Analysis and Prediction of Tides," Special Publication No. 98, U.S. Department of Commerce, National Ocean Service, NOAA, Washington, D.C., 1941.
- SHIELDS, G. C., and BURDWELL, G. B., "Western Region Sea State and Surf Forecasters Manual," Technical Memorandum WR-51, National Weather Service, NOAA, 1970.
- SIBUL, O., "Laboratory Study of Wind Tides in Shallow Water," TM-61, U.S. Army Corps of Engineers, Beach Erosion Board, Washington, D.C., Aug. 1955.
- SILVESTER, R., and VONGVISESSOMJAI, S., "Computation of Storm Waves and Swell," *The Institution of Civil Engineers*, Vol. 48, pp. 259-283, 1971.
- SIMIU, E., and SCANLAN, R. N., "Wind Effect on Structures: An Introduction to Wind Engineering," New York, Wiley, p. 62, 1978.
- SIMPSON, R.B., and ANDERSON, D.V., "The Periods of the Longitudinal Surface Seiche of Lake Ontario," *Proceedings, Seventh Conference on Great Lakes Research*, 1964.
- SVERDRUP, H.U., JOHNSON, M.W., and FLEMING, R.H., *The Oceans; Their Physics, Chemistry, and General Biology*; Prentice-Hall, New York, 1942.
- SVERDRUP, H.U., and MUNK, W.H., "Wind, Sea, and Swell: Theory of Relations for Forecasting," Publication No. 601, U.S. Navy Hydrographic Office, Washington, D.C., Mar. 1947.
- SYMONS, T. M., and ZELTER, B. D., "The Tsunami of May 22, 1960, as Recorded at Tide Stations, Preliminary Report," U.S. Department of Commerce, National Ocean Service, NOAA, Washington, D.C., 1960.
- THOMPSON, E. F., "Wave Climate at Selected Locations Along U.S. Coasts", TR 77-1, Coastal Engineering Research Centers, U.S. Army Engineer Waterways Experiment Station, Vicksburg, Miss., 1977.

- THOMPSON, E. F., "Interpretation of Wave Energy Spectra, CETA 80-5, U.S. Army Engineer Waterways Experiment Station, Vicksburg, Miss., 1980.
- THOMPSON, E. F., and SEELIG, W. N., "High Wave Grouping in Shallow Water," submitted to *Journal of the Waterway, Port, Coastal and Ocean Division*, ASCE, 1982.
- TICKNER, E.G., "Effect of Bottom Roughness on Wind Tide in Shallow Water," TM-95, U.S. Army Corps of Engineers, Beach Erosion Board, Washington, D.C., May 1957.
- U.S. ARMY ENGINEER DISTRICT, JACKSONVILLE, "Waves and Wind Tides in Shallow Lakes and Reservoirs, Summary Report, Project CW-167," South Atlantic-Gulf Region, Jacksonville, Fla., 1955.
- U.S. ARMY ENGINEER DIVISION, MISSOURI RIVER, "Concepts for Surface Wind Analysis and Record Velocities," Technical Bulletin No. 1 (CW-178), Omaha, Nebraska, 1959.
- WELANDER, P., "Numerical Prediction of Storm Surges," *Advances in Geophysics*, Vol. 8, pp. 316-379, 1961.
- WILSON, B.W., "Graphical Approach to the Forecasting of Waves in Moving Fetches," TM-73, U.S. Army Corps of Engineers, Beach Erosion Board, Washington, D.C., Apr. 1955.
- WILSON, B.W., "Deep Water Wave Generations by Moving Wind Systems," *Journal of the Waterways and Harbors Division*, ASCE, Vol. 87, No. WW2, Proc. Paper 2821, pp. 113-141, May 1961.

## BIBLIOGRAPHY

- ABBOTT, M.B., *An Introduction to the Method of Characteristics*, American Elsevier, New York, 1966, 243 pp.
- BAER, J., "An Experiment in Numerical Forecasting of Deep Water Ocean Waves," Lockheed Missile and Space Co., Sunnyvale, Calif., 1962.
- BATES, C.C., "Utilizations of Wave Forecasting in the Invasions of Normandy, Burma, and Japan," *Annals of the New York Academy of Sciences*, Vol. 51, Art. 3, "Ocean Surface Waves," 1949, pp. 545-572.
- BELLAIRE, F.R., "The Modification of Warm Air Moving Over Cold Water," *Proceedings, Eighth Conference on Great Lakes Research*, 1965.
- BODINE, B.R., "Storm Surge on the Open Coast: Fundamentals and Simplified Prediction," TM-35, U.S. Army Corps of Engineers, Coastal Engineering Research Center, Washington, D.C., May 1971.
- BODINE, B.R., HERCHENRODER, B.E., and HARRIS, D.L., "A Numerical Model for Calculating Storm Surge in a Long Narrow Basin with a Variable Cross Section," U.S. Army Corps of Engineers, Coastal Engineering Research Center, Washington, D.C., 1972.
- BRETSCHNEIDER, C.L., "Revised Wave Forecasting Curves and Procedures," Unpublished Manuscript, Institute of Engineering Research, University of California, Berkeley, Calif., 1951.
- BRETSCHNEIDER, C.L., "The Generation and Decay of Wind Waves in Deep Water," *Transactions of the American Geophysical Union*, Vol. 33, 1952b, pp. 381-389.
- BRETSCHNEIDER, C.L., "Hurricane Design-Wave Practice," *Journal of the Waterways and Harbors Division*, ASCE, Vol. 83, WW2, No. 1238, 1957.
- BRETSCHNEIDER, C.L., "Investigation of the Statistics of Wave Heights," *Journal of the Waterways and Harbors Division*, ASCE, Vol. 90, No. WW1, 1964, pp. 153-166.
- BRETSCHNEIDER, C.L., "Generation of Waves by Wind; State of the Art," Report SN-134-6, National Engineering Science Co., Washington, D.C., 1965.
- BRETSCHNEIDER, C.L., Department of Ocean Engineering, University of Hawaii, Honolulu, Hawaii, Consultations, 1970-71.
- BRETSCHNEIDER, C.L., and COLLINS, J.I., "Prediction of Hurricane Surge; An Investigation for Corpus Christi, Texas and Vicinity," Technical Report No. SN-120, National Engineering Science Co., Washington, D.C., 1963 (for U.S. Army Engineer District, Galveston, Tex.).
- CHRYSAL, G., "Some Results in the Mathematical Theory of Seiches," *Proceedings of the Royal Society of Edinburgh*, Session 1903-04, Robert Grant and Son, London, Vol. XXV, Part 4, 1904, pp. 328-337.

- COLE, A.L., "Wave Hindcasts vs Recorded Waves," Supplement No. 1 to Final Report 06768, Department of Meteorology and Oceanography, University of Michigan, Ann Arbor, Mich., 1967.
- CONNER, W.C., KRAFT, R.H., and HARRIS, D.L., "Empirical Methods of Forecasting the Maximum Storm Tide Due to Hurricanes and Other Tropical Storms," *Monthly Weather Review*, Vol. 85, No. 4, Apr. 1957, pp. 113-116.
- COX, D.C., ed., *Proceedings of the Tsunami Meetings Associated with the 10th Pacific Science Congress*, Honolulu, Hawaii, 1961.
- DARWIN, G.H., *The Tides and Kindred Phenomena in the Solar System*, W.H. Freeman, San Francisco, 1962, 378 pp.
- DAWSON, W. BELL, "The Tides and Tidal Streams," Department of Naval Services, Ottawa, 1920.
- DEFANT, A., "Gezeitlichen Probleme des Meeres in Landnähe," *Probleme der Kosmischen Physik*, VI, Hamburg, 1925.
- DEFANT, A., *Ebbe und Flut des Meeres, der Atmosphäre, und der Erd feste*, Springer, Berlin-Göttingen-Heidelberg, 1953.
- DRAPER, L., "The Analysis and Presentation of Wave Data--A Plea for Uniformity," *Proceedings of the 10th Conference on Coastal Engineering*, ASCE, New York, 1967.
- FRANCIS, G.W., "Weather Routing Procedures in the United States," *The Marine Observer*, Vol. XLI, No. 232, Apr. 1971.
- FREEMAN, J.C., JR., BAER, L., and JUNG, C.H., "The Bathystrophic Storm Tide," *Journal of Marine Research*, Vol. 16, No. 1, 1957.
- GRAHAM, H.E., and NUNN, D.E., "Meteorological Considerations Pertinent to Standard Project Hurricane, Atlantic and Gulf Coasts of the United States," National Hurricane Research Project, Report No. 33, U.S. Weather Bureau, Washington, D.C., 1959.
- GROVES, G.W., *McGraw-Hill Encyclopedia of Science and Technology*, McGraw-Hill, New York, 1960, pp. 632-640.
- HARRIS, R.A., "Currents, Shallow-Water Tides, Meteorological Tides, and Miscellaneous Matters," *Manual of Tides*, Part V, App. 6, Superintendent of the Coast and Geodetic Survey, Washington, D.C., 1907.
- HARRIS, D.L., "An Interim Hurricane Storm Surge Forecasting Guide," National Hurricane Research Project, Report No. 32, U.S. Weather Bureau, Washington, D.C., 1959.
- HARRIS, D.L., "Coastal Flooding by the Storm of March 5-7, 1962," Presented at the American Meteorological Society Annual Meeting, Unpublished Manuscript, U.S. Weather Bureau, 1963.

- HASSE, L., and WAGNER, V., "On the Relationship Between Geostrophic and Surface Wind at Sea," *Monthly Weather Review*, Vol. 99, No. 4, Apr. 1971, pp. 255-260.
- HELLSTROM, B., "Wind Effects on Lakes and Rivers," Nr. 158, Handlingar, Ingeniors Vetenskaps Akadamen, Stockholm, 1941.
- HIDAKA, K., "A Theory of Shelf Seiches, and Seiches in a Channel," *Memoirs of the Imperial Marine Observatory*, Kobe, Japan, 1934-35.
- HIDY, G.M., and PLATE, E.J., "Wind Action on Water Standing in a Laboratory Channel," *Journal of Fluid Mechanics*, Vol. 25, 1966, pp. 651-687.
- HONDA, K., et al., "Secondary Undulations of Oceanic Tides," *Journal, College of Science*, Imperial University, Tokyo, Japan, Vol. 24, 1908.
- IRISH, S.M., "The Prediction of Surges in the Southern Basin of Lake Michigan, Part II, A Case Study of the Surge of August 3, 1960," *Monthly Weather Review*, Vol. 93, 1965, pp. 282-291.
- ISAACS, J.D., and SAVILLE, T., JR., "A Comparison Between Recorded and Forecast Waves on the Pacific Coast," *Annals of the New York Academy of Sciences*, Vol. 51, Art. 3, "Ocean Surface Waves," 1949, pp. 502-510.
- JACOBS, S.L., "Wave Hindcasts vs. Recorded Waves," Final Report 06768, Department of Meteorology and Oceanography, University of Michigan, Ann Arbor, Mich., 1965.
- KAPLAN, K., "Analysis of Moving Fetches for Wave Forecasting," TM-35, U.S. Army Corps of Engineers, Beach Erosion Board, Washington, D.C., Mar. 1953.
- KAPLAN, K., and SAVILLE, T., JR., "Comparison of Hindcast and Observed Waves Along the Northern New Jersey Coast for the Storm of Nov. 6-7, 1953," *The Bulletin of the Beach Erosion Board*, Vol. 8, No. 3, July 1954, pp. 13-17.
- KEULEGAN, G.H., "Wind Tides in Small Closed Channels," *Journal of Research*, National Bureau of Standards, RP2207, Vol. 46, No. 5, 1951.
- KRECKER, F.H., "Periodic Oscillations in Lake Erie," Contribution No. 1, Franz Theodore Stone Laboratory, Ohio State University Press, Columbus, Ohio, 1928.
- MARINOS, G., and WOODWARD, J.W., "Estimation of Hurricane Surge Hydrographs," *Journal of the Waterways and Harbors Division*, ASCE, Vol. 94, WW2, Proc. Paper 5945, 1968, pp. 189-216.
- MARMER, H.A., *The Tide*, D. Appleton, New York, 1926, 282 pp.
- MASCH, F.D., et al., "A Numerical Model for the Simulation of Tidal Hydrodynamics in Shallow Irregular Estuaries," Technical Report HYD 12,6901 Hydraulic Engineering Laboratory, University of Texas, Austin, Tex., 1969.

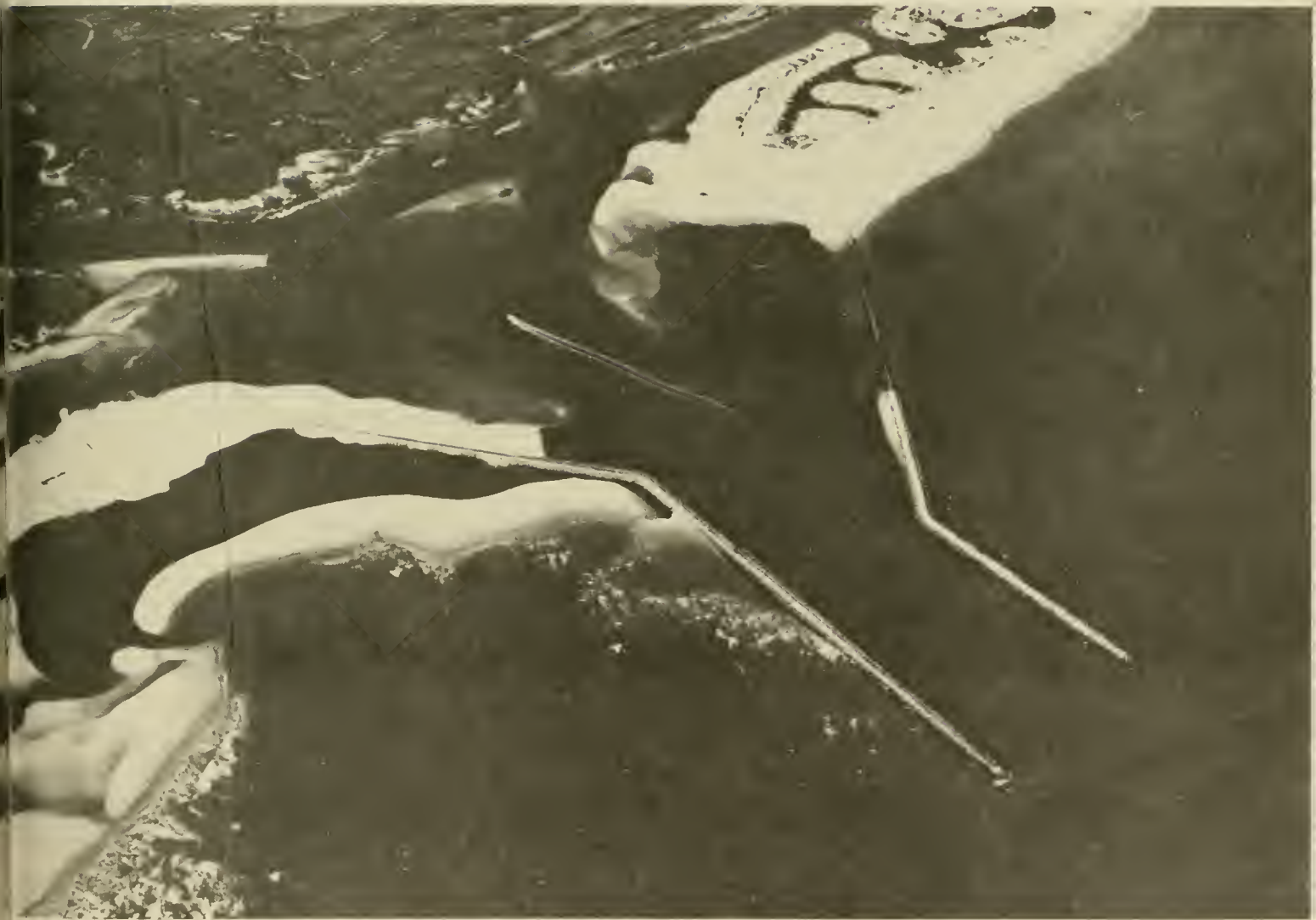
- MOSKOWITZ, L., "Estimates of the Power Spectrums for Fully Developed Seas for Wind Speeds of 20 to 40 Knots," *Journal of Geophysical Research*, Vol. 69, No. 24, 1964, pp. 5161-5179.
- NATIONAL WEATHER SERVICE, "Meteorological Characteristics of the Probable Maximum Hurricane, Atlantic and Gulf Coasts of the United States," Hurricane Research Interim Report, HUR 7-97 and HUR 7-97A, U.S. Weather Bureau, Washington, D.C., 1968.
- NATIONAL WEATHER SERVICE, "Preliminary Analysis of Surface Wind Field and Sea-Level Pressures of Hurricane Camille (August 1969)," Hurricane Research Report, HUR 7-113, U.S. Weather Bureau, Washington, D.C., 1969.
- NATIONAL WEATHER SERVICE, "Revised Surface Wind Field (30 ft) of Hurricane Camille in Gulf of Mexico (August 1969)," Hurricane Research Report, HUR 7-113A, U.S. Weather Bureau, Washington, D.C., 1970.
- NATIONAL WEATHER SERVICE, "Synoptic Code," WB-242, U.S. Weather Bureau, Washington, D.C., 1949.
- PATTERSON, M.M., "Hindcasting Hurricane Waves in the Gulf of Mexico," *Offshore Technology Conference*, Houston, Tex., Preprint, Vol. 1, 1971.
- PORE, N.A., and RICHARDSON, W.S., "Second Interim Report on Sea and Swell Forecasting," Technical Memorandum TDL-17, National Weather Service, 1969.
- PREISENDORFER, R.W., "Recent Tsunami Theory," NOAA-JTRE-60, HIG-71-15, Hawaii Institute of Geophysics, University of Hawaii, Honolulu, Hawaii 1971.
- PROUDMAN, J., and DOODSON, A.T., "Tides in Oceans Bounded by Meridians," *Philosophical Transactions of the Royal Society* (London), Parts I and II, Vol. 235, No. 753, 1936, pp. 273-342; Part III, Vol. 237, No. 779, 1938, pp. 311-373.
- RICHARDS, T.L., DRAGERT, H., and MacINTYRE, D.R., "Influence of Atmospheric Stability and Over-Water Fetch on Winds Over the Lower Great Lakes," *Monthly Weather Review*, Vol. 94, No. 1, 1966, pp. 448-453.
- SAVILLE, T., JR., "The Effect of Fetch Width on Wave Generation," TM-70, U.S. Army Corps of Engineers, Beach Erosion Board, Washington, D.C., Dec. 1954.
- SENER, P.K., "Design of Proposed Crescent City Harbor, California, Tsunami Model," Report H-71-2, U.S. Army Engineer Waterways Experiment Station, Vicksburg, Miss., 1971.
- TUCKER, M.J., "Simple Measurement of Wave Records," *Proceedings of the Conference on Wave Recording for Civil Engineers*, National Institute of Oceanography, 1961.
- U.S. ARMY CORPS OF ENGINEERS, "Shore Protection, Planning and Design," Technical Report No. 4, 3rd ed., Coastal Engineering Research Center, Washington, D.C., 1966.

- U.S. ARMY CORPS OF ENGINEERS, "Hilo Harbor, Hawaii: Report on Survey for Tidal Wave Protection and Navigation," Hawaii Region, Engineer District, Honolulu, Hawaii, 1960.
- U.S. ARMY CORPS OF ENGINEERS, "Waves in Inland Reservoirs, (Summary Report on Civil Works Investigation Projects CW-164 & CW-165)," TM-132, Beach Erosion Board, Washington, D.C., Nov. 1962.
- U.S. DEPARTMENT OF COMMERCE, COAST AND GEODETIC SURVEY, "Annotated Bibliography on Tsunamis," International Union of Geodesy and Geophysics, Paris, 1964.
- U.S. DEPARTMENT OF COMMERCE, NATIONAL OCEANIC AND ATMOSPHERIC ADMINISTRATION, *Tide Tables, East Coast, North and South America*, National Ocean Survey, Rockville, Md., 1973.
- U.S. DEPARTMENT OF COMMERCE, NATIONAL OCEANIC AND ATMOSPHERIC ADMINISTRATION, *Tide Tables, West Coast, North and South America*, National Ocean Survey, Rockville, Md., 1973.
- U.S. FLEET WEATHER FACILITY, "Forecasting Ocean Waves and Surf," U.S. Naval Air Station, Oceanographic Services Section, Operations Department, San Diego, Calif., 1966.
- U.S. NAVAL WEATHER SERVICE COMMAND, "Summary of Synoptic Meteorological Observations, North American Coastal Marine Areas," Vols. 1-10, 1970.
- VAN DORN, W.C., "Wind Stress on an Artificial Pond, *Journal of Marine Research*, Vol. 12, 1953.
- VERMA, A.P., and DEAN, R.G., "Numerical Modeling of Hydromechanics of Bay Systems," *Proceedings of the Conference on Civil Engineering in the Oceans II*, ASCE, 1969.
- WIEGEL, R.L., *Oceanographical Engineering*, Prentis-Hall, Englewood Cliffs, N.J., 1964.
- WILSON, B.W., "Hurricane Wave Statistics for the Gulf of Mexico," TM-98, U.S. Army Corps of Engineers, Beach Erosion Board, Washington, D.C., June, 1957.
- WILSON, B.W., "Propagation and Run-up of Tsunami Waves," National Engineering Science Co., Washington, D.C., 1964.
- WILSON, B.W., "Design Sea and Wind Conditions for Offshore Structures," *Proceedings of Offshore Exploration Conference*, Long Beach, Calif., 1966, pp. 665-708.
- WILSON, B.W., WEB, L.M., and HENDRICKSON, J.A., "The Nature of Tsunamis, Their Generation and Dispersion in Water of Finite Depth," National Engineering Science Co., Washington, D.C., 1962.



# CHAPTER 4

## Littoral Processes



*Murrells Inlet, 3 January 1981*



# CONTENTS

## CHAPTER 4

### LITTORAL PROCESSES

	Page
I INTRODUCTION.....	4-1
1. Definitions.....	4-1
2. Environmental Factors.....	4-1
3. Changes in the Littoral Zone.....	4-6
II LITTORAL MATERIALS.....	4-12
1. Classification.....	4-12
2. Sand and Gravel.....	4-21
3. Cohesive Materials.....	4-21
4. Consolidated Material.....	4-23
5. Occurrence of Littoral Materials on U. S. Coasts.....	4-24
6. Sampling Littoral Materials.....	4-26
7. Size Analyses.....	4-27
III LITTORAL WAVE CONDITIONS.....	4-29
1. Effect of Wave Conditions on Sediment Transport.....	4-29
2. Factors Determining Littoral Wave Climate.....	4-29
3. Nearshore Wave Climate.....	4-31
4. Office Study of Wave Climate.....	4-40
5. Effect of Extreme Events.....	4-43
IV NEARSHORE CURRENTS.....	4-46
1. Wave-Induced Water Motion.....	4-46
2. Fluid Motion in Breaking Waves.....	4-49
3. Onshore-Offshore Exchange.....	4-49
4. Longshore Currents.....	4-50
5. Summary.....	4-55
V LITTORAL TRANSPORT.....	4-55
1. Introduction.....	4-55
2. Onshore-Offshore Transport.....	4-65
3. Longshore Transport Rate.....	4-89
VI ROLE OF FOREDUNES IN SHORE PROCESSES.....	4-108
1. Background.....	4-108
2. Role of Foredunes.....	4-108
VII SEDIMENT BUDGET.....	4-113
1. Introduction.....	4-113
2. Sources of Littoral Materials.....	4-115
3. Sinks for Littoral Materials.....	4-120
4. Convection of Littoral Materials.....	4-126
5. Relative Change in Sea Level.....	4-126
6. Summary of Sediment Budget.....	4-126

CONTENTS--Continued

	Page
VIII ENGINEERING STUDY OF LITTORAL PROCESSES.....	4-133
1. Office Study.....	4-133
2. Field Study.....	4-142
3. Sediment Transport Calculations.....	4-146
IX TIDAL INLETS.....	4-148
1. Geomorphology of Tidal Inlets.....	4-148
2. Circulation Patterns at Tidal Inlets.....	4-157
3. Inlet Currents.....	4-161
4. Inlet Migration and Stabilization Effects on Adjacent Shorelines.....	4-167
5. Littoral Material Trapping at Inlets.....	4-173
6. Channel Shoaling and Dredging Effects.....	4-177
X LITERATURE CITED.....	4-182
XI BIBLIOGRAPHY.....	4-208

TABLES

4-1 Seasonal profile changes on southern California beaches.....	4-10
4-2 Density of littoral materials.....	4-18
4-3 Minerals occurring in beach sand.....	4-22
4-4 Mean significant wave height and period at coastal localities of the United States.....	4-37
4-5 Factors influencing erosion caused by storms.....	4-44
4-6 Storm-induced beach changes.....	4-77
4-7 Longshore transport rates from U. S. coasts.....	4-91
4-8 Values of parameters in equation 4-35.....	4-92
4-9 Longshore energy flux, $P_{\ell}$ , for a single periodic wave in any specified depth.....	4-94
4-10 Approximate formulas for computing longshore energy flux factor, $P_{\ell S}$ , entering the surf zone.....	4-94
4-11 Assumptions for $P_{\ell S}$ formulas in Table 4-10.....	4-95
4-12 Deepwater wave heights, in percent by direction, of east-facing coast of inland sea.....	4-102
4-13 Computed longshore transport for east-facing coast of inland sea.....	4-102

CONTENTS--Continued

	Page
4-14 Example estimate of gross longshore transport rate for shore of inland sea.....	4-107
4-15 Classification of elements in the littoral zone sediment budget.....	4-114
4-16 Sand budget of the littoral zone.....	4-128

FIGURES

4-1 Typical profile changes with time, Westhampton Beach, New York.....	4-2
4-2 Three types of shoreline.....	4-3
4-3 Shoreline erosion near Shipbottom, New Jersey.....	4-7
4-4 Stable shoreline near Peahala, New Jersey.....	4-8
4-5 Shoreline accretion and erosion near Beach Haven, New Jersey.....	4-9
4-6 Fluctuations in location of mean sea level shoreline on seven east coast beaches.....	4-11
4-7 Grain-size scales (soil classification).....	4-13
4-8 Example size distribution.....	4-16
4-9 Fall velocity versus buoyancy index for an isolated sphere or common natural grain.....	4-20
4-10 Approximate value of power $n$ relating to equation (4-9) for fall velocity in concentrated suspensions of spheres and common grains.....	4-20
4-11 Sand size distribution along the U. S. Atlantic coast.....	4-25
4-12 Annual variation in storm occurrence for Atlantic City, New Jersey, based on hindcast wave data.....	4-32
4-13 Seasonal variation in storm occurrence for Atlantic City, New Jersey, based on hindcast wave data.....	4-33
4-14 Annual distribution of the 761 recorded Atlantic tropical cyclones reaching at least tropical storm strength and the 448 reaching hurricane strength, 1886 through 1977.....	4-34
4-15 Number of tropical storms and hurricanes and hurricanes alone observed on each day, May 1-December 30, 1886 through 1977.....	4-34

CONTENTS--Continued

	Page
4-16 Smoothed frequency of landfalling tropical storms and hurricanes (1871 through 1973) for the gulf and east coasts of the United States.....	4-35
4-17 Mean monthly nearshore wave heights for five coastal segments.....	4-38
4-18 Mean monthly nearshore wave periods for five coastal segments.....	4-38
4-19 Distribution of number of simultaneous wave trains from wave gages in three coastal segments.....	4-39
4-20 Distribution of significant wave heights from coastal wave gages for 1-year records.....	4-41
4-21 Nearshore current system near La Jolla Canyon, California.....	4-51
4-22 Typical rip currents, Ludlam Island, New Jersey.....	4-52
4-23 Distribution of longshore current velocities.....	4-53
4-24 Measured versus predicted longshore current speed.....	4-56
4-25 Coasts in vicinity of New York Bight.....	4-57
4-26 Three scales of profiles, Westhampton, Long Island.....	4-61
4-27 Unit volume change versus time between surveys for profiles on south shore of Long Island.....	4-64
4-28 Distribution of grain sizes along transects of the Virginia-North Carolina coast.....	4-67
4-29 Maximum bottom velocity from small-amplitude theory.....	4-68
4-30 Comparison of vertical sequences from low-energy Georgia coast and high-energy California coast.....	4-72
4-31 Location and characteristics of beaches included in Table 4-6.....	4-79
4-32 Effects of four storms on the beach and nearshore at a profile line south of CERC's Field Research Facility in Duck, North Carolina.....	4-81
4-33 Slow accretion of ridge-and-runnel at Crane Beach, Massachusetts...4-82	4-82
4-34 Rapid accretion of ridge-and-runnel at Lake Michigan.....	4-84
4-35 Data, trends, median grain size versus foreshore slope.....	4-87
4-36 Data, median grain size versus foreshore slope.....	4-88

CONTENTS--Continued

	Page
4-37 Design curve for longshore transport rate versus energy flux factor.....	4-97
4-38 Longshore transport rate as a function of breaker height and breaker angle.....	4-98
4-39 Longshore transport rate as a function of deepwater height and deepwater angle.....	4-99
4-40 Upper limit on longshore transport rates.....	4-106
4-41 Typical barrier island profile shape.....	4-109
4-42 Frequency per 100 years that the stated water level is equalled or exceeded on the open coast, South Padre Island, Texas.....	4-111
4-43 Basic example of sediment budget.....	4-116
4-44 Erosion within littoral zone during uniform retreat of an idealized profile.....	4-118
4-45 Sediment trapped inside Old Drum Inlet, North Carolina.....	4-121
4-46 Overwash on Portsmouth Island, North Carolina.....	4-122
4-47 Growth of a spit into deep water, Sandy Hook, New Jersey.....	4-123
4-48 Dunes migrating inland near Laguna Point, California.....	4-125
4-49 Materials budget for the littoral zone.....	4-127
4-50 Summary of example problem conditions and results.....	4-131
4-51 Growth of Sandy Hook, New Jersey, 1835-1932.....	4-135
4-52 Transport directions at New Buffalo Harbor Jetty on Lake Michigan.....	4-136
4-53 Sand accumulation at Point Mugu, California.....	4-137
4-54 Tombolo and pocket beach at Greyhound Rock, California.....	4-138
4-55 Nodal zone of divergence illustrated by sand accumulation at groins, south shore, Staten Island, New York.....	4-139
4-56 South shore of Long Island, New York, showing closed, partially closed, and open inlets.....	4-140
4-57 Four types of barrier island offset.....	4-141

CONTENTS--Continued

	Page
4-58 Fire Island Inlet, New York: overlapping offset.....	4-142
4-59 Old Drum Inlet, North Carolina: negligible offset.....	4-143
4-60 Ebb-tidal delta showing volumes accumulated in outer shoals adjacent to Boca Grande Inlet, Florida.....	4-149
4-61 Typical ebb-tidal delta morphology.....	4-150
4-62 Bathymetry off the Merrimack River Inlet, Massachusetts.....	4-151
4-63 Old Drum Inlet, about 10 kilometers north of Cape Hatteras, North Carolina.....	4-153
4-64 Measurement of channel parameters.....	4-154
4-65 Measurement of ebb delta area.....	4-154
4-66 Minimum width cross-sectional area of channel $A_G$ versus channel length $L$ .....	4-155
4-67 $A_G$ versus ebb-tidal delta area.....	4-155
4-68 $A_G$ versus maximum channel depth at minimum width section DMX.....	4-156
4-69 $A_G$ versus minimum controlling channel depth DCC.....	4-156
4-70 Tidal prism versus cross-sectional area for all inlets on Atlantic, gulf, and Pacific coasts.....	4-158
4-71 Variations in cross-sectional area for Wachapreague Inlet.....	4-159
4-72 Schematic diagram of flood and ebb currents outside an inlet.....	4-159
4-73 Wave refraction patterns in vicinity of Merrimack River Estuary entrance just south of the Merrimack Inlet.....	4-160
4-74 Sea-inlet-bay system.....	4-161
4-75 Dimensionless maximum velocity versus $K_1$ and $K_2$ .....	4-163
4-76 Ratio of bay to sea tidal amplitude versus $K_1$ and $K_2$ .....	4-163
4-77 Mean high water shoreline changes at Redfish Pass, 1929-1967.....	4-168
4-78 Large-scale inlet migration at the Monomoy-Nauset Inlet, Cape Cod, Massachusetts, 1846-1965.....	4-169
4-79 Inlet changes at Hampton Harbor, New Hampshire, 1776-1931.....	4-169

CONTENTS--Continued

	Page
4-80 Shoreline changes at Barnegat Inlet, New Jersey.....	4-170
4-81 Short-term shoreline change, Brown Cedar Cut, Texas.....	4-171
4-82 Erosion and accretion patterns between 1902 and 1907 at St. Mary's River entrance, Florida.....	4-172
4-83 Accretion and erosion over a 100-year period at St. Mary's River entrance, Florida.....	4-173
4-84 Steps in calculation of accumulated volume of sand in the outer bar for an idealized inlet.....	4-175
4-85 Deposition of sand in the interior of St. Lucie Inlet Florida.....	4-176
4-86 Idealized stages of deposition in a tidal lagoon if the inlets open simultaneously and remain stationary.....	4-178
4-87 Mass dredging curve for Pensacola Inlet, Florida.....	4-179
4-88 Mass dredging curve for East Pass, Florida.....	4-179



## CHAPTER 4

### LITTORAL PROCESSES

#### I. INTRODUCTION

Littoral processes result from the interaction of winds, waves, currents, tides, sediments, and other phenomena in the littoral zone. This chapter discusses those littoral processes which involve sediment motion. Shores erode, accrete, or remain stable, depending on the rates at which sediment is supplied to and removed from the shore. Excessive erosion or accretion may endanger the structural integrity or functional usefulness of a beach or of other coastal structures. Therefore, an understanding of littoral processes is needed to predict erosion or accretion effects and rates. A common aim of coastal engineering design is to maintain a stable shoreline where the volume of sediment supplied to the shore balances that which is removed. This chapter presents information needed for understanding the effects of littoral processes on coastal engineering design.

##### 1. Definitions.

In describing littoral processes, it is necessary to use clearly defined terms. Commonly used terms, such as "beach" and "shore," have specific meanings in the study of littoral processes, as shown in the Glossary (see App. A).

a. Beach Profile. Profiles perpendicular to the shoreline have characteristic features that reflect the action of littoral processes (see Fig. 1-1, Ch. 1, and Figs. A-1 and A-2 of the Glossary for specific examples). At any given time, a profile may exhibit only a few specific features; however, a dune, berm, and beach face can usually be identified.

Profiles across a beach adapt to imposed wave conditions as illustrated in Figure 4-1 by a series of profiles taken between February 1963 and November 1964 at Westhampton Beach, New York. The figure shows how the berm built up gradually from February through August 1963, cut back in November through January, and then rebuilt in March through September 1964. This process is typical of a cyclical process of storm-caused erosion in winter, followed by progradation owing to the lower, and often longer, waves in summer.

b. Areal View. Figure 4-2 shows three generalized charts of different U.S. coastal areas, all to the same scale: 4-2a shows a rocky coast, well-indented, where sand is restricted to local pocket beaches; 4-2b a long straight coast with an uninterrupted sand beach; and 4-2c short barrier islands interrupted by inlets. These are some of the different coastal configurations which reflect differences in littoral processes and the local geology.

##### 2. Environmental Factors.

a. Waves. The action of waves is the principal cause of most shoreline changes. Without wave action on a coast, most of the coastal engineering

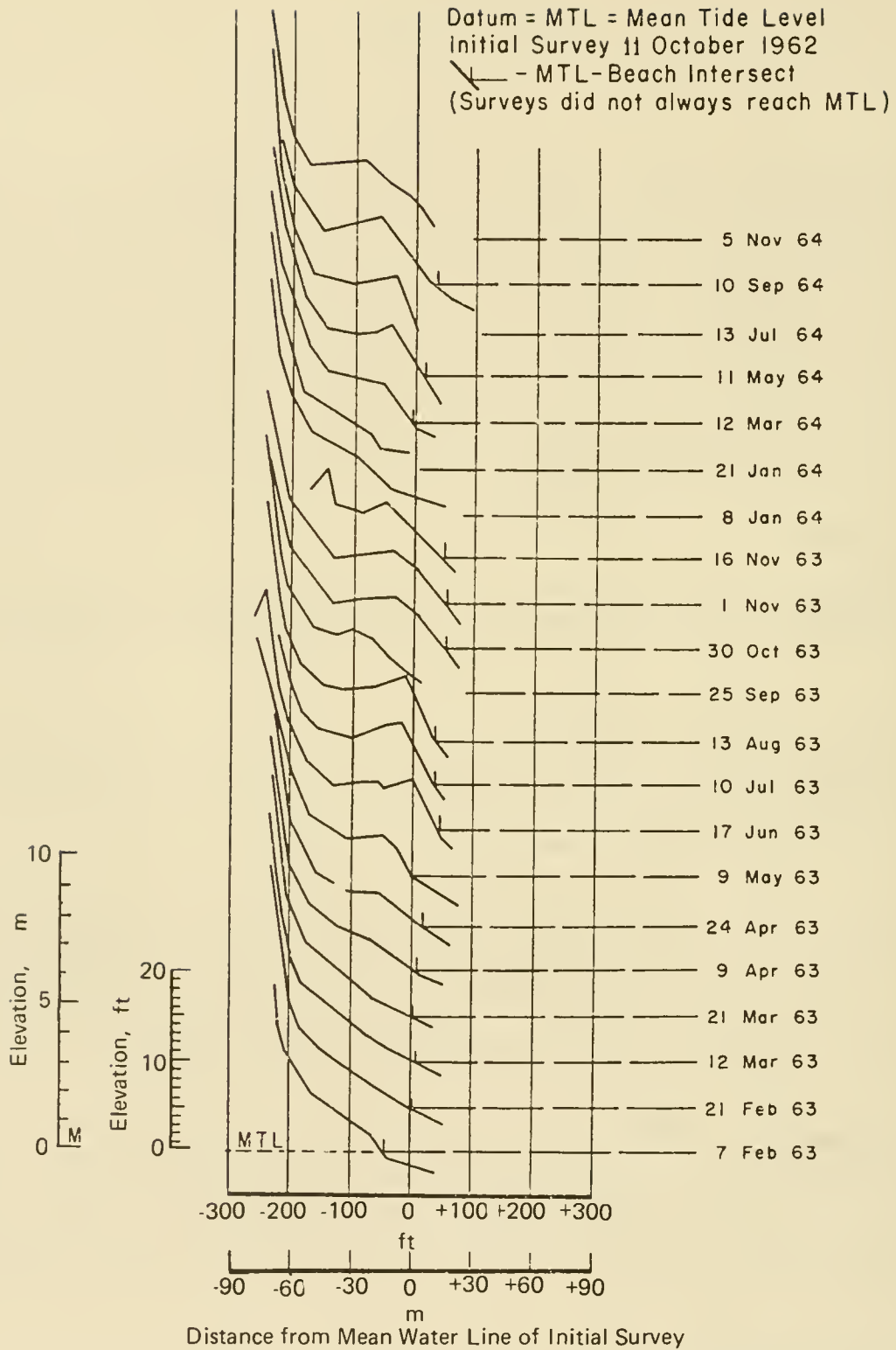
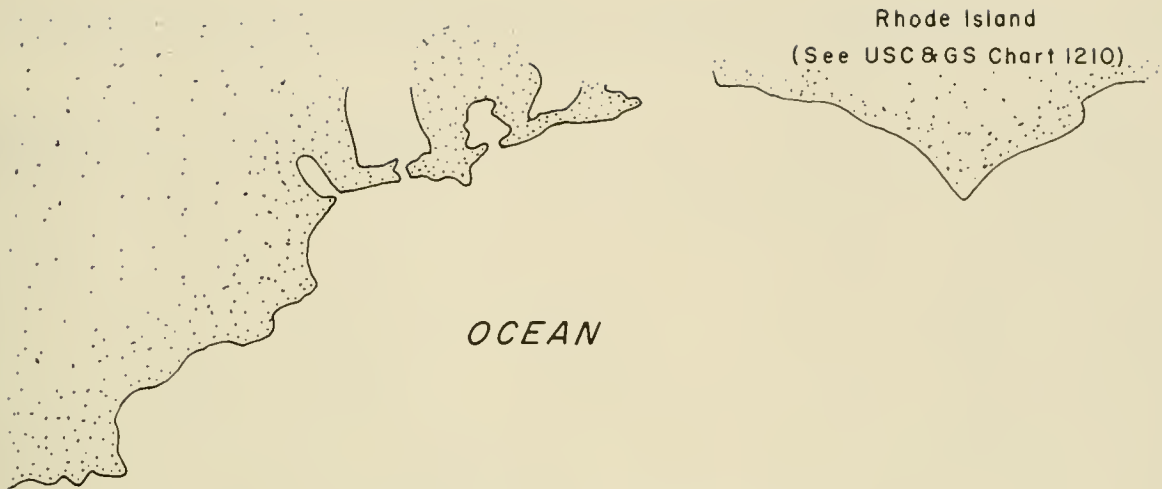
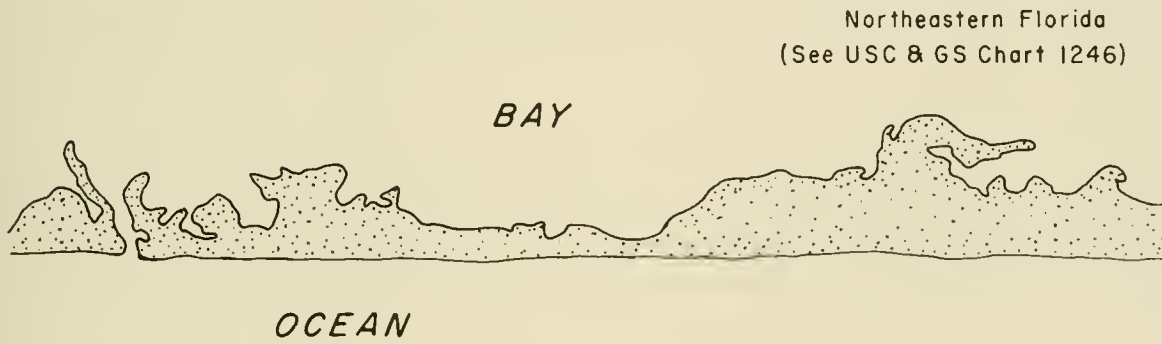


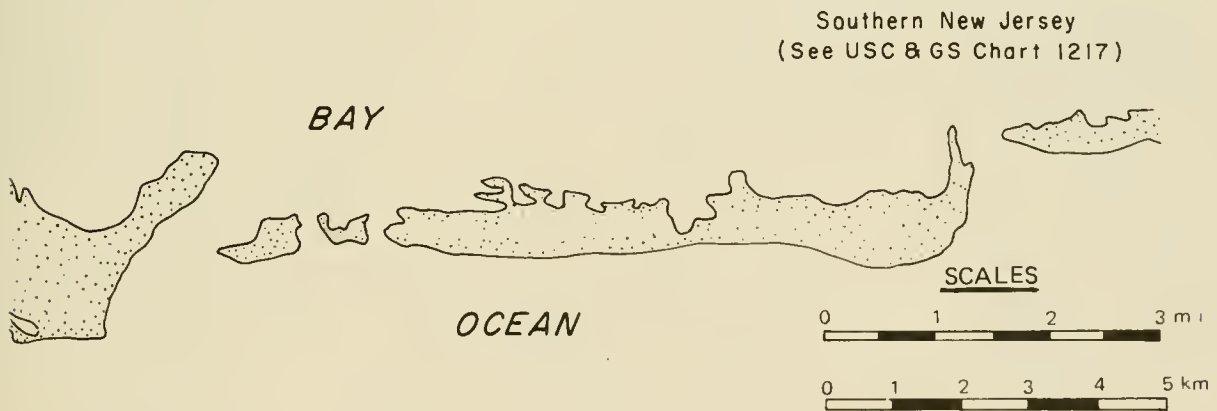
Figure 4-1. Typical profile changes with time, Westhampton Beach, New York.



a. Rocky Coast with Limited Beaches



b. Straight Barrier Island Shoreline



c. Short Barrier Island Shoreline

Figure 4-2. Three types of shoreline.

problems involving littoral processes would not occur. A knowledge of incident wave conditions is essential for coastal engineering planning, design, and construction.

Three important aspects of a study of waves on beaches are (1) the theoretical description of wave motion, (2) the climatological data for waves as they occur on a given segment of coast, and (3) the description of how waves interact with the shore to move sand.

The theoretical description of water-wave motion is useful in understanding the effect of waves on sediment transport, but currently the prediction of wave-induced sediment motion for engineering purposes relies heavily on empirical coefficients and judgment, as well as on theory.

Statistical distributions of wave characteristics along a given shoreline provide a basis for describing the wave climate of a coastal segment. Important wave characteristics affecting sediment transport near the beach are height, period, and direction of breaking waves. Breaker height is significant in determining the quantity of sand placed in motion; breaker direction is a major factor in determining longshore transport direction and rate. Waves affect sediment motion in the littoral zone in two ways: they initiate sediment movement and they drive current systems that transport the sediment once motion is initiated.

b. Currents. Water waves induce an orbital motion in the fluid in which they travel (see Ch. 2, Sec. II,3). The orbits are not closed, and the fluid experiences a slight wave-induced drift or *mass transport*. The action of mass transport, extended over a long period, can be important in carrying sediment onshore or offshore, particularly seaward of the breaker position.

As waves approach breaking, wave-induced bottom motion in the water becomes more intense, and its effect on sediment becomes more pronounced. Breaking waves create intense local currents and turbulence that move sediment. As waves cross the surf zone after breaking, the accompanying fluid motion is mostly uniform horizontal motion, except during the brief passage of the breaker front where significant turbulence occurs. Since wave crests at breaking are usually at a slight angle to the shoreline, there is usually a longshore component of momentum in the fluid composing the breaking waves. This longshore component of momentum entering the surf zone is the principal cause of longshore currents--currents that flow parallel to the shoreline within the surf zone. These longshore currents are largely responsible for the longshore sediment transport.

There is some mean exchange between the water flowing in the surf zone and the water seaward of the breaker zone. The most easily seen of these exchange mechanisms are rip currents (Shepard and Inman, 1950), which are concentrated jets of water flowing seaward through the breaker zone.

c. Tides and Surges. In addition to wave-induced currents, there are other currents affecting the shore that are caused by tides and storm surges. Tide-induced currents can be impressed upon the prevailing wave-induced circulations, especially near entrances to bays and lagoons and in regions of large tidal range. (Notices to Mariners and the Coastal Pilot

often carry this information.) Tidal currents are particularly important in transporting sand at entrances to harbors, bays, and estuaries.

Currents induced by storm surges (Murray, 1970) are less well known because of the difficulty in measuring them, but their effects are undoubtedly significant.

The change in water level caused by tides and surges is a significant factor in sediment transport since, with a higher water level, waves can then attack a greater range of elevations on the beach profile (see Fig. 1-8.).

d. Winds. Winds act directly by blowing sand off the beaches (*deflation*) and by depositing sand in dunes (Savage and Woodhouse, 1968). Deflation usually removes the finer material, leaving behind coarser sediment and shell fragments. Sand blown seaward from the beach usually falls into the surf zone; thus it is not lost, but is introduced into the littoral transport system. Sand blown landward from the beach may form dunes, add to existing dunes, or be deposited in lagoons behind barrier islands.

For dunes to form, a significant quantity of sand must be available for transport by wind, as must features that act to trap the moving sand. Topographic irregularities, the dunes themselves, and vegetation are the principal features that trap sand.

The most important dunes in littoral processes are *foredunes*, the line of dunes immediately landward of the beach. They usually form because beach grasses growing just landward of the beach will trap sand blown landward off the beach. Foredunes act as a barrier to prevent waves and high water from moving inland and provide a reservoir of sand to replenish the nearshore regime during severe shore erosion.

The effect of winds in producing currents on the water surface is well documented, both in the laboratory and in the field (van Dorn, 1953, Keulegan, 1951; and Bretschneider, 1967). These surface currents drift in the direction of the wind at a speed equal to 2 to 3 percent of the windspeed. In hurricanes, winds generate surface currents of 0.6 to 2.4 meters (2 to 8 feet) per second. Such wind-induced surface currents toward the shore cause significant bottom return flows which may transport sediment seaward; similarly, strong offshore winds can result in an offshore surface current and an onshore bottom current which can aid in transporting sediment landward.

e. Geologic Factors. The geology of a coastal region affects the supply of sediment on the beaches and the total coastal morphology, thus geology determines the initial conditions for littoral processes; but geologic factors are not usually active processes affecting coastal engineering.

One exception is the rate of change of sea level with respect to land which may be great enough to influence design and should be examined if project life is 50 years or more. On U.S. coasts, typical rates of sea level rise average about 1 to 2 millimeters per year, but changes range from -13 to +9 millimeters per year (Hicks, 1972). (Plus means a relative rise in sea level with respect to local land level.)

f. Other Factors. Other principal factors affecting littoral processes are the works of man and activities of organisms native to the particular littoral zone. In engineering design, the effects on littoral processes of construction activities, the resulting structures, and structure maintenance must be considered. This consideration is particularly necessary for a project that may alter the sand budget of the area, such as jetty or groin construction. In addition, biological activity may be important in producing carbonate sands, in reef development, or (through vegetation) in trapping sand on dunes.

### 3. Changes in the Littoral Zone.

Because most wave energy is dissipated in the littoral zone, this zone is where beach changes are most rapid. These changes may be short term due to seasonal changes in wave conditions and to occurrence of intermittent storms separated by intervals of low waves, or long term due to an overall imbalance between the added and eroded sand. Short-term changes are apparent in the temporary redistribution of sand across the profile (Fig. 4-1); long-term changes are apparent in the more nearly permanent shift of the shoreline (see Figs. 4-3, 4-4, and 4-5).

Maximum seasonal or storm-induced changes across a profile, such as those shown in Figure 4-1, are typically on the order of a few meters vertically and from 3 to 30 meters (10 to 100 feet) horizontally (see Table 4-1). Only during extreme storms, or where the available sand supply is restricted, do unusual changes occur over a short period.

Typical seasonal changes on southern California beaches are shown in Table 4-1 (Shepard, 1950). These data show greater changes than are typical of Atlantic coast beaches (Urban and Galvin, 1969; Zeigler and Tuttle, 1961). Available data indicate that the greatest changes on the profile are in the position of the beach face and of the longshore bar--two relatively mobile elements of the profile. Beaches change in plan view as well. Figure 4-6 shows the change in shoreline position at seven east coast localities as a function of time between autumn 1962 and spring 1967.

Comparison of beach profiles before and after storms suggests erosion of the beach (above MSL) can amount to 5 to 24 cubic meters per kilometer (10,000 to 50,000 cubic yards per mile) of shoreline during storms having a recurrence interval of about once a year (DeWall, Pritchett, and Galvin, 1971; Shuyskiy, 1970). While impressive in aggregate, such sediment transport is minor compared to longshore transport of sediment. Longshore transport rates may be greater than 765,000 cubic meters (1 million cubic yards) per year.

The long-term changes shown in Figures 4-3, 4-4, and 4-5 illustrate shorelines of erosion, accretion, and stability. Long-term erosion or accretion rates are rarely more than a few meters per year in horizontal motion of the shoreline, except in localities particularly exposed to erosion, such as near inlets or capes. Figure 4-4 indicates that shorelines can be stable for a long time. It should be noted that the eroding, stable, and accreting beaches shown in Figures 4-3, 4-4, and 4-5 are on the same barrier island within a few kilometers of each other.

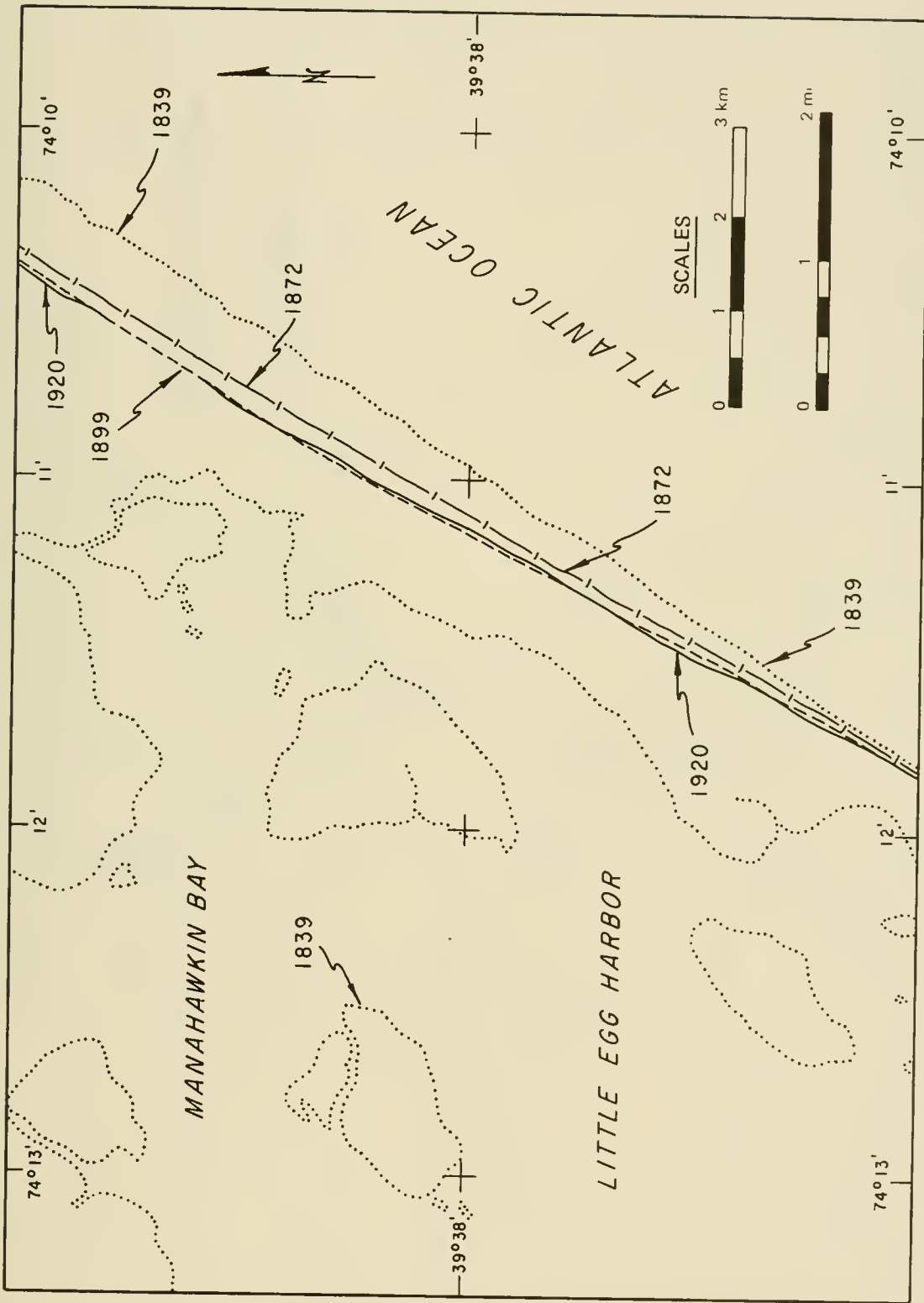


Figure 4-3. Shoreline erosion near Shipbottom, New Jersey.

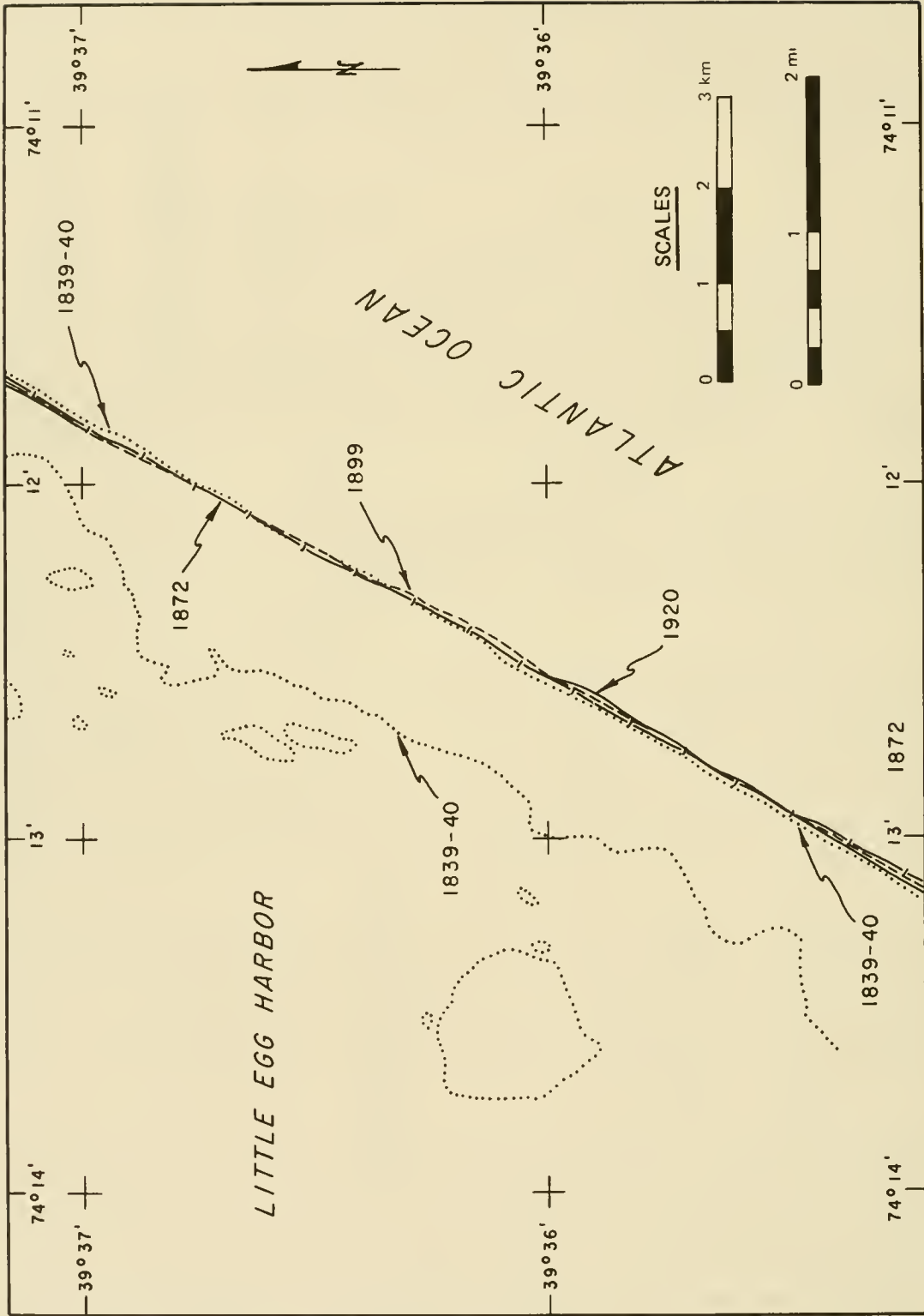


Figure 4-4. Stable shoreline near Peahala, New Jersey.

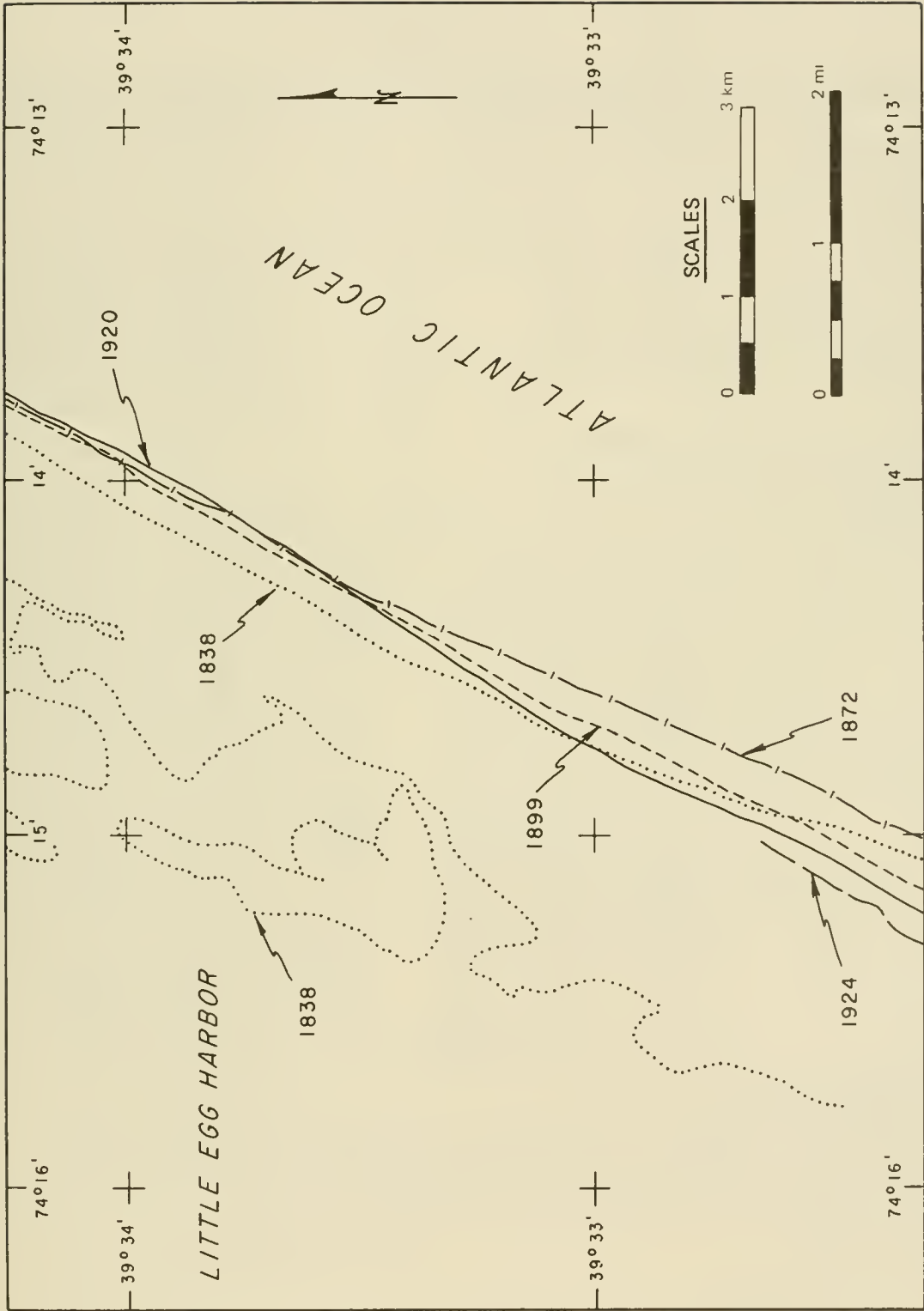


Figure 4-5. Shoreline accretion and erosion near Beach Haven, New Jersey.

Table 4-1. Seasonal profile changes on southern California beaches<sup>1</sup>.

Locality	Erosion		Date
	Vertical <sup>2</sup> m (ft)	Horizontal at MWL, m (ft)	
Marine Street	1.80 (5.9)	07.32 (24)	27 Nov 45- 5 Apr 46
Beacon Inn	2.50 (8.2)	35.66 (117)	2 Nov 45-19 Mar 46
South Oceanside	1.52 (5.0)	12.50 (41)	2 Nov 45-26 Apr 46
San Onofre			
Surf Beach	1.28 (4.2)	13.11 (43)	6 Nov 45-12 Apr 46
Fence Beach	3.29 (10.8)	26.52 (87)	6 Nov 45-12 Apr 46
Del Mar	1.04 (3.4)	--	2 Nov 45-10 May 46
Santa Monica Mountains	1.89 (6.2)	--	28 Aug 45-13 Mar 46
Point Mugu	1.83 (6.0)	--	28 Aug 45-13 Mar 46
Rincon Beach	0.82 (2.7)	--	22 Aug 45-13 Mar 46
Goleta Beach	0.15 (0.5)	--	22 Aug 45-13 Mar 46
Point Sur			27 Aug 45-14 Mar 46
South Side	0.55 (1.8)	--	
North Side	1.92 (6.3)	--	
Carmel Beach (South)	2.04 (6.7)	--	26 Aug 45-14 Mar 46
Point Reyes	1.55 (5.1)	--	26 Aug 45-16 Mar 46
Scripps Beach			
Range A	0.49 (1.6)	26.82 (88)	19 Nov 45-29 Apr 46
Range B	0.98 (3.2)	73.15 (240)	7 Nov 45-10 Apr 46
Range C	1.71 (5.6)	79.25 (260)	7 Nov 45-10 Apr 46
Range D	1.62 (5.3)	76.20 (250)	7 Nov 45- 9 May 46
Range E	1.01 (3.3)	--	7 Nov 45-24 Apr 46
Range F	0.46 (1.5)	20.42 (67)	7 Nov 45-10 May 46
Range G	0.21 (1.7)	4.57 (15)	19 Oct 45-10 Apr 46
Range H	0.49 (1.6)	13.41 (44)	7 Nov 45-24 Apr 46
Scripps Pier	1.16 (3.8)	10.06 (33)	13 Oct 37-26 Mar 38
" "	1.10 (3.6) <sup>3</sup>	9.14 (30) <sup>3</sup>	26 Mar 38-30 Aug 38
" "	1.31 (4.3)	11.58 (38)	30 Aug 38-13 Feb 39
" "	0.98 (3.2) <sup>3</sup>	9.75 (32) <sup>3</sup>	13 Feb 39-22 Sept 39
" "	0.76 (2.5)	8.53 (28)	22 Sept 39-24 Jan 40
" "	1.04 (3.4) <sup>3</sup>	10.36 (34) <sup>3</sup>	24 Jan 40-18 Sept 40
" "	0.37 (1.2)	3.66 (12)	18 Sept 40-16 Apr 41
" "	0.37 (1.2) <sup>3</sup>	3.35 (11) <sup>3</sup>	16 Apr 41-17 Sept 41
" "	0.88 (2.9)	9.14 (30)	17 Sept 41-29 Apr 42
" "	0.58 (1.9) <sup>3</sup>	4.88 (16) <sup>3</sup>	29 Apr 42-30 Sept 42

<sup>1</sup>From Shepard 1950.

<sup>2</sup>Vertical erosion measured at berm for all localities except Scripps Beach and Scripps Pier where the mean water line (MWL) was used.

<sup>3</sup>Accretion values.

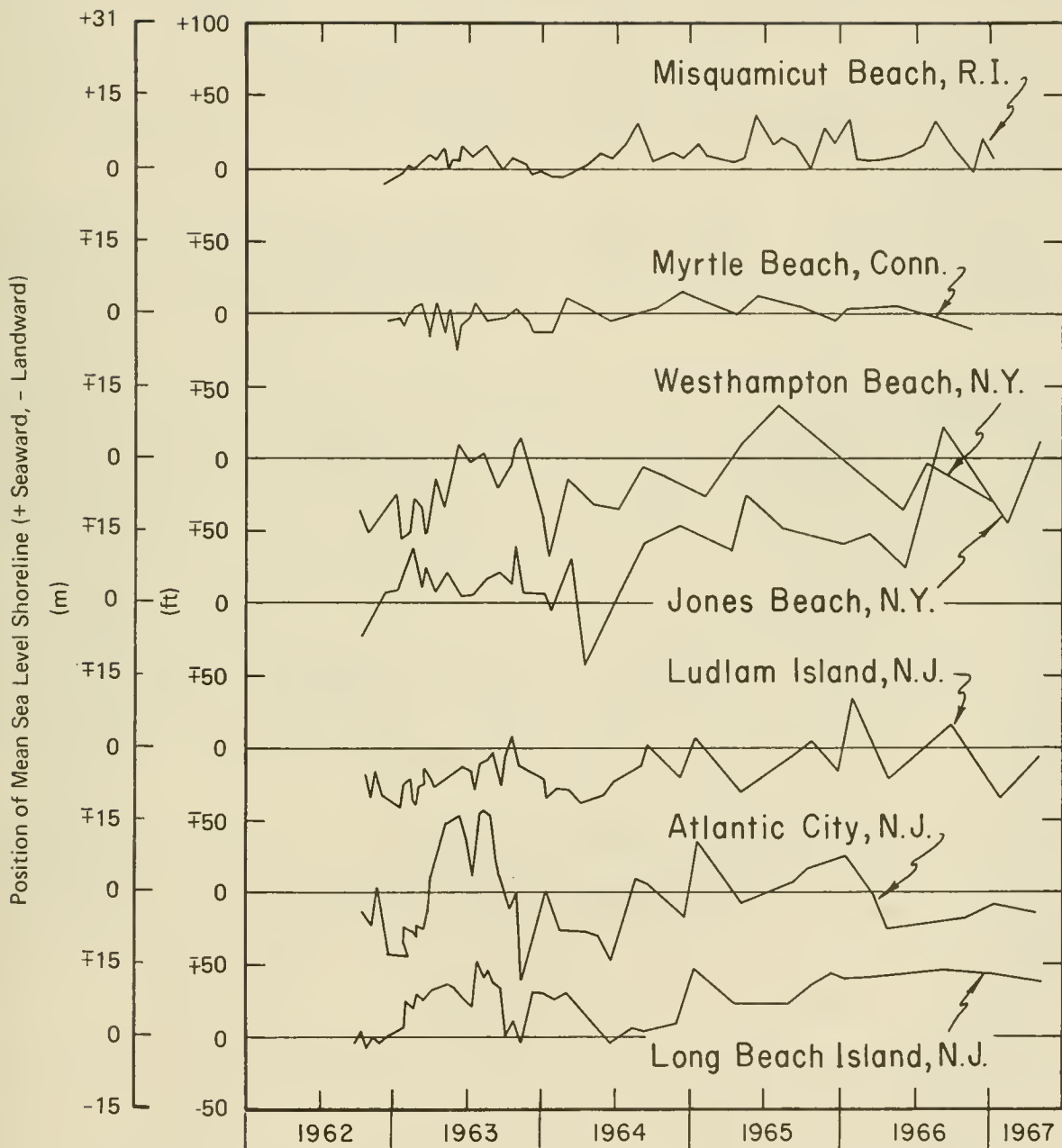


Figure 4-6. Fluctuations in location of mean sea level shoreline on seven east coast beaches.

Net longshore transport rates along ocean beaches range from near zero to 765,000 cubic meters (1 million cubic yards) per year, but are typically 76,500 to 382,00 cubic meters (100,000 to 500,000 cubic yards) per year. Such quantities, if removed from a 16- to 32-kilometer (10- to 20-mile) stretch of beach year after year, would result in severe erosion problems. The fact that many beaches have high rates of longshore transport without unusually severe erosion suggests that an equilibrium condition exists on these beaches, in which the material removed is balanced by the material supplied.

## II. LITTORAL MATERIALS

Littoral materials are the solid materials (mainly sedimentary) in the littoral zone on which the waves, wind, and currents act.

### 1. Classification.

The characteristics of the littoral materials are usually primary input to any coastal engineering design. Median grain size is the most frequently used descriptive characteristic.

a. Size and Size Parameters. Littoral materials are classified by grain size into clay, silt, sand, gravel, cobble, and boulder. Several size classifications exist, of which two, the Unified Soil Classification (based on the Casagrande Classification) and the Wentworth classification, are most commonly used in coastal engineering (see Fig. 4-7). The Unified Soil Classification is the principal classification used by engineers. The Wentworth classification is the basis of a classification widely used by geologists, but is becoming more widely used by engineers designing beach fills.

For most shore protection design problems, typical littoral materials are sands with sizes between 0.1 and 1.0 millimeters. According to the Wentworth classification, sand size is in the range between 0.0625 and 2.0 millimeters; according to the Unified Soil Classification, it is between 0.074 and 4.76 millimeters. Within these sand size ranges, engineers commonly distinguish size classes by median grain size measured in millimeters.

Samples of typical beach sediment usually have a few relatively large particles covering a wide range of diameters and many small particles within a small range of diameters. Thus, to distinguish one sample from another, it is necessary to consider the small differences (in absolute magnitude) among the finer sizes more than the same differences among the larger sizes. For this reason, all sediment size classifications exaggerate absolute differences in the finer sizes compared to absolute differences in the coarser sizes.

As shown in Figure 4-7, limits of the size classes differ. The Unified Soil Classification boundaries correspond to U.S. Standard Sieve sizes. The Wentworth classification varies as powers of 2 millimeters; i.e., the size classes have limits, in millimeters, determined by the relation  $2^n$ , where  $n$  is any positive or negative whole number, including zero. For example, the limits on sand size in the Wentworth scale are 0.0625 and 2 millimeters, which correspond to  $2^{-4}$  and  $2^{+1}$  millimeters.

Unified Soils Classification		ASTM Mesh	mm Size	Phi Value	Wentworth Classification	
COBBLE			256.0	-8.0	BOULDER	
			76.0	-6.25	COBBLE	
COARSE GRAVEL			64.0	-6.0	PEBBLE	
			19.0	-4.25		
FINE GRAVEL			4.76	-2.25	GRAVEL	
			4			
SAND	coarse		5	4.0	-2.0	SAND
			10	2.0	-1.0	
	medium		18	1.0	0.0	very coarse
			25	0.5	1.0	coarse
			40	0.42	1.25	medium
			60	0.25	2.0	fine
	fine		120	0.125	3.0	very fine
			200	0.074	3.75	
	SILT		230	0.062	4.0	SILT
				0.0039	8.0	CLAY
CLAY			0.0024	12.0	COLLOID	

Figure 4-7. Grain-size scales (soil classification).

This property of having class limits defined in terms of whole number powers of 2 millimeters led Krumbein (1936) to propose a phi unit scale based on the definition:

$$\text{Phi units } (\phi) = -\log_2 (\text{diameter in mm}) \quad (4-1)$$

Phi unit scale is indicated by writing  $\phi$  or phi after the numerical value. The phi unit scale is shown in Figure 4-7. Advantages of phi units are

(1) Limits of Wentworth size classes are whole numbers in phi units. These phi limits are the negative value of the exponent,  $n$ , in the relation  $2^n$ . For example, the sand size class ranges from +4 to -1 in phi units.

(2) Sand size distributions typically are near lognormal, so that a unit based on the logarithm of the size better emphasizes the small significant differences between the finer particles in the distribution.

(3) The normal distribution is described by its mean and standard deviation. Since the distribution of sand size is approximately lognormal, individual sand size distributions can be more easily described by units based on the logarithm of the diameter rather than the absolute diameter. Comparison with the theoretical lognormal distribution is also a convenient way of characterizing and comparing the size distribution of different samples.

Of these three advantages, only (1) is unique to the phi units. The other two, (2) and (3), would be valid for any unit based on the logarithm of size.

Disadvantages of phi units are

(1) Phi units increase as absolute size in millimeters decreases.

(2) Physical appreciation of the size involved is easier when the units are millimeters rather than phi units.

(3) The median diameter can be easily obtained without phi units.

(4) Phi units are dimensionless and are not usable in physically related quantities where grain size must have units of length such as grain size, Reynolds number, or relative roughness.

Size distributions of samples of littoral materials vary widely. Qualitatively, the size distribution of a sample may be characterized (1) by a diameter that is in some way typical of the sample and (2) by the way that the sizes coarser and finer than the typical size are distributed. (Note that size distributions are generally based on weight, rather than number of particles.)

A size distribution is described qualitatively as *well sorted* if all particles have sizes that are close to the typical size. If the particle sizes are distributed evenly over a wide range of sizes, then the sample is said to be *well graded*. A well-graded sample is poorly sorted; a well-sorted sample is poorly graded.

The *median diameter* ( $M_d$ ) and the *mean diameter* ( $M$ ) define typical sizes of a sample of littoral materials. The median size  $M_d$ , in millimeters, is the most common measure of sand size in engineering reports. It may be defined as

$$M_d = d_{50} \quad (4-2)$$

where  $d_{50}$  is the size in millimeters that divides the sample so that half the sample, by weight, has particles coarser than the  $d_{50}$  size. An equivalent definition holds for the median of the phi-size distribution, using the symbol  $M_{d\phi}$  instead of  $M_d$ .

Several formulas have been proposed to compute an approximate mean ( $M$ ) from the cumulative size distribution of the sample (Otto, 1939; Inman, 1952; Folk and Ward, 1957; McCammon, 1962). These formulas are averages of 2, 3, 5, or more symmetrically selected percentiles of the phi frequency distribution, such as the formula of Folk and Ward.

$$M_{\phi} = \frac{\phi_{16} + \phi_{50} + \phi_{84}}{3} \quad (4-3)$$

where  $\phi$  is the particle size in phi units from the distribution curve at the percentiles equivalent to the subscripts 16, 50, and 84 (Fig. 4-8);  $\phi_x$  is the size in phi units that is exceeded by  $x$  percent (by dry weight) of the total sample. These definitions of percentile (after Griffiths, 1967, p. 105) are known as graphic measures. A more complex method--the method of moments--can yield more precise results when properly used.

To a good approximation, the median  $M_d$  is interchangeable with the mean ( $M$ ) for most beach sediment. Since the median is easier to determine, it is widely used in engineering studies. For example, in one CERC study of 465 sand samples from three New Jersey beaches, the mean computed by the method of moments averaged only 0.01 millimeter smaller than the median for sands whose average median was 0.30 millimeter (1.74 phi) (Ramsey and Galvin, 1971).

Since the actual size distributions are such that the log of the size is approximately normally distributed, the approximate distribution can be described (in phi units) by the two parameters that describe a normal distribution--the mean and the standard deviation. In addition to these two parameters, skewness and kurtosis describe how far the actual size distribution of the sample departs from this theoretical lognormal distribution.

Standard deviation is a measure of the degree to which the sample spreads out around the mean (i.e., its sorting) and can be approximated using Inman's (1952) definition by

$$\sigma_{\phi} = \frac{\phi_{84} - \phi_{16}}{2} \quad (4-4)$$

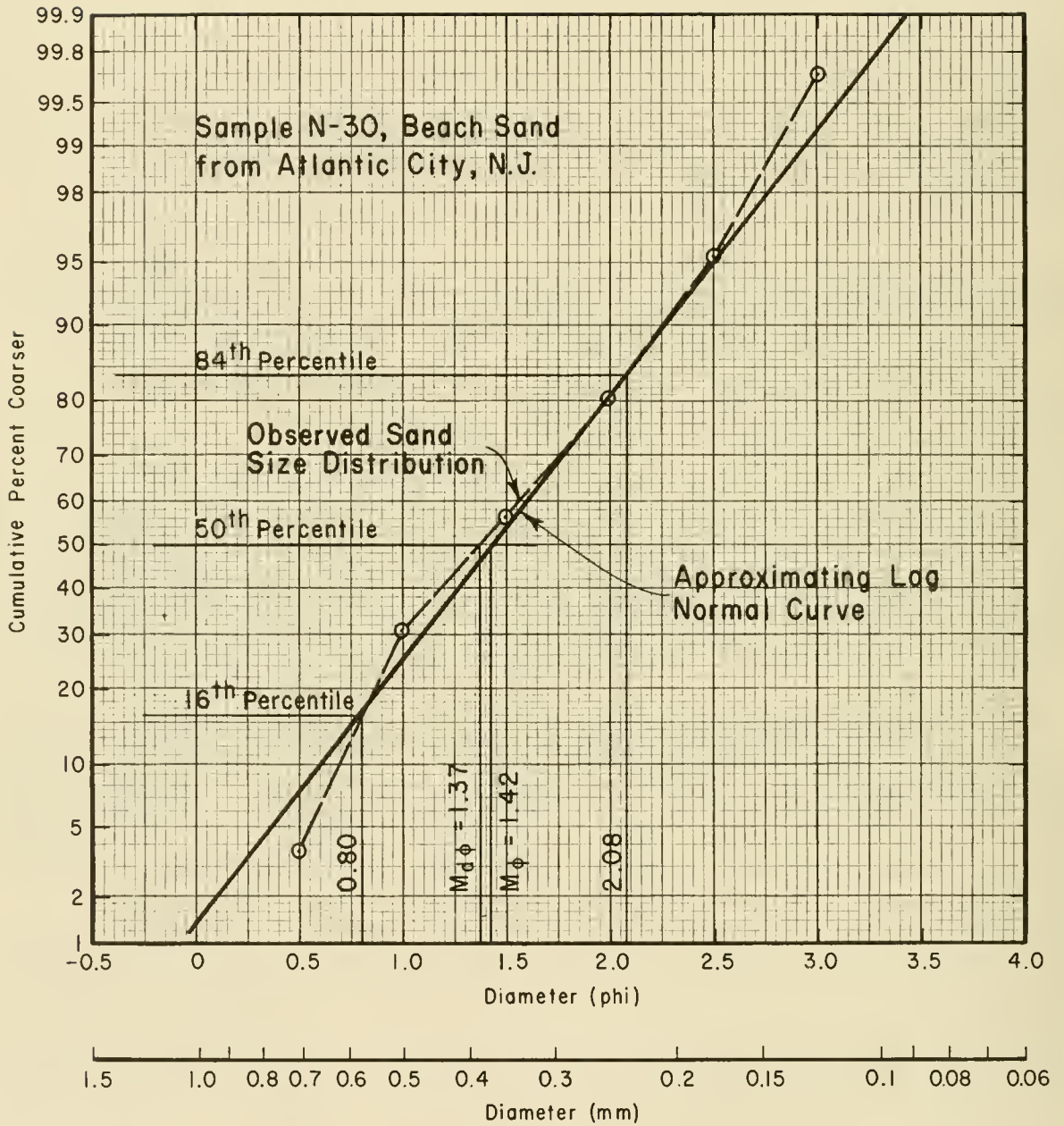


Figure 4-8. Example size distribution.

where  $\phi_{84}$  is the sediment size in phi units; i.e., finer than 84 percent by weight, of the sample. If the sediment size in the sample actually has a lognormal distribution, then  $\sigma_\phi$  is the standard deviation of the sediment in phi units. For perfectly sorted sediment,  $\sigma_\phi = 0$ . For typical well-sorted sediments,  $\sigma_\phi \approx 0.5$ .

The degree by which the phi-size distribution departs from symmetry is measured by the skewness (Inman, 1952) as

$$\alpha_\phi = \frac{M_\phi - M_{d\phi}}{\sigma_\phi} \quad (4-5)$$

where  $M_\phi$  is the mean,  $M_{d\phi}$  is the median, and  $\sigma_\phi$  the standard deviation in phi units. For a perfectly symmetric distribution, the mean equals the median and the skewness is zero.

Presently, median grain size is the most commonly reported size characteristic, and there are only limited results available to demonstrate the usefulness of other size distribution parameters in coastal engineering design. However, the standard deviation equation (4-4) is an important consideration in beach-fill design (see Hobson, 1977; Ch. 5, Sec. III,3).

Extensive literature is available on the potential implications of  $\sigma_\phi$ ,  $\alpha_\phi$ , and other measures of the size distribution (Inman, 1957; Folk and Ward, 1957; McCammon, 1962; Folk, 1965, 1966; Griffiths, 1967). For example, the conditions under which nearshore sediment has been transported and deposited might be inferred from consideration of size measures (e.g., Charlesworth, 1968).

b. Composition and Other Properties. Littoral material varies in composition, shape, and other properties. In considering littoral processes, composition normally is not an important variable because the dominant littoral material is quartz sand, which is mechanically durable and chemically inert. However, littoral material may include carbonates (shell, coral, and algal material), heavy and light minerals (Ch. 4, Sec. II,2), organics (peat), and clays and silts. Table 4-2 includes the specific gravities of common sand-size littoral materials.

The shape of littoral material ranges from nearly spherical to nearly disklike (shells and shell fragments). Littoral sands are commonly rounded, but usual departures from sphericity have appreciable effects on sediment setting, sieve analyses, and motion initiation (Ch. 4, Sec. II,1,c; Sec. II, 7,a; and Sec. V,2,b). Sediment grain shapes have been applied to the interpretation of nearshore processes (Bradley, 1958; Van Nieuwenhuise et al., 1978).

Sediment color has been used to distinguish littoral from continental shelf sands (Chapman, 1981). Tracing of sediment transport has utilized the natural radioactivity of certain littoral materials (Kamel, 1962; Kamel and Johnson, 1962).

Most other properties of littoral materials are more directly related to concerns of soil mechanics rather than littoral processes (see Terzaghi and Peck, 1967, Ch. 7, Sec. 7.7).

Table 4-2. Density of littoral materials.

Specific Gravity (dimensionless)				
Quartz	2.65			
Calcite	2.72			
Heavy Minerals	>2.87 (commonly 2.87 to 3.33)			
Unit Weight <sup>1</sup> , kg/m <sup>3</sup> (lb/ft <sup>3</sup> )				
	Dry		Saturated	
Uniform sand				
loose	1442	(90)	1890	(118)
dense	1746	(109)	2082	(130)
Mixed sand				
loose	1586	(99)	1986	(124)
dense	1858	(116)	2163	(135)
Clay				
stiff glacial	---		2066	(129)
soft, very organic	---		1426	(89)

<sup>1</sup>From Terzaghi and Peck (1967).

c. Fall Velocity. In considering the motion of littoral materials, a particularly meaningful material characteristic is the particle fall velocity,  $V_f$ . This is the terminal vertical velocity attained by an isolated solid grain settling due to gravity in a still, unbounded, less dense fluid. The fall velocity, usually for quartz in water, summarizes effects of grain size, shape, and composition and of fluid composition and viscosity. The ratio of fall velocity to characteristic fluid velocity has been widely applied as a measure of sediment mobility or transport.

For a sphere, the fall velocity  $V_{fs}$  can be expressed in the form of a single general curve, for example, relating the Reynolds number ( $V_{fs} d_s / \nu$ ) to the buoyancy index  $B$

$$[(\gamma_s / \alpha) - 1] g d_s^3 / \nu^2 \quad (4-6)$$

where

$\gamma_s$  = the specific gravity of the solid

$\gamma$  = the specific gravity of the fluid

$g$  = the gravitational acceleration

$d_s$  = the sphere diameter

$\nu$  = the fluid kinematic viscosity

(Yalin, 1977; Ch. 3; Clift, Grace and Weber, 1978, pp. 113-116). Figures 4-9 and 4-10 display empirical results for the fall velocity of spheres (solid curve).

More significant littoral processes are empirical results for the fall velocity of common natural grains (Hallermier, 1981). The dashed curve in Figure 4-9 displays these results as  $(V_f d_{50} / \nu)$  versus  $B = [(\gamma_s/\gamma - 1) g d_{50}^3 / \nu^2]$ , where the grain diameter is measured by the median sieve size  $d_{50}$ . For common grains, the three segments of the Figure 4-9 dashed curve are given by

$$V_f = (\gamma_s/\gamma - 1) g d_{50}^2 / 18 \nu \quad (B < 39) \quad (4-7)$$

$$V_f = [(\gamma_s/\gamma - 1) g]^{0.7} d_{50}^{1.1} / 6 \nu^{0.4} \quad (39 < B < 10^4) \quad (4-8)$$

$$V_f = [(\gamma_s/\gamma - 1) g d_{50} / 0.91]^{0.5} \quad (10^4 < B) \quad (4-9)$$

Equation (4-8) is most useful because it provides the fall velocity in water of common quartz grains described as fine to coarse on the Wentworth scale (Fig. 4-7). Equation (4-6) is identical to results for spheres and pertains to laminar fluid motion in settling of very fine grains. Equation (4-9) pertains to turbulent fluid motion in settling of very heavy grains; this dependence of fall velocity is identical to asymptotic results for spheres, but for common grains fall velocity is lower and turbulent motion occurs at lower values of the buoyancy index  $B$ .

According to its definition,  $V_f$  is a measure of grain behavior in an ideal situation. Actual fall velocity can be affected by several factors; e.g., the terminal fall velocity is reduced somewhat in a turbulent fluid (Murray, 1970; Niemczynowicz, 1972). However, the most appreciable effect seems to be that due to particle concentration or proximity, which can reduce fall velocity by two orders of magnitude. In a concentrated suspension of spheres, the fall velocity  $V_{fsc}$  is related to the fall velocity in isolation  $V_{fs}$  by

$$V_{fsc} = V_{fs} (1-c)^{n_s} \quad (4-10)$$

Here  $c$  is the volumetric particle concentration (between 0 and about 0.7), and the power  $n_s$  is the empirical function of the buoyancy index displayed in the solid curve of Figure 4-10 (Richardson and Jeronimo, 1979).

Although this concentration effect has not been defined empirically for common natural grains, behavior analogous to that for spheres may be expected. Presuming a smooth transition for the settling behavior of common grains between the two Figure 4-9 asymptotes (rather than the approximation in equation (4-8)), the dashed curve given in Figure 4-10 should be appropriate for the power  $n$  in

$$V_{fc} = V_f (1-c)^n \quad (4-11)$$

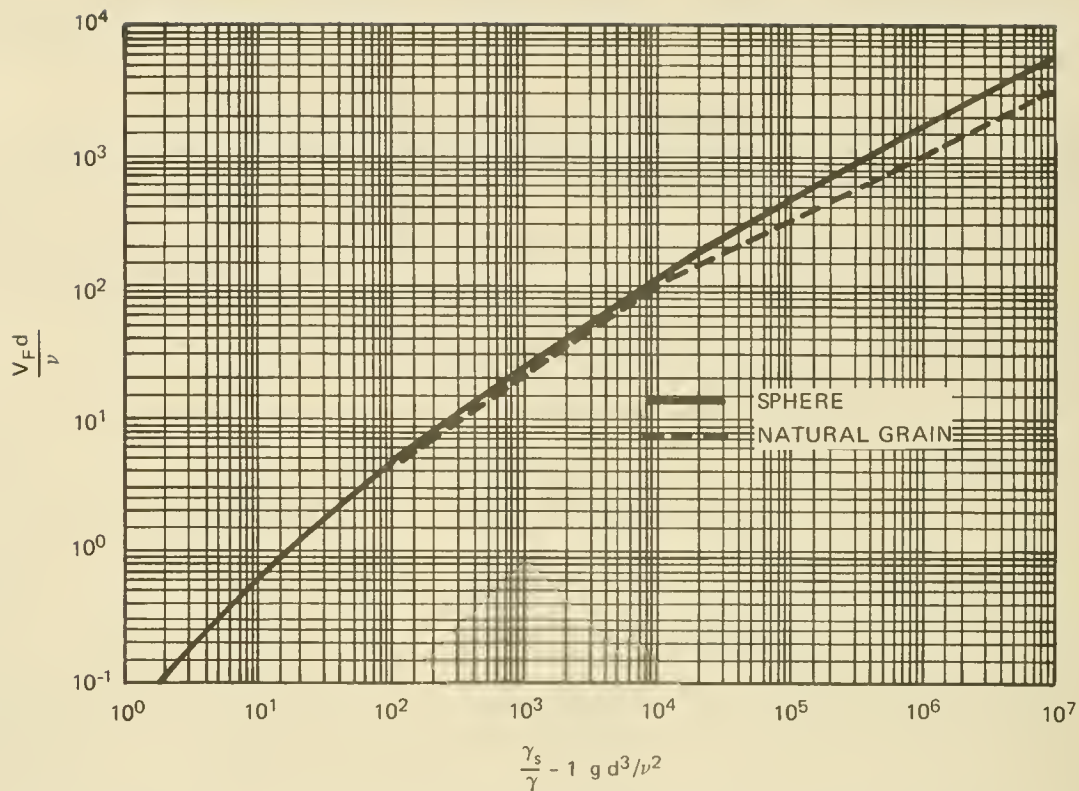


Figure 4-9. Fall velocity versus buoyancy index for an isolated sphere or common natural grain.

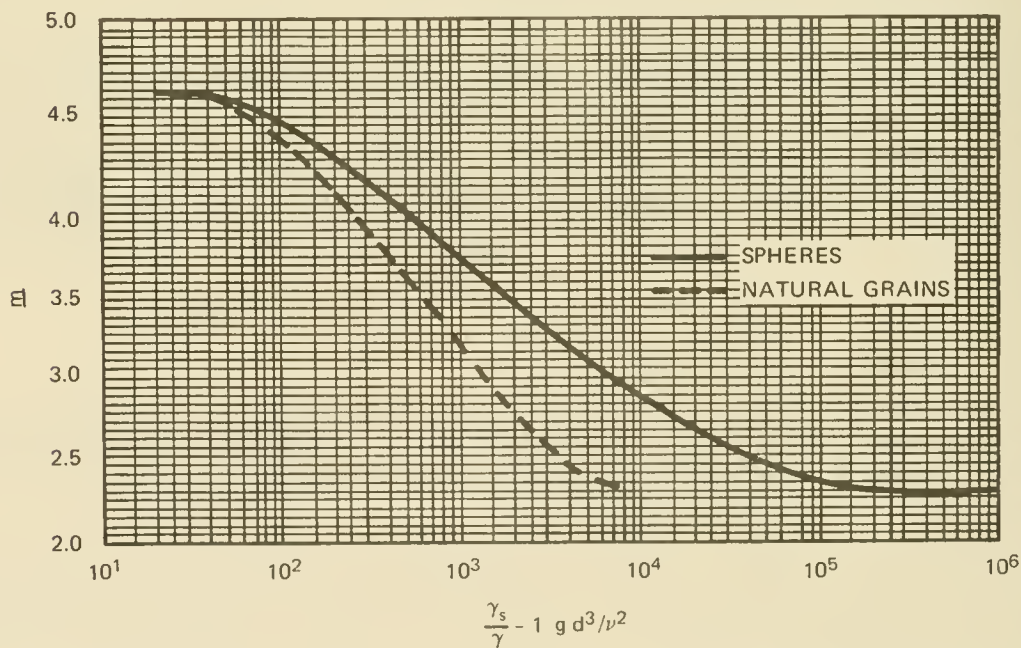


Figure 4-10. Approximate value of power  $n$  relating to equation (4-9) for fall velocity in concentrated suspensions of spheres and common grains.

which relates fall velocity in a concentrated grain suspension to that for an isolated grain.

The concentration dependence of fall velocity is important to vertical variations of grain concentrations (Lavelle and Thacker, 1978), to grain suspension processes, and to the fall of a bulk sediment sample in a settling tube (Ch. 4, Sec. II,7,b).

## 2. Sand and Gravel.

By definition, the word sand refers to a size class of material, but sand also implies the particular composition, usually quartz (silica).

In tropical climates, calcium carbonate, especially shell material, is often the dominant material in beach sand. In temperate climates, quartz and feldspar grains are the most abundant, commonly accounting for about 90 percent of beach sand (Krumbein and Sloss, 1963, p. 134).

Because of its resistance to physical and chemical changes and its common occurrence in terrestrial rocks, quartz is the most common mineral found in littoral materials. Durability of littoral materials (resistance to abrasion, crushing, and solution) is usually not a factor within the lifetime of an engineering project (Kuenen, 1956; Rusnak, Stockman, and Hofmann, 1966; Thiel, 1940). Possible exceptions may include basaltic sands on Hawaiian beaches (Moberly, 1968), some fragile carbonate sands which may be crushed to finer sizes when subject to traffic (Duane and Meisburger, 1969, p. 44), and carbonate sands which may be soluble under some conditions (Bricker, 1971). In general, recent information lends further support to the conclusion of Mason (1942) that, "On sandy beaches the loss of material ascribable to abrasion...occurs at rates so low as to be of no practical importance in shore protection problems."

The relative abundance of nonquartz materials is a function of the relative importance of the sources supplying the littoral zone and the materials available at those sources. The small amount of heavy minerals (specific gravity greater than 2.87) usually found in sand samples may indicate the source area of the material (McMaster, 1954; Giles and Pilkey, 1965; Judge, 1970), and thus may be used as a natural tracer. Such heavy minerals may form black or reddish concentrations at the base of dune scarps, along the berm, and around inlets. Occasionally, heavy minerals occur in concentrations great enough to justify mining them as a metal ore (Everts, 1971; Martens, 1928). Table 4-3 from Pettijohn (1957, p. 117) lists the 26 most common minerals found in beach sands.

Sand is by far the most important littoral material in coastal engineering design. However, in some localities, such as New England, Oregon, Washington, and countries bordering on the North Sea, gravel and shingle are locally important. Gravel-sized particles are often rock fragments, (i.e., a mixture of different minerals), whereas sand-sized particles usually consist of single mineral grains.

## 3. Cohesive Materials.

The amount of fine-grained, cohesive materials, such as clay, silt, and

peat, in the littoral zone depends on the wave climate, contributions of fine sediment from rivers and other sources, and recent geologic history. Fine grain-size material is common in the littoral zone wherever the annual mean breaker height is below about 0.3 meters. Fine material is found at or near the surface along the coasts of Georgia and western Florida between Tampa and Cape San Blas and in large bays such as Chesapeake Bay and Long Island Sound.

Table 4-3. Minerals occurring in beach sand.

Common Dominant Constituents <sup>1</sup>		
Quartz--may average about 70 percent in beach sand; varies from near 0 to over 99 percent.	Feldspar--typically only 10 to 20 percent in beach sands but may be much more, particularly in regions of eroding igneous rock.	Calcite--includes shell, coral, algal fragments and oolites; varies from 0 to nearly 100 percent; may include significant quantities of aragonite.
Common Accessory Minerals (Adopted from Pettijohn, 1957)		
Andalusite Apatite Aragonite Augite Biotite Chlorite Diopside Dolomite <sup>1</sup>	Epidote Garnet Hornblende Hypersthene-enstatite Ilmenite Kyanite Leucoxene Magnetite	Muscovite <sup>1</sup> Rutile Sphene Staurolite Tourmaline Zircon Zoisite

<sup>1</sup> These are light minerals with specific gravities not exceeding 2.87. The remaining minerals are heavy minerals with specific gravities greater than 2.87. Heavy minerals make up less than 1 percent of most beach sands.

These are all areas of low mean breaker height. In contrast, fine sediment is seldom found along the Pacific coast of California, Oregon, and Washington, where annual mean breaker height usually exceeds 0.8 meters.

Where rivers bring large quantities of sediment to the sea, the amount of fine material remaining along the coast depends on the balance between wave action acting to erode the fines and river deposition acting to replenish the fines (Wright and Coleman, 1972). The effect of the Mississippi River delta deposits on the coast of Louisiana is a primary example.

Along eroding, low-lying coasts, the sea moves inland over areas formerly protected by beaches, so that the present shoreline often lies where tidal flats, lagoons, and marshes used to be. The littoral materials on such coasts may include silt, clay, and organic material at shallow depths. As the active sand beach is pushed back, these former tidal flats and marshes then outcrop along the shore (e.g., Kraft, 1971). Many barrier islands along the Atlantic and gulf coasts contain tidal and marsh deposits at or near the surface of the littoral zone. The fine material is often bound together by the roots of

marsh plants to form a cohesive deposit that may function for a time as beach protection.

#### 4. Consolidated Material.

Along some coasts, the principal littoral materials are consolidated materials, such as rock, beach rock, and coral, rather than unconsolidated sand. Such consolidated materials protect a coast and resist shoreline changes.

a. Rock. Exposed rock along a shore indicates that the rate at which sand is supplied to the coast is less than the potential rate of sand transport by waves and currents. Reaction of a rocky shore to wave attack is determined by (1) the structure, degree of lithification, and ground-water characteristics of the exposed rock and (2) by the severity of the wave climate. Protection of eroding cliffs is a complex problem involving geology, rock mechanics, and coastal engineering. Two examples of this problem are the protection of the cliffs at Newport, Rhode Island (U.S. Army Corps of Engineers, 1965) and at Gay Head, Martha's Vineyard, Massachusetts (U.S. Army Engineer Division, New England, 1970).

Most rocky shorelines are remarkably stable, with individual rock masses identified in photos taken 50 years apart (Shepard and Grant, 1947).

b. Beach Rock. A layer of friable-to-well-lithified rock often occurs at or near the surface of beaches in tropical and subtropical climates. This material consists of local beach sediment cemented with calcium carbonate, and it is commonly known as beach rock. Beach rock is important to because it provides added protection to the coast, greatly reducing the magnitude of beach changes (Tanner, 1960) and because beach rock may affect construction activities (Gonzales, 1970).

According to Bricker (1971), beach rock is formed when saline waters evaporate in beach sands, depositing calcium carbonate from solution. The present active formation of beach rock is limited to tropical coasts, such as the Florida Keys, but rock resembling beach rock is common at shallow depths along the east coast of Florida and on some Louisiana beaches; related deposits have been reported as far north as the Fraser River Delta in Canada. Comprehensive discussions of the subject are given in Bricker (1971) and Russell (1970).

c. Organic Reefs. Organic reefs are wave-resistant structures reaching to about mean sea level that have been formed by calcium carbonate-secreting organisms. The most common reef-building organisms are hermatypic corals and coralline algae. Reef-forming corals are usually restricted to areas having winter temperatures above about 18° C (Shepard, 1963, p. 351), but coralline algae have a wider range. On U.S. coastlines, active coral reefs are restricted to southern Florida, Hawaii, Virgin Islands, and Puerto Rico. On some of the Florida coast, reeflike structures are produced by sabellariid worms (Kirtley, 1971). Organic reefs stabilize the shoreline and sometimes affect navigation.

## 5. Occurrence of Littoral Materials on U.S. Coasts.

Littoral materials on U.S. coasts vary from consolidated rock to clays, but sand with median diameters between 0.1 and 1.0 millimeter (3.3 and 0 phi) is most abundant. General information on littoral materials is in the reports of the U.S. Army Corps of Engineers National Shoreline Study; information on certain specific geological studies is available in Shepard and Wanless (1971); and information on specific engineering projects is published in Congressional documents and is available in reports of the Corps of Engineers.

a. Atlantic Coast. The New England coast is generally characterized by rock headlands separating short beaches of sand or gravel. Exceptions to this dominant condition are the sandy beaches in northeastern Massachusetts and along Cape Cod, Martha's Vineyard, and Nantucket.

From the eastern tip of Long Island, New York, to the southern tip of Florida, the littoral materials are characteristically sand with median diameters in the range of 0.2 to 0.6 millimeter (2.3 to 0.7 phi). This material is mainly quartz sand. In Florida, the percentage of calcium carbonate in the sand tends to increase going south until, south of the Palm Beach area, the sand becomes predominantly calcium carbonate. Size distributions for the Atlantic coast, compiled from a number of sources, are shown in Figure 4-11 (Bash, 1972). Fine sediments and organic sediments are common minor constituents of the littoral materials on these coasts, especially in South Carolina and Georgia. Beach rock and coquina are common at shallow depths along the Atlantic coast of Florida.

b. Gulf Coast. The Gulf of Mexico coast along Florida, Alabama, and Mississippi is characterized by fine white sand beaches and by stretches of swamp. The swampy stretches are mainly in Florida, extending from Cape Sable to Cape Romano and from Tarpon Springs to the Ochlockonee River (Shepard and Wanless, 1971, p. 163).

The Louisiana coast is dominated by the influence of the Mississippi River, which has deposited large amounts of fine sediment around the delta from which wave action has winnowed small quantities of sand. This sand has been deposited along barrier beaches offshore of a deeply indented marshy coast. West of the delta is a 120-kilometer (75-mile) stretch of shelly sand beaches and beach ridges.

The Texas coast is a continuation of the Louisiana coastal plain extending about 128 kilometers (80 miles) to Galveston Bay; from there a series of long, wide barrier islands extends to the Mexican border. Littoral materials in this area are predominantly fine sand, with median diameters between 0.1 and 0.2 millimeter (3.3 and 2.3 phi).

c. Pacific Coast. Sands on the southern California coast range in size from 0.1 to 0.6 millimeter (3.3 to 0.7 phi) (Emery, 1960, p. 190). The northern California coast becomes increasingly rocky, and coarser material becomes more abundant. The Oregon and Washington coasts include considerable sand (Bascom, 1964) with many rock outcrops. Sand-sized sediment is contributed by the Columbia River and other smaller rivers.

d. Alaska. Alaska has a long coastline (76,120 kilometers (47,300 miles)

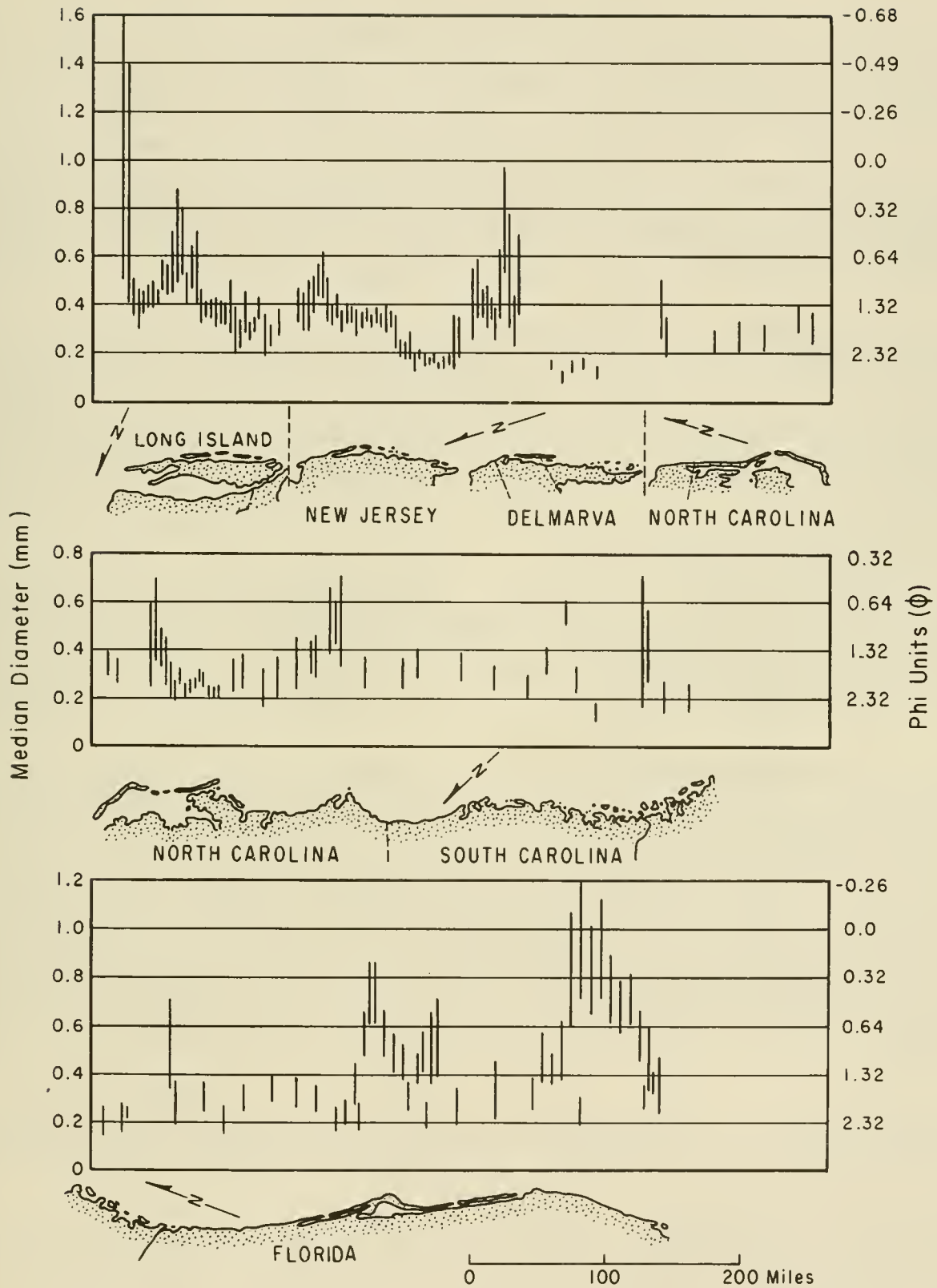


Figure 4-11. Sand size distribution along the U.S. Atlantic coast.

and is correspondingly variable in littoral materials. However, beaches are generally narrow, steep, and coarse-grained; they commonly lie at the base of sea cliffs (Sellman, et al., 1971, p. D-10). Quartz sand is less common and gravel more common here than on many other U.S. coasts.

e. Hawaii. Much of the Hawaiian islands is bounded by steep cliffs, but there are extensive beaches. Littoral materials consist primarily of bedrock, and white sand formed from calcium carbonate produced by marine invertebrates. Dark-colored basaltic and olivine sands are common where river mouths reach the sea (Shepard and Wanless, 1971, p. 497; U.S. Army Corps of Engineers, 1971).

f. Great Lakes. The U.S. coasts of the Great Lakes vary from high bluffs of clay, shale, and rock, through lower rocky shores and sandy beaches, to low marshy clay flats (U.S. Army Corps of Engineers, 1971, p. 13). The littoral materials are quite variable. Specific features are discussed, for example, by Bowman (1951), Hulsey (1962), Davis (1964), Bajorunas and Duane (1967), Berg and Duane (1968), Saylor and Upchurch (1970), Hands (1970), Corps of Engineers (1953a,b and 1971), and U.S. Army Engineer District, Milwaukee (1953).

#### 6. Sampling Littoral Materials.

Sampling programs are designed to provide information about littoral materials on one or more of the following characteristics:

- (a) Typical grain size (usually median size).
- (b) Size distribution.
- (c) Composition of the littoral materials.
- (d) Variation of (a), (b), and (c), with horizontal and vertical position on the site.
- (e) Possible variation in (a), (b), (c), and (d) with time.

A sampling program will depend on the intended purpose of the samples, the time and money available for sampling, and an inspection of the site to be sampled. A brief inspection will often identify the principal variations in the sediment and suggest the best ways to sample these variations. Sampling programs usually involve beach and nearshore sands and potential borrow sources.

The extent of sampling depends on the importance of littoral materials as related to the total engineering problem. The sampling program should specify:

- (a) Horizontal location of sample.
- (b) Spacing between samples.
- (c) Volume of sample.
- (d) Vertical location and type of sampled volume (e.g., surface layer or vertical core).

(e) Technique for sampling.

(f) Method of storing and documenting the sample.

Beaches typically show more variation across the profile than along the shore, so sampling to determine variation in the littoral zone should usually be made along a line perpendicular to the shoreline.

For reconnaissance sampling, a sample from both the wetted beach face and from the dunes is recommended. More extensive samples can be obtained at constant spacings across the beach or at different locations on the beach profile. Spacings between sampling lines are determined by the variation visible along the beach or by statistical techniques.

Many beaches have subsurface layers of peat or other fine material. If this material will affect the engineering problem, vertical holes or borings should be made to obtain samples at depth.

Sample volume should be adequate for analysis: 50 grams is required for sieve analysis; for settling tube analysis, smaller quantities will suffice, but at least 50 grams is needed if other studies are required later. A quarter of a cup is more than adequate for most uses.

Sand often occurs in fine laminae on beaches. However, for engineering applications it is rarely necessary to sample individual laminae of sand. It is easier and more representative to take an equidimensional sample that cuts across many laminae. Experience at CERC suggests that any method of obtaining an adequate volume of sample covering a few centimeters in depth usually gives satisfactory results. Cores should be taken where pile foundations are planned.

The sample is only as good as the information identifying it. The following minimum information should be recorded at the time of sampling: locality, date and time, position on beach, remarks, and initials of collector. This information must stay with the sample; this is best ensured by fixing it to the sample container or placing it inside the container. Unless precautions are taken, the sample label may deteriorate due to moisture, abrasion, or other causes. Using ballpoint ink on plastic strip (plastic orange flagging commonly used by surveyors) will produce a label which can be stored in the bag with the wet sample without deteriorating or the information washing or wearing off. Some information may be preprinted by rubber stamp on the plastic strip using indelible laundry ink.

## 7. Size Analyses.

Three common methods of analyzing beach sediment for size are visual comparison with a standard, sieve analysis, and settling tube analysis.

The mean size of a sand sample can be estimated qualitatively by visually comparing the sample with sands of known sizes. Standards can be easily prepared by sieving selected diameters, or by selecting samples whose sizes are already known. The standards may be kept in labeled transparent vials or glued on cards. If glued, care is necessary to ensure that the particles retained by the glue are truly representative of the standard.

Good, qualitative, visual estimates of mean size are possible with little previous experience. With experience, such visual estimates become semi-quantitative. Visual comparison with a standard is a useful tool in reconnaissance and in obtaining interim results pending a more complete laboratory size analysis.

a. Sieve Analysis. Sieves are graduated in size of opening according to the U.S. standard series. These standard sieve openings vary by a factor of 1.19 from one opening to the next larger (by the fourth root of 2, or 0.25-phi intervals); e.g., 0.25, 0.30, 0.35, 0.42, and 0.50 millimeter (2.00, 1.75, 1.50, 1.25, 1.00 phi). The range of sieve sizes used and the size interval between sieves selected can be varied as required. Typical beach sand can be analyzed adequately using sieves with openings ranging from 0.062 to 2.0 millimeters (4.0 to -1.0 phi), in size increments increasing by a factor of 1.41 (0.5-phi intervals).

Sediment is usually sieved dry. However, for field analysis or for size analysis of sediment with a high content of fine material, it may be useful to wet-sieve the sediment. Such wet-sieve analyses are described by Lee, Yancy, and Wilde (1970).

Size analysis by sieves is relatively slow but provides a widely accepted standard of reference.

A sieve analysis is independent of sediment density. Sediment shape variation can introduce error in that sieve analysis tends to measure the smaller axis of individual grains; these axes do not fully characterize the size or mass of elongated grains (Sengupta and Veenstra, 1968; Baba and Komar, 1981).

g. Settling Tube Analysis. Recording the rate that sediment settles in a fluid-filled tube provides a rapid measurement of sediment size with useful accuracy (Gibbs, 1972). Size analyses using a settling tube are sensitive to sediment density and to sediment shape. Settling velocity tends to be controlled by the larger axes of individual grains (Sengupta and Veenstra, 1968; Mehta, Lee, and Christensen, 1980). With commonly occurring littoral sands, the characteristic sediment size is related to the settling velocity of grains in isolation or in bulk (Ch. 4, Sec. II,1,c).

There are numerous types of settling tubes; the most common is the visual accumulation tube (Colby and Christensen, 1956), of which there are also several types. The type now used at CERC (the rapid sediment analyzer or RSA) works in the following way:

A 3- to 6-gram sample of sand is dropped through a tube filled with distilled water at constant temperature. A pressure sensor near the bottom of the tube senses the added weight of the sediment supported by the column of water above the sensor. As the sediment falls past the sensor, the pressure decreases. The record of pressure versus time is empirically calibrated to give size distribution based on fall velocity.

The advantage of settling tube analysis is its speed. With modern settling tubes, average time for size analyses of bulk lots can be about one-fifth the time required for sieve analyses.

Because of the lack of an accepted standard settling tube, rapidly changing technology, possible changes in tube calibration, and the uncertainty about fluid mechanics in settling tubes, it is recommended that all settling tubes be carefully calibrated by running a range of samples through both the settling tube and ASTM standard sieves. After thorough initial calibration, the calibration should be spot-checked periodically by running replicate sand samples of known size distribution through the tube.

### III. LITTORAL WAVE CONDITIONS

#### 1. Effect of Wave Conditions on Sediment Transport.

Waves arriving at the shore are the primary cause of sediment transport in the littoral zone. Higher waves break farther offshore, widening the surf zone and setting more sand in motion. Changes in wave period or height cause sand to move onshore or offshore. The angle between the crest of the breaking wave and the shoreline determines the direction of the longshore component of water motion in the surf zone and, usually, the longshore transport direction. For these reasons, knowledge about the wave climate--the combined distribution of height, period, and direction through the seasons--is required for an adequate understanding of the littoral processes of any specific area.

#### 2. Factors Determining Littoral Wave Climate.

The wave climate at a shoreline depends on the offshore wave climate, caused by prevailing winds and storms and on the bottom topography that modifies the waves as they travel shoreward.

a. Offshore Wave Climate. Wave climate is the temporal distribution of wave conditions averaged over the years. A wave condition is the particular combination of wave heights, wave periods, and wave directions at a given time. A specific wave condition offshore is the result of local winds blowing at the time of the observation and the recent history of winds in the more distant parts of the same waterbody. For local winds, wave conditions offshore depend on the wind velocity, duration, and fetch. For waves reaching an observation point from distant parts of the sea, wave height is reduced and wave period is increased with increasing travel distance. Waves generated by local winds have short crest lengths in a direction perpendicular to the forward wave velocity and a wide directional spread of energy. Waves arriving from distant parts of the sea are characterized by long crests and a narrow directional spread of energy. (Wave generation and decay are discussed in Chapter 3.) Offshore wave climate varies among different coastal areas because of differences in exposure to waves generated in distant parts of the sea and because of systematic differences in wind patterns around the Earth. The variations in offshore wave climate affect the amount of littoral wave energy available and the directions from which it comes.

b. Effect of Bottom Topography. As storm waves travel from deep water into shallow water, they generally lose energy even before breaking (Vincent, 1981). They also change height and direction in most cases. The changes may be attributed to refraction, shoaling, bottom friction, percolation, and nonlinear deformation of the wave profile.

Refraction is the bending of wave crests due to the slowing down of that part of the wave crest which is in shallower water (see Ch. 2). As a result, refraction tends to decrease the angle between the wave crest and the bottom contour. Thus, for most coasts, refraction reduces the breaker angle and spreads the wave energy over a longer crest length.

Shoaling is the change in wave height due to conservation of energy flux (see Ch. 2). As a wave moves into shallow water, the wave height first decreases slightly and then increases continuously to the breaker position, assuming friction, refraction, and other effects are negligible.

Bottom friction is important in reducing wave height where waves must travel long distances in shallow water (Bretschneider, 1954).

Nonlinear deformation causes wave crests to become narrow and high and wave troughs to become broad and elevated. Severe nonlinear deformation can also affect the apparent wave period by causing the incoming wave crest to split into two or more crests. This effect is common in laboratory experiments (Galvin, 1972a). It is also expected to be common in the field, although only limited field study has been done (Byrne, 1969).

Offshore islands, shoals, and other variations in hydrography also shelter parts of the shore. In general, bottom hydrography has the greatest influence on waves traveling long distances in shallow water. Because of the effects of bottom hydrography, nearshore waves generally have different characteristics than they had in deep water offshore.

Such differences are often visible on aerial photos. Photos may show two or more distinct wave trains in the nearshore area, with the wave train most apparent offshore and decreasing in importance as the surf zone is approached (e.g., Harris, 1972a,b). The difference appears to be caused by the effects of refraction and shoaling on waves of different periods. Longer period waves, which may be only slightly visible offshore, may become the most prominent waves at breaking, because shoaling increases their height relative to the shorter period waves. Thus, the wave period measured from the dominant wave offshore may be different from the wave period measured from the dominant wave entering the surf zone when two wave trains of unequal period reach the shore at the same time.

c. Winds and Storms. The orientation of a shoreline to the seasonal distribution of winds and to storm tracks is a major factor in determining the wave energy available for littoral transport and the resulting effect of storms. For example, strong winter winds in the northeastern United States usually are from the northwest and, because they blow from land to sea, they do not produce large waves at the shore.

A storm near the coastline will influence wave climate owing to storm surge and high seas; a storm offshore will influence coastal wave climate only by swell. The relation between the meteorological severity of a storm and the resulting beach change is complicated (see Sec. III,5). Although the character, tracks, and effects of storms vary along the different coasts of the United States (Pacific, Atlantic, gulf, and Great Lakes), they can be classified for a particular region.

The probability that a given section of coast will experience storm waves depends on its ocean exposure, its location in relation to storm tracks, and the shelf bathymetry. Using the Atlantic coast (characterized by Atlantic City, New Jersey) as an example, the frequency of storm occurrences (both northeasters and hurricanes) can be studied. Though the effect of a storm depends on the complex combination of variables, storm occurrence can be examined simply by studying the frequency of periods of high waves. Figure 4-12 illustrates the variation in storm occurrence over a 20-year period, and Figure 4-13 shows the seasonal variation, both for Atlantic City, New Jersey.

The data used in Figure 4-12 and Figure 4-13 are hindcast significant wave heights obtained from the Waterways Experiment Station Wave Information Study. Note that surge and tide effects have not been included in the hindcast. For the purpose of the two figures, a "storm" is defined as a period during which the wave height exceeded a critical value equal to the sum of the long-term average wave height plus one standard deviation (1.1 meters or 3.6 feet) for Atlantic City. Though six different wave height groups are shown, probably those producing peak wave heights less than 2.0 meters (6.6 feet) can be considered as insignificant.

According to Figure 4-12, there is an average of 35 storms per year, though the number varied from 22 to 42. Storms with waves greater than 4.0 meters (13.1 feet) occurred in only 9 of the 20 years of record (45 percent), while those with waves greater than 4.5 meters (14.8 feet) occurred in only 3 years.

Figure 4-13 dramatically shows the seasonal variation in storm occurrence from a summer low of 5.5 percent of all storms in July to 10.7 percent in November; 82 percent of all storms with wave heights greater than 2.5 meters (8.2 feet) occur within 6 months of the year (November to April). Storm frequencies for other east coast areas should be generally similar to those shown for Atlantic City, but more frequent and more intense to the north and less frequent to the south.

Neumann et al. (1978) discuss the frequency of occurrence of tropical storms and hurricanes along the Atlantic and gulf coasts. Figure 4-14 illustrates the annual variation in the number of hurricanes, which averages 4.9 per year. Figure 4-15 shows the seasonal variation in hurricane occurrence, with most of the storms occurring between August and October (note that this is out of phase with the occurrence of winter northeasters as shown in Figure 4-13). The probability of a hurricane reaching land varies widely along the coast, as shown in Figure 4-16.

### 3. Nearshore Wave Climate.

Desirable wave climate data for the prediction of littoral processes include summaries of wave height, period, and direction just prior to breaking for all major wave trains at a site of interest. Such data are rarely available. Summaries of significant wave height and dominant wave period from gage measurements with no identification of separate wave trains are becoming increasingly available (e.g. Thompson, 1977; California Coastal Data Collection Program, 1977-1981), but even this information is still lacking for most localities. Wave direction measurements, which are especially difficult to collect, are very rare. When data are available at one locality they may not be applicable to nearby localities because of localized effects of bottom topography.

MAXIMUM WAVE HEIGHT, m

-   $H \geq 3.5$
-   $3.0 \leq H < 3.5$
-   $2.5 \leq H < 3.0$
-   $2.0 \leq H < 2.5$
-   $1.5 \leq H < 2.0$
-   $1.1 \leq H < 1.5$

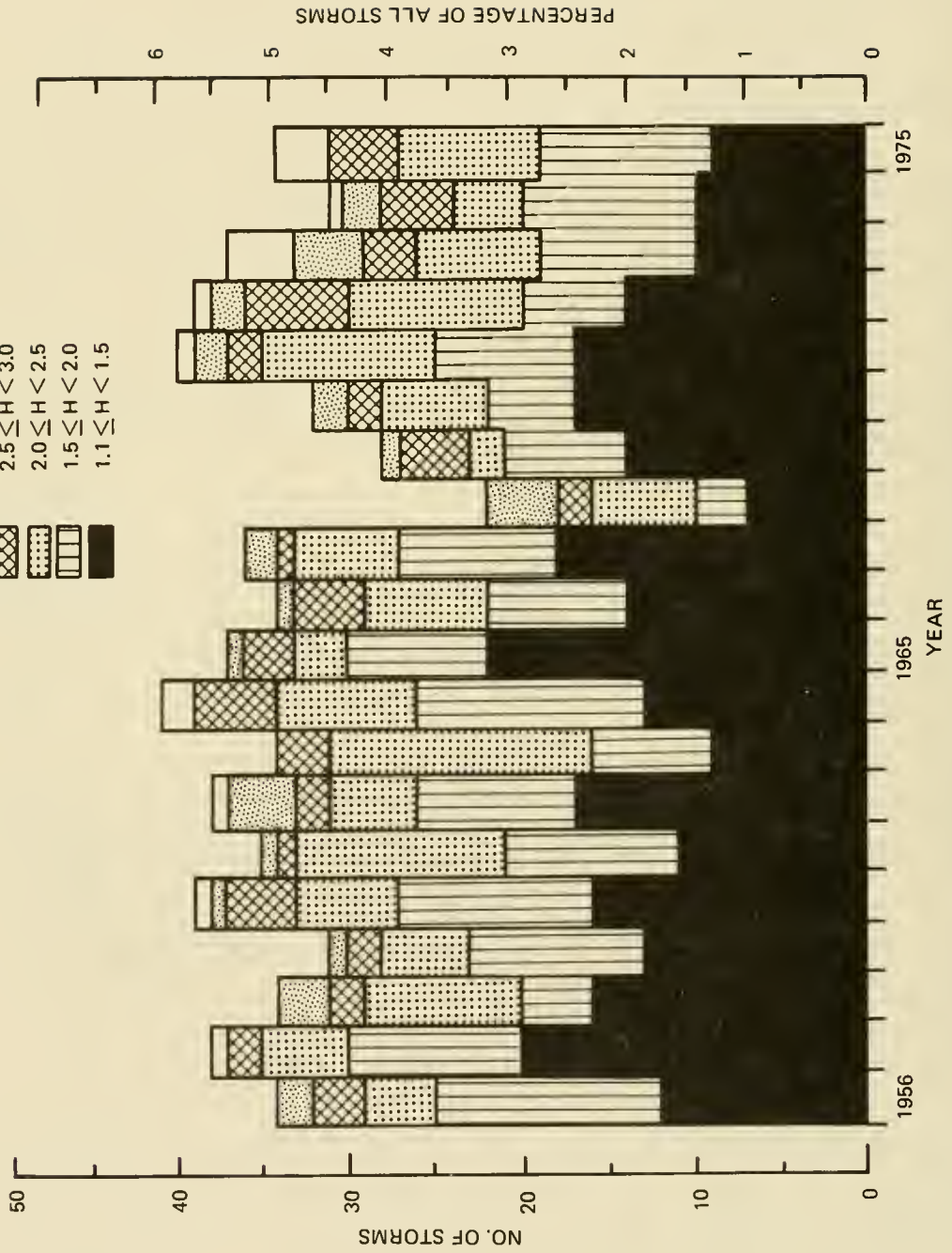


Figure 4-12. Annual variation in storm occurrence for Atlantic City, New Jersey, based on hindcast wave data.

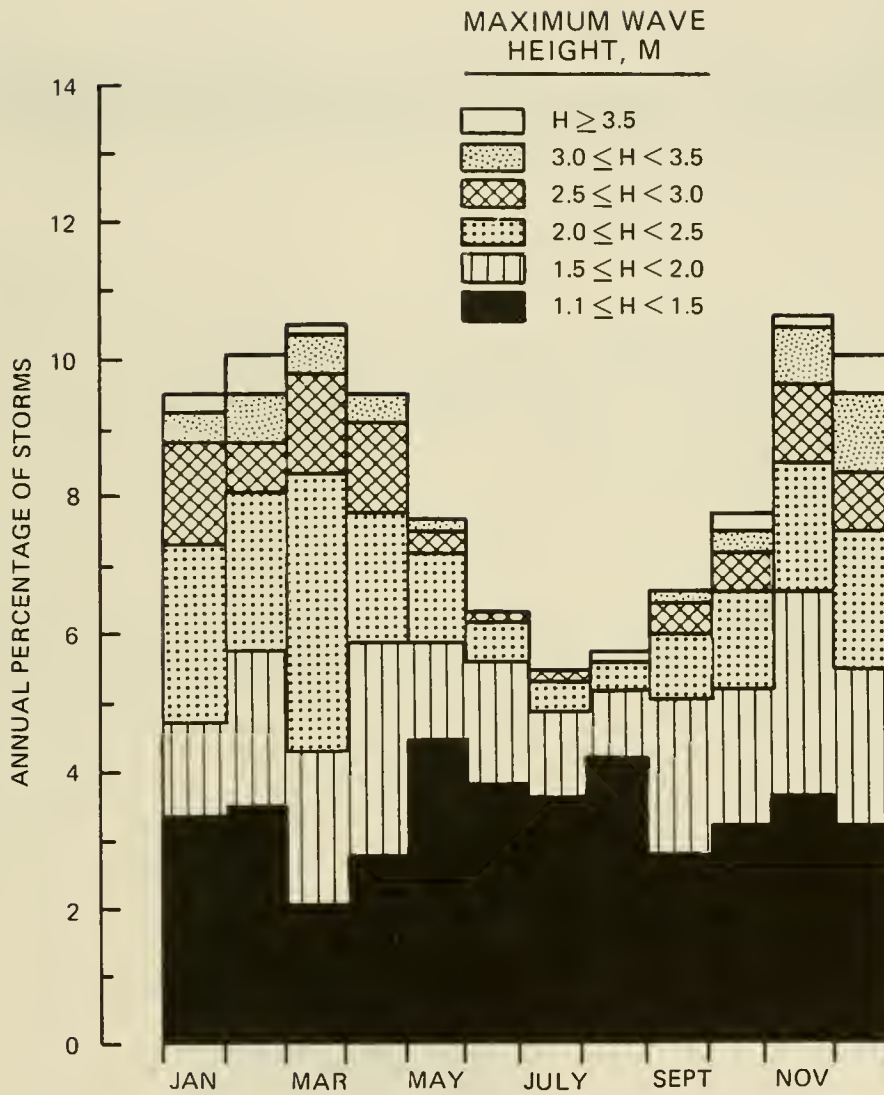
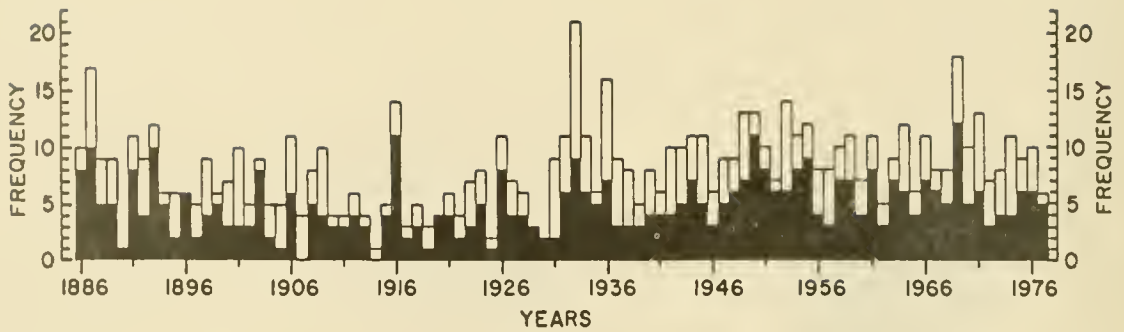
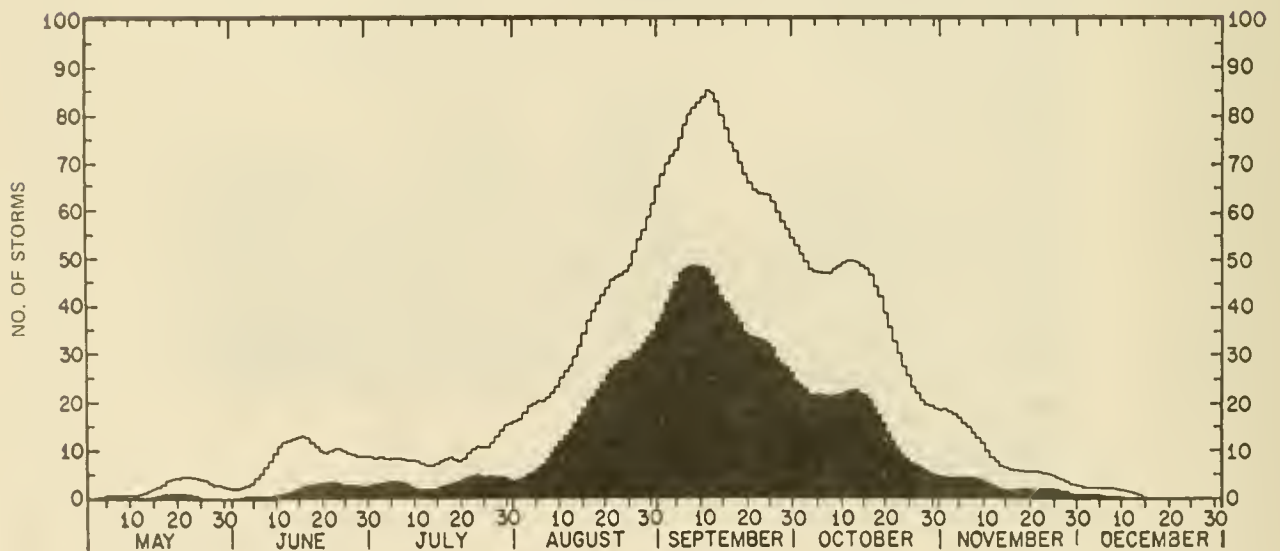


Figure 4-13. Seasonal variation in storm occurrence for Atlantic City, New Jersey, based on hindcast wave data.



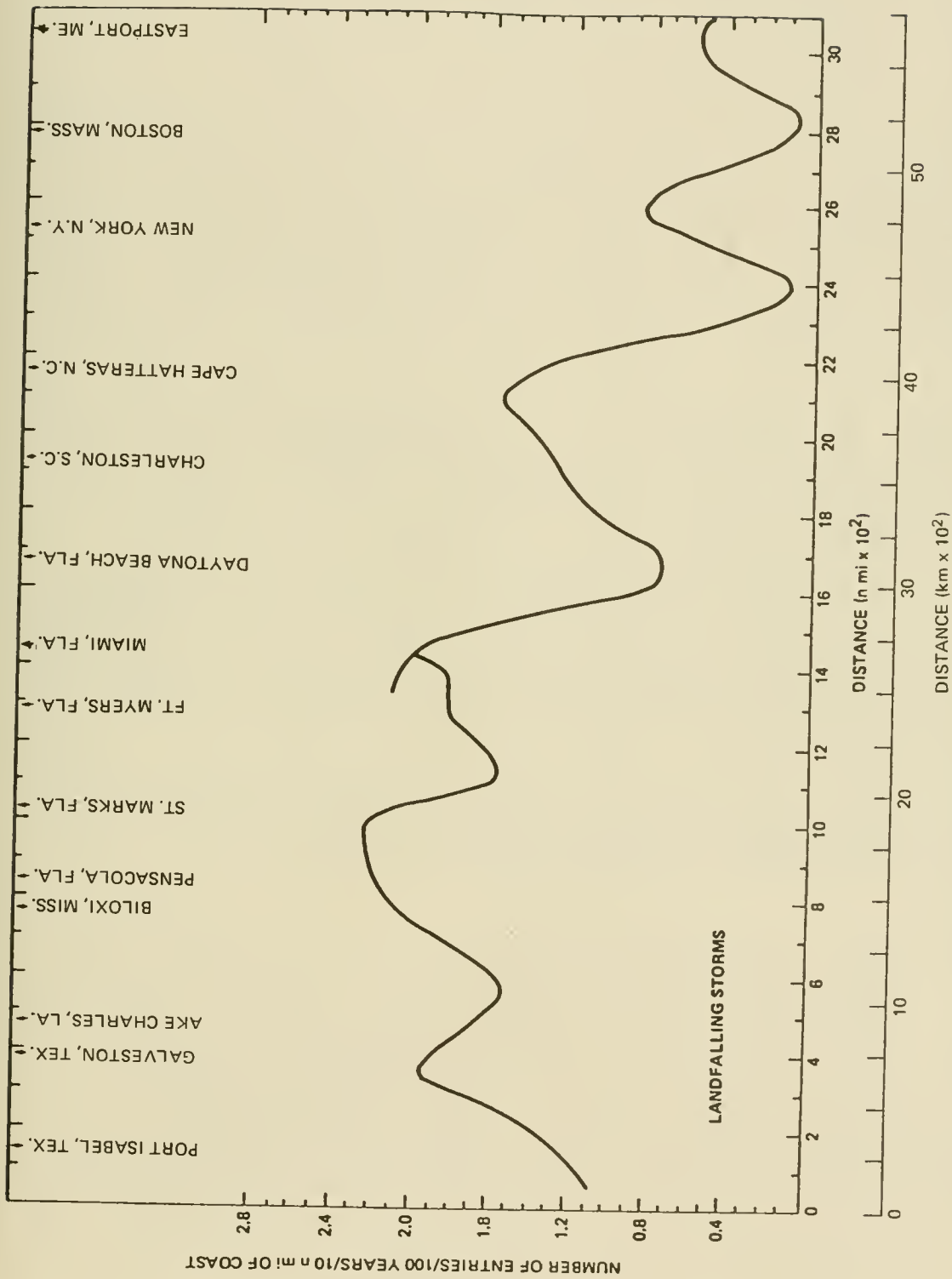
(from Neumann et al., 1978)

Figure 4-14. Annual distribution of the 761 recorded Atlantic tropical cyclones reaching at least tropical storm strength (open bar) and the 448 reaching hurricane strength (solid bar), 1886 through 1977. (The average number of such storms is 8.3 and 4.9, respectively.)



(from Neumann et al., 1978)

Figure 4-15. Number of tropical storms and hurricanes (open bar) and hurricanes alone (solid bar) observed on each day (smoothed by a 9-day moving average), May 1-December 30, 1886 through 1977.



(from Neumann et al., 1978)

Figure 4-16. Smoothed frequency of landfalling tropical storms and hurricanes (1871 through 1973) for the gulf and east coasts of the United States. (Discontinuity between Miami and Ft. Myers represents Florida Keys.)

The quality and quantity of available wave climate data often do not justify elaborate statistical analysis. Even where adequate data are available, a simple characterization of wave climate meets many engineering needs. Thus mean values of height and, to a lesser degree, period are useful. However, data on wave direction are generally of insufficient quality for even mean value use.

Mean annual wave heights and periods determined from data collected at a number of wave gages and by visual observers at exposed sites along the coasts of the United States are presented in Table 4-4. The visual height observations, made from the beach, represent an average value of the higher waves just before their first break. They can be considered as estimates of significant height  $H_s$ . The wave gage data were measured by gages fixed in depths of 3 to 8.5 meters (10 to 28 feet). Manual analysis of waves recorded on chart paper is discussed in Chapter 3 and by Draper (1967), Tucker (1961), Harris (1970), and Thompson (1977). Spectral analysis of wave records is discussed in Chapter 3 and by Kinsman (1965), National Academy of Sciences (1963); Neumann and Pierson (1966); Harris (1974); Wilson, Chakrabarti, and Snider (1974); and Thompson (1980a). While gage measurements are more accurate than visual observations, visual observations define wave conditions at breaking which account for onshore-offshore variation in surf zone position as a function of water level and wave height.

Wave data treated in this section are limited to nearshore observations and measurements. Consequently, waves were fully refracted and had been fully affected by bottom friction, percolation, and nonlinear changes in waveform caused by shoaling. Thus, these data differ from data that would be obtained by simple shoaling calculations based on the deepwater wave statistics. In addition, data are normally lacking for the rarer, high-wave events. However, the nearshore data are of use in littoral transport calculations.

Mean wave height and period from a number of visual observations made by the Coast Guard at shore stations are plotted by month in Figures 4-17 and 4-18, using the average values of stations within each of five coastal segments. Strong seasonal variations are evident in Figure 4-17.

The *minimum* monthly mean littoral zone wave height averaged for the California, Oregon, and Washington coasts exceeds the *maximum* mean littoral zone wave height averaged for the other coasts. This difference greatly affects the potential for sediment transport in the respective littoral zones and should be considered by engineers when applying experience gained in a locality with one nearshore wave climate to a problem at a locality with another wave climate.

The climatological importance of prominent secondary wave trains occurring simultaneously with the dominant wave train has been considered by Thompson (1980b). Probabilities associated with multiple wave trains, obtained by counting prominent spectral peaks over approximately 1 year of data from each site, are presented in Figure 4-19. About 70 percent of the Atlantic coast records and 60 percent of the southern California and gulf coast records indicate the existence of more than one prominent wave train.

b. Mean versus Extreme Conditions. Chapter 3, Section II contains a discussion of the distribution of individual wave heights for a wave condition

Table 4-4. Mean significant wave height<sup>1</sup> and period at coastal localities of the United States.

Location	Annual Mean		Location	Annual Mean	
	Height m (ft)	Period s		Height m (ft)	Period s
Atlantic Coast					
<u>Massachusetts</u>			<u>North Carolina</u>		
+Cape Cod	0.85 (2.8)	6.3	+Seacrest	0.85 (2.8)	7.5
<u>Rhode Island</u>			+Kill Devil Hills	0.52 (1.7)	6.3
+Misquamicut	0.49 (1.6)	8.3	*Nags Head	0.94 (3.1)	8.6
<u>New York</u>			+Nags Head	0.94 (3.1)	9.3
+Southampton	0.70 (2.3)	7.9	*Wrightsville Beach	0.79 (2.6)	7.8
+Fire Island	0.67 (2.2)	7.6	*Holden Beach	0.64 (2.1)	7.5
<u>New Jersey</u>			<u>South Carolina</u>		
+Brigantine	0.73 (2.4)	6.1	Murrels Inlet	0.91 (3.0)	7.2
*Atlantic City	0.85 (2.8)	8.3	<u>Florida</u>		
+Ludlam Island	0.55 (1.8)	6.6	*Daytona Beach	0.67 (2.2)	8.7
<u>Virginia</u>			*Palm Beach	0.64 (2.1)	6.4
+Assateague	0.67 (2.2)	7.8	*Lake Worth	0.67 (2.2)	6.4
*Virginia Beach	0.64 (2.1)	8.2	+Boca Raton	0.58 (1.9)	4.9
Gulf Coast					
<u>Florida</u>			<u>Texas</u>		
*Naples	0.30 (1.0)	4.7	*Galveston	1.40 (1.3)	5.7
*Destin	0.49 (1.6)	5.7	Corpus Christi	0.79 (2.6)	6.7
Pacific Coast					
<u>California</u>			<u>California (cont.)</u>		
Imperial Beach	0.85 (2.8)	13.6	San Simeon	0.94 (3.1)	12.2
Torrey Pines	0.91 (3.0)	15.7	Natural Bridges	1.01 (3.3)	14.6
San Clemente	0.85 (2.8)	14.5	<u>Oregon</u>		
*Huntington Beach	0.73 (2.4)	12.9	Rogue River	1.62 (5.3)	8.1
*Venice	0.37 (1.2)	10.5	Port Orford	1.25 (4.1)	13.5
PEG at Point Mugu	0.85 (2.8)	13.4	Coquille River	1.28 (4.2)	11.9
*Point Mugu	1.01 (3.3)	10.7	Coos Bay	1.28 (4.2)	10.9
Channel Islands Harbor	0.85 (2.8)	11.5	Umpqua River	0.91 (3.0)	8.9
Mandalay	0.70 (2.3)	13.0	Yaquina Bay	2.07 (6.8)	10.3
			Tillamook Bay	1.19 (3.9)	12.8

<sup>1</sup> Starred entries contain data from CERC wave gage records. Mean wave heights for entries marked with a cross (+) are from visual (nearbreaker) observations of the CERC Beach Evaluation Program; for unmarked entries, data are from the CERC Littoral Environment Observation Program.

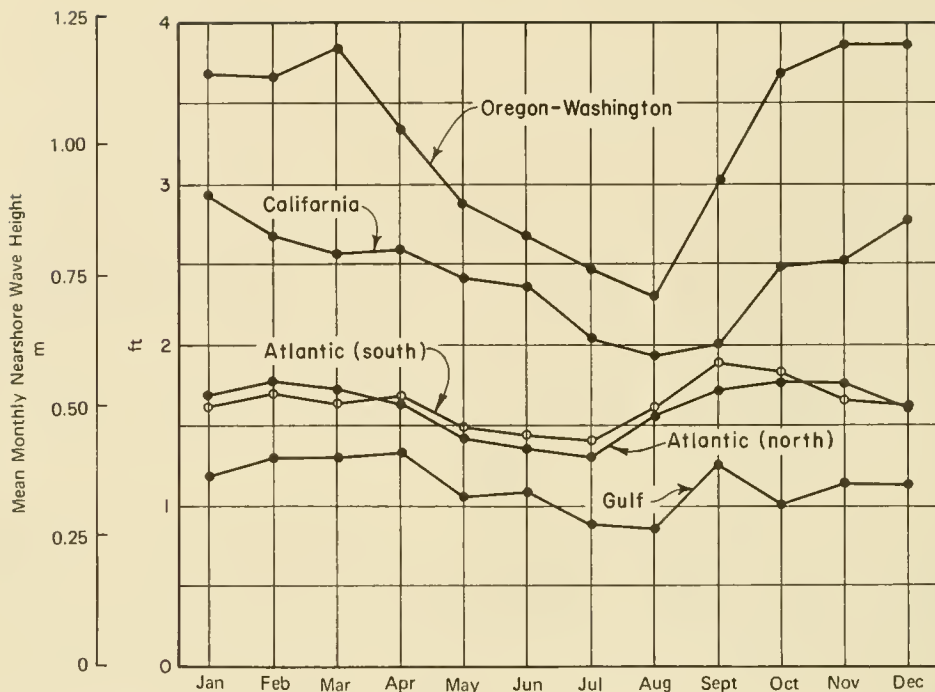


Figure 4-17. Mean monthly nearshore wave heights for five coastal segments.

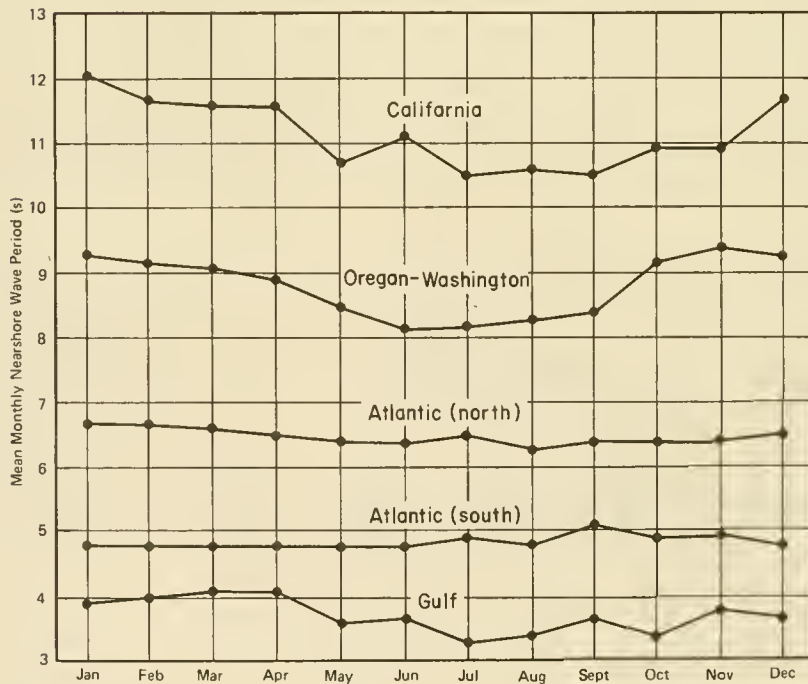


Figure 4-18. Mean monthly nearshore wave periods (including calms) for five coastal segments.

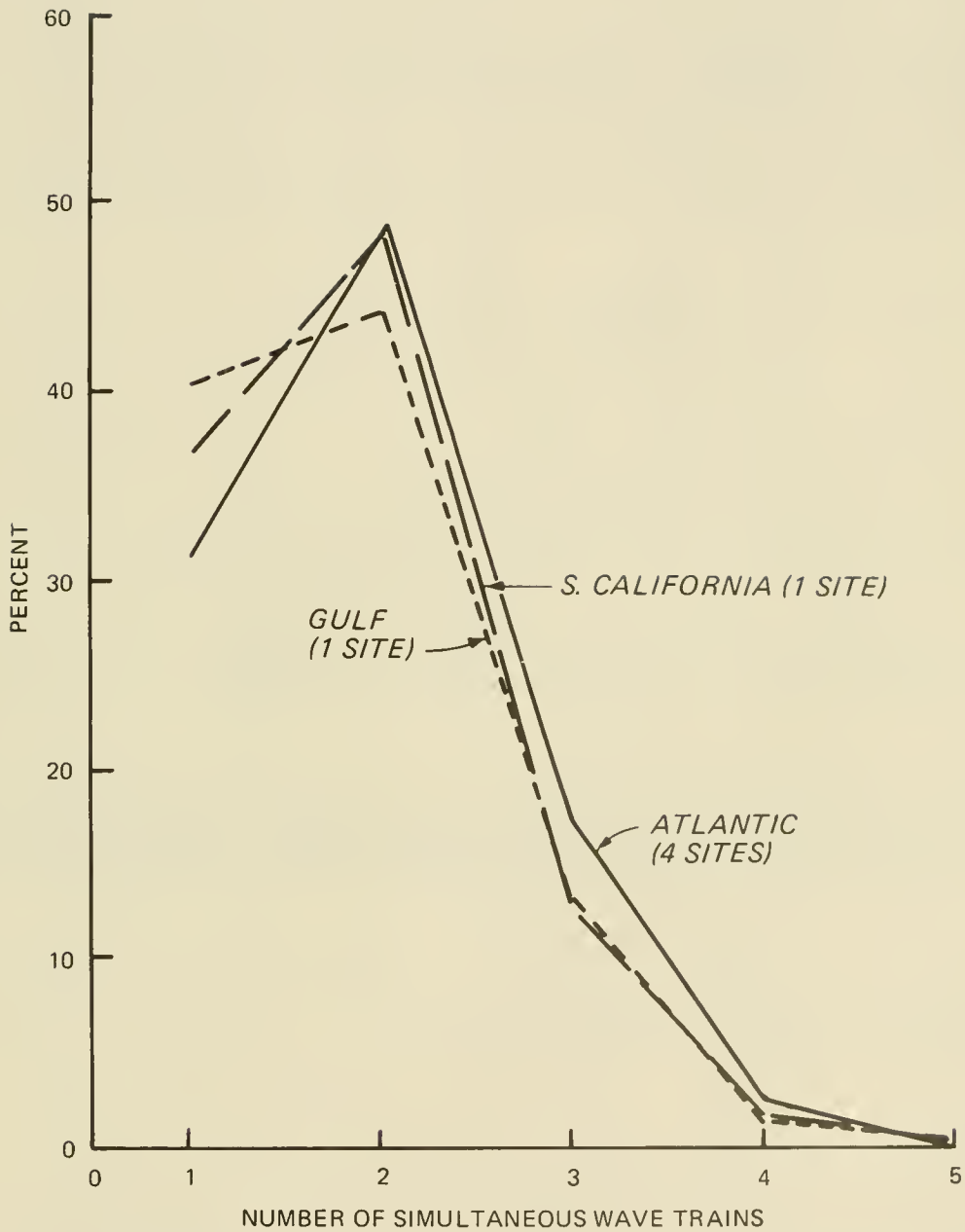


Figure 4-19. Distribution of number of simultaneous wave trains (estimated as the number of prominent spectral peaks) from wave gages in three coastal segments.

and the relations between various wave height statistics, such as the mean, significant, and RMS heights, and extreme values. In general, a group of waves from the same record can be approximately described by a Rayleigh distribution (see Ch. 3, Sec. II). A different distribution appears necessary to describe the distribution of significant wave heights, where each significant wave height is taken from a different wave record at a given locality (see Fig. 4-20). An estimate of the distribution of significant heights higher than the mean significant height can be especially important because wave energy in the littoral zone increases with the square of the wave height. A useful model is provided by a modified exponential distribution of form

$$F \left( H_s > \hat{H}_s \right) = e^{-\left[ \frac{\hat{H}_s - H_{s \min}}{\sigma} \right]} \quad (4-12)$$

where

- $H_s$  = the significant height
- $\hat{H}_s$  = significant height of interest
- $H_{s \min}$  = the approximate "minimum significant height"
- $\sigma$  = the significant wave height standard deviation

(Thompson and Harris, 1972.) This equation depends on two parameters,  $H_{s \min}$  and  $\sigma$ , which are related to the mean height,

$$\bar{H}_s = H_{s \min} + \sigma \quad (4-13)$$

If  $H_{s \min}$  or  $\sigma$  are not available but the mean significant height  $\bar{H}_s$  is known, then an approximation to the distribution of equation (4-12) can be obtained from the data of Thompson and Harris (1972, Table 1), which suggest

$$H_{s \min} \approx 0.38 \bar{H}_s \quad (4-14)$$

This approximation reduces equation (4-12) to a one-parameter distribution depending only on mean significant wave height

$$F \left( H_s > \hat{H}_s \right) \approx e^{-\left[ \frac{1.61 \hat{H}_s - 0.61 \bar{H}_s}{\bar{H}_s} \right]} \quad (4-15)$$

Equation (4-15) is not a substitute for the complete distribution function, but when used with the wave gage data in Figure 4-20, it provides an estimate of higher waves with agreement within 20 percent. Greater scatter would be expected with visual observations.

#### 4. Office Study of Wave Climate.

Information on wave climate is necessary for understanding littoral processes. Usually there is insufficient time to obtain data from the field, and it is necessary to compile information in an office study. The primary variables of engineering interest for such a compilation are wave height and direction.

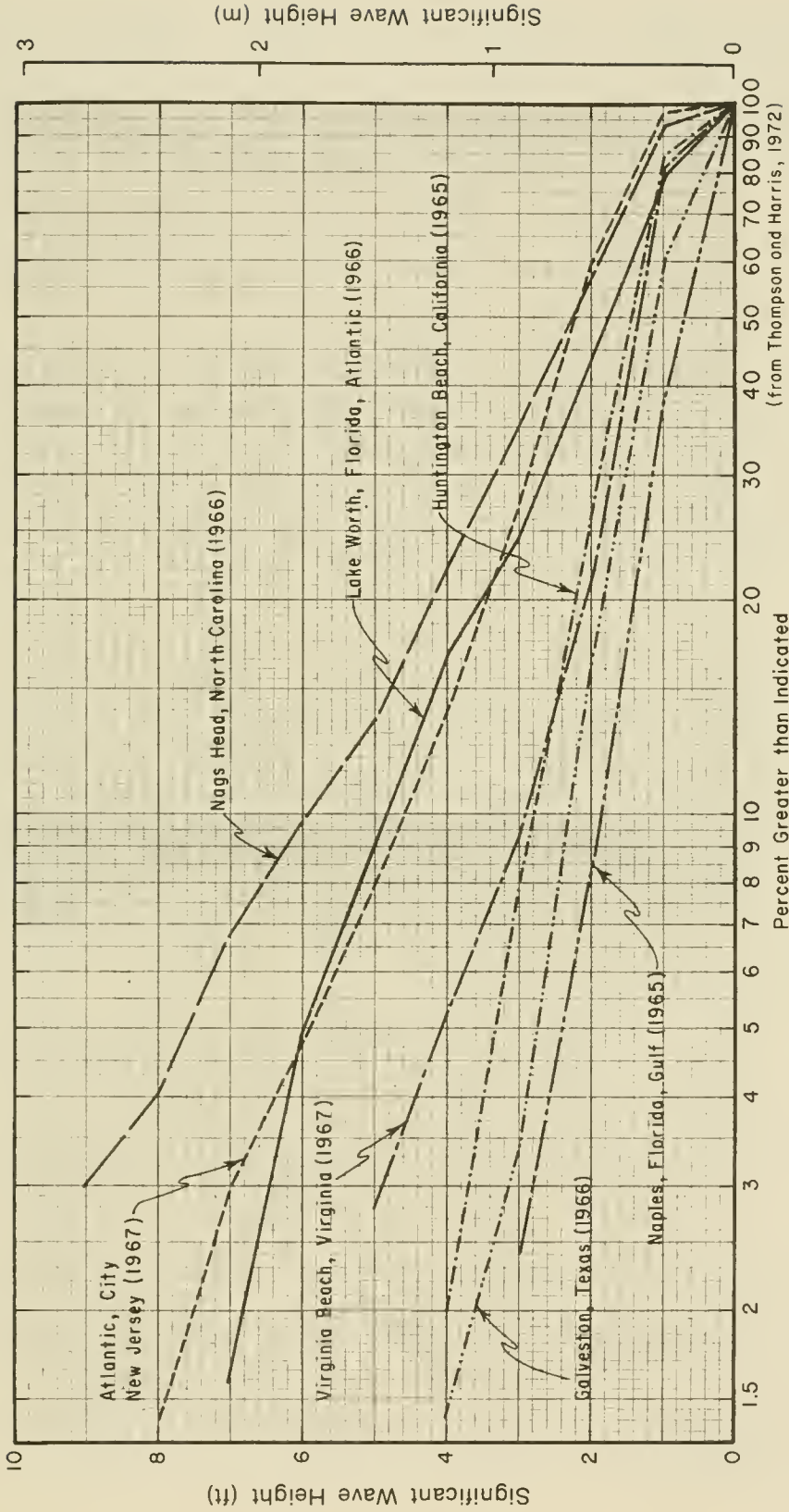


Figure 4-20. Distribution of significant wave heights from coastal wave gages for 1-year records.

Wave data from past measurement programs are available at the National Oceanographic Data Center, Washington, D.C. 20235. Shipboard observations covering U.S. coasts and other ocean areas are available as summaries (Summary of Synoptic Meteorological Observations, SSMO) through the National Technical Information Service, Springfield, Va. 22161. See Harris (1972a,b) for a preliminary evaluation of this data for coastal engineering use.

When data are not available for a specific location, the wave climate can often be estimated by extrapolating from another location--after correcting for differences in coastal exposure, winds, and storms--although this can be a tedious and uncertain procedure.

On the east, gulf, and Great Lakes coasts, local winds are often highly correlated with the direction of longshore currents. Such wind data are available in "Local Climatological Data" sheets published monthly by the National Weather Service, National Oceanographic and Atmospheric Administration (NOAA), for about 300 U.S. weather stations. Other NOAA wind data sources include annual summaries of the Local Climatological Data by station (Local Climatological Data with Comparative Data), and weekly summaries of the observed weather (Daily Weather Maps), all of which can be ordered from the Superintendent of Documents, U.S. Government Printing Office, Washington, D.C. 20402.

Local weather data are often affected by conditions in the neighborhood of the weather station, so care should be used in extrapolating weather records from inland stations to a coastal locality. However, statistics on frequency and severity of storm conditions do not change appreciably for long reaches of the coast. For example, in a study of Texas hurricanes, Bodine (1969) felt justified in assuming no difference in hurricane frequency along the Texas coast. In developing information on the Standard Project Hurricane, Graham and Nunn (1959) divided the Atlantic coast into zones 322 kilometers (200 miles) long and the gulf coast into zones 644 kilometers (400 miles) long. Variation of most hurricane parameters within zones is not great along straight open stretches of coast.

The use of weather charts for wave hindcasting is discussed in Chapter 3. Computer methods for generating offshore wave climate have improved considerably over the last decade and are now a viable tool for an office study of wave climate. However, development of nearshore wave climate from hindcasting can be a time-consuming job. Even with the best computer methods, the wave climate must be used with discretion because wind information over the ocean is often incomplete and knowledge of nearshore topography and its effect on the wave is usually limited. Nearshore wave climate data obtained by advanced state-of-the-art computer hindcasts are available for the entire Atlantic coast of the United States (Corson, et. al., 1981). Similar wave climate information development is planned for the Pacific, gulf, and Great Lakes coasts of the United States.

Other possible sources of wave climate information for office studies include aerial photography, newspaper records, and comments from local residents.

Data of greater detail and reliability than that obtained in an office

study can be obtained by measuring wave conditions at the shoreline locality for at least 1 year. In many cases a visual observation program can also provide useful data. A study of year-to-year variation in wave height statistics collected at CERC wave gages (Thompson and Harris, 1972) indicates that six observations per day for 1 year gives a reliable wave height distribution function to the 1 percent level of occurrence. Even one observation a day for 1 year appears to provide a useful height-distribution function for exposed ocean sites.

#### 5. Effect of Extreme Events.

Infrequent events of great magnitude, such as hurricanes, cause significant modification of the littoral zone, particularly to the profile of a beach. An extreme event could be defined as an event, great in terms of total energy expended or work done, that is not expected to occur at a particular location more than once every 50 to 100 years on the average. Hurricane Camille in 1969 and the Great East Coast Storm of March 1962 can be considered extreme events. Because large storms are infrequent, and because it does not necessarily follow that the magnitude of a storm determines the amount of geomorphic change, the relative importance of extreme events is difficult to establish.

Wolman and Miller (1960) suggested that the equilibrium profile of a beach is more related to moderately strong winds that generate moderate storm waves, rather than to winds that accompany infrequent catastrophic events. Saville (1950) showed that for laboratory tests with constant wave energy and angle of attack there is a particular critical wave steepness at which littoral transport is a maximum. Under field conditions, there is probably a similar critical value that produces transport out of proportion to its frequency of occurrence. The winds associated with this critical wave steepness may be winds generated by smaller storms, rather than the winds associated with extreme events.

The effect of an extreme event is determined by a complex combination of many variables. Table 4-5, after Kana (1977), identifies 13 variables which are qualitatively evaluated according to significance. Included in the table are storm, beach, and water level factors.

Most storms move large amounts of sand from the beach to offshore; but after the storm, the lower waves that follow tend to restore this sand to the face of the beach. Depending on the extent of restoration, the storm may produce little permanent change.

While rapid recovery has been documented (Birkemeier, 1979; Kana, 1977; Sonu, 1972), extreme storms may result in a net movement and loss of material to the offshore as the profile rapidly adjusts to a slow rise in sea level following a period of few major storms (Dean, 1976). Severe storms may also drive sand either far offshore, into depths deeper than can be recovered by normal wave action, or landward, overwashing the beach and moving sand inland. Both processes can result in a net loss of material from the littoral zone.

Table 4-5. Factors influencing erosion caused by storms.

Main Factors	Subfactors	Increased tendency toward erosion with (high/low) values <sup>1</sup>
Storm processes	Wind velocity	High
	Wind direction	Variable
	Wave height	High
	Wave period	Low
	Wave steepness	High
	Longshore current	High
	Storm duration	High
Beach	Sediment size	Low (to silt size)
	Degree of lithification	Low
	Morphology slope	High
	rhythmic topography	Variable
Water level	Tide stage	High
	Storm surge	High

<sup>1</sup> For example, erosion tends to increase when wave height is *high*, wave period is *low*, beach slope is *high*, etc.

Depending on the path of the storm and the angle of the waves, a significant amount of material can also be moved alongshore. If the direction of longshore transport caused by the storm is opposite to the net direction of transport, the sand will probably be returned in the months after the storm and permanent beach changes effected by the storm will be small. If the direction of transport before, during, and after the storm is the same, then large amounts of material could be moved by the storm with little possibility of restoration. Successive storms on the same beach may cause significant transport in opposite directions (e.g., Everts, 1973).

There are some unique events that are only accomplished by catastrophic storms. The combination of storm surge and high waves allows water to reach some areas not ordinarily attacked by waves. These extreme conditions may result in the overtopping of dunes and in the formation of washover fans and inlets (Morgan, Nichols, and Wright, 1958; Nichols and Marston, 1939; Howard, 1939; Leatherman et al., 1977). Some inlets are periodically reopened by storms and then sealed by littoral drift transported by normal wave action.

For a given storm, greater effects can be expected at beaches with lower average wave climates. In a high-energy climate, storm waves are not much larger than ordinary waves and their effects may not be significant; an example of this might be northeasters occurring at Cape Cod. In a low-energy climate, where transport volumes are usually low, storm waves can move significant amounts of sand, as do hurricanes on the gulf coast.

The effects of particular storms on certain beaches are described in the following paragraphs. These examples illustrate how an extreme event may affect the beach.

In October 1963, the worst storm in the memory of the Eskimo people occurred over an ice-free part of the Arctic Ocean, attacking the coast near Barrow, Alaska (Hume and Schalk, 1967). Detailed measurements of some of the key coastal areas had been made just before the storm. Freezeup just after the storm preserved the changes to the beach until surveys could be made the following July. Most of the beaches accreted 0.3 to 0.6 meter (1 to 2 feet), although Point Barrow was turned into an island. According to Hume and Schalk, "The storm of 1963 would appear to have added to the Point the sediment of at least 20 years of normal longshore transport." Because of the low-energy wave climate and the short season in which littoral processes can occur at Barrow, this storm significantly modified the beach.

A study of two hurricanes, Carla in 1961 and Cindy in 1963, was made by Hayes (1967a). He concluded that "the importance of catastrophic storms as sediment movers cannot be over-emphasized" and observed that, in low-energy wave climates, most of the total energy is expended in the nearshore zone as a series of catastrophies. In this region, however, the rare "extreme" hurricane is probably not as significant in making net changes as the more frequent moderate hurricanes.

Surprisingly, Hurricane Camille, with maximum winds of 322 kilometers per hour (200 miles per hour), did not cause significant changes to the beaches of Mississippi and Louisiana. Tanner (1970) estimated that the sand transport along the beach appeared to have been an amount equal to less than a year's amount under ordinary conditions and theorized that "the particular configuration of beach, sea wall, and coastal ridge tended to suppress large scale transport."

Hurricane Audrey struck the western coast of Louisiana in June 1957. The changes to the beach during the storm were neither extreme nor permanent. However, the storm exposed marsh sediments in areas where sand was deficient and "set the stage for a period of rapid shoreline retreat following the storm" (Morgan, Nichols, and Wright, 1958). Indirectly, the storm was responsible for significant geomorphic change.

A hurricane (unnamed) coincided with spring tide on the New England coast on 21 September 1938. Property damage and loss of life were both high. A storm of this magnitude was estimated to occur about once every 150 years. A study of the beach changes along a 19-kilometer (12-mile) section of the Rhode Island coast (Nichol and Marsten, 1939) showed that most of the changes in the beach profile were temporary. The net result was some cliff erosion and a slight retrogression of the beaches. However, the same hurricane resulted in major changes to the south shore of Long Island (Howard, 1939). A total of eight inlets were opened through the barrier island, and three into closed-mouthed bays. This included the opening of the present-day Shinnecock Inlet and the widening of Moriches Inlet.

Beach changes from Hurricane Donna which hit Florida in September 1960 were more severe and permanent. In a study of the southwestern coast of Florida before and after the storm, Tanner (1961) concluded that "Hurricane Donna appears to have done 100 years' work, considering the typical energy level thought to prevail in the area."

On 1 April 1946, a tsunami struck the Hawaiian Islands with runup in places as high as 17 meters (55 feet) above sea level (Shepard, MacDonald, and Cox, 1950). The beach changes were similar to those inflicted by storm waves, although "in only a few places were the changes greater than those produced during normal storm seasons or even by single severe storms." Because a tsunami is of short duration, extensive beach changes do not occur, although property damage can be quite high.

Several conclusions can be drawn from the above examples. If a beach has a sufficient sand supply and fairly high dunes that are not breached, little permanent modification will result from storms, except for a brief acceleration of the normal littoral processes. This acceleration will be more pronounced on a shore with low-energy wave conditions.

#### IV. NEARSHORE CURRENTS

Nearshore currents in the littoral zone are predominantly wind and wave-induced motions superimposed on the wave-induced oscillatory motion of the water. The net motions generally have low velocities, but because they transport whatever sand is moved by the wave-induced water motions, they are important in determining littoral transport.

There is only slight exchange of fluid between the offshore and the surf zone. Onshore-offshore flows take place in a number of ways that are not fully understood at present.

##### 1. Wave-Induced Water Motion.

In idealized deepwater waves, water particles have a circular motion in a vertical plane perpendicular to the wave crest (Ch. 2, Fig. 2-4), but this motion does not reach deep enough to affect sediment on the bottom. In depths where waves are affected by the bottom, the circular motion becomes elliptical, and the water at the bottom begins to move. In shallow water, the ellipses elongate into nearly straight lines. At breaking, particle motion becomes more complicated; but even in the surf zone, the water moves forward and backward in paths that are mostly horizontal, with brief, but intense, vertical motions during the passage of the breaker crest. Since it is this wave-induced water particle motion that causes the sediment to move, it is useful to know the length of the elliptical path travelled by the water particles and the maximum velocity and acceleration attained during this orbit.

The basic equations for water-wave motion before breaking are discussed in Chapter 2. Quantitative estimates of water motion are from small-amplitude wave theory (Ch. 2, Sec. II,3), even near breaking where assumptions of the theory are not completely valid (Dean, 1970; Eagleson, 1956). Equations 2-13 and 2-14 give the fluid-particle velocity components  $u$ ,  $w$  in a wave where small-amplitude theory is applicable (see Fig. 2-3 for relation to wave phase and water particle acceleration).

For sediment transport, the conditions of most interest are those when the wave is in shallow water. For this condition, and making the small-amplitude

assumption, the horizontal length  $2A$  of the path moved by the water particle as a wave passes in shallow water is approximately

$$2A = \frac{HT \sqrt{gd}}{2\pi d} \quad (4-16)$$

and the maximum horizontal water velocity is

$$u_{max} = \frac{H \sqrt{gd}}{2d} \quad (4-17)$$

The term under the radical is the wave speed in shallow water.

\*\*\*\*\* EXAMPLE PROBLEM 1 \*\*\*\*\*

GIVEN: A wave 0.3 meters (1 foot) high with a period of 5 seconds is progressing shoreward in a depth of 0.6 meter (2 feet).

FIND:

- (a) Calculate the maximum horizontal distance  $2A$  the water particle moves during the passing of a wave.
- (b) Determine the maximum horizontal velocity  $u_{max}$  of a water particle.
- (c) Compare the maximum horizontal distance  $2A$  with the wavelength in the 0.6-meter depth.
- (d) Compare the maximum horizontal velocity  $u_{max}$  with the wave speed  $C$ .

SOLUTION:

- (a) Using equation (4-16), the maximum horizontal distance is

$$2A = \frac{HT \sqrt{gd}}{2\pi d}$$

$$2A = \frac{0.3 (5) \sqrt{9.8 (0.6)}}{2\pi (0.6)} = 0.96 \text{ meter (3.17 feet)}$$

- (b) Using equation (4-17) the maximum horizontal velocity is

$$u_{max} = \frac{HT \sqrt{gd}}{2d}$$

$$u_{max} = \frac{0.3 \sqrt{9.8 (0.6)}}{2 (0.6)} = 0.61 \text{ meter per second (2.0 feet)}$$

- (c) Using the relation  $L = T \sqrt{gd}$  to determine the shallow-water wavelength,

$$L = 5 \sqrt{9.8 (0.6)} = 12.12 \text{ meters (39.78 feet)}$$

From (a) above the maximum horizontal distance  $2A$  is 0.96 meter; therefore, the ratio  $2A/L$  is

$$\frac{2A}{L} = \frac{0.96}{12.12} = 0.08$$

(d) Using the relation  $C = \sqrt{gd}$  (Eq. 2-9) to determine the shallow-water wave speed

$$C = \sqrt{9.8 (0.6)} = 2.42 \text{ meters (7.96 feet) per second}$$

From (b) above, the maximum horizontal velocity  $u_{max}$  is 0.61 meter per second. Therefore the ratio  $u_{max}/C$  is

$$\frac{u_{max}}{C} = \frac{0.61}{2.42} = 0.25$$

\*\*\*\*\*

Although small-amplitude theory gives a fair understanding of many wave-related phenomena, there are important phenomena that it does not predict. Observation and a more complete analysis of wave motion show that particle orbits are not closed. Instead, the water particles advance a little in the direction of the wave motion each time a wave passes. The rate of this advance is called the *mass transport velocity*; (Ch. 2, Sec. II,5,c). This velocity becomes important for sediment transport, especially for sediment suspended above ripples seaward of the breaker.

For conditions evaluated at the bottom ( $z = -d$ ), the maximum bottom velocity,  $u_{max}(-d)$  given by equation (2-13) determines the average bottom mass transport velocity  $\bar{u}(-d)$  obtained from equation (2-55), according to the equation

$$\bar{u}(-d) = \left( \frac{u_{max}(-d)}{2C} \right)^2 \quad (4-18)$$

where  $C$  is the wave speed given by equation (2-3). Equation (2-55), and thus equation (4-18), does not include allowance for return flow which must be present to balance the mass transported in the direction of wave travel. In addition, the actual distribution of the time-averaged net velocity depends sensitively on such external factors as bottom characteristics, temperature distribution, and wind velocity (Mei, Liu, and Carter, 1972). Most observations show the time-averaged net velocity near the bottom is directed toward the breaker region from both sides. (See Inman and Quinn (1952) for field measurements in surf zone; Galvin and Eagleson (1965) for laboratory observations; and Mei, Liu and Carter (1972, p. 220) for comprehensive discussion.) However, both field and laboratory observations have shown that wind-induced bottom currents may be great enough to reverse the direction of the shoreward time-averaged wave-induced velocity at the bottom when there are strong onshore winds (Cook and Gorsline, 1972; Kraai, 1969).

## 2. Fluid Motion in Breaking Waves.

During most of the wave cycle in shallow water, the particle velocity is approximately horizontal and constant over the depth, although right at breaking there is significant vertical velocity as the water is drawn up into the crest of the breaker. The maximum particle velocity under a breaking wave is approximated by solitary wave theory (eq. 2-66) to be

$$u_{b \text{ max}} = C = \sqrt{g (H + d)} \quad (4-19)$$

where  $(H + d)$  is the distance measured from crest of the breaker to the bottom.

Fluid motions at breaking cause most of the sediment transport in the littoral zone, because the bottom velocities and turbulence at breaking suspend more bottom sediment. This suspended sediment can then be transported by currents in the surf zone whose velocities are normally too low to move sediment at rest on the bottom.

The mode of breaking may vary significantly from spilling to plunging to collapsing to surging, as the beach slope increases or the wave steepness (height-to-length ratio) decreases (Galvin, 1967). Of the four breaker types, spilling breakers most closely resemble the solitary waves whose speed is described by equation (4-19) (Galvin, 1972). Spilling breakers differ little in fluid motion from unbroken waves (Divoky, LeMehaute, and Lin, 1970) and generate less bottom turbulence and thus tend to be less effective in transporting sediment than plunging or collapsing breakers.

The most intense local fluid motions are produced by plunging breakers. As the wave moves into shallower depths, the front face begins to steepen. When the wave reaches a mean depth about equal to its height, it breaks by curling over at the crest. The crest of the wave acts as a free-falling jet that scours a trough into the bottom. At the same time, just seaward of the trough, the longshore bar is formed, in part by sediment scoured from the trough and in part by sediment transported in ripples moving from the offshore.

The effect of the tide on nearshore currents is not discussed here, but tide-generated currents may be superimposed on wave-generated nearshore currents, especially near estuaries. In addition, the changing elevation of the water level as the tide rises and falls may change the area and the shape of the profile through the surf zone and thus alter the nearshore currents.

## 3. Onshore-Offshore Currents.

a. Onshore-Offshore Exchange. Field and laboratory data indicate that water in the nearshore zone is divided by the breaker line into two distinct water masses between which there is only a limited exchange of water.

The mechanisms for the exchange are: (1) mass transport velocity in shoaling waves, (2) wind-induced surface drift, (3) wave-induced setup, (4) currents induced by irregularities on the bottom, (5) rip currents, and (6) density currents. The resulting flows are significantly influenced by, and

act on, the hydrography of the surf and nearshore zones. Figure 4-21 shows the nearshore current system measured for particular wave conditions on the southern California coast.

At first observation, there appears to be an extensive exchange of water between the nearshore and the surf zone. However, the breaking wave itself is formed largely of water that has been withdrawn from the surf zone after breaking (Galvin, 1967). This water then reenters the surf zone as part of the new breaking wave, so that only a limited amount of water is actually transferred offshore. This inference is supported by the calculations of Longuet-Higgins (1970a, p. 6788), which show that little mixing is needed to account for observed velocity distributions. Most of the exchange mechanisms indicated act with speeds much slower than the breaking wave speed, which may be taken as an estimate of the maximum water particle speed in the littoral zone indicated by equation (4-19).

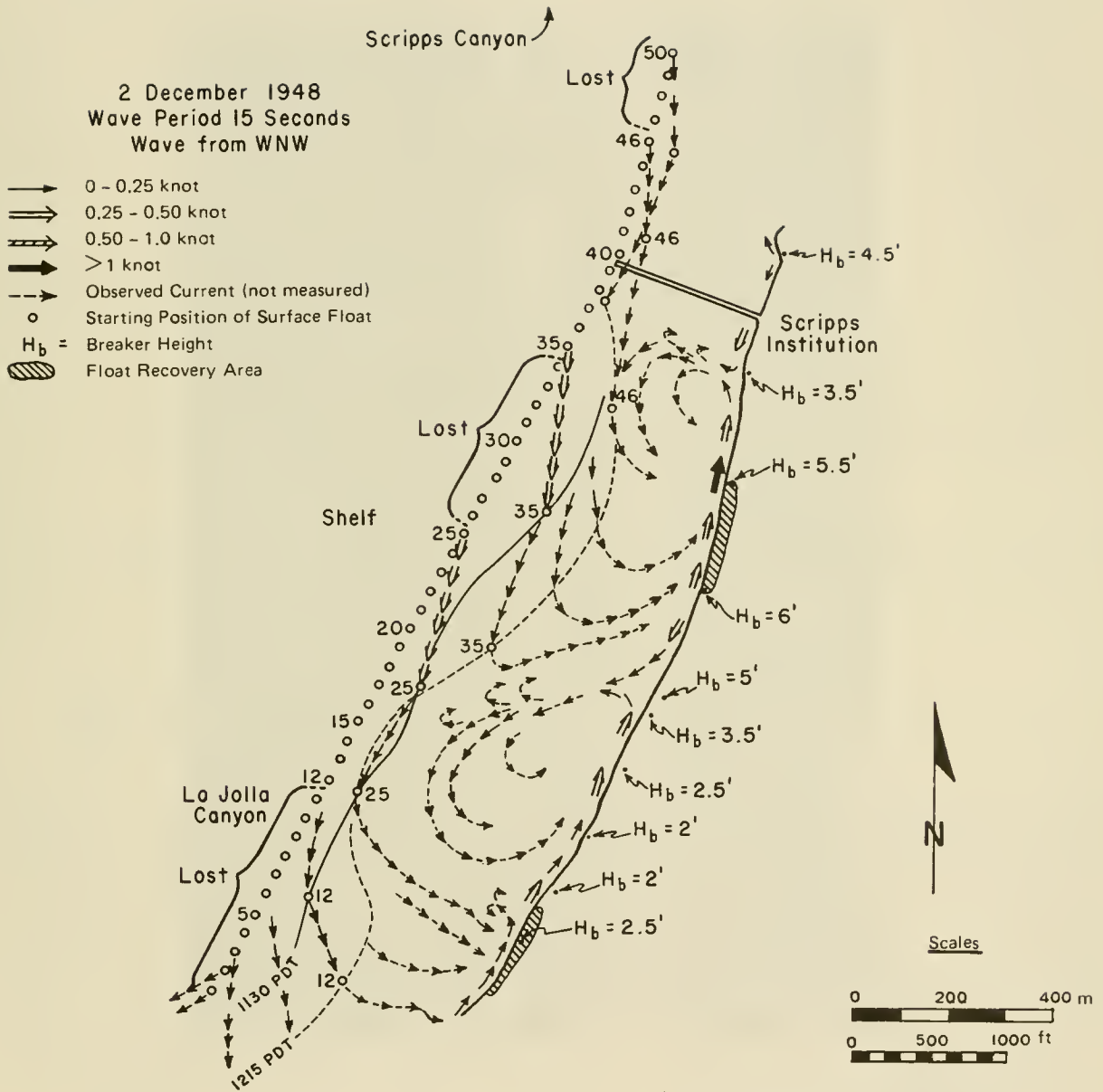
b. Diffuse Return Flow. Wind- and wave-induced water drift, pressure gradients at the bottom due to setup, density differences due to suspended sediment and temperature, and other mechanisms produce patterns of motion in the surf zone that vary from highly organized rip currents to broad diffuse flows that require continued observation to detect. Diffuse return flows may be visible in aerial photos as fronts of turbid water moving seaward from the surf zone. Such flows may be seen in the photos reproduced in Sonu (1972, p. 3239).

c. Rip Currents. Most noticeable of the exchange mechanisms between offshore and the surf zone are rip currents (see Fig. 4-22 and Fig. A-7, App. A). Rip currents are concentrated jets that carry water seaward through the breaker zone. They appear most noticeable when long, high waves produce wave setup on the beach. In addition to rip currents, there are other localized currents directed seaward from the shore. Some are due to concentrated flows down gullies in the beach face, and others can be attributed to interacting waves and edge wave phenomena (Inman, Tait, and Nordstrom, 1971, p. 3493). The origin of rip currents is discussed by Arthur (1962) and Sonu (1972).

Three-dimensional circulation in the surf is documented by Shepard and Inman (1950), and this complex flow needs to be considered, especially in evaluating the results of laboratory tests for coastal engineering purposes. However, there is presently no proven way to predict the conditions that produce rip currents or the spacing between rips. In addition, data are lacking that would indicate quantitatively how important rip currents are as sediment transporting agents.

#### 4. Longshore Currents.

a. Velocity and Flow Rate. Longshore currents flow parallel to the shoreline and are restricted mainly between the zone of breaking waves and the shoreline. Most longshore currents are generated by the longshore component of motion in waves that obliquely approach the shoreline.



(from Shepard and Inman, 1950)

Figure 4-21. Nearshore current system near La Jolla Canyon, California.

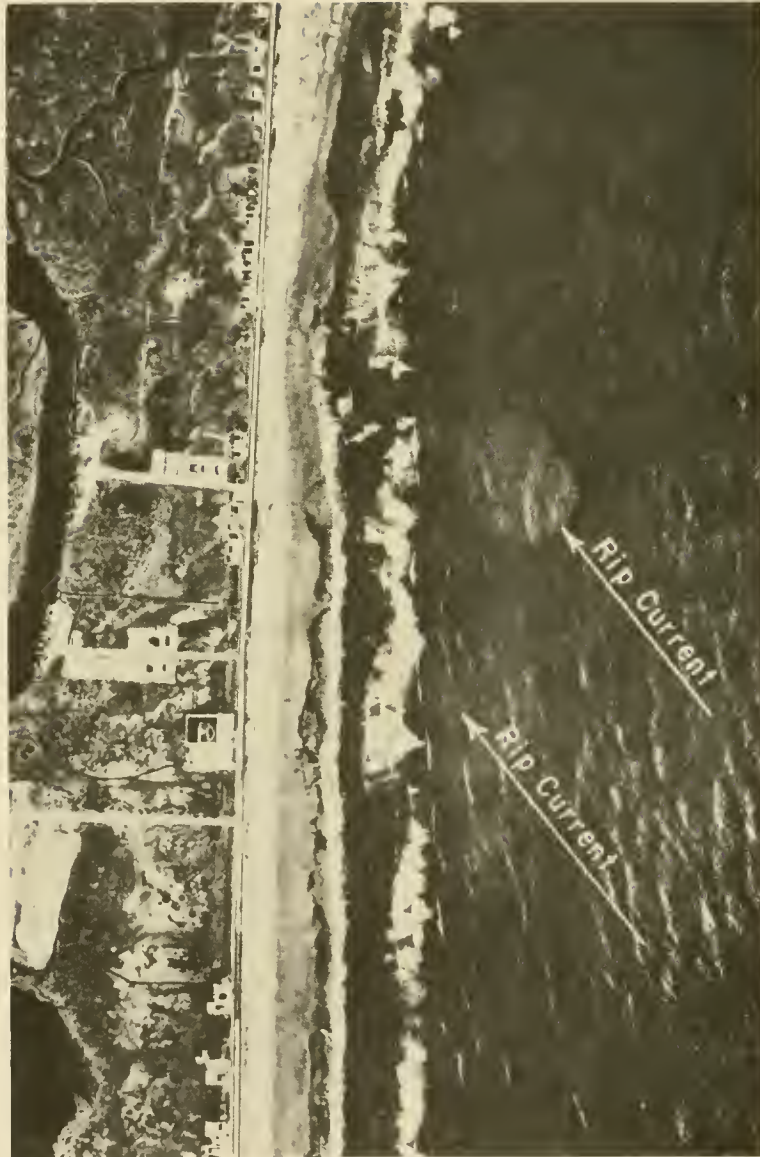


Figure 4-22. Typical rip currents, Ludlam Island, New Jersey.

Longshore currents typically have mean values of 0.3 meter (1 foot) per second or less. Figure 4-23 shows a histogram of 5,591 longshore current

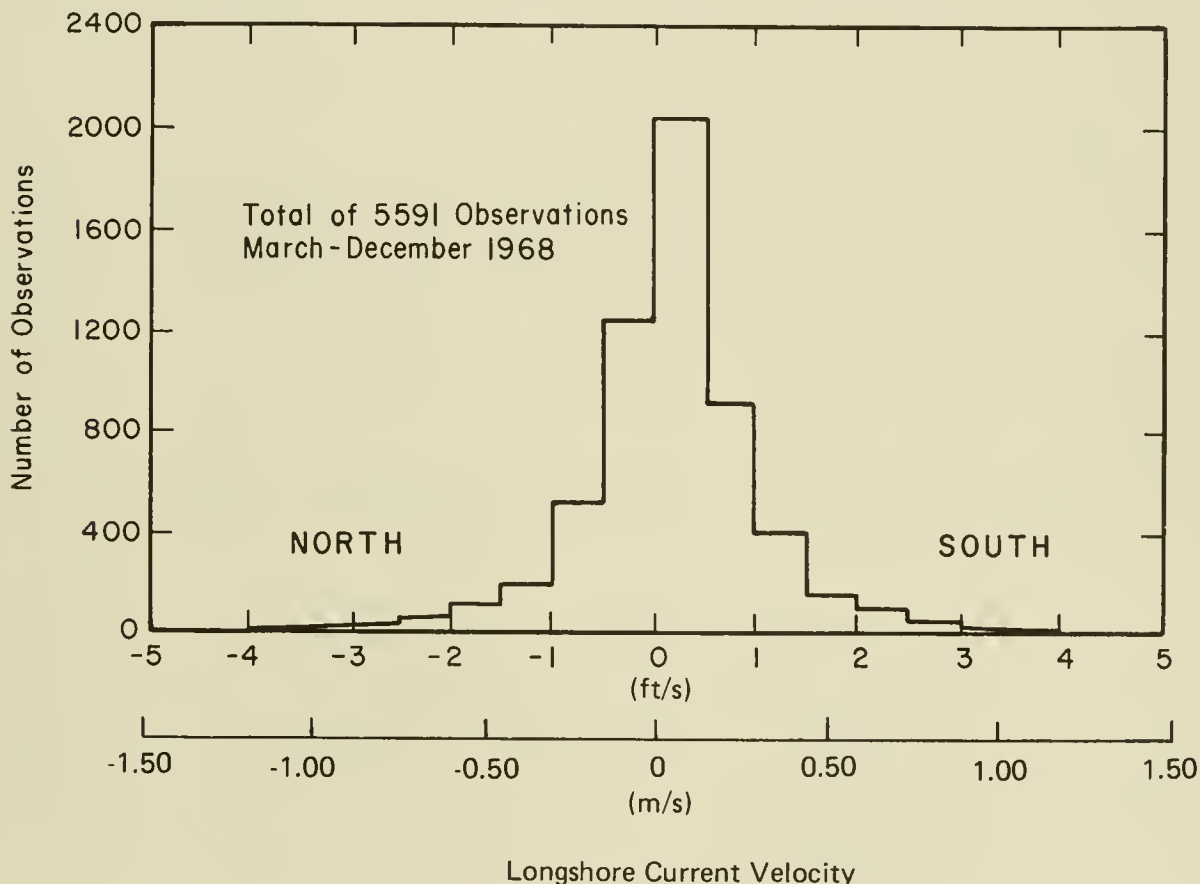


Figure 4-23. Distribution of longshore current velocities (data taken from CERC California LEO Study (Szuwalski, 1970)).

velocities measured at 36 sites in California during 1968. Despite frequent reports of exceptional longshore current speeds, most data agree with Figure 4-23 in showing that speeds above 0.9 meter (3 feet) per second are unusual. A compilation of 352 longshore current observations, most of which appear to be biased toward conditions producing high speed, showed that the maximum observed speed was 1.7 meters (5.5 feet) per second and that the highest observations were reported to have been wind-aided (Galvin and Nelson, 1967). Although longshore currents generally have low speeds, they are important in littoral processes because they flow along the shore for extended periods of time, transporting sediment set in motion by the breaking waves.

The most important variable in determining the the longshore current velocity is the angle between the wave crest and the shoreline. However, the volume rate of flow of the current and the longshore transport rate depend mostly on breaker height. The outer edge of the surf zone is determined by the breaker position. Since waves break in water depths approximately proportional to wave height, the width of the surf zone on a beach increases

with wave height. This increase in width increases the cross section of the surf zone.

If the surf zone cross section is approximated by a triangle, then an increase in height increases the area (and thus the volume of the flow) as the square of the height, which nearly offsets the increase in energy flux (which increases as the 5/2 power of height). Thus, the height is important in determining the width and volume rate of longshore current flow in the surf zone (Galvin, 1972b).

Longshore current velocity varies both across the surf zone (Longuet-Higgins, 1970b) and in the longshore direction (Galvin and Eagleson, 1965). Where an obstacle to the flow, such as a groin, extends through the surf zone, the longshore current speed downdrift of the obstacle is low, but it increases with distance downdrift. Laboratory data suggest that the current takes a longshore distance of about 10 surf widths to become fully developed. These same experiments (Galvin and Eagleson, 1965) suggest that the velocity profile varies more across the surf zone at the start of the flow than it does downdrift where the flow has fully developed. The ratio of longshore current speed at the breaker position to longshore current speed averaged across the surf zone varied from about 0.4 where the flow started to about 0.8 or 1.0 where the flow was fully developed.

b. Velocity Prediction. The variation in longshore current velocity across the surf zone and along the shore, and the uncertainties in variables such as the surf zone hydrography, make prediction of longshore current velocity uncertain. There are three equations of possible use in predicting longshore currents: Longuet-Higgins (1970b), an adaptation from Bruun (1963), and Galvin (1963). All three equations require coefficients identified by comparing measured and computed velocities, and all three show about the same degree of agreement with data. Two sets of data (Putnam, Munk, and Traylor, 1949, field data; Galvin and Eagleson, 1965, laboratory data) appear to be the most appropriate for checking predictions.

The radiation stress theory of Longuet-Higgins (1970a, eq. 62), as modified by fitting it to the data is the one recommended for use based on its theoretical foundation:

$$v_b = M_1 m (gH_b)^{1/2} \sin 2\alpha_b \quad (4-20)$$

where

$m$  = beach slope

$g$  = acceleration of gravity

$H_b$  = breaker height

$\alpha_b$  = angle between breaker crest and shoreline

and

$$M_1 = \frac{0.694 \Gamma(2\beta)^{-1/2}}{f_f} \quad (4-21)$$

According to Longuet-Higgins (1970a, p. 6788),  $v_b$  is the longshore current speed at the breaker position,  $\Gamma$  is a mixing coefficient which ranges between 0.17 (little mixing) and 0.5 (complete mixing) but is commonly about 0.2;  $d/H$  is the depth-to-height ratio of breaking waves in shallow water taken to be 1.2; and  $f_f$  is the friction coefficient, taken to be 0.01. Using these values,  $M_1 = 9.0$ .

Applying equation (4-20) to the two sets of data yields predictions that average about 0.43 of the measured values. In part, these predicted speeds are lower because  $v_b$  as given in equation (4-20) is for the speed at the breaker line, whereas the measured velocities are mostly from the faster zone of flow shoreward of the breaker line (Galvin and Eagleson, 1965). Therefore, equation (4-20) multiplied by 2.3 leads to the modified Longuet-Higgins equation for longshore current velocity:

$$v = 20.7 \text{ m } (gH_b)^{1/2} \sin 2\alpha_b \quad (4-22)$$

used in Figure 4-24. Further developments in the Longuet-Higgins' (1970b, 1971) theory permit calculation of velocity distribution, but there is no experience with these predictions for longshore currents flowing on erodible sand beds.

## 5. Summary.

The major currents in the littoral zone are wave-induced motions superimposed on the wave-induced oscillatory motion of the water. The net motions generally have low velocities, but because they transport whatever sand is set in motion by the wave-induced water motions, they are important in determining littoral transport.

Evidence indicates that there is only a slight exchange of fluid between the offshore and the surf zone.

Longshore current velocities are most sensitive to changes in breaker angle and, to a lesser degree, to changes in breaker height. However, the volume rate of flow of the longshore current is most sensitive to breaker height, probably proportional to  $H^2$ . The modified Longuet-Higgins equation (4-22) is recommended for predicting mean longshore current velocity of fully developed flows.

## V. LITTORAL TRANSPORT

### 1. Introduction.

a. Importance of Littoral Transport. If the coast is examined on satellite imagery as shown in Figure 4-25, only its general characteristics are visible. At this elevation, the shore consists of bright segments that are straight or slightly curved. The brightness is evidence of sand, the most common material along the shore. The straightness often is evidence of the effects of sediment transport.

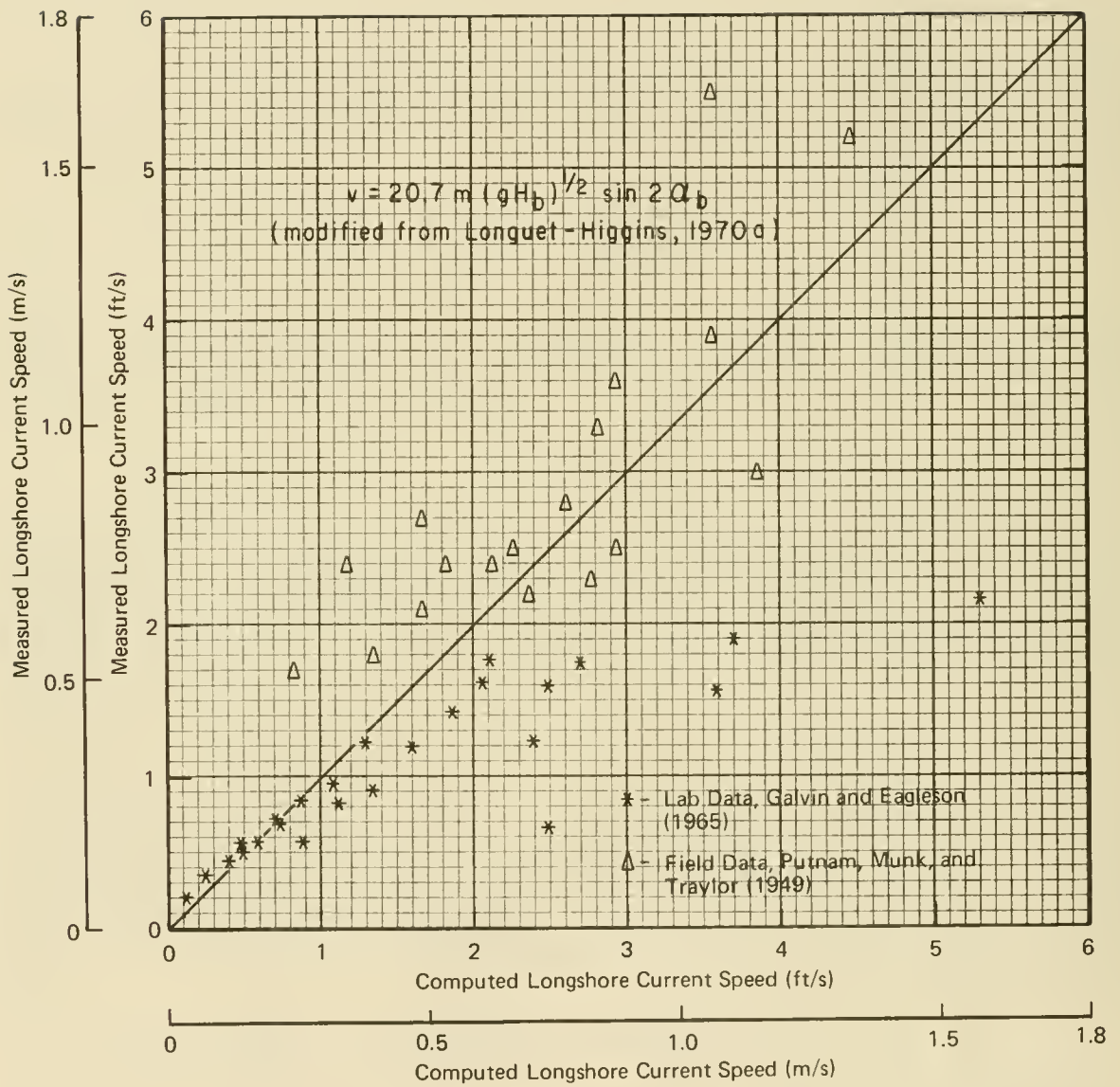


Figure 4-24. Measured versus predicted longshore current speed.

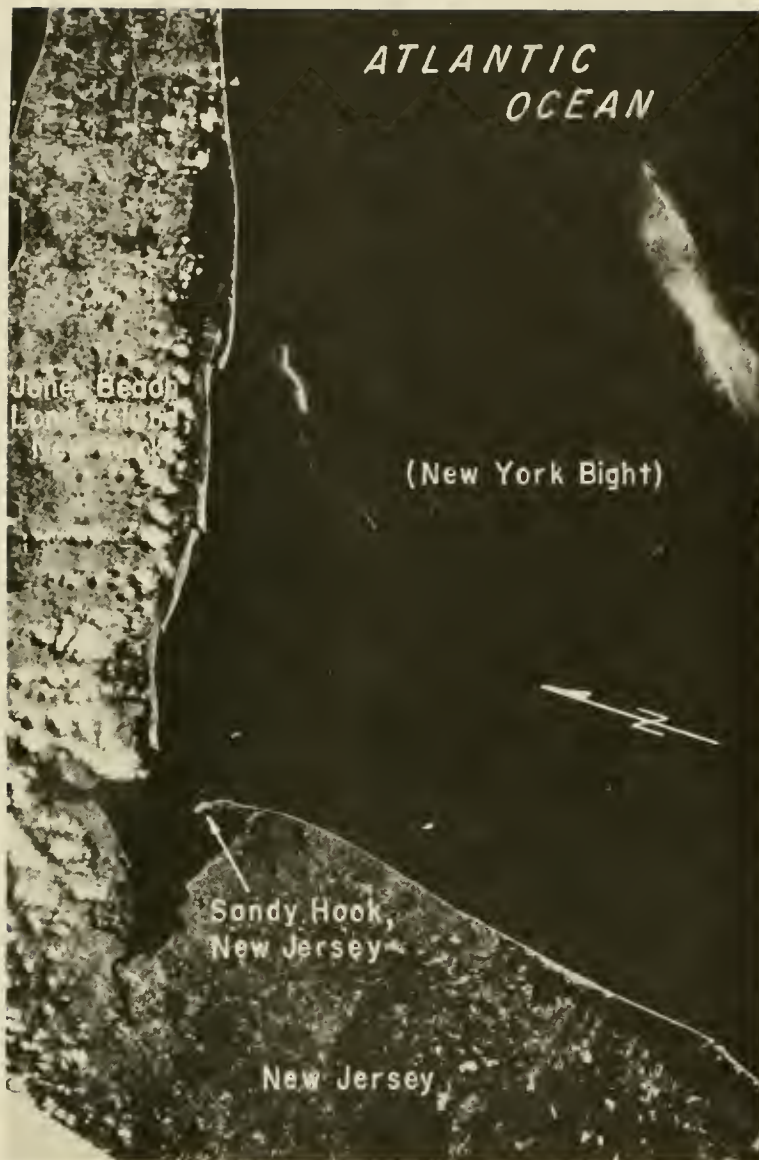


Figure 4-25. Coasts in vicinity of New York Bight.

In places, the straight segments of shoreline cut across preexisting topography. Elsewhere, the shoreline segments are separated from the irregular mainland by wide lagoons. The fact that the shore is nearly straight across both mainland and irregular bays is evidence of headland erosion, accompanied by longshore transport which has carried sand along the coast to supply the barriers and spits extending across the bays. The primary agent producing this erosion and transport is the action of waves impinging on the shore.

*Littoral transport* is the movement of sedimentary material in the littoral zone by waves and currents. The littoral zone extends from the shoreline to just beyond the seawardmost breakers.

Littoral transport is classified as *onshore-offshore transport* or as *longshore transport*. Onshore-offshore transport has an average net direction

perpendicular to the shoreline; longshore transport has an average net direction parallel to the shoreline. The instantaneous motion of sedimentary particles typically has both an onshore-offshore and a longshore component. Onshore-offshore transport is usually the most significant type of transport in the offshore zone, except in regions of strong tidal currents. Both longshore and onshore-offshore transport are significant in the surf zone.

Engineering problems involving littoral transport generally require answers to one or more of the following questions:

(1) What are the longshore transport conditions at the site? (Needed for the design of groins, jetties, navigation channels, and inlets.)

(2) What is the trend of shoreline migration over short and long time intervals? (Needed for design of coastal structures, including navigation channels.)

(3) How far seaward is sand actively moving? (Needed in the design of sewage outfalls and water intakes.)

(4) What is the direction and rate of onshore-offshore sediment motion? (Needed for sediment budget studies and beach-fill design.)

(5) What is the average shape and the expected range of shapes for a given beach profile? (Needed for design of groins, beach fills, navigation structures, and flood protection.)

(6) What effect will a postulated structure or project have on adjacent beaches and on littoral transport? (Needed for design of all coastal works.)

This section presents recommended methods for answering these and related questions. The section indicates accepted practice based on field observations and research results. Chapter 4, Section V,2 deals with onshore-offshore transport, presenting material pertinent to answering questions (2) through (6). Section V deals with longshore transport, presenting material pertinent to questions (1), (2), and (6).

b. Zones of Transport. Littoral transport occurs in two modes: *bedload transport*, the motion of grains rolled over the bottom by the shear of water moving above the sediment bed and *suspended-load transport*, the transport of grains by currents after the grains have been lifted from the bed by turbulence.

Both modes of transport are usually present at the same time, but it is hard to distinguish where bedload transport ends and suspended-load transport begins. It is more useful to identify two zones of transport based on the type of fluid motion initiating sediment motion: (1) the offshore zone where transport is initiated by wave-induced motion over ripples and (2) the surf zone where transport is initiated primarily by the passing breaker. In either zone, net sediment transport is the product of two processes: the periodic wave-induced fluid motion that initiates sediment motion and the superimposed currents (usually weak) which transport the sediment set in motion.

(1) Offshore Zone. Waves traveling toward shallow water eventually

reach a depth where the water motion near the bottom begins to affect the sediment on the bottom. At first, only low-density material (such as seaweed and other organic matter) moves. This material oscillates back and forth with the waves, often in ripplelike ridges parallel to the wave crests. For a given wave condition, as the depth decreases, water motion immediately above the sediment bed increases until it exerts enough shear to move sand particles. The sand then forms ripples with crests parallel to the wave crests. These ripples are typically uniform and periodic, and sand moves from one side of the crest to the other with the passage of each wave.

As depth decreases to a value several times the wave height, the velocity distribution with time changes from approximately sinusoidal to a distribution that has (a) a high shoreward component associated with the brief passage of the wave crest and (b) lower seaward velocities associated with the longer time interval occupied by the passage of the trough. As the shoreward water velocity associated with the passing crest decreases and begins to reverse direction over a ripple, a cloud of sand erupts upward from the lee (landward) side of the ripple crest. This cloud of sand drifts seaward with the seaward flow under the trough. At these shallow depths, the distance traveled by the cloud of suspended sediment is two or more ripple wavelengths, so that the sand concentration at a point above the ripples usually exhibits at least two maximums during the passage of the wave trough. These maximums are the suspension clouds shed by the two nearest upstream ripples. The approach of the next wave crest reverses the direction of the sand remaining suspended in the cloud. The landward flow also drags material shoreward as bedload.

For the nearshore profile to be in equilibrium with no net erosion or accretion, the average rate at which sand is carried away from a point on the bottom must be balanced by the average rate at which sand is added. Any net change will be determined by the net residual currents near the bottom which transport sediment set in motion by the waves. These currents, the subject of Section IV, include longshore currents and mass-transport currents in the onshore-offshore direction. It is possible to have ripple forms moving shoreward while residual currents above the ripples carry suspended-sediment clouds in a net offshore direction. Information on the transport of sediment above ripples is given in Bijker (1970), Kennedy and Locher (1972), and Mogridge and Kamphuis (1972).

(2) Surf Zone. The stress of the water on the bottom due to turbulence and wave-induced velocity gradients moves sediment in the surf zone with each passing breaker crest. This sediment motion is both bedload and suspended-load transport. Sediment in motion oscillates back and forth with each passing wave and moves alongshore with the longshore current. On the beach face--the landward termination of the surf zone--the broken wave advances up the slope as a bore of gradually decreasing height and then drains seaward in a gradually thinning sheet of water. Frequently, the draining return flows in gullies and carries sediment to the base of the beach face.

In the surf zone, ripples cause significant sediment suspension, but here there are additional eddies caused by the breaking wave. These eddies have more energy and are larger than the ripple eddies; the greater energy suspends more sand in the surf zone than offshore. The greater eddy size mixes the suspended sand over a larger vertical distance. Since the size is about equal

to the local depth, significant quantities of sand are suspended over most of the depth in the surf zone.

Since breaking waves suspend the sediment, the amount suspended is partly determined by breaker type. Data from Fairchild (1972, Fig. 5) show that spilling breakers usually produce noticeably lower suspended sediment concentrations than do plunging breakers (see Fairchild (1972) and Watts (1953a) for field data; Fairchild (1956, 1959) for lab data). Typical suspended concentrations of fine sand range between 20 parts per million and 2 parts per thousand by weight in the surf zone and are about the same near the ripple crests in the offshore zone.

Studies of suspended sediment concentrations in the surf zone by Watts (1953a) and Fairchild (1972) indicate that sediment in suspension in the surf zone may form a significant portion of the material in longshore transport. However, present understanding of sediment suspension and the practical difficulty of obtaining and processing sufficient suspended sediment samples have limited this approach to predicting longshore transport.

c. Profiles. Profiles are two-dimensional vertical sections showing how elevation varies with distance. Coastal profiles (Figs. 4-1 and 4-26) are usually measured perpendicular to the shoreline and may be shelf profiles, nearshore profiles, or beach profiles. Changes on nearshore and beach profiles are interrelated and are highly important in the interpretation of littoral processes. The measurement and analysis of combined beach and nearshore profiles are a major part of most engineering studies of littoral processes.

(1) Shelf Profiles. The shelf profile is typically a smooth, concave-up curve showing depth to increase seaward at a rate that decreases with distance from shore (bottom profile in Figure 4-26). The smoothness of the profile may be interrupted by other superposed geomorphic features, such as linear shoals (Duane, et al., 1972). Data for shelf profiles are usually obtained from charts of the National Ocean Service (formerly, U.S. Coast and Geodetic Survey).

The measurable influence of the shelf profile on littoral processes is largely its effect on waves. To an unknown degree, the shelf may also serve as a source or sink for beach sand. Geologic studies show that much of the outer edge of a typical shelf profile is underlain by relatively coarse sediment, indicating a winnowing of fine sizes (Dietz, 1963; Milliman, 1972; Duane, et al., 1972). Landward from this residual sediment, sediment often becomes finer before grading into the relatively coarser beach sands.

(2) Nearshore Profiles. The nearshore profile extends seaward from the beach to depths of about 9 meters (30 feet). Prominent features of most nearshore profiles are longshore bars (see middle profile of Figure 4-26 and Section V,2). In combination with beach profiles, repetitive nearshore profiles are used in coastal engineering to estimate erosion and accretion along the shore, particularly the behavior of beach fill, groins, and other coastal engineering structures. Data from nearshore profiles must be used cautiously (see Sec. V,1). Under favorable conditions nearshore profiles have been used in measuring longshore transport rates (Caldwell, 1956).

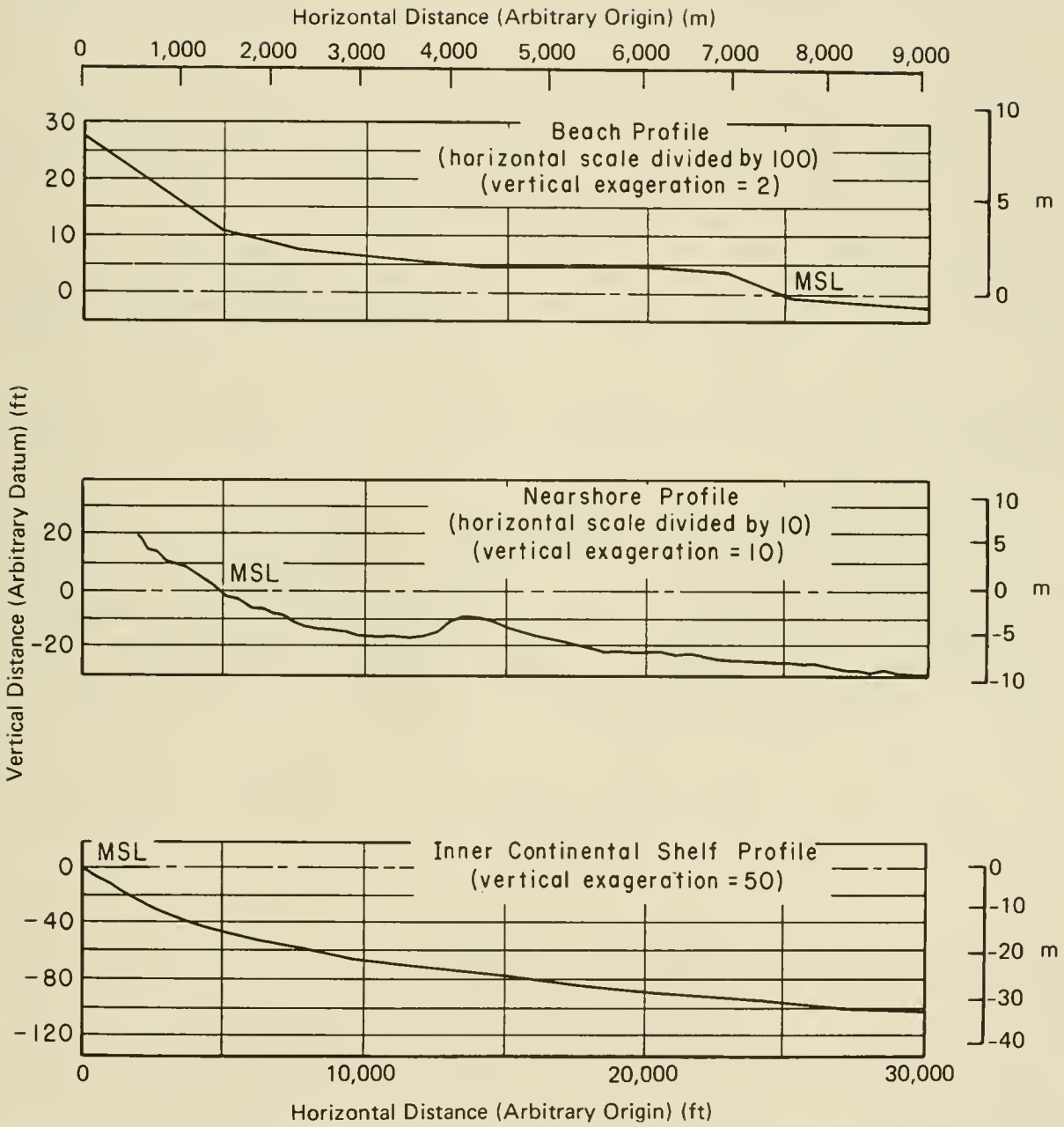


Figure 4-26. Three scales of profiles, Westhampton, Long Island.

(3) Beach Profiles. Beach profiles extend from the foredunes, cliffs, or mainland out to mean low water. Terminology applicable to features of the beach profile is in Appendix A (especially Figs. A-1 and A-2). The backshore extends seaward to the foreshore and consists of one or more berms at elevations above the reach of all but storm waves. Berm surfaces are nearly flat and often slope landward at a slight downward angle (see Fig. A-1). Berms are often bounded on the seaward side by a break in slope known as the berm crest.

The foreshore is that part of the beach extending from the highest elevation reached by waves at normal high tide seaward to the ordinary low water line. The foreshore is usually the steepest part of the beach profile. The boundary between the backshore and the foreshore may be the crest of the seawardmost berm, if a berm is well developed. The seaward edge of the foreshore is often marked by an abrupt step at low tide level.

Seaward from the foreshore, there is usually a low tide terrace which is a nearly horizontal surface at about mean low tide level (Shepard, 1950; Hayes, 1971a). The low tide terrace is commonly covered with sand ripples and other minor bed forms, and may contain a large bar-and-trough system, which is a landward-migrating sandbar (generally parallel to the shore) common in the nearshore following storms. Seaward from the low tide terrace (seaward from the foreshore, if the low tide terrace is absent) are the longshore troughs and longshore bars.

d. Profile Accuracy. Beach and nearshore profiles are the major sources of data for engineering studies of beach changes; sometimes littoral transport can be estimated from these profiles. Usually, beach and nearshore profiles are measured at about the same time, but different techniques are needed for their measurement. The nearshore profile is usually measured from a boat or amphibious craft, using an echo sounder or leadline, or from a sea sled (Kolessar and Reynolds, 1966; Reimnitz and Ross, 1971). Beach profiles are usually surveyed by standard leveling and taping techniques.

The accuracy of profile data is affected by four types of error: sounding error, spacing error, closure error, and error due to temporal fluctuations in the sea bottom. These errors are more significant for nearshore profiles than for beach profiles.

Saville and Caldwell (1953) discuss sounding and spacing errors. Sounding error is the difference between the measured depth and the actual depth. Under ideal conditions, average sonic sounding error may be as little as 0.03 meter (0.1 foot), and average leadline sounding error may be about twice the sonic sounding error (Saville and Caldwell, 1953). (This suggests that sonic sounding error may actually be less than elevation changes caused by transient features like ripples. Experience with successive soundings in the nearshore zone indicates that errors in practice may approach 0.15 meter (0.5 foot).) Sounding errors are usually random and tend to average out when used in volume computations, unless a systematic error due to the echo sounder or tide correction is involved. Long-period water level fluctuations affect sounding accuracy by changing the water level during the survey. At Santa Cruz, California, the accuracy of hydrographic surveys was  $\pm 0.45$  meter (1.5 feet) due to this effect (Magoon and Sarlin, 1970).

Spacing error is the difference between the actual volume of a segment of shore and the volume estimated from a single profile across that segment. Spacing error is potentially more important than sounding error, since survey costs of long reaches usually dictate spacings between nearshore profiles of hundreds of meters. For example, if a 3.2-kilometer (2-mile) segment of shore 1,220 meters (4,000 feet) wide is surveyed by profiles on 305-meter (1,000-foot) spacings, then the spacing error is about 23 cubic meters per meter (9 cubic yards per foot) of beach front per survey, according to the data of Saville and Caldwell (1953, Fig. 5). This error equals a major part of the littoral budget in many localities.

Closure error arises from the assumption that the outer ends of nearshore profiles have experienced no change in elevation between two successive surveys. Such an assumption is often made in practice and may result in significant error. An uncompensated closure error of 0.03 meter (0.1 foot), spread over 305 meters (1,000 feet) at the seaward end of a profile, implies a change of 9.3 cubic meters (3.7 cubic yards) per time interval per meter (foot) of beach front where the time interval is the time between successive surveys. Such a volume change may be an important quantity in the sediment budget of the littoral zone.

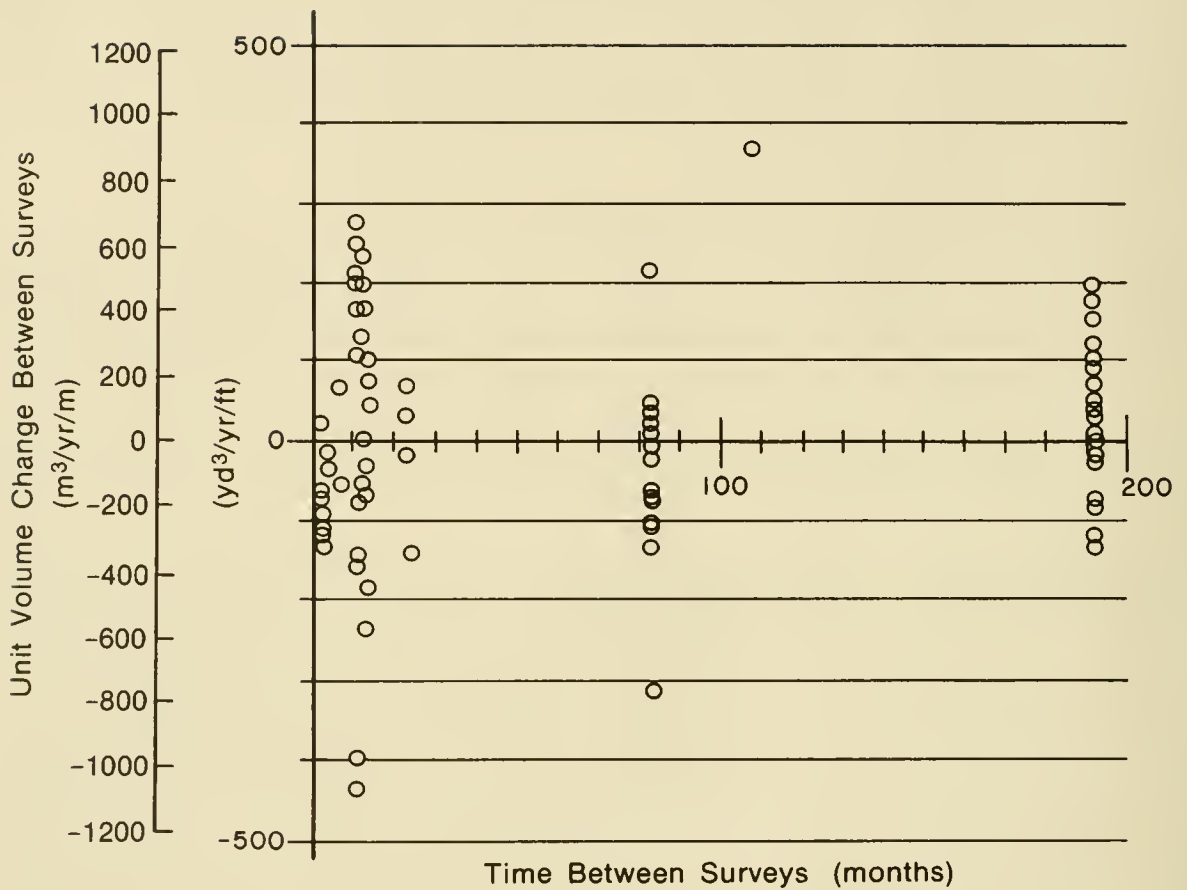
A fourth source of error comes from assuming that the measured beach profiles (which are only an instantaneous picture) represent a long-term condition. Actually, beach and nearshore profiles change rapidly in response to changing wave conditions, so that differences between successive surveys of a profile may merely reflect temporary differences in bottom elevation caused by storms and seasonal changes in wave climate. Such fluctuations obliterate long-term trends during the relatively short time available to most engineering studies. This fact is illustrated for nearshore profiles by the work of Taney (1961, App. B), who identified and tabulated 128 profile lines on the south shore of Long Island that had been surveyed more than once from 1927 to 1956. Of these, 47 are on straight shorelines away from apparent influence by inlets and extend from mean low water (MLW) to about -9 meters (-30 feet) MLW. Most of these 47 profiles were surveyed three or more times, so that 86 separate volume changes are available. These data lead to the following conclusions:

(1) The net volume change appears to be independent of the time between surveys, even though the interval ranged from 2 months to 16 years (see Fig. 4-27).

(2) Gross volume changes (the absolute sums of the 86 volume changes) are far greater than net volume changes (the algebraic sums of the 86 volume changes). The gross volume change for all 86 measured changes is 20,351 cubic meters per meter (8,113 cubic yards per foot); the net change is -1,402 cubic meters per meter (-559 cubic yards per foot) (loss in volume).

(3) The mean net change between surveys, averaged over all pairs of surveys, is  $-1,402 (-559)/86$  or -16.3 cubic meters per meter (-6.5 cubic yards per foot) of beach. The median time between surveys is 7 years, giving a nominal rate of volume change of about -2.5 cubic meters per year per meter (-1 cubic yard per year per foot).

These results point out that temporary changes in successive surveys of



(based on data from Toney, 1961 a)

Figure 4-27. Unit volume change versus time between surveys for profiles on south shore of Long Island (data are from profiles extending from MLW to about the -10-meter depth contour).

nearshore profiles are usually much larger than net changes, even when the interval between surveys is several years. These data show that care is needed in measuring nearshore profiles if results are to be used in engineering studies. The data also suggest the need for caution in interpreting differences obtained in two surveys of the same profiles.

The positions of beach profiles must be marked so that they can be recovered during the life of the project. The profile monuments should be tied in by survey to local permanent references. If there is a long-term use for data at the profile positions, the monuments should be referenced by survey to a state coordinate system or other reference system, so that the exact position of the profile may be recovered in the future. Even if there is no anticipated long-term need, future studies in any coastal region are likely and will benefit greatly from accurately surveyed, retrievable bench marks.

For coastal engineering, the accuracy of shelf profiles is usually less critical than the accuracy of beach and nearshore profiles. Generally, observed depth changes between successive surveys of the shelf do not exceed

the error inherent in the measurement. However, soundings separated by decades suggest that the linear shoals superposed on the profile do show small but real shifts in position (Moody, 1964, p. 143). Charts giving depths on the continental shelves may include soundings that differ by decades in date.

Plotted profiles usually use vertical exaggeration or distorted scales to bring out characteristic features. This exaggeration may lead to a false impression of the actual slopes. As plotted, the three profiles in Figure 4-26 have roughly the same shape, but this sameness has been obtained by vertical exaggerations of 2x, 10x, and 50x.

Sand level changes in the beach and nearshore zone may be measured quite accurately from pipes imbedded in the sand (Inman and Rusnak, 1956; Urban and Galvin, 1969; Gonzales, 1970).

2. Onshore-Offshore Transport. Quantitative engineering guidance has been more firmly established for rates of longshore transport than for rates of onshore-offshore transport. This seems mainly due to the complexity involved in the respective processes and in adequate analyses: simple considerations using small-amplitude wave theory are applicable to longshore transport (see Ch. 4, Sec. V,3), while the need for a higher order treatment in considering onshore-offshore transport is well established but still problematical (Wells, 1977; van de Graaff and Tilmans, 1980). With nearshore waves propagating usually at only a slight angle with respect to a shore-normal line, an appreciable unidirectional longshore current and net sediment transport are driven by fairly steady longshore wave thrust. In contrast, net onshore-offshore transport results from usually small differences between oscillating sediment movements near to and opposite the wave direction.

Onshore-offshore transport is sensitive to the detailed structure of the reversing flow within the wave cycle and to any net flow. Also, besides the intensely agitated surf zone, relatively gentle processes out to the seaward limit of sediment motion must be considered. The integrated effect of complex onshore-offshore transport processes, continuously varying along the active profile, determines erosion and accretion along the profile and at the shoreline (in regions of steady longshore sediment transport).

Appreciable analytical and laboratory efforts have been devoted to onshore-offshore transport in terms of separate bedload and suspended-load components. However, significant uncertainties remain, and no formulation for transport rate has established validity in prototype situations.

Many laboratory studies have measured rates of sediment transport as bedload collinear with various oscillatory flows. One problem in correlating results is the complication associated with sediment movement possibly occurring during only portions of the wave cycle. Available prediction procedures for bedload or total transport by waves (Bagnold, 1963; Einstein, 1971; Swart, 1976; Madsen and Grant, 1976; Sleath, 1978; Bailard and Inman, 1981) proceed from radically different analytical presumptions, consider various selections of available data, and usually present complicated empirical curves needed for calculations. Predicted transport rates by different procedures can disagree by more than an order of magnitude, and no procedure can be recommended presently.

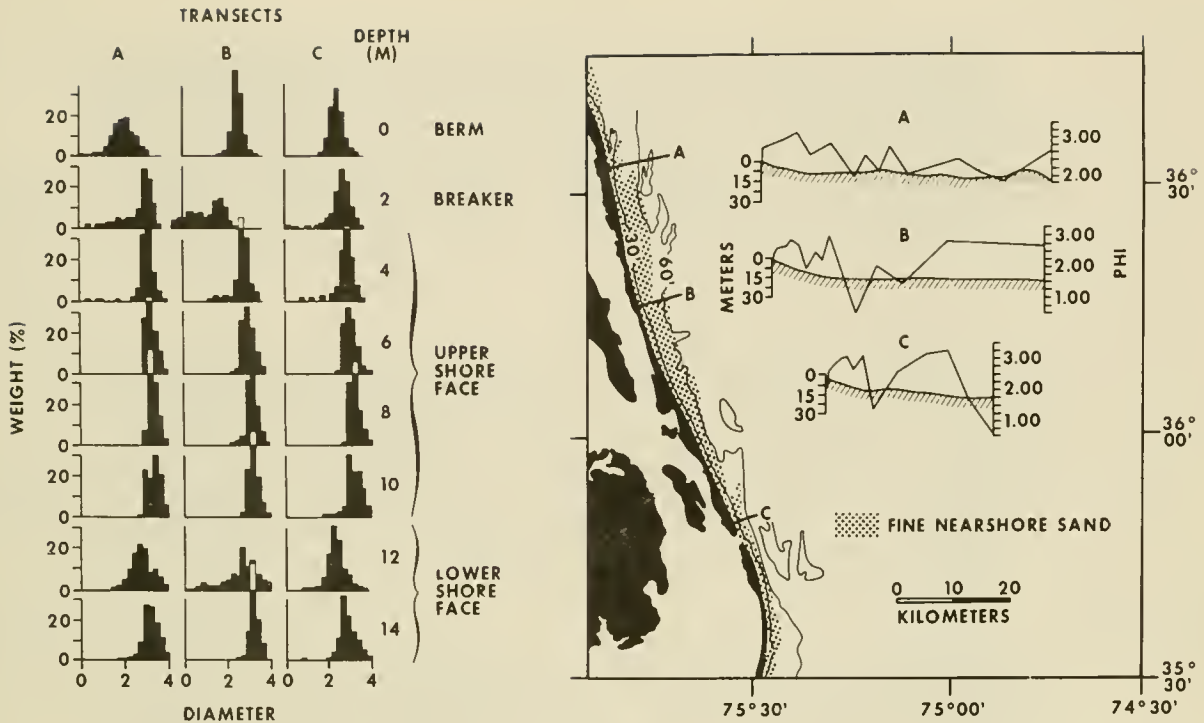
The treatment of suspended-load transport collinear with waves has received increased investigation (Nakato et al., 1977; MacDonald, 1977; Nielsen, 1979). This research has established important temporal and spatial gradients of suspended-sediment concentration in relatively simple oscillatory flows. Prediction of suspended-load transport requires several empirically determined coefficients, which at present cannot be simply related to wave and sediment characteristics. A further difficulty is that field data have shown that breaker type controls suspended-sediment concentration in the surf zone (Kama, 1979), but this effect has not been thoroughly investigated under controlled conditions.

Despite the lack of recommendable prediction procedures for transport rates, useful guidance can be provided concerning aspects of onshore-offshore transport important in coastal engineering.

a. Sediment Effects. Properties of individual particles important in sediment transport include size, shape, and composition. Collections of particles have the additional properties of size distribution, permeability, and porosity. These properties influence the fluid forces necessary to initiate and maintain sediment movement. For usual nearshore sediment, size is the only particle property which varies greatly. Grain size changes sediment motion conditions, sediment fall velocity, and hydraulic roughness of the grain bed. The hydraulic roughness affects flow energy dissipation, which also results directly from bed permeability (Bretschneider and Reid, 1954; Bretschneider, 1954). Bed permeability, depending on sediment size and sorting, can cause a net onshore sand transport from far offshore (Lofquist, 1975) and influences wave runup at the shoreline (see Ch. 7; Savage, 1958). Sediment size clearly figures in beach swash processes (Everts, 1973; Sallenger, 1981). Thus, grain size figures in a variety of processes from the landward to the seaward limit of hydrodynamic sediment transport.

Some data indicate that differential transport according to sediment size occurs near the shore. A gross indication of a size effect is the appearance of coarse sediment in zones of maximum wave energy dissipation and the deposition of fine sediment in areas sheltered from wave action (e.g., King, 1972, pp. 302, 307, 426). Regular variation in sediment size is common over ripples (Inman, 1957) and large longshore bars (Saylor and Hands, 1970). Regular sediment-size variations on a more extensive scale have been documented across some nearshore profiles (e.g., Duane, 1970a; Swift, 1976). Figure 4-28 displays surface sediment sizes from three transects of a historically eroding coast, with well-sorted sand becoming progressively finer seaward to a water depth of about 10 meters, there abutting coarser, less well-sorted sand.

This common seaward-fining of active nearshore sands demonstrates a sediment-size effect in onshore-offshore transport, but the process responsible for this is a controversial subject. The effect appears consistent with the "neutral line" concept (Cornaglia, 1889), which incorporates qualitative consideration of bedload sediment movements in terms of wave energy, bottom slope, and sediment characteristics; however, recent discussions of Cornaglia's concept emphasize its limitations and those of further laboratory-based quantitative developments (Zenkovich, 1967b, Sec. 9; Komar, 1976, Ch. 11; Bowen, 1980; Hallermeier, 1981b). The seaward fining of nearshore sands has also been ascribed to suspended-load transport by rip currents (Swift, 1976).



(from Swift, 1976)

Figure 4-28. Distribution of grain sizes along transects of the Virginia-North Carolina coast.

b. Initiation of Sand Motion. Extensive laboratory results indicate two separate criteria for motion initiation by oscillatory flow over a level bed of sediment with  $d_{50}$  between 0.1 and 2.0 millimeters (Hallermeier, 1980). In field conditions, the appropriate threshold flow velocity for sand motion is

$$u_{max(-d)} = (8 (\gamma_s/\gamma - 1) g d_{50})^{0.5} \quad (4-23)$$

where  $u_{max(-d)}$  is peak fluid velocity at the sediment bed.

For waves that are not mean breaking, measured maximum near-bottom velocities can be adequately determined using small-amplitude wave theory (Thornton and Kraphol, 1974; Grace, 1976). That (Ch. 2, Sec. II,3) provides equation (2-13) which can be rewritten as

$$\frac{u_{max(-d)} T}{H} = \frac{\pi}{\sinh\left(\frac{2\pi d}{L}\right)} \quad (4-24)$$

This expression is plotted as a function of water depth for common field values of wave period in Figure 4-29.

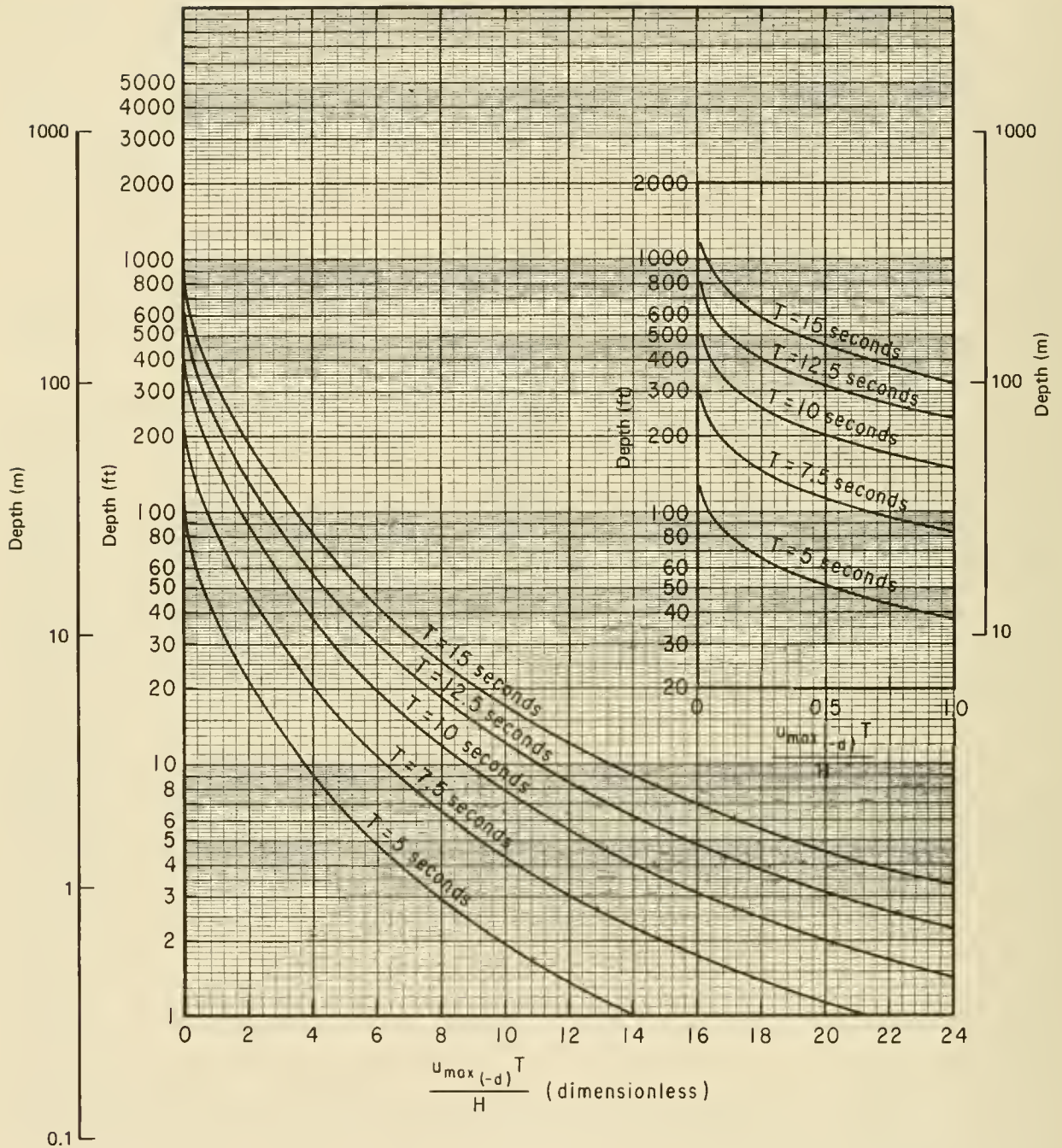


Figure 4-29. Maximum bottom velocity from small-amplitude theory.

With specified material characteristics, the right-hand side of equation (4-23) is to be evaluated and Figure 4-29 then used to examine critical wave conditions for initiation of sand motion. Two of the three wave parameters (water depth, wave height, and wave period) must be specified so that the unknown parameter can be determined. If wave period is the unknown, the exact solution must be formed by an iterative procedure (or use of the tables in Appendix C), due to the relationship between  $L$  and  $T$  (eq. 2-4). In an

irregular wave field, the significant wave description may be appropriate in this application (see Ch. 3, Sec II).

\*\*\*\*\* EXAMPLE PROBLEM 2 \*\*\*\*\*

GIVEN: Quartz sediment in seawater, with a median sediment diameter  
 $d_{50} = 0.15$  millimeter .

FIND:

(a) With wave period  $T = 10$  seconds , the minimum wave height for sand motion in water depth  $d = 10$  meters .

(b) With wave period  $T = 8$  seconds , the maximum water depth for sand motion with wave height  $H = 2$  meters .

(c) With wave height  $H = 1$  meter and water depth  $d = 20$  meters , the minimum wave period for sand motion.

SOLUTION: From Table 4-2,  $\gamma_s = 2.65$  , and  $\gamma = 1.026$  , so that the threshold condition for sand motion from equation (4-23) is

$$\begin{aligned} u_{max(-d)} &= [8 (\gamma_s/\gamma - 1) g d_{50}]^{0.5} \\ &= [8 (\frac{2.65}{1.026} - 1) (9.81) (0.00015)]^{0.5} \\ &= 0.1365 \text{ meter/second} \end{aligned}$$

(a) For  $d = 10$  meters (32.8 feet) and  $T = 10$  seconds , Figure 4-29 gives

$$\frac{u_{max(-d)} T}{H} = 4.4$$

so that

$$\begin{aligned} H &= \frac{u_{max(-d)} T}{4.4} \\ &= \frac{(0.1365) (10)}{4.4} \\ &= 0.310 \text{ meter (1.02 feet)} \end{aligned}$$

This is the required minimum wave height, since higher waves will induce near-bottom velocities larger than the threshold, according to equation (4-24).

(b) With  $T = 8$  seconds and  $H = 2$  meters , calculate

$$\frac{u_{max}(-d)^T}{H} = \frac{(0.1365)(8)}{2}$$

$$= 0.546$$

Interpolating between curves in the inset of Figure 4-29 yields

$$d = 40 \text{ meters (130 feet)}$$

This is the required maximum water depth for sand motion because at greater depths the wave-induced velocity for the given H and T will be less than the threshold velocity.

(c) Solution (a) and Figure 4-29 indicate that wave periods greater than 10 seconds will certainly cause sand motion with H = 1 meter and d = 20 meters. Estimating T = 7.5 seconds, Figure 4-29 shows for d = 20 meters (65.6 feet)

$$\frac{u_{max}(-d)^T}{H} = 1.35$$

and

$$u_{max}(-d) = 0.18 \text{ meter/second}$$

which is somewhat larger than the threshold velocity. For T = 5 seconds, Figure 4-29 shows

$$\frac{u_{max}(-d)^T}{H} = 0.25$$

and

$$u_{max}(-d) = 0.05 \text{ meter/second}$$

which is much less than the required threshold. Refining the estimate to T = 6.5 seconds, interpolation in Figure 4-29 yields

$$\frac{u_{max}(-d)^T}{H} = 0.85$$

so that

$$u_{max}(-d) = \frac{(0.85)(1)}{6.5} = 0.13 \text{ meter/second}$$

or slightly less than the threshold velocity. Thus, T = 6.6 seconds is a reasonable approximate solution.

\* \* \* \* \*

c. Seaward Limit of Significant Transport. Example problem 2, together with available measurements of usual nearshore wave conditions (Table 4-4), indicate that waves can set in motion occasionally each year fine sands over most of the continental shelf to water depths on the order of 50 to 100 meters (Silvester and Mogridge, 1970). An important question is this: what is the maximum water depth at which sand transport occurs at rates significant in coastal engineering? Such a seaward limit figures as a critical parameter in

calculation procedures for changes in shoreline location (e.g., Bruin, 1962; LeMehaute and Soldate, 1980) and must be considered in the design of nearshore structures, subaqueous beach nourishment, and offshore borrow or disposal operations.

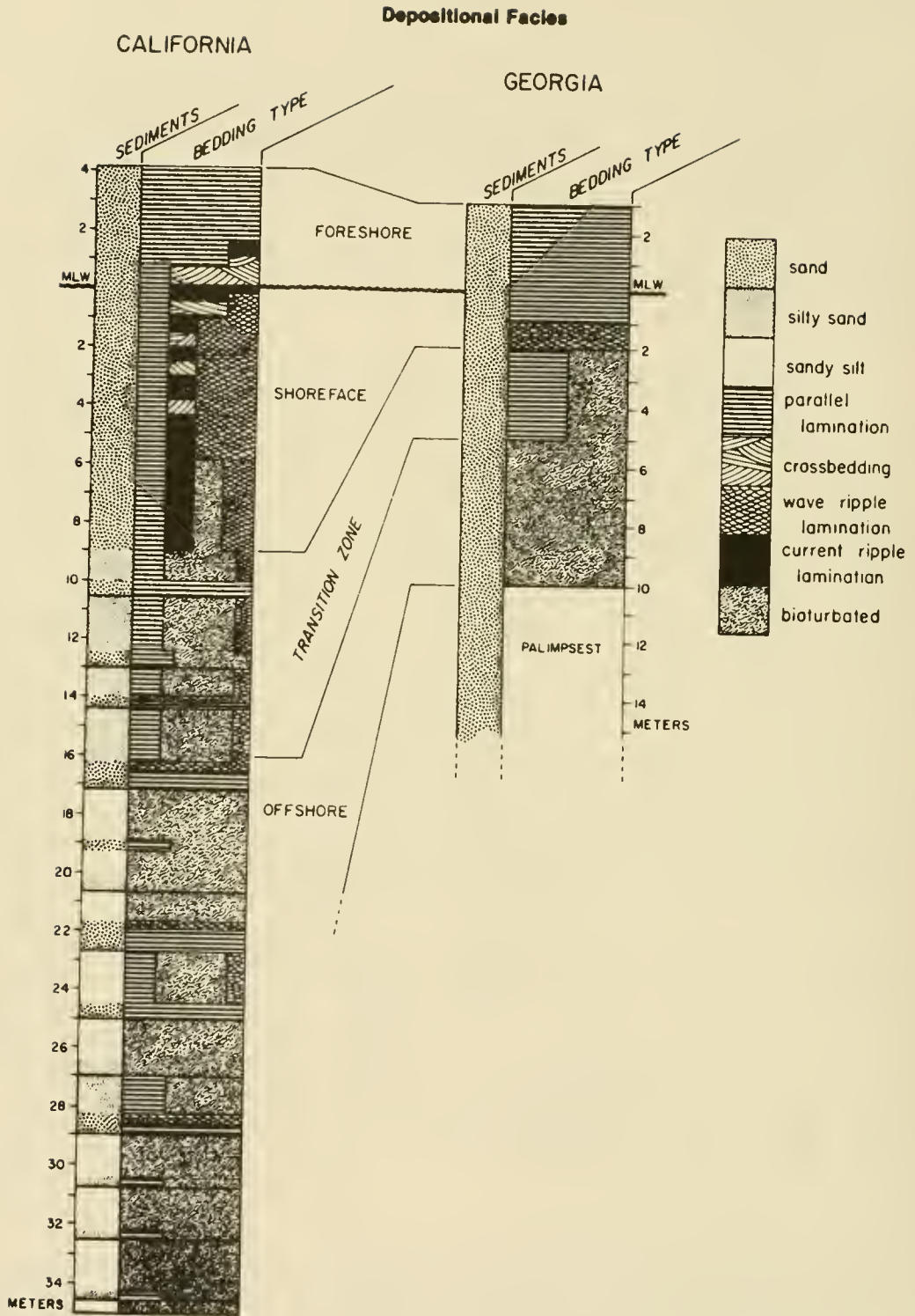
Detailed studies at certain sites have established that appreciable sediment transport by waves on exposed coasts is usually restricted to water depths shallower than 5 to 20 meters (e.g., Dietz and Fairbridge, 1968; Duane, 1976; Gordon and Roy, 1977). The seaward limit to vigorous transport must be related fundamentally to sediment and wave characteristics for a site. Despite the absence of a dependable treatment of onshore-offshore transport rates, several useful techniques exist for estimating the seaward limit of significant transport without detailed investigation of nearshore processes at specific sites.

(1) Variations in Sediment Characteristics. At many localities, a distinct break has been documented in surface sediment characteristics along the shore-normal profile of the inner continental shelf. Traversing the profile seaward, usual nearshore sediments exhibit seaward fining toward very fine, well-sorted sand, then abut sediment which is commonly less well sorted and somewhat coarser (Fig. 4-28). This break in sediment characteristics is interpreted as a boundary between littoral and shelf sediments, with significant wave agitation and transport restricted to littoral sediments.

The characteristic shelf sediment for a particular locality depends on local wave climate (Hayes, 1967b) and on other factors affecting sediments supplied to the shelf (Milliman, Pilkey, and Ross, 1972), so that different breaks in surface sediment characteristics may occur. Various interpretable breaks have been reported: sand shape (Bradley, 1958), sand color (Chapman, 1981), sediment size change from sand to silt (McCave, 1971), and carbonate content of sediment (Davies, 1974). Uncertainties connected with interpretation of surface sediment characteristics include (a) the timespan and type of wave effect indicated at a certain site and (b) how possible disagreements between various indicators are to be resolved.

Examination of vertical sedimentary sequences in the nearshore region permits more definitive interpretation of depositional processes and intensity of sediment transport (e.g., Clifton, Hunter, and Phillips, 1971; Hunter, Clifton, and Phillips, 1979). An example demonstrating the value of comprehensive sediment studies is the results (shown in Figure 4-30) from intensive coring on a high-energy and on a low-energy nearshore region (Howard and Reineck, 1981). The physical and biogenic sedimentary structures revealed comparable process-related bedding sequences at the two sites, with the extent of distinct zones showing a direct response to wave energy. Three zones below MLW were recognized at each site.

In Figure 4-30, the shoreface (or littoral) zone extends to water depths of 9 meters (MLW) at Point Mugu, California, and 2 meters (MLW) at Sapelo Island, Georgia; this zone is very low in bioturbation, except for a region of sand dollar activity between 6 and 9 meters (MLW) at the California site. Grain size decreases in the seaward direction at each site, but this trend is interrupted in the low-energy environment by the occurrence of original ("palimpsest") sediments beyond a water depth of 10 meters; at the high-energy site, no break in sediment activity or bedding type was revealed by sediment



(from Howard and Reineck, 1981)

Figure 4-30. Comparison of vertical sequences from low-energy Georgia coast and high-energy California coast.

coring conducted to water depths of about 35 meters. Between the major bioturbation in the offshore zone and the very limited bioturbation in the shoreface zone, a transition zone occurs with almost all of the characteristics of the flanking zones. Some uncertainty remains about seasonal wave effects at the high-energy site because all sampling was conducted in the summer.

(2) A Wave-Based Profile Zonation. Statistics of annual wave climate together with sand characteristics for a certain site can be used to locate a subaqueous buffer zone where expected waves should have neither strong nor negligible effects on the sand bottom during a typical year (Hallermeier, 1981b). This calculated profile zonation is based on general aspects of sand agitation by waves and is consistent with the limited available evidence on onshore-offshore sand movements at specific sites. The site description used for a calculation consists of the following: (a) the material characteristics  $(\gamma_s/\gamma)$  and (subaqueous)  $d_{50}$  and (b) the median annual significant wave height  $H_{s50}$ , the annual standard deviation of significant wave height  $\sigma_H$ , and the annual average significant wave period  $\bar{T}_s$ .

The usually smaller water depth is a seaward limit to extreme surf-related effects throughout a typical year. This water depth  $d_\ell$  is calculated from

$$\left[ u_{max}(-d) \right]_{50.137} = \left[ 0.03 \left( \frac{\gamma_s}{\gamma} - 1 \right) g d_\ell \right]^{0.5} \quad (4-25)$$

where the numerical subscript indicates the peak near-bottom velocity that is exceeded 12 hours per year (0.137 percent occurrence level). For quartz sand in seawater and small-amplitude wave theory, equation (4-25) has the approximate solution

$$\tilde{d}_\ell \approx 2 H_{s50} + 12 \sigma_H \quad (4-26)$$

so that  $d_\ell$  is roughly twice the extreme nearshore wave height exceeded 12 hours per year. This calculated water depth shows agreement with available data on the seaward limit to intense onshore-offshore sand transport, as revealed by the closeout (to within  $\pm 0.5$  foot or  $\pm 0.15$  meter) of appreciable seasonal excursions in profile elevations. Consideration of this moderately rare wave condition seems consistent with general guidance on the most effective events in geomorphic processes (Wolman and Miller, 1960).

The other water depth is a seaward limit to sand agitation by the median annual wave condition. This water depth  $d_i$  is calculated from

$$\left[ u_{max}(-d) \right]_{s50} = \left[ 8 \left( \frac{\gamma_s}{\gamma} - 1 \right) g d_{50} \right]^{0.5} \quad (4-27)$$

through the depth dependence in  $u_{max}(-d)$  according to small-amplitude wave theory. For quartz sand in seawater, the approximate solution to equation (4-26) is

$$\tilde{d}_i \approx H_{s50} \bar{T}_s \left( \frac{g}{5000 d_{50}} \right)^{0.5} \quad (4-28)$$

so that  $d_i$  varies directly with wave height and period. This water depth is a seaward limit to usual wave agitation on a sandy profile.

Both of these calculated water depths are to be taken with respect to MLW. The median sediment diameter in equation (4-27) is that characterizing the calculated buffer zone; e.g., that at a water depth of  $(1.5 d_\ell)$ . The depth  $d_i$  appears appropriate for applications requiring an estimated seaward limit to moderate wave effects in onshore-offshore transport; e.g., designation of an offshore site as inactive and thus suitable for sediment borrowing. The depth  $d_\ell$  appears appropriate for applications such as coastal structure design, in which an estimated seaward limit to relatively intense onshore-offshore transport may be required. Hallermeier (1981a,b) presented more detailed information on the calculation procedure and its suggested applications, together with extensive example results.

\*\*\*\*\* EXAMPLE PROBLEM 3 \*\*\*\*\*

GIVEN: The high-energy and low-energy coastal sites in Figure 4-30, with wave conditions as follows:

(a) Point Mugu, California (Thompson, 1977, p. 312)

$$\bar{H}_s = 1 \text{ meter (3.35 feet)}$$

$$\sigma_H = 0.34 \text{ meter (1.12 feet)}$$

$$\bar{T}_s = 11.01 \text{ seconds}$$

(b) Sapelo Island, Georgia

$$\bar{H}_s = 0.25 \text{ meter (Howard and Reineck, 1981)}$$

$$\bar{T}_s = 7 \text{ seconds (typical value for southern U. S. Atlantic coast, Thompson, 1977)}$$

Presume quartz sand in seawater, with  $d_{50} = 0.1$  millimeter for each site.

FIND: The values of  $\tilde{d}_\ell$  and  $\tilde{d}_i$  for each site.

SOLUTION: The stated average significant wave height  $\bar{H}_s$  can be used to give the needed annual wave height statistics, according to the modified exponential distribution for nearshore wave heights presented in Section III,3,b. Equation (4-12) yields

$$H_{s50} = \bar{H}_s - 0.307 \sigma_H$$

and equations (4-13) and (4-14) provide

$$\sigma_H \approx 0.62 \bar{H}_s$$

(a) Calculate

$$H_{s50} = \bar{H}_s - 0.307 \sigma_H = 1.0 - (0.307) (0.34) = 0.92 \text{ meter (3.01 feet)}$$

so that equation (4-26) gives

$$\tilde{d}_l \approx 2H_{s50} = 12 \sigma_H = 2 (0.92) + 12 (0.34) \approx 5.93 \text{ meters (19.5 feet)}$$

Also, equation (4-28) gives

$$\begin{aligned} \tilde{d}_i \approx H_{s50} \bar{T}_s \left( \frac{g}{5000 d_{50}} \right)^{0.5} &= 0.92 (11.01) \left( \frac{9.81}{5000 (0.0001)} \right)^{0.5} \\ &\approx 44.7 \text{ meters (147 feet)} \end{aligned}$$

(b) Calculate

$$\sigma_H \approx 0.62 \bar{H}_s = (0.62) (0.25) = 0.155 \text{ meter (0.51 foot)}$$

and

$$H_{s50} = \bar{H}_s - 0.307 \sigma_H = 0.25 - (0.307) (0.155) = 0.202 \text{ meter (0.664 foot)}$$

Equation (4-26) gives

$$\tilde{d} \approx 2H_{s50} + 12 \sigma_H = 2 (0.202) + 12 (0.155) = 2.26 \text{ meters (7.43 feet)}$$

Equation (4-28) gives

$$\begin{aligned} \tilde{d}_i \approx H_{s50} \bar{T}_s \left( \frac{g}{5000 d_{50}} \right)^{0.5} &= (0.202) (7) \left( \frac{9.81}{5000 (0.0001)} \right)^{0.5} \\ &= 6.28 \text{ meters (20.6 feet)} \end{aligned}$$

\*\*\*\*\*

The calculated results in this example appear fairly consistent with the Figure 4-30 results based on interpretation of sedimentary structures. The shoreface (or littoral) zone has an extent comparable to  $d_l$ , and the seaward limit to detectable wave effects occurs at a water depth on the same order of magnitude as  $d_i$ .

(3) Other Approaches. Several suggested procedures for estimating a seaward limit to effective sediment transport have considered forms of along-shore bathymetry and of onshore-offshore profiles.

The limit to the appreciably active nearshore sediment wedge might be revealed at some localities by the seaward extent of water depth contours that are parallel to a relatively straight shoreline. This limit could indicate the maximum water depth for effective reworking of nearshore sediment by waves, smoothing out bottom irregularities by sediment transport (Dietz, 1963). However, charted bathymetry along the U. S. Atlantic and Gulf of Mexico coasts exhibits an irregular along-coast variation in the limit depth to shore-parallel contours, not clearly related to varying wave climate (Everts, 1978).

Other approaches to seaward limit estimation have analyzed the geometry of charted nearshore profiles by various methods (Everts, 1978; Weggel, 1979). These suggested methods use a shape for the nearshore waveformed profile

unlike power law curves reported to be appropriate (Keulegan and Krumbein, 1949; Bruin 1954, 1973; Dean, 1977; Bowen, 1980). In any case, determining and interpreting a geometrical break on limit depth on usually small nearshore slopes are not clear-cut tasks.

(4) Summary on Seaward Limit Estimation. If a seaward limit estimate is needed for planning engineering or research activities in a sandy coastal region, the best office procedure is to adapt a proven seaward limit for a like application in a similar locale. Modifications to take into account somewhat different local conditions may be objectively based upon the profile zonation outlined in Chapter 4, Section V,2,c,(2). This course seems especially recommendable now that long-term hindcast wave data are becoming available for U. S. coasts.

If limited field study can be performed for the site of interest, it appears worthwhile to concentrate on probing variations in nearshore sediment characteristics, with interpretations as described in Section V,2,c,(1). All available information should be considered in estimating the seaward limit to significant onshore-offshore sediment transport.

#### d. Beach Erosion and Recovery.

(1) Beach Erosion. Beach profiles change frequently in response to winds, waves, and tides. The most notable rapid rearrangement of a profile is accomplished by storm waves, especially during storm surge (Ch. 3), which enables the waves to attack higher elevations on the beach (see Fig. 1-8).

The part of the beach washed by runup and runback is the beach face. Under normal conditions, the beach face is contained within the foreshore, but during storms the beach face is moved shoreward by the cutting action of the waves on the profile. The waves during storms are steeper, and the runback of each wave on the beach face carries away more sand than is brought to the beach by the runup of the next wave. Thus the beach face migrates landward, cutting a scarp into the berm (see Fig. 1-8).

In mild storms, the storm surge and accompanying steep waves will subside before the berm has been significantly eroded. In severe storms, or after a series of moderate storms, the backshore may be completely eroded, after which the waves will begin to erode the coastal dunes, cliffs, or mainland behind the beach.

The extent of storm erosion depends on the prestorm profile effects of any shore-stabilizing structures or vegetation, wave conditions, storm surge, the stage of the tide, and storm duration (see Table 4-6). Potential damage to property behind the beach depends on all these factors and on the volume of sand stored in the dune-beach-bar system when a storm occurs.

For planning and design purposes, it is useful to know the magnitude of beach erosion to be expected during severe storms. This type of information is required for the volumetric design of beach nourishment; the required depth of burial of ocean outfall and intake structures; and the functional design of dunes, groins, jetties and revetments. Unfortunately, there is no satisfactory procedure for accurately predicting expected storm losses. Moreover, there is a general paucity of field data documenting the extreme events

Table 4-6. Storm-induced beach changes.

Identification			Storm Data				Beach Damage Data					
(1) Storm Date	(2) Locality	(3) Survey Dates	(4) Profiles	(5) Recurrence Interval <sup>1</sup>	(6) Wind Wave Duration <sup>2</sup> (hr)	(7) Storm Surge (m)	(8) Peak Hind-cast wave height <sup>3</sup> (m)	(9) Profiles with Net Erosion above MSL	(10) Profiles with Net Accretion above MSL	(11) Average Erosion <sup>4</sup> (cu m/m of beach) Median Mean	(12) Range of Erosion <sup>4</sup> Single Profile (cu m/m of beach)	(13) Ratio of Erosion Extreme/Median
6-7 Nov 53	Sandy Hook to Barnegat Light, N.J. <sup>5</sup>	Summer to Nov 1953	19	N/A	N/A	1.8	N/A	18	1	N/A	-223.0 (max)	2.2
3-4 Nov 62	Long Beach Is., N.J.	23 Oct -8 Nov	18	0.8/year	32	1.2 <sup>6</sup>	3.5	12	6	-11.0	-34.1 to 26.2	3.1
	Atlantic City, N.J.	1-9 Nov 62	7	↑	34	↑	3.6	5	2	-7.4	-23.6 to 8.3	2.5
	Ludlum Beach, N.J.	1-7 Nov 62	19	↑	29	↑	3.7	15	4	-5.1	-22.2 to 17.8	4.4
7-8 Nov 63	Atlantic City, N.J.	28 Oct -14 Nov	7	12/year	36	0.6 <sup>6</sup>	2.4	6	1	-25.3	-150.9 to 0.5	6.0
	Ludlum Beach, N.J.	30 Oct -13 Nov	9	↑	27	↑	2.7	17	2	-22.3	-43.3 to 11.5	1.9
13 Mar 68	Misquicut, R.I.	8-14 Mar	6	5/year	25	N/A	3.0 <sup>4</sup>	6	0	-4.3	-8.1 to -1.1	1.9
12 Nov 68	Atlantic City, N.J.	25 Oct -15 Nov	7	2.4/year	60	1.2 <sup>6</sup>	3.1	7	0	-19.7	-32.2 to -8.1	1.6
2-3 Feb 70	Atlantic City, N.J.	28 Jan-4 Feb	7	12/year	45	0.3 <sup>d</sup>	2.5	6	1	-8.6	-12.8 to 10.3	1.5
17 Dec 70 <sup>8</sup>	Cape Cod, Mass.	10-18 Dec	10	2.4/year	31	0.6 <sup>2</sup>	3.3	9	1	-21.1	-41.6 to 21.9	2.0
	Misquicut, R.I.	9-23 Dec	7	↑	30	0.9 <sup>6</sup>	4.2 <sup>7</sup>	6	1	-10.7	-19.9 to 0.7	1.9
	Westhampton, N.Y.	1-18 Dec	11	↑	34	1.1 <sup>d</sup>	3.9	8	3	-13.7	-42.8 to 12.4	3.1
	Jones Beach, N.Y.	12-20 Dec	15	↑	32	↑	4.0	13	2	-18.6	-48.7 to 6.5	2.6
	Long Beach Is., N.J.	7-18 Dec	20	↑	38	↑	3.5	15	5	-8.6	-57.1 to 11.7	6.6
	Atlantic City, N.J.	9-18 Dec	7	↑	40	↑	3.1	4	3	-15.7	-27.4 to 61.2	1.7
	Ludlum Beach, N.J.	10-18 Dec	19	↑	33	↑	2.8	16	3	-7.2	-40.9 to 13.4	5.7
4 Feb 72	Westhampton, N.Y.	31 Jan-4 Feb	11	0.8/year	48	1.4 <sup>6</sup>	4.3	10	1	-27.2	-53.5 to 9.11	2.0
	Jones Beach, N.Y.	2-6 Feb	15	↑	↑	↑	3.8	15	0	-28.4	-43.8 to 8.32	1.5
19 Feb 72	Cape Cod, Mass.	8-23 Feb	10	0.05/year	61	0.9 <sup>6</sup>	5.1	7	3	-18.3	-74.6 to 15.1	4.0
	Misquicut, R.I.	14-25 Feb	7	↑	37	N/A	5.5 <sup>3</sup>	5	2	-5.7	-11.4 to 13.6	2.0
	Westhampton, N.Y.	5-27 Feb	11	↑	44	1.2 <sup>6</sup>	5.5	11	0	-23.0	-40.8 to -0.5	1.8
	Jones Beach, N.Y.	6-24 Feb	15	↑	36	↑	5.5	12	3	-20.8	-38.3 to 27.9	1.8
	Long Beach Is., N.J.	15-23 Feb	18	↑	52	1.5 <sup>6</sup>	4.3	12	6	-3.9	-14.1 to 34.3	3.6
	Atlantic City, N.J.	14-22 Feb	7	↑	34	↑	4.3	7	0	-9.4	-45.7 to -5.1	4.9
	Ludlum Beach, N.J.	10-23 Feb	19	↑	40	↑	4.3	16	3	-8.5	-21.0 to -5.4	2.5
18 Mar 73	Cape Cod, Mass.	8-23 Feb	10	2.4/year	61	0.9 <sup>6</sup>	5.1	7	3	-18.5	-74.6 to 15.1	4.0
	Westhampton, N.Y.	16-24 Mar	11	↑	52	0.5 <sup>c</sup>	4.0	10	1	-32.7	-65.0 to 5.0	2.0
	Long Beach Is., N.J.	13-24 Mar	17	↑	40	↑	2.6	17	2	-22.3	-43.3 to 11.5	1.9
19 Dec 77 <sup>9</sup>	Long Beach Is., N.J.	10-20 Dec	8	5/year	50	1.0 <sup>6</sup>	2.4 <sup>9</sup>	8	0	-20.0	-37.0 to -7.0	1.9
	Ludlum Beach, N.J.	18-20 Dec	13	↑	50	↑	3.8 <sup>9</sup>	13	0	-17.7	-25.9 to -9.8	1.5
	Bodie Island, N.C.	18-20 Dec	10	↑	60	0.9 <sup>f</sup>	↑	9	1	-14.0	-25.0 to 6.5	1.8
22 Sept 75	Bay County, Fla.	1973 to	94	N/A	<24	3.6	3.7 <sup>11</sup>	N/A	N/A	N/A	-49.7 (max)	3.1
Elolse <sup>10</sup>	Walton County, Fla.	Oct 1975	101	↑	↑	4.9	↑	N/A	N/A	-20.4	-73.4 (max)	3.6

1 Number of storms to be equal or exceeded per year. Based solely on WES hindcast wave height for Atlantic City and distribution of storms shown in Figure 4-31. Does not take into account the return period of the storm surge or storm duration.

2 For each locality, defined as the time that the wave height exceeded a critical value equal to the 20-year average wave height plus one standard deviation.

3 As computed for 10-nautical mile segment by WES hindcast (depth = 9.0 meters (30 feet)).

4 All volumes are computed above MSL.

5 Calbrell (1959) and U. S. Army Engineer District, New York (1954).

6 N/A = Not available.

7 Shoaling effect of Block Island not included in hindcast.

8 Dabell et al. (1977).

9 Birkmeier (1979).

10 Chiu (1977).

11 Estimated by Hughes and Chiu (1981).

a Boston, Mass.  
 b Newport, R.I.  
 c Battery, N.Y.  
 d Sandy Hook, N.J.  
 e Atlantic City, N.J.  
 f CERC, PRF, Duck, N.C.

typical of design conditions (storms with return periods of 50 to 100 years).

Various methods have been presented by Edelman (1968), Vallianos (1974), and Dean (1976) for estimating storm erosion. These methods relate dune recession to storm tide based on the equilibrium profile concept and a balance of eroded and deposited material. Storm duration and the development of an offshore bar are not included. These are important factors since few storms last long enough for the profile to reach a new equilibrium shape, and the presence of an offshore bar either before the storm or the creation of one during the storm can significantly affect the storm's impact on the beach by causing waves to break offshore and to dissipate much of their energy before reaching the beach (Dean, 1976). Hughes and Chiu (1981) present a method for estimating storm changes based on model tests which attempt to recreate the measured effects of Hurricane Eloise on the Florida coast. Their procedure, which requires field verification, recognizes the importance of the offshore bar.

Lacking satisfactory means for predicting profile changes, the engineer must estimate them using published representative changes measured for similar areas. Long-term and storm profile changes for a number of Great Lakes and east coast areas are documented in DeWall et al. (1977), DeWall (1979), Everts et al. (1980), Miller et al. (1980), Kana (1977), and Birkemeier (1981).

Table 4-6 tabulates the effect of a number of storms along the Atlantic and gulf coasts of the United States (Fig. 4-31). Columns are included detailing both the storm (columns 5-8) and the beach changes which occurred (columns 9-13). Generally, the table includes only storms for which the prestorm and poststorm surveys were done reasonably close to the date of the storm. This is particularly important for the poststorm survey since significant beach recovery can occur in the waning stages of a storm (Birkemeier, 1979; Kana, 1977).

For consistency, wave data from the Phase III east coast wave hindcast model of the Waterways Experiment Station calculated in 9.1 meters (30 feet) of water have been used. The recurrence interval has also been computed using these data from Atlantic City, New Jersey. The storm surges are computed from actual gage records. Note that the actual storm intensity is due to a combination of columns 7 and 8.

Volumetric losses computed above MSL have been tabulated for each storm and locality in columns 11 and 12. Wide variation in volume losses at single profile lines results from the proximity of structures, inlets, and nearshore bathymetry. Because of this, the median change probably better represents the average rather than the mean.

An examination of Table 4-6 provides some insight into the importance of storm surge, storm duration, and wave conditions. The highest surge occurred during Hurricane Eloise in September 1975 and, though it caused erosion over long reaches of coast because of its short duration, the average change was not unlike the data for many of the northeasters. The highest reported surge and the largest changes for a northeast storm were reported by Caldwell (1959). Some of this change may result from the long period between the first

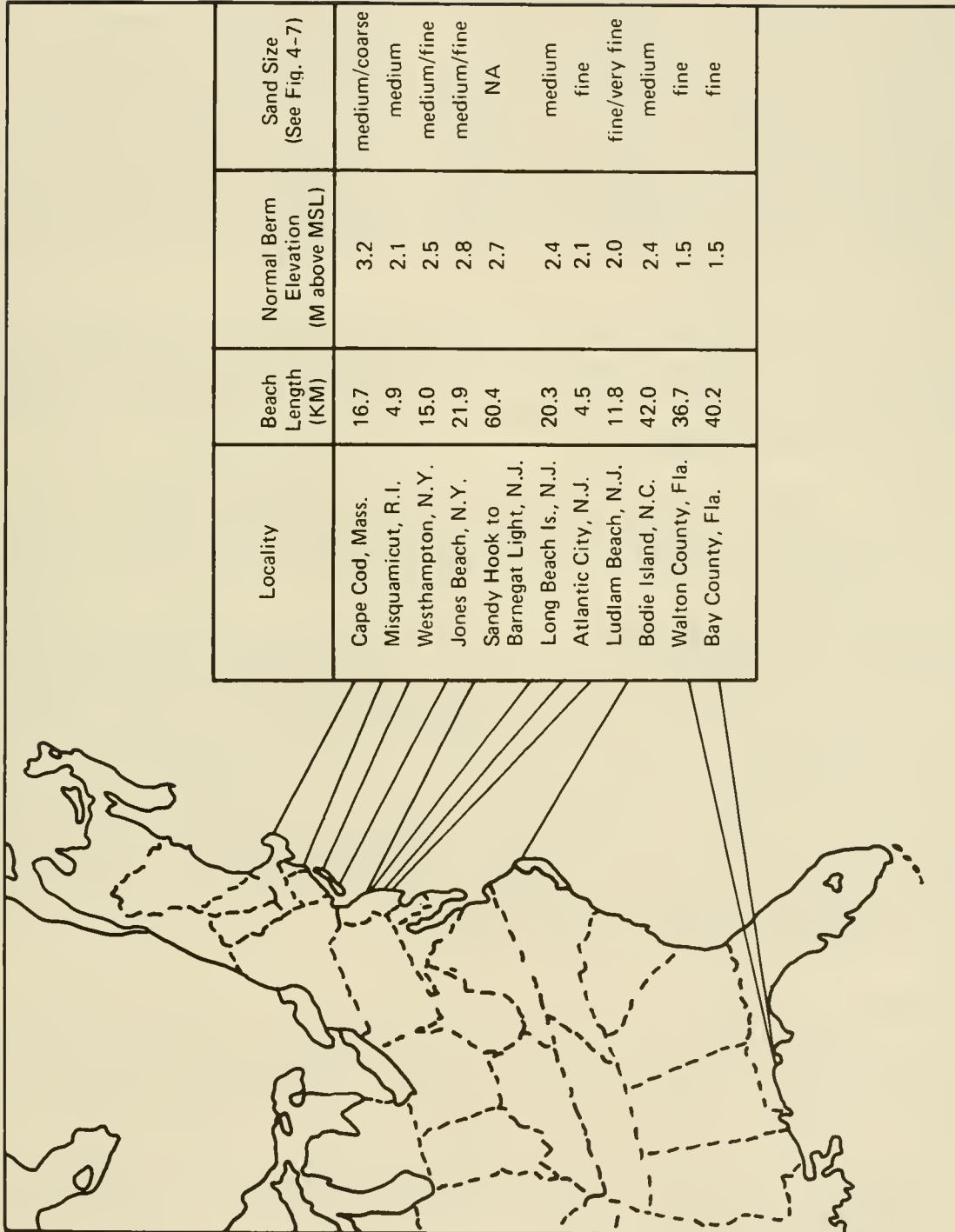


Figure 4-31. Location and characteristics of beaches included in Table 4-6.

survey and the storm. Note that only those profiles not affected by a "seawall" were reported.

Although the data in Table 4-6 are not exactly comparable, they suggest that the average volumes of sand eroded from above MSL for beaches 8 or more kilometers (5 miles) long have a limited range of values. A moderate storm may remove 10 to 25 cubic meters per meter of beach front above MSL (4 to 10 cubic yards per foot); an extreme storm (or a moderate storm that persists for a long time) may remove 25 to 50 cubic meters per meter (10 to 20 cubic yards per foot); rare storms that are most erosive due to a combination of intensity, duration, and orientation may remove 50 to 125 cubic meters per meter (20 to 50 cubic yards per foot). For comparison, a berm 30 meters (100 feet wide), 3 meters (10 feet) above MSL contains 90 cubic meters per meter of beach front (37 cubic yards per foot), a quantity that would be adequate except for extreme storms.

In terms of horizontal changes a moderate storm can erode a typical beach 20 to 30 meters (75 to 100 feet) or more (Table 4-6) and leave it exposed to greater erosion if a second storm follows before the beach has recovered. This possibility should be considered in design and placement of beach fills and other protective measures.

Extreme values of erosion may be more useful for design than mean values. Column 13 of Table 4-6 suggests that the ratio of the most eroded profile (above MSL) to the median profile for each coast beaches ranges from about 1.5 to 6.6.

Although the dominant result of storms on the portion of a beach above MSL is erosion, most poststorm surveys show that storms produce local accretion as well. Of the 90 profiles from Cape Cod, Massachusetts, to Cape May, New Jersey, surveyed immediately after the December 1970 storm, 18 showed net accretion above mean sea level. Accretion can also result during overwash when waves transport sand inland from the beach (Leatherman et al., 1977). Survey data from a number of storms also indicate that the shoreline may move seaward during a storm. This suggests movement of sand from higher to lower elevations, but not necessarily offshore. DeWall et al. (1977) reported that of the 89 profiles surveyed after the 17 December 1970 storm (Table 4-6) 52 percent showed seaward movement of the shoreline. Similar findings have been shown by Birkemeier (1979) and Chiu (1977).

Though above MSL changes are of greatest interest to the engineer, they occur over only a small part of the active profile. Figure 4-32 illustrates the types of offshore changes that can occur. The figure shows the response of a profile line located 500 meters (1700 feet) south of CERC's Field Research Facility in Duck, North Carolina. The four storms which occurred during the period caused the bar to move offshore a total distance of 172 meters (564 feet). Though the first three storms had negligible effect on the above MSL beach while causing considerable nearshore movement, only the fourth storm, which coincided with a high spring tide and which produced the highest waves, caused the beach to erode.

(2) Beach Recovery. The typical beach profile left by a severe storm is a simple, concave-upward curve extending seaward to low tide level or below. The sand that has been eroded from the beach is deposited mostly as a

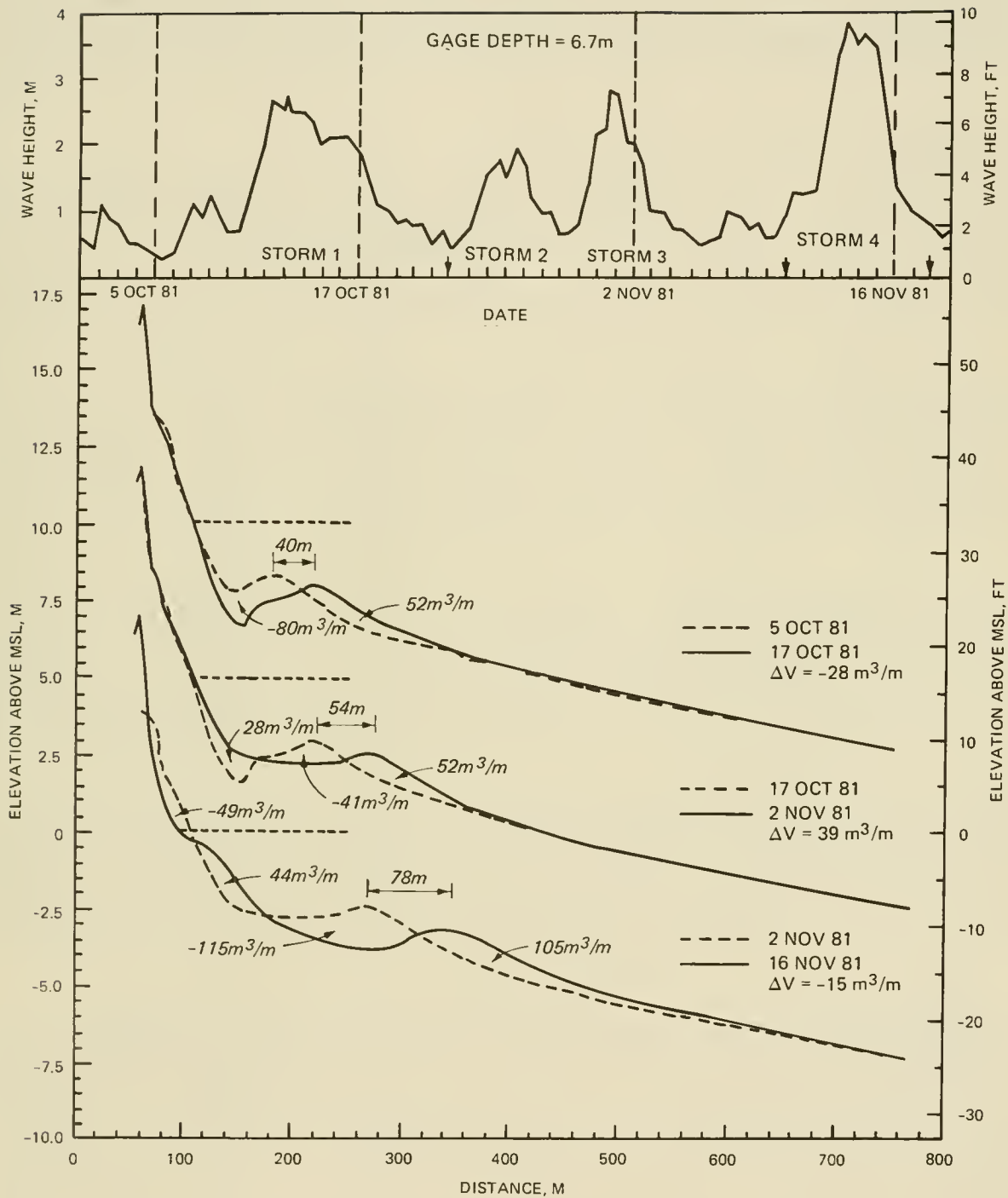


Figure 4-32. Effects of four storms on the beach and nearshore at a profile line south of CERC's Field Research Facility in Duck, North Carolina (arrows mark other surveys which show little change from those plotted).

ramp or bar in the surf zone that exists at the time of the storm. Immediately after the storm, beach repair begins by a process that has been documented in some detail (e.g., Hayes, 1971a; Davis et al., 1972; Davis and Fox, 1972; Sonu and van Beek, 1971). Sand that has been deposited seaward of the shoreline during the storm begins moving landward as a sandbar with a gently sloping seaward face and a steeper landward face (Fig. 4-33). These

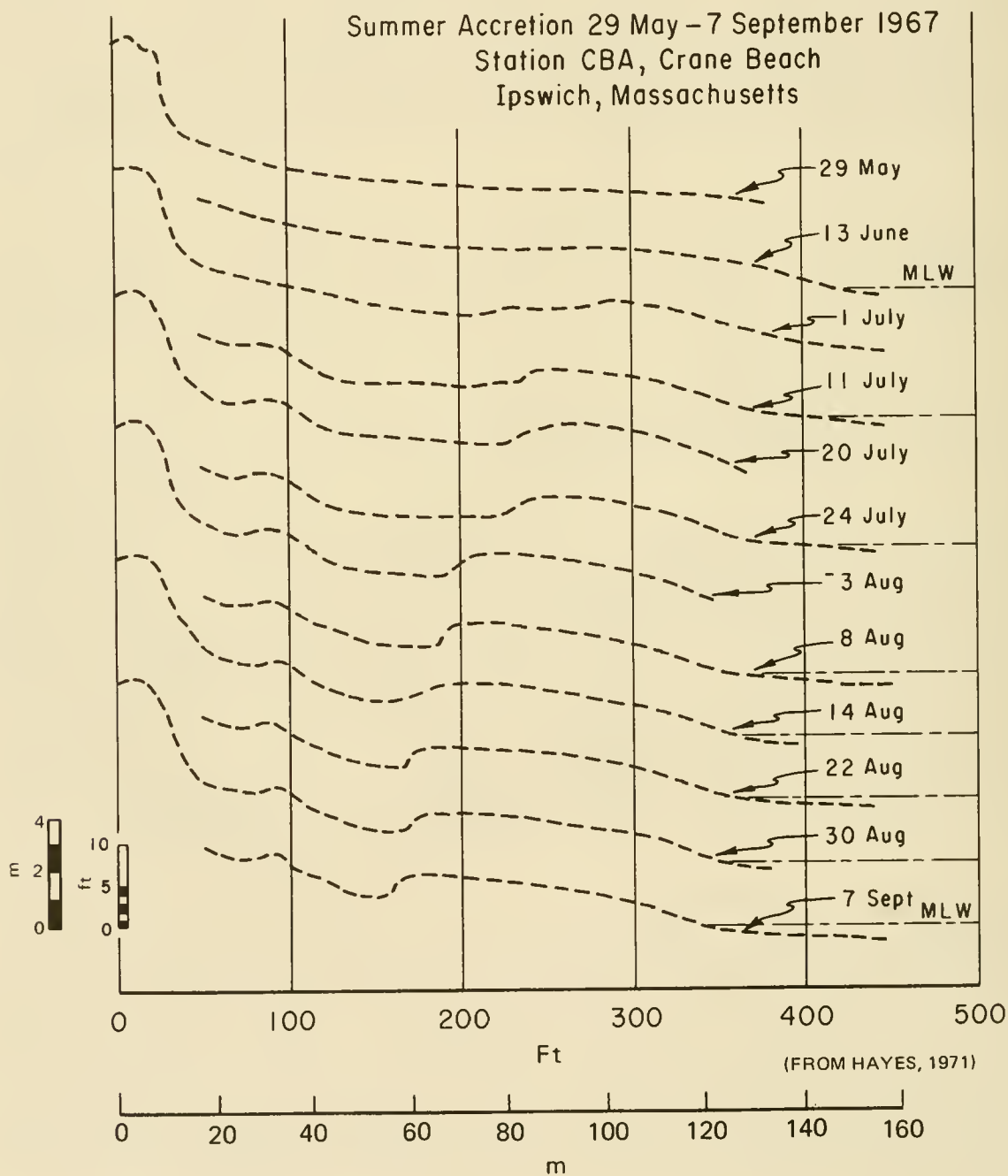


Figure 4-33. Slow accretion of ridge-and-runnel at Crane Beach, Massachusetts

bars have associated lows (runnels) on the landward side and occasional drainage gullies across them (King, 1972, p. 339). These systems are characteristic of poststorm beach accretion under a wide range of wave, tide, and sediment conditions (Davis et al., 1972). Further accretion continues by adding layers of sand to the top of the bar which, by then, is a part of the beach (see Fig. 4-34).

Berms may form immediately on a poststorm profile without an intervening bar-and-trough, but the mode of berm accretion is quite similar to the mode of bar-and-trough growth. Accretion occurs both by addition of sand laminae to the beach face (analogous to accretion on the seaward-dipping top of the bar in the bar-and-trough) and by addition of sand on the slight landward slope of the berm surface when waves carrying sediment overtop the berm crest (analogous to accretion on the landward-dipping slip face of the bar). This process of berm accretion is also illustrated in Figure 4-1.

The rate at which the berm builds up or the bar migrates landward to weld onto the beach varies greatly, apparently in response to wave conditions, beach slope, grain size, and the length of time the waves work on the bars (Hayes, 1971). Compare the slow rate of accretion at Crane Beach in Figure 4-33 (mean tidal range 2.7 meters (9 feet), spring range 4.0 meters (13 feet)), with the rapid accretion on the Lake Michigan shore in Figure 4-34 (tidal range less than 0.08 meter (0.25 foot)).

Poststorm studies show that the rate of poststorm replenishment by bar migration and berm building is usually rapid immediately after a storm (Birkemeier, 1979; Kana, 1977). This rapid buildup is important in evaluating the effect of severe storms because the true extent of erosion during the storm is likely to be obscured by the poststorm recovery (unless surveys are made within hours after the storm).

The ideal result of poststorm beach recovery is a wide backshore that will protect the shore from the next storm. Beach recovery may be prevented when the period between successive storms is too short. Maintenance of coastal protection requires (a) knowledge of the necessary width and elevation of the backshore appropriate to local conditions and (b) adequate surveillance to determine when this natural sand reservoir has diminished to the point where it may not protect the backshore during the next storm.

e. Prediction of Eroded versus Accreted Beaches. An important aspect of onshore-offshore sediment transport is the distinction between conditions which result in beach erosion and those which produce beach accretion. It is occasionally assumed that a berm characterizes an accreted profile and that a bar characterizes an eroded profile. This is oversimplified in that (1) a berm may be absent on an accreted beach where the top of the foreshore may reach the dune or cliff line, (2) nearshore bars do not directly indicate an eroded beach, and (3) a bar and a berm may both be present. Bars are connected in complicated ways with breaker processes (see Battjes, 1974), tidal range, and sediment character and supply (see Krumbain, 1944; Shepard, 1950; Saylor and Hands, 1970; Zwamborn, Fromme, and Fitzpatrick, 1970; Davis and Fox, 1972; Carter and Kitcher, 1979; Greenwood and Davidson-Arnott, 1979). Berms result from complicated, interrelated processes at the landward edge to the hydrodynamic transport of sediment.

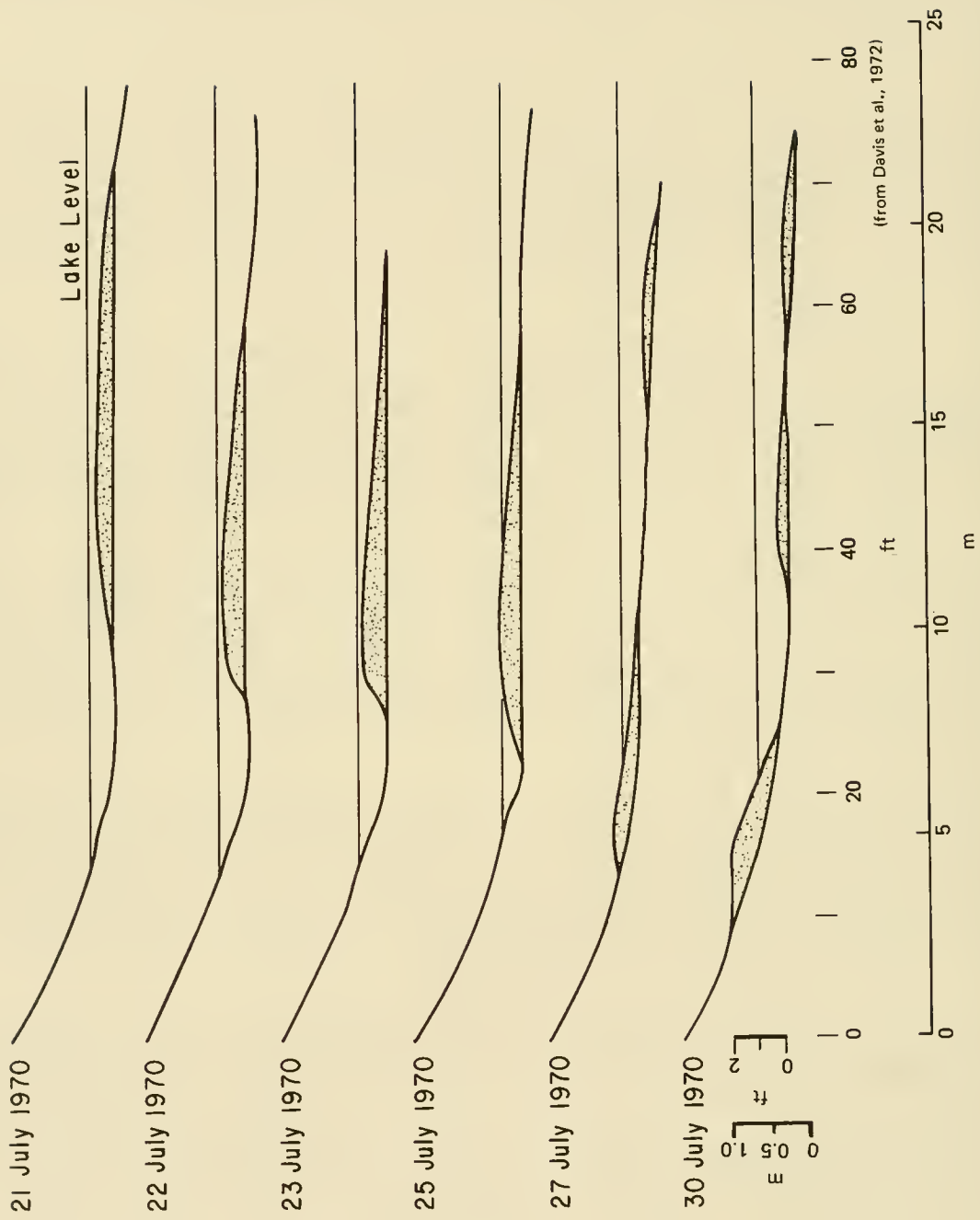


Figure 4-34. Rapid accretion of ridge-and-runnel at Lake Michigan (Holland, Michigan).

However, observations have clearly established that high, steep waves tend to erode fine beach sediment, while low, steep waves tend to cause beach accretion. Quantitative classifications of the occurrence of eroded versus accreted beaches have benefited from an increasing data base and from better developed analyses of profile formation processes. The two classifications presented here have some established pertinence to processes at prototype scale.

Early laboratory experiments indicated that the type of waveformed profile was determined by deepwater wave steepness (deepwater significant wave height ( $H_o$ ) / deepwater wave length ( $L_o$ )). With prototype-scale tests, Saille (1957) established that the wave height was as important as wave steepness in determining profile type. Extending this work by considering a fundamental sediment characteristic, the fall velocity (see Ch. 4, Sec. II,1), Dean (1973) reported that the profile type depended on the parameter

$$F_o = \frac{H_o}{V_f T}$$

where

$F_o$  = dimensionless fall time parameters

$H_o$  = deepwater significant wave height

$V_f$  = fall velocity of particles in the water column

$T$  = wave period

Beach erosion usually occurred for  $F_o > 1$ , and beach accretion usually occurred for  $F_o < 1$ . This classification is supported by laboratory tests at reduced and at prototype scales (Dean, 1973; Kohler and Galvin, 1973).

Sunamura and Horikawa (1974) considered average nearshore bottom slope ( $\tan \theta$ ) and reported shoreline changes at various field sites in an independent classification of profile types. The occurrence of beach erosion or accretion was reported to depend on the parameter

$$G_o = \frac{H_o}{L_o} (\tan \theta)^{0.27} \left( \frac{d_{50}}{L_o} \right)^{-0.67}$$

where  $G_o$  is a dimensionless parameter for determining accretion or erosion and  $d_{50}$  is the size of the 50th percentile of sediment sample. For the field data, beach erosion usually occurred for  $G_o < (1/18)$ , and beach accretion usually occurred for  $G_o > (1/9)$ . These calculations used maximum wave height between shore surveys, wave period corresponding to this height for  $L_o = (g T^2 / 2)$ , mean subaerial grain size for  $d_{50}$ , and average slope between the shoreline and a water depth of about 20 meters. The numerical values of  $G_o$  for beach erosion or accretion in small-scale laboratory tests were reported to be somewhat different than in field shoreline changes, but this may have been due to the calculation suppositions for field cases.

The functional forms of the criteria in equations (4-29) and (4-30) are fairly consistent, but both classifications might be considered in predicting the occurrence of eroded or accreted beaches.

f. Slope of the Foreshore. The foreshore is the steepest part of the beach profile. The equilibrium slope of the foreshore is a useful design parameter, since this slope, along with the berm elevation, determines minimum beach width.

The slope of the foreshore tends to increase as the grain size increases (U.S. Army Corps of Engineers, 1933; Bascom, 1951; King, 1972, p. 324.) This relationship between size and slope is modified by exposure to different wave conditions (Bascom, 1951; Johnson, 1956); by specific gravity of beach materials (Nayak, 1970; Dubois, 1972); by porosity and permeability of beach material (Savage, 1958), and probably by the tidal range at the beach. Analysis by King (1972, p. 330) suggests that slope depends dominantly on sand size and also significantly on an unspecified measure of wave energy.

Figure 4-35 shows trends relating slope of the foreshore to grain size along the Florida Panhandle, New Jersey-North Carolina, and U.S. Pacific coasts. Trends shown on the figure are simplifications of actual data, which are plotted in Figure 4-36. The trends show that, for constant sand size, slope of the foreshore usually has a low value on Pacific beaches, intermediate value on Atlantic beaches, and high value on gulf beaches.

This variation in foreshore slope from one region to another appears to be related to the mean nearshore wave heights (see Figs. 4-17, 4-18, and Table 4-4). The gentler slopes occur on coasts with higher waves. An increase in slope with decrease in wave activity is illustrated by data from Half Moon Bay (Bascom, 1951) and is indicated by the results of King (1972, p. 332).

The inverse relation between slope and wave height is partly caused by the relative frequency of the steep or high eroding waves which produce gentle foreshore slopes and the low accretionary poststorm waves which produce steeper beaches (see Figs. 4-1, 4-32, and 4-33).

The relation between foreshore slope and grain size shows greater scatter in the laboratory than in the field. However, the tendency for slope of the foreshore to increase with decreasing mean wave height is supported by laboratory data of Rector (1954, Table 1). In this laboratory data, there is an even stronger inverse relation between deepwater steepness,  $H_0/L_0$ , and slope of the foreshore than between  $H_0$  and the slope.

The following statements summarizing the results on foreshore slope for design purposes are supported by available data:

(1) Slope of the foreshore on open sand beaches depends principally on grain size and (to a lesser extent) on nearshore wave height.

(2) Slope of the foreshore tends to increase with increasing median grain size, but there is significant scatter in the data.

(3) Slope of the foreshore tends to decrease with increasing wave height, again with scatter.

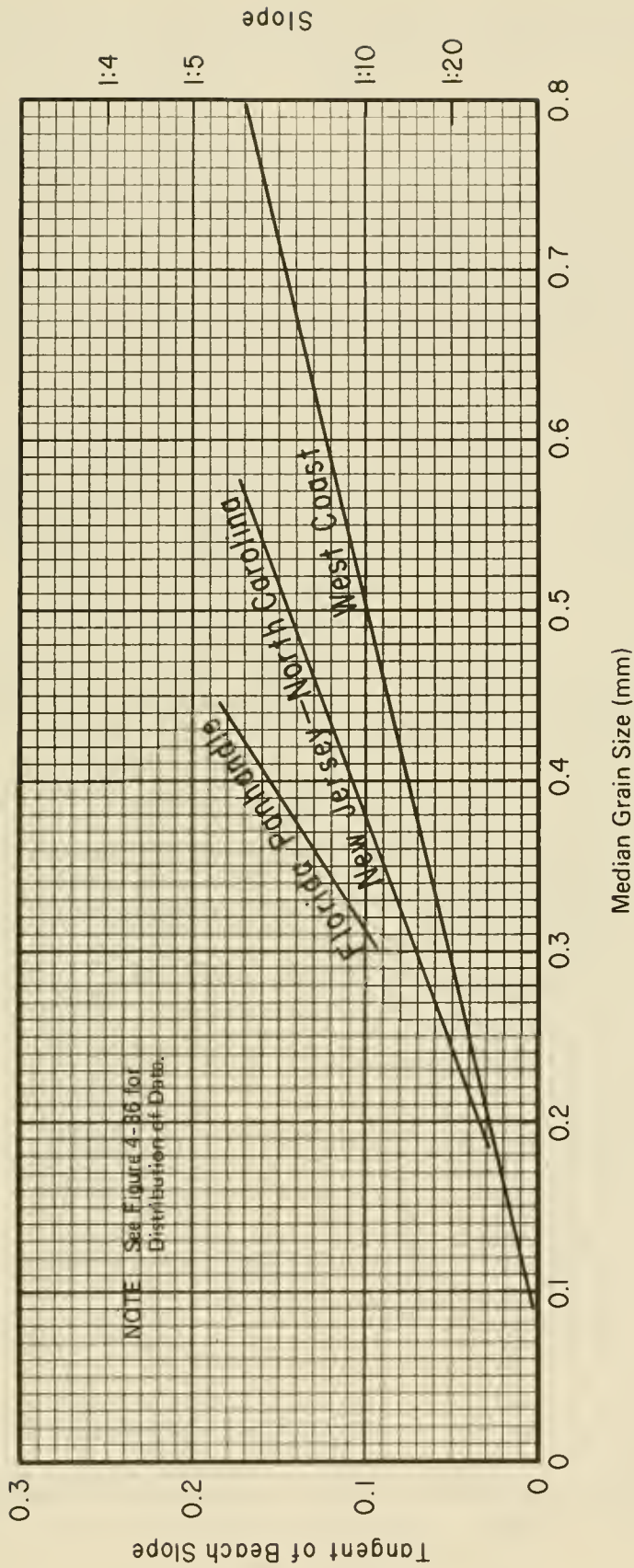


Figure 4-35. Data trends, median grain size versus foreshore slope.

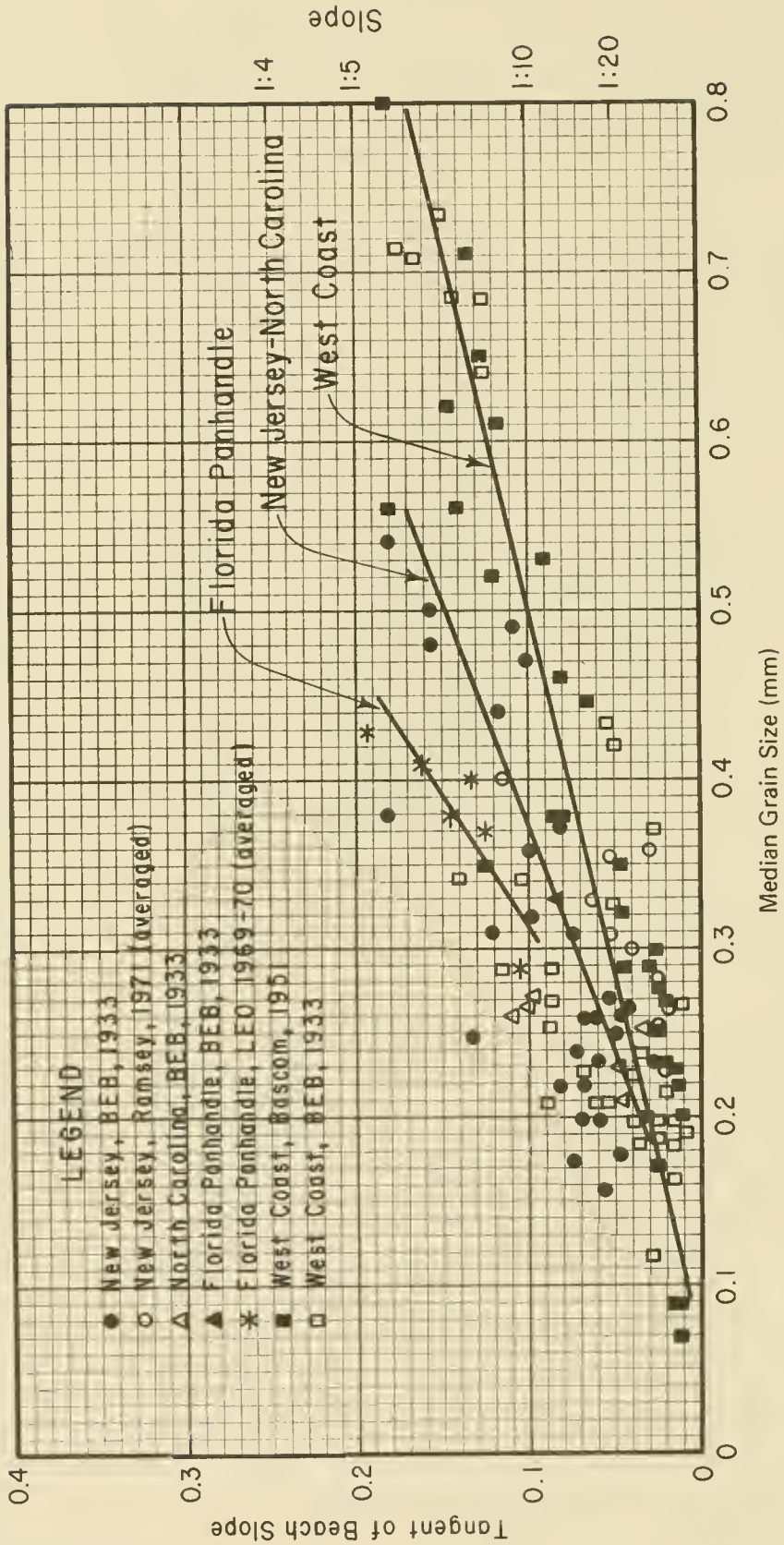


Figure 4-36. Data, median grain size versus foreshore slope.

(4) For design of beach profiles on ocean or gulf beaches, use Figure 4-35, keeping in mind the large scatter in the basic data in Figure 4-36, much of which is caused by the need to adjust the data to account for differences in nearshore wave climate.

### 3. Longshore Transport Rate.

a. Definitions and Methods. *Littoral drift* is the sediment (usually sand) moved in the littoral zone under action of waves and currents. The rate  $Q$  at which littoral drift is moved parallel to the shoreline is the *longshore transport rate*. Since this movement is parallel to the shoreline, there are two possible directions of motion, right to left, relative to an observer standing on the shore looking out to sea. Movement from the observer's right to his left is motion toward the left, indicated by the subscript  $lt$ ; movement toward the observer's right is indicated by the subscript  $rt$ .

*Gross longshore transport rate*,  $Q_g$ , is the sum of the amounts of littoral drift transported to the right and to the left, past a point on the shoreline in a given time period.

$$Q_g = Q_{rt} + Q_{lt} \quad (4-29)$$

Similarly, *net longshore transport rate*,  $Q_n$ , is defined as the difference between the amounts of littoral drift transported to the right and to the left past a point on the shoreline in a given time period:

$$Q_n = Q_{rt} - Q_{lt} \quad (4-30)$$

The quantities  $Q_{rt}$ ,  $Q_{lt}$ ,  $Q_n$ , and  $Q_g$  have engineering uses: for example,  $Q_g$  is used to predict shoaling rates in uncontrolled inlets.  $Q_n$  is used for design of protected inlets and for predicting beach erosion on an open coast;  $Q_{rt}$  and  $Q_{lt}$  are used for design of jetties and impoundment basins behind weir jetties. In addition  $Q_g$  provides an upper limit on other quantities.

Occasionally, the ratio

$$\gamma = \frac{Q_{lt}}{Q_{rt}} \quad (4-31)$$

is known, rather than the separate values  $Q_{lt}$  and  $Q_{rt}$ . Then  $Q_g$  is related to  $Q_n$  in terms of  $\gamma$  by

$$Q_g = Q_n \frac{(1 + \gamma)}{(1 - \gamma)} \quad (4-32)$$

This equation is not very useful when  $\gamma$  approaches 1.

Longshore transport rates are usually given in units of volume per time (cubic meters per year in the United States). Typical rates for oceanfront

beaches range from 100,000 to 250,000 cubic meters per year (see Table 4-7). These volume rates typically include about 40 percent voids and 60 percent solids.

Another representation of longshore transport rate is the immersed weight rate  $I_{\ell}$  which is given in units of force per unit time (such as pounds per second or newtons per second). The conversion from  $Q$  to  $I_{\ell}$  is

$$I_{\ell} = (\rho_s - \rho) g a' Q \quad (4-35)$$

where

$\rho_s$  = mass density of sand

$\rho$  = mass density of water

$g$  = acceleration of gravity

$a'$  = volume solids/total volume (accounts for the sand porosity)

This equation is valid for any consistent set of units. Table 4-8 lists commonly assumed values for the parameters in equation (4-35). If better estimates of  $\rho_s$ ,  $\rho$ , and  $a'$  are known for a specific site, they should be used in equation (4-35). Further discussion of equation (4-35) is provided by Galvin (1972b).

At present, there are four basic methods to use for the prediction of longshore transport rate

(1). The best way to predict longshore transport at a site is to adopt the best known rate from a nearby site, with modifications based on local conditions.

(2). If rates from nearby sites are unknown, the next best way to predict transport rates at a site is to compute them from data showing historical changes in the topography of the littoral zone (charts, surveys, and dredging records are primary sources).

Some indicators of the transport rate are the growth of a spit, shoaling patterns and deposition rates at an inlet, and the growth of a fillet adjacent to a jetty or groin. As an example, the longshore transport rate across Cold Spring Inlet, New Jersey, was estimated based on fillet growth next to the updrift jetty and surveys of the surrounding area to account for the sand that was not impounded by the jetty (U.S. Congress, 1953b). The rates of growth for Sandy Hook, New Jersey (U.S. Army Engineer District, New York, 1954), and for Sheshalik Spit, Alaska (Moore and Cole, 1960), were used to estimate longshore transport rate. Bruno and Gable (1976) measured the deposition behind the offshore breakwater and adjacent to the updrift jetty at Channel Island Harbor, California, to find the longshore transport rate.

(3). If neither method 1 nor method 2 is practical, then it is accepted practice to use either measured or calculated wave conditions to compute a longshore component of "wave energy flux" which is related through an empirical curve to longshore transport rate (Galvin and Schweppe, 1980).

Table 4-7. Longshore transport rates from U.S. coasts.<sup>1</sup>

Location	Predominant Direction of Transport	Longshore <sup>2</sup> Transport (cu m/yr)	Date of Record	Reference
Atlantic Coast				
Suffolk County, N.Y.	W	153,000	1946-55	New York District (1955)
Sandy Hook, N.J.	N	377,000	1885-1933	New York District (1954)
Sandy Hook, N.J.	N	333,000	1933-51	New York District (1954)
Asbury Park, N.J.	N	153,000	1922-25	New York District (1954)
Shark River, N.J.	N	229,000	1947-53	New York District (1954)
Manasquan, N.J.	N	275,000	1930-31	New York District (1954)
Barnegat Inlet, N.J.	S	191,000	1939-41	New York District (1954)
Absecon Inlet, N.J.	S	306,000	1935-46	New York District (1954)
Ocean City, N.J.	S	306,000	1935-46	U.S. Congress (1953a)
Cold Spring Inlet, N.J.	S	153,000	-----	U.S. Congress (1953b)
Ocean City, Md.	S	115,000	1934-36	Baltimore District (1948)
Atlantic Beach, N.C.	E	22,500	1850-1908	U.S. Congress (1948)
Hillsboro Inlet, Fla.	S	57,000	1850-1908	U.S. Army (1955b)
Palm Beach, Fla.	S	115,000 to 175,000	1925-30	BEB (1947)
Gulf of Mexico				
Pinellas County, Fla.	S	38,000	1922-50	U.S. Congress (1954a)
Perdido Pass, Ala.	W	153,000	1934-53	Mobile District (1954)
Pacific Coast				
Santa Barbara, Calif.	E	214,000	1932-51	Johnson (1953)
Oxnard Plain Shore, Calif.	S	765,000	1938-48	U.S. Congress (1953c)
Port Hueneme, Calif.	S	382,000	-----	U.S. Congress (1954b)
Santa Monica, Calif.	S	206,000	1936-40	U.S. Army (1948b)
El Segundo, Calif.	S	124,000	1936-40	U.S. Army (1948b)
Redondo Beach, Calif.	S	23,000	-----	U.S. Army (1948b)
Anaheim Bay, Calif.	E	115,000	1937-48	U.S. Congress (1954c)
Camp Pendleton, Calif.	S	76,000	1950-52	Los Angeles District (1953)
Great Lakes				
Milwaukee County, Wis.	S	6,000	1894-1912	U.S. Congress (1946)
Racine County, Wis.	S	31,000	1912-49	U.S. Congress (1953d)
Kenosha, Wis.	S	11,000	1872-1909	U.S. Army (1953b)
Ill. State Line to Waukegan	S	69,000	-----	U.S. Congress (1953e)
Waukegan to Evanston, Ill.	S	44,000	-----	U.S. Congress (1953e)
South of Evanston, Ill.	S	31,000	-----	U.S. Congress (1953e)
Hawaii				
Waikiki Beach	--	8,000	-----	U.S. Congress (1953f)

(from Wiegel, 1964; Johnson, 1957)

1 Method of measurement is by accretion except for Absecon Inlet and Ocean City, New Jersey, and Anaheim Bay, California, which were measured by erosion, and Waikiki Beach, Hawaii, which was measured according to suspended load samples.

2 Transport rates are estimated net transport rates,  $Q_n$ . In some cases, these approximate the gross transport rates,  $Q_g$ .

Table 4-8. Values of parameters in equation 4-35

Term	Metric <sup>1</sup>	U.S. Customary <sup>2</sup>
$s$	2,650 kg/m <sup>3</sup>	5.14 slugs/ft <sup>3</sup>
(saltwater)	1,025 kg/m <sup>3</sup>	1.99 slugs/ft <sup>3</sup>
(freshwater)	1,000 kg/m <sup>3</sup>	1.94 slugs/ft <sup>3</sup>
$a'$	0.6	0.6
$g$	9.8 m/s <sup>2</sup>	32.2 ft/s <sup>2</sup>

<sup>1</sup> Q in cubic meters per second;  $I_{\ell}$  in newtons per second.

<sup>2</sup> Q in cubic feet per second;  $I_{\ell}$  in pounds per second.

(4). An empirical method (Galvin, 1972b) is available to estimate gross longshore transport rate from mean annual nearshore breaker height. The gross rate, so obtained, can be used as an upper limit on net longshore transport rate.

Method 1 depends largely on engineering judgment and local data. Method 2 is an application of historical data, which gives usable answers if the basic data are reliable and available at reasonable cost and the interpretation is based on a thorough knowledge of the locality. By choosing only a few representative wave conditions, method 3 can usually supply an answer with less work than method 2, but with correspondingly less certainty. Because calculation of wave statistics in method 3 follows an established routine, it is often easier to use than researching the hydrographic records and computing the changes necessary for method 2. Method 4 requires mean nearshore breaker height data. Sections V,3,b through V,3,d utilize methods 3 and 4; methods 1 and 2 are discussed in Section VIII.

b. Energy Flux Method. Method 3 is based on the assumption that longshore transport rate  $Q$  depends on the longshore component of energy flux in the surf zone. The longshore energy flux in the surf zone is approximated by assuming conservation of energy flux in shoaling waves, using small-amplitude theory, and then evaluating the energy flux relation at the breaker position. The energy flux per unit length of wave crest, or, equivalently, the rate at which wave energy is transmitted across a plane of unit width perpendicular to the direction of wave advance is (from Ch. 2, Sec. II,3, combining eqs. (2-39) and (2-40)):

$$\bar{P} = \bar{E} C_g = \frac{\rho g}{8} H^2 C_g$$

If the wave crests make an angle,  $\alpha$  with the shoreline, the energy flux in the direction of wave advance *per unit length of beach* is

$$\bar{P} \cos \alpha = \frac{\rho g H^2}{8} C_g \cos \alpha$$

and the longshore component is given by

$$P_{\ell} = \bar{P} \cos \alpha \sin \alpha = \frac{\rho g}{8} H^2 C_g \cos \alpha \sin \alpha$$

or, since  $\cos \alpha \sin \alpha = 1/2 \sin 2\alpha$

$$P_{\ell} = \frac{\rho g}{16} H^2 C_g \sin 2\alpha \quad (4-36)$$

The approximation for  $P_{\ell}$  at the breaker line is written

$$P_{\ell b} = \frac{\rho g}{16} H_b^2 C_b \sin 2\alpha_b \quad (4-37)$$

For linear theory, in shallow water,  $C_g \approx C$  and

$$P_{\ell b} = \frac{\rho g}{16} H_b^2 C_b \sin 2\alpha_b \quad (4-38)$$

where  $H_b$  and  $\alpha_b$  are the wave height and direction and  $C_b$  is the wave speed from equation (2-3) evaluated in a depth equal to  $1.28 H_b$ .

Equations (4-34) and (4-37) are valid only if there is a single wave train with one period and one height. However, most ocean wave conditions are characterized by a variety of heights with a distribution usually described by a Rayleigh distribution (see Ch. 3, Sec. II). For a Rayleigh distribution, the correct height to use in equation (4-37) or in the formulas shown in Table 4-9 is the root-mean-square height. However, most wave data are available as significant heights, and coastal engineers are used to dealing with significant heights, therefore the significant wave height is substituted into equation (4-37) to produce

$$P_{\ell s} = \frac{\rho g}{16} H_{sb}^2 C_{gb} \sin 2\alpha_b \quad (4-39)$$

The value of  $P_{\ell s}$  computed using significant wave height is approximately twice the value  $P_{\ell b}$  of the exact energy flux for sinusoidal wave heights with a Rayleigh distribution. Since this means that  $P_{\ell s}$  is proportional to energy flux and not equal to it,  $P_{\ell s}$  is referred to as the *longshore energy flux factor* in the following sections.

Tables 4-9 and 4-10 present variations of  $P_{\ell}$  and  $P_{\ell s}$ , depending on the type of wave data available. Table 4-11 describes some of the assumptions used for Table 4-10. Galvin and Schweppe (1980) derive these equations in detail. Possible changes in wave height due to energy losses as waves travel over the continental shelf are not considered in these equations. Such changes may reduce the value of  $P_{\ell s}$  when deepwater wave height statistics are used as a starting point for computing  $P_{\ell s}$  (Walton, 1972; Bretschneider and Reid, 1954; Bretschneider, 1954; Grosskopf, 1980).

The term in parentheses for equation (4-41) in Table 4-9 is identical with the longshore force of Longuet-Higgins (1970a). This longshore force also correlates well with the longshore transport rate (Bruno and Gable, 1976; Vitale, 1981).

Table 4-9. Longshore energy flux,  $P_{ls}$ , for a single periodic wave in any specified depth (four equivalent expressions from small-amplitude theory).

Equation	$P_{ls}$	Data Required (metric units)
4-40	$2C_g (1/4 \bar{E} \sin 2\alpha)$	$d, T, H, \alpha_o$
4-41	$C (1/4 \bar{E}_o \sin 2\alpha_o)$	$d, T, H_o, \alpha_o$
4-42	$K_R^2 C_o (1/4 \bar{E}_o \sin 2\alpha)$	$T, H_o, \alpha_o, \alpha$
4-43	$(2C) (K_R^2 C_o)^{-1} C_g (1/4 \bar{E} \sin 2\alpha_o)$	$d, T, H, \alpha_o, \alpha$

No subscript indicates a variable at the specified depth where small-amplitude theory is valid.

Table 4-10. Approximate formulas for computing longshore energy flux factor,  $P_{ls}$ , entering the surf zone<sup>1,2</sup>

Equation	$P_{ls}$ (energy/time-distance)	Data Required (any consistent units)
4-44	$0.0884 \rho g^{3/2} H_{sb}^{5/2} \sin 2\alpha_b$	$H_{sb}, \alpha_b$
4-45	$0.05 \rho g^{3/2} H_{so}^{5/2} (\cos \alpha_o)^{1/4} \sin 2\alpha_o$	$H_{so}, \alpha_o$
4-46	$0.00996 \rho g^2 T H_{so}^2 \sin \alpha_b \cos \alpha_o$	$T, H_{so}, \alpha_o, \alpha_b$
4-47	$1.572 \rho g (H_{sb}^3/T) \sin \alpha_o$	$T, H_{sb}, \alpha_o$

<sup>1</sup> See Table 4-9 for equivalent small-amplitude equations and Table 4-11 for assumptions used in deriving  $P_{ls}$  from  $P_l$ .

<sup>2</sup> Subscript  $b$  = breaker value,  $o$  = deepwater value, and  $s$  = significant wave height.

$C_g$  = group velocity (see assumption 1b, Table 4-11)

$C_o$  = deepwater wave velocity

$d$  = water depth

$H$  = significant wave height

$T$  = wave period

$\alpha$  = angle between wave crest and shoreline

$K_R$  = refraction coefficient  $\sqrt{\frac{\cos \alpha_o}{\cos \alpha}}$

Table 4-11. Assumptions for  $P_{\ell s}$  formulas in Table 4-10<sup>1</sup>.

1. Formula 1 - Equation (4-44)

- a. Energy density at breaking is given by linear theory

$$\bar{E} = (\rho g H_b^2)/8$$

- b. Group velocity equals wave speed at breaking, and breaking speed is given by solitary wave theory according to the approximation (Galvin, 1967, eq. 11)

$$C_g = C \approx (2gH_b)^{1/2}$$

- c.  $\alpha$  can be replaced by  $\alpha_b$ .

2. Formula 2 - Equation (4-45)

- a. Same as 1b above.

- b.  $H_b$  is related to  $H_o$  by refraction and shoaling coefficients, where the coefficients are evaluated at the breaker position

$$H_b = K_R K_s H_o$$

- c. Refraction coefficient  $K_R$  is given by small-amplitude theory; shoaling coefficient  $K_s$  is assumed constant, so that

$$d. (H_b)^{1/2} = 1.14 (\cos \alpha_o)^{1/4} H_o^{1/2}$$

$$\text{if } (\cos \alpha_b)^{1/4} = 1.0$$

$$\text{and } (K_s)^{1/2} = 1.14$$

3. Formula 3 - Equation (4-46)

- a. Refraction coefficient at breaking is given by small-amplitude theory.

4. Formula 4 - Equation (4-47)

- a. Same as 1a above.

- b. Same as 1b above.

- c. Same as 3a above.

- d.  $\cos \alpha_b = 1.0$ .

<sup>1</sup> Small-amplitude theory is assumed valid in deep water. Nearshore contours are assumed to be straight and parallel to the shoreline.

The energy flux of computing longshore transport rate is based on the empirical relationship between the longshore component of wave energy flux entering the surf zone and the immersed weight of sand moved. Both have units of force per unit time, thus

$$I_{\ell} = K P_{\ell S} \quad (4-48)$$

where  $I_{\ell}$  is the immersed weight transport rate (force/time),  $K$  a dimensionless coefficient, and  $P_{\ell S}$  the longshore energy flux factor (force/time).

$Q$  can be substituted for  $I_{\ell}$  by using equation (4-33) to produce

$$Q = \frac{K}{(\rho_s - \rho) g a'} P_{\ell S} \quad (4-49)$$

Field measurements of  $Q$  and  $P_{\ell S}$  are plotted in Figure 4-37. The data were obtained in the following manner. For Watts (1953b) and Caldwell (1956), the original references give energy flux factors based on significant height, and these original data (after unit conversion) are plotted as  $P_{\ell S}$  in Figure 4-37. The field data of Komar (1969) are given in terms of root-mean-square energy flux. This energy flux is multiplied by a factor of 2 (Das, 1972), converted to consistent units, and then plotted in Figure 4-37.

A similar conversion was done for the Bruno et al. (1981) data. The equation of the line drawn through the data points in Figure 4-37 defines the design relation:

$$Q \left( \frac{\text{m}^3}{\text{yr}} \right) = 1290 \left( \frac{\text{m}^3}{\text{N-yr}} \right) P_{\ell S} \left( \frac{\text{J}}{\text{m-s}} \right) \quad (4-50a)$$

$$Q \left( \frac{\text{yd}^3}{\text{yr}} \right) = 7500 \left( \frac{\text{yd}^3}{\text{lb-yr}} \right) P_{\ell S} \left( \frac{\text{ft-lb}}{\text{ft-s}} \right) \quad (4-50b)$$

where the dimensions of the factors are given in brackets. Note that the constants (1290 and 7500) are dimensional. Using these dimensional constants and the values in Table 4-9,  $K$  in equation (4-49) is found to be 0.39. Therefore equation (4-48) becomes

$$I_{\ell} = 0.39 P_{\ell S}$$

where 0.39 is dimensionless. This equation is essentially the same as Komar and Inman's (1970) design equation  $I_{\ell} = 0.77 P_{\ell}$ , with the factor of approximately 2 difference due to Komar and Inman's use of  $H_{rms}$  in the energy flux term instead of  $H_s$  as used herein.

Judgment is required in applying equation (4-49). Although the data follow a definite trend, the scatter is obvious, even on the log-log plot. The dotted lines on Figure 4-37 are drawn at  $Q \pm 50$  percent and envelope most of the data points. Therefore, the accuracy of  $Q$  found using the energy flux method can be estimated to be  $\pm 50$  percent.

As an aid to computation, Figures 4-38 and 4-39 gives lines of constant  $Q$  based on equation (4-49) and equations (4-43) and (4-44) for  $P_{\ell S}$  given in Table 4-10. To use Figures 4-38 and 4-39 to obtain the longshore transport

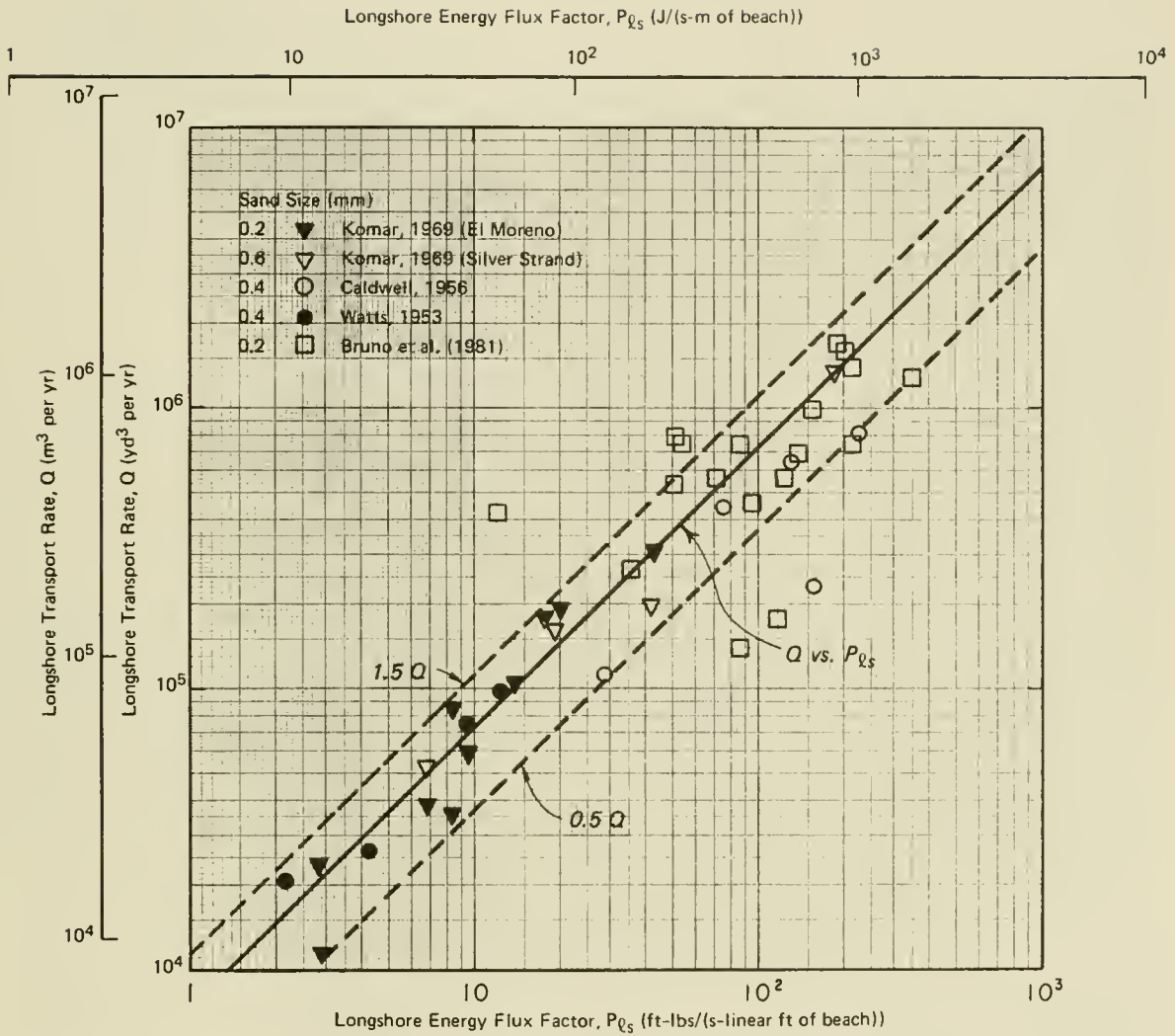


Figure 4-37. Design curve for longshore transport rate versus energy flux factor. (Only field data are included.)

rate, only the  $(H_{sb}, \alpha_b)$  data and Figure 4-38 or the  $(H_{s0}, \alpha_0)$  data and Figure 4-39 are needed. If the shoaling coefficient is significantly different from 1.3, multiply the  $Q$  obtained from Figure 4-39 by the factor  $0.88 \sqrt{K_s}$  (see Table 4-11, assumption 2d).

Figure 4-39 applies accurately only if  $\alpha_0$  is a point value. If  $\alpha_0$  is a range of values, for example a 45-degree sector implied by the direction northeast, then the transport evaluated from Figure 4-39 using a single value of  $\alpha_0$  for northeast may be 12 percent higher than the value obtained by averaging over the 45-degree sector implied by northeast. The most accurate approach is given in the example problem of Section V,3,c.

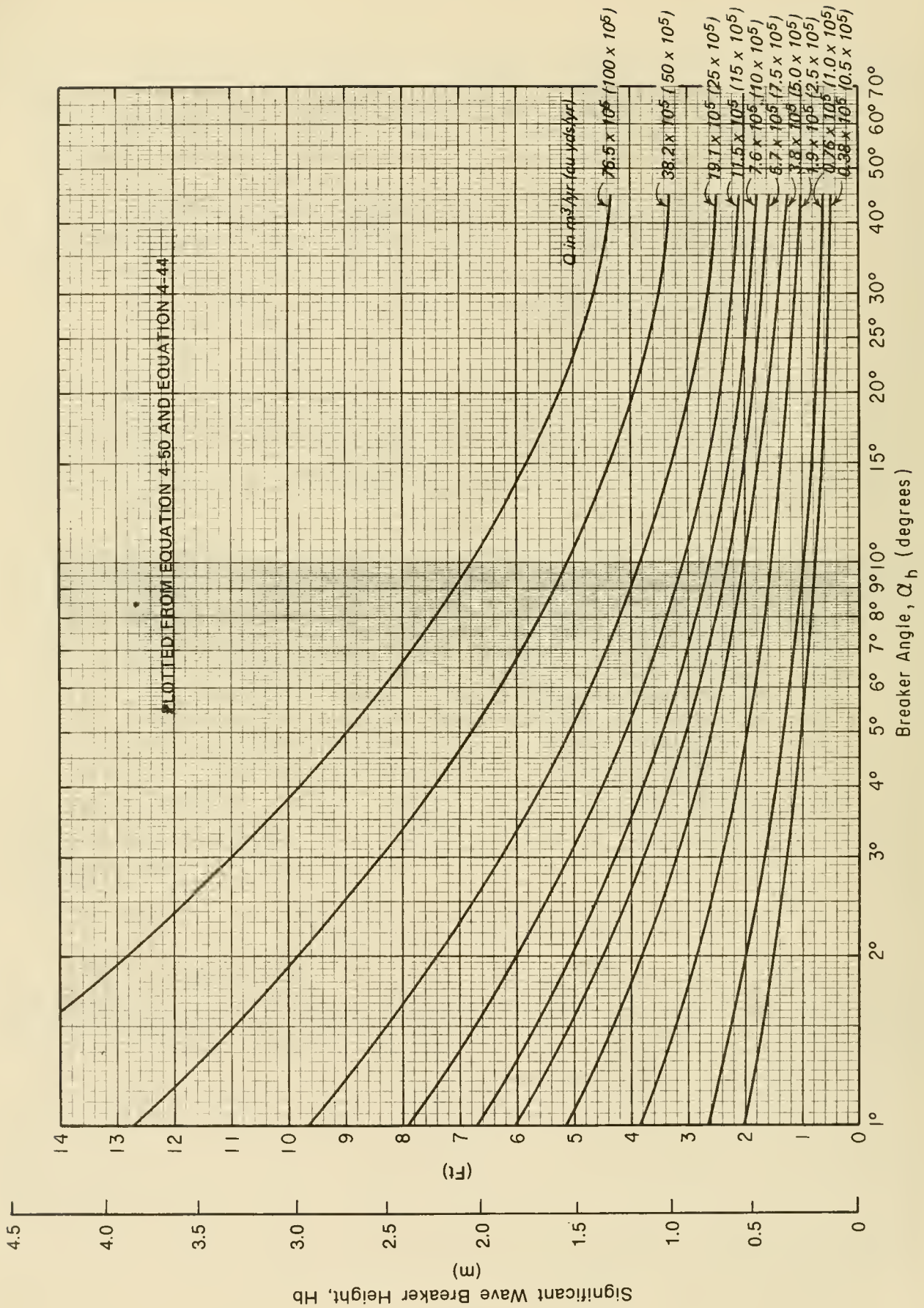


Figure 4-38. Longshore transport rate as a function of breaker height and breaker angle.

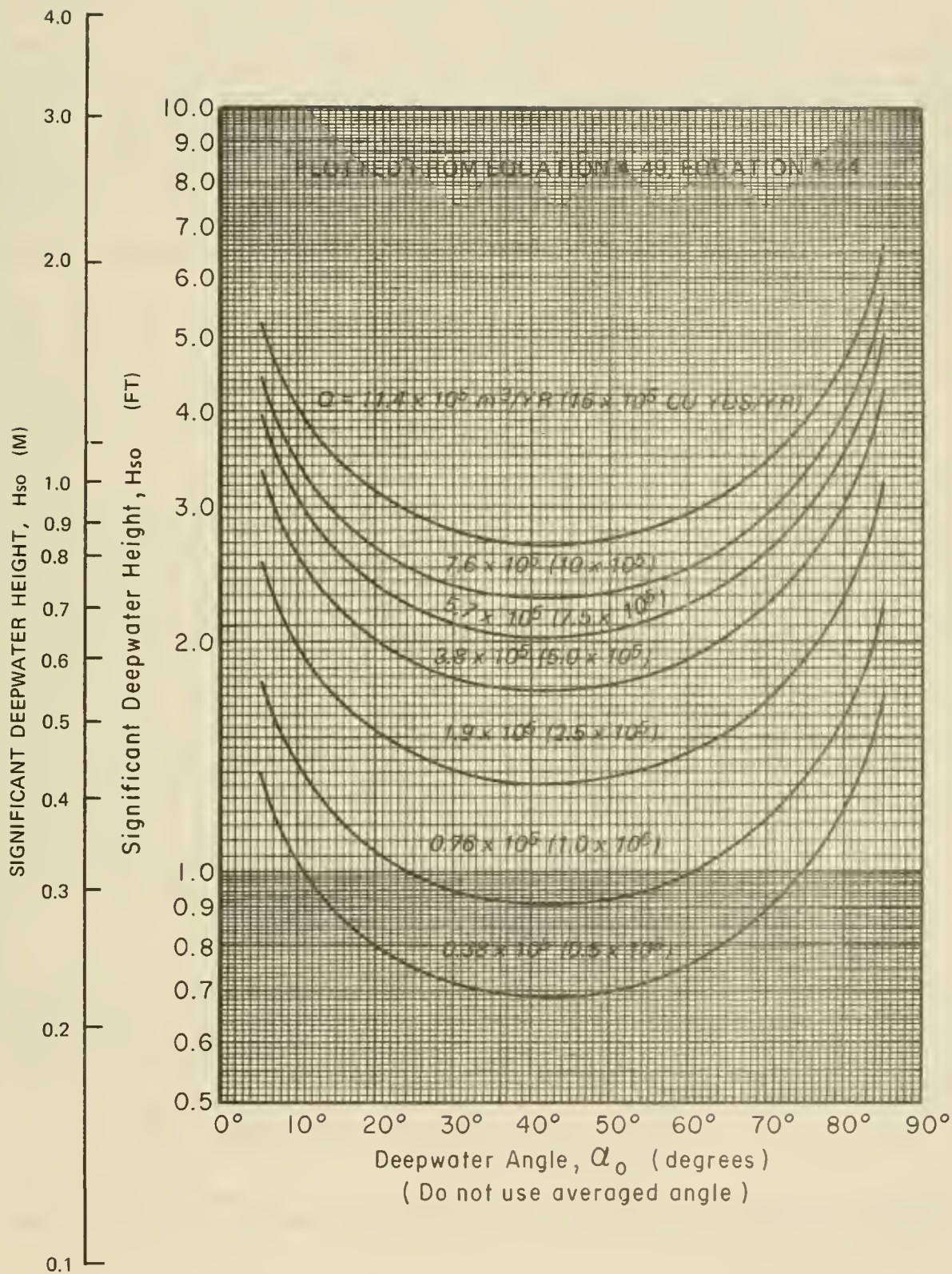


Figure 4-39. Longshore transport rate as a function of deepwater height and deepwater angle.

c. Calculation of  $P_{\ell s}$  Using LEO Data. An alternative method of calculating the energy flux factor  $P_{\ell s}$  is to use data from the CERC Littoral Environmental Observation (LEO) field data collection program. LEO data include visual observations of nearshore wave heights and periods and longshore current velocities. The program is discussed by Berg (1968), Szuwalski (1970), Bruno and Hiipakka (1974), Balsillie (1975), and Schneider (1981). Use of LEO data permits replacing the hard-to-measure wave angle term in equation (4-40) with LEO longshore current measurements. The current measurement is made by timing the travel of a dye patch in the surf zone.

The equations and example problem which follow are taken from Walton (1980), which presents derivations and additional references.

The equation giving the longshore energy flux factor with LEO data variables is

$$P_{\ell s} = \frac{\rho g H_{sb} W V_{LEO} C_f}{\left(\frac{5\pi}{2}\right) \left(\frac{V}{V_o}\right)_{LH}} \quad (4-51)$$

where

$$\left(\frac{V}{V_o}\right)_{LH} = 0.2 \left(\frac{X}{W}\right) - 0.714 \left(\frac{X}{W}\right) \ln \left(\frac{X}{W}\right) \quad (4-52)$$

and

- $\rho$  = fluid density
- $g$  = acceleration of gravity
- $H_{sb}$  = breaking wave height
- $W$  = width of surf zone
- $V_{LEO}$  = average longshore current due to breaking waves
- $C_f$  = friction factor (assume 0.01)
- $X$  = distance to dye patch from shoreline

$(V/V_o)_{LH}$  is the dimensionless longshore current based on Longuet-Higgins (1970a). It is assumed that the LEO breaking wave height is a good approximation of the significant breaking wave height and that the mixing parameter in Longuet-Higgins' theory is 0.4.

\*\*\*\*\* EXAMPLE PROBLEM 4 \*\*\*\*\*

GIVEN: A LEO observation with the following estimated values of wave height, longshore current velocity, width of surf zone, and distance of dye patch from the shoreline

$H_{sb} = 1 \text{ meter (3.28 feet)}$   
 $V_{LEO} = 0.20 \text{ meter per second (0.66 feet/second)}$   
 $W = 50 \text{ meters (164 feet)}$   
 $X = 18 \text{ meters (59.1 feet)}$

FIND: Longshore energy flux factor  $P_{\ell s}$  .

SOLUTION:

(a) Using equation (4-52), calculate  $V/V_{oLH}$  .

$$\left(\frac{V}{V_o}\right)_{LH} = 0.2 \left(\frac{18}{50}\right) - 0.714 \left(\frac{18}{50}\right) \ln\left(\frac{18}{50}\right) = 0.33$$

(b) Now, using equation (4-51), calculate  $P_{\ell s}$  .

$$P_{\ell s} = \frac{(9.8) 1025 (1) (50) (0.20) (0.01)}{\left(\frac{5\pi}{2}\right)(0.33)} = \begin{matrix} 387.6 \text{ newtons per second} \\ (87.13 \text{ pounds per second}) \end{matrix}$$

(c) The value of  $P_{\ell s}$  corresponds to a sediment transport rate of 499,000 cubic meters per year (653,000 cubic yards per year) using equation (4-50).

(d) Annual average sediment transport rates for any field site would be estimated from LEO with a  $P_{\ell s}$  value obtained by averaging the  $P_{\ell s}$  values computed for each observation by the above method.

\*\*\*\*\*

d. Energy Flux Example. Assume that an estimate of the longshore transport rate is required for a locality on the north-south coastline along the west side of an inland sea. The locality is in an area where stronger winds blow out of the northwest and north, resulting in a deepwater distribution of height and direction as listed in Table 4-12. Assume the statistics were obtained from visual observations collected over a 2-year interval at a point 3 kilometers offshore by seamen aboard vessels entering and leaving a port in the vicinity. This type of problem, based on Summary of Synoptic Meteorological Observations (SSMO) wave statistics, is discussed in detail by Walton (1972) and Walton and Dean (1973). Shipboard data are subject to uncertainty in their applicability to littoral transport, but often they are the only data available. It is assumed that shipboard visual observations are equivalent to significant heights (Cartwright, 1972; Walton, 1972).

This problem could be solved using Figure 4-39, but for illustration, and because of a slightly higher degree of accuracy possible from the direction data given, the problem is illustrated here in detail.

In this example, the available data are the joint frequency distribution of  $H_o$  and  $\alpha_o$  . For each combination of  $\alpha_o$  and  $H_o$  , the corresponding  $Q_{\alpha_o, H_o}$  is calculated for Table 4-13 in the following manner. The basic equation is a form of equation (4-50) written

$$Q_{\alpha_o, H_o} = \left(f_{AP}^{\ell s}\right) \alpha_o, H_o \tag{4-53}$$

Table 4-12. Deepwater wave heights, in percent by direction, off east-facing coast of inland sea.

Compass Direction $\alpha_0$	N 90°	NE 45°	E 0°	SE -45°	S -90°	Other <sup>1</sup>
$H_0$ (m)						
0.5	9	10	6	5	5	
1.0	5	5	2	2	2	
1.5	4	3	1	1	1	
2.0	2	1				
2.5	1					
4.0	1					
Total	22	19	9	8	8	34

<sup>1</sup> Calm conditions, or waves from SW, W, or NW.

Table 4-13. Computed longshore transport for east-facing coast of inland sea.

$H_0$ (m)	$Q_{\alpha_0}, H_0$ in $m^3/yr$ from equation (4-54)				
	N <sup>1</sup>	NE	E	SE	S <sup>1</sup>
0.5	$4.22 \times 10^3$ <sup>2</sup>	$29.51 \times 10^3$	$\pm 3.98 \times 10^3$	$-14.76 \times 10^3$	$-2.33 \times 10^3$
1.0	$13.2 \times 10^3$	$83.46 \times 10^3$	$\pm 7.52 \times 10^3$	$-33.39 \times 10^3$	$-5.29 \times 10^3$
1.5	$29.2 \times 10^3$	$137.40 \times 10^3$	$\pm 10.38 \times 10^3$	$-46.00 \times 10^3$	$-7.29 \times 10^3$
2.0	$29.9 \times 10^3$	$94.44 \times 10^3$			
2.5	$26.2 \times 10^3$				
4.0	$84.69 \times 10^3$				
Total	$187.41 \times 10^3$	$344.81 \times 10^3$	$(\pm 21.88 \times 10^3)$ $43.76 \times 10^3$	$-94.15 \times 10^3$	$-14.91 \times 10^3$

$$Q_{rt} = (187.41 + 344.81 + 21.88) \times 10^3 = 553 \times 10^3 \text{ or } 553,000 \text{ m}^3/\text{yr.}^3$$

$$Q_{lt} = (21.88 + 94.15 + 14.91) \times 10^3 = 130.3 \times 10^3 \text{ or } 130,000 \text{ m}^3/\text{yr.}^3$$

$$Q_n = Q_{rt} - Q_{Pt} = 553 \times 10^3 - 130.3 \times 10^3 = 423 \times 10^3 \text{ or } 423,000 \text{ m}^3/\text{yr.}^3$$

$$Q_g = Q_{rt} + Q_{Pt} = 553 \times 10^3 + 130.3 \times 10^3 = 683 \times 10^3 \text{ or } 683,000 \text{ m}^3/\text{yr.}^3$$

1 Coast runs N-S so frequencies of waves from N and S are halved.

2 Calculation of this number is shown in detail in the text.

3 These symbols are defined in Section V,3,a.

where  $f$  is the decimal frequency, which is the percent frequency in Table 4-12, divided by 100. The constant  $A$  is of the type used in equation (4-50).

Since the available data are  $\alpha_o$  and  $H_o$ , the appropriate equation for  $P_{\alpha_s}$  is given in Table 4-10. If  $A = 1290^3$ , as in equation (4-50a), and equation (4-45) in Table 4-10 are used,

$$Q_{\alpha_o, H_o} = 2.03 \times 10^6 f H_o^{5/2} F(\alpha_o) \quad (4-54)$$

where

$$F(\alpha_o) = \left[ (\cos \alpha_o)^{1/4} \sin 2\alpha_o \right] \quad (4-55)$$

This direction term,  $F(\alpha_o)$ , requires careful consideration. A compass point direction for the given data (Table 4-12) represents a 45-degree sector of wave directions. If  $F(\alpha_o)$  is evaluated at  $\alpha_o = 45$  degrees (NE or SE in the example problem), it will have a value 12 percent higher than the average value for  $F(\alpha_o)$  over a 45-degree sector bisected by the NE or SE directions. Thus, if the data warrant a higher degree of accuracy, equation (4-55) should be averaged by integrating over the sector of directions involved.

If  $F(\alpha_o)$  as evaluated at  $\alpha = 0$  (waves from the east in the example problem), then  $F(\alpha_o) = 0$ . Actually,  $\alpha_o = 0$  degrees is only the center of a 45-degree sector which can be expected to produce transport in both directions. Therefore,  $F(\alpha_o)$  should be averaged over 0 to 22.5 degrees and 0 to -22.5 degrees, giving  $F(\alpha_o) = \pm 0.370$  rather than 0. The + or - sign comes out of the  $\sin 2\alpha_o$  term in  $F(\alpha_o)$  (eq. 4-55), which is defined such that transport to the right is positive, as implied by equation (4-32).

A further complication in direction data is that waves from the north and south sectors include waves traveling in the offshore direction. It is assumed that, for such sectors, frequency must be multiplied by the fraction of the sector including landward-traveling waves. For example, the frequencies from N and S in Table 4-12 are multiplied by 0.5 to obtain the transport values listed in Table 4-13.

To illustrate how values of  $Q_{\alpha_o, H_o}$  listed in Table 4-13 were calculated, the value of  $Q_{\alpha_o, H_o}$  is here calculated for  $H_o = 0.5$  and the north direction, the top value in the first column on Table 4-13. The direction term,  $F(\alpha_o)$ , is averaged over the sector from  $\alpha = 67.5$  degrees to  $\alpha = 90$  degrees; i.e., from NNE to N in the example. The average value of  $F(\alpha_o)$  is found to be 0.261.  $H_o$  to the 5/2 power is 0.177 for this case. The frequency given in Table 4-12 for  $H_o = 0.5$  and direction = north (NW to NE) is 9 percent, or in decimal terms, 0.09. This is multiplied by 0.5 to obtain the part of shoreward-directed waves from the north sector (i.e., N to NE), resulting in  $f = 0.09 (0.5) = 0.045$ . Putting all these values into equation (4-54) gives

$$Q_{N,1} = 2.03 \times 10^6 (0.045) (0.5)^{5/2} (0.261) = 4220 \text{ cubic meters per year} \quad (\text{see Table 4-13})$$

Table 4-13 indicates the importance of rare high waves in determining the longshore transport rate. In the example, shoreward-moving 4.0-meter waves occur only 0.5 percent of the time, but they account for 12 percent of the gross longshore transport rate (see Table 4-13).

Any calculation of longshore transport rate is an estimate of *potential* longshore transport rate. If sand on the beach is limited in quantity, then calculated rates may indicate more sand transport than there is sand available. Similarly, if sand is abundant but the shore is covered with ice for 2 months of the year, then calculated transport rates must be adjusted accordingly.

The procedure used in this example problem is approximate and limited by the data available. Equation (4-54), and the other approximations listed in Table 4-13, can be refined if better data are available. An extensive discussion of this type of calculations is given by Walton (1972).

Although this example is based on shipboard visual observations of the SSMO type, the same approach can be followed with deepwater data from other sources, if the joint distribution of height and direction is known. At this level of approximation, the wave period has little effect on the calculation, and the need for it is bypassed as long as the shoaling coefficient (or breaker height index) reasonably satisfies the relation  $(K)^{1/2} = 1.14$  (see assumption 2d, Table 4-11). For waves on sandy coasts,<sup>8</sup> this relation is reasonably satisfied (e.g., Bigelow and Edmondson, 1947, Table 33; Goda, 1970, Fig. 7).

e. Empirical Prediction of Gross Longshore Transport Rate (Method 4). Longshore transport rate depends partly on breaker height, since as breaker height increases, more energy is delivered to the surf zone. At the same time, as breaker height increases, breaker position moves offshore widening the surf zone and increasing the cross-section area through which sediment moves.

Galvin (1972b) showed that when field values of longshore transport rate are plotted against mean annual breaker height from the same locality, a curve

$$Q = 1.646 \times 10^6 H_b^2 \quad (4-56a)$$

$$Q = 2 \times 10^5 H_b^2 \quad (4-56b)$$

forms an envelope above almost all known pairs of  $(Q, H_b)$ , as shown in Figure 4-40. In equation (4-56a),  $Q$  is given in cubic meters per year and  $H_b$  is in meters; in equation (4-56b)  $Q$  is given in units of cubic yards per year; and  $H_b$  in feet.

Figure 4-40 includes all known  $(Q, H_b)$  pairs for which both  $Q$  and  $H_b$  are based on at least 1 year of data and for which  $Q$  is considered to be the gross longshore transport rate,  $Q_g$ , defined by equation (4-31). Since all other known  $(Q, H_b)$  pairs plot below the line given by equation (4-56), the line provides an upper limit on the estimate of longshore transport rate. From the defining equations for  $Q_g$  and  $Q_n$ , any line that forms an upper limit to longshore transport rate must be the gross transport rate, since the

quantities  $Q_{rt}$ ,  $Q_{lt}$ , and  $Q_n$ , as defined in Section V,3,a are always less than or equal to  $Q_g$ .

In equation (4-56) wave height is the only independent variable, and the physical explanation assumes that waves are the predominant cause of transport (Galvin, 1972b). Therefore, where tide-induced currents or other processes contribute significantly to longshore transport, equation (4-56) would not be the appropriate approximation. The corrections due to currents may either add or subtract from the estimate of equation (4-56), depending on whether currents act with or against prevailing wind-induced transport.

f. Method 4 Example (Empirical Prediction of Gross Longshore Transport Rate. Near the site of the problem outlined in Section V,3,d, it is desired to build a small craft harbor. The plans call for an unprotected harbor entrance, and it is required to estimate costs of maintenance dredging in the harbor entrance. The gross transport rate is a first estimate of the maintenance dredging required, since transport from either direction could be trapped in the dredged channel. Wave height statistics were obtained from a wave gage in 3.66 meters (12 feet) of water at the end of a pier (see columns (1) and (2) of Table 4-14). Heights are available as empirically determined significant heights (Thompson and Harris, 1972). (To facilitate comparison, the frequencies are identical to the deepwater frequencies of onshore waves in Table 4-12 for the problem of Section V,3,d. That is, the frequency associated with each  $H_g$  in Table 4-14 is the sum of the frequencies of the shoreward  $H_o$  on the corresponding line of Table 4-12.)

The breaker height  $H_b$  in the empirical equation (4-56) is related to the gage height  $H_g$  by a shoaling coefficient ratio  $(K_s)_b / (K_s)_g$ , where  $(K_s)_b$  is the shoaling coefficient (eq. 2-44), evaluated at the breaker position and  $(K_s)_g$  is the shoaling coefficient evaluated at the wave gage:

$$H_b = H_g \frac{(K_s)_b}{(K_s)_g} \quad (4-57)$$

$K_s$  can be evaluated from small-amplitude theory if wave-period information is available from the wave gage statistics. For simplicity, assume shoaling coefficient ratios as listed in column 4 of Table 4-14. Such shoaling coefficient ratios are consistent with the shoaling coefficient of  $K_s = 1.3$  (between deepwater and breaker conditions) assumed in deriving  $P_{ls}$  (Table 4-10), and with the fact that waves on the inland sea are usually steep, locally generated waves.

Column 5 of the table is the product  $fH_g (K_s)_b / (K_s)_g$ . The sum (0.531 meter) of entries in this column is assumed equivalent to the average of visually observed breaker heights. Substituting this value in equation (4-54), the estimated gross longshore transport rate is 464,000 cubic meters per year. It is instructive to compare this value with the value of 683,000 cubic meters per year obtained from the deepwater example (see Table 4-13). The two estimates are not expected to be the same, since the same wave statistics have been used for deep water in the first problem and for a 3.66-meter depth in the second problem. However, the numerical values do not differ greatly. It should be noted that the empirical estimate just obtained is

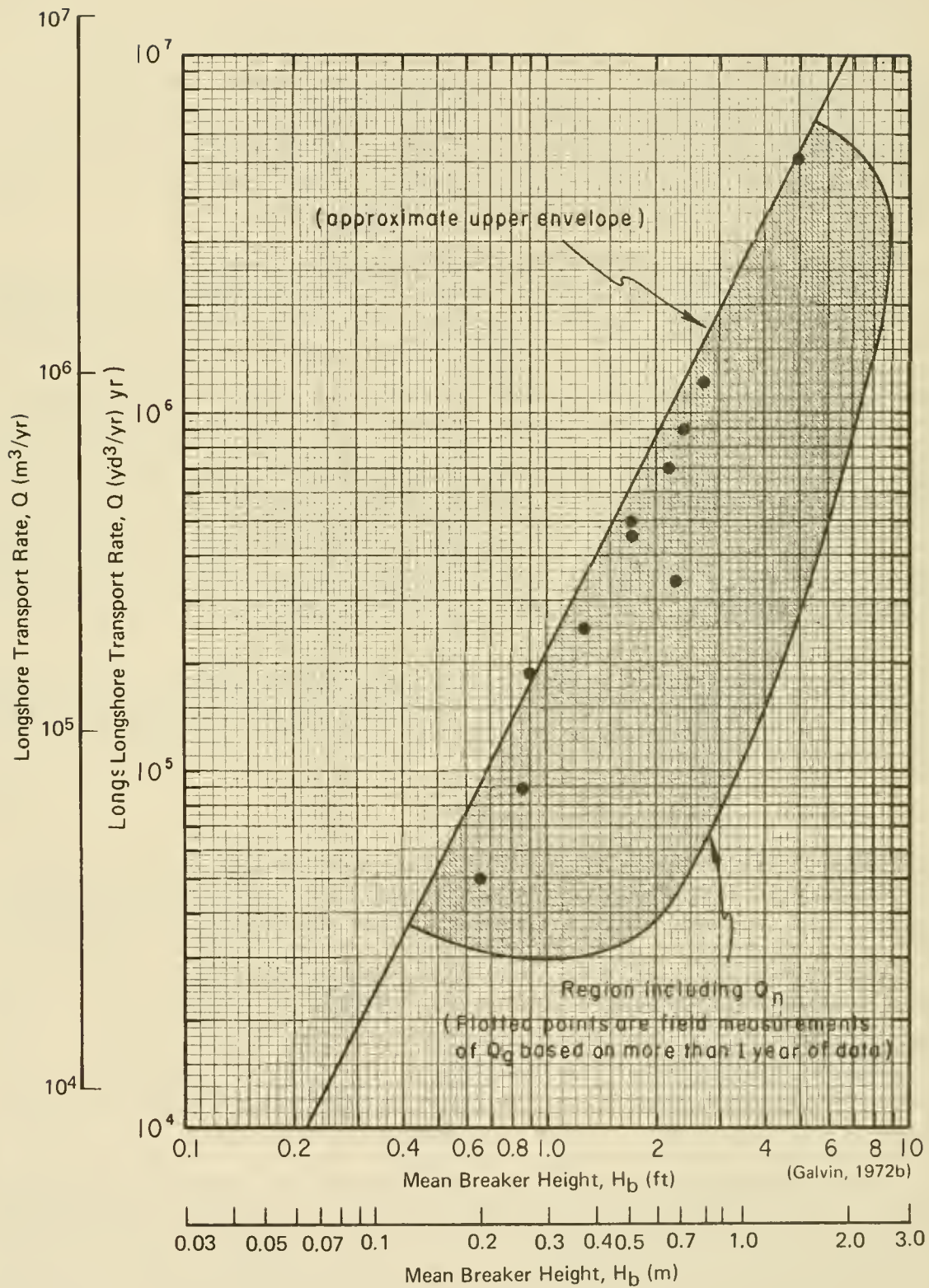


Figure 4-40. Upper limit on longshore transport rates.

Table 4-14. Example estimate of gross longshore transport rate for shore of inland sea.

(1) $H_g$ meters (ft)	(2) f	(3) $fH_g$ meters (ft)	(4) $(K_s)_b / (K_s)_g$	(5) (3) x (4) meters (ft)
0.5 (1)	0.28	0.14 (0.28)	1.2	0.168 (0.336)
1.0 (2)	0.125	0.125 (0.25)	1.2	0.150 (0.300)
1.5 (3)	0.075	0.113 (0.225)	1.2	0.135 (0.270)
2.0 (4)	0.02	0.04 (0.08)	1.1	0.044 (0.088)
2.5 (5)	0.005	0.013 (0.025)	1.1	0.014 (0.028)
4.0 (8)	0.005	0.02 (0.04)	1.0	0.020 (0.040)
$H_b = 0.531 (1.062)$				

(1)  $H_g$  = significant height reduced from gage records, assumed to correspond to the height obtained by visual observers.

(2) f = decimal frequency of wave heights.

(4)  $\frac{(K_s)_b}{(K_s)_g}$  = assumed shoaling coefficient ratio.

(5)  $H_b = \Sigma \frac{(K_s)_b}{(K_s)_g} fH_g = 0.531 \text{ meter (1.74 feet)}$

$Q = 1.646 \times 10^6 H_b^2 = 4.64 \times 10^5$  cubic meters per year from equation (4-56a),  
or

$Q = 2 \times 10^5 H_b^2 = 6.05 \times 10^5$  cubic yards per year from equation (4-56b).

Note that shoreward-moving waves exist only 51 percent of the time.

completely independent of the longshore energy flux estimate of the deepwater example.

In this example, wave gage statistics have been used for illustrative purposes. However, visual observations of breakers, such as those listed in Table 4-4, would be even more appropriate since equation (4-56) has been "calibrated" for such observations. On the other hand, hindcast statistics would be less satisfactory than gage statistics, due to the uncertain effect of nearshore topography on the transformation of deepwater statistics to breaker conditions.

## VI. ROLE OF FOREDUNES IN SHORE PROCESSES

### 1. Background.

The cross section of a barrier island shaped solely by marine hydraulic forces has three distinct subaerial features: beach, crest of island, and deflation plain (see Fig. 4-41). The dimensions and shape of the beach change in response to varying wave and tidal conditions (Section V,2,d), but usually the beach face slopes upward to the island crest--the highest point on the barrier island cross section. From the island crest, the back of the island slopes gently across the deflation plain to the edge of the lagoon separating the barrier island from the mainland. These three features are usually present on duneless barrier island cross sections; however, their dimensions may vary.

Island crest elevation is determined by the nature of the sand forming the beach and by the waves and water levels of the ocean. The beach and waves interact to determine the elevation of the limit of wave runup--the primary factor in determining island crest elevation. Normally the island crest elevation is almost constant over long sections of beach. However, duneless barrier island crest elevations vary with geographical area. For example, the crest elevation typical of Core Banks, North Carolina, is about +2 meters (+6 feet) MSL; +1.3 meters (+4 feet) MSL is typical for Padre Island, Texas; +3.3 meters (+11 feet) MSL is typical for Nauset Beach, Massachusetts.

Landward of the upper limit of wave uprush or berm crest are the backshore and the deflation plain. This area is shaped by the wind and, infrequently, by the flow of water down the plain when the island crest is overtopped by waves (e.g., Godfrey and Godfrey, 1972). Obstructions which trap wind-transported sand cause the formation of dunes in this area (see discussion in Ch. 6, Sand Dunes). Beachgrasses which trap wind-transported sand from the beach and the deflation plain are the major agent in creating and maintaining foredunes.

### 2. Role of Foredunes.

Foredunes, the line of dunes just behind a beach, have two primary functions in shore processes. First, they prevent overtopping of the island during some abnormal sea conditions. Second, they serve as a reservoir for beach sand.

a. Prevention of Overtopping. By preventing water from overtopping, foredunes prevent wave and water damage to installations landward of the dune. They also block the water transport of sand from the beach area to the back of the island and the flow (overwash) of overtopping sea water.

Large reductions in water overtopping are effected by small increases in foredune crest elevations. For example, the hypothetical 1.3-meter (4-foot) dune shown in Figure 4-41 raises the maximum island elevation about 1 meter (3 feet) to an elevation of 2 meters (6 feet). On this beach of Padre Island, Texas, the water levels and wave runup maintain an island crest elevation of +1.3 meters (+4 feet) MSL (about 0.6 meter (2 feet) above MHW). This would imply that the limit of wave runup in this area is 0.7 meter (2 feet) (the island crest elevation of +1.3 meters (+4 feet) minus the MHW of 0.6 meter (2

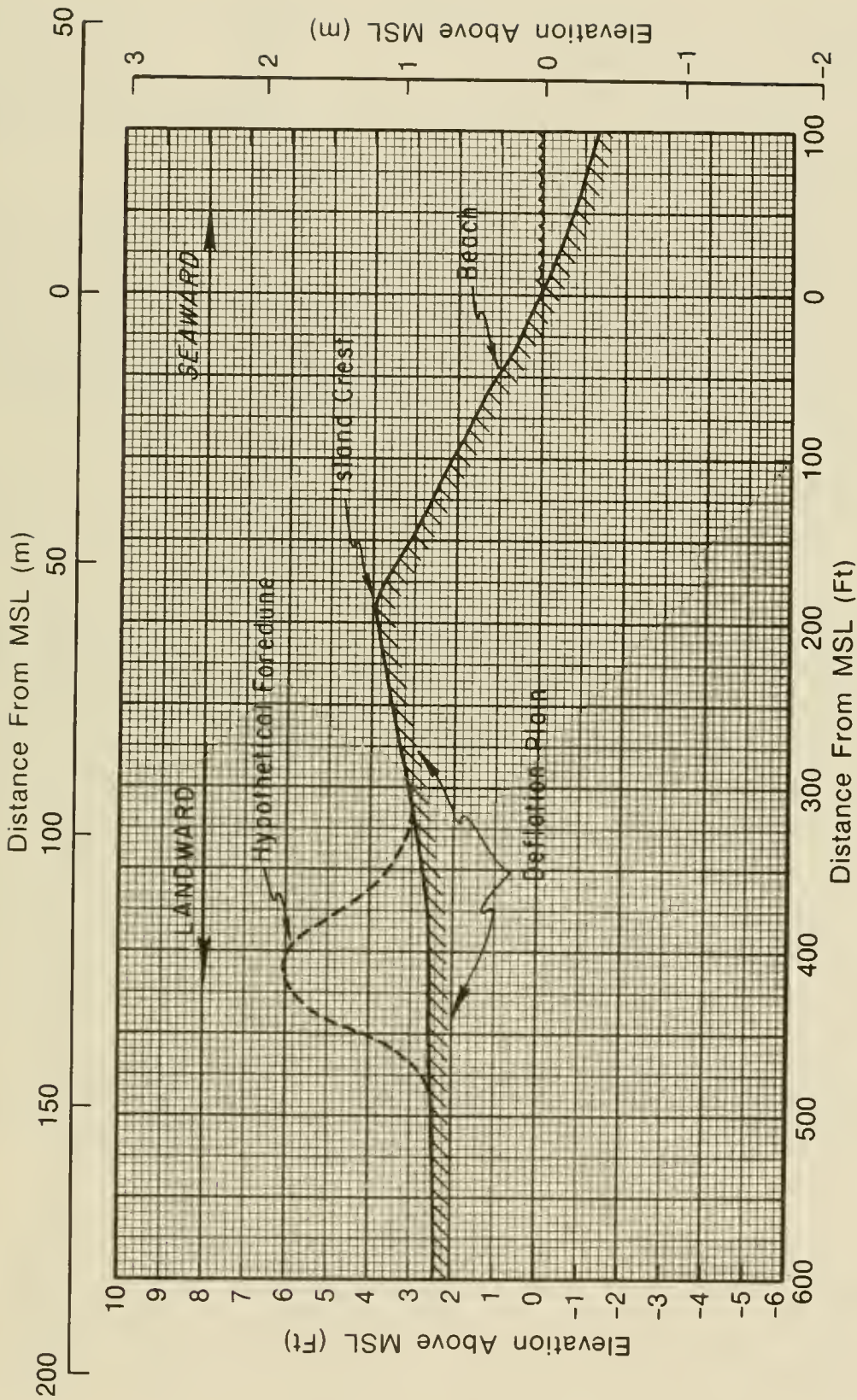


Figure 4-41. Typical barrier island profile shape (approximation of Padre Island, Texas).

feet). Assuming the wave runup to be the same for all water levels, the 1.3-meter (4-foot) dune would prevent significant overtopping at water levels up to 1.3 meters (4 feet) MSL (the 2-meter (6-foot) effective island height at the dune crest minus 0.7 meter (2 feet) for wave runup). This water level occurs on the average once each 5 years along this section of coast (see Figure 4-42). Thus, even a low dune, which can be built with vegetation and sand fences in this area in 1 year (Woodard et al. 1971) provides considerable protection against wave overtopping (see Ch. 5 and 6).

Foredunes or other continuous obstructions on barrier islands may cause unacceptable ponding from the land side of the island when the lagoon between the island and mainland is large enough to support the needed wind setup (see Ch. 3, Sec. VIII). There is little danger of flooding from this source if the lagoon is less than 8 kilometers (5 miles) wide. Where the lagoon is wider (especially 16 kilometers (10 miles) or greater) flooding from the lagoon side by wind setup should be investigated before large dune construction projects are undertaken.

b. Reservoir of Beach Sand. During storms, erosion of the beach occurs and the shoreline recedes. If the storm is severe, waves attack and erode the foredunes and supply sand to the beach; in later erosion stages, sand is supplied to the back of the island by overwash (Godfrey and Godfrey, 1972).

Volumes of sand eroded from beaches during storms have been estimated in recent beach investigations. Everts (1973) reported on two storms during February 1972 which affected Jones Beach, New York. The first storm eroded an average of 12,800 cubic meters per kilometer (27,000 cubic yards per mile) above mean sea level for the 14.5-kilometer (9-mile) study area; the second storm (2 weeks later) eroded an average of 16,600 cubic meters per kilometer (35,000 cubic yards per mile) above mean sea level at the same site. Losses at individual profiles ranged up to 57,000 cubic meters per kilometer (120,000 cubic yards per mile). Davis (1972) reported a beach erosion rate on Mustang Island, Texas, following Hurricane Fern (September 1971), of 30.8 cubic meters per meter (12.3 cubic yards per foot) of beach for a 460-meter (1,500-foot) stretch of beach (about 31,000 cubic meters per kilometer (65,000 cubic yards per mile) of beach). On Lake Michigan in July 1969, a storm eroded an average of 9 cubic meters per linear meter (3.6 cubic yards per foot) of beach (about 13,800 cubic meters per kilometer (29,000 cubic yards per mile) from a 240-meter (800-foot) beach near Stevensville, Michigan (Fox, 1970). Because much of the eroded sand is usually returned to the beach by wave action soon after the storm, these volumes are probably representative of temporary storm losses. Birkemeier (1979) studied beach changes during a December 1977 storm on Long Beach, New Jersey. He found that about one half of the material eroded from the beach during the storm returned to the beach within 2 days (see Sec. V,2,d).

Volumes equivalent to those eroded during storms have been trapped and stored in foredunes adjacent to the beach. Foredunes constructed along Padre Island, Texas (Dahl et al. 1975), and Ocracoke Island, North Carolina (Woodhouse, Seneca, and Browne, 1976), and Cape Cod, Massachusetts (Knutson, 1980), contain 120,000, 80,000, and 60,000 cubic meters of sand per kilometer (275,000, 185,000, and 135,000 cubic yards per mile) of beach, respectively. These volumes accumulated over periods of from 5 to 10 years. Sand volumes trapped during a 30-year period by European beachgrass at Clatsup Spit, Oregon

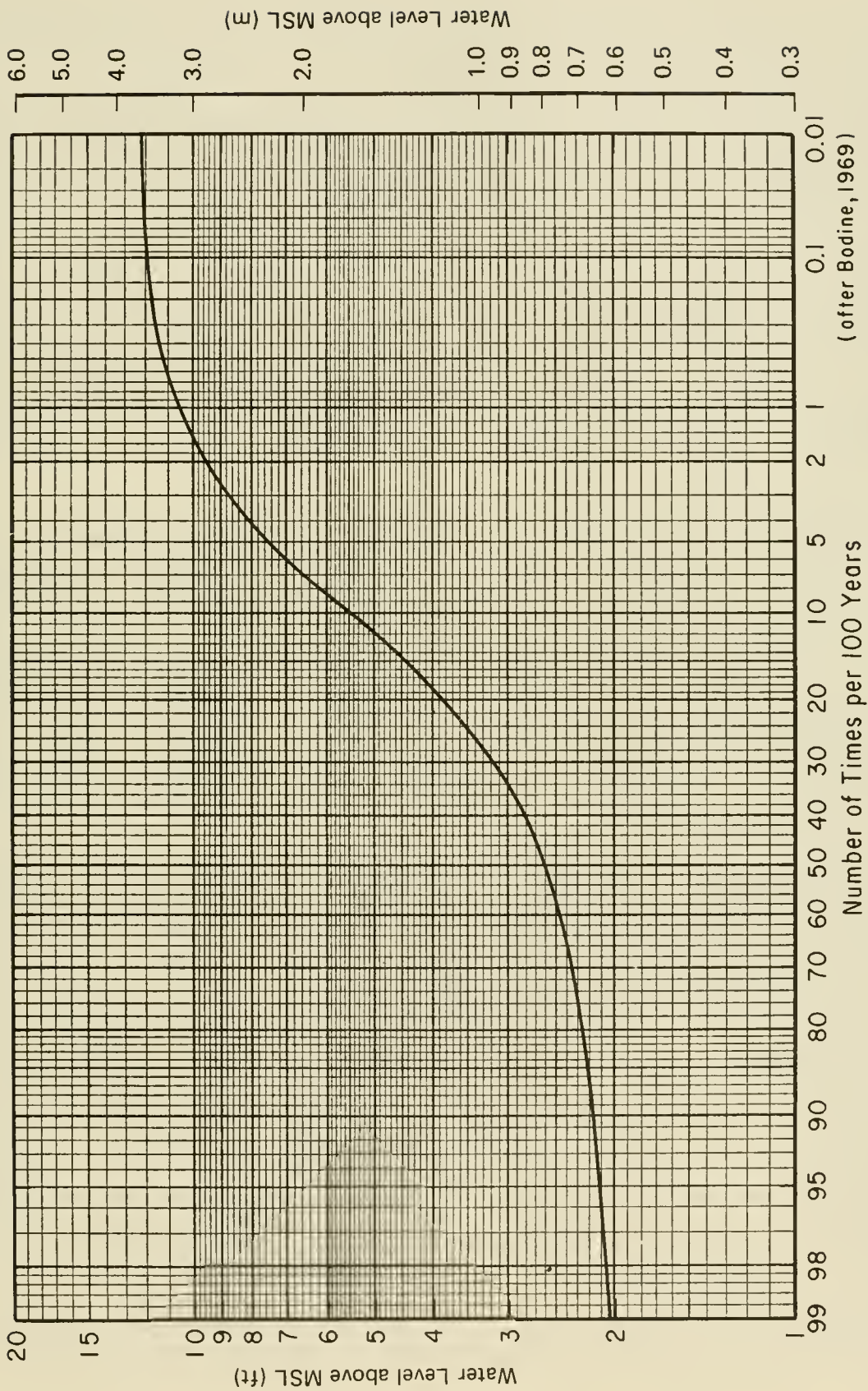


Figure 4-42. Frequency per 100 years that the stated water level is equalled or exceeded on the open coast, South Padre Island, Texas.

averaged about 400,000 cubic meters per kilometer (900,000 cubic yards per mile) of beach (Meyer and Chester, 1977). Thus, within a few years, foredunes can trap and store a volume of sand equivalent to the volumes eroded from beaches during storms of moderate intensity.

c. Long-Term Effects. Dolan (1972 and 1973) advances the concept that a massive, unbroken foredune line restricts the landward edge of the surf zone during storms, causing narrower beaches and thus increased turbulence in the surf zone. The increased turbulence causes higher sand grain attrition and winnowing rates and leads to accelerated losses of fine sand, an erosive process that may be detrimental to the long-range stability of barrier islands. However, as discussed in Section V,2,a, the effects of sediment size are usually of secondary importance in littoral transport processes--processes which are important in barrier island stability. In addition, geographical location is probably more important in determining beach sand size than dune effects, since both fine and coarse sand beaches front major foredune systems in different geographical locations. For example, fine sand beaches front a massive foredune system on Mustang Island, Texas, and coarse sand beaches front dunes on the Cape Cod spits.

Godfrey and Godfrey (1972) discuss the effect of a foredune system on the long-term stability of the barrier islands of the Cape Hatteras and Cape Lookout National Seashores, North Carolina. Important implicit assumptions of the discussion are that no new supply or inadequate new supplies of sand are available to the barrier island system and that rising sea level is, in effect, creating a sand deficit by drowning some of the available island volume. The point of the geomorphic discussion is that under such conditions the islands must migrate landward to survive. A process called "oceanic overwash" (the washing of sand from low foredunes or from the beach over the island crest onto the deflation plain by overtopping waves) is described as an important process in the landward migration of the islands. Since a foredune system blocks overtopping and prevents oceanic overwash, foredunes are viewed as a threat to barrier island stability.

If the implicit assumptions and a geologic time frame are accepted, the geomorphic concept presented has convincing logic and probably has merit. However, the assumptions are not valid on all barrier islands or at all locations in most barrier islands or at all locations in most barrier island systems. Too, most coastal engineering projects are based on a useful life of 100 years or less. In such a short period, geologic processes, such as sea-level rise, have a minor effect in comparison with the rapid changes caused by wind and waves. Therefore, the island crest elevation and foredune system will maintain their elevation relative to the mean water level on stable or accreting shores over the life of most projects. On eroding shores, the foredunes will eventually be eroded and overwash will result in shoreward migration of the island profile; sand burial and wave and water damage will occur behind the original duneline. Therefore, planning for and evaluation of the probable success of a foredune system must consider the general level of the area of the deflation plain to be protected, the rate of sea level rise, and the rate of beach recession.

## VII. SEDIMENT BUDGET

### 1. Introduction.

a. Sediment Budget. A sediment budget is a sediment transport volume balance for a selected segment of the coast. It is based on quantification of sediment transportation, erosion, and deposition for a given control volume. Usually, the sediment quantities are listed according to the sources, sinks, and processes causing the additions and subtractions. In this chapter, the sediment discussed is usually sand and the processes are either littoral processes or the changes made by man.

The purpose of a sediment budget is to assist the coastal engineer by (1) identifying relevant processes, (2) estimating volume rates required for design purposes, (3) singling out significant processes for special attention, and, on occasion, (4) through balancing sand gains against losses, checking the accuracy and completeness of the design budget.

Sediment budget studies have been presented by Johnson (1959), Bowen and Inman (1966), Vallianos (1970), Pierce (1969), Caldwell (1966), and Jarrett (1977).

b. Elements of Sediment Budget. Any process that increases the quantity of sand in a defined control volume is called a *source*. Any process that decreases the quantity of sand in the control volume is called a *sink*. Usually, sources are identified as positive and sinks as negative. Some processes (longshore transport is the most important) function both as source and sink for the control volume.

*Point sources* or *point sinks* are sources or sinks that add or subtract sand across a limited part of a control volume boundary. A tidal inlet often functions as a point sink. Point sources or sinks are generally measured in units of volume per year.

*Line sources* or *line sinks* are sources or sinks that add or subtract sand across an extended segment of a control volume boundary. Wind transport landward from the beaches of a low barrier island is a line sink for the ocean beach. Line sources or sinks are generally measured in units of volume per year per unit length of shoreline. To compute the total effect of a line source or sink, it is necessary to multiply this quantity by the total length of shoreline over which the line source or sink operates.

The following conventions are used for elements of the sediment budget:

(a)  $Q_i^+$  is a point source

(b)  $Q_i^-$  is a point sink

(c)  $q_i^+$  is a line source

(d)  $q_i^-$  is a line sink

These subscripted elements of the sediment budget are identified by name in Table 4-15 according to whether the element makes a point or line contribution

Table 4-15. Classification of elements in the littoral zone sediment budget.

Location of Source or Sink	Offshore Side of Littoral Zone	Onshore Side of Littoral Zone	Within Littoral Zone	Longshore Ends of Littoral Zone
Point source (volume/unit time)	$Q_1^+$ Offshore shoal or island	$Q_2^+$ Rivers, streams <sup>1</sup>	$Q_3^+$ Replenishment	$Q_4^+$ Longshore transport in <sup>1</sup>
Point sink (volume/unit time)	$Q_1^-$ Submarine canyon	$Q_2^-$ Inlets <sup>1</sup>	$Q_3^-$ Mining, extractive dredging	$Q_4^-$ Longshore transport out <sup>1</sup>
Line source (volume/unit time/ unit length of beach)	$q_1^+$ Sand transport from the offshore	$q_2^+$ Coastal erosion, including erosion of dunes and cliffs <sup>1</sup>	$q_3^+$ Beach erosion <sup>1</sup> ; CaCO <sub>3</sub> production	
Line sink (volume/unit time/ unit length of beach)	$q_1^-$ Sand transport to the offshore	$q_2^-$ Overwash; coastal land and dune storage	$q_3^-$ Beach storage <sup>1</sup> ; CaCO <sub>3</sub> losses	

<sup>1</sup> Naturally occurring sources and sinks that usually are major elements in the sediment budget.

to the littoral zone and according to the boundary across which the contribution enters or leaves. Each of the elements is discussed in following sections.

The length of shoreline over which a line source is active is indicated by  $b_i$  and the total contribution of the line source or line sink by  $Q_i^{*+}$  or  $Q_i^{*-}$ , so that in general

$$Q_i^* = b_i q_i \quad (4-58)$$

It is often useful to specify a source or sink as a fraction  $k_i$  of the gross longshore transport rate:

$$Q_i = k_i Q_g \quad (4-59)$$

In a complete sediment budget, the difference between the sand added by all sources and the sand removed by all sinks should be zero. In the usual case, a sand budget calculation is made to estimate an unknown erosion or deposition rate. This estimated rate will be the difference resulting from equating known sources and sinks. The total budget is shown schematically as follows:

$$\text{Sum of Sources} - \text{Sum of Sinks} = 0, \text{ or}$$

$$\text{Sum of Known Sources} - \text{Sum of Known Sinks} = \text{Unknown (Sought) Source or Sink}$$

$$\sum_{i=1}^4 Q_i^+ + \sum_{i=1}^4 Q_i^{*+} - \left( \sum_{i=1}^3 Q_i^- + \sum_{i=1}^3 Q_i^{*-} \right) = 0 \quad (4-60)$$

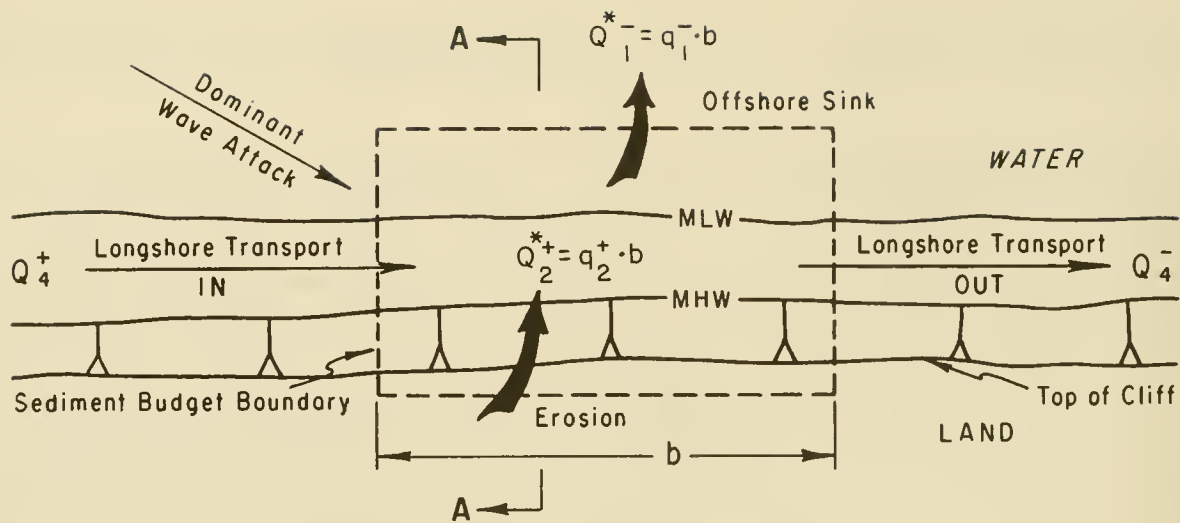
The  $Q_i^*$  are obtained using equation (4-58) and the appropriate  $q_i$  and  $b_i$ . The subscript  $i$  equals 1, 2, 3, or 4 and corresponds to the subscripts in Table 4-15.

c. Sediment Budget Boundaries. Boundaries for the sediment budget are determined by the area under study, the time scale of interest, and study purposes. In a given study area, adjacent sand budget compartments (control volumes) may be needed, with shore-perpendicular boundaries at significant changes in the littoral system. For example, compartment boundaries may be needed at inlets between eroding and stable beach segments, and between stable and accreting beach segments. Shore-parallel boundaries are needed on both the seaward and landward sides of the control volumes; they may be established wherever needed, but the seaward boundary is usually established at or beyond the limit of active sediment movement, and the landward boundary beyond the erosion limit anticipated for the life of the study. The bottom surface of a control volume should pass below the sediment layer that is actively moving, and the top boundary should include the highest surface elevation in the control volume. Thus, the budget of a particular beach and nearshore zone would have shore-parallel boundaries landward of the line of expected erosion and at or beyond the seaward limit of significant transport. A budget for barrier island sand dunes might have a boundary at the bay side of the island and the landward edge of the backshore.

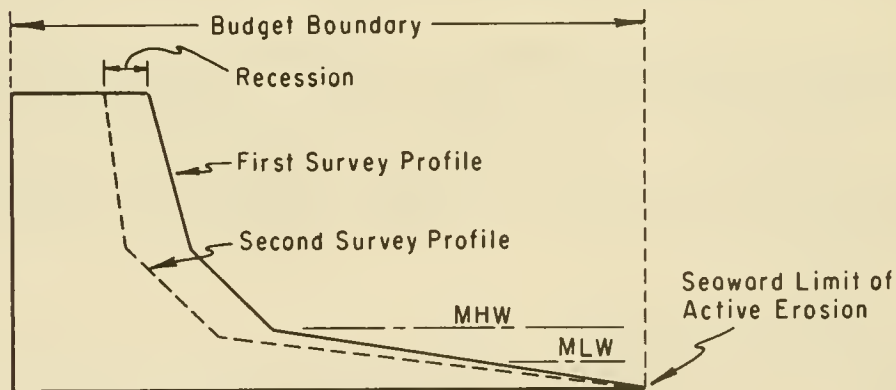
A schematic sediment budget analysis is shown in Figure 4-43. This example considers a shoreline segment along which the incident wave climate can transport more material than is entering from updrift. Therefore, the longshore transport in the segment is being fed by a continuously eroding sea cliff. The cliff is composed of 50 percent sand and 50 percent clay. The clay fraction is assumed to be lost offshore, while the sand fraction feeds into the longshore transport.

## 2. Sources of Littoral Materials.

a. Rivers. It is estimated that rivers of the world bring about 14.2 cubic kilometers (3.4 cubic miles) or 14.2 billion cubic meters (18.5 billion cubic yards) of sediment to the coast each year (volume of solids without voids) (Stoddard, 1969; from Strakhov, 1967). Only a small percentage of this sediment is in the sand size range that is common on beaches. The large rivers which account for most of the volume of sediment carry relatively little sand. For example, it is estimated (Scruton, 1960) that the sediment load brought to the Gulf of Mexico each year by the Mississippi River consists of 50 percent clay, 48 percent silt, and only 2 percent sand. Even lower percentages of sand seem probable for other large river discharges (see Gibbs, 1967, p. 1218, for information on the Amazon River), but smaller rivers flowing through sandy drainage areas may carry 50 percent or more of sand (Chow, 1964, p. 17-20). In southern California, sand brought to the coast by the floods of small rivers is a significant source of littoral material (Handin, 1951; Norris, 1964).



**ERODING SHORELINE - PLAN VIEW**  
(Not to Scale)



**SECTION A-A**  
(Not to Scale)

**Assumptions**

- $Q_4^+ = 100,000 \text{ m}^3/\text{yr}$
- $q_2^+ = 1 \text{ m}^3/\text{yr./meter}$
- $q_1^- = 0.5 \text{ m}^3/\text{yr./meter}$
- $b = 10,000 \text{ meters}$

**Budget Calculations**

Using Equation 4-60

$$\text{Sum of Sources} - \text{Sum of Sinks} = 0$$

$$\text{Find } Q_4^- \quad (Q_4^+ + Q_2^{*+}) - (Q_4^- + Q_1^{*-}) = 0$$

$$(Q_4^+ + q_2^+ b) - (Q_4^- + q_1^- b) = 0$$

$$(10^5 + 1.0 \times 10^4) - (Q_4^- + 0.5 \times 10^4) = 0$$

$$Q_4^- = 110,000 - 5,000$$

$$Q_4^- = 105,000 \text{ m}^3/\text{yr}$$

Figure 4-43. Basic example of sediment budget.

Most of the sediment carried to the coast by rivers is deposited in comparatively small areas, often in estuaries where the sediment is trapped before it reaches the coast (Strakhov, 1967). The small fraction of sand in the total material brought to the coast and the local estuarine and deltaic depositional sites of this sediment suggest that rivers are not the immediate source of sediment on beaches for much of the world's coastline. Sand-sized sediment is not supplied to the coasts by rivers on most segments of the U.S. Atlantic and gulf coasts. Therefore, other sediment sources must be important.

b. Erosion of Shores and Cliffs. Erosion of the nearshore bottom, the beach, and the seaward edge of dunes, cliffs, and mainland results in a sand loss. In many areas, erosion from cliffs of one area is the principal source of sand for downdrift beaches. Kuenen (1950) estimates that beach and cliff erosion along all coasts of the world totals about 0.12 cubic kilometer (0.03 cubic mile) or 120 million cubic meters (160 million cubic yards) per year. Although this amount is only about 1 percent of the total solid material carried by rivers, it is a major source in terms of sand delivered to the beaches. Shore erosion is an especially significant source where older coastal deposits are being eroded, since these usually contain a large fraction of sand.

If an eroding shore maintains approximately the same profile above the seaward limit of significant transport while it erodes, then the erosion volume per meter of beach front is the vertical distance from dune base or berm crest to the depth of the seaward limit  $h$ , multiplied by the horizontal retreat of the profile  $\Delta x$  (see Fig. 4-44).

Figure 4-44 shows three equivalent volumes, all indicating a net erosion of  $h\Delta x$ . To the right in Figure 4-44 is a typical beach profile (the dashed line profile below is the same as the solid line profile). The horizontal distance between solid and dashed profiles is  $\Delta x$ , the horizontal retreat of the profile due to (assumed) uniform erosion. The unit volume loss,  $h\Delta x$  between dune base and depth to seaward limit is equivalent to the unit volume indicated by the slanted parallelogram in the middle of Figure 4-44. The unit volume of this parallelogram,  $h\Delta x$ , is equivalent to the shaded rectangle on the left of Figure 4-44. If the vertical distance  $h$  is 10 meters and  $\Delta x = 1$  meter of horizontal erosion, then the unit volume lost is 10 cubic meters per meter of beach front.

c. Transport from Offshore Slope. An uncertain but possibly significant source in the sediment budget is the contribution from the offshore slope. However, hydrography, sediment size distribution, and related evidence discussed in Section V,2,c indicate that contributions from the continental shelf to the littoral zone are probably negligible in many areas. Most shoreward-moving sediment appears to originate in areas fairly close to shore. Significant onshore-offshore transport takes place within the littoral zone due to seasonal and storm-induced profile changes and to erosion of the nearshore bottom and beaches, but in the control volume defined, this transport takes place within the control volume. Transport from the offshore has been treated as a line source.

In some places, offshore islands or shoals may act as point sources of

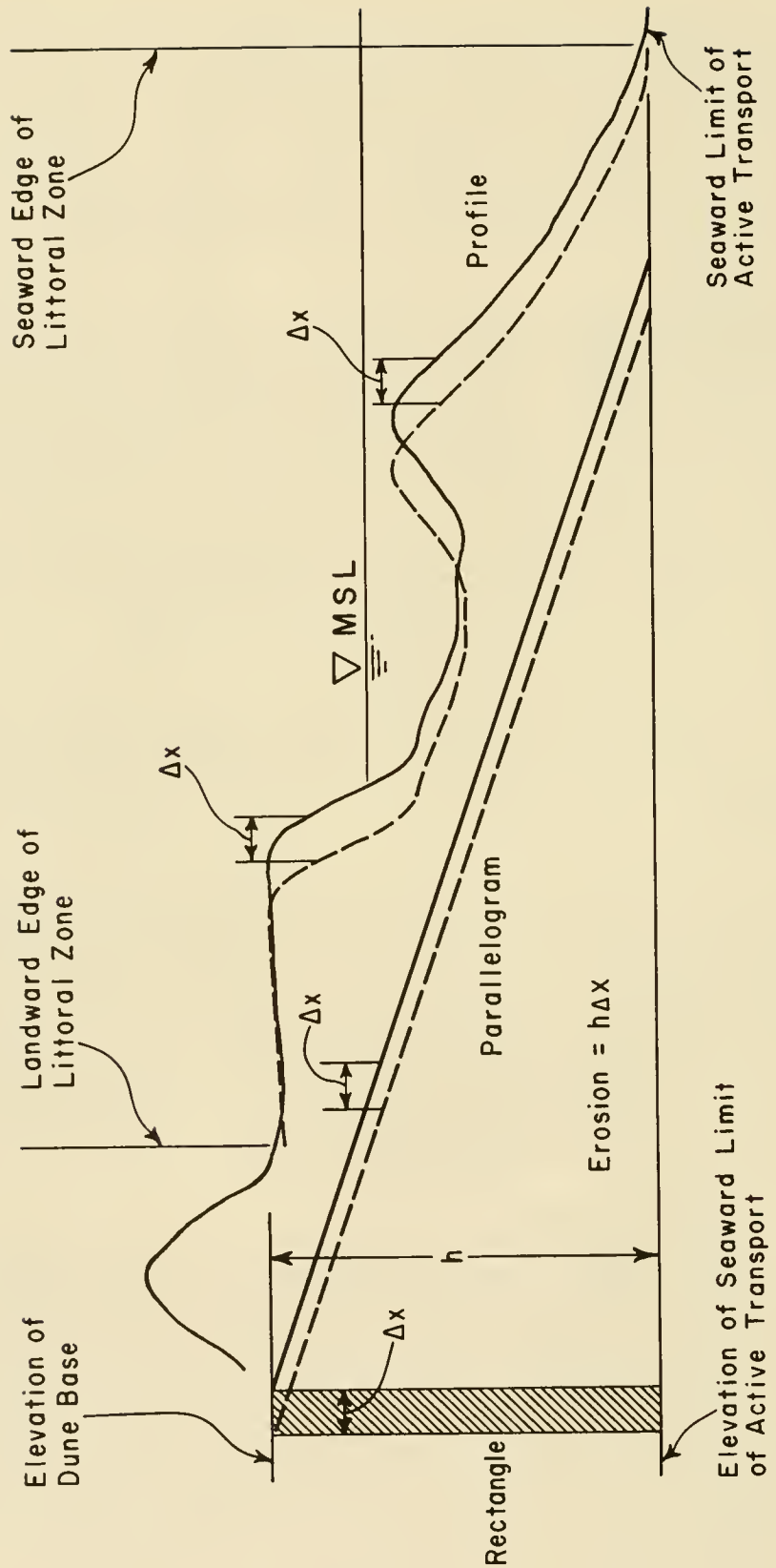


Figure 4-44. Erosion within littoral zone during uniform retreat of an idealized profile.

material for the littoral zone. For example, the drumlin islands and shoals in Boston Harbor and vicinity may be point sources for the nearby mainland.

d. Windblown Sediment Sources. To make a net contribution to the littoral zone in the time frame being considered, windblown sand must come from a land source whose sand is not derived by intermediate steps from the same littoral zone. On U.S. ocean coasts, such windblown sand is not a significant source of littoral materials. Where wind is important in the sediment budget of the ocean shore, wind acts to take away sand rather than to add it, although local exceptions probably occur.

However, windblown sand can be an important source if the control volume being considered is a beach on the lagoon side of a barrier island. Such shores may receive large amounts of windblown sand.

e. Carbonate Production. Dissolved calcium carbonate concentration in the ocean is near saturation, and it may be precipitated under favorable conditions. In tropical areas, many beaches consist of calcium carbonate sands; in temperate zones, calcium carbonate may be a significant part of the littoral material. These calcium carbonate materials are generally fragments of shell material whose rate of production appears to increase with high temperature and with excessive evaporation (see Hayes, 1967b). Oolitic sands are a nonbiogenic chemical precipitate of calcium carbonate on many low-latitude beaches.

Quantitative estimates of the production of calcium carbonate sediment are lacking, but maximum rates might be calculated from the density and rate of growth of the principal carbonate-producing organisms in an area. For example, following northeasters along the Atlantic coast of the U.S., the foreshore is occasionally covered with living clams thrown up by the storm from the nearshore zone. One estimate of the annual contribution to the littoral zone from such a source would assume an average shell thickness of about 0.012 meter (0.04 foot) completely covering a strip of beach 30 meters (100 feet) wide all along the coast. On an annual basis, this would be about 0.07 cubic meter per year per meter (0.15 cubic yard per year per foot) of beach front. Such a quantity is negligible under almost all conditions. However, the dominance of carbonate sands in tropical littoral zones suggests that the rate of production can be much higher.

f. Beach Replenishment. Beach protection projects often require placing sand on beaches. The quantity of sand placed on the beach in such beach-fill operations may be a major element in the local sediment budget. Data on beach-fill quantities may be available in Corps of Engineer District offices, in records of local government, and in dredging company records. The exact computation of the quantity of a beach fill is subject to uncertainties: the source of the dredged sand often contains significant but variable quantities of finer materials that are soon lost to the littoral zone; the surveys of both the borrow area and the replenished area are subject to uncertainty because sediment transport occurs during the dredging activities; and in practice only limited efforts are made to obtain estimates of the size distribution of fill placed on the beach. Thus, the resulting estimate of the quantity of suitable fill placed on the beach is uncertain, but the most reliable of the items in the budget. More frequent sampling and surveys could help identify this significant element in many sediment budgets.

### 3. Sinks for Littoral Materials.

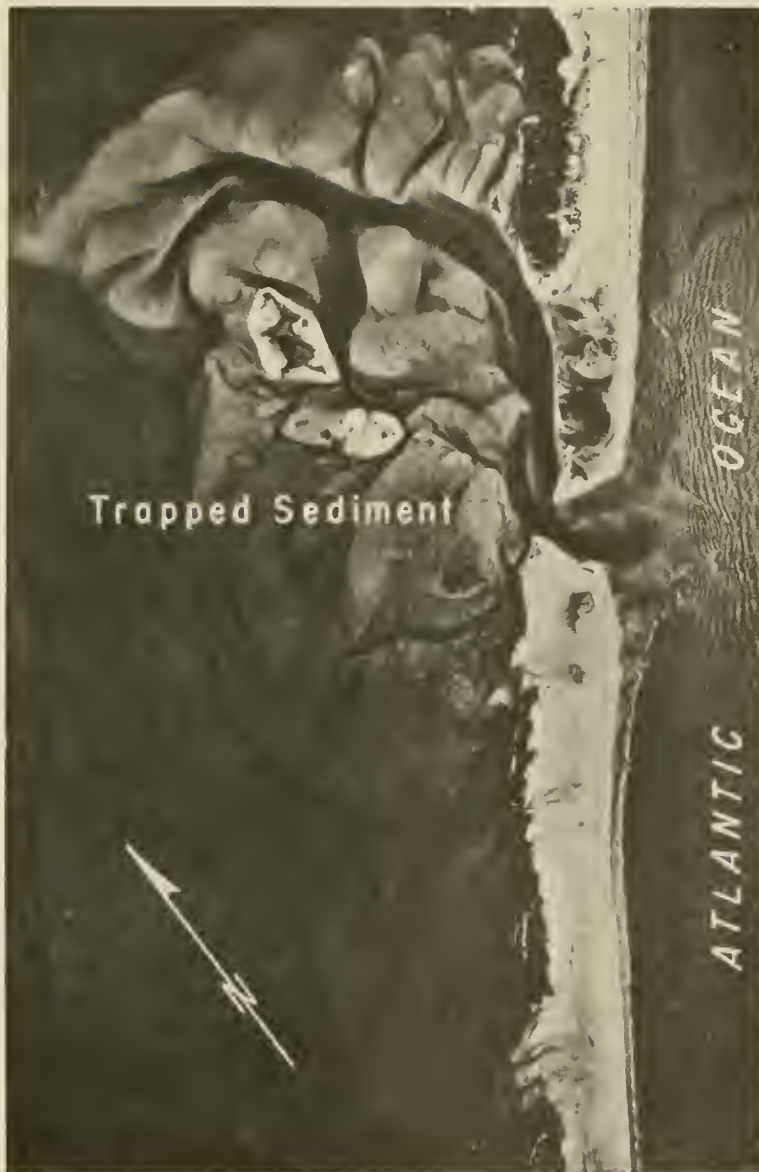
a. Inlets and Lagoons. Barrier islands are interrupted locally by inlets which may be kept open by tidal flow. A part of the sediment moved alongshore by wave action is moved into these inlets by tidal flow. Once inside the inlet, the sediment may deposit where it cannot be moved seaward by the ebb flow (Brown, 1928). The middleground shoals common to many inlets are such depositional features. Such deposition may be reduced when the ebb currents are stronger than the flood currents (Johnson, 1956). Also, particularly during times of strong ebb tidal flow, sand is jetted sufficiently far offshore to be deposited outside the control volume and removed from the littoral zone.

It is evident from aerial photography (e.g., of Drum Inlet, N.C., Fig. 4-45) that inlets do trap significant quantities of sand. Caldwell's (1966) estimate of the sand budget for New Jersey calculates that 23 percent of the local gross longshore transport is trapped by the seven inlets in southern New Jersey, or about 191,000 cubic meters (250,000 cubic yards) per year for each inlet. In a study of the south shore of Long Island, McCormick (1971) estimated from the growth of the floodtide delta of Shinnecock Inlet (shown by aerial photos taken in 1955 and 1969) that this inlet trapped 16,000 cubic meters (60,000 cubic yards) per year. This amounts to about 20 percent of the net longshore transport (Taney, 1961, p. 46) and probably less than 10 percent of the gross transport (Shinnecock Inlet is a relatively small inlet). It appears that the rate at which an inlet traps sediment is higher immediately after the inlet opens than it is later in its history.

b. Overwash. On low barrier islands, sand may be removed from the beach and dune area by overwashing during storms. Such rates may average locally up to 0.5 cubic meter per year per meter (1 cubic yard per year per foot). Data presented by Pierce (1969) suggest that for over half of the shoreline between Cape Hatteras and Cape Lookout, North Carolina, the short-term loss due to overwash was 1.5 cubic meters per year per meter (0.6 cubic yard per year per foot) of beach front. Figure 4-46 is an aerial view of overwash in the region studied by Pierce (1969). Overwash does not occur on all barrier islands, but if it does, it may function as a source for the beach on the lagoon side.

c. Backshore and Dune Storage. Sand can be temporarily withdrawn from transport in the littoral zone as backshore deposits and dune areas along the shore. Depending on the frequency of severe storms, such sand may remain in storage for intervals ranging from months to years. Backshore deposition can occur in hours or days by the action of waves after storms. Dune deposits require longer to form--months or years--because wind transport usually moves material at a lesser rate than wave transport. If the immediate beach area is the control volume of interest and budget calculations are made based on data taken just after a severe storm, allowance should be made in budget calculations for sand that will be stored in berms through natural wave action.

d. Offshore Slopes. The offshore area is potentially an important sink for littoral material. Transport to the offshore is favored by (1) storm waves which stir up sand, particularly when onshore winds create a seaward return flow, (2) turbulent mixing along the sediment concentration gradient which exists between the sediment-water mixture of the surf zone and the clear



(16 August 1959)

Figure 4-45. Sediment trapped inside Old Drum Inlet, North Carolina.

water offshore, and (3) the slight offshore component of gravity which acts on both the individual sediment particles and on the sediment-water mixture.

It is often assumed that the *sediment sorting loss* that commonly reduces the volume of newly placed beach fill is lost to the offshore slopes (U.S. Army Engineer District, Wilmington, 1970; Watts, 1956). A major loss to the offshore zone occurs where spits build into deep water in the longshore direction; Sandy Hook, New Jersey, is an example (see Fig. 4-47).

The calculation of quantities lost to the offshore zone is difficult, since it requires extensive, accurate, and costly surveys. Some data on offshore changes can be obtained by studies of sand level changes on rods



(1 November 1971)

Figure 4-46. Overwash on Portsmouth Island, North Carolina.



(14 September 1969)

Figure 4-47. Growth of a spit into deep water, Sandy Hook, New Jersey.

imbedded in the sea floor (Inman and Rusnak, 1956), but without extending the survey beyond the boundary of the moving sand bed, it is difficult to determine net changes.

e. Submarine Canyons. In some coastal areas, an important sink for littoral materials is submarine canyons. Shepard (1963) and Shepard and Dill (1966) provide extensive description and discussion of the origin of submarine canyons. The relative importance of submarine canyons in sediment budgets is still largely unknown.

Of 93 canyons tabulated by Shepard and Dill (1966), 34 appear to be receiving sediment from the coast, either by longshore transport or by transport from river mouths. Submarine canyons are thought to be especially important as sinks off southern California. Herron and Harris (1966, p. 654) suggest that Mugu Canyon, California, traps about 765,000 cubic meters (1 million cubic yards) per year of the local littoral drift.

The exact mechanism of transport into these canyons is not clear, even for the La Jolla Canyon (California) which is stated to be the most extensively studied submarine feature in the world (Shepard and Buffington, 1968). Once inside the canyons, the sediment travels down the floors of the heads of the canyons and is permanently lost to the littoral zone.

f. Deflation. The loose sand that forms beaches is available to be transported by wind. After a storm, shells and other objects are often found perched on pedestals of sand left standing after the wind has eroded less protected sand in the neighborhood. Such erosion over the total beach surface can amount to significant quantities. Unstabilized dunes may form and migrate landward, resulting in an important net loss to the littoral zone. Examples include some dunes along the Oregon coast (Cooper, 1958), between Pismo Beach and Point Arguello, California (Bowen and Inman, 1966); central Padre Island (Watson, 1971); and near Cape Henlopen, Delaware (Kraft, 1971). Typical rates of transport due to wind range from 2.5 to 25 cubic meters per year per meter (1 to 10 cubic yards per year per foot) of beach front where wind transport is noticeable (Cooper, 1958; Bowen and Inman, 1966; Savage and Woodhouse, 1968; Gage, 1970). However average rates probably range from 2.5 to 7.5 cubic meters per year per meter (1 to 3 cubic yards per year per foot).

The largest wind-transported losses are usually associated with accreting beaches that provide a broad area of loose sand over a period of years. Sand migrating inland from Ten Mile River Beach in the vicinity of Laguna Point, California, is shown in Figure 4-48.

Study of aerial photographs and field reconnaissance can easily establish whether or not important losses or gains from wind transport occur in a study area. However, detailed studies are usually required to establish the importance of wind transport in the sediment budget.

g. Carbonate Loss. The abrasion resistance of carbonate materials is much lower than quartz, and the solubility of carbonate materials is usually much greater than quartz. However, there is insufficient evidence to show that significant quantities of carbonate sands are lost from the littoral zone in the time scale of engineering interest through either abrasion or solution.

h. Mining and Dredging. From ancient times, sand and gravel have been mined along coasts. In some countries, for example Denmark and England, mining has occasionally had undesirable effects on coastal settlements in the vicinity. Sand mining in most places has been discouraged by legislation and the rising cost of coastal land, but it still is locally important (Magoon, et al. 1972). It is expected that mining will become more important in the offshore area in the future (Duane, 1968; Fisher, 1969).

Such mining must be conducted far enough offshore so the mined pit will not act as a sink for littoral materials, or refract waves adversely, or substantially reduce the wave damping by bottom friction and percolation.

Material is also lost to the littoral zone when dredged from navigable waters (channels and entrances) within the littoral zone and dumped in some area outside of the littoral zone. Material can be dumped in landfill areas or in deep water offshore. This action has been a common practice because it lowers the first costs for some dredging operations.

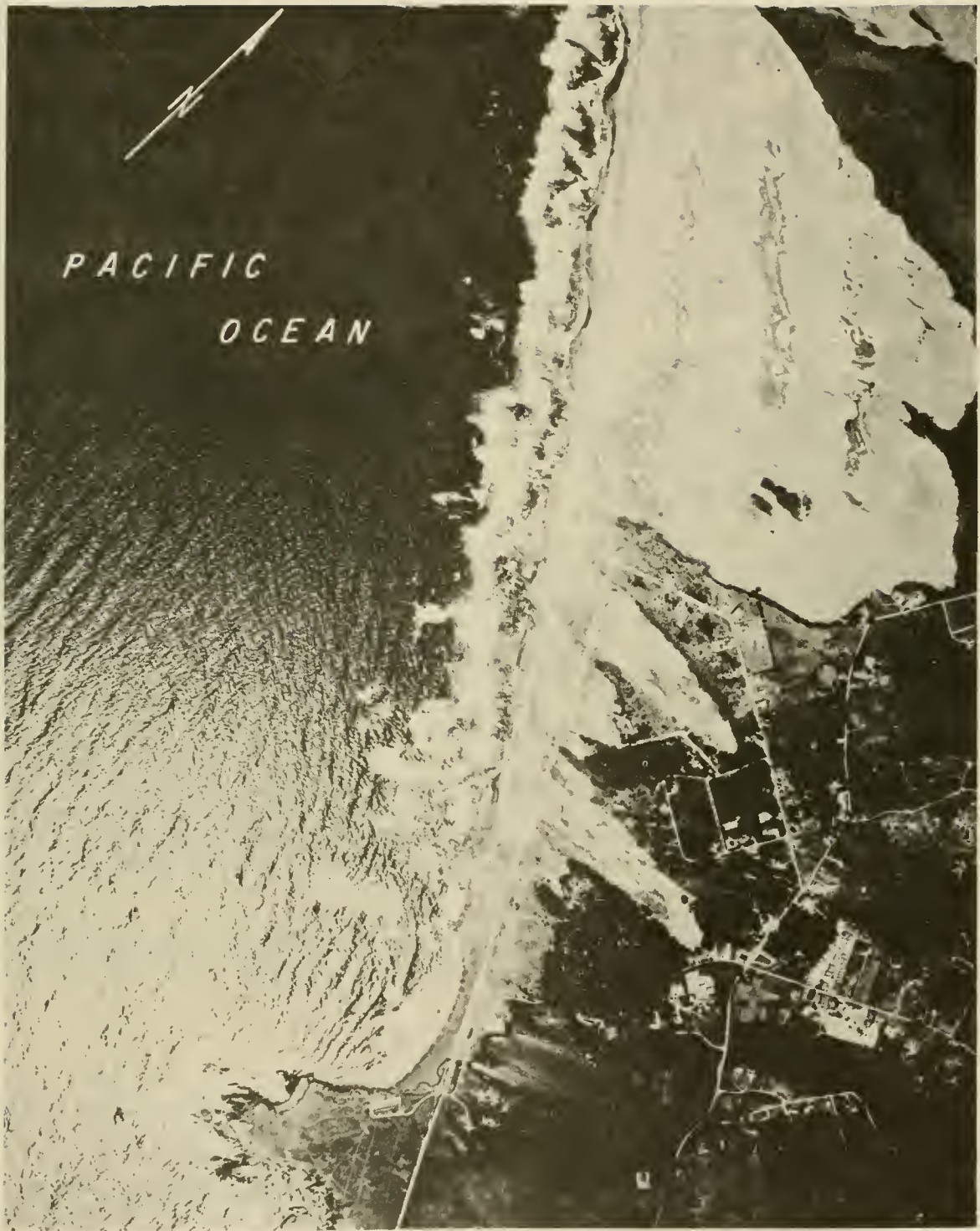


Figure 4-48. Dunes migrating inland near Laguna Point, California.

#### 4. Convection of Littoral Materials.

Sources and sinks of littoral materials are those processes that result in net additions or net subtractions of material to the selected control volume. However, some processes may subtract at the same rate that they add material, resulting in no net change in the volume of littoral material of the control volume.

The most important convecting process is longshore sediment transport. It is possible for straight exposed coastlines to have gross longshore transport rates of more than 750,000 cubic meters (1 million cubic yards) per year. On a coast without structures, such a large  $Q_g$  can occur and yet not be apparent because it causes no obvious beach changes. Other convecting processes that may produce large rates of sediment transport with little noticeable change include tidal flows, especially around inlets, wind transport in the longshore direction, and wave-induced currents in the offshore zone.

Since any structure that interrupts the equilibrium convection of littoral materials will normally result in erosion or accretion, it is necessary that the sediment budget quantitatively identify all processes convecting sediment through the study area. This is most important on shores with high waves.

#### 5. Relative Change in Sea Level.

Relative changes in sea level may be caused by changes in sea level and/or changes in land level. Sea levels of the world are now generally rising. The level of inland seas may either rise or fall, generally depending on hydrologic influences. Land level may rise or fall due to tectonic forces, and land level may fall due to subsidence. It is often difficult to distinguish whether apparent changes in sea level are due to change in sea level, change in land level, or both. For this reason, the general process is referred to as relative change in sea level.

While relative changes in sea level do not directly enter the sediment budget process, the net effect of these elevation changes is to move the shoreline either landward (relative rise in sea level) or seaward (relative fall in sea level). Relative sea level change thus can result in the appearance of a gain or loss of sediment volume.

The importance of relative change in sea level on coastal engineering design depends on the time scale and the locality involved. Its effect should be determined on a case-by-case basis.

#### 6. Summary of Sediment Budget.

Sources, sinks, and convective processes are summarized diagrammatically in Figure 4-49 and listed in Table 4-16. The range of contributions or losses from each of these elements is described in Table 4-16 measured as a fraction of the gross longshore transport rate, or as a rate given in cubic meters per year per meter (cubic yards per year per foot) of beach front. The relative importance of elements in the sand budget varies with locality and with the boundaries of the particular littoral control volume.

In most localities, the gross longshore transport rate significantly

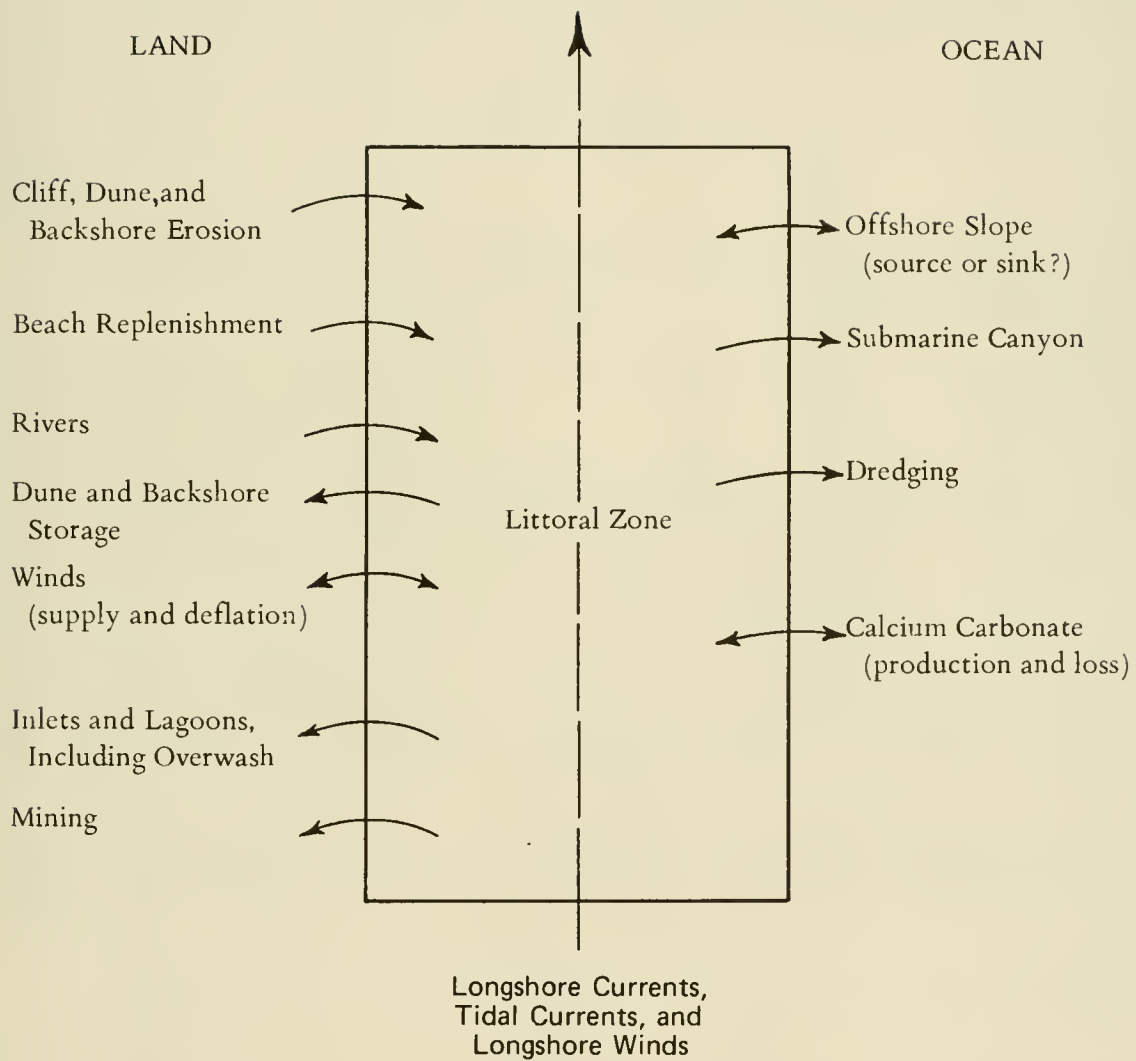


Figure 4-49. Materials budget for the littoral zone.

Table 4-16. Sand budget of the littoral zone.

Sources	
Rivers and streams	The major source in the limited areas where rivers carry sand to the littoral zone. In affected areas notable floods may contribute several times $Q_g$ .
Cliff, dune, and backshore erosion	Generally the major source where rivers are absent (2.5 to 10 cubic meters per year per meter (1 to 4 cubic yards per year per foot).
Transport from offshore	Quantity uncertain.
Wind transport	Not generally important as a source.
CaCO <sub>3</sub> production	Significant in tropical climate. The value of 0.63 cubic meter per year per meter (0.25 cubic yard per year per foot) seems reasonable upper limit on temperate beach.
Beach replenishment	Varies from 0 to greater than $Q_g$ .
Sinks	
Inlets and lagoons	May remove from 5 to 25 percent of $Q_g$ per inlet. Depends on number of inlets, inlet size, tidal flow characteristics, and inlet age.
Overwash	Less than 2.5 cubic meters per year per meter (1 cubic yard per year per foot) at most, and limited to low barrier islands.
Beach storage	Temporary, but possibly large, depending on beach condition when budget is made.
Offshore slopes	Uncertain quantity. May receive much fine material, some coarse material.
Submarine canyons	Where present, may intercept up to 80 percent of $Q_g$ .
Deflation	Usually less than 5 cubic meters per year per meter (2 cubic yards per year per foot) of beach front, but may range up to 25 cubic meters per year per meter (10 cubic yards per year per foot).
CaCO <sub>3</sub> loss	Not known to be important.
Mining and dredging	May equal or exceed $Q_g$ in some localities.
Convective Processes	
Longshore transport (waves)	May result in accretion of $Q_g$ , erosion of $Q_g$ , or no change depending on conditions of equilibrium.
Tidal Currents	May be important at mouth of inlet and vicinity, and on irregular coasts with high tidal range.
Winds	Longshore winds are probably not important, except in limited regions.

exceeds other volume rates in the sediment budget, but if the beach is approximately in equilibrium, this may not be easily noticed.

The erosion of beaches and cliffs and river contributions are the principal known natural sources of beach sand in most localities. Inlets, lagoons, and deep water in the longshore direction comprise the principal known natural sinks for beach sand. Of potential, but usually unknown, importance as either a source or a sink is the offshore zone seaward of the beach.

The works of man in beach replenishment and in mining or dredging may provide major sources or sinks in local areas. In a few U.S. localities, submarine canyons or wind may provide major sinks, and calcium carbonate production by organisms may be a major source.

\* \* \* \* \* EXAMPLE PROBLEM 5 \* \* \* \* \*

GIVEN:

- (a) An eroding beach 7.1 kilometers (4.4 miles) long at root of spit that is 16.1 kilometers (10 miles) long. Beaches on the remainder of the spit are stable, and the tip of the spit is accreting (see Fig. 4-50a.)
- (b) A uniform recession rate of 0.9 meter (3 feet) per year along the eroding 7.1 kilometers.
- (c) Depth of lowest shore-parallel contour is -9.1 meters (-30 feet) MSL, and average dune base elevation is 4.6 meters (15 feet) MSL.
- (d) Sand is accumulating at the tip of the spit at an average rate of 305,000 cubic meters (400,000 cubic yards) per year.
- (e) No sand accumulates to the right of the erosion area; no sand is lost to the offshore.
- (f) A medium-width jettied inlet is proposed which will breach the spit as shown in Figure 4-50.
- (g) The proposed inlet is assumed to trap about 15 percent of the gross transport  $Q_g$ .
- (h) The 2.1-kilometer- (1.3-mile-) long beach to the right of the jettied inlet will stabilize (no erosion) and realign with  $\gamma$  at the inlet assumed to be 3.5 (see eq. 4-34).
- (i) The accumulation at the end of the spit will continue to grow at an average annual rate of 305,000 cubic meters (400,000 cubic yards) per year after the proposed inlet is constructed.

FIND:

- (a) Annual littoral drift trapped by inlet.
- (b) After-inlet erosion rate of the beach to the left of the inlet.

(c) After-inlet nourishment needed to maintain the historic erosion rate on the beach to the left of the inlet.

(d) After-inlet nourishment needed to eliminate erosion left of the inlet.

SOLUTION: Divide the beach under study into four sand budget compartments (control volumes called reaches) as shown in Figure 4-50. Shore-perpendicular boundaries are established where important changes in the littoral system occur. To identify and quantify the *before-inlet* system, the continuity of the net transport rate along the entire spit must be established. The terminology of Figure 4-43 and Table 4-15 is used for the sand budget calculation. The average annual volume of material contributed to the littoral system per meter of eroding beach Reaches 2 and 3 is

$$q_3^+(2) = q_3^+(3) = h\Delta x = (4.6 + 9.1) 0.9 = 12.33 \text{ cubic meters per year per meter (4.91 cubic yards per year per foot)}$$

Then, from equation (4-58) the total annual contribution of the eroding beaches to the system can be determined as

$$\begin{aligned} Q_3^{*+}(2) + Q_3^{*+}(3) &= (2.1 \text{ km} + 5.0 \text{ km}) (1000 \text{ meters per kilometer}) \\ &\quad (12.33 \text{ cubic meters per year per meter}) \\ &= 87,500 \text{ cubic meters per year (114,400 cubic yards per year)} \end{aligned}$$

Since there is no evidence of sand accumulation to the right of the eroding area, the eroding beach material effectively moves to the left, becoming a component of the net transport volume  $Q_n$  toward the end of the spit. Continuity requires that erosion volume and Reach 1  $Q_n$  combine to equal the accretion at the end of the spit (305,000 cubic meters per year). Thus,  $Q_n$  at the root of the spit is

$$Q_n(1,2) = 305,000 \text{ cubic meters per year} - 87,500 \text{ cubic meters per year}$$

$$Q_n(1,2) = 217,500 \text{ cubic meters per year (284,500 cubic yards per year)}$$

$Q_n$  across the boundary between Reaches 2 and 3 ( $Q_n(2,3)$ ) is

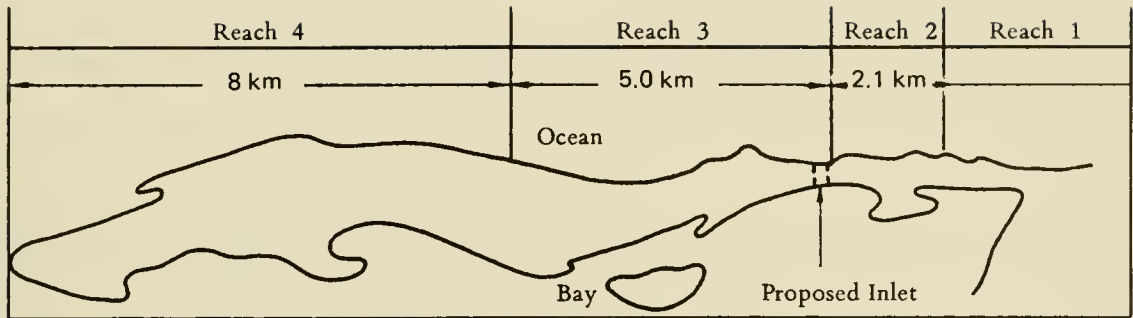
$$Q_n(2,3) = Q_n(1,2) + Q_3^{*+}(2)$$

$$Q_n(2,3) = Q_n(1,2) + b(2) (q_3^+(2))$$

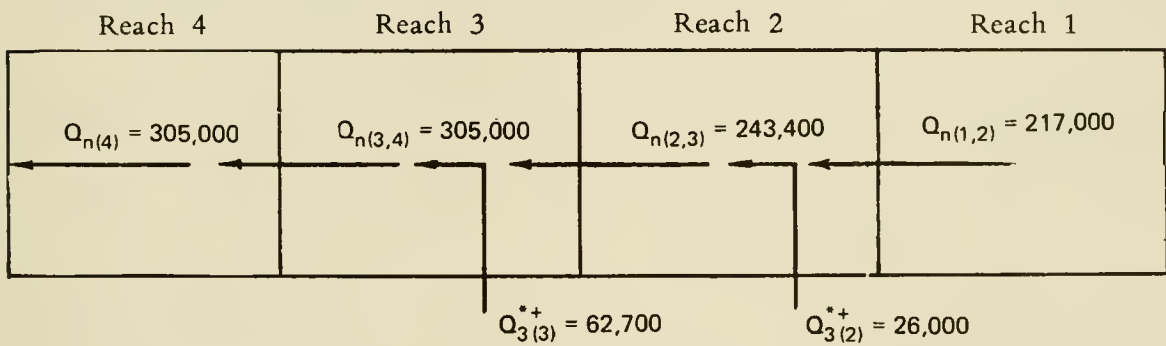
$$Q_n(2,3) = 217,500 + (2.1 \text{ kilometers}) (100 \text{ meters per kilometer}) (12.33 \text{ cubic meters per year per meter})$$

$$Q_n(2,3) = 243,400 \text{ cubic meters per year (318,000 cubic yards per year)}$$

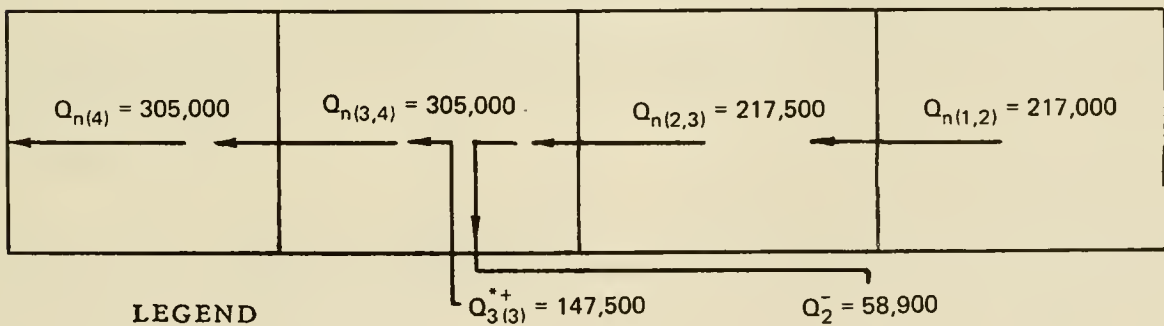
(a) Site Sketch



(b) Sand Budget Before Inlet



(c) Sand Budget After Inlet



$Q_n$  Net Volume

$Q_2^-$  Inlet Sink Volume

$Q_3^{*+}$  Erosion Source Volume

Figure 4-50. Summary of example problem conditions and results (units are metric)

$Q_n$  across the boundary between Reaches 3 and 4 is

$$Q_n(3,4) = Q_n(2,3) + Q_{3(3)}^{*+}$$

$$Q_n(3,4) = Q_n(2,3) + b(3) \left( q_{3(3)}^+ \right)$$

$$Q_n(3,4) = 243,400 \text{ cubic yards per year} + (5 \text{ kilometers}) (1000 \text{ meters per kilometer}) (12.33 \text{ cubic meters per year per meter})$$

$$Q_n(3,4) = 305,000 \text{ cubic meters per year} (400,000 \text{ cubic yards per year})$$

This  $Q_n(3,4)$  moves left across Reach 4 with no additions or subtractions, and since the accretion rate at the end of the spit is 305,000 cubic meters per year, the budget balances. The before-inlet sand budget is shown in Figure 4-50b. Now the *after-inlet* condition can be analyzed.

$$Q_n(1,2) = 217,500 \text{ cubic meters per year (same a "before-inlet")}$$

$$Q_n(2,3) = Q_n(1,2) = 217,500 \text{ cubic meters per year (284,500 cubic yards per year) (Reach 2 is stable)}$$

The gross transport rate across the inlet with the new  $\gamma = 3.5$ , using equation (4-34), is:

$$Q_g = Q_n \frac{(1 + \gamma)}{(1 - \gamma)}$$

$$Q_g(2,3) = \frac{Q_n(2,3)(1 + \gamma)}{(1 - \gamma)}$$

$$Q_g(2,3) = (217,500 \text{ cubic meters per year}) \left( \frac{4.5}{2.5} \right)$$

$$Q_g(2,3) = 319,500 \text{ cubic meters per year (512,000 cubic yards per year)}$$

The inlet sink  $Q_2^- = 15$  percent of  $Q_g(2,3)$

$$Q_2^- = 319,500 \text{ cubic meters per year} \times 0.15$$

$$Q_2^- = 58,700 \text{ cubic meters per year (76,800 cubic yards per year)}$$

The erosion value from Reach 3 now becomes

Reach 3 erosion = spit end accretion  
 + inlet sink  
 - net littoral drift right of inlet

$$Q_{3(3)}^{*+} = Q_{n(3,4)} + Q_2^- - Q_n(2,3)$$

$$Q_{3(3)}^{*+} = 305,000 + 58,700 \text{ cubic meters per year} - 217,500 \text{ cubic meters per year}$$

$$Q_{3(3)}^{*+} = 146,200 \text{ cubic meters per year (191,200 cubic yards per year)}$$

The after-inlet sand budget is shown in Figure 4-50c.

Nourishment needed to maintain historic erosion rate on Reach 3 beach is

$$\text{Reach 3 nourishment} = \text{Reach 3 erosion "after inlet"} - \text{Reach 3 erosion "before inlet"}$$

$$Q_{3(3)}^+ = Q_{3(3)}^{*+} \text{ after inlet} - Q_{3(3)}^{*+} \text{ before inlet}$$

$$Q_{3(3)}^+ = 146,200 \text{ cubic meters per year} - 62,700 \text{ cubic meters per year}$$

$$Q_{3(3)}^+ = 83,500 \text{ cubic meters per year (109,000 cubic yards per year)}$$

If Reach 3 erosion is to be eliminated, it will be necessary to provide nourishment of 146,200 cubic meters per year.

\*\*\*\*\*

## VIII. ENGINEERING STUDY OF LITTORAL PROCESSES

This section demonstrates the use of Chapter 4 in the engineering study of littoral processes.

### 1. Office Study.

The first step in the office phase of an engineering study of littoral processes is to define the problem in terms of littoral processes. The problem may consist of several parts, especially if the interests of local groups are in conflict. An ordering of the relative importance of the different parts may be necessary, and a complete solution may not be feasible. Usually, the problem will be stated in terms of the requirements of the owner or local interests. For example, local interests may require a recreational beach in an area of limited sand, making it necessary to estimate the potential rates of longshore and onshore-offshore sand transport. Or a fishing community may desire a deeper channel in an inlet through a barrier island, making it necessary to study those littoral processes that will affect the stability and long-term navigability of the inlet, as well as the effect of the improved inlet on neighboring shores and the lagoon.

a. Sources of Data. The next step is to collect pertinent data. If the problem area is located on a U.S. coastline, the *National Shoreline Study* may be consulted. This study can provide a general description of the area and may give some indication of the littoral processes occurring in the vicinity of the problem area.

Historical records of shoreline changes are usually in the form of charts, surveyed profiles, dredging reports, beach replenishment reports, and aerial photos. As an example of such historical data, Figure 4-51 shows the positions of the shoreline at Sandy Hook, New Jersey, during six surveys from 1835 to 1932. Such shoreline change data are useful for computing longshore transport rates. The Corps of Engineers maintains, in its District and Division offices, survey, dredging, and other reports relating to Corps projects. Charts may be obtained from various Federal agencies including the Defense Mapping Agency Hydrographic Center, Geological Survey, National Ocean Service, and Defense Mapping Agency Topographic Center. A map called "Status of Aerial Photography," which may be obtained from the Map Information Office, Geological Survey, Washington, D.C. 20242, shows the locations and types of aerial photos available for the U.S. and lists the sources from which the photos may be requested. A description of a coastal imagery data bank can be found in the interim report by Szuwalski (1972).

Other kinds of data usually available are wave, tide, and meteorological data. Chapter 3 discusses wave and water level predictions; Chapter 4, Section III discusses the effects of waves on the littoral zone; and Chapter 4, Section III,d presents methods of estimating wave climate and gives possible sources of data. These referenced sections indicate the wave, tide, and storm data necessary to evaluate coastal engineering problems.

Additional information can be obtained from local newspapers, courthouse records, and area residents. Local people can often identify factors that outsiders may not be aware of, and can also provide qualitative information on previous coastal engineering efforts in the area and their effects.

b. Interpretation of Shoreline Position. Preliminary interpretation of littoral processes is possible from the position of the shoreline on aerial photos and charts. Stafford (1971) describes a procedure for utilizing periodic aerial photographs to estimate coastal erosion. Used in conjunction with charts and topographic maps, this technique may provide quick and fairly accurate estimates of shoreline movement, although the results can be biased by the short-term effects of storms.

Charts show the coastal exposure of a study site, and, since exposure determines the possible directions from which waves reach the coast, exposure also determines the most likely direction of longshore transport.

Direction of longshore transport may also be indicated by the position of sand accumulation and beach erosion around littoral barriers. A coastal structure in the surf zone may limit or prevent the movement of sand, and the buildup of sediment on one side of the littoral barrier serves as an indicator of the net direction of transport. This buildup can be determined from dredging or sand bypassing records or aerial photos. Figure 4-52 shows the accumulation of sand on one side of a jetty. But wave direction and nearshore currents at the time of the photo indicate that transport was then in the

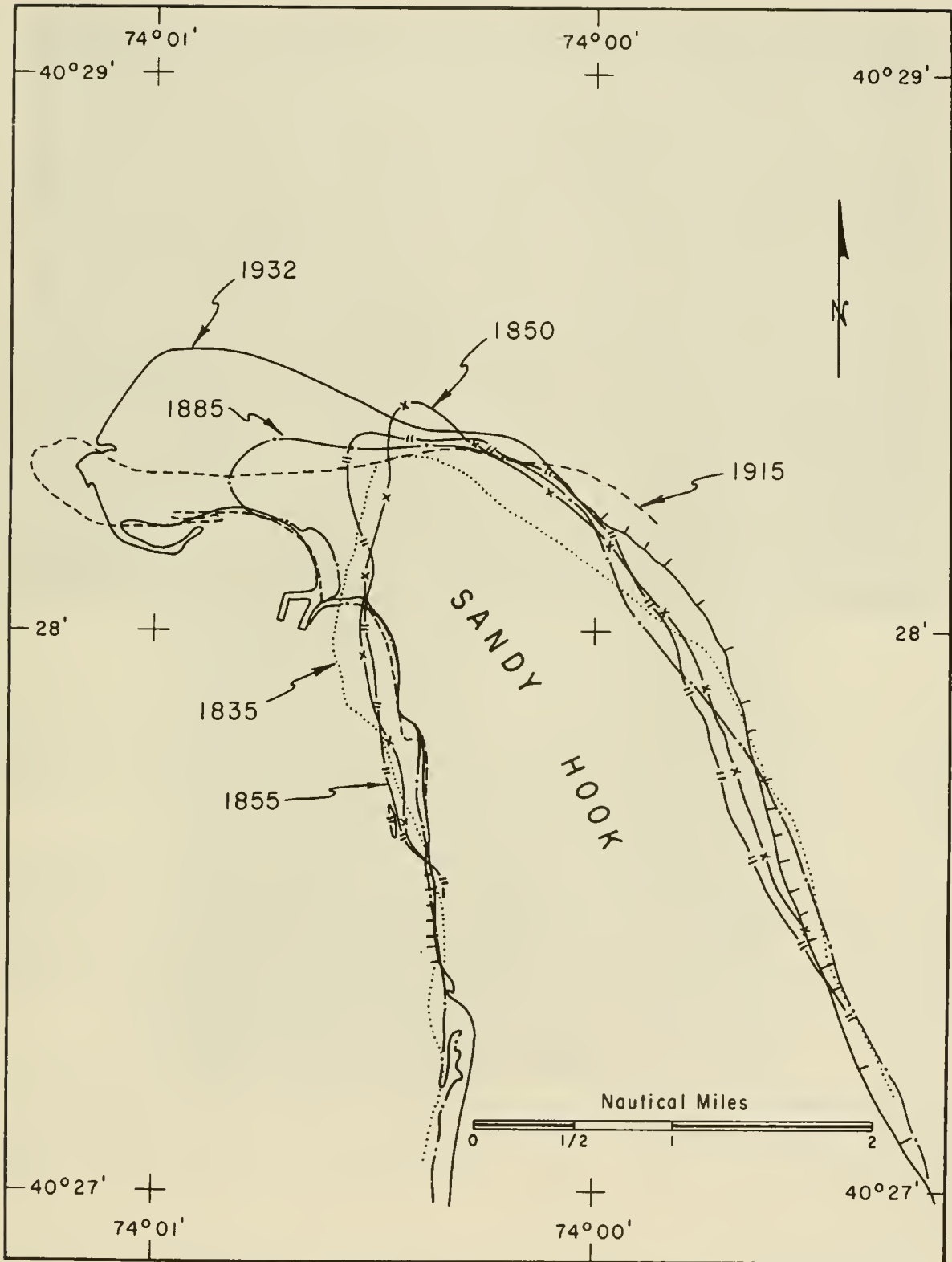


Figure 4-51. Growth of Sandy Hook, New Jersey, 1835-1932



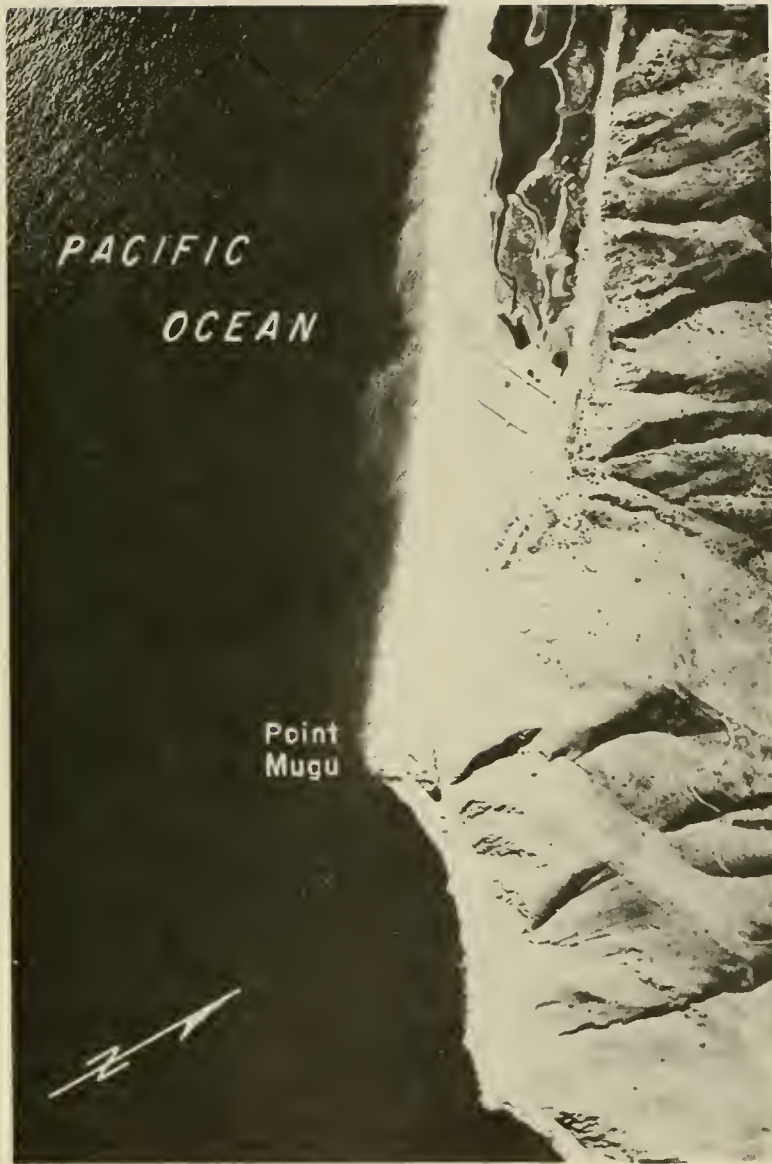
Figure 4-52. Transport directions at New Buffalo Harbor Jetty on Lake Michigan.

opposite direction. Thus, an erroneous conclusion about the net transport might be made, if only wave patterns of this photo are analyzed. The possibility of seasonal or storm-induced reversals in sediment transport direction should be investigated by periodic inspections or aerial photos of the sand accumulation at groins and jetties.

The accumulation of sand on the updrift side of a headland is illustrated by the beach north of Point Mugu in Figure 4-53. The tombolo in Figure 4-54 was created by deposition behind an offshore barrier (Greyhound Rock, California). Where a beach is fixed at one end by a structure or natural rock formation, the updrift shore tends to align perpendicular to the direction of dominant wave approach (see Figs. 4-54, and 4-55.) This alignment is less complete along shores with significant rates of longshore transport.

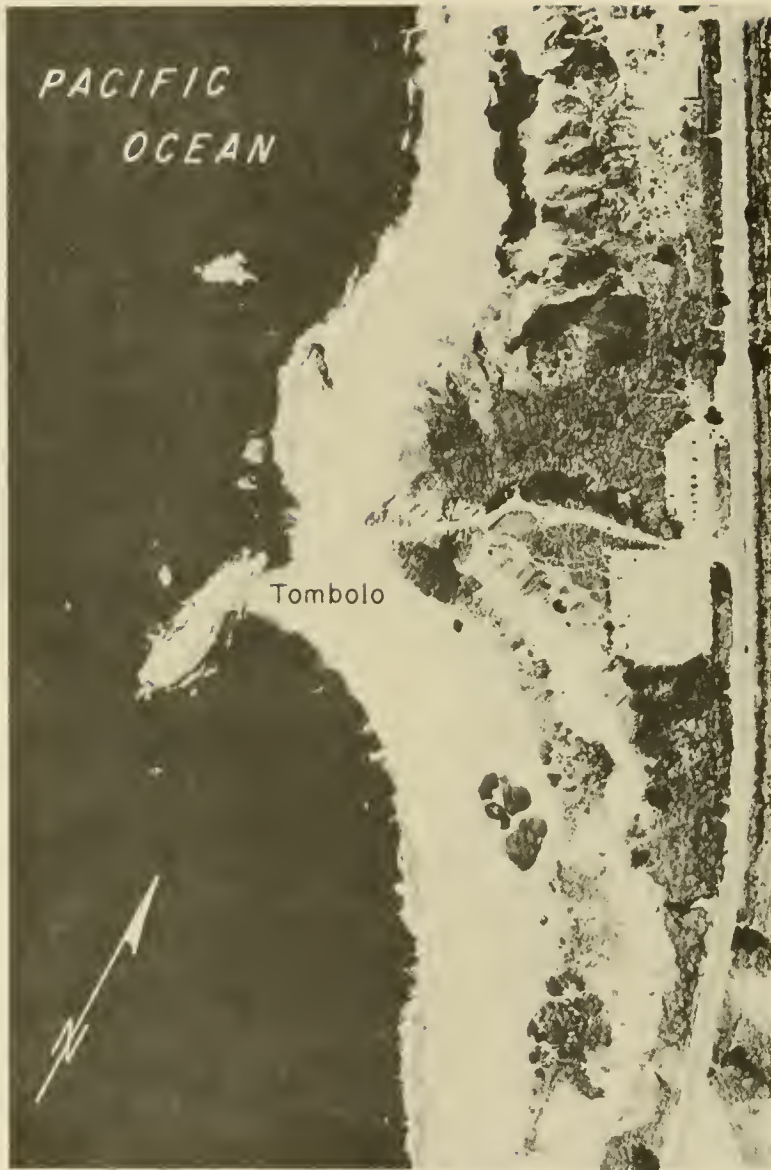
Sand accumulation at barriers to longshore transport may also be used to identify nodal zones. There are two types of nodal zones: divergent and convergent. A divergent nodal zone is a segment of shore characterized by net longshore transport directed away from both ends of the zone. A convergent nodal zone is a segment of shore characterized by net longshore transport directed into both ends of the zone.

Figure 4-55 shows a nodal zone of divergence centered around the fourth groin from the bridge on the south coast of Staten Island, Outer New York Harbor. Central Padre Island, Texas, is thought to be an example of a convergent nodal zone (Watson, 1971). Nodal zones of divergence are more common than nodal zones of convergence, because longshore transport commonly



(21 May 1972)

Figure 4-53. Sand accumulation at Point Mugu, California.



(29 August 1972)

Figure 4-54. Tombolo and pocket beach at Greyhound Rock, California.



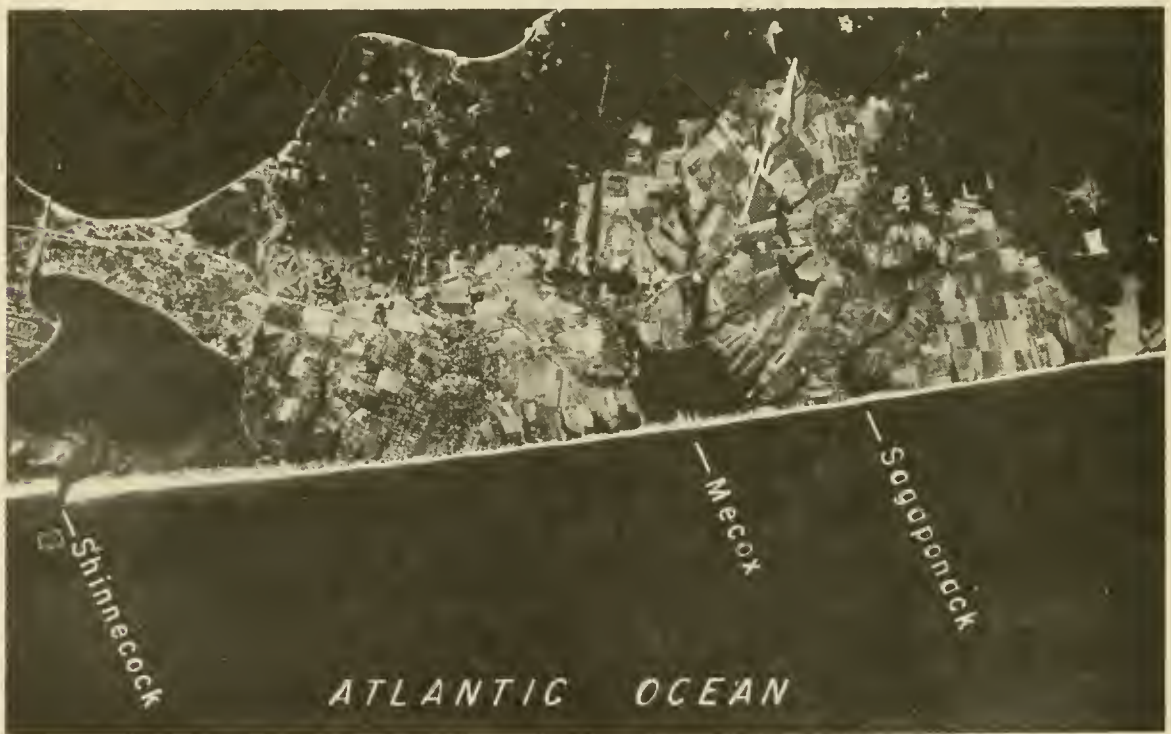
(14 September 1969)

Figure 4-55. Nodal zone of divergence illustrated by sand accumulation at groins, south shore, Staten Island, New York.

diverges at exposed shores and converges toward major gaps in the ocean shore, such as the openings of New York Harbor, Delaware Bay, and Chesapeake Bay.

Nodal zones are usually defined by long-term average transport directions, but because of insufficient data, the location of the midpoint of the nodal zone may be uncertain by up to 10's of kilometers. In addition, the short-term nodal zone most probably shifts along the coast with changes in wave climate.

The existence, location, and planform of inlets can be used to interpret the littoral processes of the region. Inlets occur where tidal flow is sufficient to maintain the openings against longshore transport which acts to close them (e.g., Bruun and Gerritsen, 1959). The size of the inlet opening depends on the tidal prism available to maintain it (O'Brien, 1969). The dependence of inlet size on tidal prism is illustrated by Figure 4-56, which shows three bodies of water bordering the beach on the south shore of Long Island, New York. The smallest of these (Sagaponack Pond) is sealed off by longshore transport; the middle one (Mecox Bay) is partly open; and the largest (Shinnecock Bay) is connected to the sea by Shinnecock Inlet, which is navigable.



(14 September 1969)

Figure 4-56. South shore of Long Island, New York, showing closed, partially closed, and open inlets.

Detailed study of inlets through barrier islands on the U.S. Atlantic and gulf coasts shows that the shape of the shoreline at an inlet can be classified in one of four characteristic planforms (See Fig. 4-57, adapted from Galvin, 1971). Inlets with overlapping offset (Fig. 4-58) occur only

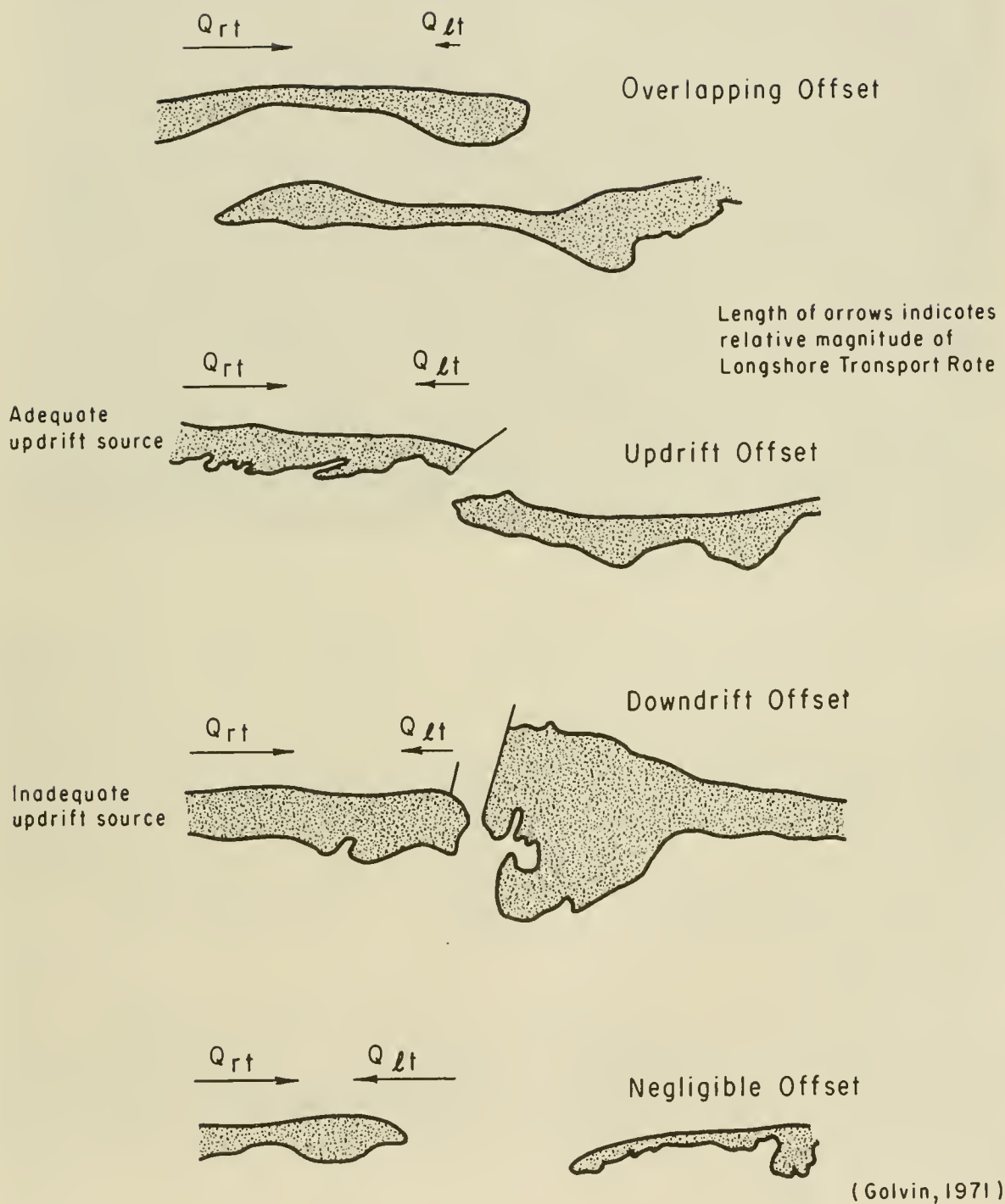


Figure 4-57. Four types of barrier island offset.



(14 September 1969)

Figure 4-58. Fire Island Inlet, New York: overlapping offset.

where waves from the updrift side dominate longshore transport. Where waves from the updrift side are less dominant, the updrift offset (Fig. 4-57) is common. Where waves approach equally from both sides, inlets typically have negligible offset (see Fig. 4-59). Where the supply of littoral drift on the updrift side is limited and the coast is fairly well exposed, a noticeable downdrift offset is common as, for example, in southern New Jersey and southern Delmarva (see Hayes, Goldsmith, and Hobbs, 1970). These planform relations to littoral processes have been found for inlets through sandy barrier islands, but they do not necessarily hold at inlets with rocky boundaries. The relations hold regionally, but temporary local departures due to inlet migration may occur.

## 2. Field Study.

A field study of the problem area is usually necessary to obtain types of data not found in the office study, to supplement incomplete data, and to serve as a check on the preliminary interpretation and correlations made from the office data. Information on coastal processes may be obtained from wave gage data and visual observations, sediment sampling, topographic and bathymetric surveys, tracer programs, and observation of effects of natural and manmade structures.

a. Wave Data Collection. A wave-gaging program yields height and period data. However, visual observations may currently be the best source of breaker direction data. Thompson and Harris (1972) determined that 1 year of wave-gage records provides a reliable estimate of the wave height frequency



(13 March 1963)

Figure 4-59. Old Drum Inlet, North Carolina: negligible offset.

distribution. It is reasonable to assume that the same is true for wave direction.

A visual observation program is inexpensive and may be used for breaker direction and for regional coverage when few wave-gage records are available. The observer should be provided with instructions so that all data collected will be uniform, and contact between observer and engineer should be maintained.

b. Sediment Sampling. Sediment sampling programs are described in Section II,6. Samples are usually surface samples taken along a line perpendicular to the shoreline. These are supplemented by borings or cores as necessary. Complete and permanent identification of the sample is important.

c. Surveys. Most engineering studies of littoral processes require surveying the beach and nearshore slope. Successive surveys provide data on changes in the beach due to storms, or long-term erosion or accretion. If beach length is also considered, an approximate volume of sand eroded or accreted can be obtained which provides information for the sediment budget of the beach. The envelope of a profile defines fluctuations of sand level at a site (Everts, 1973) and thus provides data useful in beach fill and groin design.

Methods for obtaining beach and nearshore profiles and the accuracy of the resulting profiles are discussed in Section V,1,d.

d. Tracers. It is often possible to obtain evidence on the direction of

sediment movement and the origins of sediment deposits by the use of tracer materials which move with the sediment. Fluorescent tracers were used to study sand migration in and around South Lake Worth Inlet, Florida (Stuiver and Purpura, 1968). Radioactive sediment tracer tests were conducted to determine whether potential shoaling material passes through or around the north and south jetties of Galveston Harbor (Ingram, Cummins, and Simmons, 1965).

Tracers are particles which react to fluid forces in the same manner as particles in the sediment whose motion is being traced, yet which are physically identifiable when mixed with this sediment. Ideally, tracers must have the same size distribution, density, shape, surface chemistry, and strength as the surrounding sediment; in addition they must have a physical property that easily distinguishes them from their neighbors.

Three physical properties have been used to distinguish tracers: radioactivity, color, and composition. Tracers may be either naturally present or introduced by man. There is considerable literature on recent investigations using or evaluating tracers, including reviews and bibliography (Duane and Judge, 1969; Bruun, 1966; Galvin, 1964a; Huston, 1963), models of tracer motion (James, 1970; Galvin, 1964b; Hubbell and Sayre, 1965; and Duane, 1970b), and use in engineering problems (Hart, 1969; Cherry, 1965; Cummins, 1964; and Duane, 1970b).

(1) Natural Tracers. Natural tracers are used primarily for background information about sediment origin and transport directions; i.e., for studies which involve an understanding of sediment patterns over a long period of time.

Studies using stable, nonradioactive natural tracers may be based on the presence or absence of a unique mineral species, the relative abundance of a particular group of minerals within a series of samples, or the relative abundance and ratios of many mineral types in a series of samples. Although the last technique is the most complex, it is often used because of the large variety of mineral types normally present in sediments and the usual absence of singularly unique grains. The most suitable natural tracers are grains of a specific rock type originating from a localized specific area.

Occasionally, characteristics other than mineralogy are useful for deducing source and movement patterns. Krinsley et al., (1964) developed a technique for the study of surface textures of sand grains with electron microscopy and applied the technique to the study of sand transport along the Atlantic shore of Long Island. Naturally occurring radioactive materials in beach sands have also been used as tracers (Kamel, 1962).

One advantage of natural tracers is their tendency to "average" out short-term trends and provide qualitatively accurate historical background information on transport. Their use requires a minimum amount of field work and a minimum number of technical personnel. Disadvantages include the irregularity of their occurrence, the difficulty in distinguishing the tracer from the sediment itself, and a lack of quantitative control on rates of injection. In addition, natural tracers are unable to reveal short-term changes in the direction of transport and changes in material sources.

Judge (1970) found that heavy mineral studies were unsatisfactory as indicators of the direction of longshore transport for beaches between Point Conception and Ventura, California, because of the lack of unique mineral species and the lack of distinct longshore trends which could be used to identify source areas. North of Point Conception, grain size and heavy mineral distribution indicated a net southward movement. Cherry (1965) concluded that the use of heavy minerals as an indicator of the direction of coastal sand movement north of Drakes Bay, California, was generally successful.

(2) Artificial Tracers. Artificial tracers may be grouped into two general categories: radioactive or nonradioactive. In either case, the tracers represent particles that are placed in an environment selected for study and are used for relatively short-term studies of sediment dispersion.

While particular experiments employ specific sampling methods and operational characteristics, there are basic elements in all tracing studies. These are (a) selection of a suitable tracer material, (b) tagging the particle, (c) placing the particle in the environment, and (d) detection of the particle.

Colored glass, brick fragments, and oolitic grains are a few examples of nonradioactive particles that have been used as tracers. The most commonly used stable tracer is made by coating indigenous grains with bright colored paint or fluorescent dye (Yasso, 1962; Ingle, 1966; Stuvier and Purpura, 1968; Kidson and Carr, 1962; Teleki, 1966). The dyes make the grains readily distinguishable among large sample quantities, but do not significantly alter the physical properties of the grains. The dyes must be durable enough to withstand short-term abrasion. The use of paints and dyes as tracer materials offers advantages over radioactive methods in that they require less sophisticated equipment to tag and detect the grains, nor do they require licensing or the same degree of safety precautions. However, less information is obtained for the same costs, and generally in a less timely matter.

When using nonradioactive tracers, samples must be collected and removed from the environment to be analyzed later by physically counting the grains. For fluorescent dyes and paints, the collected samples are viewed under an ultraviolet lamp and the coated grains counted.

For radioactive tracer methods, the tracer may be radioactive at the time of injection or it may be a stable isotope capable of being detected by activation after sampling. The tracer in the grains may be introduced by a number of methods. Radioactive material has been placed in holes drilled in a large pebble. It has been incorporated in molten glass which, when hardened, is crushed and resized (Sato, Ijima, and Tanaka, 1962; Taney, 1963). Radioactive material has been plated onto the surface of natural sediments (Stephens et al., 1968). Radioactive gas (krypton 85 and xenon 133) has been absorbed into quartz sand (Chleck et al., 1963; Acree et al., 1969).

In 1966, the Coastal Engineering Research Center, in cooperation with the Atomic Energy Commission, initiated a multiagency program to create a workable radioisotopic sand tracing (RIST) program for use in the littoral zone (Duane and Judge, 1969). Tagging procedures (by surface-plating with gold 198-199), instrumentation, field surveys, and data handling techniques were developed

which permit collection and analysis of over 12,000 bits of information per hour over a survey track about 5,500 meters (18,000 feet) long.

These developments in radioactive tracing permit *in situ* observations and faster data collection over much larger areas (Duane, 1970b) than has been possible using fluorescent or stable isotope tracers. However, operational and equipment costs of radionuclide tracer programs can be high.

Accurate determination of long-term sediment transport volume is not yet possible from a tracer study, but qualitative data on sediment movement useful for engineering purposes can be obtained.

Experience has shown that tracer tests can give information on direction of movement, dispersion, shoaling sources, relative velocity and movement in various areas of the littoral zone, means of natural bypassing, and structure efficiency. Reasonably quantitative data on movement or shoaling rates can be obtained for short time intervals. It should be emphasized that this type of information must be interpreted with care, since the data are generally determined by short-term littoral transport phenomena. However, tracer studies conducted repeatedly over several years at the same location could result in estimates of longer term littoral transport.

### 3. Sediment Transport Calculations.

a. Longshore Transport Rate. The example calculation of a sediment budget in Section VII,6 is typical in that the magnitude of the longshore transport rate exceeds by a considerable margin any other element in the budget. For this reason, it is essential to have a good estimate of the longshore transport rate in an engineering study of littoral processes.

A complete description of the longshore transport rate requires knowledge of two of the five variables

$$(Q_{rt}, Q_{pt}, Q_g, Q_n, \gamma)$$

defined by equations 4-31, 4-32, and 4-33. If any two are known, the remaining three can be obtained from the three equations.

Section V,3,a describes four methods for estimating longshore transport rate, and Sections V,3,b through V,3,f describe in detail how to use two of these four methods, (see methods 3 and 4).

One approach to estimating longshore transport rate is to adopt a proven estimate from a nearby locality, after making allowances for local conditions (see method 1). It requires considerable engineering judgment to determine whether the rate given for the nearby locality is a reliable estimate and, if reliable, how the rate needs to be adjusted to meet the changed conditions at the new locality.

Method 2 is an analysis of historical data. Such data may be found in charts, maps, aerial photography, dredging records, beach fill records, and related information. Section VIII,1,a describes some of these sources.

To apply method 2, it is necessary to know or assume the transport rate across one end of the littoral zone being considered. The most successful applications of method 2 have been where the littoral zone is bounded on one end by a littoral barrier which is assumed to completely block all longshore transport. The existence of such a complete littoral barrier implies that the longshore transport rate is zero across the barrier, and this satisfies the requirement that the rate be known across the end of the littoral zone being considered. Examples of complete littoral barriers include large jetties immediately after construction, or spits building into deep, quiet water.

Data on shoreline changes permit estimates of rates of erosion and accretion that may give limits to the longshore transport rate. Figure 4-51 is a shoreline change map which was used to obtain the rate of transport at Sandy Hook, New Jersey (Caldwell, 1966).

Method 3 (the energy flux method) is described in Sections V,3,b and V,3,c with a worked example in Section V,3,d. Method 4 (the empirical prediction of gross longshore transport rate) is described in Section V,3,e, with a worked example in Section V,3,f. The essential factor in methods 3 and 4, and often in method 1, is the availability of wave data. Wave data applicable to studies of littoral processes are discussed in detail in Section III.

b. Onshore-Offshore Motion. Typical problems requiring knowledge of onshore-offshore sediment transport are described in Section V,1,a. Four classes of problems are treated:

(1) The seaward limit of significant sediment transport. Available field data and theory suggest that waves are able to move sand during some days of the year over most of the continental shelf. However, field evidence from bathymetry and sediment size distribution suggest that the zone of significant sediment transport is confined close to shore where bathymetric contours approximately parallel the shoreline. The depth to the deepest shore-parallel contour tends to increase with average wave height, and typically varies from 5 to 18 meters (15 to 60 feet).

(2) Sediment transport in the nearshore zone. Seaward of the breakers, sand is set in motion by waves moving over ripples, either rolling the sand as bed load, or carrying it up in vortices as suspended load. The sand, once in motion, is transported by mean tidal and wind-induced currents and by the mass transport velocity due to waves. The magnitude and direction of the resulting sediment transport are uncertain under normal circumstances, although mass transport due to waves is more than adequate to return sand lost from the beach during storms. It appears that bottom mass transport acts to keep the sand close to the shore, but some material, probably finer sand, escapes offshore as the result of the combined wind- and wave-induced bottom currents.

(3) The shape and expectable changes in shape of nearshore and beach profiles. Storms erode beaches to produce a simple concave-up beach profile, with deposition of the eroded material offshore. Rates of erosion due to individual storms vary from a few cubic meters per meter to 10's of cubic meters per meter of beach front. The destructiveness of the storm in producing erosion depends on its intensity, duration, and orientation, especially as these factors affect the elevation of storm surge and the wave

height and direction. Immediately after a storm, waves begin to return sediment to the eroded beach, either through the motion of bar-and-trough (ridge-and-runnel) systems, or by berm building. The parameter  $F_0 = H_0/(Vft)$ , given by equation (4-29), determines whether the beach erodes or accretes under given conditions. If  $F_0$  is above critical value between 1 and 2, the beach erodes.

(4) The slope of the foreshore. There is a tendency for the foreshore to become steeper as grain size increases, and to become flatter as mean wave height increases. Data for this relation exhibit much scatter, and quantitative relationships are difficult to predict.

c. Sediment Budget. Section VII,6 summarizes material on the sediment budget. Table 4-16 tabulates the elements of the sediment budget and indicates the importance of each element. Table 4-15 classifies the elements of the sediment budget.

A sediment budget carefully defines the littoral control volume, identifies all elements transferring sediment to or from the littoral control volume, ranks the elements by their magnitude, and provides an estimate of unknown rates by the balancing of additions against losses (eq. 4-58).

If prepared with sufficient data and experience, the budget permits an estimate of how proposed improvements will affect neighboring segments of the littoral zone.

## IX. TIDAL INLETS

Some of the most important features of a sandy coastline from a standpoint of littoral processes are those breaks in its continuity which may be broadly classified as *estuaries* and *inlets*.

An estuary may be the mouth of a large river; but it is usually characterized by having a funnel shape and a wide opening to the sea (i.e., wide in relation to the length of the tidal wave in shallow water) and by being nonreflective to ocean long wave action (i.e., tidal waves can propagate up an estuary).

An inlet, on the other hand, generally has banks that are roughly parallel; it is usually small with respect to the interior basin and reflects long wave activity (inlet currents originate hydraulically because of hydraulic head difference between the ocean and bay, rather than due to tidal wave propagation).

This section will treat both of these shoreline continuity breaks under a broader definition of "inlets" since the effects of both are generally similar with respect to the littoral processes that occur in their vicinities.

### 1. Geomorphology of Tidal Inlets.

The bulge of sand formed just seaward of an inlet is called an *ebb-tidal delta*. Commonly, the ebb-tidal delta is offset; i.e., the sand accumulation protrudes farther seaward on the downdrift side than on the updrift side of the inlet. In areas of low average wave activity ebb-tidal deltas can extend

considerable distances offshore. Figure 4-60 is an example of an inlet on the gulf coast of Florida where the ebb-tidal delta extends 6.4 kilometers (4 miles) offshore. Dean and Walton (1973) attribute the large extent of this offshore delta to the relatively low amount of incoming wave energy expended on the ebb delta to move the sand shoreward.

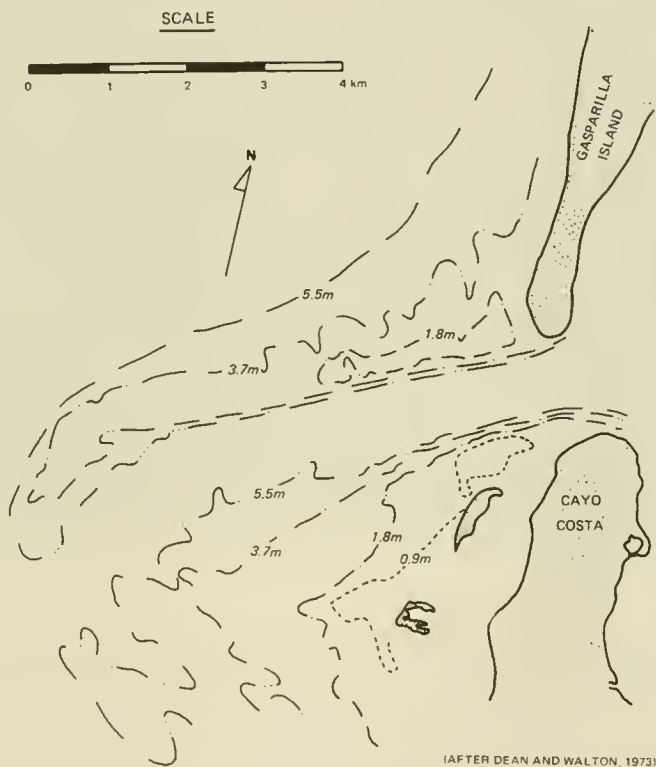
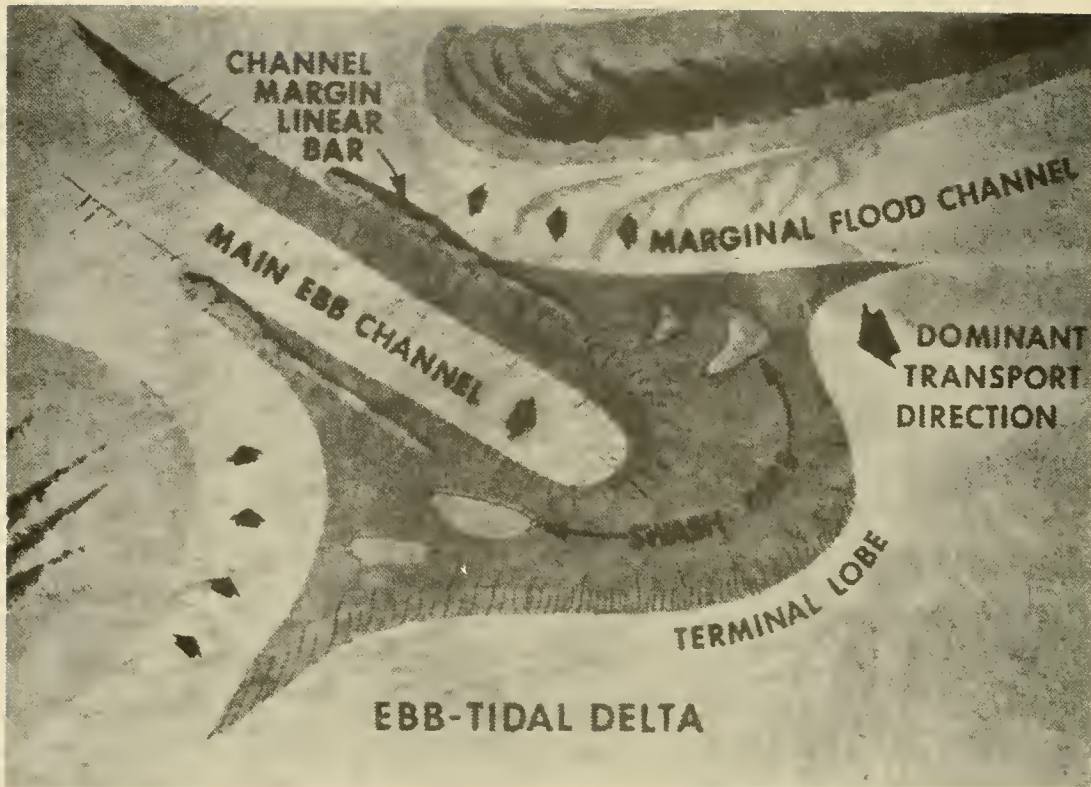


Figure 4-60. Ebb-tidal delta showing volumes accumulated in outer shoals adjacent to Boca Grande Inlet, Florida (low-energy shoreline).

Normally, three major forms of sediment accumulation are associated with ebb-tidal deltas (see Fig. 4-61):

(a) Asymmetric swash bars, oriented landward and formed by wave action, which form a broken semicircle around the perimeter of the ebb-tidal delta and sometimes meet the shore obliquely on either side of the inlet. Swash bars are essentially sediment masses arrested from the general longshore drift system. They form at the inlets because of a combination of the influence of (1) the ebb-tidal currents, which deposit the main lobe of the ebb-tidal delta, and (2) wave refraction around the lobe, which tends to slow down, or halt, the transport of sand past the inlet.

(b) Channel margin linear sand bars that trend perpendicular to shore and parallel to the main channel.



(after Hayes, 1975)

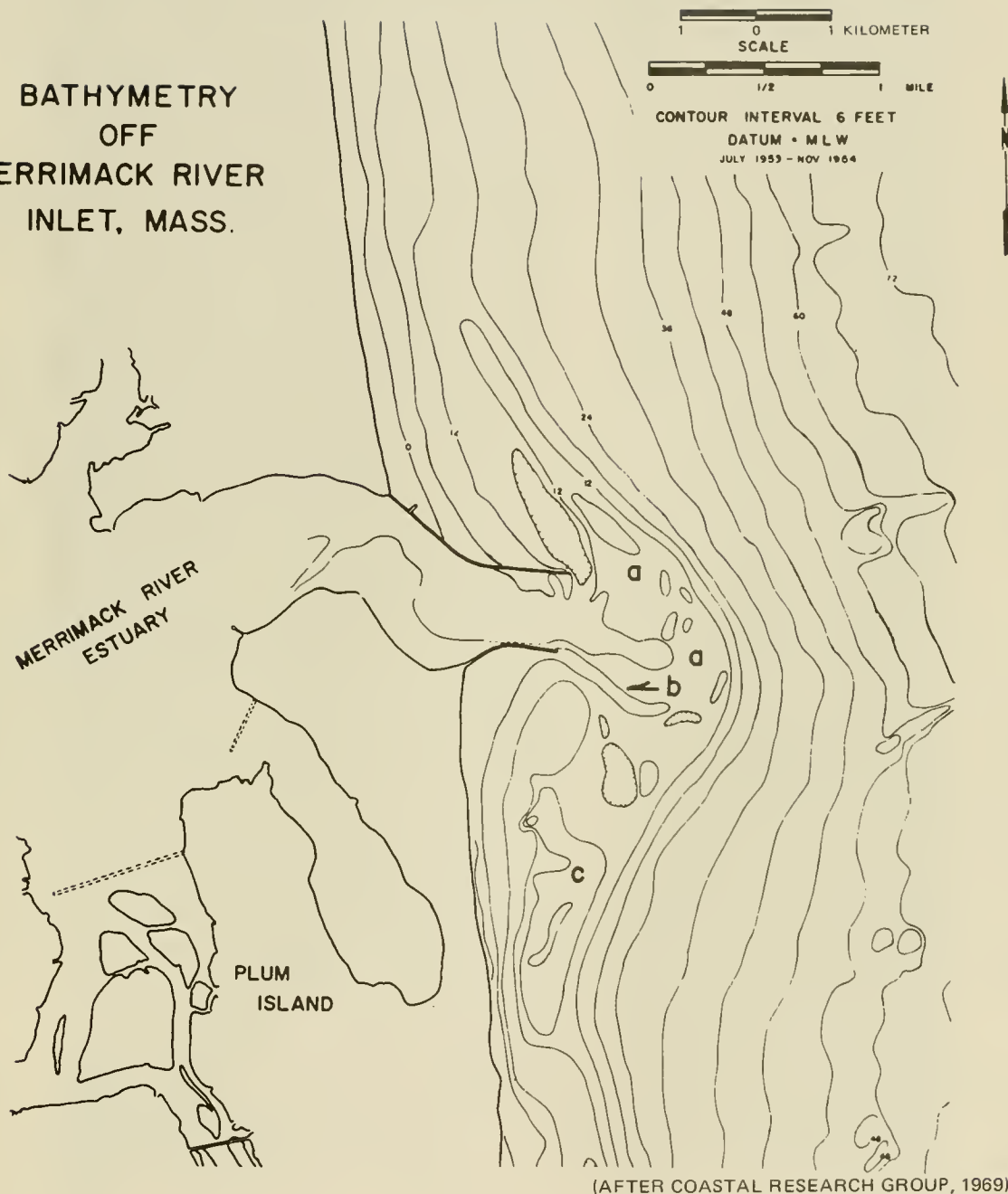
Figure 4-61. Typical ebb-tidal delta morphology. (The ebb jet maintains a deep central trough, the main ebb channel, flanked by channel margin linear bars and wide arcuate swash platforms. Wave action on the swash platforms generates landward-migrating swash bars. Marginal flood channels separate the channel margin linear bars from the adjacent beaches. Different patterns indicate which areas are dominated by ebb currents, flood currents, or waves.)

(c) A lunate, subaqueous terminal lobe deposited seaward of the main channel by ebb currents, which normally has a large ebb-oriented slip face around its seaward margin.

The topography of the ebb-tidal delta of the Merrimack River Inlet, Massachusetts, is illustrated in Figure 4-62. This inlet shows the typical *downdrift* offset on the south side of the inlet (i.e., the side downdrift of predominant wave action and littoral transport). This offset is a feature caused by a wave sheltering of the downdrift side of the inlet by the ebb-tidal delta. As noted in Section IX,2, this downdrift side of the inlet also experiences a littoral current reversal under waves from the dominant wave direction because of refraction around the ebb-tidal delta complex.

Although many inlets have a downdrift offset, there are also inlets which are offset in the updrift direction, so ebb-tidal delta geomorphology alone is not sufficient to provide the information necessary to determine the dominant sand transport direction.

BATHYMETRY  
OFF  
MERRIMACK RIVER  
INLET, MASS.



(AFTER COASTAL RESEARCH GROUP, 1969)

Figure 4-62. Bathymetry off the Merrimack River Inlet, Massachusetts. (The total ebb-tidal delta complex is subtidal, but it shows the major forms normally affiliated with ebb-tidal deltas: (a) lunate bar seaward of the main channel; (b) linear bar parallel with main channel (note bar extending seaward from the end of the south jetty); and (c) asymmetrical, wave-formed bars (i.e., swash bars; note large bar located one mile south of south jetty). Contours based on data of National Ocean Service, Hydrographic Survey No. 8096 (July 1953–November 1954).)

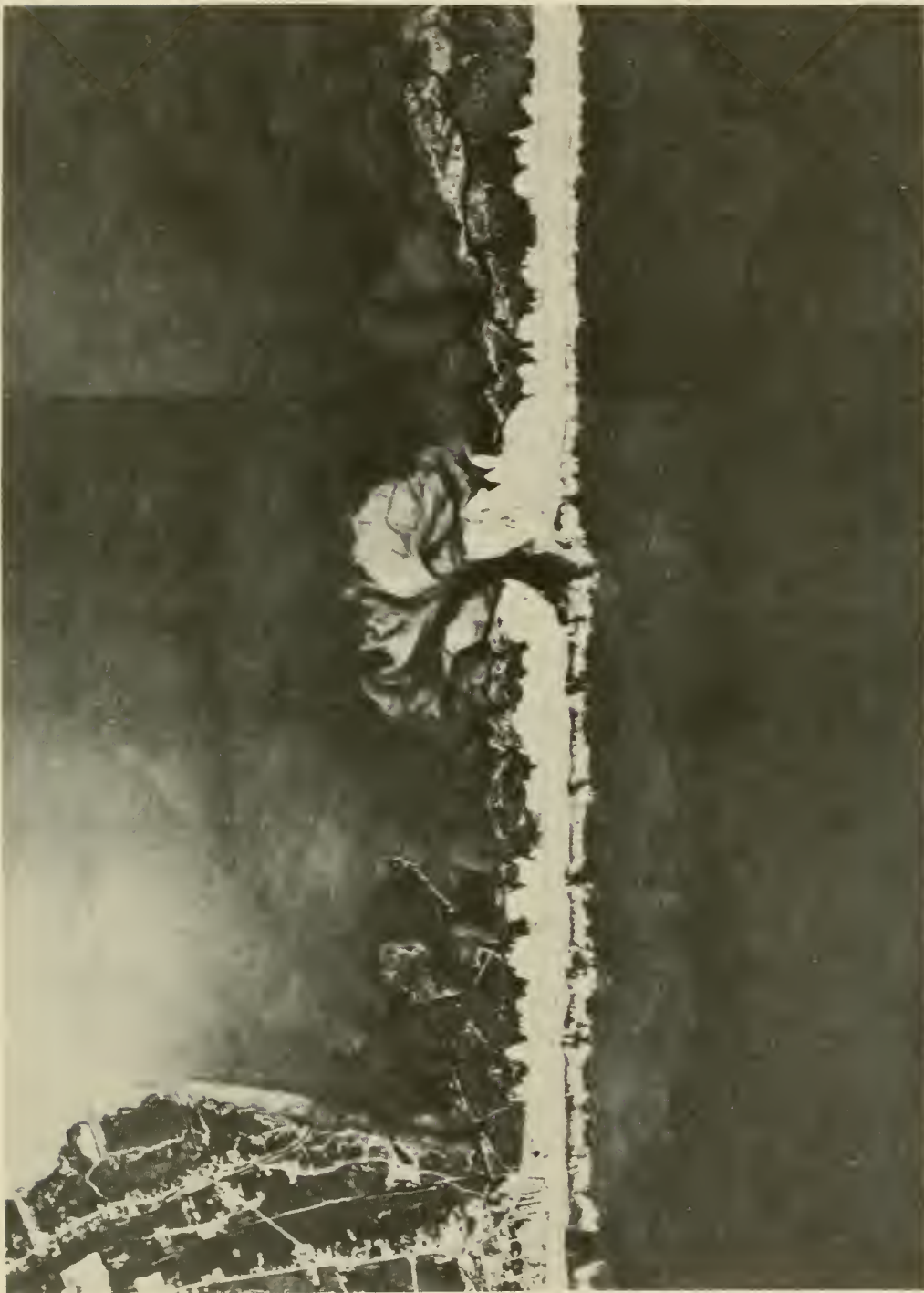
A common feature of ebb-tidal deltas is the segregation of ebb and flood flow. Each inlet usually has a main channel oriented perpendicular to the shoreline, which carries a large portion of the ebb flow. The flood flow, on the other hand, tends to be distributed as a sheet, with several individual flood channels developed in some cases. Usually the flood channels hug both beaches, flanking the main ebb channel (Fig. 4-61).

This segregation of flow is caused by the time-velocity asymmetry of the tidal currents. Maximum flood velocities are usually late in the flood-tidal phase of the tidal cycle, between midtide and high tide. Similarly, maximum ebb flow is between midtide and low tide, usually quite close to low tide. Thus, the ebb flow tends to be more channelized than the flood, which is evenly distributed across the inlet delta.

The inner shoal-flood-tidal delta system of an inlet is typically more difficult to categorize than the ebb-tidal delta because of the varied physiographical system comprising the inlet landward of its ocean-shore boundary. Just inside the landward end of the channel of many inlets, a large shoal commonly termed the *middle ground* shoal develops. This shoal is typically made up of finer material than are the beaches adjacent to the inlet. The middle ground shoal is formed in the slow divergence area of the flood tide. An example of a middle ground shoal is shown in Figure 4-63.

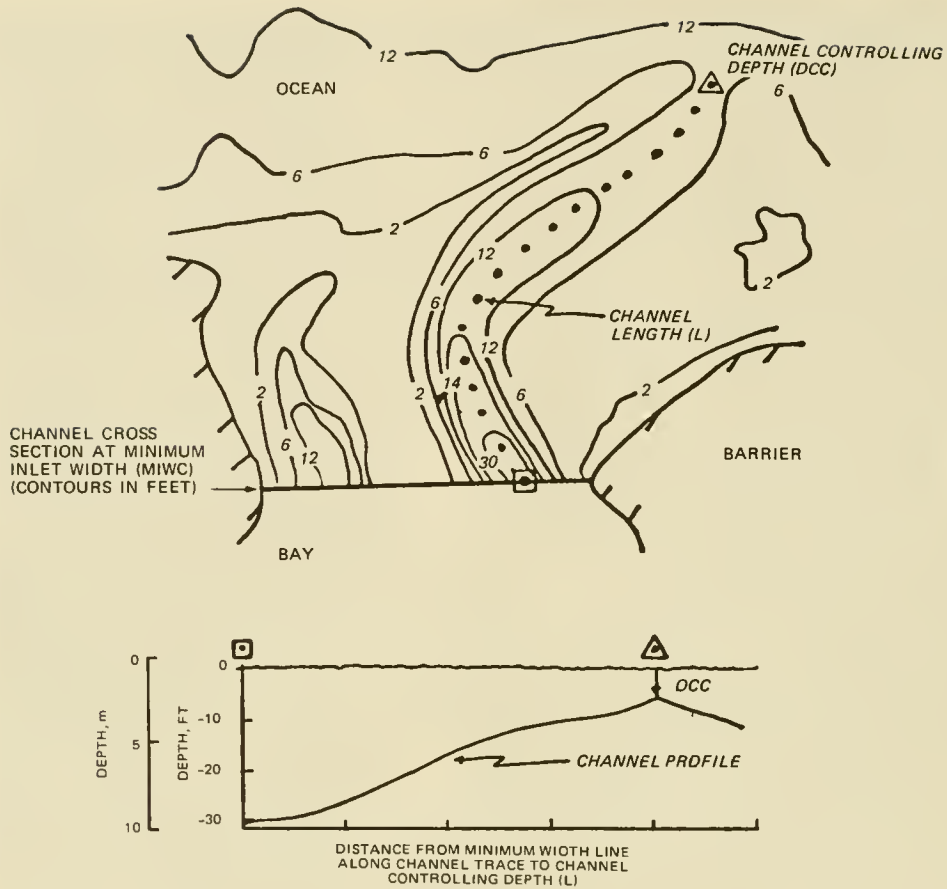
A number of investigators (Bruun and Gerritsen, 1957; Bates, 1953; Galvin, 1971; Vincent and Corson, 1980) have studied the relationships among various geometric properties of tidal inlets and noted various trends and correlations among certain inlet parameters, such as inlet cross section minimum area, channel length, maximum channel depth in minimum width cross section, ebb delta area, and controlling depth over outer bar. Vincent and Corson (1980) have systematically defined many of these inlet parameters, as shown in Figures 4-64 and 4-65. They have also made statistical correlations of the parameters to ascertain significant relationships for 67 inlets, most of which did not have engineering structures (jetties, etc.) at the time of survey. The more important of these correlations are provided in Figures 4-66 through 4-69. These correlations show a strong dependence of inlet geometry on channel minimum width cross-sectional area, which has been found by O'Brien (1969) and others to depend strongly on the tidal prism.

O'Brien (1969) originally found a relationship between the minimum *throat* cross-sectional area of an inlet below mean tide level and the tidal prism (i.e., the volume of water entering or exiting the inlet on ebb and flood tide) at spring tide. This relationship was predominantly for Pacific coast tides, where a mixed tidal pattern is observed. A more recent correlation between inlet minimum cross-sectional area at throat section and tidal prism has been given in the work of Jarrett (1976) where regression analyses were made for various coastal areas with different tidal characteristics. Jarrett (1976) has given a regression equation for each of the Atlantic, Pacific, and gulf coasts. The equations, in metric (a) and English (b) units, are as follows:



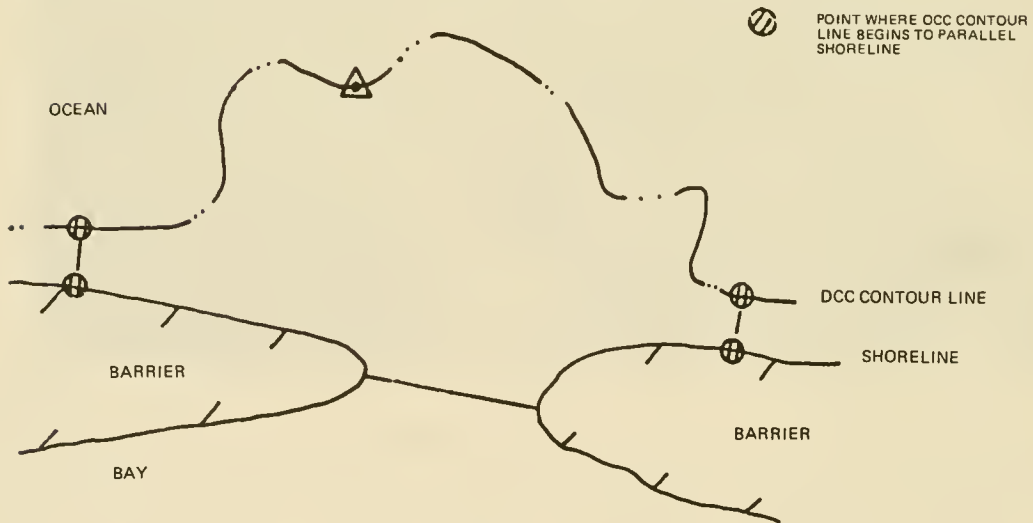
(National Ocean Service, May 1962)

Figure 4-63. Old Drum Inlet, about 10 kilometers (6 miles) north of Cape Hatteras, North Carolina. (Inlet was opened by the March 1962 Atlantic storm. Tidal delta had formed in less than 2 months. About 10 months after being opened, the inlet was artificially closed by the U.S. Army Corps of Engineers.)



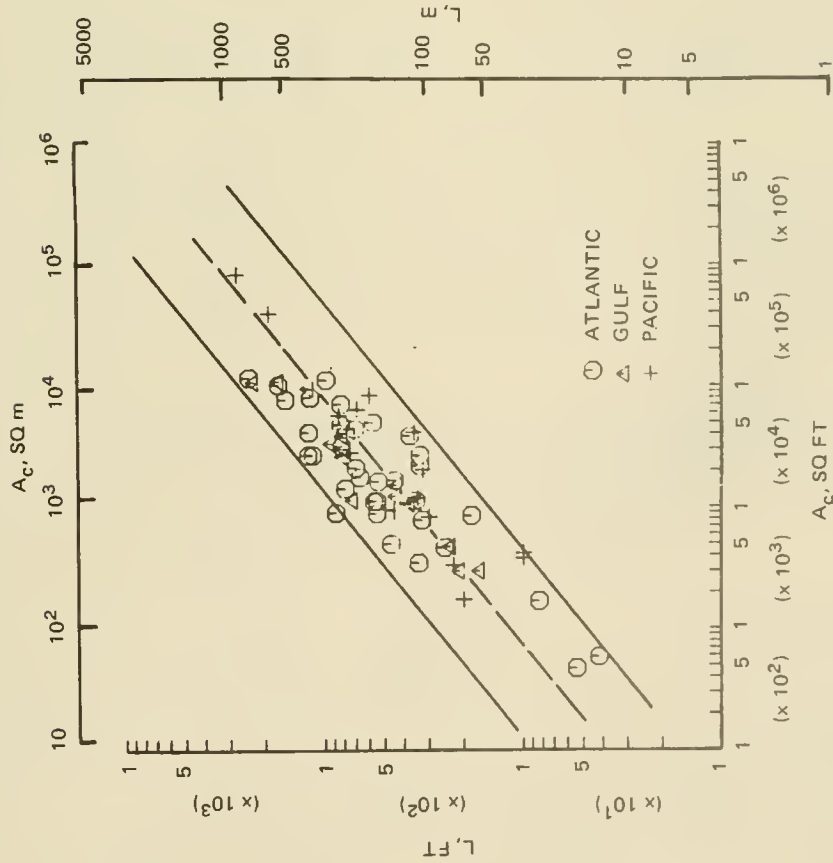
( FROM VINCENT AND CORSON, 1980)

Figure 4-64. Measurement of channel parameters.



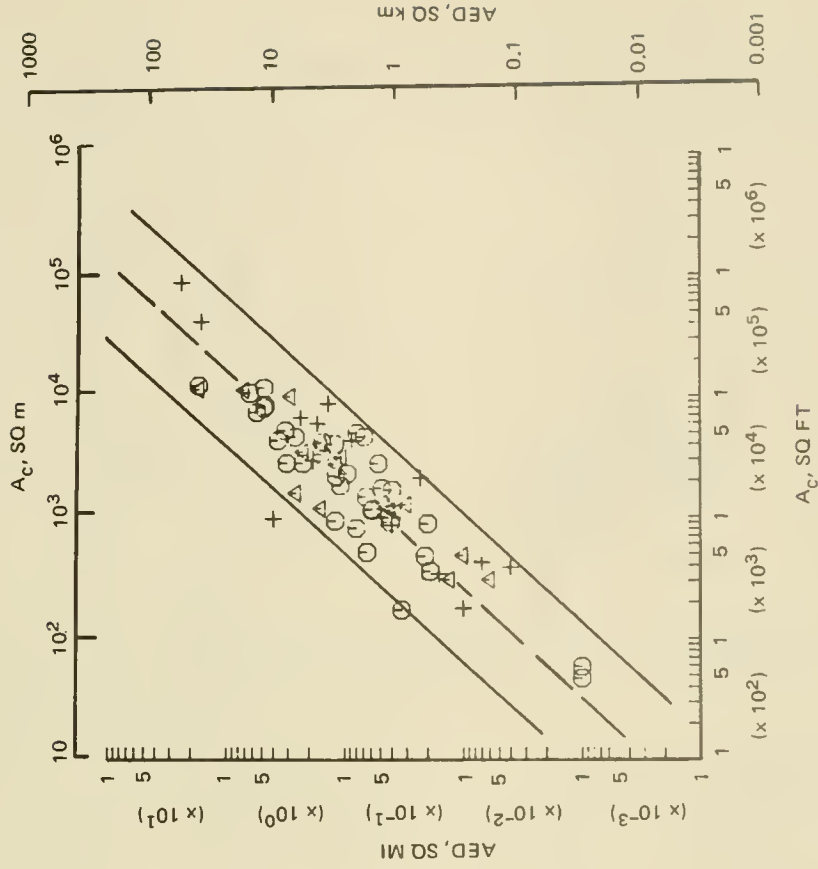
(FROM VINCENT AND CORSON, 1980)

Figure 4-65. Measurement of ebb delta area.



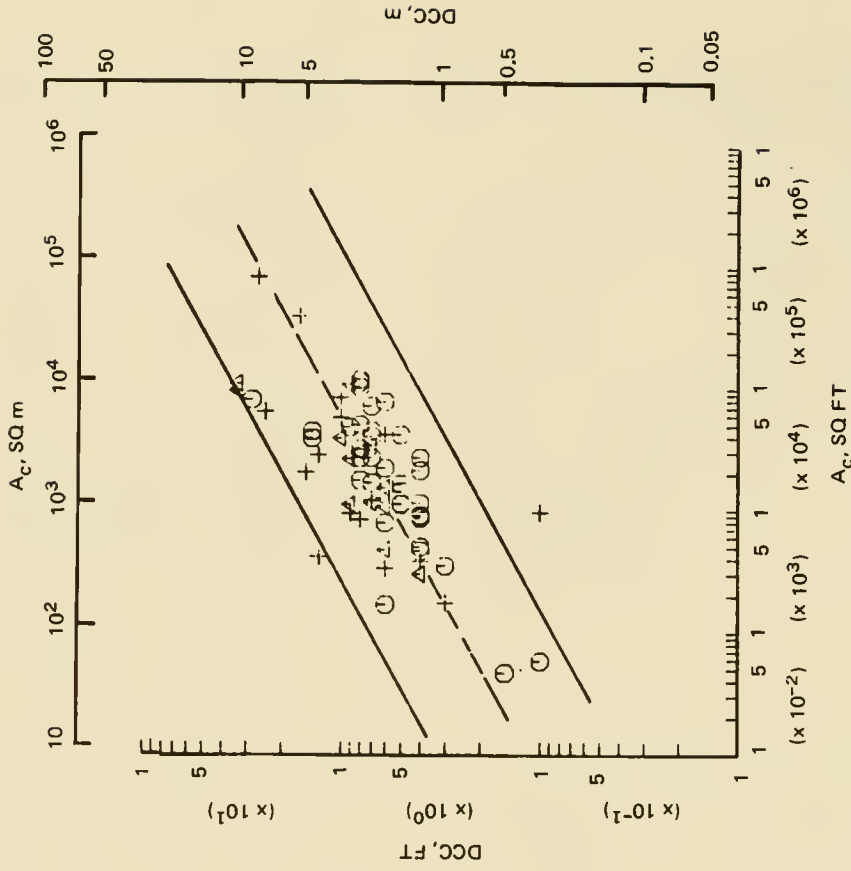
(after Vincent and Corson, 1980)

Figure 4-66. Minimum width cross-sectional area of channel  $A_c$  versus channel length  $L$ .



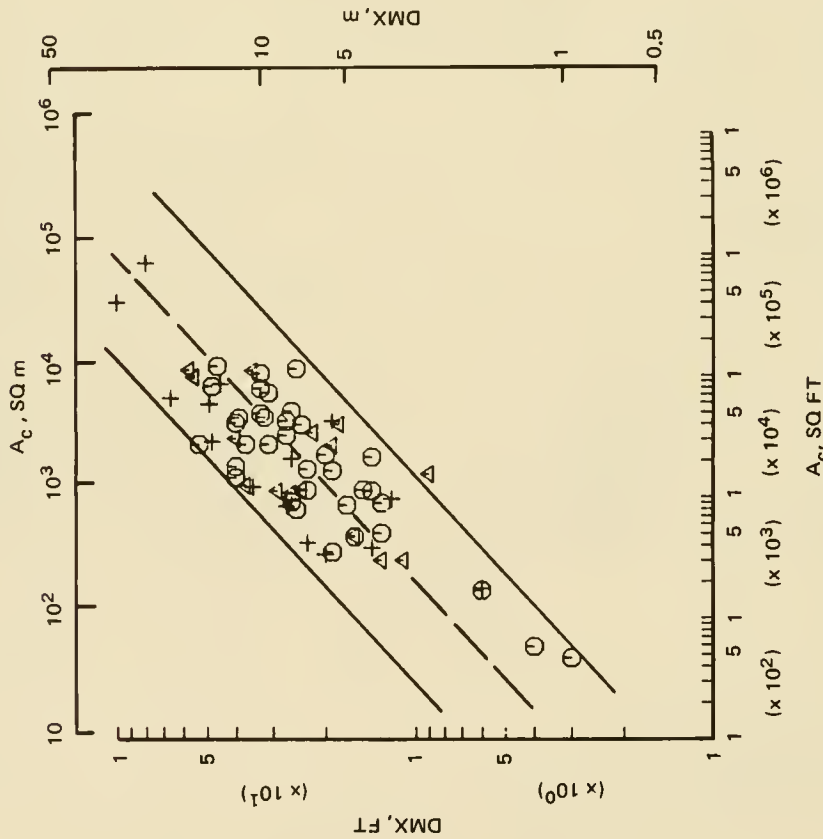
(after Vincent and Corson, 1980)

Figure 4-67.  $A_c$  versus ebb-tidal delta area.



(after Vincent and Corson, 1980)

Figure 4-69.  $A_c$  versus minimum controlling channel depth DCC .



(after Vincent and Corson, 1980)

Figure 4-68.  $A_c$  versus maximum channel depth at minimum width section DMX .

$A_c = 3.039 \times 10^{-5} P^{1.05}$	Atlantic coast	(4-61a)
$A_c = 7.75 \times 10^{-6} P^{1.05}$	Atlantic coast	(4-61b)
$A_c = 9.311 \times 10^{-4} P^{0.84}$	gulf coast	(4-62a)
$A_c = 5.02 \times 10^{-4} P^{0.84}$	gulf coast	(4-62b)
$A_c = 2.833 \times 10^{-4} P^{0.91}$	Pacific coast	(4-63a)
$A_c = 1.19 \times 10^{-4} P^{0.91}$	Pacific coast	(4-63b)

where  $A_c$  is the minimum cross-sectional area in square meters (square feet) and  $P$  is the tidal prism in cubic meters (cubic feet). A plot of inlet tidal prisms versus minimum cross-sectional areas for all of Jarrett's data is given in Figure 4-70.

Jarrett's (1976) work pertains to equilibrium minimum cross-sectional areas at tidal channels as ascertained from one survey at a given date. Byrne, De Alteris, and Bullock (1974) have shown that inlet cross section can change on the order of  $\pm 10$  percent in very short time periods (see Figure 4-71). In one case Byrne, De Alteris, and Bullock (1974) noted a 7 percent reduction of cross-sectional area in 3 days followed by a 10 percent cross-sectional area increase 1 week later for an inlet with an equilibrium cross-sectional area of approximately 4,500 square meters.

Ebb-tidal deltas of inlets can also change significantly in short periods of time. Brown (1928) notes that for Absecon Inlet, New Jersey, "a single northeaster has been observed to push as much as 100,000 cubic yards of sand in a single day into the channel on the outer bar, by the elongation of the northeast shoal, resulting in a decrease in depth on the centerline of the channel by 6 to 7 feet."

Such changes also effect changes in the hydraulics of the inlet system, which in turn remodel the shoaling patterns. Shoal changes at inlets may simply be perturbations around an *equilibrium* geometry, dynamic changes in a cyclic pattern of inlet geometry change, or a permanent inlet geometry change.

## 2. Circulation Patterns at Tidal Inlets.

Typical flood and ebb current patterns on the ocean side of a tidal inlet are shown in Figure 4-72. The important aspect of this general circulation pattern is that the currents always flow toward the inlet near the shoreline (in the *flood* channels), even on ebbside. The reason for this seeming paradox is the effect of the wave-driven currents caused by wave refraction around the outer bar. On the downdrift side of the inlet the waves are turned toward the inlet due to refraction over the outer bar and, hence, cause currents toward the inlet; although further down the downdrift coast, currents are directed away from the inlet. An example of this effect is given in Figure 4-73.

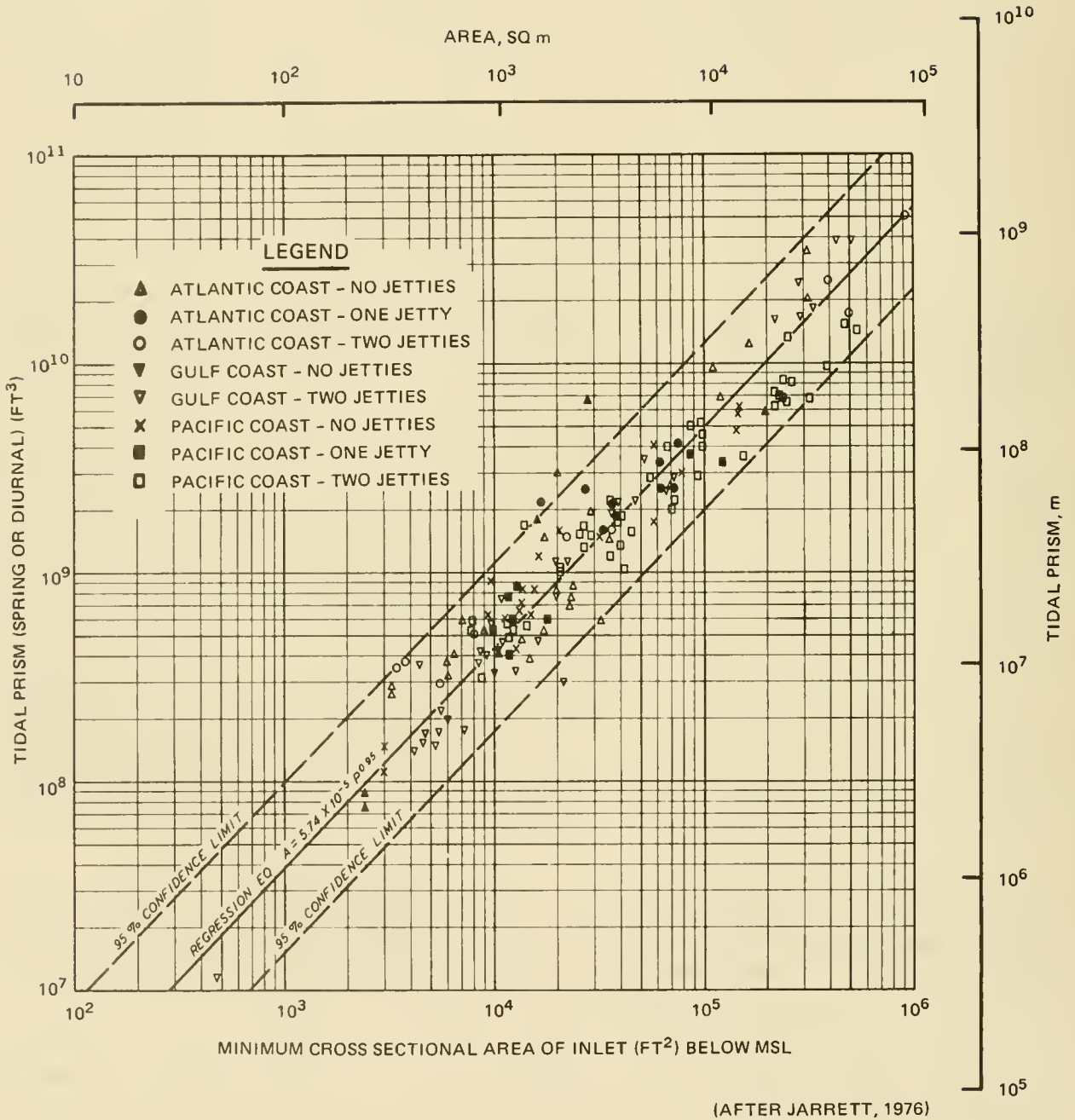


Figure 4-70. Tidal prism versus cross-sectional area for all inlets on Atlantic, gulf, and Pacific coasts. (These are regression curves with 95 percent confidence limits.)

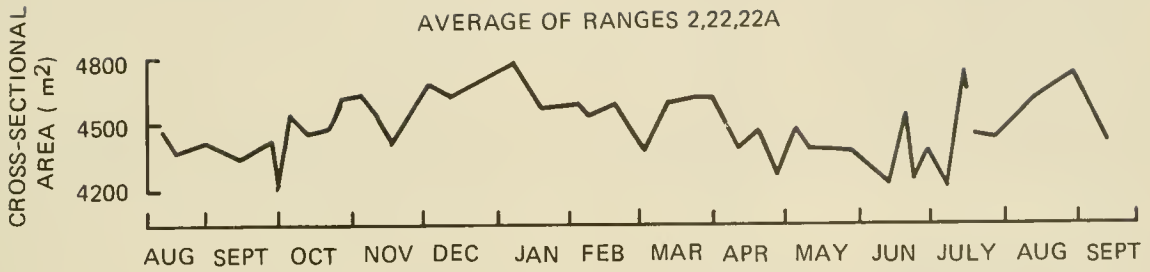


Figure 4-71. Variations in cross-sectional area for Wachapreague Inlet (from Byrne, De Alteris, and Bullock, 1974).

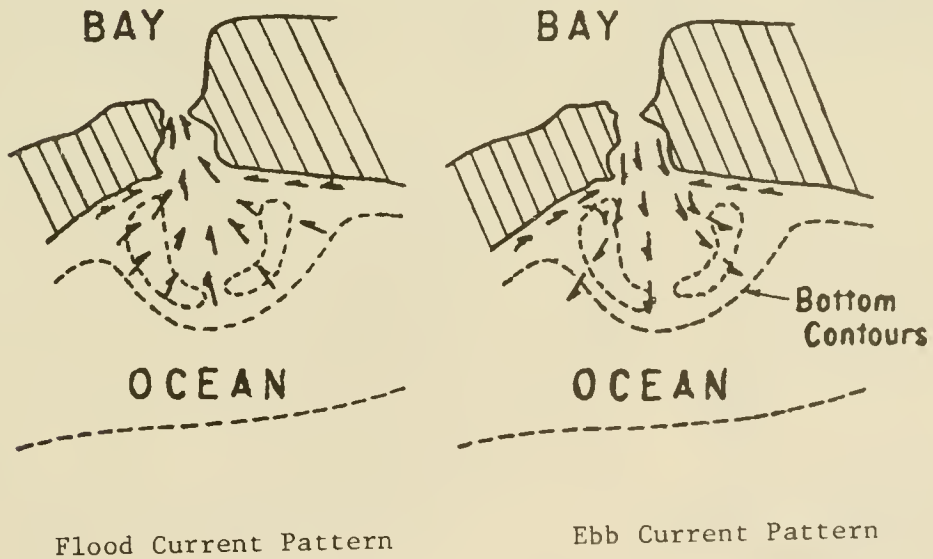


Figure 4-72. Schematic diagram of flood and ebb currents outside an inlet (from O'Brien, 1966).

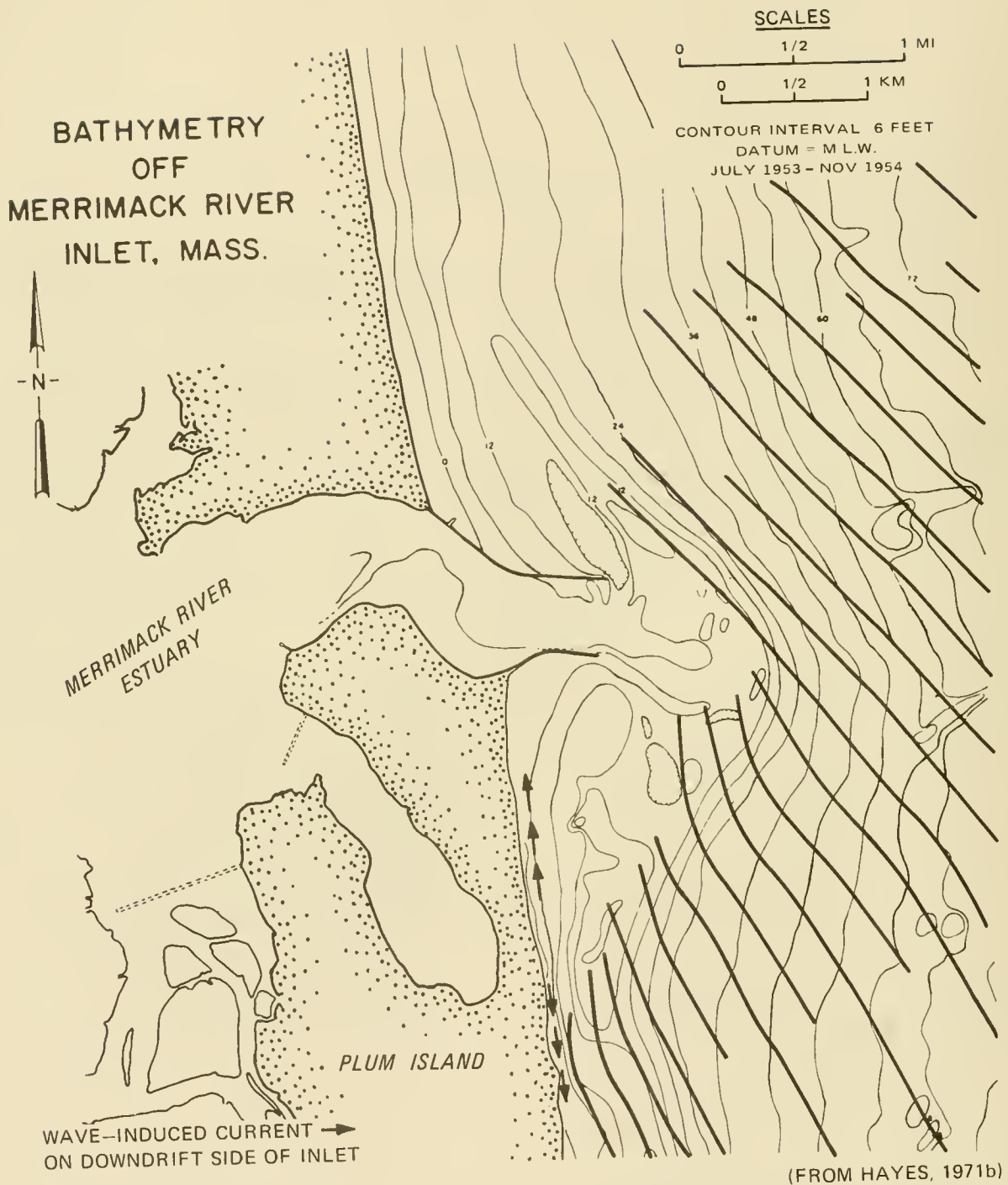


Figure 4-73. Wave refraction patterns in vicinity of Merrimack River Estuary entrance just south of the Merrimack Inlet. (Note oblique approach of the wave crests from the northeast. Refraction around the ebb-tidal delta causes an area of local reversal of longshore drift.)

General circulation patterns inside inlets are more complex due to the complexity of the interior inlet physiography.

### 3. Inlet Currents.

a. Hydraulic Currents in Inlets. This section presents methods for calculating the time-dependent average cross-sectional velocity in an inlet channel and the bay tidal level range, assuming that the inlet is sufficiently small that inlet currents are hydraulically driven by differences in elevation between inlet and bay water level elevations.

Required input data for these calculations include the ocean tidal period and amplitude, the inlet channel length and hydraulic resistance, and the bay surface area. An example is presented to demonstrate these calculations for a hypothetical sea-inlet-bay system.

Figure 4-74 shows an idealized sea-inlet bay system. The jettied inlet channel has a length  $L$ , width  $B$ , average depth  $d$ , and cross-sectional area  $A_c$  below mean sea level (MSL), and instantaneous average velocity  $V$ . Flow in the system is generated by a sea tide having a period  $T$  and amplitude  $a_s$  and results in a bay level response having the same period and amplitude  $a_b$ . The time of high water in the bay lags behind the sea high water by a phase lag  $\epsilon$ , usually given in degrees.  $A_b$  is the bay surface area, and  $2A_b a_b$ , the volume of water that flows into and then out of the bay on a tidal cycle, is commonly known as the tidal prism  $P$ . Parameters needed to define the inlet channel hydraulics include entrance- and exit-loss coefficients  $k_{en}$  and  $k_{ex}$ , a resistance coefficient  $f$  (Darcy-Weisbach) or  $n$  (Manning), and the hydraulic radius  $R$ , which equals the cross-sectional area divided by the wetted perimeter. The acceleration of gravity is  $g$ .

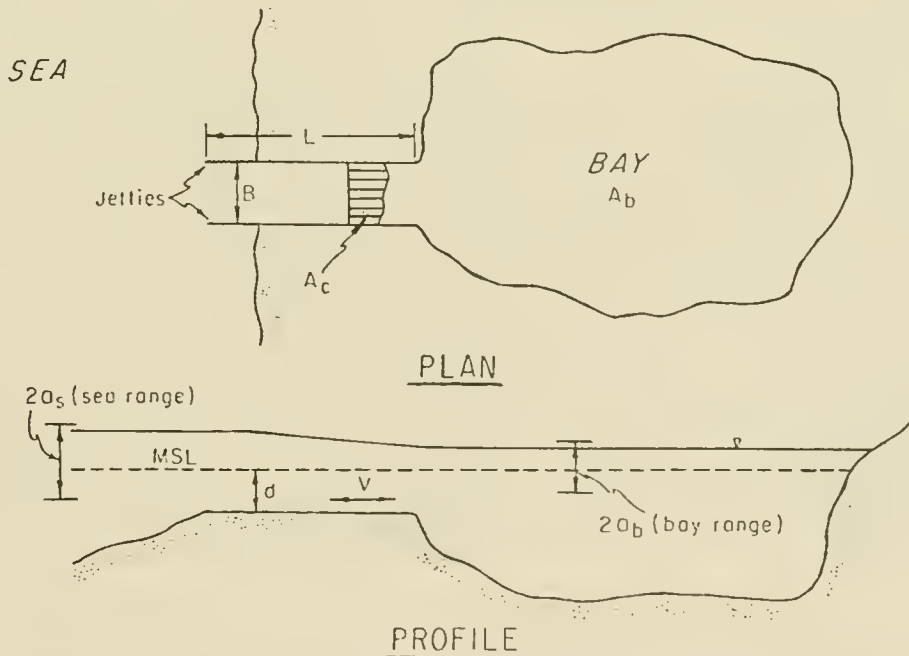


Figure 4-74. Sea-inlet-bay system.

Keulegan (1967), King (1974), Goodwin (1974), Escoffier and Walton (1979), and Walton and Escoffier (1981) have solved the basic equations of motion and continuity for an inlet-bay system (Fig. 4-74) by various techniques including (1) analytical solution and (2) numerical solution via analog and digital computer.

The latter four references include the effects of inertia and tributary inflow into the bay.

King's (1974) solution (as presented by Sorensen, 1977) for the case of no tributary inflow will be given here. The solution is in the form of curves for the dimensionless maximum channel velocity during a tidal cycle  $V'_m$  and the ratio of bay to sea tidal amplitude  $a_s/a_b$ , as functions of a friction coefficient  $K_1$  and a frequency coefficient  $K_2$  (see Figs. 4-75 and 4-76). He defines

$$V'_m = \frac{A_c TV_m}{2\pi a_s a_b} \quad (4-64)$$

$$K_1 = \frac{a_s A_b F}{2LA_c} \quad (4-65)$$

and

$$K_2 = \frac{2\pi}{T} \sqrt{\frac{LA_b}{gA_c}} \quad (4-66)$$

where  $V_m$  is the maximum velocity during a tidal cycle and

$$F = k_{en} + k_{ex} + \frac{fL}{4R} \quad (4-67)$$

With values of  $a_s$ ,  $T$ ,  $K_{en}$ ,  $k_{ex}$ ,  $f$ ,  $L$ ,  $R$ ,  $A_b$ , and  $A_c$ ,  $K_1$  and  $K_2$  can be evaluated from equations (4-65) and (4-66);  $V'_m$  and  $a_s/a_b$  determined from Figures 4-75 and 4-76; and  $V$  calculated from equation (4-64). Note in Figure 4-76 that for certain  $K_1$  and  $K_2$  values,  $a_b/a_s$  is greater than 1; that is, the bay range is amplified. This occurs when the inertia of the water in the channel exceeds the frictional resistance.

The major assumptions implicit in King's (1974) solution are

(a) The sea tide is sinusoidal; i.e.,  $\eta_s = a_s \sin 2\pi t/T$  where  $t$  denotes the time elapsed and  $\eta_s$  is the instantaneous sea level. Since the channel resistance is nonlinear, the channel velocity and bay tide will not be sinusoidal. However, for a first approximation,  $V \approx F_m \sin 2\pi t/T$  and  $\eta_b \approx a_b \sin 2\pi t/T$  can be assumed (where  $\eta_b$  is the instantaneous bay level). Thus, the average velocity over the flood or ebb phase of a tidal cycle is approximately equal to  $(2/3)V_m$ .

(b) The bay water level rises and falls uniformly (i.e., the bay water surface remains horizontal). This assumption requires that the tidal period be long compared to the time required for a shallow-water wave to propagate from the inlet to the farthest point in the bay; i.e.,

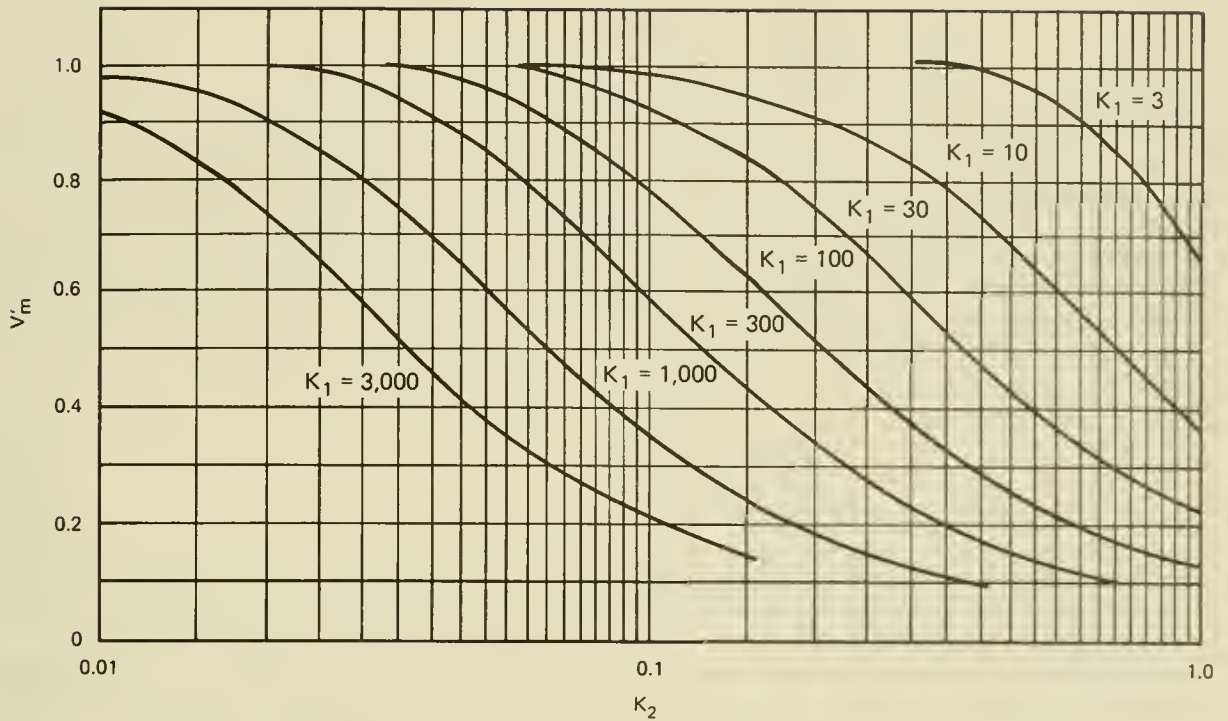


Figure 4-75. Dimensionless maximum velocity versus  $K_1$  and  $K_2$  .

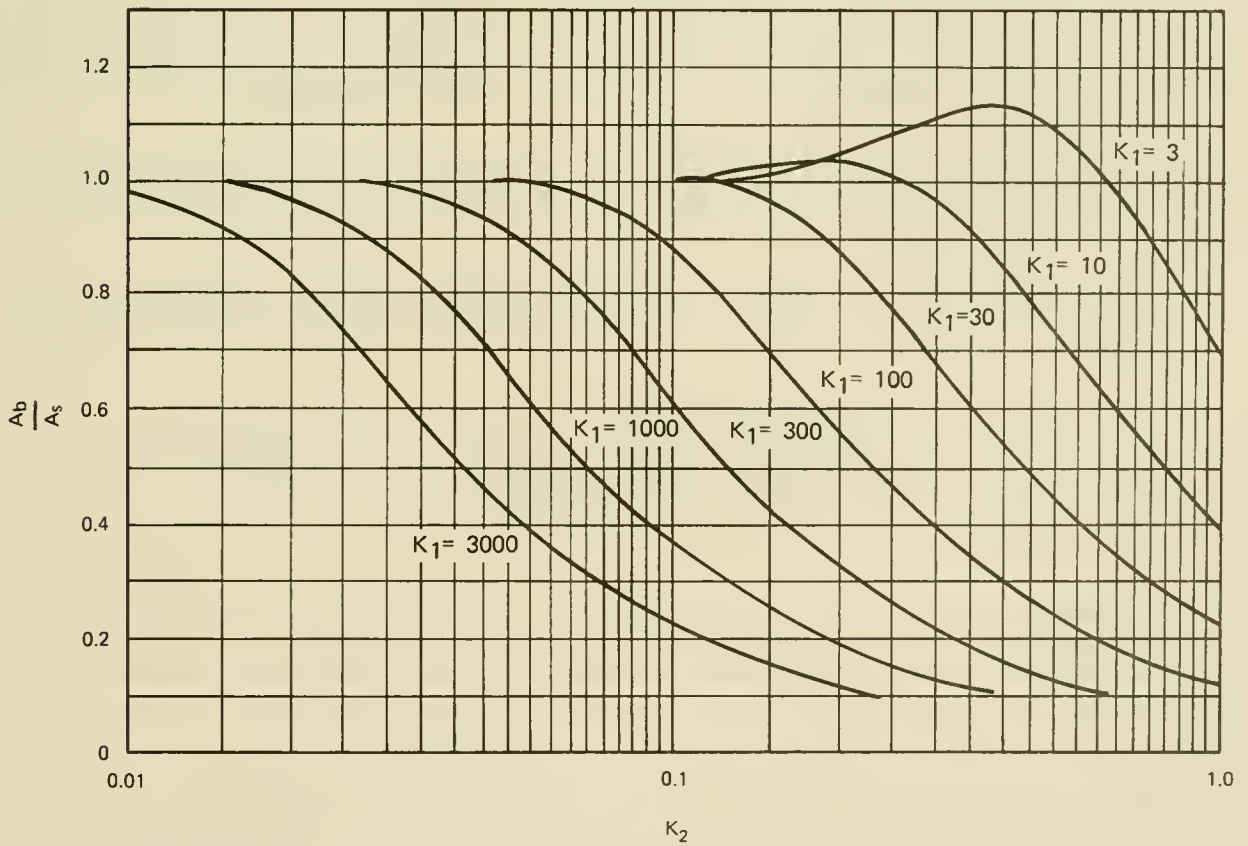


Figure 4-76 Ratio of bay to sea tidal amplitude versus  $K_1$  and  $K_2$  .

$$t \gg \frac{L_b}{gd_b} \quad (4-68)$$

where  $L_b$  is the distance to the farthest point and  $d_b$  is the average bay distance.

(c) The inlet channel depth is large compared to the ocean tidal range, and the channel depth and width do not vary along the channel. Hydraulic calculations may be made with a reasonable degree of confidence, even if channel cross-section variations exist but are not too extreme. For irregular jettied or unjettied channels, an effective channel length,  $L_*$ , which can be used in place of  $L$ , is given by

$$L_* = \sum_i^n \left( \frac{R}{R_*} \right) \left( \frac{A_c}{A_{c_*}} \right)^2 \Delta x \quad (4-69)$$

where  $R$  and  $A_c$  are average values of the channel hydraulic radius and cross-sectional area used in the hydraulic calculations and  $R_*$  and  $A_{c_*}$  are the hydraulic radius and cross-sectional area at each of  $n$  sections of equal length  $\Delta x$ , spaced along the channel. For jettied inlets the length may be taken as the distance along the channel axis from the seaward end of the jetties to the section on the bayward end of the channel where the flow velocity is diminished to a small percentage (e.g., 20 percent) of the average channel velocity. For unjettied inlets that are not too irregular in cross section, the length may be taken as the distance along the channel axis between the points on each end where the velocity is, for example, 20 percent of the average velocity.

(d) Bay walls are vertical over the bay tidal range. Hydraulic calculations may be made with a reasonable degree of confidence if there is no extensive flooding of tidal flats.

(e) There are negligible density currents at the inlet and negligible inflow to the bay from other sources (rivers, overland flow, precipitation, etc.).

The values for  $k_{en}$ ,  $k_{ex}$ , and  $f$  must be also established for calculations to proceed.  $k_{ex}$  may be assumed equal to unity ( $k_{ex} = 1.0$ ), and  $k_{en}$  will probably vary between approximately 0 and 0.2 as the entrance hydraulic efficiency decreases. A value of  $k_{en} = 0.2$  is recommended for most calculations.

The friction factor  $f$  or Manning's  $n$  ( $n = 0.093R^{1/6}f^{1/2}$ ) depends on the bed roughness and flow velocity. For a sandy channel bottom typical of most inlets,  $f$  can vary between 0.01 and 0.07, depending on the peak velocity and the phase of the tidal cycle. If no information is available to estimate the friction factors, a value of  $f = 0.03$  may be used.

Losses caused by bridge piers, sills, channel bends, etc., must also be accounted for in hydraulic calculations by adding a loss coefficient similar to  $k_{en}$  and  $k_{ex}$  in the equation defining  $F$ . Like  $k_{en}$  and  $k_{ex}$ , this coefficient defines the number of velocity heads ( $V^2/2g$ ) lost at a channel disturbance.

\*\*\*\*\* EXAMPLE PROBLEM 6 \*\*\*\*\*

GIVEN: A bay with a surface area of  $1.86 \times 10^7$  square meters ( $2 \times 10^8$  square feet) and an average depth of 6.1 meters (20 feet) is located on the Atlantic coast. The tide is semidiurnal ( $T = 12.4$  hours), with a spring range of 1.34 meters (4.4 feet), as given by the National Ocean Survey Tide Tables (National Oceanic and Atmospheric Administration, 1976). An inlet channel, which will be the only entrance to the bay, is to be constructed across the barrier beach which separates the bay from the ocean. The inlet is to provide a navigation passage for small vessels, dilution water to control bay salinity and pollution levels, and a channel for fish migration. The channel is to have a design length of 1,097 meters (3,600 feet) with a pair of vertical sheet pile jetties that will extend the full length of the channel.

FIND: If the channel has a depth below MSL of 3.66 meters (12 feet) and a width of 183 meters (600 feet), what are the maximum flow velocity, bay tidal range, and the volume of water flowing into and out of the bay on a tidal cycle (tidal prism) for a tide having the spring range?

SOLUTION: Assume  $k_{en} = 0.1$ ,  $k_{ex} = 1.0$ , and  $f = 0.03$ ;  $B = 183$  meters, and  $d = 3.66$  meters.

$$A_c = Bd = 183 (3.66) = 669 \text{ square meters (7,200 square feet)}$$

$$R = \frac{A_c}{(B + 2d)} = \frac{669}{(183 + 2(366))} = 3.51 \text{ meters (11.54 feet)}$$

$$F = k_{en} + k_{ex} + \frac{fL}{4R} = 1.0 + 0.1 + \frac{0.03(1097)}{4(3.51)} = 3.43$$

$$K_1 = \frac{a_s A_b F}{2LA_c} = \frac{(1.34/2) (1.86) (10^7) 3.43}{2(1097) (669)} = 29.1$$

and

$$K_2 = \frac{2\pi}{T} \sqrt{\frac{LA_b}{gA_c}} = \frac{2\pi}{12.4(60) (60)} \sqrt{\frac{1097(1.86) 10^7}{9.8 (669)}} = 0.25$$

From Figures 4-75 and 4-76, with the above values of  $K_1$  and  $K_2$

$$V_m' = 0.66$$

and

$$\frac{a_b}{a_s} = 0.78$$

Therefore, from equation (4-64)

$$V_m = \frac{V_m' 2\pi a_s A_b}{A_c T}$$

$$V_m = \frac{0.66(2) (3.14) (0.67) (1.86) 10^7}{669 (12.4) (3,600)} = 1.73 \text{ meters (5.68 feet) per second}$$

Since  $a_b/a_s = 0.78$ ,  $a_b = 0.78 (0.67) = 0.52$  meter (1.72 feet)

and the bay tidal range is 0.52 (2) or 1.05 meters (3.44 feet).

The tidal prism is

$$2a_b A_b = 2 (0.52 (1.86) (10^7)) = 6.37 \times 10^7 (6.86 \times 10^8 \text{ cubic feet})$$

If the average depth of the bay is 6.1 meters and the distance to the farthest point in the bay is 6.4 kilometers, the time  $t_*$  it will take for the tide wave to propagate to that point is

$$t_* = \frac{L_b}{\sqrt{gd_b}} = \frac{6400}{\sqrt{9.8 (6.1)}} = 827 \text{ seconds, or 0.23 hour}$$

Since this time is significantly less than 12.4 hours, the assumption that the bay surface remains horizontal is quite satisfactory.

\*\*\*\*\*

b. Long Wave Currents in Inlets. When an inlet is sufficiently wide and deep to allow propagation of the tidal wave through the inlet, the inlet currents must be calculated using long wave theory. The propagation of long waves through the inlet typically occurs in the case where the inlet is more appropriately termed an *estuary* and the estuary has a large tidal prism.

The water velocity at the entrance for a long wave propagating through an inlet (or estuary) for the case of an "infinitely" long channel with no frictional damping is

$$u = \frac{a_0}{h} C \cos \frac{2\pi t}{T} \quad (4-70)$$

where

$u$  = maximum water velocity at the entrance to the channel

$a_0$  = tidal amplitude

$C = \sqrt{gh}$  = celerity of long wave

$h$  = mean water depth of channel

In the case of frictional damping, an additional reduction factor (<1) must be applied to the velocity above, and a phase lag occurs between the maximum water level and the maximum velocity (Ippen, 1966).

c. Effects of Salinity Currents. Velocities at inlets discussed thus far pertain to inlets in which vertical mixing prevents vertical density stratification. In inlets with tributary inflow or estuaries which terminate into rivers, vertical stratification may take place and alter the current strengths significantly from those discussed in Sections IX,3,a and IX,3,b. In the

event of vertical stratification, the denser water along the bottom has a net flow landward (when averaged over a tidal cycle) providing a mechanism for sediment to move into the inlet. The less dense surface waters have a net flow seaward when averaged over the tidal cycle, thus satisfying continuity of water mass in the system.

#### 4. Inlet Migration and Stabilization Effects on Adjacent Shorelines.

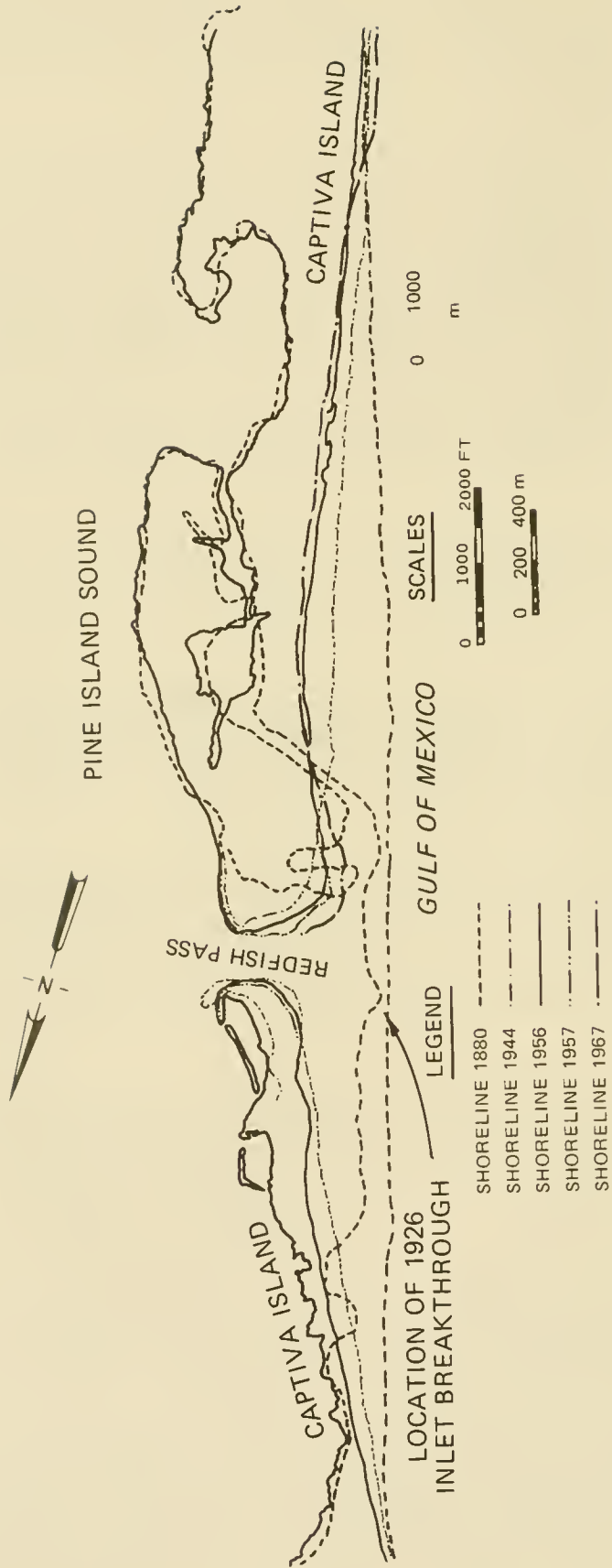
Shorelines in the vicinity of inlets are subject to considerable change, much more so than typical shorelines remote from inlets. Many shorelines have undergone little or not change prior to inlet creation. Following the opening of an inlet, significant changes occur. Figure 4-77 shows a natural barrier island on the gulf coast of Florida whose shoreline, although receding, underwent little historic change prior to 1926 when hurricane currents broke through the barrier island and created Redfish Pass. After Redfish Pass had been created, the shoreline on each side of the inlet receded. A maximum recession rate of 275 meters (900 feet) in 30 years (9 meters/year) occurred on the downdrift side of the inlet (University of Florida, Coastal Engineering Laboratory, 1974).

When long-term historical records are examined, it is clear that tidal inlets undergo spectacular changes over a period of a century. Examples of long-term natural inlet migration is illustrated by the inlets shown in Figures 4-78 to 4-80.

Short-term changes in shorelines in the vicinity of inlets are no less dramatic, as demonstrated in Figure 4-81 which shows changes of 150 meters (500 feet) in the shoreline adjacent to an inlet at Brown Cedar Cut, Texas, within a one year survey period.

Often the inlet can migrate in a direction counter to that expected from its dominant longshore sand transport direction. Brown (1928) has noted that Aransas Pass, Texas, among others, has migrated in a direction opposite that of the net longshore transport for many years; Walton and Dean (1976) have noted a northward movement of Redfish Pass, Florida, in the Gulf of Mexico for a period of 20 years, although the dominant sand transport direction in the area is southward.

The effects of inlet stabilization works (e.g., jetties, terminal groins, offshore breakwaters) on the shorelines adjacent to inlets are often difficult to assess in view of the dynamic character of natural inlets (i.e., inlets can change significantly within a short time). Shoreline accretion in the wave-sheltered areas of jetties and offshore breakwaters has been discussed in Sections V,2, V,3, and VIII,1. Also, changes are induced due to the constriction of the channel by entrance jetties. Typically, a confinement of the inlet flow between jetties causes stronger velocities within the inlet channel and a consequent displacement of sand from the area between the jetties to seaward, thereby making the inlet a more effective littoral trap (i.e., decreasing natural sand bypassing) and distorting the natural ebb-tidal delta. Figures 4-82 and 4-83 provide a historical perspective of St. Mary's River entrance, Florida, where long jetties of 5-6 kilometers were constructed between 1880 and 1902. Figure 4-82 documents the forcing of the natural ocean bar offshore during the 5-year period (1902-1907) after completion of the jetties. Figure 4-83 documents the changes, natural and jetty-induced, in the period 1870-1970, in which the area seaward of the jetties accreted  $92 \times 10^6$



(after University of Florida, Coastal Engineering Laboratory, 1974)

Figure 4-77. Mean high water shoreline changes at Redfish Pass, 1925-1967.

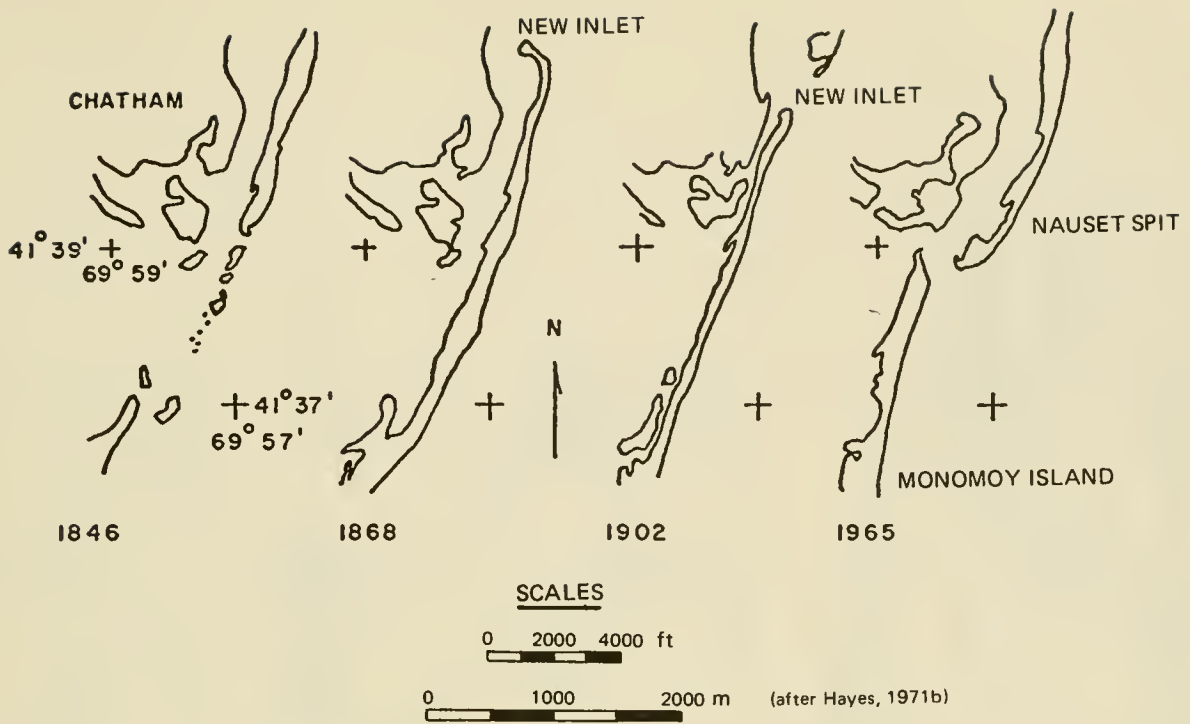


Figure 4-78. Large-scale inlet migration at the Monomoy-Nauset Inlet, Cape Cod, Massachusetts, 1846-1965. (In 1846 the inlet was located approximately 3.2 kilometers (2 miles) south of its present location. By 1868 the inlet had closed up and a new inlet was opened by a storm 9.6 kilometers (6 miles) to the north. By 1965 the inlet had migrated 6.4 kilometers (4 miles) to the south. These changes have resulted in the beach updrift of the inlet being offset in a seaward direction.)

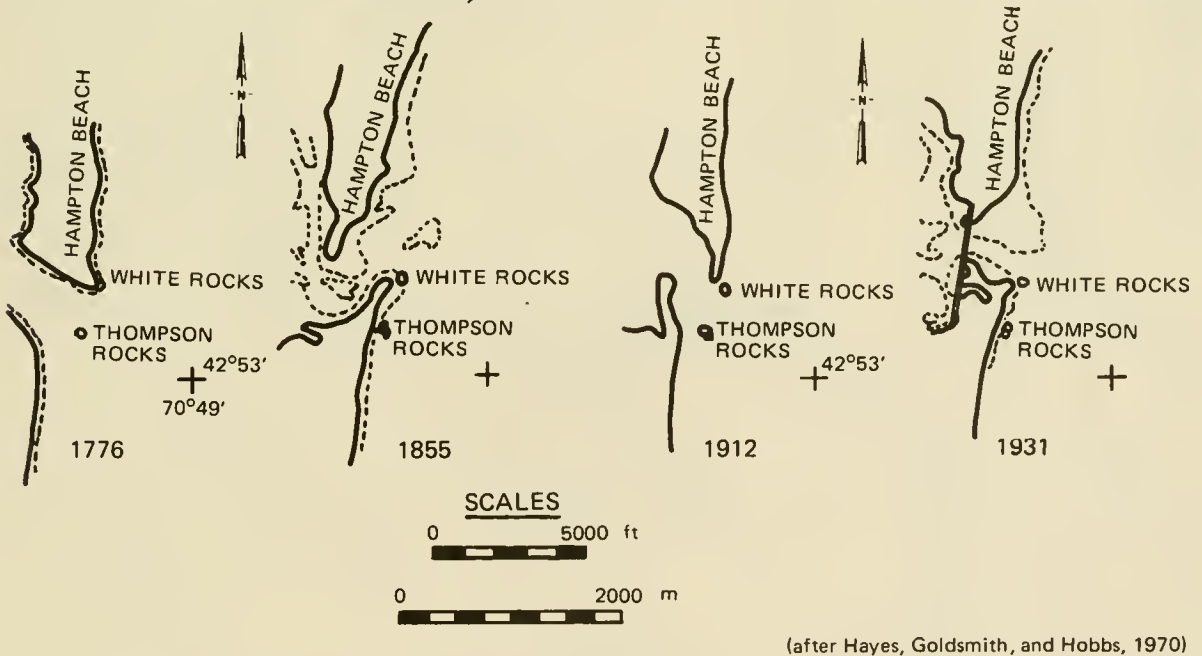


Figure 4-79. Inlet changes at Hampton Harbor, New Hampshire, 1776-1931. (Note that in 1776 and 1912 the updrift side of the inlet was further offset in a seaward direction, while in 1855 and 1931 the downdrift side of the inlet was further offset in a seaward direction.)

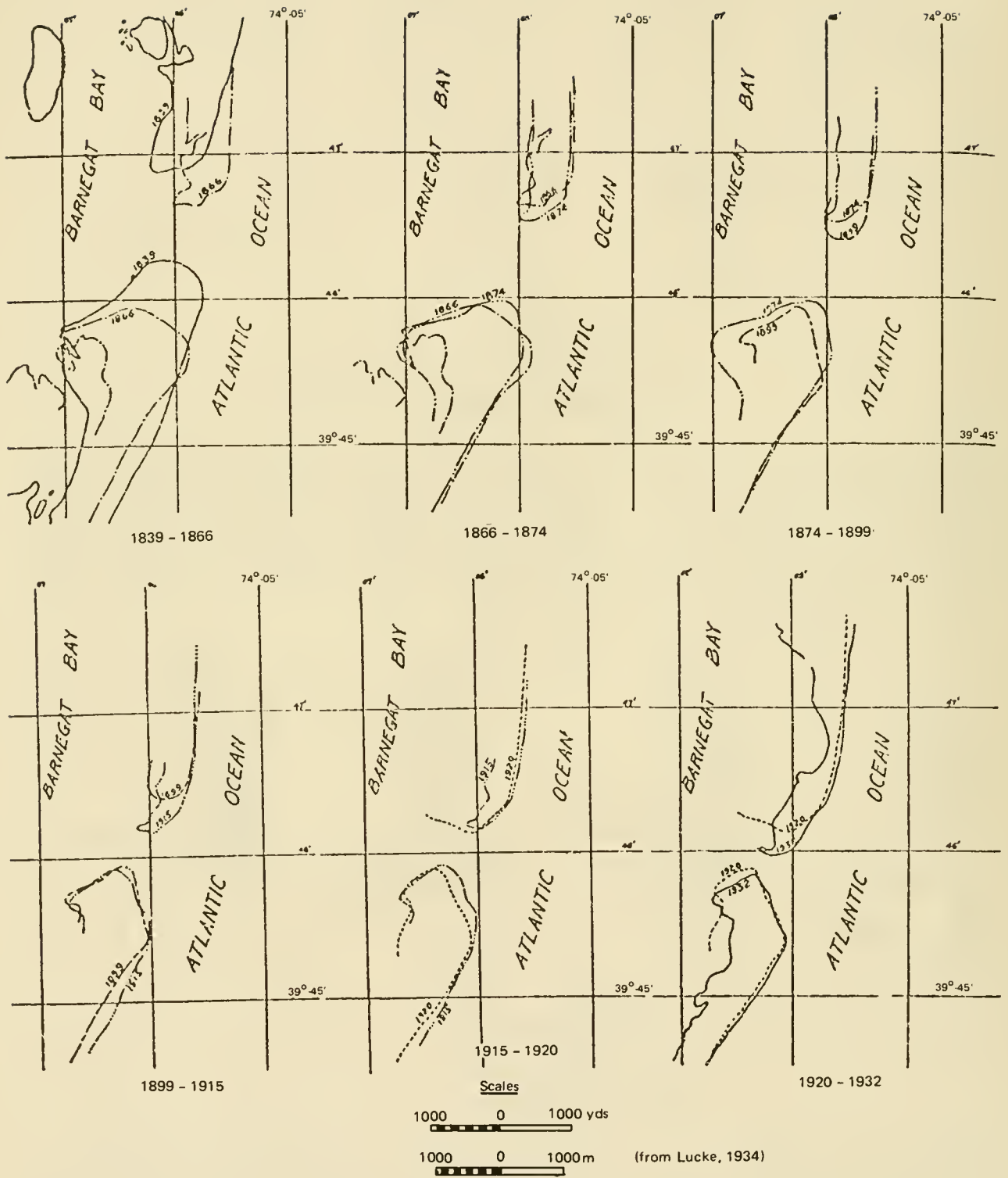


Figure 4-80. Shoreline changes at Barnegat Inlet, New Jersey.

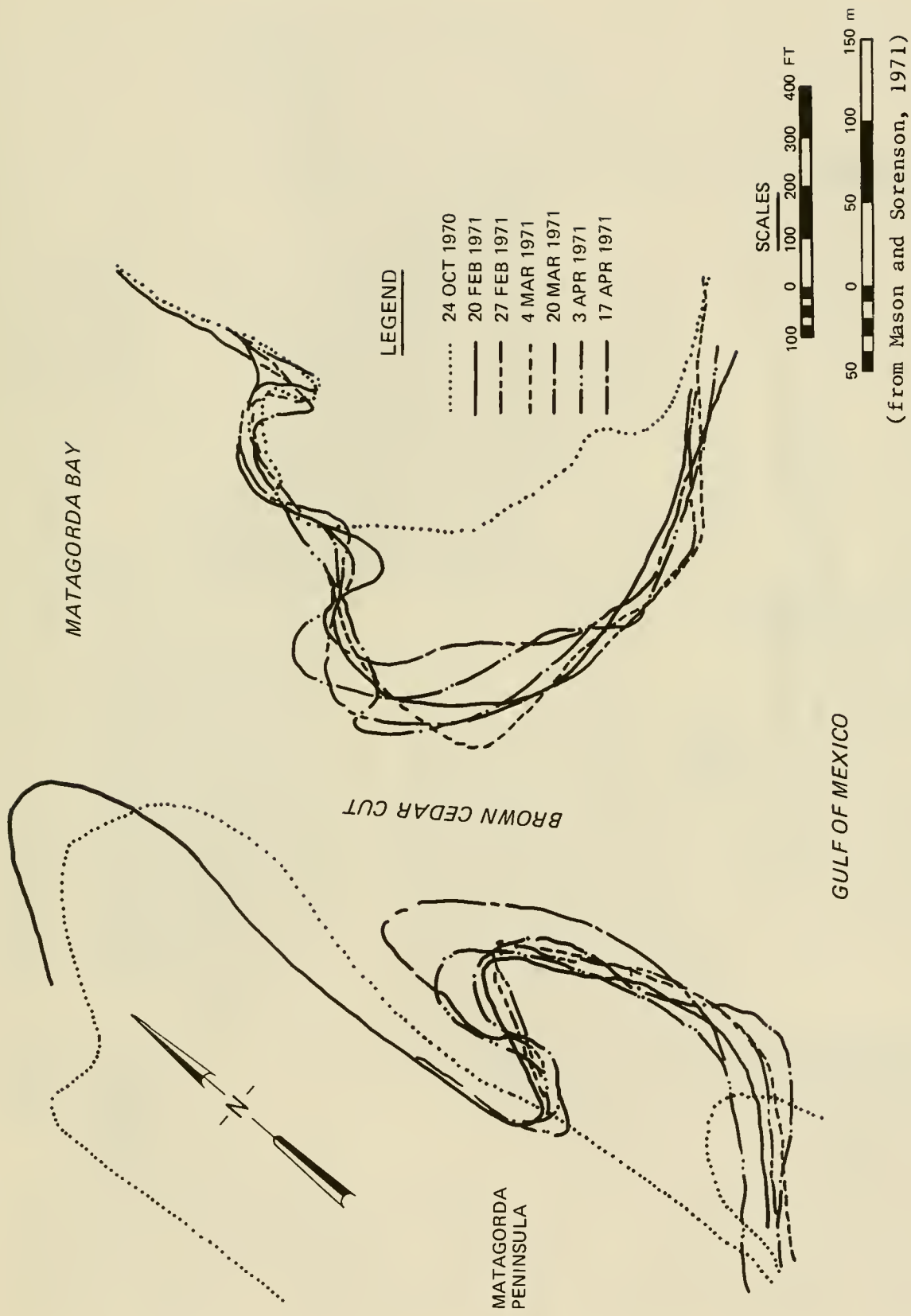
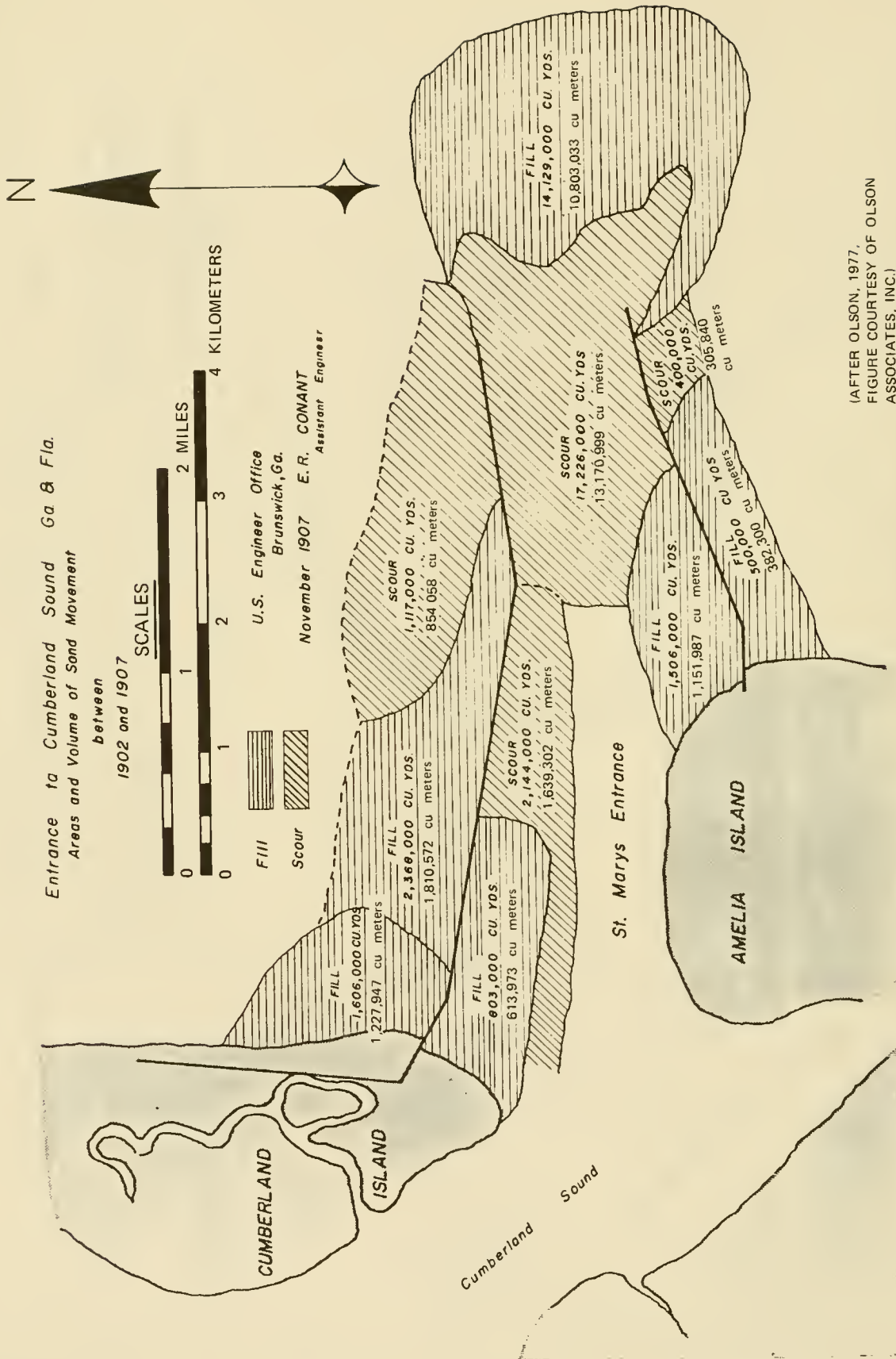
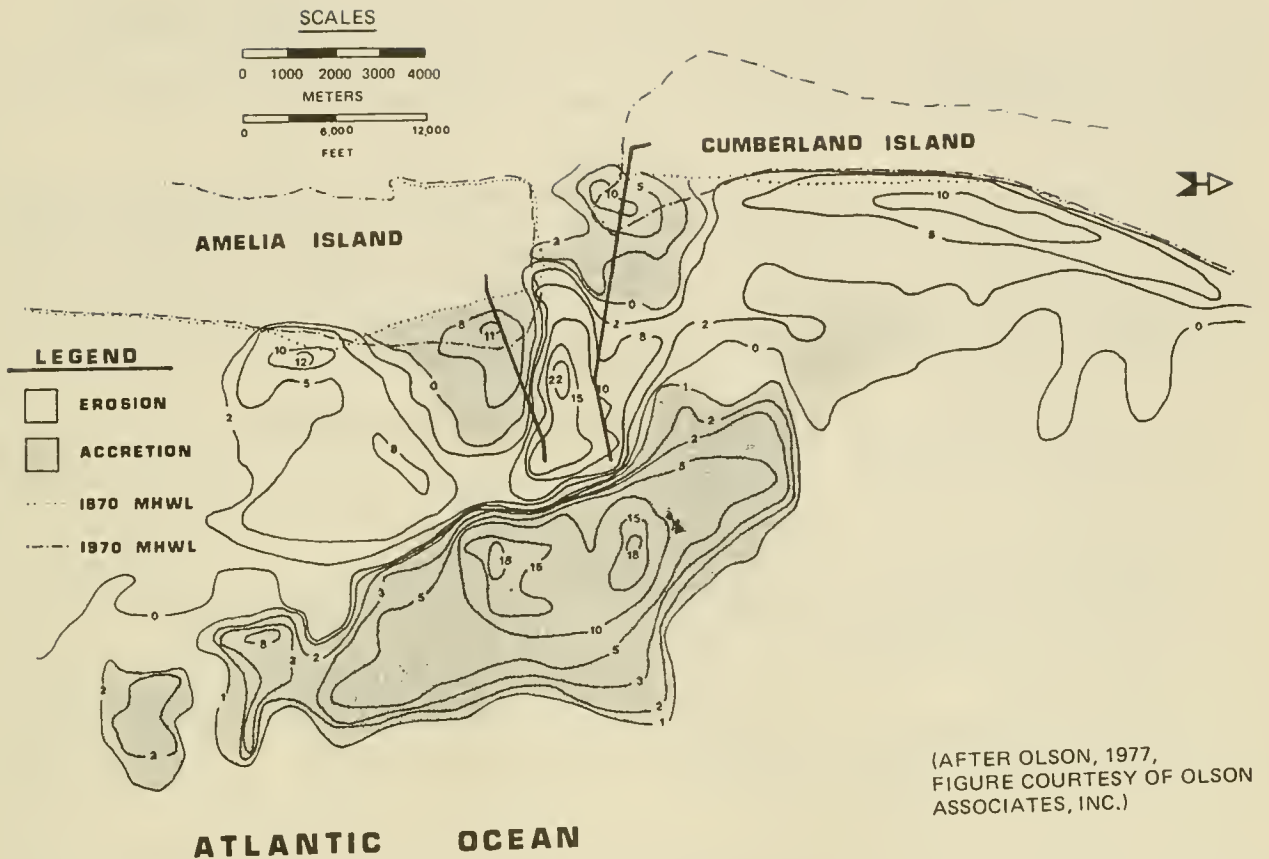


Figure 4-81. Short-term shoreline change, Brown Cedar Cut, Texas.



(AFTER OLSON, 1977,  
 FIGURE COURTESY OF OLSON  
 ASSOCIATES, INC.)

Figure 4-82. Erosion (scour) and accretion (fill) patterns between 1902 and 1907 at St. Mary's River entrance, Florida.



(AFTER OLSON, 1977,  
FIGURE COURTESY OF OLSON  
ASSOCIATES, INC.)

Figure 4-83. Accretion and erosion over a 100-year period at St. Mary's River entrance, Florida (contours are shown in feet).

cubic meters ( $120 \times 10^6$  cubic yards) of sand in a giant shoal while the areas adjacent to the shoreline on each side of the jetties (but out of the wave sheltered zone of the jetties) eroded  $46 \times 10^6$  cubic meters ( $60 \times 10^6$  cubic yards) of sand. Significant shoreline erosion is now occurring in these areas (Olsen 1977). At the time of construction of the jetties shown in Figure 4-82, navigation was a prime consideration and shorelines adjacent to the jetties were not extensively developed.

##### 5. Littoral Material Trapping at Inlets.

The potential for inlet systems to tie up sand of the littoral system in their flood-and-ebb shoals has been documented by Dean and Walton (1973); Walton and Adams (1976); Behrens, Watson and Mason (1977), Watson and Behrens (1976), and others.

Dean and Walton (1973) have noted that the sand found in the ebb-tidal deltas of inlets is derived from beach sands; the delta sand should be of the same general size distribution as that found on adjacent beaches, in view of the high wave energy expended on the ebb-tidal delta outer bar. Olsen (1980) has found that for Redfish Pass on the lower gulf coast of Florida, the sand and shell sizes in a potential borrow area (for beach nourishment) located on the ebb-tidal delta is somewhat coarser than that found on adjacent beaches.

Dean and Walton (1973) have presented a methodology for the calculation of beach material volume (sand, shell, etc.) in the ebb-tidal delta complex. This methodology, shown in Figure 4-84, is somewhat subjective because it relies on the ability to interpret the "no inlet" bathymetry. It involves calculating the volume difference between the present and "no inlet" bathymetries.

Walton and Adams (1976) found that the volume of sand comprising the ebb-tidal delta is a function of both the tidal prism of the inlet and the level of wave activity on the ebb-tidal delta. They have presented equations for the volume of sand stored in the ebb-tidal delta as a function of tidal prism for highly exposed (Pacific), moderately exposed (Atlantic and western gulf), and mildly exposed (eastern gulf) coasts in terms of average wave activity.

These relationships are, in metric (a) and English (b) units,

$$\Psi = 1.975 \times 10^{-4} P^{1.23} \quad \text{Pacific coast} \quad (4-71a)$$

$$\Psi = 8.7 \times 10^{-5} P^{1.23} \quad \text{Pacific coast} \quad (4-71b)$$

$$\Psi = 2.384 \times 10^{-4} P^{1.23} \quad \text{Atlantic \& western gulf coast} \quad (4-72a)$$

$$\Psi = 10.5 \times 10^{-5} P^{1.23} \quad \text{Atlantic \& western gulf coast} \quad (4-72b)$$

$$\Psi = 3.133 \times 10^{-4} P^{1.23} \quad \text{Eastern gulf coast} \quad (4-73a)$$

$$\Psi = 13.8 \times 10^{-5} P^{1.23} \quad \text{Eastern gulf coast} \quad (4-73b)$$

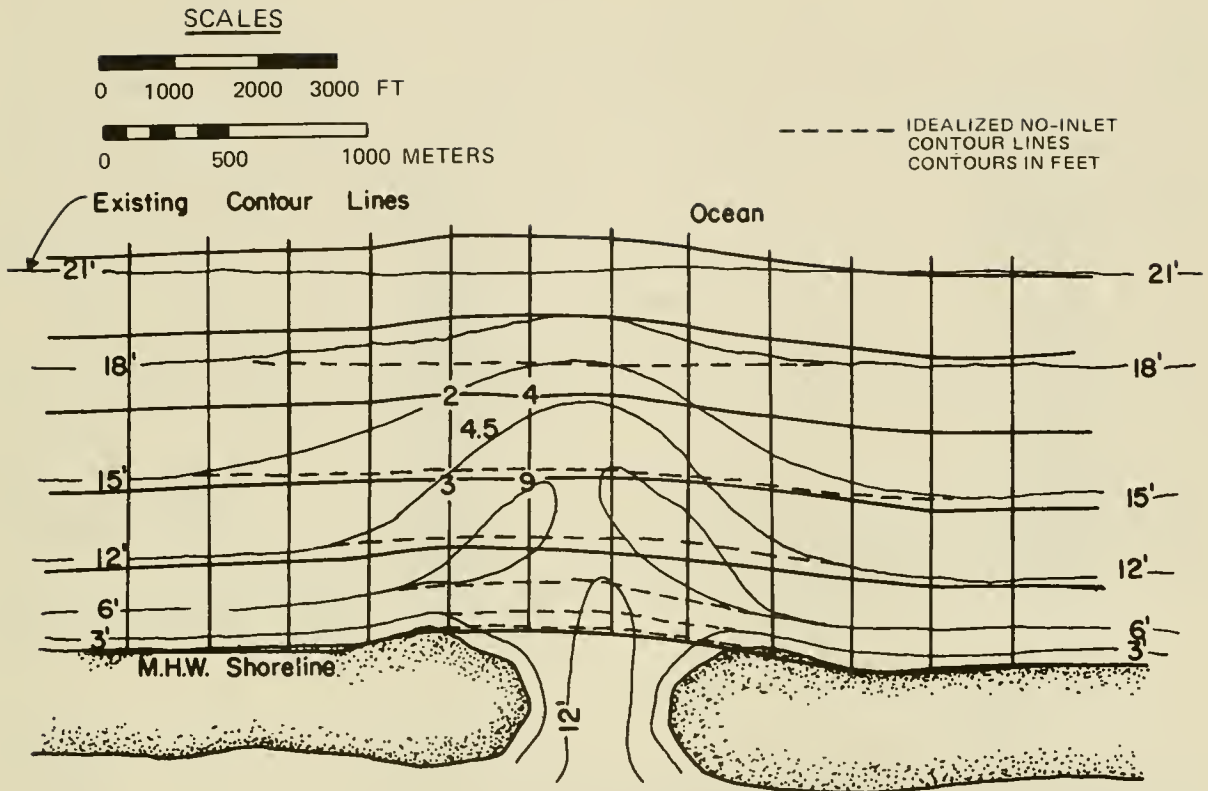
where  $\Psi$  is the volume of sand (or beach-type material) stored in ebb-tidal delta complex in cubic meters (cubic feet) and  $P$  is the tidal prism in cubic meters (cubic feet).

This type of analysis assumes that the inlet has been relatively stable in position. A similar approach to the sand storage in inner flood-tidal deltas has not been developed, owing partially to the complexity of the inner inlet physiographical system.

It is well known that flood-tidal deltas have a capacity to trap enormous quantities of sand due to the lack of wave action penetration into the lagoon on ebb tide and consequent reduced entrainment of sediments into the ebb flow.

Dean and Walton (1973) have shown that a relatively stable inlet will trap sand in its interior shoals until the system becomes filled to capacity (i.e., achieves an equilibrium shoaling volume). The history of the filling of one such inlet, presented in Figure 4-85, shows that shoaling over a continuous period of 70± years has occurred at a reduced rate with time.

In the event the channel frictional characteristics are changed such that the inlet becomes hydraulically unstable, it will close completely (a

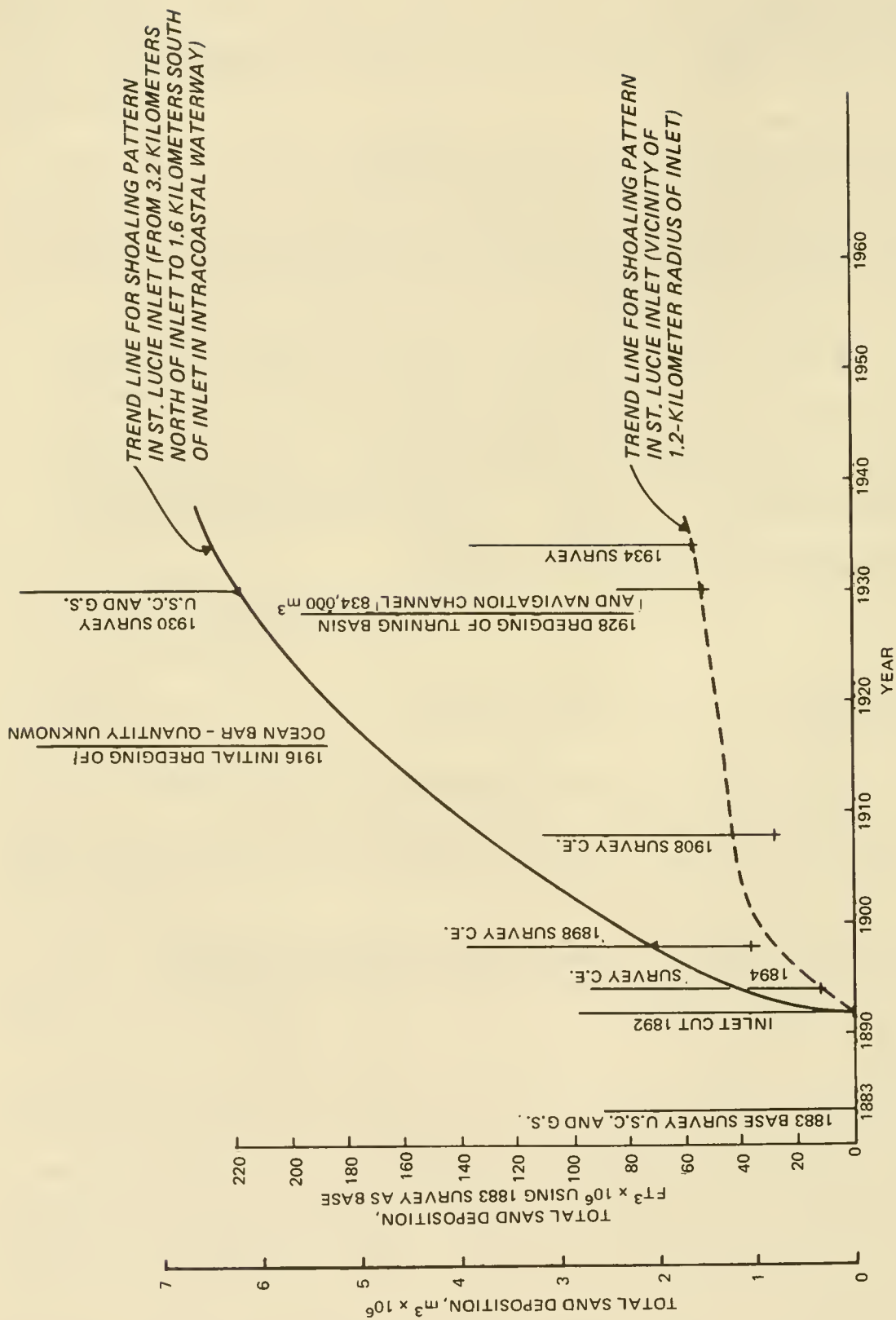


(AFTER DEAN AND WALTON, 1973)

Procedure

1. Construct idealized no-inlet contour lines.
2. Impose square grid system on chart and calculate differences between actual depth and idealized no-inlet depth at grid line intersections.
3. Average depth differences at intersections and record in center of block.
4. Compute volume of sand in outer shoal by summing averaged block depth differences, and multiply by area of single grid block.

Figure 4-84. Steps in calculation of accumulated volume of sand in the outer bar for an idealized inlet.



(AFTER DEAN AND WALTON, 1973)

Figure 4-85. Deposition of sand in the interior of St. Lucie Inlet, Florida.

generalized schematic of the stages of lagoonal filling behind a barrier island by tidal inlet flood deposits is presented in Figure 4-86). Thus, while the ebb-tidal delta or *outer bar*, being subject to the action of the currents and waves of the sea, generally does not increase beyond a definite stage; the flood-tidal delta, being subject to much milder forces in the bay, often continues to increase, even to the complete filling of the interior waters by the formation of marshes and the closure of the inlet. While this progressive deterioration of interior bays and sounds on sandy shores may not be a rapid process as measured by the span of human life, it is a very rapid process geologically as many of these interior waters show a marked deterioration within the century after their creation.

Drum Inlet, North Carolina, is an example of an inlet which deteriorated very rapidly, became hydraulically unstable, and eventually closed. Drum Inlet shoaled closed within 5 years after excavation. The volume of sand stored in the flood shoals as measured from a survey made 5 years after the inlet was opened was calculated to be 1,600,000 cubic meters (2,100,000 cubic yards) (Foreman and Machemael, 1972). Foreman and Machemael (1972) noted that the material in the flood shoal was similar in quality to, although somewhat finer than, that on the beaches adjacent to the inlet and that the median material size and standard deviation of size decreased with distance from the inlet throat.

\*\*\*\*\* EXAMPLE PROBLEM 7 \*\*\*\*\*

GIVEN : Plans have been made to construct a new unstructured inlet on the east coast of the U.S., through a barrier island into the back lagoon. The overall bay surface area which the inlet will serve is  $3 \times 10^7$  square meters ( $9.8 \times 10^7$  square feet). The ocean tide range is 1.3 meters (4.26 feet).

FIND: A rough approximation of the volume of sand which will eventually be "captured" from adjacent beaches by the ebb-tidal delta of the inlet system.

SOLUTION: Use equation (4-72) for the Atlantic coast to calculate  $\Psi$ .  
A (conservative) approximation for tidal prism P is

$$P \approx (\text{Ocean tide range}) \times (\text{Bay area})$$

$$P \approx 1.3 \text{ meters} \times (3 \times 10^7 \text{ square meters}) = 3.9 \times 10^7 \text{ square meters}$$

From equation (4-72a)

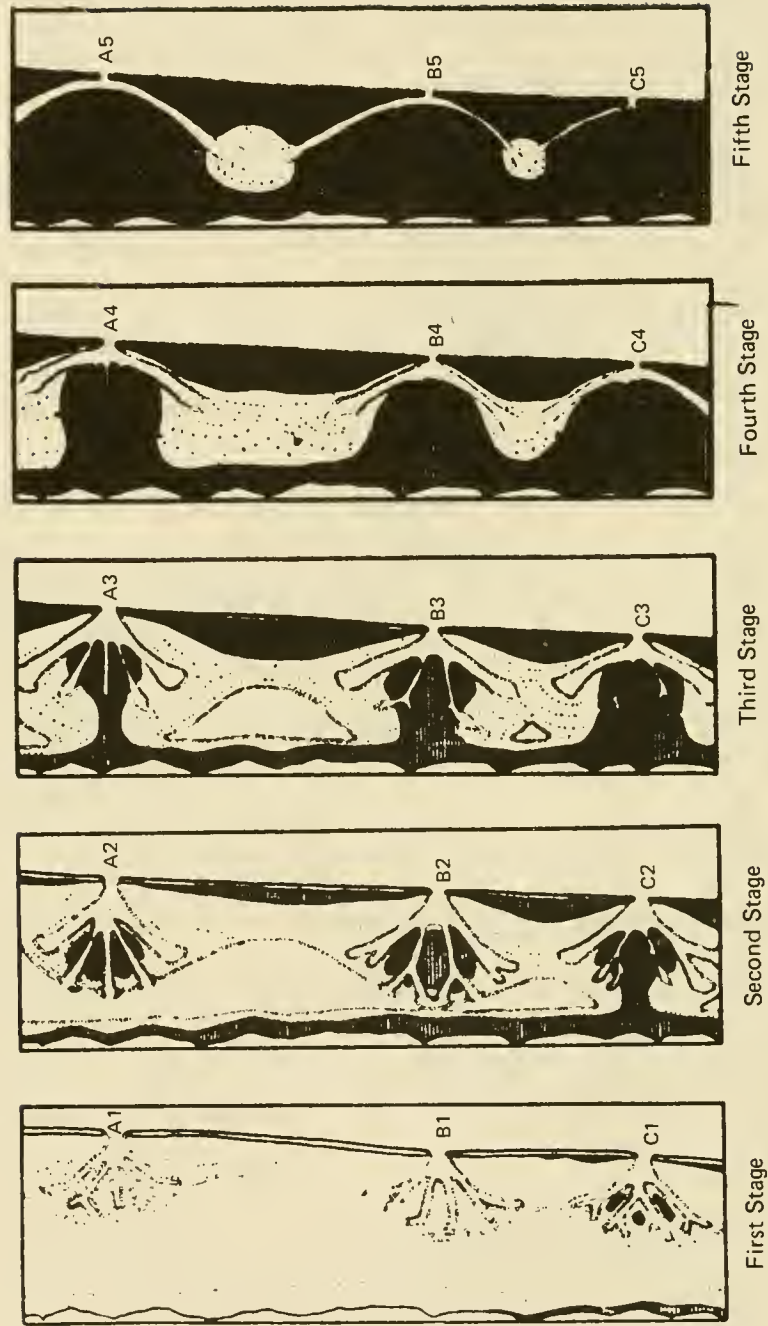
$$\Psi = 2.384 \times 10^{-4} (3.9 \times 10^7)^{1.23} = 518,000 \text{ cubic meter (677,600 cubic yards)}$$

of beach material.

\*\*\*\*\*

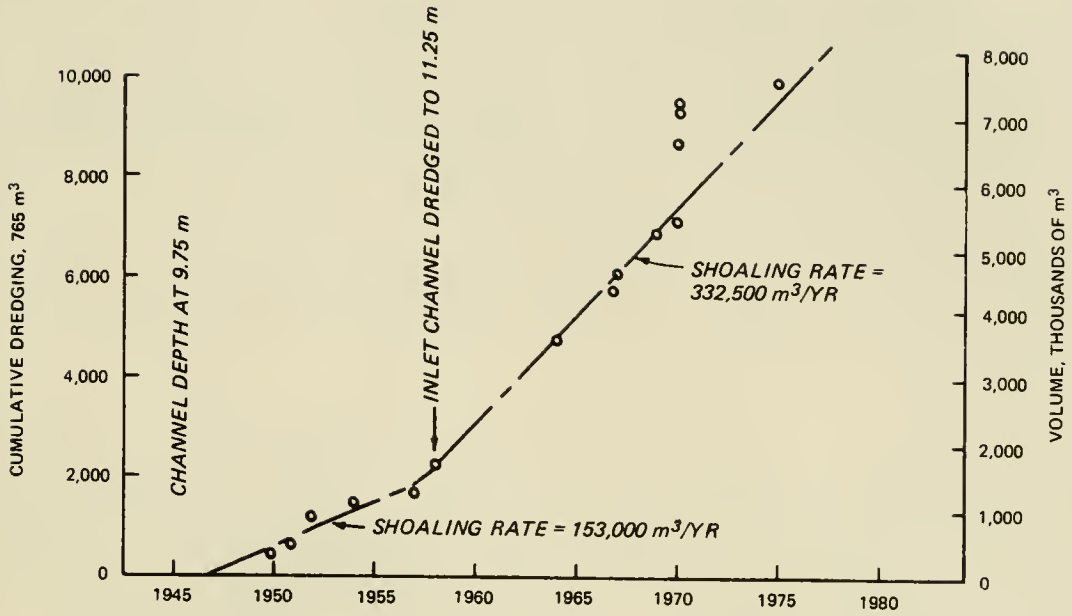
## 6. Channel Shoaling and Dredging Effects.

When a channel is dredged through a tidal inlet, increased shoaling is expected to occur in the channel over and above that which would occur in the natural channel. Little research exists on this subject, although one untested methodology for predicting channel shoaling has been presented by the U.S. Army Engineer District, Wilmington (1980). It should be noted that the



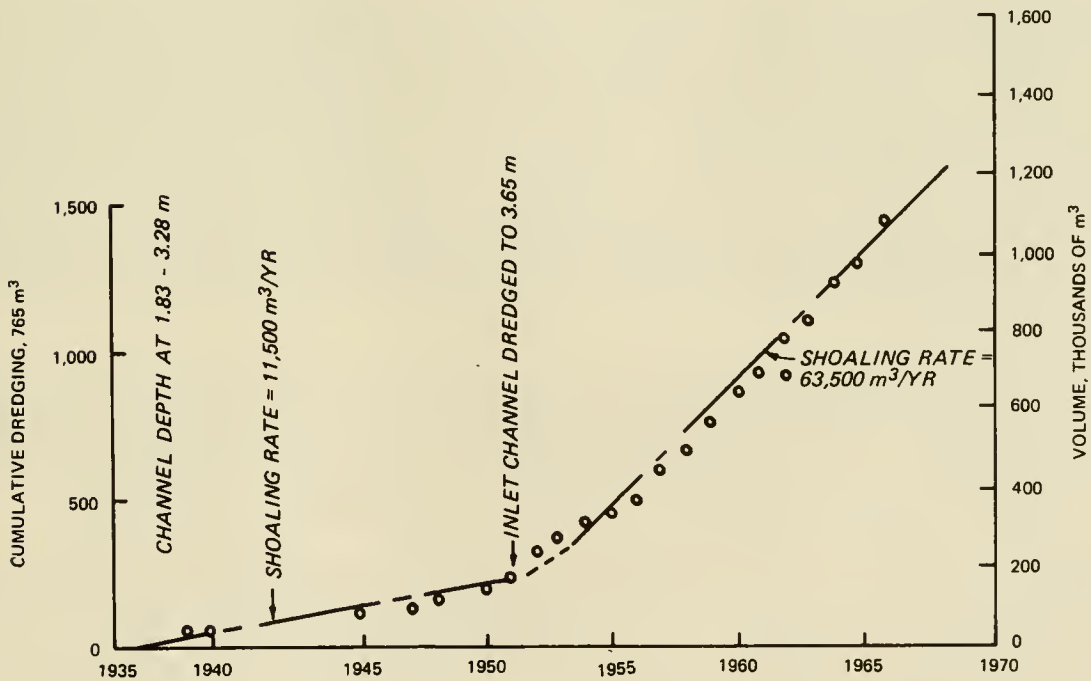
(from Lucke, 1934)

Figure 4-86. Idealized stages of deposition in a tidal lagoon if the inlets open simultaneously and remain stationary.



(from Walton, 1977)

Figure 4-87. Mass dredging curve for Pensacola Inlet, Florida.



(from Walton, 1977)

Figure 4-88. Mass dredging curve for East Pass, Florida.

increased volume of sand shoaled into the artificial channel is, in part, beach material from adjacent shorelines, although to what extent shoaling occurs is unknown and a subject for further research. The increase in channel shoaling may be a nonlinear response to increasing channel depths. Figures 4-87 and 4-88, for example, are plots of the cumulative dredging history of the ebb-tidal delta portion of the channel which has been maintained to a designed depth. The slope of the mass-dredging-versus-time curve is the average shoaling rate in the channel during that period. When the design or natural depth has been increased, the increase in shoaling has been significant. Figure 4-87 shows that increasing the depth of Pensacola Inlet, Florida, from 9.75 meters (32 feet) to 11.25 meters (37 feet) has more than doubled the shoaling rate in the channel. Similar effects are seen in Figure 4-88 for East Pass, Florida.

Channel dredging can have significant effects on adjacent shorelines, although such effects are difficult to predict or assess. Many of the deeper navigation channels in tidal inlets are dredged by hopper dredges which, due to draft limitations, must dump the channel material offshore in depths of water where the material, typically a large part beach sand, is removed from the littoral system. Although the limiting water depth for material dumped offshore of a beach to return to the beach is generally unknown, a few monitored offshore dumping tests suggest that material dumped in water depths greater than 5.5 meters (18 feet) will not return to the nearshore littoral system. The paragraphs that follow describe three trials in which offshore dumping of sand-sized material failed to provide beach material to the nearshore beach system.

Offshore dumping of sand with the intent to nourish the beach was first attempted at Santa Barbara, California, in the fall of 1935. The Santa Barbara harbor was dredged by hopper dredges; 154,000 cubic meters (202,000 cubic yards) of material was moved. Material was dumped in about 6.7 meters (22 feet) of water approximately 1 mile east of the Santa Barbara harbor breakwater and about 305 meters (1,000 feet) offshore. The sand formed a mound about 670 meters (2,200 feet) long and 1.5 meters (5 feet) high. It was expected that the waves would move the sand onshore and eastward. Surveys made in 1946 showed that the mound at that time was at no point more than 0.3 meters below its 1937 depth and did not move appreciably (U.S. Army Corps of Engineers, 1950a).

Offshore dumping of sand in 5.5 to 6.0 meters (18 to 20 feet) of water (MLW) was employed at Atlantic City, New Jersey, during the period April 1935 to September 1943. It was concluded (U.S. Army Corps of Engineers, 1950b) that the material which amounted to 2,717,000 cubic meters (3,554,000 square yards) of sand did not significantly provide nourishment for the beach.

Offshore dumping of sand by hopper dredge was carried out at Long Branch, New Jersey, in April 1948 and was monitored throughout 1948 and 1949 by the Beach Erosion Board and the U.S. Army Engineer District, New York, at Long Branch, New Jersey (Hall and Herron, 1950). The purpose of the monitoring test was to determine the feasibility of restoring an eroding shore by employing natural forces to move material, dumped in relatively deep water, shoreward toward the beach. The material was dredged from New York Harbor entrance channels (grain size  $d_{50} = 0.34$  millimeter) and was placed in a ridge about 2.1 meters (7 feet) high, 1100 meters (3,700 feet) long, and 230

meters (750 feet) wide, lying about 0.8 kilometer (0.5 mile) from shore in a depth of 11.6 meters (38 feet) below mean low water. Dumping at the site amounted to a total of 460,000 cubic meters (602,000 cubic yards) of sand. The natural beach grain size median diameter was  $d_{50} = 0.66$  millimeter. The results over the 18-month monitoring period consisting of surveys of the spoil area showed little or no movement of sand from the offshore subaqueous stockpile.

## LITERATURE CITED

- ACREE, E.H., et al., "Radioisotopic Sand Tracer Study (RIST), Status Report for May 1966-April 1968," ORNL-4341, Contract No. W-7405-eng-26, Oak Ridge National Laboratory (operated by Union Carbide Corp., for the U.S. Atomic Energy Commission), 1969.
- ARTHUR, R.S., "A Note on the Dynamics of Rip Currents," *Journal of Geophysical Research*, Vol. 67, No. 7, July 1962.
- BABA, J., and KOMAR, P.D., "Measurements and Analysis of Settling Velocities of Natural Quartz Sand Groins," *Journal of Sedimentary Petrology*, Vol. 51, pp. 631-640, June 1981.
- BAGNOLD, R.A., "Mechanics of Marine Sedimentation," *The Sea*, Vol. 3, Wiley, New York, 1963, pp. 507-528.
- BAILAND, J.A., and INMAN, D.L., "An Energetics Bedland Model for a Plane Sloping Beach: Local Transport," *Journal of Geophysical Research*, Vol. 86, pp. 2035-2044, 1981.
- BAJORUNAS, L., and DUANE, D.B., "Shifting Offshore Bars and Harbor Shoaling," *Journal of Geophysical Research*, Vol. 72, 1967, pp. 6195-6205.
- BALSILLIE, J.H., "Surf Observations and Longshore Current Prediction," Coastal Engineering Research Center, U.S. Army Engineer Waterways Experiment Station, Vicksburg, Miss., Nov. 1975.
- BASCOM, W.N., "The Relationship Between Sand Size and Beach-Face Slope," *Transactions of the American Geophysical Union*, Vol. 32, No. 6, 1951.
- BASCOM, W.N., "Waves and Beaches," *Beaches*, Ch. IX, Doubleday, New York, 1964, pp. 184-212.
- BASH, B.F., "Project Transition; 26 April to 1 June 1972," Unpublished Research Notes, U.S. Army, Corps of Engineers, Coastal Engineering Research Center, Washington, D.C., 1972.
- BATES, C.C., "Ratond Theory of Delta Formation," *Bulletin of the American Association of Petroleum Geologists*, No. 37, 1953, pp. 2119-2162.
- BATTJES, J.A., "Surf Similarity," *Proceedings of the 14th Coastal Engineering Conference*, Copenhagen, Denmark, pp. 466-480, 1944.
- BERG, D.W., "Systematic Collection of Beach Data," *Proceedings of the 11th Conference on Coastal Engineering*, London, Sept. 1968.
- BERG, D.W., and DUANE, D.B., "Effect of Particle Size and Distribution on Stability of Artificially Filled Beach, Presque Isle Peninsula, Pennsylvania," *Proceedings of the 11th Conference Great Lakes Research*, April 1968.

- BIGELOW, H.B., and EDMONDSON, W.T., "Wind Waves at Sea Breakers and Surf," H.O. 602, U.S. Navy Hydrographic Office, Washington, D.C., 1947.
- BIJKER, E.W., "Bed Roughness Influence on Computation of Littoral Drift," *Abstracts of the 12th Coastal Engineering Conference*, Washington, D.C., 1970.
- BIRKEMEIER, W.A., "The Effects of the 19 December 1977 Coastal Storm on Beaches in North Carolina and New Jersey," *Shore and Beach* Jan., 1979 (also reprint 79-2 U.S. Army Corps of Engineers, Coastal Engineering Research Center, Vicksburg, Miss., NTIS, A-70 554.
- BIRKEMEIER, W.A., "Coastal Changes, Eastern Lake Michigan, 1970-74," MR 81-2, U.S. Army Corps of Engineers, Coastal Engineering Research Center, Vicksburg, Miss., Jan. 1981.
- BODINE, B.R., "Hurricane Surge Frequency Estimated for the Gulf Coast of Texas," TM-26, U.S. Army, Corps of Engineers, Coastal Engineering Research Center, Washington, D.C., Feb. 1969.
- BOWEN, A.J., "Simple Models of Nearshore Sedimentation; Beach Profiles and Longshore Bars," in *The Coastline of Canada*, S.B McCann, editor, Geological Survey of Canada, Paper 80-10, pp. 1-11, 1980
- BOWEN, A.J., and INMAN, D.L., "Budget of Littoral Sands in the Vicinity of Point Arguello, California," TM-19, U.S. Army, Corps of Engineers, Coastal Engineering Research Center, Washington D.C., Dec. 1966.
- BOWMAN, R.S., "Sedimentary Processes Along Lake Erie Shore: Sandusky Bay, Vicinity of Willow Point," in "Investigations of Lake Erie Shore Erosion," Survey 18, Ohio Geological Survey, 1951.
- BRADLEY, W.C., "Submarine Abrasion and Wave-Cut Platforms," *Bulletin of the Geological Society of America*, Vo. 69, pp. 967-974, Aug., 1958.
- BRETSCHNEIDER, C.L., "Field Investigations of Wave Energy Loss in Shallow Water Ocean Waves," TM-46, U.S. Army, Corps of Engineers, Beach Erosion Board, Washington, D.C., Sept. 1954.
- BRETSCHNEIDER, C.L., "Fundamentals of Ocean Engineering--Part 1--Estimating Wind Driven Currents Over the Continental Shelf," *Ocean Industry*, Vol. 2, No. 6, June 1967, pp. 45-48.
- BRETSCHNEIDER, C.L., and REID, R.O., "Modification of Wave Height Due to Bottom Friction, Percolation, and Refraction," TM-45, U.S. Army, Corps of Engineers, Beach Erosion Board, Washington, D.C., Oct. 1954.
- BRICKER, O.P., ed., Carbonate Sediments, No. 19, The Johns Hopkins University Studies in Geology, 1971, 376 pp.
- BROWN, E.I., "Inlets on Sandy Coasts," *Proceedings of the American Society of Civil Engineers*, Vol. 54, Part I, Feb. 1928, pp. 505-523.

- BRUNO, R.O., et al., "Longshore Sand Transport Study at Channel Islands Harbor, California," TP 81-2, Coastal Engineering Research Center, U.S. Army Engineer Waterways Experiment Station, Vicksburg, Miss., Apr. 1981.
- BRUNO, R.O., and GABLE, C.G., "Longshore Transport at a Total Littoral Barrier," R 77-6, Coastal Engineering Research Center, U.S. Army Engineer Waterways Experiment Station, Vicksburg, Miss., July 1977.
- BRUNO, R.O., and HIIPAKKA, L.W., "Littoral Environment Observation Program in the State of Michigan," CERC R-4-74, U.S. Army Engineer Waterways Experiment Station, Vicksburg, Miss., 1974.
- BRUUN, P., "Coast Erosion and the Development of Beach Profiles," Journal Memorandum No. 44, U.S. Army, Corps of Engineers, Beach Erosion Board, Washington, D.C., 1954.
- BRUUN, P., "Sea-Level Rise as a Cause of Shore Erosion," *Journal of the Waterways and Harbors Division*, ASCE, Vol. 88, WWI, Feb. 1962, pp. 117-130.
- BRUUN, P., "Longshore Currents and Longshore Troughs," *Journal of Geophysical Research*, Vol. 68, 1963, pp. 1065-1078.
- BRUUN, P., "Use of Tracers in Coastal Engineering," *Shore and Beach*, No. 34, pp. 13-17, Nuclear Science Abstract, 20:33541, 1966.
- BRUUN, P., Paper for Section II, Subject 2, *XXIIIrd International Navigation Congress*, Ottawa, Canada, pp. 149-187, 1973.
- BRUUN, P., and GERRITSEN, F., "Investigations of Existing Data on Tidal Inlets," Interim Report, Coastal Engineering Laboratory, University of Florida, Gainesville Fla., 1957.
- BRUUN, P. and GERRITSEN, F., "Natural Bypassing of Sand At Inlets," *Journal of the Waterways and Harbors Division*, ASCE, Dec. 1959.
- BYRNE, R.J., "Field Occurrences of Induced Multiple Gravity Waves," *Journal of Geophysical Research*, Vol. 74, No. 10, May 1969, pp. 2590-2596.
- CALDWELL, J.M., "Shore Erosion by Storm Waves," MP 1-59, U.S. Army, Corps of Engineers, Beach Erosion Board, Washington, D.C., Apr. 1959.
- CALDWELL, J.M., "Wave Action and Sand Movement Near Anaheim Bay, California," TM-68, U.S. Army, Corps of Engineers, Beach Erosion Board, Washington, D.C., Feb. 1956.
- CALDWELL, J.M., "Coastal Processes and Beach Erosion," *Journal of the Boston Society of Civil Engineers*, Vol. 53, No. 2, Apr. 1966, pp. 142-157.
- CALIFORNIA COASTAL DATA COLLECTION PROGRAM, Monthly Report, Department of Boating and Waterways, State of California and South Pacific Division, U.S. Army Corps of Engineers, 1977-1981.

- CARTER, R.W.G., and KITCHEN, K.J., "The Geomorphology of Offshore Sand Bars on the North Coast of Ireland, *Proceedings of the Royal Irish Academy*, Volume 79, Section B, November 4, pp. 43-61, March, 1979.
- CARTWRIGHT, D.E., "A Comparison of Instrumental and Visually Estimated Wave Heights and Periods Recorded on Ocean Weather Ships," National Institute of Oceanography, Oct. 1972.
- CHAPMAN, D.M., "Coastal Erosion and the Sediment Budget, with Special Reference to the Gold Coast, Australia," *Coastal Engineering*, Vol. 4, pp. 207-227, Feb., 1981.
- CHARLESWORTH, L.J., Jr., "Buoy, Inlet and Nearshore Marine Sedimentation: Beach Haven-Little Egg Inlet Region, New Jersey," Unpublished Ph.D. Thesis, University of Michigan, Ann Arbor, 1968.
- CHERRY, J., "Sand Movement along a Portion of the Northern California Coast," TM-14, U.S. Army, Corps of Engineers, Coastal Engineering Research Center, Oct. 1965.
- CHIU, T.Y., "Beach and Dune Response to Hurricane Eloise of September 1975," *Proceedings of Coastal Sediments '77*, American Society of Civil Engineers, November 1977, pp. 116-134.
- CHLECK, D., et al., "Radioactive Kryptomates," *International Journal of Applied Radiation and Isotopes*, Vol. 14, 1963, pp. 581-610.
- CHOW, V.T., ed., *Handbook of Applied Hydrology*, McGraw-Hill, New York, 1964.
- CLIFT, R., GRACE, J.R., and WEBER, M.E., *Bubbles, Drops, and Particles*, Academic Press, New York, 1978.
- CLIFTON, H.E., HUNTER, R.E., and PHILLIPS, R.L., "Depositional Structures and Processes in the Non-Barred High-Energy Nearshore," *Journal of Sedimentary Petrology*, Vol. 41, pp. 651-670, Sept., 1971.
- COASTAL RESEARCH GROUP, University of Massachusetts, "Coastal Environments, N.E. Massachusetts and New Hampshire: Field Trip Guidebook," Eastern Section of the Society of Economic Paleontologists and Mineralogists, May 1969, pp. 462.
- COLBY, B.C., and CHRISTENSEN, R.P., "Visual Accumulation Tube for Size Analysis of Sands," *Journal of the Hydraulics Division*, ASCE, Vol. 82, No. 3, June 1956.
- COOK, D.O., "Sand Transport by Shoaling Waves," Ph.D. Thesis, University of Southern California, University Microfilms, Ann Michigan, 1970.
- COOK, D.O., and GORSLINE, D.S., "Field Observations of Sand Transport by Shoaling Waves," *Marine Geology*, Vol. 13, No. 1, 1972.
- COOPER, W.S., "Coastal Sand Dunes of Oregon and Washington," Memoir No. 72, Geological Society of America, June 1958.

- CORNAGLIA, P., "On Beaches," translation by W.N. Felder, in *Beach Processes and Coastal Hydrodynamics*, J.S. Fisher and R. Dolan, eds., Dowden, Hutchinson, and Ross, Stroudsburg, Pa., pp. 11-26, 1977 (1889).
- CORSON, W.D., et al., "Atlantic Coast Hindcast Deepwater Significant Wave Information," WIS Report 2, U.S. Army Engineer Waterways Experiment Station, Vicksburg, Miss., Jan., 1981.
- CUMMINS, R.S., Jr., "Radioactive Sediment Tracer Tests, Cape Fear River, North Carolina," MP No. 2-649, U.S. Army Engineer Waterways Experiment Station, Vicksburg, Miss., May 1964.
- DAHL, B.E., FALL, G.A., LOHSE, A., and APPAN, S.G., "Construction and Stabilization of Coastal Foredunes with Vegetation: Padre Island, Texas," MP 9-75, U.S. Army Engineer Waterways Experiment Station, Coastal Engineering Research Center, Vicksburg, Miss., Sept. 1975.
- DAS, M.M., "Suspended Sediment and Longshore Sediment Transport Data Review," *13th International Conference on Coastal Engineering*, Vancouver, B.C., Canada, July 1972.
- DAVIS, J.L., "The Coastal Sediment Compartment," *Australian Geographical Studies*, Vol. 12, pp. 139-151, 1974.
- DAVIS, R.A., Jr., "Sedimentation in the Nearshore Environment, Southeastern Lake Michigan," Thesis, University of Illinois, Urbana, Illinois, 1964.
- DAVIS, R.A., Jr., "Beach Changes on the Central Texas Coast Associated with Hurricane Fern, September 1971," Vol. 16, *Contributions in Marine Science*, University of Texas, Marine Science Institute, Port Aransas, Texas, 1972.
- DAVIS, R.A., Jr., et al., "Comparison of Ridge and Runnel Systems in Tidal and Non-Tidal Environments," *Journal of Sedimentary Petrology*, Vol. 42, No. 2, June 1972, pp. 413-421.
- DAVIS, R.A., Jr., and FOX, W.T., "Four-Dimensional Model for Beach and Inner Nearshore Sedimentation," *The Journal of Geology*, Vol. 80, No. 4, July 1972.
- DEAN, R.G., "Relative Validities of Water Wave Theories," *Journal of the Waterways and Harbors Division*, ASCE, Vol. 96, WWI, 1970, pp. 105-119.
- DEAN, R.G., "Heuristic Models of Sand Transport in the Surf Zone," *Conference on Engineering Dynamics in the Coastal Zone*, 1973.
- DEAN, R.G., "Beach Erosion: Causes, Processes and Remedial Measures," *CRC Critical Reviews in Environmental Control*, Vol. 6, Issue 3, 1976.
- DEAN, R.G., "Equilibrium Beach Profiles: U.S. Atlantic and Gulf Coasts," Ocean Engineering Technical Report No. 12, Department of Civil Engineering, University of Delaware, Newark, Delaware, 1977.

- DEAN, R.G., and WALTON, T.L., Jr., "Sediment Transport Processes in the Vicinity of Inlets with Special Reference to Sand Trapping," *Proceedings of the International Estuarine Research Federation Conference*, Myrtle Beach, S. C., Oct. 1973.
- DeWALL, A.E., "Beach Changes at Westhampton Beach, New York, 1967-73," MR-79-5, Coastal Engineering Research Center, U.S. Army Engineer Waterways Experiment Station, Vicksburg, Miss., 1979.
- DeWALL, A.E., et al., "Beach Changes Caused by the Atlantic Coast Storm of 17 December 1970," TP 77-1, Coastal Engineering Research Center, U.S. Army Engineer Waterways Experiment Station, Vicksburg, Miss., Jan. 1977.
- DeWALL, A.E., PRITCHETT, P.C., and GALVIN, C.J., Jr., "Beach Changes Caused by a Northeaster Along the Atlantic Coast," *Abstracts from the Annual Meeting of the Geological Society of America*, Washington, D.C., 1971.
- DIETZ, R.S., "Wave Base, Marine Profile of Equilibrium, and Wave-Built Terraces: A Critical Appraisal," *The Geological Society of America Bulletin*, Vol. 74, No. 8, Aug. 1963, pp. 971-990.
- DIETZ, R.S., and FAIRBRIDGE, R.W., "Wave Base" in *The Encyclopedia of Geomorphology*, R.W. Fairbridge, ed., Reinhold, New York, pp. 1224-1228, 1968.
- DIVOKY, D., LEMEHAUTE, B., and LIN, A., "Breaking Waves on Gentle Slopes," *Journal of Geophysical Research*, Vol. 75, No. 9, 1970.
- DRAPER, L., "Wave Activity at the Sea Bed Around Northwestern Europe," *Marine Geology*, Vol. 5, 1967, pp. 133-140.
- DUANE, D.B., "Sand Deposits on the Continental Shelf: A Presently Exploitable Resource," *Transactions of National Symposium on Ocean Sciences and Engineering of the Atlantic Shelf*, Marine Technology Society, Mar. 1968.
- DUANE, D.B., "Synoptic Observations of Sand Movement," *Proceedings of the 12th Coastal Engineering Conference*, Washington, D.C. September 1970a.
- DUANE, D.B., "Tracing Sand Movement in the Littoral Zone: Progress in the Radioisotopic Sand Tracer (RIST) Study, July 1968- February 1969," MP 4-70, U.S. Army, Corps of Engineers, Coastal Engineering Research Center, Washington, D.C., Aug. 1970b.
- DUANE, D.B., "Sedimentation and Coastal Engineering: Beaches and Harbors," in *Marine Sediment Transport and Environmental Management*, D.J. Stanley and D.J.P. Swift, eds., Wiley, New York, pp. 493-517, 1976.
- DUANE, D.B., and JUDGE, C.W., "Radioisotopic Sand Tracer Study, Point Conception, California," MP 2-69, U.S. Army, Corps of Engineers, Coastal Engineering Research Center, Washington, D.C., May 1969.
- DUANE, D.B., and MEISBURGER, E.P., "Geomorphology and Sediments of the Nearshore Continental Shelf, Miami to Palm Beach, Florida," TM-29, U.S. Army, Corps of Engineers, Coastal Engineering Research Center, Washington, D.C., Nov. 1969.

- DUANE, D.B., et al., "Linear Shoals on the Atlantic Inner Continental Shelf, Florida to Long Island," in *Shelf Sediment Transport*, by Swift, Duane, and Pilkey, eds., Dowden, Hutchinson, and Ross, Stroudsburg, Pa. 1972.
- DUBOIS, R.N., "Inverse Relation Between Foreshore Slope and Mean Grain Size as a Function of the Heavy Mineral Content," *Geological Society of America Bulletin*, Vol. 83, Mar. 1972, pp. 871-876.
- EAGLESON, P.S., "Properties of Shoaling Waves by Theory and Experiment," *Transactions of the American Geophysical Union*, Vol. 37, 1956, pp. 565-572.
- EDELMAN, T., "Dune Erosion During Storm Conditions," *Proceedings of the 11th Conference on Coastal Engineering*, American Society of Civil Engineers, New York, 1968, p. 719.
- EINSTEIN, H.A., "A Basic Description of Sediment Transport on Beaches," *Report HEL-2-34*, Hydraulic Engineering Laboratory, University of California, Berkeley, California, Aug. 1971.
- EMERY, K.O., "The Sea off Southern California," *Sediments*, Ch. 6, Wiley, New York, 1960, pp. 180-295.
- ESCOFFIER, F.F., and WALTON, T.L., Jr., "Inlet Stability Solutions for Tributary Inflow," *Proceedings Paper 14964, Journal of the Waterway, Port, Coastal and Ocean Division*, ASCE, Vol. 105, No. WW4, Nov. 1979, pp. 341-355.
- EVERTS, C.H., "Geometry of Profiles Across Inner Continental Shelves of the Atlantic and Gulf Coasts of the United States," Technical Paper No. 78-4, U.S. Army Engineer Waterways Experiment Station, Coastal Engineering Research Center, Vicksburg, Miss., Apr., 1978.
- EVERTS, C.H., "A Rational Approach to Marine Placers," Unpublished Ph.D. Thesis, University of Wisconsin, Madison, Wis., 1971.
- EVERTS, C.H., "Beach Profile Changes in Western Long Island," in "Coastal Geomorphology," *Proceedings of the Third Annual Geomorphology Symposia Series*, 1973, pp. 279-301.
- EVERTS, C.H., et al., "Beach and Inlet Changes at Ludlam Beach, New Jersey," MR-80-3, U.S. Army Engineer Waterways Experiment Station, Coastal Engineering Research Center, Vicksburg, Miss., May 1980.
- FAIRCHILD, J.C., "Development of a Suspended Sediment Sampler for Laboratory Use Under Wave Action," *Bulletin of the Beach Erosion Board*, Vol. 10, No. 1, July 1956.
- FAIRCHILD, J.C., "Suspended Sediment Sampling in Laboratory Wave Action," TM-115, U.S. Army, Corps of Engineers, Beach Erosion Board, Washington, D.C., June 1959.
- FAIRCHILD, J.C., "Longshore Transport of Suspended Sediment," *Proceedings of the 13th Coastal Engineering Conference*, Vancouver, B.C., Canada, July 1972.

- FISHER, C.H., "Mining the Ocean for Beach Sand," *Proceedings of Civil Engineering in the Oceans II*, ASCE, Dec. 1969.
- FOLK, R.L., *Petrology of Sedimentary Rocks*, Hemphill's, Austin, Texas, 1965.
- FOLK, R.L., "A Review of Grain Size Parameters," *Sedimentology*, Vol. 6, 1966, pp. 73-93.
- FOLK, R.L., and WARD, W.C., "Brazos River Bar. A Study in the Significances of Grain Size Parameters," *Journal of Sedimentary Petrology*, Vol. 27, 1957, pp. 3-26.
- FOREMAN, J.W., and MACHMAEL, J.L., "Sediment Dynamics and Shoreline Response at Drum Inlet, N. C.," Report No. S. G. 78-7, North Carolina State University of Marine Science and Engineering, 1972.
- FOX, W.T., "Anatomy of a Storm on the Lake Michigan Coast," Unpublished Paper, *Conference on Effects of Extreme Conditions on Coastal Environments*, Western Michigan University, Nov. 1970.
- GAGE, B.O., "Experimental Dunes of the Texas Coast," MP 1-70, U.S. Army, Corps of Engineers, Coastal Engineering Research Center, Washington, D.C., Jan. 1970.
- GALVIN, C.J., Jr., "Experimental and Theoretical Study of Longshore Currents on a Plane Beach," Unpublished Ph.D. Thesis, Department of Geology and Geophysics, Massachusetts Institute of Technology, Cambridge, Mass., 1963.
- GALVIN, C.J., Jr., "A Selected Bibliography and Review of the Theory and Use of Tracers in Sediment Transport Studies," Vol. I, Bulletin and Summary Report of Research Progress, Fiscal Year 1964, U.S. Army, Corps of Engineers, Coastal Engineering Research Center, Washington, D.C., 1964a.
- GALVIN, C.J., Jr., "A Theoretical Distribution of Waiting Times for Tracer Particles on Sand Bed," Vol. I, Bulletin and Summary of Research Progress, Fiscal Year 1964, U.S. Army, Corps of Engineers, Coastal Engineering Research Center, Washington, D.C., 1964b.
- GALVIN, C.J., Jr., "Longshore Current Velocity: A Review of Theory and Data," *Reviews of Geophysics*, Vol. 5, No. 3, Aug. 1967.
- GALVIN, C.J., Jr., "Wave Climate and Coastal Processes," *Water Environments and Human Needs*, A.T. Ippen, ed., M.I.T. Parsons Laboratory for Water Resources and Hydrodynamics, Cambridge, Mass., 1971, pp. 48-78.
- GALVIN, C.J., Jr., "Wave Breaking in Shallow Water," *Waves on Beaches and Resulting Sediment Transport*, Academic Press, March 1972a.
- GALVIN, C.J., Jr., "A Gross Longshore Transport Rate Formula," *Proceedings of the 13th Coastal Engineering Conference*, Vancouver B.C., Canada, July 1972b.
- GALVIN, C.J., Jr., and EAGLESON, P.S., "Experimental Study of Longshore Currents on a Plane Beach," TM-10, U.S. Army, Corps of Engineers, Coastal Engineering Research Center, Washington, D.C., Jan. 1965.

- GALVIN, C.J., and NELSON, R.A., "A Compilation of Longshore Current Data," MP 2-67, Corps of Engineers, Coastal Engineering Research Center, Washington, D.C., Mar. 1967.
- GALVIN, C., and SCHWEPPE, C.R., "The SPM Energy Flux Method for Predicting Longshore Transport Rate," TP 80-4, Coastal Engineering Research Center, U.S. Army Engineer Waterways Experiment Station, Vicksburg, Miss., June 1980.
- GIBBS, R.J., "The Geochemistry of the Amazon River System: Part I. The Factors that Control the Salinity and the Composition and Concentration of the Suspended Solids," *Geological Society of America Bulletin*, Vol. 78, Oct. 1967, pp. 1203-1232.
- GIBBS, R.J., "The Accuracy of Particle-Size Analysis Utilizing Settling Tubes," *Journal of Sedimentary Petrology*, Vol. 42, No. 1, Mar. 1972.
- GILES, R.T., and PILKEY, O.H., "Atlantic Beach and Dune Sediments of the Southern United States," *Journal of Sedimentary Petrology*, Vol. 35, No. 4, Dec. 1975, pp. 900-910.
- GODA, Y., "A Synthesis of Breaker Indices," *Proceedings of the Japan Society of Civil Engineers*, No. 180, August 1970.
- GODFREY, P.J., and GODFREY, M.M., "Comparison of Ecological and Geomorphic Interactions Between Altered and Unaltered Barrier Island Systems in North Carolina," in "Coastal Geomorphology," *Proceedings of the Third Annual Geomorphology Symposia Series*, 1972, pp. 239-258.
- GONZALES, W.R., "A Method for Driving Pipe in Beach Rock," Vol. III, Bulletin and Summary of Research Progress, Fiscal Years 1967-69, U.S. Army, Corps of Engineers, Coastal Engineering Research Center, Washington, D.C., July 1970.
- GOODWIN, C.R., "Estuarine Tidal Hydraulics," Ph.D. Thesis, Oregon State University, Corvallis, Ore., 1974.
- GORDON, A.D., and ROY, P.S., "Sand Movements in Newcastle Bight," *Proceedings of the 3rd Australian Conference on Coastal and Ocean Engineering*, Melbourne, Australia, pp. 64-69, 1977.
- GRACE, R.A., "Nearbottom Water Motion Under Ocean Waves," *Proceedings of the 15th Coastal Engineering Conference*, Honolulu, Hawaii, pp. 2371-2386, 1976.
- GRAHAM, H.E., and NUNN, D.E., "Meteorological Considerations Pertinent to Standard Project Hurricane, Atlantic and Gulf Coasts of the United States," National Hurricane Research Project Report No. 33, U.S. Department of Commerce, Weather Bureau, Washington, D.C., Nov., 1959.
- GREENWOOD, B., and DAVIDSON-ARNOTT, R.G.D., "Sedimentation and Equilibrium in Wave-Formed Bars: A Review and Case Study," *Canadian Journal of Earth Sciences*, Vol. 16, pp. 312-332, 1979.
- GRIFFITHS, J.C., "Scientific Method in Analysis of Sediments," McGraw-Hill, New York, 1967.

- GROSSKOPF, W.G., "Calculation of Wave Attenuation Due to Friction and Shoaling: An Evaluation," TP 80-8, Coastal Engineering Research Center, U.S. Army Engineer Waterways Experiment Station, Vicksburg, Miss., Oct. 1980.
- HALL, J.V., Jr., and HERRON, W.J., "Test of Nourishment of the Shore by Offshore Deposition of Sand, Long Branch, N. J.," BEB Technical Memorandum AD No. 699 395, 1950 (available from National Technical Information Service, Springfield, Va).
- HALLERMEIER, R.J., "Sand Motion Initiation by Water Waves: Two Asymptotes," *Journal of the Waterway, Port, Coastal, and Ocean Division*, ASCE, Vol. 106, No. WW3, pp. 299-318, Aug., 1980.
- HALLERMEIER, R.J., "Seaward Limit of Significant Sand Transport by Waves: An Annual Zonation for Seasonal Profiles," *Coastal Engineering Technical Aid No. 81-2*, Coastal Engineering Research Center, U.S. Army Engineer Waterways Experiment Station, Vicksburg, Miss., Jan., 1981a.
- HALLERMEIER, R.J., "A Profile Zonation for Seasonal Sand Beaches from Wave Climate," *Coastal Engineering*, Vol. 4, pp. 253-277, Feb., 1981b.
- HALLERMEIER, R.J., "Terminal Settling Velocity of Commonly Occurring Sand Grains," *Sedimentology*, Vol. 28, 1981c.
- HANDIN, J.W., "The Source, Transportation, and Deposition of Beach Sediment in Southern California," TM-22, U.S. Army, Corps of Engineers, Beach Erosion Board, Washington, D.C., Mar. 1951.
- HANDS, E.B., "A Geomorphic Map of Lake Michigan Shoreline," *Proceedings of the 13th Conference on Great Lakes Research*, International Association Great Lakes Research, 1970, pp. 250-265.
- HARRIS, D.L., "Finite Spectrum Analyses of Wave Records," *Proceedings of the International Symposium on Ocean Wave Measurement and Analysis*, American Society of Civil Engineers, Vol. 1, 1974, pp. 107-124 (also Reprint 6-74, Coastal Engineering Research Center, U.S. Army Engineer Waterways Experiment Station, Vicksburg, Miss., NTIS A002 113).
- HARRIS, D.L., "The Analysis of Wave Records," *Proceedings of the Conference on Coastal Engineering*, Washington, D.C., 1970, pp. 85-100.
- HARRIS, D.L., "Characteristics of Wave Records in the Coastal Zone," *Waves on Beaches and Resulting Sediment Transport*, Academic Press, 1972a.
- HARRIS, D.L., "Wave Estimates for Coastal Regions," in *Shelf Sediment Transport*, edited by Swift, Duane, and Pilkey, eds., Dowden, Hutchinson, and Ross, Stroudsburg, Pa., 1972b.
- HART, E.D., "Radioactive Sediment Tracer Tests, Houston Ship Channel, Houston, Texas," H-69-2, U.S. Army Engineer Waterways Experiment Station, Vicksburg, Miss., 1969.

- HAYES, M.O., "Hurricanes as Geological Agents: Case Studies of Hurricanes Carla, 1961, and Cindy, 1963," Report 61, Bureau of Economic Geology, University of Texas, Austin, Tex., 1967a.
- HAYES, M.O., "Relationship between Coastal Climate and Bottom Sediment on the Inner Continental Shelf," *Marine Geology*, 1967b, pp. 111-132.
- HAYES, M.O., "Forms of Sediment Accumulation in the Beach Zone," *Waves on Beaches and Resulting Sediment Transport*, Academic Press, New York, Oct. 1971a.
- HAYES, M.O., Lecture Notes for Course on Inlet Mechanics and Design (unpublished), 10-20 May 1971b (available from U.S. Army Engineer, Waterways Experiment Station, Vicksburg, Miss.)
- HAYES, M.O., "Morphology of Sand Accumulation in Estuaries: An Introduction to the Symposium," in Cronin, L.E., ed., *Proceedings of the 2nd International Estuarine Research Federation Conf.*, Myrtle Beach, S. C., 3-22, 1975.
- HAYES, M.O., GOLDSMITH, V., and HOBBS, C.H., III, "Offset Coastal Inlets: *Proceedings of the 12th Coastal Engineering Conference*, ASCE, Washington, D.C., Sept. 1970, pp. 1187-1200.
- HERRON, W.J., and HARRIS, R.L., "Littoral Bypassing and Beach Restoration in the Vicinity of Port Hueneme, California," *Proceedings of the 10th Conference on Coastal Engineering*, Tokyo, 1966, ASCE, United Engineering Center, New York, 1967.
- HICKS, S.D., "On Classifications and Trends of Long Period Sea Level Series," *Shore and Beach*, Apr. 1972.
- HOBSON, R.D., "Review of Design Elements for Beach-Fill Evaluation," TP 77-6, U.S. Army, Corps of Engineers, Coastal Engineering Research Center, Vicksburg, Miss., 1977.
- HOWARD, A.D., "Hurricane Modification of the Offshore Bar of Long Island, New York," *Geographical Review*, Vol. 29, No. 3, July 1939 p. 400-415.
- HOWARD, J.D., and REINECK, H.E., "Depositional Facies of High-Energy Beach-to-Offshore Sequence: Comparison with Low-Energy Sequence," *American Association of Petroleum Geologists Bulletin*, Vol. 65, No. 5, pp. 807-830, May, 1981.
- HUBBELL, D.W., and SAYRE, W.W., "Sand Transport Studies with Radioactive Tracers," *Journal of the Hydraulics Division*, ASCE, Vol. 90, No. HY3, 1965, pp. 39-68.
- HUGHES, S.A., and CHIU, T.Y., "Beach and Dune Erosion During Severe Storms," TR-043, Coastal and Oceanographic Engineering Department, University of Florida, 1981.
- HULSEY, J.D., "Beach Sediments of Eastern Lake Michigan," Ph.D. Dissertation, University Microfilming 62-6164, University of Illinois, Urbana, Ill., 1962.

- HUME, J.D., and SCHALK, M., "Shoreline Processes Near Barrow, Alaska: A Comparison of the Normal and the Catastrophic," *Arctic*, Vol. 20, No. 2, June 1967, pp. 86-103.
- HUNTER, R.E., CLIFTON, H.E., and PHILLYIS, R.L., "Depositional Processes, Sedimentary Structures, and Predicted Vertical Sequences in Barred Nearshore Systems, Southern Oregon Coast," *Journal of Sedimentary Petrology*, Vol. 49, No. 3, pp. 711-726, Sept., 1979.
- HUSTON, K.H., "A Critical Appraisal of the Technique of Using Naturally Occurring Radioactive Materials as Littoral Tracers," HEL-4-1, Hydraulic Engineering Institute, University of California, Berkeley, Calif., 1963.
- INGLE, J.C., "The Movement of Beach Sand," *Devel. Sediment*, Vol. 5, Elsevier, Amsterdam, 1966.
- INGRAM, L.F., CUMMINS, R.S., and SIMMONS, H.B., "Radioactive Sediment Tracer Tests Near the North and South Jetties, Galveston Harbor Entrance," MP 2-472, U.S. Army Engineer Waterways Experiment Station, Vicksburg, Miss., Nov. 1965.
- INMAN, D.L., "Measures for Describing the Size Distribution of Sediments," *Journal of Sedimentary Petrology*, Vol. 22, No. 3, Sept. 1952, pp. 125-145.
- INMAN, D.L., "Wave-Generated Ripples in Nearshore Sands," TM-100, U.S. Army, Corps of Engineers, Beach Erosion Board, Washington, D.C., Oct. 1957.
- INMAN, D.L., and QUINN, W.H., "Currents in the Surf Zone," *Proceedings of the Second Conference on Coastal Engineering*, ASCE, Council on Wave Research, Berkeley, Calif., 1952, pp. 24-36.
- INMAN, D.L., and RUSNAK, G.S., "Changes in Sand Level on the Beach and Shelf at La Jolla, California," TM-82, U.S. Army, Corps of Engineers, Beach Erosion Board, Washington, D.C., July 1956.
- INMAN, D.L., TAIT, R.J., and NORDSTROM, C.E., "Mixing in the Surf Zone," *Journal of Geophysical Research*, Vol. 76, No. 15, May 1971, p. 3493.
- IPPEN, A.T., ed., *Estuary and Coastline Hydrodynamics*, McGraw-Hill Book Co., 1966.
- JAMES, W.R., "A Class of Probability Models for Littoral Drift," *Proceedings of the 12th Coastal Engineering Conference*, Washington, D.C., Sept. 1970.
- JARRETT, J.T., Tidal Prism-Inlet Area Relationships, GITI, Report 3, U.S. Army Engineer Waterways Experiment Station, Vicksburg, Miss., Feb. 1976.
- JARRETT, J.T., "Sediment Budget Analysis: Wrightsville Beach to Kore Beach, N.C.," *Proceedings, Coastal Sediments '77 Speciality Conference*, Charleston, S.C., 1977.
- JOHNSON, J.W., "Sand Transport by Littoral Currents" *Proceedings of the Fifth Hydraulics Conference*, Bulletin 34, State University of Iowa, Studies in Engineering, 1953, pp. 89-109.

- JOHNSON, J.W., "Dynamics of Nearshore Sediment Movement," *American Association of Petroleum Geology Bulletin*, Vol. 40, No. 9, 1956, pp. 2211-2232.
- JOHNSON, J.W., "The Littoral Drift Problem at Shoreline Harbors," *Journal of the Waterways and Harbors Division*, ASCE, 83, WWI, Paper 1211, Apr 1957.
- JOHNSON, J.W., "The Supply and Loss of Sand to the Coast," *ASCE Journal*, Vol. 85, No. WW3, Sept. 1959, pp. 227-251.
- JUDGE, C.W., "Heavy Minerals in Beach and Stream Sediments as Indicators of Shore Processes between Monterey and Los Angeles, California," TM-33, U.S. Army, Corps of Engineers, Coastal Engineering Research Center, Washington, D.C., Nov. 1970.
- KAMEL, A.M., "Littoral Studies Near San Francisco Using Tracer Techniques," TM-131, U.S. Army, Corps of Engineers, Beach Erosion Board, Washington, D.C., Nov. 1962.
- KAMEL, A.M., and JOHNSON, J.W., "Tracing Coastal Sediment Movement by Naturally Radioactive Minerals," *Proceedings of the Eighth Coastal Engineering Conference*, ASCE, 1962, p. 324.
- KANA, T.W., "Beach Erosion During Minor Storm," *Journal of the Waterway, Port, Coastal and Ocean Division*, ASCE, Vol. 103, WW4, November 1977, pp. 505-518.
- KANA, T.W., "Suspended Sediment in Breaking Waves," Technical Report No. 18-CRD, Department of Geology, University of South Carolina, Columbia, Apr., 1979.
- KENNEDY, J.F., and LOCHER, F.A., "Sediment Suspension by Water Waves," *Waves on Beaches and Resulting Sediment Transport*, Academic Press, New York, 1972.
- KEULEGAN, G.H., "Tidal Flow in Entrances Water-Level Fluctuations of Basins in Communications with Seas," Technical Bulletin No. 14, Committee on Tidal Hydraulics, U.S. Army Engineer Waterways Experiment Station, Vicksburg, Miss., Jul. 1967.
- KEULEGAN, G.H., "Wind Tides in Small Closed Channels," Research Paper No. 2207, National Bureau of Standards, Washington, D.C., 1951.
- KEULEGAN, G.H., and KRUMBEIN, W.C., "Stable Configuration of Bottom Slope in a Shallow Sea and Its Bearing in Geological Processes," *Transactions*, American Geophysical Union, Vol. 30, No. 6, pp. 855-861, Dec., 1949.
- KIDSON, C., and CARR, A.P., "Marking Beach Materials for Tracing Experiments," *Journal of the Hydraulics Division*, ASCE, Vol. 88, July 1962.
- KING, C.A.M., *Beaches and Coasts*, Edward Arnold, Ltd., 1972.
- KING, D.B., "The Dynamics of Inlets and Bays," Technical Report No. 2, Coastal and Oceanographic Engineering Laboratory, University of Florida, Gainesville, Fla., Mar. 1974.

- KINSMEN, B., *Wind Waves, Their Generation and Propagation on the Ocean Surface*, Prentice-Hall, Englewood Cliffs, N.J., 1965.
- KIRTLEY, D.W., "Reef-Building Worms," *Sea Frontiers*, Vol. 17, No. 2, 1971.
- KNUTSON, P.L., "Experimental Dune Restoration and Stabilization, Nauset Beach, Cape Cod, Massachusetts," TP 80-5, Coastal Engineering Research Center, U.S. Army Engineer Waterways Experiment Station, Vicksburg, Miss., Aug. 1980.
- KOHLER, R.R., and GALVIN, C.J., "Berm-Bar Criterion," Unpublished CERC Laboratory Report, Aug. 1973, 70 p.
- KOLESSAR, M.A., and REYNOLDS, J.L., "The Sears Sea Sled for Surveying in the Surf Zone," Vol. II, Bulletin and Summary Report of Research Progress, Fiscal years 1965-66, U.S. Army, Corps of Engineers, Coastal Engineering Research Center, Washington, D.C. 1966.
- KOMAR, P.D., "The Longshore Transport of Sand on Beaches," Unpublished Ph.D. Thesis, University of California, San Diego, Calif., 1969.
- KOMAR, P.D., *Beach Processes and Sedimentation*, Prentice-Hall, Englewood Cliffs, New Jersey, 1976.
- KOMAR, P. D., and INMAN, D.L., "Longshore Sand Transport on Beaches, *Journal of Geophysical Research*, Vol. 75, No. 30, Oct. 20, 1970, pp. 5914-5927.
- KRAAI, P.T., "Comparison of Wind Wave and Uniform Wave Effects on a Beach," HEL 1-13, Hydraulic Engineering Laboratory, College of Engineering, University of California, Berkeley, Calif., Aug. 1969.
- KRAFT, J.C., "A Guide to the Geology of Delaware's Coastal Environments," Publication 2GL039, College of Marine Studies, University of Delaware, Newark, Del., 1971.
- KRINSLEY, D., et al., "Transportation of Sand Grains Along the Atlantic Shore of Long Island, New York: An Application of Electron Microscopy," *Marine Geology*, Vol. 2., 1964, pp. 100-121.
- KRUMBEIN, W.C., "Application of Logarithmic Moments to Size Frequency Distribution of Sediments," *Journal of Sedimentary Petrology*, Vol. 6, No. 1., 1936, pp. 35-47.
- KRUMBEIN, W.C., "Shore Processes and Beach Characteristics," TM-3, U.S. Army Corps of Engineers, Beach Erosion Board, Washington, D.C., 1944.
- KRUMBEIN, W.C., and SLOSS, L.L., "Stratigraphy and Sedimentation, Ch. 4, *Properties of Sedimentary Rocks*, W.H. Freeman & Company, 1963, pp. 93-149.
- KUENEN, P.H., *Marine Geology*, Wiley, New York, 1950.
- KUENEN, P.H., "Experimental Abrasion of Pebbles, Rolling by Current," *Journal of Geology*, Vol. 64, 1956, pp. 336-368.

- LAVELLE, J.W., and THACKER, W.C., "Effects of Hindered Settling on Sediment Concentration Profiles," *Journal of Hydraulic Research*, Vol. 16, No. 4, p. 347-355, 1978.
- LEATHERMAN, et al., "Overwash Sedimentation Associated with a Large-Scale Northeaster," *Marine Geology*, 24, 1977, pp. 109-121.
- LEE, J., YANCY, T., and WILDE, P., "Recent Sedimentation of the Central California Continental Shelf," Part A: Introduction and Grain Size Data, HEL 2-28, College of Engineers, University of California, Berkeley, Calif., Oct. 1970.
- LEMEHAUTE, B., and SOLDATE, M., "A Numerical Model for Predicting Shoreline Changes," MR 80-6, Coastal Engineering Research Center, U.S. Army Engineer Waterways Experiment Station, Vicksburg, Miss., July 1980.
- LOFQUIST, K.E.B., "An Effect of Permeability on Sand Transport Waves," TM-62, Coastal Engineering Research Center, U.S. Army Engineer Waterways Experiment Station, Vicksburg, Miss., Dec. 1975.
- LONGUET-HIGGINS, M.S., "Longshore Currents Generated by Obliquely Incident Sea Waves, 1," *Journal of Geophysical Research*, Vol. 75, No. 33, Nov. 1970a, pp. 6788-6801.
- LONGUET-HIGGINS, M.S., "Longshore Currents Generated by Obliquely Incident Sea Waves, 2," *Journal of Geophysical Research*, Vol. 75, No. 33, Nov. 1970b, pp. 6790-6801.
- LONGUET-HIGGINS, M.S., "Recent Progress in the Study of Longshore Currents," *Waves on Beaches and Resulting Sediment Transport*, Academic Press, New York, Oct. 1971.
- LUCKE, J.B., "A Study of Barnegat Inlet," *Shore and Beach*, Vol. 2, No. 2, 1934, pp. 45-94.
- MacDONALD, T.C., "Sediment Suspension and Turbulence in an Oscillating Flume," TP 77-4, Coastal Engineering Research Center, U.S. Army Engineer Waterways Experiment Station, Vicksburg, Miss., Apr. 1977.
- MADSEN, O.S., and GRANT, W.G., "Sediment Transport in the Coastal "Sediment Transport in the Coastal Environment," Report No. 209, Department of Civil Engineering, Massachusetts Institute of Technology, Cambridge, Mass., 1976.
- MAGOON, O. T., HAUGEN, J.C., and SLOAN, R.L., "Coastal Sand Mining in Northern California, U.S.A.," *Proceedings of the 13th Coastal Engineering Research Conference*, Vancouver, B.C., Canada, July 1972.
- MAGOON, O.T., and SARLIN, W.O., "Effect of Long-Period Waves on Hydrographic Surveys," *Proceedings of the 12th Coastal Engineering Conference*, Washington, D.C., September 1970.
- MARTENS, J.H.C., "Beaches of Florida," Annual Report (21st-22nd), Florida State Geological Study, 1928-1930.

- MASON, C., and SORENSEN, R.M., "Properties and Stability of a Texas Barrier Beach Inlet," U.S. Army, Corps of Engineers, Report No. 146, Texas A&M University, 1971.
- MASON, M.A., "Abrasion of Beach Sands," TM-2, U.S. Army, Corps of Engineers, Beach Erosion Board, Washington, D.C., Feb. 1942.
- McCAMMON, R.B., "Efficiencies of Percentile Measures for Describing the Mean Size and Sorting of Sedimentary Particles," *Journal of Geology*, Vol. 70, 1962, pp. 453-465.
- McCAYE, I.N., "Wave Effectiveness at the Sea Bed and Its Relationship to Bed-Forms and the Deposition of Mud," *Journal of Sedimentary Petrology*, Vol. 41, pp. 89-96, 1971.
- McCORMICK, C.L. "A Probable Cause for Some Changes in the Beach Erosion Rates on Eastern Long Island," Unpublished Paper, Southampton College, Long Island University, New York, 1971.
- McMASTER, R.L., "Petrography and Genesis of the N.J. Beach Sands," Geology Series, Vol. 63, New Jersey Department of Conservation & Economic Development, 1954.
- MEHTA, A.J., LEE, J., and CHRISTENSEN, B.A., "Fall Velocity of Shells as Coastal Sediment," *Journal of the Hydraulics Division*, ASCE, Vol. 106, No. HY11, pp. 1727-1744, Nov. 1981.
- MEI, C.C., LIU, P., and CARTER, T.G., "Mass Transport in Water Waves, Part I: Theory - Part II: Experiments," Report No. 146, Ralph M. Parsons Laboratory for Water Resources and Hydrodynamics, Massachusetts Institute of Technology, Apr. 1972.
- MEYER, A.L., and CHESTER, A.L., "The Stabilization of Clatsop Plains, Oregon," *Shore and Beach*, Oct 1977, pp. 34-41.
- MILLER, M.C., et al., "Beach Changes at Long Beach Island, New Jersey, 1962-73," MR 80-9, Coastal Engineering Research Center, U.S. Army Engineer Waterways Experiment Station, Vicksburg, Miss., Oct. 1980.
- MILLIMAN, J.D., "Atlantic Continental Shelf and Slope of the United States-- Petrology of the Sand Friction of Sediments, Northern New Jersey to Southern Florida," Geological Survey Professional Paper 529-J, U.S. Government Printing Office, Washington, D.C., 1972.
- MILLIMAN, J.D., PILKEY, O.H., and ROSS, D.A., "Sediments of the Continental Margin off the Eastern United States," *Geological Society of America Bulletin*, Vol. 83, pp. 1315-1334, May, 1972.
- MOBERLEY, R., "Loss of Hawaiian Sand," *Journal of Sedimentary Petrology*, Vol. 38, 1968, pp. 17-34.
- MOGRIDGE, G.R., and KAMPHUIS, J.W., "Experiments on Bed Form Generation by Wave Action," *Proceedings of the 13th Conference on Coastal Engineering*, July 1972.

- MOODY, D.W., "Coastal Morphology and Processes in Relation to the Development of Submarine Sand Ridges off Bethany Beach, Del.," Unpublished Ph.D. Dissertation, The John Hopkins University, Baltimore, Md., 1964.
- MOORE, G.W., and COLE, A.Y., "Coastal Processes, Vicinity of Cape Thompson, Alaska," in "Geologic Investigations of Cape Thompson, NW Alaska--Preliminary Report," Trace Element Investigation Report 753, U.S. Geological Survey, Washington, D.C., 1960.
- MORGAN, J.P., NICHOLS, L.G., and WRIGHT, M., "Morphological Effects of Hurricane Audrey on the Louisiana Coast (Advance Summary and Conclusions)," TR 10A, Coastal Studies Institute, Louisiana State University, Baton Rouge, La., 1958.
- MURRAY, S.P., "Settling Velocities and Vertical Diffusion of Particles in Turbulent Water," *Journal of Geophysical Research*, Vol. 75, No. 9, pp. 1647-1654.
- MURRAY, S.P., "Bottom Currents Near the Coast During Hurricane Camille," *Journal of Geophysical Research*, Vol. 75, No. 24, Aug. 1970.
- NAKATO, T., LOCHER, F.A., GLOVER, J.R., and KENNEDY, J.F., "Wave Entrainment of Sediment from Rippled Beds," *Journal of the Waterway Port Coastal and Ocean Division*, ASCE, Vol. 103, No. WW1, pp. 83-99, Feb., 1977.
- NATIONAL ACADEMY OF SCIENCES, "Ocean Wave Spectra," *Proceedings of National Research Council Conference*, Easton, Md., May 1-4, 1961, Prentice-Hall, Englewood Cliffs, N.J., 1963.
- NATIONAL OCEANIC AND ATMOSPHERIC ADMINISTRATION, "Tide Tables, East Coast North and South America, Including the Hawaiian Islands," National Ocean Survey, Rockville, M.D., 1976.
- NAYAK, I.V., "Equilibrium Profiles of Model Beaches," Report HEL 2-25, University of California, Berkeley, Calif., May 1970.
- NEUMANN, C.J., et al., "Tropical Cyclones of the North Atlantic Ocean, 1871-1977," U.S. Department of Commerce, National Oceanic and Atmospheric Administration, National Weather Service, 1978.
- NEWMANN, G., and PIERSON, W.J. Jr., *Principles of Physical Oceanography*, Prentice-Hall, Inc., Englewood, New Jersey, 1966.
- NICHOLS, R.L., and MARSTON, A.F., "Shoreline Changes in Rhode Island Produced by Hurricane of Sept. 21, 1938," *Bulletin of the Geological Society of America*, Vol. 50, Sept. 1939, pp. 1357-1370.
- NIELSEN, P., "Some Basic Concepts of Wave Sediment Transport, Series Paper 20, Institute of Hydrodynamics and Hydraulic Engineering, Technical University of Denmark, Lyngly, Denmark, 1979.
- NIEMCZYNOWICZ, G.L.O.J., "Effect of Grid Turbulence on Sedimentation," *Bulletin Series A*, No. 8, Division of Hydraulics, Institute of Technology, University of Lund, Sweden, 1972.

- NORRIS, R.M., "Dams and Beach-Sand Supply in Southern California," *Papers in Marine Geology*, Shepard Commemorative Volume, MacMillan, New York, 1964.
- O'BRIEN, M.P., "Equilibrium Flow Areas of Inlets on Sandy Coasts," *Journal of the Waterways and Harbors Division*, ASCE, No. WWI, Feb. 1969, pp. 43-52.
- OLSEN, E.J., "A Study of the Effects of Inlet Stabilization at St. Mary's Entrance, Florida," *Coastal Sediments '77, Fifth Symposium of the Waterways, Port, Coastal and Ocean Division*, ASCE, Nov. 1977.
- OLSEN, E.J., "Beach Nourishment Project Report for Capitva Island, Florida," Tetra Tech Report, Pasadena, Calif., 1980.
- OTTO, G.H., "A Modified Logarithmic Probability Graph for the Interpretation of Mechanical Analyses of Sediments," *Journal of Sedimentary Petrology*, Vol. 9, 1939, pp. 62-76.
- PETTIJOHN, F.J., *Sedimentary Rocks*, Harper and Brothers, New York, 1957, p. 117.
- PIERCE, J.W., "Sediment Budget Along a Barrier Island Chain," *Sedimentary Geology*, Vol. 3, No. 1, 1969, pp. 5-16.
- PUTNAM, J.A., MUNK W.H., and TRAYLOR, M.A., "The Prediction of Longshore Currents," *Transactions of the American Geophysical Union*, Vol. 30, 1949, pp. 337-345.
- RAMSEY, M.D., and GALVIN, C.J., "Size Analysis of Sand Samples from Three S. New Jersey Beaches," Unpublished Paper, U.S. Army, Corps of Engineers, Coastal Engineering Research Center, Washington, D.C., Sept, 1971.
- RECTOR, R.L., "Laboratory Study of Equilibrium Profiles of Beaches," TM-41, U.S. Army, Corps of Engineers, Beach Erosion Board, Washington, D.C., Aug. 1954.
- REIMNITZ, E., and ROSS, D.A., "The Sea Sled--A Device for Measuring Bottom Profiles in the Surf Zone," *Marine Geology*, Vol. 11, 1971.
- RICHARDSON, J.F., JERONIMO, M.A., da S., "Velocity-Voidage Relations for Sedimentation and Fluidation," *Chemical Engineering Science*, Vol. 34, pp. 1419-1422, 1979.
- RUSNAK, G.A., STOCKMAN, R.W., and HOFMANN, H.A., "The Role of Shell Material in the Natural Sand Replenishment Cycle of the Beach and Nearshore Area Between Lake Worth Inlet and the Miami Ship Channel," CERC Contract Report (DA-49-055-CIV-ENG-63-12), Institute of Marine Sciences, University of Miami, Coral Gables, Fla., 1966.
- RUSSELL, R.J., "Florida Beaches and Cemented Water-Table Rocks," Technical Report No. 88, Coastal Studies Institute, Louisiana State University, Baton Rouge, La., Oct. 1970.
- SALLENGER, A.H., Jr., "Swash Mark and Groin Flow," *Journal of Sedimentary Petrology*, Vol. 51, No. 1, pp. 261-264, Mar., 1981.

- SATO, S., IJIMA, T., and TANAKA, N., "A Study of Criteria Depth and Mode of Sand Movement Using Radioactive Glass Sand," *Proceedings of the Eighth Conference on Engineering*, Mexico City, 1962, pp. 304-323.
- SAVAGE, R.P., "Wave Run-up on Roughened and Permeable Slopes," *Journal of the ASCE*, Vol. 84, No. WW3, May 1958.
- SAVAGE, R.P., and WOODHOUSE, W.W., "Creation and Stabilization of Coastal Barrier Dunes," *Proceedings of the 11th Coastal Engineering Conference*, London, Sept. 1968.
- SAVILLE, T., Jr., "Model Study of Sand Transport Along an Infinitely Long Straight Beach," *Transactions of the American Geophysical Union*, Vol. 31, 1950.
- SAVILLE, T., Jr., "Scale Effects in Two Dimensional Beach Studies," *Proceedings of the Seventh General Meeting*, International Association for Hydraulic Research, 1957.
- SAVILLE, T., Jr., and CALDWELL, J.M., "Accuracy of Hydrographic Surveying In and Near the Surf Zone," TM-32, U.S. Army, Corps of Engineers, Beach Erosion Board, Washington, D.C., Mar. 1953.
- SAYLOR, J.H., and HANDS, E.B., "Properties of Longshore Bars in the Great Lakes," *Proceedings of the 12th Conference on Coastal Engineering*, Vol. 2, 1970, pp. 839-853.
- SAYLOR, J.H., and UPCHURCH, S., "Bottom Stability and Sedimentary Processes at Little Lake Harbors, Lake Superior," U.S. Army, Corps Engineers, Lake Survey District Detroit, Mich., 1970.
- SCHNEIDER, C., "The Littoral Environment Observation (LEO) Data Collection Program," CETA 81-5, Coastal Engineering Research Center, U.S. Army Engineer Waterways Experiment Station, Vicksburg, Miss., Mar. 1981.
- SCRUTTON, P.C., "Delta Building and the Deltaic Sequence," *Recent Sediments, Northwest Gulf of Mexico*, American Association of Petroleum Geologists, 1960, pp. 82-102.
- SELLMAN, P.V., et al., "Investigations of Terrain and Coastal Conditions on the Arctic Alaskan Coastal Plain," Draft of Special Report, U.S. Army Cold Regions Research and Engineering Laboratories, Aug. 1971.
- SENGUPTA, S., and VEENSTRA, H.J., "On Sieving and Settling Techniques for Sand Analysis," *Sedimentology*, Vol. 11, pp. 83-98, 1968.
- SHEPARD, F.P., "Beach Cycles in Southern California," TM-20, U.S. Army, Corps of Engineers, Beach Erosion Board, Washington, D.C., July 1950.
- SHEPARD, F.P., "Submarine Geology," *Physical Properties of Sediments*, Ch. V., and *Beaches and Related Shore Processes*, Ch. VII, Harper and Row, New York, 1963, pp. 167-205.

- SHEPARD, F.P., and BUFFINGTON, E.C., "La Jolla Submarine Fan Valley," *Marine Geology*, Vol. 6, 1968, pp. 107-143.
- SHEPARD, F.P., and DILL, R.F., "Submarine Canyons and Other Sea Valleys, Rand McNally, Chicago, 1966.
- SHEPARD, F.P., and GRANT, U.S., IV, "Wave Erosion Along the Southern California Coast," *Bulletin of the Geologic Society of America*, Vol. 58, 1947, pp. 919-926.
- SHEPARD, F.P., and INMAN, D.L., "Nearshore Water Circulation Related to Bottom Topography and Wave Refraction," *Transactions of the American Geophysical Union*, Vol. 31, No 2, 1950, pp. 196-212.
- SHEPARD, F.P., MacDONALD, G.A., and COX, D.C., "The Tsunami of April 1, 1946," *Bulletin of the Scripps Institute of Oceanography* Vol, 5, No. 6, 1950, pp. 391-528.
- SHEPARD, F.P., and WANLESS, H.R., *Our Changing Coastlines*, McGraw-Hill, New York, 1971.
- SHUYSKIY, Y.D., "The Effect of Strong Storms on the Sand Beaches of the Baltic Eastern Shore," *Oceanology*, Vol. 9, No. 3, 1970, p. 388.
- SILVESTER, R., and MOGRIDGE, G.R., "Reach of Waves to the Bed of the Continental Shelf," *Proceedings of the 12th Coastal Engineering Conference*, Washington, D.C., pp. 651-670, 1970.
- SLEATH, J.F.A., "Measurements of Bed Load in Oscillatory Flow," *Journal of the Waterway Port Coastal and Ocean Division*, ASCE, Vol. 104, No. WW4, pp. 291-307, Aug., 1978.
- SONU, C.J., "Field Observation of Nearshore Circulation and Meandering Currents," *Journal of Geophysical Research, Oceans and Atmospheres*, Vol. 77, No. 18, 1972.
- SONU, C.J., and VAN BEEK, J.L., "Systemic Beach Changes on the Outer Banks, North Carolina," *Journal of Geology*, Vol. 79, 1971, pp. 416-425.
- SORENSEN, R.M., "Procedures for Preliminary Analysis of Tidal Inlet Hydraulics and Stability," Coastal Engineering Technical Aid 77-8, Coastal Engineering Research Center, U.S. Army Engineer Waterways Experiment Station, Vicksburg, Miss., Dec. 1977.
- STEPHENS, N.H., et al., "Evaluation of Four Methods Using Gold-198 for Surface Labeling Sand and a New Technique for Simulating Mass Labeling," ORNL-4338, Oak Ridge National Laboratory, 1968.
- STODDARD, D.R., "World Erosion and Sedimentation," *Water, Earth, and Man*, Barnes and Noble, 1969.
- STRAKHOV, N.M., "Principles of Lithogenesis," Vol. 1, (Translation from 1962 Russian Edition by J.P. Fitzsimmons, Oliver, and Boyd), Edinburgh and London, 1967, p. 245.

- STUIVER, M., and PURPURA, J.A., "Application of Fluorescent Coastal Sand in Littoral Drift and Inlet Studies," *Proceedings of the 11th Conference on Coastal Engineering*, ASCE, 1968, pp. 307-321.
- SUNAMURA, T., and HORIKOWA, K., "Two-Dimensional Beach Transformation Due to Waves," *Proceedings of the 14th Coastal Engineering Conference*, Copenhagen, Denmark, pp. 920-938, 1974.
- SWART, D.H., "Predictive Equations Regarding Coastal Transports," *Proceedings of the 15th Coastal Engineering Conference*, Honolulu, Hawaii, pp. 1113-1132, 1976.
- SWIFT, D.J.P., "Coastal Sedimentation." in *Marine Sediment Transport and Environmental Management*, D.J. Stanley and D.J.P. Swift, eds., Wiley, New York, pp. 255-310, 1976.
- SZUWALSKI, A., "Littoral Environment Observation Program in California Preliminary Report," MP 2-70, U.S. Army, Corps of Engineers, Coastal Engineering Research Center, Washington, D.C., Feb. 1970.
- SZULWALSKI, A., "Coastal Imagery Data Bank: Interim Report," MP 3-72, U.S. Army, Corps of Engineers, Coastal Engineering Research Center, Washington, D.C., Nov. 1972.
- TANEY, N.E., "Geomorphology of the South Shore of Long Island, New York," TM 128, U.S. Army, Corps of Engineers, Beach Erosion Board, Washington, D.C., Sept. 1961.
- TANEY, N.E., "Laboratory Applications of Radioisotopic Tracers to Follow Beach Sediments." *Proceedings of the Eighth Conference on Coastal Engineering*, Council on Wave Research, ASCE, University of California, Berkeley, Calif., 1963, pp. 279-303.
- TANNER, W.F., "Florida Coastal Classification," *Transactions of the Gulf Coast Association of Geological Societies*, Vol. X, 1960, pp. 259-266.
- TANNER, W.F., "Mainland Beach Changes Due to Hurricane Donna," *Journal of Geophysical Research*, Vol. 66, No. 7, July 1961.
- TANNER, W.F., "Significance of Camille," *Southeastern Geology*, Vol. 12, No. 2, 1970, pp. 95-104.
- TELEKI, P., "Fluorescent Sand Tracers," *Journal of Sedimentary Petrology*, Vol. 36, June 1966.
- TERZAGHI, K., and PECK, R.B., *Soil Mechanics in Engineering Practice*, Wiley, New York, 1967, p. 28.
- THIEL, G.A., "The Relative Resistance to Abrasion of Mineral Grains of Sand Size" *Journal of Sedimentary Petrology*, Vol. 10, 1940, pp. 102-124.
- THOMPSON, E.F., "Wave Climate at Selected Locations Along U.S. Coasts," TR 77-1, Coastal Engineering Research Center, U.S. Army Engineer Waterways Experiment Station, Vicksburg, Miss., 1977.

- THOMPSON, E.F., "Energy Spectra in Shallow U.S. Coastal Waters, TP 80-2, Coastal Engineering Research Center, U.S. Army Engineer Waterways Experiment Station, Vicksburg, Miss., Feb., 1980.
- THOMPSON, E.F., "Interpretation of Wave Energy Spectra," CETA 80-5, Coastal Engineering Research Center, U.S. Army Engineer Waterways Experiment Station, Vicksburg, Miss., 1980a.
- THOMPSON, E.F., and HARRIS, D.L., "A Wave Climatology for U.S. Coastal Waters," *Proceedings of Offshore Technology Conference*, Dallas, Texas, May 1972.
- THORNTON, E.B., and KRAPOHL, R.F., "Water Particle Velocities Measured Under Ocean Waves," *Journal of Geophysical Research*, Vol. 79, pp. 847-852, 1974.
- TUCKER, M.J., "Recent Measurement and Analysis Techniques Developed at The National Institute of Oceanography," *National Institute of Oceanography*, Collected Reprints, V. 11, No. 465, 1963. Reprinted from *Ocean Wave Spectra*; Proceedings of Conference on Ocean Wave Spectra, 1961, pp. 219-226.
- UNIVERSITY OF FLORIDA, COASTAL ENGINEERING LABORATORY, "Coastal Engineering Study of Captiva Island, Gainesville, Fla., 1974.
- URBAN, H.D., and GALVIN, C.J., "Pipe Profile Data and Wave Observations from the CERC Beach Evaluation Program, January-March, 1968," MP 3-69, U.S. Army, Corps of Engineers, Coastal Engineering Research Center, Washington, D.C., Sept. 1969.
- U.S. ARMY CORPS OF ENGINEERS, "Relation Between Sand Size and Slope of the Foreshore," Interim Report, Beach Erosion Board, Washington, D.C., 1933.
- U.S. ARMY CORPS OF ENGINEERS, "Beach Erosion Report on Cooperative Study at Palm Beach, Florida," Beach Erosion Board, Washington, D.C., 1947, (Unpublished).
- U.S. ARMY CORPS OF ENGINEERS, Beach Erosion at Santa Barbara, California: House of Representatives, Document No. 552, 75th Congress, 3rd Session 1950a.
- U.S. ARMY CORPS OF ENGINEERS, Atlantic City, NJ Beach Erosion Control Study; House of Representatives, Document No. 538, 81st Congress, 2nd Session, 1950b.
- U.S. ARMY CORPS OF ENGINEERS, "Illinois Shore of Lake Michigan--Beach Erosion Control Study," House Document 28, 83rd Congress, 1953a.
- U.S. ARMY CORPS OF ENGINEERS, "Ohio Shoreline of Lake Erie, (Sandusky to Vermillieni) Beach Erosion Control Study," House Document 32, 83rd Congress, 1953b.
- U.S. ARMY CORPS OF ENGINEERS, "Cliff Walk, Newport, Rhode Island, Beach Erosion Control Study," Letter from Secretary of the Army, U.S. Government Printing Office, Washington, 1965.

- U.S. ARMY CORPS OF ENGINEERS, "Shore Protection, Planning, and Design," TR No. 4, Coastal Engineering Research Center, Washington, D.C., 1966.
- U.S. ARMY CORPS OF ENGINEERS, "Littoral Environment Observations, Florida Panhandle, 1969-1970," Coastal Engineering Research Center, Washington, D.C., 1970.
- U.S. ARMY CORPS OF ENGINEERS, "National Shoreline Study," Great Lakes Region-Inventory Report, Aug. 1971.
- U.S. ARMY ENGINEER DISTRICT, BALTIMORE, "Survey of Ocean City Harbor and Inlet and Sinepuxent Bay, Maryland," Baltimore, Md., 1948.
- U.S. ARMY ENGINEER DISTRICT, LOS ANGELES, "Shoreline Effects, Harbor at Playa Del Rey, Calif.," encl. 20, Los Angeles, Calif., 1948, (unpublished).
- U.S. ARMY ENGINEER DISTRICT, LOS ANGELES, "Interim Report on Harbor Entrance Improvement Camp Pendleton, California," Los Angeles, Calif., 1953 (unpublished).
- U.S. ARMY ENGINEER DISTRICT, MILWAUKEE, "Preliminary Analysis of Cooperative Beach Erosion Study, City of Kenosha, Wisconsin," Milwaukee, Wis., 1953, (unpublished).
- U.S. ARMY ENGINEER DISTRICT, MOBILE, "Beach Erosion Control Report, Cooperative Study of Perdido Pass, Alabama," Mobile, Ala., 1954.
- U.S. ARMY ENGINEER DISTRICT, NEW YORK, "Atlantic Coast of New Jersey, Sandy Hook to Barnegat Inlet, Beach Erosion Control Report on Cooperative Study," New York, N.Y., 1954, (unpublished).
- U.S. ARMY ENGINEER DISTRICT, NEW YORK, "Atlantic Coast of Long Island, N.Y., Fire Island Inlet and Shore Westerly to Jones Inlet," Beach Erosion Control Report on Cooperative Study, 1955, pp. A-16, (unpublished).
- U.S. ARMY ENGINEER DISTRICT, WILMINGTON, "Investigation of Erosion, Carolina Beach, N.C.," Rpt. 1-69, Wilmington, N.C., 1970.
- U.S. ARMY ENGINEER DISTRICT, WILMINGTON, General Design Memorandum for Bay, North Carolina, Phase II, Appendix 5, Sept. 1980.
- U.S. ARMY ENGINEER DIVISION, NEW ENGLAND, "A Study of Methods to Preserve Gay Head Cliffs, Martha's Vineyard, Massachusetts," prepared by Woodard-Moorhouse and Associates, Inc., for New England Division, Oct. 1970.
- U.S. CONGRESS, "Beach Erosion Study, Lake Michigan Shore Line of Milwaukee County, Wisconsin," House Document 526, 79th Congress, 2nd Session, p. 16, 1946.
- U.S. CONGRESS, "North Carolina Shore Line, Beach Erosion Study," House Document 763, 80th Congress, 2nd Session, 1948.
- U.S. CONGRESS, "Ocean City, New Jersey, Beach Erosion Control Study," House Document 184, 83rd Congress, 1st Session, 1953a.

- U.S. CONGRESS, "Cold Spring Inlet (Cape May Harbor), New Jersey," House Document 206, 83rd Congress, 1st Session, 1953b.
- U.S. CONGRESS, "Coast of California, Carpinteria to Point Mugu," House Document 29, 83rd Congress, 1st Session, 1953c.
- U.S. CONGRESS, "Racine County, Wisconsin," House Document 88, 83rd Congress, 1st Session, 1953d.
- U.S. CONGRESS, "Illinois Shore of Lake Michigan," House Document 28, 83rd Congress, 1st Session 1953e.
- U.S. CONGRESS, "Waikiki Beach, Island of Oahu, T.H., Beach Erosion Study," House Document No. 227, 83d Congress, 1st Session, 1953f.
- U.S. CONGRESS, "Pinellas County, Florida," House Document 380, 83d Congress, 2d Session, 1954a.
- U.S. CONGRESS, "Port Hueneme, California," House Document 362, 83d, Congress, 2d Session, 1954b.
- U.S. CONGRESS, "Anaheim Bay Harbor, California," House Document 349, 83d Congress, 2d Session, 1954c.
- VALLIANOS, F., "Recent History of Erosion at Carolina Beach, N.C.," *Proceedings of the 12th Conference on Coastal Engineering*, ASCE, Vol. 2, 1970.
- VALLIANOS, L., "Beach Fill Planning--Brunswick County, North Carolina," *Proceedings, 14th Conference on Coastal Engineering*, American Society of Civil Engineers, New York, 1974, p. 1350.
- van de GRAAFF, J., and TILMANS, W., "Sand Transport by Waves," *Proceedings of the 17th Coastal Engineering Conference*, Sydney, Australia, 1980.
- VAN DORN, W.G., "Wind Stress on an Artificial Pond," *Journal of Marine Research*, Vol. 12, 1953, pp. 249-276.
- van NIEUWENHUISE, D.S., et al., "Sources of Shoaling in Charleston Harbor Fourier Groin Shape Analysis," *Journal of Sedimentary Petrology*, Vol. 48, pp. 373-383, Jan., 1978.
- VINCENT, C.L., "A Method for Estimating Depth-Limited Wave Energy," Coastal Engineering Technical Aid No. 81-16, Coastal Engineering Research Center, U.S. Corps of Engineers, Vicksburg, Miss., Nov., 1981.
- VINCENT, C.L., and CORSON, W.D., "The Geometry of Selected U.S. Tidal Inlets," GITI Report 20, U.S. Army Corps of Engineers, Washington, D.C., May 1980.
- VITALE, P., "Movable-Bed Laboratory Experiments Comparing Radiation Stress and Energy Flux Factor as Predictors of Longshore Transport Rate," MR 81-4, Coastal Engineering Research Center, U.S. Army Engineer Waterways Experiment Station, Vicksburg, Miss., Apr. 1981.

- WALTON, T.L., Jr., "Littoral Drift Computations Along the Coast of Florida by Use of Ship Wave Observations," Unpublished Thesis, University of Florida, Gainesville, Fla., 1972.
- WALTON, T.L., Jr., "Beach Erosion--Long and Short Term Implications (With Special Emphasis on the State of Florida)," Florida Shore and Beach Preservation Association Conference, Captiva Island, 1977.
- WALTON, T.L., Jr., "Computation of Longshore Energy Flux Using LEO Current Observation," CETA 80-3, Coastal Engineering Research Center, U.S. Army Engineer Waterways Experiment Station, Vicksburg, Miss., Mar., 1980.
- WALTON, T.L., and ADAMS, W.D., "Capacity of Inlet Outer Bars to Store Sand," Fourteenth Coastal Engineering Conference, Honolulu, Hawaii, Jul. 1976.
- WALTON, T.L., and DEAN, R.G., "Application of Littoral Drift Roses to Coastal Engineering Problems," *Proceedings of the Conference on Engineering Dynamics in the Coastal Zone*, 1973.
- WALTON, T.L., Jr., and DEAN, R.G., "Use of Outer Bars of Inlets as Sources of Beach Nourishment Material," *Shore and Beach*, Vol. 44, No. 2, July 1976.
- WALTON, T.L., and ESCOFFIER, F.F., "Linearized Solution to Inlet Equation with Inertia," Proc. Paper 16414, *Journal of the Waterway, Port, Coastal and Ocean Division*, ASCE, Vol. 105, No. WW4, Aug. 1981, pp. 191-195.
- WATSON, R.L., "Origin of Shell Beaches, Padre Island, Texas," *Journal of Sedimentary Petrology*, Vol. 41, No. 4, Dec. 1971.
- WATTS, G.M., "Development and Field Tests of a Sampler for Suspended Sediment in Wave Action," TM-34, U.S. Army, Corps of Engineers, Beach Erosion Board, Washington, D.C., Mar. 1953a.
- WATTS, G.M., "A Study of Sand Movement at South Lake Worth Inlet, Florida," TM-42, U.S. Army Corps of Engineers, Beach Erosion Board, Washington, D.C., Oct. 1953b.
- WATTS, G.M., "Behavior of Beach Fill at Ocean City, New Jersey," TM-77 U.S. Army Corps of Engineers, Beach Erosion Board, Washington, D.C., Feb. 1956.
- WEGGEL, J.R., "A Method for Estimating Long-Term Erosion Rates from a Long-Term Rise in Water Level," CETA 79-2, Coastal Engineering Research Center, U.S. Army Engineer Waterways Experiment Station, Vicksburg, Miss., May, 1979.
- WELLS, D.R., "Beach Equilibrium and Second-Order Wave Theory," *Journal of Geophysical Research*, Vol. 72, No. 2, pp. 497-504, Jan., 1967.
- WIEGEL, R.L., *Oceanographic Engineering*, Prentice-Hall, Englewood Cliffs, N.J., 1964.

- WILSON, B.W., CHAKRABARTI, S.K., and SNIDER, R.H., "Spectrum Analysis of Ocean Wave Records," *Proceedings of the International Symposium on Ocean Wave Measurement and Analysis*, American Society of Civil Engineers, Vol. 1, 1974, pp. 87-106.
- WOLMAN, G.,M., and MILLER, J.P., "Magnitude and Frequency of Forces in Geomorphic Processes," *The Journal of Geology*, Vol. 68, No. 1, 1960, pp. 54-74.
- WOODARD, D.W., et al., "The Use of Grasses for Dune Stabilization Along the Gulf Coast with Initial Emphasis on the Texas Coast," Report No. 114, Gulf Universities Research Corporation, Galveston, Tex., 1971.
- WOODHOUSE, W.W., Jr., SENECA, E.D., and BROOME, S.W., "Ten Years of Development of Man-Initiated Coastal Barrier Dunes in North Carolina," Bulletin 453, Agricultural Experiment Station, North Carolina University at Raleigh, N.C., December 1976.
- WRIGHT, F., and COLEMAN, Jr., "River Delta Morphology: Wave Climate and the Role of the Subaqueous Profile," *Science*, Vol. 176, 1972, pp. 282-284.
- YALIN, M.S., *Mechanics of Sediment Transport*, 2nd Ed., Pergamon Press, Oxford, England, 1977.
- YASSO, W.E., "Fluorescent Coatings on Coast Sediment: An Integrated System," TR-16, Columbia University, Department of Geology, New York, N.Y., 1962.
- ZEIGLER, J.M., and TUTTLE, S.D., "Beach Changes Based on Daily Measurements of Four Cape Cod Beaches," *Journal of Geology*, Vol. 69, No. 5, 1961, pp. 583-599.
- ZENKOVICH, V.P., *Processes of Coastal Development*, Interscience Publishers, New York, 1967.
- ZWAMBORN, J.A., FROMME, G.A.W., and FITZPATRICK, J.B., "Underwater Mound for the Protection of Durban's Beaches," *Proceedings of the 12th Conference on Coastal Engineering*, ASCE, 1970.

## BIBLIOGRAPHY

- AKYUREK, M., "Sediment Suspension by Wave Action Over a Horizontal Bed," Unpublished Thesis, University of Iowa, Iowa City, Iowa, July 1972.
- AYERTON, H., "The Origin and Growth of Ripple Marks," *Philosophical Transactions of the Royal Society of London*, Ser. A., Vol. 84, 1910, pp. 285-310.
- BASCOM, W.N., *Manual of Amphibious Oceanography*, Vol. 2, Sec. VI, University of California, Berkeley, Calif., 1952.
- BERTMAN, D.Y., SHUYSKIY, Y.D., and SHKARUPO, I.V., "Experimental Study of Beach Dynamics as a Function of the Prevailing Wind Direction and Speed," *Oceanology*, Transaction of the Russian Journal, *Okeanologiya* (Academy of Sciences of the U.S.S.R.), Vol. 12, Feb. 1972.
- BUMPUS, D.F., "Residual Drift Along the Bottom of the Continental Shelf in the Middle Atlantic Bight," *Limnology and Oceanography*, 75th Anniversary Vol., Supplement to Vol. X, 1965
- BYRNE, R.J., DeALTERIS, J.R., and BULLOCK, P.A., "Channel Stability in Tidal Inlets: A Case Study," *Proceedings, 14th Coastal Engineering Conference*, ASCE, New York, pp. 1585-1604, 1974.
- COLONY, R.J., "Source of the Sands on South Shore of Long Island and the Coast of New Jersey," *Journal of Sedimentary Petrology*, Vol. 2, 1932, pp. 150-159.
- COOPERATIVE FEDERAL INTER-AGENCY PROJECT, "Methods of Analyzing Sediment Samples," Report No. 4, St. Paul U.S. Engineer District Sub-Office, Hydraulic Laboratory, University of Iowa, Iowa City, 1941.
- CURRAY, J.R., "Late Quarternary History, Continental Shelves of the United States," *The Quarternary of the U.S.*, Princeton University Press, Princeton, N.Y., 1965, pp. 723-735.
- DABOLL, J.M., "Holocene Sediments of the Parker River Estuary, Massachusetts," Contribution No. 3-CRG, Department of Geology, University of Massachusetts, June 1969.
- DARLING, J.M., "Surf Observations Along the United States Coasts," *Journal of the Waterways and Harbors Division*, ASCE, WWI, Feb. 1968, pp. 11-21.
- DARLING, J.M., and DUMM, D.G., "The Wave Record Program at CERC," MP 1-67, U.S. Army, Corps of Engineers, Coastal Engineering Research Center, Washington, D.C., Jan. 1967.
- DAS, MM., "Longshore Sediment Transport Rates: A Compilation of Data," MP 1-71, U.S. Army, Corps of Engineers, Coastal Engineering Research Center Washington, D.C., Sept. 1971.
- DAVIS, R.A., Jr., and FOX, W.T., "Beach and Nearshore Dynamics in Eastern Lake Michigan," TR No. 4, ONR Task No. 388-092/10-18-68, (414), Office of Naval Research, Washington, D.C., June 1971.

- DAVIS, R.A., Jr., and FOX W.T., "Coastal Processes and Nearshore Sand Bars," *Journal of Sedimentary Petrology*, Vol. 42, No. 2, June 1972, pp. 401-412.
- DAVIS, R.A., Jr., and MCGEARY, D.F.R., "Stability in Nearshore Bottom Topography and Sedimentary Distribution, Southeastern Lake Michigan," *Proceedings of the Eighth Conference on Great Lakes Research*, Pub. No. 13, Great Lakes Research Division, University of Michigan, Ann Arbor, Mich., 1965.
- DEAN, R.G., "Storm Characteristics and Effects," *Proceedings of Seminar on Planning and Engineering in the Coastal Zone*, published by Coastal Plains Center for Marine Development Services, Wilmington, N.C., 1972.
- DeWALL, A.E., "The 17 December 1970 East Coast Storm Beach Changes," Unpublished Manuscript, U.S. Army, Corps of Engineers, Coastal Engineering Research Center, Washington, D.C., 1972.
- DeWALL, A.E., and RICHTER, J.J., "Beach Changes at Boca Raton, Florida," Annual Meeting of the American Shore and Beach Preservation Association (presentation only), Fort Lauderdale, Fla., Aug. 1972.
- DILL, R.F., "Sedimentation and Erosion in Scripps Submarine Canyon Head," *Papers in Marine Geology*, Shepard Commemorative Volume, Macmillan, New York, 1964.
- DOLAN, R., "Barrier Dune System Along the Outer Banks of North Carolina: A Reappraisal," *Science*, 1972, pp. 286-288.
- DOLAN, R., "Barrier Islands: Natural and Controlled," in "Coastal Geomorphology," *Proceedings of the Third Annual Geomorphology Symposia Series*, 1973, pp. 263-278.
- DOLAN, R., FERM, J.C., and McARTHUR, L.S., "Measurements of Beach Process Variables, Outer Banks, North Carolina," TR No. 64, Coastal Studies Institute, Louisiana State University, Baton Rouge, La., Jan. 1969.
- DUNN, G.E., and MILLER, B.I., *Atlantic Hurricanes*, Louisiana State University Press, Baton Rouge, 1964, pp. 204, 257-258.
- EAGLESON, P.S., and DEAN, R.G., "Wave-Induced Motion of Discrete Bottom Sediment Particles," *Proceedings of the American Society of Civil Engineers*, Vol. 85, No. HY10, 1959.
- EAGLESON, P.S., and DEAN, R.G., "A Discussion of 'The Supply and Loss of Sand to the Coast' by J.W. Johnson," *Journal of the Waterways and Harbors Division*, ASCE, Vol. 86, No. WW2, June 1960.
- EATON, R.O., "Littoral Processes on Sandy Coasts," *Proceedings of the First Conference on Coastal Engineering*, Council on Wave Research, Engineering Foundation, Oct. 1950.
- EMERY, K.O., "A Simple Method of Measuring Beach Profiles," *Limnology and Oceanography*, Vol. 6, No. 1, 1961, pp. 90-93.

- EVANS, O.F., "The Classification of Wave-Formed Ripple-Marks," *Journal of Sedimentary Petrology*, Vol. 11, No. 1, April 1941, pp. 37-41.
- EVERTS, C.H., "Particle Overpassing on Flat Granular Boundaries," *Journal of the Waterways Harbors and Coastal Engineering Division*, ASCE, Vol. 99, No. WW4, pp. 425-438, Nov., 1973.
- FAIRCHILD, J.C., "Laboratory Tests of Longshore Transport," *Proceedings of the 12th Conference on Coastal Engineering*, ASCE, 1970.
- GALVIN, C.J., Jr., "Finite-Amplitude, Shallow Water-Waves of Periodically Recurring Form," *Proceedings of the Symposium on Long Waves*, University of Delaware, Sept. 1970.
- GALVIN, C.J., and SEELIG, W.N., "Surf on U.S. Coastline," Unpublished Research Paper, U.S. Army, Corps of Engineers, Coastal Engineering Research Center, Washington, D.C., Aug. 1969.
- GALVIN, C.J., and SEELIG, W.N., "Nearshore Wave Direction from Visual Observation," *Transactions of the American Geophysical Union*, Vol. 52, No. 4, Apr. 1971.
- GOLDSMITH, V., COLONELL, J.M., and TURBIDE, P.W., "Forms of Erosion and Accretion of Cape Cod Beaches," *Proceedings of the 13th International Conference on Coastal Engineering*, Vancouver, B.C., July 1972.
- HALLERMEIER, R.J., and GALVIN, C.J., "Wave Height Variation Around Vertical Cylinders," *Transactions of the American Geophysical Union*, 53rd Annual Meeting, 1972, p. 397.
- HANDS, E.B., "Anomalous Sand Size-Swash Slope Relationship," Unpublished MFR, U.S. Army, Corps of Engineer, Coastal Engineering Research Center, Washington, D.C., Apr. 1972.
- HARRISON, W., et al., "Circulation of Shelf Waters off the Chesapeake Bight," ESSA Professional Paper 3, U.S. Dept. of Commerce, Washington, D.C., June 1967.
- HARRISON, W., and WAGNER, K.A., "Beach Changes at Virginia Beach, Virginia," MP 6-64, U.S. Army, Corps of Engineers, Coastal Engineering Research Center, Washington, D.C., Nov. 1969.
- HODGES, T.K., "Sand Bypassing at Hillsboro Inlet, Florida," *Bulletin of the Beach Erosion Board*, Vol. 9, No. 2, Apr. 1955.
- HOUBOLT, J.J.H.C., "Recent Sediment in the Southern Bight of the North Sea," *Geologie en Mijnbouw*, Vol. 47, (4), 1968, pp. 245-273.
- HSU, S., "Coastal Air-Circulation System: Observations and Empirical Model," *Monthly Weather Review*, Vol. 98, No. 7, July 1970.
- INMAN, D.L., "Sorting of Sediments in the Light of Fluid Mechanics," *Journal of Sedimentary Petrology*, Vol. 19, 1949, pp. 51-70.

- INMAN, D.L., "Sediments: Physical Properties and Mechanics of Sedimentation," *Submarine Geology*, F.P. Shepard, 2nd ed., Harper and Row, New York, 1963.
- INMAN, D.L., and BOWEN, A.J., "Flume Experiments on Sand Transport by Waves and Currents," *Proceedings of the Eighth Conference on Coastal Engineering*, ASCE, Council on Wave Research, 1963, pp. 137-150.
- INMAN, D.L., and FRAUTSCHY, J.D., "Littoral Processes and the Development of Shorelines," *Proceedings of the Coastal Engineering Specialty Conference (Santa Barbara)*, ASCE, 1966, pp. 511-536.
- IVERSEN, H.W., "Waves and Breakers in Shoaling Water," *Proceedings of the Third Conference on Coastal Engineering*, Council on Wave Research, ASCE, 1952, pp. 1-12.
- IWAGAKI, Y., and NODA, H., "Laboratory Study of Scale Effect in Two Dimensional Beach Processes," *Proceedings of the Eighth Conference on Coastal Engineering*, Ch. 14, ASCE, 1962.
- JOHNSON, J.W., "Sand Transport by Littoral Currents," IER, Technical Report Series 3, Issue 338, Wave Research Laboratory, University of California, Berkeley, Calif., June 1952.
- JUDSON, S., "Eorsion of the Land or What's Happening to Our Continents," *American Scientist*, Vol. 56, No. 4, 1968, pp. 356-374.
- KAMPHUIS, J.W., "The Breaking of Waves at an Angle to the Shoreline and the Generation of Longshore Currents (A Laboratory Investigation)," Unpublished Thesis, Queens University, Kingston, Ontario, Apr. 1963.
- KENNEDY, V.C., and KOUBA, D.L., "Fluorescent Sand as a Tracer of Fluvial Sediment," Open-File Report, U.S. Geological Survey, Washington, D.C., 1968.
- KEULEGAN, G.H., "An Experimental Study of Submarine Sand Bars," TR-3, U.S. Army, Corps of Engineers, Beach Erosion Board, Washington, D.C., Aug. 1948.
- KOMAR, P.D., "The Mechanics of Sand Transport on Beaches," *Journal of Geophysical Research*, Vol. 76, No. 3, Jan. 1971.
- LUCKE, J.B., "Tidal Inlets: A Theory of Evolution of Lagoon Deposits on Shorelines of Emergence," *Journal of Geology*, Vol. 42, 1934, pp. 561-584.
- LeMEHAUTE, D., and LIN, "Internal Characteristics of Explosion-Generated Waves on the Continental Shelf," Tetra Technical Report No. TC-116, 1968.
- MANOHAR, M., "Mechanics of Bottom Sediment Movement Due to Wave Action," TM-75, U.S. Army, Corps of Engineers, Beach Erosion Board, Washington, D.C., June 1955.
- MEADE, R., "Landward Transport of Bottom Sediments in Estuaries of the Atlantic Coastal Plain," *Journal of Sedimentary Petrology*, Vol. 39, No. 1, pp. 222-234, 1969.

- MENARD, H.W., "Sediment Movement in Relation to Current Velocity," *Journal of Sediment Petrology*, Vol. 20, 1950, pp. 148-160.
- MONROE, F.F., "Oolitic Aragonite and Quartz Sand: Laboratory Comparison Under Wave Action," MP 1-69, U.S. Army, Corps of Engineers, Coastal Engineering Research Center, Washington, D.C., Apr. 1969.
- MORSE, B., GROSS, M.G., and BARNES, C.A., "Movement of Seabed Drifters Near the Columbia River," *Journal of the Waterways and Harbors Division*, ASCE, Vol. 94, No. WWI, Paper No. 5817, Feb. 1968, pp. 93-103.
- MURRAY, S.P., "Settling Velocities and Vertical Diffusion of Particles in Turbulent Water," *Journal of Geophysical Research*, Vol. 75, No. 9, pp. 1647-1654.
- NAKAMICHI, M., and SHIRAIISHI, N., "Recent Researches on Sand Drift in Japan," *Proceedings of the 20th International Navigation Congress*, Baltimore, 1961, pp. 101-124.
- NATIONAL MARINE CONSULTANTS, INC., "Wave Statistics for Seven Deep Water Stations Along the California Coast," prepared for U.S. Army Engineer Districts, Los Angeles and San Francisco, Calif., Dec. 1960a.
- NATIONAL MARINE CONSULTANTS, INC., "Wave Statistics for Ten Most Severe Storms Affecting Three Selected Stations off the Coast of Northern California, During the Period 1951-1960," prepared for U.S. Army Engineer District, San Francisco, Calif., Dec. 1960b.
- PIERCE, J.W., "Holocene Evolution of Portions of the Carolina Coast," *Bulletin of the Geologic Society of America*, Vol. 81, Dec. 1970.
- PIERSON, W.J., Jr., and NEUMANN, G., *Principles of Physical Oceanography*, Prentice-Hall, Englewood Cliffs, N.J., 1966.
- PILKEY, O.H., and FIELD, M.E., "Onshore Transportation of Continental Shelf Sediment: Atlantic Southeastern United States," *Shelf Sediment Transport*, Swift, Duane, and Pilkey, eds., Dowden, Hutchinson, and Ross, Inc., Stroudsburg, Pa., 1972.
- PILKEY, O.H., and FRANKENBERG, D., "The Relict-Recent Sediment Boundary on the Georgia Continental Shelf," *The Bulletin of the Georgia Academy of Science*, Vol. XXII, No. 1, Jan. 1964.
- PRICE, W.A., "Reduction of Maintenance by Proper Orientation of Ship Channels Through Tidal Inlets," *Proceedings of the Second Conference on Coastal Engineering*, Council on Wave Research, University of California, Berkeley, Calif., 1952, pp. 243-255.
- RAMSEY, M.D., "The Relationship Between Mean Sand Size vs Local Foreshore Slope for 166 New Jersey Sand Samples," Unpublished MFR, U.S. Army, Corps of Engineers, Coastal Engineering Research Center, Washington, D.C., Sept. 1971.

- RAUDKIVI, A.J., *Loose Boundary Hydraulics*, Pergamon Press, New York, Jan. 1965.
- ROSS, D.A., "Atlantic Continental Shelf and Slope of the United States--Heavy Minerals of the Continental Margin from Southern Nova Scotia to Northern New Jersey," Professional Paper 529-G, U.S. Geological Survey, U.S. Government Printing Office, Washington, D.C., 1970.
- SAUVAGE, M.G., and VINCENT, M.G., "Transport and Littoral Formation de Flecheset de Tombolos," *Proceedings of the Fifth Conference on Coastal Engineering*, 1955, pp. 296-328.
- SAVAGE, R.P., "Notes on the Formation of Beach Ridges," *Bulletin of the Beach Erosion Board*, Vol. 13, July 1959, pp. 31-35.
- SAVILLE, T., Jr., and SAVAGE, R.P., "Laboratory Determination of Littoral Transport Rates," *Journal of the Waterways and Harbors Division*, ASCE, Vol. 88, No. WW2, May 1962, pp. 69-92. Discussion: Nov. 1962, Feb. 1963, Discussion by Thorndike Saville, Jr., Nov. 1962.
- SEELIG, W.N., "Beach Evaluation Program, Visual Wave Observation Program," Unpublished Paper, U.S. Army, Corps of Engineers, Coastal Engineering Research Center, Washington, D.C., Mar. 1972.
- SHAY, E.A., and JOHNSON, J.W., "Model Studies on the Movement on Sand Transported by Wave Action Along A Straight Beach," Issue 7, Ser. 14, Institute of Engineering Research, University of California Berkeley, Calif., 1951.
- SHEPARD, F.P., "Gulf Coast Barriers," *Recent Sediments, Northwest Gulf of Mexico*, American Association of Petroleum Geologists, 1960a, pp. 197-220.
- SHEPARD, F.P., "Rise of Sea Level Along Northwest Gulf of Mexico," *Recent Sediments, Northwest Gulf of Mexico*, American Association of Petroleum Geologists, 1960b, pp. 338-344.
- STAFFORD, D.B., "An Aerial Photographic Technique for Beach Erosion Surveys in North Carolina," TM-36, U.S. Army, Corps of Engineers, Coastal Engineering Research Center, Washington, D.C., Oct. 1971.
- STONE, R.O., and SUMMERS, H.J., "Final Report, Study of Subaqueous and Subaerial Sand Ripples," ONR Project No. N00014-67-A-0269-0002, Task No. NR-388-085, Report No. USG Geology 72-1, 1972.
- SVENDSEN, S., "Munch-Petersen's Littoral Drift Formula," *Bulletin of the Beach Erosion Board*, Vol. 4, No. 4, Oct. 1950.
- SWIFT, D.J.P., "Quarternary Shelves and the Return to Grade," *Marine Geology*, Elsevier, Amsterdam, 1970.
- TANEY, N.E., "Littoral Materials of the South Shore of Long Island, New York," TM-129, U.S. Army, Corps of Engineers Beach Erosion Board, Washington, D.C., Nov. 1961.

- TELEKI, P., "Automatic Analysis of Tracer Sand," *Journal of Sedimentary Petrology*, Vol. 37, Sept. 1967, pp. 749-759.
- THOREAU, H.D., *Cape Cod*, Thicknor and Fields, Boston, Mass., 1865.
- THORNTON, E.B., "Longshore Current and Sediment Transport," TR-5, Department of Coastal and Oceanographic Engineering, University of Florida, Gainesville, Fla., Dec. 1969.
- TRASK, P.D., "Movement of Sand Around Southern California Promontories," TM-76, U.S. Army, Corps of Engineers, Beach Erosion Board, Washington, D.C., June 1955.
- U.S. CONGRESS, "Gulf Shore of Galveston Island, Texas, Beach Erosion Control Study," House Document 218, 8d Congress, 1st Session, 1953.
- VOLLBRECHT, K., "The Relationship Between Wind Records, Energy of Longshore Drift, and the Energy Balance off the Coast of a Restricted Water Body, as Applied to the Baltic," *Marine Geology*, Vol. 4, No. 2, Apr. 1966, pp. 119-148.
- WATSON, R.L., "Influence of Mean Grain Diameter on the Relationship Between Littoral Drift Rate and the Alongshore Component of Wave Energy Flux," EOS 53, No. 11, p. 1028, Nov. 1972.
- WATTS, G.M., "Laboratory Study of the Effect of Varying Wave Periods on Beach Profiles," TM-53, U.S. Army, Corps of Engineers, Beach Erosion Board, Washington, D.C., Sept. 1954.
- WATTS, G.M., and DEARDUFF, R.F., "Laboratory Study of Effect of Tidal Action on Wave-Formed Beach Profiles," TM-52, U.S. Army Corps of Engineers, Beach Erosion Board, Washington, D.C., Dec. 1954.
- ZEIGLER, J.M., et al., "Residence Time of Sand Composing the Beaches and Bars of Outer Cape Cod," *Proceedings of the Ninth Conference on Coastal Engineering*, ASCE, Vol. 26, 1964,
- ZENKOVICH, V.P., "Applications of Luminescent Substances for Sand Drift Investigation in the Nearshore Zones of the Sea," *Die Ingenieur*, Vol. 13, 1967, pp. 81-89.
- ZWAMBORN, J.A., et al., "Coastal Engineering Measurements," *Proceedings of the 13th International Conference on Coastal Engineering*, Canada, 1972.

# CHAPTER 5

## Planning Analysis



*Dana Point, California*



# CONTENTS

## CHAPTER 5

### PLANNING ANALYSIS

	Page
I GENERAL.....	5-1
II SEAWALLS, BULKHEADS, AND REVETMENTS.....	5-2
1. Functions.....	5-2
2. Limitations.....	5-2
3. Functional Planning of the Structure.....	5-3
4. Use and Shape of the Structure.....	5-3
5. Location of Structure with Respect to Shoreline.....	5-4
6. Length of Structure.....	5-4
7. Height of Structure.....	5-4
8. Determination of Ground Evaluation in Front of a Structure....	5-4
III PROTECTIVE BEACHES.....	5-6
1. Functions.....	5-6
2. Limitations.....	5-7
3. Planning Criteria.....	5-7
IV SAND DUNES.....	5-24
1. Functions.....	5-24
2. Positioning.....	5-26
V SAND BYPASSING.....	5-26
1. General.....	5-26
2. Methods.....	5-30
3. Legal Aspects.....	5-33
VI GROINS.....	5-35
1. Definition.....	5-35
2. Groin Operation.....	5-35
3. Functional Design.....	5-39
4. Filling Groins.....	5-52
5. Permeable Groins.....	5-52
6. Adjustable Groins.....	5-53
7. Alinement of Groins.....	5-53
8. Order of Groin Construction.....	5-54
9. Guidance from Existing Projects.....	5-54
10. Cost Effectiveness of Groin Construction.....	5-55
11. Legal Aspects.....	5-56
VII JETTIES.....	5-56
1. Definition.....	5-56
2. Types.....	5-56
3. Siting.....	5-57
4. Effects on the Shoreline.....	5-58
VIII BREAKWATERS, SHORE-CONNECTED.....	5-58
1. Definition.....	5-58
2. Types.....	5-59
3. Siting.....	5-59
4. Effect on the Shoreline.....	5-60

CONTENTS--Continued

	Page
IX BREAKWATERS, OFFSHORE.....	5-61
1. Definition.....	5-61
2. Functional Operation.....	5-61
3. Shoreline Response.....	5-63
4. Siting Considerations.....	5-64
5. Design Considerations.....	5-67
6. Other Considerations.....	5-71
X ENVIRONMENTAL CONSIDERATIONS.....	5-74
LITERATURE CITED.....	5-75

TABLES

5-1 Relationships of phi means and phi standard deviations of native material and borrow material.....	5-13
5-2 Comparison of composite grain-size distribution parameters and beach fill, Brunswick County, North Carolina.....	5-15
5-3 Offshore breakwaters in the United States.....	5-62

FIGURES

5-1 General classification of coastal engineering problems.....	5-1
5-2 Effects of erosion.....	5-5
5-3 Isolines of the adjusted fill factor, $R_A$ , for values of phi mean difference and phi sorting ratio .....	5-11
5-4 Isolines of the renourishment factor, $R_J$ , for values of phi mean difference and phi sorting ratio, $\Delta = 1.0$ .....	5-14
5-5 Beach berm system.....	5-20
5-6 Stabilized and migrating dunes.....	5-25
5-7 Schematic diagram of storm wave attack on beach and dune.....	5-27
5-8 Types of littoral barriers where sand transfer systems have been used.....	5-29
5-9 General shoreline configuration for a single groin.....	5-36
5-10 General shoreline configuration for two or more groins.....	5-36
5-11 Three mechanisms for creating rip currents between groins.....	5-38
5-12 Sections of a typical groin.....	5-40
5-13 Three cases of a groin-adjusted shoreline.....	5-41

## CONTENTS

### FIGURES--Continued

	Page
5-14 Alinement of updrift beach.....	5-42
5-15 Intermediate beach alinement.....	5-42
5-16 Downdrift beach alinement.....	5-43
5-17 Intermediate beach alinement with reversal of longshore transport direction.....	5-44
5-18 Summary of groin design.....	5-45
5-19 Schematic of groin-shortening procedure.....	5-46
5-20 Determination of beach profile adjacent to groin.....	5-49
5-21 Downdrift profile design in example problem.....	5-49
5-22 Calculation of updrift fillet volume.....	5-51
5-23 Calculation for downdrift erosion fillet volume.....	5-53
5-24 Effects of entrance jetties on shoreline.....	5-59
5-25 Effects of shore-connected breakwater on shoreline.....	5-60
5-26 Offshore breakwater as a littoral barrier-sediment trap.....	5-61
5-27 Offshore breakwaters with asymmetric cusplate spits (oblique wave attack).....	5-63
5-28 Diffraction at a breakwater, assuming linear wave theory is valid..	5-66
5-29 Diffraction at a breakwater, including effects of amplitude dispersion.....	5-66
5-30 Example of a segmented breakwater in a large tidal range.....	5-68
5-31 Location of cusplate spit apex.....	5-69
5-32 Segmented breakwater that is permeable and overtopped, located landward of breaker zone.....	5-70
5-33 Example of a segmented breakwater with waves passing through breakwater gaps.....	5-72



## CHAPTER 5

### PLANNING ANALYSIS

#### I. GENERAL

Coastal engineering problems may be classified into four general categories: shoreline stabilization, backshore protection (from waves and surge), inlet stabilization, and harbor protection (see Fig. 5-1). A coastal problem may fall into more than one category. Once classified, various solutions are available to the coastal engineer. Some of the solutions are structural; however, other techniques may be employed such as zoning and land-use management. This manual deals primarily with structural solutions, but the basic considerations discussed here may also apply to other types of solutions.

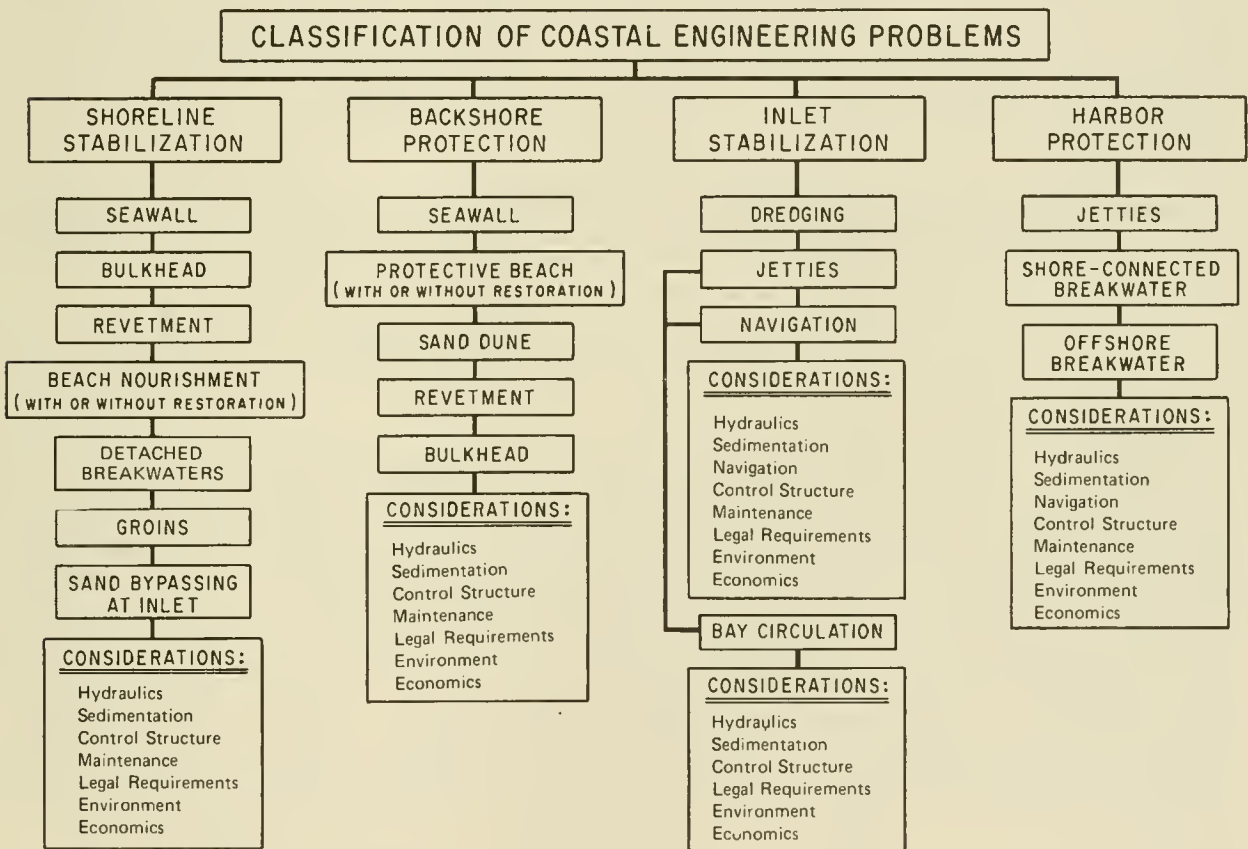


Figure 5-1. General classification of coastal engineering problems.

Figure 5-1 shows the structures or protective works in the four general coastal engineering problem classifications and lists the factors that must be considered in analyzing each problem area. Hydraulic considerations include wind, waves, currents, tides, storm surge or wind setup, and the basic bathymetry of the area. Sedimentation considerations include the littoral material and processes (i.e., direction of movement; rate of transport, net and gross; and sediment classification and characteristics), and changes in shore alignment. Navigation considerations include the design craft or vessel data,

traffic lanes, channel depth, width, length, and alinement. Control structure considerations include the selection of the protective works by evaluating type, use, effectiveness, economics, and environmental impact. In selecting the shape, size, and location of shore protection works, the objective should be not only to design an engineering work that will accomplish the desired results most economically, but also to consider effects on adjacent areas. An economic evaluation includes the maintenance costs, along with the interest on and the amortization of the first cost. If any plan considered would increase the problem by extending its effects to a larger coastal stretch or preventing an extension, the economic effect of each such consequence should be evaluated. A convenient measurement for comparing various plans on an economic basis is the total cost per year per meter of shore protected.

Effects on adjacent land areas are considered to the extent of providing the required protection with the least amount of disturbance to current and future land use, ecological factors, and esthetics of the area. The form, texture, and color of material should be considered in the design, as well as how the material is used. Proper planning analysis also requires the consideration of legal and social consequences where shore protection measures may result in significant effects on physical or ecological aspects of the environment.

The following sections describe the most common structural solutions now used to meet functional requirements and provide guidelines for the application of these solutions. The environmental effects of all such solutions must, by law as well as normal engineering concerns, be studied.

## II. SEAWALLS, BULKHEADS, AND REVETMENTS

### 1. Functions.

Seawalls, bulkheads, and revetments are structures placed parallel, or nearly parallel, to the shoreline to separate a land area from a water area. The primary purpose of a bulkhead is to retain land or prevent landsliding, with the secondary purpose of affording protection to the upland against damage by wave action. Bulkheads may also serve as moorings and cargo transfer points for vessels. The primary purpose of a seawall or revetment is to protect the land and upland areas from erosion by waves and currents, with an incidental function as a retaining wall or bulkhead. There are no precise distinctions between the three structures, and often the same type of structure in different localities will bear a different name. Thus, it is difficult to indicate whether a stone or concrete facing designed to protect a vertical scarp is a seawall or a revetment, and often just as difficult to determine whether a retaining wall subject to wave action should be termed a seawall or bulkhead. All these structures, however, have one feature in common--they separate land and water areas. The structures are generally used where it is necessary to maintain the shore in an advanced position relative to that of adjacent shores, where there is a scant supply of littoral material and little or no protective beach, as along an eroding bluff, or where it is desired to maintain a depth of water along the shoreline, as for a wharf.

### 2. Limitations.

These structures afford protection only to the land immediately behind

them, and none to adjacent areas upcoast or downcoast. When built on a receding shoreline, the recession on adjacent shores will continue and may be accelerated. Any tendency toward the loss of beach material in front of such a structure may well be intensified. Where it is desired to maintain a beach in the immediate vicinity of such structures, companion works may be necessary.

### 3. Functional Planning of the Structure.

The siting of seawalls, bulkheads, and revetments is often not a difficult process, since their primary function is usually to maintain existing fixed boundaries. Considerations for design of such a structure include: use and overall shape of the structure, location with respect to the shoreline, length, height, stability of the soil, water levels seaward and landward of the wall, availability of building materials, economic feasibility limits, environmental concerns, and institutional constraints.

### 4. Use and Shape of the Structure.

The use of the structure typically dictates the selection of the shape. Face profile shapes may be classed roughly as vertical or nearly vertical, sloping, convex-curved, concave-curved, reentrant, or stepped. Each cross section has certain functional applications, as illustrated and discussed in detail in Chapter 6. If unusual functional criteria are required, a combination of cross sections may be used.

A vertical- or nearly vertical-face structure lends itself to use as a quay wall, or docking or mooring place. Where a light structure is required, the construction of a vertical face (of sheet piling, for example) may often be quicker and less expensive than other types. This ease or speed of construction is important where emergency protection is needed. A vertical face is less effective against wave attack, and specifically against overtopping, than the concave-curved and reentrant face. The use of vertical- or nearly vertical-face walls can result in severe scouring when the toe or base of the wall is in shallow water. Waves breaking against a wall deflect energy both upward and downward. The downward component causes scouring of the material at the base of the wall. To prevent scouring, protection should be provided at the base of the wall in the form of armor stone of adequate size to prevent displacement, and of such gradation as to prevent the loss of the foundation material through the voids of the stone with consequent settlement of the armor. Vertical walls also reflect energy back offshore where resonant effects may cause beach profile changes.

Coarse rubble slopes effectively dissipate and absorb wave energy, reducing wave runup, overtopping, and scour. Convex-curved face and smooth slopes are least effective in reducing wave runup and overtopping.

Concave-curved or reentrant face structures are the most effective for reducing wave overtopping when onshore winds are light. Where the structure crest is to be used for a road, promenade, or other purpose, this design may be the best shape for protecting the crest and reducing spray. This is especially true if the fronting beach is narrow or nonexistent, or if the water level is above the structure base. If onshore winds occur at the same

time as high waves, a rubble slope should also be considered to reduce runup on the structure face and overtopping due to wind forces.

A stepped-face wall provides the easiest access to beach areas from protected areas, and reduces the scouring of wave backwash.

#### 5. Location of Structure with Respect to Shoreline.

A seawall, bulkhead, or revetment is usually constructed along that line landward of which further recession of the shoreline must be stopped. Where an area is to be reclaimed, a wall may be constructed along the seaward edge of the reclaimed area.

#### 6. Length of Structure.

A seawall, bulkhead, or revetment protects only the land and improvements immediately behind it. These structures provide no protection to either upcoast or downcoast areas as do beach fills. Usually, where erosion is expected at both ends of a structure, wing walls or tie-ins to adjacent land features must be provided to prevent flanking and possible progressive failure of the structure at the ends. Short-term beach changes due to storms, as well as seasonal and annual changes, are design considerations. Erosion updrift from such a structure will continue unabated after the structure is built, and downdrift erosion will probably be intensified.

#### 7. Height of Structure.

Seawalls, bulkheads, and revetments can be built so high that no water could overtop the crest of the structure, regardless of the severity of wave attack and storm surge levels; however, it is usually not economically feasible to do so. Wave runup and overtopping criteria on which the height of a structure should be based can be estimated from data presented in Chapter 7, Section II (WAVE RUNUP, OVERTOPPING, AND TRANSMISSION). Physical model tests can be carried out if greater accuracy is warranted.

#### 8. Determination of Ground Elevation in Front of a Structure.

Seawalls and revetments are usually built to protect a shore from the effects of continuing erosion and to protect shore property from damage by wave attack. The exact effect of such a structure on erosion processes is usually not determinable, but can be estimated using the method described in this section. For safety, even though erosion processes seem to have been halted or reversed, the designer should consider the possibility that they will continue. Changes in the beach profile subsequent to construction of a seawall or revetment should be carefully monitored, as they may produce adverse long-term effects.

As an initial short-term effect, scour may be anticipated at the toe of the structure, forming a trough with dimensions governed by the type of structure face, the nature of wave attack, and the resistance of the bed material. At a rubble slope seawall, scour may undermine the toe stone, causing stones to sink to a lower, more stable position. The resultant settlement of stone on the seaward face may be dealt with by overbuilding the cross section to allow for settlement. Another method is to provide excess

stone at the toe to fill the anticipated scour trough. The toe of a vertical structure may be protected similarly against scour by the use of stone. Impermeable cutoff walls at the base must be used to protect a gravity wall from undermining by scour. *As a general guide, the maximum depth of a scour trough below the natural bed is about equal to the height of the maximum unbroken wave that can be supported by the original depth of water at the toe of the structure.* For example, if the depth of water seaward of the face of the structure is 3.0 meters (10 feet), the offshore bottom slope is 1 vertical on 30 horizontal, and a design wave period of 8 seconds is assumed, the maximum unbroken wave height that can be supported is 3.2 meters (10.4 feet) (see Ch. 7,). Therefore, the maximum depth of scour at the toe of the structure would be about 3.2 meters below the original bottom or 6.2 meters (20.4 feet) below the design water level. Placement of a rock blanket with adequate bedding material seaward from the toe of the structure will prevent erosion at the toe and will result in a more stable structure (see Ch. 7 for design methods).

For long-term effects, it is preferable to assume that the structure would have no effect on reducing the erosion of the beach seaward of the wall. This erosion would continue as if the wall were not there. Since the determination of scour can only be approximate, general guides are usually adopted.

Consider the beach shown in Figure 5-2 where the solid line represents an average existing profile. It is desired to place a structure at point A in the figure. From prior records, either the loss of beach width per year or the annual volume loss of material over the beach area, which includes the profile, is known. In the latter case, *the annual volume loss may be converted to an annual loss of beach width by the general rule: loss of 8 cubic meters of beach material is equivalent to loss of 1 square meter of beach area on the berm (loss of 1 cubic yard of beach material is equivalent to loss of 1 square foot of beach area on the berm).* This rule is applicable primarily at the ocean front. In shallow, protected bays, the ratio of volume to area is usually much less.

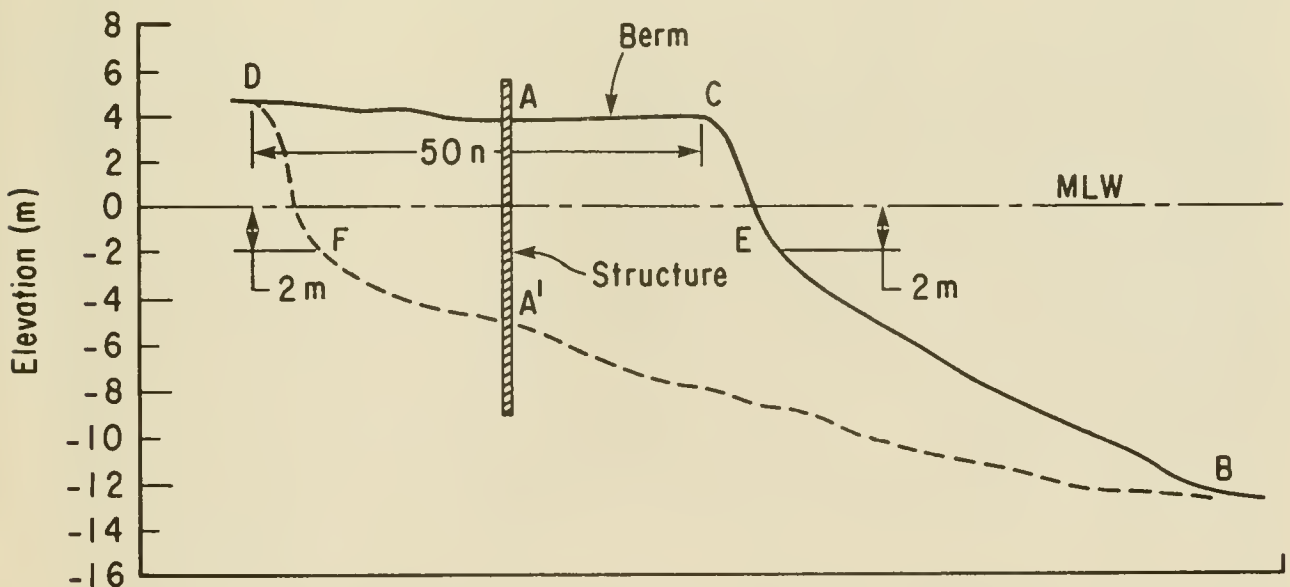


Figure 5-2. Effects of erosion.

Nearshore slopes are usually gentle seaward of the bar. Slopes are steeper inshore of the bar and may be as steep as 1 on 5 at the waterline with coarse sand. Analyses of profiles at eroding beaches indicate that it may be assumed that the slope seaward of a depth of 8 meters (26 feet) will remain nearly unchanged, that the point of slope break E will remain at about the same elevation, and that the profile shoreward of the point of break in slope will remain nearly unchanged. Thus, the ultimate depth at the wall may be estimated as follows:

(a) In Figure 5-2, let B represent a water depth of 8 meters, E the point of slope break at the depth of about 2 meters (6.5 feet), and C the present position of the berm crest. If it is desired to build a structure with an economic life estimated at 50 years at point A and it is found that  $n$  is the annual average loss of beach width at the berm, then in 50 years without the structure this berm will retreat a distance  $50n$  to point D.

(b) From D to the elevation of point E, draw a profile D-F parallel to C-E, and connect points B and F. This dashline, D-F-B, will represent the approximate profile of beach after 50 years without the structure. The receded beach elevation at the structure's location will be approximated by point A'. Similar calculations may be made for anticipated short-term beach losses caused by storms. Storm erosion generally results in a greater loss of beach material above the mean low water (MLW) level, because the super-elevation of the water level (storm surge) allows storm waves to act on the upper part of the beach.

Other factors considered in planning and design are the depth of wall penetration to prevent undermining, tiebacks or end walls to prevent flanking, stability against saturated soil pressures, and the possibility of soil slumping under the wall.

### III. PROTECTIVE BEACHES

#### 1. Functions.

Beaches can effectively dissipate wave energy and are classified as shore protection structures of adjacent uplands when maintained at proper dimensions. Existing beaches are part of the natural coastal system and their wave dissipation usually occurs without creating adverse environmental effects. Since most beach erosion problems occur when there is a deficiency in the natural supply of sand, the placement of borrow material on the shore should be considered as one shore stabilization measure. It is advisable to investigate the feasibility of mechanically or hydraulically placing sand directly on an eroding shore, termed *beach restoration*, to restore or form, and subsequently maintain, an adequate protective beach, and to consider other remedial measures as auxiliary to this solution. Also, it is important to remember that the replenishment of sand eroded from the beach does not in itself solve an ongoing erosion problem and that periodic replenishment will be required at a rate equal to natural losses caused by the erosion. Replenishment along an eroding beach segment can be achieved by stockpiling suitable beach material at its updrift end and allowing longshore processes to redistribute the material along the remaining beach. The establishment and periodic replenishment of such a stockpile is termed *artificial beach nourishment*. Artificial

nourishment then maintains the shoreline at its restored position. When conditions are suitable for artificial nourishment, long reaches of shore may be protected at a cost relatively low compared to costs of other alternative protective structures. An additional consideration is that the widened beach may have additional benefits as a recreation feature.

Under certain conditions, a properly designed groin system may improve a protective beach. However, this method must be used with caution, for if a beach is restored or widened by impounding the natural supply of littoral material, a corresponding decrease in supply may occur in downdrift areas with resultant expansion or transfer of the problem area. Detrimental effects of groins can usually be minimized by placing artificial fill in suitable quantity concurrently with groin construction to allow downdrift bypassing of littoral material; such stockpiling is called *filling the groins*. Groin construction should be sequential from farthest downdrift to the most updrift location within the system in order to achieve maximum natural filling of the groin compartments.

Groins may be included in a beach restoration project to reduce the rate of loss and therefore the nourishment requirements. When groins are considered for use with artificial fill, their benefits should be carefully evaluated to determine their justification. Such justification could be based on the fact that groins will provide a greater reduction in the annual nourishment costs than the increase annual charges for groin construction (see Ch. 5, Sec. VI,10).

## 2. Limitations.

The decision to use groins as part of a protective beach depends first on the availability of suitable sand for the purpose, and if available, on the cost per unit volume of fill and the cost of groin construction. Often the cost per cubic meter of sand for small projects is quite high due to the high expense of mobilizing and demobilizing the equipment needed for project construction, whereas for larger fills the same expense constitutes a much smaller proportion of the project funds. Also, artificial nourishment can be quite costly per unit length of short shore segments because of the rapid erosion of the widened beach which projects significantly seaward of the adjacent shores to create a *soft erodible headland* on which wave energy is focused. The resulting high nourishment requirements may be justified for short lengths of beach in cases where the artificial nourishment prevents the enlargement of the problem area to downdrift shores. Difficulties may be encountered in financing a shore protection method (in this case) which provides protection beyond the immediate problem area. The use of coarser than natural, and consequently more stable, fill material in the original restoration may reduce nourishment requirements, but may be less suitable as wildlife habitat or for human recreation. The introduction of unnatural material may also have other undesirable long-term effects to adjacent shorelines. A sacrificial veneer of fine material over coarser, more protective material would emulate natural conditions at some west coast and Hawaiian beaches.

## 3. Planning Criteria.

Planning of a protective beach by artificial nourishment requires the following:

(a) Determination of the longshore transport characteristics of the project site and adjacent coast and deficiency of material supply to the problem area.

(b) Determination of the composite average characteristics of the existing beach material, or native sand, in the zone of active littoral movement.

(c) Evaluation and selection of borrow material for the initial beach fill and periodic nourishment, including the determination of any extra amount of borrow material required for placement based on the comparison of the native beach sand and borrow material.

(d) Determination of beach berm elevation and width.

(e) Determination of wave-adjusted foreshore slopes.

(f) Determination of beach-fill transition.

(g) Determination of feeder-beach (stockpile) location.

a. Direction of Longshore Transport and Deficiency of Supply. The methods of determining the predominant direction of longshore transport are outlined in Chapter 4, Section V. The deficiency of the material supply is the rate of loss of beach material--the rate at which the material supply must be increased to balance the transport by littoral forces to prevent net loss. If no natural supply is available as downdrift from a major littoral barrier, the net rate of longshore transport required will approximate the deficiency in supply. A comparison of surveys of accreting or eroding areas over a long period of time is the best method of estimating the longshore transport rate (the nourishment required to maintain stability of the shore). Collecting long-term survey data both before and after project construction is recommended. When surveys suitable for volume measurements are unavailable, approximations computed from changes in the shore position, as determined from aerial photography or other suitable records, are often necessary. *For such computations, the relationship in which 1 square meter of change in beach surface area equals 8 cubic meters of beach material (1 square foot of change in beach surface area equals 1 cubic yard of beach material) appears to provide acceptable values on exposed seacoasts.* This relationship presumes the active beach profile extends over a range in elevation of approximately 8 meters (27 feet). The relationship should be adjusted accordingly for shores with greater or less extensive active beach profiles.

b. Description of Native Beach Sand. It is first necessary to sample and characterize native beach sand to obtain a standard for comparing the suitability of potential borrow sediments. Native sediments constitute those beach materials actively affected by beach processes during a suitable period of time (1-year minimum). During a year, at least two sets of samples should be collected from the surface of the active beach profile which extends from an upper beach elevation of wave-dominated processes seaward to an offshore depth or "seaward limit" of littoral sand movement. Ideally, a "winter" and "summer" beach condition should be sampled. The textural properties of all samples are then combined or averaged to form the native "composite" sample which serves as the native beach textural standard. Textural properties of

native sand are selected for the comparison because they result from the selective winnowing and distribution of sediment across the active profile by shoreface processes; their distribution reflects a state of dynamic equilibrium between sediments and processes within the system. See Hobson (1977) and Hands and Hansen (in preparation, 1985) for specific sampling guidelines, a discussion of composite samples, and a determination of offshore limits for sampling.

c. Selection of Borrow Material. After the characteristics of the native sand and the longshore transport processes in the area are determined, the next step is to select borrow material for beach fill and for periodic nourishment. As explained in the previous paragraph, an average native texture, called the *native composite*, is used to evaluate the suitability of potential borrow sand because the native textural patterns are assumed to be the direct response of sand sorting by natural processes. Simply stated, it is assumed that these same processes will redistribute borrow sand that is placed on the beach in a similar textural pattern as the native sand along the profile considering the differences between native and borrow sand texture. Sorting and winnowing action by waves, tides, and currents will therefore tend to generally transport finer sizes seaward, leave the coarsest sizes slightly shoreward of the plunge point, and cover the beach face and remaining offshore areas with the more medium sand sizes. Some sediment sizes that are in borrow material and not in the native beach sand may not be stable in the beach environment. Extremely fine particle sizes are expected ultimately to be moved offshore and lost from the active littoral zone while fragile grains, such as some shells, will be broken, abraded and possibly lost. These kinds of changes to the borrow sediment will, through time, make the texture of the beach fill more like the original native sediment but will, in the process, reduce the original volume of fill placed on the beach.

Borrow sediments containing organic material or large amounts of the finer sand fractions may be used as beach fill since natural sorting and winnowing processes can be expected to clean the fill material. This has been confirmed with fills containing foreign matter at Anaheim Bay and Imperial Beach, California, and Palm Beach, Florida. Also fill material darkened by organic material (Surfside/Sunset Beach, California) or "reddened" by oxidized clay minerals (Imperial Beach, California) will be bleached quickly by the sun to achieve a more natural beach color. Material finer than that exposed on the natural beach face will, if exposed on the surface during a storm, move to a depth compatible with its size to form nearshore slopes flatter than normal slopes before placement. Fill coarser than the sand on the natural beach will tend to remain on the foreshore and may be expected to produce a steeper beach. However, coarser material moved offshore during storms may not be returned to the beach during poststorm periods. The relationship between grain size and slope is discussed in Chapter 4, Section V,2,f. If borrow sand is very coarse, it will probably be stable under normal as well as more severe conditions, but it may make the beach less desirable for recreational use or as wildlife habitat. If the borrow material is much finer than the native beach material, large amounts will move offshore and be lost from the beach. Angularity and mineral content of the borrow material may also prove important factors in its redistribution, deflation, and the esthetic qualities of the beach.

The distribution of grain sizes naturally present on a stable beach represents a state of dynamic equilibrium between the supply and the loss of material of each size. Coarser particles generally have a lower supply rate and a lower loss rate; fine particles are usually more abundant but are rapidly moved alongshore and offshore. Where fill is to be placed on a natural beach that has been relatively stable (i.e., exhibiting a steady rate of change or dynamic stability, or only slowly receding) the size characteristics of the native material can be used to evaluate the suitability of potential borrow material. Borrow material with the same grain-size distribution as the native material is most suitable for fill; material slightly coarser is usually suitable. If such borrow material is available, the volume required for fill may be determined directly from the project dimensions, assuming that only insignificant amounts will be lost through sorting and selective transport and that the sorting is not significantly different from the native material. In cases where these conditions do not apply, an additional volume of fill may be required as determined by an overfill factor.

(1) Overfill Factor. Unfortunately it is often difficult to find economical sources of borrow material with the desired grain-size distribution. When the potential borrow material is finer than the native material, large losses of the beach-fill material often take place immediately following placement. Currently, there is no proven method for computing the amount of overfill required to satisfy project dimensions. Krumbein's (1957) study provides a quantitative basis for comparison on the material characteristics considered to have the greatest effect on this relationship. Subsequent work by Krumbein and James (1965), James (1974), Dean (1974), and James (1975) developed criteria to indicate probable behavior of the borrow material on the beach. The use of the overfill criteria developed by James (1975) will give the best results in the majority of cases. It should be stressed, however, that these techniques have not been fully tested in the field and should be used only as a general indication of possible beach-fill behavior.

The procedures require that enough core samples be taken from the borrow area to adequately describe the composite textural properties throughout the entire volume of the borrow pit (see Hobson, 1977). Textural analyses of both borrow and native beach samples can be obtained using either settling or sieving grain-size analysis techniques. The composite grain-size distributions are then used to evaluate borrow sediment suitability.

Almost any offshore borrow source near the shore will include some suitable size material. Since the source will control cost to a major degree, an evaluation of the proportional volume of borrow material with the desired characteristics is important in economic design. The overfill criteria developed by James (1975), presented graphically in Figure 5-3, give a solution for the overfill factor,  $R_A$ , where

$R_A$  = the estimated number of cubic meters of fill material required to produce 1 cubic meter of beach material when the beach is in a condition compatible with the native material,

$\sigma_\phi$  = the standard deviation and is a measure of sorting (see Ch. 4, Sec. II) where

$$\sigma_{\phi} = \frac{(\phi_{84} - \phi_{16})}{2} \quad (5-1)$$

$M_{\phi}$  = the phi mean diameter of grain-size distribution (see Ch. 4, Sec. II) where

$$M_{\phi} = \frac{(\phi_{84} + \phi_{16})}{2} \quad (5-2)$$

-<sub>b</sub> = subscript b refers to borrow material

-<sub>n</sub> = subscript n refers to natural sand on beach

$\phi_{84}$  = 84th percentile in phi units

$\phi_{16}$  = 16th percentile in phi units

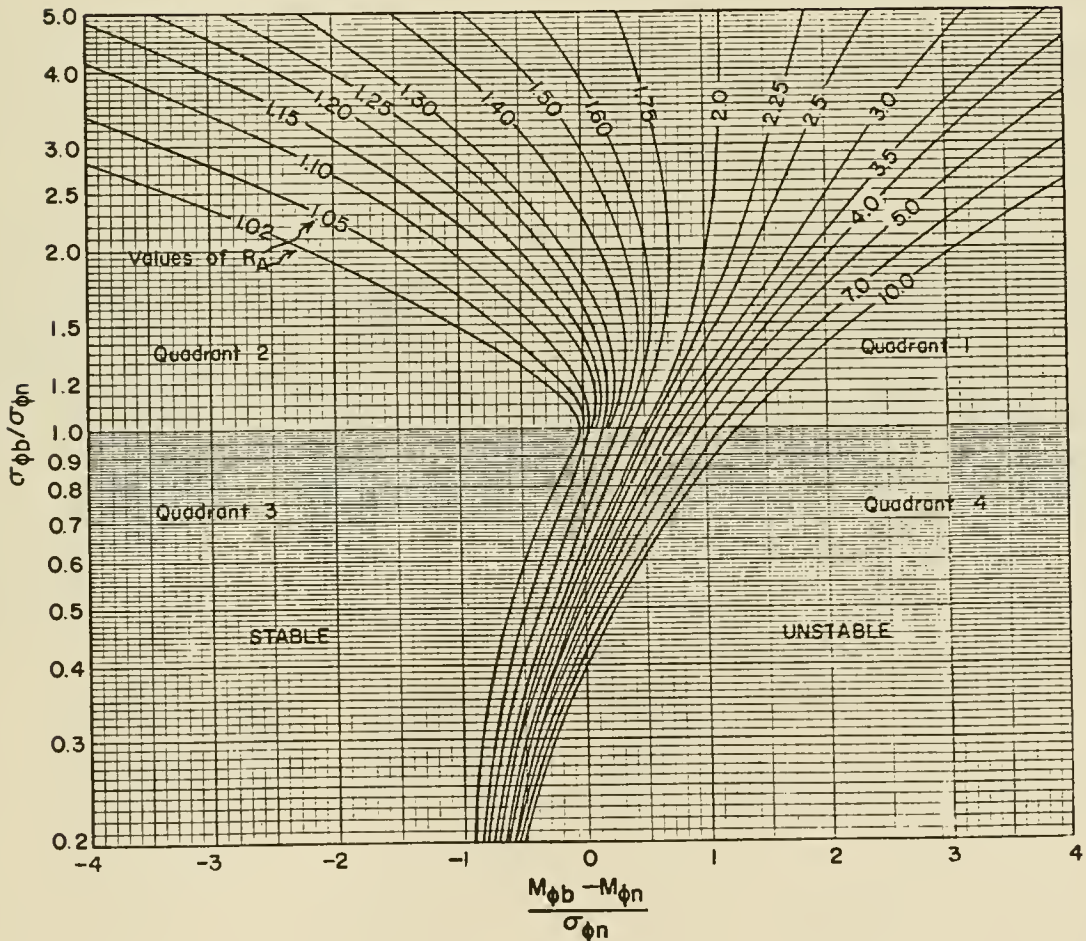


Figure 5-3. Isolines of the adjusted overfill factor,  $R_A$ , for values of phi mean difference and phi sorting ratio (from James, 1975).

This technique assumes that both composite native and borrow material distributions are nearly lognormal. This assumption is correct for the composite grain-size distribution of most natural beaches and many borrow materials. Pronounced bimodality or skewness might be encountered in potential borrow sources that contain multiple layers of coarse and fine material, such as clay-sand depositional sequences, or in borrow zones that crosscut flood plain deposits associated with ancient river channels.

The four possible combinations that result from a comparison of the composite grain-size distribution of native material and borrow material are listed in Table 5-1 and indicated as quadrants in Figure 5-3.

The engineering application of the techniques discussed above requires that basic sediment-size data be collected in both the potential borrow area and the native beach area. An estimation of the composite grain-size characteristics of native material should follow the guidelines in Hobson (1977). The determination of the composite distribution of the borrow zone material depends on the variation of materials and their individual properties. If the textural properties of the potential borrow material exhibit considerable variation in both area and depth, extensive coring may be required to obtain reliable estimates of the composite distribution of properties. Since detailed guidelines have not been established for evaluating borrow deposits, it is recommended that core sampling be carried out as a two-phase program--the first phase inventories the general borrow region and the second phase samples in detail those areas with the greatest potential.

(2) Renourishment Factor. James (1975) provides a second approach to the planning and design of nourishment projects. This approach, which relates to the long-term maintenance of a project, asks the basic question of how often renourishment will be required if a particular borrow source is selected that is texturally different from the native beach sand. With this approach, different sediment sizes will have different residence times within the dynamic beach system. Coarse particles will generally pass more slowly through the system than finer sizes. This approach also requires accurate composites of native and borrow sediment textures.

To determine periodic renourishment requirements, James (1975) defines a renourishment factor,  $R_J$ , which is the ratio of the rate at which borrow material will erode to the rate at which natural beach material is eroding. The renourishment factor is given as

$$R_J = e \left[ \Delta \left( \frac{M_{\phi b} - M_{\phi n}}{\sigma_{\phi n}} \right) - \frac{\Delta^2}{2} \left( \frac{\sigma_{\phi b}^2}{\sigma_{\phi n}^2} - 1 \right) \right] \quad (5-3)$$

where  $\Delta$  is a winnowing function. The  $\Delta$  parameter is dimensionless and represents the scaled difference between the phi means of noneroding and actively eroding native beach sediments. James (1975) estimates values of  $\Delta$  ranging between 0.5 and 1.5 for a few cases where appropriate textural data were available and recommends  $\Delta = 1$  for the common situation where the textural properties of noneroding native sediments are unknown. Equation (5-3) is plotted in Figure 5-4 for  $\Delta = 1$ . Figure 5-3 should be used for

Table 5-1. Relationships of phi means and phi standard deviations of native material and borrow material.

Category		Relationship of Phi Means	Relationship of Phi Standard Deviations
Case	Quadrant in Fig. 5-3		
I	1	$M_{\phi b} > M_{\phi n}$ Borrow material is finer than native material	$\sigma_{\phi b} > \sigma_{\phi n}$ Borrow material is more poorly sorted than native material
II	2	$M_{\phi b} < M_{\phi n}$ Borrow material is coarser than native material	
III	3	$M_{\phi b} < M_{\phi n}$ Borrow material is coarser than native material	$\sigma_{\phi b} < \sigma_{\phi n}$ Borrow material is better sorted than native material
IV	4	$M_{\phi b} > M_{\phi n}$ Borrow material is finer than native material	

determining initial quantities of beach fill, and Figure 5-4 for determining how often renourishment may be required.

The renourishment and fill factors are not mathematically related to one another. Each relationship results from unique models of predicted beach-fill behavior which are computationally dissimilar although both use the comparison of native and borrow sand texture as input. Nevertheless, the models address the different problems in determining nourishment requirements when fill that is dissimilar to native sediments is to be used (fill factor) and in predicting how quickly a particular fill will erode (renourishment). For design purposes, the fill factor,  $R_A$ , or its equivalent, should be applied to adjust both initial and renourishment volumes (see Table 5-2). The renourishment factor,  $R_J$ , should be considered an independent evaluation of when renourishment will be required. Both models are simplistic descriptions of complex beach relationships, and there will be cases where the  $R_A$  and  $R_J$  values calculated for a particular borrow material suggest quite different responses from that material. One example is where the models suggest both that overage is required and that the borrow will erode much slower than native beach sediments. This situation could arise with coarser and more poorly sorted borrow sand where early winnowing would remove the overage volume of unstable finer sizes and leave a coarser-than-native sand that erodes slowly. For cases like this and in all cases where these models are applied, engineering judgment and experience must accompany design application.

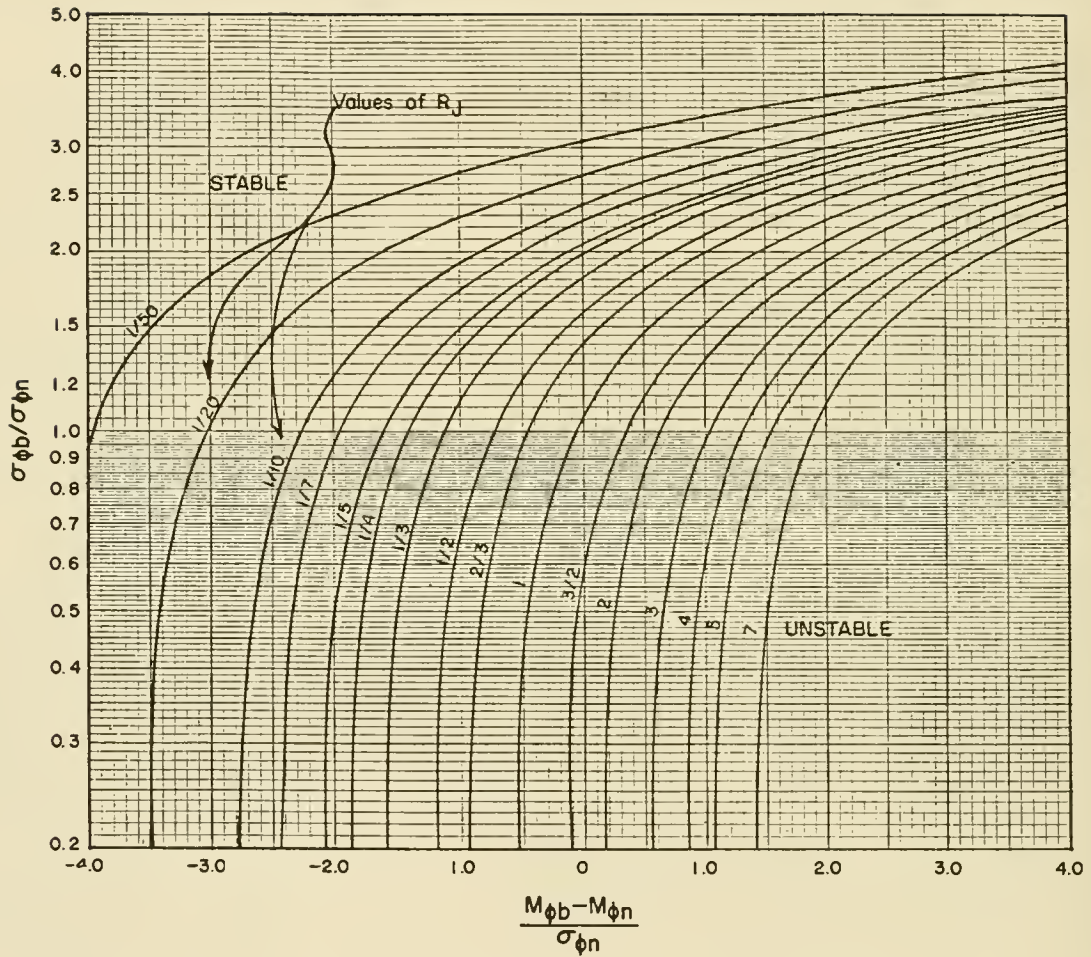


Figure 5-4. Isolines of the renourishment factor,  $R_J$ , for values of phi mean difference and phi sorting ratio,  $\Delta = 1.0$  (James, 1975).

Table 5-2. Comparison of composite grain-size distribution parameters and beach fill, Brunswick County, North Carolina.

	Sediment sources		
	Native	Borrow I (Middle ground)	Borrow II (Yellow Banks)
<b>Textural properties</b>			
$\phi_{16}$	1.10	0.58	1.22
$\phi_{84}$	2.70	2.54	2.66
Phi mean, $M_\phi$	1.90	1.56	1.94
Phi sorting, $\sigma_\phi$	0.80	0.98	0.72
$\sigma_{\phi b} / \sigma_{\phi n}$	-----	1.23	0.90
$(M_{\phi b} - M_{\phi n}) / \sigma_{\phi n}$	-----	-0.43	0.05
Percent sand	100.00	89.00	95.00
<b>Fill factors</b>			
$R_A$	-----	1.00	1.20
$R_G$ (see eq. 5-4)	-----	1.12	1.26
$R_J$	-----	0.51 <sup>1</sup>	1.16
<b>Fill requirements</b>			
Initial fill <sup>2</sup> (m <sup>3</sup> )	6,033,000	6,757,000	7,602,000
Yearly nourishment <sup>3</sup> (m <sup>3</sup> /yr)	232,000	232,000 <sup>1</sup>	269,000

<sup>1</sup> Use a retreat rate ( $R_J$ ) of unity to determine *first* renourishment needs. Use fill performance data for future renourishment planning.

<sup>2</sup> Values are adjusted products of initial fill needs (6,033,000 cubic meters) times  $R_G$ .

<sup>3</sup> Values are the adjusted *first-year* nourishment volumes ( $R_J \times 232,000$  cubic meters per year).  $R_J = 1$  is used for determining first nourishment using the middle-ground shoal borrow sediments as explained in footnote 1 above.

Application of both the overfill and renourishment techniques is demonstrated in the following example problems.

\*\*\*\*\* EXAMPLE PROBLEM 1 \*\*\*\*\*

GIVEN: Composite native beach material phi parameters

$$\phi_{84} = 2.47\phi (0.18 \text{ mm})$$

$$\phi_{16} = 1.41\phi (0.38 \text{ mm})$$

Composite borrow material parameters

$$\phi_{84} = 3.41\phi (0.09 \text{ mm})$$

$$\phi_{16} = 1.67\phi (0.31 \text{ mm})$$

FIND:

(a) The fill factor,  $R_A$

(b) The renourishment factor,  $R_J$

SOLUTION:

(a) Using equation (5-2)

$$M_\phi = \frac{\phi_{84} + \phi_{16}}{2}$$

$$M_{\phi n} = \frac{2.47 + 1.41}{2} = 1.94 (0.26 \text{ mm})$$

and

$$M_{\phi b} = \frac{3.41 + 1.67}{2} = 2.54 (0.17 \text{ mm})$$

Using equation (5-1)

$$\sigma_\phi = \frac{\phi_{84} - \phi_{16}}{2}$$

$$\sigma_{\phi n} = \frac{2.47 - 1.41}{2} = 0.53$$

and

$$\sigma_{\phi b} = \frac{3.41 - 1.67}{2} = 0.87$$

The phi sorting ratio is

$$\frac{\sigma_{\phi b}}{\sigma_{\phi n}} = \frac{0.87}{0.53} = 1.64$$

and the phi mean difference is

$$\frac{M_{\phi b} - M_{\phi n}}{\sigma_{\phi n}} = \frac{2.54 - 1.94}{0.53} = 1.13$$

From Figure 5-3, the fill factor is

$$R_A = 2.25, \text{ i.e., } 2.3$$

(b) From Figure 5-4, the renourishment factor is

$$R_J = 1.33, \text{ i.e., } 1.3$$

The results indicate that the project requires 2.3 cubic meters of this borrow material fill to satisfy each cubic meter required by the project dimensions. Periodic renourishment using the same borrow material must be provided 1.3 times as often as using original nativelike sediments in order to maintain project dimensions.

\* \* \* \* \*  
\* \* \* \* \* EXAMPLE PROBLEM 2 \* \* \* \* \*

GIVEN: Composite native beach material phi parameters

$$\phi_{84} = 3.10 \text{ (0.12 mm)}$$

$$\phi_{16} = 1.86 \text{ (0.28 mm)}$$

Composite borrow material phi parameters

$$\phi_{84} = 3.25 \text{ (0.11 mm)}$$

$$\phi_{16} = 0.17 \text{ (0.89 mm)}$$

FIND:

- (a) The fill factor,  $R_A$
- (b) The renourishment factor,  $R_J$

SOLUTION:

- (a) Using equation (5-2)

$$M_{\phi} = \frac{\phi_{84} + \phi_{16}}{2}$$

$$M_{\phi n} = \frac{3.10 + 1.86}{2} = 2.48 \text{ (0.18 mm)}$$

and

$$M_{\phi b} = \frac{3.25 + 0.17}{2} = 1.71 \text{ (0.31 mm)}$$

Using equation (5-1)

$$\sigma_{\phi} = \frac{\phi_{84} - \phi_{16}}{2}$$

$$\sigma_{\phi n} = \frac{3.10 - 1.86}{2} = 0.62$$

and

$$\sigma_{\phi b} = \frac{3.25 - 0.17}{2} = 1.54$$

The phi sorting ratio is

$$\frac{\sigma_{\phi b}}{\sigma_{\phi n}} = \frac{1.54}{0.62} = 2.48$$

and the phi mean difference is

$$\frac{M_{\phi b} - M_{\phi n}}{\sigma_{\phi n}} = \frac{1.71 - 2.48}{0.62} = 1.24$$

From Figure 5-3, the fill factor is

$$R_A = 1.15$$

- (b) From Figure 5-4 and equation (5-3), the renourishment factor is

$$R_J = \frac{1}{45} \text{ or } 0.022$$

The results indicate that the project requires 1.15 cubic meters of this borrow material fill to satisfy each cubic meter required by the project dimensions. If the beach requires periodic renourishment, the renourishment must only be provided 0.022 times as often from the borrow material as from natively like material in order to maintain the desired beach profile. Please note that very low  $R_J$  values, as in this example problem, should be applied in design with caution. A conservative approach is recommended, or initially using an  $R_J$  equal to unity in these cases for planning the first renourishment and then later adjusting the value in accordance with the results of monitoring the performance of the project.

\*\*\*\*\*

The location of the borrow source is also a factor to be considered in project design. In the past, readily available sources have frequently been bays, lagoons, and onshore sites. Onshore sites generally require less sophisticated material-handling equipment than for offshore sites but the cost per cubic meter of land-derived material is often very high, which makes these sites unattractive borrow sources. Bay and lagoonal sediments are generally finer and more poorly sorted than native beach sand. Although these textural differences often result in volumes of borrow material several times that required by project dimensions, these sources are still often selected as the most cost effective due to the proximity of bays and lagoons to project sites and because of the shelter they provide to dredging equipment. Few bays and lagoons are currently available as sources because of environmental considerations. The development of more seaworthy and innovative dredging plants has made offshore sources of borrow material more attractive, and to date, offshore sources have generally provided fill materials that are initially more compatible with native beach sands.

Hobson (1977) evaluated two borrow areas for beach fill at Oak Island, North Carolina--the Yellow Banks area on the mainland and the middle-ground shoal at the mouth of the Cape Fear River. U.S. Army Engineer District, Wilmington (1973), found it practical to account for the proportion of grain sizes finer than sand, which are considered unstable on the beach, by increasing the fill factor using the following formula:

$$R_G = R_A \times \frac{100}{\% \text{ sand}} \quad (5-4)$$

where  $R_G$  is the modified fill factor. Comparisons of the two borrow areas are shown in Table 5-2.

For this particular project, the estimated mobilization-demobilization expenses and cost per cubic meter of fill estimates, used in the original General Design Memorandum (U.S. Army Engineer District, Wilmington, 1973), favor the Yellow Banks area even when renourishment is considered. However, as the use of offshore borrow sites becomes more commonplace and the techniques of their exploitation better understood, the costs of offshore sediments are likely to become more economical when compared with conventional

sources. Offshore borrow sites have been used successfully in the construction of major beach restoration projects at Rockaway Beach, New York; Dade County, Florida; Redondo Beach, California; and Harrison County, Mississippi.

d. Berm Elevation and Width. Beach berms are formed by the deposit of material by wave action. The height of a berm is related to the cycle change in water level, normal foreshore and nearshore slopes, and the wave climate. Some beaches have no berms; others have one or several. Figure 5-5 illustrates a beach profile with two berms. The lower berm is the natural or normal berm and is formed by the uprush of normal wave action during the ordinary range of water level fluctuations. The higher berm, or storm berm, is formed by wave action during storm conditions. During most storms, waves and wave setups will cause an increase in the normal water level on the beach. Wave overtopping and backrush with sufficient duration may completely obliterate the natural beach berm.

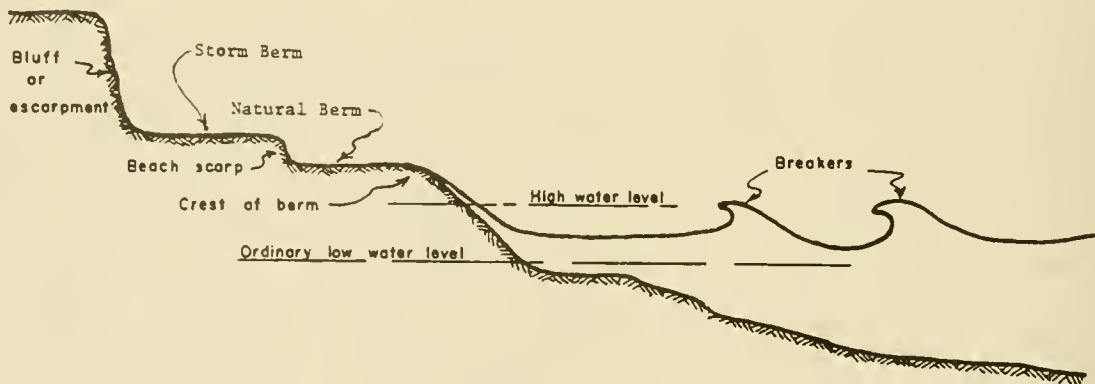


Figure 5-5. Beach berm system.

The degree of protection to the backshore depends greatly on the effectiveness of the storm berm. Beach berms must be carefully considered in the planning of a beach fill. If a beach fill is placed to a height lower than the natural berm crest, a ridge will form along the crest and high water may overtop the berm crest causing ponding and temporary flooding of the backshore area. Such flooding, if undesirable, may be avoided by placing the fill to a height slightly above the natural berm crest elevation. Several alternative techniques may be employed to estimate the height of the berm for design purposes (see Ch. 7, Sec. II). If a beach exists at the site, the natural berm crest height can be measured and future berm elevations can be estimated. An estimate may also be made by comparing the beach profile at the site with beach profiles at sites of similar exposure characteristics (waves and tides) and similar size beach material. If enough wave data applicable to the project site (either developed from synoptic surface weather charts or actual records) are available, wave runup (discussed in Ch. 7, Sec. II) can be estimated to establish a design berm crest height and adjacent beach slope.

Criteria for specifying berm width depend on several factors. If the purpose of the fill is to restore an eroded beach to protect backshore improvements from major storm damage, the width may be determined as the protective width which has been lost during storms of record plus the minimum

required to prevent wave action from reaching improvements. Where the beach is used for recreation, the justification for the increased width of the beach may be governed by the area required for recreational use. Although there is no current formally established standard in the United States, previous values of 7 to 9 square meters (75 to 100 square feet) of dry beach per bather have been used. Where the beach fill serves as a stockpile to be periodically replenished, the berm should be wide enough to accommodate the recession expected during the intervals between nourishment operations.

e. Slopes. The toe of a stockpile of beach material should not extend deeper than the effective limiting depth of sediment transport by wave-driven longshore currents. Chapter 4, Section V,2,c can be used to calculate this maximum depth. Also, the study of general offshore topographic relationships provides estimates of this 9-meter depth below low water datum for eastern and western seacoasts and about a 6-meter depth on the Great Lakes and gulf coasts. The initial slope of any beach fill will naturally be steeper than that of the natural profile over which it is placed. The subsequent behavior of the slope depends on the characteristics of the fill material and the nature of the wave climate.

Design slopes are generally used for computing fill requirements since natural processes are expected to generally shape the profile into an environmentally equilibrated form. In practice, the initial foreshore slope of a fill is designed parallel to the local or comparable natural beach slope above low water datum. The design of the offshore slope should be determined after careful investigation of all pertinent data from low water datum to the appropriate offshore depth. The design slope is derived through synthesis and the averaging of existing data within and adjacent to the problem area, and is usually significantly flatter than the foreshore slope. Design slopes based on such data are usually in the range of 1:20 to 1:30 from low water datum to the intersection with the existing bottom.

Construction slopes are seldom the same as design slopes because of the working limitations of equipment used to place and shape the fill, and because the selective sorting of the fill by waves and currents will naturally shape the profile after nourishment. Two construction approaches are recommended. One is to overbuild the upper part of the beach and the other approach is to create an initial construction profile that extends significantly offshore.

The "overbuilding" approach was adopted for fills at Carolina Beach in 1970 and Wrightsville Beach in 1981. This method places the required fill volume onshore at an elevation equal to the natural beach berm elevation and has a fill slope that is steeper than the equilibrium design slope on the seaward side. A part of the fill is placed underwater, in an amount determined by the fill's berm width and seaward slope. Readjustment of the fill sediments into a more equilibrated profile shape is accomplished almost entirely by waves and currents that erode and redistribute the artificially piled sediments and remove the finer unstable sizes through winnowing action. In general, the fill volume placed should be adequate to establish the design profile, after winnowing, and to provide an advance nourishment supply of sediment. The total volume can be determined by using both the design drawings and the calculated yearly rate of sediment loss from the beach, and by applying the overfill ratio,  $R_A$ , to these values in cases where the borrow material to be used is dissimilar to native beach sediments. Scarping is one

problem that may be encountered in the overbuilding approach. Steep scarps may develop at the toe of the fill as waves begin the readjustment, and these scarps may make access to the beach difficult, as occurred in a California beach-fill project constructed at Surfside and Sunset Beaches in 1979. The scarping process may also increase erosion rates of the fill as large volumes of sand avalanche into the littoral system when waves oversteepen or undercut the fill slope. Scarping does not always develop but it can result more easily when there is an abrupt transition between a steep fill slope and a flatter natural offshore slope.

The second approach, which may reduce scarping, is to initially place more of the fill offshore. Redistribution of the sediment across the profile by waves and currents will still take place after construction to reequilibrate profile shape, but much of the reworking will occur offshore of the fill rather than onshore. Using this construction approach, beach nourishment projects in 1975 and 1977 at Rockaway Beach, New York, were conducted hydraulically with the contractor's payment dependent on the amount of material placed on the beach to the offshore depth where the 1:30 design slope met the existing bottom. This approach also provided the contractor an incentive to minimize his fill losses. In comparing the two approaches, the offshore depth at Rockaway Beach ranged between 4 and 6 meters below MLW datum versus depths of -1 to -3 meters mean sea level (MSL) for the overbuilt fill sections at Carolina and Wrightsville Beaches in North Carolina.

Both construction approaches result in an onshore fill section that is placed to a desired berm width and has steep initial slopes. This onshore fill eventually adjusts to a natural slope and narrows the berm, leaving the impression that much of the fill has been lost, although it has only moved offshore to reestablish a stable profile.

f. Beach-Fill Transition. The alinement of a nourished beach segment generally parallels the existing shoreline but is offset seaward by the width of the fill. The nourished segment can be thought of as a subtle headland that protrudes from the existing coast. Transition from the fill to the existing shoreline can be accomplished either by constructing "hard" structures, such as groins and jetties, which compartment the fill or by filling transition zones between the terminal ends of the beach fill and the unrestored beach.

Groins, jetties, and headlands do allow an abrupt termination of the beach fill at the project limits. However, these hard structures are often quite costly, unacceptable esthetically, and more importantly, they may interrupt or modify the natural longshore transport flow in an area. If groins are selected to terminate a fill, Chapter 5, Section VI should be used to determine design components such as cross section, materials, and length.

If filled transition zones are selected, their length and transition angle will determine the additional volume of fill, and hence the cost, required for the project. The orientation of the transition shoreline will differ from the natural shoreline alinement, resulting in different erosion rates since the rate of littoral transport depends on the relative angle between the breakers and a particular shoreline segment.

One method of evaluating different transition plans is to compare total life cycle costs for the beach restoration and periodic nourishment projects with alternate combinations of transition angle and length and select the plan that provides optimum improvement (e.g., the plan with the lowest life cycle costs to accomplish the project objectives). Chapter 4, Section V,3 provides equations and procedures for determining longshore transport rates along beach segments with varied transition angles. As the transition angle decreases,

- (1) The expected rate of erosion per unit length of the transition zone decreases.
- (2) The length of the transition fill increases and hence the volume of required fill increases.
- (3) The volume of fill required for periodic nourishment increases in order to maintain the longer length of project shoreline.

These varying relationships make possible an optimization procedure to minimize the cost of a transition plan.

An example situation could be to minimize transition costs for a beach fill on a beach which

- (1) Is widened 56 meters (184 feet).
- (2) Requires 7.5 cubic meters of fill per square meter (0.9 cubic yard per square foot) of beach.
- (3) Is eroding at a rate of 22 cubic meters per linear meter (8.8 cubic yards per foot).
- (4) Has a left-to-right yearly littoral transport rate of 425,000 cubic meters (555,900 cubic yards) generated by waves with a breaker angle of  $23^\circ$ .
- (5) Has a right-to-left yearly littoral transport rate of 85,000 cubic meters (111,200 cubic yards) generated by waves with a breaker angle of  $15.5^\circ$ .

A comparison of alternate transition plans for this example indicates that minimal costs would be achieved with a long transition segment (1070 meters or 3510 feet) oriented at about  $3^\circ$  to the existing shoreline. This example is intended to illustrate that optimal transition zones are generally quite long and oriented at gentle angles to the existing shore. It may sometimes be more practical, however, to either compartment the beach-fill material with groins or construct fairly sharp transition angles and deal with high rates of fill loss at project boundaries if land ownership constraints or other factors preclude the construction of the optimum transition.

g. Feeder Beach Location. Dimensions of a stockpile or feeder beach are generally governed primarily by economic considerations involving comparisons of costs for different nourishment intervals. Therefore, planning a stockpile location must be considered in conjunction with stockpile dimensions. If the problem area is part of a continuous and unobstructed beach, the stockpile is

located at the updrift end of the problem area. Until the stockpile material is transported by littoral processes to the beach area downdrift of the stockpile location, that beach may be expected to recede at the same rate as determined from historical survey data. If economically justified, stockpiles may be placed at points along the problem area, which will decrease the time interval between stockpile placement and complete nourishment of the area. Stockpile lengths from a few hundred meters to a kilometer have been employed successfully. If the plan involves a feeder beach just downdrift of a coastal inlet, wave refraction and inlet currents must be considered to locate the feeder beach so that a minimum of material is transported into the inlet. A supplementary structure (such as a groin) may be needed to reduce the material movement into the inlet caused by either tidal currents or a change in longshore transport.

The nearly continuous interception of littoral material on the updrift side of an inlet and the mechanical transportation of the material to a point on the downdrift shore (sand bypassing) constitute a form of stockpiling for artificial nourishment to the downdrift shore. In this type of operation, the size of the stockpile or feeder beach will generally be small; the stockpile material will be transported downdrift by natural forces at a rate about equal to or greater than the rate of deposition. For the suggested location of the stockpile or feeder beach for this type of operation, see Chapter 6, Section V (SAND BYPASSING). The need for a jetty or groin between the stockpile or feeder beach and the inlet to prevent the return of the material to the inlet should be evaluated if such structures do not already exist.

#### IV. SAND DUNES

##### 1. Functions.

Sand dunes are an important protective formation. The dune ridges along the coast prevent the movement of storm tides and waves into the land area behind the beach. Dunes prevent storm waters from flooding the low interior areas. Dune ridges, which are farther inland, also protect but to a lesser degree than foredunes. Well-stabilized inland ridges are a second line of defense against erosion should the foredunes be destroyed by storms. The use of native vegetation may be desirable to stabilize the dune sand that might migrate over adjacent areas and damage property (see Fig. 5-6). Stabilizing dunes also prevent the loss of their protection. At locations that have an adequate natural supply of sand and are subject to inundation by storms, a belt of dunes can provide protection more effectively at a lower cost than a seawall (see Ch. 6, Sec. IV).

Sand dunes near the beach not only protect against high water and waves, but also serve as stockpiles to feed the beach. Sand accumulation on the seaward slope of a dune will either build or extend the dune toward the shoreline. This sand, once in the dune, may be returned to the beach by a severe storm and thus nourish the beach. Figure 5-7 is a schematic diagram of a storm wave attack on the beach and dune. As shown, the initial attack of storm waves is on the beach berm fronting the dune. Waves attack the dune when the berm is eroded. If the wave attack lasts long enough, the waves can overtop the dune, lowering the dune crest. Much of the sand eroded from the berm and dune is transported directly offshore and deposited in a bar formation. This process helps to dissipate incident wave energy during a storm,



a. High, well-stabilized barrier dune.



b. Migration of unstabilized dune across a road.

Figure 5-6. Stabilized and migrating dunes.

and offshore deposits are normally transported back to the beach by swells after the storm. Onshore winds transport the sand from the beach toward the foredune area, and another natural cycle of dune building proceeds. This dune building, however, is generally at a very slow rate unless supplemented by fences or vegetation.

## 2. Positioning.

The location of a barrier dune can have a major influence on its durability and function. Well-vegetated dunes are effective against storm surge and can withstand moderate degrees of overtopping, but they are highly vulnerable to erosion if the beach berm is either overtopped or recedes due to persistent wave attack. In the positioning of a new barrier dune, an allowance should be made for the normal shoreline fluctuations that are characteristic of the site. Serious problems of dune maintenance may often be avoided or minimized by positioning the foredune far enough back from the high water line to allow a reasonable amount of seasonal fluctuations. A minimum distance of 200 meters (650 feet) is suggested between the toe of the dune (sand fence) and the high water line (Blumenthal, 1964).

The process of dune growth is an important consideration in locating a barrier dune. Fully vegetated dunes expand only toward the sand source, which is usually the beach, and a relatively narrow strip of vegetation will, in most cases, stop all wind-transported sand. This means that, where possible, an allowance should be made for the seaward expansion of the dune with time. Also, when two dunes are desired, the first must be developed landward and have enough space left between it and the sea for the second or frontal dune.

On many low-lying coasts the crest of the storm berm is the highest point in the beach-dune area with the surface sloping back from the berm crest. This places the base of a new barrier dune below the elevation of the storm berm, making it more susceptible to overtopping during the early stages. It may also encourage ponding of the water overtopping the storm berm, resulting in water pressure, salt buildup, and destruction of vegetation along the toe of the dune. Where this problem exists, the dune location will often represent a compromise.

## V. SAND BYPASSING

### 1. General.

An inlet is a short, narrow waterway connecting the sea or major lake with interior waters. Inlets, which are either natural or improved to meet navigation requirements, interrupt sediment transport along the shore. A natural inlet has a well-defined bar formation on its seaward side. A part of the sand transported alongshore ordinarily moves across the inlet by way of this outer bar--natural sand bypassing. However, the supply reaching the downdrift shore is usually intermittent rather than regular, and the downdrift shore is usually unstable for a considerable distance. If the tidal flow through the inlet into the interior body of water is strong, part of the material moving alongshore is carried into and permanently stored in the interior body of water as a middle-ground shoal, reducing the supply available to nourish downdrift shores. The outer bar normally migrates with a migrating inlet, but the

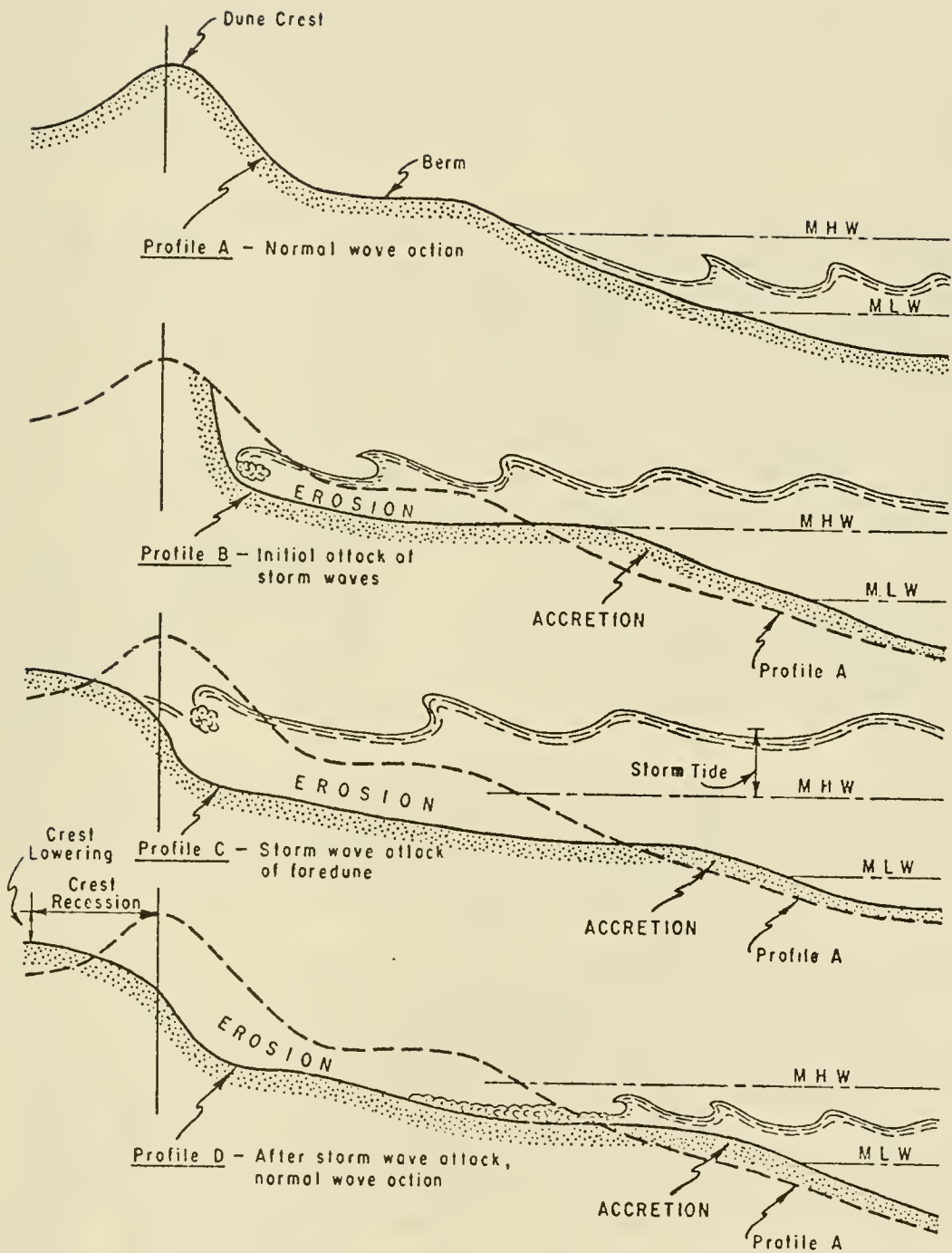


Figure 5-7. Schematic diagram of storm wave attack on beach and dune.

middle-ground shoal does not. Thus the middle-ground shoal increases in length as the inlet migrates, and the volume of material stored in the inlet increases.

When an inlet is deepened by dredging through the outer or inner bars or through the channel, an additional storage capacity is created to trap available littoral drift and the quantity which would naturally pass the inlet is reduced. If the dredged material is deposited in deep water or beyond the limits of littoral currents, the supply to the downdrift shore may be nearly eliminated. The resulting erosion is proportional to the reduction in rate of supply.

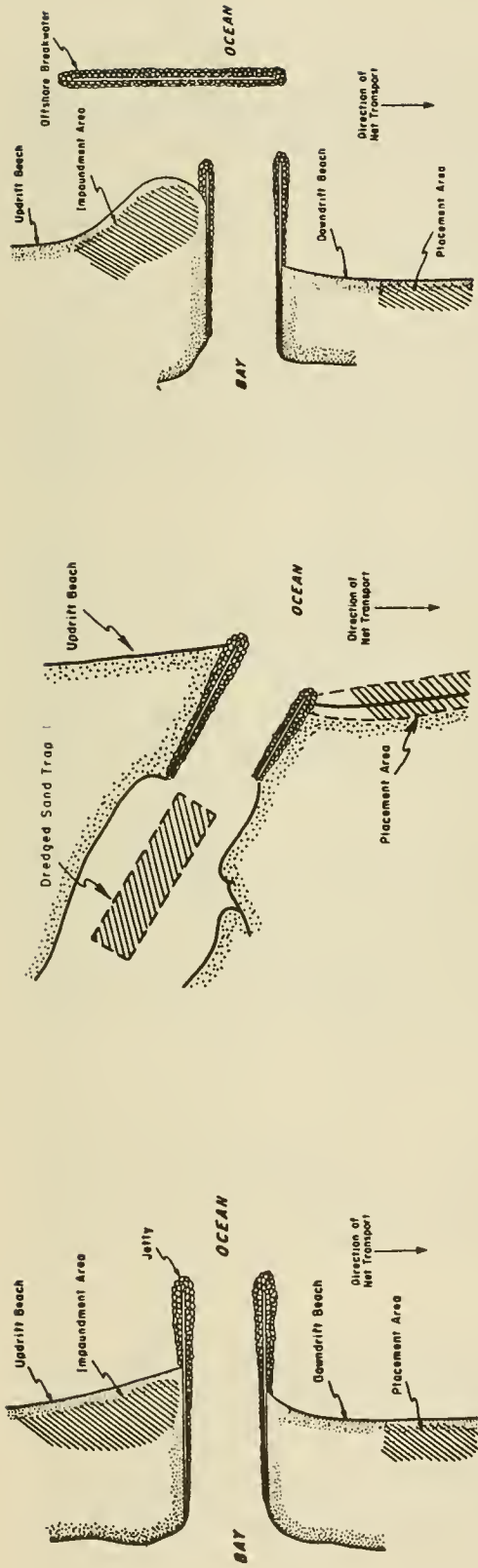
A common method of inlet improvement has been to flank the inlet channel with jetties or breakwaters. These structures form a barrier to longshore transport of littoral drift. Jetties have one or more of the following functions: to block the entry of littoral drift into the channel, to serve as training walls for inlet tidal currents, to stabilize the position of the navigation channel, to increase the velocity of tidal currents and flush sediments from the channel, and to serve as breakwaters to reduce wave action in the channel. Where there is no predominant direction of longshore transport, jetties may stabilize nearby shores, but only to the extent that sand is impounded at the jetties. The amount of sand available to downdrift shores is reduced, at least until a new equilibrium shore is formed at the jetties. Usually, where longshore transport predominates in one direction, jetties cause accretion of the updrift shore and erosion of the downdrift shore.

The stability of the shore downdrift of inlets, with or without jetties, may be improved by artificial nourishment to make up the deficiency in supply due to storage in the inlet. When such nourishment is done mechanically, using the available littoral drift from updrift sources, the process is called *sand bypassing*.

Types of littoral barriers (jetties and breakwaters) which have been generally employed in connection with inlet and harbor improvement are shown in Figure 5-8. If littoral transport predominates in one direction, any of these types can cause accretion to the updrift shore and erosion of the downdrift shore, unless a provision is made for sand bypassing.

At a jettied inlet (Fig. 5-8, type I), bypassing can normally be performed best by a land-based dredging plant or land vehicles. A floating plant can be used only where the impounding zone is subject to periods of light wave action, or by breaking into the landward part of the impoundment and dredging behind the beach berm thus leaving a protective barrier for the dredge. Such an operation was performed at Port Hueneme, California, in 1953 (see Ch. 6, Sec. V, 2,a). In any type of operation at such a jettied inlet, it is unlikely that bypassing of all the littoral drift can be attained; some material will pass around the updrift jetty into the channel, especially after the impounding capacity of the jetty has been reached.

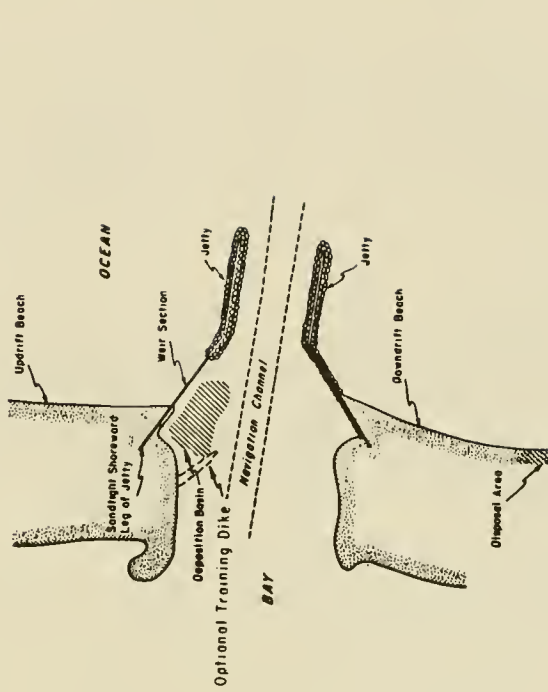
Dredging of a sand trap in the protected waters of an inlet or harbor entrance (Fig. 5-8, type II) provides a practical sand-bypassing technique, particularly when the inlet tidal currents are strong. These currents move the sediment into the inlet where it is deposited into the sand trap. Periodic dredging of the trap and depositing of the dredged material on the



Type I: Jettied inlet

Type II: Inlet sand trap

Type III: Jettied inlet and offshore breakwater



Type IV: Shore-connected breakwater (Impounding zone at seaward end of breakwater)

Type V: Shore-connected weir breakwater or jetty (Impounding zone at shoreward end of breakwater)

Figure 5-8. Types of littoral barriers where sand transfer systems have been used (Weggel, 1981).

downdrift beach completes the bypassing operation. The location of the sand trap in sheltered waters allows a dredge to operate during any season in all but the most severe wave conditions.

To ensure more complete bypassing of the littoral drift, the combination of the jettied inlet and an offshore breakwater (Fig. 5-8, type III) was developed. In this design, a floating plant works effectively, completely protected by the breakwater and most of the sand moving inshore of the offshore breakwater is bypassed. Practically no shoaling of the channel would be expected. Although this type is considered the most effective type of improvement for both navigation and sand bypassing, it is also normally the most costly.

The shore-connected breakwater with impoundment at its seaward end (Fig. 5-8, type IV) has been used effectively. Bypassing is performed by a floating plant, but heavy wave action could cause delays during the removal of the outer part of the impoundment. Most of the sand transported alongshore would be bypassed, either naturally or mechanically, but some shoaling of the navigation channel is likely between dredging operations.

The shore-connected breakwater or jetty with a low sill or weir and an impounding zone or deposition basin behind the breakwater (Fig. 5-8, type V) was designed to provide bypassing of the littoral drift moving inshore of the seaward end of the weir by a floating plant, thus not permitting any of that part of the littoral drift to shoal the navigation channel. A successful bypassing operation at Hillsboro Inlet, Florida (Hodges, 1955), where a basin behind a natural rock ledge is dredged periodically, formed the basis of this design.

Over the past 15 years the weir jetty bypassing concept has been shown to be an effective means of bypassing a part of the littoral drift. Although the performance of the first weir jetty systems, like any new concept, was not always as expected, recent advancements in their design criteria and in the understanding of their functional behavior have transformed the weir jetty concept into one of the most feasible methods of bypassing littoral drift. The methodology for weir jetty design is discussed by Weggel (1981).

## 2. Methods.

Several techniques have been employed for mechanically bypassing sand at inlets, with a combination of techniques proven to be the most practicable and economical. The basic methods of operation include (a) land-based dredging plants, (b) floating dredges, and (c) land-based vehicles.

### a. Land-Based Dredging Plants.

(1) Plant Considerations. During this operation, a dredging plant is fixed in position near the beach from which the sand transported alongshore is to be intercepted as it moves within reach of the plant. Currently, these plants are of the pump type and operate basically as an ordinary suction dredge. Most plants are positioned on an existing structure; however, some are on an independent foundation. A few movable plants located on piers or jetties with the capability of dredging along the length and on both sides have been built in the United States and abroad. Such plants have a much

larger littoral reservoir or deposition basin to accumulate the littoral drift during storm periods when the rate of transport exceeds the pumping capacity of the plant.

An installation using an eductor with pumps located in a weir jetty impoundment basin has been in use since 1975 at Rudee Inlet, Virginia (Ch. 6, Sec. V,1,c). This method, known as jet pump sand bypassing, dredges a large deposition area by repositioning the pumps within that area. Richardson and McNair (1981) describe the jet pump system and outline the necessary planning and hydraulic design for such an installation.

A critical study of shore processes at a littoral barrier must be made and the variations in longshore transport moving to the barrier must be estimated to design and position a fixed bypassing plant. The average annual impoundment of littoral materials by the littoral barrier is generally equal to the minimum quantity that must be supplied to the downdrift shores to achieve stability. Short-term fluctuations of the actual rate of littoral material movement to the barrier on an hourly, daily, or weekly basis may be many times greater or less than the estimated annual rate reduced arithmetically to an hourly, daily, or weekly basis. Therefore, even though a bypassing plan may be designed to handle the total amount of drift reaching a barrier on an annual basis, there will probably be occasions during the year when either the quantity of sand reaching the barrier will exceed the pumping capacity of the plant or the plant will operate below capacity due to insufficient material reaching the barrier.

To establish design criteria, a detailed study must be made of the beach profile updrift of the littoral barrier to determine the best location for the plant. Comparing foreshore profiles over a period of time will not only aid in predicting the future position of the foreshore, but will also allow a determination of the best position of the plant. Location of the plant too far landward may result in a *landlocked* plant when the rate of transport reaching the barrier in a short interval of time exceeds the plant's pumping capacity. Such a location may also result in large losses of material around the barrier. A location too far seaward may result in an ineffective operation until sufficient materials have been impounded by the barrier and are within reach of the intake mechanism. The disadvantage of the fixed position plant has led to consideration of a movable dredging unit on a trestle with the capability of dredging a long deposition reservoir on both sides. This would increase the capacity of the littoral reservoir and reduce the possibility of landlocking the plant. Mobility of a land-based dredging plant may overcome some deficiencies of a fixed plant; however, it seems unlikely that such a plant would be capable of bypassing all material when the rate of arrival at the site is high. Therefore, some material would be lost around the barrier.

(2) Discharge Line Considerations. The best alinement of the discharge line from the fixed plant to the downdrift side of the littoral barrier or inlet is controlled by local conditions. The discharge line must traverse a channel maintained for vessel traffic; a floating discharge line is impracticable. If the line is positioned on the channel bottom, an allowance must be made for the protection of the line against damage by pitching ships and by maintenance dredging of the channel. Also, a submerged line may require a

special flushing system to keep the line from clogging when the pumps are shut down.

The point of discharge on the downdrift side of the littoral barrier may be of critical importance. Although the point is not critical in an area with unidirectional longshore transport, in areas with transport reversal periods, some of the material at the point of discharge is transported back toward the littoral barrier or into the inlet. This reverse transport should be kept to a minimum to reduce channel maintenance and, where transport reversals occur, a detailed study must be made of the distribution of littoral forces downdrift of the barrier. Tidal currents toward the inlet may frequently predominate over other forces and produce a strong movement of material toward the downdrift jetty or into the inlet, particularly if no downdrift jetty is included in the plan. In this case, the best discharge point will be a point on the shore just beyond the influence of the downdrift jetty and the littoral forces that tend to move material in an updrift direction. The establishment of the point requires the use of statistical wave data, wave refraction and diffraction diagrams, and data on nearshore tidal currents. Such currents may sometimes dominate the littoral processes immediately downdrift of the littoral barrier. Alternative points of discharge nearer the barrier may also be considered, using groins to impede updrift movement of material at the discharge point. Such alternative considerations are of value in determining the most economical discharge point.

b. Floating Dredges. The operation of floating dredges may be classified in two general categories: hydraulic and mechanical. Hydraulic dredges include the suction pipeline dredge, with a plain suction or with a cutterhead for digging in hard material, and the self-propelled hopper dredge. Mechanical types include the dipper and bucket dredges.

The pipeline dredges employ a discharge pipeline to transport dredged material to the point of discharge or area of placement; booster pumps may be used in this line if required. The standard hopper dredge, whose bins are filled hydraulically, usually discharges by dumping the dredged material out of the bottom of the bins. This type of dredge requires disposal areas with enough depth to allow dumping. The hopper dredge is not suitable for bypassing operations unless it discharges in an area where the material may be rehandled by another type of dredge or it is equipped to pump the material ashore. Since about 1960, a number of hopper dredges have been equipped to pump the material from their bins, greatly increasing their importance in bypassing operations.

Mechanical dredges require auxiliary equipment (such as dump scows, conveyors, and eductors) to transport material to the area of placement. Equipment and techniques for transporting sand are continually being improved; therefore, incorporating a mechanical-type dredge to bypass material may be most favorable in some cases. In considering a floating dredge for a bypassing operation, each type of dredge plant must be evaluated. The evaluation should include: first, the feasibility of using various types of floating dredges; second, the details of the operation; and finally, the economics to determine which floating plant will transfer the material at the least unit cost. Since local site conditions vary, factors to be considered for each type of floating plant cannot be standardized. Some of the more important factors to evaluate are discussed below.

(1) Exposure of Plant to Wave Action. Wave action limits the effective operation of a floating dredge; the exact limitation depends on the plant type and size, and the intensity of wave action. This factor is particularly critical if the dredge will be exposed to open waters where high waves may be expected. No standard criteria are available for the maximum permissible wave action for operation of various types of dredges. Such data must be obtained from dredge operators who are familiar with the dredge plant and the area in question. However, as mentioned in Chapter 6, Section III (PROTECTIVE BEACHES), a specially designed pipeline dredge has been used successfully in an exposed location at Malaga Cove (Redondo Beach), California, for pumping sand from offshore to the beach. Hopper dredges may be operated in higher waves than the other types of floating dredge plants but cannot be safely operated in very shallow water. Pipeline dredges can operate in shallower water, but when exposed to hazardous wave action are subject to damage of the ladder carrying the suction line, breakage of spuds, and damage of the pontoon-supported discharge pipe. Thus, estimates must be made of the probable operational time with and without manmade structures or natural ground features to protect the dredge and auxiliary equipment. Determining the time of year when least wave action will prevail will provide a basis for estimating plant operation under the most favorable conditions. Also, the protection of the plant during severe storms in the area of the project must be considered.

(2) Plant Capacity. The use of a floating dredge with a specific capacity is generally controlled by economic consideration. If the impounding zone of a littoral barrier is large, a periodic bypassing operation may be considered in which a large plant is scheduled and utilized for short periods of time. An alternative would be the use of a small-capacity plant for longer periods of time. If long pumping distances to the discharge point necessitate too many booster pumps, a larger plant may provide the most economical operation. The choice sometimes depends on availability of plant equipment.

(3) Discharge Line. The discharge line considerations are the same as those given for land-based dredging plants.

c. Land-Based Vehicles. Local site conditions may favor the use of wheeled vehicles for bypassing operations. Typical factors to be considered and evaluated would be the existence or provision of adequate roadways and bridges, accessibility to the impounding zone by land-based equipment, the volume of material to be bypassed, and the time required to transport the material. Factors involved in locating deposition areas are also the same as discussed under land-based dredging plants.

### 3. Legal Aspects.

The legal consequences stemming from any considered plan of improvement are many and complex. Legal problems will vary, depending on the physical solution employed as well as the jurisdiction in which construction is to occur. The complexities of the legal problems are due not so much to the fact that legal precedent will differ from jurisdiction to jurisdiction, but rather from the application of any given factual setting to a particular body of law. It should also be noted that insofar as the Federal Government is concerned, liability for personal or property damage will be determined by reference to the Federal Tort Claims Act.

Where there is an accumulation at an inlet, whether due to an existing jetty system or as a result of natural action, and where it is desirable to transfer some of that material to the downdrift beach by whatever method is most feasible, it does not follow that any agency--Federal, State, or local--has the right to make the transfer. The accreted land is not necessarily in the public domain. For example, in at least one case in the State of New Jersey [Borough of Wildwood Crest v. Masciarella 92 NJ Super. 53,222 A 2nd. 138 (1966)], it was decided that an accumulation, which was clearly due to an existing inlet jetty system, was owned by the holder of the title to the adjacent upland. The court stated that "gradual and imperceptible accretions belong to the upland owners though they may have been induced by artificial structures."

The phrase "gradual and imperceptible accretions" is open to legal determination since it would be unusual for a person to stand on a beach and clearly see accretion taking place. Accretion might be detected by surveys at intervals of a month or more. Thus, any agency contemplating bypassing must consult the local legal precedent.

At an inlet employing a weir jetty and a deposition basin, updrift accretion may be uncertain. If the weir interferes with littoral transport and causes the beach initially to fill to the elevation of the top of the weir, it is conceivable that there will be a gradual advance of beach elevations well above the elevation of the weir. This will cause the movement of material over the weir to decrease, and there will be accretion for some distance updrift of the jetty with consequent legal questions concerning ownership. Since an impairment of the movement over the weir reduces the effectiveness of bypassing, steps should be taken to restore the efficiency of the weir. Such action will inevitably result in a loss of updrift accretions, and again legal considerations may arise.

If the deposition basin in the lee of an offshore breakwater is not cleared of accumulations regularly, it is possible that continuing accretion may ultimately produce land from the former shoreline out to the breakwater. The resumption of bypassing operations may then require ownership determination.

Legal considerations may even arise on the downdrift beach receiving bypassed sand, despite the obvious advantages to most property owners. Another case reported involved a pier used for fishing, located on a beach that had been artificially nourished. Before the beach nourishment was commenced, an adequate water depth for fishing existed; after the nourishment was commenced, depths along the pier decreased to such an extent that fishing was greatly impaired. The owner then brought suit seeking payment for the loss of value to his pier.

It is not the purpose here to set forth a comprehensive discussion of the legal problems encountered in connection with sand bypassing. The above discussion is merely to alert the planner that such problems do arise, and it is therefore prudent to seek legal counsel at the earliest stages of project formulation.

## VI. GROINS

### 1. Definition.

A *groin* is a shore protection structure designed to trap longshore drift for building a protective beach, retarding erosion of an existing beach, or preventing longshore drift from reaching some downdrift point, such as a harbor or inlet. Groins are narrow structures of varying lengths and heights and are usually constructed perpendicular to the shoreline.

### 2. Groin Operation.

The interaction between the coastal processes and a groin or groin system is complicated and poorly understood. However, there are a few basic principles which can be applied to the design of groins. These principles are discussed below and summarized in the form of several concise rules of groin design.

*RULE 1: Groins can only be used to interrupt longshore transport.*

Groins do not interrupt onshore-offshore transport. They do not attract to an area any sand which would not otherwise have passed.

*RULE 2: The beach adjustment near groins will depend on the magnitude and direction of the longshore transport.*

The longshore drift builds up on the updrift side of a groin, thereby creating a fillet. The downdrift side is deprived of this sediment and usually erodes. Figure 5-9 illustrates the single groin process and Figure 5-10 the groin system process. Note the direction of the net longshore transport. This direction depends on the predominant angle of wave approach. If the wave approach is normal to the shoreline, or if the shoreline adjusts itself normal to the wave approach through the process of fillet formation, then the longshore transport rate will be zero. Thus, a second way that groins will reduce the longshore transport rate is by allowing the shoreline to approach an orientation normal to the wave approach. The wave climate controls the longshore transport rate and is therefore an important aspect of coastal groin design.

*RULE 3: The groin-induced accumulation of longshore drift on the foreshore will modify the beach profile, which will then try to reestablish its natural shape.*

The shore-normal profile of a beach, from the highest limit of wave uprush to the seaward limit of sediment movement, is the transient result of sand particle movement as dictated by waves, currents, sand size, and beach slope (through the action of gravity). When one of these controlling factors is changed, the profile will also change through sand movement. The accumulation of sand in the foreshore zone by groins changes the beach profile at its shoreward end. The reaction to this change will be erosion of the foreshore, accretion of the nearshore, or both, in the profile's attempt to reestablish its balance. These effects may cause differential settlement of graded beach material along the beach profile. This reestablishment can be accomplished in a number of ways. For example, the natural onshore movement of sand by swell

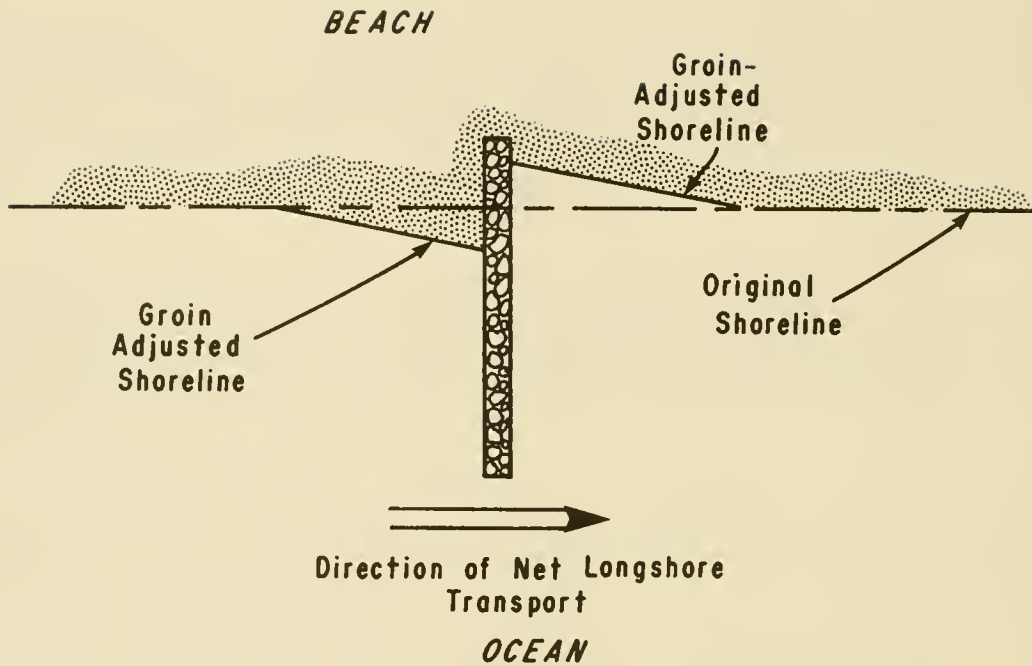


Figure 5-9. General shoreline configuration for a single groin.

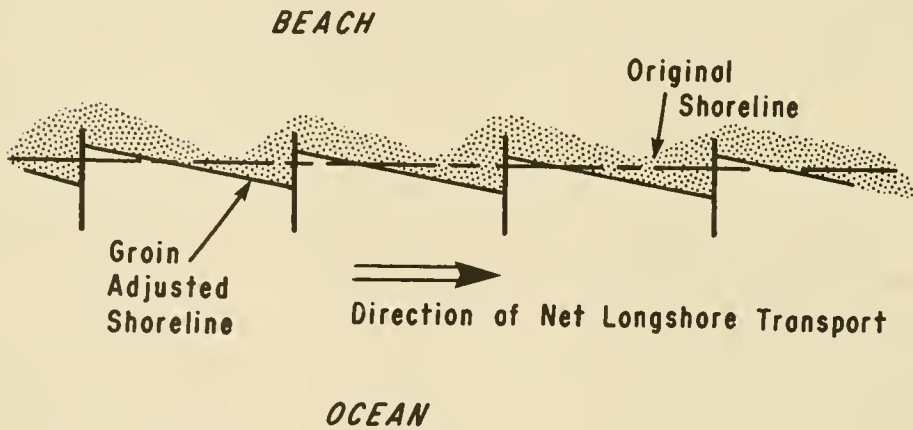


Figure 5-10. General shoreline configuration for two or more groins.

waves can decrease when the bottom velocities are insufficient to transport the sand particles up the steeper slope produced by the foreshore accumulation.

*RULE 4: Water pushed by waves into a groin compartment will sometimes return offshore in the form of rip currents along the sides of groins.*

In this way, groins may actually increase the amount of sediment which moves offshore as well as the distance seaward that it travels. Dean (1978) explains three mechanisms for creating rip currents between groins. The first is the simple channeling of the longshore current which can push up against the groin and then jet seaward (see Fig. 5-11a).

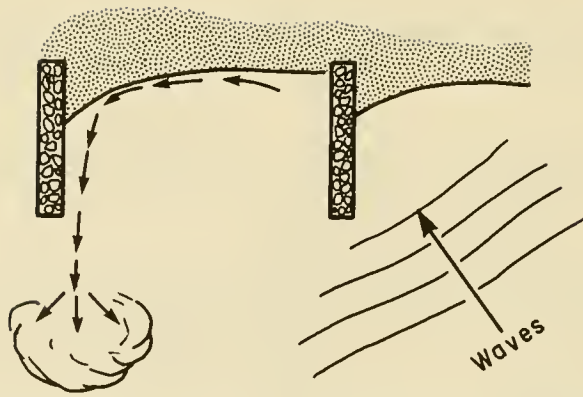
The second mechanism is the differential wave setup at the shoreline created when waves approach at an angle to the beach (see Fig. 5-11b). The wave-sheltering effect of the updrift groin produces a smaller setup at the updrift side of the groin compartment. This causes a circulation cell to be established in which water flows (a) toward the updrift groin along the shoreline, (b) seaward along the updrift groin, (c) downdrift along a line seaward of the groins, and (d) back to the beach along the downdrift groin.

The third mechanism is the differential wave setup at the shoreline created when the waves approach normal to the beach (see Fig. 5-11c). The setup is smaller adjacent to each groin due to the energy dissipation caused by the interaction of water motion with the groin structures. This produces two circulation cells within each groin compartment in which water flows (a) along the shoreline from the center of the groin compartment toward each groin, (b) seaward along each groin, (c) toward the center of the groin compartment along a line seaward of the groins, and (d) back to the beach in the center of the groin compartment. The circulation cells pick up sand at the beach and deposit it in the deeper water seaward of the groin. The effect is a sand loss at the beach even though the water recirculates.

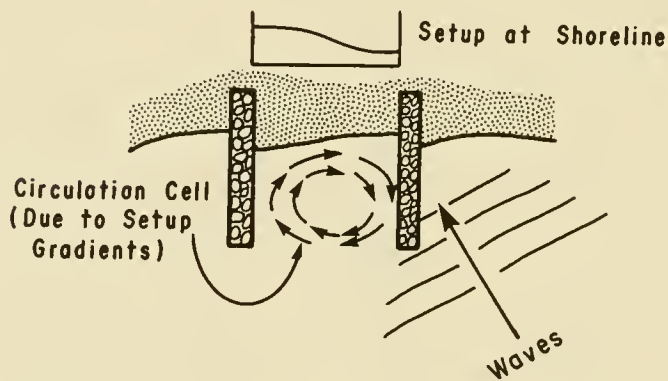
The appearance of rip currents, with their detrimental effects on the beach, is difficult to predict. They are another uncertainty in groin design. Dean (1978) suggests that the rip current problem can be compounded if the groin spacing is the same as the rip current spacing under natural conditions of the study area. This further emphasizes the importance of understanding the physical environment of the study area.

*RULE 5: The percentage of the longshore transport which bypasses a groin will depend on groin dimensions, fillet dimensions, water level, and wave climate.*

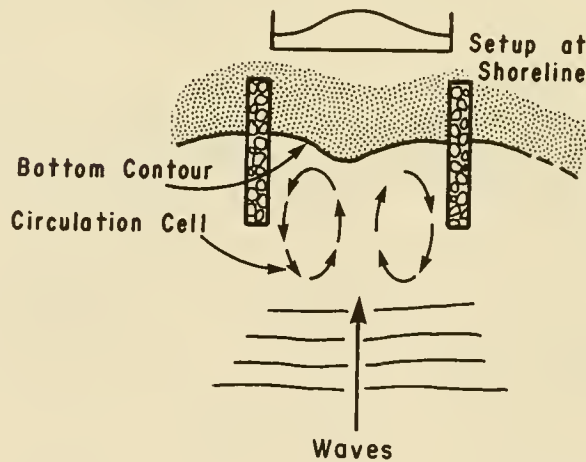
Sand can bypass a groin by traveling over its top (overpassing) or around its seaward end (endpassing). Overpassing will depend on the level of the sand immediately adjacent to the groin. If the sand level is too low, the longshore drift will not be carried over the groin; it will accumulate next to the groin. As the sand accumulates and the fillet is formed, the level may eventually rise enough to allow overpassing. However, the extent to which a fillet can grow vertically is controlled by the wave and tide climate, not the height of the groin.



a. Rip current formation due to channeling of longshore current.



b. Circulation within a groin compartment due to variation in longshore setup.



c. Circulation cell within a groin compartment due to energy dissipation at the groins and variable setup.

Figure 5-11. Three mechanisms for creating rip currents between groins (from Dean, 1978).

Endpassing considerations are similar to the overpassing process except that the controlling factor is the seaward growth of the fillet. The updrift beach will build seaward until the breaker zone has shifted seaward enough to allow the longshore drift to pass around the end of the groin.

Tide and storm effects continuously change the water level at a groin, which in turn changes the apparent groin height and length. The result is variable bypassing. For example, as water level rises, overpassing can increase; as water level falls, the breaker line moves seaward and endpassing can increase.

The combination of all the factors discussed makes prediction of the percentage of longshore transport bypassing difficult. Only gross percentage estimates are possible based on engineering experience and judgment. As an example, the estimates of the percentage of longshore transport stopped by a groin on the Atlantic coast, where a normal breaker depth of 1.8 meters (6 feet) is assumed, are as follows:

- (1) For high groins extending to a 3-meter or more water depth, use 100 percent of the total longshore transport.
- (2) For high groins extending to a 1.2- to 3-meter (4- to 10-foot) depth below MLW (or mean lower low water, MLLW), or for low groins extending to a depth more than 3 meters, use 75 percent of the total longshore transport.
- (3) For high groins extending from MLW to 1.2 meters below MLW (or MLLW), or for low groins extending to a depth less than 3 meters below MLW, use 50 percent of the total annual rate of longshore transport.

Similar percentages can be estimated proportionally by assuming that the normal breaker zone for the gulf coast and less exposed shores of the Great Lakes ranges from 0.9- to 1.2-meter (3- to 4-foot) depths; more exposed shores of the Great Lakes approach the 1.8-meter depth. The Pacific coast ranges from 2.1- to 3-meter (7- to 10-foot) depths depending on exposure.

*Rule 6: The longshore drift that is collected in the updrift fillet is prevented from reaching the downdrift area, where the sand balance is upset.*

This simple rule has surfaced many times with the addition of groins downdrift of a groin system as a followup to a progressive erosion problem. This problem can be reduced by using beach nourishment concurrent with the groin construction, which more rapidly reestablishes the natural longshore transport past the groins. (Due to the reorientation of the shoreline, the initial longshore transport rate is seldom fully reestablished.)

### 3. Functional Design.

a. Groin Height. For functional design purposes, a groin may be considered in three sections (see Fig. 5-12): horizontal shore section (HSS), intermediate sloped section (ISS), and outer section (OS).

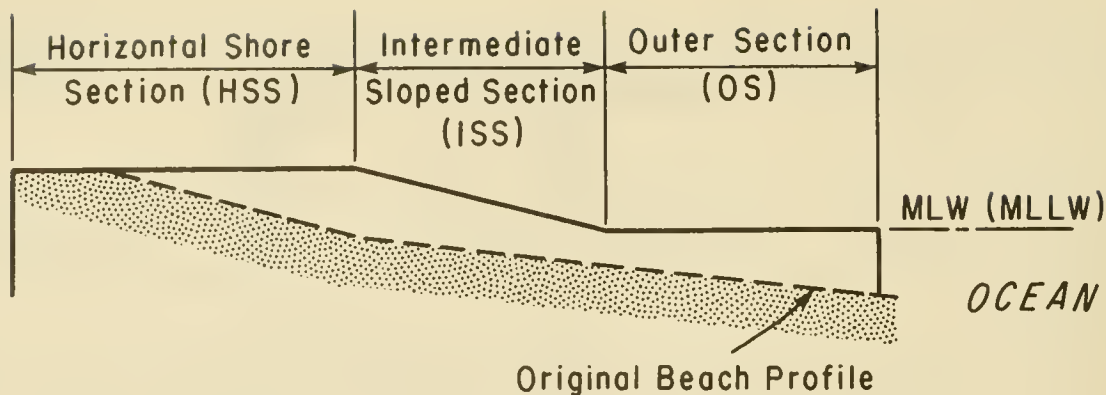


Figure 5-12. Sections of a typical groin.

(1) Horizontal Shore Section. This section extends far enough landward to anchor the groin and prevent flanking. The height of the HSS depends on the degree desirable for sand to overtop the groin and nourish the down-drift beach. The standard height is the height of the natural berm, which is usually the height of maximum high water, plus the height of normal wave uprush. An economic justification for building a groin higher than this is doubtful except for terminal groins. With rubble-mound groins, a height about 0.3 meter (1 foot) above the berm is sometimes used to reduce the passage of sand between large cap stones. The maximum height of a groin to retain all sand reaching the area (a high groin) is the height of maximum high water and maximum wave uprush during all but the most severe storms. Conversely, this section, or a part of it, can be built lower than the berm to permit overpassing of sediment during periods of high tide. A low groin of this type can be termed a *weir groin* based on its operational similarity to weir jetties. Design aspects of weir systems are discussed in Weggel (1981). The HSS is built seaward to the desired location of the design beach berm crest.

(2) Intermediate Sloped Section. The ISS extends between the HSS and the OS. It should approximately parallel the slope of the natural foreshore. The elevation at the lower end of the slope will usually be determined by the construction methods used, the degree to which it is desirable to obstruct the movement of the littoral material, or the requirements of swimmers or boaters.

(3) Outer Section. The OS includes all the groin that extends seaward of the intermediate sloped section. With most types of groins, this section is horizontal at as low an elevation as is consistent with the economy of construction and public safety.

b. Design of Beach Alinement. The first step in the design of a groin or groin system is the determination of the eventual beach alinement. The beach alinement is the orientation the shoreline will take near the groins. In this case the shoreline refers to the berm crest. The best estimation of this orientation is determined by observing fillets at nearby structures with similar coastal processes. If this information is not available, determine the nearshore direction of the predominant wave approach and then assume a beach alinement perpendicular to that direction. As shown in Figure 5-13 three aspects, which will be discussed separately, need to be considered: the

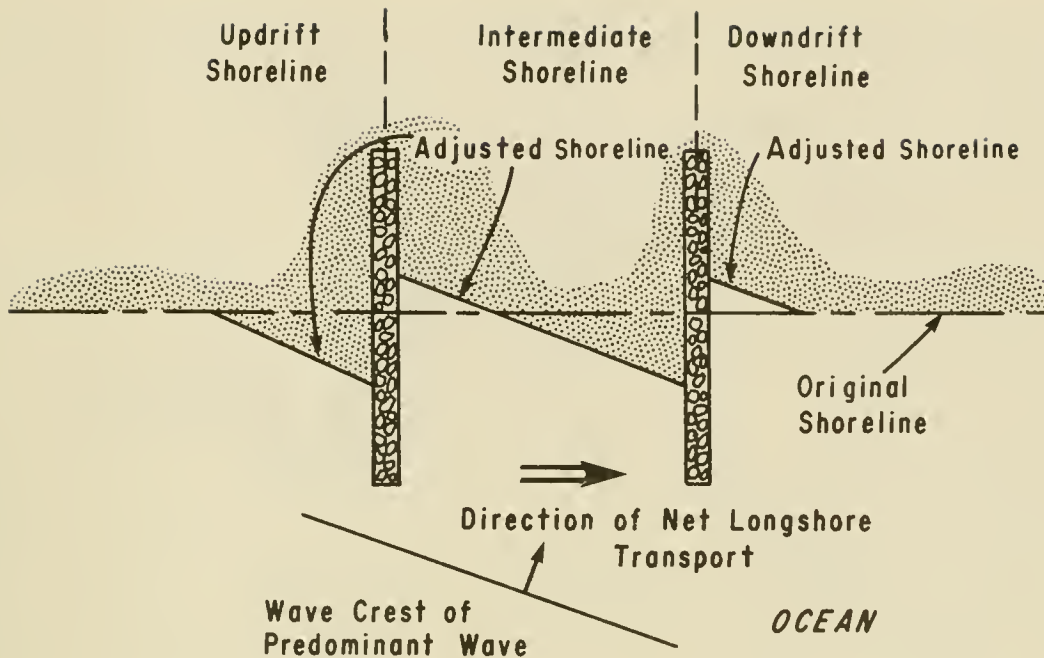


Figure 5-13. Three cases of a groin-adjusted shoreline.

updrift shoreline, the downdrift shoreline, and the intermediate shoreline or the shoreline between two groins. The principles regarding the updrift shoreline can apply to the shoreline updrift of a single groin or the updrift groin of a groin system. Similarly, the downdrift shore alignment can apply to the area downdrift of a single groin or a groin system. The concept of an updrift and downdrift direction assumes there is a predominant direction of longshore transport. The case where there is significant reversal in direction of longshore transport will also be discussed.

(1) Updrift Shore Alinement. An estimation of the shore alinement on the updrift side of a groin is illustrated in Figure 5-14. The seaward end of the adjusted shoreline is set at the seaward end of the HSS, point u in the figure. The adjusted shoreline then extends upcoast to meet the original shoreline which thus forms the updrift fillet.

(2) Intermediate Shore Alinement. The intermediate shore alinement can be estimated by establishing the shoreline (berm crest line) at the seaward end of the HSS of the downdrift groin of the groin compartment (Fig. 5-15, point u). The shore alinement then extends parallel to the predominant wave crest alinement to point t on the updrift groin. This adjusted alinement generally requires additional sand because the adjusted shoreline at the downdrift side of the updrift groin will recede and could flank the inshore end of the groin. The source of the additional sand can be from either the natural longshore transport or artificial fill. The shoreline will begin alining itself to the wave climate as soon as the groin construction is begun. Therefore, where additional sand is needed to stabilize the shoreline, the initial shoreline will be the realinement of the original shoreline; i.e., area A in Figure 5-15 will equal area B. A and B are

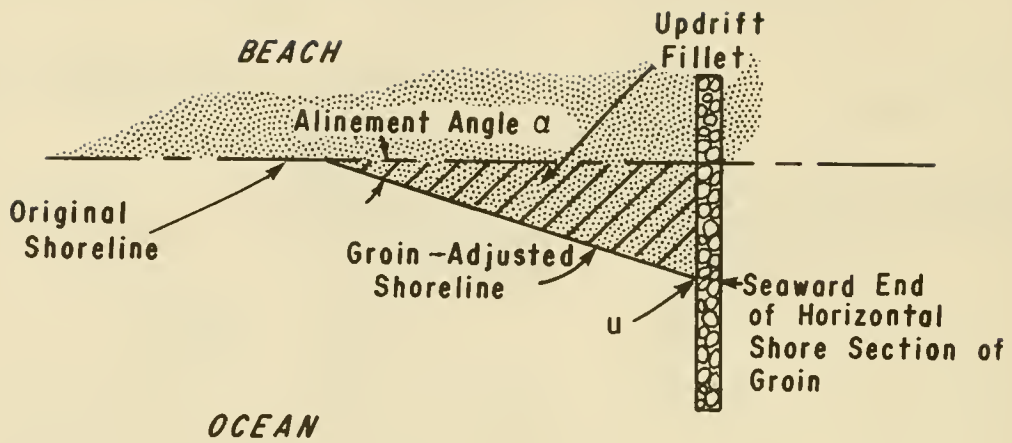


Figure 5-14. Alinement of updrift beach.

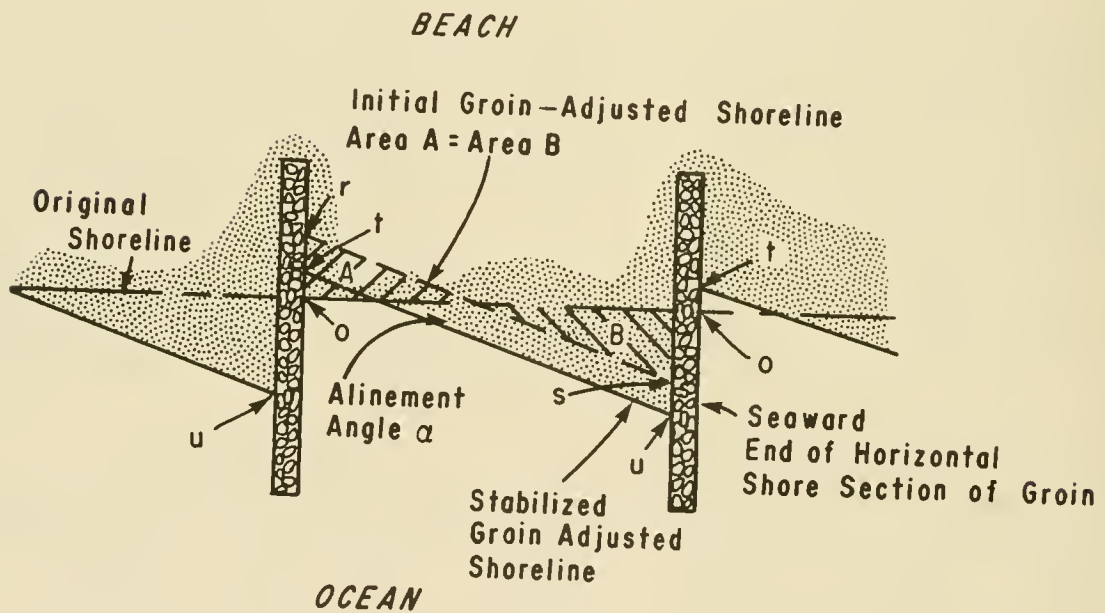


Figure 5-15. Intermediate beach alinement.

the areas between the initial postgroin shoreline and the original shoreline position. As sand is added to the compartment, the shoreline will build out to the stabilized groin-adjusted shoreline. The estimation of the initial groin-adjusted shoreline is important since it represents a maximum erosion condition and is, therefore, essential in the design of the shoreward limit of the groin.

(3) Downdrift Shore Alinement. The major factor in an adjustment of the downdrift beach is the reduction in the longshore transport while the updrift side of the groin and the updrift groin compartments of a groin system are naturally filling. The time period for a natural filling to take place can be estimated by assuming that the percentage of longshore drift not reaching the downdrift area is being trapped updrift. This sand will fill the updrift groin and groin compartments until the adjusted updrift beach alignment (Fig. 5-14) and the adjusted intermediate beach alignment (Fig. 5-15) are attained. The sediment trapped in these updrift fillets is prevented from reaching the downdrift area, which results in downdrift erosion. If artificial fill is used to form the updrift fillets, the longshore transport will bypass the groin and reach the downdrift area sooner than if the natural longshore drift were depended on to form the fillets. Therefore, artificial filling is usually preferred. The following steps can be used to determine the position of the downdrift shoreline:

(a) Estimate the time required for the updrift side of the groin to fill (see Sec.VI,3,g of this chapter).

(b) Draw an adjusted shoreline, r-s, which represents the berm crest line shown in Figure 5-16 such that the area r-s-o accounts for the deficit volume of longshore drift determined from the time period for the updrift groin or groins to fill. Use the natural beach profile of the study area to find the volume corresponding to the area r-s-o (see Sec.VI, 3,g of this chapter).

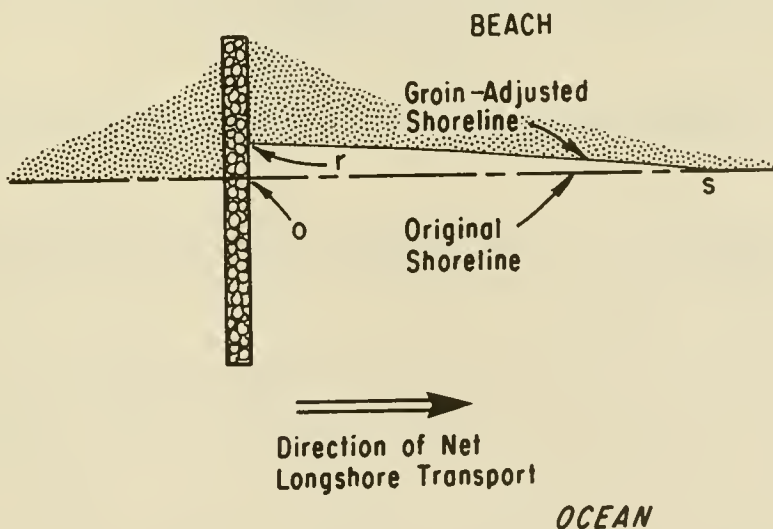


Figure 5-16. Downdrift beach alinement.

(4) Beach Alinement for Reversing Direction of Longshore Transport.

Where there is a periodic reversal in the direction of longshore transport, an area of accretion may form on both sides of a groin, as shown in Figure 5-17. The fillet between groins may actually oscillate from one end of the compartment to the other, as shown by the dashlines, or may form a U-shaped shoreline similar to the maximum recession alinement, depending on the rate of supply of littoral material. With regular reversals in the direction of longshore transport, the maximum line of recession would probably be somewhat as shown by the solid line, with areas A and C about equal to area B. The extent of probable beach recession must be considered in establishing the length of the horizontal shore section of groin and in estimating the minimum width of beach that may be built by the groin system.

(5) Mathematical Models. Mathematical models are being developed which will replace the above procedures. The models will allow the many different spacing and length combinations to be quickly and inexpensively tested to determine the optimum design. The Engineering Computer Program Library Catalog, published by the U.S. Army Engineer Waterways Experiment Station, should be consulted for an abstract of approved computer programs. The use of other engineering computer programs is governed by ER 1110-1-10.

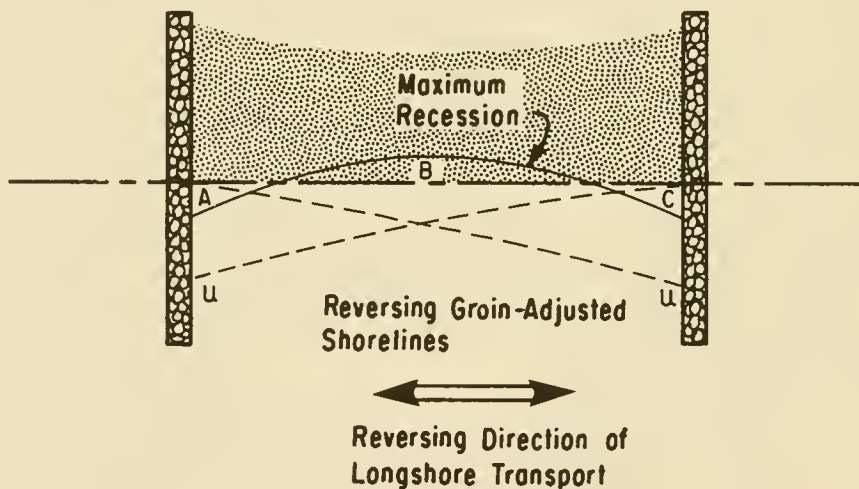


Figure 5-17. Intermediate beach alinement with reversal of longshore transport direction.

c. Groin Dimension. Once the adjusted shoreline is estimated, a determination of the groin dimensions is possible. The discussion which follows is illustrated by Figure 5-18.

(1) Shoreward Limit of Horizontal Shore Section. The primary design objective in establishing the position of the shoreward end of the groin is the prevention of flanking due to beach recession. This is done by conservatively estimating the predicted recession position represented by the r points in Figures 5-15 and 5-16.

(2) Seaward Limit of Horizontal Shore Section. The updrift berm crest is expected to move to the seaward limit of the HSS, shown as the u

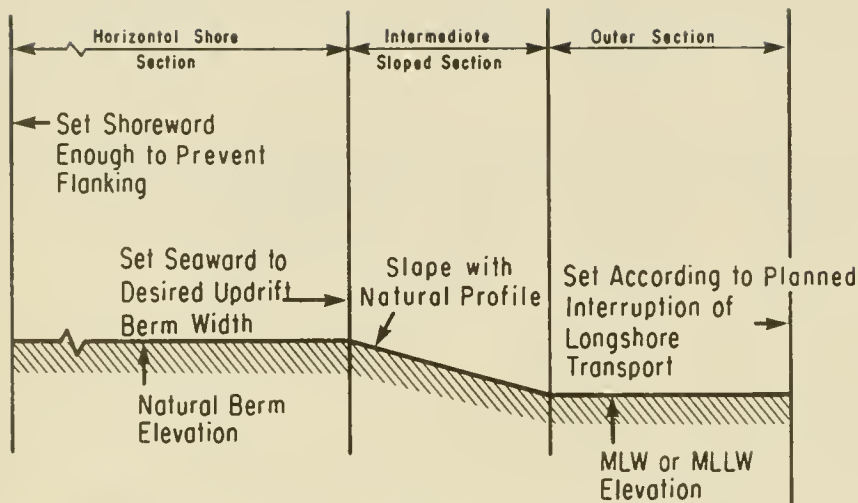


Figure 5-18. Summary of groin design.

points in Figures 5-14, 5-15, and 5-17. Therefore, the position of  $u$  becomes a design parameter which can be moved shoreward or seaward, depending on the desired beach width.

(3) Seaward Limit of Outer Section. The seaward extent of the OS depends on the amount of longshore transport to be intercepted. Some guidelines on how to estimate this are discussed in Section VI,2 of this chapter.

d. Spacing of Groins. In the design of a groin system, the estimation of the intermediate beach alignment discussed in Section VI,3,b,(2) of this chapter and shown in Figure 5-15 will usually determine the desired alongshore spacing between groins. In the future, mathematical models will be used to determine the groin spacing. However, if in the designer's opinion these spacing values are unreasonable or indeterminable, the following general rule is suggested:

*The spacing between groins should equal two to three times the groin length from the berm crest to the seaward end.*

e. Groin System Transition. To avoid an abrupt change in the shore alignment that may result in erosion of the downdrift beach, the use of transitional groins (groins of gradually reduced lengths) is recommended. A method for the design of a groin system transition that involves groin shortening has been used by the U.S. Army Engineer District, Wilmington (1973) (see Fig. 5-19). Kressner (1928) conducted model studies on groin transitions, and more recently Bruun (1952) applied the principle of groin shortening at the end of groin systems. Where there are reversals in the direction of longshore littoral transport, transitions would be appropriate for both ends of the system. Bruun (1952) indicated that in a long series of groins, the shortening should possibly be carried out on both the updrift side and the downdrift side to ensure a smooth passage of littoral drift to the unprotected coast. He further indicated that if the series consisted only of a few groins, the shortening should start with the second groin from the updrift

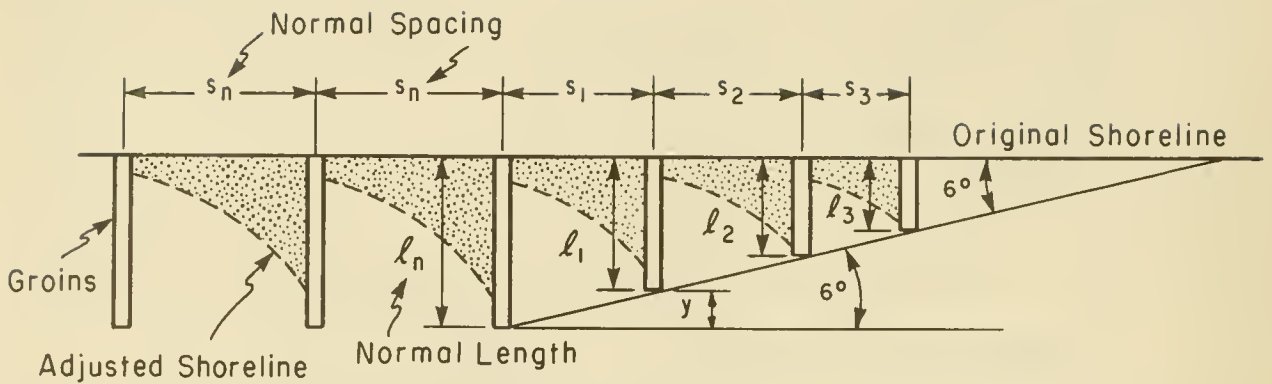


Figure 5-19. Schematic of groin-shortening procedure.

end. This would result in the entire groin system becoming a transitional section.

Kressner (1928) found in model tests that only three or four groins need to be shortened at the downdrift end of the system (see Fig. 5-19). He also found that the transition is most effective if a line connecting the seaward ends of the shortened groins and the last full-length groin meets the natural shore alignment at an angle of about  $6^\circ$ , as shown in Figure 5-19. Bruun (1952) indicates that a  $6^\circ$  angle has been successfully used. *The length of a groin,  $l$ , is measured from the crest of the beach berm to the seaward end.* (The actual groin length extends shoreward of the berm.) The limit of the shortening is a judgment decision of the designer; however, in the case of coastal tidal areas, it is suggested that the last transitional groin extend no farther than the MLLW line. With  $y$  being the shortening,  $l_n$  the normal groin length,  $l_1$  the length of the first shortened groin,  $l_2$  the length of the second shortened groin,  $l_3$  the length of the third shortened groin, etc., and  $s$  the spacing between groins, then

$$y = s_1 \tan 6^\circ \quad (5-5)$$

and

$$l_1 = l_n - y \quad (5-6)$$

or

$$l_1 = l_n - s_1 \tan 6^\circ$$

then

$$l_2 = l_1 - s_2 \tan 6^\circ \quad (5-7)$$

and

$$l_3 = l_2 - s_3 \tan 6^\circ \quad (5-8)$$

The groin spacing within the zone of shortening should decrease to maintain the design ratio between spacing and length. Since the lengths of the groins in this zone differ, *the space-to-length ratio,  $R_{s1}$ , is based on the average length of adjacent groins.* By maintaining this ratio, the spacings shown in the figure are

$$s_1 = \left( \frac{\ell_n + \ell_1}{2} \right) R_{s1} \quad (5-9)$$

$$s_2 = \left( \frac{\ell_1 + \ell_2}{2} \right) R_{s1} \quad (5-10)$$

and

$$s_3 = \left( \frac{\ell_2 + \ell_3}{2} \right) R_{s1} \quad (5-11)$$

Since the length of transitional groins and their spacings are interdependent, the equations for lengths and spacing are combined as follows:

$$\ell_1 = \left( \frac{1 - \frac{R_{s1}}{2} \tan 6^\circ}{1 + \frac{R_{s1}}{2} \tan 6^\circ} \right) \ell_n \quad (5-12)$$

and

$$s_1 = \left( \frac{\frac{R_{s1}}{2}}{1 + \frac{R_{s1}}{2} \tan 6^\circ} \right) \ell_n \quad (5-13)$$

\*\*\*\*\* EXAMPLE PROBLEM 3 \*\*\*\*\*

The example computation is based on the shortening of the three groins shown in Figure 5-19. If the normal spacing of a groin field,  $s_n$ , is 152 meters (500 feet) and the normal groin length,  $\ell_n$ , is 76 meters (250 feet)

$$R_{s1} = \frac{s_n}{\ell_n} = \frac{152}{76} = 2.0$$

then using equation (5-12)

$$l_1 = \left( \frac{1 - \frac{R_{s1}}{2} \tan 6^\circ}{1 + \frac{R_{s1}}{2} \tan 6^\circ} \right)$$

$$l_n = \left( \frac{1 - \frac{2.0}{2} (0.105)}{1 + \frac{2.0}{2} (0.105)} \right) 76 = 0.81(76) = 61.6 \text{ m (202 ft)}$$

$$l_2 = 0.81 l_1 = 0.81(61.6) = 50 \text{ m (164 ft)}$$

$$l_3 = 0.81 l_2 = 0.81(50) = 40.5 \text{ m (132 ft)}$$

Using equation (5-13)

$$s_1 = \left( \frac{R_{s1}}{1 + \frac{R}{2} \tan 6^\circ} \right) l_n = 1.81(76) = 137.6 \text{ m (451 ft)}$$

$$s_2 = 1.81 l_1 = 1.81(61.6) = 111.5 \text{ m (366 ft)}$$

and

$$s_3 = 1.81 l_2 = 1.81(50) = 90.5 \text{ m (297 ft)}$$

Using equations (5-6) and (5-9) as a check on the above calculations, the following is obtained

$$l_1 = l_n - s_1 \tan 6^\circ = 76 - 137.6 = 61.6 \text{ m}$$

and

$$s_1 = \left( \frac{l_n + l_1}{2} \right) R_{s1} = \left( \frac{76 + 61.6}{2} \right) 2.0 = 137.6 \text{ m}$$

\*\*\*\*\*

f. Beach Profiles Adjacent to Groins. Estimating the adjusted beach alinement and determining the shape of the beach profiles adjacent to the groin will permit the calculation of the differential soil loads on the groin. The updrift side of the groin will have a higher sediment level than the downdrift side. The profile, which is illustrated in Figure 5-20, is drawn by the following steps:

- (1) Draw the groin profile on the original beach profile.
- (2) Draw the MLW or MLLW line.
- (3) Locate the berm crest position relative to the HSS part of the groin. Label this point a. For example, point a can be, but is not limited to, one of the points r, s, t, or u from Figures 5-14 to 5-17.
- (4) Draw a line parallel to  $a_1b_1$  (the natural above low water level beach slope) from the berm position, point a, to the intersection with the MLW or MLLW line, point b.
- (5) Connect the intersection of the slope line and the MLW or MLLW line, point b, with the intersection of the groin end and the natural beach profile, point c.

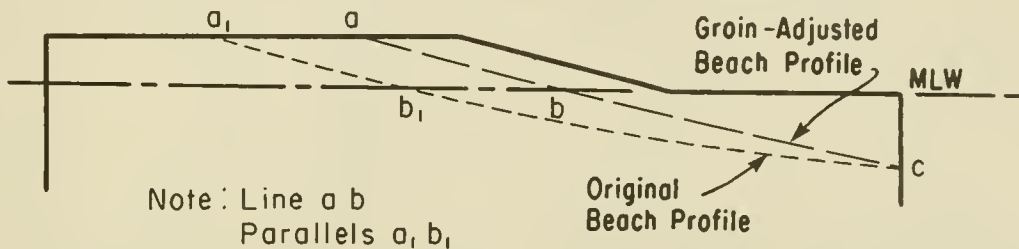


Figure 5-20. Determination of beach profile adjacent to groin.

\*\*\*\*\* EXAMPLE PROBLEM 4 \*\*\*\*\*

**GIVEN:** A groin design as follows: The HSS is to be built to the natural berm elevation of +2.5 meters (+8.2 feet) MLW and will extend from 40 meters (131.2 feet) shoreward to 50 meters (164.0 feet) seaward of the present berm crest. The OS is to be built at MLW elevation and will extend to a depth of 1.5 meters (4.9 feet) below MLW. The beach can be approximated by a 1 on 10 slope from the berm crest to MLW and a 1 on 50 slope from MLW seaward. The beach alinement analysis predicts that the berm crest on the downdrift side of the groin will erode 20 meters (65.6 feet) shoreward of the present position (see Fig. 5-21).

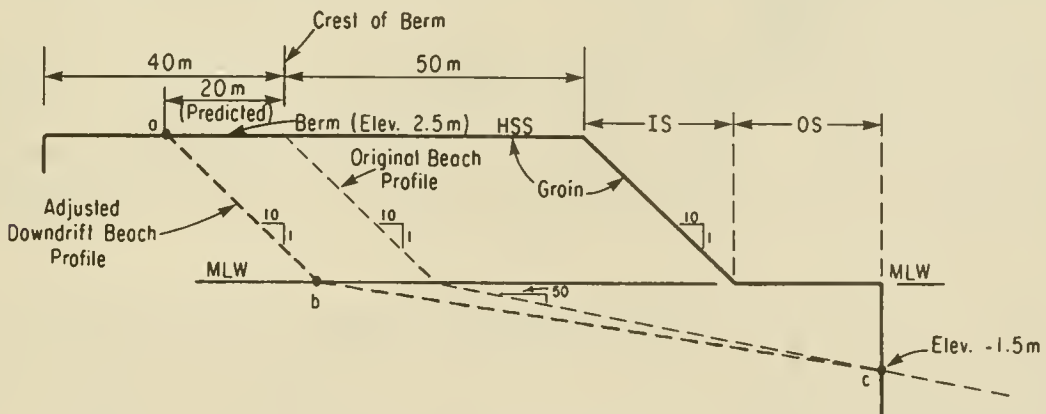


Figure 5-21. Downdrift profile design in example problem.

FIND: The beach profile adjacent to the groin on the downdrift side.

SOLUTION: Referring to Figure 5-21,

- (a) Draw the original beach profile using its approximated slope (1 on 10 and 1 on 50).
- (b) Position the groin on the profile.
- (c) Establish the position of the downdrift berm crest at 20 meters shoreward of the present berm crest location and label this point a.
- (d) Using the assumed natural beach slope of 1 on 10, draw a line from point a to the elevation of MLW, and label this point b.
- (e) The intersection of the end of the groin and the original beach profile is point c. Connect the points b and c.
- f) The line a-b-c is the estimated beach profile.

\* \* \* \* \*

g. Estimating Fillet Volumes. It is frequently necessary to estimate the volume of an updrift fillet, a groin compartment fillet, or a downdrift erosion section in order to provide the basis for determining the amount of beach material lost to the littoral process or the amount required to fill the groin compartment. The calculation of the updrift fillet is demonstrated below; similar procedures can be used to estimate the other two cases.

Figure 5-22a shows the groin profile, the original beach profile, and the groin-adjusted beach profile. Positions a, b, and c are as defined in Figure 5-20. Points d, e, f, and g are intermediate locations along the groin-adjusted profile;  $a_0$  through  $g_0$  in Figure 5-22b represent elevations of the original beach contours;  $a_1$  and  $b_1$  in Figure 5-22a are points where the original beach profile intercepts the groin. Lines  $a_1b_1$ ,  $b_1c$ , and  $bc$  are assumed straight and the original contours are assumed straight and parallel. Above the level of point b, the groin-adjusted beach profile coincides with the groin profile, assuming the groin is built to the natural berm elevation (see Fig. 5-18).

Figure 5-22b shows how the groin-adjusted contours are drawn. Starting at each point along the groin-adjusted profile at the groin, the new contour is drawn at the beach alinement angle,  $\alpha$ , until it intersects the original beach contour with the same elevation. This is the same procedure shown in Figure 5-14, except that more contours are drawn. Note how the intersection points approach the seaward end of the groin. This results from the difference in the slopes of lines  $b_1c$ , and  $bc$ .

Figure 5-22c is an isometric drawing of the fillet which is made up of a triangular prism, R, and a pyramid, Y. C and D are the same end areas that are shown in Figure 5-22a. A and B are identical triangles in parallel horizontal planes--A at the berm elevation and B at MLW. The volume of the prism R is equal to the product of the area A and the vertical distance between triangles A and B, represented by  $h_1$ ; i.e.,

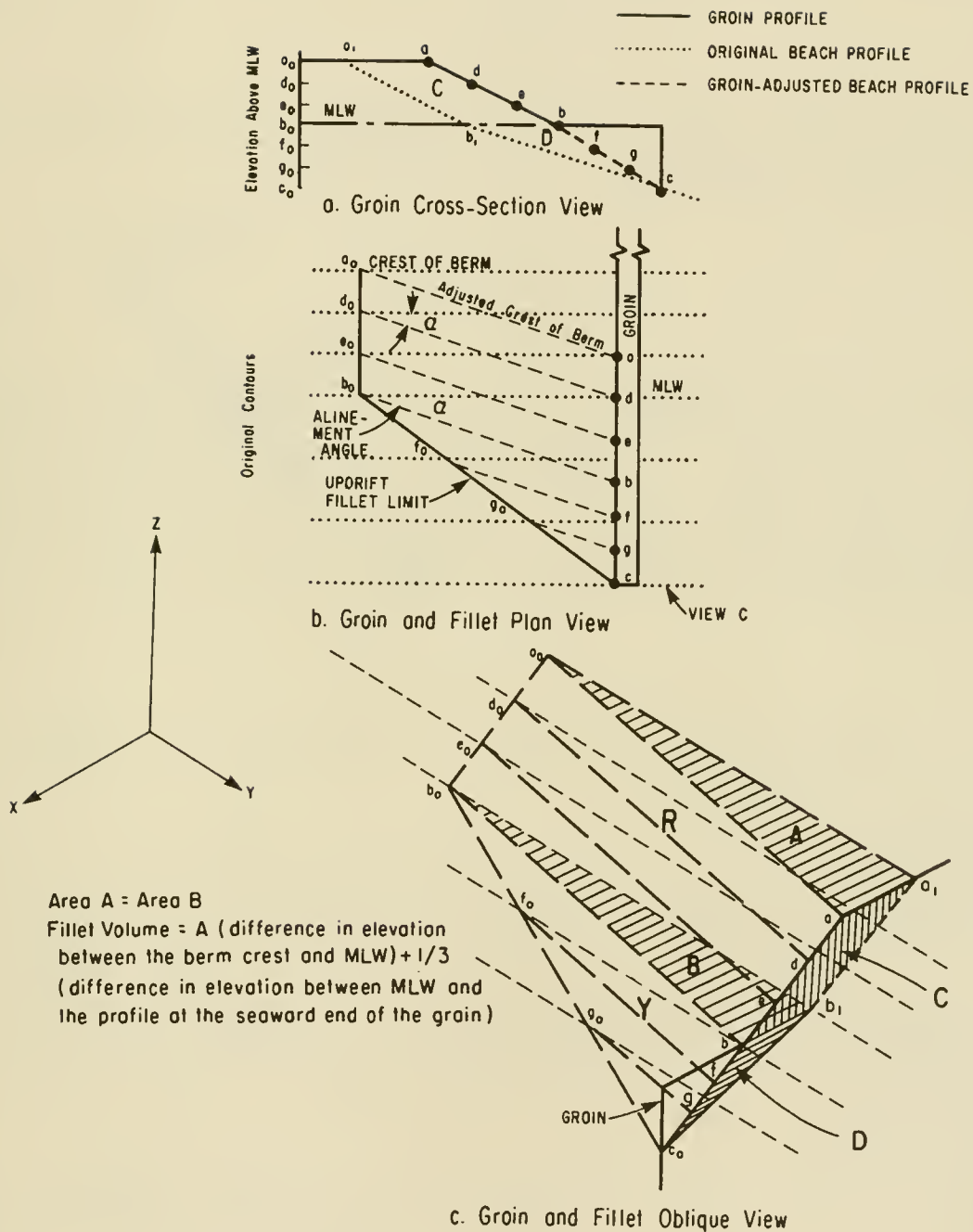


Figure 5-22. Calculation of updrift fillet volume.

$$R = Ah_1 \quad (5-14)$$

The volume of the pyramid Y is one-third of the product of the area B and the vertical distance between B and point c, represented by  $h_2$ .

$$Y = \frac{Bh_2}{3} \quad (5-15)$$

The sum of the volumes R and Y will then give a simplified straight-line approximation of the volume of the updrift fillet. Since  $A = B$ , the total fillet volume can be simplified to

$$R + Y = A \left( h_1 + \frac{h_2}{3} \right) \quad (5-16)$$

Dividing this volume by the part of the longshore transport rate assumed intercepted by the groin provides the time period it takes the fillet to form. Areas A, B, C, and D may be determined by standard geometrical formulas or by use of a planimeter. A similar procedure calculates the volume of sand loss due to downdrift-side erosion, as shown in Figure 5-23. Areas A' and B' are equal and represent horizontal triangles at the berm crest and the MLW elevation, respectively. The erosional volumes R' and Y' are calculated as before and are added to give the total volume lost due to erosion.

$$R' + Y' = A' \left( h'_1 + \frac{h'_2}{3} \right) \quad (5-17)$$

Where  $h'_1$  is the vertical distance from A' to B' and  $h'_2$  the vertical distance from B' to the point c.

#### 4. Filling Groins.

The importance of minimizing downdrift erosion after construction of a groin or groin system cannot be overemphasized. Unless the natural longshore transport is of sufficient magnitude to quickly fill the updrift side of the updrift groin and the groin compartments or unless erosion of the downdrift area is inconsequential, artificial filling will be necessary. Paragraph 8 of this section will further discuss groin filling with respect to the order of groin construction.

#### 5. Permeable Groins.

Permeability allows part of the longshore drift to pass through the groin and induces sand deposition on both sides of the groin. This in turn reduces the abrupt offset in shore alignment found at impermeable groins. Many types of permeable groins have been employed. The degree of permeability above the ground line affects the pattern and the amount of deposition. Insufficient empirical data have been compiled to establish quantitative relationships between littoral forces, permeability, and shore response. Until such data

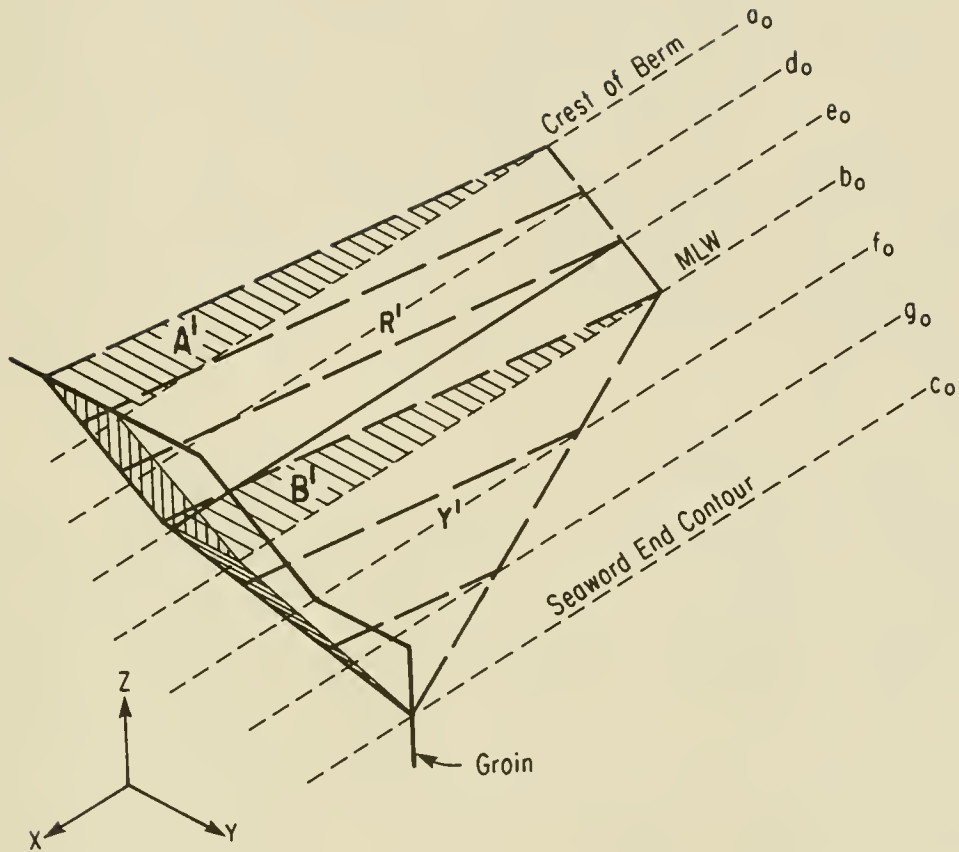


Figure 5-23. Calculation for downdrift erosion fillet volume.

are available, the evaluation and design of permeable groins will be inexact. In general, the desired degree of sand bypassing can be achieved as effectively and economically by the appropriate design of groin height and length.

#### 6. Adjustable Groins.

Most groins are permanent, fixed structures; however, adjustable groins have been used in England and Florida. These groins consist of removable panels between piles. The panels are designed to be added or removed to maintain the groin at a specific height (usually 0.3 to 0.6 meter or 1 to 2 feet) above the beach level, thus allowing a part of the sand to pass over the groin and maintain the downdrift beach. However, if the structural members undergo even slight movement and distortion, the removal or addition of panels becomes difficult or even impossible.

#### 7. Alinement of Groins.

Examples may be found of almost every conceivable groin alinement, and advantages are claimed by proponents of each. The maximum economy in cost is achieved with a straight groin perpendicular to the shoreline. Various modifications such as a T- or L-head are included to limit recession on the

downdrift side of a groin or discourage the development of rip currents. While these modifications may achieve the intended purpose, the zone of maximum recession is often simply shifted downdrift from the groin, limiting the benefits. Storm waves will normally produce greater scour at the seaward extremities of the T- or L-head structures than at the end of a straight groin perpendicular to the shore, delaying the return to normal profile after storm conditions have abated. Curved, hooked, or angle groins have been employed for the same purposes as the T- or L-head types. They also cause excessive scour and are more costly to build and maintain than the straight, perpendicular groin. Where the adjusted shore alignment expected to result from a groin system differs greatly from the alignment at the time of construction, it may be desirable to align the groins normal to the adjusted shore alignment to avoid angular wave attack on the structures after the shore has stabilized. This condition is most likely to be encountered in the vicinity of inlets and along the sides of bays.

#### 8. Order of Groin Construction.

At sites where a groin system is under consideration, two possibilities arise: either the groin system is to be filled artificially or longshore transport is to be depended on to produce the fill. With artificial fill, the only interruption of longshore transport will be the period between the time the groin system is constructed and the time the artificial fill is made. For economical reasons, the fill is normally placed in one continuous operation, especially if it is being accomplished by hydraulic dredge. Accordingly, to reduce the time period between the groin construction and the deposition of the fill, all groins should preferably be constructed concurrently. Deposition of the fill should commence as soon as the stage of groin construction permits. When depending on longshore transport, no groin will fill until all the preceding updrift groins have been filled. This natural filling will reduce the supply to downdrift beaches. The time period required for the entire system to fill naturally and the material to resume its unrestricted movement downdrift may be so long that severe downdrift damage may result. Accordingly, to reduce this damage, only the groin or group of groins at the downdrift end should be constructed initially. The second groin, or group, should not be started until the first has filled and material passing around or over the groins has again stabilized the downdrift beach. Although this method may increase costs, it will not only aid in reducing damage, but will also provide a practical guide to the spacing of groins.

#### 9. Guidance from Existing Projects.

The guidelines presented here, in addition to knowledge of the study area and experience with groins, should provide a strong basis for the proper consideration and design of a groin system. Reports which summarize existing groin fields are also helpful. For example, DeWall (1979), Everts (1979), and Nordstrom, Allen, and Gares (1979) describe the effects of groin fields at Westhampton Beach, New York; Sea Isle City and Cape May, New Jersey; and Sandy Hook, New Jersey, respectively. The more similar an existing groin field is to the study area in terms of the physical environment, the more applicable its behavior and design will be to the study area.

## 10. Cost Effectiveness of Groin Construction.

Beaches exposed to wave action constantly change due to variation in wave direction and wave characteristics. In spite of the constant movement of beach materials, a beach will remain stable if the rate of loss from an area does not exceed the rate of supply to that area. If the rate of supply is less than the rate of loss, erosion and recession of the beach will occur. An eroding beach can be restored by the placement of an artificial protective beach and subsequently stabilized by artificial nourishment, i.e., the artificial placement of sand to make up the deficiency in rate of supply or the artificial nourishment supplemented by structures (groins) to reduce the rate of loss. The choice of groins over the artificial nourishment alternative should be based on the relative costs of the two methods of shore stabilization.

On long straight beaches, making up the deficiency of sand supply presumably affects and stabilizes much of the entire reach of shore. A groin system for such a long reach is obviously expensive, but requires less artificial nourishment, especially where the nourishment of the shore downdrift of the reach is not required. A method sometimes used to estimate the comparative life cycle cost for such a groin system is to estimate the annual cost of the system, including the annual cost of artificially nourishing the reach with groins and the downdrift shore, to find if the annual cost will be less than the estimated annual cost of stabilizing by artificial nourishment alone. No firm guidance is available on the reduction in nourishment requirements where a complete groin system is built.

Where the littoral transport rate is high, a groin system will not require artificial nourishment while the groins and offshore area are filling. If the littoral transport rate has not been reduced, no nourishment will be required after filling. The volume required to fill the groin system is easily estimated; the volume required to fill the offshore area, which is equally important, is difficult to estimate. Therefore, the time needed for complete filling is difficult to estimate. It may take several years for long groins and during this long time, the downdrift shore will erode unless it is artificially nourished. This nourishment volume will be equal to the volume impounded by the groin system and its offshore area plus any deficiency suffered before groin construction. After complete filling and shore realignment at the groin system, the littoral transport rate will probably be reduced from that required during the filling period and the downdrift shores may require more nourishment.

Another approach to estimate the comparative life cycle cost of a groin system for a long reach of shore is to estimate the annual cost, as before, and convert this cost to the equivalent quantity of sand that could be artificially placed annually at the estimated cost of sand over the life of the project. This will indicate how much the groins must reduce annual nourishment requirements to be at the "break-even" point. A judgment can then be made as to whether the groin system will actually reduce annual nourishment requirements below the break-even point. The choice of a groin system over artificial nourishment would be justified only if its costs (including reduced nourishment costs) are less than the costs of artificial nourishment alone.

Where it is necessary to widen a short beach, perhaps 2 kilometers or

less, it becomes impracticable to maintain the increased width by artificial nourishment of that beach alone. The nourishment material would rapidly spread to adjacent shores, and the desired widening of the beach would not be maintained. Here groins would be necessary to stabilize the widened beach within the limited reach. Choosing an alternative by comparison of the estimated annual costs with and without the groin system would therefore be impracticable.

At the downdrift end of a beach, where it is desired to reduce losses of material into an inlet and stabilize the lip of the inlet, a terminal groin should be used. Rarely would any other method of stabilization be as suitable and available at a comparative cost. A terminal groin should not be long enough to function as a jetty; the groin should impound only enough littoral drift to stabilize the lip or edge of the inlet.

#### 11. Legal Aspects.

The legal considerations discussed previously in Section V,3 of this chapter are also applicable to the construction of groins. Legal problems are varied and often complex, due to the diversity of legal precedent in different jurisdictions and the application of the factual setting to a particular body of law.

Previous information on the functional design of groins emphasizes the fact that adverse downdrift shore erosion can be expected if the updrift side of the groin is not artificially filled to its impounding capacity at the time of groin construction. Liability for property damage insofar as the Federal Government is concerned will be determined with reference to the Federal Tort Claims Act. It is therefore incumbent on the owner of groin-type structures to recognize the legal implications of this coastal structure in order to plan, design, construct, and maintain the structure accordingly. It is thus prudent to seek legal counsel at the earliest stages of formulation.

### VII. JETTIES

#### 1. Definition.

A *jetty* is a structure that extends into the water to direct and confine river or tidal flow into a channel and prevent or reduce the shoaling of the channel by littoral material. Jetties located at the entrance to a bay or river also serve to protect the entrance channel from wave action and cross-currents. When located at inlets through barrier beaches, jetties also stabilize the inlet location.

#### 2. Types.

In the coastal United States, jetties that have been built on the open coast are generally of rubble-mound construction. In the Great Lakes, jetties have also been built of steel sheet-pile cells, caissons, and cribs using timber, steel, or concrete. In sheltered areas, single rows of braced and tied Wakefield timber piling and steel sheet piling have been used.

### 3. Siting.

The proper siting and the spacing of jetties for the improvement of a coastal inlet are important. Careful study, which may include model studies in some cases, must be given to the following hydraulic, navigation, control structure, sedimentation, and maintenance considerations:

#### a. Hydraulic Factors of Existing Inlet:

(1) The tidal prism and cross section of the gorge in the natural state.

(2) Historical changes in inlet position and dimensions (i.e., length, width, and cross-sectional area of the inlet throat).

(3) Range and time relationship (lag) of the tide inside and outside the inlet.

(4) Influence of storm surge or wind setup on the inlet.

(5) Influences of the inlet on tidal prism of the estuary and effects of freshwater inflow on estuary.

(6) Influence of other inlets on the estuary.

(7) Tidal and wind-induced currents in the inlet.

#### b. Hydraulic Factors of Proposed Improved Inlet:

(1) Dimensions of inlet (length, width, and cross-sectional area).

(2) Effects of inlet improvements on currents in the inlet and on the tidal prism, salinity in the estuary, and on other inlets into the estuary.

(3) Effects of waves passing through the inlet.

#### c. Navigation Factors of the Proposed Improved Inlet:

(1) Effects of wind, waves, tides, and currents on navigation channel.

(2) Alinement of channel with respect to predominant wave direction and natural channel of unimproved inlet.

(3) Effects of channel on tide, tidal prism, and storm surge of the estuary.

(4) Determination of channel dimensions based on design vessel data and number of traffic lanes.

(5) Other navigation factors such as (a) relocation of navigation channel to alternative site, (b) provision for future expansion of channel dimensions, and (c) effects of harbor facilities and layout on channel alinement.

d. Control Structure Factors:

(1) Determination of jetty length and spacing by considering the navigation, hydraulic, and sedimentation factors.

(2) Determination of the design wave for structural stability and wave runup and overtopping considering structural damage and maintenance.

(3) Effects of crest elevation and structure permeability on waves in channel.

e. Sedimentation Factors:

(1) Effects of both net and gross longshore transport on method of sand bypassing, size of impoundment area, and channel maintenance.

(2) Legal aspects of impoundment area and sand bypassing process (see Sec. V,3 of this chapter).

f. Maintenance Factor: Bypassing and/or channel dredging will usually be required, especially if the cross-sectional area required between the jetties is too large to be maintained by the currents associated with the tidal prism.

4. Effects on the Shoreline.

The effects of entrance jetties on the shoreline are illustrated in Figure 5-24. A jetty (other than the weir type) interposes a total littoral barrier in that part of the littoral zone between the seaward end of the structure and the limit of wave uprush on the beach. Jetties are sometimes extended seaward to the contour position equivalent to the project depth of the channel. Accretion takes place updrift from the structures at a rate proportional to the longshore transport rate, and erosion takes place downdrift at about the same rate. The quantity of the accumulation depends on the length of the structure and the angle at which the resultant of the natural forces strikes the shore. If the angle of the shoreline of the impounded area is acute with the structure, the impounding capacity is less than it would be if the angle were obtuse. Structures that are perpendicular to the shore have a greater impounding capacity for a given length and thus are usually more economical than those at an angle, because perpendicular jetties can be shorter and still reach the same depth. If the angle is acute, channel maintenance will be required sooner due to littoral drift passing around the end of the structure. Planning for jetties at an entrance should include some method of bypassing the littoral drift to eliminate or reduce channel shoaling and erosion of the downdrift shore (see Sec. V of this chapter).

VIII. BREAKWATERS, SHORE-CONNECTED

1. Definition.

A *shore-connected breakwater* is a structure that protects a shore area, harbor, anchorage, or basin from waves. Breakwaters for navigation purposes are constructed to create calm water in a harbor area, which provides protection for safe mooring, operating and handling of ships, and harbor facilities.



Indian River Inlet, Delaware (Oct. 1972)

Figure 5-24. Effects of entrance jetties on shoreline.

## 2. Types.

Breakwaters may be rubble mound, composite, concrete caisson, sheet-piling cell, crib, or mobile. In the coastal United States, breakwaters that have been built on the open coast are generally of rubble-mound construction. Occasionally, they are modified into a composite structure by using a concrete cap for stability. Precast concrete shapes, such as tetrapods or tribars, are also used for armor stone when sufficient size rock is not obtainable. In the Great Lakes area, timber, steel, or concrete caissons or cribs have been used. In relatively sheltered areas, single rows of braced and tied Wakefield (triple lap) timber piling or steel sheet piling have occasionally been used in breakwater construction. Several types of floating breakwaters have been designed and tested. Between 1970 and 1980, a total of 27 floating breakwaters of various types have been installed in the United States with varying degrees of success; 17 were tire breakwaters and 8 were concrete caissons or pontoons (Western Canada Hydraulic Laboratories Ltd., 1981).

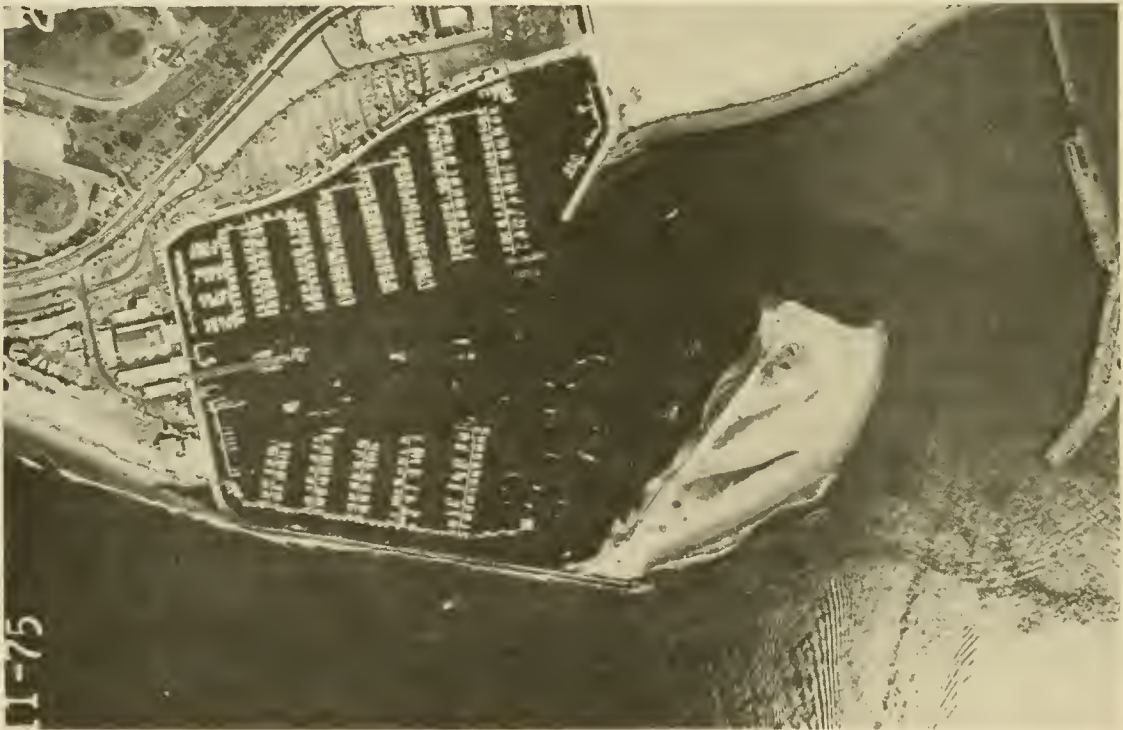
## 3. Siting.

Shore-connected breakwaters provide a protected harbor for vessels. The most important factor in siting a breakwater is determining the best location that will produce a harbor area with minimum wave and surge action over the greatest period of time in the year. This determination is made through the

use of refraction and diffraction analyses. Other siting factors are the direction and magnitude of longshore transport, the harbor area required, the character and depth of the bottom material in the proposed harbor, and the available construction equipment and operating capability. Shore-connected structures are usually built with shore-based equipment (see Sec. V,3 of this chapter).

#### 4. Effect on the Shoreline.

The effect of a shore-connected breakwater on the shoreline is illustrated in Figure 5-25. Like the jetty, the shore arm of the breakwater interposes a total littoral barrier in the zone between the seaward end of the shore arm and the limit of wave uprush until the impounding capacity of the structure is reached and the natural bypassing of the littoral material is resumed. The same accretion and erosion patterns that result from jetties also result from the installation of this type of breakwater. The accretion, however, is not limited to the shore arm; it eventually extends along the seaward face of the shore arm, building a berm over which littoral material is transported to form a large accretion area at the end of the structure in the less turbulent waters of the harbor. This type of shoal creates an ideal condition for sand bypassing. A pipeline dredge can lie in the relatively quiet waters behind the shoal and transfer accumulated material to nourish the downdrift shore (see Sec. V of this chapter).



Direction of net longshore transport →

Santa Barbara, California (1975)

Figure 5-25. Effects of shore-connected breakwater on shoreline.

## IX. BREAKWATERS, OFFSHORE

### 1. Definition.

An *offshore breakwater* is a structure that is designed to provide protection from wave action to an area or shoreline located on the leeward side of the structure. Offshore breakwaters are usually oriented approximately parallel to shore. They may also provide protection for harbors or erodible shorelines, serve as a littoral barrier-sediment trap (Fig. 5-26), or provide a combined function. Table 5-3 is a partial list of offshore breakwaters that have been constructed in the United States. These are generally of rubble-mound construction, although some cellular sheet-pile, rock-filled concrete caisson, timber crib, and floating concrete cellular designs have been used. Offshore breakwaters overseas have been constructed with timber, quarrrystone, concrete armor units, concrete caissons, and even sunken ships.

### 2. Functional Operation.

An offshore breakwater provides protection by reducing the amount of wave energy reaching the water and shore area in its lee. The breakwater structure reflects or dissipates the incident wave impacting directly on the structure and transmits wave energy by means of diffraction into the barrier's geometric shadow (see Ch. 2, Sec. IV). This reduction of wave energy in the breakwater's shadow reduces the entrainment and transport of sediment by wave action in this region. Thus, sand transported from nearby regions by a predominant longshore current or circulation will tend to be deposited in the lee of the structure. This deposition causes the growth of a cusped spit from the shoreline (see Fig. 5-27). If the structure's length is great enough in relation to its distance offshore, the cusped spit may connect to the

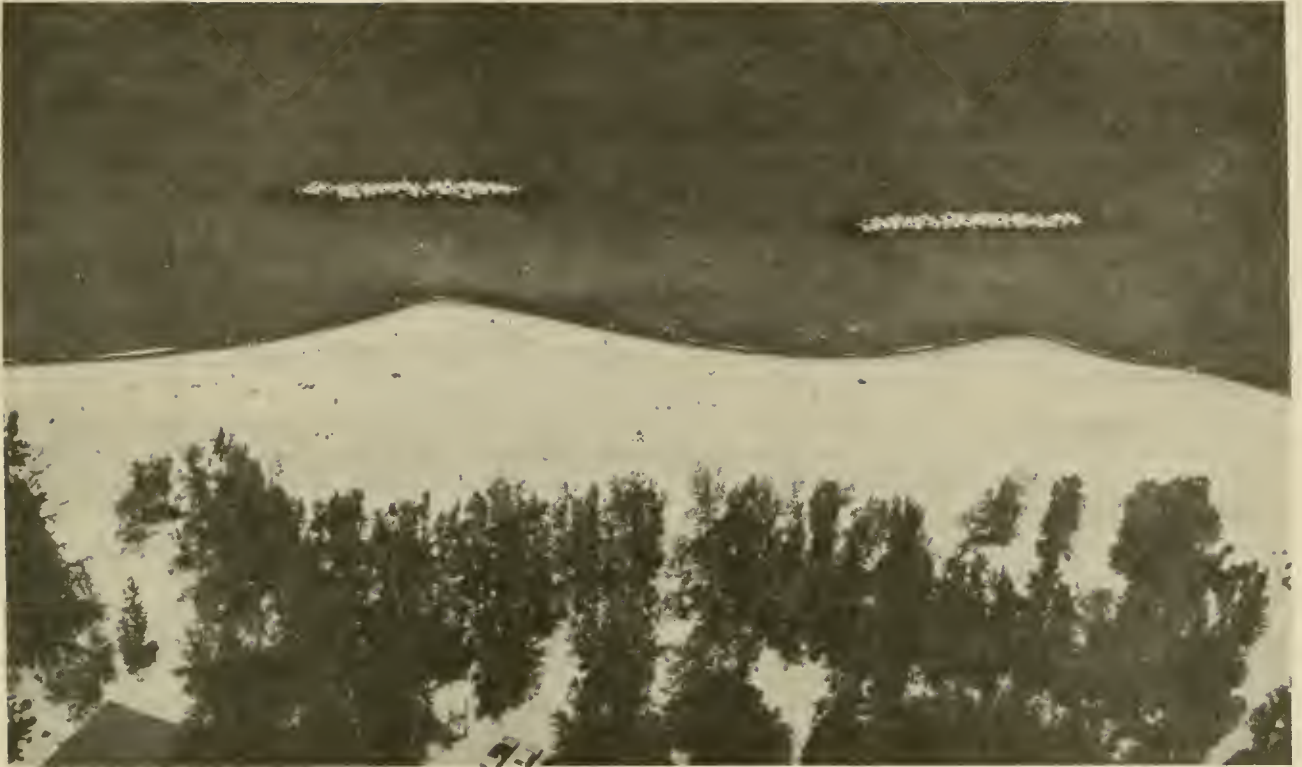


Channel Islands, California

Figure 5-26. Offshore breakwater as a littoral barrier-sediment trap.

Table 5-3. Offshore breakwaters in the United States.

Location	Construction date	Purpose	Type	Configuration	Shoreline response
Venice, Calif.	1905	Protect amusement pier	Rubble mound	Single structure; crest elevation: +3.7 meters (+12 feet) MLLW; depth: -1.8 meters (-6 feet) MLLW; length: 183 meters (600 feet); distance offshore: 213 meters (700 feet)	Tomboolo connected to structure
Santa Barbara, Calif.	1929	Harbor or refuge	Rubble mound	Originally a single offshore structure; crest elevation: +3.7 meters MLLW; water depth: -7.6 meters (-25 feet) MLLW; length: 434 meters (1,425 feet); distance offshore: 305 meters (1,000 feet)	Tomboolo connected quickly; structure extended to shore, 1930
Santa Monica, Calif.	1934	Harbor or refuge	Rubble mound	Single structure; crest elevation: +3.04 meters (+10 feet) MLLW; depth: -7.6 meters MLLW; length: 610 meters (2,000 feet); distance offshore: 610 meters	Periodic dredging has prevented connection of tomboolo
Winthrop Beach, Mass.	1935	Shore and seawall protection	Rubble mound	Segmented structure; crest elevation: +5.5 meters MLW; depth: -3 meters (10 feet) MLW; 5 segments 91 meters (300 feet) long; gap size: 30 meters (100 feet); distance offshore: 305 meters	Unconnected feature formed at expense of neighboring shorelines
Waikiki Beach, Hawaii	1938	Shore protection	Rock-filled concrete cribs	Single structure; crest elevation: 0 meter MLLW; length: 213 meters; distance offshore: 76 meters (250 feet)	Fill placed which eroded slowly over 8-year period
Lincoln Park, Ill.	1939	Shore and road protection; recreational beach	Steel sheet pile	Single structure connecting the seaward ends of four groins; crest elevation: -1.2 meter (-4 feet) MLW; water depth: -3.7 to -4.3 meters (-12 to -14 feet); length: 457 meters (1,500 feet); distance offshore: 183 meters	Fill placed and held satisfactorily
Channel Islands, Calif.	1960	Harbor entrance protection and sediment trap	Rubble mound	Single structure; crest elevation: +4.3 meters (+14 feet) MLLW; water depth: -9.1 meters (-30 feet) MLLW; length: 700 meters (2,300 feet); distance offshore: 550 meters (1,800 feet)	Large tomboolo formed which is periodically bypassed
Haleiwa Beach, Hawaii	1965	Shore protection	Rubble mound	Single structure; crest elevation: +1.5 meters (+5 feet) MLLW; water depth: -2.4 meters (-8 feet) MLLW; length: 49 meters (160 feet); distance offshore: 91 meters	Unconnected tomboolo formed
Lakeview Park, Ohio	1977	Shore protection; recreational beach	Rubble mound	Segmented structure with terminal groins; crest elevation: +2.4 meters (+8 feet) low water depth; water depth: -3.0 meters (-10 feet) low water depth; 3 segments 62 meters (205 feet) long; gap size: 49 meters; distance offshore: 76 meters	Series of unconnected tomboolos formed
Presque Isle, Pa.	1978	Shore protection; recreational beach	Rubble mound	Segmented structure; crest elevation: +1.8 meters (+6 feet) low water depth; water depth -0.3 meter (-1 foot) low water depth; 3 segments 38 meters (125 feet) long; gap size: 53 and 91 meters (175 and 300 feet); distance offshore 46 meters (150 feet)	Series of smooth tomboolos, connected at low water



Presque Isle, Pennsylvania (July 1980)

Figure 5-27. Offshore breakwaters with asymmetric cusped spits (oblique wave attack).

structure, forming a tombolo. Thus, breakwaters provide protection to the backshore property not only by reducing incident wave energy, but also by building a wider protective beach which acts as a buffer during storm events.

### 3. Shoreline Response.

The shoreline response to the construction of any offshore breakwater is predominantly governed by the resulting alterations in the longshore transport of material in the vicinity and, to a lesser extent, by the onshore-offshore transport rate. The placement of a breakwater causes the shoreline to adjust to the new conditions and seek an equilibrium configuration.

If the incident breaking wave crests are parallel to the original shoreline (which is a condition of no longshore transport), the waves diffracted into the offshore breakwater's shadow will transport sand from the edges of this region into the shadow zone. This process will continue until the shoreline configuration is essentially parallel to the diffracted wave crests and the longshore transport is again zero. In this instance the cusped spit (or tombolo) will have a symmetric shape, with the tombolos featuring concave sides and the cusped spits exhibiting a more rounded convex shape.

For obliquely incident waves the longshore transport rate in the lee of the structure will initially decrease, causing deposition of the longshore

drift. A cusped spit is formed which will continue to grow until either the longshore transport rate past the structure is reestablished or a tombolo is formed. Depending on where the offshore breakwater is positioned relative to the littoral zone, the formation of a tombolo can act as a complete littoral barrier which can trap all the littoral drift until it is filled to capacity, at which time sand will be shunted around the seaward side of the structure, restoring the longshore transport rate. During this process severe erosion of the downdrift beach would be expected. The cusped spit that results from oblique wave attack can be expected to be asymmetric with its shape dependent on the structure length, the distance offshore, and the nearshore wave conditions. Figure 5-27 illustrates the formation of asymmetric cusped spits.

A major concern in designing an offshore breakwater for shore protection is determining if the resulting shore adjustment should be connected to the structure. There are advantages and disadvantages for each shoreline configuration, and the designer is usually confronted with many aspects to consider before making a choice between tombolos and cusped spits. While both shoreline adjustments affect the adjacent shoreline, cusped spits are usually preferred over tombolos. When a tombolo forms, large quantities of sediment can be impounded, resulting in extensive erosion downdrift of the structure. A cusped spit formation will often allow the majority of littoral drift to pass and thus have a lesser effect on the downdrift beach. During seasonal changes in wave direction, a cusped spit is more likely to allow the littoral drift to pass landward of the offshore breakwater. Therefore, there is less chance of the material being retarded by passage to the seaward of the structure where parts of the littoral drift may be lost permanently. Cusped spits and tombolos do not provide uniform erosion protection along an entire project, and legal problems could arise if the protected region is not owned by a Federal, State, or local government. Depending on the project, more uniform protection may be needed.

The formation of a tombolo increases the length of beach available for recreation use and greatly facilitates the monitoring and maintenance of the structure, but beach users may be inclined to use the structure or swim immediately adjacent to it which could be dangerous.

#### 4. Siting Considerations.

The most important parameters governing the shore response to offshore breakwaters are those that affect diffraction. Wavelength, wave height, wave direction, and the breakwater gap all affect the resulting diffraction pattern. The shore responds by aligning itself with the patterns of the wave crests. The response rate is governed by the amount of wave energy available to transport sediment. Other important parameters are the local tidal range, the natural beach slope, the supply of sediment, and the sediment grain size. Background information on the protective features and the functional limitations of offshore breakwaters is discussed by Toyoshima (1972) and Lesnik (1979).

a. Wavelength. In general, the amount of wave energy transferred into the lee of a breakwater increases with increasing wavelength. According to linear diffraction theory, the wavelength does not affect the pattern created by the wave crest. However, wavelength does affect the amplitude of the diffracted wave at a particular location. Longer waves will provide more

energy to the shadow zone, especially the obliquely arriving waves, which tends to prevent tombolo formation. The amount of energy transferred into the lee of the structure can be found using Figures 2-28 to 2-39 in Chapter 2 for the appropriate position, water depth, wavelength, and wave direction. The diffraction technique must be performed for both ends of the breakwater, with the resultant energy quantities being summed.

b. Breakwater Gap Width. The ratio of the gap width,  $B$ , to the wavelength,  $L$ , for segmented offshore breakwaters greatly affects the distribution of wave heights in the lee of the structures. Generally, increasing the ratio  $B/L$  will increase the amount of energy reaching the shadow zones, while the diffraction effects will decrease. Figures 2-42 to 2-52 in Chapter 2 can be used to estimate the diffraction patterns caused by breakwater gaps. It is important to note that these diagrams do not contain refraction, shoaling, or breaking effects.

c. Wave Direction. The general shape of the shoreline behind an offshore breakwater is highly dependent on the directional nature of the wave climate. Very oblique waves produce a strong longshore current that may prevent tombolo formation and restrict the size of the cusped spit. The bulge in the shoreline tends to align itself with the predominant wave direction. This is particularly evident for tombolos, which seem to "point" into the waves. However, if the predominant waves are oblique to the shoreline, the tombolo's apex will be shifted to the downdrift direction, its equilibrium position becoming more dependent upon the strength of the longshore current and the length of the structure.

d. Wave Height. Besides its role in generating currents and entraining sediments, wave height also affects the pattern of diffracted wave crests. Linear diffraction theory assumes that the diffracted wave crests move at a speed given by

$$C = \sqrt{gd} \tag{5-18}$$

where  $C$  is the wave celerity,  $g$  the acceleration of gravity, and  $d$  the water depth. Assuming a constant water depth gives the circular diffracted wave crests as shown in Figure 5-28. In this case all the wave crests move at the same speed, even though the wave height has decreased along the crest toward the breakwater. However, in very shallow water, studies have shown that wave amplitude dispersion plays an important role in wave diffraction (Weishar and Byrne, 1978). The wave celerity in very shallow water is more accurately expressed as

$$C = \sqrt{g(d + H)} \tag{5-19}$$

which is a function of wave height,  $H$ . With a constant water depth, the wave celerity will decrease along the diffracted wave crest as the wave height decreases. In other words, the farther along a diffracted wave crest into the undisturbed region the more the wave height decreases, which in turn decreases the speed of the wave crest. This action distorts the wave pattern from the circular shape to an arc of decreasing radius as shown in Figure 5-29. In situations where amplitude dispersion is important, tombolos are more likely to form because the diffracted parts of the wave crests are less likely to

intersect before the undiffracted waves adjacent to the structure reach the shore.

e. Tidal Range. It is extremely difficult to predict the exact effect of a large tidal range on the shoreline response to the construction of an offshore breakwater. Generally, a large range (typically more than 1.5 meters) will tend to hinder tombolo formation, especially if the structure is significantly overtopped during high tide. In addition, the cusped spit will probably not attain a smooth equilibrium shape. An example of a segmented

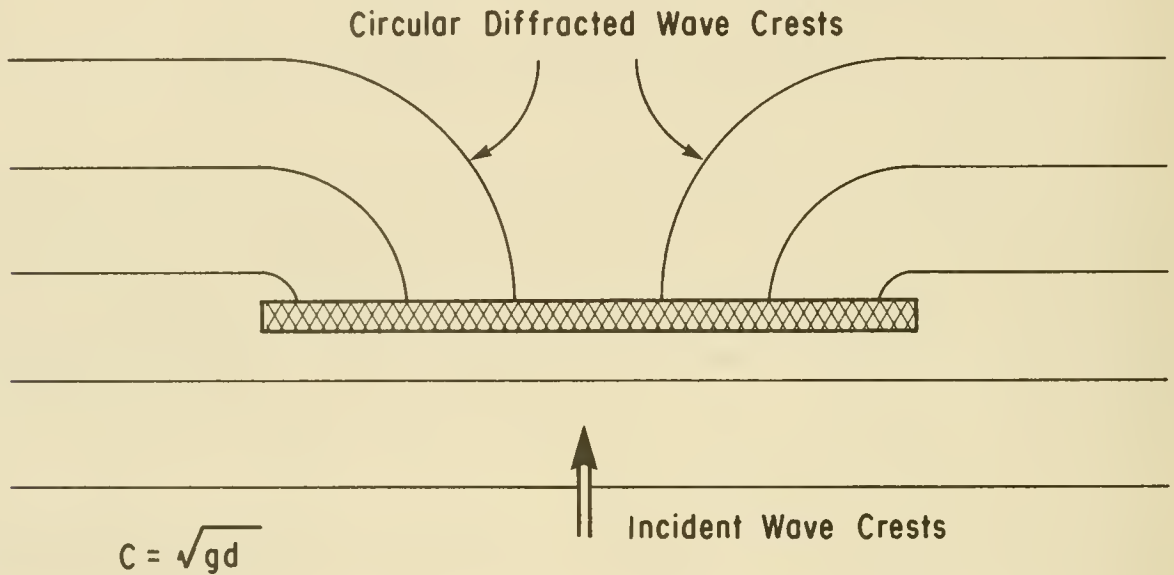


Figure 5-28. Diffraction at a breakwater, assuming linear wave theory is valid.

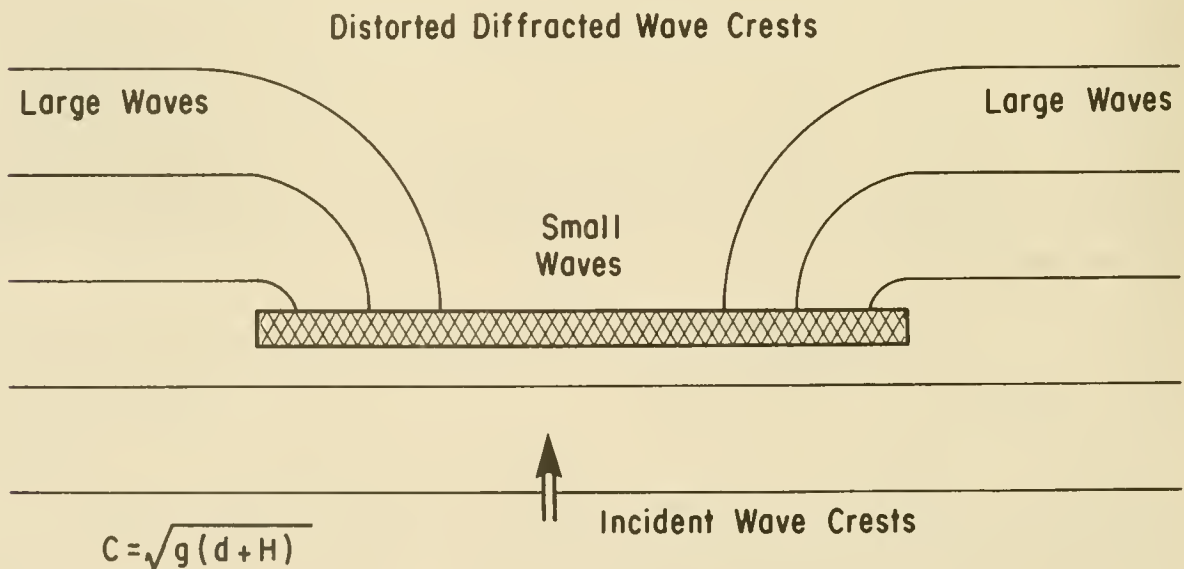


Figure 5-29. Diffraction at a breakwater, including effects of amplitude dispersion.

breakwater in a large tidal range is shown in Figure 5-30. The mean tidal range is 2.9 meters (9.5 feet) and there is a limited sediment supply. At low tide (Fig. 5-30a) a double tombolo has formed because the structure is long, close to shore, and has narrow breakwater gaps. At high tide (Fig. 5-30b) the combined structure length is only about twice as long as the distance from the original shoreline. A "high water tombolo" has not formed as might be expected for this configuration due to the combination of the large tidal range and the limited sediment supply.

f. Natural Beach Slope. The natural beach slope can play a major role in the positioning and configuration of offshore breakwaters. If the profile is gently sloping and the structure is to be placed outside the surf zone, the breakwater may have to be lengthened in order to be an effective sediment trap. A gently sloping beach with a large tidal range makes an optimum structure placement extremely difficult because such a large section of the profile is active over the tidal cycle.

g. Sediment Supply. If there is an insufficient supply of sediment, the expected shoreline adjustment in the form of a cusped spit will not fully develop. Offshore transport will continue to erode and flatten the beach profile in the lee of the structure, resulting in a different equilibrium condition than expected. In locations where there is a seasonal variation in sediment supply, it is possible that cusped spits may accrete and recede accordingly.

h. Sediment Size. The sediment grain-size distribution on a beach affects the shape and growth of a cusped spit by affecting the slope of the equilibrium beach profile and the sediment transport rate. Coarser sediments have steeper profiles which cause more diffraction than finer grain-sized sediments. The finer grained beaches will respond more rapidly to changing wave conditions and are more likely to form tombolos. Graded materials may settle differently between the shore and the breakwater.

## 5. Design Considerations.

The main design considerations for an offshore breakwater center around the resulting shoreline adjustment. In some cases it is desirable to ensure a tombolo connection, but more often this connection should be avoided. The formation of a tombolo is usually prevented by allowing sufficient energy to pass into the protected region, using one or more of the techniques discussed below.

a. Breakwater Length Versus Distance Offshore. Tombolo formation can usually be prevented if the structure length,  $\ell$ , is less than the distance offshore,  $X$ ; i.e.,

$$\ell < X \quad (5-20)$$

This configuration usually permits the intersection of the diffracted wave crests well before the undistorted waves adjacent to the structure reach the shoreline. If the predominant wave direction is nearly shore normal, an approximate location of the bulge apex is found at the point of the intersection of the two wave crests as the waves reach the shoreline, as shown in Figure 5-31. When the structure length becomes greater than the distance



Winthrop Beach, Massachusetts (1981)

a. Low tide



Winthrop Beach, Massachusetts (1981)

b. High tide

Figure 5-30. Example of a segmented breakwater in a large tidal range.

offshore, the chance of tombolo formation increases, becoming almost certain in usual circumstances when  $\lambda < 2X$ . There is the possibility of a double tombolo formation with trapped water between them when the structure length is further increased.

Offshore breakwaters designed for an open coast are generally sited in water depths between 1 to 8 meters (3 to 25 feet). If the project length is so great that economic considerations preclude moving the structure far enough offshore to satisfy the  $\lambda < X$  criterion, alternate methods for increasing the energy flux into the protected region must be employed.

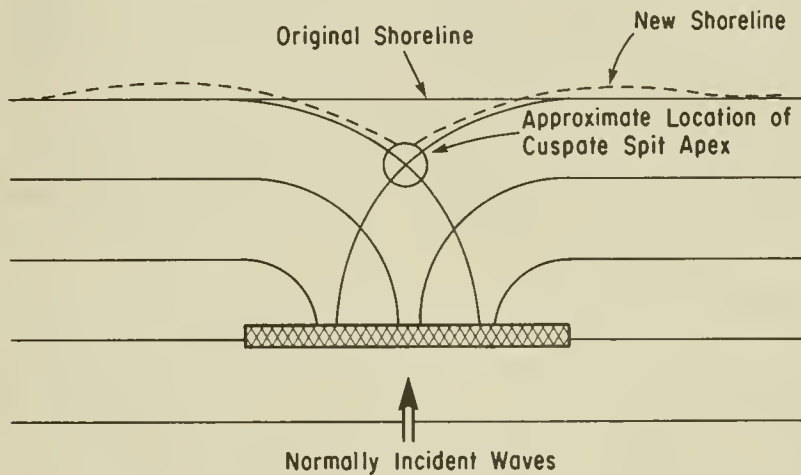


Figure 5-31. Location of cusped spit apex.

b. Wave Overtopping. The offshore breakwater can be designed so that a part of the incident wave energy can be transmitted by overtopping which helps to prevent the connection of the cusped spit to the structure. An advantage to using this method is that the shoreline of the cusped spit tends to flatten and spread laterally along the shore in a more uniform manner. However, the transmitted waves have a shorter wave period than the incident wave and are highly irregular. Tide level, wave height and period, structure slope and roughness all have nonlinear effects on the amount and form of energy transmission by overtopping. This makes the design procedure difficult unless these parameters are nearly constant. Chapter 7, Section II,3 discusses procedures for altering the structure cross section so that sufficient energy is transmitted by overtopping. If an existing structure is not performing as required, it is conceivable that the crest elevation could be raised or lowered, but this is often costly and impractical.

c. Breakwater Permeability. Another means of preventing a tombolo formation is to make the structure permeable, so a part of the incident energy is passed through the breakwater. This energy is transmitted at the period of the incident wave period and is generally more predictable and regular than overtopping transmission. With transmission through the permeable structure, the advancement of the shoreline is generally more uniform than with segmented structures. However, the transmission is highly dependent on wave period. If an existing structure is not performing as intended, it is impractical to increase the permeability as a solution to the problem. Figure 5-32 shows



Kakuda-Hama, Japan

Figure 5-32. Segmented breakwater that is permeable and overtopped, located landward of breaker zone.

the shoreline adjustment behind a segmented breakwater that is permeable and overtopped.

d. Segmented Breakwaters. A segmented breakwater offers a very functional solution for a long section of shoreline that requires wave transmission to prevent tombolo formation. The structure can be built nearshore in an economical water depth because it permits a constant proportion of wave energy into the protected area. Also, the diffracted waves have the same period as the incident waves. Segmented breakwaters can be designed to allow the beach in their lee to accrete enough sediment to provide an erodible buffer during storms and still maintain the natural longshore transport rate during normal wave conditions.

The amount of energy reaching the lee of the structure is controlled by the width of the gaps between the breakwaters and the wave diffraction through these gaps. The gaps should be at least two wavelengths wide, and the length of each structure segment should be less than the distance offshore. Providing fewer gaps of greater width will cause the shoreline to respond with spaced bulges and embayments with an enlarged relief (the seaward distance from the more shoreward point of the embayment to the tip of the cusped spit), which does not provide uniform storm protection along the project. If this is not acceptable, increasing the number of gaps and shortening the length of each segment will promote features of less relief, providing more uniform protection. Segmented offshore breakwaters are illustrated in Figures 5-30, 5-32, and 5-33. Figure 5-33 illustrates the use of offshore breakwaters in conjunction with a beach fill.

e. Positioning with Respect to Breaker Zone. Placing the breakwater landward of the normal breaker zone will advance the shoreline and may cause tombolo formation (see Fig. 5-32). If positioned well shoreward of the breaker zone, a large percentage of the total longshore transport will pass seaward of the structure and the effect on the adjacent shoreline will be less severe. This method is not recommended for coasts with steep beach slopes and narrow surf zones because the area shoreward of the breakwater will tend to fill completely, turning the breakwater into a seawall.

f. Structure Orientation. The orientation of the breakwater with respect to both the predominant wave direction and the original shoreline can have a marked effect on the size and shape of the resulting cusped spit or tombolo. A change in structure orientation modifies the diffraction pattern at the shoreline, and subsequently, the shore response. An approximation of the shape of the shore response when waves are normally incident to the shoreline can be determined by using the procedures discussed in Chapter 2, Section IV to determine the diffracted wave crest configuration. For waves that are extremely oblique to the shoreline, it is recommended that the breakwater be oriented parallel to the incoming wave crests. This will provide protection to a longer section of shoreline for a given structure length; however, it will probably increase the amount of construction material required for the structure since one end of the breakwater will be in water deeper than if it were oriented parallel to the bottom contours.

## 6. Other Considerations.

Apart from shore response, there are several other factors which affect



Lakeview Park, Ohio (November 1979)

a. Short wavelengths



Lakeview Park, Ohio (April 1981)

b. Long wavelengths

Figure 5-33. Example of a segmented breakwater with waves passing through breakwater gaps.

shore alignment configuration and construction of offshore breakwaters. These include ecology, safety, esthetics, and breakwater gap currents. Structural aspects such as foundation design, scour protection, cross-section shape, and armor stability and placement are discussed in Chapter 7, Section III.

a. Ecological Considerations. The design analysis should include an appraisal of the total impact of the project, environmental as well as economical. Rounsefell (1972) discusses the ecological effects of offshore construction, and Thompson (1973) examines the ecological effects of offshore dredging and beach nourishment. Although these studies suggest that offshore breakwaters generally do not cause long-term undesirable ecological changes, each proposed project site is unique and must be examined for a possible negative impact to the ecological system.

If a double tombolo (or any other shoreline adjustment that traps water) forms, it is possible that the reduced exchange of water will cause the entrapped water to become stagnant. This is more likely to occur in regions of small tidal ranges. Generally offshore breakwaters have adequate circulation to prevent accumulation of waterborne pollutants in their lees.

b. Esthetics. If a breakwater is to be constructed to protect a recreational beach, esthetics should be taken into consideration. For example, bathers usually prefer that their view of the horizon is not obstructed, so this may be a factor in selecting the structure height. However, the effectiveness will be limited as overtopping becomes more common.

c. Flow Through Breakwater Gaps. Of possible concern when sizing offshore breakwater gaps are return flow currents. These currents occur when the structure is nearly impermeable and low crested, causing the water that passes into its lee by wave overtopping to return only through the gaps or around the ends of the structure. The return flow can become particularly strong if the breakwater is long, has only a few gaps, and has two tombolos that prevent flow around the exterior ends of the structure. These currents can cause severe scour at the ends of each segment, which may result in the partial failure of the breakwater. The strong currents are also a hazard to swimmers. A method for estimating the magnitude of these currents is presented by Seelig and Walton (1980). Return flow currents can be reduced by raising the breakwater crest elevation, enlarging the gaps between segments, and increasing structure permeability.

d. Construction Considerations. Because of the difficulty in quantitatively predicting shoreline changes associated with segmented offshore breakwaters, it may be wise to first build small segments with large gaps and partially close the gaps in response to the shoreline adjustment. In this way the desired protection is eventually attained. If feasible, the expected shoreline adjustment behind the structure should be artificially placed to reduce starvation of the downdrift beach. Beginning construction at the downdrift end of the project will result in a more uniform accretion of the shoreline.

Construction capability plays a major role in determining the water depth in which the structure is placed. Land-based equipment can operate in depths up to 1 meter, and floating construction vessels usually can operate no closer to shore than the 2-meter (6-foot) contour. Wave activity and tidal range can

greatly influence these limits. Most large shore protection projects require floating construction equipment.

## X. ENVIRONMENTAL CONSIDERATIONS

Shore protection measures by their very nature are planned to result in some modification of the physical environment. However, thorough planning and design require that the full impact of that modification on the ecological and esthetic aspects of the environment be fully considered and understood. If there is potential for a significant adverse effect to any environmental feature, the design analysis of a shore improvement project should include alternatives for avoiding or mitigating that adverse effect. Therefore, the design analysis should include a multidiscipline appraisal of the total impact of the project, which includes environmental quality as well as economic benefits. The necessity for this appraisal at the planning and design stage is apparent and required by law. If there is a probability for conflict between planned construction and environmental quality, a final decision by appropriate authority based on social, technical, and economic analysis will be required.

In recent years the question of total environmental quality has reached high levels of public concern. Published technical information on this question is scattered through many disciplines, and the lack of quantifiable base-line data precludes reliable quantitative forecasting of most environmental and ecological changes resulting from manmade structures. Two works that specifically address this question are Rounsefell (1972) on the ecological effects of offshore construction and Thompson (1973) on ecological effects of offshore dredging and beach nourishment. Both works include state-of-the-art evaluations, from the ecologist's perspective, and extensive bibliographies with some entries annotated. Both describe and discuss direct and indirect effects of several categories of coastal protective works, and both discuss procedures for evaluating those effects. The two agree that it is of utmost importance to obtain necessary data on probable environmental impact of proposed construction at an early stage of the project planning. An accurate assessment of preproject environment is essential, not only for initial planning and design, but also for later design modification or alternatives that could bear on either mitigation or environmental change or enhancement of other aspects of the environment. Rounsefell and Thompson's works suggest that the methods of shore protection discussed in this manual would generally not result in long-term undesirable ecological changes for individual projects. However, this opinion is qualified to the extent that cumulative effects of numerous works of certain types could conceivably result in some detrimental long-term changes. A further requirement is recognized for additional baseline data and knowledge of the quantitative ecological-physical relationships. This information can be developed by monitoring before-, during-, and after-construction effects on coastal projects.

## LITERATURE CITED

- BLUMENTHAL, K.P., "The Construction of a Draft Sand Dyke on the Island Rottmerplatt, *Proceedings of the Ninth Conference on Coastal Engineering*, American Society of Civil Engineers, 1964, pp. 346-367.
- BRUUN, P., "Measures Against Erosion at Groins and Jetties," *Proceedings of the Third Conference on Coastal Engineering*, American Society of Civil Engineers, Oct. 1952.
- DEAN, R.G., "Compatibility of Borrow Material for Beach Fills," *Proceedings of the 14th International Conference on Coastal Engineering*, American Society of Civil Engineers, Vol. II, 1974, pp. 1319-1330.
- DEAN, R.G., "Coastal Structures and Their Interaction with the Shoreline," *Application of Stochastic Processes in Sediment Transport*, H.W. Shen and H. Kikkawa, eds., Water Resources Publication, Littleton, Colo., 1978, pp. 18-1--18-46.
- DeWALL, A.E., "Beach Changes at Westhampton Beach, New York, 1962-73," MR 79-5, Coastal Engineering Research Center, U. S. Army Engineer Waterways Experiment Station, Vicksburg, Miss., Aug. 1979.
- EVERTS, C.H., "Beach Behavior in the Vicinity of Groins--Two New Jersey Field Examples," *Proceedings of Coastal Structures '79*, American Society of Civil Engineers, 1979, pp. 853-867 (also Reprint 79-3, Coastal Engineering Research Center, U. S. Army Engineer Waterways Experiment Station, Vicksburg, Miss., NTIS A073 276).
- HOBSON, R.D., "Review of Design Elements for Beach Fill Evaluation," TP 77-6, Coastal Engineering Research Center, U. S. Army Engineer Waterways Experiment Station, Vicksburg, Miss., June 1977.
- HANDS, E.B., and HANSEN, M.A., "Beach Sampling," Coastal Engineering Research Center, U. S. Army Engineer Waterways Experiment Station, Vicksburg, Miss. (in preparation, 1985).
- HODGES, T.K., "Sand Bypassing at Hillsboro Inlet, Florida," *Bulletin of the Beach Erosion Board*, Vol. 9, No. 2, U.S. Army, Corps of Engineers, Beach Erosion Board, Washington, D.C., Apr. 1955.
- JAMES, W.R., "Borrow Material Texture and Beach Fill Stability," *Proceedings of the 14th International Conference on Coastal Engineering*, American Society of Civil Engineers, Vol. II, 1974, pp. 1334-1344.
- JAMES, W.R., "Techniques in Evaluating Suitability of Borrow Material for Beach Nourishment," TM-60, Coastal Engineering Research Center, U. S. Army Engineer Waterways Experiment Station, Vicksburg, Miss., Dec. 1975.
- KRESSNER, B., "Tests with Scale Models to Determine the Effect of Currents and Breakers upon a Sandy Beach, and the Advantageous Installation of Groins," *The Technical High School of the Free City of Danzig, Construction Methods*, Vol. 25, Berlin, June 1928.

- KRUMBEIN, W.C., "A Method for Specification of Sand for Beach Fills," TM-102, U. S. Army, Corps of Engineers, Beach Erosion Board, Washington, D.C., Oct. 1957.
- KRUMBEIN, W.C., and JAMES, W.R., "A Lognormal Size Distribution Model for Estimating Stability of Beach Fill Material," TM-16, Coastal Engineering Research Center, U. S. Army Engineer Waterways Experiment Station, Vicksburg, Miss., Nov. 1965.
- LESNIK, J.R., "An Annotated Bibliography on Detached Breakwaters and Artificial Headlands," MR 79-1, Coastal Engineering Research Center, U. S. Army Engineer Waterways Experiment Station, Vicksburg, Miss., Feb. 1979.
- NORDSTROM, K.F., ALLEN, J.R., and GARES, P.A., "The Effect of Groin Removal on Shoreline Stability," *Proceedings of Coastal Structures '79*, American Society of Civil Engineers, 1979, pp. 904-920.
- RICHARDSON, T.W., and McNAIR, E.C., "A Guide to the Planning and Hydraulic Design of Jet Pump Remedial Sand Bypassing Systems," Instruction Report HL 81-1, U.S. Army Engineer Waterways Experiment Station, Vicksburg, Miss., Sept. 1981.
- ROUNSEFELL, G.A., "Ecological Effects of Offshore Construction," *Marine Science*, Vol. 2, No. 1, 1972.
- SEELIG, W.N., and WALTON, T.L., Jr., "Estimation of Flow Through Offshore Breakwater Gaps Generated by Wave Overtopping," CETA 80-8, Coastal Engineering Research Center, U. S. Army Engineer Waterways Experiment Station, Vicksburg, Miss., Dec. 1980.
- THOMPSON, J.R., "Ecological Effects of Offshore Dredging and Beach Nourishment," MP 1-73, Coastal Engineering Research Center, U. S. Army Engineer Waterways Experiment Station, Vicksburg, Miss., Jan. 1973.
- TOYOSHIMA, O., "Coastal Engineering for the Practicing Engineer: Erosion," 1972 (published in Japanese).
- U.S. ARMY ENGINEER DISTRICT, WILMINGTON, "Hurricane-Wave Protection - Beach Erosion Control Brunswick County, N.C., Beach Projects, Yaupon Beach and Long Beach Segments," General Design Memorandum - Phase I, Wilmington, N.C., July 1973.
- WEGGEL, J.R., "Weir Sand-Bypassing Systems," SR-8, Coastal Engineering Research Center, U. S. Army Engineer Waterways Experiment Station, Vicksburg, Miss., Apr. 1981.
- WEISHAR, L.L., and BYRNE, R.J., "Field Study of Breaking Wave Characteristics," *Proceedings of the 16th Coastal Engineering Conference*, American Society of Civil Engineers, Ch. 27, 1978.
- WESTERN CANADA HYDRAULIC LABORATORIES LTD., "Development of a Manual for the Design of Floating Breakwaters, *Canadian Manuscript Report of Fisheries and Aquatic Sciences*, No. 1629, Nov. 1981.



